

VOL. **452** OCTOBER 28, 1988
COMPLETE IN ONE ISSUE

Erich Heftmann Honour Volume

ATTENTION

Please note that Vol. 451 (Cumulative Indexes Vols. 401-450) will appear in 1989. Please do not claim; nothing is missing.

JOURNAL OF

CHROMATOGRAPHY

INTERNATIONAL JOURNAL ON CHROMATOGRAPHY, ELECTROPHORESIS AND RELATED METHODS

EDITOR, Michael Lederer (Switzerland)

ASSOCIATE EDITORS, R. W. Frei (Amsterdam), R. W. Giese
Boston, MA), J. K. Haken (Kensington, N.S.W.),
K. Macek (Prague), L. R. Snyder (Orinda, CA)

EDITOR, SYMPOSIUM VOLUMES, E. Heftmann (Orinda, CA)

EDITORIAL BOARD

W. A. Aue (Halifax)
V. G. Berezkin (Moscow)
V. Betina (Bratislava)
A. Bevenue (Belmont, CA)
P. Boček (Brno)
P. Boulanger (Lille)
A. A. Boulton (Saskatoon)
G. P. Cartoni (Rome)
S. Dilli (Kensington, N.S.W.)
L. Fishbein (Washington, DC)
A. Frigerio (Milan)
C. W. Gehrke (Columbia, MO)
E. Gil-Av (Rehovot)
G. Guiochon (Knoxville, TN)
I. M. Hais (Hradec Králové)
S. Hjertén (Uppsala)
E. C. Horning (Houston, TX)
Cs. Horváth (New Haven, CT)
J. F. K. Huber (Vienna)
A. T. James (Harrold)
J. Janák (Brno)
E. sz. Kováts (Lausanne)
K. A. Kraus (Oak Ridge, TN)
E. Lederer (Gif-sur-Yvette)
A. Liberti (Rome)
H. M. McNair (Blacksburg, VA)
Y. Marcus (Jerusalem)
G. B. Marini-Bettolo (Rome)
A. J. P. Martin (Cambridge)
C. Michalec (Prague)
R. Neher (Basel)
G. Nickless (Bristol)
N. A. Parris (Wilmington, DE)
R. L. Patience (Sunbury-on-Thames)
P. G. Righetti (Milan)
O. Samuelson (Göteborg)
R. Schwarzenbach (Dübendorf)
A. Zlatkis (Houston, TX)

EDITORS, BIBLIOGRAPHY SECTION

Z. Deyl (Prague), J. Janák (Brno), V. Schwarz (Prague), K. Macek (Prague)

ELSEVIER

JOURNAL OF CHROMATOGRAPHY

Scope. The *Journal of Chromatography* publishes papers on all aspects of chromatography, electrophoresis and related methods. Contributions consist mainly of research papers dealing with chromatographic theory, instrumental development and their applications. The section *Biomedical Applications*, which is under separate editorship, deals with the following aspects: developments in and applications of chromatographic and electrophoretic techniques related to clinical diagnosis or alterations during medical treatment; screening and profiling of body fluids or tissues with special reference to metabolic disorders; results from basic medical research with direct consequences in clinical practice; drug level monitoring and pharmacokinetic studies; clinical toxicology; analytical studies in occupational medicine.

Submission of Papers. Papers in English, French and German may be submitted, in three copies. Manuscripts should be submitted to: The Editor of *Journal of Chromatography*, P.O. Box 681, 1000 AR Amsterdam, The Netherlands, or to: The Editor of *Journal of Chromatography, Biomedical Applications*, P.O. Box 681, 1000 AR Amsterdam, The Netherlands. Review articles are invited or proposed by letter to the Editors. An outline of the proposed review should first be forwarded to the Editors for preliminary discussion prior to preparation. Submission of an article is understood to imply that the article is original and unpublished and is not being considered for publication elsewhere. For copyright regulations, see below.

Subscription Orders. Subscription orders should be sent to: Elsevier Science Publishers B.V., P.O. Box 211, 1000 AE Amsterdam, The Netherlands, Tel. 5803 911, Telex 18582 ESPA NL. The *Journal of Chromatography* and the *Biomedical Applications* section can be subscribed to separately.

Publication. The *Journal of Chromatography* (incl. *Biomedical Applications* and *Cumulative Author and Subject Indexes*, Vols. 401–450) has 37 volumes in 1988. The subscription prices for 1988 are:

J. Chromatogr. (incl. *Cum. Indexes*, Vols. 401–450) + *Biomed. Appl.* (Vols. 424–460):

Dfl. 6290.00 plus Dfl. 962.00 (p.p.h.) (total ca. US\$ 3537.50)

J. Chromatogr. (incl. *Cum. Indexes*, Vols. 401–450) only (Vols. 435–460):

Dfl. 5070.00 plus Dfl. 676.00 (p.p.h.) (total ca. US\$ 2803.00)

Biomed. Appl. only (Vols. 424–434):

Dfl. 2145.00 plus Dfl. 286.00 (p.p.h.) (total ca. US\$ 1185.75).

Our p.p.h. (postage, package and handling) charge includes surface delivery of all issues, except to subscribers in Argentina, Australia, Brasil, Canada, China, Hong Kong, India, Israel, Malaysia, Mexico, New Zealand, Pakistan, Singapore, South Africa, South Korea, Taiwan, Thailand and the U.S.A. who receive all issues by air delivery (S.A.L. — Surface Air Lifted) at no extra cost. For Japan, air delivery requires 50% additional charge; for all other countries airmail and S.A.L. charges are available upon request. Back volumes of the *Journal of Chromatography* (Vols. 1 through 423) are available at Dfl. 230.00 (plus postage). Claims for missing issues will be honoured, free of charge, within three months after publication of the issue. Customers in the U.S.A. and Canada wishing information on this and other Elsevier journals, please contact Journal Information Center, Elsevier Science Publishing Co. Inc., 52 Vanderbilt Avenue, New York, NY 10017. Tel. (212) 916-1250.

Abstracts/Contents Lists published in Analytical Abstracts, ASCA, Biochemical Abstracts, Biological Abstracts, Chemical Abstracts, Chemical Titles, Chromatography Abstracts, Current Contents/Physical, Chemical & Earth Sciences, Current Contents/Life Sciences, Deep-Sea Research/Part B: Oceanographic Literature Review, Excerpta Medica, Index Medicus, Mass Spectrometry Bulletin, PASCAL-CNRS, Referativnyi Zhurnal and Science Citation Index.

See inside back cover for Publication Schedule, Information for Authors and information on Advertisements.

© ELSEVIER SCIENCE PUBLISHERS B.V. — 1988

0021-9673/88/\$03.50

All rights reserved. No part of this publication may be reproduced, stored in a retrieval system or transmitted in any form or by any means, electronic, mechanical, photocopying, recording or otherwise, without the prior written permission of the publisher, Elsevier Science Publishers B.V., P.O. Box 330, 1000 AH Amsterdam, The Netherlands.

Upon acceptance of an article by the journal, the author(s) will be asked to transfer copyright of the article to the publisher. The transfer will ensure the widest possible dissemination of information.

Submission of an article for publication entails the authors' irrevocable and exclusive authorization of the publisher to collect any sums or considerations for copying or reproduction payable by third parties (as mentioned in article 17 paragraph 2 of the Dutch Copyright Act of 1912 and the Royal Decree of June 20, 1974 (S. 351) pursuant to article 16 b of the Dutch Copyright Act of 1912) and/or to act in or out of Court in connection therewith.

Special regulations for readers in the U.S.A. This journal has been registered with the Copyright Clearance Center, Inc. Consent is given for copying of articles for personal or internal use, or for the personal use of specific clients. This consent is given on the condition that the copier pays through the Center the per-copy fee stated in the code on the first page of each article for copying beyond that permitted by Sections 107 or 108 of the U.S. Copyright Law. The appropriate fee should be forwarded with a copy of the first page of the article to the Copyright Clearance Center, Inc., 27 Congress Street, Salem, MA 01970, U.S.A. If no code appears in an article, the author has not given broad consent to copy and permission to copy must be obtained directly from the author. All articles published prior to 1980 may be copied for a per-copy fee of US\$ 2.25, also payable through the Center. This consent does not extend to other kinds of copying, such as for general distribution, resale, advertising and promotion purposes, or for creating new collective works. Special written permission must be obtained from the publisher for such copying.

No responsibility is assumed by the Publisher for any injury and/or damage to persons or property as a matter of products liability, negligence or otherwise, or from any use or operation of any methods, products, instructions or ideas contained in the materials herein. Because of rapid advances in the medical sciences, the Publisher recommends that independent verification of diagnoses and drug dosages should be made. Although all advertising material is expected to conform to ethical (medical) standards, inclusion in this publication does not constitute a guarantee or endorsement of the quality or value of such product or of the claims made of it by its manufacturer.

Printed in The Netherlands

For contents see p. VII

JOURNAL OF CHROMATOGRAPHY

VOL. 452 (1988)

JOURNAL *of* CHROMATOGRAPHY

INTERNATIONAL JOURNAL ON CHROMATOGRAPHY,
ELECTROPHORESIS AND RELATED METHODS

EDITOR

MICHAEL LEDERER (Switzerland)

ASSOCIATE EDITORS

R. W. FREI (Amsterdam), R. W. GIESE (Boston, MA), J. K. HAKEN (Kensington,
N.S.W.), K. MACEK (Prague), L. R. SNYDER (Orinda, CA)

EDITORIAL BOARD

W. A. Aue (Halifax), V. G. Berezkin (Moscow), V. Betina (Bratislava), A. Bevenue
(Belmont, CA), P. Boček (Brno), P. Boulanger (Lille), A. A. Boulton (Saskatoon), G. P.
Cartoni (Rome), S. Dilli (Kensington, N.S.W.), L. Fishbein (Washington, DC), A. Frige-
rio (Milan), C. W. Gehrke (Columbia, MO), E. Gil-Av (Rehovot), G. Guiochon (Knox-
ville, TN), I. M. Hais (Hradec Králové), S. Hjertén (Uppsala), E. C. Horning (Houston,
TX), Cs. Horváth (New Haven, CT), J. F. K. Huber (Vienna), A. T. James (Harrold), J.
Janák (Brno), E. sz. Kováts (Lausanne), K. A. Kraus (Oak Ridge, TN), E. Lederer (Gif-
sur-Yvette), A. Liberti (Rome), H. M. McNair (Blacksburg, VA), Y. Marcus (Jerusa-
lem), G. B. Marini-Bettolo (Rome), A. J. P. Martin (Cambridge), Č. Michalec (Prague),
R. Neher (Basel), G. Nickless (Bristol), N. A. Parris (Wilmington, DE), R. L. Patience
(Sunbury-on-Thames), P. G. Righetti (Milan), O. Samuelson (Göteborg), R. Schwar-
zenbach (Dübendorf), A. Zlatkis (Houston, TX)

EDITORS, BIBLIOGRAPHY SECTION

Z. Deyl (Prague), J. Janák (Brno), V. Schwarz (Prague), K. Macek (Prague)



ELSEVIER

AMSTERDAM — OXFORD — NEW YORK — TOKYO

J. Chromatogr., Vol. 452 (1988)

All rights reserved. No part of this publication may be reproduced, stored in a retrieval system or transmitted in any form or by any means, electronic, mechanical, photocopying, recording or otherwise, without the prior written permission of the publisher, Elsevier Science Publishers B.V., P.O. Box 330, 1000 AH Amsterdam, The Netherlands.

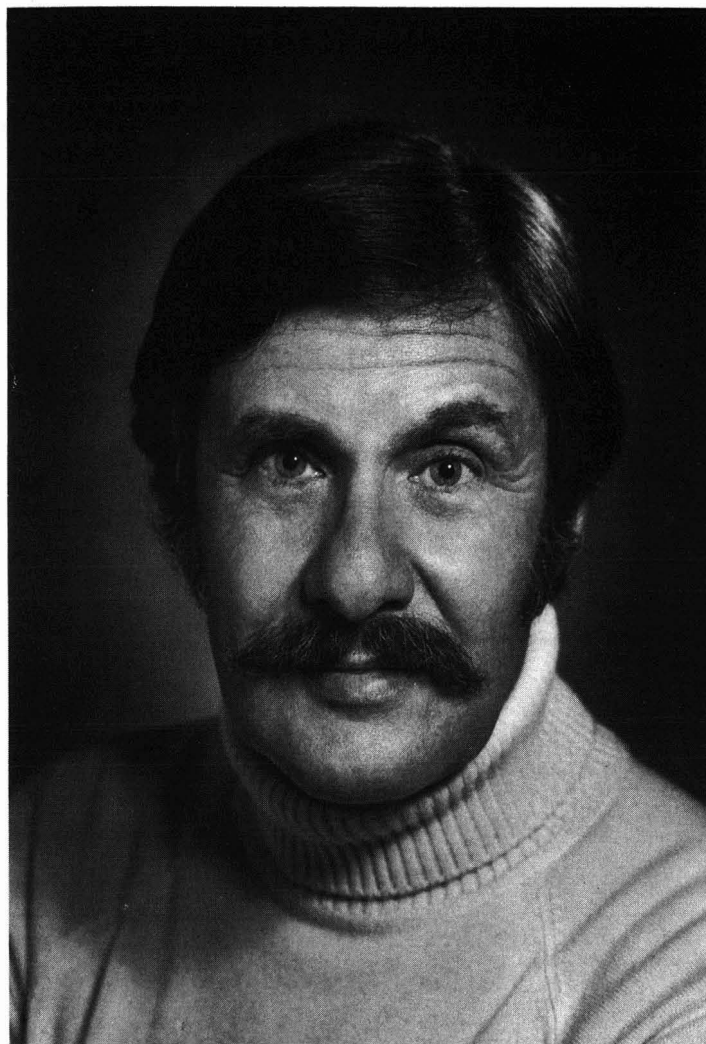
Upon acceptance of an article by the journal, the author(s) will be asked to transfer copyright of the article to the publisher. The transfer will ensure the widest possible dissemination of information.

Submission of an article for publication entails the authors' irrevocable and exclusive authorization of the publisher to collect any sums or considerations for copying or reproduction payable by third parties (as mentioned in article 17 paragraph 2 of the Dutch Copyright Act of 1912 and the Royal Decree of June 20, 1974 (S. 351) pursuant to article 16 b of the Dutch Copyright Act of 1912) and/or to act in or out of Court in connection therewith. **Special regulations for readers in the U.S.A.** This journal has been registered with the Copyright Clearance Center, Inc. Consent is given for copying of articles for personal or internal use, or for the personal use of specific clients. This consent is given on the condition that the copier pays through the Center the per-copy fee stated in the code on the first page of each article for copying beyond that permitted by Sections 107 or 108 of the U.S. Copyright Law. The appropriate fee should be forwarded with a copy of the first page of the article to the Copyright Clearance Center, Inc., 27 Congress Street, Salem, MA 01970, U.S.A. If no code appears in an article, the author has not given broad consent to copy and permission to copy must be obtained directly from the author. All articles published prior to 1980 may be copied for a per-copy fee of US\$ 2.25, also payable through the Center. This consent does not extend to other kinds of copying, such as for general distribution, resale, advertising and promotion purposes, or for creating new collective works. Special written permission must be obtained from the publisher for such copying.

No responsibility is assumed by the Publisher for any injury and/or damage to persons or property as a matter of products liability, negligence or otherwise, or from any use or operation of any methods, products, instructions or ideas contained in the materials herein. Because of rapid advances in the medical sciences, the Publisher recommends that independent verification of diagnoses and drug dosages should be made.

Although all advertising material is expected to conform to ethical (medical) standards, inclusion in this publication does not constitute a guarantee or endorsement of the quality or value of such product or of the claims made of it by its manufacturer.

SPECIAL VOLUME



HONOUR VOLUME

on the occasion of the 70th birthday of

ERICH HEFTMANN

CONTENTS

HONOUR VOLUME ON THE OCCASION OF THE 70TH BIRTHDAY OF ERICH HEFTMANN

Preface	
by L. R. Snyder	1
Tswett's letter to Claparède on tropisms and taxes	
by I. M. Hais (Hradec Králové, Czechoslovakia)	5
Unified theory of adsorption chromatography: gas, liquid and supercritical fluid mobile phases	
by D. E. Martire (Washington, DC, U.S.A.)	17
Dispersion and selectivity indices of alkyl and alkenyl benzenes	
by J. K. Haken and R. J. Smith (Kensington, N.S.W., Australia)	31
Quantitative determination of dicarboxylic acids and polyols in silicone-polyester resins	
by J. K. Haken, N. Harahap and R. P. Burford (Kensington, N.S.W., Australia)	37
Analysis of short alkylsilane bonded silica gel high-performance liquid chromatographic stationary phases using hydrofluoric acid digestion and headspace analysis by capillary gas chromatography	
by T. R. Floyd, N. Sagliano Jr. and R. A. Hartwick (Piscataway, NJ, U.S.A.)	43
Determination of 5-methylcytosine in DNA by gas chromatography-electron-capture detection	
by D. H. Fisher and R. W. Giese (Boston, MA, U.S.A.)	51
Applications of gas chromatography to the study of terpenoid metabolism	
by D. M. Satterwhite and R. B. Croteau (Pullman, WA, U.S.A.)	61
Superconductor metal oxide catalyst in a chemiluminescence chromatography detector	
by E. A. McNamara, S. A. Montzka, R. M. Barkley and R. E. Sievers (Boulder, CA, U.S.A.)	75
Migration of tetrahydroisoquinoline, a possible parkinsonian neurotoxin, into monkey brain from blood as proved by gas chromatography-mass spectrometry	
by T. Niwa, N. Takeda, A. Tatematsu, S. Matsuura (Nagoya, Japan), M. Yoshida (Tochigiken, Japan) and R. Nagatsu (Nagoya, Japan)	85
Identification of the more complex triacylglycerols in bovine milk fat by gas chromatography-mass spectrometry using polar capillary columns	
by J. J. Myher, A. Kuksis and L. Marai (Toronto, Canada) and P. Sandra (Ghent, Belgium)	93
Studies on steroids. CCXXXVIII. Determination of bile acids in liver tissue by gas chromatography-mass spectrometry with negative ion chemical ionization detection	
by J. Goto, H. Miura, M. Inada, T. Nambara, R. Nagakura and H. Suzuki (Sendai, Japan)	119
Studies of adsorption and partition effects in liquid chromatography with mixed mobile phases	
by M. Borówko and M. Jaroniec (Lublin, Poland)	131
Interchangeable use of aqueous and organic solvents in a hydrophilic poly(vinyl alcohol) gel column	
by S. Mori (Mie, Japan)	137
Reversed-phase high-performance liquid chromatography with a C ₁₈ polyacrylamide-based packing	
by J. V. Dawkins and N. P. Gabbott (Loughborough, U.K.) and L. L. Lloyd, J. A. McConville and F. P. Warner (Church Stretton, U.K.)	145
Comparison of retention mechanisms of homologous series and triglycerides in non-aqueous reversed-phase liquid chromatography	
by M. Martin, G. Thevenon and A. Tchaplá (Palaiseau, France)	157

Expert system for chromatography by L. Peichang and H. Hongxin (Dalian, China)	175
Considerations for using the solvent selectivity triangle approach for stationary phase characterization by B. R. Kersten and C. F. Poole (Detroit, MI, U.S.A.)	191
Effect of mobile phase flow-rate on the recoveries and production rates in overloaded elution chromatography. A theoretical study by S. Ghodbane and G. Guiochon (Knoxville and Oak Ridge, TN, U.S.A.)	209
Contribution of electronic effects to the lipophilicity determined by comparison of values of log <i>P</i> obtained by high-performance liquid chromatography and calculation by J. Tipker, C. P. Groen, J. K. van den Bergh-Swart and J. H. M. van den Berg (Weesp, The Netherlands)	227
Effects of system peaks in ion-pair reversed-phase liquid chromatography for noscapine and metabolites by M. Johansson (Solna, Sweden) and D. Westerlund (Uppsala, Sweden)	241
Measurement of the distribution coefficients of several classes of drug using reversed-phase thin-layer chromatography by D. B. Jack, J. L. Hawker, L. Rooney, M. Beerah, J. Lobo and P. Patel (Birmingham, U.K.)	257
Some considerations on the "charge" on a metal ion in ion-exchange chromatography by M. Lederer (Lausanne, Switzerland)	265
Methyl green-coated column for separation of inorganic anions by ion chromatography by R. Golombek (Stuttgart, F.R.G.) and G. Schwedt (Clausthal-Zellerfeld, F.R.G.)	283
Determination of nitrite and nitrate by reversed-phase high-performance liquid chromatography using on-line post-column photolysis with ultraviolet absorbance and electrochemical detection by M. Lookabaugh (Winchester, MA, U.S.A.) and I. S. Krull (Boston, MA, U.S.A.)	295
Enantioselectivity of complex formation in ligand-exchange chromatographic systems with chiral stationary and/or chiral mobile phases by V. A. Davankov, A. A. Kurganov and T. M. Ponomareva (Moscow, U.S.S.R.)	309
Determination of impurity profiles in drugs and related materials. II. Detection and quantification of diastereomeric impurity in the peptide RGH-0205 (Arg-Lys-Asp) by S. Görög, B. Herényi, O. Nyéki, I. Schön and L. Kisfaludy (Budapest, Hungary)	317
Use of hydroxypropyl- and hydroxyethyl-derivatized β -cyclodextrins for the thin-layer chromatographic separation of enantiomers and diastereomers by D. W. Armstrong, J. R. Faulkner, Jr. and S. M. Han (Rolla, MO, U.S.A.)	323
Mixed-bed ion-exchange columns for protein high-performance liquid chromatography by Y.-F. Maa, F. D. Antia, Z. el Rassi and Cs. Horváth (New Haven, CT, U.S.A.)	331
Hydrophobic interaction of Alcian Blue with soluble and erythrocyte membrane proteins by G. M. Ghiggeri and G. Candiano (Lavagna, Italy) and F. Ginevri (Genoa, Italy) and A. Mutti, E. Bergamaschi and R. Alinovi (Parma, Italy) and P. G. Righetti (Milan, Italy)	347
Purification and partial amino acid sequence of human urine protein I. Evidence for homology with rabbit uteroglobin by P. J. Jackson, R. Turner, J. N. Keen, R. A. Brooksbank and E. H. Cooper (Leeds, U.K.)	359
Mass spectrometry of electrophore-labeled nucleosides. Pentafluorobenzyl and cinnamoyl derivatives by T. M. Trainor, R. W. Giese and P. Vouros (Boston, MA, U.S.A.)	369

Comparison of the chromatographic properties of sterols, select additional steroids and triterpenoids: gravity-flow column liquid chromatography, thin-layer chromatography, gas-liquid chromatography and high-performance liquid chromatography by S. Xu, R. A. Norton, F. G. Crumley and W. D. Nes (Athens, GA, U.S.A.)	377
Quantitative microanalysis of bile acids in biological samples. Collaborative study by F. Nakayama (Fukuoka, Japan)	399
Improved solid-phase extraction and liquid chromatography with electrochemical detection of urinary catecholamines and 5-S-L-cysteinyl-L-dopa by T. Huang, F. Wall and P. Kabra (San Francisco, CA, U.S.A.)	409
Immunoaffinity pre-column for selective on-line sample pre-treatment in high-performance liquid chromatography determination of 19-nortestosterone by A. Farjam, G. J. de Jong, R. W. Frei and U. A. Th. Brinkman (Amsterdam, The Netherlands) and W. Haasnoot, A. R. M. Hamers, R. Schilt and F. A. Huf (Wageningen, The Netherlands)	419
Chromatography for diagnosis of metabolic diseases by E. Jellum (Oslo, Norway)	435
Determination of fatty acids as phenacyl esters in rat adipose tissue and blood vessel walls by high-performance liquid chromatography by T. Hanis, M. Smrz, P. Klir, K. Macek, J. Klima, J. Base and Z. Deyl (Prague, Czechoslovakia)	443
Isolation of bile acid glucosides and N-acetylglucosaminides from human urine by ion-exchange chromatography and reversed-phase high-performance liquid chromatography by H.-U. Marschall, G. Green, B. Egestad and J. Sjövall (Stockholm, Sweden)	459
Development of a solid-phase extraction technique for α -human atrial natriuretic peptide in human plasma by M. A. O'Flynn, R. C. Causon, J. Brown and S. Kageyama (London, U.K.)	469
Direct enantiomeric separation of betaxolol with applications to analysis of bulk and biological samples by A. M. Krstulović, M. H. Fouchet, J. T. Burke, G. Gillet and A. Durand (Meudon la Forêt, France)	477
High-performance liquid chromatographic analysis of the ajmalicine distribution in roots of <i>Catharanthus roseus</i> lines with different flower colours by M. Weissenberg, A. Levy and I. Schaeffler (Bet Dagan, Israel) and E. C. Levy (Jerusalem, Israel)	485
Liquid chromatographic procedures for the analysis of compounds in the serotonergic and octopamine pathways of lobster hemolymph by D. A. Fadool, S. J. Cobb, G. Kass-Simon and P. R. Brown (Kingston, RI, U.S.A.)	491
Liquid chromatographic analysis of organic additives in copper plating baths by S. Shohat and E. Grushka (Jerusalem, Israel) and S. Glikberg (Kiriath Malachi, Israel)	503
High-performance liquid chromatography separations of nitrosamines. III. Conformers of N-nitrosamino acids by H. J. Issaq, D. G. Williams, N. Schultz and J. E. Saavedra (Frederick, MD, U.S.A.)	511
Reversed-phase C ₁₈ and normal-phase silica high-performance liquid chromatography of gibberellins and their methyl esters by J.-T. Lin and A. E. Stafford (Albany, CA, U.S.A.)	519
Performance of graphitized carbon black cartridges in the extraction of some organic priority pollutants from water by F. Mangani, G. Crescentini, P. Palma and F. Bruner (Urbino, Italy)	527
Reversed-phase liquid chromatography of astacene by H. J. C. F. Nelis and A. P. De Leenheer (Ghent, Belgium)	535

Potential application of thin-layer chromatography and thin-layer chromatography with flame ionization detection of cholestanol in the diagnosis of cerebrotendinous xanthomatosis by Č. Michalec and M. Ranný (Prague, Czechoslovakia)	543
Retention in sedimentation–flotation focusing field-flow fractionation using a step density gradient by J. Jancá and N. Nováková (Brno, Czechoslovakia)	549
High-performance liquid chromatographic analysis of the alkaloid spectrum in the roots and capsules of the species and hybrids of <i>Papaver</i> section <i>Oxytona</i> by J. Milo, A. Levy and D. Palevitch (Bet Dagan, Israel) and G. Ladizinsky (Rehovot, Israel)	563
Micellar, inclusion and metal-complex enantioselective pseudophases in high-performance electro-migration methods by J. Snopek, I. Jelinek and E. Smolková-Keulemansová (Prague, Czechoslovakia)	571
Use of a double-detector system for the measurement of mobilities in zone electrophoresis by J. L. Beckers, Th. P. E. M. Verheggen and F. M. Everaerts (Eindhoven, The Netherlands)	591
Capillary zone electrophoresis. Quantitative study of the effects of some dispersive processes on the separation efficiency by F. Foret, M. Deml and P. Boček (Brno, Czechoslovakia)	601
Simple sampling device for capillary isotachopheresis and capillary zone electrophoresis by Th. P. E. M. Verheggen, J. L. Beckers and F. M. Everaerts (Eindhoven, The Netherlands)	615
Separation of α -keto acids by capillary supercritical fluid chromatography as their quinoxalinol derivatives by P. A. David and M. Novotny (Bloomington, IN, U.S.A.)	623
<i>Author Index</i>	631

*
* In articles with more than one author, the name of the author to whom correspondence should be addressed is indicated in the
* article heading by a 6-pointed asterisk (*)
*

PREFACE

The present volume of the *Journal of Chromatography* is dedicated to Erich Heftmann on the occasion of his 70th birthday. Dr. Heftmann's involvement with chromatography spans the four decades beginning in the mid 1940s, during which a multiplicity of new techniques were developed, and problems of major importance in organic and biological chemistry were solved by chromatographic analysis. During this time his name came to be synonymous with the documentation of chromatography in general, and the application of this technique to the biochemistry of steroids in particular.

Erich Heftmann was born in Vienna in 1918, emigrated to the United States in 1939, and completed his Ph.D. in Biochemistry at the University of Rochester in 1947. His subsequent career was divided (roughly equally) between work for the National Institutes of Health and the U.S. Department of Agriculture. He was Acting Chief of the Steroid Section at the National Institute of Arthritis and Metabolic Diseases, spent 10 years as Research Associate at the California Institute of Technology (Pasadena, 1959–1969), and later organized a Plant Biochemistry Research Unit at the Western Regional Research Center of the U.S. Department of Agriculture (Albany, CA). He retired from civil service in 1983 and has since been active as the Editor of the *Journal of Chromatography* Symposium volumes, authored several review articles, and has completed the fourth edition of his classic *Chromatography* (Elsevier, 1983). Since his first publication in 1947, Dr. Heftmann has contributed almost 200 technical publications relating to chromatography and the biochemistry of steroids — including 8 books. He was honored by the Alexander von Humboldt Award in 1975.

Erich Heftmann's major research contributions have centered on the application of chromatography to the study of plant steroids and an understanding of their role in the biology of plants. All of this began in the late 1940s, when interest arose in the commercial synthesis of cortisone from starting materials of plant origin. Dr. Heftmann was able to facilitate this work by developing assays for plant steroids based on paper chromatography. This in turn soon led him to an important observation: the distribution of various steroids in plants was remarkably similar in many respects to the occurrence of these same compounds in animals (including man). Then and later it would be argued that steroids occur "accidentally" in plants and have no obvious biological function other than their toxicity to animals. However Dr. Heftmann's work would eventually suggest a more important biochemical role for these plant steroids — although this question is by no means resolved after many years of research. Of specific interest in this regard was his early demonstration that a sterol is responsible for cellular differentiation in the slime mold (*J. Am. Chem. Soc.*, 1959). Later (1963) he was to show that inhibitors of steroid biosynthesis can suppress floral induction in certain plants, another instance of differentiation.

During the 1960s Erich Heftmann broadened his studies to include non-steroidal plant components that are biochemically related to the steroids: gibberellins, triterpenoid saponins, and other isoprenoid compounds. Information on the occurrence of these compounds in plants served to fill in many of the gaps in our understanding of how these compounds and various steroids arise in plants. He first showed

that cholesterol occurs in higher plants (*Science*, 1963), whereas previous workers had argued for the absence of this compound in the plant kingdom. Cholesterol plays a central role in an understanding of steroid biochemistry, since it is the starting material from which other steroids are made in both plants and animals. In a similar vein, he first demonstrated (1965) the presence of estrone in the seeds of various plants; this suggested a parallelism for the similar occurrence of this potent hormone in the reproductive organs of animals. About this same time he was able to trace the biosynthesis of numerous plant products of steroidal origin. These various studies served again to confirm the remarkable similarities between plants and animals with respect to their basic biochemistry.

Throughout this period Dr. Heftmann was a pioneer in the application of new chromatographic techniques for the analysis of steroids in samples of plant or animal origin. An early paper (*Science*, 1950) described the identification of estrogens by paper chromatography. This publication generated wide interest (over 1000 reprint requests), and served to arouse the awareness of the scientific community to the general applicability of chromatography along similar lines. During the 1950s he conceived the possibility of automated liquid chromatography — an idea that was later to come to fruition (in other laboratories) as amino acid analysis, gel permeation chromatography, and (finally) high-performance liquid chromatography. By the late 1950s he had undertaken the construction of the “steroid analyzer”, which was to be finished in 1961. This device attracted the attention of many workers concerned with the problems of manual column chromatography; it was unfortunately ahead of its time, and was therefore not pursued beyond this first prototype. In this regard, it is useful to paraphrase the philosopher, John Dewey: “Science is a process, not a series of completed tasks”.

Later Dr. Heftmann would be active in exploiting thin-layer and high-performance liquid chromatography for steroid analysis. He was also a proponent of centrifugal column chromatography as a means of scaling up preparative separations — beginning with thin-layer chromatographic results. Throughout his research career, Dr. Heftmann was of course involved with many collaborators. Erich Mosettig at the National Institutes of Health and Jim Bonner and Anton Lang of the California Institute of Technology were particularly prominent in shaping his early career.

Another major contribution of Erich Heftmann was in archiving, critiquing and disseminating information on chromatography in general, and specifically the chromatography of steroids. By the mid-1950s he had digested most of the written material that had so far appeared about chromatography (a task that is today hard to conceive of!). This led him to organize what was probably the first course on chromatography, presented at the Graduate School of the U.S. Department of Agriculture. Another seven years of teaching this course led to the appearance in 1961 of the first edition of his *Chromatography*. Since a detailed knowledge (at this time) of all of chromatography was beyond the grasp of any human, he wisely involved a large number of international experts as collaborators. It was during the preparation of the second edition of this work (1965) that I first met Erich. At that time he invited me to contribute some chapters on column chromatography, which was already in transition between open-column procedures and high-performance liquid chromatography. *Chromatography* was to reappear in a third (1975) and fourth (1983) edition.

Overall, it is undoubtedly the most widely used (and most useful) single work in the field. During this same time a number of other books and reviews were being prepared by Dr. Heftmann on more specific applications of chromatography — particularly in the steroid area. A dominant feature of these various works was a critical interpretation of the literature for ready application to practical problems. He also continued to be active as a teacher, with academic appointments at several major universities on both the East and West Coasts (California Institute of Technology, University of California at Berkeley, University of Southern California, etc.)

A biography of this sort would not be complete without focusing on the personal characteristics of our honoree. Toward this end, we might ask the question: “What is a scientist?” Or: “What exemplifies the scientist?”. During Erich Heftmann’s lifetime we have seen science grow from an avocation pursued by a small number of dedicated people to an enterprise that today employs literally millions of workers. In the process, some of the original standards that defined scientific research have become somewhat eroded. In my opinion, Erich exemplifies certain of these older standards and is an excellent model for what is commendable in science. These characteristics include absolute objectivity, a distaste for self-aggrandizement through one’s research, and a total absence of arrogance. Someone close to Dr. Heftmann has commented on his personal humility, without which good science is difficult — under the best of circumstances. Another personal characteristic is his dedication to precise writing, a standard which of late seems to have been honored more in the breach than in the observance. Finally, few scientists have been willing to spend more time on the job of preserving the literature and making it accessible to each new generation. Erich’s long tenure as the chromatography reviewer for *Analytical Chemistry* comes immediately to mind as one example among many.

I have been privileged to know Erich Heftmann for well over 20 years, originally as a contributor to his *Chromatography* series, and more recently as a joint editor of the *Journal of Chromatography*. Throughout this period we have been good friends, and I have looked to him as a “senior statesman” of the field — one who has taught me many things which cannot be found in books. I join with other chromatographers in expressing our thanks for Erich Heftmann’s 40+ years as a fellow scientist, and I hope that we can look forward in the near future to the appearance of the fifth edition of his *Chromatography*. We wish him many more years.

Orinda, CA (U.S.A.)

L. R. SNYDER

CHROM. 20 510

TSWETT'S LETTER TO CLAPARÈDE ON TROPISMS AND TAXES

I. M. HAIS

Department of Biochemistry, Faculty of Pharmacy, Charles University, 501 65 Hradec Králové (Czechoslovakia)

SUMMARY

Part of a letter of March 30th, 1909, in which M. S. Tswett tried to give his opinion requested by his closest friend, Edouard Claparède, on the role of tropisms and taxes in metazoa, is presented and discussed. An attempt is made to provide the background to the problems discussed in the letter.

INTRODUCTION

Since it became known¹ that Tswett's letters to his most intimate friend, E. Claparède, are kept in the Public and University Library of the City of Geneva, it occurred to me² that in the letters addressed to a psychologist, Tswett might have revealed his motivation and his approach to science. From this point of view the letters, although interesting in many other ways, were a disappointment. Tswett's letters to the botanist John Briquet^{3,4} say more about his scientific ambitions and plans than those to Claparède. Among the letters to the latter there is only the one of March 30th, 1909, which deals predominantly with scientific problems — not concerning Tswett's profession, but animal psychology, which interested his addressee. As the subject was rather complex, it was not included in the recent paper devoted to the remaining letters⁵, and is dealt with here.

At the University of Geneva, Tswett attended lectures by Th. Flournoy on psychology and, in a letter from St. Petersburg to Briquet dated August 27th, 1898, he mentions an *Introduction à la Médecine de l'Esprit* by de Fleury (ref. 3, p. 21).

The letter by Claparède which Tswett answers (as all of Claparède's letters to Tswett) is not available. One would expect, however, that Claparède's views were expressed in an article entitled "Les tropismes devant la psychologie"⁶. This may be one of the "long printed letters" mentioned here by Tswett. Unfortunately, the journal of this name is not catalogued in the Prague University library and it has been impossible to obtain it elsewhere. The same applies to further relevant papers by Claparède⁹.

It has therefore been necessary to draw on secondary or tertiary sources, the most important of which were the autobiography of Claparède^{7,8} (followed by an article by Piaget¹¹ on Claparède's psychology), a book by Georges Bohn¹² and a textbook by Piéron¹³.

Before reproducing the letter, we should outline the background, *i.e.*, the opinions and arguments dealing with the role of tropisms and taxes in animal psychology. In 1886–1888 Jacques Loeb^{14–19} studied in Würzburg and was influenced by the ideas of the phytophysiologist Julius Sachs³⁰, who tried to extend the notion of tropisms (heliotropism in the first place) from plants, for which the term had been coined by Darwin, to animals (bacterial chemotaxis was discovered subsequently³¹).

Tropism is now mostly understood as an orientated growth reaction of plants and fixed or sedentary animals to a spatially (directionally) defined physical stimulus or to a gradient of concentration. Changes in position or movements relative to the direction of the stimulus are usually called taxes (in French tactismes), but the terminology had not been standardized in 1909 and the word tropism was mostly used to include both tropisms and taxes, especially in animals.

Loeb's ideas on tropisms enjoyed great interest and popularity, and he was acclaimed as the Galileo of his science^{32–34}. However, his attempts to reduce life phenomena to the simplest physico-chemical processes were also heavily attacked, mainly from two quarters: (a) vitalists objected to Loeb's mechanistic approach and (b) some authors, leaving aside the philosophical issues, reported observations that were at variance with Loeb's theories and sometimes even with his observations.

Let us concentrate on two authors mentioned in Tswett's letters, namely Claparède himself and Georges Bohn. Both claimed the notion of tropisms in metazoa to be limited. Claparède excluded active phenomena governed by his favourite "Law of Momentary Interest"³⁵ from the class of tropisms. By "interest" he does not mean a "psychological interest" (curiosity), but a "biological interest". This, in common with the "interest" of Jennings³⁴, has been criticized as finalism, teleology, in spite of Jennings' and Claparède's protests. Speaking about Claparède's functionalism in general, Piaget stressed that causal explanations were arrived at when functional introduction to the problem was followed by structural study.

G. Bohn defined two criteria to be fulfilled if a phenomenon had to be called tropism³⁶.

A PASSAGE FROM TSWETT'S M.Sc. DISSERTATION OF 1901

As a basis for Tswett's views on the physical and chemical explication of life phenomena in general, let us first quote a passage from his dissertation for the degree of Master of Sciences at the University of Kazan, "Physico-chemical structure of the chlorophyll grain" (1901) (ref. 4, pp. 43–44). In addition, in one of the eight "Propositions" (Theses), Tswett had to express his opinion on the vitalist and mechanistic doctrine in biology (ref. 5, p. 78). These propositions were not available to us.

Every objective life process eventually consists of a series of elementary material and energetic phenomena which follow each other subject to similar laws to those which are studied by science disciplines concerned with the unorganized Nature.

This postulate lies at the basis of all physiological investigations. To prove its general validity is the ideal goal of the life sciences and their history is nothing else but the history of asymptotic approximation towards this goal.

The distinctive mysterious process which takes place in the chloroplast under the surge of light waves appears to be a process most easily accessible to analysis, one of

the processes least connected with those categories of plant life phenomena in whose study the concepts of instinct and reflexes persistently impose themselves, together with the notion of the extraordinary complexity of the structural properties of the life mechanism.

The solution of a question of such an importance for both the theoretical and practical worker cannot be left to the uncertain happy chance of ingenious discovery; it must be sought by a painstaking, laborious, but faithful route including the investigation of all necessary conditions of the process.

Methodological conditions must be investigated in the first line. The haphazard, insufficiently thought-out methods may have been responsible for nearly all failures that slowed down the normal development of chlorophyll chemistry.

The biochemist must employ purely physical methods for the isolation of substances...

If we understand it correctly, then it would seem that Tswett expressed here his belief in the possibility of explaining life phenomena in physical and chemical terms; however, in the case of excitatory processes that lead to the study of the neural and mental phenomena, he considered the problem to be so complex that he avoided tackling it. He might have also been aware of the controversies which were prompted by the opinions of Academician Famintsyn on these questions³⁹; see also below⁵¹⁻⁵³.

PARTS OF THE LETTER OF MARCH 30TH, 1909

As part of this letter has already been published recently⁵, we shall limit ourselves to the remaining part and the postscript. Taking into account the fact that Loeb's ideas^{14,24,32} on tropisms and their physico-chemical basis originated from Sachs³⁰ research on heliotropism in plants, it is not surprising that Claparède took advantage of his close friendship with Tswett, plant physiologist and biochemist in addition to physical chemist, to ask for his opinion on Loeb's ideas.

Warsaw, 30th March 1909

Dear old chap,

For a long time I have been reproaching myself for not yet answering your brief written missives and long printed letters⁴⁰ on the tropisms. I wonder how it has happened that the "law of momentary interest" (of biological interest, of course)^{35,41} has always thwarted my intentions of replying, thus inhibiting any demonstration of positive "philotropism"⁴² uniting two such old friends as ourselves.

Once again, on reading your letters, I have found that our natural-philosophical tropisms⁴² are orientated in very similar directions, although the parallelism⁴³ with which you have armoured yourself seems to me a very precarious refuge, simply because to be exact, as you say, it is not metaphysics.

If the abstract, slightly schopenhauerite⁴⁴ notion of tropism at which you have arrived were accepted, this would considerably disturb phytophysiological terminology. For under the name of tropisms and taxes we understand simply categories of well defined objective phenomena. For my part, after having reconsidered this subject, I would define⁴⁵ tropisms and taxes as follows: phenomena of orientation or locomotion

with respect to light, gravity or other polarized systems of energy, in which the movement is produced or at least triggered by the organism. Plants are endowed with a limited number of tropisms governed by simple laws⁴⁶. The protophytes and protozoa (as also the zoospores or spermatozoids of metaphytes) are equipped with various taxes, which are also limited in number and subject to not very complicated rules. If one ascends the scale of metazoa, one sees the number of tropic reactions increasing and their manifestations—due to interferences—becoming gradually more variable, more dependent on the physiological state, so that a physiology based on taxes and tropisms becomes in practice cumbersome and is transformed to the physiology of movements and the physiology of the nervous system controlling these movements, and it is here that objective study becomes insufficient and powerless and where psychology must necessarily intervene. All the active (“organically permitted”) oriented movements are thus, ultimately, tropisms and taxes⁴⁷. And as this notion of tropism does not involve any particular conception of mechanism, the term “tropism” could by no means help to introduce surreptitiously into animal biology the negation of Mind (“the psychic”) or the affirmation of a simplistic physico-chemical mechanism. This applies all the less, since the prototypes of tropisms, that is plant tropisms, are—as you have correctly understood—just simple phenomena, explicable in physico-chemical terms and participating more or less in the way of the metazoal reflexes. Thus I do not see what on earth the animal physiologists had to gain by ascribing positive heliotropism to the unfortunate caterpillars of *Porthesia*⁴⁸. Heliotropism—well, and so what? Does Loeb believe that he has simplified or resolved the problem of movement of these caterpillars by this terminology? To explain the movements of animals by tropisms is just putting the thing off with fine words, thus opening the door from one blind alley to another.

In the definition of tropisms outlined above I have introduced the notion of at least partial (not necessarily total) activity of the organism in order to include the case where the organism, directing itself—by a permitted, voluntary act—utilises an external source of energy in its movement. For example, the movement of a fish that contracts its swimming bladder and thus increases its weight due to gravity, or that of a bird that is going to land. Another limitation, difficult to express in strictly physiological language, should exclude for example the case of a tourist who leans over a precipice in order to see better, loses his balance and is thereby forced to make a movement to which he has by no means consented.

I would very much like to attend the Geneva Congress and the discussion where Loeb's report will undoubtedly be the focal point⁴⁹. I do not yet know whether I shall be able to.

...If our resort is not far from Geneva I could take time off during the Congress.

Yours

M. Tswett

Concerning comparative psychology extended to plants, are you acquainted with the work of one of my compatriots, Warwara Polowzew: *Untersuchungen über Reizerscheinungen bei den Pflanzen* (Jena 1909)?^{39,50-53}

A PASSAGE FROM THE LETTER OF MAY 16TH, 1911

In Tswett's later letter⁵ is a passage worth repeating in the present context:

I am now reading the short treatise by Bohn⁵⁴ on animal psychology. This "application of physical chemistry to psychology" struck me as being a bit naive. Isn't it an abuse of the name of physical chemistry?

CONCLUSIONS

The letter under discussion is interesting for the chromatographer as it shows that the originator of the method was deeply interested in one of the cardinal problems of biology on which Claparède sought his advice. In his experimental work, however, Tswett avoided even phenomena of excitability in plants which would have led to those of nervous and mental processes in animals and man.

According to Piéron³², the phenomenon of tropism (taxis) as a fact presents no particular problem, but its interpretation made it one of the most hotly debated issues at the end of the 19th and the beginning of the 20th century. This is illustrated by the extent of a rather concise overview of the problem¹³.

Claparède, applying his "Law of Momentary Interest"³⁵, and Bohn³⁶, stressing "differential sensitivity" (temporal sensing of differences), cellular memory and his two criteria, limited Loeb's broad conception of tropisms as simple physico-chemically explicable phenomena underlying the behaviour of metazoa. Tswett goes even further in his scepticism. He does not acknowledge the usefulness of this concept at all, at least with respect to the mechanisms underlying mental and behavioural phenomena in multicellular animals. In 1909 he comes near to Piéron¹³ who, in 1941, after a thorough analysis, arrived at the conclusion that Loeb's conception of tropisms (in metazoa) is at best of historical interest.

Does this mean that Tswett identified himself with the "old" animal psychology, against which the German physiologists⁵⁵, who contested the justification of animal psychology in general, had lanced and attack? In view of his materialistic beliefs reflected in the preface of his M.Sc. Dissertation, this is unlikely.

The controversy of which this letter gives evidence stems from a stage in which animal psychology, in common with other disciplines that had formed a part of philosophy, was starting its development as a (natural, biological) science. Some mechanists were trying to corroborate their views by physico-chemical interpretations of particular processes, which, with the state of biological and other knowledge in those days, were premature. No wonder that Tswett, as a plant physiologist (the concept of tropisms having originated in plant physiology) as well as a physical chemist, was critical of the generalizations put forward in this context by partisans of the "new animal psychology".

In recent years, David Edward Koshland, Jr., and Julius Adler have significantly contributed to the elucidation of the mechanism of chemotaxis in flagellar bacteria^{38,56-63}. A letter by Koshland⁶⁴ may serve as a contribution to the dialogue bridging the span of about 70 years.

ACKNOWLEDGEMENT

I thank for advice Dr. Jan Gayer of the Department of Paediatrics, Dr. Věroslav Golda of the Institute of Experimental Neurosurgery, Faculty of Medicine, Hradec Králové and Prof. Laco Kováč, for linguistic help Ms. Claudine Dauphin and Dr. Marie Doubravová, for the copy of the letter Mr. Philippe Monnier of Geneva and for typing the manuscript Mrs. Bl. Lorenzová.

APPENDIX: PART OF TSWETT'S LETTER IN FRENCH

Varsovie 30 III 09

Bien cher vieux!

Voici bien longtemps que je me reproche de n'avoir pas encore répondu à tes courtes missives écrites et à tes longues lettres imprimées sur les tropismes. Je ne sais comment, toujours la "loi de l'intérêt momentané" (de l'intérêt biologique s'entend) s'est venue mettre en travers de mes projets de répondre, inhibant toute manifestation du "philotropisme" positif unissant deux vieux amis tels que nous.

Une fois de plus, en te lisant, j'ai constaté que nos tropismes naturphilosophiques sont orientés vers des points très voisins, encore que le parallélisme dont tu t'es cuirassé me paraisse un abri très précaire, puisque tout justement, comme tu le dis, il n'est pas une métaphysique.

La notion abstraite, quelque peu schopenhauerienne du tropisme à laquelle tu arrives, étant admise bouleverserait considérablement la nomenclature physiologique botanique. Car sous le nom de tropismes et des tactismes nous entendons simplement des catégories de phénomènes objectifs bien définies. Pour ma part, après avoir remédié ce sujet, je définirais les tropismes et tactismes ainsi: phénomènes d'orientation ou de locomotion par rapport à la lumière, la pesanteur ou autres systèmes d'énergie polarisés, dans lesquels le mouvement est produit ou au moins déclenché par l'organisme. Les plantes sont douées de tropismes en nombre restreint, gouvernés par des lois simples. Les protophytes et les protozoaires (ainsi que les zoospores ou les spermatozoïdes des métaphytes) sont doués de tactismes divers, également peu nombreux et assujettis à des règles (lois) peu compliquées. En montant l'échelle des métazoaires on voit le nombre des réactions tropiques augmenter et leurs manifestations, par suite d'interférences, devenir de plus en plus variables, de plus en plus dépendantes de l'état physiologique, de sorte qu'une physiologie des tactismes et tropismes devient en pratique encombrante et se transforme en physiologie du mouvement et physiologie du système nerveux régissant les mouvements, et c'est ici que l'étude objective devenant insuffisante, impuissante, la psychologie doit nécessairement intervenir. Tous les mouvements orientés actifs ("consentis organiquement") des organismes sont donc, en fin de compte, des tropismes ou tactismes. Et comme dans cette notion du tropisme il n'entre aucune conception particulière du mécanisme, le terme de tropisme ne saurait nullement servir à introduire clandestinement en biologie animale la négation du psychisme ou l'affirmation d'un mécanisme physico-chimique simpliste. Cela d'autant moins que les tropismes prototypes, les tropismes végétaux, ne sont, comme tu l'as bien saisi, rien moins que des phénomènes simples, physico-chimiquement expliqués, et participant bien plutôt de la nature des réflexes métazoaires. Ainsi bien je ne vois pas du tout ce que les zoophysologistes auraient à gagner en dotant d'héliotropisme positif les infortunées chenilles du *Porthesia*. Héliotropisme —soit! Et puis après Loeb croit-il avoir par cette dénomination simplifiée ou résolu le problème des mouvements des dites chenilles? Expliquer les mouvements des animaux par des tropismes c'est se payer des mots, c'est d'une impasse s'ouvrir une issue dans une autre impasse.

Dans la définition ébauchée plus haut des tropismes j'ai fait entrer la notion d'activité *au moins partielle* (pas nécessairement totale) de l'organisme afin d'embrasser les cas où l'organisme se dirigeant (par acte consenti, voulu) utilise dans le mouvement une énergie extérieure, par ex. le mouvement d'un poisson qui contractant sa vessie natatoire gagne le poids par l'effet de la pesanteur, ou bien celui de l'oiseau qui vient se reposer à terre. Une autre restriction, difficile à apporter en langage strictement physiologique devrait exclure par ex. le cas d'un touriste qui se penchant sur l'abîme pour mieux voir, perdrait l'équilibre et serait précipité dans un mouvement nullement consenti.

J'aimerais beaucoup assister au Congrès de Genève et à la discussion dont le rapport de Loeb sera sans doute le centre. Je ne sais encore si je le pourrais.

...Dans le cas où notre lieu de cure ne serait pas très éloigné de Genève, je pourrais faire une absence à l'époque du Congrès.

Ton M. Tswett

A propos de psychologie comparée, étendue sur végétaux, as-tu connaissance du travail d'une de mes compatriotes: Warwara Polowzew: *Untersuchungen über Reizerscheinungen bei den Pflanzen* (Jena 1909)?

REFERENCES AND NOTES

- 1 J. Miège, *Musées de Genève, N.S.*, 14, No. 133 (1973) 18.
- 2 I. M. Hais, *J. Chromatogr.*, 86 (1973) 283.
- 3 K. I. Sakodynskii, *Mikhail Semenovich Tsvet and Chromatography: 100th Anniversary of his Birth* (in Russian), Nauch. Sov. po Khromatogr. Akad. Nauk SSSR, 1972, 72 pp.
- 4 E. M. Senchenkova, *Mikhail Semenovich Tsvet 1872-1919* (in Russian), Nauka, Moscow, 1973, 308 pp.
- 5 I. M. Hais, *J. Chromatogr.*, 440 (1988) 509.
- 6 E. Claparède, "Les tropismes devant la psychologie", *J. Psychol. Neurol.*, 13 (1908), page not given by Claparède; ref. 7, p. 79; ref. 8, p. 20.
- 7 E. Claparède, in C. Murchison (Editor), *A History of Psychology in Autobiography*, Clark University Press, Worcester, MA, 1930, pp. 63-97.
- 8 E. Claparède, "Autobiographie", in *Edouard Claparède*, Delachaux et Niestlé, Neuchâtel, undated (1941?), pp. 1-39.
- 9 Claparède's papers on animal psychology which he quotes in his autobiography (ref. 7, p. 73; ref. 8, p. 14), mostly without page numbers, are "Les animaux sont-ils conscients?", *Rev. Philos.* (1901), "The consciousness of animals", *Int. Quar.*, 8 (1903), "La psychologie comparée est-elle légitime?", *Arch. Psychol.*, 5 (1905), a book *La Psychologie Animale de Ch. Bonnet*¹⁰, Geneva, 1909, and a chapter "Tierpsychologie", in *Handwörterbuch der Naturwissenschaften*, Bd. 9, 1913, p. 1198. In addition, "De l'intelligence animale à l'intelligence humaine", *Le Mystère Animal*, Présences, Paris, 1938, pp. 141-190, is quoted by P. Bovet, "Les dernières années d'Edouard Claparède", in *Edouard Claparède*, Delachaux et Niestlé, Neuchâtel, undated (1941?), pp. 41-49.
- 10 Charles Bonnet, b. 1720 in Geneva, d. 1793 in Genthod or Geneva, one of the fathers of modern biology. He discovered parthenogenesis in aphids, studied regeneration in various species and respiration in insects and plants. His "palingenesis" was a modified theory of preformation. *Essai de Psychologie*, Leiden, 1754, and *Essai Analytique sur les Facultés de l'Ame*, Copenhagen, 1760, deal with animal psychology. Cf., P. E. Pilet, "Bonnet, Charles", in C. C. Gillespie (Editor), *Dictionary of Scientific Biography*, Vol. 2, C. Scribner & Sons, New York, 1970, pp. 286-287.
- 11 J. Piaget, "La psychologie d'Edouard Claparède", in *Edouard Claparède*, Delachaux et Niestlé, Neuchâtel, undated (1941?), pp. 51-71.
- 12 G. Bohn, *Die Neue Tierpsychologie*, Verlag von Veit, Leipzig, 1912, 183 pp.
- 13 H. Piéron, "Psychologie Zoologique", in G. Dumas (Editor), *Nouveau Traité de Psychologie*, Tome 8, Fasc. 1, Presses Universitaires de France, Paris, 1941, Chapter VII, Les grands problèmes du comportement animal, A. La question des tropismes, pp. 132-155.
- 14 Jacques¹⁵ Loeb¹⁶⁻¹⁹, b. 1859 in Mayen, near Koblenz, d. 1924 in Hamilton, Bermuda. He studied in Berlin, Munich and Strasbourg, where he graduated in 1884. He was impressed by Goltz' studies of the physiology of the brain. In 1886-88, as an "Assistent" at the Institute of Animal Physiology in Würzburg, he started to study tropisms²⁰ and physiological morphology²¹. In 1889-91 he worked in the Biological Station at Naples. In 1891 he came to the U.S.A. He worked at Bryn Mawr College, the University of Chicago and Berkeley. In 1909 he was given honorary doctorates in Cambridge (England) (D.Sc.), Geneva (M.D.) and Leipzig (Ph.D.). From 1910 he was Head of the Division of General Physiology at the Rockefeller Institute of Medical Research in New York, where he started the *Journal of General Physiology*. He tried to demonstrate that life phenomena can be reduced to physico-chemical laws. Tropisms (including taxes) remained his favourite subject throughout his life^{20, 23-25}. He studied regeneration (chemical theory)²⁶ and became famous by inducing, in 1899, parthenogenesis by an artificial stimulus (MgCl₂)²⁷. He described heterogenous cross-breeding elicited by an increase in alkalinity. By studying the antagonistic influence of salts on the cell (*e.g.*, developing egg) he laid the foundations for the ion theory of excitation. He is credited for having placed the issue of proteins (zwitterions, isoelectric point, etc.) on a stoichiometric footing²⁸ and systematized the interactions of inorganic ions with proteins. Moses Kunitz was his research assistant in 1913-24²⁹.
- 15 In different sources the spelling of the first name varies between Jaques and Jacques.
- 16 Harms, "Jaques Loeb", in R. Dittler *et al.* (Editors), *Handwörterbuch der Naturwissenschaften*, Vol. 6, G. Fischer, Jena, 2nd ed., 1932, p. 549.

- 17 *Who Was Who in America*, Vol. I, 1897–1912, Marquis–Who’s Who Inc., Chicago, 1968, p. 740.
- 18 *World Who’s Who in Science*, Marquis–Who’s Who Inc., Chicago, 1968, p. 1059.
- 19 *Bol’shaya Sovetskaya Entsiklopediya*, Vol. 24, 2nd. ed., 1953, p. 376 (Loeb) and Vol. 43, 1956, pp. 285–286 (tropisms).
- 20 J. Loeb, *Der Heliotropismus der Tiere und seine Übereinstimmung mit dem Heliotropismus der Pflanzen*, Würzburg, 1889¹⁶; *The Heliotropism of Animals and its Identity with the Heliotropism of Plants*, Würzburg, 1890¹⁷.
- 21 J. Loeb, *Physiological Morphology*, Part I, 1891, Part II, 1892¹⁷.
- 22 J. Loeb, *Studies in General Physiology*, 1905¹⁷; *The Mechanistic Conception of Life*, 1912¹⁷; *The Organism as a Whole*, 1916¹⁷.
- 23 J. Loeb, *Vergleichende Gehirnphysiologie*, 1899; see ref. 7, p. 73, and ref. 8, p. 14; *Comparative Physiology of the Brain and Comparative Psychology*, 1900¹⁷.
- 24 J. Loeb, *Dynamics of Living Matter*, 1906¹⁷; *Le Dynamique des Phénomènes de la Vie*; see ref. 13, p. 138.
- 25 J. Loeb, *Forced Movements, Tropisms and Animal Conduct*, Lippincott, Philadelphia and London, 1918^{13,16,17}.
- 26 J. Loeb, *Regeneration*, 1924¹⁸.
- 27 J. Loeb, *Artificial Parthenogenesis and Fertilisation*, 1913¹⁷.
- 28 J. Loeb, *Proteins and the Theory or Colloidal Behavior*, 1922¹⁸; 2nd ed., McGraw-Hill, New York, 1924, quoted by N. Morgan, *Trends Biochem. Sci.*, 11 (1986) 187–189; *Eiweisskörper und die Theorie der kolloidalen Erscheinungen*, Berlin, 1924¹⁶.
- 29 S. S. Cohen, “Finally, the beginnings of molecular biology”, *Trends Biochem. Sci.*, 11 (1986) 92–94.
- 30 Julius Sachs, b. 1832 in Breslau (Wrocław), d. 1897 in Würzburg; Prof. in Poppelsdorf, Freiburg, from 1868 in Würzburg, plant physiologist (*cf.*, *Der Grosse Brockhaus*, Bd. 16, F. A. Brockhaus, Leipzig, 1933, p. 282). Studied, among other problems, the influence of temperature and light on the growth of plants.
- 31 T. W. Engelmann, *Pflügers Arch. Ges. Physiol.*, 57 (1902) 375–390; W. Pfeffer, *Untersuch. Bot. Inst. Tübingen*, 2 (1888) 582–589^{57–59}.
- 32 Unfortunately, Loeb’s classical publications²⁴ on this topic were not available to me. However, the field was reviewed in retrospect in a chapter¹³ from which the following is quoted (p. 137): “The existence of static or dynamic orientation reaction controlled by localized stimulation does not, by itself, pose special problems. But Loeb’s formulation of certain theory of tropisms which puts forward a very simple mechanical interpretation of the orientation reactions, has aroused a very lively interest, a lot of research and often passionate controversies.” The theory is exemplified by the case of phototropism (heliotropism): “Light energy which reaches unequally the two sides of the symmetrical body of the organism and which is transformed on each side to the tonus of tissues and muscles, causes a tonic dissymmetry which is manifested by a change in position that orientates the organism against the light source (or the other way, respectively). If the position adopted exposes both sides equally to the influx of the light energy, the tonic equalization maintains this orientation... If the animal approaches the light (or retires from it), this is the result of the initial tonic dissymmetry which has brought about a directed position which is then preserved during the movement... Loeb insisted on the perfect similarity of the animal and plant tropisms, trying to prove the same laws in the effect of light... In aspiring to explain mechanically all the acts of animals or possibly even Man, Loeb has presented the tropisms as the components of instinctive and voluntary actions.” In animals which have a nervous system, Loeb admitted neural links between the receptor and effector. Eventually, he identified tropisms with reflexes and other “forced movements”^{24,25}.
- 33 “At the beginning of the century, he (J. Loeb) thought that he had found here the elementary unit of behaviour, which for the ethologists would be equivalent to the living cell of the biologists. Presently, the theory of tropisms is invoked only for some orientation reactions of animals and plants.” C. Viaud, *Le Phototropisme Animal*, Faculté des Lettres de Strasbourg, 1938; *Les Tropismes*, PUF, Paris, 1951, quoted by R.-J. Darchen, “Les tropismes”, in R. Chauvin (Director), A. Quillot and R. Ropartz (Editors), *La Biologie. Les Êtres Vivants. Les Dictionnaires Marabout Université*, Vol. 8, Gérard et Cie, (Paris ?), 1973, pp. 82–90.
- 34 Piéron¹³ quotes Herbert Spencer Jennings (1868–1947, botanist, microbiologist, geneticist, ethologist) as one of the earliest and most important opponents of Loeb. Jennings experimented especially on the simplest animals, including protozoa. He gave many examples of external and internal sources of variation (different “physiological states”) and of behaviour modifications incompatible with the con-

- ception of “irreversibility” of tropisms; these modifications often amounted to a true regulation. According to him, the “law of interest” decides the selection of favourable acts in different reactions available to lower animals. As “trials and errors” he designated primary reactions which are subject to progressive selection during the true learning process.
- 35 Claparède’s Law of Momentary Interest was defined by him as follows: “At any given moment, that instinct which is of greatest importance takes precedence over the others”, or “At any given moment, an organism acts according to its strongest interest” (ref. 7, p. 76; ref. 8, p. 17). “Biological interest is what is useful for the individual from the point of view of its maintenance and development of its personality”, E. Claparède, *Psychology of the Child and Experimental Pedagogy* (Czech translation from the 8th edition of 1920), Vol. 2, Ústř. spolek jednot učitelů nas Moravě and Dědictví Komen-ského, Brno and Prague, 1928, p. 123. The “interest” is not identical with the need, but corresponds to its anticipation. The law is part of the generalizations which Claparède advocates in describing mental phenomena and derives from his basic biological, functional point of view expounded in Piaget’s analysis of Claparède’s psychology; ref. 11, pp. 52–66.
- 36 For Georges Bohn (1868–1948) (ref. 12, p. 17) tropisms are produced by the different rates of chemical reactions on the right and the left sides of the plane of symmetry. This led him to postulate two objective criteria (explained here in the case of phototropism). (a) If light of equal intensity from two sources reaches an animal attracted by light and the animal “chooses” one of these lights and moves towards it, this is no tropism. If the animal orientates itself so as to be equally illuminated on both sides, this is tropism. (b) If one receptor (e.g., one eye) is eliminated while the contralateral one is active, manage movements ensue. Both of these criteria were criticized by other authors who observed fluctuations between true tropisms, as defined in this way, and other patterns of behaviour in the same animals¹³. Bohn emphasized another class of phenomena which, in agreement with Loeb^{20,24}, he called “differential sensitivity” (Unterschiedsempfindlichkeit). This term is not happily chosen. It denotes reactions to the temporal change in the intensity of the stimulus³⁷. As the third class of simple phenomena, Loeb mentioned cellular memory. Going up the evolutionary scale, Bohn sees fewer and fewer true tropisms and other simple phenomena to occur (already in arthropods they may be super-imposed by associative memory), whereas Loeb tries to extend the notion of tropisms to very complex reactions, including vertebrates and man.
- 37 Interestingly, the simplest of taxes, bacterial chemotaxis, has been shown to be based on temporal sensing of the difference in concentration³⁸, thus in Loeb’s and Bohn’s terminology it would be “differential sensitivity”.
- 38 R. M. Macnab and D. E. Koshland, Jr., *Proc. Natl. Acad. Sci. USA*, 69 (1972) 2509–2512.
- 39 Incidentally, Vladislav Adolfovich Rotert, of Polish descent, who is reported to have been engaged in the study of heliotropism in Famintsyn’s Cabinet of Anatomy and Physiology of Plants of the Academy of Sciences in St. Petersburg, was a Privat-Docent of botany at the Kazan’ University in 1889–97 (ref. 4, pp. 51 and 80).
- 40 It is probable that journal articles rather than typed letters are meant. One likely candidate is ref. 6.
- 41 By “biological interest” Tswett may be jokingly referring to “psychological” interest in biology.
- 42 By calling “philotropism” mutual sympathies of the two friends and “naturphilosophical tropisms” their interest in the philosophy of Nature, Tswett probably makes fun of the extension of the term tropism to higher mental functions.
- 43 Here again, the term “parallelism” oscillates between two meanings: the parallel ways of thinking of the two friends, and the psycho-physical parallelism which Claparède describes (ref. 7, pp. 73–74; ref. 8, p. 14), in the context of the heated discussions between the opponents and defenders of animal psychology in 1890–1910 and repetition of these discussions a quarter of a century later (behaviorism): “For my part, in these discussions I adopted Flournoy’s point of view of parallelism, not as a meta-physical principle—he declared that parallelistic dualism had never been asserted in philosophy [see T. Flournoy, “Sur le panpsychisme”, *Arch. Psychol.*, 4 (1905) 137–138]—but as a methodological principle [see T. Flournoy, *Metaphysique et Psychologie*, Geneva, 1890, new edition 1919, and E. Claparède, “Th. Flournoy”, *Arch. Psychol.*, 8 (1921) 2]. While it is a scientific expression of the close union which exists between processes of conscience and cerebral processes, this principle also has the great advantage of removing all sterile discussion as to the nature of this union. It enables psychology and physiology to remain in close harmony with one another”.
- 44 It is likely that by “schopenhauerite” Tswett hints at the spontaneity, the activity which, according to Claparède’s “Law of Momentary Interest”, should disqualify a phenomenon, as “tropism”.
- 45 Both Tswett and Claparède emphasized definitions as a way to prevent misunderstanding. Tswett

- chose the following quotation of the mathematician Henri Poincaré as the motto of the introductory part of his *Chromophylls of the Plant and Animal World, Doctor's Dissertation* (in Russian), University of Warsaw, 1910: "La rigueur ne pourrait pas s'introduire dans les raisonnements si on ne la faisait entrer d'abord dans les définitions". Claparède says (ref. 7, p. 92; ref. 8, p. 34): "This same desire for clearness of thought led me to study terminology, and I would have liked our Congresses to be a means of attaining unity in this respect, as is the case with those of chemists and botanists (e.g., "Rapport sur la terminologie psychologique", *C.R. Congr. Int. Psychol.*, Geneva, 1909). This is the reason which made Binet say I had a taste for doing the police work of psychology [A. Binet, *Année Psychol.*, 17 (1911) 490]. A taste, no, but I considered it a necessity, and I must admit, it satisfies at the same time my systematizing demon and, perhaps, the sublimated remnants of my infantile desire for domination."
- 46 Simplicity of the prototype tropisms may be more apparent than real: now that considerable progress has been achieved in the elucidation of one of the simplest taxes, the chemotaxis of bacteria, we may consider the complicated physiology of the sensory detection, transmission and processing of the signal, memory function, motor performance, adaptation at several levels and genetic control of these functions. The mechanism of the effect of auxins in plants is no less complicated.
- 47 By saying that, in a sense, all tropisms are active, Tswett contradicts Claparède who excluded "actions" from tropisms. Cf., Claparède's autobiography (ref. 7, p. 79; ref. 8, p. 21) where he mentions his paper⁶. "The conception of interest has also been my criterion to distinguish an *action*, a *conduct* from any other kind of movement of an organism, such as, for instance, the tropisms in the sense in which Loeb uses the word. An action, a spontaneous reaction (as opposed to tropism or the simple, mechanical reflex, such as the patellar reflex) is any reaction governed by the Law of Momentary Interest, which law adapts itself to the varying needs of the organism (the stimulation remaining the same)." As we have said in the Introduction, Claparède did not accept the degree to which Jacques Loeb extended the notion of "tropism" to cover mental phenomena, but even Claparède's compromising views did not appeal to Tswett. He saw no advantage in Claparède's differentiation: all positions or movements orientated with respect to some directional external energy could be called "tropisms" or "taxes", but none of them was passive and no useful purpose was served by attaching a label without demonstrating mechanism.
- 48 The larvae of *Porthesia chrysoorrhoea* hibernate in a nest and then climb up the branches towards sunlight (positive heliotropism). After they have fed on leaves, this heliotropism ceases. According to Loeb, if they are left to ascend in a cul-de-sac (an inverted test-tube illuminated near its end) where there is no food, they starve to death. (This is probably why Tswett calls them "unfortunate".) "The animal is placed in a field of forces of which he is a toy, sometimes even leading to death" (Loeb²⁴). Piéron (ref. 13, p. 148), on the other hand, quotes Deegener and Manquat, who observed that, if these caterpillars do not find any leaves at the end of the branches which they explore, they descend and do not hesitate to search in shaded areas.
- 49 J. Loeb and G. Bohn were among the "rapporteurs" whose reviews on topical themes were printed in advance for the 1909 Sixth International Congress of Psychology in Geneva, presided by Th. Flournoy, of which Claparède was General Secretary. Loeb's and Bohn's rapports enjoyed great popularity. The year 1909 brought a general recognition of Loeb's work. As already mentioned, honorary doctorates were conferred on him in Cambridge, Geneva and Leipzig.
- 50 Unfortunately, we were unable to find the book in the catalogue of the Prague University library. One suspects that the work of Varvara Polovtseva was connected with the research carried out by Academician A. S. Famintsyn (in whose laboratory Tswett had worked in St. Petersburg) on excitation phenomena in plants⁵¹⁻⁵³. It would be interesting to know whether there was any connection between Varvara Polovtseva and her namesake V. V. Polovtsev, who in 1895 (ref. 4, pp. 51, 57, 61 and 62) founded the botanical section of P. F. Lesgaft's "St. Petersburg Laboratory of Biology" and directed it until 1897, when he left for Famintsyn's Cabinet and Tswett succeeded him in Lesgaft's Laboratory. Polovtsev worked on bacteria and the effect of X-rays on plants in Lesgaft's laboratory and on respiration in plants in Famintsyn's Cabinet. The spelling of V. V. Polovtsev's name is controversial. Senchenkova consistently spells it Polovtsov whereas the Bol'shaya Sovetskaya Entsiklopediya gives Polovtsev wherever the name is mentioned. (Heliotropism was studied in Famintsyn's Cabinet by V. A. Rotert³⁹, geotropism by F. F. Zelinskii; ref. 4, p. 51).
- 51 These studies were severely criticized by K. A. Timiryazev. While defending A. S. Famintsyn (1835-1918) in other respects, Senchenkova⁵² admits that K. A. Timiryazev was justified in criticizing some of Famintsyn's theses on the excitability in plants; yet she does not agree with those who, mainly for his ideas on excitability, labelled Famintsyn as a partisan of phytopsychology, superficial evolutionist,

anti-darwinist, booster, reactionary clerical, pseudoscientist singing from the parts of German obscurants.

- 52 E. M. Senchenkova: "The discovery of chromatography and the Academy of Sciences" (in Russian), *Privoda*, No. 5 (1975) 92–101.
- 53 G. V. Platonov, *The Weltanschauung of K. A. Timiryazev* (in Russian), Moscow, 1952⁵².
- 54 This book was not available to us. It is possible, however, that the book of 1912^{12,36}, which I studied, is a translation of the book referred to by Tswett in 1911. Its first chapter is entitled "Anwendung der physikalischen Chemie auf die Psychologie". Some examples may illustrate the reasons for Tswett's disinclination to this book. Page 8: "According to Jacques Loeb animals are chemical machines and scientific analysis of mental phenomena has the sole task to find out the physico-chemical laws which underlie them. Loeb himself brought the proof that this claim can be met, and I should like to mention here at least the most important results which have been obtained by the application of physico-chemical methods to psychology. [Cf., J. Loeb's lecture on the Congress of Geneva (1909) and *Die Bedeutung der Tropismen für die Tierpsychologie*, Leipzig 1909]...".
- As one of results which are brought forward as an argument in favour of the physico-chemical interpretation of life phenomena, Bohn quotes (p. 12) the case of a weakly heliotropic animal made strongly heliotropic by treatment with a chemical substance. Loeb describes fresh-water Copepoda (crustaceans) which show no phototropism in an aquarium illuminated on one side. When water rich in carbonic acid is added, they become strongly positively heliotropic. Loeb assumes that the surplus in the overall mass of substances, which are produced photochemically on one side of the body, is normally insufficient to produce a noticeable increase in the muscle tonus on one half of the body in these animals in comparison with the other half. The acid could act as a catalyst, as in the catalysis of esters, where, according to Stieglitz, the acid increases the active mass of the material which undergoes reaction. "Tentatively, we can assume that the acid acts by increasing the active mass of the photochemical products and hence the difference in their amount." Another example of "physico-chemical" reasoning is the concept of an excess of energy in the sexually excited dog as opposed to a deficiency of energy manifested by the economy of Pavlovian conditioned reflexes (p. 153).
- 55 Th. Beer, A. Bethe and J. von Uexküll, "Vorschläge zur einer objektivierenden Nomenklatur in der Physiologie des Nervensystems", *Biol. Centralbl.*, 19 (1899) 517; ref. 12, p. 1.
- 56 J. Adler, *Science*, 160 (1969) 1588–1597.
- 57 D. E. Koshland, Jr., "The chemotactic response in bacteria", in L. Jaenicke (Editor), *Biochemistry of Sensory Functions*, 25. Mosbacher Coll. der Ges. für Biol. Chem., 25–27.4.1974, Springer, Berlin, 1974, pp. 134–160.
- 58 J. Adler, "Chemotaxis in Bacteria", *Annu. Rev. Biochem.*, 44 (1975) 342–356. He quotes here Alfred Binet (1857–1911), *The Psychic Life of Micro-organisms*, Open Court, Chicago, 1889, pp. iv–v: "If the existence of psychological phenomena in lower organisms is denied, it will be necessary to assume that these phenomena can be superadded in the course of evolution, in proportion as an organism grows more perfect and complex. Nothing could be more in consistent with the teachings of general physiology, which shows us that all vital phenomena are previously present in non-differentiated cells."
- 59 J. Adler, "The sensing of chemicals by bacteria", *Sci. Am.*, 234, No. 4 (1976) 40–47: "The basic elements that make behavior possible in a higher organism are thus present in a single bacterial cell; they are sensory receptors, a system that transmits and processes sensory information and effectors to produce movement. Whether the mechanisms of any of these elements in the bacterium are similar to those in more complex organisms remains to be established. Obviously there must be major differences; for example, since bacteria are independent cells, the cell-to-cell synaptic action that is so important in determining behavior in more complex organisms cannot possibly exist in bacteria, at least not at a cellular level. Still, it appears that the bacterial system may be a good model for the study of behavior."⁶³
- 60 D. E. Koshland, Jr., "Special topic: Chemotaxis and motility", *Annu. Rev. Physiol.*, 44 (1982) 499–500. A. Boyd and M. Simon, "Bacterial chemotaxis", *Annu. Rev. Physiol.*, 44 (1982) 501–519.
- 61 J. M. Lackie and P. C. Wilkinson (Editors), *The Biology of the Chemotactic Response*, Society for Experimental Biology Seminar Series, No. 12, Cambridge University Press, 1982, pp. xiii + 177. The meeting confined itself to unicellular chemotaxis.
- 62 J. Stock and A. Stock, "What is the role of receptor methylation in bacterial chemotaxis", *Trends Biochem. Sci.*, 12 (1987) 371.
- 63 For the investigation of chemoreception in bacteria, J. Adler won the R. H. Wright Award in Olfactory Research 1987; B. P. Clayman, *Trends Biochem. Sci.*, 13 (1988) 9.

64 University of California, Berkeley
Department of Biochemistry

July 31, 1975

I am pleased to send some reprints on our work on chemotaxis and I was very interested to learn of the historical connections with Michael Tswett.

I am not sure I would find a conflict with Tswett's conclusion, although I might invert it and say that I believe the higher neural functions must be "physical, chemical, well understood physical phenomena subject to simple laws." The important feature is the complexity of the system. In my opinion the relationship of bacteria to the human brain is that of a small, hand calculator to the giant computers. Our studies have shown that bacteria do not do something very simple, such as slow down as the concentration of sugar increases. That could be explained by very simple physical laws. At least twenty different gene products affect their behaviour and probably many more which we have not discovered yet. However, each of these products by itself follows simple physical laws. Hence the difference between bacteria and higher species is that there are just a great many more gene products involved in the human brain than in the small microorganism.

There is a danger of making shortcuts, but there is a danger of being blind to relationships. The genetic code and the metabolism of carbohydrates were both worked out in microorganisms and turn out to be essentially the same in man. It would be surprising if sensory processes did not have a similar biochemistry in all species.

Sincerely yours,
Daniel E. Koshland, Jr.

CHROM. 20 574

UNIFIED THEORY OF ADSORPTION CHROMATOGRAPHY: GAS, LIQUID AND SUPERCRITICAL FLUID MOBILE PHASES

DANIEL E. MARTIRE

Department of Chemistry, Georgetown University, Washington, DC 20057 (U.S.A.)

SUMMARY

Utilizing statistical thermodynamics and a mean-field lattice model, and exploiting isomorphic elements of binary-liquid and single-fluid critical behavior, the unified theory of the title is derived and discussed in some detail. The final results confirm that the natural mobile-phase state variables are its reduced temperature and reduced density. As an example of its utility and efficacy, the theory is applied to gas-solid chromatography with a highly adsorbable mobile phase. Potential refinements of the model are noted.

INTRODUCTION

Recently, we developed a unified molecular theory of absorption or fluid-liquid chromatography^{1,2}. The present advance extends this work to adsorption or fluid-solid chromatography.

Researchers in many areas of the physical sciences have been attempting to develop unified theories in the form of master equations to describe, succinctly and quantitatively, related physical phenomena. For instance, the isomorphism among various types of critical phenomena has been recognized and treated³, suggesting some quantitative universal laws. Also, the search continues in physics for a unified theory to describe the effects of different, fundamental force fields. However, with the exception of our recent theory and a classic study by Giddings on the dynamics of chromatography⁴, such unified approaches have been lacking in the area of chromatography, despite their conceptual and practical advantages.

Starting with equations derived for the solute distribution coefficient in the case of a binary liquid mobile phase and a solid adsorbent stationary phase, and then, exploiting the isomorphism between the upper critical solution temperature (UCST) in a binary liquid system and the liquid-gas critical point in a single-component fluid system³, a general equation is derived for the solute distribution coefficient in a chromatographic system where the stationary phase is an adsorbent and the mobile phase is a single-component ideal gas, moderately non-ideal gas, supercritical fluid or even a liquid.

In view of the more advanced state of theory and theoretical treatments of experimental data in gas and liquid chromatography, this unified theory should ultimately find its widest application in the area of supercritical fluid chromatography

(SFC), where there is renewed interest in packed-column systems containing unmodified or modified adsorbents⁵⁻¹⁰. However, as an example of its utility, the unified theory is applied here to low-pressure gas-solid chromatography with a highly adsorbable vapor (volatile modifier) in the carrier gas^{11,12}.

THEORY OF LIQUID-SOLID CHROMATOGRAPHY WITH A BINARY MOBILE PHASE

In common with our earlier treatments of liquid-solid (adsorption) and liquid-bonded phase chromatography¹³⁻¹⁶, statistical thermodynamics and a mean-field lattice model are utilized to derive the relevant equations to describe the equilibrium distribution of solute between a binary liquid mobile phase and an adsorbent stationary phase, and, hence, solute retention in such systems. Also, the present, more refined treatment examines (as before) the competitive equilibrium at the molecular level among solvent and solute molecules distributed between generally non-ideal mobile and stationary phases, all components being non-electrolytes. Both entropy and interaction energy effects are rigorously included.

The stationary phase (subscript s) is assumed to be an energetically homogeneous, planar surface on which is adsorbed a monolayer of solvent and solute molecules. Although a variety of molecular structures may be considered within the general framework of the model^{1,13-15,17}, for present purposes the molecules are assumed to be completely flexible chains, each having r_i singly-connected (terminal) or doubly-connected (internal) cubic segments, each of volume l^3 . (Therefore, the hard-core volume of a molecule of type i is $r_i l^3$.) Parallel-layer adsorption and, hence, a uniform thickness of all of the molecules in the adsorbed monolayer are also assumed. The adsorbent surface is modelled as a two-dimensional, square-planar lattice having a nearest-neighbor coordination number of $z_s = 4$ and containing M_s equivalent surface sites, each of area l^2 . Occupying these sites in a restricted random walk^{1,18} are $N_{a(s)}$ solute molecules, each occupying r_s sites, and $N_{b(s)}$ and $N_{c(s)}$ solvent molecules, each occupying r_b and r_c sites, respectively, where $M_s = r_a N_{a(s)} + r_b N_{b(s)} + r_c N_{c(s)}$. Accordingly, the volume of the stationary phase is equal to the surface area of the adsorbent ($M_s l^2$) times the monolayer thickness (l), *i.e.*, $M_s l^3$.

The mobile phase (subscript m) is modelled as a three-dimensional, simple-cubic lattice having a nearest-neighbor coordination number of $z_m = 6$ and containing M_m cubic cells or sites, each of volume l^3 . Similarly, $M_m = r_a N_{a(m)} + r_b N_{b(m)} + r_c N_{c(m)}$ and the volume of the mobile phase is $M_m l^3$.

The dimensionless configurational entropy of the stationary-phase ($x = s$) or mobile-phase ($x = m$) mixture, S_x/k_B , is given by^{1,18}

$$\begin{aligned}
 -S_x/k_B = & \sum_{i=a}^c (N_{i(x)} \ln N_{i(x)} - N_{i(x)}) - \\
 & \sum_{i=a}^c N_{i(x)} (r_i - 1) \ln \{ (z_x - 1) / M_x \} - \\
 & M_x \ln M_x + M_x
 \end{aligned} \tag{1}$$

where $M_x = \sum_{i=a}^c r_i N_{i(x)}$ and k_B is the Boltzmann constant. If the attractive interaction energy between nearest-neighbor segments on molecules i and j is denoted by ε_{ij} , and between a molecular segment on i and a surface site by ε_{is} , the dimensionless total interaction energy in phase x , $E_x/k_B T$, is^{1,18}

$$\begin{aligned} E_x/k_B T = & (z_e f_x / k_B T) \sum_{i=a}^c r_i N_{i(s)} \varepsilon_{is} + \\ & (z_e f_x / k_B T M_m) \sum_{i,j=a}^c r_i N_{i(m)} r_j N_{j(s)} \varepsilon_{ij} + \\ & [z_e (1 - 2f_x) / 2k_B T M_x] \sum_{i,j=a}^c r_i N_{i(x)} r_j N_{j(x)} \varepsilon_{ij} \end{aligned} \quad (2)$$

where T is the temperature (K), ε_{ij} and ε_{is} are negative (attractive), and z_e denotes the number of nearest-neighbor, external contacts of a molecular segment. (For sufficiently large r_i , where the number of terminal segments is small compared to the number of internal segments, $z_e \approx 4$ in this model.) Also, f_x is the fraction of the molecular surface which is in contact with the adsorbent surface. For the mobile phase ($x = m$), $f_m = 0$ and only the third term on the right hand side (r.h.s.) of eqn. 2 survives. For the stationary phase ($x = s$), $f_s > 0$. (Again, for sufficiently large r_i , $f_s \approx 1/4$ in this model.) The first term on the r.h.s. of eqn. 2 represents the total (dimensionless) molecular energy of adhesion to the adsorbent surface. Also, it is assumed that the same fraction, f_s , of the molecular surface opposite that in contact with the adsorbent interacts with the mobile-phase molecules in contact with the adsorbed monolayer (second term on the r.h.s. of eqn. 2). Therefore, the "lateral" molecular interactions in the stationary phase are reflected in the third term on the r.h.s. of eqn. 2. Finally, if we denote the cell partition function per segment of molecule i in phase x by $q_{i(x)}$ and include the contribution¹

$$A'_x/k_B T = - \sum_{i=a}^c r_i N_{i(x)} q_{i(x)} \quad (3)$$

the entire dimensionless Helmholtz free energy of the mixture, $A_x/k_B T$, consistent with the Bragg-Williams approximation¹⁸, is simply given by the sum of eqs. 1, 2 and 3:

$$A_x/k_B T = (A'_x/k_B T) + (E_x/k_B T) - (S_x/k_B) \quad (4)$$

The dimensionless chemical potential of the h th component in phase x , $\mu_{h(x)}/k_B T$, is determined from

$$\mu_{h(x)}/k_B T = \left[\frac{\partial(A_x/k_B T)}{\partial N_{h(x)}} \right]_{T, N_{-h(x)}, N_{i(y)}} \quad (5)$$

where $N_{-h(x)}$ denotes the number of molecules of components other than h th one in

phase x and $N_{i(y)}$ denotes the number of molecules of all of the components in phase y ($y \neq x$). From eqns. 1-5

$$\begin{aligned} \mu_{h(x)}k_B T = & \ln(\theta_{h(x)}/r_h) + r_h \sum_{i=a}^c \theta_{i(x)}(1 - r_i^{-1}) - \\ & (r_h - 1)\ln(z_x - 1) - r_h \ln q_{h(x)} + (z_e f_x r_h / k_B T) \varepsilon_{hs} + \\ & (z_e f_x r_h / k_B T) \sum_{i=a}^c \theta_{i(m)} \varepsilon_{hi} + [z_e(1 - 2f_x) r_h / k_B T] \sum_{i=a}^c \theta_{i(x)} \varepsilon_{hi} - \\ & [z_e(1 - 2f_x) r_h / 2k_B T] \sum_{i,j=a}^c \theta_{i(x)} \theta_{j(x)} \varepsilon_{ij} \end{aligned} \quad (6)$$

where $h = a, b$ or c , $x = m$ or s , and where $\theta_{i(x)} = r_i N_{i(x)} / M_x$ is the volume fraction of component i in phase x . At equilibrium, each of the components must satisfy the following condition at the operational temperature:

$$\mu_{h(s)} / k_B T = \mu_{h(m)} / k_B T \quad (7)$$

Applying eqns. 6 and 7 to the solute component ($h = a$), one obtains

$$\begin{aligned} \ln[\theta_{a(s)} / \theta_{a(m)}] = & - (r_a - 1) \ln[(z_m - 1) / (z_s - 1)] - \\ & (z_e f_s r_a / k_B T) \varepsilon_{as} - r_a \ln[q_{a(m)} / q_{a(s)}] + \\ & r_a \sum_{i=a}^c [(\theta_{i(m)} - \theta_{i(s)}) (1 - r_i^{-1})] + \\ & [z_e(1 - f_s) r_a / k_B T] \sum_{i=a}^c \theta_{i(m)} \varepsilon_{ai} - \\ & [z_e(1 - 2f_s) r_a / k_B T] \sum_{i=a}^c \theta_{i(s)} \varepsilon_{ai} - \\ & (z_e r_a / 2k_B T) \sum_{i,j=a}^c \theta_{i(m)} \theta_{j(m)} \varepsilon_{ij} + \\ & [z_e(1 - 2f_s) r_a / 2k_B T] \sum_{i,j=a}^c \theta_{i(s)} \theta_{j(s)} \varepsilon_{ij} \end{aligned} \quad (8)$$

The chromatographic distribution coefficient, K , is defined as the ratio of the equilibrium concentration of solute in the stationary phase, $c_{a(s)}$, to that in the mobile phase, $c_{a(m)}$, in the limit of infinite dilution of the solute ($N_a \rightarrow 0$ or $\theta_a \rightarrow 0$). Clearly, in the model system, this ratio is also equal to the ratio of the respective θ_a 's, *i.e.*

$$K = \lim_{N_a \rightarrow 0} (c_{a(s)}/c_{a(m)}) = \lim_{N_a \rightarrow 0} (\theta_{a(s)}/\theta_{s(m)}) \quad (9)$$

Therefore, from eqns. 8 and 9, one obtains

$$\begin{aligned} \ln K_{b+c} = & - (r_a - 1) \ln[(z_m - 1)/(z_s - 1)] - (z_e f_s r_a / k_B T) \epsilon'_{as} + \\ & r_a \sum_{i=b}^c [(\theta_{i(m)} - \theta_{i(s)}) (1 - r_i^{-1})] + [z_e (1 - f_s) r_a / k_B T] \sum_{i=b}^c \theta_{i(m)} \epsilon_{ai} - \\ & [z_e (1 - 2f_s) r_a / k_B T] \sum_{i=b}^c \theta_{i(s)} \epsilon_{ai} - (z_e r_a / 2k_B T) \sum_{i,j=b}^c \theta_{i(m)} \theta_{j(m)} \epsilon_{ij} + \\ & [z_e (1 - 2f_s) r_a / 2k_B T] \sum_{i,j=b}^c \theta_{i(s)} \theta_{j(s)} \epsilon_{ij} \end{aligned} \quad (10)$$

where the subscript $b+c$ in K_{b+c} emphasizes the binary solvent. Also, in eqn. 8, the cell partition function term has been incorporated into the surface interaction term, as follows¹⁴

$$(z_e f_s / k_B T) \epsilon'_{hs} + \ln(q_{h(m)}/q_{h(s)}) = (z_e f_s / k_B T) \epsilon'_{hs} \quad (11)$$

thus making ϵ'_{hs} an adhesion free energy per molecular segment in eqns. 10 ($h=a$) and 11.

Eqn. 10 is still incomplete because it does not explicitly take into account the competitive equilibrium involving solvent components b and c , in addition to the solute component (a). Accordingly, setting $\theta_{a(x)} = 0$, applying eqn. 6 for solvent component b ($h=b$, $x=m$ or s) and eqn. 7 ($h=b$) in the form,

$$(r_a / r_b) [(\mu_{b(m)} / k_B T) - (\mu_{b(s)} / k_B T)] = 0 \quad (12)$$

and adding eqns. 10 and 12, one obtains

$$\begin{aligned} \ln K_{b+c} = & \ln K_b + (r_a / r_b) \ln(\theta_{b(s)} / \theta_{b(m)}) + \\ & (z_e r_a / k_B T) [(1 - f_s) \theta_{b(m)} - (1 - 2f_s) \theta_{b(s)} - f_s] [\epsilon_{ab} - \epsilon_{ac} + \epsilon_{bc} - \epsilon_{bb}] \end{aligned} \quad (13)$$

where K_b , the solute distribution coefficient with neat solvent b ($\theta_b \rightarrow 1$; $\theta_c \rightarrow 0$), is given by

$$\begin{aligned} \ln K_b = & [1 - (r_a / r_b)] \ln[(z_m - 1)/(z_s - 1)] + \\ & (z_e f_s r_a / k_B T) (\epsilon'_{bs} - \epsilon'_{as} + \epsilon_{ab} - \epsilon_{bb}) \end{aligned} \quad (14)$$

and where eqn. 11 ($h=b$) has also been applied. In terms of interaction parameters^{15,16}, χ_{ij} , where

$$\chi_{ij} = (z_e / 2k_B T) (2\epsilon_{ij} - \epsilon_{ii} - \epsilon_{jj}) \quad (15)$$

Eqn. 13 may be written as

$$\ln K_{b+c} = \ln K_b + (r_a/r_b)\ln(\theta_{b(s)}/\theta_{b(m)}) + r_a[(1-f_s)\theta_{b(m)} - (1-2f_s)\theta_{b(s)} - f_s](\chi_{ab} + \chi_{bc} - \chi_{ac}) \quad (16)$$

Similarly, setting $\theta_{a(x)} = 0$, applying eqn. 6 for solvent component c ($h=c, x=m$ or s) and eqn. 7 ($h=c$) in the form,

$$(r_a/r_c)[(\mu_{c(m)}/k_B T) - (\mu_{c(s)}/k_B T)] = 0 \quad (17)$$

and adding eqns. 10 and 17, one obtains

$$\ln K_{b+c} = \ln K_c + (r_a/r_c)\ln[(1-\theta_{b(s)})/(1-\theta_{b(m)})] + (z_c r_a/k_B T)[(1-2f_s)\theta_{b(s)} - (1-f_s)\theta_{b(m)}][\epsilon_{ac} - \epsilon_{ab} + \epsilon_{bc} - \epsilon_{cc}] \quad (18)$$

where K_c , the solute distribution coefficient with neat solvent c ($\theta_c \rightarrow 1; \theta_b \rightarrow 0$), is given by

$$\ln K_c = [1 - (r_a/r_c)]\ln[(z_m - 1)/(z_s - 1)] + (z_c f_s r_a/k_B T)(\epsilon'_{cs} - \epsilon'_{as} + \epsilon_{ac} - \epsilon_{cc}) \quad (19)$$

and where eqn. 11 ($h=c$) has also been applied. In terms of interaction parameters (eqn. 15), eqn. 18 may be written as

$$\ln K_{b+c} = \ln K_c + (r_a/r_c)\ln[(1-\theta_{b(s)})/(1-\theta_{b(m)})] + r_a[(1-2f_s)\theta_{b(s)} - (1-f_s)\theta_{b(m)}](\chi_{ac} + \chi_{bc} - \chi_{ab}) \quad (20)$$

Letting $z_e = 4$ and $f_s = 1/4$ (*vide supra*), eqns. 13, 14, 18 and 19 become, respectively

$$\ln K_{b+c} = \ln K_b + (r_a/r_b)\ln(\theta_{b(s)}/\theta_{b(m)}) + (r_a/k_B T)(3\theta_{b(m)} - 2\theta_{b(s)} - 1)(\epsilon_{ab} - \epsilon_{ac} + \epsilon_{bc} - \epsilon_{bb}) \quad (21)$$

$$\ln K_b = [1 - (r_a/r_b)]\ln[(z_m - 1)/(z_s - 1)] + (r_a/k_B T)(\epsilon'_{bs} - \epsilon'_{as} + \epsilon_{ab} - \epsilon_{bb}) \quad (22)$$

$$\ln K_{b+c} = \ln K_c + (r_a/r_c)\ln[(1-\theta_{b(s)})/(1-\theta_{b(m)})] + (r_a/k_B T)(2\theta_{b(s)} - 3\theta_{b(m)})(\epsilon_{ac} - \epsilon_{ab} + \epsilon_{bc} - \epsilon_{cc}) \quad (23)$$

$$\ln K_c = [1 - (r_a/r_c)]\ln[(z_m - 1)/(z_s - 1)] + (r_a/k_B T)(\epsilon_{cs} - \epsilon_{as} + \epsilon_{ac} - \epsilon_{cc}) \quad (24)$$

where, again, $\theta_{b(x)}$ is the volume fraction of solvent component b in phase x ($x = m$ or s).

In eqns. 22 and 24 (neat solvents) the first term on the r.h.s. stems from the configurational entropy term in $A_x/k_B T$ (eqns. 1 and 4) and the second term reflects the exchange interaction free energy associated with the competitive equilibrium¹³⁻¹⁶. In eqns. 21 and 23 the second term on the r.h.s. is associated with the statistics of the displacement process, while the third term reflects the exchange interaction energy associated with the competitive equilibrium¹³⁻¹⁶. Parenthetically, it is noted that for the special case of monomeric solute and solvent molecules ($r_a = r_b = r_c = 1$; $z_e = 6$; $f_s = 1/6$), eqns. 13, 14, 18 and 19 reduce to similar equations derived and discussed previously^{13,14}.

If we now designate component b as the “good” solvent, *i.e.*, the preferentially adsorbed solvent component, and component c as the “poor” solvent, and consider the special case where $\theta_{b(s)} \rightarrow 1$ ($\theta_{c(s)} \rightarrow 0$), eqn. 16 becomes

$$\ln K_{b+c} = \ln K_b - v_{ab} \ln \theta_{b(m)} - r_a(1 - f_s)(1 - \theta_{b(m)})(\chi_{ab} + \chi_{bc} - \chi_{ac}) \quad (25)$$

where $v_{ab} = r_a/r_b$. If, in addition, cancellation of the interaction energy terms (χ_{ij} 's) is assumed, then eqn. 25 reduces to the familiar Snyder-Soczewinski expression¹⁶:

$$\ln K_{b+c} = \ln K_b - v_{ab} \ln \theta_{b(m)} \quad (26)$$

Therefore, the equations derived in the present, more refined treatment of liquid–solid chromatography with binary mobile phases are seen to reduce to earlier and more familiar equations in certain special (but restrictive) cases.

Finally, full application of the general set of equations, *i.e.*, eqns. 13 (or 16) and 14, or eqns. 18 (or 20) and 19, requires the adsorption isotherm describing the equilibrium distribution of the solvent components between the mobile and stationary phases. Using eqn. 7 ($h = b$ or c) in the forms

$$(\mu_{b(m)}/k_B T) - (\mu_{b(s)}/k_B T) = 0 \quad (27)$$

$$(r_b/r_c)[(\mu_{c(m)}/k_B T) - (\mu_{c(s)}/k_B T)] = 0 \quad (28)$$

and scaling the system to the smallest molecule by letting $r_c = 1$ (refs. 13 and 15), one obtains from eqns. 6 (with $h = b$ or c , $x = m$ or s , $\theta_{a(x)} = 0$), 27 and 28

$$\begin{aligned} \ln[(1 - \theta_{b(m)})^{r_b}/\theta_{b(m)}] + (r_b - 1)\ln[(z_m - 1)/(z_s - 1)] + \\ (z_e f_s r_b / k_B T)(\varepsilon_{bs} - \varepsilon_{cs} + \varepsilon_{cc} - \varepsilon_{bc}) + 2r_b(1 - f_s)\chi_{bc}\theta_{b(m)} = \\ \ln[(1 - \theta_{b(s)})^{r_b}/\theta_{b(s)}] + 2r_b(1 - 2f_s)\chi_{bc}\theta_{b(s)} \end{aligned} \quad (29)$$

where eqn. 11 ($h = b$ or c) has been applied and where, from eqn. 15

$$\chi_{bc} = (z_e/2k_B T)(2\varepsilon_{bc} - \varepsilon_{bb} - \varepsilon_{cc}) \quad (30)$$

UNIFIED THEORY OF FLUID–SOLID CHROMATOGRAPHY WITH A NEAT MOBILE PHASE

In this section we take the final results from the previous section, exploit the isomorphism between the critical behavior in a binary liquid mixture and that in a neat

(single-component) fluid, and obtain a universal equation for fluid–solid (adsorption) chromatography, where the neat mobile phase may be a gas, liquid or supercritical fluid.

It is possible to work with either one of the following two sets of fundamental equations derived in the previous section:

(1) eqns. 14 (for $\ln K_b$), 16 (for $\ln K_{b+c}$, in terms of χ_{ij}) and 29 (mixed-solvent adsorption isotherm);

(2) eqns. 19 (for $\ln K_c$), 20 (for $\ln K_{b+c}$, in terms of χ_{ij}) and 29 (mixed-solvent adsorption isotherm).

These equations are based on a model which considers an energetically homogeneous and planar adsorbent surface, a stationary phase consisting of a monolayer of solvent and solute molecules adsorbed parallel to the surface, and the Bragg-Williams (random-pairing) approximation¹⁸. For reasons soon to become apparent, the second set of basic equations will be utilized here.

Continuing to scale the system by letting $r_c = 1$ (refs. 13 and 15), eqns. 19, 20 and 29 may be manipulated into reduced form by first noting the critical solution condition applicable to the binary-liquid mobile phase¹⁸

$$T^* = 2T\chi_{bc}r_b/(1 + \sqrt{r_b})^2 \quad (31)$$

$$\theta_b^* = (1 + \sqrt{r_b})^{-1} \quad (32)$$

where χ_{bc} is given by eqn. 30, T^* refers to the UCST (above which the b+c solvent mixture is homogeneous over the entire composition region) and θ_b^* refers to the critical volume fraction of “good” solvent, *i.e.*, the composition corresponding to T^* in the $T - \theta_{b(m)}$ phase diagram¹⁸. Introducing reduced variables (subscript R)

$$T_R = T/T^* = (1 + \sqrt{r_b})^2/2r_b\chi_{bc} \quad (33)$$

$$\theta_{b(m),R} = \theta_{b(m)}/\theta_b^* = \theta_{b(m)}(1 + \sqrt{r_b}) \quad (34)$$

and making use of eqn. 33 in eqns. 19, 20 and 29 (with $r_c = 1$ in all), one finds

$$\ln K_c = (1 - r_a)\ln[(z_m - 1)/(z_s - 1)] + [r_a(1 + \sqrt{r_b})^2 f_s / r_b T_R][(\epsilon'_{cs} - \epsilon'_{as} + \epsilon_{ac} - \epsilon_{cc}) / (2\epsilon_{bc} - \epsilon_{bb} - \epsilon_{cc})] \quad (35)$$

$$\ln K_{b+c} = \ln K_c + r_a \ln[(1 - \theta_{b(s)}) / (1 - \theta_{b(m)})] + [r_a(1 + \sqrt{r_b})^2 / r_b T_R][(1 - 2f_s)\theta_{b(s)} - (1 - f_s)\theta_{b(m)}][(\chi_{ac} + \chi_{bc} - \chi_{ab}) / 2\chi_{bc}] \quad (36)$$

$$\begin{aligned} & \ln[(1 - \theta_{b(m)})^{r_b} / \theta_{b(m)}] + (r_b - 1)\ln[(z_m - 1)/(z_s - 1)] + \\ & [(1 + \sqrt{r_b})^2 f_s / T_R][(\epsilon'_{bs} - \epsilon'_{cs} + \epsilon_{cc} - \epsilon_{bc}) / (2\epsilon_{bc} - \epsilon_{bb} - \epsilon_{cc})] + \\ & [(1 + \sqrt{r_b})^2 (1 - f_s) / T_R]\theta_{b(m)} = \\ & \ln[(1 - \theta_{b(s)})^{r_b} / \theta_{b(s)}] + [(1 + \sqrt{r_b})^2 (1 - 2f_s) / T_R]\theta_{b(s)} \end{aligned} \quad (37)$$

By invoking the isomorphism between the critical behavior in a binary liquid system and that in a single-component fluid system³, one may utilize the direct

correspondence between the volume fraction of “good” solvent (b) in the former and the volume fraction of space occupied by the molecules in the latter, and similarly with the “poor” solvent (c) and unoccupied space. It follows from eqn. 34 that

$$\theta_{b(m),R} = \rho_{b(m),R} = \rho_{b(m)}/\rho_b^* = \theta_{b(m)}(1 + \sqrt{r_b}) \quad (38)$$

where $\theta_{b(m)}$ is now the volume fraction of space occupied by the hard cores of the molecules in the mobile phase (*i.e.*, the fraction relative to what it would be in a hypothetical close-packed molecular arrangement of these cores, for which $\theta_{b(m)} = 1$), $1 - \theta_{b(m)}$ is the volume fraction of “empty” (unoccupied) space (and similarly for $\theta_{b(s)}$ and $1 - \theta_{b(s)}$ in the adsorbed monolayer), $\rho_{b(m)}$ is the actual density of the mobile-phase fluid, ρ_b^* is its critical density and $\rho_{b(m),R}$ is its reduced density. Also, $T_R = T/T_b^*$ becomes the usual reduced temperature of a single-component fluid, where T_b^* is its critical temperature. This correspondence also indicates that K_c may be replaced by K_0 , the solute distribution coefficient for ideal gas–solid chromatography (GSC) ($\rho_{b(m)} \rightarrow 0$). Lastly, it follows that all interactions involving component c (now representing unoccupied or void space in the model) may be set to zero, *i.e.*, $\epsilon'_{cs} = 0$ and $\epsilon_{ic} = 0$ ($i = a, b, c$). Accordingly, with the aid of eqn. 15, eqns. 35–37 become

$$\ln K_0 = (1 - r_a) \ln[(z_m - 1)/(z_s - 1)] + [r_a(1 + \sqrt{r_b})^2 f_s / r_b T_R] [\epsilon'_{as} / \epsilon_{bb}] \quad (39)$$

$$\ln K = \ln K_0 + r_a \ln[(1 - \theta_{b(s)}) / (1 - \theta_{b(m)})] + [r_a(1 + \sqrt{r_b})^2 / r_b T_R] [(1 - 2f_s)\theta_{b(s)} - (1 - f_s)\theta_{b(m)}] [\epsilon_{ab} / \epsilon_{bb}] \quad (40)$$

$$\begin{aligned} & \ln[(1 - \theta_{b(m)})^{r_b} / \theta_{b(m)}] + (r_b - 1) \ln[(z_m - 1)/(z_s - 1)] - \\ & [(1 + \sqrt{r_b})^2 f_s / T_R] [\epsilon'_{bs} / \epsilon_{bb}] + [(1 + \sqrt{r_b})^2 (1 - f_s) / T_R] \theta_{b(m)} = \\ & \ln[(1 - \theta_{b(s)})^{r_b} / \theta_{b(s)}] + [(1 + \sqrt{r_b})^2 (1 - 2f_s) / T_R] \theta_{b(s)} \end{aligned} \quad (41)$$

where K (replacing K_{b+c}) is the solute distribution coefficient when the mobile-phase density is $\rho_{b(m)}$, which, in turn, is related to $\theta_{b(m)}$ through eqn. 38. Note that eqns. 38–41, which comprise the unified molecular theory, are applicable to gas, liquid and supercritical fluid, single-component mobile phases.

Eqn. 41, which describes the distribution of fluid between the mobile and stationary phases (*i.e.*, the equilibrium adsorption isotherm), is required to determine the equilibrium value of $\theta_{b(s)}$ for a given mobile-phase density, $\rho_{b(m)}$. In eqn. 39 (ideal GSC), the first term on the r.h.s. stems from the change in the configurational entropy of the solute when it is transferred from an ideal-gas mobile phase to a bare, adsorbent stationary phase. The second term reflects the interaction free energy of adsorption of an isolated solute molecule on the surface. In eqn. 40, which links ideal GSC to nonideal GSC, supercritical fluid–solid chromatography (SFSC) and liquid–solid chromatography (LSC), the second term on the r.h.s. is associated with the statistics of the displacement process (the relative availability of void space in the two phases), while the third term reflects the exchange interaction energy associated with the competitive equilibrium. Note that eqn. 40 may also be written in terms of capacity factors (replacing K and K_0 by, respectively, k' and k'_0) or retention volumes.

At this point, several special cases of eqns. 40 and 41 could be considered. However, with the exception of one such case to be applied in the next section, these are deferred for future study.

Consider a situation where $\theta_{b(s)} \gg \theta_{b(m)} \approx 0$, *i.e.*, where there is an appreciable buildup of the carrier fluid on the adsorbent surface, even at very low mobile-phase densities (or pressures). Accordingly, in this limit, eqns. 40 and 41 become:

$$\ln K = \ln K_0 + r_a \ln(1 - \theta_{b(s)}) + [r_a(1 + \sqrt{r_b})^2/r_b T_R] [\epsilon_{ab}/\epsilon_{bb}] [(1 - 2f_s)\theta_{b(s)}] \quad (42)$$

$$\ln \theta_{b(m)} = \ln \theta_{b(s)} - r_b \ln(1 - \theta_{b(s)}) - [(1 + \sqrt{r_b})^2(1 - 2f_s)/T_R](\theta_{b(s)}) + (r_b - 1) \ln[(z_m - 1)/(z_s - 1)] - [(1 + \sqrt{r_b})^2 f_s / T_R] [\epsilon'_{bs}/\epsilon_{bb}] \quad (43)$$

APPLICATION OF THE UNIFIED THEORY

As an example of its utility, the unified theory is applied here to analyze the GSC retention behavior, at 10°C, of *n*-butane on graphitized carbon black (Carbopack C) modified by adsorption of propane from the carrier-gas stream. Parcher *et al.*¹² and Johnson¹⁹ obtained both retention and adsorption-isotherm data for this system. Although helium was employed as a second fluid component in their studies and, strictly, the model applies to a single-component fluid, the low pressure of carrier gas and the negligible adsorption of helium in their experiments permit application of the present model.

Designating *n*-butane (the solute) as component a and propane as component b, and noting that a value of $r_b = 4.614$ has been determined for carbon dioxide¹, r_i ($i = a$ or b) may be calculated from

$$r_i = r_{CO_2}(V_i/V_{CO_2}) \quad (44)$$

where V is the van der Waals molar volume. The published V data²⁰ and eqn. 44 yield values of $r_a = 11.195$ and $r_b = 8.799$ for the molecular size parameters. From the critical density of propane, $\rho_b^* = 0.217$ g/ml, and eqn. 38, we have

$$\theta_{b(m)} = 1.162 \rho_{b(m)} \quad (45)$$

Since the propane pressure, $P_{b(m)}$, corresponding to monolayer coverage of adsorbed propane is *ca.* 1000 Torr¹², ideal-gas behavior may be safely assumed, with negligible error, to relate $\rho_{b(m)}$ in eqn. 45 to $P_{b(m)}$ (Torr):

$$\theta_{b(m)} = 2.901 \cdot 10^{-6} P_{b(m)} \quad (46)$$

Eqn. 46 establishes the relationship between a model variable and an experimental state variable. With $P_{b(m)} = 1000$ Torr, $\theta_{b(m)} \approx 0.003$, thus justifying the application of eqns. 42 and 43, which are based on the condition $\theta_{b(m)} \approx 0$.

The critical temperature of propane, T_b^* , is 369.8 K. Thus, the other state variable, the reduced temperature, T_R , has a value of 0.766 at 283.2 K. The remaining

molecular parameters in eqn. 41 are $\epsilon_{ab}/\epsilon_{bb}$, which is reasonably assigned a value of 1.000, and f_s , which, as before, is assigned a value of 0.250. Therefore, writing eqn. 42 in terms of standard specific (per unit surface area of adsorbent) retention volumes, V_s^0 , and substituting into it the numerical values determined or assigned above, one obtains

$$\ln V_s^0 = \ln(V_s^0)_0 + 11.195 \ln(1 - \theta_{b(s)}) + 13.071 \theta_{b(s)} \quad (47)$$

Turning to eqn. 43, the applicable adsorption isotherm when $\theta_{b(s)} \gg \theta_{b(m)} \approx 0$, and recalling that $z_m = 6$ and $z_s = 4$, substitution of numerical values yields

$$\ln \theta_{b(m)} = \ln \theta_{b(s)} - 8.799 \ln(1 - \theta_{b(s)}) - 10.274 \theta_{b(s)} + 3.984 - 5.137 (\epsilon'_{bs}/\epsilon_{bb}) \quad (48)$$

where $\theta_{b(m)}$ is related to $P_{b(m)}$ in eqn. 46.

Analysis of the retention volume and adsorption isotherm results^{12,19} using eqns. 47 and 48 gives best-fit values of $\ln(V_s^0)_0 = 1.217$ and $(\epsilon'_{bs}/\epsilon_{bb}) = 2.114$. The excellent fits are evident in Figs. 1 and 2.

The monolayer capacity of adsorbed propane on the Carbpac C used was estimated to be $5.49 \mu\text{mol}/\text{m}^2$ (ref. 12). The $\theta_{b(s)}$ value in our model corresponding to this capacity is 0.562. (Recall that $\theta_{b(s)}$ is the ratio of the monolayer volume physically occupied by the hard cores of adsorbed molecules to the total volume of the monolayer.) This suggests that if the "hard cores" of the propane molecules were close-packed (a physical impossibility, given the prohibitive repulsive forces which would have to be overcome), the monolayer capacity would be $9.77 \mu\text{mol}/\text{m}^2$. Viewed another way, with the estimate of 30.1 \AA^2 for the actual specific surface area of a propane molecule adsorbed on Carbpac C¹², this suggests a realistic hard-core area of 16.9 \AA^2 .

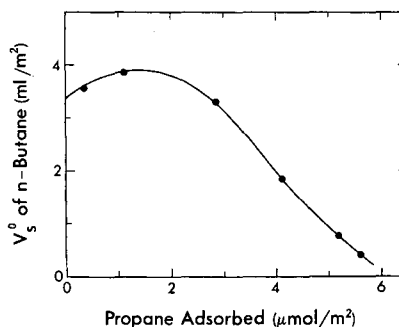
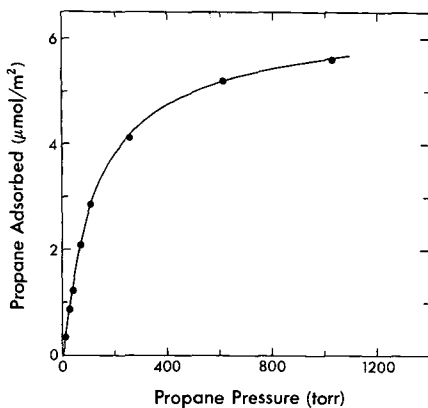


Fig. 1. Adsorption isotherm of propane on Carbpac C at 10°C ^{12,19}. Solid line was calculated from eqns. 46 and 48 with $\epsilon'_{bs}/\epsilon_{bb} = 2.114$.

Fig. 2. Specific retention volume, V_s^0 , of *n*-butane as a function of the amount of propane adsorbed on Carbpac C at 10°C ^{12,19}. Solid line was calculated from eqn. 47 with $\ln(V_s^0)_0 = 1.217$.

The reasonableness and consistency of the model results are further confirmed by evaluation of the specific volume and film thickness of the adsorbed monolayer. Assuming that propane-surface and butane-surface segmental interactions are equivalent, so that $(\epsilon'_{as}/\epsilon_{bb}) = (\epsilon'_{bs}/\epsilon_{bb}) = 2.114$, and, as before, letting $z_m = 6$, $z_s = 4$, $r_a = 11.195$, $r_b = 8.799$, $f_s = 1/4$ and $T_R = 0.766$, eqn. 39 yields a limiting value (zero propane pressure) of $K_0 = 5470$ (dimensionless). Using the fitted value of $(V_s^0)_0 = 3.377 \text{ ml/m}^2$, a specific volume of adsorbed propane of $6.2 \cdot 10^{-4} \text{ ml/m}^2$ is calculated. From the molar volume of liquid propane at 10°C (85.69 ml^{21}) and a monolayer coverage of $5.49 \mu\text{mol/m}^2$, a specific volume of $4.7 \cdot 10^{-4} \text{ ml/m}^2$ is estimated. In addition to the decent agreement between the two independent computations, one should also note the reasonableness of the estimated film thickness of about 5 or 6 Å.

The source of the maximum in Fig. 2 has been analyzed in some detail by Parcher *et al.*¹², who applied a scaled-particle theory in their treatment of the experimental results. The present model provides an explanation which is in full accord with theirs. Briefly, at low propane pressures (low $\theta_{b(s)}$) the third term on the r.h.s. of eqn. 47 ("lateral" interactions between adsorbed propane and butane molecules) dominates and leads initially to an increase in V_s^0 with increasing pressure. At higher propane pressures (higher $\theta_{b(s)}$) the second term, which reflects the availability of unoccupied adsorption sites, dominates and leads to a rapid decrease in V_s^0 with increasing pressure. The maximum occurs at the transition between these two pressure regions, here at $\theta_{b(s)} = 0.144$ (surface coverage of about $1.4 \mu\text{mol/m}^2$). This corresponds to a propane pressure of 45.8 Torr, at which $V_s^0 = 3.89 \text{ ml/m}^2$.

Similar maxima (and, presumably, for a similar reason) have been observed by Semonian and Rogers²² for pyrene with *n*-pentane as the carrier gas and C_{18} bonded to Porasil B as the column packing. On the other hand, at low pressures, King¹⁰ found only a very rapid drop in k' with increasing carbon dioxide pressure for *n*-alkane solutes and an alumina column, suggesting that any retention gain due to adsorbed carbon dioxide-solute lateral interactions was far outweighed by the loss from reduced availability of adsorption sites. These results and ones forthcoming from the author's laboratory (nonideal GSC and SFSC measurements) warrant detailed analysis in the light of this unified molecular theory of adsorption chromatography.

CONCLUSIONS

The unified theory of adsorption chromatography is compactly expressed by eqns. 39–41, where $\theta_{b(m)}$ is linked to an experimental state variable (reduced density of the mobile phase) by eqn. 38. As in our unified theory of absorption chromatography^{1,2}, these equations reveal that the natural state variables of the mobile phase are its reduced temperature and density.

To demonstrate its utility and efficacy, the theory has been successfully applied here to a single (but not trivial) GSC system. As mentioned in the preceding section, additional tests of the theory are clearly in order. Also, as emphasized throughout the derivation, the present model is based on an energetically homogeneous adsorbent and parallel-layer adsorption of the solute and solvent molecules in the assumed monolayer. However, virtually all chromatographic adsorbents have some degree of heterogeneity. There is evidence, for example, that Carboxpack C has a very small

fraction of "high-energy" sites¹², and silica gel is notorious for its heterogeneity. Also, a monolayer picture may not always be adequate, as Findenegg and Löring²¹ have shown in a careful study of propane adsorbed on Graphon (a graphitized carbon black) over a wide temperature range. Thus, a more complete model incorporating a discrete or continuous, energetic distribution of adsorption sites^{14,23} and allowing for multilayer adsorption needs to be explored. (Not included in the data fits via the models in this paper and ref. 12 were the actual, zero-pressure retention volume, where the tiny fraction of high-energy surface sites has its most pronounced effect, and the datum beyond the estimated monolayer coverage, where, in any event, the retention volume becomes impractically low.)

In addition, it is conceivable and, in fact, probable that the orientation of the adsorbed solute and solvent molecules would depend on the chemistry of the molecules and surface, as well as the density of the mobile phase (hence, the surface coverage). A further refinement of the present model would then be to allow for a distribution of molecular orientations in the adsorbed state. To this end, molecular statistics similar to those applied to anisotropic fluids (such as nematic liquid crystals) would have to be applied^{14,15,17}.

Finally, it should be noted that in any application of the results of the present or a modified model to SFSC, it must be kept in mind that the formulated K (or k') is strictly a local value, referring to a given position along the column. A rigorous method needs to be developed to relate the observed retention parameter to appropriate column-averaged quantities for particular inlet and outlet conditions.

ACKNOWLEDGEMENT

This material is based upon work supported by the National Science Foundation under Grant CHE-8305045.

REFERENCES

- 1 D. E. Martire and R. E. Boehm, *J. Phys. Chem.*, 91 (1987) 2433, and references cited therein.
- 2 D. E. Martire, *J. Liq. Chromatogr.*, 10 (1987) 1569.
- 3 R. B. Griffiths and J. C. Wheeler, *Phys. Rev. A*, 2 (1970) 1047.
- 4 J. C. Giddings, in A. Goldup (Editor), *Gas Chromatography 1964*, Elsevier, Amsterdam, 1965, p. 3.
- 5 C. M. White and R. K. Houck, *J. High Resolut. Chromatogr. Chromatogr. Commun.*, 9 (1986) 4.
- 6 P. J. Schoenmakers and F. C. C. J. G. Verhoeven, *J. Chromatogr.*, 352 (1986) 315.
- 7 P. Mourier, P. Sassi, M. Caude and R. Rosset, *J. Chromatogr.*, 353 (1986) 61.
- 8 P. J. Schoenmakers, P. E. Rothfus and F. C. C. J. G. Verhoeven, *J. Chromatogr.*, 395 (1987) 91.
- 9 D. Leyendecker, D. Leyendecker, B. Lorenschat, F. P. Schmitz and E. Klesper, *J. Chromatogr.*, 398 (1987) 89, 105.
- 10 J. W. King, in T. G. Squires and M. E. Paulatis (Editors), *Supercritical Fluids: Chemical Engineering Principles and Applications*, ACS Symp. Ser. Vol. 329, American Chemical Society, Washington, DC, 1987, p. 150.
- 11 J. F. Parcher, *J. Chromatogr. Sci.*, 21 (1983) 346.
- 12 J. F. Parcher, P. J. Lin and D. M. Johnson, *Anal. Chem.*, 58 (1986) 2207.
- 13 D. E. Martire and R. E. Boehm, *J. Liq. Chromatogr.*, 3 (1980) 753.
- 14 R. E. Boehm and D. E. Martire, *J. Phys. Chem.*, 84 (1980) 3620.
- 15 D. E. Martire and R. E. Boehm, *J. Phys. Chem.*, 87 (1983) 1045.
- 16 M. Jaroniec and D. E. Martire, *J. Chromatogr.*, 351 (1986) 1, and references cited therein.
- 17 D. E. Martire, *J. Chromatogr.*, 406 (1987) 27.

- 18 T. H. Hill, *An Introduction to Statistical Thermodynamics*, Addison-Wesley, Reading, MA, 1960, Ch. 20 and 21.
- 19 D. M. Johnson, *Doctoral Dissertation*, The University of Mississippi, 1985.
- 20 A. Bondi, *J. Phys. Chem.*, 68 (1964) 441.
- 21 G. H. Findenegg and R. Löring, *J. Chem. Phys.*, 81 (1984) 3270.
- 22 B. P. Semonian and L. B. Rogers, *J. Chromatogr. Sci.*, 16 (1978) 49.
- 23 M. Jaroniec, D. E. Martire and M. Borówka, *Advan. Colloid Interface Sci.*, 22 (1985) 177.

CHROM. 20 197

Note

Dispersion and selectivity indices of alkyl and alkenyl benzenes

J. K. HAKEN* and R. J. SMITH

Department of Polymer Science, The University of New South Wales, P.O. Box 1, Kensington, N.S.W. 2033 (Australia)

The retention of any substance in chromatography is the result of both apolar and polar forces, moderated by steric factors. Recently Evans *et al.*¹ introduced a modification of the Kováts' retention index system in an attempt to separate the contributions of these two forces.

Assuming that the non-polar forces involved in retention are proportional to molecular weight, Evans *et al.*¹ expressed Kováts' index as the sum of two factors:

$$I = I_m + I^* \quad (1)$$

where I_m (selectivity index) is defined as the retention index of a hypothetical n -alkane having the same molecular weight as the solute and I^* is the dispersion index, which reflects the combined effects of molecular shape and functionality.

Since an n -alkane has a molecular formula of C_iH_{2i-2} or $(CH_2)_i + 2H$ its molecular weight is $m = 14.026 i + 2.016$. Therefore I_m can be calculated from;

$$I_m = \frac{m - 2.016}{0.14026} \quad (2)$$

where m is the molecular weight of the solute.

In a further paper Evans and Haken² studied the dispersion and selectivity indices for the halogenated derivatives of cyclohexane, benzene and anisole. Their initial results indicated the potential value of these new parameters for the study of molecular structure-retention relationships, the prediction of retention data and the characterisation of stationary phases.

This paper extends this analysis to alkyl- and alkenylbenzenes.

DATA

The retention data used in this paper are reproduced from work reported by Engewald *et al.*³ who used a Hewlett-Packard Model 5840 gas chromatograph and a Varian Moduline 2740 gas chromatograph with a HP3370B digital integrator. The following columns were used: (a) 50 m × 0.3 mm I.D., soda glass, pretreated by high-temperature silanization with hexamethyldisilazane, dynamically coated with


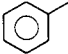
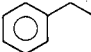
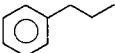
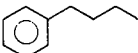
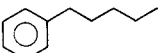
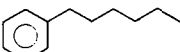
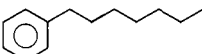
0.5% OV-1; (b) 100 m \times 0.23 mm I.D., soda glass, pretreated by dichloromethane pyrolysis, dynamically coated with 5% Ucon LB 550X.

RESULTS

Table I shows retention data of homologous alkylbenzenes on both a low-polarity (OV-1) phase and one of moderate polarity (LB550X). A consideration of the retention increments (ΔI) show an initial decrease with increasing chain length. However, with butylbenzene an increase occurs and further ΔI values show little variation with alkyl chain length. On both phases the ΔI values level out at approximately 100, giving little insight into the interactions between the homologous series and the stationary phases.

On the other hand, the I^* values show a regular gradual decrease in polar character as the alkyl chain length increases. All the I^* values are positive showing the predominance of the polar interactions produced by the π bonding of the benzene ring. Accepting that most of the I^* contribution is due to the benzene ring, the effect

TABLE I
ANALYSIS OF DATA FROM ENGEWALD *et al.*³, ON ALKYL BENZENES

Compound No.*	Structure	I_m	I_{100}^{OV}	ΔI_{100}^{OV}	I_C	$I_C - I_B$	I_{100}^{LB}	ΔI_{100}^{LB}	I_C	$I_C - I_B$
1		542	664		122		759		217	
2		642	767	103	125	+3	862	103	220	+3
3		742	859	92	117	-5	950	88	208	-9
6		842	950	91	108	-14	1037	87	195	-22
12		942	1047	97	105	-17	1134	97	192	-25
20		1041	1146	99	104	-18	1233	99	191	-26
29		1142	1244	98	102	-20	1332	99	190	-27
32		1242	1342	98	100	-22	-	-	-	-

* Numbers refer to the original numbers used by Engewald *et al.*³.

of the alkyl chain may be gauged by subtraction of I^* for benzene (I^*_B) from the I^* value for the compound (I^*_C). Thus the values shown in Table I as $I^*_C - I^*_B$ confirm the reduction in polar forces with increasing alkyl chain length on both stationary phases. The small negative values show that the effect is small compared to the contributions of the benzene ring.

A comparison of the respective I^* values for LB550X compared to OV-1 clearly indicates the increased polarity of LB550X, as the magnitude of the I^* values are almost double those for OV-1.

Table II shows retention data obtained using homologous series of alkenylbenzenes with terminal unsaturation and 1-phenylalkenes. As with Table I, the ΔI values give little indication of the respective interactions.

Again the positive I^* values indicate the predominance of polar forces in these substances. With the terminal bonded alkenylbenzenes and the *trans*-1-phenylalkenes, there is little variation of I^* values with alkenyl chain length. This indicates that the main influence in both series is the benzene ring and the double bond.

The effect of the double bond can be seen in each series by again calculating $I^*_C - I^*_B$. With the terminally unsaturated alkenylbenzenes, the values are slightly negative (note that ethenylbenzene is not truly a member of the terminal alkenylbenzenes as its double bond is conjugated with the benzene ring). This shows that the double bond has little effect in this position.

The *trans* 1-phenylalkenes on the other hand, show significantly positive values. This can be attributed to the conjugated type bonding existing between the aromatic ring and the alkene double bond.

The *cis*-1-phenylalkenes, however, show significantly different behaviour. The I^* values are again positive, showing the predominance of polar forces. The I^* values, however, decrease with increasing alkenyl chain length. In addition, the $I^*_C - I^*_B$ values decrease from moderately positive values to approximately zero indicating that the polar effect of the conjugated double bond is greatly reduced compared to the *trans* 1-phenylalkenes.

Engewald *et al.*³ postulated that the capability of conjugation between the double bond and aromatic ring is greater for *trans* isomers than for the corresponding *cis* isomers because the steric hindrance between the methylene group in position 3 of the side chain of the *cis* isomers and the α -hydrogen atom of the aromatic ring is stronger than repulsion forces between the hydrogen atoms. This would result in a greater angle between the double bond and the plane of the ring in the case of *cis* isomers and a weaker conjugation effect. Thus the use of I^* values supports the analysis of Engewald *et al.*³.

Comparison of the respective I^* values for LB550X and OV-1 confirm the increased polarity of the LB550X stationary phase.

Recently Evans and Haken⁴ showed that selectivity was constant within several homologous series, within experimental error. Homologous series investigated were aliphatic acetates, alcohols, aldehydes and methyl ketones. The only exception to this constant relationship was the *n*-alkanols on the relatively polar stationary phase PEG400. This deviation was explained as being due to long-range inductive effects.

The *trans*-1-phenylalkenes and the terminally bonded alkenylbenzenes show a similar consistency, although the random variation is larger. With the terminal bonded alkenylbenzenes the variation is most likely a result of the non-planar pre-

ferred conformation of the side chain, where the double bond may interact with the π -electrons of the benzene ring as outlined by Engewald *et al.*³.

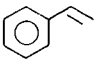
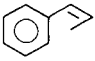
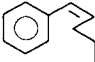
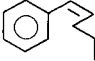
The *cis*-1-phenylalkenes, by contrast show a trend from moderately positive I values to values around zero. This can be attributed to steric effects as previously outlined.

Table I shows that the alkylbenzenes also follow a gradual downward trend

TABLE II
ANALYSIS OF DATA FROM ENGEWALD *et al.*³ ON ALKENYLBENZENES AND 1-PHENYLALKENES
 $I_B^B = +122$ (OV-1); $I_B^B = +217$ (LB500X).

Compound No.	Structure	I_m	I_{100}^{OV}	ΔI_{100}^{OV}	I_C	$I_C - I_B$	I_{100}^{LB}	ΔI_{100}^{LB}	I_C	$I_C - I_B$
<i>(a) Terminal double bonded alkenylbenzenes</i>										
4		728	885		157	+35	1009	-	281	+64
7		828	939	54	111	-11	1044	35	216	-1
16		928	1032	93	104	-18	1137	93	209	-8
25		1028	1140	108	112	-10	1243	106	215	-2
34		1228	1330	≈95	102	-19				
<i>(b) trans-1-Phenylalkenes</i>										
4		728	885		157	+35	1009		281	+64
8		828	1019	134	191	+69	1146	137	381	+101
13		928	1112	93	184	+62	1232	86	304	+87
21		1028	1205	93	177	+55	1324	92	296	+79
30		1128	1308	103	180	+58	1425	101	297	+80
32		1228	1400	98	178	+56				

TABLE II (continued)

Compound No.	Structure	I_m	I_{100}^V	ΔI_{100}^V	I_C	$I_C - I_B$	I_{100}^B	ΔI_{100}^B	I_C	$I_C - I_B$
(c) <i>cis</i> -1-Phenylalkenes										
4		728	885		157	+35	1009		281	+64
9		828	984	99	156	+34	1095	86	267	+50
22		1028	1155	≈86	127	+5	1258	≈86	230	+13
31		1128	1249	94	121	-1	1353	95	225	+8

in I^* values as the alkyl chain length increases. This can be explained by the moderating effect of the alkyl chain on the π electrons of the benzene ring.

These examples show the significant effect on retention properties of the π electrons in aromatic substituted compounds when compared to aliphatic compounds. It has been shown that the comparison of dispersion indices provides an insight into these structure-retention relationships. In addition the index provides a useful indication of the polarity of the stationary phase.

REFERENCES

- 1 M. B. Evans, J. K. Haken and T. Tóth, *J. Chromatogr.*, 351 (1986) 155.
- 2 M. B. Evans and J. K. Haken, *J. Chromatogr.*, 389 (1987) 240.
- 3 W. Engewald, I. Topalova, N. Petsev, C. Dimitrov, *Chromatographia*, 23 (1987) 561.
- 4 M. B. Evans and J. K. Haken, *J. Chromatogr.*, 406 (1987) 105.

Note

Quantitative determination of dicarboxylic acids and polyols in silicone–polyester resins

J. K. HAKEN*, N. HARAHAHAP and R. P. BURFORD

Department of Polymer Science, The University of New South Wales, P.O. Box 1, Kensington, N.S.W. 2033 (Australia)

Alkyd and polyester resins are produced by the condensation of a wide variety of mono- and dicarboxylic acids with polyols. These resins may be variously modified but when silicone intermediates are incorporated products used in the paint industry exhibit excellent exterior durability and are described as silicone–polyester resins.

The determination of carboxylic and polymeric esters has been reported using alkali and acid reaction^{1,2}. Phthalate³ and polyvinyl esters⁴ have been hydrolysed with molten potassium hydroxide in a reactor attached to the injection port of a gas chromatograph. Similar alkali fusion procedures conducted externally to the chromatograph have been used for the identification of dicarboxylic acids and polyols in polyester resins in the liquid and cured laminate form⁵. The qualitative analysis of vegetable oil based⁶ and linear⁷ silicone–polyester resins has recently been reported. The microfusion was conducted at 250°C for 1 h after which the polyols were identified as their trifluoroacetamide derivatives and the carboxylic acids as their methyl or dimethyl esters. The organic pendant groups on the co-condensed siloxane intermediate were estimated simultaneously using gas solid chromatography. The analysis of silicone polyesters has been extended⁸ to allow simultaneously estimation of the silicon content which converted to silicate is reacted to form a trimethylsilyl derivative.

Acid reactions were used with cellulose esters by Williams and Siggia⁹ in the *in situ* chromatographic reactor and by Haken *et al.*^{6,7} with various polyesters. The acidic cleavage of oil modified and linear silicone polyesters^{6,7} has been carried out by reaction for 2 h at 125°C of the polymer (200 mg) with 15 ml of mixed anhydride reagent consisting of an equimolar mixture of the anhydrides of acetic and *p*-toluenesulphonic acids^{10,11}.

Before the recent work of Haken *et al.*^{6,7} the analysis of silicone polyester resins had not been widely studied. Quantitative analysis of polyols in silicone polyester resins and paint films has been reported by McFadden and Scheuing¹² using a method involving a small-scale saponification with tetramethyl ammonium hydroxide at 100°C for 2 min followed by the formation of polyol derivatives with silylation reagents and subsequent gas chromatography (GC).

The analysis of polyester resins has followed from that of alkyd resin¹³ where the functional classes have been separated, and identified separately. This procedure was first followed with the application of alkali and acid fusion but it has been

established¹⁴ that while these reactions effect complete hydrolysis, losses occur with the extraction steps.

The hydrolysis of simple alkyd resins using 1 *N* ethanolic hydroxide followed by acetylation to form derivatives of the liberated polyols has been reported¹⁵. The analysis of phthalic anhydride and polyols was performed simultaneously on a column packed with 5% nitrile silicone oil and 22% orthophosphoric acid 85% on Chromaton N. The method is of limited use as few resins are as readily hydrolysed while few dicarboxylic acids are successfully examined as the free acids.

This paper reports the quantitative determination of dicarboxylic acids and polyols in linear silicone-polyester resins using acid fusion reaction GC. GC is readily performed simultaneously for the both functional classes of compounds as their appropriate derivatives.

The hydrocarbons, *i.e.* methane and benzene, corresponding to the organic pendant groups on the siloxane intermediate have been previously examined and are not repeated here. The quantitative nature of these cleavages has been previously reported for dimethyl polysiloxanes by Haken *et al.*¹⁶.

EXPERIMENTAL

Samples

Polyester resins based on adipic acid, isophthalic acid, neopentyl glycol and trimethylol propane, modified with silicone-intermediate SY231 [a methoxy functional methyl phenyl polysiloxane (Wacker Chemie)], with a silicone content of 30% were used in this work. The resins were prepared to the intermediate manufacturer's formulation and their composition is shown in Table I.

Procedure

Approximately 200 mg of the resin sample was hydrolysed with 5 ml acetic anhydride containing 15% water in a round bottom flask with reflux for about 1 h. As internal standards, stearic acid (12–15 mg) and glycerol (13–17 mg) were added before the reaction. Acetic acid formed during the reaction and the remaining acetic anhydride in the mixture were carefully distilled out, and the residue was then allowed to cool at room temperature. About 8 ml of bromine trifluoride-methanol reagent was added into the flask and the mixture was then refluxed again for 1 h. After cooling, the mixture was concentrated under reduced pressure and followed by the

TABLE I
COMPOSITION OF SILICONE-POLYESTER RESINS

Polyester components	wt.-%	
	Sample 1	Sample 2
Adipic acid	32.4	21.4
Isophthalic acid	14.3	26.3
Neopentyl glycol	—	7.9
Trimethylol propane	53.3	44.4

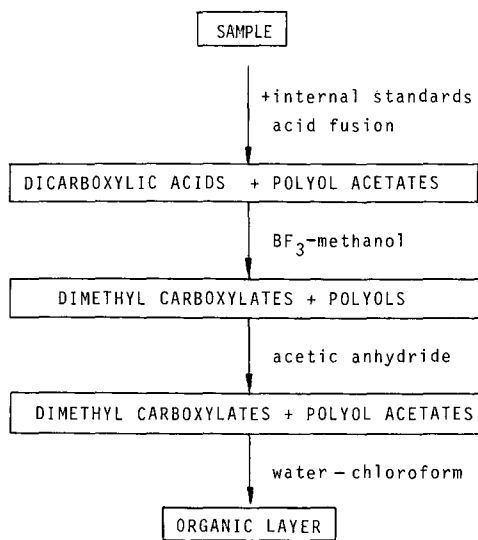


Fig. 1. Analytical scheme.

addition of 5 ml of acetic anhydride and 0.5 ml of 1-methylimidazole. The excess of acetic anhydride and the methylacetate formed were distilled out with care and then the remaining solution was transferred into a separating funnel containing 25 ml of distilled water and was extracted twice with dichloromethane (20 ml). The dichloromethane extract was dried over anhydrous magnesium sulphate and concentrated under reduced pressure to about 1 ml. Finally 1 μ l of this resultant mixture was injected into the gas chromatograph for simultaneous analysis of both functional classes. The analytical scheme is shown in Fig. 1.

Gas chromatography

GC was carried out using a Hewlett-Packard 5750 Research Model gas chromatograph equipped with a flame ionisation detector. Helium was used as carrier gas at a flow-rate of 60 ml/min.

The separations were performed on a column (10 ft. \times $\frac{1}{4}$ in. O.D., aluminium) packed with Silar 10% 10 CP on Chromosorb W AW DCMS (100–200 mesh), temperature programmed at 6°C/min from 185 to 224°C and held at upper limit for 4 min.

RESULTS AND DISCUSSION

The qualitative analysis of the acid and polyol components of silicone polyesters may be identified simultaneously by effecting the hydrolytic cleavage with the mixed anhydride reagent and subsequently esterifying the liberated free acids¹⁷. Some competing transesterification reactions occur with a partial reduction in the concentration of the polyol acetates and the formation of minor amounts of sulphonic esters. It has been shown that linear polyester resins cross-linked with aminoplasts

TABLE II
ANALYSIS OF SILICONE-POLYESTER RESINS CONTAINING THREE COMPONENTS

<i>Component</i>	<i>Analysis (wt.-%)</i>	<i>Standard deviation</i>	<i>Expected (wt.-%)</i>	<i>Recovery (%)</i>
Adipic acid	31.3	1.25	32.4	96.6
Isophthalic acid	13.3	0.5	14.3	97.6
Trimethylol propane	51.8	1.36	53.3	97.2

are degraded by reaction with acetic anhydride and acetic acid. A re-esterification step ensures that all polyols are converted to their acetates^{18,19}.

The non-volatile reaction products, *i.e.* excluding methane and benzene from the polysiloxane intermediate, of the silicone-polyester resin samples based on adipic acid, isophthalic acid, neopentylglycol and trimethylol propane were analysed simultaneously using the acid fusion reaction GC procedure described.

Good agreement between observed and expected values was obtained as summarised in Tables II and III. The calibration for this analysis was by the internal standard method using stearic acid and glycerol as the added components. Quantitative determinations of the carboxylic acids were obtained by measuring the areas under the corresponding acid derivatives and comparing them to the internal standard derivative peak run under the same analytical conditions, while determinations of polyols were obtained by comparison with acetylated glycerol.

All of the results presented in Tables II and III were obtained from eight individual determinations. The analysis values are 93.7–97.6%. However apart from experimental error, some material losses during the synthesis of the resin could occur and this fact must be taken into consideration when evaluating the results as this affects the concentration of that material in the resin. Further, the initial materials are not 100% pure, and as pilot batches of any new resin are required the results are considered satisfactory. Reproducibility of the analysis is found very good as shown by the standard deviations.

Derivative formation of dicarboxylic acids and polyols was maximised by refluxing for 1 and 0.5 h respectively. Occasional shaking of the reaction mixture was found necessary to prevent premature sample particle aggregation. All of the derivatives were relatively stable and under appropriate conditions, were readily separated by GC. Trimethylsilyl derivatives of neopentyl glycol, trimethylol ethane, trimethylol

TABLE III
ANALYSIS OF SILICONE-POLYESTER RESINS CONTAINING FOUR COMPONENTS

<i>Component</i>	<i>Analysis (wt.-%)</i>	<i>Standard deviation</i>	<i>Expected (wt.-%)</i>	<i>Recovery (%)</i>
Adipic acid	20.4	1.14	21.4	95.3
Isophthalic acid	25.3	1.97	26.3	96.2
Neopentyl glycol	7.4	0.62	7.9	93.7
Trimethylol propane	42.3	1.25	44.4	95.3

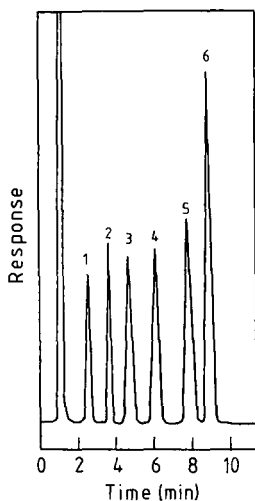


Fig. 2. Gas chromatogram showing separation: 1 = neopentyl glycol diacetate; 2 = dimethyl adipate; 3 = methyl stearate; 4 = glycerol triacetate; 5 = dimethyl isophthalate; 6 = trimethylol propane diacetate.

propane, adipic acid and isophthalic acid have been successfully separated on the SE-30 column¹⁶. The later derivatives are separated more effectively on Silar 10 CP and the separation achieved here are shown in Fig. 2.

Acetic acid formed during the first step of the procedure should be distilled out to avoid both the avoid formation of methyl acetate and an excessive use bromine trifluoride-methanol reagent. During the reaction of dicarboxylic acids and bromine trifluoride-methanol whilst hot polyol acetates were found to be cleaved with to the formation of methyl acetate and polyols, therefore, the acetylation was repeated with 1-methylimidazole as catalyst by refluxing for 0.5 h. Methyl acetate previously formed and the excess of the acetic anhydride reagent should be distilled out prior to GC. Water was used to destroy the excess of the remaining reagents, especially that of the 1-methylimidazole. There were no apparent interferences from silicone intermediate fragments or reagent peaks throughout this GC analysis.

Acid fusion reaction GC with acetic anhydride-acetic acid has been demonstrated as a satisfactory method for a single-step quantitative determination of common dicarboxylic acids and polyols in silicone polyester resins. The analysis procedure is simple, rapid, accurate and precise. The determination of the organic pendant groups on the siloxane intermediate may be conducted simultaneously as previously reported.

REFERENCES

- 1 L. R. Whitlock and S. Siggia, *Sep. Purif. Methods*, 3 (1974) 299.
- 2 J. K. Haken, *Ind. Eng. Chem. Prod. Res. Dev.*, 25 (1986) 171.
- 3 S. P. Frankoski and S. Siggia, *Anal. Chem.*, 44 (1977) 507.
- 4 R. J. Williams and S. Siggia, *Anal. Chem.*, 44 (1977) 2337.
- 5 J. K. Haken and M. A. Rohanna, *J. Chromatogr.*, 298 (1984) 263.
- 6 J. K. Haken, N. Harahap and R. P. Burford, *J. Chromatogr.*, 387 (1987) 223.

- 7 J. K. Haken, N. Harahap and R. P. Burford, *J. Coat. Technol.*, No. 749 (1987) 73.
- 8 J. K. Haken, N. Harahap and R. P. Burford, *J. Chromatogr.*, 441 (1988) 207.
- 9 R. J. Williams and S. Siggia, cited in ref. 1.
- 10 K. Tsuji and K. Konishi, *Analyst (London)*, 96 (1971) 547.
- 11 K. Tsuji and K. Konishi, *Analyst (London)*, 99 (1974) 54.
- 12 J. McFadden and D. R. Scheuing, *J. Chromatogr. Sci.*, 22 (1984) 310.
- 13 *ASTM D563-52*, American Society for Testing Materials, Philadelphia, PA, 1952.
- 14 J. K. Haken, *J. Chromatogr.*, 406 (1987) 167.
- 15 B. Laurinat and J. Hellwig, *Plaste Kautsch.*, 29(12) (1982) 710.
- 16 J. K. Haken, R. P. Burford and P. A. D. T. Vimalasiri, *J. Chromatogr.*, 349 (1985) 347.
- 17 J. K. Haken, N. Harahap and R. P. Burford, *J. Coat. Technol.*, No. 759 (1988) 53.
- 18 J. K. Haken and M. R. Green, *J. Chromatogr.*, 396 (1987) 121.
- 19 J. K. Haken and M. R. Green, *J. Chromatogr.*, 403 (1987) 145.

CHROM. 20 526

ANALYSIS OF SHORT ALKYL-SILANE BONDED SILICA GEL HIGH-PERFORMANCE LIQUID CHROMATOGRAPHIC STATIONARY PHASES USING HYDROFLUORIC ACID DIGESTION AND HEADSPACE ANALYSIS BY CAPILLARY GAS CHROMATOGRAPHY

THOMAS R. FLOYD*, NICHOLAS SAGLIANO Jr. and RICHARD A. HARTWICK*
Department of Chemistry, Rutgers University, Piscataway, NJ 08855-0939 (U.S.A.)

SUMMARY

A quantitative hydrofluoric acid digestion-headspace gas chromatography (GC) method was developed for the analysis of *n*-butyldimethylsilane and other short alkyl bonded silica gel high-performance liquid chromatographic stationary phases. The method requires only 10–30 mg of material and simple reaction vials. Digestion of the bonded silica requires 75 min, followed by a 4-min GC analysis. The average of the absolute value of the relative error for a range of alkyl bonded silica surface concentrations was 6.44% compared to elemental analysis, with an average precision of 1.55% (relative standard deviation). The method was used to identify and quantify both laboratory bonded and commercial stationary phases.

INTRODUCTION

Short alkylsilane bonded silica high-performance liquid chromatographic (HPLC) stationary phases are widely used in the separation of polypeptides¹, proteins^{2,3} and oligonucleotides^{4,5}. Although well suited for the separation of such compounds, these phases have been reported as being more susceptible to the hydrolytic loss of the bonded silanes than their longer chain counterparts⁴. Research in our laboratory regarding the acid stability of *n*-butyl phases employed for preparative separations of proteins required an analytical method by which the identity and surface concentration of these bonded alkylsilane phases could be determined. Such a method was needed (1) as a reliable means of measuring the extent of alkylsilane hydrolysis under accelerated hydrolytic conditions, (2) to determine the efficacy of various alkylsilane bonding reactions, and (3) to determine, quantitatively and qualitatively, multiple alkyl ligand bonded stationary phases.

Elemental analysis⁶ has been the most popular means of quantifying bonded stationary phase concentrations due to the simplicity of sample preparation and its widespread availability. One problem with elemental analysis however, is its lack of

* Present address: Tennessee Eastman Co., Kingsport, TN, U.S.A.

qualitative information and the inability to differentiate between multiple sources of carbon. Consequently, a number of other techniques have been useful in the analysis of bonded phases on silica gel supports. These include, spectroscopic techniques such as diffuse reflectance infrared Fourier transform spectroscopy and magic angle spinning ^{29}Si Nuclear magnetic resonance^{7,8}, surface techniques such as electron spectroscopy for chemical analysis⁹ and fast atom bombardment mass spectroscopy (FAB-MS)¹⁰, thermal methods¹¹, pyrolysis gas chromatography (GC)¹², and basic and acidic hydrolysis of phases followed by GC analysis^{13,14}. One simple chemical means for determining bonded alkylsilane identity and quantity has been by the GC analysis of the fluorinated alkylsilanes derivatives generated by hydrofluoric acid digestion of the stationary phases. This method has been used for the analysis of a variety of bonded alkylsilanes¹⁵⁻¹⁷.

During previous studies¹⁶, it was determined that alkylfluorosilanes of less than about 7 carbon atoms were too volatile for hexane extraction, requiring instead a headspace sampling technique. Headspace GC was successfully used in this original work for the determination of trimethylsilane (TMS) concentrations following "capping" reactions. We wish to report further on the development of an expanded and refined headspace procedure for the analysis of various short alkylsilane bonded phases.

EXPERIMENTAL

Bonded phase synthesis

A single lot of silica gel was used throughout this study, CD-802 Lot 863-94, supplied by the PQ Corp. (Valey Forge, PA, U.S.A.). This was an earlier experimental lot of gel, which is currently marketed under the IMPAQ tradename. Chloroalkylsilanes were purchased from Petrarch Systems (Britol, PA, U.S.A.). Imidazole was purchased from Fisher Scientific (Springfield, NJ, U.S.A.).

The silylation procedure used is a modification to that described by Kinkel and Unger²⁰. Silica gel (10 g) was weighed, transferred to a 1000-ml round-bottom flask, and dried at 150°C under vacuum for at least 24 h. Imidazole (10 g) was dissolved in 100 ml of dichloromethane. An approximate fourfold molar excess (10 ml) of *n*-butyldimethylchlorosilane was added to another 100 ml of dichloromethane. The imidazole solution, followed by the silane solution were transferred to the silica, which was then placed on a rotary evaporator. The reaction flask was rotated at moderate velocity for at least 24 h at room temperature. Following reaction, the bonded silica gel was washed with 100-ml volumes each of dichloromethane, acetone, methanol, water, methanol and acetone.

Hydrofluoric acid digestion and fluoroalkyl derivative generation

The hydrofluoric acid solutions were made up by volume percent of concentrated hydrofluoric acid (Fisher), distilled water, and an organic modifier, which in this study was either acetone or acetonitrile (Fisher). The digestion/derivatization step was carried out in 30 ml Tuf-Tainer PTFE/PFA vials (Pierce, Rockford, IL, U.S.A.) equipped with Tuf-Bond PTFE/silicone septa caps and PTFE-coated magnetic stir discs.

An amount of 10–30 mg (depending upon silane surface density) of bonded stationary phase was weighed out along with an approximately equivalent molar amount of internal standard. Ethyldimethylsilane or *n*-propyldimethylsilane bonded silicas were employed as internal standards. Hydrofluoric acid solution (10 ml) was added and then caps were securely tightened onto the vials. Vials were spun on a stir plate for 30 min allowing for digestion/derivatization of the silicas, at which time they were then transferred to a water bath (Precision Scientific, Chicago, IL, U.S.A.) maintained at 27.0°C for 45 min, to ensure thermal equilibration.

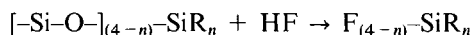
Gas chromatography of fluoroalkylsilane derivatives

A 500- μ l side-hole gas-tight syringe (Hamilton, Reno, NV, U.S.A.) was used to sample the headspace of the sample vial. A 12 m \times 250 μ m I.D. SE-30 capillary column (Scientific Glass Engineering, Austin, TX, U.S.A.) was used in a HP 5890A gas chromatograph, equipped with a FID detector (Hewlett-Packard, Avondale, PA, U.S.A.). Split injection at a 50:1 ratio was used, and head pressure was set at 10 p.s.i. All GC runs were performed isothermally at 40°C. Chromatographic data were collected by an HP 3392A recording integrator.

RESULTS AND DISCUSSION

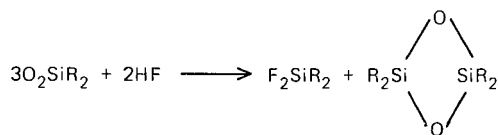
Reactions of silane with hydrofluoric acid

Aqueous fluorination of bonded alkylsilanes has been shown to proceed as



where *n* represents the number of alkyl groups bonded to the silicon. Hydrolysis, followed by dimerization (or polymerization for mono- and dialkylsilanes) of halo-silanes in general is thermodynamically favored. However, for the silicon-fluorine bond, hydrolysis accounts for an insignificantly small percentage of the total fluoro-silane starting material at equilibrium¹⁸. Under conditions of 7.2 *M* (25%) hydrofluoric acid, trialkylfluorosilanes have been shown to be chemically stable, allowing for quantitation¹⁹.

Mono and dialkylsilanes have been less successfully quantitated due to polymerization side-reactions. In the case of a dialkylsilane



the siloxyl dimer can also be formed in significant quantities. In addition further complications arise when using alcohols in the digestion solution, since the alkoxy-silane by-product will also occur. In general, it will be found that trialkylsilanes can be quantitatively converted to their fluoro derivatives, while dialkyl silanes may or may not yield 100% conversion, depending upon the particular silane and reaction conditions. Monoalkylsilanes under these conditions demonstrate a strong tendency to polymerize, and are generally not suited for quantitative hydrofluoric acid digestion and analysis, although they can often be qualitatively analyzed by this method.

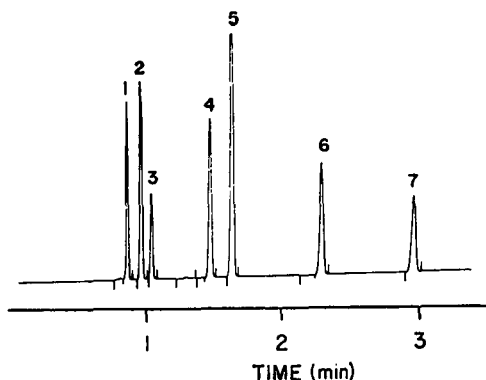


Fig. 1. Hydrofluoric acid digest of a number of fluorosilanes, analyzed by headspace GC. The compounds present: (1) trimethylfluorosilane, (2) *n*-butyltrifluorosilane, (3) ethyldimethylfluorosilane, (4) *n*-butylmethyl-difluorosilane, (5) *tert.*-butyldimethylfluorosilane, (6) *n*-butyldimethylfluorosilane, and (7) triethylfluorosilane, were separated in less than 3 min isothermally at 40°C on a 12 m × 250 μm I.D. SE-30 capillary column. Bonded silanes were digested in 25% (v/v) aq. hydrofluoric acid.

Qualitative identification

Fig. 1 is the result of a 25% (v/v) aq. hydrofluoric acid digest of a number of pure alkylchlorosilanes standards, yielding the fluoro derivatives, determined by headspace GC. The total separation time was less than 3 min.

The retention times for *n*-butyltrifluorosilane, *n*-butylmethyl-difluorosilane, and *n*-butyldimethylfluorosilane were 0.84, 1.54, and 2.32 min, respectively. Thus, unknown phases bonded with mono-, di- or trifunctional *n*-butyl silanes can be readily identified. Additionally, co-bonded phases can also be quantitated for each of the alkyl ligands present provided that they partition into the gas phase.

During the course of this work, several commercially available butyl bonded phases were examined. One phase, Vydac C₄ 214-TPB, produced fluorosilane peaks not observed in any of the other phases studied. Since this phase is widely employed for biopolymer separations, it was felt that further investigations using GC-MS were warranted. The mass spectrum indicated that the bonded silane species was a dibutylsilane. In addition the presence of the dioxo-bridge dibutylsiloxyl dimer, (C₄H₉)₂SiO₂Si(C₄H₉)₂, was also confirmed by GC-MS.

Distribution coefficients of fluorosilanes

In order to achieve reliable quantitative results using a static headspace sampling technique it was necessary to establish the conditions of linearity between the analyte concentration in the liquid phase and the gas phase, as well as the linearity of the GC detector response over the range investigated. The range over which a given distribution coefficient (*K*) is constant establishes the operating limits for bonded phase loadings to be determined, as well as the sensitivity of the method. Operation under linear conditions also permits the use of one point standardizations and allows for examining unknown phase concentrations more easily.

Assuming conditions of linearity, *K* is given by

$$K = \frac{C_1 V_1}{C_g V_g} \quad (1)$$

where C_l and C_g are the concentrations of the solute in the liquid and gas phase and V_l and V_g are the volumes of the two respective phases.

The factors leading to non-linear effects acting on the concentration in the gas phase (C_g) have been well documented in the literature²¹. It has been reported that to prevent such effects, C_g should be kept small (*ca.* 0.01% of the vapor phase mole fraction)²². Since the combined mole fractions of the fluorosilane derivatives sample and internal standard are on the order of $1 \cdot 10^{-4}$ in the liquid phase and their values for K are typically in the range 1–10, a linear relationship²² between C_l and C_g would be expected.

The presence of an organic modifier was observed to increase both the accuracy and precision of the assay. Acetonitrile and acetone were found to be chemically compatible with the hydrofluoric acid digestion step, and to elute in a non-interfering region of the gas chromatogram. Alcoholic modifiers were not used, since they interfere with the derivatization reaction.

Distribution coefficients for compounds 2, 3, 4, 6 (identified in Fig. 1) and for *n*-propyldimethylfluorosilane were determined by static headspace GC under a variety of liquid phase compositions²³. Derivatization solvent systems were examined that consisted of 25% (v/v) hydrofluoric acid, containing various volume percents of water and either acetonitrile or acetone.

In general, the partition coefficients were found to be linear for the quantitation of *n*-butyldimethylsilane stationary phases over a range from 2–50 μmol (total) of alkylsilane present. Table I lists the slopes and correlation coefficients (R^2) using different fluorination solutions and internal standards for butyldimethylfluorosilane and butylmethyldifluorosilane. Examination of the residuals from the linear least squares fit indicated good linearity for the calibration curves over the reported ranges. The response slope was calculated from the ratio of the detector response to the ratio of the moles added for the butyl and ethyl fluorosilanes. This response slope represents a combination of factors. The slope is proportional to relative response factor of the sample and internal standard and their partition coefficients. The absolute values of K were increased by one to two orders of magnitude in the presence of 25% or 50% of either acetonitrile or acetone, as compared to their values in neat aqueous solutions. At the same time, the R.S.D. was decreased for the same samples. The conclusion is that the organic modifier can be used both to control the overall relative response factor and also to establish linear operating conditions for the headspace partition technique. Thus the selection of an organic modifier and the proportions used is critical to this method.

Quantitation

Having established the partition coefficients for the alkylfluorosilanes of interest, and establishing the required organic modifier conditions, the next goal was to find a suitable working internal standard for this system and to determine the linearity of responses and detection limits for the final analytical protocol. Since both the starting alkylsilanes and their fluoro derivatives are volatile, internal standards in the form of silanes bonded to silica gel were used. This allows the internal standard alkyl phase to be conveniently weighed and placed in the sample vial concurrently with analyte silica gel. *n*-Propyldimethylfluorosilane was chosen as the internal standard since the ethyldimethylfluorosilane eluted slightly behind the tailing acetone peak. It

TABLE I
LINEARITY OF HEADSPACE METHOD

<i>Alkyl silane</i>	<i>Internal standard</i>	<i>Derivatization solvent</i>	<i>Slope*</i>	<i>Intercept</i>	<i>r</i> ²
<i>n</i> -Butyldimethyl	<i>n</i> -Ethyldimethyl	25% HF in water	1.664	0.091	0.9934
		25% HF/25% acetonitrile in water	1.336	0.101	0.9970
		25% HF/50% acetone in water	0.912	-0.042	0.9964
	<i>n</i> -Propyldimethyl	25% HF/50% acetone in water	0.797	-0.004	0.9977
<i>n</i> -Butyldimethyl	<i>n</i> -Propyldimethyl	25% HF/50% acetone in water	0.466	0.003	0.9995

* The slope was calculated from a linear least square fit, the X-axis being the mole ratio of *n*-butyldimethylfluorosilane to ethyldimethylfluorosilane and the Y-axis being the detector response ratio of *n*-butyldimethylfluorosilane to ethyldimethylfluorosilane.

TABLE II
ELEMENTAL PERCENT CARBON VS. GC HEADSPACE (25% HF/50% ACETONE)

Sample	Elemental* carbon	GC Headspace*	Difference (%)
1	$8.81 \cdot 10^{-4}$	$9.19 \cdot 10^{-4}$	4.31
2	$7.56 \cdot 10^{-4}$	$7.33 \cdot 10^{-4}$	3.04
3	$6.59 \cdot 10^{-4}$	$6.62 \cdot 10^{-4}$	0.46
4	$3.98 \cdot 10^{-4}$	$3.79 \cdot 10^{-4}$	4.77
5	$2.60 \cdot 10^{-4}$	$2.09 \cdot 10^{-4}$	19.6
Average difference		$0.27 \cdot 10^{-4}$	6.44

* Silane concentration recorded as weight-corrected mol per g bonded silica gel.

was not possible to separate the butyltrifluorosilane on the SE-30 capillary column under these conditions, since it co-eluted with the acetone peak. However, GC conditions can be modified if such analyses are required, at the expense of longer separation times.

Comparison to elemental analysis

Table II compares the relative accuracy of the headspace technique against elemental analysis for a series of five *n*-butyldimethylsilane stationary phases. A relative response factor was determined using an internal standard and a known *n*-butyldimethylsilane phase standard. This standard was analyzed in triplicate for percent carbon by elemental analysis ($9.35 \cdot 10^{-4} \pm 0.12 \cdot 10^{-4}$ mol/g bonded silica). The day-to-day average response factor for the *n*-butyldimethylfluorosilane when using propyldimethylfluorosilane as the internal standard was 1.295 ± 0.035 (2.68% R.S.D.). The average absolute difference between elemental analysis and the final recommended headspace technique was 6.44%. It should be noted that the elemental analysis is unreliable for low percent carbon coverages. This fact could explain the large absolute difference for sample 5 seen in Table II.

CONCLUSIONS

A qualitative and quantitative method has been described for the analysis of a variety of short aliphatic silane bonded stationary phases, particularly *n*-butyldimethylfluorosilane, by the use of a hydrofluoric acid digest-headspace GC method. This method provides a simple means of monitoring alkylsilane bonding procedures, of measuring the extent of bonded alkylsilane hydrolysis and identifying the type of silanes used in the bonding of commercial or unknown phases. An additional feature of this method is the suitability for determining, simultaneously, the surface concentrations of multiple alkyl ligands bonded to a silica surface.

ACKNOWLEDGMENTS

This research was supported by the Petroleum Research Fund, grant AC No. 16161, by the Busch Memorial Fund and the Center for Advanced Food Technology (CAFT) at Rutgers University, and by the PQ Corporation.

A Fellowship for the support of T. R. Floyd from the PQ Corporation is gratefully acknowledged. The authors would like thank Shih Hsien Hsu and Jonathan Crowther for their assistance with the GC-MS analyses.

REFERENCES

- 1 E. Nice, M. W. Capp, N. Cooke and M. J. O'Hare, *J. Chromatogr.*, 218 (1981) 569.
- 2 F. Warren and B. Bidlingmeyer, *J. Liq. Chromatogr.*, 6 (1985) 619.
- 3 M. Schmuck, K. Gooding and D. Gooding, *LC, Liq. Chromatogr. HPLC Mag.*, 3 (1985) 814.
- 4 J. Pearson and F. Regnier, *J. Liq. Chromatogr.*, 6 (1983) 1441.
- 5 C. R. Becker, J. W. Efcavitch, C. R. Heiner and N. F. Kaiser, *J. Chromatogr.*, 326 (1985) 293.
- 6 J. H. Knox and A. Pryde, *J. Chromatogr.*, 112 (1975) 171.
- 7 L. Sander, J. Callis and L. Field, *Anal. Chem.*, 55 (1983) 1068.
- 8 G. E. Maciel, D. W. Sindorf and V. J. Bartuska, *J. Chromatogr.*, 205 (1981) 438.
- 9 M. Miller, R. Linton, S. Bush and J. Jorgenson, *Anal. Chem.*, 56 (1984) 2204.
- 10 S. Simko, M. Miller and R. Linton, *Anal. Chem.*, 57 (1986) 2448.
- 11 L. Zhuraviev, A. Leselev and V. Naidina, *Russ. J. Phys. Chem.*, 42 (1968) 1200.
- 12 L. Hansson and L. Trojer, *J. Chromatogr.*, 207 (1981) 1.
- 13 M. Verzele, P. Musche and P. Sandra, *J. Chromatogr.*, 190 (1980) 331.
- 14 J. B. Crowther, S. D. Fazio, R. Schiknis, S. Murcus and R. A. Hartwick, *J. Chromatogr.*, 289 (1984) 367.
- 17 C. Gaget, D. Morel, M. Traore and J. Serpinet, *Analisis*, 12 (1984) 386.
- 18 C. Eaborn, *J. Chem. Soc.*, 3 (1952) 2846.
- 19 S. Fazio, J. Crowther and R. Hartwick, in S. Ahuja (Editor), *Chromatography and Separation Chemistry* (ACS Symp. Ser. Vol. 297), American Chemical Society, Washington, DC, 1986, p. 127.
- 20 J. N. Kinkel and K. K. Unger, *J. Chromatogr.*, 316 (1984) 193.
- 21 B. Ioffe and A. Vitenberg, *Headspace Analysis and Related Methods in Gas Chromatography*, Wiley, New York, 1982.
- 22 A. Hussam and P. W. Carr, *Anal. Chem.*, 57 (1985) 793.
- 23 T. Floyd, *Thesis*, Rutgers University, Piscataway, NJ, 1986.

CHROM. 20 602

DETERMINATION OF 5-METHYLCYTOSINE IN DNA BY GAS CHROMATOGRAPHY-ELECTRON-CAPTURE DETECTION

DANIEL H. FISHER*

Department of Medical Laboratory Science, College of Pharmacy and Allied Health Professions, and Barnett Institute of Chemical Analysis and Materials Science, Northeastern University, 360 Huntington Avenue, Boston, MA 02115 (U.S.A.)

and

ROGER W. GIESE

Department of Medicinal Chemistry, College of Pharmacy and Allied Health Professions, and Barnett Institute of Chemical Analysis and Materials Science, Northeastern University, 360 Huntington Avenue, Boston, MA 02115 (U.S.A.)

SUMMARY

The following sequence of analytical steps was used to determine the amount of 5-methylcytosine (mol-%) in calf thymus and human lymphocyte DNA: acid hydrolysis of the DNA, derivatization (pentafluorobenzyl bromide, solid phase extraction, pivalic anhydride), internal standard addition, solid phase extraction, high-performance liquid chromatography, and gas chromatography with electron-capture detection. The steps were carefully optimized, leading to a recovery of $30 \pm 1.0\%$ starting with a nucleobase standard containing 1.25 ng of 5-methylcytosine. A second analysis of this sample gave a $30 \pm 0.3\%$, demonstrating a high precision for the method. In good agreement with earlier work by others, 1.2 ± 0.10 mol-% of 5-methylcytosine was then found in a 350 ng sample of calf thymus DNA, and values of 0.9 ± 0.07 and 0.8 ± 0.04 mol-% (two runs) were found in human lymphocyte DNA.

INTRODUCTION

There is increasing concern about the risks to human health, especially carcinogenesis and mutagenesis, from exposure to chemicals. Since DNA is an ultimate target for this exposure, the measurement of chemicals attached to DNA, or of "DNA adducts", is of considerable interest^{1,2}. High sensitivity is required since a tiny amount of a chemical attached to DNA may pose a significant risk.

Our approach to quantify a DNA adduct with high sensitivity is to isolate it from a physiological sample as a modified nucleobase or nucleoside, derivatize the adduct with an electrophore, and quantify the derivatized adduct by gas chromatography (GC) or high-performance liquid chromatography (HPLC) utilizing electrophore detection. The latter refers to either the use of electron-capture detection (ECD) or electron-capture negative-ion mass spectrometry (ECNIMS).

Thus far we have formed sensitive electrophoric derivatives from standards of

pyrimidine³ and purine⁴ nucleobases. We have utilized a mild, chemical oxidation reaction to release pyrimidine and purine nucleobases from their corresponding nucleosides⁴. We have detected $1.3 \cdot 10^{-15}$ mol of an electrophoric derivative of the DNA adduct, 5-hydroxy-methyluracil, as a standard by HPLC-ECNIMS using a belt interface⁵.

Our continuing work on the quantitation of DNA adducts by chromatography with electrophore detection is proceeding along two lines. First, we are preparing suitable electrophoric derivatives of other DNA adducts. Second, the subject of this paper, we are developing sample cleanup procedures to bring this electrophore methodology to real samples.

As an intermediate stage towards the determination of a trace amount of DNA adduct obtained from a real sample, we chose to set up an electrophore-based method for quantifying 5-methylcytosine (5-MC) in calf thymus DNA and in DNA obtained from human lymphocytes. This analyte is a normal, minor base in DNA, typically reported to be about 1–2 mol-% of mammalian DNA. Thus its measurement presents an intermediate level of difficulty relative to much smaller amounts of DNA adducts that need to be measured². 5-MC has been determined in these DNA samples by several techniques (see Table I). Recently, an HPLC-UV method using rechromatography was used to quantify 5-MC in trace amounts (1 in 100 000 nucleotides) in other types of DNA samples¹⁵.

Here we present the determination of 5-MC in both calf thymus DNA and human blood lymphocyte DNA by electrophoric derivatization followed by GC-ECD. A small amount of DNA (350 ng) was analyzed in order to test the suitability of our sample handling steps for eventual application to trace amounts of DNA adducts. We also analysed larger amounts of the same calf thymus DNA by HPLC with UV detection in order to establish our own reference values for this sample.

TABLE I
DETERMINATION OF 5-METHYLCYTOSINE IN DNA SAMPLES

<i>Sample</i>	<i>Method</i>	<i>Reference</i>	<i>Amount 5-methylcytosine (mol-%)</i>
Calf thymus	HPLC-UV*	6,7	1.7
		8	1.4 ± 2.2
	GC-MS of an alkylsilyl derivative	7,10	1.28 ± 0.09
		11	1.39 ± 0.09
	³² P-Postlabeling-TLC- autoradiography	12	1.07 ± 0.06
	Fluoroimmunoassay	13	1.0
	GC-ECD	This work	1.2 ± 0.10
Human blood lymphocyte	HPLC-UV	14	0.96 ± 0.01
	GC-ECD	This work	$0.9 \pm 0.07^{**}$
			$0.8 \pm 0.04^{**}$

* Using such a method, DNA was hydrolyzed in aqueous hydrofluoric acid to prevent deamination of 5-methylcytosine.

** Different runs.

EXPERIMENTAL

Chemicals and reagents

The DNA bases and calf thymus DNA (Type I: sodium salt; highly polymerized), were obtained from Sigma (St. Louis, MO, U.S.A.). Pentafluorobenzyl bromide (>99%), trimethylacetic anhydride (99%), and 4-dimethylaminopyridine (99%) were from Aldrich (Milwaukee, WI, U.S.A.). Tetrafluorobenzyl bromide was from Alfa Products, (Danvers, MA, U.S.A.). Organic solvents, GC/HPLC or GC² grade, were from American Burdick and Jackson (American Scientific Products, Boston, MA, U.S.A.). Distilled-deionized water was purified to HPLC grade with an Organopure system (Barnstead, Boston, MA, U.S.A.). HPLC grade water was also purchased from J. T. Baker (Phillisburg, NJ, U.S.A.). Formic acid (88%) was from Baker. For the reactions, the acetonitrile was dried with type 4A molecular sieves.

All solution compositions were v/v except as noted. Values for precision were based on analysis of samples in triplicate unless indicated otherwise.

Apparatus

The glassware was soaked in hot liquid detergent, washed with water, kept in hot conc. HCl for >2 h, washed with water and methanol, thermally cleaned (250°C), silanized¹⁶, and thermally cleaned again.

Solid phase extraction columns were prepared using 5.25-in. borosilicate Pasteur pipets. They were packed with 500 mg of either silica gel (60-Å pore size, 40-µm irregular particles) or end-capped cyanopropylsilica (60-Å pore size, 40-µm irregular particles), from Baker. The column bed was sandwiched between two plugs of silanized glass wool. Solvents and samples were eluted immediately after application with 1 p.s.i. of nitrogen. This pressure was removed when the level of solvent (or sample) was 2–3 mm above the column bed, and the next aliquot of solvent was applied before the level of liquid reached the bed.

The analytical HPLC separations were done at 1.0 ml/min on a LC-18-DB HPLC column (250 × 4.6 mm, 5-µm diameter particles; Supelco, Bellefonte, PA, U.S.A.) fitted with a LC-18-DB guard column (20 × 4.6 mm, 5-µm diameter particles; Supelco). The column temperature was kept at 30°C. Detection was at 254 or 260 nm for the nucleobases, 284 nm for N1-pentafluorobenzyl-5-methylcytosine (PFBz-5-MC), and 314 nm for the pivalyl-N1-pentafluorobenzyl-5-methylcytosine (Piv-PFBz-5-MC) and internal standard, pivalyl-N1-(2,3,5,6-tetrafluorobenzyl)-5-methylcytosine. A Perkin-Elmer Series 4 HPLC pump was used (Perkin-Elmer, Norwalk, CT, U.S.A.).

A Model 3740 gas chromatograph was fitted with a ⁶³Ni electron-capture detector and Model 1095 on-column capillary injector (Varian, Palo Alto, CA, U.S.A.). Compounds were separated on a HP-Ultra, 5% phenylmethylsilicone, fused-silica capillary column (32 m × 0.32 mm I.D., 0.52-µm film thickness; Hewlett-Packard, Palo Alto, CA, U.S.A.). The flow of the carrier gas, helium, was set to 4 ml/min at 250°C. The flow of make-up gas, nitrogen, was set to 26 ml/min at 250°C.

Peak areas for both HPLC and GC were obtained manually using the scanner mode of a Waters 840 data system (Millipore-Waters, Milford, MA, U.S.A.).

Synthesis

PFBz-5-MC. 5-MC hydrochloride (485 mg, 3 mmol), pentafluorobenzyl bromide (1.36 ml, 9 mmol) and potassium carbonate (2.07, 15 mmol) were refluxed at 50°C in 100 ml of dry acetonitrile with stirring until no starting material remained by silica TLC. Ethyl acetate (100 ml) was added and the mixture was transferred to a silica flash chromatography column (20 cm × 19 mm I.D. bed). This was repeated two more times and the column was washed with 500 ml of hexane. The compound was eluted with acetonitrile, and further purified after evaporation by preparative HPLC on a C₈ silica column (25 cm × 10 mm I.D.) using a gradient of acetonitrile in water. Evaporation gave a white solid that was a single peak by HPLC. IR, 2.86 and 3.03 cm⁻¹ (NH₂), 5.9–6.1 (C=O); ¹H NMR, δ 1.9 (s, 3H, CH₃), 4.9 (s, 2H, CH₂), 7.5 (s, 1H, ring CH); MS(EI), *m/z* 305 (M, 100%), 263 (17%, [M – NCNH₂]).

Piv-PFBz-5-MC. N1-PFBz-5-MC (305 mg, 1 mmol), pivalic anhydride (203 ml, 10 mmol), N-methylmorpholine (1.1 ml, 10 mmol) were refluxed in 100 ml of dry acetonitrile for 20 h at 50°C with stirring. The product was purified by flash chromatography, as described above, followed by spotting onto two 1000 μm thick, 20 × 20 cm silica TLC plates (Analtech, Newark, DE, U.S.A.). After development with methanol–methylene chloride (1:9), the scraped band was boiled in ethyl acetate, filtered through sintered glass, and evaporated yielding a white solid that was a single peak by HPLC and GC-ECD. IR, new peak at 6.3 cm⁻¹ (C=O, pivalyl); ¹H NMR, new peak at δ 1.2 (s, 9H, pivalyl); MS(ECNI), *m/z* 208 (100%, [M – CH₂C₆F₅]).

Pivalyl-N1-(2,3,5,6-tetrafluorobenzyl)5-methylcytosine. This compound was synthesized and purified using the procedures just described except 2,3,5,6-tetrafluorobenzyl bromide was substituted for pentafluorobenzyl bromide. MS(EI), *m/z* 372 (2%, [M + 1]), 314 (85%, [M – C(CH₃)₃]) 208 (100%, [M – CH₂C₆F₄H]).

Analytical procedure

DNA hydrolysis. An aliquot of an aqueous DNA sample (*ca.* 350 ng) or of an external nucleobase standard (1.25 ng or 10 pmol of 5-MC and 200 pmol each of the other four DNA bases) was added to a 1-ml crimp-top Wheaton Micro-V vial (Aldrich). The sample was dried by evaporation in a Speed-Vac Concentrator (Savant Instruments, Hicksville, NY, U.S.A.) at 45°C for 1 h. Formic acid (200 μl) was added to the vial, and the vial was sealed with a PTFE-faced silicone septum and aluminum seal (Aldrich). After heating for 3 h at 150°C in a Reacti-Therm (Pierce, Rockford, IL, U.S.A.) in which the vial holes were half-filled with sand, the sample was evaporated as before for 45 min. A crimp-top cap was used because the plastic caps were digested by the acid vapors. The elevation of the vial with sand minimized contact of the acid vapors with the vial seal.

Alkylation. Pentafluorobenzyl bromide (100 μl of a 100 nmol/μl solution in dry acetonitrile) was added followed by a spatula tip (1–2 mg) of potassium carbonate that had been dried at 250°C. The vial was capped with a PTFE-faced silicone septum and an open-top screw cap (Pierce) and kept at 60°C for 3 h with vortexing every 30 min.

Cyano solid phase extraction. The column was conditioned with 2 ml of methanol followed by 2 ml of ethyl acetate–dichloromethane–acetonitrile (3:1:1) (solvent A). The sample was treated with 0.5 ml of solvent A and transferred with a Pasteur pipet to the column. This was repeated two more times, and the column was washed with 2 ml of solvent A and 4 times 0.5 ml of methanol, the last two portions of which were

collected in a 2-ml Reacti-Vial (Pierce) since they contained the product. The sample was evaporated at 45°C for 45 min.

Acylation. The sample was treated with 100 μ l of a solution of pivalic anhydride (100 nmol/ μ l) and 4-dimethylaminopyridine (20 nmol/ μ l) in dry acetonitrile. The vial was sealed and heated at 60°C for 1 h with vortexing every 15 min. The internal standard was added (0.65 pmol, 241 pg).

Silica solid phase extraction. The column was conditioned with 2 ml of acetonitrile–2-propanol (9:1) (solvent B) followed by 4 ml of hexane–dichloromethane (3:1) (solvent C). The reaction mixture was transferred to the column using 500 μ l of solvent C and this step was repeated twice. The column was washed 2 times with 1 ml of solvent C and 4 times with 0.5 ml of solvent B. The last two fractions, which contained the product, were collected in a 2-ml Reacti-Vial and evaporated as before.

HPLC cleanup. The column was cleaned at 1 ml/min starting with acetonitrile–water (2:8), by progressive gradient changes, each 10 min in duration, to 100% acetonitrile and then isopropanol–methylene chloride (1:9). The latter mobile phase was maintained for 2 h, and the starting mobile phase was re-established by reversing the gradient program. The “analytical gradient” later to be used for the samples was then begun: a gradient from acetonitrile–water (2:8) to (7:3) in 10 min, to (8:2) in 10 min, and similarly back to (2:8).

A solution containing approximately 20 pmol each of the internal standard and derivatized analyte was injected and detected by UV to establish their retention times, typically 15 and 16 min, respectively. After washing the injector with 1 ml of hot acetonitrile, mobile phase was injected and the “analytical gradient” was done. This hot wash/injection/gradient sequence was repeated. It was then done twice more except the fraction eluting from 14.5 to 16.5 min was collected, evaporated, and analyzed by GC–ECD (see below) to assure that the HPLC system was clean. The injector was hot washed.

The sample was reconstituted in 150 μ l of hot acetonitrile (50–60°C) with vortexing. After the solvent drained off the walls (10–20 min), essentially the entire volume was injected onto the HPLC column and the “analytical gradient” (see above) was performed. A fraction was collected from 14.5 to 16.5 min in a 3-ml Reacti-Vial and evaporated in a Speed-Vac Concentrator at 45°C for 1.5 h. The vial was washed with 100 μ l of hot methanol (50–60°C) followed by thorough vortexing and evaporation at 60°C under a gentle stream of nitrogen.

The column was equilibrated for 10 min with the starting mobile phase and the injector was hot washed. The next and subsequent samples were treated the same, with a hot wash of the injector and 10 min column re-equilibration between each sample.

GC–ECD. The sample was reconstituted in 10 μ l of toluene and 1 μ l was injected into the gas chromatograph. The data were calculated relying on a linear calibration curve obtained by injecting standards containing known amounts of Piv-PFBz-5-MC and internal standard.

Mol-% values of nucleobases determined by HPLC

DNA (4–6 μ g) was acid-hydrolyzed as above in 200 μ l of formic acid, evaporated, dissolved in mobile phase, and the amount of the nucleobase (mol-%) was determined using HPLC. The peak areas for the bases were calibrated using standard solutions prepared from weighed, vacuum-dried bases. The bases, used as received,

were single peaks by HPLC. The base ratios ([C plus 5-MC]/G and T/A) for both types of DNA samples were 1.0 in all cases except A/T was 0.95 for human lymphocyte DNA.

RESULTS AND DISCUSSION

Our method for quantifying 5-MC in DNA by GC-ECD is summarized in Fig. 1. The DNA sample was either commercial calf thymus DNA, or human lymphocyte DNA that we isolated from blood by a conventional technique.

Hydrolysis

The DNA was hydrolyzed in formic acid for 3 h at 150°C (Fig. 1, step 1), conditions known to completely hydrolyze DNA to its bases^{14,17,18}. The amount of DNA was 350 ng for each sample later subjected to quantitation by GC-ECD; whereas 4–6 µg was hydrolyzed for independent measurement of the mol-% values of all nucleobases in the DNA by HPLC.

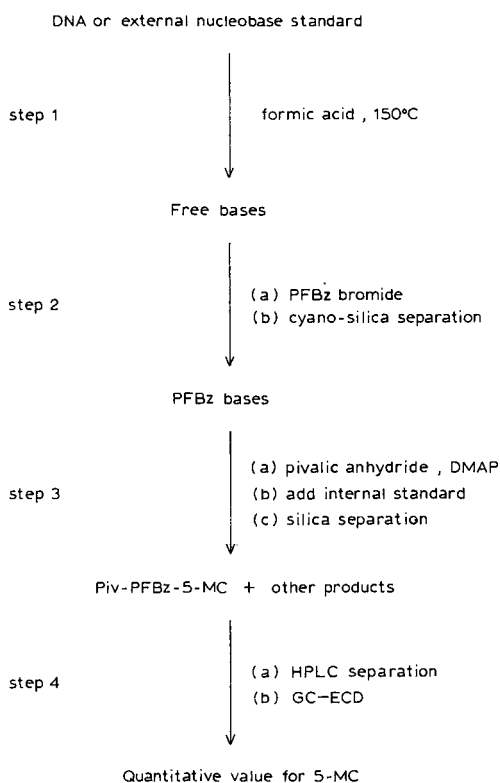


Fig. 1. Scheme for the quantitation of the amount of 5-MC (mol-%) in DNA by GC-ECD.

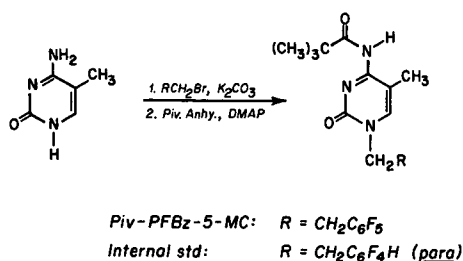


Fig. 2. Derivatization of 5-methylcytosine. Piv. Anhy. = pivalic anhydride; DMAP = 4-dimethylaminopyridine.

Derivatization

Previously we derivatized 5-MC with pentafluorobenzoyl chloride followed by methyl iodide¹⁶. Although the product had good electrophore detection characteristics, the yield varied, particularly when a few nanograms as opposed to milligrams of 5-MC were reacted. Apparently this problem was due to the formation of both mono-(desired) and di-substituted products in the acylation reaction.

Derivatization was done here in two steps, with a solid phase extraction after each. This is shown in Fig. 1 as steps 2 and 3. The overall derivatization reaction, including the likely structure of the final product, is presented in Fig. 2. In the first derivatization reaction, 5-MC is alkylated with pentafluorobenzyl bromide in the presence of solid potassium carbonate. Analysis of the product by electron impact mass spectrometry reveals a fragment corresponding to loss of NCNH_2 , proving that the PFBz group is not attached to N^4 (exocyclic nitrogen) or to $\text{N}3$ (ring nitrogen closest to N^4) of 5-MC. Based on analysis by ^{13}C NMR, the PFBz group is attached to N (ref. 19). Thus the PFBz group is attached to the $\text{N}1$ position of 5-MC.

A reaction time of 3 h was selected for the conversion of 5-MC to PFBz-5-MC since the yield of this product ($48.1 \pm 6.3\%$ by HPLC starting with 50 nmol of 5-MC) was maximum at this point. Analyte is lost in this step, especially with a longer reaction time, because of the formation of two, less polar side products in the first derivatization reaction. The major one is a dialkylated product, based on mass spectrometry, and the minor one, which was not investigated, is probably a trialkylated product.

The intermediate product, PFBz-5-MC, is next semi-purified by extraction on a cyanosilica cartridge. Smaller or less polar contaminants including residual PFBz bromide are washed away initially with ethyl acetate-dichloromethane-acetonitrile (3:1:1) and then PFBz-5-MC is eluted with methanol. The cartridge, acting as a filter, also removes the solid potassium carbonate. To avoid contact of the sample with plastic, a source of interferences in work with GC-ECD²⁰, the cartridge is prepared in a silanized Pasteur pipet. The recovery of PFBz-5-MC is quantitative in this extraction step.

In the second derivatization reaction, PFBz-5-MC is acylated with pivalic anhydride in the presence of 4-dimethylaminopyridine (DMAP). The yield as determined by HPLC of this step (step 3a in Fig. 1) is $89.4 \pm 0.7\%$ starting with 50 nmol of PFBz-5-MC. This reaction is followed by semi-purification of the product with a quantitative recovery on a silica cartridge. The DMAP remains on the column, and the pivalic anhydride/acid is washed out prior to elution of the product.

The structure of the final product, Piv-PFBz-5-MC, is probably as shown in Fig. 2, with the pivalyl group attached to the N⁴ site on PFBz-5-MC. This site is where acylation of cytosine and 5-MC has always been observed to take place^{3,14}.

This derivative, Piv-PFBz-5-MC, is a good choice for the determination of 5-MC by electrophore detection. As just cited, its yield is moderate and reproducible starting with a trace amount of 5-MC. The compound is sensitive by both ECD (peak area molar response is 0.16 relative to that of lindane) and ECNIMS. Essentially only a peak for [M - 181], due to loss of a PFBz group, is seen in the latter spectrum²¹. Although the compound possesses an active hydrogen, shielding of this hydrogen by the adjacent pivalyl group, a strategy that we have used before²², allows the compound to be determined by GC. Interestingly, the corresponding methylated product (obtained by reacting Piv-PFBz-5-MC with methyl iodide) tails more on GC than Piv-PFBz-5-MC. Apparently methylation of Piv-PFBz-5-MC significantly changes its electronic structure, the orientation of its pivalyl group, or both.

Continuing with step 3 (Fig. 1) of the analytical procedure, an internal standard was added at the end of the derivatization reaction. This standard has the same structure as the final derivatized product except for the presence of a tetra- vs. pentafluorobenzyl group (see Fig. 2). While such an internal standard fails to monitor the earlier step in the procedure, these steps are checked by the external standards. This compound also is conveniently obtained and structurally similar to the derivatized analyte.

HPLC

Because electrophore detection by ECD is non-specific, we have resorted in general to the use of HPLC as a post-derivatization cleanup step in analytical procedures of this type²⁰. Thus we next semi-purified the sample here by HPLC (step 4a in Fig. 1). The chromatogram (not shown) from the C₁₈ silica column is featureless, aside from the early elution of non-retained components. A prior injection of a larger amount of product and internal standard, detectable by UV, established the collection window. Typical retention times for product and internal standard are 15 and 16 min, and the collection window is 30 s wider on each side. Apparently derivatized 5-MC is largely resolved from earlier-eluting, derivatized cytosine in this step.

GC-ECD

The evaporated sample collected from the HPLC column is dissolved in hot methanol, thoroughly vortexed and re-evaporated. Now that the sample is focused low in the vial it is efficiently dissolved in 10 μ l of toluene. Injection of 1 μ l of this latter solution into the GC-ECD gives a chromatogram such as that shown in Fig. 3A. This chromatogram is obtained from a sample derived from human lymphocyte DNA; similar chromatograms (not shown) are obtained from calf thymus DNA. A corresponding chromatogram from a nucleobase standard solution is shown in Fig. 3B: a mixture of the DNA bases corresponding to the base composition of human lymphocyte DNA is prepared and subjected to the overall procedure including initial acid hydrolysis. Fig. 3C shows the chromatogram of a blank sample (all steps were done except no DNA was present at the outset of the procedure). Although there is a small peak in the latter chromatogram that has the same retention time as that of the

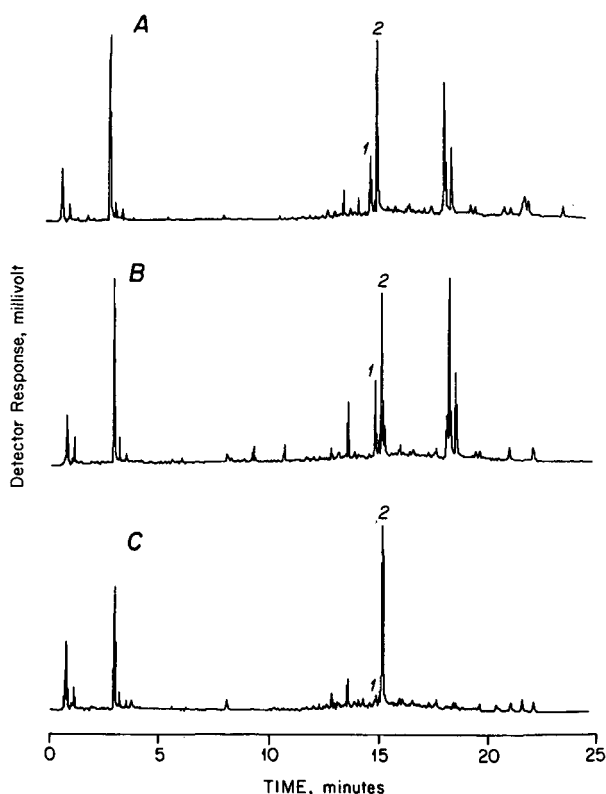


Fig. 3. Representative GC-ECD chromatogram from a human lymphocyte DNA sample (A), nucleobase standard (B), and reaction blank (C). 1 = Piv-PFBz-5-MC; 2 = internal standard. In B, the peaks represent 0.3 pmol or 117 pg of 1, and 0.65 pmol or 241 pg of 2.

product, this peak is resolved from the product on a new 50-m GC column of the same type (data not shown).

Two runs were made using the scheme of Fig. 1, one on human lymphocyte DNA sample plus an external standard nucleobase sample (defined above), and one on a calf thymus and human lymphocyte DNA sample plus an external standard nucleobase sample. The two yields for 5-MC from the external standard nucleobase samples from the two runs were 30 ± 1.0 and $30 \pm 0.3\%$. This high precision is significantly better than that cited above for one of the individual steps due to refinements in our sample handling techniques, as detailed in the Experimental, which were developed during the course of the work. Thus a yield of 30% was used in the calculation for the amount of 5-MC in the DNA samples. Accordingly, the amount of 5-MC in the calf thymus DNA was 1.2 ± 0.10 mol-%, and in the human lymphocyte DNA was 0.9 ± 0.07 mol-% (one run) and 0.8 ± 0.04 mol-% (second run). These values compare favorably with literature values of 1.39 ± 0.09 mol-% of 5-MC in calf thymus DNA based on isotope dilution-MS¹¹, and 0.96 ± 0.01 mol-% of 5-MC in human lymphocyte DNA by HPLC¹⁴.

CONCLUSION

A multi-step but sensitive and precise method relying on GC-ECD has been developed to quantify 5-MC in DNA. The experience of developing this procedure is intended to help us set up similar methodology for the determination of DNA adducts. The GC-ECD chromatograms shown in Fig. 3 are relatively clean when compared to other GC-ECD chromatograms in the literature in which low-molecular-weight analytes from biological samples are similarly derivatized and quantified. Nevertheless, refinements in the GC stage will be necessary to overcome the interferences which are present before such methodology can be successfully applied to DNA adducts, which tend to be present in much smaller amounts in DNA than 5-MC. Most attractive for this purpose will be the use of GC with detection by ECNIMS.

ACKNOWLEDGEMENTS

Financial support for this research was provided by National Cancer Institute Grant CA 35843 and Grant CR 812740 from the Reproductive Effects Assessment Group of the U.S. Environmental Protection Agency. This is Contribution No. 346 from the Barnett Institute of Chemical Analysis.

REFERENCES

- 1 R. A. Cartwright, *Chemical Carcinogens*, American Chemical Society, Washington, DC, 1984.
- 2 B. Singer and D. Grunberger, *Molecular Biology of Mutagens and Carcinogens* Plenum, New York, 1983.
- 3 A. Nazareth, M. Joppich, S. Abdel-Baky, K. O'Connell, A. Sentissi and R. W. Giese, *J. Chromatogr.*, 314 (1984) 201.
- 4 O. Minnetian, M. Saha and R. W. Giese, *J. Chromatogr.*, 410 (1987) 453.
- 5 R. S. Annan, G. M. Kresbach, R. W. Giese and P. Vouros, unpublished results.
- 6 H. Yuki, H. Kawasaki, T. Kobayashi and A. Yamaji, *Chem. Pharm. Bull.*, 25 (1977) 2827.
- 7 R. L. P. Adams and R. H. Burdon, in A. Rich (Editor), *Molecular Biology of DNA Methylation*, Springer-Verlag, New York, 1985.
- 8 K. C. Kuo, R. A. McCune and C. W. Gehrke, *Nucl. Acids Res.*, 8 (1980) 4763.
- 9 J. Catania, B. C. Keenan, G. P. Margison and D. S. Fairweather, *Anal. Biochem.*, 167 (1987) 347.
- 10 J. Singer, W. C. Schnute Jr., J. E. Shively, C. W. Todd and A. D. Riggs, *Anal. Biochem.*, 94 (1979) 297.
- 11 P. E. Crain and J. A. McCloskey, *Anal. Biochem.*, 132 (1983) 124.
- 12 M. V. Reddy, R. C. Gupta and K. Randerath, *Anal. Biochem.*, 117 (1981) 271.
- 13 J. A. Vilpo, S. Rasi, E. Suvante and L. M. Vilpo, *Anal. Biochem.*, 154 (1986) 436.
- 14 M. Ehrlich, M. A. Gama-Sosa, L. Huang, R. M. Midgett, K. C. Kuo, R. A. McCune and C. W. Gehrke, *Nucl. Acids Res.*, 10 (1982) 2709.
- 15 C. V. Patel and K. P. Gopinathan, *Anal. Biochem.*, 164 (1987) 164.
- 16 D. H. Fisher, J. Adams and R. W. Giese, *J. Environ. Health Sci.*, 62 (1985) 67.
- 17 D.-B. Lakings and C. W. Gehrke, *Clin. Chem.*, 18 (1972) 810.
- 18 D. Eick, H. J. Fritz and W. Doerfler, *Anal. Biochem.*, 135 (1983) 165.
- 19 M. Saha, P. Vouros and R. W. Giese, in preparation.
- 20 E. J. Rogers and R. W. Giese, *Anal. Biochem.*, 184 (1987) 439.
- 21 T. Trainor, R. W. Giese and P. Vouros, unpublished results.
- 22 A. Sentissi, M. Joppich, K. O'Connell, A. Nazareth and R. W. Giese, *Anal. Chem.*, 56 (1984) 2512.

CHROM. 20 656

APPLICATIONS OF GAS CHROMATOGRAPHY TO THE STUDY OF TERPENOID METABOLISM

D. MICHAEL SATTERWHITE and RODNEY B. CROTEAU*

Institute of Biological Chemistry, Washington State University, Pullman, WA 99164-6340 (U.S.A.)

SUMMARY

Studies on the enzymology and mechanism of biosynthesis of the essential oil terpenes are often hampered by the need to resolve and detect trace levels of these metabolites, an analytical requirement for which gas chromatography is ideally suited. Essential principles in the application of gas chromatography to terpenoid metabolism are described, with particular emphasis on experimental strategies employing flame ionization, mass spectrometric and thermal conductivity-radiochemical detection methods. The general approaches described can be readily adapted to studies on the origin of other volatile natural products.

INTRODUCTION

The monoterpenes and sesquiterpenes are two large and diverse families of natural compounds produced primarily by plants in which they often cooccur as complex mixtures known as essential oils¹. Although the monoterpenes and sesquiterpenes were of key significance in the historical development of isoprenoid biogenetic theory², studies on the biochemistry of these volatile terpenoids were often hindered by the inability to resolve and detect trace levels of isomeric metabolites. Gas chromatography (GC), with ancillary detection systems, is ideally suited to this analytical problem, and the application of this technique to metabolic investigations is in large part responsible for recent progress in this area^{3,4}.

The application of gas chromatographic methods to terpene biosynthetic investigations was last reviewed in 1983⁵ and since that time significant refinement in methods has been made, particularly in the use of fused-silica capillary columns and associated on column injection techniques. A number of assays for specific metabolites, based on these and related techniques, have been reported⁶⁻¹¹, yet the guiding principles and strategies underlying the method are rarely provided in the primary literature. We address these issues in the context of terpenoid metabolism by describing the applications of GC in conjunction with flame ionization, mass spectrometric and thermal conductivity-radiochemical detection methods. The general procedures are applicable to any volatile, thermally stable metabolites.

EXPERIMENTAL

Enzyme systems

General procedures for isolating the enzymes of terpenoid metabolism have been described^{12,13}. Descriptions of specific enzymes, and the substrates and standards required for their assay, are provided by citation in the appropriate sections of the text.

Special considerations

The extraction of proteins from terpene-producing tissues with aqueous buffer systems is always accompanied by the co-extraction of greater or lesser amounts of terpenoid metabolites which adhere to the various cellular constituents. These endogenous terpenoids can interfere with subsequent kinetic assays by acting as inhibitors or substrates of the relevant enzymes or, alternatively, by compromising quantitative analysis of the enzyme reaction by masking or diluting the product(s) of interest. Such endogenous materials can be removed by incorporating polymeric adsorbents, such as soluble or insoluble polyvinylpyrrolidone and polystyrene beads^{14,15}, into the extraction buffer^{12,13}. For particularly oily or resinous tissue, an equal tissue weight of such polymers may be required to reduce the levels of endogenous terpenoids to negligible levels. Beaded polystyrene containing the adsorbed terpenoids is sufficiently large to remove from cell free homogenates by simple filtration through cheesecloth. Insoluble polyvinylpyrrolidone can be removed from soluble enzyme extracts by centrifugation, since this material pellets readily at 27000 *g*. For membranous enzymes, soluble polyvinylpyrrolidone is substituted for the insoluble form of the polymer in the extraction buffer, and is then discarded in the supernatant when the membranes are collected by centrifugation. Detailed protocols for these procedures have been published^{8,12,13}.

Since the products of most of the metabolic reactions of interest are relatively hydrophobic, extraction of the aqueous incubation mixture with organic solvent is generally the first step of the assay. Pentane is most often chosen for this purpose because such an extract can be eluted through a short column of silica (3 cm × 0.5 cm I.D. of silica gel Type 60A-special, 100–200 mesh, Mallinckrodt 6447) to separate terpene olefins from oxygenated metabolites which remain adsorbed to the column. Subsequent extraction of the assay mixture with ether and passage of this extract through the same column allows the collection of the oxygenated products in a separate fraction. More polar co-solvents such as methanol or acetic acid may be required to elute highly oxygenated or acidic metabolites. Prior to the column chromatography step, the extract may be decolorized if needed with a minimum amount of activated charcoal and, following filtration, the extract can be back-extracted with water to remove possible additional contaminants. Drying of these organic extracts is most easily accomplished by surmounting the above silica columns with a small plug of anhydrous magnesium sulfate. Internal standards may be added at any stage of the work up; however, this is preferably done at the extraction step to prevent evaporative losses of product. In any case, the minimum volumes of high purity solvents should be employed during extraction and column elution to reduce product loss during the solvent concentration steps.

Sample concentration in preparation for chromatographic analysis is efficiently carried out by solvent evaporation under a stream of dry nitrogen or argon. Removal

of solvent under vacuum (Savant Speed-Vac) is also efficient and rapid, and permits concentration of a few milliliters of solvent to *ca.* 100 μ l with 80–90% sample recovery. Samples at this volume are adequate for most applications; concentration to 10–20 μ l, if required, is best performed in a microvial equipped with a Mininert valve (Wheaton 986294 or 986293 vial with Pierce 10127 valve).

Numerous derivatization procedures can be applied to the analysis of specific product types and several of these are described in the following text. In many instances it is also desirable to remove specific classes of potentially interfering compounds, and for the preparation of saturated terpenoid products a useful procedure for removing olefinic contaminants has been developed. For this application, the initial extract is treated with 0.1–0.5 mg of osmium tetroxide and a few drops of pyridine. Following agitation for one to several hours, osmate esters are decomposed with saturated sodium metabisulfite solution and the organic layer processed through the silica column as above. In this way olefinic bonds are converted to the corresponding diols, rendering these compounds water-soluble or of sufficient polarity to adhere tightly to silica.

Radio gas chromatography

Radio GC was performed on a Gow-Mac 550P programmable chromatograph equipped with a low volume 10-955 thermal conductivity detector, with gold-plated tungsten-rhenium filaments, which was coupled directly to the oxidation–reduction furnace of a Packard 894 flow-through gas proportional counter. The thermal conductivity detector has more than adequate sensitivity for this application; however, the primary reasons for this choice of detection are the non-destructive nature and the fact that the optimum gas flow for separation is perfectly compatible with the flow-through counter. Thus, direct coupling of the instruments without sample loss is possible, thereby eliminating the need for make-up gas or effluent splitting with the attendant variation in split-ratio with temperature.

The helium carrier-gas stream exiting the chromatograph detector is introduced directly into a 10 \times 0.7 cm quartz tube containing copper oxide wire at 750°C (both ends plugged with quartz wool). The combustion products (*i.e.*, $^{14}\text{CO}_2$ and $^3\text{H}_2\text{O}$) are passed through a short capillary tube into a 15 \times 0.7 cm quartz tube packed with chloroform–methanol washed, preconditioned (750°C) steel wool (000 or finer) also at 750°C. The emerging gases ($^{14}\text{CO}_2$, $^3\text{H}_2$) are conducted across short columns of carbon dioxide adsorbent [Mallcosorb (Mallinckrodt) is employed for $^3\text{H}_2$ detection to eliminate the possibility of carbon dioxide-based quenching] and magnesium perchlorate (to remove traces of water), and then mixed with the appropriate proportion (6–8% of column flow) of the propane quench gas before passage, via zero-dead-volume capillary fittings, into the 20-ml counting tube held at \sim 1700 volts.

Using conventional packed columns [3.7 m \times 2 mm I.D. stainless steel containing, for example, 15% Silar 10C (olefins), Superox 20M or FFAP (most oxygenated terpenoids) on 80–100 mesh Chromosorb WHP] the optimum column flow is about 35 ml/min, prior to combustion, and not greater than 40 ml/min emerging from the counting tube (exhausted to a hood). With sample loads up to about 50 μ g per component (with mass detection to about 1 μ g), baseline resolution with peak widths (at half-height) of roughly 30 s can be expected. Under these conditions, quantitation of 2000 ± 200 dpm is easily attainable (counting efficiencies ranging to 80% for $^3\text{H}_2$ at

optimum flow and peak width), with reliable detection to about 600 dpm. The system is calibrated externally with [^3H]toluene or [^{14}C]toluene, or a similar primary standard. A System Instruments, America 7000A chromatogram processor is employed for simultaneous (dual channel) monitoring of the thermal conductivity detector and gas proportional counter outputs, and for data reduction.

Fused-silica, wall coated open tubular, capillary columns (530 μm) can be employed with the radio chromatographic system described. Resolution at optimum flow-rates (*ca.* 6 ml/min) is far superior to that of packed columns; however, sample capacity is reduced (5- to 10-fold) and counting efficiency is slightly diminished because of the greater sample dilution in the gas stream. For such applications, helium make up gas (to total 35 ml/min) is added to the thermal conductivity detector and a small quantity of hydrogen (2–4% of total flow) is added at the inlet of the reduction furnace to insure efficient purging of the $^3\text{H}_2$ formed.

Capillary gas chromatography

Capillary GC (hydrogen as carrier) was done on a Hewlett-Packard 5890 chromatograph equipped with flame ionization detector, split injection and on-column injection ports, and a 7673A autoinjector. Data were analyzed using a Hewlett-Packard 3392A recording integrator.

Combined capillary gas chromatography–mass spectrometry (GC–MS) (helium as carrier) was carried out on a Hewlett-Packard 5840A-5985B system with SIDS data system. The instrument was equipped with a dual injector system as above, and modified to allow column selection and source isolation with a Valco switching valve. The transfer line, to within 0.5 cm from the ion source, was a 30 cm \times 0.1 mm I.D. deactivated fused-silica tubing.

For cold, on-column injection (splitless), a 10-cm section of 530 μm deactivated fused-silica tubing was coupled to a 1-m section of similar 250 μm tubing, and thence connected to the capillary column (30 m \times 250 μm I.D., with bonded Superox or methyl silicone type phase). This system permits up to 1 μl injections using a conventional 10- μl syringe with 26-gauge needle and eliminates most problems associated with on-column injection using fused-silica needles. Removable couplings (Valco ZU.5TF5.4) permit easy removal of the deactivated inlet tubing for cleaning. For most applications, 0.5- μl injections are employed (50–100 pg sample load) and a 5-pg component can be accurately quantitated.

RESULTS AND DISCUSSION

Assays with radioisotopes

Radiochemically based enzyme assay employing coupled GC–gas proportional counting is the method of choice when maximum sensitivity is required, because this technique permits detection of a few hundred dpm in a single component diluted in the gas volume of the counting tube. Additional advantages of the method include continuous monitoring of the chromatographic separation, thus avoiding the collection of fractions, and the ease of operation when the counter is coupled, via the combustion–reduction train, directly from the outlet of a thermal conductivity detector, thus avoiding the complications of effluent splitting.

Since the enzymatic cyclization reactions appear to be the slow steps of many

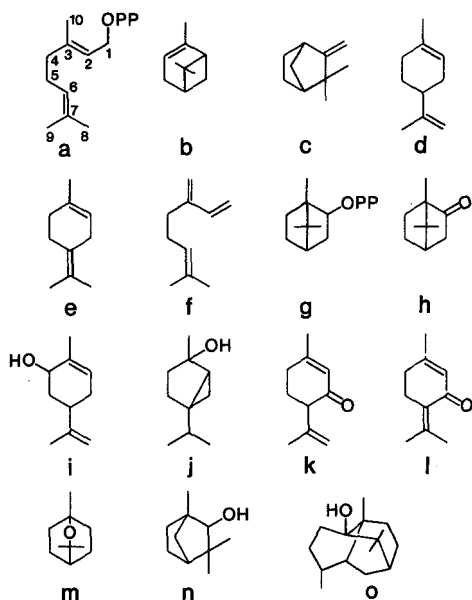


Fig. 1. Structures of (a) geranyl pyrophosphate, (b) α -pinene, (c) camphene, (d) limonene, (e) terpinolene, (f) myrcene, (g) bornyl pyrophosphate, (h) camphor, (i) carveol, (j) sabinene hydrate, (k) isopiperitenone, (l) piperitenone, (m) 1,8-cineole, (n) fenchol and (o) patchoulol.

biosynthetic sequences in the terpene series^{2,3}, this basic technique, involving conversion of ^3H - or ^{14}C -labeled immediate precursors (acyclic prenyl pyrophosphates) and radio GC analysis of the resulting products, has found wide application in the assay of these "cyclase" enzyme types. Several important considerations arise in exploiting this technique, including the fact that assays of this type, especially with relatively crude enzyme extracts, often produce complex mixtures of isomeric products, whereas the radio chromatographic separations, because of the flow requirements of the proportional counter, are largely restricted to relatively low-resolution packed columns. Most cyclic products are soluble in organic solvent and thus easily separated from the residual substrate by extraction. More importantly, radioisotopic labeling permits the addition of carrier standards (to a dilution of 4 nCi/ μmol) as a precaution against loss of these volatile products in handling, and it thereby allows preliminary column or thin-layer fractionation by class (olefins, oxygenated metabolites, etc.) thereby minimizing the gas chromatographic separation requirements.

The technique has been applied to the conversion of variously labeled geranyl pyrophosphates to mixtures of cyclic monoterpene olefins (Fig. 1) by a partially purified enzyme preparation from common sage (*Salvia officinalis*). In this application the products of the cyclase assay mixture are extracted with pentane, and the pentane passed through a short column of silica to adsorb oxygenated species. The olefin fraction, following dilution with appropriate authentic standards, is concentrated and separated in a straightforward manner, yielding essentially baseline resolution of the standards and revealing which of the many potential biosynthetic products are labeled

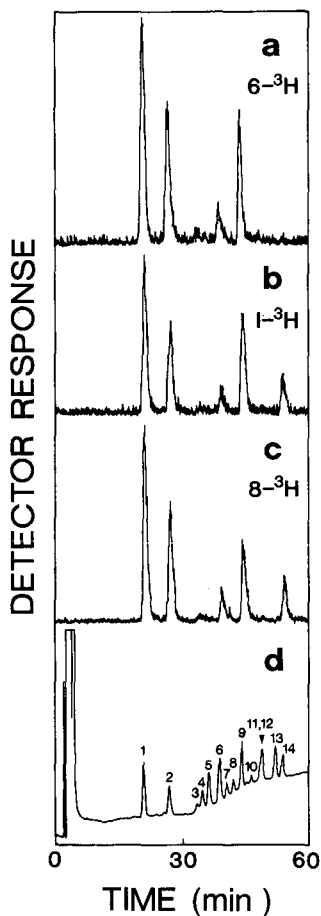


Fig. 2. Radio GC of the monoterpene olefins derived from geranyl pyrophosphate labeled with ^3H at C-6 (a), C-1 (b) and C-8 (c) by a partially purified cyclase from sage (*S. officinalis*) leaves. The smooth lower tracing (d) is the thermal conductivity detector response to a mixture of authentic α -pinene (1), camphene (2), β -pinene (3), sabinene (4), 3-carene (5), myrcene (6), α -phellandrene (7), α -terpinene (8), limonene (9), *cis*- β -ocimene (10), β -phellandrene (11), γ -terpinene (12), *p*-cymene (13), and terpinolene (14). The 3.7 m \times 2 mm I.D. stainless-steel column was packed with 15% AT 1000 on 60–80 mesh Gas-Chrom Q-II and was programmed from 80°C (20 min hold) to 150°C at 4°C/min at a helium flow of 35 ml/min. The gas proportional counter was set at 1000 cpm full-scale.

or devoid of isotope (Fig. 2). Analysis of the product mixtures generated separately from $1\text{-}^3\text{H}$, $6\text{-}^3\text{H}$ and $8\text{-}^3\text{H}$ labeled geranyl pyrophosphate has allowed the regiochemistry of the deprotonations leading to the various olefins, and other mechanistic features of the cyclization reaction, to be deciphered^{11,16}.

In some applications only a single product need be sought, thus both simplifying the chromatographic analysis and often permitting detailed probing of the enzymatic reaction. Two separable enzymes from sage (differing in molecular weight) were known to convert geranyl pyrophosphate to bornyl pyrophosphate en route to camphor (Fig. 1), a natural product of sage known to occur in the leaf oil primarily as

the (+)-isomer and thus prompting an examination of the optical purity of the two enzymatic products¹⁷. Incubation of the separate enzymes with [1-³H]geranyl pyrophosphate gave the respective products which, following ether extraction of the reaction mixtures to remove non-polar materials, were liberated as borneol from the aqueous phases by treatment with acid phosphatase plus apyrase. Each product was then diluted with racemic carrier and the mixtures treated with excess osmium tetroxide to convert the double bonds of geraniol (liberated from the substrate by the enzymatic hydrolysis) to the corresponding diols before purification by thin-layer chromatography (TLC). Each isolated borneol was then oxidized to camphor which was converted to a mixture of diastereomeric ketals with D-(−)-2*R*,3*R*-butanediol^{17,18}. Radio GC separation of the diastereoisomers gave compelling evidence that the two original enzymatically derived bornyl pyrophosphates, from which these derivatives were obtained, were in fact enantiomeric products (Fig. 3), indicating that the responsible enzymes were functionally distinct.

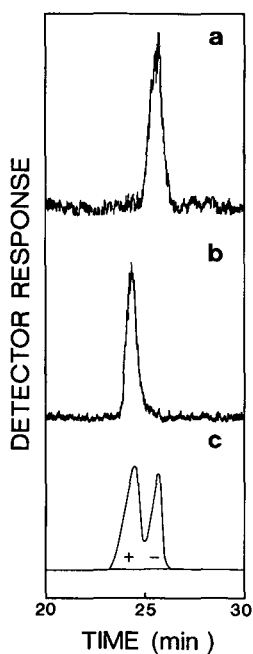


Fig. 3. Radio GC separation of the diastereomeric ketals obtained by condensation of D-(−)-2*R*,3*R*-butanediol with [³H]camphor derived from [³H]bornyl pyrophosphate generated by two enzymes from sage (*S. officinalis*). Each enzyme was incubated with [1-³H]geranyl pyrophosphate, and the bornyl pyrophosphate product was enzymatically hydrolyzed to borneol, diluted with racemic standard, oxidized to camphor and converted to the ketal. Separation of products obtained from the lower-molecular-weight enzyme (a) and from the higher-molecular-weight enzyme (b) is illustrated. The smooth lower tracing (c) is the thermal conductivity detector response obtained from a mixture of the diastereomeric ketals derived from (+)- and (−)-camphor, and the order of elution was established by separate injection of each authentic diastereomer. The separation was performed on a 3.7 m × 2 mm I.D. stainless-steel column packed with 15% Silar 10C on 80–100 mesh Chromosorb WHP which was programmed from 90°C (10 min hold) to 150°C at 4°C/min at a helium flow of 35 ml/min. The radioactivity response is 3000 cpm full-scale for (b) and 1000 cpm full-scale for (a).

Although the two examples described above represent applications to the *in vitro* metabolism of terpenoids, the technique is readily adapted to *in vivo* investigations. Because of the permeability barriers encountered with intact tissue, such *in vivo* labeling studies can rarely employ advanced precursors such as geranyl pyrophosphate, and so are most often carried out with more basic precursors such as mevalonate, acetate, sucrose and even $^{14}\text{CO}_2$. This naturally leads to the labeling of a broader variety of terpenoid and non-terpenoid products, which increases the need for pre-fractionation of metabolites before radio GC analysis. Micro-scale steam distillation of the crude tissue extracts has proven to be a suitable method for isolating volatile terpenoids prior to chromatographic separation¹⁹.

Quantitation is readily accomplished by combination of aliquot counting of the sample and integration of the radio-monitor trace, and the system is externally calibrated by injection of known quantities of [^3H]toluene or of a similar volatile standard.

Assays with unlabeled substrates

GC assays with unlabeled substrates are generally preferred for studies on the subsequent enzymatic conversions of the parent cyclic terpenoids since the available enzyme activities (levels) are higher for these secondary transformations⁴ and the sensitivity requirements are therefore in the range of capillary chromatography using on-column injection and a flame ionization detector (unfortunately, the activity levels available are rarely in the range of spectrophotometric assays). Analysis time is comparable to that of radio chromatographic based assays (including sample handling and pre-fractionation); however, the major advantage of the simple mass detection technique is in avoiding the preparation of many labeled substrates which would otherwise be required (*e.g.*, in substrate specificity studies). Wide bore pre-columns coupled to standard 30-m phase-bonded capillary columns provide more than sufficient resolution, and the increased sample delivery is a requirement for on-column injection. A major consideration with this approach is the need to reduce the level of endogenous metabolites in the enzyme extract to a negligible level so as not to interfere with the analysis. Partial purification of soluble enzymes by gel permeation or ion-exchange chromatography is generally sufficient to remove small hydrophobic substances which bind to protein (and are extracted in the subsequent assay)²⁰, but such purification is often not possible when working with membranous enzymes where adsorption of small molecules to the hydrophobic membrane matrix is most severe⁸. This difficulty is overcome by treating the preparations with polymeric adsorbents such as polyvinyl pyrrolidone or polystyrene which are subsequently removed by filtration or centrifugation^{8,13}. This procedure may need to be repeated several times to lower the background to acceptable levels, but it does permit the assay of even crude enzyme extracts.

The technique has been applied to study the hydroxylation of limonene to *cis*-carveol (en route to carvone) by microsomal membrane preparations from spearmint (*M. spicata*) leaves²¹. For this purpose, the relevant enzymes are isolated by selective extraction of the cellular contents of leaf epidermis oil glands in the presence of polystyrene beads, soluble polyvinylpyrrolidone and bovine serum albumin¹³. The former is removed by simple filtration through cheesecloth, whereas the soluble polymers are removed when the microsomal membranes are collected by high-speed

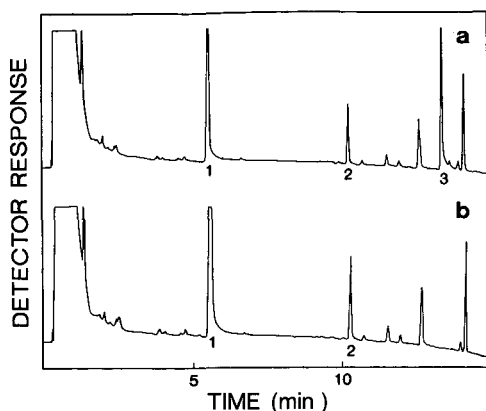


Fig. 4. Capillary gas chromatograms (flame ionization detection) of the diethyl ether-soluble products obtained from the incubation of a microsomal preparation from spearmint (*M. spicata*) leaves with 1 mM NADPH and 0.5 mM of (–)-limonene (a), and from a solvent denatured control similarly incubated (b). The peaks identified are (–)-limonene, at 200 nmol in the assay (1), camphor, 25 nmol added as internal standard (2), and the product, (–)-*cis*-carveol (3). The separation was performed on a 30 m × 0.25 mm I.D. fused-silica column coated (0.1 μm) with Superox-FA which was programmed from 70°C (5 min hold) to 220°C at 10°C/min at a hydrogen flow of 2 ml/min. Injection was on-column at 35°C.

centrifugation. Following suspension of the membrane fraction in buffer, and the addition of the substrate and appropriate cofactors, the reaction mixture is incubated in a sealed screw-capped tube (Corning 9826-13). At the appropriate time, the tube is chilled, a known amount of internal standard is added (in this case camphor), and the contents are extracted with ether, the extract concentrated and an aliquot analyzed (Fig. 4). The detection limit for the carveol product by this method is about 100 fg, which is more than adequate for kinetic evaluation of the hydroxylase system even at low substrate and cofactor levels. A very similar approach has been applied to assay numerous other enzymes of terpenoid metabolism in mint, including dehydrogenases and double bond reductases and isomerases^{6–8}.

In instances when quantitation is of lesser importance, and preparative scale incubations can be carried out, the method can be applied to the stereochemical analysis of biosynthetic products. Thus, to resolve the fenchol (Fig. 1) derived from geranyl pyrophosphate by a cyclase from fennel (*Foeniculum vulgare*), the pooled biosynthetic product from several large-scale incubations was (after treatment with osmium tetroxide and preliminary column fractionation on silica) converted to the corresponding isopropyl urethane¹⁰. This derivative was then separated on a chiral phase capillary column (XE-60-*S*-valine-*S*- α -phenylethylamide) to prove conclusively that the sole product was (–)-*endo*-fenchol (Fig. 5). Detection in this instance was by coupled GLC–MS using selected ion monitoring of the characteristic double-cleavage ion at *m/e* 80 for the isopropyl urethanes. A very similar strategy was employed to distinguish the sesquiterpene alcohol patchoulol (molecular weight, MW 222) from sesquiterpene olefins (MW 204) produced from farnesyl pyrophosphate by a crude cell free extract from *Pogostemon cablin*⁹. In this instance, the analysis by flame ionization detection was complicated by the co-extraction of interfering substances from the assay mixture (Fig. 6, inset), yet by selective-ion monitoring of the

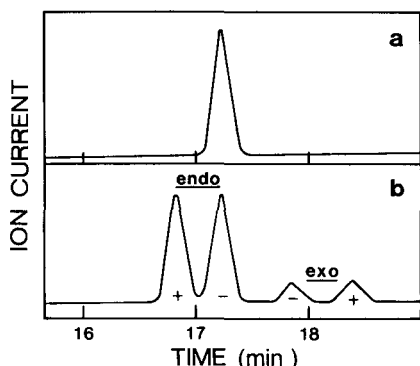


Fig. 5. Chiral phase capillary GC separation of the isopropyl urethane of fenchol derived from geranyl pyrophosphate by a cyclase from fennel (*F. vulgare*) (a). The separation of authentic standards of the isopropyl urethanes of both (+)- and (-)-isomers of both *endo*- and *exo*-fenchol are also illustrated (b). Retention times were established by separate injection of the derivative of each authentic stereoisomer. The column employed was 50 m \times 0.17 mm I.D. fused silica coated with XE-60-*S*-valine-*S*- α -phenylethylamide (Chrompack) and was programmed from ambient temperature (25°C) to 160°C at 30°C/min at a helium flow of 0.5 ml/min. Injection was on-column at 25°C, and detection was by selected ion monitoring of the double-cleavage ion at *m/e* 80 for the isopropyl urethanes. Quantitation was by summation of ion current (5–10 scans) over the appropriate retention interval.

capillary-column effluent at *m/e* 204 and *m/e* 222 very simple chromatograms were produced which allowed straightforward detection of the products of interest (Fig. 6).

The higher boiling point of the sesquiterpenes and of derivatized monoterpenes allows considerable manipulation of extracts containing these compounds, yet even in

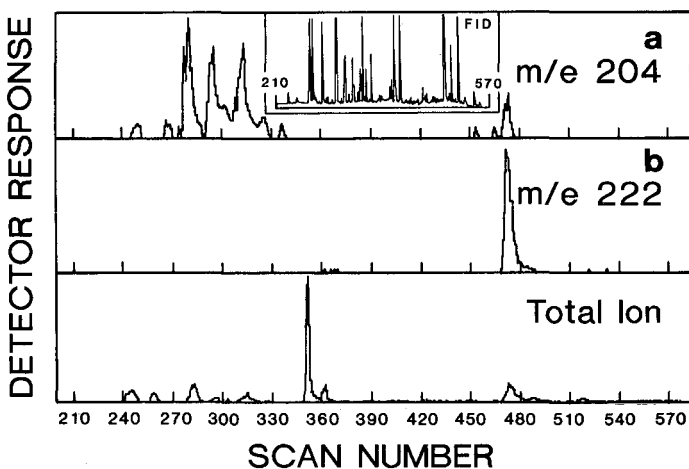


Fig. 6. Capillary GC separation of the diethyl ether-soluble products obtained from the incubation of a crude enzyme extract from patchouli (*P. cablin*) leaves with farnesyl pyrophosphate. The inset illustrates the flame ionization detector response in the relevant section of the chromatogram, the bottom trace is the total ion current, and panels (a) and (b) illustrate detection by selected ion monitoring of *m/e* 204 and 222, respectively, over the same interval. The column was the same as described under Fig. 4, and was programmed from 45°C (5 min hold) to 220°C at 10°C/min at a helium flow of 2 ml/min. Injection was on-column at 45°C.

these cases solvent volumes should be kept to a minimum to avoid evaporative losses of product during the required concentration steps. Quantitative analysis by this general method dictates the accurate addition of a suitable (non-interfering) internal standard as early as possible in the assay procedure to compensate for handling losses. For most applications the internal reference standard should be of comparable boiling point and polarity to the product(s) of interest, and bear a response factor near unity. In addition to the normal boiled enzyme or solvent denatured controls run with assays of this type, additional controls should include incubations of enzyme without substrate and of substrate without enzyme to confirm the absence of interfering materials in the chromatographic analysis.

Assays with stable isotopes

MS detection and product analysis is invaluable for mechanistic studies using stable isotopes. General considerations for this type of experiment are essentially the same as for assays with unlabeled substrates, and particular care must be taken to avoid interferences which will result in apparent isotopic dilution of the ions to be monitored. Preliminary experiments with unlabeled compounds will usually reveal such potential problems which can often be overcome by simple prefractionation or derivatization of the product of interest; however, any manipulation of this type will lead to at least some product loss.

In examining the source of the hydroxyl oxygen atom of *cis*-sabinene hydrate (Fig. 1) produced by a soluble cyclase from majoram (*Majorana hortensis*)²² crude enzyme preparations adjusted to suitable assay conditions and containing the substrate geranyl pyrophosphate were frozen and lyophilized, and the dry powder then dissolved in H₂¹⁸O or H₂¹⁶O prior to the assay. The reaction product formed was extracted into ether along with a variety of coproducts and then separated directly by on column injection capillary GLC-MS while monitoring specific ions in the range of the possible parents (*i.e.*, *m/e* 154-157). The observed isotopic enrichment of the sabinene hydrate, evidenced by the complete shift of the parent ion from *m/e* 154 (in H₂¹⁶O) to *m/e* 156 (in H₂¹⁸O) clearly indicated that water was the exclusive source of the oxygen atom incorporated in the cyclization²². Related experiments have confirmed that the hydroxyl oxygen of the aforementioned (-)-*endo*-fenchol cyclization product is similarly derived by water trapping of a cationic reaction intermediate^{23,24}. However, studies with [1-¹⁸O]geranyl pyrophosphate as a substrate demonstrated that the exclusive source of the ester oxygen of bornyl pyrophosphate formed in this enzymatic cyclization was the corresponding ester oxygen of the acyclic precursor, thus providing strong evidence for ion-pairing in this unusual reaction^{25,26}. In this instance, the product was examined by GLC-MS analysis of the corresponding bornyl benzoate, since preparation of the higher molecular weight derivative minimized evaporative losses and gave a superior parent ion.

Attempts to demonstrate directly the intramolecular hydrogen transfer thought to be involved in the isomerization of isopiperitenone to piperitenone (Fig. 1) by an enzyme from peppermint (*Mentha piperita*) were thwarted by very low product yields as the result of a pronounced isotope effect when the specifically deuterated substrate was employed⁶. However, indirect evidence for such an internal transfer was obtained when the enzymatic isomerization was examined in ²H₂O, since analysis of the resulting piperitenone by GLC-MS (monitoring a series of [P + *n*]⁺ ions) revealed that

the product contained no detectable deuterium⁶. A recent examination of the cyclization of geranyl pyrophosphate to 1,8-cineole (Fig. 1) by an enzyme from *S. officinalis* has confirmed that one hydrogen atom from water is acquired in this product during the course of the reaction²⁷. In this case, the lyophilized enzyme preparation was incubated with substrate in either H₂O or ²H₂O, and the resulting products extracted into pentane and adsorbed to a small silica column. Following rinsing of the column with pentane to remove interfering olefins, each cyclic ether was eluted in a minimum volume of 10% ether in pentane, then separated from oxygenated coproducts and analyzed by combined GLC-MS. Monitoring the column at the elution volume of 1,8-cineole revealed a shift of one a.m.u. in the parent ion from *m/e* 154 (in H₂O) to *m/e* 155 (in ²H₂O).

As with assays employing unlabeled substrates, experiments with stable isotopes can be calibrated by the use of internal standards. However, since the response to normal and isotopically enriched materials can differ markedly, by either single ion or total ion-current monitoring, it is often simpler to avoid this complication by external calibration with authentic labeled material.

CONCLUSION

The application of GC, along with ancillary prefractionation and detection methods, to the study of terpenoid metabolism has been illustrated by way of several diverse examples. Without these chromatographic assay methods, studies on this class of natural products would be severely limited since few other techniques offer the combination of sensitivity and high resolution required. The general approach appears to be underutilized in other areas of study where the experimental constraints are similar, as for example in the biosynthesis of flavor substances and pheromones. It is hoped that this article will stimulate applications of this powerful method to research on the origin of these and other naturally occurring metabolites.

ACKNOWLEDGEMENTS

This investigation was supported by grants from the U.S. National Institutes of Health, National Science Foundation, and Department of Energy, and by Project 0268 from the Research Center, College of Agriculture and Home Economics, Washington State University, Pullman, WA 99164, U.S.A. We thank Nancy Madsen for typing the manuscript.

REFERENCES

- 1 S. R. Srinivas, *Atlas of Essential Oils*, ANADAMS Consulting Service, New York, 1986.
- 2 L. Ruzicka, *Pure Appl. Chem.*, 6 (1963) 493.
- 3 R. Croteau, in L. E. Craker and J. E. Simon (Editors), *Herbs, Spices and Medicinal Plants, Recent Advances in Botany, Horticulture and Pharmacology*, Vol. 1, Oryx Press, Phoenix, AZ, 1986, p. 81.
- 4 R. Croteau, *Chem. Rev.*, 87 (1987) 929.
- 5 R. Croteau and R. C. Ronald, in E. Heftmann (Editor), *Chromatography: Fundamentals and Applications of Chromatographic and Electrophoretic Methods, Part B: Applications*, Elsevier, Amsterdam, 1983, p. 147.
- 6 R. B. Kjonaas, K. V. Venkatachalam and R. Croteau, *Arch. Biochem. Biophys.*, 238 (1985) 49.
- 7 R. Croteau and K. V. Venkatachalam, *Arch. Biochem. Biophys.*, 249 (1986) 306.

- 8 F. Karp, J. L. Harris and R. Croteau, *Arch. Biochem. Biophys.*, 256 (1987) 179.
- 9 R. Croteau, S. L. Munck, C. C. Akoh, H. J. Fisk and D. M. Satterwhite, *Arch. Biochem. Biophys.*, 256 (1987) 56.
- 10 D. M. Satterwhite, C. J. Wheeler and R. Croteau, *J. Biol. Chem.*, 260 (1985) 13901.
- 11 R. Croteau, C. J. Wheeler, D. E. Cane, R. Ebert and H.-J. Ha, *Biochemistry*, 26 (1987) 5383.
- 12 R. Croteau and D. E. Cane, *Methods Enzymol.*, 110 (1985) 383.
- 13 J. Gershenzon, M. A. Duffy, F. Karp and R. Croteau, *Anal. Biochem.*, 163 (1987) 159.
- 14 W. D. Loomis, *Methods Enzymol.*, 31 (1974) 528.
- 15 W. D. Loomis, J. D. Lile, R. P. Sandstrom and A. J. Burbott, *Phytochemistry*, 18 (1979) 1049.
- 16 R. M. Coates, J. F. Denissen, R. B. Croteau and C. J. Wheeler, *J. Am. Chem. Soc.*, 109 (1987) 4399.
- 17 R. Croteau, D. M. Satterwhite, D. E. Cane and C. C. Chang, *J. Biol. Chem.*, 261 (1986) 13438.
- 18 D. M. Satterwhite and R. Croteau, *J. Chromatogr.*, 407 (1987) 243.
- 19 R. Croteau and F. Karp, *Arch. Biochem. Biophys.*, 176 (1976) 734.
- 20 M. A. Johnson and R. Croteau, *Arch. Biochem. Biophys.*, 235 (1984) 254.
- 21 D. M. Satterwhite, K. Wagschal and R. Croteau, in preparation.
- 22 T. W. Hallahan and R. Croteau, *Arch. Biochem. Biophys.*, 264 (1988) 618.
- 23 R. Croteau, J. Shaskus, D. E. Cane, A. Saito and C. Chang, *J. Am. Chem. Soc.*, 106 (1984) 1142.
- 24 D. M. Satterwhite and R. Croteau, *Arch. Biochem. Biophys.*, submitted for publication.
- 25 D. E. Cane, A. Saito, R. Croteau, J. Shaskus and M. Felton, *J. Am. Chem. Soc.*, 104 (1982) 5831.
- 26 R. Croteau, J. J. Shaskus, B. Renstrøm, N. M. Felton, D. E. Cane, A. Saito and C. Chang, *Biochemistry*, 24 (1985) 7077.
- 27 R. Croteau and D. M. Satterwhite, in preparation.

CHROM. 20 717

SUPERCONDUCTOR METAL OXIDE CATALYST IN A CHEMILUMINESCENCE CHROMATOGRAPHY DETECTOR

E. A. McNAMARA, S. A. MONTZKA, R. M. BARKLEY and R. E. SIEVERS*

Department of Chemistry and Biochemistry and Cooperative Institute for Research in Environmental Sciences, Campus Box 215, University of Colorado, Boulder, CO 80309 (U.S.A.)

SUMMARY

The superconducting oxygen-deficient perovskite, $\text{YBa}_2\text{Cu}_3\text{O}_7$, was used to catalyze redox reactions between organic species and NO_2 in a chromatography detector based upon chemiluminescence. The reactions were studied at catalyst temperatures ranging from 200°C to 350°C and at make-up gas flow-rates of 3.5–36.5 ml/min. By changing the flow-rate or the catalyst temperature, one can alter the sensitivity of analyte response in redox chemiluminescence and the selectivity ratios. Alcohols and alkenes responded the most strongly, with ethanol being detected at the level of 0.5 ng. Ammonia, acetaldehyde, acetone, methylethylketone, acetonitrile and nitromethane were also sensitively detected. Chromatographic analyses of oxygenates, e.g., methyl *tert.*-butyl ether or alcohols, in paraffinic matrices such as gasoline were demonstrated.

INTRODUCTION

Selective detectors for gas chromatography are widely used for the quantitative analysis of specific compounds that are present in complex matrices. A recent review of selective detectors¹ describes many that are currently in use and the range of compounds that can be detected selectively. Chemiluminescence offers many advantages upon which chromatography detectors can be based. Among the new detectors that are especially effective is the redox chemiluminescence detector, the selectivity of which depends on the post-column reaction of NO_2 with eluted analytes over a heated gold catalyst to produce NO^{2-8} . The pulses of NO formed are subsequently detected downstream through the chemiluminescent reaction with ozone.

While gold is the catalyst that has shown the best selectivity for oxygenated compounds, other catalysts such as palladium may be employed to achieve differing degrees of selectivity⁷. We now report on the catalytic properties of a new catalyst that will be of particular value to chromatographers. The superconducting characteristics of the oxygen-deficient perovskite, $\text{YBa}_2\text{Cu}_3\text{O}_7$, and its oxygen-exchange properties are now well known^{9,10}. Other perovskites have been studied for use in the catalytic oxidation of CO and hydrocarbons in auto exhaust, and as fuel cell components¹¹.

Chauvin and Michel^{1,2}, studied three perovskites and found that the greater the oxygen mobility in the structure, the greater is the catalytic activity of the perovskite for the oxidation of CO. Our experiments have now demonstrated that $\text{YBa}_2\text{Cu}_3\text{O}_7$ is a strongly active catalyst in the redox chemiluminescence detector system, and that alcohols are particularly sensitively detected.

EXPERIMENTAL

The chromatographic system used in these studies is shown in Fig. 1. The gas chromatograph was a Hewlett-Packard (Avondale, PA, U.S.A.) Model 5710A that was modified with a Grob-type split/splitless injection port¹³. Analytical separations were made with a 25 m \times 0.32 mm I.D. fused-silica column from Hewlett-Packard with a 5% cross-linked phase of phenylmethylsilicone (0.52 μm film thickness). The column was operated at a linear velocity of 21 cm/s of helium carrier gas.

At D in Fig. 1, the effluent from the column was mixed with NO_2 in a heated, 2-mm I.D. quartz, "T" shaped catalyst chamber. The source (C) of NO_2 was a permeation tube fabricated from fluorinated ethylene propylene (FEP) tubing (Galtek, Chaska, MN, U.S.A.), over which diluent helium was passed. Approximately 10 mg of the $\text{YBa}_2\text{Cu}_3\text{O}_7$ catalyst was held in place by plugs of quartz wool at either end of the 3-mm long catalyst bed in the tube. The reduction of NO_2 and oxidation of analyte occurs rapidly on the catalyst bed in the reaction zone, and the NO produced is detected downstream in the ozone reaction chamber (F) of a Model 207 redox chemiluminescence detector (Sievers Research, Boulder, CO, U.S.A.).

The flow of NO_2 in helium was controlled by adjusting a needle valve (E) downstream of the catalyst zone and was measured with a flow meter (B) (Brooks Instrument, Hatfield, PA, U.S.A.) that had been previously calibrated. Flow-rates ranged from 3.5 to 36.5 ml/min when the helium head pressure was set at 4 p.s.i.g. The NO_2 was research purity grade (Matheson, Secaucus, NJ, U.S.A.), and was purged with oxygen at approximately 0°C to oxidize any residual NO to NO_2 , prior to filling a permeation device that was constructed from 2 mm I.D., 6 mm O.D. FEP. At room temperature the permeation device supplies a constant mass of NO_2 per unit time that

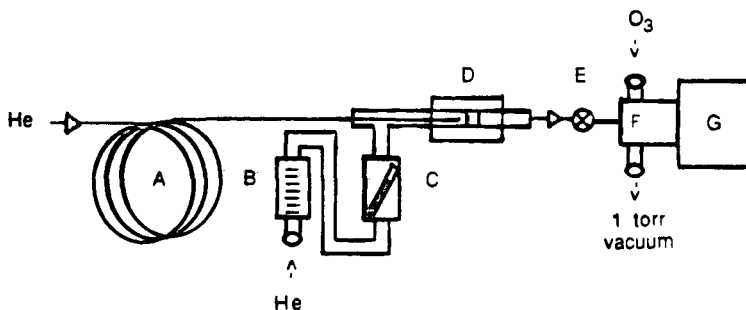


Fig.1. Experimental apparatus: (A) gas chromatography column, (B) flow meter to measure the rate of helium make-up gas flow over the NO_2 permeation tube, (C) NO_2 permeation tube, (D) reaction zone containing the catalyst bed in a quartz tube surrounded by a heater block, (E) needle valve to control the flow of make-up gas through the reaction zone, (F) NO- O_3 chemiluminescence chamber, (G) photomultiplier tube and electronics of the Model 207 RCD.

yields a concentration of about 200 ppm when the flow of diluent gas is maintained at approximately 30 ml/min.

The helium used as NO₂ diluent and column carrier (U.S. Welding, Denver, CO, U.S.A.) was purified by scrubbing with Hopcalite (Mine Safety Appliances, Pittsburgh, PA, U.S.A.) to remove CO, R3-11 copper catalyst (Chemical Dynamics, South Plainsfield, NJ, U.S.A.) to remove oxygen, and molecular sieve 4A (Fisher Scientific, Fair Lawn, NJ, U.S.A.) to remove water.

The chemicals used in the test mixture were obtained from the following vendors: methyl *tert.*-butyl ether (MTBE) (97%), toluene (99+%), and 1-octene (97%) were obtained from Aldrich (Milwaukee, WI, U.S.A.). Benzene (99%) and methanol (certified ACS Spectranalyzed grade) were obtained from Fisher Scientific, ethanol (absolute) from AAPER Alcohol and Chemical Co. (Shelbyville, KY, U.S.A.), *tert.*-butanol (analytical-reagent grade from Mallinckrodt (St. Louis, MO, U.S.A.), methylcyclohexane from J. T. Baker (Phillipsburgh, NJ, U.S.A.), octane from Eastman-Kodak (Rochester, NY, U.S.A. and isooctane (2,2,4-trimethylpentane) from EM Science (Gibbstown, NJ, U.S.A.). The benzene used as solvent in the dilutions of ethanol for detection limit studies was pesticide quality obtained from MCB (Norwood, OH, U.S.A.).

Additional studies of catalyst materials were performed with a system that allowed for continuous flow of NO₂ and/or an organic compound over the catalyst⁶. The products of reactions that occurred were monitored by mass spectrometry. High-purity grade helium (O₂ less than 5 ppm, v/v) was used as the diluent gas in these studies. The temperature of the catalyst was maintained with a modified oven control unit from a Hewlett-Packard Model 402 gas chromatograph. Downstream of the catalyst, a portion of the flow was diverted to a Hewlett-Packard Model 5980A mass spectrometer that had been modified to allow for direct introduction of the sample into the ion source. The remaining flow was sampled to determine NO concentrations by a Sievers Research Model 207 redox chemiluminescence detector.

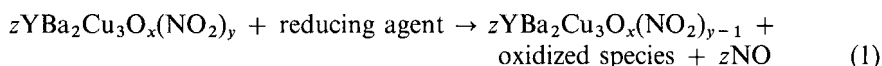
The chemicals used to synthesize the catalyst were 99.9% Y₂O₃ (American Potash and Chemical Co., West Chicago, IL, U.S.A.), BaCO₃ (Mallinckrodt) and CuO (J. T. Baker). The superconductor catalyst was prepared by a solid-state reaction of powders of the compounds listed above using established techniques¹⁰. Presence of the superconducting phase was verified by observation of the Meissner effect, in which a sample of the material is repelled by a magnet at temperatures below the superconducting transition temperature. Analysis by X-ray diffraction indicated the presence of the superconducting, orthorhombic phase.

RESULTS AND DISCUSSION

The catalytic reactions that occur in a redox chemiluminescence detector determine the selectivity of the detector; thus, studies of new catalysts are important for the development of new applications for this detector. Oxidation of CO and organic compounds on various perovskites has been investigated and reviewed¹¹. Other mechanistic studies indicate that a two-step redox mechanism often plays a major role in the catalytic oxidation of compounds over perovskites^{14,15}. In the first step, lattice or adsorbed oxygen is responsible for the catalytic oxidation. Regeneration of the oxygen vacancy occurs in the second step as the catalyst is reoxidized by molecular oxygen in the gas phase.

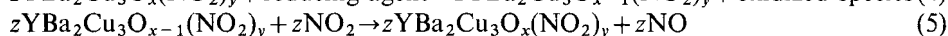
In our present system, our studies indicate that NO_2 can act as the oxidant that regenerates the oxidized lattice. When excess NO_2 is allowed to react with ethanol over this catalyst, oxidation occurs at a temperature identical to that at which it occurs in the absence of NO_2 . The yields and identities of product are also the same for NO_2 oxidation as for O_2 oxidation, except that substantial amounts of NO are also produced as the oxidation occurs. These results suggest that the superconducting perovskite may act catalytically in two different ways. In one way (reactions 1–3), the perovskite may promote the direct oxidation of analytes by lattice NO_2 , under similar conditions as employed for reaction with lattice oxygen. In the other (reactions 4–6), the redox reaction may occur directly with the oxide catalyst to form an oxygen vacancy which is then cyclically refilled in a second step by reaction with NO_2 . After exposure to NO_2 in the analytical system the catalyst is still superconducting, as evidenced by observation of the Meissner effect. However, the resulting material is different from $\text{YBa}_2\text{Cu}_3\text{O}_7$, and has NO_2 incorporated into the lattice. Temperature-programmed desorption mass spectrometry experiments indicate that the stoichiometry of this material is $\text{YBa}_2\text{Cu}_3\text{O}_x(\text{NO}_2)_y$, where $x = 7.4 \pm 0.4$ and $y = 1.3 \pm 0.2$ (ref. 16).

Reactions 1–3:



In these reactions z is determined by the extent of reduction in reaction 1. In reaction 1, the analyte eluting from the chromatographic column reacts directly with NO_2 at the catalyst surface and becomes oxidized, creating an NO_2 vacancy and generating NO which is measured by chemiluminescence (reaction 3). In reaction 2, NO_2 refills the vacancy.

In reactions 4–6, the catalyst acts as an oxidizing agent:



In reaction 4, the analyte reacts at the catalyst surface to form an oxygen vacancy, and becomes oxidized. In reaction 5 the oxygen vacancy is re-filled with oxygen by NO_2 reacting with the catalyst to form NO . Reaction 6 occurs outside the catalyst chamber in front of the photomultiplier tube (F in Fig. 1), where the NO formed by each analyte reacts with ozone to produce chromatographic peaks.

The size of each peak is related to the amount of the analyte, and the yield of O or NO_2 vacancies it created under the conditions in the catalyst chamber (D). Compounds that have been tested in this system and produce a relatively large response include methanol, ethanol, *tert.*-butanol, MTBE, 1-octene, toluene, ammonia, acetaldehyde, acetone, methylethylketone, cyclohexene, acetonitrile and nitromethane. Hydrogen and carbon monoxide produce weak responses in this system.

Chromatographic studies

A mixture of the following composition (prepared by volumetric dilution) was studied to provide information about selectivity of response to various classes of compounds: methanol, 0.1%; ethanol, 0.1%; *tert.*-butanol, 0.1%; MTBE, 5.0%; benzene, 5.0%; isooctane (2,2,4-trimethylpentane), 73.7%; methylcyclohexane, 5.0%; 1-octene, 1.0%; toluene, 5.0%; and octane, 5.0%. These compounds are present in various commercially available gasolines. In a test program, either 10% ethanol or 8% MTBE is being added to gasolines in Colorado in order to evaluate the effect of these additives on reducing the ambient concentration of CO resulting from automobile exhaust, so a rapid method for checking the concentration of either of these is needed. Oxygenates in feedstocks also poison some catalysts, so the detection of alcohols in hydrocarbon matrices is important.

A systematic study was made of the effect of catalyst temperature and flow-rate through the catalyst on the detector response for each component in the mixture. Flow-rates through the catalyst bed were varied from 3.5 to 36.5 ml/min at a catalyst temperature of 325°C in one set of experiments, and, in another set, the catalyst temperature was varied from 200 to 375°C with the flow-rate fixed at 6.0 ml/min. The chromatographic separations were all performed isothermally and with split injections of the sample at a split ratio of 25:1.

Effects of flow-rate

Two important experimental conditions are dependent on the flow-rate of helium in the system. The permeation device emits a constant amount of NO₂ per unit time; therefore, the concentration of NO₂ in the flow stream is dependent on the rate of helium flow. The flow-rate of gas over the catalyst bed also affects the residence time of reactants in the reaction zone of the detector. For all compounds studied, an increase in the flow-rate of NO₂ in helium through the catalyst zone caused a decrease in the observed chemiluminescence response, without altering the order of relative responses. However, the degree of selectivity with which certain compounds respond is highly dependent on the flow-rate. These data, relative to the response for benzene, are shown in Table I. Above a flow-rate of 18.8 ml/min, benzene response was not detectable. The data were calculated as photon counts per mole of analyte/photon counts per mole of benzene. Relative standard deviations for replicate measurements ranged from 1 to 10% for the various compounds. The absolute responses of the alcohols decrease less with increased flow than any of the other compounds. Since the relative rates of reactions determine, in part, the relative responses, it can be concluded that the response of the alcohols suffers least from shorter catalyst contact time at the higher flow-rates because they react most rapidly.

Effects of catalyst temperature

Selectivity of response factors for each compound studied, relative to benzene, as a function of catalyst temperature are listed in Table II. The ratios were calculated from area responses on a molar basis (integrated photon counts per mole). Typical relative standard deviations for replicate measurements of the components of the test mixture using the peak area percent for each compound ranged from 2 to 10%, with benzene often showing the highest variability because it produces the smallest peak in the chromatogram. With a make-up gas flow-rate of 6.0 ml/min and a catalyst

TABLE I

THE EFFECT OF MAKE-UP REAGENT GAS FLOW-RATE ON SELECTIVITY OF DETECTOR RESPONSE TO VARIOUS ANALYTES AT 325°C

Compound	Flow-rate through the catalyst (ml/min)		
	3.5	6.0	18.8
Methanol	50	153	200
Ethanol	182	379	582
<i>tert.</i> -Butanol	452	839	1430
MTBE	28	31	22
Benzene	1	1	1
Methylcyclohexane	6	10	5
1-Octene	207	227	253
Toluene	51	48	59
<i>n</i> -Octane	17	16	12

TABLE II

THE EFFECT OF TEMPERATURE ON SELECTIVITY OF DETECTOR RESPONSE TO ANALYTES AT A MAKE-UP GAS FLOW-RATE OF 6.0 ml/min

Compound	Temperatures of catalyst (°C)				
	275	300	325	350	375
Methanol	264	138	153	158	147
Ethanol	681	408	379	366	383
<i>tert.</i> -Butanol	1180	819	839	879	890
MTBE	32	28	31	35	30
Benzene	1	1	1	1	1
Methylcyclohexane	9	8	10	9	7
1-Octene	191	182	227	227	241
Toluene	47	45	48	49	54
<i>n</i> -Octane	19	15	16	13	11

temperature of 275°C the relative standard deviations of the peak areas were: methanol, 6.9%; ethanol, 5.6%; *tert.*-butanol, 4.7%; MTBE, 2.8%; benzene, 8.6%; methylcyclohexane, 4.0%; 1-octene, 3.5%; toluene, 3.5%; *n*-octane, 3.5%. At temperatures below 225°C, benzene was not detectable; therefore, the data for selectivity are tabulated starting at 275°C. The alcohols were most selectively detected at 225°C, because at higher temperatures, the other compounds studied produced proportionately larger peaks than the alcohols. Changes in selectivity ratios with temperature are greatest for the alcohols and 1-octene, while the other compounds studied show only small changes in the selectivity.

The components in the mixture all exhibited a maximum response at 325°C and a slight decrease in response with increased temperature above 325°C. While this was not expected, it may arise from partial loss of the most active O or NO₂ in the superconductor catalyst at higher temperatures. Temperature-programmed desorption experiments have shown that NO₂ and O₂ begin to evolve from the catalyst at

350°C. This results in lower concentrations of active oxidants in the catalyst at these temperatures, which may result in lower yields of NO.

The most sensitively detected compounds were the alcohols. Toluene, 1-octene and MTBE also responded, but much less sensitively than the alcohols, at a catalyst temperature of 200°C. Methylcyclohexane responded when the catalyst temperature was raised to 225°C, while the remaining compounds in the mixture responded only at 250°C or greater. For the oxygenated compounds studied at temperatures below 325°C, the responses observed for MTBE and *tert.*-butanol were more dependent upon the temperature of the catalyst than were those observed for methanol and ethanol. At 200°C the response for ethanol is 100-fold greater than that for MTBE and 10-fold greater than that for *tert.*-butanol. However, at 325°C, the response for ethanol is only 10-fold greater than that for MTBE and half that for *tert.*-butanol. This order of relative responses is maintained at catalyst temperatures of 300°C and above. The order of response for all compounds studied (area counts/mole) at 300°C is: *tert.*-butanol > ethanol > 1-octene > methanol > toluene > MTBE > *n*-octane > methylcyclohexane > isooctane > benzene.

It is interesting to compare the selectivity of the catalytic reactions for alcohols and MTBE with those for octane and methylcyclohexane, because it is desirable to detect these oxygenated compounds in the presence of hydrocarbons. The alcohols and MTBE are detected most selectively, relative to *n*-octane and methylcyclohexane at 225°C; however, peaks tend to be broader at the lower temperatures.

Detection limit for ethanol

The limit of detection for ethanol was determined using splitless injection techniques with samples of known amounts of ethanol in benzene. The standards were prepared volumetrically by serial dilution of stock solutions of ethanol in benzene. At 325°C, with a reagent gas flow-rate of 6.0 ml/min, the detection limit (signal-to-noise ratio = 3) was 0.5 ng of ethanol. If the oxidation of ethanol is complete, producing only CO₂ and H₂O, then 6 mol NO per mol ethanol should be produced if this is the only reaction product. Although the mechanism for oxidation of ethanol on superconductor catalyst is unknown, we have investigated the reaction by mass spectrometric techniques and have shown the reaction products to be CO₂ and H₂O although some acetaldehyde formation was observed at low catalyst temperatures.

Analysis of gasoline for MTBE

A sample of a commercial gasoline containing 8% MTBE by volume was analyzed by redox chemiluminescence detection, employing YBa₂Cu₃O₇ as the catalyst, at 325°C (Fig. 2). Temperature programmed chromatography was used for the analysis of this sample. Split injections (30:1) of undiluted gasoline samples were made at an initial oven temperature of 25°C for 6 min, and subsequently programmed at 8°C per min to a final temperature of 150°C.

The sensitivity of the system to isooctane, octane and methylcyclohexane decreases more rapidly at higher flows than does the sensitivity for MTBE; therefore, higher make-up gas flows may be used advantageously to detect MTBE selectively in the complex hydrocarbon matrices of gasolines. The selectivity factor for MTBE compared to methylcyclohexane at the highest flow-rate studied (36.5 ml/min) was its greatest value of 3.65, compared to a value of 2.25 at a flow-rate of 3.5 ml/min. Neither

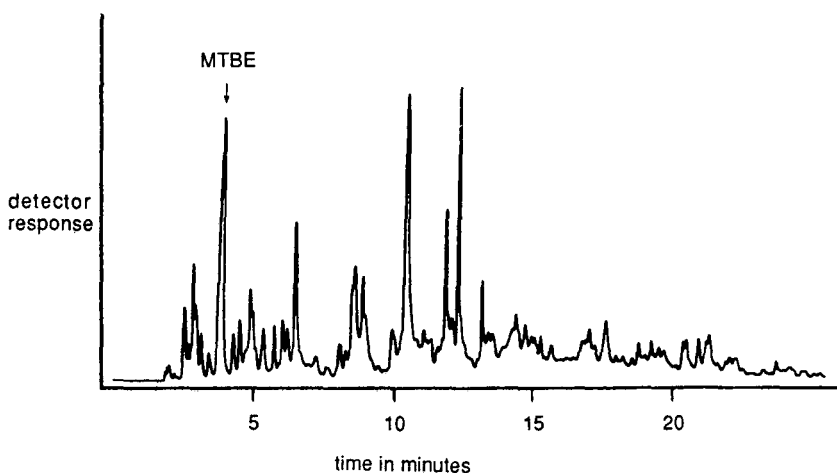


Fig. 2. Chemiluminescence detection of methyl *tert.*-butyl ether in a commercial gasoline sample.

isooctane nor octane was detected at the highest flow-rate. The chromatogram shown in Fig. 2 was obtained using a make-up gas flow-rate of 18.8 ml/min. By Colorado law, the concentration of MTBE in the gasoline is required to be 8% (v/v) during the wintertime when atmospheric inversions are common. The area of the peak for MTBE is the largest of any peak in the chromatogram. The percent response for this peak, based on peak height, in the matrix was reproducible within $\pm 8\%$ relative S.D. for four determinations that were made over a period of two days.

CONCLUSIONS

The perovskite, $\text{YBa}_2\text{Cu}_3\text{O}_7$, exhibits strong catalytic activity, particularly toward oxidation of alcohols and other organic compounds in reactions with NO_2 to form NO. The selectivity of the catalyst can be modified by changing the temperature or the flow-rate of the reagent gas to selectively detect compounds of interest. The response to *tert.*-butanol is 1000 times greater than to benzene. Olefins and alkyl-aromatic compounds are detected with greater sensitivity than benzene or aliphatic hydrocarbons measured in gasoline with this detector.

ACKNOWLEDGEMENTS

The support of the National Science Foundation under Grant ATM-8618793 to the University of Colorado is gratefully acknowledged. The loan of a redox chemiluminescence detector by Sievers Research, Boulder, CO, U.S.A. and partial financial support is acknowledged. We also acknowledge B. Hybertson and B. Hansen for supplying the superconductor material used as catalyst, and J. J. DeAngelis for advice and valuable suggestions.

REFERENCES

- 1 M. Dressler, *Selective Gas Chromatographic Detectors (Journal of Chromatography Library, Vol.36)*, Elsevier, Amsterdam, 1986, p. 312.
- 2 S. A. Nyarady, R. M. Barkley and R. E. Sievers, *Anal. Chem.*, 57 (1985) 2074.
- 3 S. A. Nyarady and R. E. Sievers, *J. Am. Chem. Soc.*, 107(1985) 3726.
- 4 R. E. Sievers, S. A. Nyarady, R. L. Shearer, J. J. DeAngelis and R. M. Barkley, *J. Chromatogr.*, 349 (1985) 395.
- 5 R. S. Hutte, R. E. Sievers and J. W. Birks, *J. Chromatogr. Sci.*, 24 (1986) 499.
- 6 N. Pourreza, S. A. Montzka, R. M. Barkley, R. E. Sievers and R. S. Hutte, *J. Chromatogr.*, 399 (1987) 165.
- 7 R. E. Sievers, R. L. Shearer and R. M. Barkley, *J. Chromatogr.*, 395 (1987) 9.
- 8 S. Montzka and R. Sievers, *Chromatography*, 2 (1987) 22.
- 9 M. Wu, J. Ashburn, C. Torng, P. Hor, R. Meng, L. Gao, Z. Huang, Y. Wang and C. Chu, *Phys. Rev. Lett.*, 58 (1987) 908.
- 10 J. M. Williams, M. A. Beno, K. Carlson, U. Geiser, H. C. I. Kao, A. M. Kini, L. C. Porter, A. J. Schultz, R. J. Thorn, H. H. Wang, M. H. Whangbo and M. Evain, *Acc. Chem. Res.*, 21 (1988) 1.
- 11 R. J. H. Voorhoeve, in J. J. Burton and R. L. Garten (Editors), *Advanced Materials in Catalysis*, Academic Press, New York, 1977, pp. 129–180.
- 12 C. Chauvin and C. Michel, *Mater. Chem. Phys.*, 13 (1985) 197.
- 13 K. Grob and K. Grob, Jr., *J. High Resolut. Chromatogr. Chromatogr. Commun.*, 1 (1978) 57.
- 14 T. Nakamura, M. Misono and Y. Yoneda, *J. Catal.*, 83 (1983) 151.
- 15 B. Viswanathan and S. George, *Indian J. Tech.*, 23 (1985) 470.
- 16 S. A. Montzka, B. M. Hybertson, R. M. Barkley and R. A. Sievers, submitted for publication.

CHROM. 20 623

MIGRATION OF TETRAHYDROISOQUINOLINE, A POSSIBLE PARKINSONIAN NEUROTOXIN, INTO MONKEY BRAIN FROM BLOOD AS PROVED BY GAS CHROMATOGRAPHY-MASS SPECTROMETRY

TOSHIMITSU NIWA

Department of Internal Medicine, Nagoya University Branch Hospital, Higashi-ku, Nagoya 461 (Japan)

NAOHITO TAKEDA and AKIRA TATEMATSU

Faculty of Pharmacy, Meijo University, Tempaku-ku, Nagoya 468 (Japan)

SADAO MATSUURA

Department of Chemistry, College of General Education, Nagoya University, Chikusa-ku, Nagoya 464 (Japan)

MITSUO YOSHIDA

Department of Neurology, Jichi Medical School, Minami Kawachi, Tochigi-ken 329-04 (Japan)

and

TOSHIHARU NAGATSU*

Department of Biochemistry, Nagoya University School of Medicine, 65 Tsurumai-cho, Showa-ku, Nagoya 466 (Japan)

SUMMARY

1,2,3,4-Tetrahydroisoquinoline (TIQ) was quantitated by use of gas chromatography-mass spectrometry in brains and livers of marmosets which showed parkinsonism after daily subcutaneous injection of TIQ. TIQ showed greatly increased levels in the brains and livers of the TIQ-treated marmosets, with no detectable metabolites of TIQ. TIQ was present as an endogenous amine in the brains and livers of saline-treated marmosets at very low concentrations. It thus seems that TIQ can pass easily through the blood-brain barrier but cannot be metabolized in the brain or the liver. It is possible that TIQ accumulated in the brain may produce parkinsonism.

INTRODUCTION

Since a highly selective, irreversible neurotoxin, 1-methyl-4-phenyl-1,2,3,6-tetrahydropyridine (MPTP) that produces parkinsonism in humans, monkeys and mice¹⁻⁴ was discovered, an extensive search has been undertaken for endogenous or exogenous compounds that induce Parkinson's disease.

We screened of various compounds structurally related to MPTP for neurotoxicity by assaying the inhibition of the tyrosine hydroxylase system in tissue slices of the striatum⁵⁻⁷. After this screening, 1,2,3,4-tetrahydroisoquinoline (TIQ) and N-methyl-1,2,3,4-tetrahydroisoquinoline (N-Me-TIQ) were suggested as possible

endogenous neurotoxins^{8–10}. TIQ has been recently discovered in rat brain¹¹, and in the parkinsonian and normal human brains¹². Repeated administration of TIQ to marmosets produced parkinsonian symptoms with reduction in tyrosine hydroxylase, dopamine and total bipterin concentrations in the substantia nigra¹³. To determine whether subcutaneously administered TIQ can pass through the blood–brain barrier, and whether TIQ can be metabolized in the brain and liver, we analysed the brains and livers of the TIQ-treated marmosets by use of gas chromatography–mass spectrometry (GC–MS).

EXPERIMENTAL

Chemicals

TIQ was purchased from Wako, and heptafluorobutyric anhydride (HFBA) from Gasukuro Kogyo.

A mixture of 1,3,4-trideutero-1,2,3,4-tetrahydroisoquinoline ($[^2\text{H}_3]\text{TIQ}$) and 1,3,4,4-tetradeutero-1,2,3,4-tetrahydroisoquinoline ($[^2\text{H}_4]\text{TIQ}$) was synthesized by a modified method of Wedekind and Oechslen¹⁴. Isoquinoline (1.29 g, 10 mmol) was dissolved in 37% deuterium chloride (15 g, deuterium content 99%) and stirred with tin powder at 60°C for 8 h, until the absorption at 325 nm had disappeared. The excess tin was removed by filtration, and the filtrate was evaporated to dryness. Water was added to the residue, and the mixture was made alkaline with sodium hydroxide and extracted with chloroform. The chloroform solution was then extracted with 2 *N* hydrochloric acid, and the extract was evaporated to dryness. The residue, after treatment with ethanol, gave the product as small prisms, 244 mg (18% yield), m.p. 174–177°C with decomposition. The synthesized compound was found to be a mixture of $[^2\text{H}_3]\text{TIQ}$ (47.5%), $[^2\text{H}_4]\text{TIQ}$ (47.5%), and TIQ (5%) by GC–MS. The structures of $[^2\text{H}_3]$ - and $[^2\text{H}_4]\text{TIQ}$ was assigned by ¹H NMR spectroscopy.

All the other chemicals used were of analytical grade.

Samples

Brains and livers were obtained from four marmosets¹³: A, a 2.1-year-old male weighing 435 g; B, a 2.8-year-old female weighing 470 g; C, a 2.5-year-old male weighing 370 g; and D, a 2.6-year-old female weighing 530 g. Saline alone was injected subcutaneously once a day for 16 days into A and B; TIQ was injected subcutaneously at a dose of 50 mg/kg once a day for 16 days into C and D. TIQ (1 g) was suspended in 20 ml of saline. Since TIQ does not dissolve in saline, the suspension was made by shaking the container just before injection. For GC–MS analysis, all four marmosets were sacrificed under deep ketamine-induced anesthesia on the 16th day of daily injection of either saline or TIQ. Brains and livers were immediately removed, and kept at –80°C until GC–MS analysis could be performed.

Sample preparation

To quantitate the TIQ levels in the brains and livers of TIQ-treated marmosets, tissue (0.5 g) was spiked with 50 µg of a mixture of $[^2\text{H}_3]\text{TIQ}$ and $[^2\text{H}_4]\text{TIQ}$ as an internal standard, and homogenized with 0.4 *N* perchloric acid (10 ml) containing EDTA (0.1% w/v) and ascorbic acid (0.1% w/v). To quantitate the TIQ levels in the brains and livers of saline-treated marmosets, tissue (0.5 g) was spiked with 50 ng of a

mixture of [$^2\text{H}_3$]TIQ and [$^2\text{H}_4$]TIQ as an internal standard and then homogenized likewise. To profile the amines in the brain and liver, the tissue sample was homogenized without addition of deuterated TIQ. The homogenate was centrifuged at 12 000 g for 15 min at 4°C. The supernatant was transferred to a glass test-tube and the pellet was vortexed with 0.4 N perchloric acid (10 ml) containing EDTA (0.1%) and ascorbic acid (0.1%) and centrifuged again. The combined supernatant was extracted with diethyl ether (10 ml). The aqueous phase was adjusted to pH 11 with 6 N sodium hydroxide and extracted twice with dichloromethane (10 ml). The organic phase was dehydrated over anhydrous sodium sulphate, and the filtrate was evaporated to dryness under a stream of nitrogen. The residue was dissolved in ethyl acetate-HFBA (20 μl :20 μl), and derivatized at 70°C for 30 min.

Gas chromatography-mass spectrometry

A Shimadzu GC-9A gas chromatograph combined with a double-focusing mass spectrometer (Shimadzu 9020-DF) was used. The chromatograph was equipped with an OV-1 bonded fused-silica capillary column (25 m \times 0.25 mm I.D.) and a moving-needle type solventless injector. The injection temperature was 280°C, and the column temperature was programmed from 130°C to 190°C at 3°C/min. Electron-impact ionization (EI) mass spectra were recorded at an ionizing energy of 70 eV, an ion source temperature of 250°C, a trap current of 60 μA , and an accelerating voltage of 3 kV.

Quantification of TIQ by GC-MS

To quantitate TIQ in the brains and livers of TIQ-treated marmosets, mass chromatography was carried out using 50 μg of a mixture of [$^2\text{H}_3$]TIQ and [$^2\text{H}_4$]TIQ as an internal standard, and the molecular ions of TIQ (m/z 329) and [$^2\text{H}_3$]TIQ (m/z 332) were monitored. A calibration line relating the concentration of TIQ to the peak-area ratio of TIQ at m/z 329 to the internal standard ([$^2\text{H}_3$]TIQ) at m/z 332 was obtained from the mass chromatograms. The correlation coefficient of the calibration line for concentrations of TIQ ranging from 10 μg to 500 μg per 0.5 g of tissue was 0.9997.

To quantitate TIQ in the brains and livers of saline-treated marmosets, selected-ion monitoring (SIM) was performed using 50 ng of a mixture of [$^2\text{H}_3$]TIQ and [$^2\text{H}_4$]TIQ as an internal standard. A calibration line relating the concentration of TIQ to peak area ratio of TIQ at m/z 329 to the internal standard ([$^2\text{H}_3$]TIQ) at m/z 332 was obtained from the SIM chromatograms. The correlation coefficient of the calibration line for concentrations of TIQ ranging from 5 ng to 300 ng per 0.5 g of tissue was 0.9987.

RESULTS

Fig. 1 shows the gas chromatograms of the HFB-derivatized extracts from the brains of TIQ-injected marmosets (a), and saline-injected marmosets (b). Deuterated TIQ was not added to the tissue homogenate. The EI mass spectrum of peak 1 in Fig. 1a is shown in Fig. 2a. The EI mass spectrum of the HFB-derivatized mixture of [$^2\text{H}_3$]TIQ and [$^2\text{H}_4$]TIQ used as an internal standard is shown in Fig. 2b. Peak 1 was identified as TIQ, since the peak showed a retention time and an EI mass spectrum

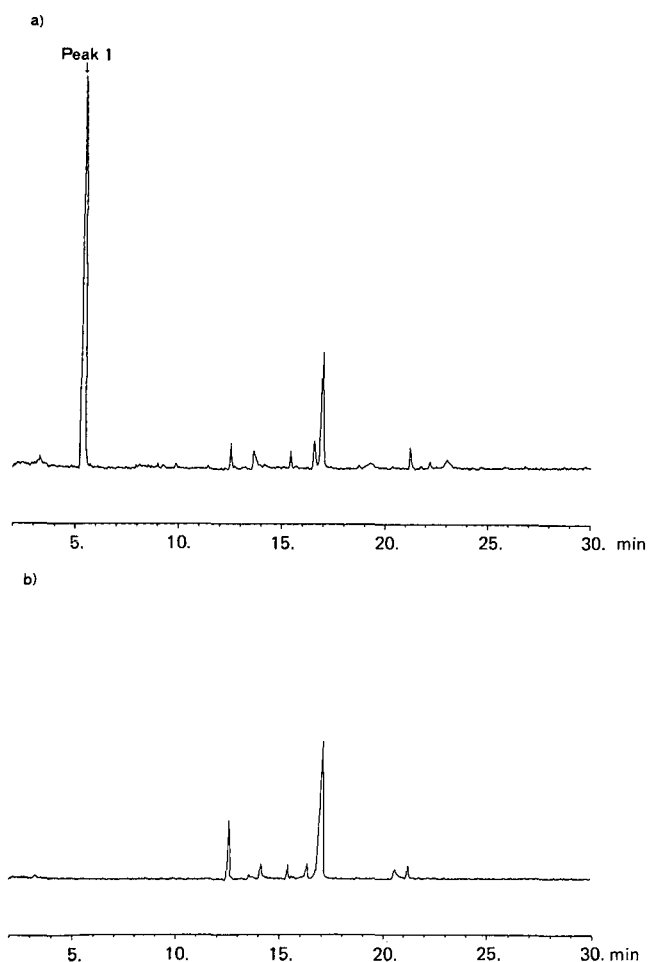


Fig.1. Gas chromatograms of the HFB-derivatized extracts from the brains of TIQ-treated marmosets (a), and saline-treated marmosets (control) (b). Deuterated TIQ was not added to the tissue homogenate. Peak 1 was identified as TIQ. The molecular ion of TIQ (m/z 329) was monitored by mass chromatography.

identical with those of HFB-derivatized TIQ. TIQ was detected in the brains of TIQ-treated marmosets at a high concentration, but no TIQ metabolites were detected.

Fig. 3 shows the gas chromatograms of the HFB-derivatized extracts from the livers of TIQ-treated marmosets (a) and saline-treated marmosets (b). TIQ was also detected in the livers of TIQ-treated marmosets at a high concentration, but no TIQ metabolites were detected.

Table I shows the concentrations of TIQ in the brains and livers of saline-injected and TIQ-injected marmosets. The concentrations of TIQ were greatly increased in the brains and livers of TIQ-treated marmosets. However, TIQ was detected in the brains and livers of saline-treated marmosets at low concentrations.

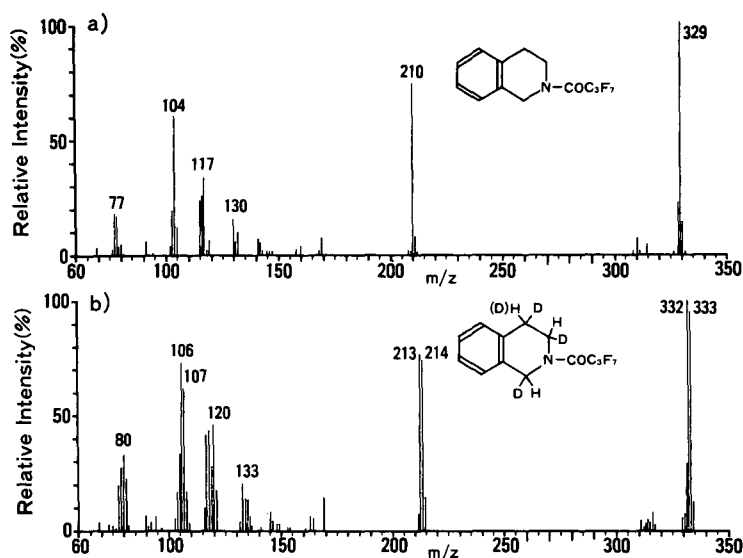


Fig. 2. EI mass spectra of peak 1 in Fig. 1a (a), and the HFB-derivatized mixture of [²H₃]TIQ and [²H₄]TIQ used as an internal standard (b).

DISCUSSION

We have reported the behavioural changes in the marmosets by the administration of TIQ¹³. The TIQ-injected marmosets showed features of parkinsonism, such as akinesia, tremor, and hypertonus. However, the saline-treated marmosets did not show any behavioural change at all. On the 8th day of TIQ injection, the legs of marmoset C had a slight tendency to drag. On the 11th day, a similar behavioural change was observed in marmoset D. The analysis of video recordings of the behavioural changes showed akinesia and hypertonus, which were more severe in marmoset C than in D. However, tremors in arms, legs, and trunk were more severe in D than in C. On the whole, the parkinsonian behavioural changes were more marked in marmoset C than in D. These results can be explained by our observation that the TIQ level in the brain of marmoset C was much higher than in marmoset D.

The concentration of TIQ in the brains of TIQ-injected marmosets was greatly increased, to the same degree as in the livers. This means that TIQ can pass easily through the blood-brain barrier. No metabolites of TIQ, such as 1,2-dihydroisoquinoline, could be detected in the brains or livers of TIQ-treated marmosets. This suggests that TIQ is not a substrate of monoamine oxidase. This result was also confirmed by our *in vitro* studies on TIQ metabolism in rat brains. The incubation of deuterated TIQ with mitochondria fraction or microsome fraction obtained from rat brain did not produce any metabolite of deuterated TIQ according to GC-MS analysis of the incubated medium using the same extraction method as from the marmosets' tissues.

TIQ was also detected as an endogenous amine in the brains and livers of control marmosets at low concentrations. However, there is an argument against the

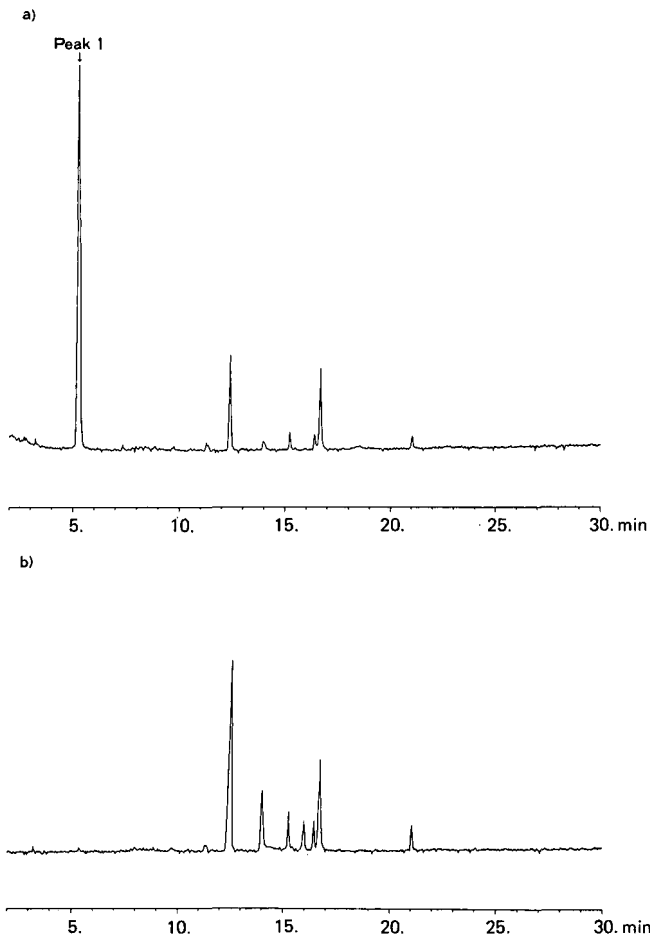


Fig. 3. Gas chromatograms of the HFB-derivatized extracts from the livers of TIQ-treated marmosets (a) and saline-treated marmosets (control) (b). Deuterated TIQ was not added to the tissue homogenate. Peak 1 was identified as TIQ. The molecular ion of TIQ (m/z 329) was monitored by mass chromatography.

TABLE I

CONCENTRATION OF TIQ IN BRAINS AND LIVERS OF MARMOSETS INJECTED WITH SALINE OR TIQ

Monkeys	Concentration of TIQ ($\mu\text{g/g}$ wet tissue)	
	Brain	Liver
<i>Saline (control)</i>		
A	0.149	0.193
B	0.193	0.180
<i>TIQ</i>		
C	201	296
D	149	142

endogenous origin of TIQ, since TIQ could be artifactually formed from N-methylene-phenylethylamine by heptafluorobutyric acid during HFB derivatization (Dr. Boulton, personal communication). We are now investigating whether or not the endogenous TIQ is such an artifact, which may exist endogenously in tissues during the derivatization.

TIQ injected into marmosets could not be metabolized in the liver or brain, passed easily through the blood-brain barrier, then accumulated in the brain, and produced parkinsonian symptoms with reductions of dopamine and biopterin concentrations, and tyrosine hydroxylase activity¹³. Thus, TIQ may be an important endogenous amine that was demonstrated for the first time to produce Parkinson's disease in monkeys. Our results suggest that TIQ, an endogenous neurotoxin, is a candidate for causing Parkinson's disease in human beings.

REFERENCES

- 1 J. W. Langston, P. Ballard, J. W. Tetrud and I. Irwin, *Science (Washington, D.C.)*, 219 (1983) 979.
- 2 R. S. Burns, C. C. Chiueh, S. P. Markey and M. H. Ebert, *Proc. Natl. Acad. Sci. U.S.A.*, 80 (1983) 4546.
- 3 R. E. Heikkila, A. Hess and R.C. Duvoisin, *Science (Washington, D.C.)*, 224(1984) 1451.
- 4 S. P. Markey, J. M. Johannessen, C. C. Chiueh, R. S. Burns and M. A. Herkenham, *Nature (London)*, 311 (1981) 464.
- 5 Y. Hirata and T. Nagatsu, *Neurosci. Lett.*, 68 (1986) 245.
- 6 Y. Hirata and T. Nagatsu, *Brain Res.*, 337 (1985) 193.
- 7 Y. Hirata and T. Nagatsu, *Neurosci. Lett.*, 57 (1985) 301.
- 8 Y. Hirata and T. Nagatsu, *Brain Res.*, 397 (1986) 341.
- 9 Y. Hirata and T. Nagatsu, *Shinkei Kagaku*, 24 (1985) 169.
- 10 T. Nagatsu and Y. Hirata, *Eur. Neurol.*, s1-159 (1986) 1.
- 11 M. Kohno, S. Ohta and M. Hirobe, *Biochem. Biophys. Res. Commun.*, 140 (1986) 448.
- 12 T. Niwa, N. Takeda, N. Kaneda, Y. Hashizume and T. Nagatsu, *Biochem. Biophys. Res. Commun.*, 144 (1987) 1084.
- 13 T. Nagatsu and M. Yoshida, *Neurosci. Lett.*, 87 (1988) 178.
- 14 E. Wedekind and R. Oechslen, *Ber. Dtsch. Chem. Ges.*, 34 (1901) 3986.

CHROM. 20 652

IDENTIFICATION OF THE MORE COMPLEX TRIACYLGLYCEROLS IN BOVINE MILK FAT BY GAS CHROMATOGRAPHY–MASS SPECTROMETRY USING POLAR CAPILLARY COLUMNS

J. J. MYHER, A. KUKSIS* and L. MARAI

Banting and Best Department of Medical Research, University of Toronto, 112 College Street, Toronto M5G 1L6 (Canada)

and

P. SANDRA

Laboratory of Organic Chemistry, State University of Ghent, Ghent (Belgium)

SUMMARY

The fourth most volatile 2.5% molecular distillate of butteroil obtained by redistillation of the most volatile 10% cut was examined by gas chromatography on a polar capillary column (RSL-300) with electron impact and chemical ionization mass spectrometry. For this purpose the distillate was first freed from the acetyldiacylglycerols by thin-layer chromatography on plain silica gel and the remainder resolved into long and short chain length saturates, *cis*- and *trans*-monoenes, dienes and trienes by thin-layer chromatography on silver nitrate–silica gel. The order of gas chromatographic elution was established for more than 100 major and minor species making up the bulk of the molecular distillate. The results were used to derive the quantitative composition of the triacylglycerol species making up the various peaks obtained by polar capillary column gas chromatography of the total molecular distillate, which closely resembles the lower half of the molecular mass distribution of whole bovine milk fat.

INTRODUCTION

Ruminant milk fat represents one of the most complex mixtures of natural fatty acid esters of glycerol. Because of the high molecular mass and closely similar chemical and physical properties they have yielded even to partial chromatographic separation with great difficulty. The fatty acids range in chain length from C₂ to C₂₄, including odd carbon numbers, and in unsaturation from one to four double bonds, including *cis* and *trans* isomers¹. In addition, one to four methyl branches may be present on the fatty chains. Commonly about 25 different fatty acids are distinguished, which could theoretically yield 15 625 different triacylglycerols. Since many of the milk fat triacylglycerols are represented only as one of the two possible enantiomers^{2,3} the number of species would be reduced by as much as one half. Furthermore, several of the fatty acids are present in small quantities only and are not readily detected in a total

mixture even after interesterification with other fatty acids in the triacylglycerol molecules. In the past ruminant milk fat triacylglycerols have been resolved on the basis of carbon number using short non-polar packed^{4,5} or capillary⁶ gas chromatographic (GC) columns. The use of long non-polar capillary columns results in a considerable splitting of the peaks within most carbon numbers^{7,8}. However, none of these separations is suitable for triacylglycerol identification because each of the peaks contains many molecular species. GC of butterfat triacylglycerols on polar packed⁹ and capillary¹⁰ columns has led to a separation of the triacylglycerol peaks on the basis of both carbon and double bond number, which are readily recognized and quantitated. An extensive separation of peaks within each of the lower carbon numbers is also obtained⁹. As a result many peaks contain two or more major molecular species when total ruminant milk fat is chromatographed prohibiting exact identification and quantitation of any triacylglycerol species.

The present study reports the identification and quantitation of the major molecular species of triacylglycerols in a molecular distillate of butteroil using a combination of thin-layer chromatography (TLC) on silver nitrate-silica gel, polar and non-polar capillary GC and mass spectrometry (MS). A progressive preliminary segregation of the triacylglycerols into small groups of molecular species having well defined chemical differences, and introducing restrictions into the types of possible molecular species that could be present in a specific GC peak, was found to be essential for an unequivocal identification and quantitation of the GC peaks.

EXPERIMENTAL

Milk fats

The fourth most volatile 2.5% distillate, derived by molecular redistillation of the original most volatile 10% cut, had been obtained by distilling 777 pounds of butteroil in 1960 (Distillation Products Industries, Rochester, NY, U.S.A.) and its general properties have been described¹¹. This distillate had been stored either at 4°C or -2°C for *ca.* 25 years prior to the present analyses. The sample of total butterfat was from another earlier analysis⁹. Synthetic *rac*-1,2-dipalmitoyl-3-acetyl, 1,3-dipalmitoyl-2-acetyl, *rac*-1,2-dipalmitoyl-3-butyryl and 1,3-dipalmitoyl-2-butyrylglycerols were prepared in the laboratory¹², while the monoacid triacylglycerols ranging in carbon number from C₂₄ to C₅₄ were prepared by mixing synthetic triacylglycerols of 99%+ purity obtained from NuChek Prep., Elysian, MN, U.S.A. Standards of common fatty acids along with a special Mix 110 containing normal and branched (iso and anteiso) odd and even carbon number saturated fatty acids were obtained from Supelco, Bellefonte, PA, U.S.A.

Solvents and reagents

All solvents were analytical-reagent grade. Hexane, chloroform, acetonitrile and propionitrile were of chromatographic quality. Acidified methanol and *n*-butanol for transesterification of fatty acids were prepared by addition of 5 ml of sulfuric acid to 100 ml of the anhydrous alcohol.

Thin-layer chromatography

TLC was performed on either plain silica gel (G and H, Merck, Darmstadt,

F.R.G.) or on silica gel containing 15% silver nitrate (home made) using 20 × 20 cm glass plates containing a 0.25-mm thick layer prepared in the laboratory. The acetyldiacylglycerols were resolved from the rest of the triacylglycerols in the distillate by chromatography on plain silica gel using hexane–ethyl acetate (88:1) as the developing solvent¹³. The lipid bands representing the acetates and the other triacylglycerols were located by spraying the plates with fluorescein and viewing them under UV light (254 nm). The triacylglycerols were recovered from the silica gel by extraction with chloroform–methanol (2:1). The remainder of the triacylglycerols were resolved into long and short chain lengths saturates, *trans*- and *cis*-monoenes, dienes containing two monoenoic fatty acids, and dienes plus trienes, which were retained at the origin, using chloroform (plus 0.75% ethanol preservative) as the developing solvent¹⁴. The triacylglycerol bands were located and extracted as above.

Gas chromatography

The GC analyses of triacylglycerols were done on a Hewlett-Packard Model 5880A gas chromatograph equipped with a hydrogen flame ionization detector and an on-column injector (Hewlett-Packard, Palo Alto, CA, U.S.A.). Analyses by carbon number were performed using a flexible quartz column (8 m × 0.32 mm I.D.) coated with a permanently bonded non-polar SE-54 liquid phase (Hewlett-Packard) as previously described for plasma lipid extracts¹⁵. Analyses by carbon and double bond number were performed using a flexible quartz column (25 m × 0.25 mm I.D.; RSL-300) custom-made by one of us (P.S.). It was conditioned under hydrogen carrier flow by repeatedly programming the oven temperature between 250 and 360°C at 3°C/min in multiprogram-run over a period of 48 h. Samples were injected on-column at 40°C. After 1 min the column was heated ballistically to 290°C. When the microprocessor controller indicated that the column was ready (equilibration time set at 0.5 min) the integration plot was initiated. After an additional 0.5 min the temperature was programmed at 10°C/min to 330°C and then at 2°C/min to 350°C. Single column compensation was used to correct for column bleed. The carrier gas was hydrogen at 0.68 bar. Fatty acid methyl esters were analyzed on a 15 m × 0.32 mm I.D. flexible quartz column (RTx 2330, Supelco) as previously described¹⁶, while the butyl esters were analyzed on the 25 m RSL-300 column using temperature programming (0.5 min after injection at 40°C, 10°C/min to 200°C and then at 5°C/min to 250°C). The carrier gas in all instances was hydrogen at 0.2 bar head pressure.

Gas chromatography–mass spectrometry

The mass spectrometry was performed with a Hewlett-Packard Model 5985B quadrupole instrument interfaced with a capillary gas chromatograph using the above described polar capillary GC column. The samples were injected on-column at 40°C and the temperature allowed to rise to 250°C. The triacylglycerols were resolved by temperature programming from 250 to 340°C at 4°C/min. The transfer line was maintained at 280°C and the ion source at 230°C. Electron impact (EI) spectra were recorded at 70 eV and a hydrogen carrier gas head pressure of 0.34 bar. Chemical ionization (CI) spectra were determined at 210 eV and similar carrier gas head pressure, but the ion source pressure was increased to 0.6 Torr by admitting methane via a separate capillary inlet. Full mass spectra (200–850 mass units) were recorded every 7 s over the entire elution profile. The data were analyzed by means of

a Hewlett-Packard data system (Model HP 1000E) and a graphics terminal (Model HP 2648A) as previously described^{17,18}.

RESULTS

Table I gives the fatty acid composition of the R-4 distillate and of a representative sample of bovine milk fat as obtained by polar capillary GC. In addition to the major even carbon number saturated and unsaturated long chain and the saturated short chain acids, minor amounts of the odd carbon number saturated and unsaturated acids as well as small amounts of branched-chain acids, are also seen in the distillate. Because of the interesterification of the short and long chain fatty acids in

TABLE I

FATTY ACID COMPOSITION OF R-4 DISTILLATE AND OF A REPRESENTATIVE SAMPLE OF BOVINE MILK FAT TRIACYLGLYCEROLS

GC conditions as in text.

<i>Fatty acid*</i>	<i>R-4 distillate (mol%)</i>	<i>Milk fat triacylglycerols (mol%)</i>
4:0	17.32	8.68
6:0	6.58	4.75
8:0	2.25	2.44
10:0	3.12	4.80
10:1	0.44	0.47
11:0	0.01	0.10
12:0	3.03	5.11
13:0	0.10	0.15
14:0 (i)	0.19	0.20
14:0	11.45	12.53
14:1	0.83	0.95
15:0 (i)	0.33	0.36
15:0 (ai)	0.63	0.61
15:0	1.35	1.35
16:0 (i)	0.29	0.23
16:0	29.50	32.71
16:1w9	0.10	0.20
16:1w7	1.17	1.45
17:0 (i)	0.34	0.23
17:0 (ai)	0.45	0.43
Phytanic	0.05	—
17:0	0.67	0.59
17:1	0.31	0.23
18:0 (i)	0.06	0.06
18:0	6.22	7.43
18:1w9 (t)	0.93	1.02
18:1w9 (c)	11.13	11.52
18:2w6	0.82	0.96
18:3w3	0.33	0.29

* i = iso-methyl branched; ai = anteiso-methyl branched; t = *trans*-monounsaturated; c = *cis*-monounsaturated.

butterfat, the selective enrichment of the short chain acids in this fraction is smaller than would have been otherwise anticipated. The distillate also contains small amounts of acetic acid, which is best demonstrated by examining the purified acetate subfraction isolated from the distillate by TLC. The overall composition of the major fatty acids compares closely to previous analyses of the distillate^{9,10}, where many of the minor acids, however, were not determined. The carbon number distributions of the distillate obtained on non-polar capillary column resembled closely the separations obtained previously on non-polar packed columns^{9,10}. On the polar capillary column the total distillate yielded for each carbon number a minimum of two (long chain lengths) to a maximum of eight (short chain lengths) components (see below).

Fig. 1 illustrates the separations obtained for the distillate by TLC on plain silica gel and on silica gel treated with silver nitrate. On the plain gel the triacylglycerols were resolved on the basis of overall polarity, with the acetates retarded more strongly than the butyrates, hexanoates, octanoates and decanoates, which overlapped, while any long chain triacylglycerols migrated ahead. On silver nitrate TLC the triacylglycerols were resolved according to chain length, the number of double bonds and their geometric configuration. The saturates are separated into butyrates (band 2) and all others (band 1), which are clearly resolved from the monoenes and dienes. The monoenes and dienes are divided into the *cis* and *trans* isomers, which overlap with the chain length isomers. Not all of these separations were fully realized. It would be anticipated, however, that the *trans*-monoenes of the non-butyrate would migrate ahead of the *trans*-monoenes of butyrates, which would overlap with the *cis*-monoenes of non-butyrate. The *cis*-monoenes of butyrates would be expected to overlap with the *trans*-dienes of the non-butyrate (band 5). The *cis*-dienes of the butyrates would overlap with any *trans*-trienes of the non-butyrate (band 6), while the *cis*-trienes of the butyrates would remain at the origin (band 7). The anticipated separations were partly confirmed by analysis of the TLC fractions. It is possible that the actual separations were more complex. In any event Table II gives the relative amounts of material recovered from the different TLC bands.

Fig. 2 shows the polar capillary GC resolution of the acetate fraction of the distillate, which was recovered as a minor slow moving component by TLC on plain silica gel (TLC band 3, Fig. 1A). The chromatographic identification of the associations of the major fatty acids in each of the acetate peaks obtained on polar

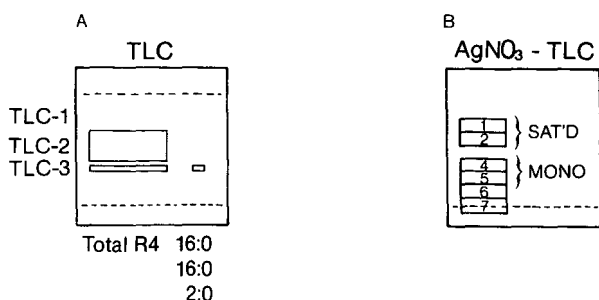


Fig. 1. Fractionation of R-4 butteroil distillate triacylglycerols by TLC on plain (A) and silver nitrate-treated (B) silica gel G. Band identification as shown in figure. TLC conditions: (A) hexane-ethyl acetate (88:1)¹³; (B) chloroform plus 0.75% ethanol preservative (15% silver nitrate).

TABLE II

RELATIVE AMOUNTS OF TRIACYGLYCEROLS RECOVERED FROM SILVER NITRATE TLC RESOLUTION OF R-4 DISTILLATE

TLC conditions as in text.

Silver nitrate TLC fraction	R-4 (%)	Characterization
1	23.7	Saturates; C ₆ and longer chain fatty acids
2	31.3	Saturates; C ₄ and longer chain fatty acids
3	0.0	
4	4.0	Monoenes: 72% <i>trans</i> ; 28% <i>cis</i>
5	32.0	Monoenes: 100% <i>cis</i>
6	5.2	Dienes containing two monoenoic fatty acids
7	3.8	Other dienes and trienes

capillary GC was confirmed by GC-MS. Table III gives the composition of the major molecular species in the acetyldiacylglycerol fraction.

Fig. 3 shows the polar capillary GC profile of band 1 from the silver nitrate TLC. It is made up exclusively of the triacylglycerol species containing two long chain-length saturated fatty acids in combination with one residue of caproic, caprylic or capric

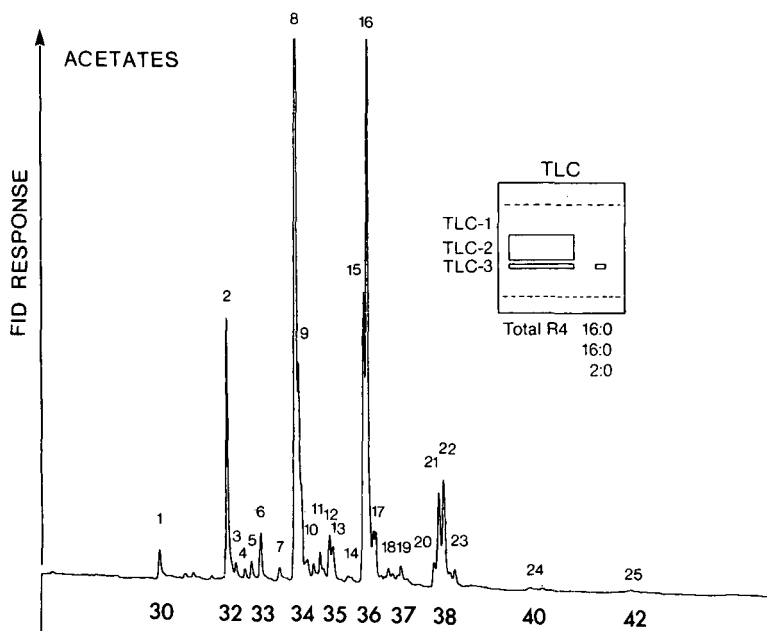


Fig. 2. Polar capillary GC profile of the acetyldiacylglycerol fraction isolated from R-4 butteroil distillate by TLC on plain silica gel. Peak numbers are identified in Table III. GC conditions: instrument, Hewlett-Packard Model 5880; column, 25 m \times 0.25 mm I.D. RSL-300; carrier gas, hydrogen at 0.68 bar head pressure; on-column injection at 40°C, then ballistically heated to 290°C. Integration plot initiated at 290°C, then after 0.5 min oven programmed at 10°C/min to 330°C and then at 2°C to 350°C. Abscissa indicates the carbon number and is linear with time. Peak 22 is eluted in 5.56 min after the start of the integration plot.

TABLE III
COMPOSITION OF THE MAJOR MOLECULAR SPECIES OF ACETYLDIACYLGLYCEROL FRACTION

Peak No.	Species type*	RRT**	Mol%	Major molecular species
1	30 (0, 0, 0)	0.530	0.96	
1a		0.546	0.10	
1b	ai 31 (0, 0, 0)	0.628	0.26	
1c		0.662	0.26	
1d	i 32 (0, 0, 0)	0.737	0.11	
2	32 (0, 0, 0)	0.798	8.08	14, 16, 2 + 12, 18, 2
3		0.831	0.75	
4	i 33 (0, 0, 0)	0.869	0.56	i 15, 16, 2 + i 17, 14, 2
5	ai 33 (0, 0, 0)	0.899	0.80	ai 15, 16, 2 + ai 17, 14, 2
6	33 (0, 0, 0)	0.933	1.80	15, 16, 2 + 17, 14, 2
7	i 34 (0, 0, 0)	1.008	0.78	
7a		1.031	0.23	
8	34 (0, 0, 0)	1.072	21.21	16, 16, 2 + 14, 18, 2
9	34 (0, 0, 1)	1.072	6.85	14, 18:1, 2 + 16:1, 16, 2
9a	34 (shoulder)	1.095		
10		1.110	0.57	
10a		1.121	0.93	
10b	i 35 (0, 0, 0)	1.144	0.87	i 15, 18, 2 + i 17, 16, 2
10c	i 35 (0, 0, 1)	1.159	0.41	i 15, 18:1, 2 + i 17, 16:1, 2
11	ai 35 (0, 0, 0)	1.170	1.25	ai 15, 18, 2 + ai 17, 16, 2
11a	ai 35 (0, 0, 1)	1.185	0.82	ai 15, 18:1, 2 + ai 17, 16:1, 2
12	35 (0, 0, 0)	1.204	1.82	15, 18, 2 + 17, 16, 2
13	35 (0, 0, 1)	1.219	2.22	15, 18:1, 2 + 17, 16:1, 2 + 17:1, 16, 2
14	i 36 (0, 0, 0)	1.279	0.99	
14a	i 36 (0, 0, 1)	1.293	0.78	
15	36 (0, 0, 0)	1.347	8.69	16, 18, 2
16	36 (0, 0, 1)	1.362	17.36	16, 18:1, 2 + 16:1, 18, 2
17	36 (0, 1, 1)	1.385	1.59	16:1, 18:1, 2
17a	36 (0, 0, 2)	1.395	1.68	
17b	i 37 (0, 0, 0)	1.415	0.66	
17c	37 (0, 0, 1)	1.433	0.48	
18	ai 37 (0, 0, 0)	1.444	0.85	ai 17, 18, 2
18a	ai 37 (0, 0, 1)	1.464	0.99	
18b	37 (0, 0, 0)	1.482	0.75	17, 18, 2
19	37 (0, 0, 1)	1.494	1.58	17, 18:1, 2
20	38 (0, 0, 0)	1.629	1.06	18, 18, 2
21	38 (0, 0, 1)	1.648	3.16	18, 18:1, 2
22	38 (0, 1, 1)	1.666	4.14	18:1, 18:1, 2
22a	38 (0, 0, 2)	1.693	0.71	18, 18:2, 2
23	38 (0, 1, 2)	1.712	1.00	18:1, 18:2, 2
23a		1.757	0.31	
24	40		0.84	
25	42		0.58	

* Species type indicated by the total acyl carbon number and, in brackets, the degree of unsaturation of each of the three acyl chains.

** Relative to 14:0 16:0 4:0 on the polar capillary column (RSL-300).

TABLE IV
MAJOR TRIACYLGLYCEROLS FROM SILVER NITRATE TLC BAND 1

Peak No.	Species type*	RRT**	Mol%	Major species
1	32	0.681	0.19	
1a	32	0.699	0.11	
2	34 (8, X, X)	0.933	0.73	8, 10, 16 + 8, 12, 14
3	34 (8, X, X)	0.948	0.68	
4	34 (6, X, X)	0.960	1.72	6, 14, 14 + 6, 18, 10 + 6, 16, 12
4a		1.034	0.10	
4b		1.073	0.30	
5	35 (6, X, X)	1.094	0.42	
6		1.165	0.23	
7	36 (8-10, X, X)	1.206	4.24	8, 14, 14 + 8, 12, 16 + 10, 14, 12
8	36 (6, X, X)	1.230	10.31	6, 14, 16 + 6, 12, 18
9		1.260	0.46	
10	i 37 (6, X, X)	1.298	0.55	
11	ai 37 (6, X, X)	1.325	1.244	
12	37 (6, X, X)	1.360	1.770	
13		1.396	0.151	
13a		1.411	0.156	
13b		1.434	0.43	
14	38 (10, X, X)	1.461	3.17	10, 14, 14 + 10, 12, 16
15	38 (8, X, X)	1.473	6.31	8, 14, 16 + 8, 12, 18
16	38 (6, X, X)	1.503	18.95	6, 16, 16 + 6, 14, 18
17	38 (4, X, X)	1.535	1.28	
18		1.577	0.89	
19		1.606	1.86	
20	39 (6, X, X)	1.645	1.16	
20a		1.683	0.29	
20b		1.698	0.17	
21	40 (10-12, X, X)	1.758	7.71	10, 14, 16 + 12, 14, 14
22	40 (8, X, X)	1.775	5.86	8, 16, 16 + 8, 14, 18
23	40 (6, X, X)	1.808	6.12	6, 16, 18
24		1.849	0.65	
25		1.879	0.41	
25a		1.897	0.22	
26		1.921	0.94	
27		1.941	0.29	
27a		1.977	0.16	
28		2.018	0.28	
29	42 (10, X, X)	2.104	8.24	10, 16, 16 + 10, 14, 18
30	42 (8, X, X)	2.128	1.45	8, 16, 18
31	42 (6, X, X)	2.167	0.42	
31a		2.190	0.19	
32		2.238	0.18	
33		2.285	0.35	
34	i 44	2.395	0.14	
35	44 (10-14, X, X)	2.499	4.58	10, 16, 18 + 12, 16, 16 + 14, 14, 16
36	i 45	2.614	0.17	
37	i 45	2.665	0.21	
38	45	2.723	0.31	
39	i 46	2.848	0.10	
40	46	2.966	1.98	14, 16, 16
41	i 47	3.088	0.10	
42	ai 47	3.160	0.13	
43	47	3.224	0.12	
44	48	3.503	0.65	16, 16, 16
45	50	4.290	0.17	16, 16, 18

* Species type indicated by the total acyl carbon number and, in brackets, the chain of each of the three alkyl chains. Unspecified chain lengths are indicated by X.

** Retention time relative to 16:0 14:0 4:0.

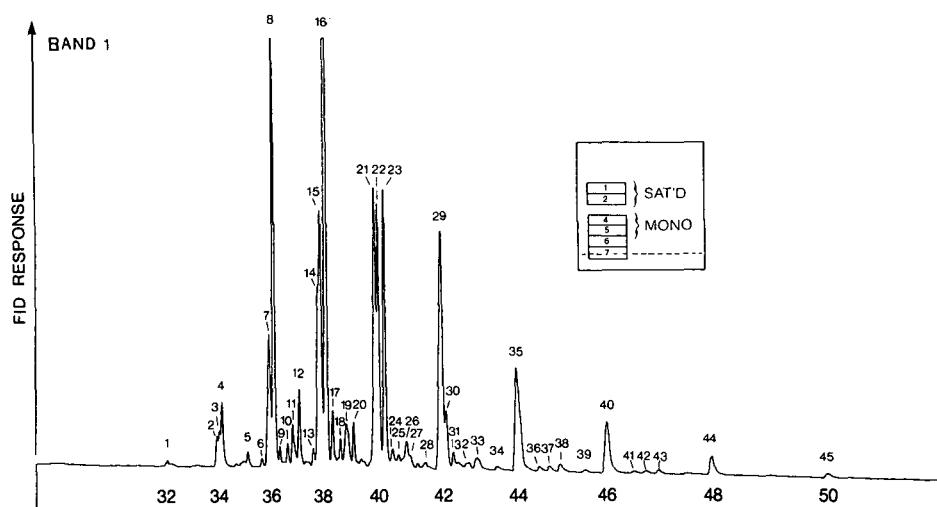


Fig. 3. Polar capillary GC profile of the saturated long chain-length triacylglycerol fraction isolated from R-4 butteroil distillate by silver nitrate TLC (band 1). Peak numbers are identified in Table IV. GC conditions as in Fig. 2. TLC conditions as in Fig. 1.

acid, which have been partially resolved within the corresponding carbon numbers on the polar capillary column. Between the major even carbon number peaks are seen minor peaks, which are due to odd carbon number triacylglycerols arising from the substitution of one of the long chain acids by a C_{15} or C_{17} fatty acid of normal, iso or anteiso structure. The identity of the peaks was confirmed by MS (see below), which also provided estimates for the relative proportions of the molecular species within

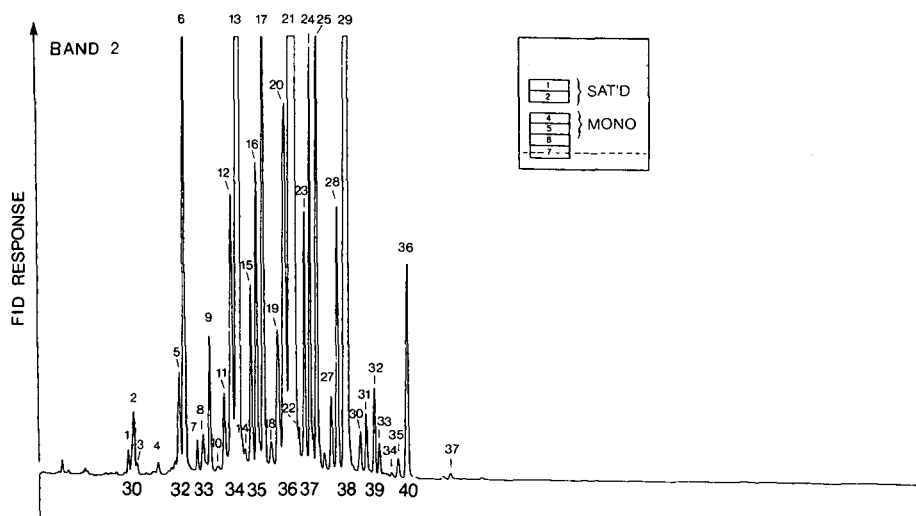


Fig. 4. Polar capillary GC profile of the saturated short chain-length triacylglycerols isolated from R-4 butteroil distillate by silver nitrate TLC (band 2). Peak numbers are identified in Table V. GC conditions as in Fig. 2. TLC conditions as in Fig. 1.

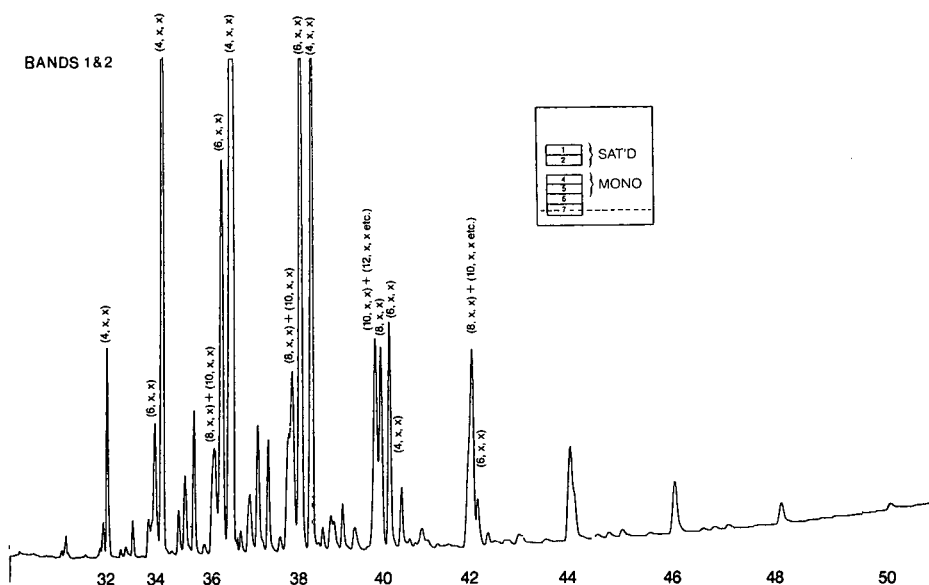


Fig. 5. Polar capillary GC profile of a 1:1 mixture of triacylglycerols from band 1 (Fig. 1) and band 2 (Fig. 1). Peak identification as shown on figure. GC conditions as in Fig. 2. TLC conditions as in Fig. 1.

each carbon number. Table IV gives the identity and quantity of the major molecular species as estimated by GC and GC-MS using the polar capillary column.

Fig. 4 shows the polar capillary GC profile of the triacylglycerols in band 2 from the silver nitrate TLC separation. On the basis of the fatty acid composition these triacylglycerols are largely butyrates with small amounts of caproates overlapping from silver nitrate TLC band 1. Fig. 5 shows the polar capillary GC profile of a mixture of bands 1 and 2. It is seen clearly that the butyrates are eluted later than the longer chain-length species of triacylglycerols within each carbon number. On the basis of the mass chromatograms recorded for the peaks obtained on the polar column for band 2, it was possible to confirm the identity of all major molecular species in each major resolved peak. Table V gives the identities and quantities of the major molecular species in band 2 as determined by GC on the polar capillary columns and confirmed by GC-MS.

Fig. 6 illustrates the use of GC-MS for the identification of the milk fat triacylglycerols. It shows the mass chromatograms recorded for the $(M - RCOOH)^+$ ions for the major species of the triacylglycerols in the silver nitrate TLC band 2. It can be seen that C_{32} yields two major ions with m/z 327 and 495, which correspond to C_{16} and C_{28} diacylglycerols, respectively, representing a 16:0 12:0 4:0 triacylglycerol as a sole major component. C_{34} yields ions with m/z 327, 355, 383 and 523 as major products and 411, 439 and 467 as minor products, representing C_{16} to C_{30} diacylglycerols, respectively. Within the C_{34} , it is therefore possible to construct the triacylglycerols 18:0 12:0 4:0, 16:0 14:0 4:0 as major components preceded by 16:0 12:0 6:0 as a minor component. Likewise, it is seen that C_{36} contains 16:0 16:0 4:0 as a major component, which is preceded by 16:0 14:0 6:0 and 14:0 14:0 8:0 as minor components. Similarly, C_{38} is seen to be made up of 18:0 16:0 4:0 as a major component, preceded by

TABLE V
MAJOR TRIACYLGLYCEROLS FROM SILVER NITRATE TLC BAND 2

Peak No.	Species type*	RRT**	Mol%	Major molecular species
1		0.441	0.03	
2	30 (4, X, X)	0.467	0.06	
3		0.481	0.01	
4		0.586	0.11	
4a		0.661	0.05	
4b		0.673	0.08	
5	32 (6, X, X)	0.693	0.69	
6	33 (4, X, X)	0.717	3.56	16, 12, 4 + 14, 14, 4
7	i 33 (4, X, X)	0.789	0.19	i 15, 14, 4 + i 17, 12, 4
8	ai 33 (4, X, X) + 33 (6, X, X)	0.815	0.28	
9	33 (4, X, X)	0.848	0.74	15, 14, 4 + 17, 12, 4
10		0.890	0.10	
11		0.923	0.52	
12		0.958	1.99	
13	34 (4, X, X)	1.000	19.06	14, 16, 4 + 18, 12, 4
14		1.027	0.20	
15	i 35 (4, X, X)	1.060	0.98	i 15, 16, 4 + i 17, 14, 4
16	ai 35 (4, X, X)	1.086	1.68	ai 15, 16, 4 + ai 17, 14, 4
17	35 (4, X, X)	1.125	3.10	15, 16, 4 + 17, 14, 4
18		1.161	0.28	
19	36 (8, X, X)	1.193	1.02	
20	36 (6, X, X)	1.229	3.07	
21	36 (4, X, X)	1.283	38.30	16, 16, 4 + 14, 18, 4
22		1.304	0.22	
23	i 37 (4, X, X)	1.336	1.17	i 15, 18, 4 + i 17, 16, 4
24	ai 37 (4, X, X)	1.363	1.66	ai 15, 18, 4 + i 17, 16, 4
24a		1.375	0.16	
25	37 (4, X, X)	1.396	2.44	15, 18, 4 + 17, 16, 4
26		1.438	0.18	
27		1.473	0.45	
28	38 (6, X, X)	1.503	1.41	
29	38 (4, X, X)	1.554	13.86	16, 18, 4
29a		1.580	0.07	
30	i 39 (4, X, X)	1.619	0.26	i 17, 18, 4
31	ai 39 (4, X, X)	1.649	0.31	ai 17, 18, 4
32	39 (4, X, X)	1.690	0.39	17, 18, 4
33		1.714	0.16	
33a		1.732	0.03	
33b		1.747	0.03	
34	i 40 (4, X, X)	1.777	0.04	
35	40 (6, X, X)	1.809	0.10	
36	40 (4, X, X)	1.854	1.01	18, 18, 4
37		2.071	0.03	

* As in Table IV.

** Retention time relative to 16:0 14:0 4:0.

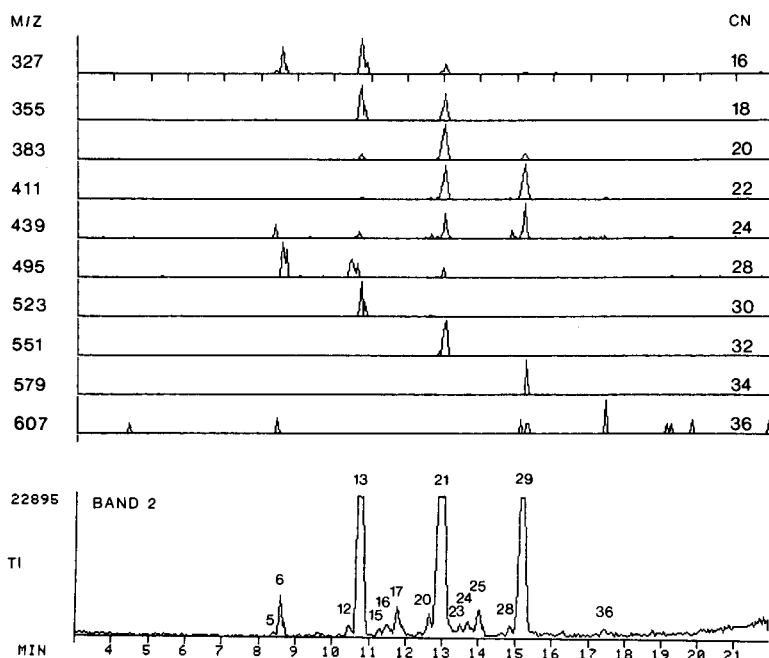


Fig. 6. Mass chromatograms of the mixed saturated triacylglycerols (Fig. 4). Peak identification by carbon number and by $(M - RCOOH)^+$ fragment ions. GC-MS conditions: instrument, Hewlett-Packard quadrupole mass spectrometer interfaced with a gas chromatograph equipped with the same capillary column as the GC instrument in Fig. 2; carrier gas, hydrogen; methane chemical ionization; other conditions as given in text. Full spectra were recorded every 7 s and the appropriate ions were recalled from storage in a computer.

16:0 16:0 6:0 as another major component, which is further preceded by 14:0 14:0 10:0 and 16:0 12:0 10:0 as minor components. The three major peaks within C_{40} (Fig. 5) gave GC-CI-MS fragments which could have come only from a sequential elution of the capric, caprylic and caproic acid containing triacylglycerol species. Within each peak the short chain acid was combined, however, with two or more different long chain acids to give a total carbon number of 40 (*e.g.* 8:0 14:0 18:0; 8:0 16:0 16:0). In all instances the GC-MS findings were consistent with the results of silver nitrate TLC separation and analyses of the fatty acids of the individual TLC bands. The minor even carbon number peaks were identified on the basis of the GC retention times and the rules of resolution just established. The minor odd carbon number peaks were due to the presence of significant amounts of C_{15} and C_{17} acids, which were combined with the short and long chain length even carbon number acids in the triacylglycerol molecules. The separation within the carbon number was due to a resolution of the iso, anteiso and normal chains, in order of increasing retention time. This was consistent with the order of resolution of the simple fatty acid esters and the finding of "diacylglycerol" ions with identical masses in all three peaks for carbon numbers 35 and 37. Fig. 7 illustrates the GC-CI-MS identification of the saturated odd carbon number butyrates in silver nitrate TLC band 2 (Fig. 1B). These are due to the combination of one residue of butyric acid with one residue of the odd carbon number

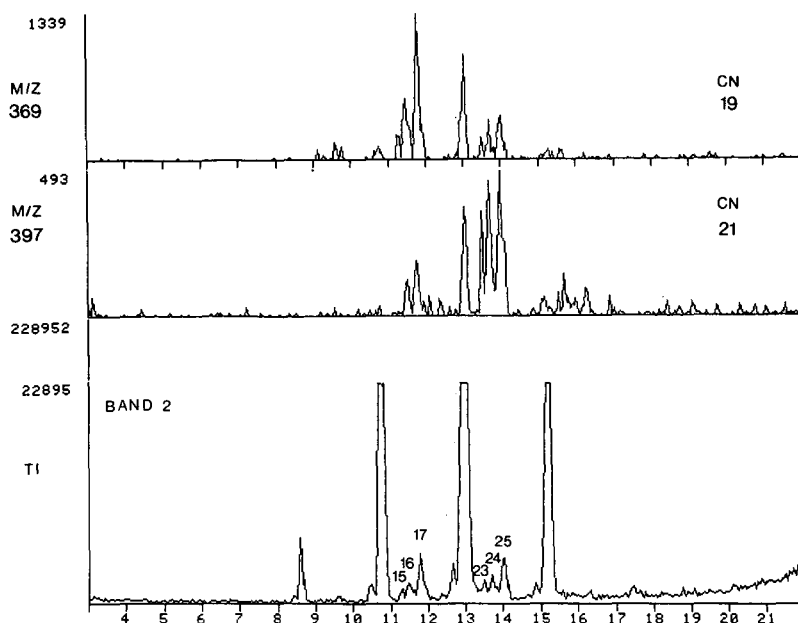


Fig. 7. Mass chromatograms of the odd carbon number triacylglycerols resolved from the saturated short chain-length fraction (Fig. 4). Peak identification by carbon number and by $(M - RCOOH)^+$ fragment ions. GC-MS conditions as in Fig. 6.

(C_{15} or C_{17}) and one residue of the corresponding even carbon number long chain length fatty acid. The mass spectra indicate that C_{35} is made up of peaks containing 4:0 15:0 16:0 and 4:0 17:0 14:0 triacylglycerol species, which have been resolved according to the nature of the odd carbon number fatty acid (*e.g.* normal chains preceded by iso and anteiso chains). Similar identifications were made of the components in C_{37} . The odd carbon number triacylglycerols were identified and quantitated similarly in band 1 where they were shown to consist of the 6, 8 and 10 carbon short chain along with the corresponding even carbon number long chain acids. Fig. 8 gives the full mass spectra recorded for the major components of C_{35} from the silver nitrate TLC band 2. The major triacylglycerols in each of the peaks yield the same "diacylglycerol" fragments, although some contamination from the preceding and succeeding major peaks is also seen. The major ions represent the 14:0 17:0 and 16:0 15:0 (m/z 537); 17:0 4:0 (m/z 397), 14:0 4:0 (m/z 365), 16:0 4:0 (m/z 383) and 15:0 4:0 (m/z 369) "diacylglycerols". The parent ions of these species were not seen under the present working conditions.

Fig. 9 gives the polar capillary GC profile of silver nitrate TLC band 5 (Fig. 1B), which represents the major monoene fraction. On the basis of the fatty acid analyses the monoenes were the *cis* isomers of 18:1 and lower carbon number monounsaturates. Unlike the saturates, the monoenes were not resolved into the butyrate and longer chain length species as effectively as the saturates, presumably because of the overriding influence of the π -bonding to the silver ions. As a result each carbon number on GC is resolved into the butyrate, caproate, caprylate and caprate subfractions. GC-MS examination of the major peaks showed combinations of the mono-unsaturated fatty acid with a short chain and a long chain length acid corresponding to

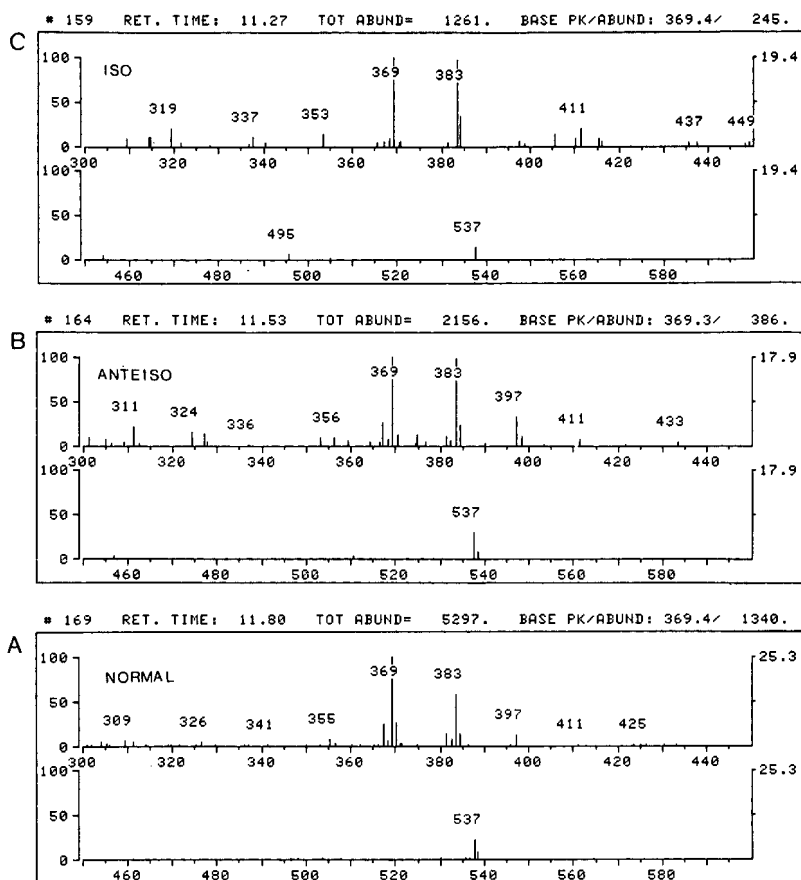


Fig. 8. Full GC-MS spectra of odd carbon number triacylglycerols resolved under C_{35} from saturated short chain length fraction (Fig. 4). (A) Normal chain C_{15} and C_{17} triacylglycerols; (B) anteiso chain C_{15} and C_{17} triacylglycerols; (C) iso chain C_{15} and C_{17} triacylglycerols. GC-MS conditions as in Fig. 6.

the appropriate carbon number (*e.g.* $C_{38} = 18:1\ 16:0\ 4:0$, preceded by $18:1\ 14:0\ 6:0$ and $18:1\ 12:0\ 8:0$). The odd carbon number triacylglycerols again were resolved according to the configuration of the odd carbon number fatty chain into the normal, iso and anteiso species. However, among these peaks were interdigitated the peaks arising from the separation of the *cis* and *trans* monoenes of the butyrates, caproates and caprylates in accordance with the appropriate carbon number. This complexity was not seen for the odd carbon number triacylglycerols of silver nitrate TLC band 2, which contained butyric as the only short chain-length acid. The odd carbon number resolution obtained with band 5 also contrasted with that recorded for band 1, which showed in addition to the normal, iso and anteiso separation also a segregation of the caproates and caprylates present in this saturated triacylglycerol fraction. Since it was not possible to confirm the identity of each minor peak by GC-MS, the identities of the minor odd carbon number peaks were assigned on the basis of their relative retention times and consistency with other chromatographic data and chemical composition. An

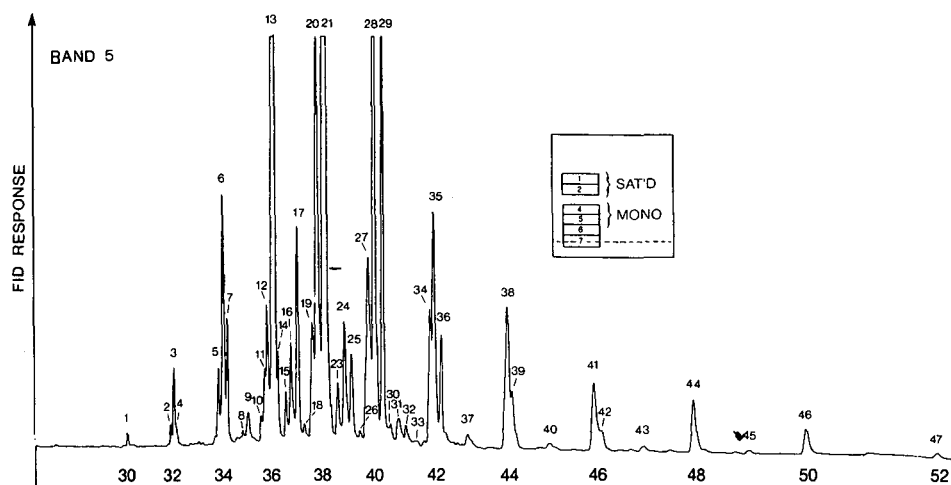


Fig. 9. Polar capillary GC profile of the *cis*-monoene fraction isolated from R-4 butteroil distillate by silver nitrate TLC (band 5). Peak numbers identified in Table VIII. GC conditions as in Fig. 2.

essentially identical elution pattern was obtained for band 4, which was identified as a monoene fraction containing *trans*-18:1 as the major monounsaturated fatty acid. This band made up *ca.* 11% of the total monoenoic triacylglycerols and is consistent with the ratio of elaidic to oleic acid in the distillate. Greater mobility of elaidic compared to oleic acid-containing butterfat triacylglycerols on silver nitrate TLC plates has been previously reported by Breckenridge and Kuksis¹⁴. The identity of the major peaks in bands 4 and 5 were confirmed by GC-MS as described above. In addition, the GC-MS revealed the presence of small amounts of monoenoic triacylglycerols containing medium chain length monounsaturated fatty acids. The identity and quantity of the major triacylglycerol species in bands 4 and 5 are listed in Table VI.

The polar capillary GC profile of the triacylglycerols from silver nitrate TLC band 6, which made up 8.1% of the total, indicated (chromatogram not shown) a C₃₄-C₅₂ range, with only one or two peaks each: butyrates and caproates at the lower end and caprylates, caprates and laurates at the upper end as the major components. On the basis of the fatty acid composition, the fraction represents a diene band containing two monounsaturated fatty acids per triacylglycerol molecule. The requirement for two monounsaturated fatty acids per molecule also explains the relative simplicity of the elution pattern, which is due to the predominance of the 18:1 over the other monoenoic fatty acids in the mixture. The chromatographic pattern also shows evidence for small quantities of odd carbon number triacylglycerols, which reflect the trace amount of 17:1 expected to occur in this fraction. Table VII gives the identity and estimated triacylglycerol composition of band 6.

The polar capillary GC elution patterns recorded for the triacylglycerols recovered in silver nitrate TLC band 7, which contributed 3.3% of the total distillate and represented the origin of the plate, indicated a very complex pattern (chromatogram not shown). On the basis of the fatty acid composition and the relative retention times of the triacylglycerols, it contained mainly tri-unsaturated species plus

TABLE VI
MAJOR MONOENOIC TRIACYLGLYCEROLS FROM SILVER NITRATE TLC BANDS 4 AND 5

Peak No.	Species type*	RRT**	Band 4 (mol%)	Band 5 (mol%)	Major molecular species
1	30	0.468		0.10	
2		0.716		0.18	
3	32 (4, X, X)	0.735	0.25	0.78	8, 18:1, 4 + 10, 16:1, 4
4		0.755	0.06		
5	34 (6, X, X)	0.986	0.96	0.73	10, 18:1, 6
6	34 (4, X, X)	1.011	1.52	2.51	12, 18:1, 4 + 14, 16:1, 4
7	34 (4, X, X)	1.036	0.28	1.01	16, 14:1, 4
8	35	1.130	0.99	0.26	
9	35	1.152	0.24	0.59	
10	36	1.223		0.28	
11		1.241	3.34	0.65	
12	36 (6, X, X)	1.256		1.54	12, 18:1, 6 + 14, 16:1, 6 + 16, 14:1, 6
13	36 (4, X, X)	1.292	11.56	13.20	14, 18:1, 4 + 16, 16:1, 4
14	36 (4, X, X)	1.312	1.58	0.76	18, 14:1, 4
15	ai 37 (6, X, X) + i 37 (4, X, X)	1.355	1.15	0.56	ai 15, 16:1, 6 + i 15, 18:1, 4
16	ai 37 (4, X, X) + 37 (6, X, X)	1.380	1.00	1.23	ai 15, 18:1, 4 + 15; 16:1, 6
16a		1.393	0.72		
17	37 (4, X, X)	1.408	1.79	2.28	15, 18:1, 4 + 17, 16:1, 4
18		1.455		0.31	
19	38 (8-10, X, X)	1.495	2.11	2.08	16:1, 14, 8 + 12, 16:1, 10
20	38 (6, X, X)	1.520	6.82	6.87	18:1, 14, 6 + 16:1, 16, 6
21	38 (4, X, X)	1.569	26.57	31.569	18:1, 16, 4 + 16:1, 18, 4
22		1.595	3.14	0.44	
23	ai 39 (6, X, X) + i 39 (4, X, X)	1.634	0.88	0.82	ai 15, 18:1, 6 + i 17, 18:1, 4
24	ai 39 (4, X, X) + 39 (6, X, X)	1.666	1.55	1.55	ai 17, 18:1, 4 + 15, 18:1, 6
25	39 (4, X, X)	1.700	0.51	1.13	17, 18:1, 4
25a		1.711	0.87		
26		1.749	0.18	0.24	
27	40 (8-10, X, X)	1.796	3.19	2.94	18:1, 14, 8 + 16:1, 14, 10
28	40 (6, X, X)	1.832	8.53	7.52	18:1, 16, 6
29	40 (4, X, X)	1.876	1.07	4.57	18:1, 18, 4
30		1.919		0.34	
31	ai 41 (6, X, X) + (8-10, X, X)	1.959	0.84	0.57	
32	41 (6, X, X)	1.998	0.32	0.34	
33		2.052	0.30	0.10	
34	42 (10, X, X + 12, X, X)	2.128	2.70	1.37	10, 18:1, 14 + 12, 16:1, 14
35	42 (8, X, X)	2.152	1.80	2.72	18:1, 16, 8
36	42 (6, X, X)	2.190	1.46	1.03	18:1, 18, 6
37	43	2.322	0.35	0.31	
38	44	2.543	1.97	2.01	10, 18:1, 16
39	44	2.567	0.28	0.67	18:0, 18:1, 8
40	45	2.770		0.10	
41	46	3.002	1.05	1.11	16, 18:1, 12 + 14, 14, 18:1
42	46	3.043		0.22	16, 18:1, 10
43	47	3.267		0.10	
44	48	3.540	0.60	0.74	14, 16, 18:1
45	49	3.829		0.07	15, 16, 18:1
46	50	4.135	0.23	0.35	16, 16, 18:1
47	52	4.824	0.07	0.12	

* As in Table IV.

** Retention time relative to 16:0 14:0 4:0.

TABLE VII
MAJOR TRIACYLGLYCEROLS FROM SILVER NITRATE TLC BAND 6

<i>Species type</i>	<i>RRT*</i>	<i>Mol%</i>	<i>Major molecular species</i>
30	0.495	0.12	
32	0.761	0.19	
	0.775	0.26	
34	0.958	0.06	
	1.011	0.49	
	1.035	1.12	
36	1.227	0.13	
	1.268	1.31	
	1.306	6.10	16:1, 16:1, 4
	1.377	0.19	
37	1.410	0.83	
	1.439	0.96	
	1.483	0.21	
	1.516	0.93	
38	1.551	3.1	14:1, 16:1, 8
	1.578	7.1	14:1, 18:1, 6
38	1.589	10.4	16:1, 18:1, 4
39	1.663	0.77	
	1.698	0.85	
	1.725	2.40	
40	1.899	32.67	18:1, 18:1, 4
	1.920	4.54	18:2, 18, 4
41	2.029	1.50	
	2.062	0.45	
42	2.186	2.25	18:1, 16:1, 8
	2.213	8.97	18:1, 18:1, 6
43	2.385	0.29	
44	2.602	4.38	18:1, 18:1, 8 + 16:1, 18:1, 10
46	3.072	2.59	18:1, 18:1, 10
47		0.22	
48	3.602	0.79	18:1, 18:1, 12
	3.644	0.77	14:1, 18:1, 16
49	3.894	0.14	
50	4.200	1.31	18:1, 18:1, 14
51	4.522	0.16	18:1, 18:1, 15
52	4.902	0.97	18:1, 18:1, 16
54	5.792	0.07	18:1 18:1, 18

* Retention time relative to 16:0 14:0 4:0.

dienes, which were not completely resolved from band 6. However, triacylglycerols containing one butyric, caproic or caprylic acid residue in combination with one monounsaturated and one diunsaturated fatty acid could be clearly identified, as could be some dienoic odd carbon number triacylglycerols containing only one diunsaturated long chain length fatty acid per molecule. The chromatographic identifications of the major components were again confirmed by GC-MS. Table VIII gives the identities and quantities of the major triacylglycerols in silver nitrate TLC band 7.

Fig. 10 gives the polar capillary GLC profile of the total R-4 distillate of butteroil

TABLE VIII
MAJOR TRIACYLGLYCEROLS FROM SILVER NITRATE TLC BAND 7

<i>Species type*</i>	<i>RRT**</i>	<i>Mol%</i>	<i>Molecular species</i>
32	0.764	0.62	
	0.793	0.10	
	0.819	0.17	
	0.921	0.01	
34	0.982	0.06	
	1.003	0.53	
	1.035	0.54	Band 6 overlap
	1.052	0.74	
	1.084	0.77	
	1.111	0.10	
	1.157	0.10	
	1.178	0.12	
36	1.219	0.12	
	1.254	0.61	
	1.268	0.27	
	1.306	4.55	Band 6 overlap: 16:1, 16:1, 4
	1.323	0.94	14:1, 18:2, 4
	1.353	4.76	
	1.394	0.57	
	1.434	0.85	
	1.455	0.50	
1.490	0.70		
38	1.507	0.76	
	1.551	2.18	14:1, 16:1, 8
	1.575	7.44	14:1, 18:1, 6 + 16:1, 18:1, 4
	1.589		
	1.607	4.10	
	1.652	9.82	16:1, 18:2, 4
	1.676	1.54	
	1.723	1.48	
	1.765	1.27	
	1.812	1.21	
40 (4, Δ1, Δ1)	1.895	8.82	18:1, 18:1, 4
40 (4, Δ1, Δ2)	1.954	17.76	18:1, 18:2, 4
40 (4, Δ0, Δ3)	1.996	3.50	
	2.020	5.07	
41	2.067	1.48	
42	2.168	1.38	
	2.213	1.01	18:1, 18:1, 6
	2.278	5.97	18:1, 18:2, 6
	2.338	1.23	
	2.362	2.09	
44	2.596	1.04	
	2.674	1.50	(includes front and back shoulder)
	2.775	0.46	
46	3.705	0.35	
	4.323	0.33	
	5.048	0.47	

* Species type indicated by total acyl carbon number and, in brackets, carbon number of the short chain acid and degree of unsaturation of the long chain acids.

** Retention time relative to 16:0 14:0 4:0.

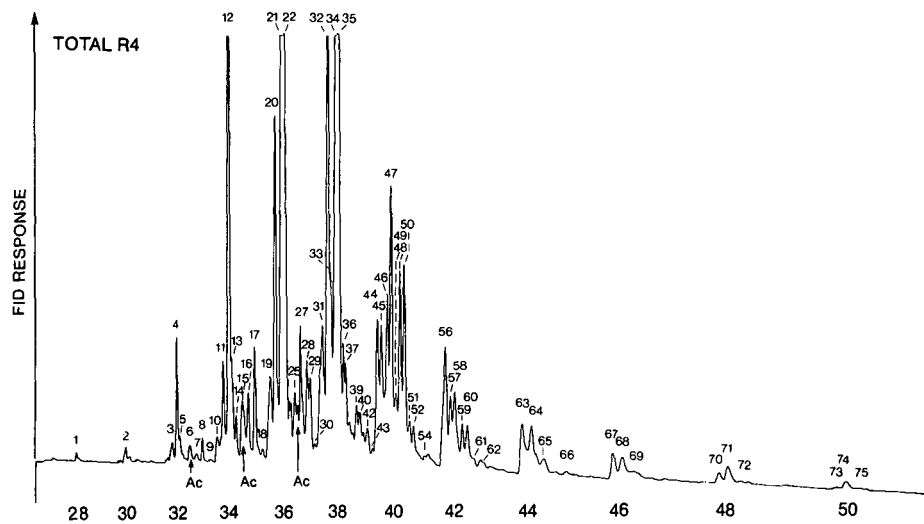


Fig. 10. Polar capillary GC profile of total R-4 distillate triacylglycerols. Peak numbers are identified in Table IX. Acetates (Ac) are identified by arrows. GC conditions as in Fig. 2.

TABLE IX

MAJOR TRIACYLGLYCEROL TYPES AND SPECIES IDENTIFIED AND QUANTITATED IN R-4 DISTILLATE

Peak No.	Species type*	RRT**	Mol%	Major molecular species
1	28	0.72	0.07	
2	30	1.57	0.33	
3	32 (6, X, X)	0.694	0.26	
4	32 (4, X, X)	0.717	1.24	
5		0.735	0.37	
6	i 33 (4, X, X)	0.791	0.09	
7	n 33 (6, X, X) + ai 33 (4, X, X)	0.891	0.15	
8	n 33 (4, X, X)	0.855	0.28	
9	ai 33 (2, X, X)	0.895	0.07	
10	n 33 (2, X, X) +	0.935	0.32	
11	34 (6, X, X)	0.966	1.27	
12	34 (4, X, X)	1.000	7.07	}
13	(shoulder)			
14		1.037	0.49	
15	i 35 (4, X, X) + 34 (2, X, X)	1.073	0.43	
16	n 35 (6, X, X) + ai 35 (4, X, X) + 34 (2, X, X) Δ1	1.100	0.76	
17	n 35 (4, X, X)	1.134	1.25	
18	n 35 (2, X, X) +	1.176	0.20	
19	36 (8, X, X) + 35 (2, X, X) Δ1	1.216	1.32	
20	36 (6, X, X)	1.243	3.92	
21	36 (4, X, X) + 36 (6, X, X) Δ1	1.283	12.90	
22	36 (4, X, X) Δ1	1.294	4.30	
23	i 37 (6, X, X) + 36 (4, X, X) Δ1	1.314	0.44	

(continued on p. 112)

TABLE IX (continued)

Peak	Species type*	RRT**	Mol%	Major molecular species
24		1.325	0.49	
25	ai 37 (6, X, X) +	1.341	0.70	
26	36 (2, X, X) +	1.355	0.16	
27	36 (2, X, X) Δ 1 + 37 (6, X, X) + ai 37 (4, X, X)	1.369	1.11	
27a	36 (2, X, X) Δ 1,1 +	1.383	0.43	
28	n 37 (4, X, X) +	1.403	0.92	
29		1.413	0.98	
30		1.439	0.25	
31	38 (8, X, X) + 38 (10, X, X)	1.483	2.53	8, 14, 16 + 10, 14, 14 + 10, 12, 16
32	38 (6, X, X) + 38 (8, X, X) Δ 1	1.503	5.37	6, 14, 18 + 6, 16, 16 + 8, 16:1, 14
33	38 (6, X, X) Δ 1	1.513	1.48	6, 18:1, 14 + 6, 16:1, 16
34	38 (4, X, X)	1.542	5.40	4, 16, 18
35	38 (4, X, X) Δ 1	1.557	9.65	4, 16, 18:1 + 4, 16:1 18
36	38 (4, X, X) Δ 1,1	1.581	0.96	4, 16:1 18:1
37	39 +	1.592	0.83	
38			0.70	
39	38 (4, X, X) Δ 1,2 + (2, X, X) Δ 1 + 39	1.648	0.63	
40	38 (2, X, X) Δ 1,1	1.669	0.61	
41		1.695	0.34	
42		1.704	0.57	
43		1.731	0.18	
44	40 (10, X, X)	1.757	1.74	10, 14, 16
45	40 (8, X, X)	1.775	1.61	8, 16, 16 + 8, 14, 16
46	40 (6, X, X) + (8, X, X) Δ 1 + (10, X, X) Δ 1	1.810	2.18	6, 16, 18 + 8, 18:1, 14 + 10, 18:1, 12
47	40 (6, X, X) Δ 1	1.828	2.90	6, 18:1 16
48	40 (4, X, X) +	1.851	0.83	
49	40 (4, X, X) Δ 1	1.875	1.08	4, 18:1, 18
50	40 (4, X, X) Δ 1,1	1.895	2.14	4, 18:1, 18:1
51	40 (4, X, X) Δ 2 + 41 (10, X, X)	1.922	0.59	
52	40 (4, X, X) Δ 1,2	1.945	0.79	
53				
54	41	2.001	0.18	
55	41	2.018	0.37	
56	42 (10, X, X)	2.104	2.04	10, 14, 18 + 10, 16, 16
57	42 (8, X, X) + (10, X, X) Δ 1	2.130	0.92	8, 16, 18 + 10, 18:1, 14
58	42 (8, X, X) Δ 1	2.151	1.34	8, 18:1, 16
59	42 (6, X, X) Δ 1 + (8, X, X) Δ 1,1	2.192	0.62	6, 18:1, 18 + 8, 16:1, 18:1
60	42 (6, X, X)	2.220	0.74	6, 18:1, 18:1
61	43			
62	42 (6, X, X) Δ 1,2	2.283	0.29	6, 18:1, 18:2
63	44 (10-14, X, X)	2.498	1.23	10, 1, 18 + 12, 16, 16 + 14, 14, 16
64	44 (10, X, X) Δ 1	2.547	1.32	10, 18:1, 16
65	44 (8, X, X) Δ 1,1	2.594	0.45	8, 18:1, 18:1
65a		2.647	0.55	
66	45	2.727	0.66	
67	46 (14, X, X)	2.970	0.55	14, 16, 16
68	46 (12, X, X) Δ 1 + (14, X, X) Δ 1	3.012	0.66	12, 16, 18:1 + 14, 14, 18:1
69	46 (10, X, X) Δ 1,1	3.07	0.18	10, 18:1, 18:1
70	48	3.505	0.26	16, 16, 16
71	48 (14, X, X) Δ 1	3.549	0.54	14, 16, 18:1
72	48 (12, X, X) Δ 1,1	3.609	0.06	12, 18:1, 18:1
73	50 (16, X, X)	4.111	0.09	16, 16, 18
74	50 (16, X, X) Δ 1	4.157	0.33	16, 16, 18:1
75	50 (14, X, X) Δ 1,1	4.224	0.16	14, 18:1, 18:1

* Species type indicated as in Table IV with fatty acid (X, X) degree of unsaturation specified by Δ 1, Δ 1,1, Δ 2, and Δ 1,2.

** Retention time relative to 16:0 14:0 4:0.

including the identity of the major peaks. The peak pattern resembles very closely that of the lower-molecular mass triacylglycerols in total bovine milk fat published previously by Geeraert and Sandra¹⁰, where these peaks, however, were not identified. Table IX gives the composition of the total triacylglycerol mixture of the R-4 distillate. The mole percentages of 75 different peaks are estimated from the knowledge of the carbon number distribution and the flame ionization response in the gas chromatograph. The triacylglycerol species were identified on the basis of GC and GC-MS analysis of the intact triacylglycerols recovered from the various silver nitrate TLC bands and the knowledge of the fatty acid composition of the distillate. Over 100 individual triacylglycerol species were recognized, which accounted for a large percentage of the total distillate. Only the major triacylglycerol species have been specifically listed.

Table X illustrates the method used in the reconstitution of the mass of the triacylglycerols recovered from the various TLC bands. In the example the composition of the C₄₀ triacylglycerol grouping in the R-4 distillate is compared to that reconstituted from the analysis of the various silver nitrate TLC bands. A total of eleven peaks are recognized, each of which contains more than one triacylglycerol species. Only the major components have been identified in Table X. Although the grouping appears very complex, only the third peak of the first seven major peaks had major contributions from more than one silver nitrate TLC band. For the reconstitution the contribution of each C₄₀ peak in the TLC band was multiplied by the mass proportion of the corresponding TLC band and the products summed. The resulting composition was compared to the composition of the C₄₀ triacylglycerol grouping in the total R-4 distillate. An excellent agreement was obtained. Similar reconstitution of the composition of the other triacylglycerol carbon numbers gave equally good agreement with the values measured directly in the total R-4 distillate.

DISCUSSION

Chromatographic characteristics of short chain length triacylglycerols

The present study reveals that the complex chromatographic elution patterns of the short chain triacylglycerols of butteroil arise from the resolution of its triacylglycerols into several groups of molecular species within most carbon numbers. This is due to both the characteristic composition and molecular association of the fatty acids. Essentially all of the triacylglycerols are mixed acid species, in which the occurrence of the short chains is limited to one per molecule. From stereospecific analyses^{2,3} we know that the short chain acids are confined specifically to the *sn*-3-position of the triacylglycerol molecule, which renders them enantiomeric. The association of the butyric acid residue with the *sn*-3-position has been confirmed by NMR using chiral shift reagents^{19,20}. Further complications occur from the polarity differences between the short and long chain length fatty acid substituents in the triacylglycerol molecules, which become manifested under certain chromatographic conditions, resulting in a segregation of the triacylglycerols on the basis of chain length on plain silica gel, or on polar capillary columns. The short and long chain lengths of saturated triacylglycerols are also resolved on silver nitrate TLC, but the unsaturated triacylglycerol bands were too complex to see clearly the anticipated resolution. Such chain length separations on plain silica gel have been observed previously by Nutter and Privett²¹ and Brecken-

TABLE X
 RECONSTITUTION OF TRIACYLGLYCEROL MASS RECOVERED BY POLAR CAPILLARY GC FROM THE VARIOUS SILVER NITRATE TLC
 BANDS

Representative triacylglycerols	RRT*	ECN**	Band No.***							Sum	R _f
			1	2	4	5	6	7			
16, 14, 10	1.757	40.000	1.83	0.01					0.05	1.89	1.73
16, 16, 8 + 18, 14, 8	1.778	40.13	1.39	0.01						1.40	1.59
18, 16, 6 + 14, 18:1, 8 + 12, 18:1, 10	1.811	40.33	1.45	0.03	0.13	0.94			0.05	2.60	2.16
16, 18:1, 6	1.828	40.43			0.34	2.41				2.75	2.87
18, 18, 4	1.852	40.58	0.16	0.32						0.48	0.82
18, 18:1, 4	1.876	40.72	0.10			1.46				1.60	2.06
18:1, 18:1, 4	1.897	40.84	0.05		0.03		1.70		0.34	2.12	2.12
16, 15, 10 + 18, 18:2, 4	1.924	41.00	0.22		0.11		0.24			0.57	0.58
18:1, 18:2, 4	1.947	41.13	0.07		0.03		0.18		0.67	0.95	0.78
Unknown	2.000	41.40							0.13	0.25	0.18
Unknown	2.018	41.51	0.07		0.01	0.11		0.08	0.19	0.34	0.35

* Retention times relative to 16:0 14:0 4:0.

** Equivalent carbon number based on the set of long chain saturated triacylglycerols, such as 10:0 16:0 14:0 (ECN = 40.00) and 10:0 16:0 16:0 (ECN = 42.00).

*** Values are in mol%.

ridge and Kuksis¹⁴. The separations on silver nitrate TLC were accompanied by a resolution of triacylglycerols containing *cis*-18:1 (oleic) and *trans*-18:1 (elaidic) acids, as already reported by Breckenridge and Kuksis¹⁴.

Chain length separations beyond the carbon number on polar packed columns were first observed by Kuksis *et al.*⁹, who demonstrated that within a carbon number the butyrates were preceded by caproates, caprylates, caprates and mixtures of triacylglycerols containing exclusively long chain length fatty acids. The present separations on polar capillary columns, supported by MS, have permitted a further characterization of this resolution. Thus, the shifts in equivalent carbon number (ECN) that result from differences in chain length, positional placement and unsaturation of the fatty acids have been assessed. It was found that for species with the same total carbon and double bond number, the ECN decreased as the minimum chain length increased (*e.g.* Δ ECN are observed as follows: 2,X,X - 4,X,X = 0.47; 4,X,X - 6,X,X = 0.29; 6,X,X - 8,X,X = 0.20). The acetates and butyrates having the short chain acid in the secondary position were eluted later than the equivalent species having the short chain acid in the primary position (*e.g.* X,2,X - 2,X,X = 0.29; X,4,X - 4,X,X = 0.16). The effects of unsaturation on the separation of the short chain triacylglycerols on the polar capillary columns paralleled those described by Geeraert and Sandra^{7,10}. Thus, the triacylglycerol 4, 18:0, 18:1 was retained longer than 4, 18:0, 18:0 (Δ ECN = 0.13) and 4, 18:1, 18:1 longer than 4, 18:0, 18:1 (Δ ECN = 0.12), while 4, 18:0, 18:2 was retained much longer than 4, 18:1, 18:1 (Δ ECN = 0.17), and 4, 18:1, 18:2 very much longer than 4, 18:1, 18:1 (Δ ECN = 0.29). Similar resolution factors were observed for the caproates and caprylates of the C₁₈ fatty acids and the mixtures of C₁₆ and C₁₈ acids. Furthermore, the polar capillary columns permitted an effective resolution of the odd carbon number triacylglycerols into normal, anteiso and iso isomer-containing odd carbon number fatty acids, which occurred with a stoichiometry of only one per molecule. In all instances the species containing the normal chain isomers were preceded by species containing the anteiso isomers, which were preceded by species containing the iso isomers of the odd carbon fatty acids. These separations are similar to those seen for the simple fatty acid methyl and butyl esters on the polar capillary column. The finding of these odd carbon number and branched chain fatty acids in butterfat is in agreement with the original report of Ryhage²². Small amounts of phytanic (C₂₀) acid were also noted among the fatty acids of the distillate, and presumably accounted for small peaks in the total GC pattern of the triacylglycerols. The chromatographic behaviour of the tetramethyl-substituted C₁₅ (pristanic) and C₁₆ (phytanic) saturated fatty acids in bovine milk fat have been previously characterized by Avigan²³ and Hansen and Ackman²⁴, respectively.

The substitution of a *trans*- for a *cis*-18:1 acid in the butterfat triacylglycerols did not result in a significant change in the retention times for the corresponding species. However, the GC run of silver nitrate TLC band 4, which contained both *cis* and *trans* monounsaturates, showed peaks that were slightly broadened in comparison to runs obtained for silver nitrate TLC band 5 (pure *cis*-species). Other monounsaturated fatty acids in bovine milk fat have been identified as positional isomers of oleic acid, as well as of palmitoleic acid. In addition, trace amounts of even and odd carbon number medium chain length fatty acids have also been reported in bovine milk fat^{1,22}. No unidentified fatty acids appeared to accumulate in significant amounts in any of the major triacylglycerol fractions isolated and identified in the present study. There was

little loss of linoleic and linolenic acids in the distillate in comparison to the total bovine milk fat.

GC-MS characteristics of short chain length triacylglycerols

The MS behaviour of short and long chain triacylglycerols has been extensively studied in the past and the principles of fragmentation under EI^{25,26} and CI²⁷ conditions have been well established. The use of the polar capillary GC for the admission of the triacylglycerols to the ion source of the mass spectrometer was anticipated to provide a superior method of insuring the purity of the analyte, any remaining overlaps being confined to clearly defined chromatographic and molecular weight analogues. In general this was true. However, due to the close spacing and uneven proportions of the peaks, and the need for overloading the low-capacity capillary column to ensure sufficient ions for the minor components, there was considerable overlap between adjacent peaks, and uncertainty arose regarding the exact identity and order of elution of closely spaced species. It was therefore necessary to effect a fractionation of the samples prior to the GC-MS analysis. Isolation of the acetates by TLC on plain silica gel and of the long and short chain saturates, monoenes, dienes and trienes by TLC on silver nitrate-treated silica gel helped to simplify the interpretation of the mass spectra for all species including the odd carbon number triacylglycerols. In most instances the GC-MS spectra did not give a molecular ion in either EI or CI mode and the triacylglycerol species present had to be identified from the "diacylglycerol" type of fragment ions. Within the restrictions of carbon and double bond numbers and the chromatographic retention times of the peaks, however, the identification of the parent triacylglycerols did not present problems. In many instances the diacylglycerol fragments were unique to the triacylglycerols present, while in other instances the full complement of triacylglycerol species could be recognized by appropriate allowance for minor diacylglycerol species.

We had previously shown²⁸ that the ion yields vary with the triacylglycerol type and the diacylglycerol fragment selected, and that exact quantitation of the molecular species of triacylglycerols in a mixture requires calibration of the system with appropriate standards. Since this was not practical, we relied upon the hydrogen flame ionization response in the gas chromatograph for the quantitation of the total amount of material in each GC peak and used the ion current response only for obtaining the relative proportions of the unresolved components in a GC peak. The overall validity of each estimate was established by reference to the mass proportions of the species in the corresponding silver nitrate TLC fraction.

Previously a GC-MS analysis of bovine milk fat had been reported⁶ using a non-polar capillary column for admission of triacylglycerols to the ion source, but the limited resolution had not given any extensive identifications. Despite the great resolving power of the polar capillary column and its exceptional suitability for analysis of natural triacylglycerols¹⁰, few meaningful identifications of bovine milk fat triacylglycerols could be made without a preliminary fractionation of the sample.

Previous analysis of R-4 distillate

The fatty acid composition and carbon number distribution of the R-4 distillate was reported some 25 years ago¹¹. At various later times this butteroil fraction had been employed to demonstrate the specific location of the short chain fatty acids in the

sn-3-position³, the TLC separation of short and long chain length triacylglycerols of bovine milk fat¹⁴, the separation of short and long chain length-containing triacylglycerols within a carbon number on packed polar GC columns⁹, and more recently the liquid chromatography-MS identification of short and medium chain length triacylglycerols in ruminant milk fat²⁹. These studies had shown that the composition and chemical structure of the triacylglycerols in the R-4 distillate closely resembles that of the lower-molecular-mass triacylglycerols of bovine milk fat, as far as the analytical methods of the time had permitted to determine.

Significance of present analyses

The present study establishes the chromatographic behaviour of the short chain length triacylglycerols on GC and GC-MS using polar capillary columns. The molecular distillate of butteroil provides a secondary reference standard for the identification of the mixed short and long chain triacylglycerols in bovine milk fat. We had noted in the past that the R-4 distillate closely resembles the early part of the carbon number profile of whole butterfat and of ruminant milk fats in general^{9,11,14}. The elution profiles obtained on the polar capillary columns for the R-4 distillate in the present study and for whole butterfat in the present study and by Geeraert and Sandra¹⁰ are almost superimposable over the C₂₄ to C₄₆ range of carbon numbers, including the fine details of the pattern within many of the carbon numbers. The analyses of the distillate account for the species in the most complex part of the butterfat profile. Polar capillary GC appears superior to the reversed-phase HPLC resolution of the milk fat triacylglycerols²⁹ because of the ease of quantitation provided by the flame ionization detector and the much larger number of theoretical plates, which can be profitably exploited for the resolution of closely related species. However, a complete resolution of even all major species is not obtained without prefractionation by silver nitrate TLC. It would be of interest to submit to polar capillary GC the milk fat triacylglycerol fractions obtained by reversed-phase HPLC.

ACKNOWLEDGEMENTS

These studies were supported by funds from the Medical Research Council of Canada, Ottawa, Canada and the Heart and Stroke Foundation of Ontario, Toronto, Canada.

REFERENCES

- 1 W. R. Morrison, in F. D. Gunstone (Editor), *Topics in Lipid Chemistry*, Vol. 1, Logos Press, London, 1970, pp. 51-106.
- 2 R. E. Pitas, J. Sampugna and R. G. Jensen, *J. Dairy Sci.*, 50 (1967) 1332.
- 3 W. C. Breckenridge and A. Kuksis, *J. Lipid Res.*, 9 (1968) 388-393.
- 4 R. Watts and R. Dils, *J. Lipid Res.*, 9 (1968) 40-51.
- 5 A. Kuksis and M. J. McCarthy, *Can. J. Biochem. Physiol.*, 40 (1962) 679.
- 6 P. P. Schmid, M. D. Mueller and W. Simon, *J. High Resolut. Chromatogr. Chromatogr. Commun.*, 2 (1979) 675-676.
- 7 E. Geeraert, in P. Sandra (Editor), *Sample Introduction in CGC*, Vol. 1, Hüthig, Heidelberg, 1985, pp. 133-158.
- 8 K. Grob, Jr., H. P. Neukom and R. Bataglia, *J. Am. Oil Chem. Soc.*, 57 (1980) 282-286.
- 9 A. Kuksis, L. Marai and J. J. Myher, *J. Am. Oil Chem. Soc.*, 50 (1973) 193-201.

- 10 E. Geeraert and P. Sandra, *J. Am. Oil Chem. Soc.*, 64 (1987) 100–105.
- 11 M. J. McCarthy, A. Kuksis and J. M. R. Beveridge, *Can. J. Biochem.*, 40 (1962) 1693–1703.
- 12 N. H. Morley, A. Kuksis, D. Buchnea and J. J. Myher, *J. Biol. Chem.*, 250 (1975) 3414–3418.
- 13 P. W. Parodi, *J. Chromatogr.*, 111 (1975) 223–226.
- 14 W. C. Breckenridge and A. Kuksis, *Lipids*, 3 (1968) 291–300.
- 15 J. J. Myher and A. Kuksis, *J. Biochem. Biophys. Methods*, 10 (1984) 13–23.
- 16 J. J. Myher and A. Kuksis, *Can. J. Biochem.*, 60 (1982) 638–650.
- 17 J. J. Myher, A. Kuksis, L. Marai and S. K. F. Yeung, *Anal. Chem.*, 50 (1978) 557–561.
- 18 L. Marai, J. J. Myher and A. Kuksis, *Can. J. Biochem. Cell Biol.*, 61 (1983) 840–849.
- 19 J. Bus, C. M. Lok and A. Groewegen, *Chem. Phys. Lipids*, 16 (1976) 123.
- 20 P. E. Pfeffer, J. Sampugna, D. P. Schwartz and J. N. Shoolery, *Lipids*, 12 (1977) 869–871.
- 21 L. J. Nutter and O. S. Privett, *J. Dairy Sci.*, 50 (1967) 1194–1199.
- 22 R. Ryhage, *J. Dairy Res.*, 34 (1967) 115–121.
- 23 J. Avigan, *Biochim. Biophys. Acta*, 125 (1966) 607–609.
- 24 R. G. Ackman and R. P. Hansen, *Lipids*, 2 (1967) 357–362.
- 25 W. M. Lauer, A. J. Aasen, G. Graf and R. T. Holman, *Lipids*, 5 (1970) 861–868.
- 26 A. J. Aasen, W. M. Lauer and R. T. Holman, *Lipids*, 5 (1970) 869–877.
- 27 T. Murata and S. Takahashi, *Anal. Chem.*, 49 (1977) 728–731.
- 28 J. J. Myher, A. Kuksis, L. Marai and F. Manganaro, *J. Chromatogr.*, 283 (1984) 289–301.
- 29 A. Kuksis, L. Marai, J. J. Myher, J. Cerbulis and H. M. Farrell, Jr., *Lipids*, 21 (1986) 183–190.

CHROM. 20 753

STUDIES ON STEROIDS

CCXXXVIII.* DETERMINATION OF BILE ACIDS IN LIVER TISSUE BY GAS CHROMATOGRAPHY–MASS SPECTROMETRY WITH NEGATIVE ION CHEMICAL IONIZATION DETECTION

JUNICHI GOTO, HIROYA MIURA, MEGUMI INADA and TOSHIO NAMBARA*

Pharmaceutical Institute, Tohoku University, Sendai 980 (Japan)

and

TAKATOMO NAGAKURA and HIROSHI SUZUKI

The Third Department of Internal Medicine, Tohoku University School of Medicine, Sendai 980 (Japan)

SUMMARY

A method for the determination of bile acids in 2–10 mg of human liver tissue by gas chromatography (GC) in combination with negative ion chemical ionization (NICI) mass spectrometry is described. Unconjugated, glycine- and taurine-conjugated bile acids labelled with ^{18}O and ^2H were used as internal standards. The preparation of these compounds was attained by the exchange reaction of the carbonyl group with H_2^{18}O , followed by metal hydride reduction. Bile acids in solubilized liver tissue were extracted with a Sep-Pak C_{18} cartridge, separated into the unconjugated, glycine- and taurine-conjugated fractions by ion-exchange chromatography on piperidinohydroxypropyl-Sephadex LH-20 and then derivatized to the pentafluorobenzyl ester–dimethylethylsilyl ethers. Subsequent resolution of each fraction into lithocholate, deoxycholate, chenodeoxycholate, ursodeoxycholate and cholate was attained by GC on a cross-linked 5% phenylmethyl silicone fused-silica capillary column where bile acids were monitored with a characteristic carboxylate anion $[\text{M} - 181]^-$ in the NICI mode using isobutane as a reagent gas. The newly developed method was applied to the quantitation of bile acids in liver tissue with satisfactory sensitivity and reliability.

* For Part CCXXXVII, see H. Hosoda, R. Tsukamoto, K. Shoriken, W. Takasaki and T. Nambara, *Chem. Pharm. Bull.*, 36 (1988) 3525. In this paper the following trivial names and abbreviations are used: lithocholic acid (LCA) = 3α -hydroxy- 5β -cholan-24-oic acid; chenodeoxycholic acid (CDCA) = $3\alpha,7\alpha$ -dihydroxy- 5β -cholan-24-oic acid; deoxycholic acid (DCA) = $3\alpha,12\alpha$ -dihydroxy- 5β -cholan-24-oic acid; ursodeoxycholic acid (UDCA) = $3\alpha,7\alpha$ -dihydroxy- 5β -cholan-24-oic acid; cholic acid (CA) = $3\alpha,7\alpha,12\alpha$ -trihydroxy- 5β -cholan-24-oic acid; G = glycine-conjugated; T = taurine-conjugated.

INTRODUCTION

In recent years, considerable interest has been directed to the biodynamics of bile acids in man in connection with the diagnosis of hepatobiliary diseases¹. A reliable method is, therefore, urgently needed for the trace analysis of bile acids in liver tissue. Among various methods, gas-liquid chromatography-mass spectrometry (GC-MS) is a powerful tool for the profile analysis of trace compounds and has been applied to the determination of bile acids in liver tissue using the electron impact ionization mode². In the previous study, we disclosed that the combined use of derivatization to the pentafluorobenzyl (PFB) ester-dimethylethylsilyl (DMES) ether and capillary GC-MS with negative ion chemical ionization (NICI) detection is much more promising with respect to the sensitivity and versatility for the determination of bile acids³. The present paper deals with the separation and determination of unconjugated, glycine- (G) and taurine-conjugated (T) bile acids in liver tissue by GC-NICI-MS using stable isotope-labelled bile acids as internal standards (I.S.).

EXPERIMENTAL

Materials

Bile acids and cholyglycine hydrolase were supplied by Sigma (St. Louis, MO, U.S.A.) and DMES-imidazole was obtained from Tokyo Kasei Kogyo (Tokyo, Japan). Glycine- and taurine-conjugated bile acids were prepared in these laboratories⁴. The Sep-Pak C₁₈ cartridge and Pre Pak-500/C₁₈ were obtained from Waters Assoc. (Milford, MA, U.S.A.). All other chemicals employed were of analytical reagent grade. Solvents were purified by distillation prior to use. Piperidinohydroxypropyl-Sephadex LH-20 (PHP-LH-20) (acetate form, 0.6 mequiv./g)⁵ and carboxymethyl-Sephadex LH-20 (CM-LH-20) (K⁺ form, 1 mequiv./g)⁶ were prepared in the manner previously reported. All glassware used was silanized with trimethylchlorosilane.

Gas chromatography-mass spectrometry

Capillary GC-MS was carried out using a VG Analytical MM12030 quadrupole mass spectrometer equipped with an Hewlett-Packard HP 5790A gas chromatograph. Isobutane was used as a reagent gas. A cross-linked 5% phenylmethyl silicone fused-silica capillary column (20 m × 0.3 mm I.D.) (J & W Scientific, Folsom, CA, U.S.A.) was inserted into the ion source through the direct inlet. The carrier gas was helium at a linear velocity of 60 cm/s. The test samples were injected through a Van den Berg solventless injector with an inlet pressure of 0.8 kg/cm². The injection port, column oven and ion source were kept at 280, 285 and 270°C, respectively. The ionization energy was 70 eV and the emission current was 400 μA.

Preparation of [¹⁸O]-labelled bile acids

The methyl esters of LCA, CDCA, DCA and CA were subjected to oxidation with chromium trioxide in acetic acid, followed by alkaline hydrolysis, yielding mono-, di- and trioxo-5β-cholanoic acids. In a similar fashion, glycine- and taurine-conjugated oxo bile acids were also prepared from the corresponding ethyl glycinate- and taurine-conjugates. These were unequivocally characterized by ¹H NMR spectroscopy^{7,8}, and their purities were greater than 99.5% as judged by high-perform-

ance liquid chromatography (HPLC)⁹. The oxo bile acid (10–20 mg) in 70% ethanol (5 ml) was applied to a column (10 cm × 18 mm I.D.) of CM-LH-20 (K⁺ form, 5 g) and eluted with 70% ethanol (50 ml). The eluate was dried and recrystallized from methanol–diethyl ether. The potassium salt of the oxo bile acid (20 mg) thus obtained was dissolved in H₂¹⁸O (isotopic purity 98 atom%, 300 μl) and heated at 90°C for 50 h. After cooling, the solution was stirred with NaB²H₄ (isotopic purity 97 atom%, 4 mg) for 1 h with cooling in ice, and then poured into 5% hydrochloric acid. Unconjugated and glycine-conjugated bile acids were extracted with ethyl acetate. In the case of taurine-conjugates, the reaction mixture was poured into 5% hydrochloric acid, neutralized with 5% potassium hydroxide and then passed through a column (19 mm × 20 mm I.D.) of Pre Pak-500/C₁₈ (2 g). After washing with water (20 ml), the desired bile acids were eluted with ethanol (20 ml). The ¹⁸O,²H-labelled bile acids thus obtained were purified by means of column chromatography on silica gel and HPLC on a reversed-phase column⁹.

Sample preparation

Liver biopsies were performed at the Third Department of Internal Medicine, Tohoku University School of Medicine, for histological examination. A part of the liver tissue was used for this work.

The sample preparation was carried out according to the method previously reported². Liver tissue weighing 2–10 mg taken by diagnostic needle biopsy was rinsed with ice-cold saline, placed on a filter-paper until weighing and then put into a 10-ml PTFE test-tube. To this tube was added 5% sodium hydroxide (1 ml) containing 1–10 ng each of unconjugated, glycine- and taurine-conjugated ¹⁸O,²H-labelled bile acids as I.S., and the whole was heated at 80°C for 30 min to solubilize the tissue. A 100–200 μl aliquot was taken to determine the protein content by the method of Lowry *et al.*¹⁰. The remaining solution was neutralized with 10% hydrochloric acid and then passed through a Sep-Pak C₁₈ cartridge. After washing with water (4 ml), bile acids were eluted with 90% ethanol (5 ml). The eluate was applied to a column (18 mm × 6 mm I.D.) of PHP-LH-20 (100 mg) and elution was carried out at a flow-rate of 0.2 ml/min. After washing with 90% ethanol (4 ml), unconjugated, glycine- and taurine-conjugated bile acids were fractionally separated by stepwise elution with 0.1 M acetic acid in 90% ethanol (5 ml), 0.2 M formic acid in 90% ethanol (5 ml) and 0.3 M acetic acid–potassium acetate in 90% ethanol (pH 6.5) (5 ml)^{5,11}. Hydrolytic cleavage of glycine- and taurine-conjugates in each fraction was then performed by incubation at 37°C for 2 h with cholyglycine hydrolase (5 U) in 0.1 M acetate buffer (pH 5.6, 1 ml) containing 0.1 M 2-mercaptoethanol and 0.2 M EDTA disodium salt. To the incubation mixture was added 0.1 M sodium hydroxide (0.1 ml), and the whole was applied to a Sep-Pak C₁₈ cartridge in the manner described above for removal of proteins and inorganic salts. The unconjugated, glycine- and taurine-conjugated fractions were evaporated to dryness under reduced pressure and then were derivatized to PFB ester–DMES ethers.

Derivatization

To the deconjugated bile acid were added 5% (v/v) PFB bromide in acetonitrile (60 μl) and diisopropylethylamine (10 μl), and the whole was allowed to stand at 37°C for 45 min. The reaction mixture was diluted in ethanol–acetonitrile (1:1, 1 ml), and

then applied to a Sep-Pak C₁₈ cartridge impregnated with ethanol. The PFB esters were eluted with ethanol-acetonitrile (1:1, 4 ml). To the dried eluate were added DMES-imidazole (50 μ l) and 1% pyridine in hexane (50 μ l), and the whole was heated at 60°C for 1 h^{12,13}. Following the addition of 1% each of methanol and pyridine in hexane (200 μ l) to decompose the excess of silylating reagent, the solution was evaporated under a stream of nitrogen. The residue was redissolved in 1% pyridine in hexane and injected onto the GC-MS system.

RESULTS AND DISCUSSION

Preparation of stable isotope-labelled bile acids

The reversed isotope dilution technique in combination with GC-MS provides a useful methodology for the trace analysis of important biological materials with high accuracy, specificity and sensitivity. For this purpose, target compounds labelled with ²H have been commonly used as I.S. In the previous paper, we demonstrated that bile acid PFB ester-DMES ethers exhibited characteristic negative ions [M - PFB]⁻, which contain oxygen atoms in both hydroxyl and carboxyl groups, as base peaks in NICI-MS³. This finding strongly suggested that an ¹⁸O-labelled I.S. would be useful for the trace analysis of bile acids by GC with selected-ion monitoring (SIM). The incorporation of ¹⁸O atoms into prostaglandins was attained through the carboxyl moiety by chemical or enzymatic hydrolysis of the ester bond in H₂¹⁸O^{14,15}. In order to obtain ¹⁸O-labelled bile acids with high isotopic purity, this procedure requires four to five cycles of esterification of the carboxyl group followed by hydrolysis of the ester. Moreover, the formation of amide bonds with glycine and taurine through the carboxyl group results in loss of the ¹⁸O label. Consequently, introduction of ¹⁸O atoms into the hydroxyl groups on the steroid nucleus was attempted by the use of an exchange reaction of the carbonyl oxygen atom¹⁶. Initially, the reactivities of the carbonyl groups at C-3, C-7 and C-12 towards the exchange reaction were examined with 3- and 7-dehydro CDCA and 12-dehydro DCA. It is well known that such an exchange reaction proceeds more easily under basic conditions. In addition, the alkali metal salt of the carboxylic acid is fairly soluble in water. Hence, oxo bile acids were converted into the potassium salts by passage through a lipophilic cation-exchange gel, CM-LH-20 (K⁺ form). The potassium salt was then dissolved in H₂¹⁸O, whose isotopic purity was 98 atom%, and allowed to stand at 37 or 90°C. Aliquots of the resulting solution were taken at certain times and subjected to reduction with sodium borohydride. Following derivatization to the PFB ester-DMES ether, the content of ¹⁸O in CDCA and DCA labelled with heavy isotope was determined by GC-SIM using a characteristic ion, [M - 181]⁻. As illustrated in Fig. 1, the reaction rate was found to be dependent upon the position of the carbonyl group. The content of ¹⁸O at C-3 increased along with the reaction time up to 2 h and reached the theoretical value at 37°C. On the other hand, the contents at C-7 and C-12 remained almost unchanged, even though the reaction time was prolonged for 6 h at 37°C. When the exchange reaction was performed at 90°C, even for carbonyl groups at C-7 and C-12, the ¹⁸O content was elevated to a plateau at 45 h. The marked difference in the reactivity may be explained in terms of the steric hindrance of the carbonyl carbon atom. The position of the ¹⁸O atom incorporated was further confirmed. Bile acids were transformed into the methyl ester-DMES ether derivatives and then subjected

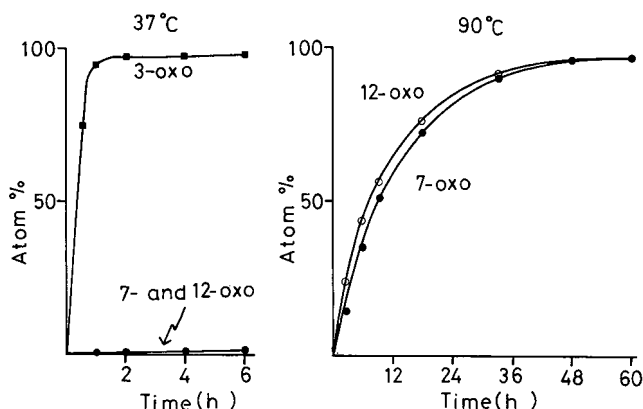


Fig. 1. Time courses for incorporation of ^{18}O atom into oxo bile acids.

to MS with the electron impact ionization mode. As compared with the non-labelled dihydroxy bile acids, the molecular ion was observed at two units to higher masses, while the fragment ion formed by elimination of two dimethylethylsilanol groups was at the same mass number. No exchange with the heavy isotope occurred at the carboxyl group under these conditions.

On the basis of these results, the preparation of unconjugated, glycine- and taurine-conjugated bile acids labelled with ^{18}O atom was then undertaken. Potassium 5β -cholanates having the carbonyl groups at C-3, C-7 and C-12, prepared by chromium trioxide oxidation from common bile acids and ion exchange on CM-LH-20 (potassium form), were dissolved in H_2^{18}O (isotopic purity of 98%) and heated at 90°C for 50 h. Following metal hydride reduction and, if necessary, hydrolytic cleavage of glycine- and taurine-conjugates with cholyglycine hydrolase, the ^{18}O contents were determined as PFB esters-DMES ethers. It is evident from the data listed in Table I that ^{18}O was incorporated into oxo bile acids at each position in the theoretical amounts. Labelled UDCA, that is the positional isomer of CDCA, was also obtained by metal hydride reduction of 3,7-didehydro CDCA as a minor product. It is well known that the introduction of a number of ^2H atoms into a molecule causes a somewhat smaller retention value in GC. Such a kinetic isotope effect was negligible

TABLE I
ATOM% EXCESS OF ^{18}O -LABELLED BILE ACIDS*

Bile acid	Number of ^{18}O			
	0	1	2	3
LCA	2.4	97.6		
CDCA	<0.1	5.8	94.2	
DCA	<0.1	5.9	94.1	
CA	<0.1	0.5	8.3	91.2

* Corrected for background and natural abundance of stable isotopes.

for ^{18}O -labelled bile acids and, hence, no marked difference in the retention time was found even in labelled CA having three ^{18}O atoms.

Since the natural abundance of stable isotopes causes intense isotope peaks especially in the high mass region, a difference of more than 3 mass units between the labelled and unlabelled compounds is recommended. As for lithocholates, the two substrates differ from each other by only 2 mass units. Moreover, labelled lithocholates would be contaminated with more than 2% of unlabelled species owing to the isotopic purity of H_2^{18}O used. Therefore, further labelling with ^2H was undertaken. The ^{18}O -labelled oxo bile acids were reduced with sodium borodeuteride (NaB^2H_4) (isotopic purity 97%) and the heavy isotope contents in the product were estimated in the manner described above. As shown in Table II, the ratios of the unlabelled fragment to the fully labelled fragment in [^{18}O , ^2H]mono-, -di- and -trihydroxylated bile acids were found to be 1/500, 1/2000 and 1/10 000, respectively. This result implies that these labelled bile acids can also serve as carriers, preventing the loss of target compounds in the clean-up procedure. Any labelled isotopes were not eliminated during alkaline hydrolysis and solvolysis. A calibration graph was constructed by plotting the ratio of the peak height of each bile acid to that of the corresponding I.S. against the weight ratio of bile acid to the corresponding I.S. For unconjugated, glycine- and taurine-conjugated UDCA, corresponding [^{18}O , ^2H]CDCAs were used as the I.S.s. The calibration graphs for unconjugated bile acids using 1 ng each of the corresponding I.S. are shown in Fig. 2. The linearity was good in the range of 0.01–20 for LCA, 0.005–100 for dihydroxylated bile acids and 0.01–500 for CA. Almost the same calibration graphs were obtained for glycine- and taurine-conjugates. A typical selected-ion recording of a synthetic mixture of unconjugated bile acids is illustrated in Fig. 3, where the monitoring ions were 461/464 for LCA, 563/569 for DCA, CDCA and UDCA and 665/674 for CA.

TABLE II

RATIOS OF UNLABELLED TO LABELLED FRAGMENT IN STABLE ISOTOPE-LABELLED BILE ACIDS

Compound	Peak height ratio		
	461/464	563/569	665/674
[3- ^{18}O ,3- ^2H]LCA	0.0022		
[3- ^{18}O ,3- ^2H]GLCA	0.0016		
[3- ^{18}O ,3- ^2H]TLCA	0.0020		
[3,7- $^{18}\text{O}_2$,3,7- $^2\text{H}_2$]CDCA		0.0001	
[3,7- $^{18}\text{O}_2$,3,7- $^2\text{H}_2$]GCDCA		< 0.0001	
[3,7- $^{18}\text{O}_2$,3,7- $^2\text{H}_2$]TCDCAs		< 0.0001	
[3,12- $^{18}\text{O}_2$,3,12- $^2\text{H}_2$]DCA		0.0005	
[3,12- $^{18}\text{O}_2$,3,12- $^2\text{H}_2$]GDCA		0.0006	
[3,12- $^{18}\text{O}_2$,3,12- $^2\text{H}_2$]TDCA		0.0001	
[3,7,12- $^{18}\text{O}_3$,3,7,12- $^2\text{H}_3$]CA			< 0.0001
[3,7,12- $^{18}\text{O}_3$,3,7,12- $^2\text{H}_3$]GCA			< 0.0001
[3,7,12- $^{18}\text{O}_3$,3,7,12- $^2\text{H}_3$]TCA			< 0.0001

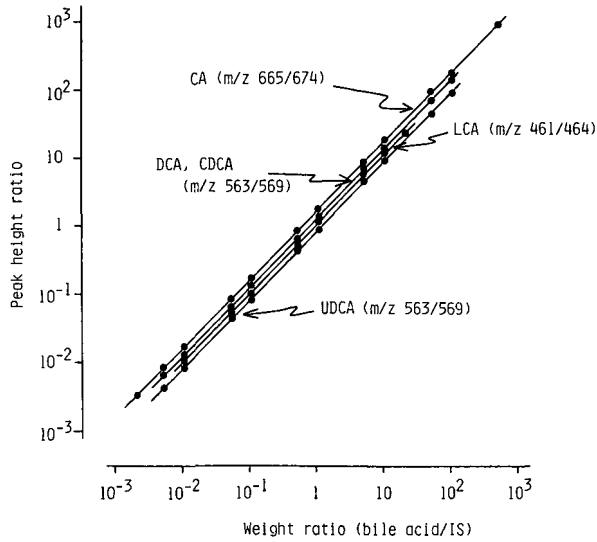


Fig. 2. Calibration graphs for bile acids.

Determination of bile acids in liver tissue

A standard procedure for the determination of bile acids in liver tissue is shown in Fig. 4. A liver tissue specimen was solubilized with an alkaline solution containing unconjugated, glycine- and taurine-conjugated [^{18}O , ^2H]bile acids as I.S.s, according to the method of Yanagisawa *et al.*², and bile acids were extracted with a Sep-Pak C_{18} cartridge. The GC-MS technique has inevitable disadvantages such as the loss of information about the conjugated form. Therefore, bile acids were separated into the unconjugated, glycine- and taurine-conjugated fractions by ion-exchange chromatography on PHP-LH-20 prior to deconjugation^{5,11}. After enzymatic hydrolysis of the amide bonds, bile acids in each fraction were derivatized to the PFB esters. In the previous study, removal of the excess of PFB bromide was carried out by means of

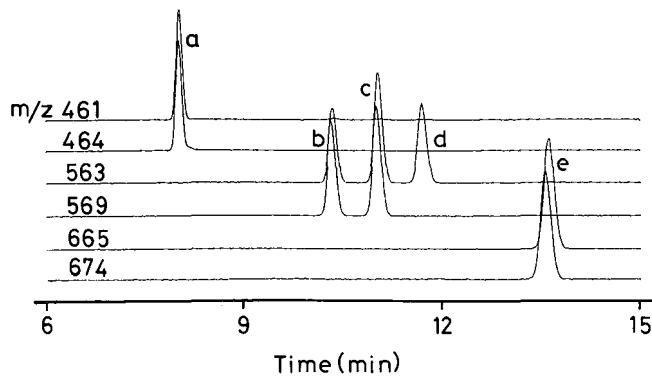


Fig. 3. GC with NICI selected-ion recording of bile acids as the PFB ester-DMES ether derivatives. a = LCA; b = DCA; c = CDCA; d = UDCA; e = CA.

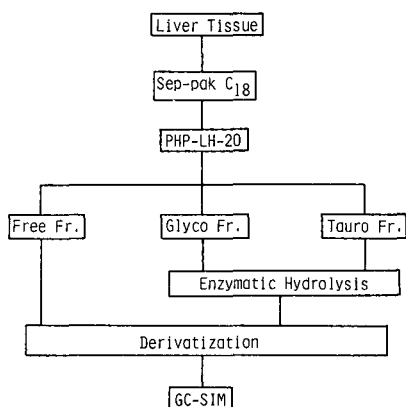


Fig. 4. Procedure for determination of bile acids in liver tissue.

column chromatography on silica gel¹⁷. However, this clean-up procedure proved to be unfavourable for trace analysis of bile acids because of the low recovery. Therefore, reversed-phase partition chromatography on a Sep-Pak C₁₈ cartridge was employed for this purpose. The reaction mixture was applied to the cartridge and the cartridge was washed with methanol-acetonitrile. The bile acid PFB esters were recovered quantitatively, the excess of reagent remaining on the cartridge. Subsequently, the PFB esters were derivatized to the DMES ethers according to the method previously reported^{2,12,13}.

Applying the standard procedure to human liver, bile acids were determined with satisfactory reproducibility. Known amounts of bile acids were added to the solubilized test samples corresponding to approximately 2 mg of liver tissue, and their recoveries were estimated. In these experiments, the I.S.s were added prior to solubilization or derivatization. As listed in Table III, all bile acids exhibited satisfactory recoveries. The present method was applied to the simultaneous determination of bile acids in liver tissue obtained by diagnostic needle biopsy, and the results obtained are collected in Table IV. An amount of 1 μ g wet weight of liver tissue corresponded to about 90 μ g of protein. A typical selected-ion recording of the unconjugated bile acids in human liver tissue is illustrated in Fig. 5. The peaks of LCA, DCA, CDCA, UDCA and CA on the chromatogram represent approximately 3, 28, 34, 5 and 49 fmol as injected amounts, respectively.

In this study, we developed a new method for the determination of bile acids in liver tissue by GC-SIM with NICI detection. Although ²H-labelled bile acids have been commonly used as I.S.s, the preparation of these compounds with high isotopic purity needs a time-consuming and tedious procedure. Hence, ²H labelling has been employed only for unconjugated bile acids. For the determination of bile acids, the observed value should be corrected owing to the low recoveries of glycine- and taurine-conjugates². The present method for introducing ¹⁸O atoms into the hydroxyl groups made possible the preparation of unconjugated, glycine- and taurine-conjugated bile acids labelled with a stable isotope by a simple procedure. The group separation on PHP-LH-20 can serve to provide information about the conjugated form at C-24. Common bile acids in liver tissue were separated into LCA, DCA,

TABLE III
RECOVERY OF UNCONJUGATED BILE ACIDS ADDED TO SOLUBILIZED LIVER TISSUE

<i>Bile acid</i>	<i>Tissue (ng/mg[*])</i>	<i>Added (ng/mg[*])</i>	<i>Expected (ng/mg[*])</i>	<i>Found (ng/mg[*])</i>	<i>Recovery (% ± S.D.**)</i>
<i>Internal standards added prior to solubilization</i>					
LCA	0.019	0.051	0.070	0.069	98.6 ± 5.2
DCA	0.201	0.100	0.301	0.291	96.7 ± 4.9
CDCA	0.256	0.102	0.358	0.350	97.8 ± 3.7
UDCA	0.052	0.053	0.105	0.101	96.2 ± 4.8
CA	0.521	0.101	0.622	0.628	101.0 ± 4.2
GLCA	0.150	0.105	0.255	0.249	97.6 ± 5.1
GDCA	4.02	1.03	5.05	5.00	99.0 ± 3.9
GCDCA	4.82	1.00	5.82	5.70	79.9 ± 3.8
GUDCA	0.432	0.102	0.534	0.530	99.3 ± 5.8
GCA	6.50	1.06	7.56	7.58	100.3 ± 4.7
TLCA	0.130	0.101	0.231	0.227	98.3 ± 4.3
TDCA	0.789	0.508	1.297	1.30	100.2 ± 4.5
TCDCa	1.89	0.511	2.401	2.40	100.0 ± 5.2
TUDCA	0.184	0.102	0.286	0.280	97.9 ± 6.5
TCA	1.90	0.502	2.402	2.39	99.5 ± 5.7
<i>Internal standards added prior to derivatization</i>					
LCA	0.021	0.051	0.072	0.059	81.9 ± 12.3
DCA	0.144	0.100	0.244	0.210	86.1 ± 7.5
CDCA	0.184	0.102	0.286	0.240	83.9 ± 6.7
UDCA	0.036	0.053	0.089	0.071	79.8 ± 10.4
CA	0.267	0.101	0.368	0.302	82.1 ± 9.2
GLCA	0.038	0.105	0.143	0.113	79.0 ± 24.8
GDCA	2.40	1.03	3.43	2.92	85.1 ± 9.8
GCDCA	3.56	1.00	4.56	4.10	89.9 ± 8.4
GUDCA	0.362	0.102	0.464	0.371	80.0 ± 18.7
GCA	2.96	1.06	4.02	3.22	80.1 ± 9.6
TLCA	0.057	0.101	0.158	0.124	78.5 ± 12.2
TDCA	0.567	0.508	1.075	0.881	82.0 ± 12.6
TCDCa	1.02	0.510	1.530	1.30	85.0 ± 11.3
TUDCA	0.125	0.102	0.227	0.177	78.0 ± 24.6
TCA	1.00	0.502	1.502	1.127	75.0 ± 11.0

* Given in ng/mg liver tissue in wet weight.

** $n = 8$.

CDCA, UDCA and CA as PFB ester-DMES ethers on a capillary column coated with 5% phenylmethyl silicone. Monitoring with characteristic negative ions, $[M - PFB]^-$, unconjugated bile acids, which comprised less than 10% of the total amount, in 2-10 mg of the liver tissue specimen were determined with a quantitation limit of 10 pg/mg tissue.

In man, bile acids are also conjugated with glucuronic acid and sulphuric acid to form glucuronides and sulphates, respectively. The preparation of these bile acid conjugates labelled with ^{18}O and their use for GC-MS are being undertaken in these laboratories. It is hoped that the availability of an excellent method for the simultaneous determination of bile acids in liver tissue with satisfactory sensitivity and reliabil-

TABLE IV

AMOUNTS OF BILE ACIDS IN HUMAN LIVER TISSUE DETERMINED BY THE PRESENT METHOD

Results are given in ng/mg protein.

Bile acid	Patient 1*	Patient 2*	Patient 3*	Patient 4**
CA	2.50	6.52	4.86	5.23
CDCA	3.22	7.74	6.83	3.69
DCA	4.20	1.65	2.35	2.88
UDCA	0.45	0.92	1.03	0.71
LCA	1.21	1.62	2.08	0.43
GCA	29.35	35.76	85.12	59.15
GCDCA	46.72	141.24	198.20	71.22
GDCA	44.46	11.76	40.25	48.16
GUDCA	3.41	1.92	11.63	7.30
GLCA	2.02	4.81	4.79	0.76
TCA	11.23	24.63	29.19	20.13
TCDC	11.41	50.05	40.84	20.55
TDCA	8.12	3.87	12.15	11.35
TUDCA	0.83	0.79	3.00	2.49
TLCA	2.06	2.67	6.25	1.15

* Chronic inactive hepatitis.

** Acute hepatitis.

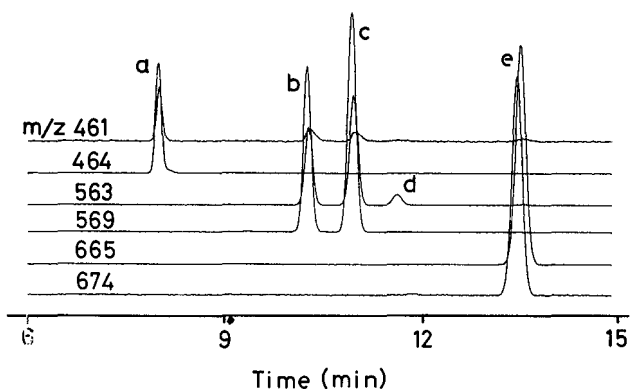


Fig. 5. GC with NICI selected-ion recording of unconjugated bile acids in solubilized human liver tissue as the PFB ester-DMES ether derivatives.

ity may provide much more precise knowledge on the metabolic profile of bile acids and serve as a diagnosis for hepatobiliary diseases.

ACKNOWLEDGEMENT

This work was supported in part by a grant from the Ministry of Education, Science and Culture of Japan.

REFERENCES

- 1 J. M. Street, D. J. H. Trafford and H. L. Makin, *J. Lipid Res.*, 24 (1983) 491.
- 2 J. Yanagisawa, M. Itoh, M. Ishibashi, H. Miyazaki and F. Nakayama, *Anal. Biochem.*, 104 (1980) 75.
- 3 J. Goto, K. Watanabe, H. Miura, T. Nambara and T. Ida, *J. Chromatogr.*, 388 (1987) 379.
- 4 J. Goto, H. kato, F. Hasegawa and T. Nambara, *Chem. Pharm. Bull.*, 27 (1979) 1402.
- 5 J. Goto, M. Hasegawa, H. kato and T. Nambara, *Clin. Chim. Acta*, 87 (1978) 141.
- 6 E. Nyström, *Ark. Kemi*, 29 (1968) 99.
- 7 J. Goto, K. Suzaki and T. Nambara, *Chem. Pharm. Bull.*, 30 (1982) 4422.
- 8 T. Iida, T. Shinohara, T. Momose, T. Matsumoto, T. Nambara and F. C. Chang, *Synthesis*, (1986) 998.
- 9 J. Goto, H. Kato, Y. Saruta and T. Nambara, *J. Liq. Chromatogr.*, 3 (1980) 991.
- 10 O. H. Lowry, N. J. Rosenbrough, A. L. Farr and R. J. Randall, *J. Biol. Chem.*, 193 (1951) 265.
- 11 J. Goto, Y. Sano, K. Tsuchiya and T. Nambara, *J. Chromatogr.*, 425 (1988) 59.
- 12 H. Miyazaki, M. Ishibashi, M. Itoh and T. Nambara, *Biomed. Mass Spectrom.*, 4 (1977) 23.
- 13 Y. Nishikawa, K. Yamashita, M. Ishibashi and H. Miyazaki, *Chem. Pharm. Bull.*, 26 (1978) 2922.
- 14 R. J. Strife and R. C. Murphy, *Prostagland. Leuk. Med.*, 13 (1984) 1.
- 15 J. Y. Westcott, K. L. Clay and R. C. Murphy, *Biomed. Mass Spectrom.*, 12 (1985) 714.
- 16 J. A. McCloskey, *Methods Enzymol.*, 14 (1969) 382—450.
- 17 H. Miyazaki, M. Ishibashi, K. Yamashita, I. Ohguchi, H. Saitoh, H. Kurono, M. Shimono and M. Katori, *J. Chromatogr.*, 239 (1982) 595.

CHROM. 20 462

STUDIES OF ADSORPTION AND PARTITION EFFECTS IN LIQUID CHROMATOGRAPHY WITH MIXED MOBILE PHASES

M. BORÓWKO and M. JARONIEC*

Institute of Chemistry, M. Curie-Skłodowska University, 20-031 Lublin (Poland)

SUMMARY

A general theory of liquid chromatography with mixed mobile phases formulated previously was utilized to study quantitatively the adsorption and partition effects in solute retention. The competitive adsorption of the solute and solvent was found to influence significantly the values of the distribution coefficient, whereas the solute–solvent interactions control mainly the shape of the dependence of this coefficient on the mobile phase composition.

The mechanism of solute retention in liquid chromatography with mixed mobile phases is mainly determined by the competitive adsorption of solute and solvent molecules (adsorption mechanism) and the differentiated interactions of solute molecules with solvent molecules in the stationary and mobile phases^{1–4}. If the adsorption effects are negligible then the source of the distribution of solute molecules between the surface-influenced stationary phase and the mobile phase is the differentiation in the solute–solvent interactions in both phases. The physical nature of this solute retention mechanism is analogous to classical partitioning and therefore it was called the “partition mechanism”². The adsorption mechanism of solute retention dominates in normal-phase liquid–solid chromatography, whereas the partition mechanism dominates in reversed-phase liquid chromatography. In previous papers^{2,3} a general theory of liquid chromatography was formulated for describing the adsorption and partition mechanisms of solute retention. Here, this theory is applied to study quantitatively the influence of these mechanisms on the dependence of the distribution coefficient on the mobile phase composition.

Let us consider retention of the *s*-th solute in a binary mixed solvent^{1,2}. For simplicity, let us assume that the molecules of both solvents have the same size. The equilibrium between the two solvents in the mobile phase and the surface-influenced stationary phase is described by the general expression^{1–4}

$$K_{12} = (x_1^\sigma \gamma_1^\sigma / x_1^l \gamma_1^l) (x_2^l \gamma_2^l / x_2^\sigma \gamma_2^\sigma) \quad (1)$$

with

$$x_1^\sigma + x_2^\sigma \approx 1 \text{ for } \rho = \sigma \text{ and } l \quad (2)$$

Here K_{12} is the equilibrium constant for the phase-exchange reaction between molecules of solvents 1 and 2, x_i^ρ ($i = 1, 2$) denotes the mole fraction of the i -th solvent in the ρ -th phase and γ_i^ρ is the activity coefficient of the i -th component in the ρ -th phase and $\rho = 1$ (bulk phase) or σ (stationary phase).

The retention of the s -th solute is characterized by the distribution coefficient¹:

$$k_s = \lim_{x_s^1 \rightarrow 0} (x_s^\sigma/x_s^1) \quad (3)$$

A general equation for the distribution coefficient is

$$k_s = K_{s1} (y_s^1/y_s^\sigma) (x_1^\sigma y_1^\sigma/x_1^1 y_1^1) \quad (4)$$

where K_{s1} denotes the phase exchange between molecules of the s -th solute and first solvent, and γ_s^ρ is the activity coefficient of the s -th solute in the ρ -th phase. When competitive adsorption fully controls solute distribution we have:

$$k_s = K_{s1} (x_1^\sigma/x_1^1) \quad (5)$$

In this case all activity coefficients are equal to unity. For the pure partition model the distribution coefficient is defined as follows:

$$k_s = \gamma_s^1/\gamma_s^\rho \quad (6)$$

Eqn. 6 is obtained from eqn. 4 for $K_{12} = K_{s1} = K_{s2} = 1$.

The model studies of adsorption and partition effects in liquid chromatography are discussed for a strictly regular solution. The stationary phase composition is calculated from the expression

$$x_1^\sigma = F/(1 + F) \quad (7)$$

where

$$F = K_{12}[x_1^1/(1 - x_1^1)] \exp \{ \chi_{12}^1[(1 - 2x_1^1) - q(1 - 2x_1^\sigma)] \} \quad (8)$$

and

$$\chi_{12}^\sigma = q\chi_{12}^1 \quad (9)$$

Here q is a constant equal to the ratio of the numbers of neighbours in the same lattice layer to the total number of neighbours for each lattice site.

For $K_{12} \neq 1$ the general eqn. 4 gives the following expression for the distribution coefficient, k_s

$$k_s = K_{s1} (x_1^\sigma/x_1^1) \exp [\alpha(x_1^1 - qx_1^\sigma) + \beta] \quad (10)$$

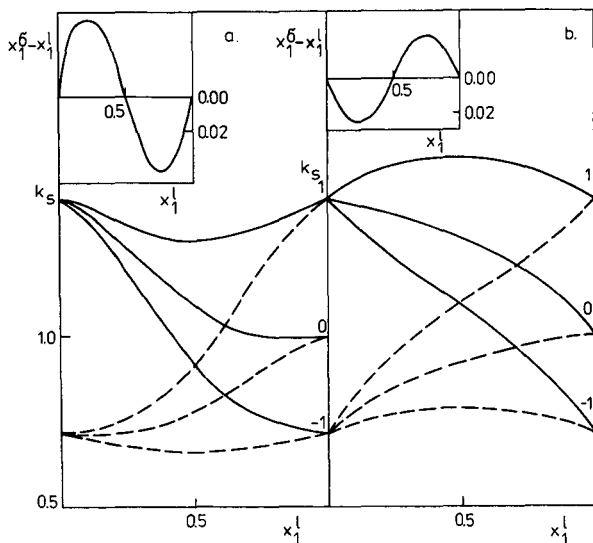


Fig.1. Partition model. Theoretical curves of k_s vs. x_1^I and the excess adsorption isotherms $n_1^e = x_1^\sigma - x_1^I$ plotted for $\chi_{12}^I = 1$ (a). $\chi_{12}^I = -1$ (b) and different values of the parameters $\chi_{1s}^I = -1, 0, 1$ and $\chi_{2s}^I = -1$ (---) and 1 (—); $q = \frac{2}{3}$.

where

$$\alpha = \chi_{12}^I + \chi_{1s}^I - \chi_{2s}^I \tag{11}$$

$$\beta = (1 - q) (\chi_{2s}^I - \chi_{12}^I) \tag{12}$$

and χ_{is}^I ($i = 1, 2$) is the interaction parameter that characterizes the solution (i, s).

For the pure partition model, eqn. 6 leads to:

$$k_s = \exp\{(\chi_{1s}^I - \chi_{12}^I) (x_1^I - qx_1^\sigma) - \chi_{12}^I [x_1^I (1 - x_1^I) - qx_1^\sigma (1 - x_1^\sigma)] + \chi_{2s}^I (1 - q)\} \tag{13}$$

Now we will discuss the influence of the mobile phase composition on the distribution coefficient for particular retention models. First, the pure displacement model will be analysed. In this case the interaction parameter, χ_{12}^I , is equal to zero. Then the function $k_s = k_s(x_1^I)$ has the analytical form

$$k_s = K_{s1} / [K_{21} + (1 - K_{21}) x_1^I] \tag{14}$$

where $K_{21} = 1/K_{12}$. It follows from previous papers^{1,4} that for $K_{12} > 1$ the function $k_s(x_1^I)$ decreases. For $K_{12} = K_{s1} = K_{s2} = 1$ the distribution of a solute between two phases occurs according to the partition mechanism. Fig. 1 shows the function $k_s(x_1^I)$ calculated according to eqn. 13. From this figure we can conclude that: (i) the function $k_s(x_1^I)$ may be strictly decreasing for $\chi_{2s}^I > \chi_{1s}^I$ or increasing for $\chi_{2s}^I < \chi_{1s}^I$; (ii) this

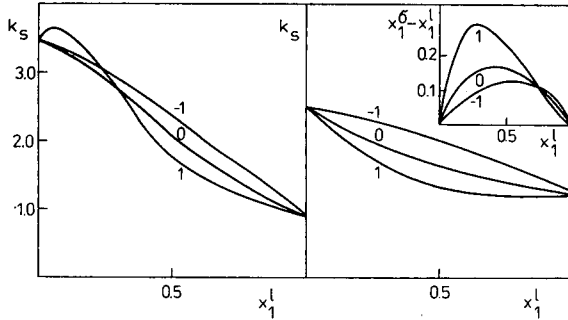


Fig. 2. Mixed model. Theoretical curves of k_s vs. x_1^I and the excess adsorption isotherm for $K_{12} = 2$, $K_{s1} = 1.25$, $\chi_{1s}^I = -1$, $\chi_{2s}^I = 1$ (left), $\chi_{1s}^I = \chi_{2s}^I = 0$ (right) and different values of the parameter $\chi_{12}^I = -1, 0, 1$; $q = \frac{2}{3}$.

function may have one extremum, a maximum for $\chi_{12}^I < 0$ or a minimum for $\chi_{12}^I > 0$; (iii) solute-solvent and solvent-solvent interactions affect the solute retention in quite different ways, an increase in χ_{1s}^I and χ_{2s}^I causing an increase in the distribution coefficient, whereas the opposite effect is observed when χ_{12}^I increases. The excess adsorption isotherms ($x_1^G - x_1^I$) associated with the curves $k_s(x_1^I)$ are also presented in Fig. 1.

In the case of mixed solute retention for particular values of the parameters χ_{1s}^I and χ_{2s}^I , the curves $k_s(x_1^I)$ corresponding to different values of the parameter χ_{12}^I may interact. For $x_1^I \rightarrow 0$ an increase in χ_{12}^I causes an increase in the distribution coefficient; the opposite effect is observed for high concentrations of the first solvent (Fig. 2). When the adsorption constants are sufficiently high a maximum in such a curve can occur even for mixed solvents characterized by a positive deviation from Raoult's law.

Fig. 3 presents a comparison of the curves k_s vs. x_1^I and the excess adsorption isotherms calculated for different models of solute retention. Curve 1 is for the mixed model. In this case the solute retention is caused by the difference in adsorption potentials of the solute and solvents, and the difference in the solute-solvent

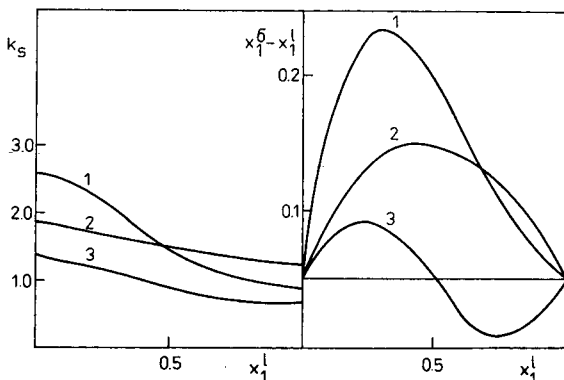


Fig. 3. Comparison of solute retention models: mixed model with $K_{s1} = 1.25$, $K_{12} = 1.5$, $\chi_{1s}^I = 1$, $\chi_{2s}^I = -1$, $\chi_{12}^I = 1$ (curve 1); displacement model with $K_{s1} = 1.25$, $K_{12} = 1.5$, $\chi_{12}^I = \chi_{1s}^I = \chi_{2s}^I = 0$ (curve 2) and partition model with $K_{s1} = K_{s2} = K_{12} = 1$, $\chi_{1s}^I = 1$, $\chi_{2s}^I = -1$ and $\chi_{12}^I = 1$ (curve 3); $q = \frac{2}{3}$.

interactions in both phases. For the system investigated the equilibrium constants are $K_{s1} = 1.25$, $K_{12} = 1.5$. Curve 2 represents the pure displacement (adsorption) model; it was calculated for $\chi_{12}^1 = \chi_{1s}^1 = \chi_{2s}^1 = 0$ and the remaining parameters were the same as for curve 1. Curve 3 corresponds to the pure partition model. From Fig. 3, the interactions with the adsorbent surface (adsorption effects) have a predominant influence on the value of the distribution coefficient, however the partition effects control the course of the dependence of the distribution coefficient on the mobile phase composition.

REFERENCES

- 1 M. Jaroniec, D. E. Martire and M. Borówko, *Adv. Colloid Interface Sci.*, 22 (1985) 177.
- 2 M. Jaroniec and D. E. Martire, *J. Chromatogr.*, 351 (1986) 1.
- 3 M. Jaroniec and D. E. Martire, *J. Chromatogr.*, 387 (1987) 55.
- 4 M. Borówko and M. Jaroniec; *Adv. Colloid Interface Sci.*, 19 (1983) 137.

CHROM 20 604

INTERCHANGEABLE USE OF AQUEOUS AND ORGANIC SOLVENTS IN A HYDROPHILIC POLY(VINYL ALCOHOL) GEL COLUMN

SADAO MORI

Department of Industrial Chemistry, Faculty of Engineering, Mie University, Tsu, Mie 514 (Japan)

SUMMARY

Water, methanol, chloroform and their mixtures were used as mobile phases and the elution behaviours of polyethylene glycols (PEG) and polystyrenes (PS) on a hydrophobic poly(vinyl alcohol) column were investigated. The column efficiency was not affected by variation of the mobile phase. Samples were eluted in order of decreasing molecular weight and separation was mainly achieved by size exclusion, a slight adsorption effect being superimposed. With water–methanol as the mobile phase, the minimum retention volume of PEG was obtained with a mobile phase composition of water–methanol (25:75, v/v) and a size-exclusion separation was mainly expected. With other compositions of this mobile phase an adsorption effect was superimposed on size exclusion. With chloroform–methanol as the mobile phase, the minimum retention volume of PS was obtained with a mobile phase composition of chloroform–methanol (80:20, v/v) and a slight adsorption effect was observed. Size-exclusion, adsorption and partition effects were evaluated from the variations of retention volumes, peak widths and solubility parameters.

INTRODUCTION

A number of applications of high-performance liquid chromatographic (HPLC) columns packed with polymer-based materials have been reported. Most of them involve porous polymer beads such as styrene–divinylbenzene copolymers which are hydrophobic in nature. These porous polystyrene (PS) gels have been used in both reversed-phase and normal-phase chromatography and also in size-exclusion chromatography (SEC) with various mobile phases¹. The first attempt to use PS gels as packing materials for aqueous SEC was reported by Chow², who separated dextrans having different molecular weights by using 0.1% sodium lauryl sulphate solution as the mobile phase.

However, because of the hydrophobic nature of PS gels, their use is limited to reversed-phase chromatography in addition to non-aqueous SEC. Polymer-based packing materials may have great stability with mobile phases over a wide range of pH and therefore they have attracted much attention. Polystyrene- and polyacrylamide-based packing materials have been developed for reversed-phase chromatography³ and applied to pharmaceutical analysis⁴. A solvent eluotropic scale for PS gels has

been developed⁵. To reduce their hydrophobicity, neutral hydrophilic groups were covalently bonded to the surface of porous PS gels⁶.

Several types of hydrophilic gels are now commercially available for aqueous SEC. These gels are used exclusively for water-soluble ionic and non-ionic polymers such as polysaccharides, proteins and sodium polystyrene sulphonates. However, these polymer gels undergo shrinkage with many organic solvents and the mobile phases available are limited to aqueous solutions plus small amounts of organic solvents.

Recently, it was found that some hydrophilic polymer gels containing a vinyl alcohol copolymer were compatible with polar and non-polar organic solvents⁷. Hence columns packed with these gels can be used interchangeably with both aqueous solutions and non-polar organic solvents as mobile phases without loss of column efficiency.

In this work three solvents, water, methanol and chloroform, were used as mobile phase components and the elution behaviour of polyethylene glycols (PEG), PS and related compounds were investigated on columns packed with these poly(vinyl alcohol) gels.

EXPERIMENTAL

The column used was Asahipak GS-310 (500 mm × 7.6 mm) (Asahi Chemical, Kawasaki, Japan) packed with a vinyl alcohol copolymer gel. The packing solvent was water-methanol (70:30, v/v). A Jasco (Japan Spectroscopic, Tokyo, Japan) Trirotar-V high-performance liquid chromatograph was used with two different types of detectors: a Jasco Uvidec-100 IV ultraviolet (UV) detector and a Shodex (Showa Denko, Tokyo, Japan) Model SE-11 refractive index (RI) detector. The UV detector was operated at 254 nm. Sample solutions were injected using a Model VL-611 variable-loop injector (Jasco).

The methanol phases were water, methanol, chloroform and mixtures of water and methanol and of chloroform and methanol. Elution was performed in the isocratic mode at a flow-rate of 0.5 ml/min. The concentration of the sample solutions was 0.5% and the volume of sample injected was 0.025 ml. Samples were dissolved in the solvent used as the mobile phase.

The samples were benzene, *n*-hexylbenzene, ethylene glycol, polyethylene glycols (PEG), polyethylene oxides (PEO) and polystyrenes (PS). These polymers were relatively monodisperse and their molecular weights were known.

When the mobile phase was changed, the flow rate was decreased to 0.3 ml/min and a pump was operated overnight to allow the new mobile phase to flow through the column in order to condition it. After this column conditioning the flow-rate was increased to 0.5 ml/min again.

RESULTS

Number of theoretical plates, N

When water and methanol were used as mobile phases, the values of *N* were 24 000 and 21 000 plates per column, respectively, on injecting 0.025 ml of 0.5% ethylene glycol solution. When the sample was benzene and the mobile phases were

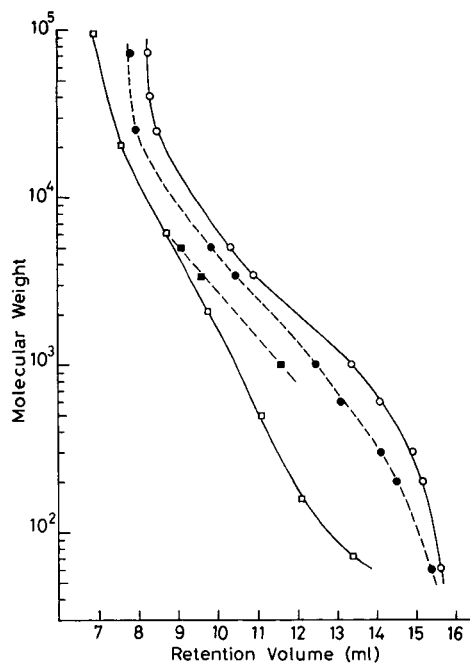


Fig. 1. Calibration graphs for PEG, PEO and PS in water, methanol and chloroform as mobile phases. Sample and mobile phase: (○) PEG, PEO in water; (●) PEG, PEO in methanol; (□) PS in chloroform; (■) PEG in chloroform.

chloroform and methanol, the values of N were 20 000 and 17 000 plates per column, respectively. Ethylene glycol was retained in the column when chloroform was used as the mobile phase.

Experiments were performed with mobile phases being changed in the order water, methanol, methanol–water, chloroform and chloroform–methanol. After a series of the experiments, the mobile phase was returned to water and the value of N was remeasured. It was unchanged (24 000 plates per column) and the retention volume of ethylene glycol was also stable. Only the column pressure increased from 25 kg/cm² initially to 35 kg/cm² after 7 months.

Calibration graphs

Calibration graphs of retention volume vs. log (molecular weight) for PEG and PEO in water and methanol as the mobile phases and those for PS and some PEG in chloroform are shown in Fig. 1. PEG and PEO in methanol eluted earlier from the column than when in water. Elution chromatograms of PEG 600, 1000 and 3400 in water and methanol are shown in Fig. 2 (the number after PEG represents the average molecular weight; henceforth the number given after each polymer's name also represents its average molecular weight).

Peak widths at half-height for these peaks were 0.75 ml (PEG 600), 0.725 ml (PEG 1000) and 0.45 ml (PEG 3400) in methanol and 0.825 ml (PEG 600), 0.85 ml (PEG 1000) and 0.59 ml (PEG 3400) in water. These results suggest that peak

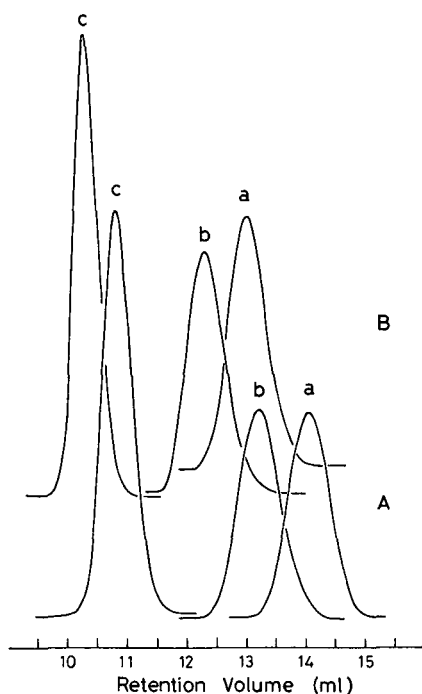


Fig. 2. Chromatograms of PEG in (A) water and (B) methanol as mobile phases. Samples: (a) PEG 600; (b) PEG 1000; (c) PEG 3400.

broadening and retardation of elution for PEG and PEO in the water mobile phase are due to the superimposition of an adsorption effect on the size-exclusion effect. However, viscosity differences among the mobile phases may also contribute to the variations in plate number.

When chloroform was used as the mobile phase, the peak shapes of PS were sharp for all samples and the adsorption effect seemed to be small. The peaks of PEG 600 and 1000 in chloroform were broad and PEG 200 was not eluted from the column. When the stationary phase was PS gel and the mobile phase was chloroform, PEG eluted earlier than PS of the same molecular weight⁸. Therefore, the results imply that an adsorption interaction between PEG and the surface of the poly(vinyl alcohol) gel occurred when chloroform was used as the mobile phase. The reason why PEGs in chloroform eluted earlier than those in methanol is probably due to the difference in the interstitial volumes of the column for the two mobile phases.

Mobile phase composition vs. retention volume

The changes in the retention volumes of benzene and ethylene glycol with variation in the mobile phase composition were determined and the results are shown in Fig. 3. The changes in the peak width at half-height of the solutes with variation in the mobile phase composition are also shown.

With chloroform-methanol as the mobile phase, the retention volume of benzene increased with increasing content of methanol in the mobile phase. The

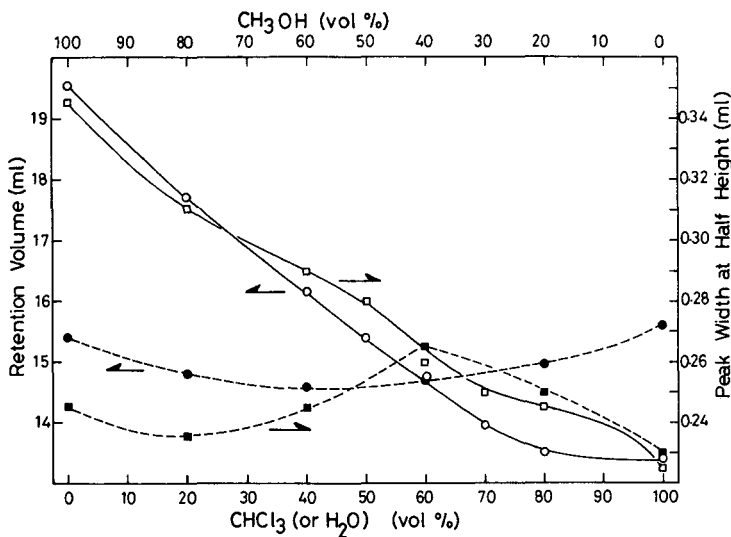


Fig. 3. Relationships between the mobile phase composition and retention volume (○, ●) or peak width at half-height (□, ■) of benzene and ethylene glycol. ○, □. Mobile phase, chloroform-methanol; solute, benzene. ●, ■. Mobile phase, water-methanol; solute, ethylene glycol.

peak-width at half-height of benzene also increased similarly. Therefore, the increase in retention volume of benzene with increasing methanol content in the mobile phase may be assumed to arise from the adsorption effect between benzene and the gel surface.

With water-methanol as the mobile phase, the minimum retention volume of

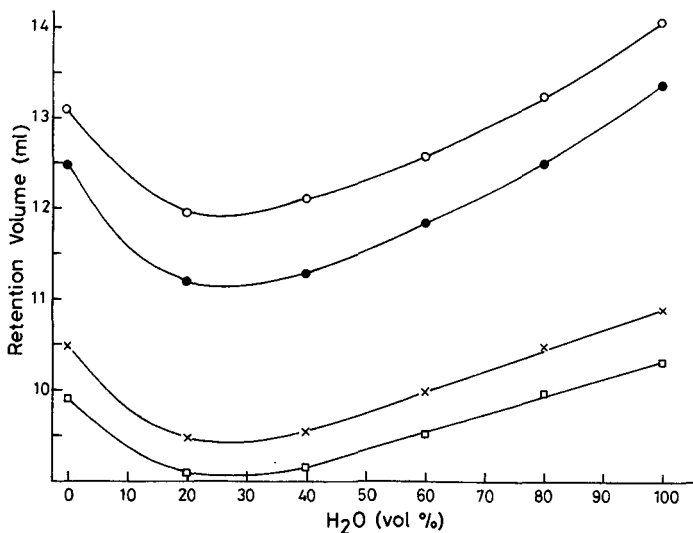


Fig. 4. Relationship between mobile phase composition and retention volume of PEG. (○) PEG 600; (●) PEG 1000; (×) PEG 3400; (□) PEG 5000.

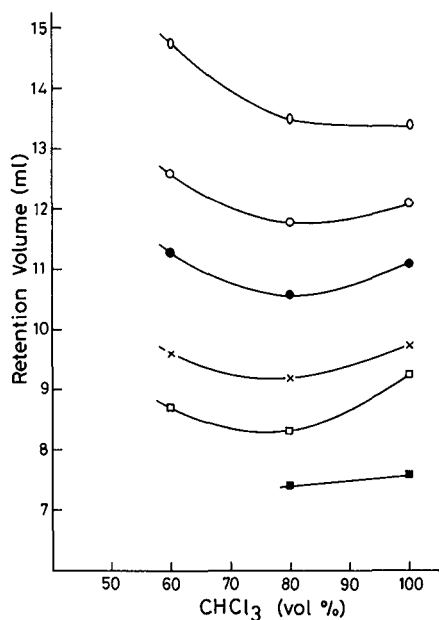


Fig. 5. Relationship between mobile phase composition and retention volume of PS and related compounds. (○) Benzene; (○) *n*-hexylbenzene; (●) PS 600; (×) PS 2100; (□) PS 6200; (■) PS 20400.

ethylene glycol was obtained at a mobile phase composition of water–methanol (40:60, v/v) and the maximum value with 100% water. The minimum peak width at half-height was obtained when 100% water was used as the mobile phase and the trend in the variation of peak width was not consistent, in contrast to the results with benzene. The next to the minimum peak width was obtained with water–methanol (20:80, v/v).

Fig. 4 shows the relationship for PEGs. The minimum retention volume was obtained at a mobile phase composition of water–methanol (25:75, v/v). This composition is similar to that for the next to the minimum peak width for ethylene glycol. The peak widths for each PEG with different compositions of the mobile phases were almost constant except with 100% water.

Fig. 5 shows the results for PS in chloroform and chloroform–methanol. The minimum retention volume was obtained at a composition of the mobile phase of chloroform–methanol (80:20, v/v). The peak widths for each PS with different compositions of the mobile phases were almost constant and the peaks were sharp.

DISCUSSION

The column efficiency for a given solute–solvent combination remained unchanged with the use of different solvents. The efficiency was checked by determining N values.

The samples used here were eluted from the column in order of decreasing molecular weight. Therefore, the separation mechanism is probably due mainly to size

exclusion. However, with the PEGs–water system, the peak broadening phenomena indicate that an adsorption effect is superimposed on the size-exclusion effect.

The minimum retention volume for ethylene glycol was obtained with water–methanol (40:60, v/v), for PEG with water–methanol (25:75, v/v) and for PS with chloroform–methanol (80:20, v/v). The concept of the solubility parameter may be applied to elucidate the elution mechanism⁹. Hildebrand solubility parameters for water, methanol, chloroform, ethylene glycol and poly(vinyl alcohol) are 47.9, 29.1, 18.8, 33.2 and 25.8 (J/cm³)^{1/2}, respectively¹⁰. According to this concept⁹, when the solubility parameter of the mobile phase is equal to that of the gel or a solute, then the separation occurs mainly by the size-exclusion effect.

The solubility parameter of the mobile phase water–methanol (25:75, v/v) is 33.8, which is nearly equal to that of ethylene glycol. If the solubility parameter of PEG has a similar value to that of ethylene glycol, then the separation in this system may be achieved by size exclusion. In the benzene–chloroform system, the solubility parameter of benzene is equal to that of chloroform and separation by size exclusion is expected. The solubility parameter of chloroform–methanol (80:20, v/v) is 24.8, which is nearly equal to that of the poly(vinyl alcohol) gel and the size-exclusion effect can be considered as the main separation mechanism in this system.

With water–methanol and chloroform–methanol mobile phases, separation of PEG and PS, respectively, by size exclusion alone may not be expected on a poly(vinyl alcohol) gel. We can say that the mobile phases water–methanol (25:75, v/v) and chloroform–methanol (80:20, v/v), which gave minimum retention volumes of PEG and PS, are effective for the SEC of PEG and PS because they minimize the adsorption effect.

ACKNOWLEDGEMENT

The author expresses his gratitude to O. Kawanami for technical assistance.

REFERENCES

- 1 S. Mori, *J. Chromatogr.*, 129 (1976) 53.
- 2 C. D. Chow, *J. Chromatogr.*, 114 (1975) 486.
- 3 J. V. Dawkins, L. L. Lloyd and F. P. Warner, *J. Chromatogr.*, 352 (1986) 157.
- 4 M. J. Cope and I. E. Davidson, *Analyst (London)*, 112 (1987) 417.
- 5 J. L. Robinson, W. J. Robinson, M. A. Marshall, A. D. Barnes, K. J. Johnson and D. S. Salas, *J. Chromatogr.*, 189 (1980) 145.
- 6 Y.-B. Yang and M. Verzele, *J. Chromatogr.*, 387 (1987) 197.
- 7 N. Hirata, M. Kasai, Y. Yanagihara and K. Noguchi, *J. Chromatogr.*, 396 (1987) 115.
- 8 S. Mori and A. Yamakawa, *J. Liq. Chromatogr.*, 3 (1980) 329.
- 9 S. Mori, *Anal. Chem.*, 50 (1978) 745.
- 10 J. Brandrup and E. H. Immergut (Editors), *Polymer Handbook*, Wiley, New York, 2nd ed., 1975, Section IV.

CHROM. 20 618

REVERSED-PHASE HIGH-PERFORMANCE LIQUID CHROMATOGRAPHY WITH A C₁₈ POLYACRYLAMIDE-BASED PACKING

J. V. DAWKINS* and N. P. GABBOTT

Department of Chemistry, Loughborough University of Technology, Loughborough, Leicestershire LE11 3TU (U.K.)

and

L. L. LLOYD, J. A. McCONVILLE and F. P. WARNER

Polymer Laboratories Ltd., Essex Road, Church Stretton, Shropshire SY6 6AX (U.K.)

SUMMARY

A rigid macroporous polyacrylamide-based packing having an octadecyl (C₁₈) chemically bonded phase has been developed for reversed-phase high-performance liquid chromatography. Separations of non-polar, polar, basic and acidic compounds are demonstrated with this packing and compared with the retention properties of a C₁₈ silica packing and a polystyrene-based packing. The C₁₈ polyacrylamide-based packing equilibrates rapidly to changes in the composition of the mobile phase and may be used at pressures up to $25 \cdot 10^6$ N/m². The packing retains its performance after prolonged contact with aqueous mobile phases at both low and high pH.

INTRODUCTION

Reversed-phase high-performance liquid chromatography (HPLC) is generally performed with a silica packing coated with an octadecyl (C₁₈) chemically bonded phase¹. This column packing may be viewed as a hydrophilic polar support covered by a hydrophobic surface layer. Ideally, retention is dependent only on the bonded phase, but for some solutes, for example amines, interactions with residual silanol groups cause broadening or distortion of chromatographic peaks². Improved surface coverage methods can reduce but may not eliminate peak-tailing for amines on C₁₈ silica packings. A further limitation of bonded phase silica packings is the instability of the silica surface owing to possible dissolution when in contact with a mobile phase having a high pH³.

In recent years there has been considerable interest in polymer-based packings for reversed-phase HPLC. Particular attention has been directed to polymers based on poly(styrene-divinylbenzene) (PS-DVB) because these packings are stable with eluents from pH 1–14^{4–11}. Furthermore, amines often show little or no peak-tailing on PS-DVB packings compared with C₁₈ silica packings^{11,12}. Both the matrix and surface of PS-DVB packings are viewed as neutral non-polar PS. However, the presence of aromatic groups must generate somewhat different retention behaviour from

that for C_{18} silica¹⁰. It is possible to bring the retention properties of PS-based packings closer to C_{18} silica by using a C_{18} bonded PS-DVB¹³, but non-polar PS still constitutes the matrix. Somewhat more polar polymeric packings may be employed for specific separations by reversed-phase HPLC, see for example applications reported for polymethacrylate packings¹⁴.

Hydrophobic interaction chromatography developed for biological macromolecules involves a soft gel filtration matrix in which hydrophobic groups (either alkyl or aryl) are covalently attached to a hydrophilic (wetable) gel such as agarose or cross-linked dextrans^{15,16}. Unfortunately, gel filtration matrices have poor mechanical stability at high column pressures and so are unsuitable for HPLC. Improved rigidity is characteristic of TSK-Gel, type PW (based on a hydroxylated polyether)^{17,18} which has been widely used for aqueous high-performance size-exclusion chromatography (HPSEC), and this type of gel may be modified for hydrophobic interaction chromatography¹⁹.

Reversed-phase HPLC with C_{18} silica has become an extremely popular analytical technique for a wide range of compounds²⁰. If a polymer-based packing having long-term stability is to replace C_{18} silica in separations requiring eluents at high pH, then these two types of packings must have similar retention properties. We believe that the most likely replacement (by analogy both with reversed-phase HPLC with silica and hydrophobic interaction chromatography) will result from a packing constituted from a hydrophilic polar polymeric support covered with a hydrophobic surface-layer. This approach is evident in the development of a C_{18} bonded phase on a vinyl alcohol copolymer packing for reversed-phase HPLC^{21,22}. In previous papers^{23,24} we have reported the preparation of cross-linked polyacrylamide microspheres, which are both rigid and macroporous, and demonstrated their use for aqueous HPSEC. We have produced a packing having a C_{18} stationary phase bound to a polyacrylamide-based support, and brief chromatographic details for this packing were reported in a previous paper²⁵ which emphasised column efficiency data for the PS-DVB packing known as PLRP-S (tradename of Polymer Labs.). In the present paper reversed-phase HPLC separations are demonstrated with this C_{18} polyacrylamide-based packing. A major aim was to compare the retention characteristics for non-polar, polar, basic and acidic compounds for this packing with those of a C_{18} silica packing. Variations in the composition of the mobile phase are investigated and studies of the stability of the packing at low and high pH are reported.

EXPERIMENTAL

The polymeric column packing for reversed-phase HPLC is a polyacrylamide-based packing containing N-octadecylamide groups. Macroporous polyacrylamide particles were produced in an inverse suspension process by co-polymerising acrylamide and N,N'-methylenebisacrylamide with the cross-linking agent as the major monomeric component. The inverse suspension polymerisations were performed according to the conditions described elsewhere²⁶. The bonded phase was prepared by first forming strongly nucleophilic amide anions on the surfaces of the porous polyacrylamide particles by the use of strong base²⁷, followed by treatment with *n*-octadecyl bromide. The polymer particles were separated by air classification, and optical and scanning electron micrographs indicated spherical particles with a narrow parti-

cle size distribution with a mean particle diameter of 10 μm . The mean pore diameter estimated from results obtained by HPSEC²⁵ was about 100 \AA . The dry polyacrylamide-based particles were dispersed in methanol, and this slurry was packed into a column (150 \times 4.6 mm I.D.) at pressures up to 3500 p.s.i. (1 p.s.i. \equiv 6894.8 N/m²). The performance of this column was compared with a column (100 \times 4.6 mm I.D.) containing 5 μm Hypersil ODS 100 \AA supplied by Hewlett-Packard (Avondale Division, Avondale, PA, U.S.A.). HPSEC separations indicated that the two packings had similar pore size distributions²⁵.

The chromatographic apparatus consisted of a Knauer pump Model 64 (Dr. Herbert Knauer, Berlin, West Germany), a Rheodyne Model 7125 injection valve (20 μl loop), supplied by HPLC Technology (Macclesfield, U.K.) a thermostatted oven (Applied Chromatography Systems) supplied by HPLC Technology and a Pye Unicam variable-wavelength UV detector Model LC3 operated at 254 nm, supplied by Pye Unicam (Cambridge, U.K.). Injection volumes were 5 μl and solute concentrations were typically below 40 $\mu\text{g}/\text{cm}^3$. Analytical grade solutes and reagents (Fisons Scientific Equipment Division, Loughborough, U.K.) and doubly distilled water were used throughout this work. Separations were performed at ambient temperature with an eluent flow-rate of 0.5 cm^3/min . Separations of caffeine, theophylline, benzoic acid and toluic acid were performed at 37°C with acetonitrile–10 mM sodium acetate pH 4.5 (20:80, v/v) as eluent. The composition of the eluent in separations with mixtures of methanol and water is given in tables and figures. Data for capacity factor k' were derived from $(t_R - t_0)/t_0$, where t_R is the retention time for the solute and t_0 is the time for an unretained peak obtained by injecting a liquid mixture with a volume composition different from that of the eluent, for example methanol–water (10:90) for the eluent methanol–water (70:30). Values for separation factor (or selectivity, α) for two solutes 1 and 2 were determined from k'_2/k'_1 .

RESULTS AND DISCUSSION

Retention behaviour

Chromatograms for non-polar aromatic compounds are shown in Fig. 1. Derived values for k' for toluene, naphthalene and anthracene are given in Table I.

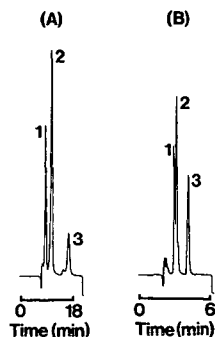


Fig. 1. Separation of non-polar aromatic compounds with (A) C₁₈ polyacrylamide-based packing and (B) Hypersil ODS packing. Peaks: 1 = toluene, 2 = naphthalene, 3 = anthracene. Eluent: methanol–water (90:10, v/v) at ambient temperature.

TABLE I

CAPACITY FACTORS FOR ELUTIONS WITH METHANOL-WATER (90:10, v/v) AT AMBIENT TEMPERATURE

<i>Solute</i>	<i>k'</i>	
	<i>Polyacrylamide-based packing</i>	<i>Silica packing</i>
Toluene	0.28	0.45
Naphthalene	0.54	0.54
Anthracene	1.33	0.96
Biphenyl	0.70	0.67
Terphenyl	1.71	1.50

These results indicate similar behaviour for the polyacrylamide-based and silica column packings. These two column packings also produce similar separations of biphenyl and terphenyl, as shown by the chromatograms in Fig. 2 and the calculated values of k' in Table I. Data for α are shown for terphenyl and biphenyl in Table II, confirming excellent resolution of these two solutes with the polyacrylamide-based packing incorporating a C_{18} bonded phase.

Chromatograms for two polar alkyl phthalates are shown in Fig. 3. The derived values of k' for diethyl phthalate and dibutyl phthalate in Table III indicate that the two column packings produce somewhat different separation behaviour. This is further confirmed by the values of α in Table II. Although the selectivity for the C_{18} polyacrylamide-based packing is not as high as for the column of C_{18} silica, the column containing the C_{18} polyacrylamide-based packing provides a baseline separation of the two alkyl phthalates under the operating experimental conditions.

Chromatograms for basic compounds are shown in Fig. 4. The excellent baseline separation of pyridine and aniline with the C_{18} polyacrylamide-based packing is

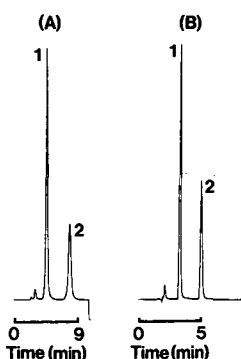


Fig. 2. Separation of non-polar aromatic compounds with (A) C_{18} polyacrylamide-based packing and (B) Hypersil ODS packing. Sample: 1 = biphenyl, 2 = terphenyl. Eluent: methanol-water (90:10 v/v) at ambient temperature.

TABLE II
SELECTIVITIES

Solutes	α	
	Polyacrylamide-based packing	Silica packing
Terphenyl- Biphenyl	2.43	2.24
Dibutyl phthalate- diethyl phthalate	5.13	6.26
Toluic acid- benzoic acid	3.01	2.66

confirmed by the values of k' given in Table III. The C₁₈ polyacrylamide-based packing together with an eluent containing 70% methanol produces peaks in Fig. 4 which are symmetrical and which correspond to efficiencies similar to those for non-polar solutes. Chromatograms for the C₁₈ silica packing in Fig. 4 show a reversal in elution order of the two solutes compared with the C₁₈ polyacrylamide-based packing. The broadening and tailing of the peak for pyridine with the column of C₁₈ silica packing may arise from solute interaction with residual surface silanol groups. For basic compounds interactions with residual surface silanol groups may influence retention^{11,28}. For example, the capacity factor ($k' = 0.25$) for caffeine with the C₁₈ polyacrylamide-based packing was somewhat below $k' = 1.0$ for the C₁₈ silica packing, and the selectivity ($\alpha = 1.35$) determined with caffeine and theophylline was lower than 1.65 for the C₁₈ silica packing. Whilst the separation mechanism with the C₁₈ polyacrylamide-based packing here should be simpler than a mixed-mode separation occurring with a bonded phase silica, a mixed mechanism of retention might occur for other types of compounds with the C₁₈ polyacrylamide-based packing.

Chromatograms for acidic compounds are shown in Fig. 5. Excellent resolution of benzoic acid and toluic acid with the C₁₈ polyacrylamide-based packing is obtained,

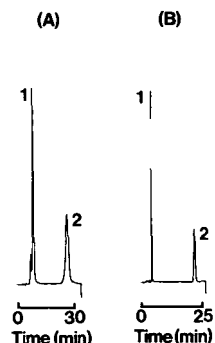


Fig. 3. Separation of polar alkyl phthalates with (A) C₁₈ polyacrylamide-based packing and (B) Hypersil ODS packing. Peaks: 1 = diethyl phthalate, 2 = dibutyl phthalate. Eluent: methanol-water (70:30, v/v) at ambient temperature.

TABLE III

CAPACITY FACTORS FOR ELUTIONS WITH METHANOL–WATER (70:30, v/v) AT AMBIENT TEMPERATURE

Solute	k'	
	Polyacrylamide-based packing	Silica packing
Diethyl phthalate	0.67	1.00
Dibutyl phthalate	3.42	6.26
Pyridine	0.21	0.77
Aniline	0.58	0.28

as confirmed by the derived values of k' given in Table IV. The C_{18} polyacrylamide-based and C_{18} silica packings have similar values for α , as shown in Table II.

Mobile phase composition

In reversed-phase HPLC, the solute is distributed between a non-polar stationary phase (bonded C_{18}) and a polar mobile phase, so elution will be very dependent on the organic content of the mobile phase. Results for k' for non-polar aromatic compounds in eluents consisting of mixtures of methanol and water are displayed in Fig. 6. For both types of column packing it is evident that increasing the organic content of the mobile phase reduces k' , so the analysis time may be lowered by raising the proportion of methanol in the eluent. The same trend was observed for separations of polar alkyl phthalates and basic compounds with the C_{18} polyacrylamide-based packing as shown in Figs. 7 and 8.

Studies of the mobile phase composition illustrate how the retention properties of the C_{18} polyacrylamide-based packing are quite different from PS–DVB stationary phases. The data for k' for methanol–water mixtures as eluents given in Tables V and VI are always considerably higher for the PS–DVB packing (PLRP-S) than for the

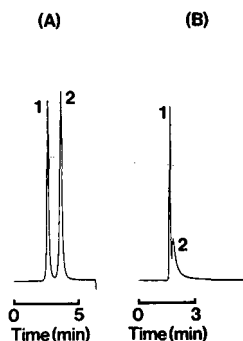


Fig. 4. Separation of basic compounds with (A) C_{18} polyacrylamide-based packing (peaks: 1 = pyridine, 2 = aniline) and (B) Hypersil ODS packing (peaks: 1 = aniline, 2 = pyridine). Eluent: methanol–water (70:30, v/v) at ambient temperature.

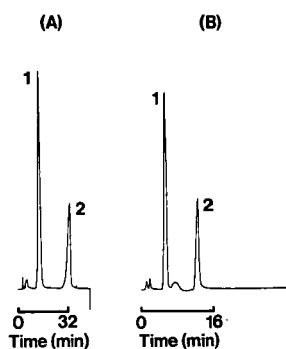


Fig. 5. Separation of acidic compounds with (A) C₁₈ polyacrylamide-based packing and (B) Hypersil ODS packing. Peaks: 1 = benzoic acid, 2 = toluic acid. Eluent: acetonitrile–10 mM sodium acetate, pH 4.5 (20:80, v/v) at 37°C.

C₁₈ polyacrylamide-based packing (Tables I and III). It has been noted previously that methanol has poor elution strength for PS–DVB column packings with methanol–water mixtures as eluents²⁹. Data for k' for compounds in Table VI demonstrate that retention for the C₁₈ polyacrylamide-based packing with methanol–water as eluent is similar to PLRP-S with acetonitrile–water (90:10, v/v), but in Table V other solutes separating with these two stationary phase–mobile phase combinations exhibit very different retention behaviour. Benzoic acid and toluic acid (Table IV) were not eluted from the PLRP-S column with these mobile phases. It must be concluded that these two polymer-based packings require quite different eluent compositions in order to obtain similar solute retention times.

Column packing stability

Macroporous polymer-based packings may undergo limited swelling in contact with some liquids. Swelling tests on C₁₈ polyacrylamide-based packings indicated that particle volumes were very similar for methanol, methanol–water (from 10:90 to 90:10, v/v), and acetonitrile. Therefore, a column packed using methanol may be flushed immediately with the required mixture of methanol and water. It is not necessary to flush the column with mixtures having intermediate compositions. Rapid equilibration was proved by observing reproducible chromatograms on repeated in-

TABLE IV

CAPACITY FACTORS FOR ELUTIONS WITH ACETONITRILE–10 mM SODIUM ACETATE pH 4.5 (20:80, v/v) AT 37°C

Solute	k'	
	Polyacrylamide-based packing	Silica packing
Benzoic acid	2.24	1.60
Toluic acid	6.74	4.25

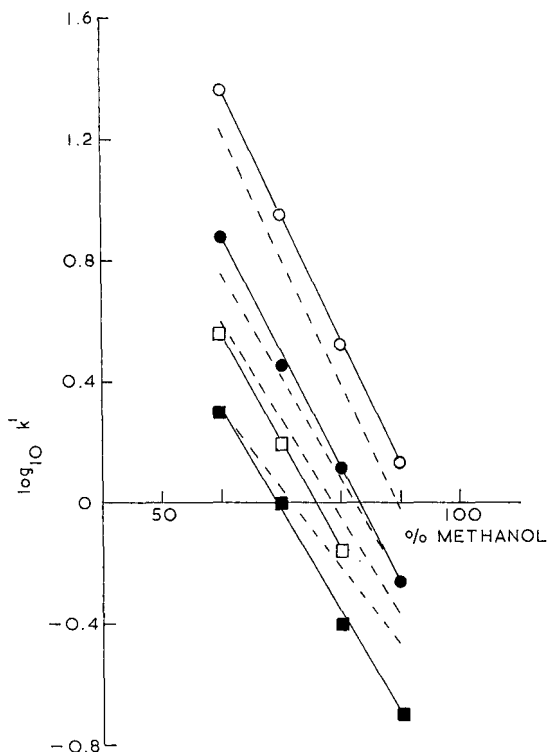


Fig. 6. Dependence of capacity factor on the composition of the eluent for C_{18} polyacrylamide-based packing (—) and Hypersil ODS packing (----). (○) Anthracene, (●) naphthalene, (□) toluene, (■) benzene.

jection of a test mixture of alkyl phthalates, when the data in Fig. 8 were again reproducibly obtained and so the C_{18} polyacrylamide-based packing equilibrates quickly to changes in mobile phase composition in separations operating by gradient elution. The degree of particle swelling will also determine the maximum pressure limit (and therefore fastest eluent flow-rate) for column operation. The packing pressure of $25 \cdot 10^6 \text{ N/m}^2$ should not be exceeded because particle distortion and variations in close packing of particles may arise, resulting in a fall in column efficiency.

Column lifetime will be determined by the stability of the bonded phase in contact with a range of mobile phases. The column containing the C_{18} polyacrylamide-based particles was subjected to a series of experiments involving prolonged contact with methanol, water, and aqueous mobile phases at both low and high pH. After each experiment, column performance was assessed with a test mixture of three alkyl phthalates which were eluted isocratically with methanol–water (65:35, v/v).

After completing HPLC analyses, it may be necessary to clean up a reversed-phase packing by removing non-polar solutes adsorbed on the stationary phase. This may be achieved by flushing out the column with only the organic component of the mobile phase. The column containing the C_{18} polyacrylamide-based packing is extremely stable under these conditions. Thus, it was observed that the peak shapes,

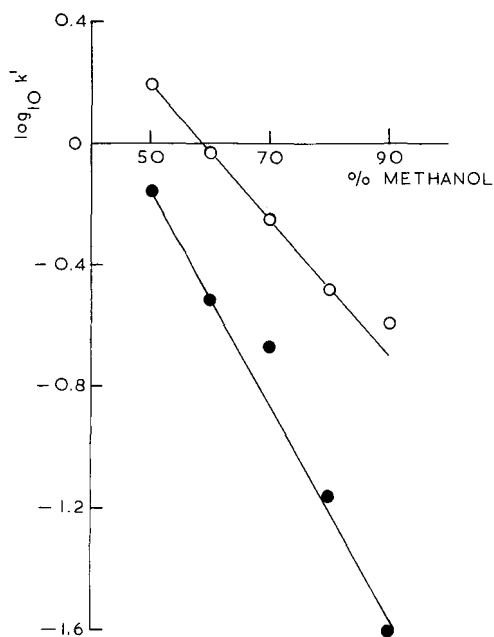


Fig. 7. Dependence of capacity factor on the composition of the eluent for C_{18} polyacrylamide-based packing. (○) Aniline, (●) pyridine.

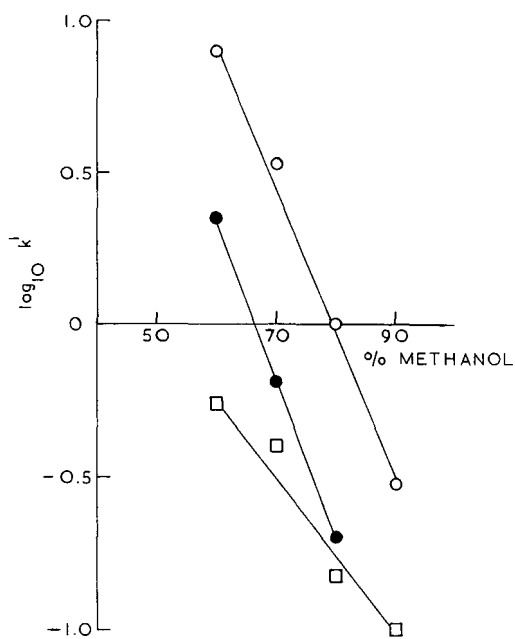


Fig. 8. Dependence of capacity factor on the composition of the eluent for C_{18} polyacrylamide-based packing. (○) Dibutyl phthalate, (●) diethyl phthalate, (□) dimethyl phthalate.

TABLE V

CAPACITY FACTORS FOR ELUTIONS WITH POLYMER-BASED PACKINGS AT AMBIENT TEMPERATURE

<i>Solute</i>	<i>k'</i>		
	<i>Polyacrylamide-based packing*</i>	<i>PLRP-S*</i>	<i>PLRP-S**</i>
Toluene	0.28	4.95	1.21
Naphthalene	0.54	> 10	2.86
Anthracene	1.33	> 10	8.10
Biphenyl	0.70	> 10	1.62
Terphenyl	1.71	> 10	10.52

* Methanol-water (90:10, v/v) as eluent.

** Acetonitrile-water (90:10, v/v) as eluent.

TABLE VI

CAPACITY FACTORS FOR ELUTIONS WITH POLYMER-BASED PACKINGS AT AMBIENT TEMPERATURE

<i>Solute</i>	<i>k'</i>		
	<i>Polyacrylamide-based packing*</i>	<i>PLRP-S*</i>	<i>PLRP-S**</i>
Diethyl phthalate	0.67	> 10	0.72
Dibutyl phthalate	3.42	> 10	1.76
Pyridine	0.21	1.21	0.28
Aniline	0.58	2.22	0.41

* Methanol-water (70:30, v/v) as eluent.

** Acetonitrile-water (90:10, v/v) as eluent.

TABLE VII

COLUMN CONDITIONS AT LOW AND HIGH pH FOR C₁₈ POLYACRYLAMIDE-BASED PACKING

<i>Aqueous eluent</i> (0.1 mol/dm ³)	<i>Temperature</i> (°C)	<i>Time</i> (h)	<i>Flow-rate</i> (cm ³ /min)
Hydrochloric acid	Ambient	7	0.5
Sodium hydroxide	Ambient	16	0.1
Sodium hydroxide	Ambient	24	0
Hydrochloric acid	50	16	0.1
Sodium hydroxide	40	24	0.1

capacity factors and efficiencies for all three solutes in the test mixture were the same before and after flushing the column with methanol. The same tests were also performed after flushing the column with distilled water, with the same results, thus confirming the excellent stability of the bonded phase in aqueous media.

Reversed-phase packings based on silica are generally employed with aqueous eluents having a pH in the range 3.5–7.5. The stability of the C₁₈ polyacrylamide-based packing was examined with aqueous eluents having low and high pH. The experimental conditions are shown in Table VII. After each experiment, the column was flushed with methanol–water (65:35, v/v), and the test mixture was injected to establish column performance. Again, there was no change in peak shape and efficiency before and after exposure to either a low pH or high pH eluent, indicating no deterioration in the column packing. Therefore, the C₁₈ polyacrylamide-based packing significantly extends the operating pH range in reversed-phase HPLC.

CONCLUSIONS

These initial results indicate that the C₁₈ polyacrylamide-based packing is promising for reversed-phase HPLC. The data for capacity factor and selectivity for non-polar and polar solutes confirm that this packing operates by the reversed-phase mechanism, with similar results for retention and selectivity for aromatic and polar organic solutes to a conventional silica-based packing such as Hypersil ODS. The C₁₈ polyacrylamide-based packing could therefore be considered as a direct replacement for a C₁₈ silica packing with the additional advantage of providing long term physical and chemical stability over a wide pH operating range (1–13). The C₁₈ polyacrylamide-based packing is particularly advantageous for nitrogen-containing bases, such as pyridine and aniline. Reversed-phase silica packings may generate broad tailing peaks for such basic compounds. The retention behaviour of the C₁₈ polyacrylamide-based packing which like Hypersil ODS may be viewed as a hydrophobic layer on a hydrophilic rigid support is quite different from polystyrene-based packings such as PLRP-S.

We have reported the promising behaviour of the C₁₈ polyacrylamide-based packing with simple test mixtures in typical reversed-phase separations and further work is now required on studies of more complex mixtures. This will have to be performed in conjunction with synthetic work on further column packings in order to optimise capacity factors and selectivities in relation to pore size distribution and mean pore diameter and to maximise column resolution in relation to packing particle diameter (*ca.* 5 μm).

ACKNOWLEDGEMENT

The authors thank the Science and Engineering Research Council for the support of this research with a Cooperative Research Grant.

REFERENCES

- 1 A. M. Krstulovic and P. R. Brown, *Reversed-Phase High-Performance Liquid Chromatography*, Wiley-Interscience, New York, 1982.

- 2 K. E. Bij, Cs. Horváth, W. Melander and A. Nahum, *J. Chromatogr.*, 203 (1981) 65.
- 3 N. H. C. Cooke and K. Olsen, *J. Chromatogr. Sci.*, 18 (1980) 512.
- 4 T. Hanai, K. C. Tran and J. Hubert, *J. Chromatogr.*, 239 (1982) 385.
- 5 H. S. Ramsdell and D. R. Buhler, *J. Chromatogr.*, 210 (1981) 154.
- 6 H. A. McLeod and G. Laver, *J. Chromatogr.*, 244 (1982) 385.
- 7 D. P. Lee, *J. Chromatogr. Sci.*, 20 (1982) 203.
- 8 J. G. Buta, *J. Chromatogr.*, 295 (1984) 506.
- 9 T. Isobe, Y. Kurosu, Y.-I. Fang, N. Ishioka, H. Kawasaki, N. Takai and T. Okuyama, *J. Liq. Chromatogr.*, 7 (1984) 1101.
- 10 R. M. Smith, *J. Chromatogr.*, 291 (1984) 372.
- 11 W. A. Moats and L. Leskinen, *J. Chromatogr.*, 386 (1987) 79.
- 12 R. M. Smith, K. C. Madahar, W. G. Salt and N. A. Smart, *Chromatographia*, 19 (1984) 411.
- 13 J. R. Benson and A. Woo, *J. Chromatogr. Sci.*, 22 (1984) 386.
- 14 K. Iriyama, M. Yoshiura and T. Iwamoto, *J. Liq. Chromatogr.*, 8 (1985) 333.
- 15 B. H. J. Hofstee, *Pure Appl. Chem.*, 51 (1979) 1537.
- 16 B. H. J. Hofstee, in A. R. Cooper (Editor), *Polymeric Separation Media*, (Polymer Science and Technology, Vol. 16), Plenum Press, New York, 1982, p. 87.
- 17 T. Hashimoto, H. Sasaki, M. Aiura and Y. Kato, *J. Polym. Sci., Polym. Phys. Ed.*, 16 (1978) 1789.
- 18 Y. Kato, H. Sasaki, M. Aiura and T. Hashimoto, *J. Chromatogr.*, 153 (1978) 546.
- 19 H. Imai, G. Tamai and S. Sakura, *J. Chromatogr.*, 371 (1986) 29.
- 20 R. E. Majors, H. G. Barth and C. H. Lochmuller, *Anal. Chem.*, 56 (1984) 300R.
- 21 Y. Arai, M. Hirukawa and T. Hanai, *J. Liq. Chromatogr.*, 10 (1987) 635.
- 22 Y. Yanagihara, K. Yasukawa, T. Tamura, T. Uchida and K. Noguchi, presented as a poster at the *Eleventh International Symposium on Column Liquid Chromatography, Amsterdam, 1987*.
- 23 J. V. Dawkins and N. P. Gabbott, *Polymer*, 22 (1981) 291.
- 24 J. V. Dawkins, N. P. Gabbott, A. M. C. Montenegro, L. L. Lloyd and F. P. Warner, *J. Chromatogr.*, 371 (1986) 283.
- 25 J. V. Dawkins, L. L. Lloyd and F. P. Warner, *J. Chromatogr.*, 352 (1986) 157.
- 26 M. V. Dimonie, C. M. Boghina, N. N. Marinescu, M. M. Marinescu, C. I. Cincu and C. G. Oprescu, *Eur. Polym. J.*, 18 (1982) 639.
- 27 B. C. Challis and J. A. Challis, in D. H. R. Barton and W. D. Ollis (Editors), *Comprehensive Organic Chemistry, Vol. 2, Nitrogen Compounds, Carboxylic Acids, Phosphorus Compounds*, Pergamon Press, Oxford, 1979, p. 957.
- 28 H. Engelhardt, B. Dreyer and H. Schmidt, *Chromatographia*, 16 (1982) 11.
- 29 L. D. Bowers and S. Pedigo, *J. Chromatogr.*, 371 (1986) 243.

CHROM. 20 624

COMPARISON OF RETENTION MECHANISMS OF HOMOLOGOUS SERIES AND TRIGLYCERIDES IN NON-AQUEOUS REVERSED-PHASE LIQUID CHROMATOGRAPHY

MICHEL MARTIN^{*,*}, GÉRALDINE THEVENON and ALAIN TCHAPLA

Ecole Polytechnique, Laboratoire de Chimie Analytique Physique, 91128 Palaiseau (France)

SUMMARY

The retention behaviour of saturated homogeneous triglycerides was compared to that of single chain homologous compounds in reversed-phase liquid chromatography on silica-based octadecyl bonded phases with non-aqueous binary eluents containing chloroform. For both series, in all eluents and at all investigated temperatures, a discontinuity (1-6% slope change) in $\log k'$ vs. the carbon atom number, n_c , of each solute hydrocarbonaceous chain was observed for a given critical number of carbon atoms, $n_{c,crit} \approx 12-13$. Similar discontinuities were observed in ΔH° and ΔS° vs. n_c for the same $n_{c,crit}$ value. These and other phenomena (existence of two convergence points for $\log k'$ vs. n_c plotted at different eluent compositions; existence of two convergence temperatures in $\log k'$ vs. $1/T$ plotted for several members of a given solute series) reflect the mechanism of penetration of the solute aliphatic chains into the bonded layer. The eluotropic strength of acetonitrile-chloroform mobile phases was determined and seen to have a larger rate of variation with the solvent composition than that of some other non-aqueous binary eluents. The ratio of the slope of plots of $\log k'$ vs. n_c curves for triglycerides and single chain homologous series is not a whole number but has a value lying between 2 and 3. This explains why triglyceride retentions cannot be predicted from retention data for the fatty acid methyl esters. More importantly, this indicates that the triglycerides may interact with the stationary phase using various conformations, one, two or three chains penetrating into the bonded layer. These conformations, in dynamic equilibrium with each other, contribute differently to the retention. This offers, in principle, the possibility to separate unsaturated triglycerides having the same number of carbon atoms and of double bonds but differing in the distribution of the unsaturations along the chains, if the double bonds located in a non-penetrating chain can selectively interact with a mobile phase component.

INTRODUCTION

The liquid chromatographic analysis of triglycerides has been the subject of many studies which have recently been reviewed¹. The analysis of these substances

^{*} Present address: École Supérieure de Physique et de Chimie Industrielles, Laboratoire d'Hydrodynamique et Mécanique Physique, 10 rue Vauquelin, 75231 Paris Cedex 05, France.

has been a challenge to chromatographers for several reasons: the great complexity of natural triglyceride samples (vegetable or animal oils, biological samples); the absence of UV chromophores in the molecular structure of the compounds; their important hydrophobicity and, consequently, their poor solubility in aqueous solvents. The sample complexity problem is classically solved by using high efficiency columns under programmed elution conditions. In liquid chromatography, this is usually done by increasing the solvent strength of the mobile phase during the migration of the compounds through the column (gradient elution), although the relatively large temperature dependence of the triglyceride retention has made temperature programming (temperature increase) an alternative possibility². Using an evaporative light scattering photometer, it has become possible to detect the triglycerides with a relatively good sensitivity and, moreover, to perform gradient elution analysis with a quite stable baseline³⁻⁵. Because the triglycerides all have the same polar group but differ in their apolar moieties, the separation selectivity is much larger under reversed-phase conditions than under normal-phase ones and most authors have used *n*-octadecyl bonded silica as the stationary phase. However, the insolubility of these compounds in hydroorganic solvents makes it impossible to use, as is very frequently done in reversed-phase liquid chromatography, water as a component of the mobile phase. Moreover, due to the high hydrophobicity of these solutes, it is necessary to use rather strong solvents to maintain reasonable retention. These are the reasons why the method of non-aqueous reversed-phase (NARP) liquid chromatography is generally selected for the analysis of triglycerides⁶. Although the development of the analytical instrumentation in the past few years has made feasible the liquid chromatographic analysis of this very important class of compounds, there are still problems to be solved regarding the choice of the best separation conditions and the prediction of the retention of specific triglycerides, which are usually not available as standards, in order to identify the numerous peaks observed in the chromatograms of samples of natural origin.

All previous work in this area has focused on relationships between the retention of a triglyceride and the number of carbon atoms as well as the number of double bonds in its chains. However, this work only permits the understanding of primary effects, and a fine tuning of the prediction of retention is not yet possible in many instances. Besides, some separation problems are still unsolved. For example, it has frequently been found very difficult, if not impossible, to separate triglycerides containing the same number of carbon atoms and the same total number of unsaturations, differing in the distribution of these unsaturations within the three chains. It is not possible to predict the retention of a triglyceride as a function of the retention of the three fatty acid methyl esters corresponding to the structures of each of its three chains. Indeed, it has been shown that the logarithm of the capacity factor of a mixed triglyceride must be calculated from the retention of the three homogeneous ones rather than from the retention of the three corresponding esters. So, for a mixed triglyceride ABC, where A, B, C represent three different esters, the logarithm of the capacity factor may be expressed as⁷:

$$\log k'_{ABC} = 1/3 \log k'_{AAA} + 1/3 \log k'_{BBB} + 1/3 \log k'_{CCC} \quad (1)$$

One of the purposes of the present study is to examine the causes of these phenomena, by investigation of the retention mechanism of the triglycerides on *n*-octadecyl bonded phases in non-aqueous eluents. This was done by comparing the selectivity obtained by addition of a methylene group in the triglycerides and in homologous series of single chain (*n*-alkyl) compounds under various conditions. The choice of single compounds as model reference compounds is based on the fact that a triglyceride can be considered as the sum of three linear chains (alkyl chains) attached to a head group (glyceryl group). Moreover, the retention mechanism of such linear solutes on alkyl bonded phases is relatively well documented. It has been shown that, in water-methanol and methanol-tetrahydrofuran eluents, these solutes penetrate into the layer of ligands of monomeric alkyl bonded phases⁸. As the elution of triglycerides requires binary eluents containing such solvents as chloroform or acetone, which are not classically used in reversed-phase liquid chromatography, it is first necessary to study, for later comparison purposes, the retention mechanism of linear solutes in such binary non-aqueous mobile phases. This comprises the first part of the study reported. The eluotropic strength of solvent mixtures used for the analysis of triglycerides has also been determined. The retention mechanism of the triglycerides under the same chromatographic conditions is then discussed by a comparison of the methylene selectivities of the triglycerides with those of an appropriate linear homologous series.

EXPERIMENTAL

Reagents

Methanol, acetonitrile and chloroform were HPLC grade (Carlo Erba, Milan, Italy). All solvents were filtered through a Millipore GF/C 1.2- μ m filter. The solutions were then degassed by sonication.

Alkanes, fatty acid methyl esters, phenylalkanes, chloroalkanes and *n*-alkyl benzoates were from different sources. Triglycerides and diglycerides were from Interchim (Montluçon, France).

Equipment

The liquid chromatographic system comprised a Model 112 pump (Beckman, San Ramon, CA, U.S.A.), a Model 7125 injection valve with a 20- μ l loop (Rheodyne, Cotati, CA, U.S.A.) and a Model R 401 refractive index detector (Waters, Milford, MA, U.S.A.). Two columns were used. The Ultrasphere 5- μ m ODS column, 15 cm \times 4.6 mm, was a gift from Beckman, and a μ Bondapak 10- μ m C₁₈ column, 30 cm \times 3.9 mm, was obtained from Waters. For all experiments, the temperature of the precolumn, of the injection valve and of the column was controlled using a laboratory made water jacket by means of a Model HS 40 thermostat (Huber, Offenburg-Elgersweier, F.R.G.) with a precision of 0.1°C. The eluent flow-rate was 0.8 ml/min.

Methods

Samples were always dissolved in the solvent or solvent mixture used as the mobile phase in order to avoid the precipitation of the solutes on the column, a change in the solute peak shape⁹ or the modification of the retention time due to the presence of an excess of strong solvent in the injected sample¹⁰.

All retention values are reported in terms of the capacity factor, k' . The calculation of this factor requires the measurement of the void volume of the column (column hold-up volume). It has been shown that, in order to determine this volume, a convention must be adopted regarding the adsorption equilibrium¹¹ and that the various possible conventions lead to void volumes which may differ by as much as 20%¹². In the present study, the recommended¹¹ weighing method¹³ has been used because it provides a value which does not depend on the mobile phase composition and is linked to the total column porosity. It was shown that it closely corresponds to the convention that no liquid phase component is adsorbed in terms of volume¹². In order to minimize the possible error in the capacity factor and although we are in the following concerned only with relative, not absolute, k' values, only capacity factors greater than 0.4 were considered. Each value of k' is the result of at least three reproducible injections.

RESULTS AND DISCUSSION

Retention mechanism of single chain compounds

Martin's equation¹⁴ predicts a linear relationship between the free enthalpy of transfer of a single chain compound from the mobile phase to the stationary phase and the number of carbon atoms of the chain. As this free enthalpy is linearly related to the logarithm of the capacity factor, a linear relationship is expected between this logarithm and the number, n_c , of carbon atoms of the solute. Such a linearity has often been observed^{15,16} and has even served as a basis for the determination of the hold-up volume¹⁷. However, a slight discontinuity in the plot of $\log k'$ vs. n_c has recently been observed when working with monomeric alkyl bonded phases^{8,18}. Because this effect is small and plotting the retention in logarithmic coordinates tends to level off small variations, the relationship between the retention and chain length of a solute is more appropriately investigated in terms of the quadratic methylene selectivity, α , defined as

$$\alpha(n_c) = (k'_{n+1}/k'_{n-1})^{1/2} \quad (2)$$

where k'_{n+1} and k'_{n-1} represent the capacity factors of homologous single chain compounds with $n + 1$ and $n - 1$ carbon atoms, respectively. This expression has the advantage of revealing details that do not appear on a logarithmic scale. Furthermore, the calculation of a ratio minimizes the effects of experimental errors. The plot of α vs. n_c is nevertheless closely related to that of $\log k'$ vs. n_c . A linear variation of $\log k'$ should correspond to a constant α value when n_c is changing. In fact, the plot of α vs. n_c reveals a discontinuity, dependent on the chain length of the ligand and corresponding to the point where a break appears in the plot of $\log k'$ vs. n_c . This phenomenon, observed with numerous homologous series and with various ligand chain lengths, has been attributed to the penetration of the solutes into the bonded ligands. Evidence in support of this mechanism is provided by the fact that the break in the plot of $\log k'$ vs. n_c is not observed for methyl bonded phases as well as for bonded phases synthesized using a trifunctional alkyl silane leading to so-called polymeric bonded phases. In the first case the methyl chain is obviously too short for the solute to penetrate into the ligand layer, while in the second case the sup-

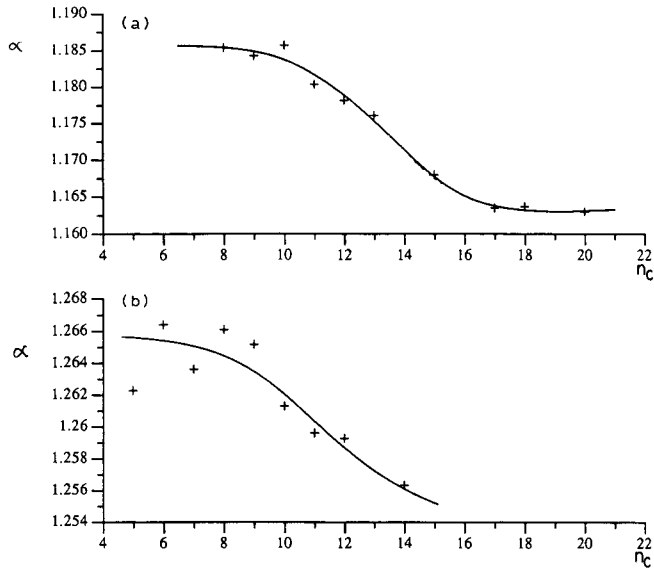


Fig. 1. Quadratic selectivity, α , vs. the number of carbon atoms for different homologous series on an Ultrasphere ODS column. Temperature: 20°C. (a) Solutes, *n*-alkanes; mobile phase, acetonitrile–chloroform (70:30, v/v). (b) Solutes, phenylalkanes; mobile phase, acetonitrile–chloroform (90:10, v/v).

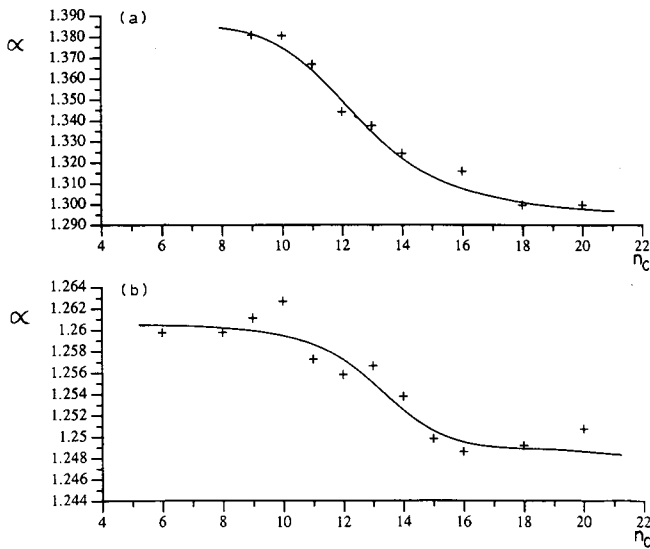


Fig. 2. Quadratic selectivity, α , vs. the number of carbon atoms for different homologous series on an Ultrasphere ODS column. (a) Solutes, fatty acid methyl esters; mobile phase, acetonitrile; temperature, 17°C. (b) Solutes, alkyl benzoates; mobile phase, acetonitrile–chloroform (90:10, v/v); temperature, 20°C.

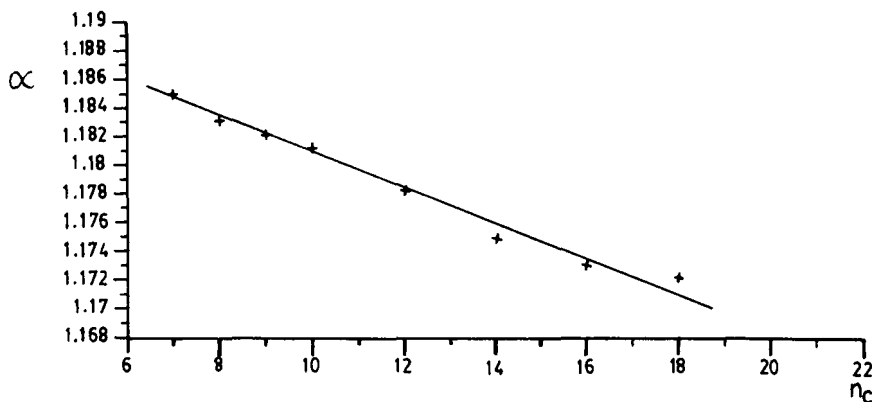


Fig. 3. Quadratic selectivity, α , vs. the number of carbon atoms for the series of chloroalkanes on a μ Bondapak column with methanol as the mobile phase, at 20°C.

posedly more erratic structure of the polymeric phases either does not allow the solute insertion or allows it to various extents in such a way that there is no reason to observe a break in α vs. n_c at any particular n_c value.

We have investigated the retention behaviour of different homologous series in binary non-aqueous mobile phases typically used for the analysis of triglyceride mixtures. Figs. 1 and 2 show some examples of plots of α vs. n_c for different homologous series, with different eluents and temperatures, for the Ultrasphere column. Fig. 3 shows the same type of plot for the μ Bondapak column. The curves in Figs. 1 and 2 for the monomeric Ultrasphere phase are quite similar. The methylene quadratic selectivity is roughly constant for small solute carbon numbers, then a discontinuity (decrease) occurs before the selectivity again becomes approximately constant as n_c increases. In contrast, the curves for μ Bondapak do not exhibit any discontinuity but regularly decrease with increasing n_c . The results presented in Figs. 1–3 and similar results obtained with different homologous series and different non-aqueous mobile phases appear to be in close agreement with those reported previously principally for aqueous mobile phases⁸. They are interpreted in terms of a mechanism of penetration of the solute alkyl chain into the octadecyl bonded phase. Under the non-aqueous eluent conditions used here or in the low water content of the hydroorganic eluents previously used, the ligands of the monomeric stationary phase can be reasonably pictured as extending with a relatively high mobility into the mobile phase as confirmed by NMR conformational studies^{19,20}. Because of the solvophobic effect²¹, the alkyl chains of the solutes tend to penetrate into the bonded layer. This penetration can occur relatively freely up to some solute carbon number, the alkyl chain mainly adopting a regular, commonly called all-*trans* or zigzag conformation which favours a close dispersion interaction with the bonded phase. Above this critical carbon number, which was shown to be correlated with the bonded chain length⁸, the solute chain must slightly change its conformation in order fully to penetrate into the bonded layer and provide optimum interaction with it. This is supposed to result in a looser contact with the bonded phase, reflected by a slight decrease in the interaction energy associated with the addition of a methylene group to the solute and, consequently, in the quadratic methylene selectivity.

The magnitude of this decrease depends on the experimental conditions and from Figs. 1 and 2 is seen to vary from 1 to 6%. In spite of the relatively small value of this variation, the discontinuity in α is clear and unambiguous in Figs. 1 and 2. A detailed statistical study of the error associated with the α determination has been carried out for experimental conditions very similar to the present ones²². It shows that the relative error (standard deviation) for the magnitude of the discontinuity in α is equal to 0.25%. This is several times smaller than the magnitude of the discontinuity and indicates clearly that the latter cannot be accounted for by experimental errors.

Further support to the hypothesis of a penetration mechanism is the fact that the discontinuity in α appears in the same range of n_c values, for monomeric octadecyl bonded phase, whatever the nature of the homologous series and the mobile phase composition. This range lies between about 10 and 14 with an average at about 12. This confirms previous observations that this critical carbon number increases less rapidly than the chain length of the alkyl bonded phase⁸. This possibly reveals that long ligand alkyl chains, such as octadecyl chains, do not adopt the all-*trans* conformation (straight chain) but show a *gauche* conformation so that they are bent to some extent, as observed in Fourier transform infrared spectroscopic studies²³. It should be noted that we do not observe in Figs. 1 and 2 a different behaviour of the phenylalkanes and benzoates from the other series. The critical carbon number is the same for all series, in contrast with a previous report⁸. A detailed study of the particular behaviour of the phenylalkanes and benzoates will be published elsewhere.

Fig. 3 confirms the previous results about the μ Bondapak phase, for which there is no discontinuity in the plots of α vs. n_c , but a regular decrease of the methylene selectivity. Similar curves have been obtained with acetonitrile-chloroform eluents of various compositions. Clearly this bonded phase is not a monomeric one.

Eluotropic strength in non-aqueous reversed-phase liquid chromatography

The average methylene selectivity value varies from one curve to another in Figs. 1 and 2. We have observed that, for a given mobile phase composition, this average value does not depend on the homologous series selected, at least to a first approximation. This is clearly seen in Figs. 1b and 2b plotted at the same temperature and with the same mobile phase composition for two different series (phenylalkanes and alkylbenzoates). The range of α values scanned is nearly the same for these two series. However, the methylene selectivity does significantly depend on the mobile phase composition. As it is a monotonous function of the eluting power of the mobile phase, the average α value gives an indication of this solvent eluting power. In Fig. 4a, the logarithm of the average methylene selectivity, obtained from the slope of a least mean square linear regression of $\log k'$ vs. n_c for *n*-alkanes (from *n*-octane to *n*-docosane), is plotted as a function of the volume fraction of chloroform in acetonitrile. (The variation of the methylene selectivity associated with the penetration mechanism is nearly negligible compared to the influence of the mobile phase composition on this selectivity. Therefore we have used data for all members of the homologous series for solvent strength determinations without taking into account the effect of the penetration mechanism.) The continuous decrease in $\log \alpha$ with increasing volume fraction of chloroform clearly indicates, as expected, that chloroform is a stronger eluent than acetonitrile on octadecyl bonded phases.

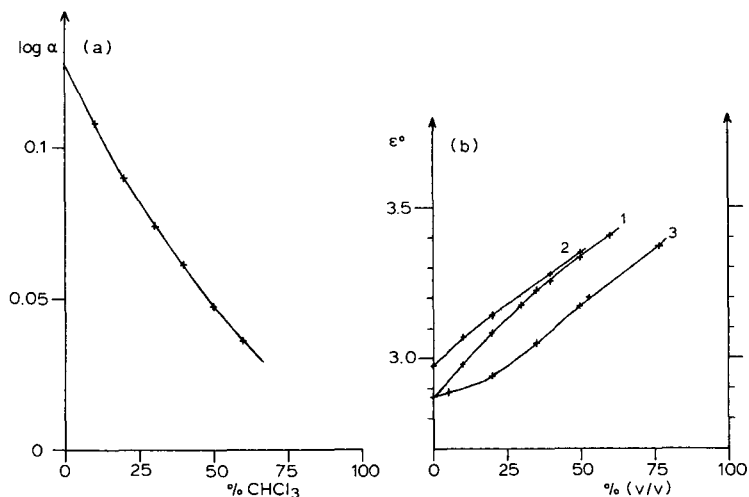


Fig. 4. (a) Logarithm of the average methylene selectivity (slope of $\log k'$ vs. n_c) vs. the volume fraction of chloroform in acetonitrile on the Ultrasphere ODS column. (b) Elutropic strength of the acetonitrile–chloroform mixture vs. the volume fraction of chloroform (curve 1). For comparison, previously reported values²⁵ of the elutropic strength of methanol–tetrahydrofuran and acetonitrile–ethyl acetate mixtures are also plotted vs. the volume fractions of tetrahydrofuran (curve 2) and ethyl acetate (curve 3); respectively.

Furthermore, as the solvophobic effect is the main retention mechanism in reversed-phase liquid chromatography²¹, the average α value provides a very useful means to determine the elutropic strength of a mobile phase. Following the reasoning of Snyder²⁴ for the definition of the elutropic strength, ϵ° , in normal-phase liquid chromatography, the ϵ° value in reversed-phase liquid chromatography has been shown to be easily derived from $\log \alpha$

$$\epsilon^\circ = (\log \alpha_{\text{H}_2\text{O}} - \log \alpha) / \nu_0 \quad (3)$$

where $\alpha_{\text{H}_2\text{O}}$ is the methylene selectivity with pure water as the eluent and ν_0 is the volume of the methylene group, which was estimated to be 0.168 in units of 100 ml²⁵. In this equation, the methylene group is used for measuring the change in retention when changing the eluent, and water serves as the reference solvent for which ϵ° is by definition equal to zero. Although not experimentally determined using the *n*-alkane series in the present study, the $\log \alpha$ value in pure acetonitrile can be estimated by extrapolation of the curve in Fig. 4 with a relatively good precision. It is found to be equal to 0.126. It is remarkable that this extrapolation gives an α value equal to 1.34 which is very close to the average value obtained in pure acetonitrile for the fatty acid methyl ester series, as seen in Fig. 2a. Again this reflects the fact that the methylene selectivity does not depend on the series investigated. The corresponding $\log \alpha$ value is somewhat larger than the value ($\log \alpha = 0.1101$) previously measured by Colin *et al.*²⁵ on a different octadecyl bonded phase column. They determined the ϵ° value of acetonitrile to be 2.87. Using this value together with our extrapolated value of $\log \alpha$, one finds that $\log \alpha_{\text{H}_2\text{O}}$ in our system is equal to 0.608 [$\log \alpha_{\text{H}_2\text{O}} = \log \alpha(\text{acetonitrile}) + \nu_0 \epsilon^\circ(\text{acetonitrile})$], which is remarkably close to the two previously

determined values of 0.592²⁵ and, especially, 0.60²⁶. These small differences probably reflect the slightly different properties of different brands of octadecyl bonded phases. The variations of the eluotropic strength of the acetonitrile–chloroform system are plotted as a function of the mobile phase composition in Fig. 4b. For comparison, the curves previously determined in the same ϵ° range for the acetonitrile–ethyl acetate and methanol–tetrahydrofuran binary mixtures²⁵ are also plotted in this Figure. To be rigorously comparable, all curves should be plotted at the same temperature. In fact, the previous curves were obtained at 25°C while our work was performed at 17°C. Although we have observed, for acetonitrile–chloroform (60:40, v/v), a relative $\log \alpha$ variation of -0.5% per °C, the temperature effect on ϵ° should be sufficiently small for the curves in Fig. 4b to be correctly compared because the temperature variations of $\log \alpha_{\text{H}_2\text{O}}$ and $-\log \alpha$ most likely compensate each other.

Curves like those of Fig. 4b are interesting as they provide a basis for the optimization of the mobile phase composition, when one attempts to separate compounds differing by their apolar moieties, such as triglycerides, in non-aqueous reversed-phase liquid chromatography. Indeed, the weakest eluents found in these systems are acetonitrile and methanol. It appears that, among the three solvent mixtures compared in Fig. 4b, the acetonitrile–chloroform system gives the largest rate of increase of ϵ° with the volume fraction of the strong solvent when this fraction is lower than 50%. It is interesting to compare this system with the acetonitrile–acetone mixture as this system has been used relatively frequently for the analysis of triglyceride samples¹. Although the eluotropic strength of acetonitrile–acetone mixtures has not been reported, it should lie between 2.87 and 3.19, which are the ϵ° values of pure acetonitrile and pure acetone, respectively²⁵. Therefore, according to Fig. 4b, larger ϵ° values can be obtained by adding chloroform rather than acetone to acetonitrile. Indeed, acetonitrile–chloroform (70:30, v/v) has about the same eluting power as pure acetone. Therefore, when performing a gradient elution analysis, one should be able to scan a wider range of triglyceride chain lengths using chloroform rather than acetone as the strong solvent. Alternatively, curves like those of Fig. 4b can be used to select two isoeluotropic solvent mixtures for the optimization of the composition of ternary mobile phase systems.

Retention mechanism of triglycerides

Evidence of the penetration of the triglycerides. If it is easy to visualize the penetration of a single chain solute into the layer of ligands of a bonded phase, the conformational structure of more complex molecules, such as triglycerides, in interaction with a bonded phase is not so trivial. In order to get some insight into this conformation and better to understand the retention behaviour of the triglycerides in non-aqueous mobile phases, we have investigated the retention of saturated homogeneous triglycerides on the monomeric Ultrasphere bonded phase. The results are reported on Fig. 5 for different temperatures and in Fig. 6 for different mobile phases in terms of $\log k'$ vs. the number of carbon atoms (including the carbon of the ester bond) of each chain of the triglyceride molecules. A discontinuity in the slope of these curves is clearly visible for a number of carbon atoms equal to 13 in each chain. Such a break in the curves is equivalent to discontinuity in the corresponding plots of α vs. n_c . As in the above study of homologous series, it can be interpreted as reflecting a penetration mechanism of the triglyceride molecules into the bonded

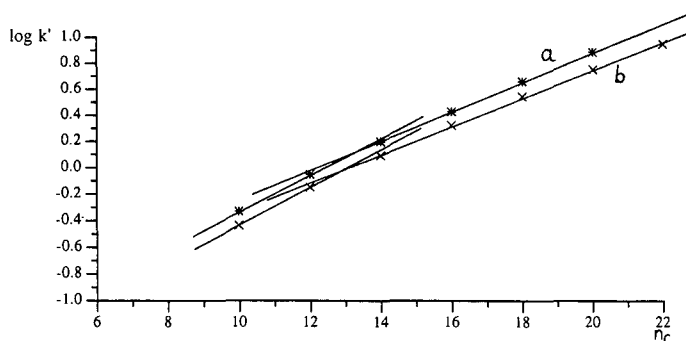


Fig. 5. Plots of $\log k'$ vs. the number of carbon atoms for homogeneous saturated triglycerides on the Ultrasphere ODS column. Mobile phase: acetonitrile–chloroform (60:40, v/v). Temperatures: (a) 35°C; (b) 40°C.

layer. Furthermore, the break appears for the same number of carbon atoms as for the homologous series. This reveals that the triglycerides do not penetrate into the ligand layer using their glyceryl head. Indeed, in this case, the break should have appeared for a lower n_c value due to the steric hindrance (equivalent to about two carbon atoms) of the glyceryl moiety.

By plotting curves like those of Fig. 6 for seven different compositions of acetonitrile–chloroform mobile phases at a given temperature (17°C), it appears that the curves all converge to a given point, as previously observed for single chain homologous series in aqueous mobile phases²⁷. However, because of the slight discontinuity in the plots of $\log k'$ vs n_c , separate extrapolation of the straight lines before and after the break point at the critical number of carbon atoms, reveals not one, but two convergence points; the coordinates of these points are: $\log k' = -1.60$ and $n_c = 0.6$, $\log k' = -1.50$ and $n_c = -0.4$, for the lines extrapolated before the break and after the break, respectively. Such a behaviour for the triglycerides is entirely similar to the behaviour of single chain homologous series⁸.

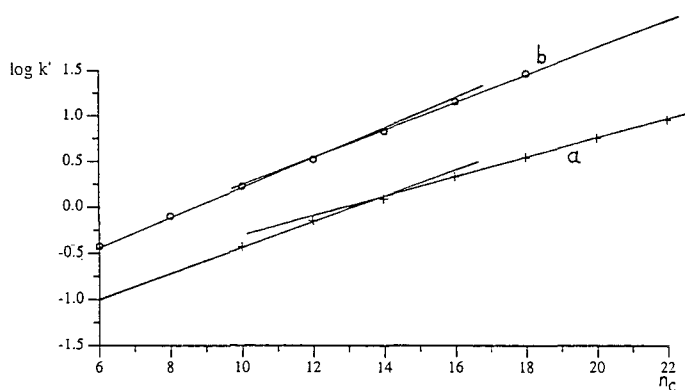


Fig. 6. Plots of $\log k'$ vs. the number of carbon atoms for homogeneous saturated triglycerides on the Ultrasphere ODS column at 20°C. Mobile phases: (a) acetonitrile–chloroform (50:50, v/v); (b) methanol–chloroform (75:25, v/v).

From the variations of the retention with the temperature, one can obtain access to the thermodynamic variables associated with the transfer of a solute from the mobile phase to the stationary phase. The capacity factor of a soluble is related to the standard Gibbs free energy of transfer, ΔG°

$$\log k' = C - \Delta G^\circ / 2.3 RT \quad (4)$$

where C is a constant taking account of the amounts of mobile and stationary phases. The standard enthalpy of transfer, ΔH° , can be determined from the slope of the linear plot of $\log k'$ vs. $1/T$.

$$\log k' = C - (\Delta H^\circ / 2.3 RT) + (\Delta S^\circ / 2.3 R) \quad (5)$$

where ΔS° represents the entropy of transfer of the solute. Plots of $\log k'$ vs. $1/T$ have been made for the alkane and triglyceride series at eight different temperatures ranging from 17 to 55°C, *i.e.*, at temperatures above that corresponding to the end of the phase transition noted for octadecyl bonded phases¹⁸, for acetonitrile–chloroform (60:40, v/v) as the mobile phase. These plots are effectively linear (correlation coefficient of the least mean square linear regression larger than 0.999 for all solutes, but the least retained for which this coefficient is 0.996). By extrapolating these lines to low $1/T$ values, two different intersection points or, more precisely, two different intersection domains are found. The curves for solutes with numbers of carbon atoms lower than the critical carbon atom number, $n_{c, \text{crit}}$, converge to a temperature which is about 100 K larger than the convergence temperature of curves for n_c larger than $n_{c, \text{crit}}$. These convergence temperatures (490 and 590 K) are approximately the same for the n -alkane and triglyceride series. Again, such a behaviour is quite similar to that observed for the n -alkane series in methanol–water or pure methanol eluents²². It was shown²² that the meaning of the convergence temperature for homologous series is identical to the concept of compensation temperature associated with the enthalpy–entropy compensation²⁸. It is interesting that the invariance of the two convergence temperatures observed under largely different operating conditions (aqueous or non-aqueous mobile phases, simple or more complex solute series) indicates that the interaction mechanism of the solutes with the stationary phase is the same for all conditions examined. The existence of a penetration mechanism of the solute apolar chains into the bonded layer is reinforced by the fact that the plots of ΔH° vs. n_c and $(\Delta S^\circ + 2.3 RC)$ vs. n_c are not linear over all the n_c but present a discontinuity for a n_c value close to $n_{c, \text{crit}}$, again as was observed for simple series in aqueous mobile phases²².

Further insight into the penetration mechanism can be gained from the comparison of the slopes of the plots of $\log k'$ vs. n_c for the triglycerides with those of single chain homologous series. Although such a comparison should naturally be done with the series of fatty acid methyl esters, which are structurally similar, the retention values of these compounds in the eluents used for triglyceride analysis are too small to provide an acceptable precision. However, as we noted above that the α values do not depend, to a first approximation, on the series selected, we used, for this purpose, the series of n -alkanes which, being less polar than the esters, have a greater retention.

Procedure for determination of the number of penetrating chains. According to eqn. 4, the slope of $\log k'$ vs. n_c , which was seen to be equal to $\log \alpha$, is directly proportional to the difference in the ΔG° values of two consecutive members of the series investigated, *i.e.*, for an homologous series, to the free enthalpy of transfer, $\Delta G_{\text{CH}_2}^\circ$, associated with the addition of a methylene group to a given compound. The following expression is therefore obtained:

$$\log \alpha = -\Delta G_{\text{CH}_2}^\circ / 2.3 RT \quad (6)$$

For triglycerides, the slope of $\log k'$ vs. n_c corresponds to the decrease in the free enthalpy, $(\Delta G_{\text{CH}_2}^\circ)_{\text{tri}}$, associated with the addition of one methylene group in each chain of the molecule. Interesting information from the comparison of the slopes can be gained by calculating either the ratio or the difference of the $\log \alpha$ values. The former, R_α , reflects the ratio of the $\Delta G_{\text{CH}_2}^\circ$ values for the triglycerides and for the n -alkanes

$$R_\alpha = (\log \alpha)_{\text{tri}} / (\log \alpha)_{\text{alk}} = (\Delta G_{\text{CH}_2}^\circ)_{\text{tri}} / (\Delta G_{\text{CH}_2}^\circ)_{\text{alk}} \quad (7)$$

where the suffixes tri and alk refer to the homogeneous saturated triglyceride series and n -alkane series, respectively, while the latter (logarithm of the α ratio) measures their difference. The relevant comparison basis which is to be selected depends on the objective pursued. Our purpose, in the present study, is to get some information on the interaction of the triglyceride chains with the bonded layer and, specifically, to evaluate the number of chains which penetrate into the layer. This can be done by calculating the ratio R_α .

Indeed, in reversed-phase liquid chromatography, it is accepted that the solvophobic effect is the dominating mechanism for retention, especially when considering the retention change associated with the addition of methylene groups to the solute molecules. The retention theory based on this effect predicts that the free enthalpy of transfer of a solute is proportional to the reduction in the overall molecular surface area of species (solute and ligand) immersed in the eluent resulting from the association of the solute with a ligand²¹. Accordingly, the change in $\log k'$ of consecutive members of the triglyceride series, $(\log \alpha)_{\text{tri}}$, is directly related to the variation of the contact areas between the solutes with the ligands when adding a methylene group to each chain. The variation of contact area due to the interaction of one methylene group with the ligand is measured by $(\log \alpha)_{\text{alk}}$. Therefore, the ratio R_α provides a scale for measuring this variation for the triglyceride series in units of the contact area of a methylene group. It should be noted that such a scaling procedure can be applied to any series of compounds differing in the number of structural units of a given kind *e.g.*, aromatic groups. However, in the specific case of molecular compounds with multiple chains, such as the triglycerides, R_α directly measures the number of methylene groups interacting with the stationary phase when one methylene is added to each chain and, consequently, the number of chains penetrating into the bonded layer.

Number of penetrating chains for the triglycerides. Because we have seen above that, for both the n -alkane and triglyceride series, the value of $\log \alpha$ depends slightly on the number of carbon atoms penetrating into the bonded layer, the comparison

TABLE I

RATIO OF THE LOG α VALUES OF THE TRIGLYCERIDES AND *n*-ALKANES

Column: Ultrasphere ODS. A = acetonitrile; B = methanol; C = chloroform.

Mobile phase	<i>T</i> (°C)	log α <i>n</i> -alkanes	Correlation coefficient	log α triglycerides	Correlation coefficient	R_α
A-C (60:40, v/v)	20	0.065	0.9999	0.152	0.9999	2.34
	25	0.061	0.9998	0.148	0.9997	2.42
	35	0.058	0.9996	0.139	0.9995	2.39
	45	0.057	0.9987	0.136	0.9985	2.39
A-C (70:30, v/v)	20	0.077	0.9998	0.182	1	2.35
B-C (90:10, v/v)	20	0.086	0.9999	0.206	0.9999	2.41
A-C (70-30, v/v)	17	0.081	0.9998	0.194	0.9999	2.39
A-C (55-45, v/v)	17	0.061	0.9997	0.144	0.9994	2.37
A-C (50-50, v/v)	17	0.058	0.9991	0.135	0.9995	2.34

of log α must be done either before or after the appearance of the break in log k' vs. n_c (or, which is equivalent, of the discontinuity in α vs. n_c) using the same range of carbon numbers. The results of such comparisons are shown in Table I for different temperatures and mobile phase compositions. The log α values reported in this table correspond to the slopes of the least mean square linear regressions of the log k' vs. n_c data for alkanes and triglycerides with 10, 12 and 14 carbon atoms in the aliphatic chains. Under all conditions tested, the R_α value is almost the same, close to 2.4.

This value confirms the conclusion, derived above from the position of the break in log k' vs. n_c , that the glyceryl moiety does not penetrate into the bonded layer. Indeed, such a penetration would have necessarily induced the penetration of the three alkyl chains and led to an R_α value equal to three.

However, it is somewhat surprising that this ratio is not a whole number. A value higher than 2 eliminates the possibility of penetration of only one or two chains of the triglycerides into the bonded ligands. Therefore, this suggests that the penetration of the three chains must be considered and that at least one chain can undergo only a partial penetration. However, because of the way R_α is defined, this cannot be due to the fact that a length of a chain cannot penetrate entirely into the bonded layer but, instead, reveals that there is a dynamic conformational equilibrium such that either one, two or three chains penetrate into the stationary phase. The value of R_α therefore reflects the statistical time average of the different conformations at the interface between the mobile and stationary phases.

The ratio R_α is a measure of a ΔG° ratio for methylene groups. It is interesting to compare the other thermodynamic variables associated with the transfer of a methylene group from the mobile phase to the stationary phase. It has been noted above that plots of ΔH° vs. n_c and $(\Delta S^\circ + 2.3 RC)$ vs. n_c for the triglyceride series are made of two linear parts with a discontinuity for $n_c = n_{c, \text{crit}}$. There is also a discontinuity at the same $n_{c, \text{crit}}$ value for the *n*-alkane series in the same eluent. The slopes of these plots correspond to the enthalpy and entropy of transfer of a methylene group, $\Delta H_{\text{CH}_2}^\circ$ and $\Delta S_{\text{CH}_2}^\circ$, respectively. One can compare the corresponding values for tri-

glyceride and alkane series for a range of n_c values which are either lower or larger than $n_{c,crit}$. In acetonitrile–chloroform (60:40, v/v) as the mobile phase, one obtains the following results:

$$(\Delta H_{CH_2})_{tri}/(\Delta H_{CH_2})_{alk} = 2.7 \quad \text{for } n_c \leq n_{c,crit}$$

$$(\Delta H_{CH_2})_{tri}/(\Delta H_{CH_2})_{alk} = 2.2 \quad \text{for } n_c > n_{c,crit}$$

$$(\Delta S_{CH_2})_{tri}/(\Delta S_{CH_2})_{alk} = 2.2 \quad \text{for } n_c \leq n_{c,crit}$$

It is noticeable that these enthalpy and entropy ratios, corresponding to the addition of a methylene group to the hydrocarbonaceous chains, are similar to R_α . The difference between these ratios and R_α , which amounts to about $\pm 10\%$, is similar to that observed for the series of *n*-alkyl *o*-phthalates in aqueous eluents²² and is most likely due to the precision of the experimental determinations. The fact that these ratios are not whole numbers again indicates that there are several conformations, in dynamic equilibrium with each other, for the triglycerides interacting with the stationary phase.

Possible conformations of diglycerides and triglycerides at the interface with the bonded layer. Numerous studies have been carried out on the conformation of glycerol-based molecules in different states. X-ray and NMR spectroscopic studies performed on the crystalline structures of the triglycerides have shown that, in the solid state, the conformation of these molecules is such that the two extreme chains are oriented in the same direction while the central chain is oriented in the opposite direction^{29,30}. Such a configuration may lead to the penetration of either one or two chains. Under liquid chromatographic conditions, however, different conformations may be encountered due to the free rotation of the bonds. It was shown that *gauche* conformations of the glyceryl moiety exist in aqueous solutions³¹. Furthermore, one can expect that the solvophobic effect will tend to force all aliphatic chains to interact with the ligands. This was shown in a conformational study of triglyceride films on water³².

We have performed similar retention studies on homogeneous saturated 1,2- and 1,3-diglycerides in acetonitrile–methanol (90:10, v/v). A slight (11%) retention difference is found between isomers. The secondary alcohols (1,3-diglycerides) are less retained than the primary alcohols (1,2-diglycerides), as observed for *n*-alcohols¹⁵. The number of available diglycerides is not enough for a break to be detected in $\log k'$ vs. the number of carbon atoms in each chain of the diglyceride molecules. Nevertheless, $\log \alpha$ values can be calculated from retention data for 1,2- and 1,3-diglycerides with 12 and 14 carbon atoms in each aliphatic chain and compared to the corresponding value ($\log \alpha = 0.116$) for *n*-alkanes in the same mobile phase. The resulting R_α values obtained for the 1,2- and 1,3-diglycerides are both equal to 1.8. This value again is not a whole number and corresponds to a time average of molecular conformation in which either one or the two chains interact with the stationary phase. One can easily calculate that the configurations corresponding to the two interacting chains are four times more probable than the configurations in which only one chain is interacting. If one now assumes that this probability ratio is kept

unchanged for triglycerides, it becomes possible to solve the system of equations giving an R_α value equal to 2.4. One then finds that the probabilities, P_1 , P_2 and P_3 , for configurations corresponding to one, two and three interacting chains are equal to 10, 40 and 50%, respectively. Because of the uncertainty about the above assumption and, to a lesser extent, of the somewhat limited precision of the R_α determination, these probability values for the occurrence of the different conformations must be regarded with caution. Nevertheless, the relatively large value of P_3 is quite remarkable. Indeed, in the free mobile phase, the probability of finding the three aliphatic chains of a diluted triglyceride oriented in the same direction is expected to be quite low. Therefore, the relatively large value of P_3 for three chains penetrating into the bonded layer certainly reflects the strong influence, and the cooperative contribution, of the solvophobic effect on the conformation of the molecules at the interface between the two phases.

CONCLUSIONS

Several conclusions can be drawn from the results presented above.

(1) This study confirms that the previously observed mechanism of penetration of the hydrocarbonaceous solute chains into the layer of bonded ligands prevails under widely varying reversed-phase liquid chromatography conditions, for aqueous as well as non-aqueous mobile phases and for simple as well as more complex solute molecular structures, such as the triglycerides. Various indicators can be used to illustrate this mechanism (break in $\log k'$ vs. n_c or discontinuity in α vs. n_c ; existence of two intersection points or domains for $\log k'$ vs. n_c under different mobile phase compositions; existence of two different convergence temperatures for $\log k'$ vs. $1/T$; invariability of these temperatures when changing the mobile phase composition; break in ΔH° and ΔS° vs. n_c). The positive response of all these indicators and their sensitivity to a constant $n_{c, \text{crit}}$ value considerably reinforces the support for the penetration mechanism and gives a coherent image of the retention mechanism.

(2) A procedure has been established to determine the number of penetrating chains for complex solute molecules with multiple hydrocarbonaceous chains. The concept on which this procedure is based, *i.e.*, measurement of the incremental contact area with the stationary phase for structurally related compounds in terms of the contact area of a reference structural unit (here, a methylene group), can be extended to other types of structural units (for instance, aromatic rings).

(3) The application of this procedure to triglycerides has revealed that these molecules can interact with the bonded stationary phase using various conformations in dynamic equilibrium with each other. When interacting with the ligand layer, a triglyceride may have one, two or more frequently, three chains penetrating into the layer. Of course, each of these conformations does not lead to the same energy of interaction. The overall retention of a triglyceride in the column is the result of a statistical time averaging of these various free energies. It is most likely that such conformational equilibria influencing significantly the retention exist for other types of compounds having several more or less flexible hydrocarbonaceous chains, such as, for instance, branched polymers or hydrocarbons present in petroleum fractions. The diglycerides have a similar behaviour, one of their chains or, most frequently, the two chains penetrating into the stationary phase.

(4) The eluotropic strength, ε° , of acetonitrile–chloroform mixtures in reversed-phase liquid chromatography has been determined and compared to that of other non-aqueous elements. In the present case, the use of the methylene group as the reference solute for ε° determinations is justified by the fact that triglycerides must first be separated according to their numbers of methylene groups. It is shown that the rate of variation of ε° with the volume fraction of the strongest solvent component is larger for acetonitrile–chloroform mixtures than for solvent mixtures for which ε° determinations have been carried out. Consequently, during an acetonitrile–chloroform gradient elution, one can scan a larger range of triglyceride hydrophobicities, *i.e.*, analyse triglycerides with longer chains than by carrying out a gradient elution with other mixtures. Furthermore, the comparison of the relative influences of temperature and mobile phase variations on retention indicates that an acetonitrile–chloroform gradient elution analysis is much more efficient than a temperature gradient (in the practical range 15–55°C) for scanning a large range of triglyceride chain lengths.

(5) This study permits a clear understanding of why the retention of a triglyceride cannot be correctly predicted from the retention of the three corresponding fatty acid methyl esters. Indeed, the aliphatic chain of these single chain esters does penetrate into the stationary phase. By combining the retention data of the three esters, one implicitly assumes that the three chains interact with the stationary phase, while, in fact, only 2.4 chains have been shown statistically to penetrate into the bonded layer.

(6) The identification of triglycerides in complex samples is frequently done by calculating the capacity factor of a mixed triglyceride from those of homogeneous ones according to eqn. 1 using diagrams where linear interpolations of $\log k'$ vs. the number of carbon atoms are performed⁷. However, because it is shown that there is a break in such curves, much care must be used not to interpolate curves on both sides of the critical carbon atom number.

(7) It is frequently thought that unsaturated triglyceride isomers having the same number of carbon atoms and of unsaturations, but differing in the positions of the double bonds along the three chains, cannot be separated. This can be understood since, when the chains penetrate into the stationary layer, there is no interaction specificity according to the position of the double bonds. However, the fact that the triglycerides may have different conformations when interacting with the ligands and that one, or more rarely, two chains may not penetrate into the bonded layer but stay entirely surrounded by solvent molecules, can give a selectivity basis according to specific interactions of the mobile phase with the unsaturations remaining outside the bonded layer. Admittedly, the corresponding selectivity values are likely to be small since these “outside chain” conformations are statistically not very favourable and since there might be several different conformations giving one outside chain (this might be the central chain or a lateral chain) which tends to average and somewhat cancel out these different interactions. Nevertheless, in principle, the separation of such isomers can occur provided that the efficiency of the chromatographic system is sufficient, as seems to have been recently observed³³. It is expected that the separations will be improved by using a mobile phase which gives strong specific interactions with unsaturated compounds and which simultaneously has an appropriate eluotropic strength to provide an adequate retention.

ACKNOWLEDGEMENT

We are grateful to MM. Anselme and Azemar (Beckman, Gagny, France) for the gift of the monomeric Ultrasphere column.

REFERENCES

- 1 L. J. R. Barrón and G. Santa-Maria, *Chromatographia*, 23 (1987) 209.
- 2 E. Frede, *Chromatographia*, 21 (1986) 29.
- 3 A. Stolyhwo, H. Colin, M. Martin and G. Guiochon, *J. Chromatogr.*, 288 (1984) 253.
- 4 J. L. Robinson and R. Macrae, *J. Chromatogr.*, 303 (1984) 386.
- 5 A. Stolyhwo, H. Colin and G. Guiochon, *Anal. Chem.*, 57 (1985) 1342.
- 6 N. A. Parris, *J. Chromatogr.*, 149 (1978) 615.
- 7 J. P. Goiffon, C. Reminiac and D. Furon, *Rev. Fr. Corps Gras*, 4 (1981) 199.
- 8 A. Tchaplá, H. Colin and G. Guiochon, *Anal. Chem.*, 56 (1984) 621.
- 9 P. K. Tseng and L. B. Rogers, *J. Chromatogr. Sci.*, 16 (1978) 436.
- 10 M. Tsimidou and R. Macrae, *J. Chromatogr. Sci.*, 23 (1985) 155.
- 11 F. Riedo and E. Sz. Kováts, *J. Chromatogr.*, 239 (1982) 1.
- 12 E. sz. Kováts, in F. Bruner (Editor), *The Science of Chromatography*, (Journal of Chromatography Library, Vol. 32), Elsevier, Amsterdam, 1985, p. 205.
- 13 E. H. Slaats, J. C. Kraak, W. J. T. Brugman and H. Poppe, *J. Chromatogr.*, 149 (1978) 255.
- 14 A. J. P. Martin, *Biochem. Soc. Symp.*, 3 (1949) 4.
- 15 H. Colin and G. Guiochon, *J. Chromatogr. Sci.*, 18 (1980) 54.
- 16 P. Jandera, *J. Chromatogr.*, 314 (1984) 13.
- 17 G. E. Berendsen, P. J. Schoenmakers, L. De Galan, G. Vigh, Z. Varga-Puchony and J. Inczedy, *J. Liq. Chromatogr.*, 3 (1980) 1669.
- 18 D. Morel, J. Serpinet, J. M. Letoffe and P. Claudy, *Chromatographia*, 22 (1986) 103.
- 19 R. K. Gilpin and M. E. Gangoda, *J. Chromatogr. Sci.*, 21 (1983) 352.
- 20 E. Bayer, A. Paulus, B. Peters, G. Laupp, J. Reiners and K. Albert, *J. Chromatogr.*, 364 (1986) 25.
- 21 Cs. Horváth, W. Melander and I. Molnár, *J. Chromatogr.*, 125 (1976) 129.
- 22 A. Tchaplá, S. Héron, H. Colin and G. Guiochon, *Anal. Chem.*, (1988) in press.
- 23 L. C. Sander, J. B. Callis and L. R. Field, *Anal. Chem.*, 55 (1983) 1068.
- 24 L. R. Snyder, *J. Chromatogr.*, 6 (1961) 22.
- 25 H. Colin, G. Guiochon, Z. Yun, J. C. Diez-Masa and P. Jandera, *J. Chromatogr. Sci.*, 21 (1983) 179.
- 26 B. L. Karger, J. R. Gant, A. Hartkopf and P. H. Weiner, *J. Chromatogr.*, 128 (1976) 65.
- 27 H. Colin, A. M. Krstulovic, M.-F. Gonnord, G. Guiochon, Z. Yun and P. Jandera, *Chromatographia*, 17 (1983) 9.
- 28 W. Melander, D. E. Campbell and Cs. Horváth, *J. Chromatogr.*, 158 (1978) 215.
- 29 L. H. Jensen and A. J. Mabis, *Acta Crystallogr.*, 21 (1966) 770.
- 30 D. L. Dorset, W. A. Pangborn, A. J. Hancock, T. C. Van Soest and S. M. Greenwald, *Z. Naturforsch., Teil C*, 33 (1978) 50.
- 31 G. Fourche, C. Clément, B. Lemaire and C. Lussan, *Nouv. J. Chim.*, 5 (1981) 91.
- 32 T. Bursh, K. Larsson and M. Lundquist, *Chem. Phys. Lipids*, 2 (1968) 102.
- 33 G. Semporé and J. Bézard, *J. Chromatogr.*, 366 (1986) 261.

CHROM. 20 730

EXPERT SYSTEM FOR CHROMATOGRAPHY

LU PEICHANG* and HUANG HONGXIN

Dalian Chromatographic R&D Centre of China, Dalian Institute of Chemical Physics, Academia Sinica, Dalian, Liaoning (China)

SUMMARY

A strategy for development of an expert system for chromatography is discussed. A program including the recommendation of the column system, the optimization of operating conditions, peak identification and quantitation on-line and the diagnosis of the hardware system has been developed. Both artificial intelligence and some advanced algorithms have been incorporated.

INTRODUCTION

Since the chromatograph Sentinel¹ with automatic method development was produced by DuPont in 1981, the development of chromatographs with artificial intelligence (AI) has attracted much attention²⁻⁴. Hardware such as laboratory robotic systems with fully automatic sample preparation and analysis has been produced by Perkin-Elmer⁵ and Zymark⁶. To develop hardware to provide the technical support for advanced software is very important, but the key to the development of a chromatograph with AI is the software⁷⁻¹⁰. Research on chromatographic theory and methodology are still the central focus of chromatographers¹¹⁻¹⁵. The development of computer programs for solvent optimization, which are heavily dependent on some algorithms, has been achieved by optimizing the separation with respect to specific criteria. Glajch and co-workers^{11,12} reported an overlapping resolution mapping (ORM) method which is a powerful tool for aiding the chromatographer in obtaining satisfactory high-performance liquid chromatographic (HPLC) separation, but an human expert is still required to recommend the stationary and mobile phases. Recently, Snyder and Dolan¹⁶ developed a series of software, Drylab, which is based on a set of equations to predict how various changes in chromatographic conditions and column length affect the resolution, plate number, analysis time, solvent consumption, relative peak sensitivity and other chromatographic parameters. Computer simulation can also be used for optimizing gradient-elution separation after two initial experimental gradient separations of the sample¹⁷. Method development using this procedure, of course, can result in a better separation with much less effort.

The development of expert systems for chromatography using AI techniques has just begun¹⁸⁻²¹, e.g., the Expert Chromatographic Assistance Team (ECAT) devel-

oped by Bach¹⁹ and the Michigan University System (MUS) developed by Wade²⁰. The task of ECAT is to perform, at the human expert level, the design, analysis, optimization and troubleshooting of an HPLC separation method. Because there is not a "living" chromatogram base in ECAT, it is difficult to demonstrate the reliability of the reasoning of an expert system and to display chromatograms corresponding to samples analyzed in the literature.

A new generation of chromatographs employ AI²¹. Our basic research in this area has been reviewed²²⁻²⁴. In this article we shall discuss our strategy for developing an expert system for chromatography (ESC), the design of the knowledge base and the chromatogram base and some advanced algorithms such as those for separation optimization and data handling. We also discuss how to combine the algorithms with the AI approach to build up the system.

System strategy

The expert system is divided into three parts: knowledge base and chromatogram base, inference engine and user interface. The knowledge base consists of a set of facts and rules on the chromatographic subject. The chromatogram base contains some chromatograms for the samples published in the literature. The inference engine or rule interpreter is responsible for extracting the desired information from the knowledge base and explaining how the answer is obtained. The user interface allows the user to interact with the system through dialogues and to display reasoning results, chromatogram and explanation. The stages involved in the development and application of the ESC are presented in Fig. 1.

The goal of any chromatographic analysis is to separate a mixture into individual peaks for qualitative and quantitative determination. First, it is necessary to select a suitable mode of separation, *i.e.*, gas chromatography (GC) or liquid chromatography (LC). We think that GC should be recommended if two conditions can be met: the sample analyzed is (1) volatile enough to be eluted from the column, (2) stable enough not to change at the operating temperature. The reason is that GC is characterized by high resolving power and low cost. Of course, the volatility of the sample also depends on the detectability of the detector. In addition, derivatization of the sample and column switching techniques can further enlarge the application range of GC. However, for thermally unstable or non-volatile substances only LC can be

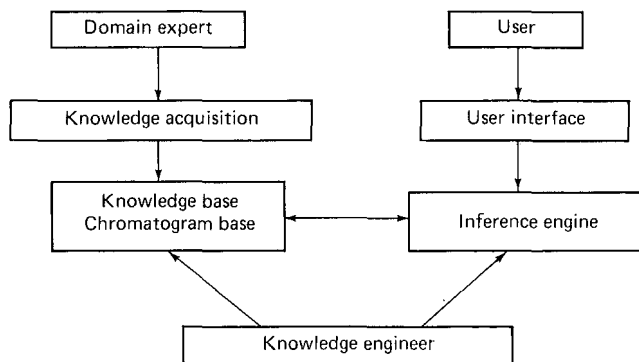


Fig. 1. The stages involved in the expert system for chromatography.

used. After choosing the mode of separation, the column system should be selected, *i.e.*, the stationary liquid and type of column in GC, and the stationary phase and mobile phase in LC. Secondly, the method of sample pretreatment and detection will be determined by the sample, its matrix and where it is. Thirdly, it is desirable to obtain a good separation within the shortest time with a minimum number of experiments, *i.e.*, the optimum separation. To guarantee good analytical results from the column system, it is necessary to diagnose the instrument hardware. So a program for hardware diagnosis must be included in the system. It is concluded that an expert system for chromatography has to perform at least the following modules:

- (1) The recommendation of the mode of separation and column system
- (2) The recommendation of the method of sample pretreatment and detection
- (3) The optimization of the operating conditions
- (4) Peak identification and quantitation on-line
- (5) The diagnosis of the hardware system

We have developed the knowledge base and chromatogram base, inference engine, user interface and some algorithms to support task modules in an ESC. In order to implement and use them conveniently, each module is independent of the rest of the system. The flow chart of chromatographic method development is presented in Fig. 2.

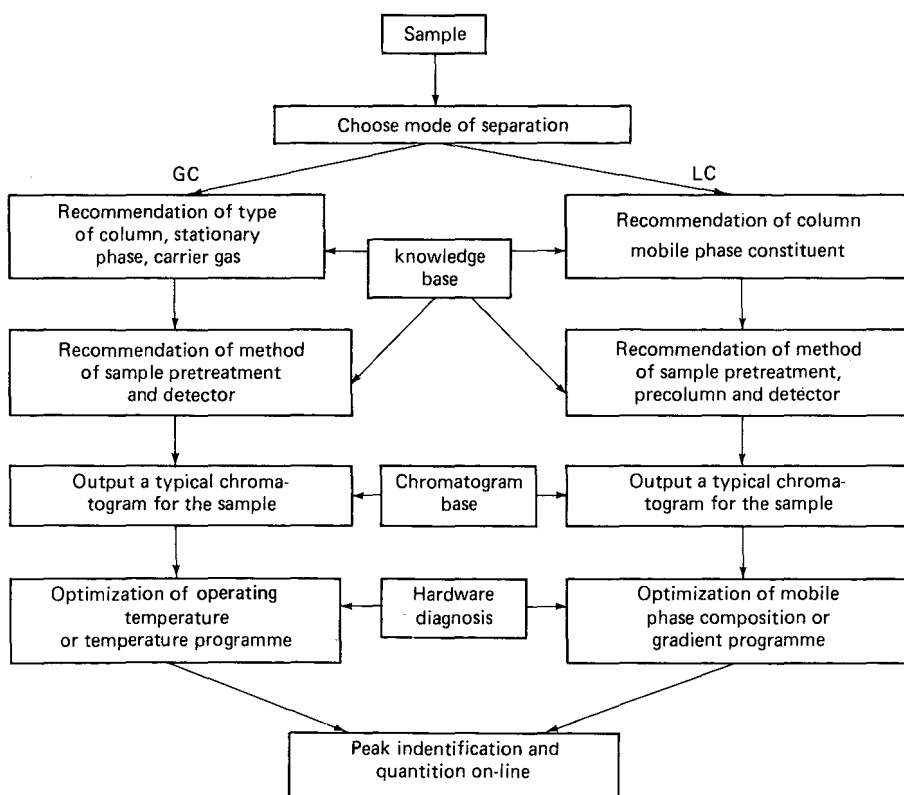


Fig. 2. The flow chart of the chromatographic method development.

As mentioned above, the major feature of an ESC is its knowledge base and chromatogram base. On the other hand, numerical calculation, based on chromatographic theory and algorithms, still plays an important rôle in the development of an ESC. Some problems, such as optimization, chromatographic data handling, should be solved using advanced algorithms. Therefore, we think that an ESC should be based not only on general chromatographic reasoning, but also on advanced algorithms.

Theory and algorithms

Optimization. For the simultaneous experimental optimization for a sample with known constituents, the resolution criterion K1 can be used to select the optimum conditions, considering the effect of the peak height ratio of two adjacent peaks

$$\begin{aligned}
 K1 &= 2(t_{R_1} - t_{R_2})/(w_{h_1} + w_{h_2}) \\
 &= 1/2.354(\alpha' - 1) n \\
 &= 1/2.354(\alpha' - 1)[(1 + k')/(\beta + k')] \cdot \sqrt{n_\infty} \\
 &= 1/2.354S\sqrt{n_\infty}
 \end{aligned} \tag{1}$$

where t_R is the retention time, w_h the peak width at half height, α' the separation factor, n the plate number, k' the capacity factor, β the coefficient of variation of the plate number with variation of the capacity factor, n_∞ the plate number for a solute having a capacity factor approaching infinity and S is the selectivity criterion of the column system

$$S = (\alpha' - 1)(1 + k')/(\beta + k') \tag{2}$$

For sequential experimental optimization of a sample with unknown constituents, another criterion, the serial chromatographic response function (SCRFF), is proposed²⁵

$$SCRFF = 100\,000N + 10\,000 \cdot K3 + (100 - t) \tag{3}$$

where N is the peak number, $K3$ is the peak resolution of the least separated peak pair in a chromatogram and t is the analysis time. Once the SCRFF is combined with the simplex optimization method, the optimum conditions can be searched for. The principles of selecting the optimum conditions are:

(1) The higher the number of peaks, the better are the operating conditions. This implies that more information about a sample can be extracted from an analysis.

(2) When the peak number has reached a maximum the resolution of the least-separated peak pair should meet the criterion K1 or K3.

(3) With maximum peak number and satisfactory K1 or K3, the analysis time should be as short as possible.

If the above principles are employed the multi-step linear program optimization for a known sample in HPLC, K1, can be expressed as²⁶

$$Kl_i = 2[t_0(1 + k'_{i+1})Q_{i+1}^x - t_0(1 + k'_i)Q_i^x]/(w_{h_{i+1}}^x + w_{h_i}^x) \tag{4}$$

where k'_i , $w_{h_i}^x$ and Q_i^x are the column dead time, capacity factor, peak width at half height and rest fraction of the column length to be moved for the i th component at the x -step mobile phase composition, respectively. The effect of the mobile phase composition on k'_i , $w_{h_i}^x$ can be predicted by:

$$\ln k'_i = A_i + B_iCb + C_i \ln Cb \tag{5}$$

$$w_{h_i}^x = a + bk'_i \tag{6}$$

where A_i is related to the adsorption energy of the solute, molecular interactions between the solute, solvent and stationary phase; B_i is only involved in solution interaction; C_i is an entropy function of an adsorbed solute; Cb is the concentration of strong solvent in a binary mobile phase; a and b are constants.

The parameters in eqns. 5 and 6 can be calculated by curve fitting from the data for at least three isocratic experiments. The parameter Q_i^x can be expressed as

$$\left. \begin{aligned} Q &= 1 - \sum_{j=1}^{2x-1} M_{i,j} \\ M_{i,2x-2} &= \int_{c_{x-1}}^c \frac{dC}{t_0 r_{x-1} [1 + \exp(A_i + B_iCb + C_i \ln Cb)]} \\ M_{i,2x-1} &= \left[1 - \sum_{j=1}^{2x-2} M_{i,j} \right] \frac{(t_x - t_0)(1 + k'_{i-1})u}{k'_i(1 + k'_i)} \end{aligned} \right\} \tag{7}$$

where $M(i,0) = 0$, u is the mobile phase velocity, t_x is the elution time of component i at the x -step mobile phase composition and r_{x-1} is the composition rate from the step $x+1$ to the step x . The Kl_i for any adjacent components becomes a function of the mobile phase composition upon inserting eqns. 5-7 into eqn. 4.

Data handling. Data handling is an important topic. The data handling software, which can be used to detect various peaks including shoulders and give information on peak identification and quantitation, has been developed. The flow chart of the software is presented in Fig. 3.

Here, an advanced algorithm, a curve fitting method, for measurement of overlapping peaks is proposed on the basis of an exponentially modified Gaussian (EMG) function.

$$h(t) = \frac{A}{\sqrt{\pi\tau}} \exp\left(\frac{\sigma^2}{2\tau^2} - \frac{t - t_G}{\tau}\right) \cdot \int_{-\infty}^z e^{-x^2} dx = A \cdot f(t, t_G, \sigma, \tau) \tag{8}$$

or

$$A = h(t)/f(t, t_G, \sigma, \tau) \tag{9}$$

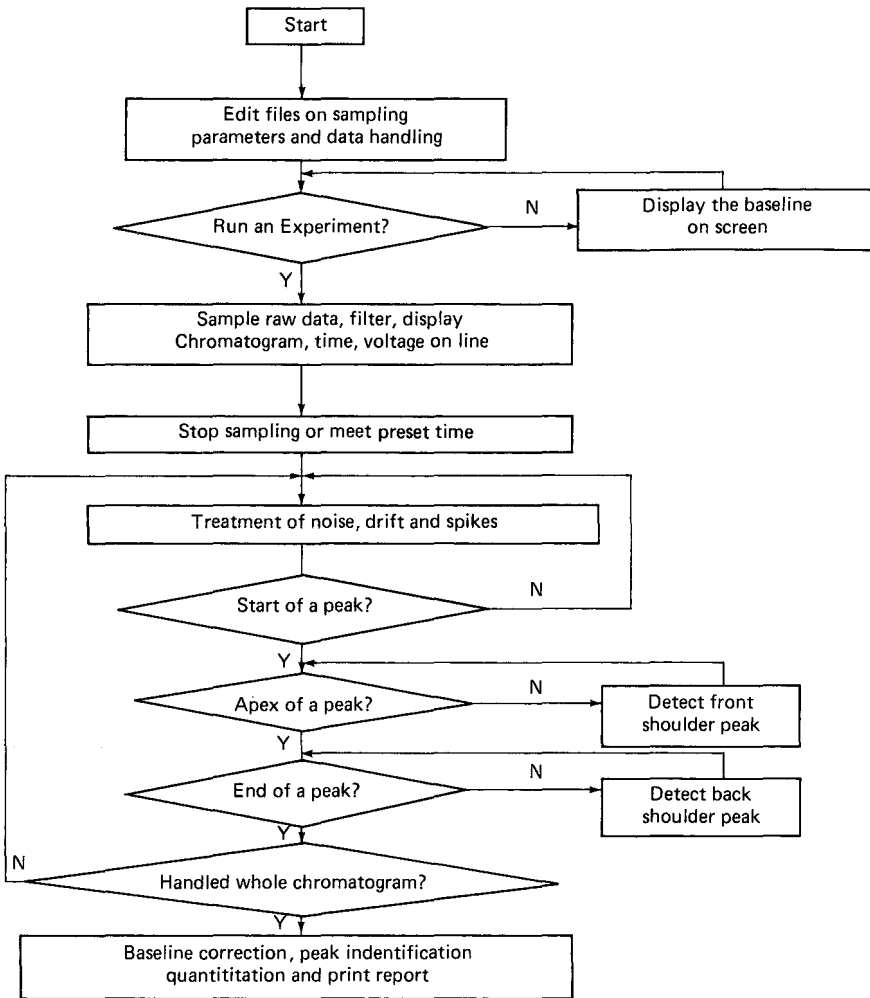


Fig. 3. Flow chart for peak identification and quantitation in the ESC.

where $z = \left(\frac{t - t_G}{\sigma} - \frac{\sigma}{\tau} \right) / \sqrt{2}$, A is the peak area, t is the time, $h(t)$ is the peak height at

t , t_G is the central position of a Gaussian constituent, σ is the standard deviation of a Gaussian constituent and τ is the time constant for exponential decay. When $t = t_R$, $h(t)$ is the maximum peak height. The methods for estimating the parameters are given in ref. 27. We found²⁸ in practice that the linear relationship among σ , τ and t_R are

$$\sigma = a_1 + b_1 t_R \quad (10)$$

$$\tau = a_2 + b_2 t_R \quad (11)$$

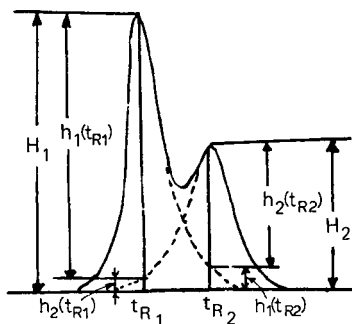


Fig. 4. The resolution of overlapping peaks.

where a_1, b_1, a_2 and b_2 are dynamically related coefficients²⁹ that can be obtained by the regression of several baseline-separated peaks. That means that the function f for all peaks in a chromatogram can be calculated. When we want to resolve the overlapping peaks presented in Fig. 4, the curve-fitting area is represented as

$$\begin{aligned}
 A_1 &= h_1(t_{R1})/f(t_{R1}, \sigma_1, \tau_1) \\
 &= [H_1 - h_2(t_{R1})]/f(t_{R1}, t_{G1}, \sigma_1, \tau_1) \\
 &= [H_1 - A_2 f(t_{R1}, t_{G2}, \sigma_2, \tau_2)]/f(t_{R1}, t_{G1}, \sigma_1, \tau_1) \quad (12)
 \end{aligned}$$

$$A_2 = [H_2 - A_1 f(t_{R2}, t_{G1}, \sigma_1, \tau_1)]/f(t_{R2}, t_{G2}, \sigma_2, \tau_2) \quad (13)$$

where H_1, H_2 can be measured from the chromatogram, but A_1, A_2 on the right-hand side of equation are not known before resolving the overlapping peaks. So the peak areas obtained from the perpendicular drop method are first substituted for A_2 and A_1 in eqns. 12 and 13 to get approximate new peak areas A_1, A_2 . The new A_1 and A_2 are again substituted for A_1 and A_2 in the right-hand side of eqns. 12 and 13. The iterative calculation proceeds until the error in the peak area is less than desired one (at least two calculations are performed).

Implementation

All software except the numerical processing modules has been written in SCHEME-LISP, a language used to develop programs for symbolic processes. It can call programs written in procedural languages such as BASIC, FORTRAN and C. The decision made by the inference engine can be passed to numerical processing modules via a file or parameters. The results obtained from the numerical processing modules can also be returned to the inference engine to enable further decision making via a file. The combination of the rule-based system with the algorithms approach can thus be realized. The system has been hosted on an IBM PC/XT-286 microcomputer with a 20M hard disk drive, two floppy disk drives and a 20-bit analog-to-digital (A/D) converter to acquire raw data from a detector.

RESULTS AND DISCUSSION

The development of the knowledge base and chromatogram base

Our strategy for building the knowledge base is based on fundamental chromatographic theory. The selection rules for the stationary and mobile phase have been proposed after considering the interaction among solutes, stationary phase and mobile phase. The sample, we think, can be separated into individual peaks if the compounds in the sample have small chemical and physical differences such as functional groups, polarity, solubility, molecular weight. The specific stationary phase and mobile phase should be selected for separation of very similar compounds such as chiral and isomer samples.

An expert system with a chromatogram base has not reported until now, but it is well known that the chromatograms and operating conditions published in the literature are very useful to a novice chromatographer. A brief method for storing a living chromatogram based on an EMG function has been proposed³⁰. A chromatogram with n peaks can be stored in a computer by use of $2n+4$ parameters. Based on this principle, we have built a chromatogram base about 500 typical and reliable chromatograms chosen from the published literature. The base can be searched in

```
(define fact)
(set! fact '((fact1
  (if (sample is PTH_amino_acid)
    (then ((PTH_group)
      (molecular_weight<1000)
      (moderate_polar)
      (inactive-form)
      (slight_aqueous_solubility)
      (dispersion_force)
      (orientation_force))))
    ;
  (fact100
    (if (eluent is acetonitrile))
    (then ((methyl)
      (cyano)
      (dispersion_force)
      (orientation_force)
      (pi-pi_interaction)))
    ;
  ))
;
(define rule)
(set! rule '((rule-mode
  (if ((slight_aqueous_solubility)
    (moderate_polar)
    (dispersion_force)))
    (then (reversed_phase)))
  (rule-mobile-phase
    (if ((reversed-phase)
      (inactive-form)
      (dispersion)
      (orientation-force)))
    (then (acetonitrile)))
;
  ))
```

Fig. 5. Some examples of facts and rules in the ESC knowledge base.

accordance with compound, analyte class or author(s). So the system can generate a typical chromatogram for a sample analyzed to determine whether the symbolic reasoning over the knowledge base is correct.

The inference engine in the ESC is used to control and coordinate various components of the system. The forward chaining is used to select the mode of separation, mobile phase, stationary phase, method of sample pretreatment and detector.

Now three user entries in the ESC are designed to interface the computer with the user: (1) provision of the molecular structure of the sample; (2) provision of the commercial name of the sample; (3) provision of the analyte class to which the sample belongs. Once one of the entries is inputted, the program can obtain the molecular frame, functional groups and dominant molecular interaction through reasoning over the knowledge base. The column system, method of sample pretreatment and detector can be recommended.

Fig. 5 shows an example of some facts and heuristic rules in the knowledge base. All facts and rules are represented by IF/THEN statements. A rule asserts that the statement at the left-hand side implies the statements on the right-hand side. The inference engine is used to interpret those rules to generate new facts or to answer questions. For example, it can reason the new fact from the rule, fact100, in Fig. 5 that the eluent, acetonitrile, has the cyano, methyl and dominant dispersion force, orientation force and π - π interaction. Fig. 6 shows an example of the application of the ESC to method development in phenylthiohydantoin (PTH)-amino acid separation by HPLC. The user input and system recommendation are automatically processed and generated by the program. After items in Fig. 6 are printed, the system can also

```

User      Entries
Instrument      HPLC
Analytical sample      PTH_amino_acid
Sample from      Synthetic_mixture
Smallest amounts (ug)      5
Detector type      UV

Recommendation

Mode of separation:      HPLC

Analytical column
(Separation mode      Reversed_phase_chromatography)
(Column              Bonded_phase_C18)

Mobile phase
(Operating mode      isocratic)
(Eluent_a            acetonitrile)
(Eluent_b            0,01m_NaAC_aqueous_solution)
(Additive agent      0.5%_EtC12)

Pretreatment method

(Guard column, 5_cm_low_capacity_bonded_phase_C18)

Detectors

(Detector           UV/254)

```

Fig. 6. The dialogue between the computer and user and method development.

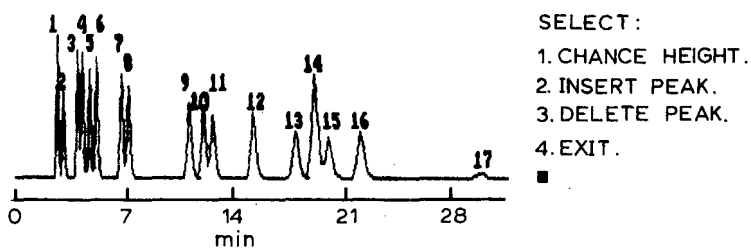


Fig. 7. The chromatogram generated by the chromatogram base of the ESC. Isocratic separation of PTH-amino acids after ref. 37. Column, 25 cm \times 4.6 mm I.D. Ultrasphere-ODS; mobile phase, 0.01 M sodium acetate (pH 4.9)-acetonitrile (62.2:37.8); flow-rate, 1.0 ml/min; temperature, 55°C; detection, UV at 254 nm. Peaks: PTH derivatives of: 1 = Asp; 2 = Glu; 3 = Asn; 4 = Gln; 5 = Thr; 6 = Gly; 7 = Ala; 8 = Tyr; 9 = Met; 10 = Val; 11 = Pro; 12 = Trp; 13 = Phe; 14 = Lys; 15 = Ile; 16 = Leu; 17 = Ser.

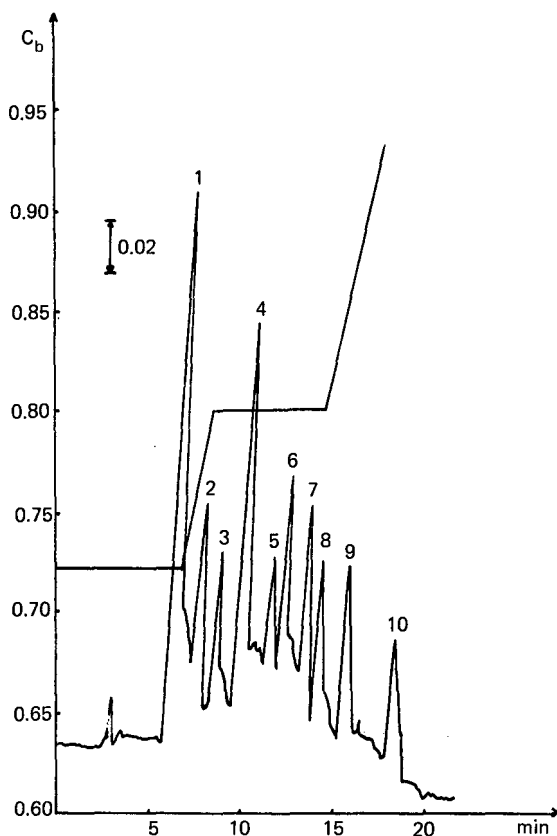


Fig. 8. Separation of ten bile acids with the selected optimum binary mobile phase composition of a multi-step linear programme. Column: 20 cm \times 4.6 mm I.D., 10 μ m YWG-C₁₈. Eluents: a, pH 5.6, 0.01 M KH₂PO₄, methanol-water (73:27); b, pH 5.6, 0.01 M KH₂PO₄, methanol-water (98:2). Flow-rate: 1 ml/min. Detector: UV, 210 nm. Solutes: 1 = tauroursodeoxycholic acid, 2 = glycooursodeoxycholic acid, 3 = taurocholic acid, 4 = glycocholic acid, 5 = taurochenodeoxycholic acid, 6 = glycochenodeoxycholic acid, 7 = glycodeoxycholic acid, 8 = taurodeoxycholic acid, 9 = tauroolithocholic acid, 10 = glycolithocholic acid.

generate a chromatogram corresponding to an analyte class or compounds. An example of PTH-amino acid separation is presented in Fig. 7 as generated by the ESC. It can be noted that not only are there operating conditions and compounds in Fig. 7, but we can also arbitrarily adjust the peak height and insert and delete peaks in the chromatogram. So we call it a living chromatogram. Comparing the results of the recommendations in Fig. 6 with those in Fig. 7, it is found that the method designed by the ECS is similar to the one from literature. So the knowledge base of the ESC and reasoning are reliable.

The optimization of separation conditions

After choosing the column system, the operating conditions should be optimized. Two strategies are often used in ESC. One is simultaneous experimental optimization. A variety of experimental designs has been adapted to mapping sample retention and to extracting the basic parameters of the column system, and then to predicting the optimum conditions by computation. Another strategy is sequential experimental optimization. The black box approach is used. It is characterized by the lack of knowledge of any chemical information on the sample analyzed, but the drawback of this method is that it can cause local optimization¹⁰.

On the basis of the above-mentioned theory of the ESC, we have proposed optimization of the isothermal operating conditions³¹ and of the multi-step temperature programme³² in GC. In the same way, the optimization of isocratic elution³³ and of a multi-step linear solvent programme²⁶ in HPLC have been reported. The optimization for samples with unknown constituents has just begun²⁵.

In order to demonstrate the validity of the theory and algorithm, a sample containing ten bile acids was separated by four different isocratic experiments at constant pH and potassium dihydrogenphosphate concentration initially, and then the coefficient A_i , B_i , C_i and a , b were calculated. Finally, the optimum binary mobile phase composition of the multi-step linear programme was obtained by the overlapping resolution mapping method. The chromatogram obtained from the optimum multi-step programme is presented in Fig. 8. The result shows that the separation is quite good and the optimum programme is successful.

The peak identification and quantitation

To demonstrate the validity of the software, some experiments have been carried out. The results obtained by a C-R1B integrator, where the area measurement is based on the perpendicular drop method, and by our software based on the above-mentioned principle are presented in Table I. When the eluent is methanol-water (80:20) as shown in Fig. 9A, the resolution of the peaks 11 and 12 is about 85%. The peak areas of the pair are 15.87 and 10.92% according to the C-R1B, and 17.92 and 9.20% according to our software. However, when the eluent is methanol-water (90:10) as shown in Fig. 9B, the peak resolution of pair 11, 12 becomes about 0.2; the peak areas are 9.09 and 16.73% from C-R1B, but 17.12 and 9.04% from our software. This means that the error of the peak area measurement by the normal line method increases greatly with decrease in resolution, but the precision of the curve fitting method is very good. In addition, a shoulder, 15 in Fig. 9B, can also be detected and be identified and quantitated by our software.

TABLE I

COMPARISON OF QUALITATIVE AND QUANTITATIVE RESULTS FROM THE SAME CHROMATOGRAMS BY USE OF DIFFERENT SOFTWARE

MK represents the mark of the peak: T = baseline separated, V = overlapping, B = back shoulder peak.

<i>Fig. 9A</i>					<i>Fig. 9B</i>				
Peak No.	t_R (min)	MK	ESC Area %	C-RIB Area %	Peak No.	t_R (min)	MK	ESC Area %	C-RIB Area %
1	1.07	T	0.21	0.16	1	1.01	T	0.02	*
2	1.30	V	0.49	0.38	2	1.23	V	0.27	0.07
3	1.89	T	0.05	*	3	1.91	T	0.05	0.06
4	2.12	V	0.05	0.07	4	2.15	V	0.55	0.05
5	4.24	T	5.68	5.55	5	3.03	T	5.50	5.51
6	5.49	T	6.49	6.43	6	3.42	V	6.57	6.44
7	6.94	T	1.81	1.62	7	3.80	V	1.85	1.35
8	7.53	V	3.57	3.81	8	3.98	V	3.55	3.65
9	9.52	T	6.49	5.80	9	4.32	V	6.44	6.09
10	10.27	V	0.82	1.70	10	4.68	V	1.06	2.28
11	13.70	T	17.92	15.87	11	5.44	V	17.23	9.10
12	14.99	V	9.20	10.92	12	5.68	V	9.15	16.73
13	19.86	T	7.14	7.27	13	6.82	V	7.04	5.84
14	27.14	T	0.38	0.34	14	7.48	V	40.94	42.83
15	29.09	T	39.62	40.07	15	7.97	B	0.90	*
					16	11.60	T	0.03	*
Total			100.00	99.99				100.00	100.00

* Not detected.

The diagnosis of hardware

So-called intelligent instruments imply that the system must possess self-diagnosis. However, almost all chromatographs do not possess self-diagnosis at the heart of the system, the column. Though the evaluation of column efficiency has been reported³⁴, there are few methods to diagnose the chromatograph.

In the expert system for chromatography under development, the diagnosis of hardware is necessary, especially for the column in HPLC. It was demonstrated that the column, especially a small-bore column in HPLC, can exhibit high efficiency only if the column system is suitable³⁵. In addition, the extra-column dead volume of the column system has a contribution to the retention time³⁶. We have proposed a general strategy for diagnosing hardware. First, to ensure that the column system is suitable for chromatographic peak identification and quantitation, a standard column with a set of parameters, such as efficiency, asymmetry, retention time, selectivity etc., must be connected to the instrument system and be operated once. The results from this experiment can be compared to the set of parameters obtained from the standard column system. If great deviation is found, the column system must be improved, otherwise the system is adopted. On the other hand, monitoring changes in the chromatographic parameters, such as efficiency, asymmetry, retention time, selectivity and operating pressure on-line, allows the verification of column performance.

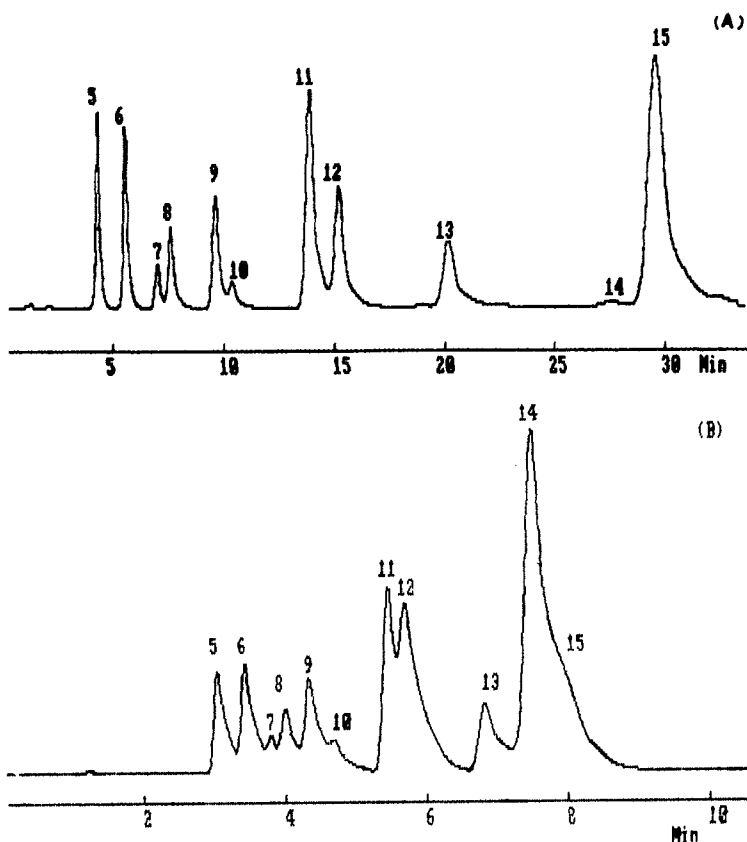


Fig. 9. The chromatograms which are handled by different software. Analysis: mixture of aromatic hydrocarbons. Column, 15 cm \times 4.6 mm I.D. 10- μ m Nucleosil C₁₈; flow-rate, 1.0 ml/min; detection, UV at 254 nm; mobile phase, (A) methanol-water (80:20), (B) methanol-water (90:10). Peaks: 5 = benzene, 6 = toluene, 7 = naphthalene, 8 = *p*-xylene, 9 = biphenyl, 10 = 1,3,5-trimethylbenzene, 11 = phenanthrene, 12 = anthelene, 13 = fluoranthene, 14 + 15 = *m*-diphenylbenzene + impurity (the large peak is diphenylbenzene).

TABLE II

COMPARISON OF RESULTS FROM A STANDARD SYSTEM WITH THOSE FROM A WATERS SYSTEM

n_1 and $(\tau/\sigma)_1$ are the plate number and the ratio (τ/σ) when $k' = 1$. n_∞ and $(\tau/\sigma)_\infty$ are the plate number and the area ratio (τ/σ) when k' approaches infinity; $(b/a)_{0.1}$ is the asymmetry at 1/10 peak height.

		k'	w_h	$(b/a)_{0.1}$	n	
Standard system	Benzene	0.60	10.69	1.47	7280	n_1 7760
	Naphthalene	1.32	14.78	1.20	8010	n_∞ 8210, 1.07
	Biphenyl	1.85	18.08	1.11	8080	$(\tau/\sigma)_1$ 1.00
	Phenanthrene	2.92	25.19	1.05	7950	$(\tau/\sigma)_\infty$ 0.21
Waters system	Benzene	0.58	10.71	1.56	7030	n_1 7180
	Naphthalene	1.30	15.04	1.30	7490	n_∞ 8420, 1.16
	Biphenyl	1.87	18.21	1.25	7730	$(\tau/\sigma)_1$ 1.17
	Phenanthrene	2.87	24.90	1.15	7800	$(\tau/\sigma)_\infty$ 0.20

Troubleshooting faults in a chromatograph is an high-level task requiring professional knowledge. The results of diagnosis can be passed to the inference engine for decision making in the ESC. For example, a standard column with a set of parameters is connected to an instrument system for evaluation. If a considerable decrease in column efficiency compared with standard parameters is found, our experience shows that it results from three causes, *i.e.*, (1) the dead volume of the pre-column is larger than the standard system, (2) the dead volume of the post-column is larger, (3) the dead volume of both the pre- and post-columns is larger. There are three rules in the ESC to judge what causes the decrease in column efficiency:

A considerable decrease in column efficiency with smaller k' and a constant column efficiency with larger k' is caused by factor (1)

An almost constant column efficiency with smaller k' and a considerable decrease in column efficiency with larger k' is caused by factor (2)

A decrease in column efficiency with various k' is caused by factor (3)

The Waters system has been evaluated by the diagnosis software. The results are presented in Table II. It is noted that the column efficiency and asymmetry were worse than with the standard system. The program indicates that the cause may be factor (3) and it is recommended that a user check the injection system, connecting tube and detector.

CONCLUSION

We have presented a system strategy for developing an expert system of chromatography. The knowledge base and chromatogram base, optimization of operating conditions, peak identification and quantitation on-line and the diagnosis of the hardware system have been discussed. To enlarge the range of application, the knowledge base and chromatogram base should be further expanded. The ESC is still under development.

REFERENCES

- 1 DuPont's Sentinel, *Am. Lab.*, 6 (1982) 15.
- 2 J. P. Bonnine and G. Guiochon, *Analisis*, 12 (1984) 175.
- 3 J. C. Berridge and E. G. Morrissey, *J. Chromatogr.*, 316 (1984) 69.
- 4 J. W. A. Klaessens, G. Kateman and B. G. M. Vandeginste, *Trends Anal. Chem.*, 4 (1985) 114.
- 5 M. G. Cirillo, *J. Liq. Chromatogr.*, 9 (1986) 3185.
- 6 J. N. Little, *J. Liq. Chromatogr.*, 9 (1986) 3197.
- 7 Cs. Horváth (Editor), *High Performance Liquid Chromatography, Advances and Perspective*, Vols. 1-3, Academic Press, New York, 1980-1983.
- 8 C. M. White and R. K. Houck, *J. High Resolut. Chromatogr. Chromatogr. Commun.*, 9 (1986) 4.
- 9 M. A. Quarry, M. A. Stadalius, T. H. Mourey and L. R. Snyder, *J. Chromatogr.*, 358 (1986) 17.
- 10 C. E. Goewie, *J. Liq. Chromatogr.*, 9 (1986) 1431.
- 11 J. L. Glajch, J. J. Kirkland, K. M. Squire and J. M. Minor, *J. Chromatogr.*, 199 (1980) 57.
- 12 J. L. Glajch, J. J. Kirkland and L. R. Snyder, *J. Chromatogr.*, 238 (1982) 269.
- 13 J. J. Kirkland and J. L. Glajch, *J. Chromatogr.*, 255 (1983) 27.
- 14 P. J. Schoenmakers, A. C. J. H. Drouen and L. de Galan, *Chromatographia*, 15 (1983) 688.
- 15 H. A. H. Billiet, A. C. J. H. Drouen and L. de Galan, *J. Chromatogr.*, 316 (1984) 231.
- 16 L. R. Snyder and J. W. Dolan, *Am. Lab.*, 8 (1986) 37.
- 17 J. W. Dolan, R. L. Snyder and M. A. Quarry, *Chromatographia*, 24 (1987) 261.
- 18 R. E. Dessy, *Anal. Chem.*, 56 (1984) 1200A, 1312A.
- 19 R. Bach in J. H. Pierce and R. A. Hohne (Editors), *Artificial Intelligence Application in Chemistry*, Maple Press, York, PA, 1986, p. 279.

- 20 "Expert System in HPLC", *Anal. Chem.*, 58 (1986) 1192A.
- 21 P. Lu and H. Li, *Chin. J. Sci. Instrum.*, 4 (1983) 237.
- 22 P. Lu, *Proceedings of the 4th Chinese National Conference on Chromatography, Shanghai, 1985*, P1.
- 23 P. Lu and X. Lu, in Y. Dong (Editor), *Advance in Science of China*, Science Press, Beijing, 1985.
- 24 P. Lu and X. Lu, *J. Chromatogr.*, 292 (1984) 169.
- 25 H. Huang, Y. Zhang and P. Lu, *Proceedings of 2nd Beijing Conference and Exhibition on Instrumental Analysis (BCEIA), Beijing, 1987*, p. 937.
- 26 M. Zou, Y. Zhang and P. Lu, *Proceedings of 2nd Beijing Conference and Exhibition on Instrumental Analysis (BCEIA), Beijing, 1987*, p. 871.
- 27 J. P. Foley and J. G. Dorsey, *Anal. Chem.*, 55 (1983) 730.
- 28 Y. Zhang, L. Dong, M. Bao, G. Zhou and P. Lu, *Fenxichesin Tonbao*, 3 (1984) 16.
- 29 H. Li, B. Li, C. Luo and P. Lu, *Kexue Tongbao*, 5 (1986) 449.
- 30 B. Lin, H. Li and P. Lu, *LC · GC, Mag. Liq. Gas Chromatogr.*, 4 (1987) 1206.
- 31 B. Lin, H. Li, C. Luo and P. Lu, *Chin. J. Chromatogr.*, 4 (1986) 193.
- 32 P. Lu, B. Lin, X. Chu, C. Luo, G. Lai and H. Li, *J. High Resolut. Chromatogr. Chromatogr. Commun.*, 9 (1986) 702.
- 33 P. Lu, R. Liu and L. Dou, *LC · GC, Mag. Liq. Gas Chromatogr.*, 4 (1986) 354.
- 34 J. D. Stuart and J. S. Stokis, *Pittsburgh Conference and Exposition on Analytical Chemistry and Applied Spectroscopy*, Atlantic City, NJ, 1985, Abstr. No. 785.
- 35 H. Chen, H. Bao, S. Fang and P. Lu, *Chromatographia*, 13 (1981) 12.
- 36 H. Zou, Y. Zhang and P. Lu, *Chin. J. Chromatogr.*, 6 (1986) 334.
- 37 C. M. Noyes, *J. Chromatogr.*, 266 (1983) 451.

CHROM. 20 792

CONSIDERATIONS FOR USING THE SOLVENT SELECTIVITY TRIANGLE APPROACH FOR STATIONARY PHASE CHARACTERIZATION

BRIAN R. KERSTEN and COLIN F. POOLE*

Department of Chemistry, Wayne State University, Detroit, MI 48202 (U.S.A.)

SUMMARY

The use of solvent selectivity parameters (X_e , X_n , X_d) for stationary phase characterization is compromised by a failure to allow for interfacial adsorption of test solutes and *n*-alkane retention index markers in the recommended calculation method and by inadequate retention of the test solutes ethanol, nitromethane, and dioxane on phases of low polarity. There is also a lack of constancy in the relative position of phases in the selectivity triangle as the identity of the test solutes is changed. The low partitioning of *n*-alkanes on polar phases such as DEGS, OV-275, TCEP, EAN and PAN precludes calculation of solvent selectivity parameters using retention index differences. The partial molar Gibbs free energy of solution for the test solutes derived from the gas-liquid partition coefficients corrected for interfacial adsorption allows the universal calculation of solvent selectivity parameters for all phases. The position of individual phases in selectivity groups is similar for selectivity parameters calculated using either corrected retention indices or Gibbs free energy differences except that all phases are displaced to the right in the triangle constructed using free energy differences resulting from weak interactions for the tested phases with the proton acceptor probe dioxane. There is good agreement between the solvent strength calculated from the energy differences, the partial molar Gibbs free energy of solution for a methylene group, and Snyder's P' values for non-polar and moderately polar phases. Polar phases show anomalous behaviour on the different scales. Recommendations for further improvements in the solvent selectivity parameter approach to stationary phase characterization are made.

INTRODUCTION

Snyder¹ introduced the solvent strength parameter (P') and solvent selectivity parameters (X_e , X_n , X_d) to characterize the fundamental properties of solvents used in gas and liquid chromatography. The test solutes ethanol, dioxane and nitromethane were selected as probes to express the contribution made by proton donor-acceptor complexation and orientation interactions to the solvent strength. By plotting the data with triangular coordinates solvents of similar selectivity are easily identified and preferred solvents for stationary phase selectivity optimization identified. In this context Klee *et al.*² classified several commonly used gas chromatographic stationary

phases and commented on the current lack of phases close to the apices of the selectivity triangle which would provide the most varied properties for selectivity optimization. Shah *et al.*³ noted that the position of a solvent within the selectivity triangle varied with the selection of the test solutes including the use of homologues of the original test solutes used by Snyder. Betts⁴ suggested that 2-octyne, *n*-butanol, and pyridine were more appropriate probes than those suggested by Snyder for estimating polar interactions. All of these studies can be seen to be related to earlier work by Brown⁵ who used the retention volumes of various test probes on different stationary phases plotted as triangular coordinates to indicate selective stationary phase interactions. For a review of the use of the solvent selectivity triangle approach to stationary phase characterization see ref. 6.

It is noteworthy that in all the above studies it is assumed that the retention of the test probes and the *n*-alkanes used to calculate retention index differences are controlled by gas-liquid partitioning for all phases. Previously⁷⁻⁹ we have shown that failure to appreciate the importance of interfacial adsorption as a retention mechanism can lead to poor stationary phase classification using the McReynolds stationary phase classification scheme. In this report the role of interfacial adsorption in the misclassification of selectivity parameters is assessed for 15 stationary phases spanning a wide range of solvent strength and an improved calculation procedure based on the partial molar Gibbs free energy of solution for the Snyder probes is recommended to eliminate errors arising from the use of the retention index scheme for stationary phase classification.

EXPERIMENTAL

The silicone polymers OV-105 (cyanopropylmethyltrimethylsilicone), OV-17 (phenylmethylsilicone), OV-330 (dimethylsilicone/Carbowax copolymer), OV-225 (cyanopropylmethylphenylmethylsilicone), and OV-275 (dicyanoallylsilicone) were obtained from Ohio Valley Specialty Chemicals (Marietta, OH, U.S.A.). Squalane, QF-1 (trifluoropropylmethylsilicone), Carbowax 20M [poly(ethylene glycol)], DEGS [poly(diethylene glycol succinate)], TCEP [1,2,3-tris(2-cyanoethoxy)propane], Chromosorb W-AW (60-80 mesh), and column conditioner (a mixture of silanizing reagents No. A7682) were obtained from Anspec (Ann Arbor, MI, U.S.A.). Ethylammonium nitrate (EAN), *n*-propylammonium nitrate (PAN), *n*-butylammonium thiocyanate (BAT), *sec*-butylammonium thiocyanate (sBAT), and di-*n*-propylammonium thiocyanate (DPAT) were prepared as described previously^{10,11}. Other standards and reagents were general laboratory grade in the highest purity available.

Column packings containing from 5 to 20% (w/w) of liquid phase on Chromosorb W-AW were prepared using the rotary evaporator technique. The damp packings were dried in a fluidized-bed drier, sieved, and packed into glass columns (3.0 m × 2.0 mm I.D.) with the aid of vacuum suction and gentle vibration. The packings prepared with squalane, OV-105, OV-17, QF-1 and OV-225 were thoroughly silanized *in situ* by repeated injection of 50 μ l of column conditioner at 100°C followed by conditioning at the same temperature until invariant retention times and symmetrical peak shapes for the test solutes were obtained. Accurate phase loadings were determined by evaporation for squalane and the liquid organic salts^{7,12} and by Soxhlet extraction for the higher-molecular-weight polymeric phases¹³.

For column evaluation a Varian 3700 gas chromatograph with a heated on-column injector and flame-ionization detector was used. The nitrogen carrier gas flow-rate was accurately measured with a thermostatted soap-film bubble meter and set to approximately 20 ml/min. All measurements were made isothermally at $80.8 \pm 0.2^\circ\text{C}$. Samples were injected as headspace vapors with a gas-tight syringe to approximate the conditions for infinite dilution. Sample sizes were varied to insure that all data were measured in the Henry's law region and retention times independent of sample size were obtained. All peaks were symmetrical.

The net retention volume per gram of packing corrected to zero column pressure drop for the test solutes and *n*-alkanes were calculated according to eqn. 1.

$$\ln V_N^* = \ln \left[\frac{3}{2} (t_R - t_M) \frac{F_0(T_c)}{W(T_a)} \left(1 - \frac{P_w}{P_a} \right) \left(\frac{P^2 - 1}{P^3 - 1} \right) \right] - \frac{3\beta}{4} P_a \left(\frac{P^4 - 1}{P^3 - 1} \right) \quad (1)$$

- where V_N^* = net retention volume per gram of packing corrected to zero column pressure drop
 t_R = solute retention time
 t_M = column dead time (assumed equal to the retention time of methane at T_c)
 F_0 = carrier gas flow-rate at the column outlet
 W = weight of column packing
 T_c = column temperature (K)
 T_a = ambient temperature (K)
 P_w = saturated water vapor pressure at T_a
 P_a = ambient pressure (mmHg)
 P = column pressure drop (P_i/P_a)
 P_i = column inlet pressure (mmHg)
 β = $(2B_{12} - V_1^0)/RT_c$
 B_{12} = second interaction virial coefficient (solute-carrier gas)
 V_1^0 = solute molar volume
 R = universal gas constant

A mercury manometer was used to determine the column pressure drop (± 1 mmHg). The second interaction virial coefficients were taken from the compilations of Dymond and Smith¹⁴ and Driesbach¹⁵, or if unavailable calculated by the method of corresponding states¹⁶.

Gas-liquid partition coefficients were estimated by linear extrapolation of plots of V_N^*/V_L vs. $1/V_L$ based on eqn. 2^{7,17,18}

$$\frac{V_N^*}{V_L} = K_L + B \cdot \frac{1}{V_L} \quad (2)$$

- where V_L = volume of liquid phase per gram of packing
 K_L = gas-liquid partition coefficient
 B = coefficient accounting for interfacial adsorption

Values for the adjusted retention time and gas-liquid partition coefficients for

TABLE I
RETENTION DATA FOR TEST SOLUTES

Stationary phase	Adjusted retention time (min)*			Gas-liquid partition coefficient \pm standard deviation		
	Ethanol	Nitromethane	Dioxane	Ethanol	Nitromethane	Dioxane
Squalane	0.17	0.33	1.72	7.2 \pm 0.2	15.9 \pm 0.7	81.4 \pm 0.7
OV-17	0.15	0.65	1.48	13.5 \pm 0.7	57.5 \pm 1.6	129.2 \pm 3.2
OV-105	0.32	0.56	1.29	18.4 \pm 2.7	34.9 \pm 0.9	84.7 \pm 2.3
OV-330	0.52	1.87	1.90	43.9 \pm 2.1	160.0 \pm 6.4	161.0 \pm 5.7
OV-225	0.46	2.03	2.13	32.8 \pm 1.3	143.3 \pm 8.7	148.1 \pm 9.6
QF-1	0.13	0.84	0.95	14.5 \pm 1.1	91.0 \pm 2.4	101.6 \pm 1.7
Carbowax 20M	1.24	5.41	3.14	76.1 \pm 0.6	341.7 \pm 2.7	199.6 \pm 0.7
DPAT	2.31	3.05	3.07	174.0 \pm 5.3	242.0 \pm 3.3	229.8 \pm 6.0
DEGS	0.69	2.25	1.95	84.4 \pm 2.0	273.3 \pm 6.1	236.1 \pm 4.5
BAT	2.75	2.08	4.73	237.5 \pm 5.5	178.2 \pm 3.0	406.3 \pm 9.6
sBAT	3.97	2.76	6.80	293.5 \pm 7.3	205.9 \pm 6.5	505.2 \pm 11.7
TCEP	0.74	3.95	2.60	72.2 \pm 0.9	375.4 \pm 5.7	245.9 \pm 3.3
OV-275	0.46	2.25	1.26	41.1 \pm 2.6	232.4 \pm 6.8	126.4 \pm 4.7
PAN	3.79	3.81	4.39	167.7 \pm 1.5	168.4 \pm 0.9	196.4 \pm 1.7
EAN	4.52	5.10	5.20	177.2 \pm 1.0	203.3 \pm 1.3	207.5 \pm 2.5

* 3.0 m \times 2 mm I.D. column with 12-15% (w/w) of phase on Chromosorb W-AW (60-80 mesh).

ethanol, nitromethane, and dioxane on all phases are given in Table I. The partition coefficients for the *n*-alkane and 2-alkanone retention index markers were fitted to eqn. 3. The coefficients obtained by linear regression are summarized in Table II.

TABLE II
COEFFICIENTS FOR CALCULATING PARTITION COEFFICIENTS FOR *n*-ALKANES AND 2-ALKANONES (EQN. 3)

Stationary phase	<i>n</i> -Alkanes			2-Alkanones		
	A	D	Correlation coefficient (r^2)	A	D	Correlation coefficient (r^2)
Squalane	0.361	-0.3746	1.000	0.358	0.7673	1.000
OV-17	0.325	-0.5596	0.999	0.317	1.0517	0.999
OV-105	0.314	-0.3339	1.000	0.311	0.9841	0.999
OV-330	0.302	-0.6023	1.000	0.298	1.1844	0.999
OV-225	0.293	-0.6556	1.000	0.284	1.2894	0.999
QF-1	0.262	-0.3152	1.000	0.270	1.3499	0.999
Carbowax 20M	0.264	-0.5754	0.999	0.265	1.2939	0.999
DPAT	0.228	-0.6058	1.000	0.239	1.5658	0.999
DEGS	—	—	—	0.218	1.3653	0.999
BAT	0.223	-0.8211	0.999	0.215	1.6994	0.997
sBAT	0.188	-0.5733	0.998	0.204	1.8350	0.998
TCEP	—	—	—	0.199	1.5552	0.999
OV-275	—	—	—	0.180	1.3233	0.998
PAN	—	—	—	0.166	1.4033	0.997
EAN	—	—	—	0.088	1.5565	0.991

$$\log K_L = A(n) + D \quad (3)$$

where A and D = experimentally derived constants

n = number of carbon atoms for the n -alkanes or the number of carbon atoms minus 2 for the 2-alkanones.

The retention index for each test solute was determined from the adjusted retention time using the standard procedure¹⁹. Retention index values corrected for interfacial adsorption were calculated using eqn. 4⁷

$$I_{PH}^C(P) = 100z + 100 \left[\frac{\log K_L^P - \log K_L^z}{\log K_L^{z+1} - \log K_L^z} \right] \quad (4)$$

where $I_{PH}^C(P)$ = retention index for probe P corrected for interfacial adsorption on phase PH

K_L^P = gas-liquid partition coefficient for probe P

K_L^z = gas-liquid partition coefficient for a n -alkane with z carbon atoms eluting immediately before probe P

K_L^{z+1} = gas-liquid partition coefficient for an n -alkane with $z+1$ carbon atoms eluting after probe P.

Retention index values of ethanol, nitromethane and dioxane on all phases are summarized in Table III.

The solvent polarity parameter (P') and solvent selectivity parameters (X_e , X_n and X_d) were calculated according to the method of Snyder¹. The solvent polarity parameter is obtained from eqn. 5

TABLE III
RETENTION INDEX VALUES FOR THE TEST SOLUTES

Stationary phase	Retention index values					
	Uncorrected			Corrected		
	Ethanol	Nitromethane	Dioxane	Ethanol	Nitromethane	Dioxane
Squalane	369	449	643	353	451	643
OV-17	519	715	824	492	714	825
OV-105	533	608	722	555	668	772
OV-330	749	933	935	755	940	940
OV-225	740	963	970	736	968	976
QF-1	564	874	895	556	878	896
Carbowax 20M	919	1150	1065	934	1178	1093
DPAT	1225	1276	1277	1255	1312	1308
DEGS	1107	1292	1270			
BAT	1395	1342	1501	1426	1374	1538
sBAT	1498	1428	1599	1635	1554	1767
TCEP	1182	1477	1406			
OV-275	1131	1385	1294			
PAN	1437	1438	1460			
EAN	1612	1640	1645			

$$P' = 1.2 + \Sigma \Delta I_i^c \cdot \frac{A}{100} \quad (5)$$

where P' = solvent polarity parameter
 $\Sigma \Delta I_i^c$ = $\Delta I_e^c + \Delta I_n^c + \Delta I_d^c$
 ΔI_i^c = $I_{PH}^c(i) - I_{SQ}^c(i)$
 $I_{PH}^c(i)$ = corrected retention index for probe i on phase PH
 $I_{SQ}^c(i)$ = corrected retention index for probe i on squalane
 A = slope of the plot of $\log K_L$ vs. carbon number for the n -alkanes (Table II)

The subscripts e, n and d refer to ethanol, nitromethane and dioxane, respectively. The solvent selectivity parameters (X_e, X_n, X_d) are defined in turn by eqn. 6. Values for the solvent polarity parameter and solvent selectivity parameters are summarized in Table IV.

$$X_i = \frac{\Delta I_i^c}{\Sigma \Delta I_i^c} = \frac{\Delta I_i^c}{\Delta I_e^c + \Delta I_n^c + \Delta I_d^c} \quad (6)$$

The partial molar Gibbs free energy of solution for a methylene group was calculated using eqn. 7 and the coefficients summarized in Table II²⁰

$$\Delta G_k^0(\text{CH}_2) = -2.3 RT_c A \quad (7)$$

TABLE IV
SOLVENT POLARITY AND SOLVENT SELECTIVITY PARAMETERS

Stationary phase	Gibbs free energy per methylene group (cal/mol)		Solvent polarity parameter (P')*	Solvent selectivity parameters		
	<i>n</i> -Alkanes	2-Alkanones		X_e	X_n	X_d
Squalane	-585	-579	1.20			
OV-17	-525	-513	3.10	0.24	0.45	0.31
OV-105	-508	-503	2.76	0.40	0.44	0.16
OV-330	-488	-482	4.79	0.34	0.41	0.25
OV-225	-469	-459	4.78	0.31	0.42	0.27
QF-1	-424	-437	3.51	0.24	0.48	0.28
Carbowax 20M	-427	-428	5.84	0.33	0.41	0.26
DPAT	-369	-386	6.74	0.37	0.35	0.27
DEGS		-352	(7.28)			
BAT	-361	-347	7.65	0.37	0.32	0.31
TCEP		-322	(8.03)			
sBAT	-304	-330	7.80	0.37	0.31	0.32
OV-275		-291	(8.81)			
PAN		-268	(9.41)			
EAN		-142	(12.58)			

* Values in parentheses were estimated from eqn. 13.

TABLE V

PARTIAL MOLAR AND MOLAL GIBBS FREE ENERGY OF SOLUTION FOR THE TEST SOLUTES

Stationary phase	Partial molar Gibbs free energy (kcal/mol)			Partial molal Gibbs free energy (kcal/mol)		
	Ethanol	Nitromethane	Dioxane	Ethanol	Nitromethane	Dioxane
Squalane	-1.3919	-1.9517	-3.1037	-1.8204	-2.3801	-3.5321
OV-17	-1.8284	-2.8493	-3.4280	-2.0391	-3.0599	-3.6386
OV-105	-2.0481	-2.5033	-3.1314	-2.3486	-2.8037	-3.4319
OV-330	-2.6588	-3.5669	-3.5823	-2.8582	-3.7663	-3.7817
OV-225	-2.4536	-3.4910	-3.5238	-2.6676	-3.7051	-3.7379
QF-I	-1.8812	-3.1719	-3.2651	-1.9945	-3.2852	-3.3783
Carbowax 20M	-3.0463	-4.1020	-3.7344	-3.2450	-4.3007	-3.9331
DPAT	-3.6273	-3.8593	-3.8324	-3.9227	-4.1547	-4.1278
DEGS	-3.1186	-3.9448	-3.8508	-3.2263	-4.0526	-3.9585
BAT	-3.8463	-3.6441	-4.2327	-4.1536	-3.9514	-4.5400
sBAT	-3.9952	-3.7456	-4.3863	-4.2563	-4.0068	-4.6475
TCEP	-3.0087	-4.1681	-3.8788	-3.2117	-4.3711	-4.0818
OV-275	-2.6126	-3.8310	-3.4114	-2.7781	-3.9994	-3.5798
PAN	-3.6014	-3.6043	-3.7124	-3.8116	-3.8145	-3.9226
EAN	-3.6401	-3.7368	-3.7514	-3.8160	-3.9127	-3.9273

where $\Delta G_K^0(\text{CH}_2)$ = partial molar Gibbs free energy of solution for a methylene group

R = universal gas constant (1.987 cal/mole)

A = coefficient from Table II.

The partial molar Gibbs free energy of solution for the test probes was calculated using eqn. 8²¹. The data are summarized in Table V.

TABLE VI

PARTIAL MOLAR AND MOLAL GIBBS FREE ENERGY OF SOLUTION DIFFERENCE VALUES

Stationary phase	$\delta(\Delta G_K^0)_{SQ}^{PH}$			$\delta(\Delta G_M^0)_{SQ}^{PH}$		
	Ethanol	Nitromethane	Dioxane	Ethanol	Nitromethane	Dioxane
Squalane	0	0	0	0	0	0
OV-17	-0.437	-0.898	-0.324	-0.219	-0.680	-0.107
OV-105	-0.656	-0.552	-0.028	-0.528	-0.424	-0.100
OV-330	-1.267	-1.615	-0.479	-1.038	-1.386	-0.250
OV-225	-1.062	-1.539	-0.420	-0.847	-1.325	-0.206
QF-I	-0.489	-1.220	-0.161	-0.174	-0.905	-0.154
Carbowax 20M	-1.654	-2.150	-0.617	-1.425	-1.921	-0.401
DPAT	-2.235	-1.908	-0.729	-2.102	-1.775	-0.596
DEGS	-1.727	-1.993	-0.747	-1.406	-1.673	-0.426
BAT	-2.454	-1.692	-1.129	-2.333	-1.571	-1.008
sBAT	-2.603	-1.794	-1.283	-2.436	-1.627	-1.115
TCEP	-1.617	-2.216	-0.775	-1.391	-1.991	-0.550
OV-275	-1.221	-1.879	-0.308	-0.961	-1.619	-0.048
PAN	-2.210	-1.653	-0.609	-1.991	-1.434	-0.391
EAN	-2.248	-1.785	-0.648	-1.996	-1.533	-0.395

TABLE VII

SOLVENT SELECTIVITY PARAMETERS CALCULATED FROM DIFFERENCES IN PARTIAL MOLAR GIBBS FREE ENERGIES OF SOLUTION

Stationary phase	$\Sigma\delta(\Delta G)_{SQ}^{PHi}$	X_e	X_n	X_d
OV-17	-1.659	0.26	0.54	0.20
OV-105	-1.236	0.53	0.45	0.02
OV-330	-3.361	0.38	0.47	0.15
OV-225	-3.021	0.34	0.50	0.16
QF-1	-1.870	0.26	0.64	0.10
Carbowax 20M	-4.421	0.37	0.49	0.14
DPAT	-4.872	0.46	0.39	0.15
DEGS	-4.467	0.39	0.44	0.17
BAT	-5.275	0.47	0.32	0.21
sBAT	-5.680	0.46	0.32	0.23
TCEP	-4.608	0.35	0.48	0.17
OV-275	-3.408	0.36	0.55	0.09
PAN	-4.472	0.50	0.37	0.13
EAN	-4.681	0.48	0.38	0.14

$$\Delta G_K^0(P) = -2.303RT_c \log K_L^P \quad (8)$$

where $\Delta G_K^0(P)$ = partial molar Gibbs free energy of solution for solute P.

To assess the importance of molecular weight differences on the solvent selectivity parameters the molal Gibbs free energy of solution was used in some calculations (eqn. 9²¹). The data are summarized in Table V.

$$\Delta G_M^0(P) = -2.303RT_c \log\left(\frac{10^3 K_L^P}{RT_c \rho_c}\right) \quad (9)$$

where $\Delta G_M^0(P)$ = partial molal Gibbs free energy of solution
 ρ_c = liquid density at T_c .

The stationary phase densities and gas-liquid partition coefficients for butanol and nitropropane were taken from ref. 8. Solvent selectivity parameters were redefined in thermodynamic terms using eqns. 10 and 11. The letters e, n and d refer to ethanol, nitromethane and dioxane, respectively. The $\delta(G_K^0)_{SQ}^{PHi}$ and $\delta(G_M^0)_{SQ}^{PHi}$ values are summarized in Table VI and the solvent selectivity parameters in Table VII.

$$\delta(G_K^0)_{SQ}^{PHi} = (\Delta G_K^0)^{PH} - (\Delta G_K^0)^{SQ} \quad (10)$$

where $(\Delta G_K^0)^{PH}$ = partial molar Gibbs free energy of solution of probe i
on phase PH

$(\Delta G_K^0)^{SQ}$ = partial molar Gibbs free energy of solution of probe i
on squalane

$$x_i = \frac{\delta(\Delta G_K^0)_{SQ}^{PHi}}{\Sigma\delta(\Delta G_K^0)_{SQ}^{PHi}} \quad (11)$$

where $\Sigma\delta(\Delta G_K^0)_{SQ}^{PHi} = \delta(\Delta G_K^0)_{SQ}^{PHe} + \delta(\Delta G_K^0)_{SQ}^{PHn} + \delta(\Delta G_K^0)_{SQ}^{PHd}$.

RESULTS AND DISCUSSION

The calculation of solvent strength and solvent selectivity parameters according to Snyder for gas chromatographic solvents is based on the differences in retention index values for the test solutes ethanol, nitromethane and dioxane on two phases, one of which is the non-polar reference phase squalane. The retention value of the test solute on squalane is used as an approximate measure of dispersive interactions. Inductive interactions are ignored. This may be reasonable for test solutes with small dipole moments or at high temperatures where all orientations of the dipoles become equally probable. For nitromethane it could be reasonably argued that inductive interactions with squalane may be significant. Meyer *et al.*²² indicated that inductive interactions between dipolar solutes and *n*-tetracosane are on the order of 1 kcal/mol. However, the calculation method used by these authors to estimate the dispersive contribution to the total interaction energy is not well founded and may lead to an overestimation of the inductive energy contribution. Appropriate models are not available for the unequivocal determination of inductive energies. We draw the readers attention to this general problem in solution interactions but are unable to propose a solution at this time. The influence of an imperfect correction term on the use of the solvent selectivity triangle is unlikely to be great. The value of the test solutes on squalane acts as a scaling term which affects the absolute but not the relative accuracy of the solvent selectivity parameters. In other cases the inductive effect is combined with the orientation interaction and is hopefully weak for ethanol and dioxane whose retention is principally influenced by hydrogen bonding interactions.

In developing the theoretical model for the solvent selectivity triangle approach to stationary phase characterization it is assumed that the test solutes and *n*-alkanes used to establish the fixed points on the retention index scale are retained solely by gas-liquid partitioning. Adsorption of either the test solutes or *n*-alkanes at the support or liquid phase interfaces will lead to incorrect values for the retention index. The concurrent retention of solutes of strikingly different polarity to the liquid phase used for their separation by a mixed retention mechanism is a well established phenomenon (see, for example, refs. 7-9, 17 and 18), but one that has generally been ignored in methods used to characterize the solvent properties of liquid phases. Initial studies were directed towards establishing the contribution of interfacial adsorption to the solvent selectivity parameters for fifteen liquid phases spanning a wide polarity range.

Influence of interfacial adsorption on solvent selectivity parameters

The model used to estimate the contribution of interfacial adsorption to retention is based on the constancy of the observed partition coefficient at high phase loadings when the coefficient *B* in eqn. 2 can be considered zero. When *B* has a finite value the observed partition coefficient is no longer constant and varies with phase loading causing a slope or curvature in the observed data. Extrapolation to infinite liquid volume enables a value for the gas-liquid partition coefficient to be determined that is independent of the contribution from interfacial adsorption. For the liquid phases studied here three different categories of general behavior can be discerned. For those phases of low and moderate solvent strength (for example, squalane, OV-17, OV-105, OV-330, OV-225, QF-1 and Carbowax 20M), reasonable agreement with

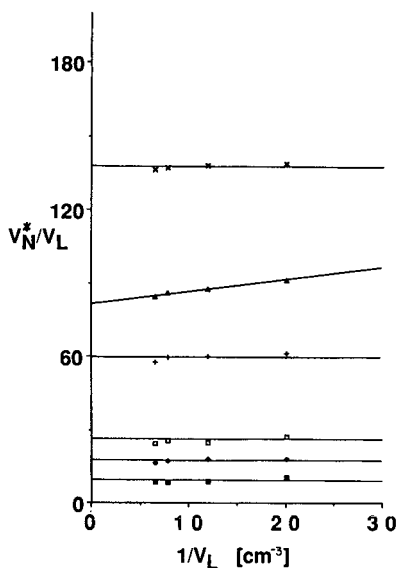


Fig. 1. Plot of V_N^*/V_L vs. $1/V_L$ for *n*-alkanes, ethanol, nitromethane and dioxane on squalane. Solutes: ■ = ethanol; ▲ = dioxane; ◆ = nitromethane; □ = pentane; + = hexane; × = heptane.

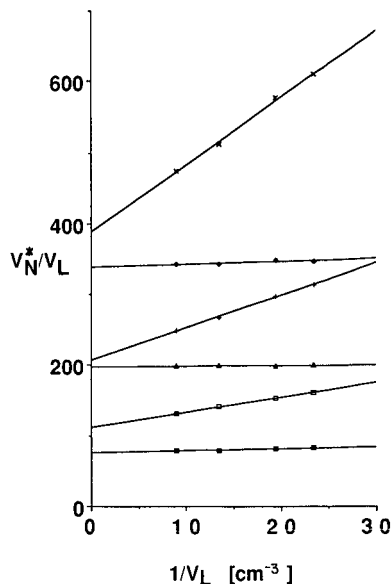


Fig. 2. Plot of V_N^*/V_L vs. $1/V_L$ for *n*-alkanes, ethanol, nitromethane and dioxane on Carbowax 20M. Solutes as in Fig. 1 except: □ = decane; + = undecane; × = dodecane.

a partition only model is found. By way of example the graphical data for squalane and Carbowax 20M are shown in Figs. 1 and 2. The difference between the measured retention index and the retention index value corrected for interfacial adsorption is generally small as indicated by the results in Table III. A second group of phases represented by the three thiocyanate salts show different behaviour to the first group. Using sBAT as a representative example (Fig. 3), both the test solutes and *n*-alkanes show substantial interfacial adsorption; the *n*-alkanes more so than the test probes. Linear extrapolation to infinite phase volume provides an accurate value for the gas-liquid partition coefficient. Large differences are now seen between the measured and corrected retention index values in Table III. Ignoring the contribution of interfacial adsorption to retention for these phases results in the calculation of misleading solvent selectivity parameters.

The remaining phases are perhaps among the most important from a classification point of view since they are the most polar of the phases evaluated. Taking DEGS and OV-275 (Figs. 4 and 5), as representative examples of the group which includes DEGS, TCEP, OV-275, PAN and EAN it can be seen that retention of the *n*-alkanes occurs almost entirely by interfacial adsorption. The polar test solutes are retained by a mixed retention mechanism and the gas-liquid partition coefficients can be obtained by linear extrapolation as for the other phases. Since, however, the *n*-alkanes do not partition significantly with these phases, meaningful retention index values can not be obtained. Consequently, it is not possible to calculate solvent selectivity parameters for these phases.

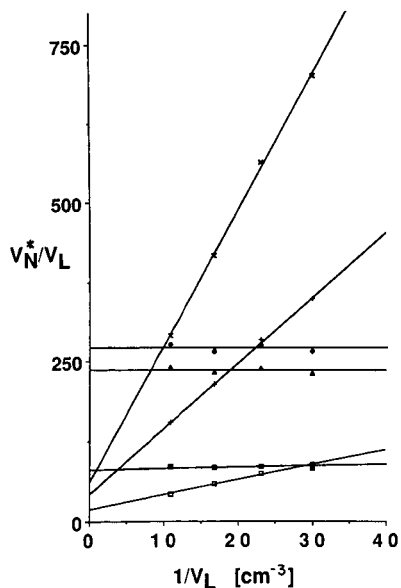


Fig. 3. Plot of V_N^*/V_L vs. $1/V_L$ for *n*-alkanes, ethanol, nitromethane and dioxane on *sec.*-butylammonium thiocyanate. Solutes as in Fig. 1 except: \square = pentadecane; \times = hexadecane.

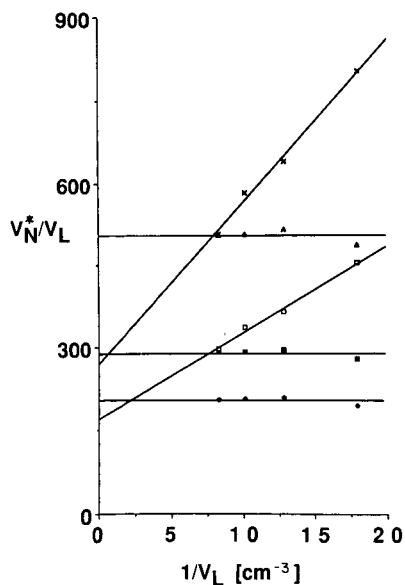


Fig. 4. Plot of V_N^*/V_L vs. $1/V_L$ for *n*-alkanes, ethanol, nitromethane and dioxane on poly(diethyleneglycol succinate). Solutes as in Fig. 1 except: \square = decane; \times = dodecane.

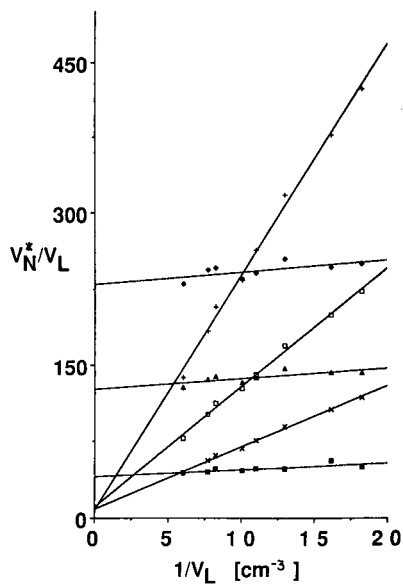


Fig. 5. Plot of V_N^*/V_L vs. $1/V_L$ for *n*-alkanes, ethanol, nitromethane and dioxane on OV-275. Solutes as in Fig. 1 except: \times = dodecane; \square = tridecane; $+$ = tetradecane.

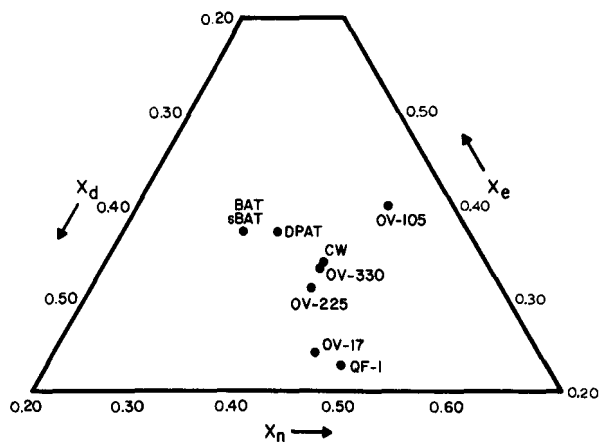


Fig. 6. Solvent selectivity triangle calculated using corrected retention indices.

The solvent selectivity parameters corrected for interfacial adsorption (Table IV), are plotted with triangular coordinates in Fig. 6. The phases evaluated can be grouped into four selectivity groups with Carbowax 20M, OV-330 and OV-225 forming one group, OV-17 and QF-1 a second, BAT, sBAT, and DPAT a third, and finally OV-105. A phase exhibiting minimum selectivity would be located at the center of the triangle. The most selective phases are found towards the corners of the triangle. None of the phases evaluated in Fig. 6 are highly selective as their location is centrally weighted compared to the selectivity space available. More selective phases, however,

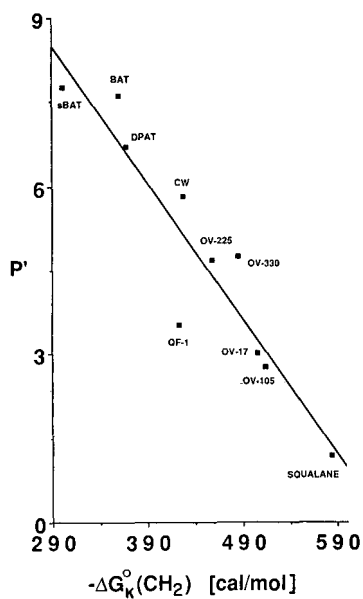


Fig. 7. Plot of $\Delta G_k^0(\text{CH}_2)$ against P' for phases that partition with n -alkanes.

could not be evaluated due to a failure of the calculation method caused by a lack of partitioning of the *n*-alkanes. A solution to this problem will be discussed subsequently.

Solvent polarity parameter

The solvent strength of a stationary phase can not be precisely defined since it is not a unique property of a solvent but a composite expression for several different interactions. Consequently, there is no single probe that can be defined as polar. The solvent polarity parameter equates polarity with the sum of the retention index increments for ethanol, nitromethane and dioxane corrected for the contribution from dispersion as indicated by eqn. 5. The approach proposed by Golovnya equates solvent strength with the reluctance of a stationary phase to retain a hydrocarbon. Quantitatively, this corresponds to the partial molar Gibbs free energy of solution for a methylene group (eqn. 7). In general, the agreement between the two scales is quite good (Table IV and Fig. 7) for those phases where a direct comparison is possible. A lack of partitioning of the hydrocarbons with some of the more polar phases evaluated (DEGS, TCEP, OV-275, PAN, EAN) excludes calculation of the solvent polarity parameter in those cases. For the remaining phases the solvent polarity parameter, P' , and the partial molar Gibbs free energy of solution for a methylene group, $\Delta G_k^0(\text{CH}_2)$, are related by eqn. 12

$$P' = 15.4559 + 0.0239[\Delta G_k^0(\text{CH}_2)] \quad n = 10 \quad r^2 = 0.859 \quad (12)$$

From Fig. 7 it is obvious that the data for QF-1 and OV-330 are more discordant than other members of the data set. Although the reason for this is not obvious if these two phases are removed a better correlation represented by eqn. 13 is obtained.

$$P' = 16.1149 + 0.0251[\Delta G_k^0(\text{CH}_2)] \quad n = 8 \quad r^2 = 0.966 \quad (13)$$

Eqn. 13 allows an estimate of P' values for liquid phases that partition with the 2-alkanones but not the *n*-alkanes. The estimated values are given in parentheses in Table IV. For those phases where a comparison is possible the $\Delta G_k^0(\text{CH}_2)$ values for the *n*-alkanes and 2-alkanones show good agreement.

An alternative estimation of the solvent polarity parameter is given by $\Sigma\delta(\Delta G_k^0)_{\text{SQ}}^{\text{PH}i}$ in eqn. 11. This represents the sum of the differences in the partial molar Gibbs free energy of solution of the test solutes ethanol, nitromethane, and dioxane on the polar phase and squalane as a non-polar reference phase. A good correlation exists between the free energy scale and the P' scale (Fig. 8) if the values estimated for DEGS, TCEP, OV-275, PAN and EAN are eliminated (eqn. 14).

$$P' = 0.4606 - 0.7908[\Sigma\delta(\Delta G_k^0)_{\text{SQ}}^{\text{PH}i}] \quad n = 9 \quad r^2 = 0.973 \quad (14)$$

The $\Delta G_k^0(\text{CH}_2)$ values used to estimate the P' values for the polar phases measures a quite general interaction whereas the $\Sigma\delta(G_k^0)_{\text{SQ}}^{\text{PH}i}$ scale sums only the three interactions measured by the test solutes. For the most polar phases these interactions are dominant and probably not adequately expressed by $\Delta G_k^0(\text{CH}_2)$.

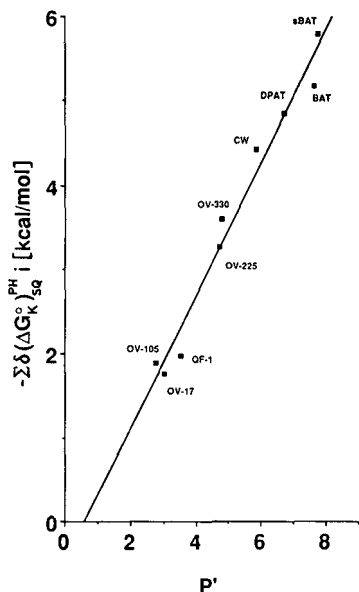


Fig. 8. Plot of $\Sigma\delta(\Delta G_K^0)_{SQ}^{PH}i$ against P' for phases that partition with n -alkanes.

Solvent selectivity parameters measured on the free energy scale

Since the test solutes partition on all phases and solvent selectivity parameters cannot be obtained on polar phases due to a lack of partitioning of the n -alkanes it should be possible to derive a universally applicable selectivity scale based on the partition coefficients of the test solutes. These can be corrected for dispersion by subtraction of the solute partition coefficient for the test solutes on squalane and the results expressed as differences in the partial molar Gibbs free energy of solution. Since the phases to be evaluated span a wide molecular weight range both molar and molal Gibbs free energy differences were calculated (Table VI). The two scales are correlated well as indicated in eqns. 15-17.

$$\delta(\Delta G_K^0)_{SQ}^{PH} = 0.9628[\delta(\Delta G_M^0)_{SQ}^{PH}] - 0.2677 \quad \text{ethanol } n = 14 \quad r^2 = 0.994 \quad (15)$$

$$\delta(\Delta G_K^0)_{SQ}^{PH} = 1.0044[\delta(\Delta G_M^0)_{SQ}^{PH}] - 0.2100 \quad \text{nitromethane } n = 14 \quad r^2 = 0.975 \quad (16)$$

$$\delta(\Delta G_K^0)_{SQ}^{PH} = 0.9211[\delta(\Delta G_M^0)_{SQ}^{PH}] - 0.2478 \quad \text{dioxane } n = 14 \quad r^2 = 0.972 \quad (17)$$

Thus, ignoring differences in the molecular weights of the liquid phases will not seriously effect the accuracy of the solvent selectivity parameters.

The solvent selectivity parameters were calculated from the partial molar Gibbs free energy of solution for the test solutes using eqn. 11 and are summarized in Table VII. The data are shown diagrammatically in Fig. 9. Where a comparison is possible with Fig. 6 the grouping of the phases is not very different. What is more striking is that all phases are displaced substantially to the right in Fig. 9. This is due to a diminished contribution from proton-donor forces to retention on the scale derived from free energy differences. Analysis of the two sets of solvent selectivity parameters (Tables IV

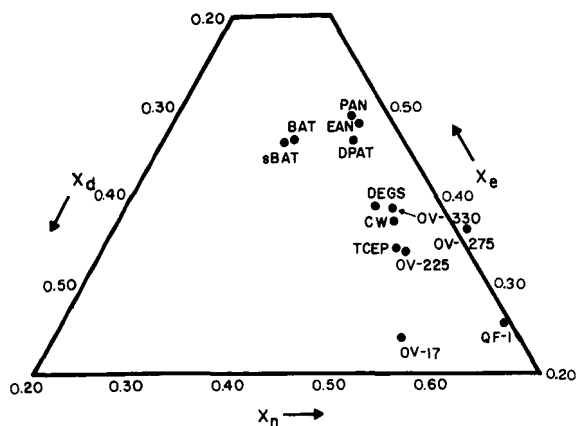


Fig. 9. Solvent selectivity triangle calculated using $\delta(\Delta G_{k,SO}^0)^{PH}$ values.

and VII) indicates that for OV-17, OV-225, QF-1, OV-330 and OV-105 the decrease in magnitude of X_d is largely compensated for by an increase in the X_n value while for DPAT, BAT and sBAT the decrease in X_d is largely compensated for by an increase in X_e . This would tend to indicate that either none of the phases evaluated have strong proton-donor properties or, alternatively, dioxane is a rather insensitive probe for proton-donor interactions.

The case for the selection of different test solutes

Snyder¹ selected ethanol, nitromethane and dioxane for his solvent selectivity scheme based on the availability of published data for over seventy solvents gathered by Rohrschneider²³; Rohrschneider used headspace analysis to measure the gas-liquid partition coefficients as most of the solvents evaluated were volatile liquids unsuitable as stationary phases for gas chromatography. One deficiency in the recommended test solutes for gas chromatography is their low retention on some phases even at moderate temperatures. The desire to measure solute-solvent interactions with an acceptable degree of accuracy presupposes sufficient residence time of the solute in the liquid phase to express this interaction with the desired experimental accuracy. Chromatographically the extent of liquid phase interactions as a function of the residence time of a solute in a column is indicated by the capacity factor. A selection of capacity factor values for the test solutes and some homologues or analogues recommended by McReynolds²⁴ for stationary phase characterization are given in Table VIII. As is readily apparent, the retention of ethanol and nitromethane on the non-polar phases is inadequate. This will, of course, influence the accuracy with which the retention of the test solutes on squalane can be taken as an approximate measure of dispersive interactions. If it is accepted that a capacity factor of at least 5 is desirable and a value greater than 20 is preferred, then ethanol and nitromethane are inadequate as test solutes. Dioxane is marginally acceptable. New probes should be selected for the accurate determination of solvent selectivity parameters for gas chromatographic purposes.

Gas-liquid partition coefficients for *n*-butanol, nitropropane, 2-pentanone and pyridine at 80.8°C have been determined for many of the phases used in this study⁶.

TABLE VIII
CAPACITY FACTOR VALUES FOR TEST SOLUTES ON DIFFERENT STATIONARY PHASES
(PHASE LOADING 12–15%, w/w) AT 80.8°C

Stationary phase	Capacity factor					
	Ethanol	Nitromethane	Dioxane	Butanol	Nitropropane	Pyridine
Squalane	0.46	0.89	4.65	2.81	4.6	6.56
OV-17	0.41	1.76	4.00	2.14	6.1	5.97
OV-105	0.84	1.47	3.39	3.60	5.07	4.71
OV-330	1.41	5.05	5.14	6.35	11.19	9.24
OV-225	1.35	5.97	6.26	5.65	15.97	10.56
QF-1	0.39	2.55	2.76	1.52	7.64	4.03
Carbowax 20M	3.26	14.24	8.26	12.21	20.03	16.97
DPAT	7.00	9.24	9.30	23.39	18.91	
DEGS	2.16	7.03	6.09	6.22	9.59	
BAT	8.33	6.30	14.33	24.33	11.12	
sBAT	11.03	7.67	18.89	29.81	13.42	
TCEP	2.24	11.97	7.88	6.52	17.30	13.61
OV-275	1.39	6.82	3.82	3.61	9.52	7.33
PAN	4.68	4.70	5.42	10.69	5.33	
EAN	4.52	6.80	6.93	10.31	5.81	

These probes are better retained on most phases (Table VIII), but are not necessarily ideal. Pyridine, in particular, is of questionable value as its peak shape on several phases is asymmetric resulting in inaccurate partition coefficients. These additional probes can be used to determine whether the choice of the test solute influences the position of a particular phase in the solvent selectivity triangle.

There is a reasonable correlation between the partial molar or molal Gibbs free energy and energy differences $\delta(\Delta G)$ for ethanol and butanol.

$$\delta(\Delta G_K^0)_{\text{butanol}} = 0.7705[\delta(\Delta G_K^0)_{\text{ethanol}}] + 0.1338 \quad n = 14 \quad r^2 = 0.924 \quad (18)$$

$$\delta(\Delta G_M^0)_{\text{butanol}} = 0.7301[\delta(\Delta G_M^0)_{\text{ethanol}}] + 0.1030 \quad n = 14 \quad r^2 = 0.913 \quad (19)$$

Scrutiny of the data indicates two separate trends for phases that can be separated by their ability to partition with the *n*-alkanes. This is most apparent in the data for $\delta(\Delta G_M^0)$ where the polar phases DEGS, OV-275, TCEP, EAN and PAN are displaced to the right of the other phases and form a second quasi linear relationship (Fig. 10). The fluorine-containing phase QF-1 is perhaps a little ambiguous or exceptional as it fits better with the data for the polar phases rather than with those phases having similar solvent strength. If the polar phases are removed from the correlation the agreement between the two test solutes improves ($r^2 = 0.985$, $n = 9$) for both the molar and molal scale. Changing ethanol for butanol will have a small effect on the selectivity parameters of the moderately polar phases but will produce a systematic change for the polar phases.

There is no correlation between either the Gibbs free energies or the differences in free energy after subtraction of the value on squalane for the test solutes

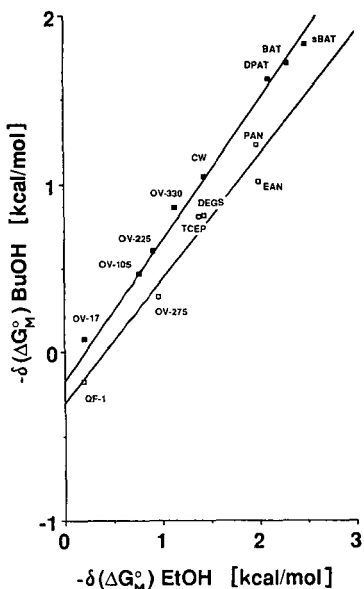


Fig. 10. Plot of $-\delta(\Delta G_M^0)_{\text{BuOH}}$ against $-\delta(\Delta G_M^0)_{\text{EtOH}}$.

nitromethane and 1-nitropropane. This is not surprising since the retention of the first member of a homologous series is frequently anomalous compared to expectations predicted from higher members of the series. On some phases it was noted that nitromethane eluted after 1-nitroethane. Thus, nitromethane does not behave characteristically of the other nitroalkanes on most selective phases. The use of higher-molecular-weight nitroalkanes in place of nitromethane will significantly change the relative position of a phase in the selectivity triangle in an unpredictable manner.

2-Pentanone and pyridine were evaluated as alternative test solutes for dioxane. Again there was no correlation between the free energies or their differences after subtraction of the value for the test solutes on squalane. The value of the solvent selectivity parameter will consequently be influenced by the choice of test solute. Part of the reason in this case may be that both pyridine and 2-pentanone have reasonably large dipole moments (≈ 2.5 D) compared to dioxane (≈ 0.45 D) and consequently their retention will be more influenced by orientation interactions than is the case for dioxane.

CONCLUSIONS

The solvent selectivity parameter approach is a useful tool for characterizing the solvent properties of liquid phases. The method as proposed by Snyder has certain limitations when applied to gas chromatographic solvents. A lack of partitioning of the *n*-alkanes with polar phases precludes the calculation of selectivity parameters for these phases. Inadequate retention of the test solutes on many phases, particularly those of low polarity, adversely influences the accuracy with which selectivity parameters can be measured. The position of a phase within the selectivity triangle is

a function of the test solutes used and will vary even for homologues of the test solutes suggested by Snyder.

To make the solvent selectivity parameters more useful for classifying liquid phases it will be necessary to select a new group of test solutes with sufficient retention to enable accurate measurements on phases spanning a wide range of solvent strength. To discontinue the use of the retention index scale for the measurement of retention in favor of using the gas-liquid partition coefficient of each test solute or some function, such as the Gibbs free energy of solution, easily derived from it. To evaluate further the contribution made by dispersion to the solvent selectivity parameters and define suitable methods of allowing for its effect. With these changes the solvent selectivity triangle approach to stationary phase characterization can be made more universally useful.

ACKNOWLEDGEMENTS

Support of this research in the form of a gift of stationary phases by A. A. Mendicino of Ohio Valley Specialty Chemical Inc. is gratefully acknowledged. C.F.P. wishes to thank Wayne State University for a Career Development Chair Award and a Graduate School Research Fellowship (to B.R.K.) in support of this research. Acknowledgement is made to the donors of the Petroleum Research Fund, administered by the American Chemical Society, for partial support of this research.

REFERENCES

- 1 L. R. Snyder, *J. Chromatogr. Sci.*, 16 (1978) 223.
- 2 M. S. Klee, M. A. Kaiser and K. B. Laughlin, *J. Chromatogr.*, 279 (1983) 681.
- 3 P. Shah, H. Na and L. B. Rogers, *J. Chromatogr.*, 329 (1985) 5.
- 4 T. J. Betts, *J. Chromatogr.*, 354 (1986) 1.
- 5 I. Brown, *J. Chromatogr.*, 10 (1963) 284.
- 6 C. F. Poole and S. K. Poole, *Chem. Rev.*, (1989) in press.
- 7 B. R. Kersten and C. F. Poole, *J. Chromatogr.*, 399 (1987) 1.
- 8 B. R. Kersten, C. F. Poole and K. G. Furton, *J. Chromatogr.*, 411 (1987) 43.
- 9 S. K. Poole, B. R. Kersten, R. M. Pomaville and C. F. Poole, *LC · GC, Mag. Liq. Gas Chromatogr.*, 6 (1988) 400.
- 10 C. F. Poole, B. R. Kersten, S. S. J. Ho, M. E. Coddens and K. G. Furton, *J. Chromatogr.*, 352 (1986) 407.
- 11 M. E. Coddens, K. G. Furton and C. F. Poole, *J. Chromatogr.*, 356 (1986) 59.
- 12 R. J. Laub, J. H. Purnell, P. S. Williams, M. W. P. Harbison and D. E. Martire, *J. Chromatogr.*, 155 (1978) 233.
- 13 E. F. Sanchez, J. A. G. Domínguez, J. G. Muñoz and M. J. Molera, *J. Chromatogr.*, 299 (1984) 151.
- 14 J. H. Dymond and E. B. Smith, *The Virial Coefficients of Pure Gases and Mixtures*, Clarendon Press, Oxford, 1980.
- 15 D. R. Dreisbach, *Physical Properties of Chemical Compounds*, American Chemical Society, Washington, DC, Vol. 1, 1955; Vol. 2, 1959; and Vol. 3, 1961.
- 16 J. R. Conder and C. L. Young, *Physicochemical Measurement by Gas Chromatography*, Wiley, New York, 1979, p. 336.
- 17 H.-L. Liao and D. E. Martire, *Anal. Chem.*, 44 (1972) 498.
- 18 J. R. Conder, D. C. Locke and J. H. Purnell, *J. Phys. Chem.*, 73 (1969) 700.
- 19 C. F. Poole and S. A. Schuette, *Contemporary Practice of Chromatography*, Elsevier, Amsterdam, 1984, p. 23.
- 20 R. V. Golovnya and T. A. Misharina, *J. High Resolut. Chromatogr. Chromatogr. Commun.*, 3 (1980) 51.
- 21 K. G. Furton and C. F. Poole, *J. Chromatogr.*, 399 (1987) 47.
- 22 E. F. Meyer, K. S. Stec and R. D. Hotz, *J. Phys. Chem.*, 77 (1973) 2140.
- 23 L. Rohrschneider, *Anal. Chem.*, 45 (1973) 1241.
- 24 W. O. McReynolds, *J. Chromatogr. Sci.*, 8 (1970) 685.

CHROM. 20 740

EFFECT OF MOBILE PHASE FLOW-RATE ON THE RECOVERIES AND PRODUCTION RATES IN OVERLOADED ELUTION CHROMATOGRAPHY

A THEORETICAL STUDY

SAMIR GHODBANE and GEORGES GUIOCHON*

**Department of Chemistry, University of Tennessee, 575 Buehler Hall, Knoxville, TN 37996-1600 (U.S.A.) and Oak Ridge National Laboratory, Analytical Chemistry Division, Oak Ridge, TN 37831-6120 (U.S.A.)*

SUMMARY

The effect of mobile phase flow-rate on the recoveries and production rates in overloaded elution liquid chromatography was investigated from a theoretical standpoint. Numerical solutions of the semi-ideal model of non-linear chromatography were calculated for simulated columns, using a classical form of the HETP equation. Production rates and recoveries were derived for several mixtures with different relative retentions. It is generally observed that the recoveries decrease with increasing mobile phase flow-rate but that the production rates pass through a maximum which is reached at very high velocities. In the cases studied here, the optimum flow-rate corresponds to the efficiency for which the analytical resolution between the two compounds separated is around unity or even slightly lower.

INTRODUCTION

The explosive growth of the biotechnological and pharmaceutical industries in the last 10 years has generated tremendous needs for large amounts of highly pure compounds. Thus, preparative chromatography has arisen as a powerful separation and purification tool. In these applications, the ultimate goal is to recover the largest possible amount of a given compound at the highest possible degree of purity while minimizing the investment and operational costs. So far, most of the applications have been developed by analytical chemists, organic chemists, biochemists or chemical engineers. Each group has brought along its expertise but also its biases. It turns out that most preparative chromatographic units are still operated far below their optimum capacities, because the phenomena underlying the separation process are poorly understood. Consequently, it is still impossible to predict the optimum experimental conditions for a preparative separation¹.

An overall solution to this optimization problem will be obtained by establishing a theoretical framework taking all of the effects of finite concentration into account. Such a model would correctly predict the elution profiles of the components of a mixture and would relate the experimental parameters of a chromatographic separation to these band profiles. It would then permit the calculation of the

performance of a given column. This would be an essential tool in the determination of the optimum experimental conditions necessary to achieve maximum production¹.

The fundamental theory of non-linear chromatography can serve as a basis for the development of this approach¹⁻³. This theory is based on a study of the solutions of the system of partial differential equations obtained by writing a mass balance and a kinetic equation for each component of the mixture of interest. It may be assumed that the mobile phase is not adsorbed on the stationary phase⁴. In most modes of chromatography, the kinetics of mass transfer between phases are extremely fast and, as a first approximation, it has been assumed that instantaneous equilibrium is achieved between the mobile and stationary phases. This last assumption implies that: the kinetic equations are replaced by the equilibrium isotherms and the molecular diffusion coefficients are set equal to zero.

The remaining system of partial differential equations is the ideal model of chromatography. It has been widely studied in the past and its shortcomings are well known^{5,6}. It cannot be solved analytically.

Recently, a numerical solution based on a finite difference method was described and used to solve the system of partial differential equations discussed above in a variety of boundary conditions^{2,3,7}. In this method, the continuous (z, t) plane is replaced by a (z, t) grid which is characterized by a space, δz , and a time, δt , increment. The proper selection of the finite space increment δz , set equal to the height equivalent to a theoretical plate of the column (HETP), H , and of the time increment ($\delta t = 2H/u$) allows for the introduction of a numerical diffusion term which simulates the column efficiency and has exactly the same role as the apparent diffusion coefficient, which accounts for the kinetic effects and axial diffusion⁸. The profiles obtained are very realistic and quantitatively compare very well with those generated experimentally for a single compound⁹.

In order to achieve the highest production possible, it is essential to optimize the column length (L), the mobile phase flow-rate (u), the diameter of the particles (d_p) and the column efficiency. These parameters are interrelated. In this paper, we shall investigate only the effect of flow-rate on the recoveries and production, keeping the column length and particle size constant.

The mobile phase flow-rate is an important part of the separation process and has a very prominent effect on the column efficiency. In chromatography, packed beds are used. Because the packing structure is complex, the flow pattern is very complicated and it has never been possible to relate exactly the band spreading to the column characteristics and the flow-rate. It is known that the optimum mobile phase flow-rate is a function of the particle size, the column dimensions and the molecular diffusion of the solute in the mobile phase. The decrease in column efficiency resulting from the use of a high flow-rate of the mobile phase is often neglected in preparative liquid chromatography. As band profiles rapidly broaden and become less symmetrical when the sample size is increased, users tend to operate at high flow-rates in an attempt to increase production, on the basis that as the apparent column efficiency drops dramatically, it is not necessary to be concerned about this more moderate source of band broadening. As a result, however, the apparent diffusion coefficient increases, which leads to smooth band flanks and to increasing band interactions, *i.e.*, to increasing overlap of the bands. The resolution between bands and, consequently, the recoveries decrease. This leads us to the following questions: to what extent does

TABLE I
PARAMETERS OF THE LANGMUIR ISOTHERMS

Component	<i>a</i>	<i>b</i>
1	23	2.38
2	25	2.56

the reduction in the injection cycle compensate for the decrease in yield?; and does the production per unit time (production rate) or per unit volume of mobile phase increase with increasing flow-rate? This paper aims at answering these questions.

DESCRIPTION OF THE PROBLEM

To illustrate our point, let us investigate the preparative separation of a binary mixture on a 25-cm long column. The relative retention of the two compounds (equal to 1.09) and their relative concentrations (1:3) are kept constant throughout. The average size of the porous particles (d_p) making up the stationary phase is 20 μm . The diffusion coefficient of both solutes, D_m , in the mobile phase is $0.7 \cdot 10^{-5} \text{ cm}^2/\text{s}$. The two solutes compete for the sites available on the surface. Their equilibrium adsorption isotherms are both of the Langmuir type and they slowly diverge with increasing solute concentration. They are of the general form

$$q_i = \frac{a_i c_i}{1 + b_1 c_1 + b_2 c_2} \quad (1)$$

where a_i and b_i are the Langmuir coefficients for compound i (see Table I).

Although there is serious doubt that such a simple relationship could be exact in any real situation, this is also, on a qualitative basis, the most general type of behavior observed in liquid chromatography. We have also assumed a typical relationship between the column plate height and the flow-rate. For the sake of simplicity, it is expressed using the reduced plate height (h) and velocity (τ) introduced by Giddings¹⁰:

$$h = \frac{H}{d_p} \quad (2)$$

$$\tau = \frac{u d_p}{D_m} \quad (3)$$

The HETP equation we have assumed is

$$h = \frac{1.5}{\tau} + \tau^{0.33} + 0.03\tau \quad (4)$$

This equation is classical¹¹ and corresponds to a good column with a minimum reduced plate height of 2.024 and an optimum reduced velocity of 2.735¹². A plot of h versus τ is shown in Fig. 1.

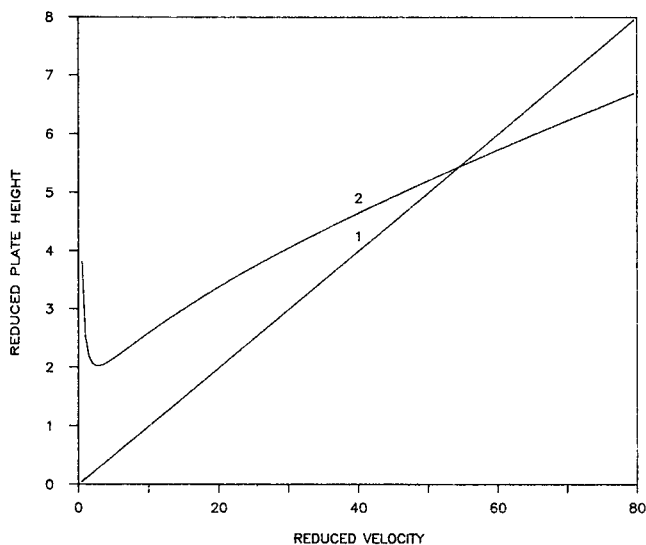


Fig. 1. Plots of column reduced plate height *versus* reduced flow velocity: (1) equation used by Knox and Pyper¹⁴; (2) eqn. 4.

For each set of simulations, we proceeded as follows. We start with a value of τ between 1 and 300 (see Table II) and from eqn. 4 determine the reduced plate height. The plate height H is then calculated using eqn. 2. This, in turn, gives the time and space increments of the (z, t) grid, defined above, on which the numerical problem is solved. Eqn. 3 allows for the determination of the mobile phase flow-rate u . Consequently, the retention time for an unretained solute,

$$t_0 = \frac{L}{u} \quad (5)$$

and the retention time at infinite dilution ($c_i \rightarrow 0$) for the two components of the mixture,

TABLE II
PARAMETERS USED IN THE SIMULATION

τ	u (cm/s)	h	N	R_s
1	0.0035	2.53	4941	1.36
2.735	0.0096	2.024	6173	1.52
20	0.07	3.362	3718	1.18
40	0.14	4.615	2708	1.01
50	0.175	5.166	2420	0.95
100	0.35	7.58	1645	0.79
200	0.7	11.845	1055	0.63
300	1.05	15.68	797	0.55

$$t_{r_i} = \frac{L}{u} (1 + k'_i) \quad (6)$$

are determined.

As H and t_{r_i} are known, the apparent diffusion coefficient, D_a , for a given set of experimental conditions is derived through the Einstein equation:

$$D_a = \frac{HL}{2t_{r_a}} \quad (7)$$

where L is the column length and t_{r_a} the average retention time of the two components of the mixture of interest at infinite dilution.

At this point, all the parameters needed to undertake a series of simulation are known. Those used are listed in Table II.

RESULTS AND DISCUSSION

The amount of solute eluted from a column is the integral of the concentration *versus* the volume of solvent flowing out from the column, and the peak area is the integral of the detector signal *versus* time. The ratio of the sample size to the peak area is thus equal to the flow-rate. This relationship, which holds for concentration-sensitive detectors, holds here also, as the natural time unit for our calculations is inversely proportional to the mobile phase flow-rate (see the above description of the time increment). This requires proper adjustment of the peak area introduced into the calculation, depending on the value of the flow-rate selected. To avoid any misunderstanding, the sample size is given here exclusively as a fraction of the column saturation capacity¹³, which is equal to a/b (see eqn. 1). To avoid any problem, this ratio is the same for both compounds.

Recoveries

The column efficiency decreases with increasing flow-rate over most of the range investigated. We may therefore expect that the yield, at constant sample size and purity, will follow the same trend as the column efficiency. This effect can be clearly seen by comparing the profiles in Fig. 2a and b. As the injection period increases with decreasing flow-rate, the production rate, which is the amount of a given product (1 or 2) recovered at a certain degree of purity per unit time, will depend on a combination of two different, opposite effects, the yield, which decreases with increasing flow-rate, and the period, which increases. The aim of this work is to determine whether there is an optimum and where it is, in order to maximize the production rate.

As a general rule, the recovery decreases with increasing mobile phase flow-rate (see Figs. 3 and 4). The dependence of the recovery on the flow-rate, *i.e.*, on the efficiency, is stronger for the first component (see Figs. 3a and 4a) than for the second (see Figs. 3b and 4b). The recoveries tend to be higher for the second component at low or moderate column loadings but lower at high loadings. Between 80 and 15%, the recovery decreases linearly with increasing logarithm of sample size (fraction of column saturation capacity, $\log X$) for the first component over most of the range

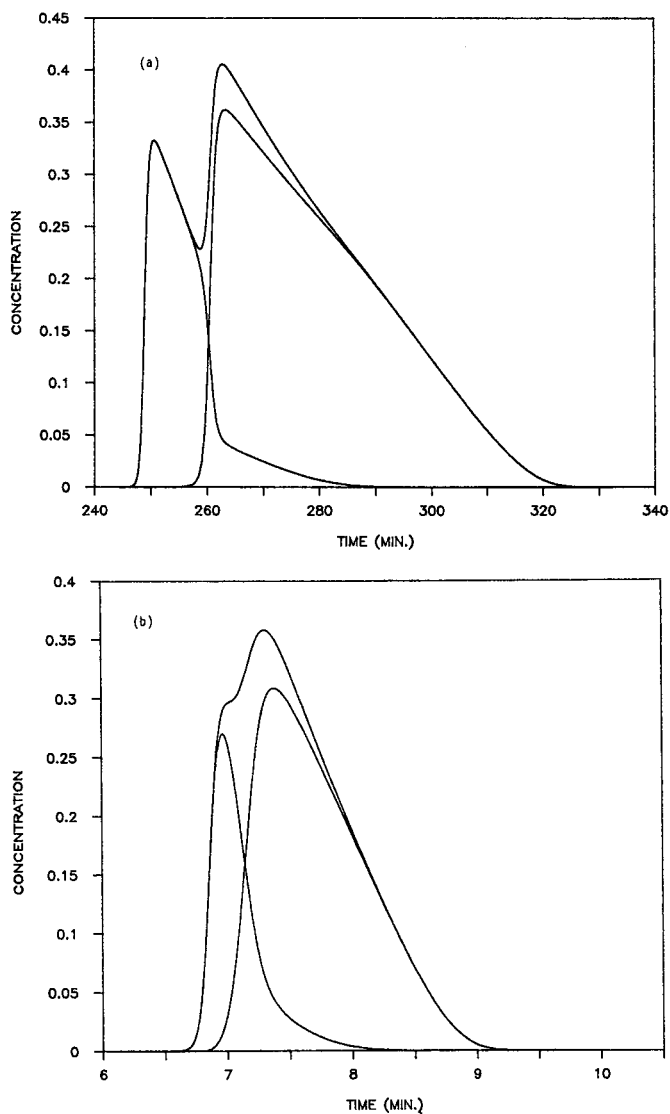


Fig. 2. Chromatograms of a sample amount corresponding to 2.5% of column saturation capacity for a 1:3 mixture ($\alpha = 1.09$) and (a) $\tau = 2.735$ ($u = 0.0096$ cm/s) (b) $\tau = 100$ ($u = 0.35$ cm/s).

studied. For the second component, the plot of the recovery *versus* the logarithm of X has a strong S-shape (see Figs. 3b and 4b).

At $\tau = 100$ ($u = 0.35$ cm/s) and for a required purity of 98%, the recovery of the lesser retained component of the mixture is poor even at low sample sizes (the "analytical" resolution is only 0.79) and is only 25% for a 1.5% column saturation capacity sample [$\log(X) = -1.8$]. At $\tau = 2.735$ ($u = 0.0096$ cm/s, *i.e.*, the efficiency optimum flow-rate, the recovery exceeds 80% for the same sample size, *i.e.*, it is more than three times larger (see Fig. 3a). The corresponding figures for the second component are 42% and 59%, respectively (see Fig. 3b).

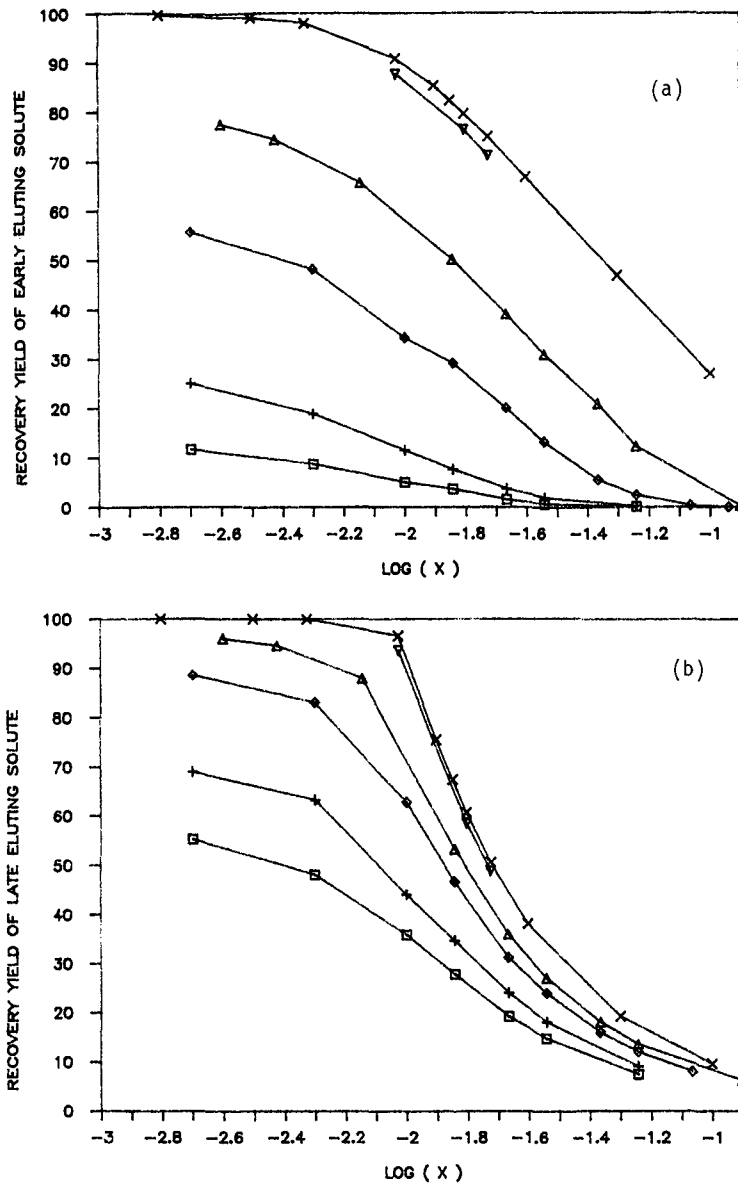


Fig. 3. Plots of the recovery (98% purity) versus logarithm of sample size (fraction of column saturation capacity) ($\alpha = 1.09$) for (a) component 1 and (b) component 2. τ : $\square = 1.05$; $+$ = 0.7; $\diamond = 0.35$; $\triangle = 0.175$; $\times = 0.0096$; $\nabla = 0.0035$ cm/s.

For a required purity of 95% and a 5% column saturation capacity sample [$\log(X) = -1.3$], the yields are about 25 and 29% at $\tau = 100$ and 2.735, respectively, for the second component (see Fig. 4b), and 15 and 52%, respectively, for the first component (see Fig. 4a).

As mentioned above, simulations were run using a value of the mobile phase

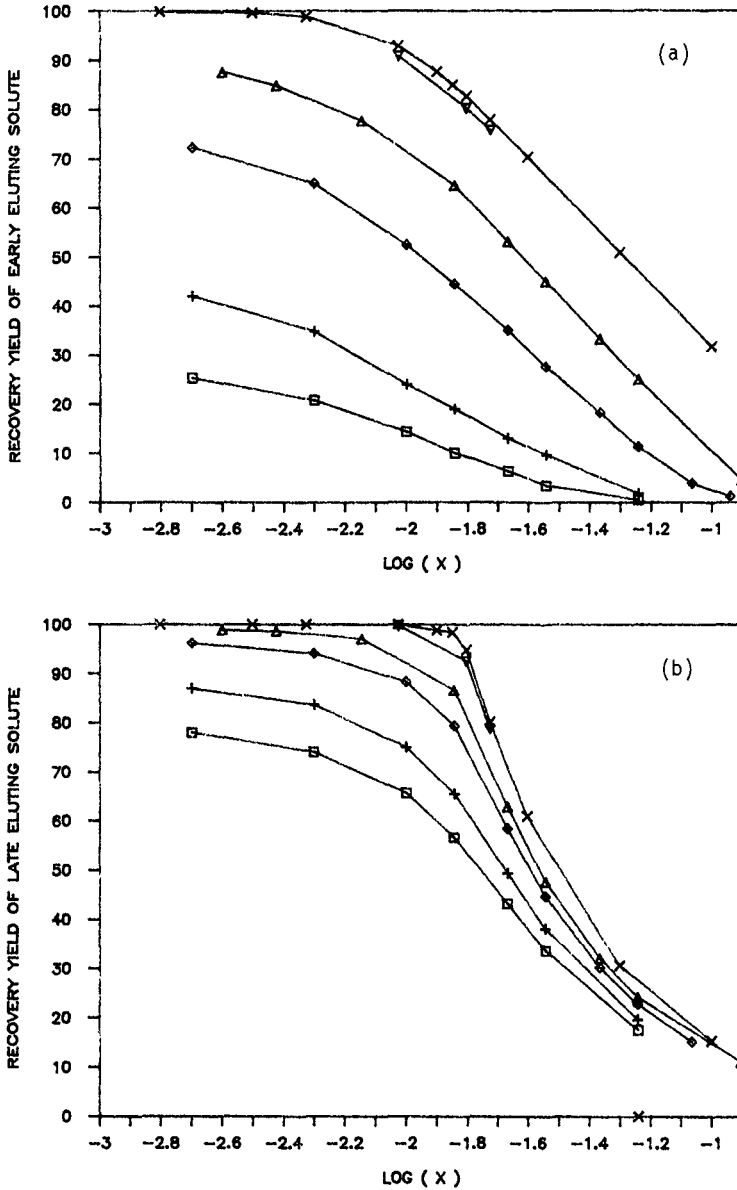


Fig. 4. As Fig. 3 for a purity of 95%.

flow-rate below the minimum of the Van Deemter curve ($\tau = 1$, see Table II). As expected, in all instances the recoveries were lower than those obtained for the optimum flow-rate ($\tau = 2.735$) but higher than those obtained at $\tau = 20$ ($u = 0.07$ cm/s), confirming that the origin of the influence of the flow-rate on the recovery lies in its effect on the column efficiency (see Figs. 3 and 4).

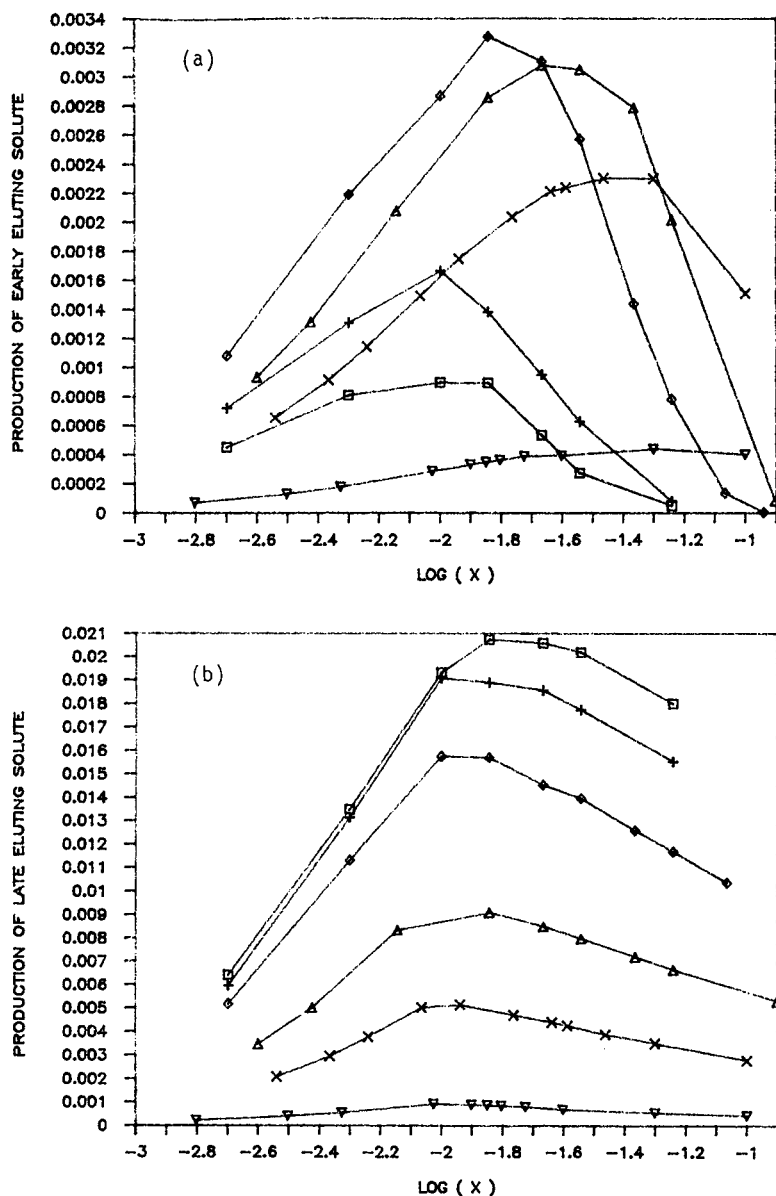


Fig. 5. Plots of the production rate (mol/cm³/min) (98% purity) versus logarithm of sample size (column saturation capacity) ($\alpha = 1.09$) for (a) component 1 and (b) component 2. $\square = 1.05$; $+$ = 0.7; $\diamond = 0.35$; $\Delta = 0.175$; $\times = 0.07$; $\nabla = 0.0096$ cm/s.

Production rates

As the production rate is the product of a factor that decreases with increasing flow-rate (the recovery) and on that increases (the injection frequency), all production rates pass through a maximum as expected from the above discussion (see Figs. 5 and 6). In general, these figures show that the production rates increase rapidly with

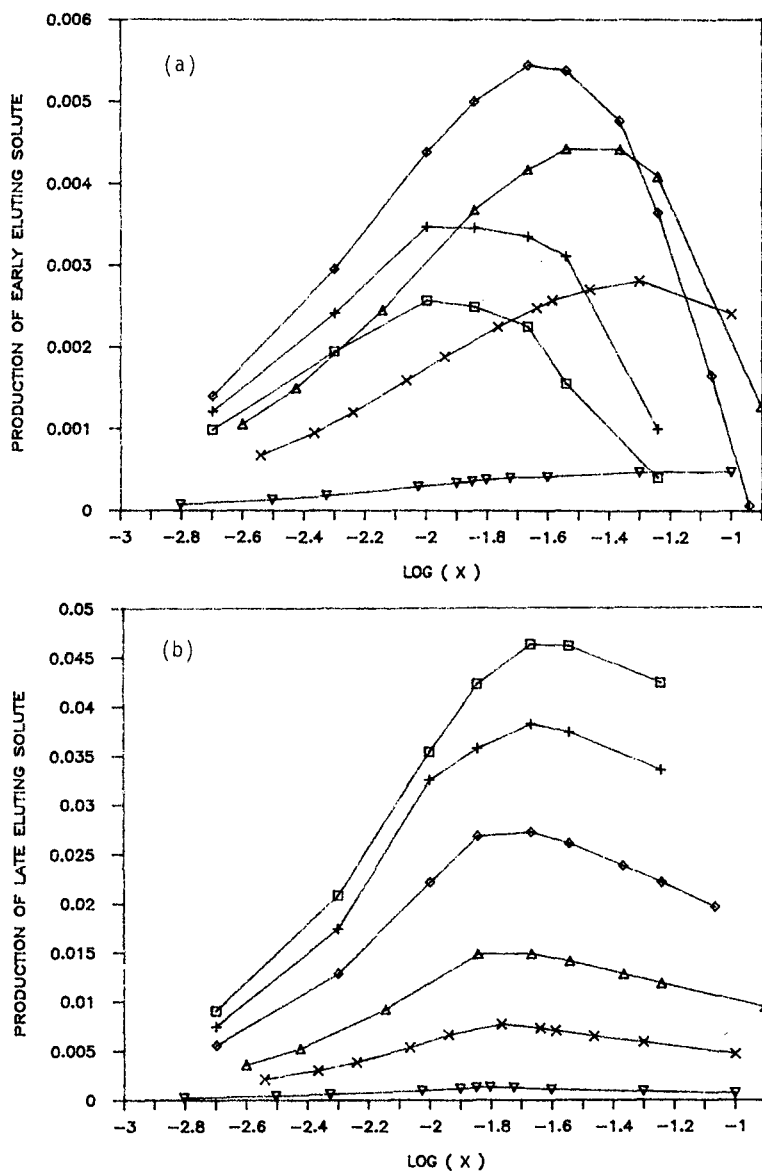


Fig. 6. As Fig. 5 for a purity of 95%.

increasing flow-rate at constant load per cycle [except for compound 1, at large loading factors and velocities (Figs. 5a and 6a) or at high purity]. The production rates are higher for component 2 than they are for component 1, which is normal as the concentration of component 2 is three times higher than that of component 1. The production rates under a given set of experimental conditions are not in this ratio of 1:3, however. Also, the production rates increase with decreasing purity requirements (compare Figs. 5a and 6a on the one hand and Figs. 5b and 6b on the other). When the

required purity decreases from 98 to 95%, the maximum production rate of compound 1 observed increases from 0.0033 to 0.0055 mol/cm³/min.

It can also be seen that for a given value of the required purity, the optimum sample size for maximum production increases with decreasing mobile phase flow-rate for the early eluting component of the mixture (Figs. 5a and 6a). This is no longer true for the more retained compound (Figs. 5b and 6b). In the latter instance, the optimum sample size appears to be independent of the mobile phase flow-rate (loading factor *ca.* 1.2%). It is remarkable that the maximum production rate increases with increasing flow-rate up to values of the reduced velocity in excess of 100. As the viscosity of a water-methanol mixture is of the order of 1 cP, and with a column permeability factor of about 1000 for a 25-cm long column packed with 20- μ m particles, the pressure drop for a reduced velocity of 100 would be of the order of 22 atm, which, although reasonable for preparative applications, could easily be exceeded if needed.

Figs. 5a and 6a are strikingly different from Figs. 5b and 6b. For both a 98% and 95% purity of the recovered first compound, there is an optimum flow-rate above which the production rate starts to decrease. For a purity of 98%, for example, the optimum production rate increases from $u = 0.0096$ cm/s to 0.35 cm/s, where it is maximum and equal to 0.0033 mol/cm³/min. It then decreases for higher flow-rates. It is interesting that the maximum possible production rates, at both 98% and 95% purity, are reached for a flow-rate at which the "analytical" efficiency between the bands of the two compounds has dropped below 1 (see Table II), which is a small value. This is even more true for component 2, for which the production rate optimum velocity has yet to be reached at a reduced velocity of 300 ($u = 1.05$ cm/s).

Clearly, there are two different optimum velocities, one for each component of the mixture. It is quite possible that the optimum flow velocity depends also on the relative concentration ratio of the mixture under consideration.

Comparison with the prediction of a simpler model

In this last section, we compare our predictions with those made by Knox and Pyper¹⁴. Their derivation suggests that the optimum throughput is determined exclusively by the minimum number of theoretical plates, N^* , required to provide "adequate" preparative resolution for the components of interest, *i.e.*, to achieve the separation when the tail of the early eluting component and the leading front of the late eluting one just start to touch. This plate number corresponds to the largest sample size for which the recovery is still complete. Under such optimum conditions, Knox and Pyper¹⁴ have shown that the thermodynamic contribution to the band width has become identical with twice the kinetic contribution. Assuming triangular shape bands, the critical plate number is given by¹⁴

$$N^* = 16 \left(\frac{t_{r2}}{t_{r2} - t_{r1}} \right)^2 = 16 \left(\frac{1 + k'_2}{k'_2 - k'_1} \right)^2$$

The optimization procedure recommended by Knox and Pyper¹⁴ is thus as follows:

- (i) determine the critical number of plates, N^* , for the required separation using eqn. 8;
- (ii) compare it with the maximum column efficiency, N_{\max} ;
- (iii) if $N_{\max} \leq 3N^*$, operate the column under the optimum flow-rate and inject

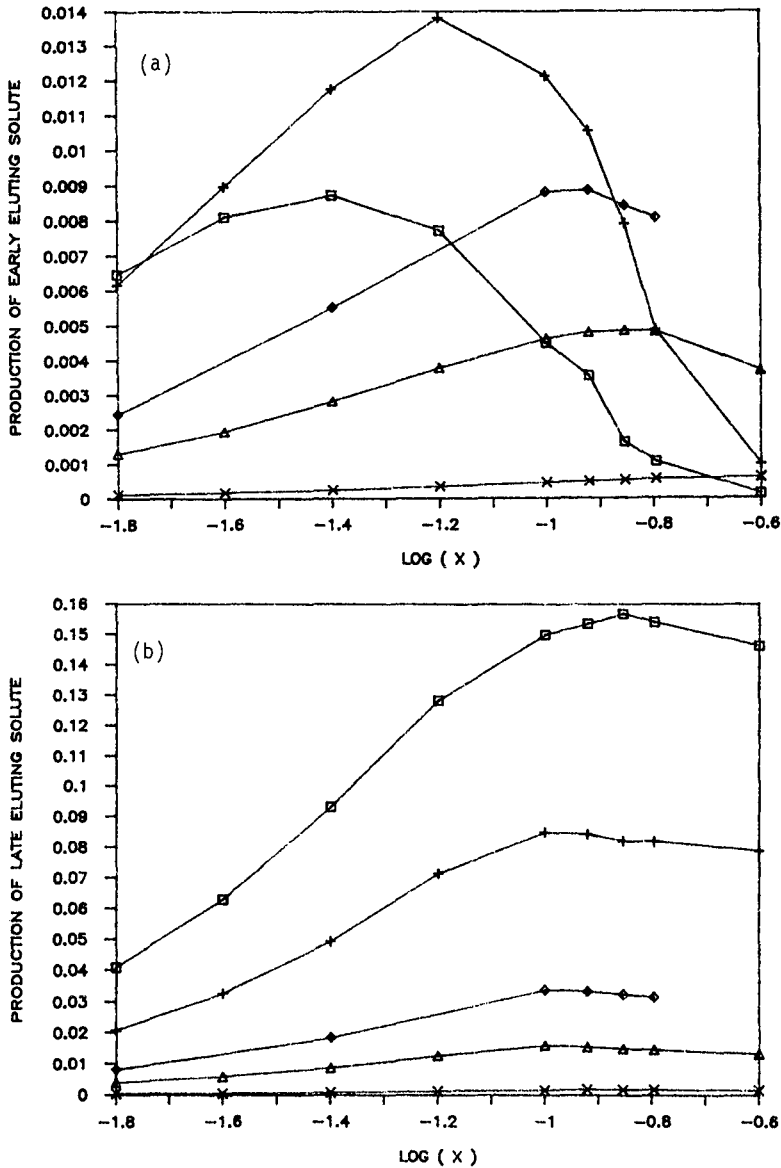


Fig. 7. Plots of the production rate *versus* logarithm of sample size ($\alpha = 1.25$): (a) component 1 collected at 99% purity and (b) component 2 collected at 95% purity. N : $\square = 275$; $+$ = 538; $\diamond = 1034$; $\triangle = 1614$; $\times = 3102$ plates.

the sample amount required to achieve a resolution of 1 as described in the previous paragraph;

(iv) if $N_{\max} > 3N^*$, operate the column at a high flow-rate at which the efficiency N ($N < N_{\max}$) is just equal to $3N^*$ and load the column as described under (iii). In most practical situations, this requires high or very high velocities, much larger than that

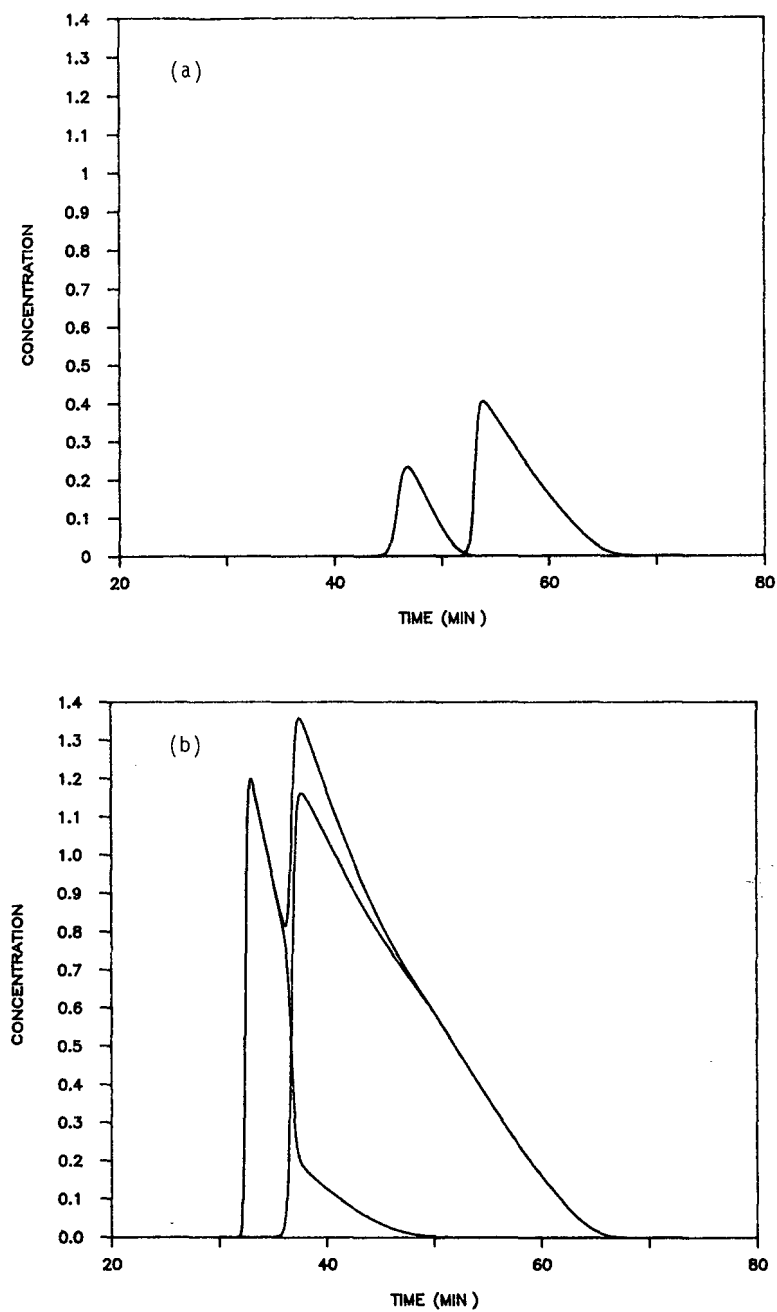


Fig. 8. Chromatograms of a 1:3 mixture ($\alpha = 1.25$) on a 1614-plate column under optimum conditions according to (a) Knox and Pyper¹⁴ and (b) our model.

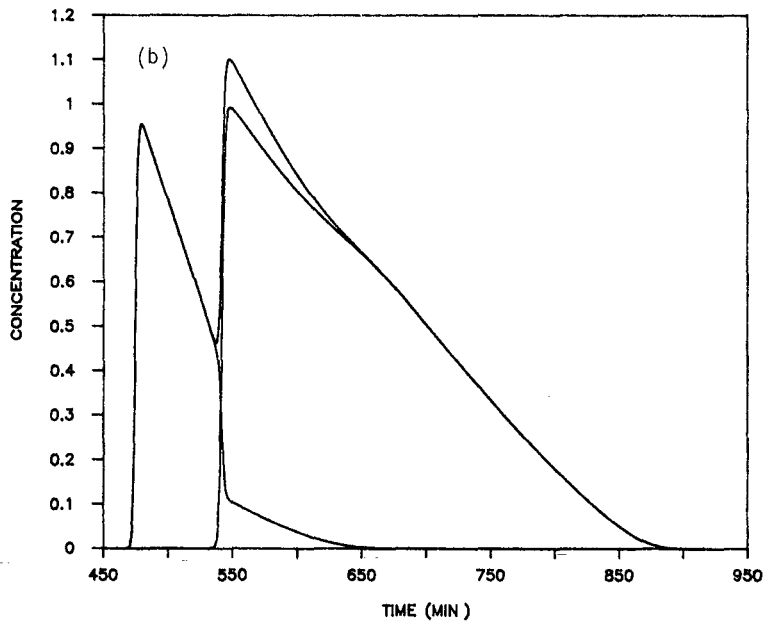
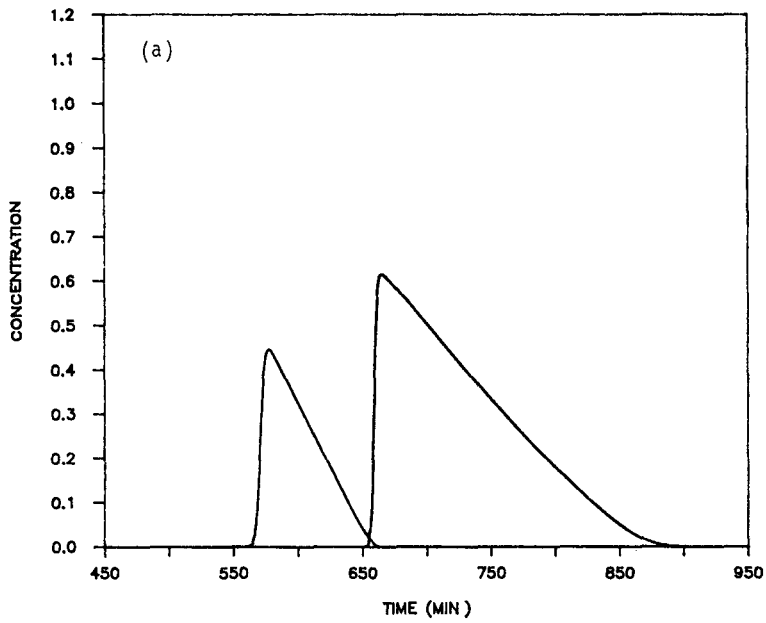


Fig. 9. As Fig. 8 for a 3102-plate column.

corresponding to the minimum of the Van Deemter curve. Hence the characteristics of the pumping system may limit the performance and force operation at sub-optimum conditions.

The results discussed in the previous two sections correspond to the separation of a pair of compounds ($\alpha = 1.09$) which requires a large critical plate number, $N^* = 3364$. This is more than a third of the efficiency (6173 plates) of the column used for the previous simulation. Accordingly, we are under conditions which are sub-optimum according to Knox and Pyper¹⁴. Our result that maximum production is not achieved at the flow-rate for which the column efficiency is maximum is at variance with their conclusions. To check (iii) further and also (iv), we carried out other series of calculations for a much easier separation.

We now consider a 1:3 binary mixture with a relative retention of 1.25 and $k'_2 = 6.25$ on a 25-cm long column packed with 40- μm particles. The critical plate number, N^* , is now equal to 538 plates only ($\tau = 195.5$). The corresponding number for the analytical separation is therefore 1614 plates ($\tau = 27.5$). Hence, according to Knox and Pyper¹⁴, one should operate the column at a linear velocity corresponding to $N = 3N^* = 1614$ to reach the maximum throughput. The reduced plate height equation remains the same (eqn. 4). As a result, the coordinates of the Van Deemter minimum are the same as those used above. Accordingly, at the linear velocity corresponding to the minimum HETP, the column efficiency is 3102 plates ($\tau = 2.735$). The reduced velocity recommended by Knox and Pyper¹⁴ would thus be 27.5 (Fig. 1).

A numerical study of the variation of the production rate of the two compounds as a function of the sample load shows that the production increases rapidly with increasing throughput and continues to do so even for throughputs larger than those suggested by Knox and Pyper¹⁴ (see Fig. 7a and b), despite the appearance and growth of an interference between the two bands, *i.e.*, although the yield decreases. Further, the maximum production rate observed at a given flow-rate increases with increasing flow-rate, up to very large values of the flow-rate and, accordingly, to very low values of the efficiency. The column should be operated at flow-rates much higher than that corresponding to the minimum of the Van Deemter curve, sometimes even higher than that corresponding to an analytical resolution between the bands of units. As observed previously, the maximum production for component 2 keeps increasing with increasing flow-rate, whereas it passes through a maximum for component 1, at least for a 99% requested purity. This maximum seems to occur for an analytical resolution close to 1, *i.e.*, in this instance between $N = 538$ ($R_s = 1.25$) and $N = 275$ plates ($R_s = 0.89$ and $\tau = 497.3$).

Finally, Figs. 8a and 9a show the two bands under conditions for which the production rates should be maximum, according to Knox and Pyper¹⁴, for $N = 1614$ and 3102 plates, respectively. They correspond to loads of 1.6 and 4% of the total column saturation capacity, *i.e.*, $\log(X) = -1.8$ and -1.4 , respectively. For the sake of illustration, the chromatograms corresponding to the maximum production as predicted by our model for $N = 1614$ and 3102 plates are shown in Figs. 8b and 9b, respectively. These figures confirm that one must allow for the two bands to interfere a great deal in order to achieve maximum production.

It is interesting to pursue a quantitative comparison between our results and those predicted by Knox and Pyper¹⁴. They calculated the maximum throughput under their optimum conditions from the following equation (eqn. 62 in ref. 14):

$$\log[\varphi T(\text{m/s})] = -0.64 - 1.58 \log N^* \quad (9)$$

with $\varphi = [k'_2/(1 + k'_2)]^2 (b_2/4a_2)$. In the numerical case discussed here, this gives $\varphi = 1.9 \cdot 10^{-5} \text{ m}^3/\text{mol}$. Their expression relating the throughput $T = Q/t_0$ to the "practical" throughput $PT = Q/[t_0(k'_2 + 2)]$ is then used to arrive to the following expression:

$$\log[PT(\text{mol/m}^2/\text{s})] = 3.16 - 1.58 \log N^* \quad (10)$$

The expected "practical" throughput is therefore equal to 0.00042 mol/cm²/min for a yield of 100% at this velocity. According to our simulation, the expected throughput is equal to 0.0012 mol/cm³/min with a loading factor of 1.6% (Fig. 6a). For a 25-cm long column with $\varepsilon = 0.8$, this corresponds to a production rate of 0.0060 mol/cm²/min. Comparison between these two values must be made with caution. First, it is satisfactory, given the differences in approaches over which we elaborate below, that they agree within a factor 15. This may explain part of the difference. Secondly, Knox and Pyper used a simplified plate equation, $h = C\tau$ (see eqn. 50 in ref. 14), in their work whereas we used a more realistic plate equation (see eqn. 4). As a result, the value of the reduced velocity used in our simulation is 1.4 times lower than that used by Knox and Pyper for the same reduced column efficiency (see Fig. 1). Accordingly, had we used the same plate height equation in our calculations, we would have obtained a production rate 1.4 times higher, *i.e.*, 0.0084, which is to be 20 times greater than the Knox and Pyper expected practical throughput (0.00042). There are several possible explanations for this difference. We must emphasize that our value corresponds to a yield of 99% and theirs to 100%. Also, Knox and Pyper¹⁴ neglected the effect of the displacement of the first component by the second^{15,16}. The latter results in a concentration of the first eluting solute in the mobile phase, *i.e.*, a narrowing of its band¹⁷. This, in turn, allows for the amount of the mixture required to reach the optimum production rate at a unit yield larger than when the two solutes do not interfere and explains in part why our predicted value is higher than theirs. The remainder of the difference may lie in the nature of the assumptions used in their model, *viz.*, triangular peak shape and optimum throughput achieved when the kinetic dispersion is half the thermodynamic dispersion.

In practice, if a certain loss in the recovery is accepted, a 5–10-fold gain in production can be achieved by injecting large samples and making the proper fraction cuts. Figs. 8b and 9b show the chromatograms obtained with the injections giving maximum productivity under the flow-rate recommended by Knox and Pyper¹⁴. Fig. 10a and b show the chromatograms corresponding to the maximum production we could achieve for the first (purity 99%) and the second compound (purity 95%), respectively.

CONCLUSION

The main conclusion is that an increase in the mobile phase flow-rate far beyond the values conventionally used in analytical HPLC leads to an important increase in production rate of a preparative column. The recoveries always increase with increasing column efficiency and are maximum at the optimum column flow-rate.

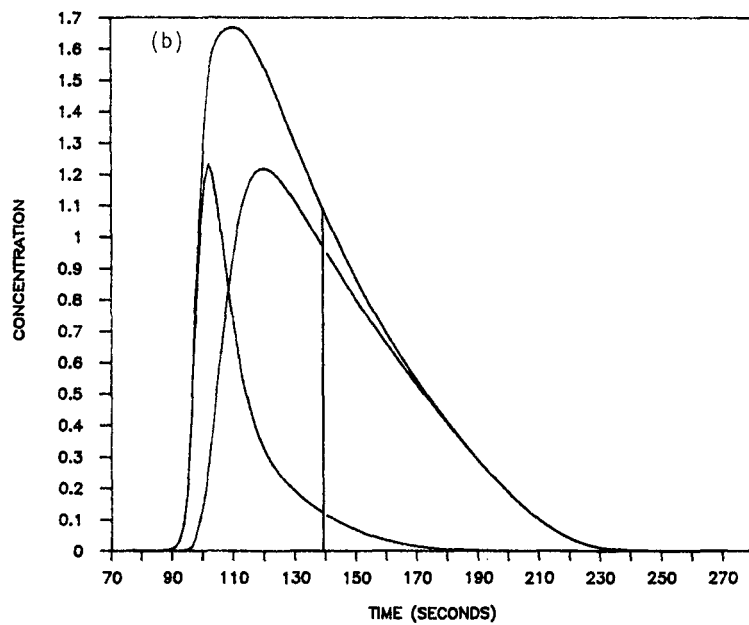
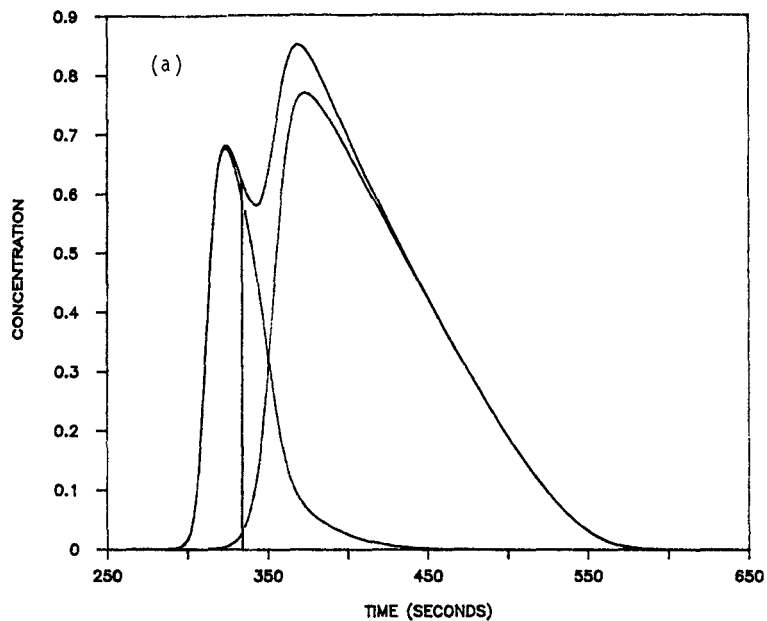


Fig. 10. Chromatograms of a 1:3 mixture ($\alpha = 1.25$) corresponding to the maximum achievable production rate for: (a) component 1 collected at 99% purity ($N = 538$ plates) and (b) component 2 collected at 95% purity ($N = 275$ plates).

On the other hand, the number of injections per unit time increases with increasing flow-rate as retention times are inversely proportional to the flow-rate. Accordingly, there must be a production rate optimum flow-rate. This turns out to be true in the general case but this optimum flow-rate is much higher than the efficiency optimum flow-rate. It corresponds to an analytical resolution of about 1 for component 1 for highly pure fractions and less than 1 for 95% purity. By accepting the loss of recovery associated with the use of strongly interfering bands, it is possible to improve the production rates of a preparative chromatograph by nearly an order of magnitude. The relative maximum production rates of compounds 1 and 2 are not in the ratio of their proportions in the injected mixture, however, and these maximum rates are reached for different linear velocities and different amounts injected.

REFERENCES

- 1 G. Guiochon, in B. L. Shapiro (Editor), *New Directions in Chemical Analysis*, Texas A&M University Press, College Station, TX, 1985, p. 84.
- 2 P. Rouchon, M. Shonauer, P. Valentin and G. Guiochon, in F. Bruner (Editor), *The Science of Chromatography*, Elsevier, Amsterdam, 1985, p. 131.
- 3 S. Ghodbane and G. Guiochon, *J. Chromatogr.*, 440 (1988) 9.
- 4 E. Kováts, in F. Bruner (Editor), *The Science of Chromatography*, Elsevier, Amsterdam, 1985, p. 205.
- 5 D. DeVault, *J. Am. Chem. Soc.*, 65 (1943) 532.
- 6 G. Guiochon and L. Jacob, *J. Chromatogr.*, 14 (1971) 77.
- 7 G. Guiochon, S. Golshan-Shirazi and A. Jaulmes, *Anal. Chem.*, in press.
- 8 B. Lin and G. Guiochon, *Sep. Sci. Technol.*, in press.
- 9 S. Golshan-Shirazi, S. Ghodbane and G. Guiochon, *Anal. Chem.*, in press.
- 10 J. C. Giddings, *Dynamics of Chromatography*, Marcel Dekker, New York, 1965.
- 11 J. H. Knox and M. Saleem, *J. Chromatogr. Sci.*, 7 (1969) 745.
- 12 G. Guiochon, in C. Horváth (Editor), *High Performance Liquid Chromatography*, Academic Press, New York, 1980, p. 1.
- 13 J. E. Eble, R. L. Grob, P. E. Antle and L. R. Snyder, *J. Chromatogr.*, 384 (1987) 25.
- 14 J. H. Knox and H. M. Pyper, *J. Chromatogr.*, 363 (1986) 1.
- 15 S. Ghodbane and G. Guiochon, *J. Chromatogr.*, 444 (1988) 275.
- 16 G. Guiochon and S. Ghodbane, *J. Phys. Chem.*, 92 (1988) 3682.
- 17 S. Ghodbane and G. Guiochon, *J. Chromatogr.*, 450 (1988) 27.

CHROM. 20 719

CONTRIBUTION OF ELECTRONIC EFFECTS TO THE LIPOPHILICITY DETERMINED BY COMPARISON OF VALUES OF LOG *P* OBTAINED BY HIGH-PERFORMANCE LIQUID CHROMATOGRAPHY AND CALCULATION*

J. TIPKER, C. P. GROEN, J. K. VAN DEN BERGH-SWART and J. H. M. VAN DEN BERG*
Duphar B.V., Analytical Development Department, P.O. Box 2, 1380 AA Weesp (The Netherlands)

SUMMARY

In a series of 49 aryl sulphoxides, the partition coefficients (log *P*) estimated by high-performance liquid chromatography were compared with log *P* values calculated according to the hydrophobic fragmental method of Rekker and a modification of the method of Moreau. Moderate correlations were found. The introduction of Hammett sigma values as a measure of electronic effects proved to be good correction factors for the calculated log *P* values. In the presence of strong electron-withdrawing substituents, the sulphoxide moiety is far less hydrophobic than in the absence of such groups.

INTRODUCTION

The partition of a compound between water and an organic phase, generally expressed as log *P*, seems to be the most important parameter in quantitative structure activity relationships (QSAR). The log *P* values obtained from an *n*-octanol–water system are commonly used because of the ability of *n*-octanol to simulate biological membranes. In order to predict biological activities from equations derived in QSAR experiments, not only experimentally obtained log *P* values but also calculated ones are necessary.

Different methods of calculating partition coefficients have been described. In 1973 Rekker introduced the hydrophobic fragmental constant. These constants were obtained from regression analysis of experimental log *P* values. Corrections have to be made for proximity effects, cross-conjugation, etc. If correction is necessary, it has to be done by adding a “magic constant”¹ to the original calculated log *P*. In our study, the Rekker method is one of the procedures used to calculate log *P*.

The Hansch and Leo approach² is also based upon a fragmental method. Their constants were obtained from very precise log *P* measurements on simple molecules. They introduced a lot of correction factors, depending upon the type of binding,

* This paper was presented in part at the *11th International Symposium on Column Liquid Chromatography, Amsterdam, June 1987*, and the *International Mini-Symposium on Estimation and Determination of Partition Coefficients of Drugs and Related Compounds, Stockholm, October 1987*.

proximity effects, *ortho-ortho* interactions, the possibility of hydrogen bonds and influences of electronic effects.

Broto *et al.*³ developed a somewhat different method. From about 1800 experimental $\log P$ values, more than 200 atomic contributions were extracted by regression analysis. These atomic constants are defined by their atom type, binding pattern and the character of the bonded atoms. The only correction is for conjugated double bonds. In our laboratory a combined Moreau/Hansch method has been developed and more than 500 atomic constants were calculated from over 2500 experimental $\log P$ values. Corrections are necessary for *ortho-ortho* and hydrogen-bond interactions, and electronic effects⁴. Values of $\log P$ calculated by this method are also used in this study.

Beside calculated $\log P$ values, there is a need for experimentally determined ones. The traditional shake-flask method is time consuming, requires very pure chemicals and can be used only within a certain range of $\log P$ values. Some of these objections are associated with high-performance liquid chromatographic (HPLC) methods.

The prediction of $\log P$ in *n*-octanol–water using HPLC has been shown to be of value^{5,6}, depending on the nature of the compounds⁷. The use of reversed-phase HPLC systems with surfactants in the mobile phase is especially useful for ionizable substances^{8–10}. Interaction between different functional groups within the molecule affects the actual lipophilicity. Deviations between HPLC measurements and computer calculated values of $\log P$ have been reported¹¹.

In this study, HPLC $\log P$ values for aryl sulphoxides are compared with calculated ones. The influence of electronic factors is considered by means of regression analysis. As a measure of electronic factors, the Hammett σ and *para* σ values are used.

EXPERIMENTAL

Apparatus

The liquid chromatograph consisted of an high-pressure pump (S1000; Sykam, F.R.G.), an autosampler (231-401; Gilson, U.S.A.) equipped with a 5- μ l loop, a stainless-steel column (50 mm \times 4.6 mm I.D.) and a variable-wavelength UV detector (Kratos, Spectroflow 757, ABI, U.S.A.). The column was thermostatted at $22 \pm 0.1^\circ\text{C}$ by means of a water jacket connected to a cryostat bath (Colora WK 4; Braun Melsungen, F.R.G.). The detector signal at 254 nm was recorded by an integrator (HP 3392; Hewlett-Packard, Avondale, PA, U.S.A.).

Materials

HPLC-grade methanol, acetonitrile (J. T. Baker, U.S.A.) and doubly distilled water were used to prepare the mobile phase, which was sparged with helium before use. All other chemicals were of analytical reagent grade. The solutes were commercially available or made by the Duphar laboratory¹². The stationary phase consisted of chemically modified silica gel, phenyl-Rosil, 5 μm (Alltech, Belgium).

Procedures

The column was packed by a pressurized slurry technique with *n*-propanol–

tetrachloromethane (1:4) as the slurry liquid and *n*-hexane as the displacer liquid. The maximum packing pressure was 60 MPa. The column was washed with tetrahydrofuran followed by methanol–water (9:1) and equilibrated with the mobile phase until the retention was constant.

The mobile phase was prepared by dissolving 0.7 g $\text{NaH}_2\text{PO}_4 \cdot \text{H}_2\text{O}$ in 450 ml water, adjusting the pH to 3.0 with phosphoric acid and mixing with 1.0 g sodium dodecyl sulphate and 14.0 g sodium perchlorate dissolved in 550 ml methanol. Potassium dichromate was used as a non-retained compound.

A linear regression was established from $\log k'$ (k' = capacity factor) and literature values of $\log P$ in *n*-octanol–water for neutral (Nos. 1–9) and basic (Nos. 10–14) solutes as given in Table I. The HPLC $\log P$ values were determined from linear regression according to

$$\log P_{n\text{-octanol-water}} = 2.16 \log k' \frac{t \text{ value}}{19.65} + 1.19 \quad (1)$$

$$n = 14 \quad r = 0.985 \quad s = 0.267 \quad F = 386.2$$

where n is the number of data, r is the correlation coefficient, s is the standard error of the estimate, F is a measure of the significance of the correlation and the t value is the Student t test. Each day a calibration was performed twice, before and after a series of seven compounds for which $\log P$ was to be determined. The $\log P$ values were determined from the means of at least two measurements on different days.

RESULTS AND DISCUSSION

Measurements of $\log P_{\text{HPLC}}$ were performed for 49 aryl sulphoxides as described. The correlation coefficient of the linear regression according to eqn. 1 ranged from

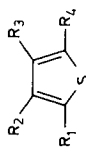
TABLE I
COMPOUNDS USED FOR THE LINEAR REGRESSION

Literature values of $\log P$ in *n*-octanol–water and measured values of $\log k'_{\text{HPLC}}$:

Code	Compound	$\log P_{n\text{-octanol-water}}$	$\log k'_{\text{HPLC}}$
1	Acetanilide	1.16	0.002
2	Indole	2.14	0.347
3	Nitrobenzene	1.85	0.450
4	Linuron	3.00	0.808
5	<i>p</i> -Xylene	3.18	0.885
6	Naphthalene	3.33	0.932
7	Benzophenone	3.18	1.035
8	Biphenyl	3.91	1.269
9	4,4'-Dichlorobiphenyl	5.28	1.827
10	Procaine	1.87	0.072
11	Atropine	1.80	0.413
12	Haloperidol	4.31	1.610
13	Imipramine	4.70	1.635
14	Pimozide	6.23	2.166

TABLE II
STRUCTURES OF THIENYL SULPHOXIDES USED IN THE CORRELATION STUDIES AND VALUES OF HPLC AND COMPUTER CALCULATED
LOG *P*

(*p*) means *para*-substituted.



No.	R ₁	R ₂	R ₃	R ₄	log <i>P</i>	σ			
						HPLC	Rekker	Moreau	
1	H	H	NO ₂	SOCH ₃	1.69	0.06	0.01	0.83	1.27
2	H	H	NO ₂	SOC ₂ H ₅	2.06	0.58	0.43	0.83	1.27
3	H	H	NO ₂	SOC ₃ H ₇	2.52	1.10	0.89	0.83	1.27
4	H	H	NO ₂	SOCH ₂ CH(CH ₃) ₂	2.93	1.62	1.09	0.83	1.27
5	H	CH ₃	NO ₂	SOCH ₃	2.19	0.58	0.43	0.76	1.20
6	CH ₃	CH ₃	NO ₂	SOCH ₃	2.65	1.15	0.84	0.59	1.03
7	H	C ₆ H ₅	NO ₂	SOCH ₃	3.20	1.72	1.44	0.83	1.27
8	CN	H	CN	SOCH ₃	1.31	-0.42	-0.80	1.37	2.00
9	CN	H	CN	SOC ₂ H ₅	1.78	0.10	-0.38	1.37	2.00
10	CN	H	CN	SOC ₃ H ₇	2.18	0.62	0.08	1.37	2.00
11	CN	H	CN	SOC ₄ H ₉	2.64	1.14	0.55	1.37	2.00

12	CN	Cl	CN	SOCH ₃	2.15	0.33	-0.09	1.74	2.37
13	CN	Cl	CN	SOC ₃ H ₇	2.95	1.37	0.79	1.74	2.37
14	CN	Cl	CN	SOC ₄ H ₉	3.44	1.88	1.25	1.74	2.37
15	COCH ₃	CH ₃	NO ₂	SOC ₂ H ₅	2.81	0.60	0.66	1.25	2.04
16	COCH ₃	Cl	CN	SOC ₂ H ₅	2.64	0.95	0.55	1.57	2.24
17	CN	CH ₃	COCH ₃	SOC ₂ H ₅	2.22	0.72	0.02	1.14	1.77
18	COCH ₃	CH ₃	C ₆ H ₅	SOCH ₃	3.26	2.22	1.89	0.48	0.87
19	COCH ₃	NH ₂	CN	SOC ₂ H ₅	1.82	-0.82	0.22	1.05	1.71
20	COCH ₃	C ₆ H ₄ Cl(p)	CN	SOCH ₃	3.31	2.08	1.69	1.36	2.02
21	COOC ₂ H ₅	H	CN	SOCH ₃	2.27	0.59	0.21	1.16	1.64
22	COCH ₃	CH ₃	C ₆ H ₄ Cl(p)	SOCH ₃	3.82	2.96	2.60	0.63	0.80
23	CN	OCH ₃	CN	SOCH ₃	2.02	-0.33	-0.47	1.49	2.12
24	CN	CH ₃	C ₆ H ₅	SOCH ₃	3.36	2.12	1.58	0.64	1.00
25	CN	CH ₃	C ₆ H ₅	SOCH ₃	3.80	2.86	2.29	0.72	0.92
26	COCH ₃	NH ₂	C ₆ H ₄ Cl(p)	SOCH ₃	3.18	1.42	2.31	0.54	0.73
27	NO ₂	H	C ₆ H ₄ Cl(p)	SOCH ₃	1.40	0.06	0.24	0.83	1.27
28	H	H	CN	SOCH ₃	0.96	-0.06	-0.27	0.71	1.00
29	H	H	SOCH ₃	H	0.91	0.29	0.26	0.05	0.00
30	H	H	H	SOCH ₃	0.91	0.29	0.26	0.05	0.00
31	H	H	Br	SOCH ₃	1.71	1.23	0.92	0.28	0.28
32	COCH ₃	H	H	SOC ₂ H ₅	1.31	0.56	0.46	0.55	0.87
33	CN	OCH ₃	CN	SOC ₂ H ₅	2.35	0.18	-0.05	1.49	2.12
34	Cl	H	CN	SOC ₂ H ₅	2.31	1.20	0.85	0.94	1.27
35	COCH ₃	CH ₃	CN	SOC ₂ H ₅	2.22	0.72	0.38	1.21	1.77

0.984 to 0.988. The reproducibility of the determination was 1.5% ($n = 49$).

In Table II the parameters for 35 thienyl sulphoxides are mentioned. In the column containing the sigma values the sum of the Hammett sigma values is used without the values for the SO-alkyl substituents; for the thienyl S a value of 0.05 is taken and R_1 and R_3 are considered as *para* and *ortho* to R_4 (the sulphoxide position). For the *ortho* and *para* positions the same sigma value is taken. The *para* sigma column contains the sum of the *para* sigma values of R_1 and R_3 and of the normal Hammett *meta para* sigma values of R_2 . *Para* sigma values are also chosen as they are sometimes of importance in reactions containing thiophens¹³. All sigma values are taken from Hansch and Leo¹⁴.

The correlation between both calculated values is expressed in eqn. 2:

$$\log P_{\text{Rekker}} = 1.00 \log P_{\text{Moreau}} + 0.24 \quad t \text{ value } 12.78 \quad (2)$$

$$n = 35 \quad r = 0.912 \quad s = 0.372 \quad F = 163.3$$

The relative low correlation coefficient, r is caused by two outliers, the compounds 19 and 26 containing a NH_2 group. In our Moreau approach these are electronic corrections so that the NH_2 group is less polar due to the presence of electron-withdrawing substituents. In Fig. 1 the relationship is shown between the calculated values according to Rekker and the HPLC values:

$$\log P_{\text{HPLC}} = 0.75 \log P_{\text{Rekker}} + 1.67 \quad t \text{ value } 9.01 \quad (3)$$

$$n = 35 \quad r = 0.843 \quad s = 0.437 \quad F = 81.2$$

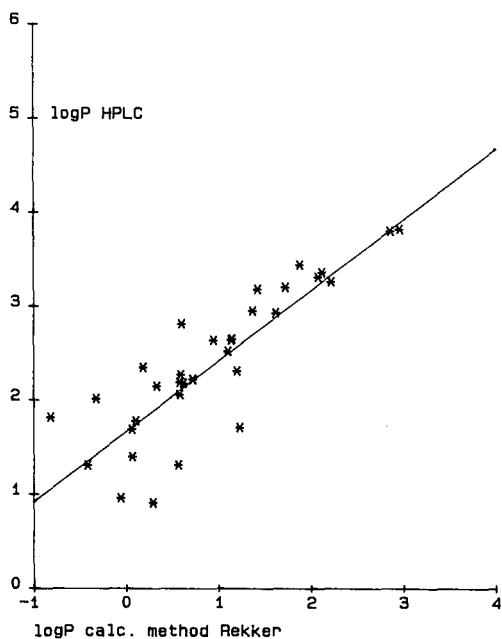


Fig. 1. Relationship between $\log P$ calculated according to Rekker and $\log P_{\text{HPLC}}$ for 35 thienyl sulphoxides.

The intercept is far from zero and the slope is much smaller than the expected value of one. The values of $\log P$ calculated by the Moreau method are plotted against the HPLC values in Fig. 2. Eqn. 4 is the corresponding equation.

$$\log P_{\text{HPLC}} = 0.79 \log P_{\text{Moreau}} + 1.83 \quad \begin{array}{l} t \text{ value} \\ 7.74 \end{array} \quad (4)$$

$$n = 35 \quad r = 0.803 \quad s = 0.484 \quad F = 59.8$$

The results are less good than those shown in eqn 3. Also the intercept is high and the slope lower than one. One reason for such large deviations may be an underestimate of the contribution of the SO moiety to the calculated $\log P$ values in the presence of strong electron-withdrawing groups. Eqns 5–8 show how the correlations can be improved by adding σ values to the regression analyses:

$$\log P_{\text{HPLC}} = 0.81 \log P_{\text{Rekker}} + 0.64 \sigma + 0.98 \quad \begin{array}{l} t \text{ value} \\ 12.81 \\ 5.26 \end{array} \quad (5)$$

$$n = 35 \quad r = 0.919 \quad s = 0.325 \quad F = 87.2$$

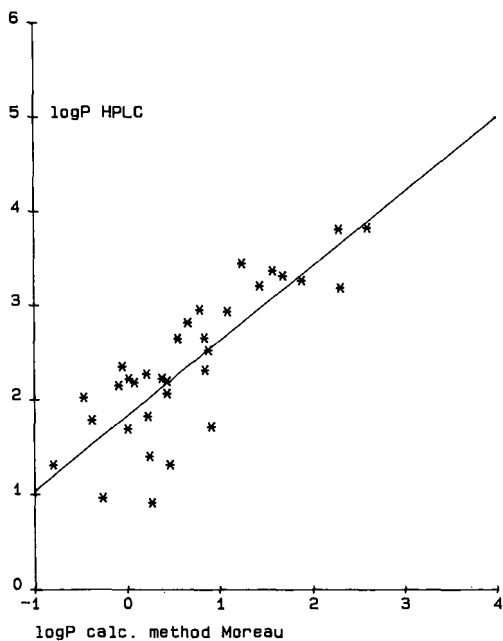


Fig. 2. Relationship between $\log P$ calculated according to Moreau and $\log P_{\text{HPLC}}$ for 35 thienyl sulphoxides.

$$\log P_{\text{HPLC}} = \begin{array}{r} 0.82 \log P_{\text{Rekker}} \\ +0.49 \text{ para } \sigma \\ +0.90 \end{array} \begin{array}{r} 13.96 \\ 6.08 \end{array} \quad (6)$$

$$n = 35 \quad r = 0.931 \quad s = 0.302 \quad F = 103.3$$

$$\log P_{\text{HPLC}} = \begin{array}{r} 0.96 \log P_{\text{Moreau}} \\ +0.94 \sigma \\ +0.80 \end{array} \begin{array}{r} 16.84 \\ 9.28 \end{array} \quad (7)$$

$$n = 35 \quad r = 0.951 \quad s = 0.256 \quad F = 150.2$$

$$\log P_{\text{HPLC}} = \begin{array}{r} 0.97 \log P_{\text{Moreau}} \\ +0.68 \text{ para } \sigma \\ +0.73 \end{array} \begin{array}{r} 18.63 \\ 10.48 \end{array} \quad (8)$$

$$n = 35 \quad r = 0.959 \quad s = 0.233 \quad F = 183.5$$

The result of eqn. 8 is visualized in Fig. 3.

It is obvious that electronic effects strongly influence the hydrophobic character of the sulphoxide moiety. The best correction is effected by sigma constants, especially to the Moreau values. The slope is nearly one, but the intercept is still far from zero. In order to investigate whether this is due to the thienyl basic structure, the log *P* values of some other sulphoxides were estimated. The results are shown in Table III.

The σ value for one aromatic nitrogen is assigned the value for a NO₂ group, and for two nitrogens 1.5 times that value, because of mutual interactions. The results of the regression analyses are shown in eqns. 9–12:

$$\log P_{\text{HPLC}} = \begin{array}{r} 1.09 \log P_{\text{Rekker}} \\ +1.70 \end{array} \begin{array}{r} t \text{ value} \\ 5.51 \end{array} \quad (9)$$

$$n = 14 \quad r = 0.850 \quad s = 0.601 \quad F = 31.1$$

$$\log P_{\text{HPLC}} = \begin{array}{r} 1.00 \log P_{\text{Moreau}} \\ +1.75 \end{array} \begin{array}{r} 7.76 \end{array} \quad (10)$$

$$n = 14 \quad r = 0.913 \quad s = 0.465 \quad F = 60.2$$

$$\log P_{\text{HPLC}} = \begin{array}{r} 1.16 \log P_{\text{Rekker}} \\ +0.67 \sigma \\ +0.85 \end{array} \begin{array}{r} 6.71 \\ 2.22 \end{array} \quad (11)$$

$$n = 14 \quad r = 0.899 \quad s = 0.522 \quad F = 23.1$$

$$\log P_{\text{HPLC}} = \begin{array}{r} 1.07 \log P_{\text{Moreau}} \\ +0.76 \sigma \\ +0.78 \end{array} \begin{array}{r} 13.12 \\ 4.50 \end{array} \quad (12)$$

$$n = 14 \quad r = 0.970 \quad s = 0.288 \quad F = 88.3$$

The correlation between the calculated $\log P$ values and the experimental values is much better for $\log P$ derived from the Moreau method. However, the intercept remains approximately. By use of all the compounds and regression analysis with only the Moreau values, eqns. 13 and 14 are obtained:

$$\log P_{\text{HPLC}} = 0.87 \log P_{\text{Moreau}} + 1.80 \quad t \text{ value } 10.96 \quad (13)$$

$$n = 49 \quad r = 0.848 \quad s = 0.479 \quad F = 120.2$$

$$\log P_{\text{HPLC}} = 0.98 \log P_{\text{Moreau}} + 0.86 \sigma + 0.82 \quad t \text{ value } 21.23 \quad (14)$$

$$n = 49 \quad r = 0.955 \quad s = 0.271 \quad F = 238.4$$

The results of eqns. 13 and 14 are visualized in Figs. 4 and 5. Fig. 5 shows a very good correlation, but the intercept remains about 0.80, the same as in eqn. 8 and 12. It is known^{11,15} that sulphones and sulphoxides often show disagreement with respect to partition behaviour. The "real" *n*-octanol-water partition coefficient of compound 42 is known^{1,14} as 0.50. So it is possible that all HPLC values are about 0.55 too high in relation to the "shake-flask" values. When corrected in such a way, Fig. 6 shows the result. The remaining intercept of 0.27 is hardly significant and probably caused by the error in the value for atomic sulphur in the Moreau approach.

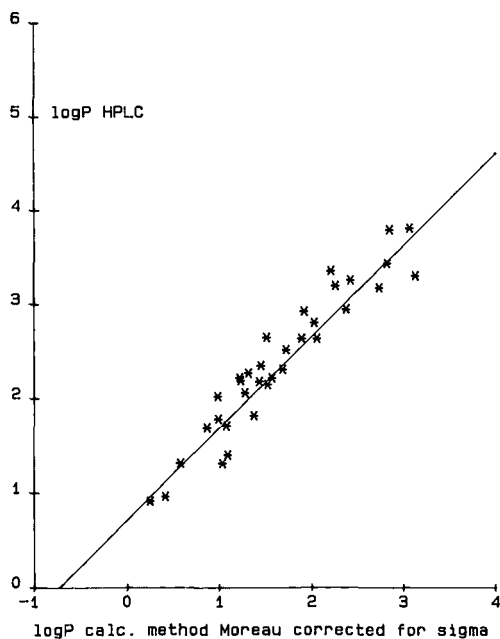


Fig. 3. Relationship between $\log P$ calculated according to Moreau with σ correction factors and $\log P_{\text{HPLC}}$ for 35 thienyl sulphoxides.

TABLE III

STRUCTURES OF ARYL SULPHOXIDES USED IN THE CORRELATION STUDIES AND VALUES OF HPLC AND COMPUTER CALCULATED LOG *P*

No.	<i>R</i> ₁	<i>R</i> ₂	<i>R</i> ₃	<i>log P</i>			σ
				HPLC	Rekker	Moreau	
36	COC ₂ H ₅	NO ₂	SOC ₂ H ₅	2.80	1.04	0.77	1.28
37	COC ₅ H ₁₁	NO ₂	SOC ₂ H ₅	4.36	2.59	2.16	1.28
38	COC ₆ H ₅	NO ₂	SOC ₂ H ₅	3.82	1.66	1.86	1.21
39	NO ₂	CN	SOC ₂ H ₅	2.15	0.42	0.19	1.44
40		NO ₂	SOC ₂ H ₅	5.11	2.24	3.45	0.85
41	Cl	SO ₂ CH ₃	SOC ₂ H ₅	2.31	0.40	0.20	0.95
42	H	H	SOCH ₃	1.04	0.49	0.32	0.00
43				2.10	1.17	0.58	1.24
44				2.43	0.96	1.47	0.78
45				1.74	-0.55	-0.16	1.56
46				1.77	0.37	0.20	1.10
47				2.44	0.14	0.19	2.08
48				2.29	0.31	0.61	1.17
49				3.01	1.06	1.07	1.71

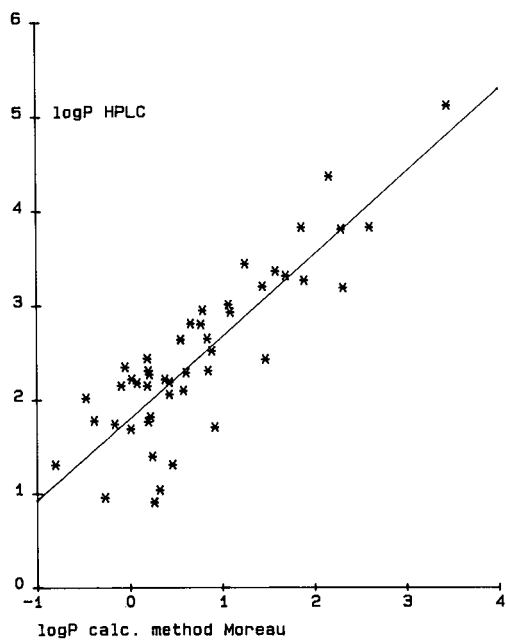


Fig. 4. Relationship between $\log P$ calculated according to Moreau and $\log P_{\text{HPLC}}$ for 49 aryl sulphoxides.

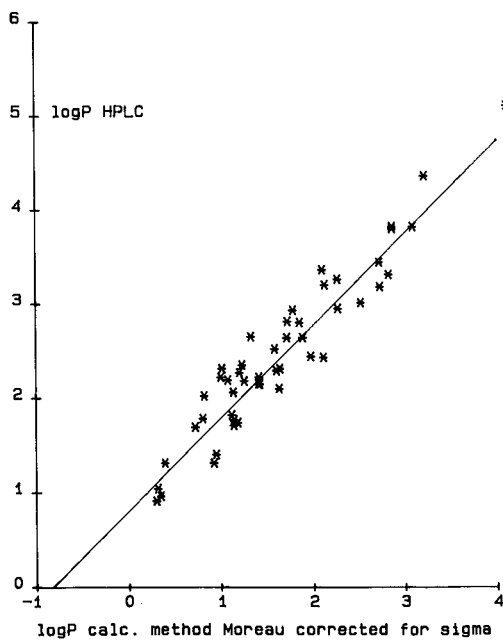


Fig. 5. Relationship between $\log P$ calculated according to Moreau with σ correction factors and $\log P_{\text{HPLC}}$ for 49 aryl sulphoxides.

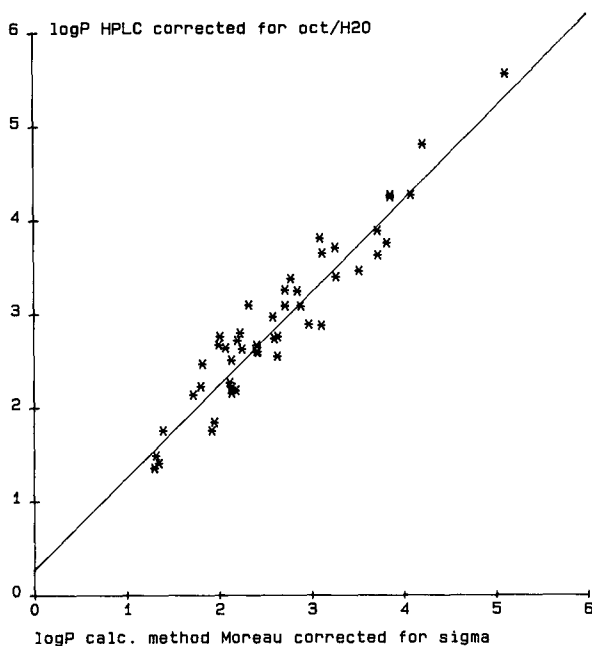


Fig. 6. Relationship between $\log P$ calculated according to Moreau with correction factors for σ and $\log P_{\text{HPLC}}$ corrected for the SO moiety of 49 aryl sulphoxides.

CONCLUSIONS

The hydrophobic properties of the sulphoxide moiety, substituted into an aromatic nucleus, is strongly dependent on the electronic character of other substituents attached to that nucleus. Electron-withdrawing groups increase hydrophobicity. In the case of thienyl derivatives, the *para* σ substituent constants seem to be the best correction factors for calculated $\log P$ values. For aromatic systems in general, the Hammett constants are suitable to correct calculated $\log P$ values in order to get good correlations with $\log P$ values estimated by HPLC. The equation finally obtained for 49 aryl sulphoxides is:

$$\begin{aligned} \log P_{\text{HPLC}} = & 0.98 \log P \text{ calc.} & t \text{ value} & 21.23 \\ & + 0.86 \sigma & & 10.05 \\ & + 0.82 & & \\ n = 49 & r = 0.955 & s = 0.271 & F = 238.4 \end{aligned}$$

The remaining intercept of 0.82 is possibly caused by a systematic overestimation of the hydrophobicity of the sulphoxide moiety by HPLC in relation to the "shake-flask" method.

ACKNOWLEDGEMENT

The authors thank Dr. F. J. Spruit for this stimulating discussions and helpful suggestions in the preparation of this article.

REFERENCES

- 1 R. F. Rekker, *The Hydrophobic Fragmental Constant —Its Derivation and Application— A Means of Characterizing Membrane Systems*, Elsevier, Amsterdam, 1977.
- 2 A. Leo, P. Y. C. Jow, C. Silipo and C. Hansch, *J. Med. Chem.*, 18 (1975) 865.
- 3 P. Broto, G. Moreau and C. Vandycke, *Eur. J. Med. Chem.*, 19 (1984) 71.
- 4 J. Tipker, in preparation.
- 5 T. Brauman, *J. Chromatogr.*, 373 (1986) 191.
- 6 H. Terada, *Quant. Struct.-Act. Relat.*, 5 (1986) 81.
- 7 K. Miyake, N. Mizuno and H. Terada, *Chem. Pharm. Bull.*, 34 (1986) 4787.
- 8 J. L. G. Thus and J. C. Kraak, *J. Chromatogr.*, 320 (1985) 271.
- 9 J. C. Kraak, H. H. van Rooij and J. L. G. Thus, *J. Chromatogr.*, 352 (1986) 455.
- 10 F. Gago, J. Alvarez-Builla, J. Elguero and J. C. Diez-Masa, *Anal. Chem.*, 59 (1987) 921.
- 11 J. J. Sabatka, D. J. Minick, T. K. Shumaker, G. L. Hodgson and B. A. Brent, *J. Chromatogr.*, 384 (1987) 349.
- 12 H. Dolman and J. Kuipers, *Neth. Pat. Appl.*, 8 600 416 (1986).
- 13 C. Dell'Erba and D. Spinelli, *Tetrahedron*, 21 (1965) 1061.
- 14 C. Hansch and A. Leo, *Medicinal Chemistry Project Database*, Pomona College, Claremont, CA, July 1984.
- 15 A. Verloop, in E. J. Ariens (Editor), *Drug Design*, Vol. III, Academic Press, New York, 1972, pp. 133–187.

CHROM. 20 755

EFFECTS OF SYSTEM PEAKS IN ION-PAIR REVERSED-PHASE LIQUID CHROMATOGRAPHY FOR NOSCAPINE AND METABOLITES

MARGARETA JOHANSSON

Department of Research and Development, ACO Läkemedel AB, Box 3026, 171 03 Solna (Sweden)
and

DOUGLAS WESTERLUND*

Department of Analytical Pharmaceutical Chemistry, Uppsala University, Box 574, 751 23 Uppsala (Sweden)

SUMMARY

System peaks were generated in an ion-pair reversed-phase system by co-injection of an alkylsulphate with the analytes. The acidic mobile phase contained acetonitrile and an aliphatic tertiary amine as a co-ion. The retention time of the system peak was regulated by the concentration and hydrophobicity of the co-ion and the alkylsulphate. The peak performance of the analytes was affected by co-elution with a system peak. Both peak distortions and improvements appeared, and the principles for the latter could be applied in a dual-column system involving trace enrichment and column switching.

INTRODUCTION

Ion-pair-reversed phase liquid chromatography is widely used for the separation of ionizable compounds. The ionic reagent is normally a component of the mobile phase. In order to achieve special effects with respect to retention and/or efficiency, an ionic compound may be injected before¹ or at the same time as the analytes^{2,3} or at pulsed intervals during the separation^{4,5}. Injection of a solution with a composition deviating from the mobile phase gives rise to disturbances in the established equilibria in the column. These disturbances are registered as peaks or zones with a refractive index (RI) detector using a common UV-transparent mobile phase, or they can be monitored with a UV detector, if the mobile phase contains at least one UV-absorbing compound that participates in the disturbed equilibria. Each component in the injected solution, which deviates from the mobile phase, gives rise to two kinds of peaks. One is the ordinary peak corresponding to the injected compound and the other originates from the disturbances of the equilibria described above, and is due to changes in the concentrations of mobile phase components. The retention time of the latter kind of peaks is characteristic of the mobile phase component from which the peak or zone originates^{6–10}. It is called the system peak (or system zone), as it is characteristic of the actual chromatographic system.

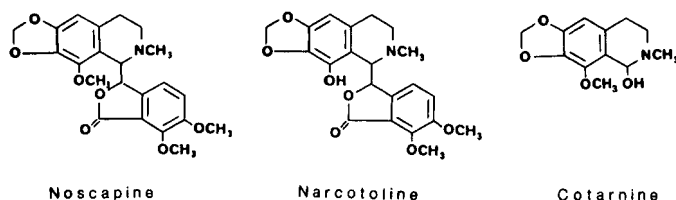


Fig. 1. Structures of noscapine, narcotoline and cotarnine.

Co-elution of an analyte with the zone may affect the peak shape in different ways, giving either distorted or improved peak performance. In a system with an acidic mobile phase containing a tertiary aliphatic amine it was possible to achieve an extremely compressed analyte peak for a cationic benzamide which co-eluted with the back of a system peak, created by the co-injection of an organic alkylsulphonate².

The aim of this work was to study the conditions for the peak compression of noscapine, narcotoline and cotarnine (Fig. 1). The analytes were injected on to the analytical column in a solution containing octyl- or decylsulphate in high concentrations. Correlations between the peak performance of the analytes and the retention of the system peak were studied using an RI and a UV detector coupled in series.

The conditions established for peak compression of noscapine were applied in a dual-column system. The analytes were enriched as ion pairs on a small polar precolumn, with a mobile phase containing alkylsulphate and a low content of acetonitrile, followed by back-flushing to the analytical column with a mobile phase including a tertiary aliphatic amine and a higher content of acetonitrile.

EXPERIMENTAL

Chemicals

The sodium salts of octyl- and decylsulphate were obtained from Eastman Kodak (Rochester, NY, U.S.A.). N,N-Dimethyl-N-octylamine (DMOA), N,N-dimethyl-N-hexylamine (DMHA) and N,N-dimethyl-N-dodecylamine (DMDDA) were obtained from ICN Pharmaceuticals (Plainview, NY, U.S.A.). Noscapine was obtained from Macfarlan Smith (Edinburg, U.K.), cotarnine chloride dihydrate from EGA-Chemie (Albuch, F.R.G.) and narcotoline from Diosynth-Apeldoorn (Oss, The Netherlands). All other chemicals were of analytical-reagent or HPLC grade.

LC apparatus

The chromatographic system consisted of an LKB 2150 pump (LKB, Bromma, Sweden), a Waters M 45 pump (Waters Assoc., Milford, MA, U.S.A.), a Kontron Tracer MCS 670 valve-switching unit with a Tracer timer 210 (Kontron, Zürich, Switzerland) and a Waters WISP 710 B automatic injector. The UV absorbance was monitored at 310 or 210 nm with a Spectroflow 783 (Kratos Analytical, Ramsey, NJ, U.S.A.) and the refractive index was monitored with a Waters Model R 401 refractometer. The recorder was a dual-channel Servogor 220 (Gortz, Vienna, Australia) and the integrator was a Shimadzu C-R3A (Shimadzu, Kyoto, Japan).

Chromatographic system

The analytical column (100 × 4.6 mm or 100 × 4.0 mm I.D.) was packed with Nucleosil C₁₈ (3 μm) from Machery, Nagel & Co. (Düren, F.R.G.). In the dual-column system the precolumn (20 × 3.8 mm I.D.) was packed with Nucleosil C₄ (5 μm). The columns were packed with dichloromethane as the slurry medium and methanol as the eluent. The mobile phase consisted of various concentrations of an aliphatic tertiary amine in different percentages of acetonitrile in phosphate buffer (pH 2) ($\mu = 0.05$).

The analytes were dissolved in phosphate buffer (pH 2) ($\mu = 0.05$) containing octyl- or decylsulphate (0, 0.01–0.10 M) and 200 μl were injected on to the analytical column. In the dual-column system the analytes were dissolved in phosphate buffer (pH 2) ($\mu = 0.05$) and 500 μl were injected on to the precolumn.

Calculation of plate height

The plate number was calculated from the retention time and the peak width at half-height. This is not correct when the analyte elutes in a gradient; however, in this study such calculations were made only for comparisons of the peak performances.

Mass spectrometry

The mass spectrometer was a Shimadzu QP 1000 equipped with a direct inlet probe. The probe temperature was programmed from room temperature to 250°C at 80°C/min. Electron-impact ionization was performed at 70 eV. The mass was scanned from m/z 38 to 400 with a cycle time of 4 s. The presence of sulphate ions was monitored using the reconstructed ion chromatogram (RIC) of the ions of m/z 48 and 64.

Fractions of mobile phase from the LC system collected between 2–12 min (2-ml portions), 22–24 min, 2.5–3 h (5-ml portions) and 4–4.08 h (5-ml portions). The time for fraction collection was decided by monitoring the RI detector (2–12 min) and the UV detector at 210 nm (12 min–4.5 h).

An aliquot of the fractions (1 or 2 ml) was mixed with 0.5 ml of phosphate buffer (pH 2, $\mu = 0.05$), containing 2.5 mM DMOA, before extraction with dichloromethane. After centrifugation, 2 μl of the organic phase were evaporated at the direct probe.

THEORY

It has been found in ion-pair chromatography that solid phases of the hydrophobized silica gel type seem in most instances to contain at least two different adsorption sites with different total adsorption capacities and affinities^{11,12}. The retentions of both analytes and mobile phase components (system peak) are determined by the partial derivative of the adsorption isotherm at the actual mobile phase composition. However, as the analyte concentration from the start of elution is zero, whereas those of the mobile phase components are non-zero, different retention equations will result^{9,13}. When the analyte concentrations are high and influence the retention and peak shape, no exact theory is yet available. Empirically it has been found that when high analyte concentrations are injected the retention volume will be influenced as if the denominator contained an additional term including the analyte concentration,

according to eqns. 1 and 2. These equations are derived from simplified models relating the capacity ratios directly to distribution. They can be useful for qualitative discussions about retention.

Cationic analyte, HA⁺:

$$V_{N,HA} = \frac{W_s K_0 K_{HAX} [X^-]_m}{1 + K_{QX} [Q^+]_m [X^-]_m + K_{HAX} [HA^+]_m [X^-]_m} + \frac{W_s K_0^* K_{HAX}^* [X^-]_m}{1 + K_{QX}^* [Q^+]_m [X^-]_m + K_{HAX}^* [HA^+]_m [X^-]_m} \quad (1)$$

Anionic analyte, Z⁻:

$$V_{N,Z} = \frac{W_s K_0 K_{QZ} [Q^+]_m}{1 + K_{QX} [Q^+]_m [X^-]_m + K_{QZ} [Q^+]_m [Z^-]_m} + \frac{W_s K_0^* K_{QZ}^* [Q^+]_m}{1 + K_{QX}^* [Q^+]_m [X^-]_m + K_{QZ}^* [Q^+]_m [Z^-]_m} \quad (2)$$

System peak:

$$V_{N,Q} = W_s \cdot \frac{\partial C_{Q,s}}{\partial C_{Q,m}} = \frac{W_s K_0 K_{QX} [X^-]_m}{(1 + K_{QX} [Q^+]_m [X^-]_m)^2} + \frac{W_s K_0^* K_{QX}^* [X^-]_m}{(1 + K_{QX}^* [Q^+]_m [X^-]_m)^2} \quad (3)$$

where V_N = net retention volume, W_s = weight of solid phase, K_0 , K_0^* = total adsorption capacity of the two sites, K , K^* = equilibrium constants, Q^+ = mobile phase component (tertiary aliphatic amine) and X^- = buffer component (dihydrogenphosphate); the subscript m denotes mobile phase.

The system peaks will be positive or negative depending on the disturbance of the adsorption equilibria⁶⁻⁹.

RESULTS AND DISCUSSION

Origin of system peaks

The injection of a solution deviating in composition from the mobile phase may give rise to system peaks. One such peak is obtained for each component in the mobile phase, which participates in an interaction common with a compound in the injected solution. The retention times of the system peaks are characteristic of the mobile phase component from which respective peak originates. System peaks are only detected when retarded from the front disturbances and when at least one of the mobile phase components involved in the disturbed equilibria gives a detector response. As RI detection provides an almost general response, most system peaks present will be registered, whereas an UV-absorbing mobile phase component is necessary for UV

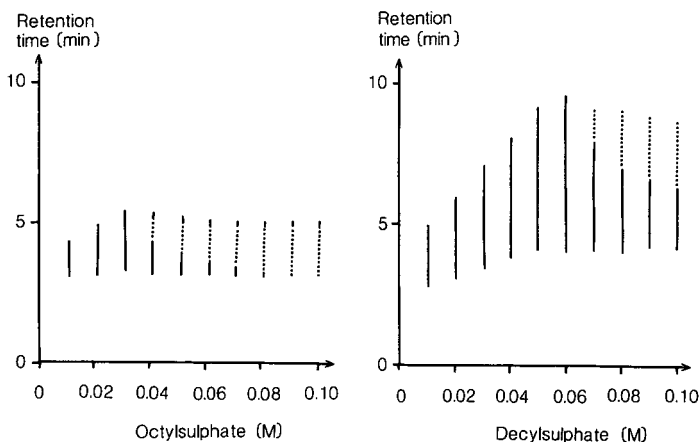


Fig. 2. Width and retention times of the system peak (DMOA) (solid lines) and octyl- or decylsulphate peaks (broken lines). Mobile phase, 2.5 mM DMOA in 25% (v/v) of acetonitrile in phosphate buffer (pH 2).

detection. The direction of the system peak, *i.e.*, positive or negative in relation to the baseline, is determined by the charge and relative retention of the solutes relative to the component from which the system peak originates⁶⁻⁹.

In this study, system peaks were generated by the injection of octyl- or decylsulphate (0.01–0.1 M) into an acidic mobile phase with acetonitrile (25%, v/v) and containing an aliphatic tertiary amine, *i.e.*, DMHA, DMOA or DMDDA. The widths and retention times of the system peaks (DMOA) monitored by a RI detector after the injection of various concentrations of octyl- or decylsulphate are shown in Fig. 2. Injection of a low concentration of alkylsulphate gave only one peak (peak 1). When the retention time of this peak reached a nearly constant value a second peak (peak 2) appeared with the opposite response direction. The retention time of the second peak decreased with increasing injected concentrations of alkylsulphate, whereas the area of peak 1 increased until the retention had attained a constant level with an increasing injected alkylsulphate concentration. At the level of constant retention time the peak area was difficult to evaluate owing to a disturbance from peak 2. The area of peak 2 increased continuously with increasing concentration of alkylsulphate.

The equations given under Theoretical were used for qualitative interpretations in this paper. An alkylsulphate peak with a longer retention time than that of the induced system peak will contain an excess of tertiary amine in the alkylsulphate peak, leaving a deficiency of this mobile phase component to elute in the system peak. Injection of increasing amounts of alkylsulphate will decrease the amount of tertiary amine in the system peak. The retention of the system peak will increase with a decreasing concentration of the tertiary amine in the peak (see eqn. 3) and the area will also increase. A constant retention time and a constant area may be obtained when the system peak contains a very low concentration of cation (Q^+). This retention behaviour is in accordance with peak 1 on the RI trace, which means that this system peak contains a deficiency of DMOA. The large amount of alkylsulphate

TABLE I

RETENTION TIMES OF SYSTEM PEAKS AND ANALYTES WITH DIFFERENT TERTIARY ALIPHATIC AMINES IN THE MOBILE PHASE

The analytes were injected with 0.1 M of the respective counter ion.

Amine	Concentration (mM)	Counter ion	Retention time (min)			
			System-peak	Cotarine	Narcotine	Noscapine
DMHA	2.5	OS	4	4.2	4.5	13
DMOA	2.5	OS	5	4.5	3.7	5
DMOA	2.5	DS	8	8.6	8.4	9.3
DMOA	0.5	OS	9	5.5	6.8	9
DMDDA	0.5	OS	23	2.5	2.7	6.5

injected may also lead to this compound having a more direct influence on the retention time of the mobile phase component (Q^+) by retaining it as an ion pair during the period of co-elution of the two zones, that is, at the start of elution and during elution for different times depending on the alkylsulphate concentration in each injection.

The retention behaviour of the second peak (alkylsulphate) can be understood qualitatively in light of eqn. 2, which shows that increasing analyte concentrations will decrease the retention. This peak appears first when the system peak has reached a constant retention. It was further observed that very broad peaks with long retention times of about 1.5 and 2.3 h for octylsulphate and decylsulphate, respectively, appeared. The presence of two or three peaks from a homogeneous sample has been reported previously¹⁴⁻¹⁶. One interpretation of this phenomenon involved slow interconversion between two forms of a pure compound¹⁴ and another was based on a dual retention mechanism, *i.e.*, both ion-pair and dynamic ion exchange¹⁶.

In this work the two peaks appeared only when a high concentration of alkylsulphate was injected. It is assuming that at a certain critical concentration of each anion the adsorption capacity of the solid phase is exceeded and only a fraction of this compound is retained with the hydrophobic cation in the injection zone. Then the remaining fraction of the molecules will elute faster, initially only being retained by buffer cations (Q^+ in eqn. 2 then corresponds to Na^+), and in fact being identical with the peak which is detected according to Fig. 2. For the less hydrophobic anion OS the visible critical concentration was about 0.04 M with 2.5 mM DMOA in the mobile phase (*cf.*, Fig. 2) and <0.01 M with 0.5 mM DMOA. For the stronger adsorbed DS the critical concentration was 0.07 M with 2.5 mM DMOA in the mobile phase (*cf.*, Fig. 2).

The hypothesis was supported by mass spectrometric identification of DS both in the early (2-10 min) and the late (2.5-3.0 h) fractions. This is discussed further below.

The stronger adsorption of decylsulphate compared with octylsulphate will deplete the DMOA zone more efficiently. Accordingly, the concentration of DMOA in the deficiency zone will be lower after decylsulphate resulting in a longer retention time (eqn. 3). However, ion-pairing effects during co-elution between the two kinds of

peaks will also be stronger with decylsulphate. The peak width of the system peak was broader with decylsulphate than octylsulphate, although the peak height was about the same. However, the peak height decreased with decreasing concentration of amine in the mobile phase.

The retention of the system peak increases with increasing lipophilicity of the tertiary aliphatic amine (Table I). Further, the retention of the system peaks increases with decreasing concentration of the amine in the mobile phase, qualitatively in accordance with eqn. 3.

Mass spectral identification of alkylsulphate in the LC peaks

The mass spectral (MS) properties of *n*-alkylsulphates with sodium and amines as counter ions have been studied previously¹⁷. In both instances the characteristic fragments from the sulphate were SO^+ , SO_2^+ and SO_3^+ (m/z 48, 64 and 80).

Batch extractions of DS with dichloromethane gave considerably higher recoveries as measured from MS signals from the evaporated dichloromethane when the extraction was performed with a buffer containing DMOA compared with a buffer without the amine. This was probably due to the better extraction properties of DS as an ion pair with DMOA in combination with a higher volatility of the DS-DMOA ion pair compared with the sodium salt of DS.

MS analysis of the collected fractions confirmed that DS was present both in an early peak (2–8 min) and in a very late and broad peak (2.5–3.0 h). No DS was found in a fraction collected between 20 and 22 min or in a very late fraction (4.0–4.1 h). These studies were performed on a solid phase from a different batch than that for the results shown in Figs. 2–4. The retention times for the system and alkylsulphate peaks differ slightly between the two batches, as well as the critical concentration of alkylsulphate exceeding the adsorption capacity. However, the retention behaviour was similar for the two different batches of solid phase.

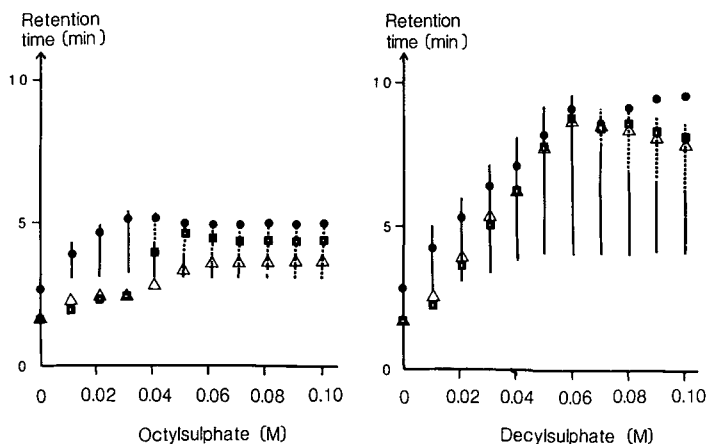


Fig. 3. Retention times of (●) noscapine, (△) narcotoline and (◻) cotarnine co-injected with octyl- or decylsulphate. Chromatographic conditions as in Fig. 2.

Retention times of the analytes as influenced by the co-injected organic anion

Noscapine, narcotoline and cotarnine were injected together with octyl- or decylsulphate in phosphate buffer. With increasing concentration of the organic anion the retention times of the analytes increased until an upper level was reached (octylsulphate); a more complex retention behaviour was obtained with decylsulphate (Fig. 3). The retention times were measured from the middle of the peak when there was no sharp top to the peak. In most instances the analytes elute within the system peak and the special conditions prevailing there with different gradients of the mobile phase components will influence the retention times. A detailed discussion of the retention behaviour of the analytes is therefore difficult. At octylsulphate levels $>0.06 M$ the retention does not change with increasing anion concentrations. This may indicate that the relative influences of DMOA and OS compensate each other in the combined system and octylsulphate peaks at these high levels. However, with decylsulphate the retention of noscapine, the most retarded analyte, increases with increasing decylsulphate concentration (an ion-pairing effect), whereas the opposite behaviour was observed for the polar metabolites. The noscapine peak elutes under these circumstances outside the combined system and DS peaks and was affected by strong ion pairing in the injection zone. The selectivities between the analytes were generally lower with co-injection of decylsulphate than with octylsulphate.

Retention times of the analytes as influenced by the aliphatic tertiary amine in the mobile phase

Addition of an aliphatic amine to the mobile phase has been found to improve the peak shape of cationic analytes owing to competition for adsorption sites¹². With increasing lipophilicity of the competing amine the retention of the analytes will be reduced more effectively (Table I). Further, an increasing concentration of the amine will have a similar effect owing to increasing competition.

Influences of system and alkylsulphate peaks on the analyte peak performance

In trace analysis, involving no preconcentration step, the injection of a large volume may be necessary to achieve the required detection limits. In order to retain the chromatographic efficiency a low eluting strength of the injected solution is essential, as the analytes will then be enriched on the top of the column before elution starts with the bulk mobile phase. Combining this principle with co-injection of an ion-pairing agent a highly compressed analyte peak has been obtained in favourable instances, when the analyte co-elutes with a system zone of suitable composition².

As discussed earlier, both alkylsulphate peaks contain an excess of the tertiary amine, leaving a deficiency of this mobile phase component to elute in the system peak. However, when the adsorption capacity of the solid phase is exceeded the excess of the alkylsulphate will elute in an additional peak that in some instances also has an influence on the analyte peaks.

Decylsulphate

Some typical chromatograms with different concentrations of decylsulphate as the anionic system peak inducer are illustrated in Fig. 4. The RI trace shows the system peak (DMOA-deficient zone) and with increasing anion concentration the area of the peak with the excess of decylsulphate also increases. It is first visible as a

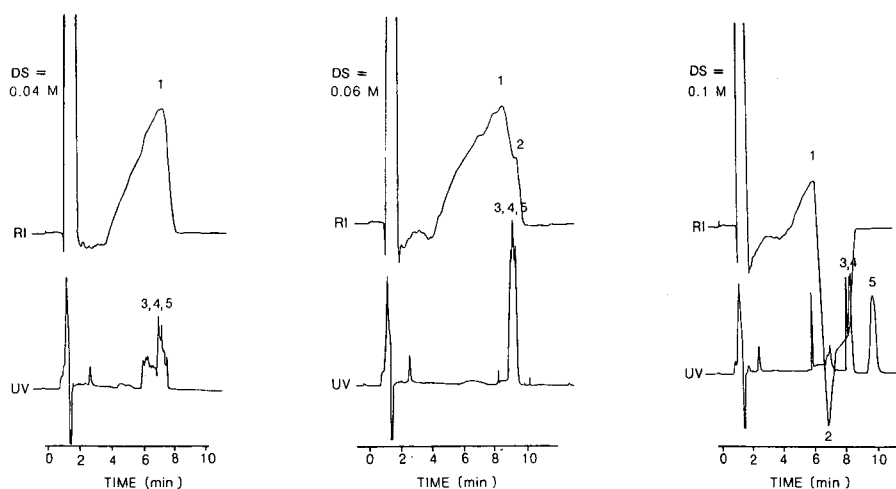


Fig. 4. Simultaneous recording of UV (310 nm) and RI traces. The analytes were dissolved in phosphate buffer (pH 2) containing decylsulphate at the different concentrations indicated. 1 = DMOA deficiency; 2 = decylsulphate; 3 = narcotoline; 4 = cotarnine; 5 = noscapine. Chromatographic conditions as in Fig. 2.

disturbance of the system peak at a concentration of the anion of 0.06 *M*. One fraction of the decylsulphate elutes, as mentioned before, very late after about 2.3 h in a very broad peak outside this part of the chromatogram.

Analyte peaks are seriously disturbed at the lowest concentration of the anion (0.04 *M*) in this example. The compounds elute in the middle of the amine-deficient zone and each analyte seems to give a split peak. At the next higher concentration (0.06 *M*) the three analytes are clearly visible, and all three peaks seem to have a very high performance with a high degree of peak compression. However, the selectivity is low and the peaks are not separated. Here all three components elute at the back part of the system zone, which further is disturbed by a small decylsulphate peak.

The last example (0.10 *M*) shows a complete separation of noscapine from the two metabolites. Noscapine elutes here after both the system zone and the excess alkylsulphate peak, and its chromatographic performance seems to be unaffected by the presence of these zones, its efficiency corresponding to values obtained in a conventional system (reduced plate height, $h = 10$). The metabolites are not baseline separated and elute at the back of the system and anion peaks. They are both still compressed, especially narcotoline, which elutes first and gives an efficiency corresponding to " h " < 1. Obviously, as remarked under Experimental as the peaks in systems of this kind are affected by different special effects, such as gradients of mobile phase components, it is not possible to compare the apparent "efficiency" data obtained in this study with normal isocratic systems. The peak compression effects are, however, difficult to illustrate by other means and have therefore been expressed by this parameter in this paper.

At a concentration of the anion of 0.06 *M* the analytes largely elute under the conditions described in ref. 2, *i.e.*, with a decreasing DMOA deficiency zone. Although the alkylsulphate peak is also present, with a slight excess of DMOA, causing

a disturbance of the DMOA gradient, in this instance it probably has only a marginal effect on the analyte peak shapes. At a high concentration of the anion (0.10 *M*), however, the conditions are different. The most hydrophobic analyte, noscapine, is so strongly retained by ion pairing with the decylsulphate on injection that it elutes later than the system and alkylsulphate zones. The two metabolites elute here at the back of the decylsulphate excess peak.

Two effects may operate in this position. First, alkylsulphate, which is absent from the mobile phase, is available here as a decreasing gradient, offering possibilities for ion pairing with the cationic analytes. This effect is then strongest at the earliest eluting parts of the analyte peaks, giving a peak compression effect, which is evident from the peak shape in Fig. 4c. Second, as the conditions for the DMOA concentrations in this area of the chromatogram are complex it is not possible to give a detailed interpretation of the results. Obviously peak compression effects dominate, giving high apparent efficiencies for the two metabolites. Narcotoline, which elutes first, where the decylsulphate concentration is highest, gives the best apparent efficiency.

The split-peak behaviour at a low concentration of decylsulphate (0.04 *M*, Fig. 4a) may be explained as follows. The ion-pairing effect in the injection zone is lower, which means that the analytes will start the elution earlier than with larger amounts of the organic anion in the injected solution. During elution the system peak may catch up the analyte peaks, which will be exposed to both increasing and decreasing gradients of DMOA. The ultimate result will be split peaks, as different parts of a peak simultaneously experience forces of different strengths of competing properties.

Octylsulphate

The comparatively more polar anion octylsulphate is also more strongly retained than the DMOA system peak. As already mentioned, it elutes after about 1.5 h, but the excess of alkylsulphate will interfere with the system peak at a lower

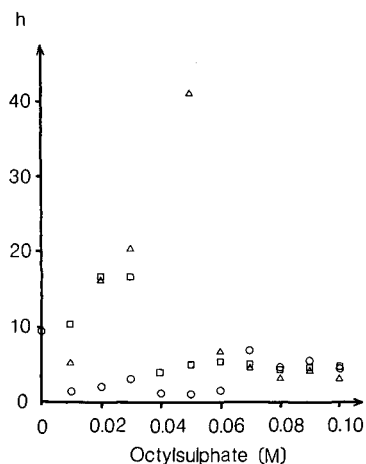


Fig. 5. Effects on the apparent peak efficiency, *h*, of the concentration of octylsulphate co-injected with the analytes: (○) noscapine; (△) narcotoline; (□) cotarnine. Chromatographic conditions as in Fig. 2.

concentration of injected anion compared with decylsulphate (Fig. 3). As indicated in Fig. 3, this peak is first visible at 0.04 M of injected anion, when it elutes at the back of the system peak. With increasing concentration the peak will gradually acquire decreasing retention times (*cf.*, eqn. 2) and finally, at concentrations ≥ 0.09 M it is the dominant part of the mixed peak and elutes first. Obviously this behaviour is more complicated than for decylsulphate and will make the interpretation of analyte peak performances more difficult, and here only the most evident effects are discussed.

Calculation of the dependence of the apparent efficiencies of the analytes on the injected octylsulphate concentration illustrates some of the effects that may be obtained in systems of this kind (Fig. 5). Noscapine elutes within the DMOA system peak in all systems used (see Fig. 3) and in many instances a peak compression effect was obtained, corresponding maximally to an apparent reduced plate height of 1. The more polar metabolites have lower retention times than the DMOA system peak with small amounts of the co-injected anion. However, with increasing anion concentration and resulting increasing retention times of the metabolites, in addition to a broader system zone of DMOA, they will elute within the zone, cotarnine at OS > 0.03 M and narcotoline at > 0.04 M. Their apparent efficiencies are initially low but with increasing amounts of injected octylsulphate attain a higher and fairly constant value, cotarnine at OS > 0.03 M and narcotoline at OS > 0.05 M. The reason for the low efficiencies at low anion concentrations may be insufficient trace enrichment effects on the top of the column. DMOA is more strongly retained than the metabolites in the system and consequently competes efficiently with the metabolites for ion pairing with the OS anion. The remaining octylsulphate will not be sufficient for an effective enrichment and the analytes are already spread out over a significant part of the column at the start; the volume injected was 200 μ l. With increasing concentration of the anion an enrichment effect is gradually obtained. Further, the efficiency obtained seems to be higher even than a reference value obtained for noscapine when no organic alkylsulphate was injected. At these concentrations of the anion the metabolites also elute within the alkylsulphate peak, and will consequently experience an additional retaining factor, in addition to the deficiency of the DMOA, namely ion pairing with the octylsulphate.

Application of the peak compression principle in a dual-column system

The levels of noscapine in biological fluids after administration of the drug to humans are low, probably owing to an extensive first-pass metabolism. The compound has no useful physico-chemical properties that can be utilized for detection apart from UV absorbance in the low wavelength range. An application of the peak compression effect may be useful for bioanalytical purposes and some limited experiments in that direction were performed.

For simple sample preparation a direct injection technique is desirable. In such applications a precolumn is necessary to protect the analytical column from the biological fluid. Often the precolumn is placed in a loop of an injection valve, making it possible to inject the analytes from one direction and then to back-flush the compounds on to the analytical column. Hence the precolumn must first retain the analytes from the injected sample, and then release them in a small volume of the mobile phase for further transport to the analytical column. By a careful choice of the polarity of the precolumn and the mobile phase, *e.g.*, the ion-pairing agent and the content

TABLE II
BREAKTHROUGH VOLUMES OF COTARNINE ON ENRICHMENT COLUMNS (20 × 3.8 mm I.D.)

Column	Counter ion		Content of acetonitrile (%)	V_b (ml)
	Type	Concentration (mM)		
Nucleosil CN (5 μ m)	Decyl sulphate	1	5	1.2
Nucleosil C ₄ (5 μ m)	Decyl sulphate	1	5	16.8
	Decyl sulphate	1	10	3.9
	Octyl sulphate	1	10	<2.1
	Octyl sulphate	10	10	9.0
Nucleosil C ₈ (5 μ m)	Octyl sulphate	1	10	<4.1
	Decyl sulphate	1	10	18.7
Spherisorb Ph (5 μ m)	Decyl sulphate	1	5	14.6*
	Octyl sulphate	10	5	21.5**

* V_b for narcotoline was 11.7 ml.

** V_b for narcotoline was 9.2 ml.

of organic modifier, the analytes can be enriched on the top of the precolumn. After reversal of the flow the analytes can be desorbed by applying a mobile phase containing a competing compound and a larger content of organic modifier than the initial mobile phase.

The breakthrough volumes and retention volumes were measured on a number of solid phases for the least retarded compound, cotarnine (Table II). As expected, decylsulphate gave a higher breakthrough volume than octylsulphate. Further, the breakthrough volumes increased with increasing lipophilicity of the solid phase. On Spherisorb phenyl support a reversal of the retention order occurred, narcotoline eluting before cotarnine.

The necessary compromise between enrichment ability and desorption effects with the different mobile phases indicated that Nucleosil C₄ might be a suitable solid phase, with decylsulphate (1 mM) in phosphate buffer (pH 2) containing of 5% acetonitrile for the enrichment conditions. The precolumn was utilized in the dual-column system shown in Fig. 6, where the analytical column was Nucleosil C₁₈. The precolumn will be saturated with decylsulphate and the analytes were retained effectively by ion-pair formation. After switching the valve the analytes were desorbed by the mobile phase for the analytical column, containing 2.5 mM DMOA in 20% of acetonitrile in phosphate buffer (pH 2). Simultaneously with desorption of the analytes, a fraction of decylsulphate from the first mobile phase will be transferred to the analytical column. A strong equilibrium disturbance will be obtained, creating a DMOA-deficient system zone eluting on the column.

Under the applied conditions noscapine co-eluted with the back of the DMOA system peak, resulting in a peak compression effect (see Fig. 7). The metabolites elute before the system zone, cotarnine even within the front. Injection of only 0.03 nmol of noscapine gave a very high apparent efficiency, corresponding to an apparent reduced plate height, " h ", of 1.8. However, when a ten times larger amount of the compound

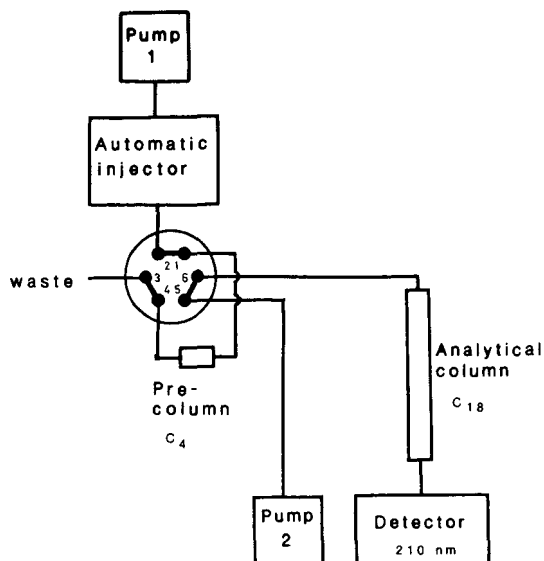


Fig. 6. Scheme of the dual-column system. Chromatographic conditions: precolumn, Nucleosil C_4 , $5\ \mu\text{m}$ ($20 \times 3.8\ \text{mm}$ I.D.); analytical column, Nucleosil C_{18} , $3\ \mu\text{m}$ ($100 \times 4.0\ \text{mm}$ I.D.); precolumn mobile phase, $1\ \text{mM}$ decylsulphate in 5% (v/v) of acetonitrile in phosphate buffer (pH 2); analytical column mobile phase, $2.5\ \text{mM}$ DMOA in 20% (v/v) of acetonitrile in phosphate buffer (pH 2).

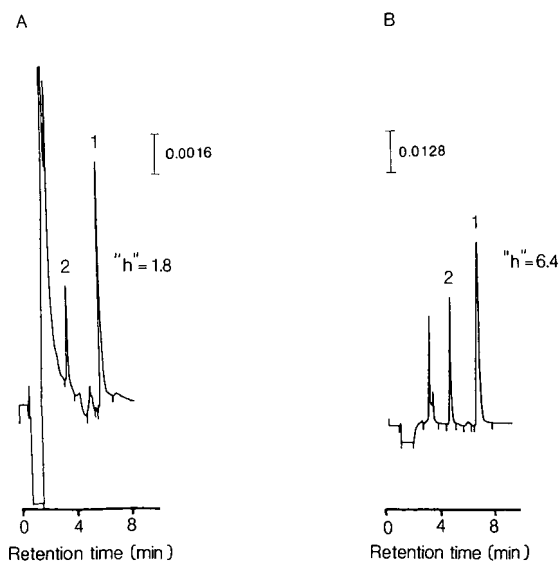


Fig. 7. Chromatogram obtained by injection of $500\ \mu\text{l}$ of phosphate buffer (pH 2) containing the analytes. Enrichment on the precolumn was performed for 4 min, before back-flushing. UV detection at 210 nm. 1 = Noscapine; 2 = narcotoline. Amounts injected: (A) noscapine 31 and narcotoline 23 pmol; (B) noscapine 310 and narcotoline 230 pmol.

was injected the efficiency dropped to " h " = 6.4. One reason is probably small changes in retention time, giving co-elution with different parts of the DMOA gradient, which considerably affect the apparent efficiency. An alternative reason is that with such a large amount the concentration of DMOA in the system zone is affected, resulting in a disturbance of its gradient¹⁸. Another drawback with this system was a late-eluting (1 h) and broad decylsulphate peak, visible when UV monitoring at 211 nm was used.

CONCLUSIONS

The injection of a solution deviating in composition from the mobile phase creates system peaks in chromatographic systems. The presence of an organic anion in the injected sample was used to generate system peaks containing a deficiency of a tertiary aliphatic amine, a component of an acidic mobile phase with acetonitrile as the organic modifier. The peak shapes of analytes co-eluting with the system peak were affected by the special conditions prevailing there, *i.e.*, gradients of DMOA at the back and front in addition to low levels in the middle of the peak. The analyte peak shapes vary from severely distorted, such as peak splitting, to greatly improved (peak compression), depending on the conditions during elution and in the system peak. The analyte peak shapes could be regulated by the character and concentration of the co-injected organic anion. Apparent reduced plate heights < 1 were obtained in optimal instances for some of the analytes (noscapine and two of its metabolites, narcotoline and cotarnine).

The principle was applied in a dual-column system where the analytes were injected on to a pre-column (C_4) equilibrated with an acidic mobile phase including an organic anion and a low content of acetonitrile. Back-flushing with a mobile phase containing a tertiary amine and a higher concentration of acetonitrile transferred the analytes to the separation column (C_{18}), where a system peak with a deficiency of the tertiary amine was created by the simultaneously transferred fraction of the organic anion from the first mobile phase. Under these conditions noscapine eluting in this system peak experienced a peak compression effect corresponding to an apparent reduced efficiency of 1.8.

ACKNOWLEDGEMENTS

Dr. S. Jacobsson and Mr. O. Falk are thanked for performing the mass spectrometric analyses.

REFERENCES

- 1 V. V. Berry and R. E. Shansky, *J. Chromatogr.*, 284 (1984) 303.
- 2 L. B. Nilsson and D. Westerlund, *Anal. Chem.*, 57 (1985) 1835.
- 3 M. Krejci, K. Slais and A. Kunath, *Chromatographia*, 22 (1986) 311.
- 4 J. J. Stranahan, S. N. Deming and B. Sachok, *J. Chromatogr.*, 202 (1980) 233.
- 5 V. V. Berry, *J. Chromatogr.*, 321 (1985) 33.
- 6 L. Hackzell and G. Schill, *Chromatographia*, 15 (1982) 437.
- 7 M. Denkert, L. Hackzell, G. Schill and E. Sjögren, *J. Chromatogr.*, 218 (1981) 31.
- 8 G. Schill and J. Crommen, *Trends Anal. Chem.*, 6 (1987) 111.

- 9 J. Crommen, L. Hackzell, G. Schill and D. Westerlund, *Chromatographia*, 24 (1987) 252.
- 10 S. Levin and E. Grushka, *Anal. Chem.*, 59 (1987) 1157.
- 11 A. Tilly-Melin, Y. Askemark, K.-G. Wahlund and G. Schill, *Anal. Chem.*, 51 (1979) 976.
- 12 A. Sokolowski and K.-G. Wahlund, *J. Chromatogr.*, 189 (1980) 299.
- 13 A. Sokolowski, T. Fornstedt and D. Westerlund, *J. Liq. Chromatogr.*, 10 (1987) 1629.
- 14 R. A. Keller and J. C. Giddings, *J. Chromatogr.*, 3 (1960) 205.
- 15 G. K. C. Low, A. M. Duffield and P. R. Haddad, *Chromatographia*, 15 (1982) 289.
- 16 G. K. C. Low, P. R. Haddad and A. M. Duffield, *J. Chromatogr.*, 336 (1984) 15.
- 17 D. P. Kirby, P. Vouros, B. L. Karger, B. Hidy and B. Petersen, *J. Chromatogr.*, 203 (1981) 139.
- 18 A. Sokolowski, T. Fornstedt and D. Westerlund, *J. Liq. Chromatogr.*, in press.

CHROM. 20 789

MEASUREMENT OF THE DISTRIBUTION COEFFICIENTS OF SEVERAL CLASSES OF DRUG USING REVERSED-PHASE THIN-LAYER CHROMATOGRAPHY

D. B. JACK*, J. L. HAWKER, L. ROONEY, M. BEERAHEE, J. LOBO and P. PATEL

Department of Pharmacology, The Medical School, Birmingham University, Birmingham B15 2TJ (U.K.)

SUMMARY

Using reversed-phase thin-layer chromatography, with octan-1-ol as stationary phase and phosphate buffer (pH 7.4) as mobile phase, the behaviour of different drugs at 37°C was studied. Three classes of drug were examined: β -adrenoceptor antagonists, non-steroidal anti-inflammatory agents and dihydropyridine calcium antagonists. As well as ranking these compounds in terms of their distribution coefficients, an attempt was also made to assign a quantitative value to each. For the β -adrenoceptor antagonists this was done by using a series of published values obtained using the shake-flask technique: for the non-steroidal anti-inflammatory agents a series of standard compounds was used. No good calibration data were available for the dihydropyridine calcium antagonists, but approximate values were assigned. The results obtained were compared with other published data and the applicability of the method discussed.

INTRODUCTION

The magnitude of the partition coefficient of a drug is a major factor in determining its passage across membranes within the body for absorption, tissue penetration and elimination. Many drugs are weak acids or bases and their ionized and unionized forms exist in equilibrium within the body. When a drug is partially ionized, the apparent partition, or distribution coefficient is measured; this is referred to as P' , while the true partition coefficient is P . The relationship between the two can be simply expressed by the following, where K_a is the dissociation constant:

$$\text{for a base: } P = P' (1 + H^+/K_a)$$

$$\text{for an acid: } P = P' (1 + K_a/H^+)$$

The standard method for determining the distribution coefficient of a drug is to partition it between a lipid-like organic phase and an aqueous phase, then measure the concentration of drug in both. Whether the classical "shake flask" technique or the more recent AKUFVE method is employed¹, this approach suffers from the

disadvantage that quantitative measurements of drug in both phases must be carried out.

When it is desired to determine the distribution coefficients of a number of drugs, even closely related, it is rarely possible to use a single analytical method. Radiolabelled compounds can, of course, be used but are not always readily available. To overcome these disadvantages, several groups of workers have used reversed-phase chromatography where a lipid-like stationary phase is used in conjunction with an aqueous buffer as mobile phase.

High-performance liquid chromatography (HPLC) has been used², but thin-layer chromatography (TLC) is much cheaper and has been employed since the early studies on penicillins³ and phenothiazines⁴. The method is simple and can be used even when the drug is impure.

We have applied the technique of reversed-phase thin-layer chromatography to the quinolone antibiotics⁵ and now wish to report its application to β -adrenoceptor antagonists, non-steroidal anti-inflammatory agents and dihydropyridine (DHP) calcium antagonists.

MATERIALS AND METHODS

Drugs and related chemicals

The following drugs were used: penbutolol (Hoechst, U.K.), bevantolol (Warner Lamber, U.K.), propranolol and practolol (ICI, U.K.), labetalol (Duncan Flockhart, U.K.), alprenolol, metoprolol and felodipine (Hässle, Sweden), oxprenolol, diclofenac sodium and pirofen (Ciba-Geigy, U.K.), pindolol and isradipine (Sandoz, U.K.), timolol, diflunisal, indomethacin and sulindac (MSD, U.K.), acebutolol, diacetolol and ketoprofen (May & Baker, U.K.), sotalol (Bristol-Meyers, U.K.), nadolol (Squibb, U.K.), atenolol (Stuart, U.K.), benoxaprofen (Dista, U.K.), fenbufen (Lederle, U.K.), flufenamic acid (Merrell Dow, U.K.), naproxen (Syntex, U.K.), flurbiprofen and ibuprofen (Boots, U.K.), tolmetin sodium (Ortho, U.K.), nisoldipine, nitrendipine, nimodipine and nifedipine (Bayer, U.K.). Antipyrine, 4-aminoantipyrine, mephenesin, phenacetin and salicylic acid were all purchased from Sigma, U.K.

Thin-layer chromatography

Cellulose plates (CEL300, 20 × 20 cm) were obtained from Macherey-Nagel (Düren, F.R.G.) and octan-1-ol from Sigma. The plates were coated with octan-1-ol by placing them in a tank containing a solution of octan-1-ol (5%) in diethyl ether and allowing the organic phase to migrate up to plate until it had reached a few centimeters from the top. The plate was then removed from the tank and allowed to dry in air. Standard solutions of the drugs under investigation were made up in methanol, water or other suitable solvent to a concentration of 1 mg/ml and applied to the starting line, 1.5 cm from the bottom edge of the plate. The applied spots were dried in a gentle stream of air and the plate transferred to a glass tank containing the phosphate buffer (pH 7.4, 0.07 M), previously saturated with octan-1-ol. This developing tank was kept in an incubator at 37°C and development of the plate was allowed to continue until the mobile phase had travelled a distance of 10 cm (approximately 1 h). The plate was then removed, allowed to dry and the drugs visualized by examination under UV light or by spraying with a suitable reagent⁶. Many of the

drugs can be detected by simply observing the plate as it dries when they appear as white areas against a wet background. These spots disappear again as the plate continues to dry. The R_F value of each drug is recorded and the R_M calculated using the relationship

$$R_M = 1/R_F - 1$$

Relatively lipophilic drugs, such as penbutolol, show a concentration-dependent R_F value and, in such cases, a range of concentrations were used and the R_F extrapolated to zero-concentration.

The extremely lipophilic DHP calcium antagonists do not migrate at all when phosphate buffer is used as mobile phase. To overcome this, different amounts of acetone are added to the phosphate buffer and extrapolation made to zero acetone concentration. This method has previously been used to study the partition of a number of penicillins⁷.

RESULTS

Kieselguhr and silica gel layers were also examined initially but the former were too easily damaged while the latter were very slow to coat with octan-1-ol and took much longer to develop, once coated. The coating with octan-1-ol was reproducible and only very small variations in R_F values were obtained from day to day. A study using 18 plates was performed over a period of several weeks and coefficients of variation of R_F of 1.4–2.2% were obtained for the calibration compounds 4-aminoantipyrine, antipyrine, mephensin and phenacetin. Three different classes of drug have been studied: β -adrenoceptor antagonists non-steroidal anti-inflammatory agents and dihydropyridine calcium antagonists. The R_F and R_M values for each class of compound are shown in Tables I–III, respectively. Examination of this data allows an

TABLE I
RETENTION DATA FOR β -ADRENOCEPTOR ANTAGONISTS

<i>Drug</i>	<i>Abbreviation used in Fig. 1</i>	R_F	R_M
Penbutolol		0.10	9.00
Bevantolol		0.12	7.33
Propranolol	pr	0.18	4.50
Labetalol	la	0.21	3.80
Alprenolol		0.26	2.85
Oxprenolol	ox	0.45	1.20
Pindolol	pi	0.56	0.80
Timolol	ti	0.57	0.75
Metoprolol	me	0.61	0.65
Acebutolol	ac	0.66	0.51
Diacetolol		0.80	0.25
Sotalol	so	0.85	0.17
Nadolol	na	0.87	0.15
Atenolol	at	0.90	0.11
Practolol		0.91	0.10

TABLE II
RETENTION DATA FOR NON-STEROIDAL ANTI-INFLAMMATORY AGENTS

<i>Drug</i>	R_F	R_M	<i>Drug</i>	R_F	R_M
Benoxaprofen	0.33	2.03	Naproxen	0.74	0.35
Diflunisal	0.46	1.17	Flurbiprofen	0.79	0.27
Fenbufen	0.48	1.08	Salicylic acid	0.80	0.25
Indomethacin	0.57	0.75	Ibuprofen	0.81	0.23
Flufenamic acid	0.62	0.61	Pirprofen	0.81	0.23
Sulindac	0.62	0.61	Tolmetin sodium	0.81	0.23
Diclofenac sodium	0.73	0.37	Ketoprofen	0.82	0.22

immediate ranking in terms of distribution coefficient and absolute values can be obtained using suitable calibration curves and the relationship

$$\log P' = A \log R_M + B$$

For the β -adrenoceptor antagonists, we used the data obtained by Woods and Robinson⁸ who determined their distribution coefficients at pH 7.4 and 37°C using the "shake flask" technique. Their data are given in Table IV. A good fit was obtained when distribution coefficient was plotted against R_M and this is illustrated in Fig. 1.

Unfortunately there is no similar set of data for the non-steroidal anti-inflammatory agents and calibration was performed using four compounds whose distribution coefficients have been measured under carefully controlled conditions: 4-aminopyrine, antipyrine, mephenesin and phenacetin. The calibration curve obtained is shown in Fig. 2. Some data has recently been published using a reversed-phase C₁₈ column⁹ coated with octan-1-ol and this is shown in Table IV along with some quantitative structure-activity relationship (QSAR) data¹⁰. The distribution coefficients for flufenamic acid, flurbiprofen and ibuprofen are reasonably similar when the two chromatographic techniques are compared but large differences are observed for the other compounds studied. Agreement between both these sets and the QSAR data is also poor. Reasons for this are suggested in the discussion.

TABLE III
RETENTION DATA FOR DIHYDROPYRIDINE Ca ANTAGONISTS

<i>Acetone in mobile phase (%)</i>	R_M					
	<i>Nifedipine</i>	<i>Isradipine</i>	<i>Nimodipine</i>	<i>Nitrendipine</i>	<i>Nisoldipine</i>	<i>Felodipine</i>
5	5.67	15.66	49.0	49.0	199.0	199.0
10	2.85	10.11	11.50	11.50	49.0	49.0
15	1.44	4.56	5.67	6.14	10.10	19.0
20	0.69	2.03	2.33	2.70	3.76	6.14
25	0.41	1.13	1.33	1.38	2.23	3.00
30	0.23	0.61	0.75	0.79	1.08	1.50
40	0.02	0.18	0.19	0.18	0.32	0.33

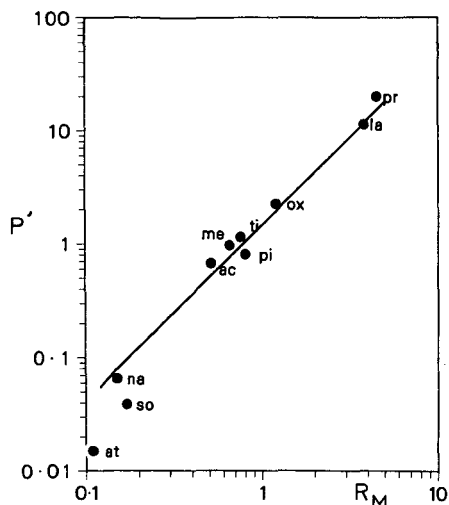


Fig. 1. Relationship between R_M and distribution coefficient for a range of β -adrenoceptor antagonists.

The dihydropyridine calcium antagonists are all extremely lipid soluble and no good calibration compounds are available. The two most lipophilic compounds available to us with known distribution coefficients were penbutolol and diazepam and we used these to give us a two point calibration. The R_M data were extrapolated to zero-acetone concentration (Fig. 3). We felt confident in doing this because a good linear relationship was apparent for the compounds nifedipine and isradipine. Extrapolation of the other data was far less certain but, nevertheless, we felt it would be an instructive exercise.

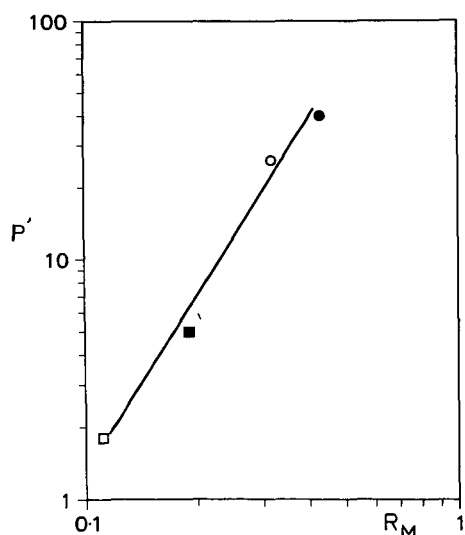


Fig. 2. Relationship between R_M and distribution coefficient for antipyrine (□), 4-aminoantipyrine (■), mephesisin (○) and phenacetin (●).

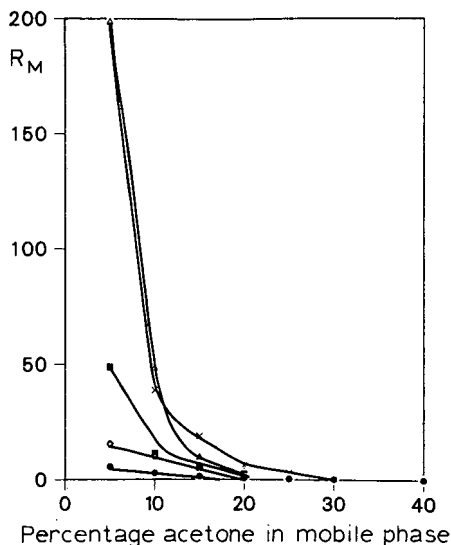


Fig. 3. Relationship between acetone concentration and R_M for the DHP calcium antagonists nifedipine (●), isradipine (○), nimodipine (■), nitrendipine (□), nisoldipine (Δ) and felodipine (×).

A very limited amount of published data exists for the calcium antagonists and this is reproduced in Table IV.

DISCUSSION

The good fit achieved with the β -adrenoceptor antagonists suggests that the present approach may be of some value. A number of other antagonists, not studied by Woods and Robinson⁸, were examined using our method and the results are in general agreement with published values, bearing in mind that our measurements are carried out at 37°C.

The measured R_F values of the β -adrenoceptor antagonists ranged from 0.1 (penbutolol) to 0.91 (practolol). In view of the good fit obtained for the compounds used to construct Fig. 1, we believe that R_F values over this range can be used to give meaningful data. For very lipophilic compounds, with R_F values less than 0.1, acetone can be added to the mobile phase as we described above for the dihydropyridine calcium antagonists. How useful the method is for compounds with R_F values greater than 0.91 remains to be seen. An examination of this is planned.

Comparisons between different methods is difficult since most "shake-flask" determinations are carried out at 18–25°C; most drugs are weak acids or bases and their dissociation constants are temperature-dependent. We deliberately chose a working temperature of 37°C in order that our results would be more relevant to what happens *in vivo*.

As far as the non-steroidal anti-inflammatory agents are concerned, the poor agreement between the different studies obviously requires that further work be carried out. We ourselves plan a comparison of TLC with HPLC, as well as more comprehensive calculations of partition coefficients using Hansch analysis.

One property of the acidic anti-inflammatory drugs that may well be of relevance is their ability to form dimers in the octanol phase. This phenomenon is concentration-dependent and will, almost certainly, have an effect on the results obtained by different groups of workers.

We have carried out some simple Hansch calculations for the dihydropyridine calcium antagonists and our results suggest that the experimental ranking of lipophilicity that we have observed is largely correct, bearing in mind that the experimental extrapolation described above for the compounds other than nifedipine and isradipine can only be regarded as approximate. There is a large difference between our results and the limited published data. All the compounds we studied behaved chromatographically as though they had distribution coefficients much greater than diazepam ($P' = 661$)¹³. It is therefore very difficult to explain the very low values of other workers^{11,12}. In support of our own observations, we have examined an internal report from Hässle¹⁴, makers of felodipine. They measured the distribution coefficient for this compound between toluene and water and obtained a value for $\log K_D$ of 4.52. We believe that our value of 7.06 ($P' = 11\,500 \cdot 10^3$) for the octan-1-ol-water system is sufficiently close, bearing in mind the technical difficulties and the extrapolation, to merit further study of the technique. This we intend to do. Comparison of distribution coefficients from different sources suffers from the disadvantage that they are often obtained under very different experimental conditions such as temperature, pH and mobile phase. We believe that reversed-phase TLC offers a versatile approach that can be applied to a wide range of drugs. When distribution coefficients are determined under a single set of conditions, more meaningful comparisons can be made to allow a greater understanding of processes such as tissue binding and penetration, metabolism and excretion.

REFERENCES

- 1 W. J. Dunn III, J. H. Block and R. S. Pearlman (Editors), *Partition Coefficient, Determination and Estimation*, Pergamon Press, Oxford, 1986.
- 2 M. S. Mirrlees, S. J. Moulton, C. T. Murphy and P. J. Taylor, *J. Med. Chem.*, 19 (1976) 615.
- 3 A. E. Bird and A. C. Marshall, *J. Chromatogr.*, 63 (1971) 313.
- 4 A. Hulshoff and J. H. Perrin, *J. Chromatogr.*, 120 (1976) 65.
- 5 D. B. Jack, J. F. Gonzalez and S. J. Laughler, *Rev. Infect. Dis.*, 10, Suppl. 1 (1988) S10.
- 6 D. B. Jack, S. Dean, M. J. Kendall and S. J. Laughler, *J. Chromatogr.*, 196 (1980) 189.
- 7 G. L. Biagi, A. M. Barbaro, M. F. Gamba and M. C. Guerra, *J. Chromatogr.*, 41 (1969) 371.
- 8 P. B. Woods and M. L. Robinson, *J. Pharm. Pharmacol.*, 33 (1981) 172.
- 9 S. H. Unger, P. S. Chueng, G. H. Chiang and J. R. Cook, in W. J. Dunn III, J. H. Block and R. S. Pearlman (Editors), *Partition Coefficient, Determination and Estimation*, Pergamon Press, Oxford, 1986, p. 69.
- 10 M. Kuchar, V. Rejholec and O. Nemecek, *Drugs of the Future*, VII (1982) 179.
- 11 D. C. Pang and N. Sperelakis, *Biochem. Pharmacol.*, 33 (1984) 821.
- 12 L. G. Herbette, D. W. Chester and D. G. Rhodes, *Biophys. J.*, 49 (1986) 91.
- 13 E. Tomlinson and T. L. Hakenscheid, in W. J. Dunn III, J. H. Block and R. S. Pearlman (Editors), *Partition Coefficient, Determination and Estimation*, Pergamon Press, Oxford, 1986, p. 101.
- 14 M. Ahnoff, *Internal Report*, Hässle, Sweden.

CHROM. 20 426

SOME CONSIDERATIONS ON THE “CHARGE” ON A METAL ION IN ION-EXCHANGE CHROMATOGRAPHY

M. LEDERER

Institut de Chimie Minérale et Analytique, Université de Lausanne, Boîte Postale 115, Centre Universitaire, CH-1015 Lausanne 15, Dorigny (Switzerland)

SUMMARY

Published work on the determination of the “charge” on an ion by means of ion-exchange equilibria is reviewed and a number of examples are discussed in which such determinations led to erroneous results. The effect of outer-sphere complexing (or ion pairing) in solution and with exchange groups is discussed.

INTRODUCTION

Throughout the development of the theory and practice of ion-exchange chromatography, a certain picture of electrostatic attraction between ions in solution and fixed groups on the resin was taken for granted. The best summary of early work on the topic was given by Walton¹.

The basic structure of a sulphonic ion exchanger such as Dowex 50 was pictured as shown in Fig. 1.

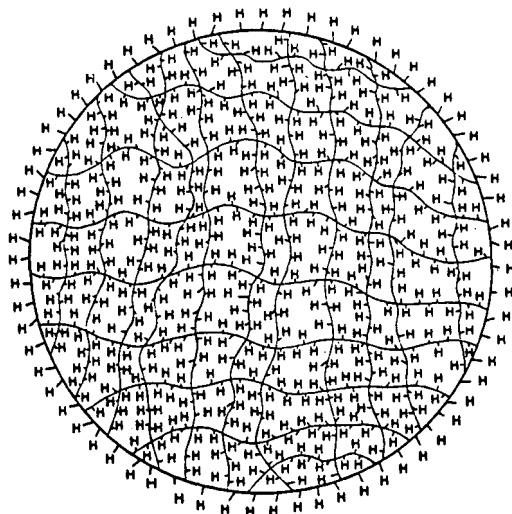


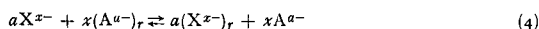
Fig. 1. Basic structure of Dowex 50. (From ref. 15).

The application of equations based on the law of mass action and similar¹ created the general belief that in such a network two or more species would swim around like fish and, depending on their attraction to the negatively charged sulphonic groups present throughout the resin particle, they would be more or less retarded with respect to the flowing eluent. This picture led to the determination of the "charge" on a metal ion using chromatographic or equilibrium data with ion exchangers.

Our laboratory was interested in such correlations in connection with the development of ion-exchange papers and several papers were published on this topic. The best summary of this work up to 1965 can be found in a review by Carunchio and Grassini-Strazza (ref. 2, pp. 282-284):

Total charge on the complex

To determine this quantity, most authors have used methods very similar to or the same as that developed by NELSON AND KRAUS¹³⁹ for investigating alkaline-earth metal citrates on anion-exchangers. In this method, the ion-exchange equilibrium is expressed as:



where X^{x-} and A^{a-} denote respectively the complex ion and the eluting anion, the resin phase being indicated by r . The exchange constant can then be written as:

$$K = G \frac{[X^{x-}]_r^a [A^{a-}]^x}{[X^{x-}]^a [A^{a-}]_r^x} \quad (5)$$

where G is the ratio of the activity coefficients and the quantities in brackets are concentrations. Assuming that G and the term $[A^{a-}]_r$ are constant, *i.e.* that $[X^{x-}]_r$ is small in comparison with $[A^{a-}]_r$, we can write eqn. (5) in the form:

$$\text{const.} = \frac{K}{G} [A^{a-}]_r^x = D^a [A^{a-}]^x \quad (6)$$

since:

$$D = \frac{[X^{x-}]_r}{[X^{x-}]} \quad (7)$$

Differentiating eqn. (6), we obtain:

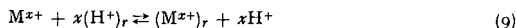
$$\frac{d \log D}{d \log [A^{a-}]} = S = -\frac{x}{a} \quad (8)$$

The slope S of the curve obtained by plotting $\log D$ against $\log [A^{a-}]$ is numerically equal to the ratio between the charge on the complex ion (x) and that on the eluting anion (a).

LI AND WHITE¹²⁷ used this method to determine the charge on the citrates of Co(II), Zn(II), and Th(IV) and verified the result for the Co(II) citrate by a somewhat different technique, in which the resin was not in the citrate but in the Cl⁻ form. However, the attempts to determine x for a uranyl citrate complex failed, since the very strong affinity of the uranyl ion for the resin citrate makes it impossible to obtain reasonable distribution coefficients for this system. The very stable uranyl citrate complex, which is evidently formed, may serve as a basis for the separation of uranium from metals on anion-exchangers.

The method of NELSON AND KRAUS¹³⁹ has been used in conjunction with other techniques to determine the charge x on several complexes such as the oxygenated cobalt glycyglycinate¹⁴⁰ ($x = -1$), a plutonium(IV) oxalate¹²⁴ ($x = -6$), two protactinium(V) complexes formed in H₂SO₄ solutions¹⁴¹ ($x = -1$ and -3), complexes of Sr(II) with dicarboxylic acids¹⁴² ($x = 0$), and a Pm(III)-EDTA complex formed in solutions with pH 1.8 to 9.0 ($x = -1$)¹⁴³. The value of x has also been determined for some complexes of Fe(II) and Ti(IV) by BEUKENKAMP AND HERRINGTON^{137, 138} using a similar method and by NABIVANETS¹³³ for the complexes of Ti(IV) formed in HCl solutions of various concentrations.

A cation exchanger in the H^+ form is used in the method of CADY AND CONNICK^{48,91,134-136} for determining x of cationic complexes. This method is based on the fact that the equilibrium distribution of the complex cation depends on the concentration of H^+ (the exchangeable ion) in the aqueous phase and the resin phase. Thus the ion-exchange constant K for the reaction:



is given by:

$$K = G \frac{[M^{x+}]_r [H^+]^x}{[M^{x+}] [H^+]_r^x} \quad (10)$$

where G is the ratio of the activity coefficients. The distribution of M^{x+} , *i.e.* $[M^{x+}]_r/[M^{x+}]$, varies as the x -th power of the hydrogen ion distribution $[H^+]_r/[H^+]$. We can calculate x and K by substituting in eqn. (10) the values obtained from two equilibrations at different hydrogen-ion concentrations. Strictly accurate values are obtained only if K is the same for both equilibrations. This is not so in practice, because the activity coefficients in the aqueous phase vary from one equilibration to another. However, the method can still be used, since x is known to be a whole number of n (charge per metal atom), so the experimental values need not be very accurate.

LEDERER AND KERTES¹⁴⁴ correlated the charge on reversibly adsorbed cationic complexes with their R_F values on ion-exchange paper. Equations (9) and (10) are equally valid for exchange reactions occurring on paper impregnated with ion-exchangers. The logarithmic form of eqn. (10) is as follows (provided that $G = 1$):

$$\log K = \log \frac{[M^{x+}]_r}{[M^{x+}]} + x \log [H^+] - x \log [H^+]_r \quad (11)$$

To express $\log K$ as a function of R_F , the only parameter that is directly measurable on paper, we use the following relationship valid for partition chromatography:

$$R_F = \frac{A_L}{A_L + \alpha A_S} \quad (12)$$

where A_L is the cross-section of the mobile phase, A_S is the cross-section of the stationary phase, and α is the partition coefficient (ratio of the concentration in the stationary phase to that in the mobile phase). Equation (12) can also be written as:

$$\frac{1}{R_F} - 1 = \alpha \frac{A_S}{A_L} \quad (13)$$

Substitution of this into eqn. (11) gives:

$$\log K = \log \frac{A_L}{A_S} + \log \left[\frac{1}{R_F} - 1 \right] + x \log [H^+] - x \log [H^+]_r \quad (14)$$

Moreover, since $\log K$, $\log A_L/A_S$, and $x \log [H^+]_r$ are assumed to be constant, we obtain:

$$\log \left[\frac{1}{R_F} - 1 \right] = -x \log [H^+] + \text{constant} \quad (15)$$

Utilizing the relationship $\log (1/R_F - 1) = R_M$, we may simplify eqn. (15) and write:

$$R_M = x \text{pH} + \text{constant} \quad (16)$$

This relationship holds for each given cation eluted with hydrogen ions but the method is limited to eluent concentrations that give rise to intermediate R_F values. It has been used with $Al(III)$ in mixtures of HCl and HF of various concentrations¹⁴⁵. Moreover, eqn. (15) has been found valid¹⁴⁶ when a paper impregnated with zirconium phosphate (K^+ form) is used and the elution is carried out with highly concentrated solutions of KCl . In this case, the concentration of H^+ is naturally replaced by that of K^+ in eqn. (15).

Reading this extract one gains the impression that such "charge" determinations give meaningful results and have been generally applied. However, since then, severe limitations to this approach have become apparent. This emerged during the determination of the purity of a number of Co^{III} complexes, using the usual planar methods then at our disposal, namely paper partition chromatography, ion-exchange paper chromatography and paper electrophoresis. Doubts arose about the validity of such "charge" determinations when complexes such as $\text{Co}(\text{NH}_3)_6^{3+}$ behaved in some systems as if they had a charge of +5.

During the 1987 meeting on ion chromatography in Sils, the author noted that the authorities on ion exchange were unaware of these results, probably because they were obtained in terms of R_F and $R_M (= \log(1/R_F - 1))$ values or in terms of paper electrophoretic relative mobilities, and not in terms of K_d or capacity factors, as used in column chromatography; it was felt that a summary of the results, which were originally presented in various publications, would be of interest to chromatographers.

At this point the author would like to express his appreciation to Professor J. Inczedy for the help he gave in lengthy discussions and correspondence on this topic, which provided the impetus for this paper.

(i) Behaviour of Co^{III} complexes on sulphonic resin paper Amberlite SA-2

In 1969, Mazzei and Lederer³ chromatographed $\text{Co}(\text{NH}_3)_6^{3+}$ and $\text{Co}(\text{en})_3^{3+}$ and a number of divalent and trivalent metal ions and obtained the results shown in Fig. 2.

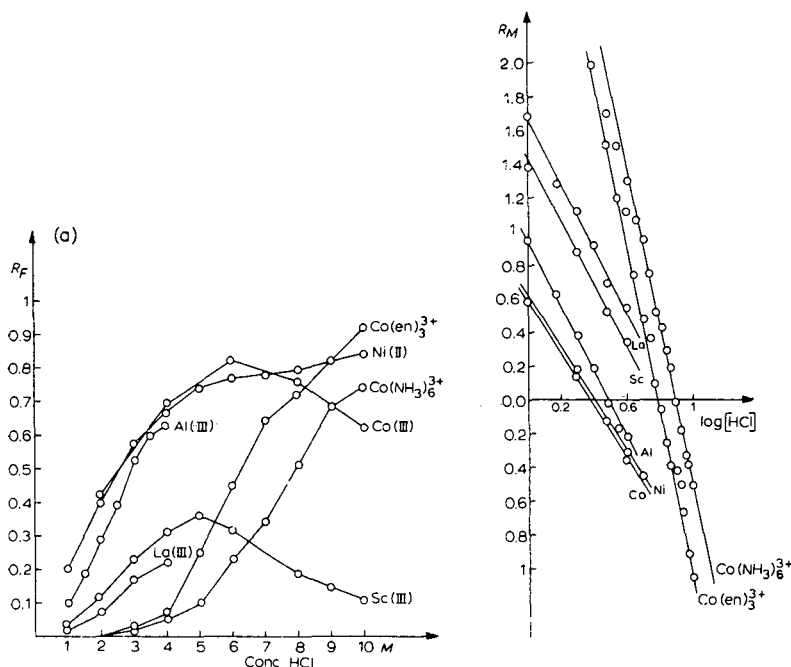


Fig. 2.

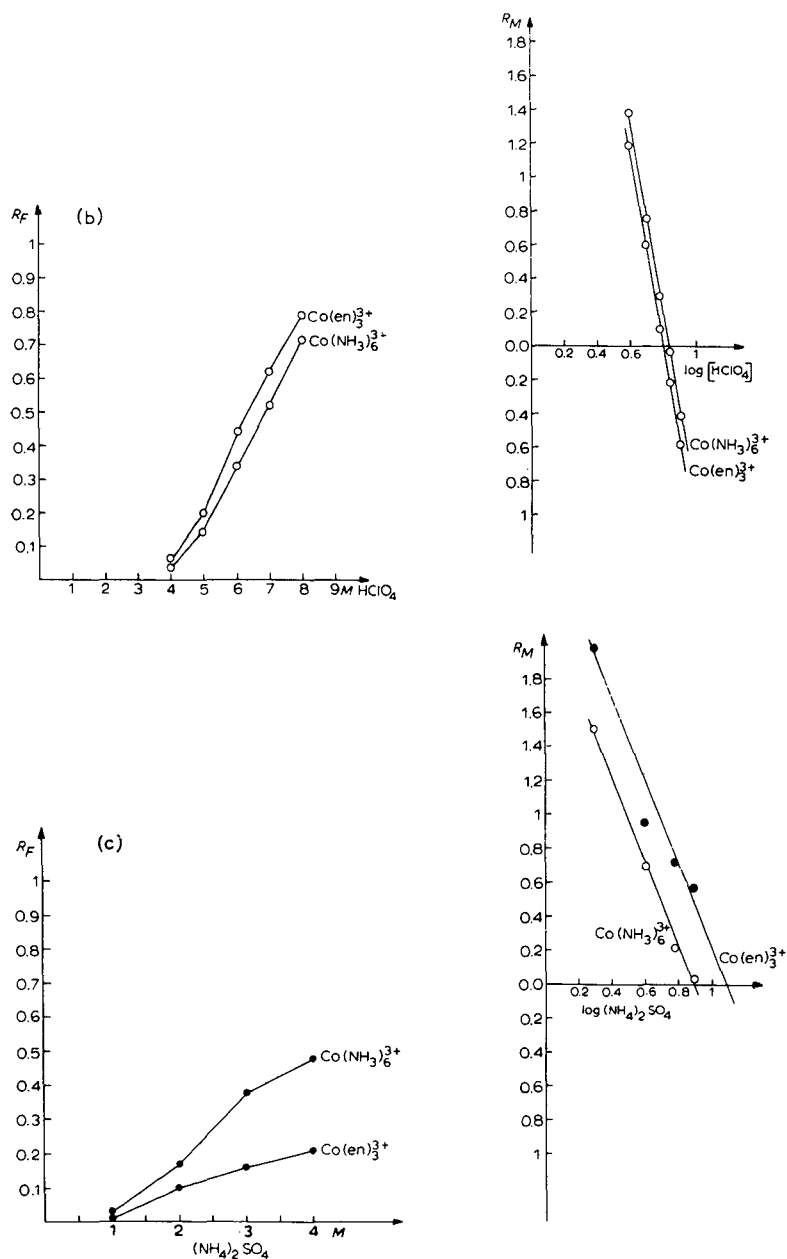


Fig. 2. (a) R_F vs. [HCl] and R_M vs. log [HCl] plots for Co^{II}, Ni^{II}, Al^{III}, Sc^{III}, La^{III}, [Co(NH₃)₆]³⁺ and [Co(en)₃]³⁺ on Amberlite SA-2 paper developed with hydrochloric acid. The slopes of the R_M vs. log [HCl] plots are Co^{II} = 1.7, Ni^{II} = 1.6, Al^{III} = 2.0, Sc^{III} = 1.92, La^{III} = 1.94, [Co(en)₃]³⁺ = 4.6 and [Co(NH₃)₆]³⁺ = 4.75. (b) R_F vs. [HClO₄] and R_M vs. log [HClO₄] plots for [Co(NH₃)₆]³⁺ and [Co(en)₃]³⁺ on Amberlite SA-2 paper developed with perchloric acid. The slopes of the R_M vs. log [HClO₄] plots are [Co(NH₃)₆]³⁺ = 5.3 and [Co(en)₃]³⁺ = 5.6. (c) R_F vs. [(NH₄)₂SO₄] and R_M vs. log [(NH₄)₂SO₄] plots for [Co(NH₃)₆]³⁺ and [Co(en)₃]³⁺ on Amberlite SA-2 paper developed with aqueous ammonium sulphate. The slopes of the R_M vs. log [(NH₄)₂SO₄] plots are [Co(NH₃)₆]³⁺ = 2.45 and [Co(en)₃]³⁺ = 2.5. (From ref. 3).

Whereas the "slopes" for divalent metals such as Co^{II} and Ni^{II} were of the order of 1.7, those of trivalent metals such as Sc^{III} and La^{III} were between 1.9 and 2.0, and those of the Co^{III} complexes were 4.6–4.8 in hydrochloric acid and 5.3–5.6 in perchloric acid. In ammonium sulphate as eluent, the "charges" for the Co^{III} complexes were around 2.5.

(ii) "Charge" of Co^{III} complexes on a range of exchangers

We found the results of the above work to be surprising and felt that more data should be obtained for a wide range of cation exchangers. Table I shows the results obtained by Giannetta and Lederer⁴, which clearly indicate that the "charge" so measured can vary from about 1 to 6, depending mainly on the resin and also on the eluent.

TABLE I

CHARGE EXHIBITED BY SOME COBALT COMPLEXES ON CATION-EXCHANGE PAPERS (FROM REF. 4)

Cation-exchange paper	Eluent	"Apparent charge" or tangent of the R_M vs. $\log [\text{LiCl}]$ plot for	
		$\text{Co}(\text{NH}_3)_6^{3+}$	$\text{Co}(\text{en})_3^{3+}$
Amberlite SA-2 paper	HCl	4.75	4.6
Amberlite SA-2 paper	LiCl	3.3	3.9
Cellulose phosphate paper, Whatman No. P20	LiCl	2.2	2.1
Cellulose citrate paper, Whatman No. CT30	LiCl	1.5	1.5
Carboxymethyl cellulose paper, Whatman No. CM50	LiCl	1.2	1.2
Zirconium phosphate paper	LiCl		2.4
Sulphonic acid cellulose paper (Macherey, Nagel and Co., Stark Sauer)	HCl	1.6	1.6

(iii) Effect of the "concentration" of the ion-exchange groups on the "charge"

This led us to suspect that the "charge" depends to a large extent on the number of exchange groups that can approach closely enough to a metal ion in order to exert an attraction or interaction. Cerrai *et al.*⁵ showed that on a series of paper impregnated with di(2-ethylhexyl)orthophosphoric acid (HDEHP) liquid ion exchanger the "charge" changes with the concentration of the exchange groups, as shown in Fig. 3 and Table II, *viz.*, from about 1.3 at low impregnation to about 3 at high impregnation.

If the "charge" measured in ion-exchange equilibria corresponds to the charge on the ion present in a solution properties, then the other properties of such solutions should be such as to agree with the ion-exchange results. This has been discussed extensively in relation to the charge on proteins and will be discussed at the end of this paper. Here we shall consider two properties which give evidence for the actual "charge" in solution.

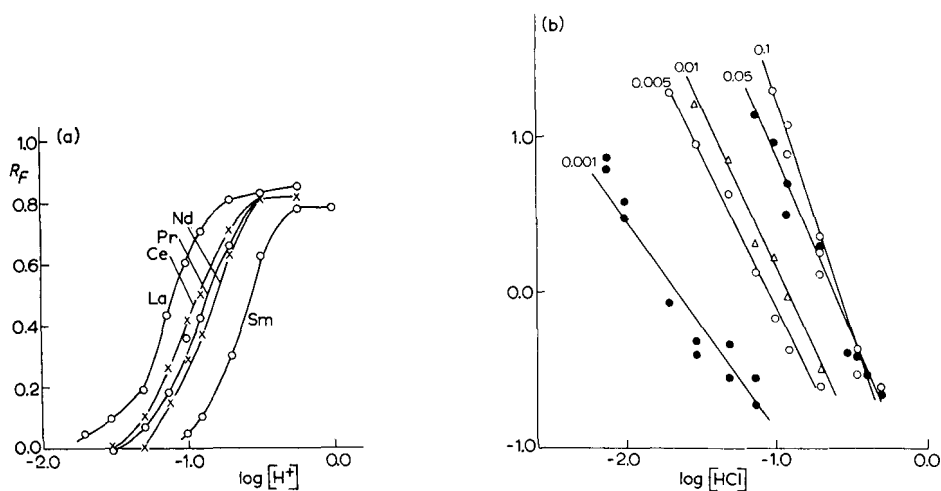


Fig. 3. (a) R_F versus $\log [H^+]$ plots for papers impregnated with 0.005 M HDEHP. (b) R_M versus $\log [H^+]$ plots for papers impregnated with various concentrations of HDEHP. (From ref. 5).

(iv) Activity coefficients

Activity coefficients obtained from electrochemical measurements are available in the literature for various concentrations of pure salts, but data for, e.g., La^{3+} in 1 M hydrochloric acid are usually not available and would be difficult to measure with any accuracy.

If we examine Table III for 0.1 M solutions⁶, we find that monovalent cations as in $AgNO_3$ or $CsCl$ have activity coefficients near unity, viz., 0.734 and 0.756, respectively. With a divalent cation such as in $CaCl_2$ or $CoCl_2$, the activity is only 0.518 and 0.523, respectively, in other words reduced by about 50%. Trivalent cation salts, such as $AlCl_3$, have an activity of 0.337.

To give a kinetic picture, the Al^{3+} in 0.1 M $AlCl_3$ attracts the Cl^- so closely that to all intents the particle preponderant in such a solution is best pictured as an ion pair $[Al^{3+} + 2 Cl^-]^+$.

TABLE II

SLOPES OF R_M VERSUS $\log [HCl]$ PLOTS FOR PAPER IMPREGNATED WITH VARIOUS AMOUNTS OF HDEHP (FROM REF. 5)

Metal ion	HDEHP concentration in impregnating solution (M)				
	0.1	0.05	0.01	0.005	0.001
La ^{III}	-3.02 ± 0.47	-2.29 ± 0.23	-2.12 ± 0.46	-1.99 ± 0.26	-1.34 ± 0.18
Ce ^{III}	-2.82 ± 0.58	-2.68 ± 0.21	-2.40 ± 0.35	-2.17 ± 0.51	-1.40 ± 0.18
Pr ^{III}	-2.98 ± 0.37	-2.47 ± 0.36	-2.20 ± 0.56	-2.10 ± 0.43	-2.06 ± 0.30
Nd ^{III}	-3.08 ± 0.61	-2.40 ± 0.41	-2.28 ± 0.73	-2.00 ± 0.41	-2.27 ± 0.52
Sm ^{III}	-3.11 ± 0.69	-2.69 ± 0.35	-2.66 ± 0.53	-2.12 ± 0.62	-1.71 ± 0.48

TABLE III
MEAN ACTIVITY COEFFICIENTS (FROM REF. 6)

<i>M</i>	<i>AgNO</i> ₃	<i>AlCl</i> ₃	<i>BaCl</i> ₂	<i>Ba(ClO</i> ₄) ₂	<i>Ba(NO</i> ₃) ₂	<i>CaBr</i> ₂	<i>CaCl</i> ₂	<i>Ca(ClO</i> ₄) ₂	<i>Ca(NO</i> ₃) ₂
0.1	0.734	0.337	0.508	0.524	0.431	0.532	0.518	0.557	0.488
0.2	0.657	0.305	0.450	0.481	0.345	0.491	0.472	0.532	0.429
0.3	0.606	0.302	0.425	0.464	0.295	0.481	0.455	0.532	0.397
0.4	0.567	0.313	0.411	0.459	0.262	0.482	0.448	0.544	0.378
0.5	0.536	0.331	0.403	0.462		0.490	0.448	0.564	0.365
0.6	0.509	0.356	0.397	0.469		0.504	0.453	0.589	0.356
0.7	0.485	0.388	0.397	0.477		0.521	0.460	0.618	0.349
0.8	0.464	0.429	0.397	0.487		0.542	0.470	0.654	0.344
0.9	0.446	0.479	0.397	0.500		0.567	0.484	0.695	0.340
1.0	0.429	0.539	0.401	0.513		0.596	0.500	0.743	0.338
1.2	0.399	0.701	0.411	0.545		0.664	0.539	0.853	0.337
1.4	0.374	0.936	0.424	0.581		0.746	0.587	0.992	0.337
1.6	0.352	1.284	0.439	0.622		0.846	0.644	1.161	0.339
1.8	0.333	1.819	0.455	0.674		0.968	0.712	1.372	0.342
2.0	0.316			0.718		1.119	0.792	1.634	0.347
2.5	0.280			0.868		1.654	1.063	2.62	0.362
3.0	0.252			1.047		2.53	1.483	4.21	0.382
3.5	0.229			1.287		3.88	2.08	6.76	0.407
4.0	0.210			1.545		6.27	2.93	10.77	0.438
4.5	0.194			1.826		10.64	4.17	17.02	0.472
5.0	0.181			2.13		18.43	5.89	26.7	0.510
5.5	0.169					31.7	8.18	41.7	0.551
6.0	0.159					55.7	11.11	63.7	0.596

(v) Paper electrophoretic mobilities

Here we can measure the mobility of an ion in an excess of background electrolyte. For example, Table IV shows mobilities of metal ions in various concentrations of perchloric acid⁵. The conditions here are similar to those in ion-exchange equilibria. The values shown are relative and illustrate that all divalent and polyvalent metal ions travel with similar speeds and that this speed is about half of that of a monovalent cation (in this instance we used Tl⁺; other monovalent ions were not run in these experiments because of the difficulty in finding suitable detection reagents).

In the case of the two series of data which (although they cannot be directly compared) both show that in eluent solutions from 0.1 to 1.0 *M* the existence of an M²⁺ or M³⁺ is most unlikely owing to the strong interactions between the metal ions and their counter anions. Hence the high "charges" exhibited in ion-exchange equilibria were perplexing. Some light was thrown on this problem by the paper electrophoretic behaviour of metal ions in 0.5 *M* sulphate solution at pH 1.

A series of metals were examined by Chakraborty⁷, as shown in Table V. Here monovalent metals, such as Ag⁺ and Tl⁺, move fastest, followed by divalent metal

$CdCl_2$	$Cd(NO_3)_2$	$CdSO_4$	$CoCl_2$	$Co(NO_3)_2$	$CrCl_3$	$Cr(NO_3)_3$	$CsCl$	$CuCl_2$
0.2280	0.516	0.150	0.523	0.521	0.331	0.319	0.756	0.510
0.1638	0.467	0.103	0.479	0.474	0.298	0.285	0.694	0.457
0.1329	0.445	0.0822	0.463	0.455	0.294	0.279	0.656	0.431
0.1139	0.433	0.0699	0.459	0.448	0.300	0.281	0.628	0.419
0.1006	0.428	0.0615	0.462	0.448	0.314	0.291	0.606	0.413
0.0905	0.426	0.0553	0.470	0.451	0.335	0.304	0.589	0.411
0.0827	0.426	0.0505	0.479	0.458	0.362	0.322	0.575	0.411
0.0765	0.428	0.0468	0.492	0.468	0.397	0.344	0.563	0.412
0.0713	0.431	0.0438	0.511	0.480	0.436	0.371	0.553	0.415
0.0669	0.436	0.0415	0.531	0.493	0.481	0.401	0.544	0.419
0.0599	0.449	0.0379	0.578	0.526	0.584	0.474	0.529	0.427
0.0546	0.463	0.0355	0.634	0.566		0.565	0.518	0.436
0.0504	0.481	0.0338	0.699	0.613			0.509	0.446
0.0469	0.498	0.0327	0.773	0.668			0.501	0.457
0.0441	0.518	0.0321	0.860	0.730			0.496	0.468
0.0389	0.573	0.0317	1.120	0.926			0.485	0.496
0.0352		0.0329	1.458	1.189			0.479	0.522
0.0325		0.0356	1.832	1.535			0.475	0.549
0.0306			2.22	1.984			0.474	0.575
0.0291				2.57			0.474	0.599
0.0279				3.33			0.475	0.623
0.0270							0.477	0.650
0.0263							0.480	0.676

ions. The trivalent metal ions move very little, either positively (*e.g.*, Al^{III} and Y^{III}) or negatively (*e.g.*, La^{III} and Sc^{III}).

Two important points are that: (i) it can be shown that in 0.5 M sodium sulphate at pH 1 the preponderant species is HSO₄⁻, which is almost the same anion as the functional groups in a sulphonic resin; (ii) it is known that most of these anionic moving trivalent metal ions did not form sulphate complexes, because in the crystalline double salts (alums) the cation is present as a hexahydrate, *viz.*, the movement is governed by ion-pair formation between an [M^{III}(H₂O)₆]³⁺ ion and a number of anions, probably HSO₄⁻ or SO₄²⁻ ions.

We feel that the comparison of the ion exchange equilibrium data and the electrophoretic data suggest that retention of trivalent metal ions probably involves ion-pair formation between the hydrated metal ion and the sulphonic groups, which is the same as seen in electrophoresis, *i.e.*, ion-pair formation with hydrogensulphate anions. This would explain why apparent charges of 5–6 are possible with Co(NH₃)₃³⁺ and Co(en)₃³⁺.

The apparent charge of 3 on metal ions such as Al^{III} seems to be due to a coincidence of several factors and further is observed only in some resins.

TABLE IV

DISTANCE MOVED BY METAL IONS IN HClO_4 BY HIGH-VOLTAGE ELECTROPHORESIS (FROM REF. 5)

Paper: Whatman No. 1. Experiments conducted at 3–4°C for 2 h at 300 V. Camag apparatus.

Metal ion	Distance in mm corrected for electroosmotic flow (with H_2O_2)		
	0.1 M HClO_4	0.5 M HClO_4	1.0 M HClO_4
Tl ^I	93	76	61
UO_2^{2+}	45	35	35
Bi ^{III}	46	49	50
Cd ^{II}	60	56	52
Pb ^{II}	74	57	57
Cu ^{II}	61	47	50
Fe ^{III}	52	45	47
Co ^{II}	61	56	51
Ni ^{II}	62	56	51
Mn ^{II}	70	57	50
Zn ^{II}	62	57	51
Al ^{III}	69	56	49
Y ^{III}	67	59	52
La ^{III}	75	65	58
Zr ^{IV}	28 comet	37 comet	38 comet
Th ^{IV}	49	55	55

TABLE V

DISTANCES MOVED BY METAL IONS IN 0.5 M SODIUM SULPHATE SOLUTION ADJUSTED TO pH 1 WITH SULPHURIC ACID IN 1 h AT 360 V (FROM REF. 7)

Metal ion	Distance moved (mm)	Metal ion	Distance moved (mm)
Ag ^I	39	In ^{III}	–14
Tl ^I	50	Ga ^{III}	–6
Fe ^{III}	21	Bi ^{III}	–12
Co ^{II}	22	$\text{Co}(\text{NH}_3)_6^{3+}$	12
Ni ^{II}	21	Sc ^{III}	–14
Zn ^{II}	23	Y ^{III}	9
Cd ^{II}	19	La ^{III}	–6
Cu ^{II}	23	Th ^{IV}	–30
Mn ^{II}	13	Zr ^{IV}	–19
Mg ^{II}	26	Ti ^{IV}	–24
Be ^{II}	7	V ^{IV}	–11
Pb ^{II}	0 (precipitated)	Ge ^{IV}	–4
Hg ^{II}	0	CrO_4^{2-}	–70
Fe ^{III}	–9	MoO_4^{2-}	–30
Al ^{III}	9	UO_2^{2+}	–44
Cr ^{III}	4		

This leaves some interesting questions open. Fig. 3 shows $\log [\text{HCl}]$ against R_M relationships over the ranges 1–12 M hydrochloric acid and 4–9 M perchloric acid. The activities of hydrochloric acid and perchloric acid are certainly not constant in this range. Linearity over the whole range is thus unexpected and so far unexplained.

"CORRECTION" OF THE SLOPE BY THE USE OF ACTIVITY COEFFICIENTS

It has been stated on various occasions that the "charge" determined by plotting $\log K_d$ (or R_M) against $\log [\text{eluent concentration}]$ gives incorrect values. It was suggested that the "theoretical" slopes of 3 and 2 for tri- and divalent cations can be obtained by multiplying the eluent concentration by the activity coefficient of the eluent.

The first such proposal was refereed some 30 years ago for this journal by Professor G. Alberti and I am grateful for his criticism, in which he pointed out that in an equation such as (see page 3):

$$K = G \cdot \frac{[\text{M}^{x+}]_r}{[\text{M}^{x+}]} \cdot \frac{[\text{H}^+]^x}{[\text{H}^+]_r^x}$$

we must know not only the activity coefficients of the eluent, but also that of the sulphonic groups of the resin and that of the metal ion in solution and in the resin. These cannot be determined readily but probably cancel each other. However, for an "accurate determination" the activity coefficients of all four terms in the equation would have to be introduced.

SOME CONSIDERATIONS OF INORGANIC EXCHANGERS

A typical inorganic ion exchanger fully investigated for its properties is zirconium oxide. For anion exchange it was postulated that there are free zirconium cations on the surface which attract anions from solution. The law of mass action plot for the CrO_4^{2-} anion yields exactly a slope of 2, and this was taken as evidence that the adsorption was ion exchange, *i.e.*, of an electrostatic nature⁸.

However, in paper electrophoretic experiments with chromate anions, chromate migrates in a Zr^{IV} or Th^{IV} solution as a cation, *viz.*, in solution an ion pair with a residual positive charge is formed. This strongly suggests that the equilibrium between chromate and Zr cations on the surface of zirconium oxide involves the same kind of association⁹.

The adsorption of Co^{III} complexes on a range of inorganic exchangers was examined by Lederer and Battilotti^{10,11}. The general behaviour of Co^{III} complexes in electrophoresis should also be mentioned here. The electrophoretic sequence changes radically according to the type of ion pairs (or outer-sphere complexes) formed with the electrolyte. In acetate or chloride, for example, the Co^{III} complexes with three "charges" travel at about the same speed. In sulphate or other anions prone to hydrogen bonding with ammine groups, the complexes with ammine groups are strongly retarded, whereas those with heterocyclic nitrogen such as dipyriddy complexes have high speed. In electrolytes with hydrophobic anions such as ClO_4^- or

TABLE VI

RELATIVE ELECTROPHORETIC MOVEMENT OF COBALT(III) COMPLEXES IN VARIOUS ELECTROLYTES (AFTER REF. 13)

en = Ethylenediamine; dip = dipyriddy; ophen = *o*-phenanthroline.

Electrolyte	$[Co(en)_3]^{3+}$	$[Co(dip)_3]^{3+}$	$[Co(ophen)_3]^{3+}$
1 M CH ₃ COONa	49	50	42
1 M LiCl	33	31	27
1 M NaClO ₄	72	14	8
1 M Cl ₃ CCOONa	38	0	-8
0.5 M Na ₂ SO ₄	-2	22	21
1 M NaH ₂ PO ₄	23	45	42

Cl₃COO⁻ it is the large complexes such as the dipyriddy complexes that move very little while the ammine complexes move at high speed (see Table VI, taken from refs. 12 and 13).

On zirconium(IV) oxide, as well as on titanium(IV) oxide, zirconium phosphate, alumina and thorium(IV) oxide, the hydrogen bonding ammine-type complexes are strongly retained, similar in sequence to those on a sulphonic ion exchanger, whereas on silica, the opposite sequence is observed, as shown in Fig. 4. The R_M vs. log [LiCl] plots are linear, showing that the adsorption follows a law of mass action equation with a slope of *ca.* 1. On inorganic ion exchangers there seems also to be strong evidence for ion pairing with the exchange groups. Depending on the exchanger, different mechanism may operate.

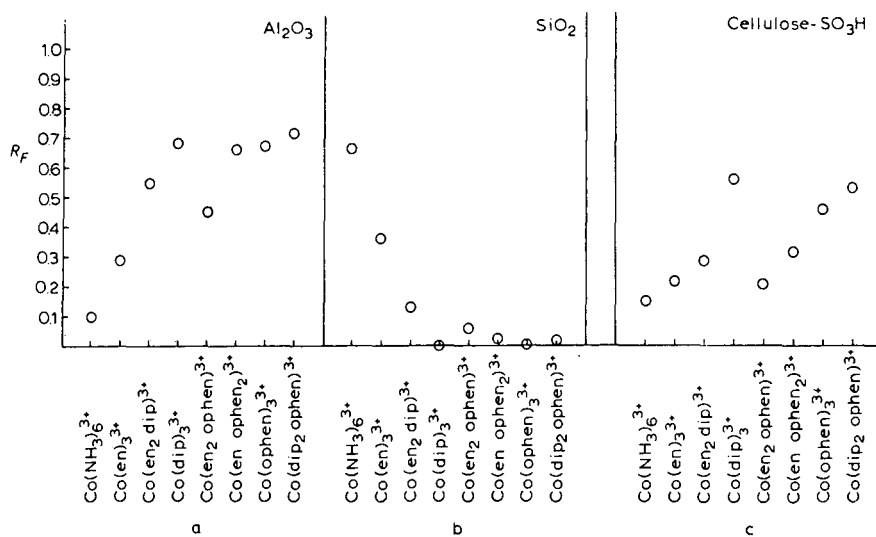


Fig. 4. Graphical representation of the R_F values of cobalt(III) complexes: (a) on MN Polygram Alox N thin layers developed with 0.1 M lithium chloride solution; (b) on MN Polygram Sil G thin layers developed with 0.1 M lithium chloride solution; (c) on MN ion-exchange paper with strongly acidic (sulphonic) groups developed with 0.5 M LiCl. (From ref. 10).

ION-EXCHANGE CHROMATOGRAPHY OF PROTEINS

The application of law of mass action-type equations has received the attention of numerous workers. We quote here from a thorough study by Kopaciewicz *et al.*¹⁴:

Since there are both acidic and basic residues within the same protein molecule, its net charge is pH-dependent. Under acidic conditions, basic amino acids are ionized, while carboxyl ionization is suppressed, and the protein obtains a net positive charge. Conversely, under basic conditions carboxyl groups are ionized, while the amino groups are neutral, and the protein accumulates a negative charge. Depending on the ratio of acidic to basic amino acids, at some intermediate pH, the net charge will be zero and a protein is said to be at its isoelectric point (*pI*). The exact pH of the isoelectric point is determined by both the type of amino acids and molecular structure. The amphoteric nature of a protein is best examined by a pH titration curve. Since a protein can exhibit net positive, neutral or net negative charge, depending on its *pI* and solution pH, the "net charge" concept has been used to predict retention behavior on ion-exchange columns. The general features of this concept are that proteins: (1) will not be retained on ion-exchange columns at their *pI* because they have no net charge; (2) will be retained above their *pI* on anion-exchange columns because they have a net negative charge; (3) will be retained below their *pI* on cation-exchange columns because they have a net positive charge; and (4) will show a correlation between net charge, as demonstrated by the titration curve and retention on ion-exchange columns. This hypothetical relationship between net charge and chromatographic retention is illustrated in Fig. A. A titration curve depicts net charge (*Z*), and a retention map (retention time *versus* pH) represents pH-dependent chromatographic behavior.

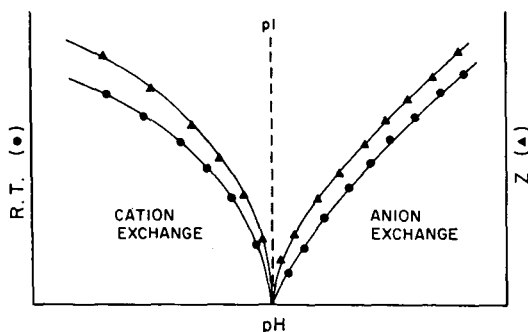


Fig. A. The hypothetical relationship between protein net charge and chromatographic retention. Net charge, *Z*, is depicted by a titration curve, and pH-dependent chromatographic behavior is represented by a retention map (retention time *vs.* pH).

Straight-line $\log K'$ *versus* $\log [\text{NaCl}]$ graphs were obtained, *e.g.*, Fig. 5. The effect of the cation and the anion of the eluent was also examined (see Table VII). The conclusions in ref. 14:

CONCLUSIONS

The retention of proteins on high-performance ion-exchange columns cannot be satisfactorily explained by the "net charge" concept alone. Approximately three-fourths of the proteins studied deviated from this concept in that they were retained at their respective *pI*. Thus, the importance of protein *pI* has apparently been

overemphasized. Non-systematic deviations from this concept are not the result of non-ionic interactions but, rather, are due to the nature of the protein molecule itself. Intramolecular charge asymmetry promotes differences in electrical potential on the surface of the protein. These regions of localized charge are present even when the net charge of the molecule is zero (at the pI) and are postulated to orient or "steer" the protein with respect to oppositely charged surfaces, such as ion-exchange support. An estimation of stationary-phase surface double-layer thickness indicates that it is small relative to protein dimensions; thus, this "steering effect" may be important during the adsorption-desorption process.

In addition to the charge characteristics of the protein itself, the nature of the support surface and the mobile-phase displacing ion are also important. Retention on both strong anion- and cation-exchange columns was shown to be affected by the choice of displacing salt. The extent of this effect varied among columns. In some cases, protein retention was altered as much as 100%. Individual proteins may respond differently to specific salts. This phenomenon may be linked to the thermodynamic activity of the displacing ion itself.

A non-mechanistic model for the retention of proteins on HPIEC columns was developed. Calculations of Z (the number of charges associated with the adsorption/desorption process) for β -lactoglobulin indicates that the number of charged sites involved in binding may be greater or less than the net charge of the protein. This would explain the lack of correlation between retention and titration curves for β -LAC. There appears to be a positive correlation between Z and protein retention.

show that, as with trivalent ions, the net charge as measured by titration or in electrophoresis has no relevance for the Z measured by ion-exchange equilibria. Also, the anion and cation of the eluent can change the retention, evidently by ion-pair formation.

TABLE VII

INFLUENCE OF VARIOUS IONS ON THE RETENTION OF CYTOCHROME c AND LYSOZYME ON A STRONG CATION-EXCHANGE (SCX) COLUMN

Ion	Relative retention** on SCX*** column		Retention ratio [§] , LYS/CYT c	Ion	Relative retention*** on SCX*** column		Retention ratio [§] , LYS/ CYT c
	CYT c	LYS			CYT c	LYS	
<i>Anion* (sodium salt):</i>				<i>Cation* (chloride salt):</i>			
Fluoride	0.79	0.88	1.38	Lithium	1.00	1.00	1.22
Chloride	0.68	0.64	1.16	Sodium	0.58	0.55	1.16
Bromide	0.58	0.51	1.10	Potassium	0.57	0.55	1.19
Phosphate	0.54	0.57	1.29	Ammonium	0.59	0.58	1.19
Sulphate	0.90	0.85	1.16	Magnesium	0.56	0.54	1.18
Acetate	0.74	0.74	1.22				
Tartrate	0.98	0.99	1.25				
Citrate	1.00	1.00	1.23				

* Chromatography was performed at pH 6. The ionic strength of buffer B was 0.5.

** Unity refers to the longest retention time obtained with a 20-min gradient.

*** SCX refers to the Pharmacia Mono S column.

§ Ratios were calculated from the actual retention times.

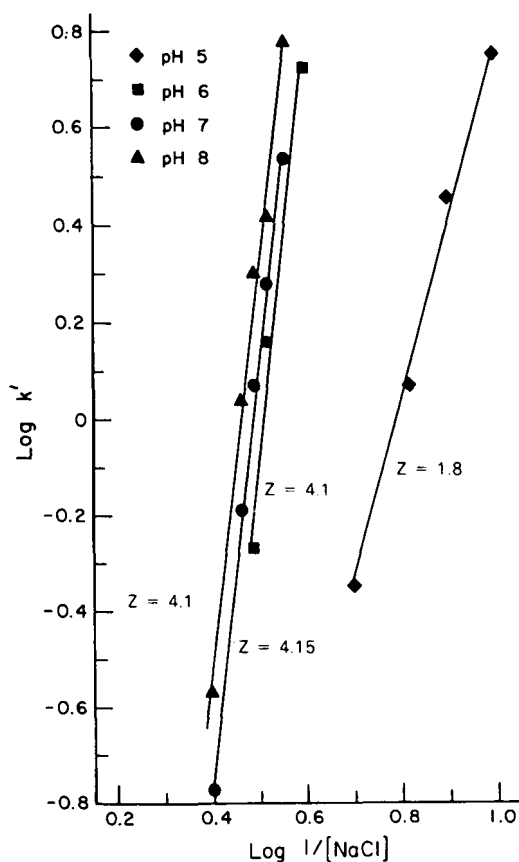


Fig. 5. Estimation of the number of charge interactions (Z) occurring between β -lactoglobulin and the surface of a strong anion-exchange column. β -Lactoglobulin was chromatographed isocratically at several pH values on a 25×0.41 cm I.D. silica-based SAX column. (From ref. 14).

CONCLUSIONS

Werner, at the turn of the century, observed that complexes of the type $\text{Co}(\text{NH}_3)_6^{3+}$ interacted strongly with anions in aqueous solution to the extent that the spectra of, e.g., chlorides and sulphates differed considerably. In the consideration of ion-exchange equilibria, the importance of such ion pairing or outer-sphere complexing has often been underestimated, and the possibility of ion pairing with the functional groups of the exchanger has not been sufficiently appreciated. The determination of the “charge” of a metal ion by the use of ion-exchange equilibria is strongly influenced by such ion pairing, especially when the metal ion has a charge of more than +2. Similar limitations have also been reported with proteins.

APPENDIX

Here I reproduce a letter to me from Professor Inczedy (with her permission) in which he discusses the problem of the "charge" on a metal ion.

"Concerning the problem of the ion exchange of cobalt-hexamine and similar complex cations, I have read your papers carefully and I have read also my papers which were published many years ago. After long consideration I would like to answer your questions as follows:

(1) If we use strongly acidic ion exchangers of the traditional type (styrene-DUB copolymers, sulphonated), the log (distribution ratio) vs. log [eluent ion (hydrogen ion) concentration] in the acidity range 0.1–1 *M* follows the ideal equation. Hence the slopes for Li, Na, K, Rb, Cs and NH₄ ions in hydrochloric and perchloric acid and for Tl and Ag ions in perchloric and nitric acid are very close to –1.

Similarly, the slopes for divalent ions (Cu, Zn, VO, Ca, Sr, Ba, Ni, Co, Mg, Mn, Fe, TiO) are very close to –2 in hydrochloric acid, and for Pb in nitric acid solutions. See [1] [2] [3].

For trivalent ions the slope is between 2 and 3. For example, for La³⁺ and Y³⁺ in hydrochloric acid it is close to three [1], but the slope for iron(III) and aluminium is between 2 and 3. For titanium the slope is close to 2, corresponding to the TiO²⁺ [or Ti(OH)₂²⁺] ion [3].

[1] F. W. Strelow, *Anal. Chem.*, 32 (1961) 1185.

[2] F. W. Strelow, R. Rethemeyer and C. J. C. Bothma, *Anal. Chem.*, 37 (1965) 106.

[3] F. W. Strelow and H. Sondorp, *Talanta*, 19 (1972) 1113.

The mentioned phenomena are valid, of course, only for traditional ion-exchange resins of high capacity and of the strongly acidic type. In those systems the ion-exchanger phase can be assumed to be a strong electrolyte system. The deviations from the ideal slope for the trivalent ions can be attributed to partial hydroxo or chloride complex formation and also to steric problems discovered by you.

Salmon published a paper [4], 30 years ago in which the partial charge of the complex is determined by saturation of the ion exchanger with the solution of the complex. From the capacity of the resin and from the adsorbed amount of the metal ion the partial charge is calculated.

It is a very interesting statement in your paper that by lowering the capacity of the ion-exchanger phase the slope number "decreases". Thus the ion-exchange sites are not accessible by the polyvalent ions owing to steric problems. This effect is very similar to that which we found earlier, *viz.*, that the divalent tetracyanozincate ions are bound only monovalently to the anion exchanger, and the ion exchange sites are shared between cyanide and Zn(CN)₄²⁻ ions [5].

[4] J. E. Salmon, *Rev. Pure Appl. Chem. (Australia)*, 6 (1956) 24.

[5] J. Inczedy and Frankow, *Period. Polytech.*, 11 (1967) 53.

(2) The nickel-, cobalt-, copper-, cadmium- and zinc-ammine complexes are bound very strongly to sulphonic acid-type resin. This phenomenon is based on the fact that the ammine complex cations, surrounded with NH₃ ligands, are not hydratable in comparison with aquo complex ions. Especially those cations are the most strongly adsorbed for which the coordination sphere is completely saturated, *e.g.*, Ni(NH₃)₆²⁺ or Cd(NH₃)₆²⁺. The volume of the resin saturated with the mentioned ammine complex cations is smaller than that of the hydrated cations (*i.e.*, aquo complexes). The interaction between the resin sites and the ammine complex ion is rather strong. One cannot speak any more about a strong electrolyte system. The ions and the fixed ionic groups are very close to each other, and the electrostatic force is dominating. The behaviour of ethylenediamine complexes is similar, but different for those complex cations in which the coordinated neutral ligand is much larger (dipyridyl or *o*-phenanthroline, etc.).

An ion-exchanger experiment with trivalent cobalt hexammine complex and with a conventional ion-exchange resin is almost impossible, because the adsorption of the complex ions and the water release are very high, and the resin cannot be regenerated completely.

(3) The "unusual high slopes" of the Co(NH₃)₆³⁺ and Co(en)₃³⁺ ions obtained by you may be attributed to the formation of associated species. The concentration of the acid (hydrochloric or perchloric acid) used in the experiments is also high, 4–10 *M*, where the water activity is low, and the formation of the associated species and ion pairs is highly favoured. The medium does not correspond to the usual strong electrolyte systems, where well hydrated simple ions in fairly dilute aqueous solutions are present. In your

system in the strongly acidic solutions the hydrophobic complex cations may form binuclear species with attached chloride or perchlorate ions, which are expelled from the aqueous phase to the hydrophobic phase, but negatively charged resin particles are embedded in the paper.

(4) The electrophoretic mobility of the simple cations depends on the volume of the hydrated ion and on the total charge. Since the volume of the hydrated ions is not perfectly known, and the number of the water molecules in the hydrate sphere change according to the temperature, it is very difficult to predict the mobility values of the cations. Li^+ has a high charge density, being a very small ion, and its hydrate sphere is large. Therefore, its mobility is very low. Since the mass increases in the order $\text{Li} < \text{Na} < \text{K} < \text{Rb} < \text{Cs}$, the hydrate sphere decreases and the mobility increases from Li^+ to Cs^+ . However, the mass of NH_4^+ is small (less than that for Na^+) and its mobility is similar to that of K^+ because NH_4^+ has a lower hydration tendency than Na^+ . Divalent metal ions have a double charge, but their hydration ability is therefore also higher. Ca^{2+} is more mobile than Mg^{2+} , having a larger mass, but has a lower hydration ability. This is true also for Pb^{2+} , which has an even greater mass but a very small hydrate sphere and a high mobility. Cu^{2+} and Zn^{2+} are of medium mass (63.5 and 65), but their mobilities are low, similar to that of Mg^{2+} . Hence it is more difficult to predict the behaviour of the trivalent ions. In certain cases, by increasing the ion mass, the mobility also increases, e.g., $\text{Al}^{3+} < \text{Cr}^{3+} < \text{Fe}^{3+}$. I am afraid one cannot draw unambiguous conclusions from the data mentioned.

Conclusions; (1) you are completely right, that in those systems where the ion-exchange phase is "dilute", i.e., is of low capacity, the polyvalent ions cannot access corresponding ion-exchange sites, and therefore the value of the ionic charge seem to be lower than the real value. The data in Table III in the paper by Cerrai, Ghersini, Lederer and Mazzei [*J. Chromatogr.*, 44 (1969) 161] are very convincing.

(2) In the experiments reported in the paper by Mazzei and Lederer [*J. Chromatogr.*, 40 (1969) 197], the ion-exchanger system is very different from the conventional hydrated systems. In the strongly acidic heterogeneous mixed solid phase used, unusual interactions and also kinetic hindrance must be assumed, which are very probably responsible for the very high slopes obtained for the $\log R_M$ vs. \log (acid concentration) diagrams."

REFERENCES

- 1 H. F. Walton, in F. C. Nachod (Editor), *Ion Exchange*, Academic Press, New York, 1949, pp. 3–28.
- 2 V. Carunchio and G. Grassini-Strazza, *Chromatogr. Rev.*, 8 (1966) 260–290.
- 3 M. Mazzei and M. Lederer, *J. Chromatogr.*, 40 (1969) 197.
- 4 F. Giannetta and M. Lederer, *J. Chromatogr.*, 49 (1970) 573.
- 5 E. Cerrai, G. Ghersini, M. Lederer and M. Mazzei, *J. Chromatogr.*, 44 (1969) 161.
- 6 L. Meites, *Handbook of Analytical Chemistry*, McGraw-Hill, New York, 1963.
- 7 H. C. Chakraborty, *J. Chromatogr.*, 5 (1961) 121.
- 8 K. A. Kraus, H. O. Phillips, T. A. Carlson and J. S. Johnson, in *Proceedings of Second International Conference on the Peaceful Uses of Atomic Energy*, Vol. 28, United Nations, Geneva, 1958, p. 3.
- 9 M. Sinibaldi, G. Matricini and M. Lederer, *J. Chromatogr.*, 129 (1976) 412.
- 10 M. Lederer and M. Battilotti, *J. Chromatogr.*, 89 (1974) 380.
- 11 M. Battilotti and M. Lederer, *J. Chromatogr.*, 95 (1974) 81.
- 12 M. Lederer and M. Mazzei, *J. Chromatogr.*, 35 (1968) 201.
- 13 M. Mazzei and M. Lederer, *J. Chromatogr.*, 31 (1967) 196.
- 14 W. Kopaciewicz, M. A. Rounds, J. Fausnaugh and F. E. Regnier, *J. Chromatogr.*, 266 (1983) 3.
- 15 W. C. Baumann, in F. C. Nachod (Editor), *Ion Exchange*, Academic Press, New York, 1949.

CHROM. 20 473

METHYL GREEN-COATED COLUMN FOR SEPARATION OF INORGANIC ANIONS BY ION CHROMATOGRAPHY

ROLF GOLOMBEK

Institut für Lebensmittelchemie und Analytische Chemie der Universität, Pfaffenwaldring 55, D-7000 Stuttgart 80 (F.R.G.)

and

GEORG SCHWEDT*

Institut für Anorganische und Analytische Chemie der Universität, Paul-Ernst-Strasse 4, D-3392 Clausthal-Zellerfeld (F.R.G.)

SUMMARY

A polystyrene–divinylbenzene column (PRP-1) was coated with methyl green to obtain an anion-exchange column with adsorbed quaternary ammonium groups. The efficiency of the coated column was examined. Two different eluents previously applied to single-column anion chromatography with chemically bonded exchanging groups were used with only little modifications. Baseline separation for eight common anions can be achieved and water analyses, *e.g.*, mineral water, can be realized with these systems. No organic modifier is needed to obtain an efficient separation and only small amounts of dyestuff have to be added. The performance of this column is comparable to that of a chemically bonded anion-exchange column, *e.g.*, PRP-X 100. Besides efficient separation, this system provides the advantage that the column lifetime increases because the lost anion exchanging sites are replaced by the eluent which contains the dyestuff.

INTRODUCTION

One of the chromatographic separation methods for ions is ion-pair chromatography which has been developed by Eksborg *et al.*¹. The well known effect of ion-pair formation has found wide applications in the separation of organic and also inorganic ions. Haddad and Heckenberg² have reviewed ion chromatography as well as “ion-pair” chromatography.

Ion interaction columns are generally produced by sorption of an organic, hydrophobic and ionic molecule onto the surface of a reversed-phase column. A charged double layer is obtained³. Corresponding to this principle, this technique was also called “soap chromatography”⁴. Other terms used were listed by Bidlingmeyer *et al.*⁵. Systems for the separation of inorganic anions have been developed by several authors^{6–14}. Aliphatic amines and mainly quaternary ammonium salts were applied as counter ions. One of the major works on coated columns for ion chromatography is that of Duval and Fritz¹⁵.

The retention mechanism in "ion-pair" liquid chromatography was examined by Bidlingmeyer *et al.*⁵, Hung and Taylor¹⁶ and Knox and Hartwick¹⁷. The authors came to different conclusions, so that no comprehensive explanation for all "ion-pair" chromatographic systems can be given.

Cassidy and Elchuk^{7,10,12} produced dynamically coated and also "permanent" sorbed fixed-site ion exchangers. The systems differed only in the length of the hydrophobic hydrocarbon chain of the ion interaction reagent. A fixed-site column does not need any ion interaction reagent in the mobile phase and acts as an ion exchanger. Obviously these chromatographic systems cannot be definitively divided into "ion-pair" or ion-exchange chromatography. Cassidy and Elchuk used the more adequate term "ion interaction" chromatography. The use of dyestuffs in chromatographic separation was first described by Gnanasambandan and Freiser¹⁸. They employed methylene blue for the separation of aliphatic alcohols. The dye-alcohol complex formation and the partitioning equilibrium were investigated. In other studies methyl green was used for conditioning the column in ion interaction chromatography of inorganic ions to provide sharper peaks and shorter elution times, by eliminating interaction with the basis material¹¹.

Brilliant green as the stationary phase on a chemically bonded ODS column and the separation of aliphatic acids on this column was described by DiNunzio and Freiser¹⁹. The mobile phase consisted only of organic solvents. The process was described as real "ion-pair" chromatography.

Kang²⁰ developed a chromatographic system with methylene blue as the counter ion for the separation of organic and inorganic anions. The separation on a chemically bonded octadecyl silica gel column with an aqueous eluent and methanol as the organic modifier showed peak tailing.

Previous studies²¹ pointed out that a styrene-divinylbenzene copolymer column with chemically bonded quaternary ammonium groups (PRP-X 100) showed a loss of ion-exchange capacity. The concentration of the organic acid in the eluent had to be decreased to obtain separations comparable to those achieved on a new column. Preliminary studies showed that the ion-exchange capacity can be increased by adsorption of methyl green. The basis material of a PRP-X 100 column is a PRP-1 resin²². Owing to these facts it should be possible to develop a methyl green-coated column for single-column anion chromatography that possesses a performance comparable to that of a chemically bonded ion-exchange column. The same simple eluents as used for chemically bonded columns are expected to be applicable.

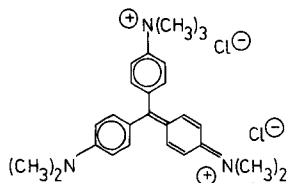
EXPERIMENTAL

Apparatus

The HPLC equipment consisted of a dual-head reciprocating pump (Bischoff 2200), a syringe-loading sample injector (Bischoff 7125) and a variable-wavelength UV detector (Bischoff 8201) linked to a pen recorder (Kipp-Zonen BD8 multi range) or to a computing integrator (Shimadzu C-R3A). An autosampler (Talbot ASI-3) was also used instead of a syringe-loading sample injector. The variable-loop injector with an 100- μ l loop was integrated in a thermobox (Bischoff 4000) kept to room temperature. The chart speed of the recorder was 1 cm/min. For studying the detector response in the visible range a UV-VIS detector (Kratos Spectroflow 757) was used.

Reagents

2,4-Dihydroxybenzoic acid (purum, Fluka; 98%) and 4-hydroxybenzoic acid (puriss, Fluka) were used. Chloride in methyl green (Fluka, for microscopy) was replaced with iodide on an anion-exchange resin. The anion exchanger (Amberlite, Type IRA 400, counter ion Cl^-) was completely transformed into the iodide form for conversion of 100 mg methyl green in 50 ml water on a short column (8 cm \times 2 cm). The final volume of the dyestuff solution was 200 ml. This column was regenerated before each conversion and had been used for 3 months.



The other reagents used were analytical grade. They were used without further purification. Water was always first deionized and then distilled.

Column and column coating

A Bischoff Hyperchrome SC column (125 mm \times 4.6 mm I.D.) packed with Hamilton PRP-1 was used. The particle size was 5 μm . Aqueous methyl green solution (0.5 g/l) was degassed for column coating. Potassium hydroxide was added to a pH of about 10. The methyl green was used as received without any anion exchange. The dyestuff solution was pumped through the column at a flow-rate of 0.5 ml/min until it appeared at the column exit. After completion of column coating, the system, except the column, was washed with water and afterwards with mobile phase. Then the coated column was connected with the system to obtain equilibration. If the column with sorbed dyestuff were to be washed with water, adsorbed methyl green would be removed.

Mobile phase

The organic acids were dissolved by adding potassium hydroxide in half the final volume. The pH value of this solution should be acid, otherwise difficulties arise owing to the carbonate content in the eluent. When the organic acid was completely dissolved, the required amount of methyl green was added. The eluent was degassed by a water-jet pump. The mobile phases were kept in polyethylene bottles.

Sample preparation

Samples with high contents of cations, *e.g.*, mineral water, have to be pretreated with a cation-exchange resin (Serva, Dowex 50W-X8; analytical grade, 100–200 mesh, H)²¹. An high content of carbonate can be decreased by the above pretreatment in combination with degassing of the sample. By using a 1 g/l potassium carbonate solution, it can be determined whether the cation exchanger has to be washed before use. Therefore the carbonate solution has to be pretreated as mentioned above and analyzed by the chromatographic system. With the exception of the injection and system peaks and perhaps a little carbonate peak, no peaks should appear in the chromatogram.

RESULTS AND DISCUSSION

Methyl green was chosen for the column coating on account of its quaternary ammonium group and its good water solubility. In addition, the dyestuff possesses a distinct hydrophobicity, therefore column coating can be realized. The pH value of the methyl green solution must be in the basic range during the column coating procedure, otherwise the adsorption rate will decrease due to reduced hydrophobicity of the dyestuff. The amount of dyestuff adsorbed was determined by the breakthrough method; 50 mg of methyl green were adsorbed on a short column as used in the present work. After column coating, the chromatographic equipment is washed with water, with the exception of the column in order to prevent loss of dyestuff. It is possible but not absolutely necessary to wash the coated column with alkaline water before equilibration with the eluent. Storing the column with the eluent is practicable for about 3 days. If the column is to be stored for a longer period, it has to be washed with methanol to remove the dyestuff, otherwise the column pressure will increase irreversibly when using the column again.

Indirect photometric detection is used for detecting "transparent" ions, as described in detail by Small and Miller^{2,3}. The detection wavelength does not coincide with the absorption maximum of the eluent. The most suitable wavelength for the 4-hydroxybenzoic acid eluent is 311 nm; it has the most favourable signal-to-noise ratio. The wavelength was also used in preliminary studies made with a PRP-X 100

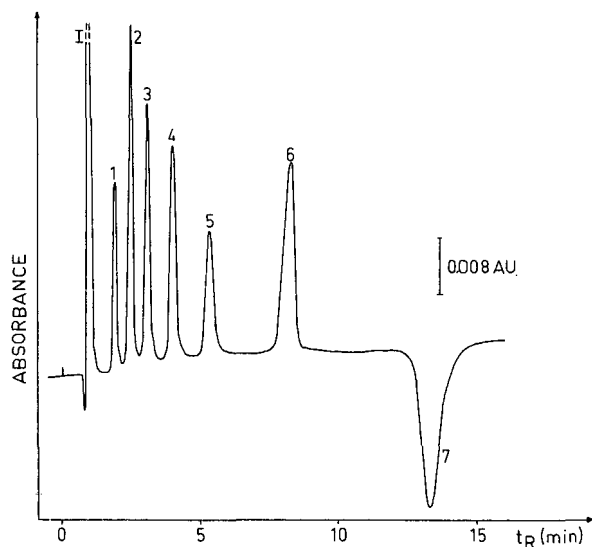


Fig. 1. Chromatogram of an anion standard solution. Eluent: $6 \cdot 10^{-3}$ mol/l 4-hydroxybenzoic acid and 50 mg/l methyl green adjusted to pH 9.0 with potassium hydroxide. Column: Bischoff Hyperchrome SC (125 mm \times 4.6 mm I.D.) packed with Hamilton PRP-1 resin. The column was equilibrated with methyl green. Flow-rate: 1.0 ml/min. Sample size: 100 μ l. UV detection: wavelength 311 nm. Peaks: 1 = injection peak; 1 = fluoride (10 mg/l); 2 = hydrogencarbonate (50 mg/l); 3 = chloride (30 mg/l); 4 = nitrite (50 mg/l); 5 = bromide (50 mg/l); 6 = sulphate (100 mg/l); 7 = system peak.

TABLE I
RETENTION OF INORGANIC ANIONS

For conditions see Fig. 1.

<i>Anion</i>	<i>k'</i>	<i>Anion</i>	<i>k'</i>
Borate	0.7	Selenite	4.7
Fluoride	1.1	Phosphate	5.4
Iodate	1.25	Arsenate	5.5
Hydrogencarbonate	1.6	Nitrate	6.5
Chloride	2.2	Sulphate	7.2
Bromate	3.1	Selenate	8.2
Nitrite	3.2	Chlorate	10.4
Bromide	4.6	System peak	12.2

chemically bonded anion-exchange resin and a mobile phase without methyl green. Methyl green does not affect UV detection at 311 nm. Preliminary studies showed that conductivity detection can also be used.

To examine the efficiency of the new column, two different eluents were chosen which had been applied to single-column anion chromatography with a chemically bonded anion-exchange resin (PRP-X 100)^{21,22}. The first eluent uses 4-hydroxybenzoic acid as the eluting agent. Fig. 1 shows the separation of an anion standard mixture obtained on a methyl green-coated column by using a 4-hydroxybenzoic acid eluent and indirect UV detection (see also Table I). The separation is similar to that achieved by Lee²² on a chemically bonded column.

The chromatographic run time achieved with the present system was slightly longer than that reported by Lee, but a more efficient separation of fluoride from the injection peak can be realized. In addition, chloride and nitrate are baseline separated and the chromatogram shows a better peak shape. Almost the same eluent was used as proposed by Lee²² for the separation of anions on a PRP-100 column. Only the elution power was reinforced by increasing the concentration of 4-hydroxybenzoic acid and the pH was adjusted to 9 with potassium hydroxide. The flow-rate was decreased to 1.0 ml/min, thus a smaller quantity of eluent is needed.

Methyl green was obtained as a chloride salt. If it is used in this form, interferences are observed in the detection of chloride. The chloride content in the eluent creates a small peak exactly at the elution time of chloride. The signal is positive in contrast to the chloride signal of the sample. This behaviour is in accord with results obtained with other chromatographic systems²⁴.

It is impossible to exchange chloride for hydroxide because the dyestuff precipitates during the exchange of the counter ion. Iodide was chosen as the counter ion because it is eluted together with the system peak. Thus the separation and detection of the other sample anions is not influenced by a resulting negative peak.

The column efficiency calculated by using the width at half peak height was 3000 plates for chloride and 4500 for sulphate with 4-hydroxybenzoic acid as the eluting agent (column length 125 mm).

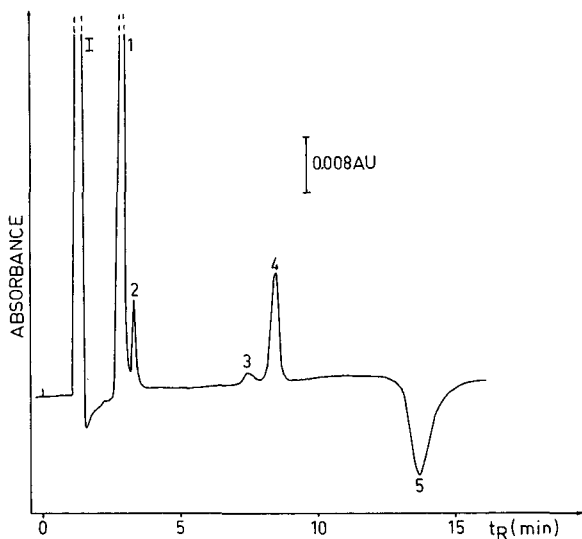


Fig. 2. Chromatogram of anions in tap-water. For conditions see Fig. 1. Peaks: I = injection peak; 1 = hydrogencarbonate; 2 = chloride (9 mg/l); 3 = nitrate (3.4 mg/l); 4 = sulphate (56.5 mg/l); 5 = system peak.

Fig. 2 shows the chromatogram of a tap-water sample. The sample is only degassed because the low content of cations does not influence the anion separation and detection. When samples of mineral water are analyzed, as illustrated in Fig. 3,

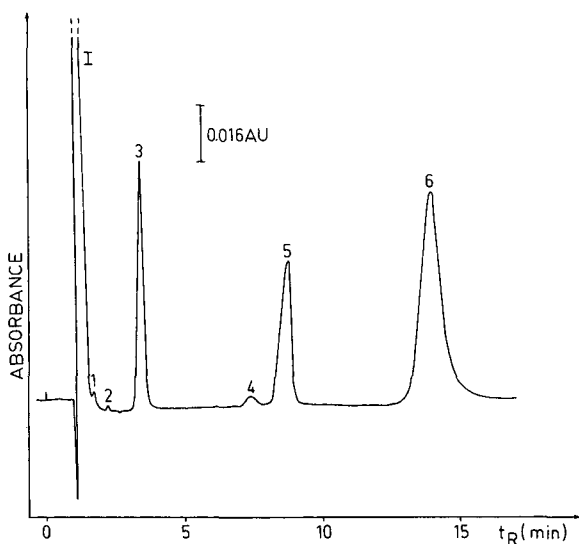


Fig. 3. Anion analysis in the mineral water "Radenska". The sample was pretreated with a cation-exchange resin and degassed (see Experimental). For other conditions see Fig. 1. Peaks: I = injection peak; 1 = borate (9.8 mg/l); 2 = fluoride (0.74 mg/l); 3 = chloride (68.3 mg/l); 4 = nitrate (5.6 mg/l); 5 = sulphate (155 mg/l); 6 = system peak.

TABLE II

DETECTION LIMITS (IN $\mu\text{g/l}$, BASED ON THREE TIMES THE BASELINE NOISE) OF SEVERAL INORGANIC ANIONS

<i>4-Hydroxybenzoic acid</i> (for conditions see Fig. 1)		<i>2,4-Dihydroxybenzoic acid</i> (for conditions see Fig. 7)	
Fluoride	100	Fluoride	20
Chloride	150	Chloride	40
Carbonate	200	Nitrite	75
Nitrite	400	Silicate	90 (as Si)
Sulphate	500	Bromide	250
Bromide	1000	Sulphate	400
		Phosphate	1500

pretreatment with a cation-exchange resin is absolutely necessary. Without this a large negative peak results from the high content of cations. Thus the detection of early eluting anions is impossible. When eluting with 4-hydroxybenzoic acid, the

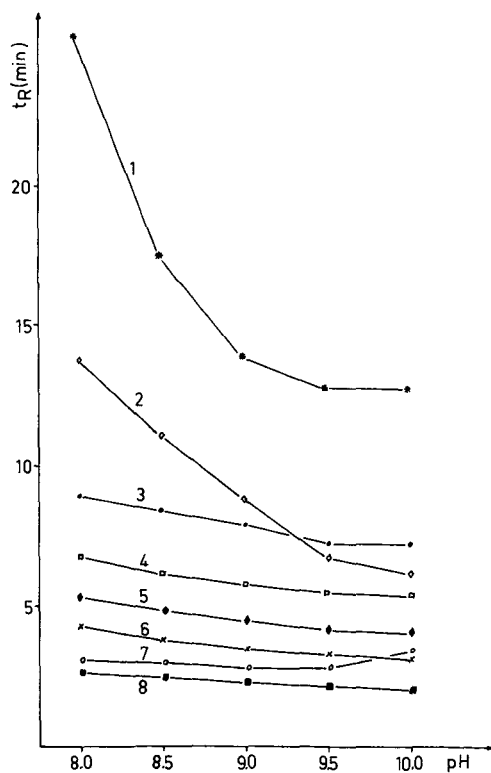


Fig. 4. Dependence of the elution time on the pH of the eluent. For other conditions see Fig. 1. 1, System peak; 2, sulphate; 3, nitrate; 4, bromide; 5, nitrite; 6, chloride; 7, carbonate; 8, fluoride.

methyl green-coated column enables fluoride detection in water samples for more than 2 months, in contrast to a PRP-X 100 column that shows an evident loss of ion-exchange capacity²¹.

The detection limits of six main anions are listed in Table II. They are low enough for anion analyses of natural water samples. Fig. 4 illustrates the correlation of pH and elution time of the anions. At pH < 8 no chromatogram can be obtained because of decreasing dissociation of 4-hydroxybenzoic acid. In the range pH 9.5–10.0 the baseline worsens and at pH 9.2–9.3 no separation of nitrate and sulphate can be realized. The most efficient separations were obtained at pH 9.0.

Concentrations of 4-hydroxybenzoic acid from $0.4 \cdot 10^{-2}$ to 10^{-2} mol/l were studied. As expected, higher contents of organic acid shorten the elution time. At the lowest concentration no sulphate peak appears after 40 min.

Different concentrations of methyl green in the eluent (5–100 mg/l) were tested to determine the dependence of retention on dyestuff concentration. The elution time of the anions remains nearly constant in the range of 40–100 mg/l. At dyestuff contents higher than 50 mg/l the baseline noise increases. If no dyestuff is dissolved in the mobile phase, the elution time will decrease very slowly. After 6 h, sulphate is still eluted at 6.5 instead of 8.6 min.

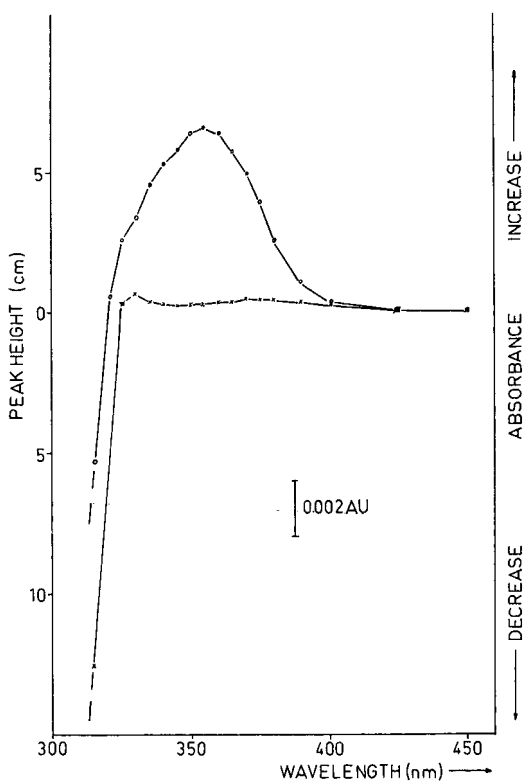


Fig. 5. Dependence of the peak height and absorbance on the detection wavelength. O, Nitrite (50 mg/l); x, chloride (30 mg/l). For other conditions see Fig. 1.

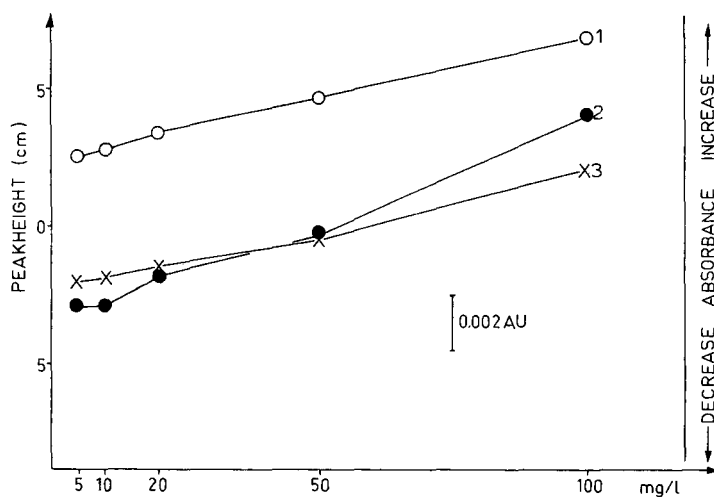


Fig. 6. Dependence of the peak height and absorbance on the methyl green concentration in the mobile phase. Detection wavelength: 324 nm. 1, nitrite (50 mg/l); 2, carbonate (50 mg/l). 3, chloride (30 mg/l). For other conditions see Fig. 1.

Two of the anions tested interact with methyl green and produce species that influence eluent absorption. The phosphate peak cannot be quantified because it is in part positive and negative. If phosphate is dissolved in the eluent, the colour of the solution changes slowly to blue in about half an hour. Eluents with a pH > 9.3 give an uniform signal for phosphate, but the baseline noise increases as mentioned above. The other interacting anion is nitrite. It changes the colour of the solution slowly to yellow when dissolved in mobile phase. Thus the peak height of the nitrite peak is not influenced in the same way as the peaks of the other anions while changing the detection wavelength (Fig. 5). The curves for other anions are similar to that obtained for chloride. At a wavelength of about 318–319 nm the peak height is zero for nitrite, while this characteristic point is reached at 324 nm for the other anions. In contrast to the other anions, nitrite has another maximum in peak height at 355 nm. Therefore selective detection of nitrite can also be achieved when a sample contains a large quantity of chloride or other neighbouring ions.

As expected, the peak height at these wavelengths is also influenced by the concentration of methyl green in the mobile phase (Fig. 6). Studies were carried out at a constant wavelength of 324 nm, where all anions except nitrite results in only very small peaks when using the normal eluent composition. The peak height of the nitrite peak is nearly linear with respect to the dyestuff content in the eluent. As stated above, the baseline noise increases at higher methyl green concentrations.

The second eluent, chosen for testing the methyl green-coated column, uses 2,4-dihydroxybenzoic acid as the organic acid in the mobile phase, so that also the determination of silicate in water samples can be realized. The concentration and pH value are the same as in previous studies with this eluent on a PRP-X 100 column²¹. The concentration of methyl green in the eluent can be decreased to 10 mg/l due to the stronger hydrophobicity of the dyestuff at higher pH.

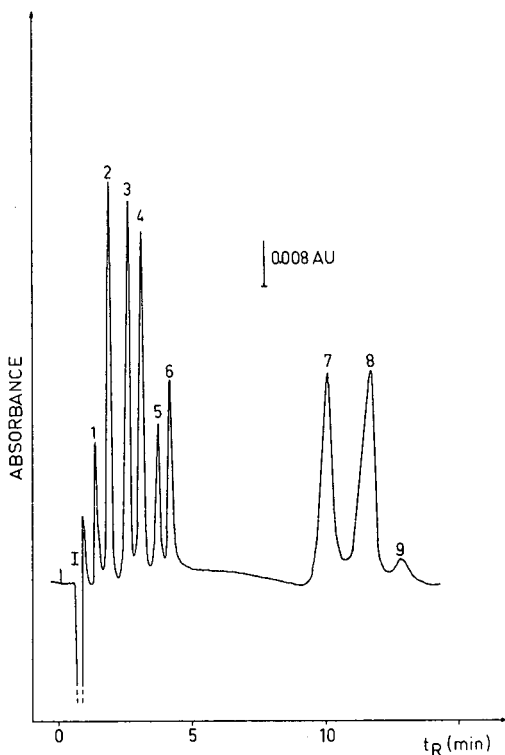


Fig. 7. Chromatogram of an anion standard solution. Eluent: 70 mg/l 2,4-dihydroxybenzoic acid and 10 mg/l methyl green adjusted to pH 10.1 with potassium hydroxide. Column: Bischoff Hyperchrome SC (125 mm \times 4.6 mm I.D.) packed with Hamilton PRP-1 resin. The column was coated with methyl green. Flow-rate: 1.5 ml/min. Sample size: 100 μ l. UV detection: wavelength 312 nm. Peaks: 1 = injection peak; 2 = silicate (10 mg/l); 3 = fluoride (3 mg/l); 4 = chloride (7 mg/l); 5 = nitrite (10 mg/l); 6 = bromide (10 mg/l); 7 = carbonate system peak; 8 = phosphate (20 mg/l); 9 = sulphate (20 mg/l); 9 = system peak.

Fig. 7 shows the chromatogram of an anion standard sample. The total elution time until the system peak has passed the detector is shortened in comparison with the separation obtained on a PRP-X 100 column. In addition, the flow-rate of the mobile phase is decreased to 1.5 ml/min, which is in part caused by the use of a shorter column. The difficulties previously described²¹ with a negative peak in front of the sulphate peak at pH > 10.2 can be avoided.

Anion separation of a tap-water sample can be realized (Fig. 8). The detection limits of the main anions are listed in Table II. They are inferior to those obtained by this eluent (without methyl green) on a PRP-X 100 column²¹ because of a better peak shape. The column efficiency expressed by the number of theoretical plates is 3500 for chloride and 5000 for sulphate (column length 125 mm).

The carbonate system peak results from the carbonate content in the sample and carbonate decontamination of the eluent, a fact that can be explained by the basic pH of the mobile phase.

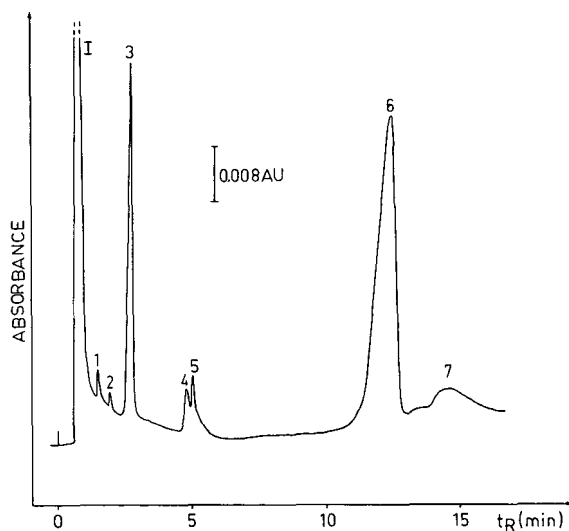


Fig. 8. Chromatogram of anions in tap-water. The sample was pretreated with a cation-exchange resin and degassed (see Experimental). For other conditions see Fig. 7. Peaks: 1 = injection peak, 1 = silicate (1.95 mg/l); 2 = fluoride (90 $\mu\text{g/l}$); 3 = chloride (5.8 mg/l); 4 = carbonate system peak; 5 = nitrate (3.2 mg/l); 6 = sulphate (45.6 mg/l); 7 = system peak.

It is possible to create an efficient anion-exchange column by sorbing methyl green on a styrene-divinylbenzene column. The separation system shows an increased stability compared to a PRP-X 100 column. Sorption of other organic molecules with different functional groups besides other triphenylmethane dyestuffs^{2,5} should be possible.

ACKNOWLEDGEMENT

Our thanks are due to Bischoff Analysentechnik, Leonberg (F.R.G.) for the loan of equipment and columns.

REFERENCES

- 1 S. Ekborg, P.-O. Lagerström, R. Modin and G. Schill, *J. Chromatogr.*, 83 (1973) 99–110.
- 2 P. R. Haddad and A. L. Heckenberg, *J. Chromatogr.*, 300 (1984) 357–394.
- 3 Z. Iskandarani and D. J. Pietrzyk, *Anal. Chem.*, 54 (1982) 1065–1071.
- 4 J. H. Knox and G. R. Laird, *J. Chromatogr.*, 122 (1976) 17–34.
- 5 B. A. Bidlingmeyer, S. N. Deming, W. P. Price, Jr., B. Sachok and M. Petrussek, *J. Chromatogr.*, 186 (1979) 419–434.
- 6 N. E. Skelly, *Anal. Chem.*, 54 (1982) 712–715.
- 7 R. M. Cassidy and S. Elchuk, *Anal. Chem.*, 54 (1982) 1558–1563.
- 8 Z. Iskandarani and D. J. Pietrzyk, *Anal. Chem.*, 54 (1982) 2427–2431.
- 9 W. E. Barber and P. W. Carr, *J. Chromatogr.*, 260 (1983) 89–96.
- 10 R. M. Cassidy and S. Elchuk, *J. Chromatogr.*, 262 (1983) 311–315.
- 11 G. Schmuckler, B. Rössner and G. Schwedt, *J. Chromatogr.*, 302 (1984) 15–20.
- 12 R. M. Cassidy and S. Elchuk, *J. Chromatogr. Sci.*, 21 (1983) 454–459.
- 13 F. G. P. Mullins and G. F. Kirkbright, *Analyst (London)*, 109 (1984) 1217–1221.

- 14 F. G. P. Mullins, *Analyst (London)*, 112 (1987) 665–671.
- 15 D. L. Duval and J. S. Fritz, *J. Chromatogr.*, 295 (1984) 89–101.
- 16 C. T. Hung and R. B. Taylor, *J. Chromatogr.*, 202 (1980) 333–345.
- 17 J. H. Knox and R. A. Hartwick, *J. Chromatogr.*, 204 (1981) 3–21.
- 18 T. Gnanasambandan and H. Freiser, *Anal. Chem.*, 54 (1982) 1282–1285.
- 19 J. DiNunzio and H. Freiser, *Talanta*, 26 (1979) 587–589.
- 20 S. W. Kang, *Taehan Hwahakhoe Chi*, 29 (1985) 365–371.
- 21 R. Golombek and G. Schwedt, *J. Chromatogr.*, 367 (1986) 69–76.
- 22 D. P. Lee, *J. Chromatogr. Sci.*, 22 (1984) 327–331.
- 23 H. Small and T. E. Miller, *Anal. Chem.*, 54 (1982) 462–469.
- 24 J. Hertz and U. Baltensperger, *Liq. Chromatogr. HPLC Mag.*, 2 (1984) 600–602.
- 25 R. Golombek, *Dissertation*, University of Stuttgart, 1987.

CHROM. 20 665

DETERMINATION OF NITRITE AND NITRATE BY REVERSED-PHASE HIGH-PERFORMANCE LIQUID CHROMATOGRAPHY USING ON-LINE POST-COLUMN PHOTOLYSIS WITH ULTRAVIOLET ABSORBANCE AND ELECTROCHEMICAL DETECTION

MARK LOOKABAUGH

U.S. Food and Drug Administration, Winchester Engineering and Analytical Center, Winchester, MA 01890 (U.S.A.)

and

IRA S. KRULL*

Department of Chemistry and Barnett Institute, Northeastern University, Boston, MA 02115 (U.S.A.)

SUMMARY

Ion-pair (paired-ion) reversed-phase HPLC has proved to be an effective technique for the analysis of inorganic anions. Also referred to as ion-interaction chromatography, it has been used with conductimetric, ultraviolet (UV) absorbance, refractive index, and electrochemical detection. Nitrite and nitrate are amenable to UV detection at wavelengths of approximately 240 nm and below. In addition, nitrite is readily oxidized at potentials of +0.9 V or higher at a glassy carbon electrode. While nitrate is electrochemically unreactive under these conditions, it will undergo photolysis, with the conversion product (in all likelihood the nitrite anion) generating an oxidative signal.

This paper describes the use of a Teflon™ knitted open tubular (KOT) reactor, which when wrapped around a UV source, provides a means of continuous, on-line photolysis. This derivatization step, combined with high-performance liquid chromatography, permits the determination of both nitrite and nitrate using oxidative amperometric detection. We have applied this technique to a number of samples (cured meats, smoked and fresh salmon, smoked cod, spiked water solutions) and have also obtained comparative data for nitrite by UV and direct (*i.e.* non-photolytic) oxidative electrochemical detection, as well as by a standard spectrophotometric procedure.

INTRODUCTION

Food additives, both direct and indirect, are permitted at levels which are set forth in United States Code of Federal Regulations (Part 172). It is the responsibility of the Food and Drug Administration to monitor the food supply for such additives. Nitrite and nitrate are typically determined in products such as cured meats and smoked fish using a spectrophotometric procedure¹. Nitrite (or nitrate, following its reduction to nitrite) is reacted with sulfanilamide, forming a diazonium salt, which is in

turn combined with N-(1-naphthyl)ethylenediamine to produce a colored solution. Quantitation is accomplished by comparison of the sample absorbance with a standard curve.

We hoped to develop an alternative chromatographic procedure which would be sensitive, selective, and broadly applicable. We chose to employ ion-interaction chromatography for the separation of nitrite and nitrate, since previous experience with this technique had proved very positive². Numerous articles have appeared in recent years describing the use of this scheme as an alternative to conventional ion chromatography, as first described by Small *et al.*³. Moreover, nitrite and nitrate, specifically, have been the focus of a number of papers in which high-performance liquid chromatography (HPLC) has been employed. Typically, single column ion exchange or ion-interaction chromatography was used and detection techniques most commonly reported were UV absorbance and electrochemical detection (ED) (oxidative, amperometric)⁴⁻¹⁵.

With a sample matrix as complex as that presented by cured meats, sample preparation or clean-up is an obstacle which can pose serious problems. A comprehensive discussion of this subject (with specific reference to the colorimetric analysis of nitrite in frankfurters) has been presented by Fiddler and Fox¹⁶. Those authors cautioned against the use of commonly used chemical treatments, *e.g.* the addition of protein precipitants, such as Carrez I (zinc acetate) and Carrez II (potassium ferrocyanide). Instead, they recommended the digestion procedure which has been incorporated in the Association of Official Analytical Chemists' (AOAC) Official Methods of Analysis¹. We decided to adopt the AOAC procedure for our work. Although the resulting filtered aqueous extracts can yield rather complex chromatograms, reliable quantitation of nitrite and nitrate has usually been possible.

In summary then, the fundamental components of the overall analytical methodology consist of sample extraction (followed by an optional solid phase extraction clean-up), ion-interaction reversed-phase HPLC for the separation of nitrite and nitrate, UV absorbance detection for quantitation of both species, on-line, post-column photolysis for ED of both species, and ED without photolysis for the quantitation of nitrite. The applications described herein include: (1) single-blind spiked water samples, (2) incurred and spiked levels in smoked salmon and cod, and (3) incurred and spiked levels in cured meat products with comparison to AOAC methodology.

EXPERIMENTAL

Apparatus

A modular HPLC system was assembled, using as components, a Waters Chromatography Division/Millipore (Milford, MA, U.S.A.) Model 6000A solvent delivery system, either a Rheodyne (Cotati, CA, U.S.A.) Model 7125 syringe loading injector or a Waters/Millipore WISP 710B autosampler, and Spectra-Physics (San Jose, CA, U.S.A.) Model SP 4270 recording integrators. Detectors employed were the Kratos (Ramsey, NJ, U.S.A.) Spectroflow 757 variable-wavelength UV detector and the Bioanalytical Systems (West Lafayette, IN, U.S.A.) electrochemical detector, consisting of two Model LC-4B amperometric controllers and a Model TL-5A thin-layer transducer. Specific sub-components of the Model TL-5A included a Model

RE-1 Ag/AgCl reference electrode, a Model TG-5M 0.127-mm gasket, and dual glassy carbon electrodes. The chromatographic column used was an Alltech Assoc. (Deerfield, IL, U.S.A.) Econosil (Cat. No. 60148) C₁₈ reversed-phase column, 250 mm × 4.6 mm I.D.

The on-line, post-column photolytic reactor has been described elsewhere in detail^{17,18}. The reactor consists of a knitted open tubular reaction coil (total path length approximately 10 m), constructed from 0.5 mm I.D. Teflon tubing (Rainin Instruments, Woburn, MA, U.S.A.), which is in turn wound about a mercury lamp. The UV source and the knitted open tubular (KOT) reactor are placed in a covered stainless-steel vessel (kettle). The kettle's lid is fitted with a glass tube (finger) which accommodates the lamp and KOT reactor and allows the reactor to be immersed in an ice-water bath. The kettle and lamp are commercially available, as a unit, from Photronix (Medway, MA, U.S.A.) as the Model 816 H.P.L.C. Reservoir.

Mobile phase

Preliminary separations of nitrite and nitrate were carried out using a mobile phase which consisted of 0.005 M (5 mM) tetrabutylammonium hydrogensulfate (TBAHS) dissolved in a methanol-phosphate buffer (10:90). The composition of the phosphate buffer was 0.025 M each of potassium dihydrogenphosphate and disodium hydrogenphosphate. The final pH of the mobile phase was adjusted to 6.8 with phosphoric acid. Prior to use, the mobile phase was routinely aspirated through a Rainin Instruments 0.45 μm pore size membrane filter (Nylon 66) and degassed under vacuum or by sonication.

Two other ion-pair reagents were also investigated, *viz.*, octyltriethylammonium phosphate and dodecyltriethylammonium phosphate (Q8 and Q12, Regis Chemical Co., Morton Grove, IL, U.S.A.). Greater retention and resolution could be achieved for nitrite and nitrate using these two reagents. The only disadvantage associated with them was noticeably longer equilibration times for the chromatographic system. In fact, most sample analyses were carried out with the Q12-based mobile phase because of the complexity of many of the sample matrices, which frequently proved intractably resistant to sample clean-up. They were incorporated in the methanol-phosphate buffer mobile phase at the 2–5 mM levels and the pH was again controlled at 6.8 using phosphoric acid.

Chemicals

Deionized, distilled water and HPLC-grade methanol (EM Science, Cherry Hill, NJ, U.S.A.) were used to prepare the mobile phases. Ion-pairing reagents of the highest available purity were obtained from Fluka (Hauppauge, NY, U.S.A.), in the case of tetrabutylammonium hydrogensulfate, and from Regis Chemical Co. or Alltech Assoc. in the case of octyltriethylammonium (Q8) and dodecyltriethylammonium (Q12) phosphate. Standard reagents of sodium nitrate and sodium nitrite were purchased from Aldrich (Milwaukee, WI, U.S.A.) and Baker (Phillipsburg, NJ, U.S.A.), respectively.

Procedures

Authentic mixtures (aqueous solutions) of sodium nitrate and sodium nitrite were prepared and analyzed in accordance with a single blind protocol. Determina-

tions of nitrite and nitrate were performed concomitantly using sequential UV detection and post-column, photolytic ED. The UV detector was placed prior to and in series with the post-column KOT reactor, which was in turn connected to the electrochemical detector (dual, parallel-configured, glassy carbon electrodes) cell. Six studies were conducted, three with both species (*i.e.* nitrite, nitrate) present, two with only one or the other present, and one with neither present. Initial dilutions were made with deionized, distilled water, with subsequent dilutions being made with mobile phase.

Additionally, a number of samples of smoked or fresh fish (salmon, cod), as well as cured meat products (beef/pork bologna or hot dogs, turkey bologna) were analyzed. In these cases, the sample preparation followed was that described in the previously cited standard procedure¹. Final analysis was carried out by HPLC. Recovery data were obtained by spiking separate portions of these samples (in a single blind format, when possible) and repeating the analysis. All filtrations were performed using either nylon membrane filters or filter paper known to be free of nitrite or nitrate. Membrane filters manufactured from mixed esters of cellulose acetate and nitrate are not suitable, as nitrate will be leached from them during the filtration process.

In some cases an optional solid phase extraction clean-up step was employed. The use of this technique for HPLC determinations of nitrite and nitrate has been previously reported. Osterloh and Goldfield⁷ evaluated anion-exchange versions of the solid-phase extraction cartridges, but encountered difficulty achieving reproducible recoveries of each analyte. Jackson *et al.*⁶ employed C₁₈ cartridges with apparent success to clean-up cheese, meat and vegetable samples. However, Wootton *et al.*¹³, in examining an impressive variety of foodstuffs, found the C₁₈ cartridges to be of only limited utility. Our experience was largely in line with that of Wootton's group and Osterloh and Goldfield. The only cartridge we found to be of even limited utility was the cyano bonded phase variety. Unfortunately it could not be applied to a wide range of samples.

RESULTS AND DISCUSSION

Optimization of UV and electrochemical detection

Both nitrite and nitrate exhibit significant UV absorptivity at wavelengths of roughly 240 nm and below. Our choice of 220 nm as a detection wavelength simply represents a compromise between signal response for the two analytes and background noise levels. In addition, nitrite possesses intrinsic electrochemical activity (oxidative) at a glassy carbon surface. While nitrate generates no such response under these conditions, a study evaluating the electrochemical activity of a number of inorganic anions, both with and without photolysis, clearly indicated that an oxidative response could be photolytically induced in the nitrate anion¹⁸. There is evidence from chemical literature to support the assumed photoreductive generation of nitrite from nitrate under solution conditions comparable to those described herein^{19,20}. Additional confirmation has been provided by the batch irradiation of nitrate and the subsequent chromatographic identification of the nitrite generated, as well as by the dual electrode response ratio for nitrate which has undergone on-line, post-column photolysis.

Hydrodynamic voltammograms of nitrite indicated that an oxidative response is produced at potentials of +0.8 V (*vs.* Ag/AgCl) on a glassy carbon surface. For analytical use, working potentials of +1.10 V (W1) and +1.00 V (W2) were chosen.

Residence time in the post-column reactor

The theoretical basis for, and the practical considerations involved in, the use and construction of KOT reactors have been discussed elsewhere²¹⁻²³. In essence, a crocheting technique is used to produce a tube which is coiled in three dimensions. The resulting geometry enables flow to occur through a considerable length of tubing without the creation of drastic band broadening.

For our work we used a KOT reactor constructed from a 10 m × 0.5 mm I.D. Teflon tubing. This corresponds to a nominal coil volume of approximately 2 ml. Using a pump (Waters 6000A) as a source of metered flow, we determined the actual volume to be 2.3 ml. The residence time can be controlled by varying the flow-rate. Moreover, an optimum value can be determined by evaluating the response for nitrate with photolysis as opposed to the response for nitrite without photolysis (flow injection). With increasing flow-rates, the area response for nitrite with the lamp turned off decreased. For nitrate, with the lamp turned on, the same general trend was observed. The fact that signal response decreases with increasing flow-rate is indicative of the fact that the thin-layer cell design of the amperometric detector results in concentration-sensitive behaviour (as opposed to mass-sensitive). Presumably mass transfer of the analyte(s) through the diffusion layer (and to the surface of the electrode itself) is adversely affected by increased flow. However, when the second set of data was normalized for any decrease in signal response due simply to changes in flow, it was the case that signal response was maximized at flow-rates between 0.6 and 1.0 ml/min. The maximum response observed corresponded to a residence time of 2.8 min (0.8 ml/min flow-rate). The degree of photoconversion of nitrate to nitrite was determined (once again via flow injection). Under optimum conditions we estimated the conversion efficiency to be 85-90%.

It was our usual practice to acquire simultaneous (sequential) signals from both the UV and the amperometric detector. Residence time for the analytes in the UV detector's flow cell is very brief. Were any detector-induced photolysis to occur, this would be apparent in the electrochemical chromatogram as a peak with a retention time corresponding to nitrate (and attributable, of course, to any photoconversion of nitrate to nitrite). No such peak was ever observed. We feel that our findings are in all probability applicable to other commercially available detectors. Nonetheless it would be prudent to establish this on a case-by-case basis.

Effect of pH on photolysis of nitrate

A brief study on the influence of eluent pH upon the photolytic conversion of nitrate revealed that at a pH of 7, a stable response was produced. At a pH of 5, roughly a 40% reduction in response was encountered. At a pH of 3, no photolytically induced response for nitrate could be detected. For this reason we used buffered mobile phases with a pH adjusted to 6.8.

Our primary concern regarding mobile phase pH was with respect to its effect upon the photoconversion of nitrate to nitrite and its influence on the stability of the nitrite anion itself, which is threatened at lower pH levels. Chromatography is also influenced by pH, but this was of secondary concern. Previous studies have demonstrated ion-interaction chromatographic separations of nitrite and nitrate are readily achieved in a pH range of roughly 4 to 7^{24,25}.

Linearity of response, current response ratios

The linearity of response for nitrite was evaluated using UV detection, ED without photolysis (lamp off), and ED with photolysis (lamp on). In the case of nitrate, UV detection and lamp on ED were used (nitrate shows no response via ED with the lamp off). ED was carried out using parallel dual electrodes maintained at +1.10 V and +1.00 V, respectively. The results are summarized in Table I.

For each analyte, linear responses were obtained for all detection schemes. A minimum detection level of 50 ppb is conservatively proposed for each analyte using either ED or UV detection. Solutions as low as 5–10 ppb yielded responses, but the signals began to deviate from linearity. Our findings are in general agreement with detection limits recently published by Schroeder¹⁵, who also employed reversed-phase HPLC, along with UV detection at 210 nm, for the determination of nitrate alone. It should be noted that the “lamp-on” and “lamp-off” slope values for nitrite at a particular potential (*e.g.* see Table I) are not necessarily comparable. In this case the two sets of experiments were performed on different days and electrode response can vary from day-to-day.

The reproducibility of injection for standard solutions of nitrate or nitrite by either detection technique was very good, with relative standard deviations of less than one percent being typical.

By using a parallel-configured dual-electrode transducer and maintaining the electrodes at a voltage differential of 100–150 mV, it is possible to obtain current response ratios, *i.e.* i_1/i_2 . These ratios will ideally lend an additional degree of selectivity for the electrochemical detection scheme, since they should be characteristic

TABLE I

LINEARITY OF RESPONSE FOR NITRITE AND NITRATE BY UV ABSORBANCE AND ELECTROCHEMICAL DETECTION (WITH AND WITHOUT PHOTOLYSIS)

A = absorbance units, i = current in nA. Concentrations expressed as ppm. Chromatographic conditions: Alltech Assoc. Econosil C₁₈ column, 250 mm × 4.6 mm I.D.; mobile phase: 5 mM TBAHS dissolved in methanol–phosphate buffer (0.025 M each of potassium dihydrogenphosphate and disodium hydrogenphosphate) (10:90); flow-rate: 0.8 ml/min; injection volume: 200 μ l; nitrite: 0.005400–10.80 ppm, nitrate: 0.005125–10.25 ppm (220 nm); nitrite: 0.005400–1.080 ppm (ED, lamp off); nitrite: 0.05400–1.080 ppm, nitrate: 0.05125–1.025 ppm (ED, lamp on).

Anion	Detection	Equation line	Correlation coefficient, r
Nitrite	UV (220 nm)	$A = 0.04100[\text{NO}_2^-] + 0.00139$	0.9998
Nitrate	UV (220 nm)	$A = 0.0233[\text{NO}_3^-] + 0.00115$	0.9999
Nitrite	ED (lamp on) (+1.10 V)	$i = 465[\text{NO}_2^-] + 2.23$	0.9999
Nitrite	ED (lamp on) (+1.00 V)	$i = 325[\text{NO}_2^-] + 0.718$	0.9999
Nitrite	ED (lamp off) (+1.10 V)	$i = 195[\text{NO}_2^-] + 2.81$	0.9999
Nitrite	ED (lamp off) (+1.00 V)	$i = 425[\text{NO}_2^-] + 1.90$	0.9999
Nitrate	ED (lamp on) (+1.10 V)	$i = 290[\text{NO}_3^-] + 12.3$	0.9997
Nitrate	ED (lamp on) (+1.00 V)	$i = 205[\text{NO}_3^-] + 7.62$	0.9998

of a particular analyte. In Table II the stability of the current response ratio for nitrite and nitrate, under photolytic conditions and over a range of concentrations, is summarized. The ratios for both species display reasonable stability over a 20-fold concentration range. Moreover, the actual values for nitrite and nitrate are in very close agreement, serving to substantiate the hypothesis that nitrate is indeed photolyzed to nitrite.

Photolytic conversion of nitrate to nitrite

In addition to relying on the comparison of current response ratios (for the two peaks with retention times corresponding to nitrite and nitrate) as evidence of the fact that nitrate was indeed being photolytically reduced to nitrite, we also subjected a solution of sodium nitrate standard (5 ppm) to batch irradiation (3 min). This irradiated solution was then analyzed chromatographically. Whereas the unphotolyzed solution revealed only the single peak corresponding to nitrate (UV detection), the photolyzed solution showed two peaks, one with a retention time matching nitrate, and a second peak matching nitrite. By amperometric oxidative detection, a peak was observed for nitrite in the photolyzed solution, while for the unphotolyzed solution, no peaks were observed (nitrate is unreactive in the absence of photolysis). Current response ratios obtained by chromatographing a standard solution of nitrite did indeed compare favorably with those obtained from the photolyzed solution of nitrate [$i_1/i_2 = 2.43$, relative standard deviation (R.S.D.) = 0.82% ($n = 3$) for the photolyzed solution as opposed to $i_1/i_2 = 2.46$, R.S.D. = 0.62% ($n = 3$) for the nitrite standard]. The fact that the current ratios obtained in this study differ significantly from those presented in Table II is again illustrative of the fact that the current generated by a particular glassy carbon electrode is dependent upon a number of factors, such as the age and surface condition of the electrode. It is not at all unreasonable to observe different current ratios for essentially similar experiments conducted at separate intervals. The key issue is that standard and sample current ratios, obtained concomitantly, do in fact correspond closely.

Interestingly, when a solution of sodium nitrite (2 ppm) was photolyzed (again for 3 min), there was a partial conversion of nitrite to nitrate. The nitrite response was reduced by approximately 30% under both UV detection and ED. In bulk aqueous

TABLE II
CURRENT RESPONSE RATIOS (i_1/i_2) FOR NITRITE AND NITRATE (PHOTOLYZED) AS A FUNCTION OF CONCENTRATION

Chromatographic conditions as Table I. $W_1 = +1.10$ V, $W_2 = +1.00$ V vs. Ag/AgCl.

Anion	Concentration (ppm)	i_1/i_2	RSD (%) ($n = 3$)
Nitrite	1.080	1.43	0.43
	0.5400	1.44	0.15
	0.1080	1.46	1.20
	0.05400	1.48	2.70
Nitrate	1.025	1.42	0.43
	0.5120	1.43	0.63
	0.1025	1.46	0.79
	0.05120	1.48	2.69

solutions, it would thus appear that the photolytic conversion of nitrate to nitrite involves an equilibrium reaction. In fact, the reduction in the nitrite peak was very nearly stoichiometric. The unphotolyzed solution of $0.0300 \mu\text{M}$ nitrite yielded, after photolysis, a chromatogram with a nitrite peak corresponding to $0.0225 \mu\text{M}$ nitrite and a nitrate peak corresponding to $0.00774 \mu\text{M}$ nitrate ($0.0225 + 0.00774 = 0.0302$). This is also most likely the case when the solution is a buffered methanolic mobile phase under conditions of flow. One of the earliest studies we performed was a comparison of "lamp-on" and "lamp-off" response for nitrite under actual analytical conditions of chromatographic flow and post-column photolysis. A reduction in the nitrite response of between 15 and 20% was observed.

Method validation

The accuracy of the analytical methodology was initially assessed through the use of authentic aqueous solutions of sodium nitrate and sodium nitrite which were prepared and analyzed according to a single blind protocol. Analyses were performed using essentially simultaneous UV detection and post-column photolytic ED. The UV detector was placed in series with, and prior to, the post-column reactor, which was then connected to the amperometric detector. Six samples were analyzed, three containing both analytes, one containing neither analyte, and two containing only one or the other of the analytes. No false positive results were obtained. The amounts determined, expressed as a percentage of the actual weight of analyte added, are summarized in Table III. For sodium nitrite, they ranged from 98.4% to 99.9% (UV, 220 nm), from 97.9% to 100.6% (ED, $W_1 = +1.10 \text{ V}$), and from 97.7% to 100.4% (ED, $W_2 = +1.00 \text{ V}$). For sodium nitrate the corresponding figures are 98.7% to 101.0% (220 nm), 97.8% to 99.9% ($+1.10 \text{ V}$), and 97.6% to 99.8% ($+1.00 \text{ V}$).

TABLE III

SUMMARY OF ANALYSES: AUTHENTIC SOLUTIONS OF NITRITE AND NITRATE (SINGLE BLIND SPIKES) BY UV AND PHOTOLYTIC ED

Chromatographic conditions: see Table I. Figures in parentheses are average calculated amounts of sodium nitrite and sodium nitrate expressed as a percentage of the actual amount added. The amounts themselves represent weight (mg) of standard in original solutions. N.D. = not determined.

Sample	NaNO_2 (mg)	NaNO_3 (mg)	Average calculated values ($n = 3$)					
			NaNO_2			NaNO_3		
			220 nm	+1.10 V	+1.00 V	220 nm	+1.10 V	+1.00 V
A	0	123.4	N.D.	N.D.	N.D.	124.6 (101.0)	122.8 (99.5)	121.2 (98.2)
B	158.9	138.9	158.8 (99.9)	159.9 (100.6)	159.6 (100.4)	139.0 (100.1)	138.7 (99.9)	138.3 (99.6)
C	176.9	124.9	174.1 (98.4)	173.1 (97.9)	172.8 (97.7)	123.3 (98.7)	122.2 (97.8)	121.9 (97.6)
D	149.1	136.8	147.6 (99.0)	148.5 (99.6)	148.4 (99.5)	135.8 (99.3)	136.5 (99.8)	136.5 (99.8)
E	147.1	0	144.9 (98.5)	144.6 (98.3)	144.3 (98.1)	N.D.	N.D.	N.D.

Actual samples were also analyzed in order to more fully assess the suitability of the method. Tables IV and V represent the results of two separate sets of analyses. The first involved the analysis of bologna and frankfurters, while the second involved only bologna. In each case a single blind comparison was carried out with respect to the official colorimetric procedure¹. In the case of the second study, involving only bologna, and in which all HPLC analyses were completed within the same day, good agreement was seen between the AOAC results and the HPLC-ED (lamp on, as well as

TABLE IV

DETERMINATION OF NITRITE BY COLORIMETRIC* PROCEDURE AND BY HPLC WITH UV DETECTION AND ED** (SINGLE BLIND STUDY)

Value in parenthesis is relative standard deviation.

	AOAC	Nitrite (as NaNO ₂) (ppm in product)				
		UV (220 nm)	ED (lamp off)		ED (lamp on)***	
			+1.10 V	+1.00 V	+1.10 V	+1.00 V
Bologna (turkey)	66.3	74.6 (1.47)	75.3 (0.86)	75.4 (0.93)	67.9 (1.15)	67.6 (2.02)
Frankfurter (beef/pork)	34.4	39.0 (0.90)	39.2 (0.78)	39.2 (0.78)	29.8 (1.27)	29.9 (1.72)
Bologna [§] (turkey)	18.0		18.0 (0.58)	17.9 (0.62)	18.0 (0.76)	18.3 (1.78)

* AOAC 14th ed., sections 24.044 and 24.045, single determination.

** Chromatographic conditions: same as in Table I except for the mobile phase: methanol-water (25:75), 2 mM Q12, 0.025 M each potassium dihydrogenphosphate and disodium hydrogenphosphate.

*** Determination performed on following day (frozen storage of extract overnight).

§ Same day determination; matrix interference prevented UV determination.

TABLE V

DETERMINATION OF NITRATE BY HPLC WITH UV DETECTION AND PHOTOLYTIC ED

Chromatographic conditions: see Table IV. Values in parenthesis are relative standard deviations.

	AOAC	Nitrate (as NaNO ₃) (ppm in product)		
		UV (220 nm)	ED (lamp on)*	
			+1.10 V	+1.00 V
Bologna (turkey)	144 (3.82)	133 (3.91)	132 (1.75)	
Frankfurter (beef/pork)	79.8 (1.26)	66.2 (5.83)	65.2 (6.03)	
Bologna (turkey)**	122 (0.83)	130 (0.67)	135 (1.00)	

* Determination performed on following day (frozen storage of extract overnight).

** Same day determination for UV and ED.

lamp off). Matrix interferences unfortunately prevented accurate quantitation of nitrite by UV detection (Fig. 1). Nitrite values obtained in the first study exhibit less than ideal correlation, and this may in large part be due to the fact that the HPLC data could not all be generated on the same day. In Table V, the values for nitrate are those obtained by the two separate detection schemes for HPLC, *i.e.*, UV detection and ED (lamp on) at +1.10 V and +1.00 V (Figs. 2 and 3). In this study same-day results ranged from 122–135 ppm. While internal agreement could be better, these data are none the less encouraging as a first attempt.

Table VI summarizes similar data, this time for smoked cod and salmon. Since intrinsic levels of nitrite and nitrate in fish products were routinely found to be either

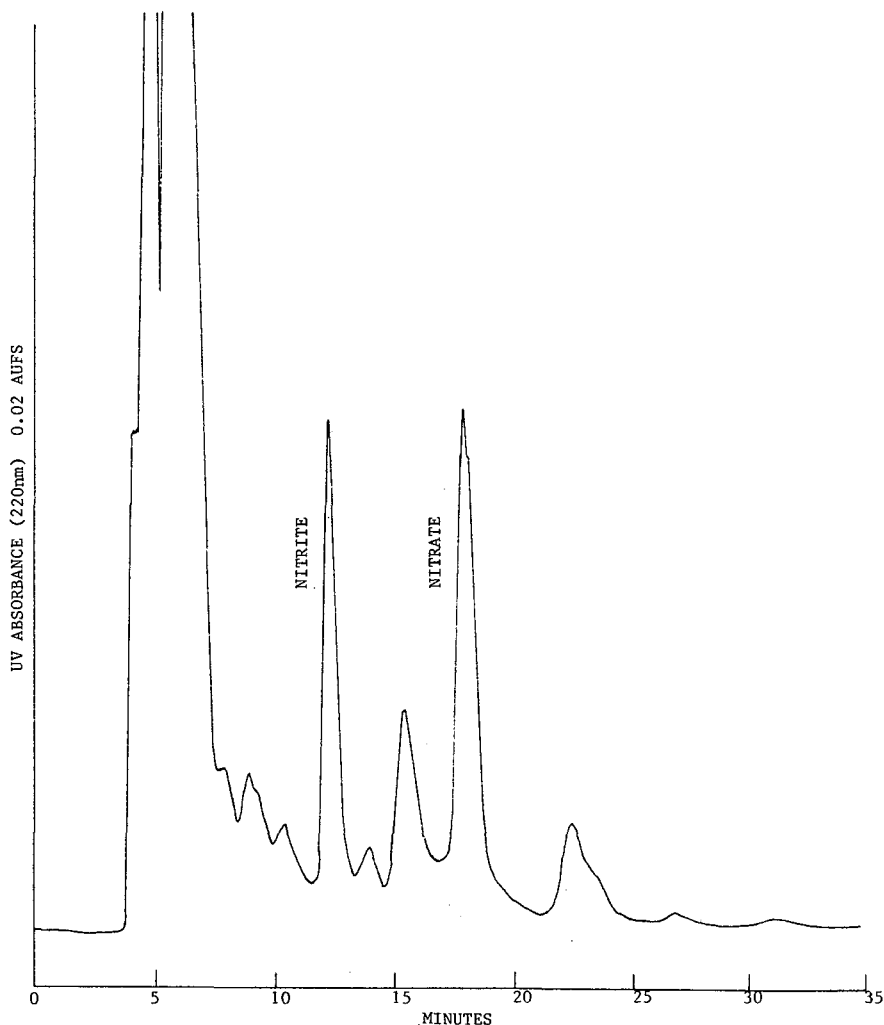


Fig. 1. Chromatogram of bologna extract (5 g/500 ml water) with UV detection at 220 nm (100 μ l injection). Alltech Econosil C₁₈ column, 250 mm \times 4.6 mm I.D., mobile phase: 2 mM dodecyltriethylammonium phosphate in methanol-phosphate buffer, 0.8 ml/min flow-rate.

very low or non-existent, the essential point being conveyed here is that the spiked recoveries (one of which was conducted in triplicate via a single blind protocol) were, as a rule, quite good.

We are encouraged by the results which we have thus far obtained. Certainly in the case of nitrite, which may be detected electrochemically without photolysis, sample matrix problems are generally minimal, and the overall technique is probably applicable to real samples without further modification or development. For nitrate, which must be detected either by UV or photolytic ED, matrix interferences are more of a problem. Additional work in the area of sample clean-up, ideally through the use of solid-phase extraction, will hopefully resolve any deficiencies. But, even as the method now stands, with essentially no clean-up subsequent to aqueous extraction, it is capable of detecting nitrate with no difficulty at levels of regulatory concern (500 ppm in the product/5 ppm in the sample extract). The ability to screen products for levels of both nitrite and nitrate with a single injection is certainly very desirable.

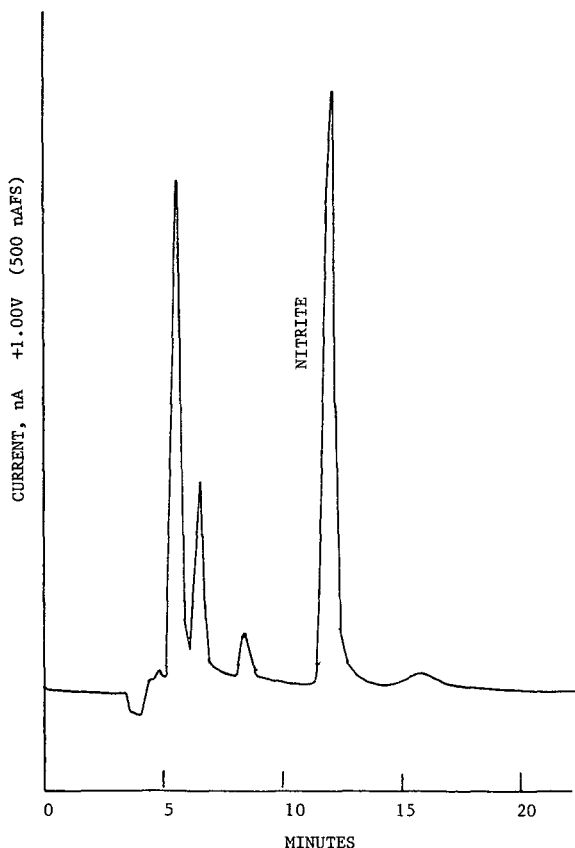


Fig. 2. Chromatogram of bologna extract (5 g/500 ml water) with ED (100 μ l injection). Alltech Econosil C_{18} column, 250 mm \times 4.6 mm I.D. mobile phase: 2 mM dodecyltriethylammonium phosphate in methanol-phosphate buffer, 0.8 ml/min flow-rate.

Finally, it should be indicated that the photoreduction of nitrate to nitrite as an analytical approach appears to have more widespread, perhaps general, applicability to many inorganic, oxidized anions. We have demonstrated the photoreductive-oxidative ED of already oxidized halogen anions, such as iodate–periodate, chlorate–perchlorate, and bromate–perbromate²⁶. In as yet unpublished work, we have shown by flow injection–post-column photolytic methods that anions such chromate, permanganate, bicarbonate, hydrogenphosphate, dihydrogenphosphate, benzoate, and others, can all be photoreduced, to varying degrees, and detected at reasonable working potentials, thus far with glassy carbon electrodes²⁷. Additional work is underway to demonstrate the full extent of applicability of this newer analytical approach for inorganic and organic, oxidized, anionic species.

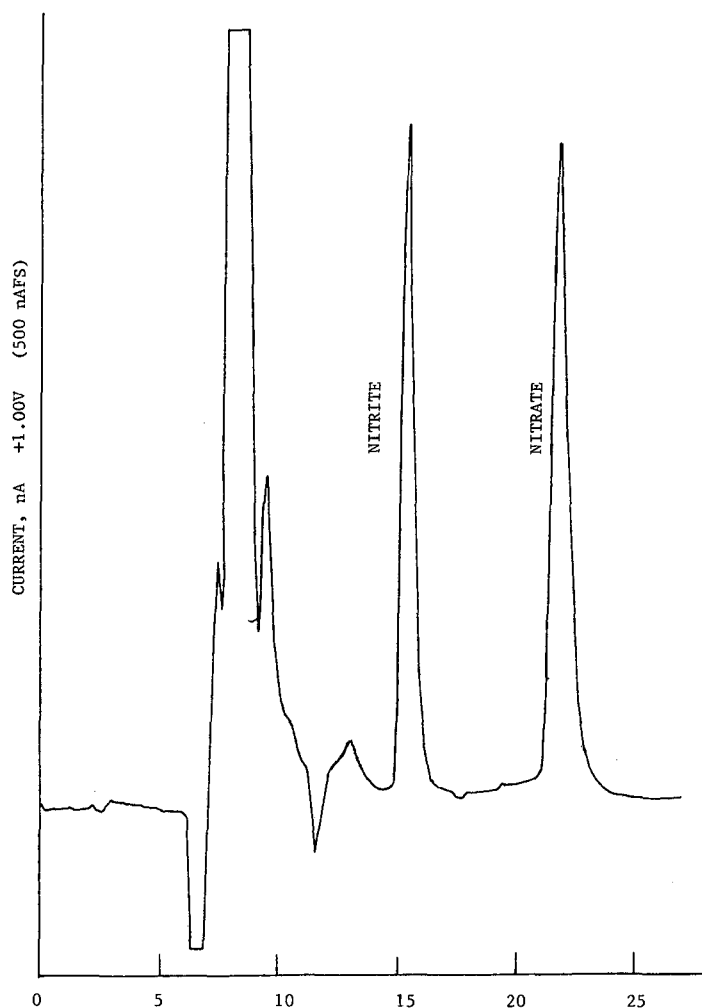


Fig. 3. Chromatogram of bologna extract (5 g/500 ml water) with photolytic ED (100 μ l injection). Alltech Econosil C_{18} column, 250 mm \times 4.6 mm I.D., mobile phase: 2 mM dodecyltriethylammonium phosphate in methanol–phosphate buffer, 0.8 ml/min flow-rate.

TABLE VI

RECOVERIES OF ADDED NITRITE AND NITRATE (FROM SMOKED SALMON, COD) FOR HPLC PROCEDURE WITH UV DETECTION AND ED

N.D. = not detected in product (could have been seen, if present, under these analytical conditions).

- = cannot be detected in the absence of irradiation (under lamp off conditions).

Sample	Detection	NaNO ₂ (ppm)	Recovery (%)	NaNO ₃ (ppm)	Recovery (%)
Salmon	UV (220 nm)	N.D.	97.4	N.D.	95.9
	W ₁ = +1.05 V (lamp off)	N.D.	94.2	-	-
	W ₂ = +0.95 V (lamp off)	N.D.	96.5	-	-
	W ₁ = +1.05 V (lamp on)	N.D.	112.5	N.D.	111.2
	W ₂ = +0.95 V (lamp on)	N.D.	113.3	N.D.	112.4
	UV (220 nm)*	N.D.	108.7	N.D.	104.9
	UV (220 nm)**	N.D.	104.0, 101.0, 99.8***	44	103.5, 95.5, 101.1***
Cod [§]	UV (220 nm)	N.D.	105.6	N.D.	103.8
	W ₁ = +1.10 V (lamp off)	N.D.	101.4	-	-
	W ₂ = +1.00 V (lamp off)	N.D.	101.1	-	-

* Solid phase extraction (SPE) as clean-up, using Analytichem Cyano cartridge.

** SPE with Waters C18 Sep-Pak.

*** Triplicate single blind spikes of product. Chromatographic conditions: see Table IV.

§ SPE with Baker Cyano cartridge.

ACKNOWLEDGEMENTS

We wish to acknowledge the generous and very able assistance of FDA analysts Pamela Mackill, John Noonan and Susan Krzysko, who assisted in much of the analytical work. We are also grateful to Carl Selavka, formerly of Northeastern University, who provided advice in the use of the post-column photolysis unit. Finally, we would like to express our gratitude to James Fitzgerald and Martin Finkelson of Winchester Engineering and Analytical Center for their encouragement and support of this research. This is contribution number 357 from the Barnett Institute at Northeastern University.

REFERENCES

- 1 *Official Methods of Analysis*, Association of Official Analytical Chemists, Arlington, Virginia, 14th ed., 1984, sections 24.044-24.045.
- 2 M. Lookabaugh, W. R. LaCourse and I. S. Krull, *J. Chromatogr.*, 387 (1987) 301.
- 3 H. Small, T. S. Stevens and W. C. Bauman, *Anal. Chem.*, 47 (1975) 1801.
- 4 Z. Iskandarani and D. Pietrzyk, *Anal. Chem.*, 54 (1982) 2601.
- 5 J. P. deKleijn and K. Hoven, *Analyst (London)*, 109 (1984) 527.
- 6 P. E. Jackson, P. R. Haddad and S. Dilli, *J. Chromatogr.*, 295 (1984) 471.
- 7 J. Osterloh and D. Goldfield, *J. Liq. Chromatogr.*, 7 (1984) 753.
- 8 R. G. Gerritse, *J. Chromatogr.*, 171 (1979) 527.
- 9 U. Leuenberger, R. Gauch, K. Rieder and E. Baumgartner, *J. Chromatogr.*, 202 (1980) 461.
- 10 J. P. Witter, S. J. Gatley and E. Balish, *J. Chromatogr.*, 229 (1982) 450.
- 11 T. C. Kuchnicki, L. P. Sarna and G. R. B. Webster, *J. Liq. Chromatogr.*, 8 (1985) 1593.
- 12 L. Eek and N. Ferrer, *J. Chromatogr.*, 322 (1985) 491.
- 13 M. Wootton, S. H. Kok and K. A. Buckle, *J. Sci. Food Agric.*, 36 (1985) 297.
- 14 N. J. Eggers and D. L. Cattle, *J. Chromatogr.*, 354 (1986) 490.

- 15 D. C. Schroeder, *J. Chromatogr. Sci.*, 25 (1987) 405.
- 16 R. N. Fiddler and J. B. Fox, *J. Assoc. Off. Anal. Chem.*, 61 (1978) 1063.
- 17 C. M. Selavka, K.-S. Jiao and I. S. Krull, *Anal. Chem.*, 59 (1987) 2221.
- 18 I. S. Krull, X.-D. Ding, C. Selavka and R. Nelson, *LC, Liq. Chromatogr., HPLC Mag.*, 2 (1984) 214.
- 19 J. W. Mellor, *A Comprehensive Treatise on Inorganic and Theoretical Chemistry*, Vol. 8, Wiley, New York, 1962, p. 456.
- 20 F. Daniel and R. A. Alberty, *Physical Chemistry*, Wiley, 3rd ed., 1967, p. 620.
- 21 W. R. LaCourse, C. M. Selavka and I. S. Krull, *Anal. Chem.*, 59 (1987) 1366.
- 22 C. M. Selavka and I. S. Krull, *J. Ener. Mat.*, 4 (1986) 273.
- 23 J. R. Poulsen, K. S. Birks, M. S. Gandelman and J. W. Birks, *Chromatographia*, 22 (1986) 231.
- 24 N. E. Skelly, *Anal. Chem.*, 54 (1982) 712.
- 25 R. Vespalec, J. Neča and M. Vrchlabský, *J. Chromatogr.*, 286 (1984) 171.
- 26 C. Selavka, K.-S. Jiao, I. S. Krull, P. Shieh, W. Yu and M. Wolf, *Anal. Chem.*, 60 (1988) 250.
- 27 L. Dou and I. S. Krull, unpublished results.

CHROM. 20 458

ENANTIOSELECTIVITY OF COMPLEX FORMATION IN LIGAND-EXCHANGE CHROMATOGRAPHIC SYSTEMS WITH CHIRAL STATIONARY AND/OR CHIRAL MOBILE PHASES

V. A. DAVANKOV*, A. A. KURGANOV and T. M. PONOMAREVA

Institute of Organo-Element Compounds, USSR Academy of Sciences, 117813 Moscow (U.S.S.R.)

SUMMARY

Equations are derived describing the retention and separation selectivity of two enantiomeric species in a chromatographic system containing a chiral selector in the stationary and/or in the mobile phase. It is shown that the total column enantioselectivity generally differs from the enantioselectivity of the selector–selectand interaction in solution. In chiral chromatographic systems, there are significant deviations from the principal of reciprocity of mutual chiral selector–selectand recognition.

INTRODUCTION

Impressive achievements of ligand-exchange chromatography (LEC) in separating optical isomers, which have been analysed in two successive reviews^{1,2} and the book by Davankov *et al.*³, have led to the elaboration of three general types of chiral LC systems that employ (i) chiral (bonded) stationary phases (CSPs)⁴, (ii) chiral coated stationary phases (CCSPs)⁵ and (iii) chiral mobile phases (CMPs)^{6,7} respectively. In the last case the chiral selector of the chromatographic system can either largely remain in the mobile phase or partition between the mobile and stationary phases.

The principal interaction mode between two solute enantiomers, A_R and A_S , to be separated and the chiral selector, B, in LEC is the formation of ternary, mixed-ligand complexes with a transition metal cation, M. The two labile ternary complexes formed, A_RMB and A_SMB , are diastereomeric and, therefore, may differ in their thermodynamic stability constants:

$$\beta_{A_RMB} = \frac{[A_RMB]}{[A_R][M][B]} \text{ and } \beta_{A_SMB} = \frac{[A_SMB]}{[A_S][M][B]}$$

The ratio of the two constants, $\alpha^* = \beta_{A_RMB}/\beta_{A_SMB}$, is a convenient quantitative measure for the enantioselectivity of the complexation reaction.

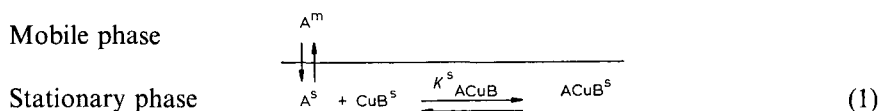
Enantioselectivity of labile complex formation in homogeneous solutions was first demonstrated in nickel(II) bis-histidinato complexes⁸ and in copper(II) bis complexes with bidentate α -amino acid ligands⁹ and 1,2-diamine-type ligands¹⁰.

Several attempts were made to correlate enantioselectivity, $\alpha = k'_{A_R}/k'_{A_S}$, of chiral LEC systems with the enantioselectivity, $\alpha^* = \beta_{A_RMB}/\beta_{A_SMB}$, of complex formation in homogeneous solutions containing the solute enantiomers, A_R and A_S , metal ions, M , and a ligand, B , which would simulate the structure of the chiral selector. Though some chiral polystyrene-type ligand-exchange resins are known for which a qualitative relationship $\alpha \approx \alpha^*$ has been found^{1,2,11}, such an agreement turned to be an exception, rather than a general rule¹².

It is the purpose of the present paper to analyse theoretically the role of enantioselectivity of ternary complex formation in the discrimination of enantiomers in chiral LEC systems.

CHIRAL STATIONARY PHASES

Independent of whether the chiral selector B is covalently bonded to the sorbent matrix or is permanently adsorbed onto the surface of the packing, the CSP and CCSP systems are very similar in that the chiral selector B and its diastereomeric mixed-ligand complexes with the solute enantiomers A_R and A_S are always located in the stationary phase, whereas the mobile phase only transports the enantiomeric solute species. Supposing A and B are bifunctional amino acids and M is copper(II), a whole series of dissociation and complexation equilibria would be established in the two-phase system. However, the processes that are responsible for the retention and chiral recognition of the solute molecules can be reduced to the following simple scheme



where the superscripts m and s denote the location of the species in the mobile and stationary phases, respectively.

The capacity factor of the solute amino acid A is related to its adsorption and complexation through

$$k'_A = \varphi \cdot \frac{[A^s] + [ACuB^s]}{[A^m]} \quad (2)$$

where φ is the phase ratio. With the aid of the equilibrium constant, K^s_{ACuB} , of the ternary complex formation reaction 1, eqn. 2 can be written as:

$$\begin{aligned}
 k'_A &= \varphi \cdot \frac{[A^s] + K^s_{\text{ACuB}}[A^s][\text{CuB}^s]}{[A^m]} \\
 &= \varphi \cdot \frac{A^s}{A^m} \cdot (1 + K^s_{\text{ACuB}}[\text{CuB}^s]) \\
 &= k''_A(1 + K^s_{\text{ACuB}}[\text{CuB}^s])
 \end{aligned} \quad (3)$$

Eqn. 3 is a rather fundamental one. Here, k_A'' is the capacity factor of solute A in the absence of complexation reactions ($[\text{CuB}^s] = 0$ or $K_{\text{ACuB}}^s = 0$); $[\text{CuB}^s]$ represents the concentration of chiral sorption sites and K_{ACuB}^s the formation constant of the solute enantiomer–chiral selector adduct in the stationary phase. According to eqn. 3, an increase in both the chiral selector concentration and its complexing ability would result in an enhanced solute retention.

The enantioselectivity of the column is given by

$$\alpha = \frac{k_{A_R}'}{k_{A_S}'} = \frac{k_{A_R}''}{k_{A_S}''} \cdot \frac{1 + K_{A_R\text{CuB}}^s [\text{CuB}^s]}{1 + K_{A_S\text{CuB}}^s [\text{CuB}^s]} = \frac{1 + K_{A_R\text{CuB}}^s [\text{CuB}^s]}{1 + K_{A_S\text{CuB}}^s [\text{CuB}^s]} \quad (4)$$

since the retention of the enantiomers in the absence of complexation reactions with the chiral selector B is identical, *i.e.*, $k_{A_R}'' = k_{A_S}''$.

It is obvious that the enantioselectivity of the CSP chromatographic system approaches the value of

$$\alpha \leq K_{A_R\text{CuB}}^s / K_{A_S\text{CuB}}^s \quad (5)$$

if the non-specific adsorption of the solute enantiomers is negligible compared to the complexation reaction with the chiral selector, *i.e.*, $[\text{A}^s] \ll [\text{ACuB}^s]$ in eqn. 2. Thus, the maximum value of the chiral column enantioselectivity is generally given by the enantioselectivity of the complex formation process in the CSP:

$$\alpha \leq \alpha^*, \text{ where } \alpha^* = K_{A_R\text{CuB}}^s / K_{A_S\text{CuB}}^s = \beta_{A_R\text{CuB}} / \beta_{A_S\text{CuB}}$$

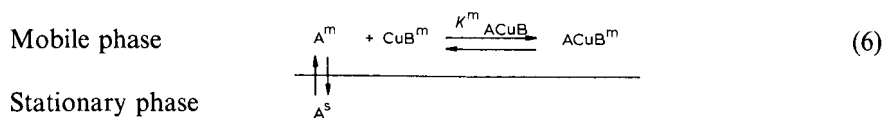
This conclusion is valid for all types of CSPs, not just the ligand-exchange one.

Equations that are similar to 3 and 4 were earlier derived by Feibush *et al.*¹³.

CHIRAL MOBILE PHASES

Two cases should be considered here: one with the chiral selector B always remaining in the mobile phase and the other with the selector B partitioning between the two phases.

In the first case, the theoretical treatment very much resembles that of a CSP system:



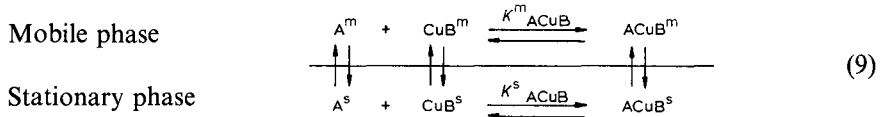
$$k_A' = \varphi \cdot \frac{[\text{A}^s]}{[\text{A}^m] + [\text{ACuB}^m]} = \varphi \cdot \frac{[\text{A}^s]}{[\text{A}^m] + K_{\text{ACuB}}^m [\text{A}^m][\text{CuB}^m]} = k_A'' (1 + K_{\text{ACuB}}^m [\text{CuB}^m])^{-1} \quad (7)$$

The retention reaction 6 obviously diminishes the solute retention. However, the stronger the complexation, the higher is the enantioselectivity of the CMP system, as follows from eqn. 8:

$$\begin{aligned} \alpha &= \frac{k'_{A_R}}{k'_{A_S}} = \frac{k''_{A_R}}{k''_{A_S}} \cdot \frac{1 + K_{A_R\text{CuB}}^m[\text{CuB}^m]}{1 + K_{A_S\text{CuB}}^m[\text{CuB}^m]} \\ &= \frac{1 + K_{A_R\text{CuB}}^m[\text{CuB}^m]}{1 + K_{A_S\text{CuB}}^m[\text{CuB}^m]} \end{aligned} \quad (8)$$

The limiting enantioselectivity of a CMP is, again, given by the enantioselectivity, α^* , of the complexation reaction 6 with the principal difference from the situation with a CSP column being that the chiral selector **B** now produces an inversed elution order of the solute enantiomers.

More complex is a CMP chromatographic system where the chiral selector **B** and its complexes reside both in the mobile phase and stationary phases:



$$\begin{aligned} k'_A &= \varphi \cdot \frac{[\text{A}^s] + [\text{ACuB}^s]}{[\text{A}^m] + [\text{ACuB}^m]} = \varphi \cdot \frac{[\text{A}^s] + K_{\text{ACuB}}^s[\text{A}^s][\text{CuB}^s]}{[\text{A}^m] + K_{\text{ACuB}}^m[\text{A}^m][\text{CuB}^m]} \\ &= k''_A \cdot \frac{1 + K_{\text{ACuB}}^s[\text{CuB}^s]}{1 + K_{\text{ACuB}}^m[\text{CuB}^m]} \end{aligned} \quad (10)$$

According to eqn. 10, complexation reactions in the stationary phase enhance the solute retention, whereas the complexation in the mobile phase facilitates the elution.

The enantioselectivity of the system is now a complex function of the phase distribution of the chiral selector and the enantioselectivity of the latter in the mobile and stationary phases:

$$\begin{aligned} \alpha &= \frac{k'_{A_R}}{k'_{A_S}} = \frac{k''_{A_R}}{k''_{A_S}} \cdot \frac{(1 + K_{A_R\text{CuB}}^s[\text{CuB}^s]) (1 + K_{A_S\text{CuB}}^m[\text{CuB}^m])}{(1 + K_{A_R\text{CuB}}^m[\text{CuB}^m]) (1 + K_{A_S\text{CuB}}^s[\text{CuB}^s])} \\ &= \frac{1 + K_{A_R\text{CuB}}^s[\text{CuB}^s]}{1 + K_{A_S\text{CuB}}^s[\text{CuB}^s]} \bigg/ \frac{1 + K_{A_R\text{CuB}}^m[\text{CuB}^m]}{1 + K_{A_S\text{CuB}}^m[\text{CuB}^m]} \end{aligned} \quad (11)$$

In the case that the formation constants of ternary complexes are sufficiently high, the enantioselectivity, α , of the chromatographic system is, roughly, given by the ratio of the complexation enantioselectivities in the stationary and mobile phases:

$$\alpha = \frac{K_{A_R\text{CuB}}^s / K_{A_S\text{CuB}}^s}{K_{A_R\text{CuB}}^m / K_{A_S\text{CuB}}^m} = \alpha_s^* / \alpha_m^*$$

ENANTIOSELECTIVITY OF REAL CHROMATOGRAPHIC SYSTEMS

A most important question is whether a rational design of useful chiral chromatographic systems is possible based on experimental data on stereochemical relationships between an appropriate chiral selector and a certain type of racemic compounds which interact in an homogeneous solution; *vice versa*, what kind of information concerning the stereochemistry of a selector–selectand interaction can be inferred from data on occasional successful resolution of a racemic compound in a chiral chromatographic system?

From the above considerations, one can conclude that an immediate relationship between the enantioselectivity of a real chromatographic system and that of an homogeneous solution of a model compound only exists in a single case, namely that with the chiral selector residing entirely in the mobile phase. In this case, the column enantioselectivity, α , approaches the value, α^* , for the selector–selectand interaction. The solute enantiomer, which binds most strongly to the chiral selector, is eluted first and, according to eqn. 7, the solute–selector association constant, K_{ACuB}^m , can be easily estimated from the linear relationship between $(k'_A)^{-1}$ and the selector concentration, $[CuB^m]$, in the mobile phase. Unfortunately, the situation when both the chiral selector and its complexes with the solute enantiomers, A_RCuB and A_SCuB , remain entirely in the mobile phase and are not adsorbed onto the column packing is seldom realized. A rare example of this type of chromatographic systems is the chiral resolution of hydrophobic solutes using a reversed-phase (RP) column in combination with a polar eluent that is modified with cyclodextrin¹⁴. This chiral selector, as well as its inclusion complexes with the solute enantiomers, appear to have but a minimum affinity for the RP packing.

With chiral stationary phases, too, it is sometimes possible to determine the solute–selector association constant and the enantioselectivity of the association. Thus, in the case of ligand-exchange bonded phases, one can vary the copper(II) content from zero to the maximum value of the chiral selector concentration in the stationary phase and then treat the retention parameters according to eqns. 3 and 4. With other types of CSPs, k'_A and K_{ACuB}^s are less readily available, since the sorption site concentration cannot be varied. Another general problem with chiral sorbents is the selection of adequate low-molecular-mass models for the chiral sorption site in the stationary phase, which would simulate in solution all the interactions with the solute enantiomers that are contributing to chiral recognition of the latter in the column. Obviously, this problem does not arise with cyclodextrins and α_1 -acid glycoprotein, where the solute molecule appears to be completely enveloped in or, respectively, adsorbed on the rigid surface of the chiral resolving agent. The solute interactions with these chiral selectors are expected to remain unchanged, independent of whether the selector is dissolved or chemically bonded to an insoluble matrix. It is, probably, not difficult to find adequate soluble chiral selector models for Pirkle's type chiral phases, especially when the selector molecule provides all three distinct interaction sites with the solute molecule, which are required for chiral recognition of the latter. The situation becomes much more complicated with the majority of ligand-exchange phases with bonded chiral amino acid type ligands. Here, spacer fragments have to be included in the structure of the selector model, as is the case with N-benzyl-L-proline

taken as a model for the L-proline-incorporating polystyrene type chiral resin^{1-3,11}. Finally, only oversimplified models can be designed for coated chiral stationary phases where the solid sorbent surface appears to play a decisive role in the chiral recognition of enantiomers by taking an immediate part in the formation of diastereomeric sorption complexes, as we have shown earlier^{5,12}.

At least for the time being, the situation with chiral eluent additives distributed between the mobile and stationary phases seems impossible to resolve. Here, according to eqn. 9, a whole series of labile equilibria exist, each contributing to the overall enantiomeric resolution of solutes on the chromatographic column. Most striking is the conclusion, eqn. 12, that the selector-selectand interaction selectivities in the mobile and stationary phases exert opposite effects on the total resolution. We can arrive at the same conclusion by a purely logical approach: in order to produce maximum chiral discrimination of two enantiomers in a chromatographic column, the chiral selector should bind more strongly and transport more rapidly one enantiomer in the mobile phase, but bind more strongly and retain more strongly the opposite enantiomer when in the stationary phase. This idea has already been exploited by combining a chiral bonded phase with a mobile phase containing the chiral selector of identical chemical structure, but opposite in configuration^{15,16}.

Be this as it may, a chiral eluent system appears more productive if the solute-selector interaction enantioselectivity changes significantly on transferring the selector-selectand adducts from the solution to the stationary phase. Indeed, the relative stability of the two diastereomeric adducts on the sorbent surface changes dramatically, compared to that in the bulk solution, which makes the CMPs a general powerful approach to chromatographic chiral separations.

However, with a CMP system, it would be extremely difficult to tell which one of the complexing and partitioning equilibria 9 makes the desive contribution to the overall enantioselectivity of the chromatographic column. Moreover, due to the complexity of equilibria 9, CMP systems appear to be much more flexible compared to CSP systems in that changing the chromatographic conditions (pH of the eluent, type and concentration of organic modifiers and inorganic salts) significantly influences the solute retention in both the CMP and CSP systems, but, in the former case, the resolution enantioselectivity would also change dramatically, in addition to the retention parameters.

That the total enantioselectivity of CMP systems is not directly related to the enantioselectivity of the selector-selectand interaction in solution can best be demonstrated by the invalidity of the principals of chiral recognition reciprocity in these systems.

RECIPROCITY OF CHIRAL RECOGNITION

Chiral recognition is expected to be reciprocal in that if a chiral resolving agent B_R can distinguish between A_R and A_S , then selector A_R may distinguish B_R from B_S .

In LEC of the solute enantiomers A_R and A_S according to the CMP mode, a copper(II) complex of the chiral ligand B_R is added to the eluent. Two diastereomeric ternary complexes, A_RCuB_R and A_SCuB_R , are formed both in the mobile and stationary phases. These complexes can differ in their stabilities and/or phase

TABLE I

ENANTIOSELECTIVITY, $\alpha = k'_R/k'_S$, FOR THE RESOLUTION OF AMINO ACIDS USING A LICHROSORB RP-18 COLUMN AND AN AQUEOUS ACETONITRILE ELUENT MODIFIED WITH $10^{-3} M$ BIS(S-AMINO ACIDATO)COPPER(II)COMPLEX

Chiral eluent	Racemic solute	k'_R	k'_S	α_1	α_2
S-Pro	Hyp	1.03	2.33	0.44	
S-Hyp	Pro	2.06	3.25		0.63
S-Pro	aHyp	0.80	0.80	1.00	
S-aHyp	Pro	1.37	0.85		1.47
S-Hyp	aHyp	0.82	0.82	1.00	
S-aHyp	Hyp	0.52	0.32		1.63
S-aHyp	BzlaHyp	12.33*	37.89*	0.33	
S-BzlaHyp	aHyp	1.42*	1.17*		1.21
S-BzlPro	Pro	8.38*	2.29*	3.65	
S-Pro	BzlPro	42.50*	27.67*		1.59
S-BzlaHyp	Pro	7.67*	1.75*	4.40	
S-Pro	BzlaHyp	65.16*	19.16*		3.43

* 4% acetonitrile in the eluent.

distributions, which should result in the enantiomers A_R and A_S arriving at the detector cell separately, with an enantioselectivity, α_1 , of the chromatographic system.

If now the chiral selector A_R is allowed to play the rôle of the chiral additive to the mobile phase with the aim of resolving racemic solute $B_{R,S}$, then diastereomeric complexes A_RCuB_R and A_RCuB_S should form in the system. Again, these diastereomeric species may behave differently, thus delivering enantiomers B_R and B_S to the detector cell with a total enantioselectivity of α_2 .

It is important to note that one of the diastereomeric complexes, namely, A_RCuB_R , appears in both chromatographic systems considered. The two other species, A_SCuB_R and A_RCuB_S , are enantiomeric, *i.e.*, identical in all their properties, including stability and phase distribution. This implies that the two chromatographic systems should produce identical enantioselectivity values, $\alpha_1 = \alpha_2$, exactly as required by the reciprocity rule.

Table I presents enantioselectivity values, $\alpha = k'_R/k'_S$, for chromatographic resolutions of a series of racemic amino acids on a LiChrosorb RP-18, 5- μ m column using water-acetonitrile eluents containing chiral bis(amino acidato)copper complexes ($10^{-3} M$). Each amino acid appears twice in the table, as a racemic solute to be resolved and as a chiral selector added to the eluent. Accordingly, each pair of amino acids produces two values of the resolution enantioselectivity, α_1 and α_2 .

Contrary to the requirements of the above reciprocity rule, the two corresponding enantioselectivity values never coincide. Most striking is the situation with the pair *allo*-hydroxyproline-*N*-benzyl-*allo*-hydroxyproline. If $Cu(S\text{-}a\text{Hyp})_2$ is present in the eluent as the chiral selector, then the ternary complex $Cu(S\text{-}a\text{Hyp})$

(*S*-BzlaHyp) is the most strongly retained diastereomeric species, so that the elution sequence of BzlaHyp enantiomers is *S* after *R* with $\alpha_1 = 0.33$. If now $\text{Cu}(\text{S-BzlaHyp})_2$ is added to the eluent, the elution order of the enantiomers of aHyp is observed to be *S* ahead of *R*, $\alpha_2 = 1.21$, which implies that the complex $\text{Cu}(\text{S-aHyp})(\text{S-BzlaHyp})$ is less strongly retained than its diastereomer. This situation can be understood only with the assumption¹⁷ that, after conditioning the column with the corresponding chiral eluents, the hydrophobic complex $\text{Cu}(\text{S-BzlaHyp})_2$ covers the RP packing material much more densely than is the case with the hydrophilic complex $\text{Cu}(\text{S-aHyp})_2$. Therefore, the phase partitioning conditions for the two diastereomeric ternary complexes formed differ drastically in the two chromatographic systems concerned, producing opposite signs of the total enantioselectivity effects, *i.e.*, inversed elution order of the amino acid enantiomers.

CONCLUSION

Enantioselectivity of chiral chromatographic systems appears to be a complex function of the enantioselectivity effects of the selector–selectand adduct formation in both the mobile and stationary phases, as well as of the phase distribution of these adducts, unless the chiral selector resides entirely in one of these phases. The microenvironment of the diastereomeric adducts in the stationary phase can influence significantly the association enantioselectivity. For these reasons, the reciprocity relationships for mutual chiral selector–selectand recognition, which are known to be valid for their association in solutions as well as for diastereomeric salt crystallization, do not necessarily hold for chiral chromatographic systems.

REFERENCES

- 1 V. A. Davankov, *Adv. Chromatogr. (N.Y.)*, 18 (1980) 139.
- 2 V. A. Davankov, A. A. Kurganov and A. S. Bochkov, *Adv. Chromatogr. (N.Y.)*, 22 (1983) 71.
- 3 V. A. Davankov, J. D. Navratil and H. F. Walton, *Ligand Exchange Chromatography*, CRC Press, Boca Raton, FL, 1988.
- 4 S. V. Rogozhin and V. A. Davankov, *Dokl. Akad. Nauk SSSR*, 192 (1970) 1288.
- 5 V. A. Davankov, A. S. Bochkov, A. A. Kurganov, P. Roumeliotis and K. K. Unger, *Chromatographia*, 13 (1980) 677.
- 6 P. E. Hare and E. Gil-Av, *Science (Washington, D.C.)*, 204 (1979) 1226.
- 7 J. N. LePage, W. Lidner, G. Davies, D. E. Seitz and B. L. Karger, *Anal. Chem.*, 51 (1979) 433.
- 8 C. C. McDonald and W. D. Phillips, *J. Am. Chem. Soc.*, 85 (1963) 3736.
- 9 V. A. Davankov, S. V. Rogozhin and A. A. Kurganov, *Izv. Akad. Nauk SSSR, Ser. Khim.*, (1971) 204.
- 10 A. A. Kurganov, T. M. Ponomareva and V. A. Davankov, *Inorg. Chim. Acta*, 86 (1984) 145.
- 11 V. A. Davankov and P. R. Mitchell, *J. Chem. Soc. Dalton Trans.*, (1972) 1012.
- 12 V. A. Davankov and A. A. Kurganov, *Chromatographia*, 17 (1983) 686.
- 13 B. Feibush, M. J. Cohen and B. L. Karger, *J. Chromatogr.*, 282 (1983) 3.
- 14 J. Debowski, D. Sybilska and J. Jurczak, *Chromatographia*, 16 (1982) 198.
- 15 M. Fujita, Y. Yoshikawa and H. Yamatera, *Chem. Lett.*, 11 (1975) 473.
- 16 C. Pettersson and C. Gioeli, *J. Chromatogr.*, 435 (1988) 225.
- 17 A. A. Kurganov, T. M. Ponomareva and V. A. Davankov, *6th Int. Symp. Capillary Chromatography, Riva del Garda, 1985*, p. 871.

Note

Determination of impurity profiles in drugs and related materials

II*. Detection and quantification of a diastereomeric impurity in the peptide RGH-0205 (Arg-Lys-Asp)

S. GÖRÖG*, B. HERÉNYI, O. NYÉKI, I. SCHÖN and L. KISFALUDY
Chemical Works Gedeon Richter Ltd., P.O.B. 27, H-1475 Budapest (Hungary)

In the determination of the impurity profile of the immunostimulant peptide RGH-0205 (Arg-Lys-Asp)¹, the separation of a major impurity was a difficult task. The usual methods for the separation of impurities in small peptides such as thin-layer chromatography (TLC) and reversed-phase high-performance liquid chromatography (HPLC) using acidic or neutral buffers as eluents failed to separate this impurity. We report here a successful separation using an HPLC eluent of higher pH than usual.

EXPERIMENTAL

Apparatus

A Hewlett-Packard (Waldbronn, F.R.G.) 1090 high-performance liquid chromatograph equipped with an HP-1040 diode-array detector was used. Optical rotations were measured using a Perkin-Elmer (Überlingen, F.R.G.) 241 polarimeter. The NMR spectra were taken using a Varian (Palo Alto, CA, U.S.A.) XL-400 instrument.

Reagents

Water used in HPLC was purified by double distillation followed by passing it through a LiChroprep RP-8 column (Merck, Darmstadt, F.R.G.). Other solvents and reagents were of ACS reagent grade and were purchased from Aldrich (Beerse, Belgium).

HPLC procedure

A 250 × 4 mm I.D. column was used, packed by Bio Separation Technologies (Budapest, Hungary) with LiChrosorb RP-18 (Merck). The eluent was 0.015 M disodium hydrogenphosphate solution adjusted to pH 7.0–9.5 by adding hydrochloric acid and sodium hydroxide. The flow-rate was 1 ml/min. The analytical separations were performed at pH 9.0. The concentration of the sample solution was 0.1% in the eluent. The volume injected was 20 μl.

* For Part I, see S. Görög, A. Laukó and B. Herényi, *J. Pharm. Biomed. Anal.*, 6 (1988) in press.

TLC procedure

The solvent systems were (1) *n*-butanol–pyridine–acetic acid–water (9:20:6:11) and (2) *n*-butanol–ethyl acetate–acetic acid–water (1:1:1:1). A solution of 100 μg of RGH-0205 in 20 μl of water was applied to the plate (Kieselgel 60 HPTLC plate 13748; Merck). The length of the run was 10 cm. The spots were revealed with chlorine–tolidine reagent².

Investigation of the protected peptide

A 100-mg amount of Boc-Arg(HCl)–Lys(Boc)–Asp(OBu^t)-OBu^t (Bu^t = *tert.* butyl), synthesized as described in ref. 1, was dissolved in 2 ml of trifluoroacetic acid in a small glass-stoppered bottle. The mixture was allowed to stand at room temperature for 60 min, then 200 μl were transferred into a 10-ml volumetric flask, 2 ml of 1 *M* sodium hydroxide solution were added and the content were diluted to volume with water. A 20- μl volume of this solution was injected into the chromatograph.

RESULTS AND DISCUSSION

As can be seen in Table I, measuring the optical rotation, TLC using various systems (of which two are shown here) and reversed-phase HPLC using neutral or acidic eluents cannot differentiate between pure RGH-0205 and a batch containing about 10% of an unknown impurity. The presence of the latter was detected by HPLC using a pH as high as 9 for the eluent.

Fig. 1a and b show the chromatograms of batches 1 and 2, respectively, at pH 9. The fact that the impurity peak at $k' = 1.20$ does not appear at all in batch 1, even if the test solution is allowed to stand at this high pH for 24 h before the injection, indicated that this impurity is by no means a chromatographic artifact or an alkaline degradation product of RGH-0205.

The UV spectrum of the impurity obtained with the diode array detector was identical with that of the main component. The amino acid analysis of a sample enriched in impurity to about 35% was also identical with that of batch 1. However, the HPLC analysis of the acidic hydrolysate of the sample (6 *M* hydrochloric acid,

TABLE I
ANALYTICAL DATA OF TWO BATCHES OF RGH-0205

Batch No.	$[\alpha]_D^{20}$ *	TLC		HPLC	
		System 1	System 2	pH 8	pH 9
1	+3.8°	Single spot, $R_F=0.15$	Single spot, $R_F=0.20$	Single peak, $k'=0.76$	$k'=0.80$
2	+3.6°	Single spot, $R_F=0.15$	Single spot, $R_F=0.20$	Single peak, $k'=0.76$	Main peak $k'=0.80$, impurity peak (10%), $k'=1.20$

* Solvent: 10% (v/v) acetic acid.

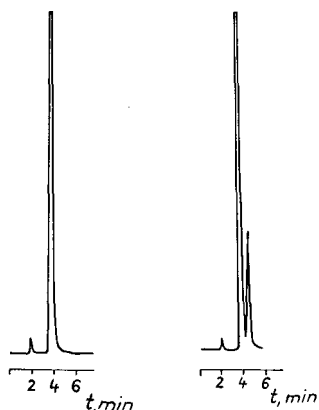


Fig. 1. HPLC of (a) pure and (b) contaminated RGH-0205 at pH 9. For chromatographic conditions, see Experimental.

24 h, 110°C) after enantiomeric derivatization with Marfey's reagent³ showed the presence of D-aspartic acid. This was supported by a comparison of the 400 MHz ¹H NMR spectra of the pure and contaminated samples. In addition to the multiplets of α -CH at 4.403 ppm (dd) and β -CH₂ at 2.695 and 2.575 ppm (dd) of the pure substance, new signals appeared at 4.442 (dd) and at 2.712 and 2.495 ppm (dd), respectively.

On the basis of these findings we concluded that epimerization had taken place during the synthesis, resulting in the formation of Arg-Lys-D-Asp (LLD impurity). This was later proved by retention matching with synthesized Arg-Lys-D-Asp⁴.

In possession of the pure LLD derivative it was possible to establish its quantitative determination. The identity of their UV spectra permitted the determination of the percentage of the LLD impurity in RGH-0205 based on area normalization in the chromatogram taken at 215 nm, as shown by the following regression equation derived from model experiments with RGH-0205 samples spiked with LLD impurity:

$$\text{LLD, A (\%)} = 1.02 \times \text{LLD, T (\%)} + 0.03 \quad (r=0.99)$$

where LLD, A (%) and LLD, T (%) are percentages of the impurity found by area normalization and taken, respectively. The relative standard deviation at the 5% impurity level was 1.6% ($n=6$) and the detection level was found to be 0.2%.

The fact that the separation of the two diastereomeric derivatives can be performed only at the unusually high pH of 9 merits special attention. In most of the hundreds of papers on the HPLC separation of peptides, including diastereomeric derivatives, slightly acidic or neutral buffers, preferably with ion-pairing anions such as phosphate, with or without organic modifiers, were used as the eluents^{5,6}. With our highly polar peptide no modifier was found to be necessary to obtain suitable k' values. The presence of phosphate ion is essential; using ammonium carbonate buffer poor peak shapes and no resolution of the diastereomers were obtained. Equally necessary was the above-mentioned high pH. Table II shows the changes in the retention and separation parameters as a function of pH, and large changes take place

TABLE II
RETENTION AND SEPARATION DATA AT VARIOUS pH VALUES

pH	$k'_{Arg-Lys-Asp}$	$k'_{Arg-Lys-D-Asp}$	α
7.0	0.75	0.75	1.00
7.5	0.75	0.75	1.00
8.0	0.76	0.80	1.05
8.5	0.78	0.90	1.15
9.0	0.80	1.20	1.50
9.5	0.82	1.25	1.52

between pH 8 and 9. This is attributable to the changes in the ionization state of RGH-0205 in this pH range. The pK_a values of RGH-0205 are as follows⁷: 2.9 and 4.3 (carboxyl groups of the aspartic acid), 7.6 (α -NH₃⁺ group of arginine), 10.6 (ϵ -NH₃⁺ group of lysine) and about 14 [-NHC(=NH₂⁺)NH₂ group of arginine]. From these data it is evident that the main change that occurs when the pH is raised from 8 to 9 is deprotonation of the α -amino group to form a neutral, zwitterionic species. The discussion of the exact mechanism of the separation will be the subject of another publication, where the retention and separation data of all diastereomers of RGH-0205 will also be presented. It is probable, however, even from these data that the separation of the two diastereomers at pH 9 is due to the above-mentioned deprotonation of the terminal α -NH₂ group, preventing its participation in the process of ion pairing so that ion-pair formation is limited to the side-chain positive centres and the two carboxylates bringing the molecules into the isoelectric state. Ion-pair formation in this state may be subject to steric hindrance, causing differences in the polarities, *i.e.*, the retention characteristics of the diastereomers.

In the course of a study aiming at finding the reasons for the formation of the LLD impurity in some of the batches of RGH-0205 it was necessary to investigate the optical purity of its protected form. It was found that, in accordance with the above-outlined separation mechanism, no separation took place at any pH with the LLL and LLD form of Boc-Arg(HCl)-Lys(Boc)-Asp(OBu^t)-OBu^t. The determination of the ratio of the diastereomers in this form was traced to the underivatized form of RGH-0205. The protecting group can be quantitatively removed by treatment with trifluoroacetic acid at room temperature and the neutralized reaction mixture is suitable for direct injection into the chromatograph. It was found that no racemization takes place during the removal of the protecting groups, hence this indirect method is suitable for the determination of the diastereomeric composition of the protected peptide. From the analytical point of view, the chromatographic separation after the splitting with trifluoroacetic acid at room temperature is a new example of a series of "retro-derivatization" reactions successfully used in our laboratory for the spectrophotometric and chromatographic determination of various steroid, benzhydrol and other derivatives⁸⁻¹¹.

CONCLUSIONS

The problem of the HPLC separation of a diastereomeric impurity in some batches of Arg-Lys-Asp can be solved by raising the pH of the eluent to 9. The

question of the extent to which this finding can be generalized, *i.e.*, the extent to which investigation at high pH can be recommended as a part of the impurity profiling of peptides, can only be answered when more data than we have at present are available. Work is in progress on this aspect.

On the other hand, it should be taken into account that working with eluents at pH 9, which is much above the usual pH range recommended for silica or modified silica columns, can drastically reduce the lifetime of the column. The solution to this problem may be the use of an alkali-resistant porous polystyrene-divinylbenzene column with which the optimal separation of diastereomeric di- and tripeptides was achieved in the pH range of the isoelectric point¹².

ACKNOWLEDGEMENTS

We thank Dr. Gy. Szókán (Institute of Organic Chemistry, Eötvös Lóránd University, Budapest) for the Marfey tests and Mr. G. Balogh and Mr. A. Csehi for the NMR spectra.

REFERENCES

- 1 L. Kisfaludy, O. Nyéki, I. Schön, L. Dénes, J. Ember, L. Szporny, Gy. Hajós and B. Szende, *Hoppe-Seyler's Z. Physiol. Chem.*, 364 (1983) 933.
- 2 K. G. Krebs, D. Heusser and H. Wimmer, in E. Stahl (Editor), *Thin-Layer Chromatography*, Springer-Verlag, Berlin, Heidelberg, New York, 1969, p. 863.
- 3 P. Marfey, *Carlsberg Res. Commun.*, 49 (1984) 591.
- 4 I. Schön, O. Nyéki, L. Kisfaludy, B. Herényi and S. Görög, *Proceedings of the 20th European Peptide Symposium, Tübingen, September 4-10, 1988*, in press.
- 5 D. D. Blevins, M. F. Burke and V. J. Hruby, in W. S. Hancock (Editor), *Handbook of HPLC for the Separation of Amino Acids, Peptides, and Proteins*, Vol. II, CRC Press, Boca Raton, FL, 1984, pp. 137-143.
- 6 F. Lottspeich and A. Henschen, in A. Henschen, K.-P. Hupe, F. Lottspeich and W. Voelter (Editors), *High Performance Liquid Chromatography in Biochemistry*, VCH, Weinheim, 1985, pp. 139-317.
- 7 B. Noszál, personal communication.
- 8 S. Görög, M. Rényi and A. Laukó, *J. Pharm. Biomed. Anal.*, 1 (1983) 39.
- 9 S. Görög, A. Laukó, M. Rényi and B. Hegedüs, *J. Pharm. Biomed. Anal.*, 1 (1983) 497.
- 10 G. Balogh, A. Csehi, S. Görög, A. Laukó and Z. Tuba, in S. Görög (Editor), *Advances in Steroid Analysis '84*, Elsevier, Amsterdam, 1985, p. 301.
- 11 S. Görög and A. Laukó, *Magy. Kém. Foly.*, 92 (1986) 337.
- 12 Z. Iskandarani and D. J. Pietrzyk, *Anal. Chem.*, 53 (1981) 489.

USE OF HYDROXYPROPYL- AND HYDROXYETHYL-DERIVATIZED β -CYCLODEXTRINS FOR THE THIN-LAYER CHROMATOGRAPHIC SEPARATION OF ENANTIOMERS AND DIASTEREOMERS

DANIEL W. ARMSTRONG*, JAMES R. FAULKNER, Jr. and SOON M. HAN

Department of Chemistry, University of Missouri-Rolla, Rolla, MO 65401-0249 (U.S.A.)

SUMMARY

Partially substituted hydroxypropyl- β -cyclodextrin and hydroxyethyl- β -cyclodextrin proved to be effective chiral mobile phase additives (CMAs) for the thin-layer chromatographic (TLC) resolution of racemic benzyl-2-oxazolidinone, 5-(4-methylphenyl)-5-phenylhydantoin, mephentoin and several dansyl and β -naphthylamide amino acids. Several diastereomeric compounds including steroid epimers and alkaloids were separated as well. The derivatized β -cyclodextrins tended to be much more soluble in water and hydro-organic solvents than native β -cyclodextrin. Their chromatographic selectivity also was somewhat different. The use of CMAs in TLC is a potentially useful and powerful method that has not been considered adequately. The relative lack of chiral stationary phases available in planar format makes the use of CMAs particularly attractive.

INTRODUCTION

Cyclodextrins (CDs) have been used effectively in chromatography for the separation of enantiomers, diastereomers, structural isomers and routine compounds. Most of these separations have been done via high-performance liquid chromatography (HPLC) with the CD bonded phase^{1–18}. However, there has been some success with CD mobile phase additives^{19–25}. Two things that limit the use of CDs as mobile phase additives are solubility and cost. β -CD is the least expensive and most widely used homologue. However, its solubility in water is only about 0.017 *M* at room temperature. This value can decrease significantly when organic modifiers are added. The solubility of β -CD in water can be increased by going to very high pH values or by adding large amounts of urea²⁶. Another alternative is to synthetically modify the CD so as to increase its water solubility. In fact, hydroxypropyl- and hydroxyethyl-substituted β -CDs can be made relatively inexpensively and are much more soluble in water than native β -CD (see Experimental). In fact, their solubility increases as the degree of substitution increases. In chromatography, the concentration of the chiral mobile phase additive (CMA) frequently is the critical parameter for obtaining enantiomeric separations. In the specific case of CD additives, enantioselectivity generally increases with increasing CD concentrations in the mobile phase^{24,26}.

While a large number of chiral stationary phases (CSPs) have been introduced for HPLC²⁷, relatively few CSPs are available, commercially, in TLC (thin-layer chromatography) format. Consequently, the use of CMAs will continue to play an important role in the TLC separation of optical isomers. In fact, there are a number of advantages to using CMAs that complement the TLC approach. For example, there is a wider variety of CMAs available than there are CSPs. The use of CMAs permits enantiomeric separations to be done on less expensive and often more durable achiral stationary phases. The selectivities of CMA methods are often different from those of analogous CSP techniques¹⁹⁻²⁶. Also, much less of a CMA is needed in TLC than in the equivalent HPLC method. This can be important if the CMA is costly.

EXPERIMENTAL

Chemically bonded octadecylsilane reversed-phase TLC plates, KC 18F (200 μm layer thickness, 5 \times 20 cm and 20 \times 20 cm) were obtained from Whatman Chemical Separation Division (Clifton, NJ, U.S.A.). All dansyl amino acids, cinchonine, cinchonidine, quinine, quinidine, 17 α ,20 α -dihydroxy-4-pregnen-3-one, 17 α ,20 β -dihydroxy-4-pregnen-3-one, 20 α -hydroxy-4-pregnen-3-one, 20 β -hydroxy-4-pregnen-3-one, 17 α ,20 α ,21-trihydroxy-4-pregnene-3,11-dione, 17 α ,20 β ,21-trihydroxy-4-pregnene-3,11-dione, 11 β ,17 α ,20 α ,21-tetrahydroxy-4-pregnen-3-one, 11 β ,17 α ,20 β ,21-tetrahydroxy-4-pregnen-3-one and sodium chloride were obtained from Sigma (St. Louis, MO, U.S.A.). DL-Alanine- β -naphthylamide, DL-methionine- β -naphthylamide, 5-(4-methylphenyl)-5-phenylhydantoin, *R*-(+)-benzyl-2-oxazolidinone and *S*-(-)-benzyl-2-oxazolidinone were obtained from Aldrich (Milwaukee, WI, U.S.A.). Mephenytoin was obtained from Dr. R. D. Armstrong of the La Jolla Cancer Research Foundation. Hydroxypropyl- and hydroxyethyl- β -CDs were obtained from Dr. Otto Huber of the Consortium für Elektrochemische Industrie (Munich, F.R.G.). Relevant information on these compounds is given in Table I. The basic structure of these compounds is shown in Fig. 1. N'-(Menthoxycarbonyl)anabasine and N'-

TABLE I
PROPERTIES OF SUBSTITUTED β -CYCLODEXTRINS

Data obtained from the Consortium für Elektrochemische Industrie GMBH technical literature. The following solvents also will dissolve the substituted CD to some extent: methanol, ethanol, dimethylformamide, dimethyl sulfoxide and pyridine.

Compound	Average molar substitution*	Average molecular mass**	Solubility in water at 25°C (g/100 ml)
Hydroxypropyl- β -CD	0.6 \pm 0.1	1379 \pm 40	96
Hydroxypropyl- β -CD	0.9 \pm 0.1	1501 \pm 40	> 100
Hydroxyethyl- β -CD	1.0 \pm 0.2	1443 \pm 62	> 200
Hydroxyethyl- β -CD	1.6 \pm 0.2	1628 \pm 62	> 200

* Average molar substitution is defined as the average number of hydroxypropyl or hydroxyethyl groups per anhydroglucose unit.

** Each sample contained a narrow distribution of homologues. For example, the molar substitution of the first compound in this table varied from 0.5 to 0.7 for an average of 0.6. Consequently, the molecular mass varied from 1338 to 1419 for an average of 1379.

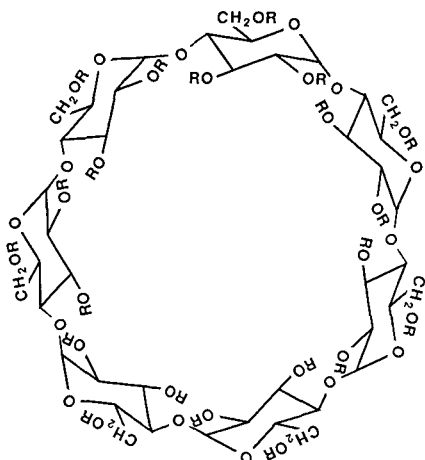


Fig. 1. Basic structure of derivatized CD. For hydroxyethyl- β -CD, $R = (\text{CH}_2\text{-CH}_2\text{-O})_n\text{H}$. For hydroxypropyl- β -CD, $R = (\text{CH}_2\text{-C}(\text{CH}_3)\text{H-O})_n\text{H}$. The cyclodextrin is randomly substituted and side-chains with $n > 1$ are possible. The AMS of each derivative (*i.e.*, 0.6, 0.9, 1.0 and 1.6 in Table I) refers to the number of hydroxyalkyl groups per anhydroglucose unit.

(menthoxy carbonyl)3-pyridyl-1-aminoethane were produced as previously reported²⁶. HPLC-grade water, acetonitrile, methanol and triethylamine were obtained from Fisher Scientific (St. Louis, MO, U.S.A.). All chemicals were used without purification.

All developments were done at room temperature. Cylindrical glass developing chambers (23×6 cm I.D.) and rectangular glass chambers ($28.5 \times 9.5 \times 27.0$ cm) were used. Spot visualization was accomplished using a fixed-wavelength (254 nm) UV lamp.

RESULTS AND DISCUSSION

Past work on the use of native CDs as CMAs (in both HPLC and TLC) indicated that some minimum concentration was needed to obtain an enantiomeric separation. Increasing the CD concentration generally improved the separation. Eventually a point is reached where no further CD can be solubilized or where further increases in the CD concentration do not improve the separation²⁶. In the case of β -CD, often the solubility limit was reached before any enantioselectivity was observed. The solubility of hydroxypropyl- and hydroxyethyl- β -CDs in water is much greater than that of underivatized β -CD (Table I). Solutions exceeding 0.4 M can be made without including additives to enhance solubility. While greater solubility is desirable, there are a number of other ramifications and "trade-offs" that must be considered. For example, the viscosity of derivatized β -CD solutions also increases with concentration. Consequently TLC development times increase substantially. This is shown in Fig. 2. Indeed, the time of development can become prohibitively long at the higher derivatized β -CD concentrations.

It appears (Table I) that the solubility of the derivatized β -CD increases as the

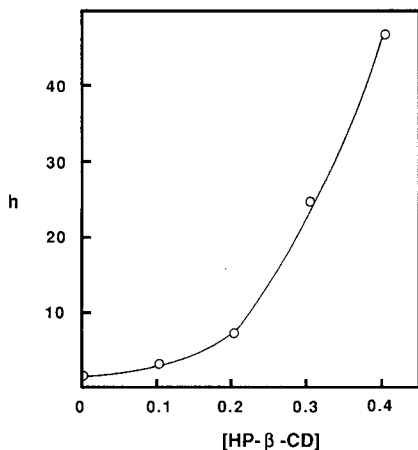


Fig. 2. Plot of the TLC development time (h) *versus* the molar concentration of 0.6 AMS hydroxypropyl- β -CD in the mobile phase. The solute used was dansyl DL-leucine. The mobile phase was acetonitrile-water (30:70, v/v). The separation was done on a 5 \times 20 cm reversed-phase TLC plate.

degree of substitution increases. Also, the hydroxyethyl- β -CD may be more soluble than an analogous hydroxypropyl- β -CD. Unfortunately, little is known about the effect of derivatization on enantioselectivity and inclusion complex formation. Since hydrogen bonding to the secondary hydroxyl groups at the mouth of the CD cavity is known to be important for chiral recognition^{13,15}, it is likely that derivatization will induce changes in chromatographic behavior. In fact, it was found that some optical isomers were better resolved with the derivatized β -CDs while others separated better with native β -CD. As expected, there were substantial differences in the performance of the various β -CD derivatives. This is shown for dansyl DL-leucine in Fig. 3. Several

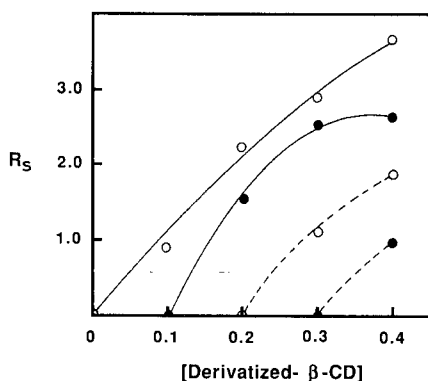


Fig. 3. Plots of enantiomeric resolution (R_s) of dansyl DL-leucine *versus* concentration of four different hydroxyalkyl- β -CDs. The curves, from left to right, are: (—○—) 0.6 AMS hydroxypropyl- β -CD; (—●—) 0.9 AMS hydroxypropyl- β -CD; (—○—) 1.0 AMS hydroxyethyl- β -CD; and (—●—) 1.6 AMS hydroxyethyl- β -CD.

TABLE II
SEPARATION DATA FOR ENANTIOMERS

Compound	R_F^*	R_s	Mobile phase**
(1) Dansyl DL-leucine**	0.44	3.6	0.4 M HP- β -CD acetonitrile-water (30:70)
(2) Dansyl DL-valine***	0.37	1.3	0.4 M HP- β -CD acetonitrile-water (30:70)
(3) Dansyl DL-methionine***	0.37	1.6	0.4 M HP- β -CD acetonitrile-water (30:70)
(4) Dansyl DL-threonine***	0.58	0.9	0.4 M HP- β -CD acetonitrile-water (30:70)
(5) Dansyl DL-phenylalanine***	0.36	1.3	0.4 M HP- β -CD acetonitrile-water (35:65)
(6) Dansyl DL-norleucine***	0.20	1.8	0.4 M HP- β -CD acetonitrile-water (30:70)
(7) DL-Methionine- β -naphthylamide	0.60	1.8	0.3 M HP- β -CD acetonitrile-water (35:65)
(8) DL-Alanine- β -naphthylamide	0.66	1.0	0.3 M HP- β -CD acetonitrile-water (25:75)
(9) Mephentoin	0.39	2.0	0.4 M HP- β -CD acetonitrile-water (30:70)
(10) 5-(4-Methylphenyl)-5-phenylhydantoin	0.24	0.8	0.3 M HP- β -CD acetonitrile-water (35:65)
(11) R-(+)Benzyl-2-oxazolidinone S-(-)Benzyl-2-oxazolidinone	0.54	0.9	0.3 M HP- β -CD acetonitrile-water (35:65)

* This is the R_F of the enantiomer that moved nearest the solvent front.

** HP- β -CD stands for the 0.6 AMS hydroxypropyl- β -CD (Table I).

*** D-isomer was eluted first.

things are apparent from this figure. First, as the average molar substitution (AMS) of the CD is increased, the amount of the CMA needed to achieve an enantiomeric resolution increases. Consequently, a balance must be reached in which the degree of derivatization is sufficient to increase solubility and perhaps alter selectivity, but not high enough to interfere with complexation or chiral recognition. For the compounds in this study, the 0.6 AMS hydroxypropyl- β -CD seemed to be the most effective CMA. Solutions of the higher AMS β -CDs had to be two to ten times higher in concentration than the 0.6 AMS β -CD in order to obtain equivalent or often inferior separations.

Table II gives the optimum separation conditions and data for eleven racemates. Table III gives analogous information for eight pairs of diastereomers. Note that in all cases the mobile phase consists of an acetonitrile-water mixture plus the substituted CDCMA. Organic modifier concentrations between 20 and 40% (v/v) are optimal for this technique. When less than 20% acetonitrile was added, some streaking occurred. If the acetonitrile concentration exceeded 40%, it became difficult to dissolve a sufficient concentration of the CMAs. When methanol was used in place of acetonitrile, streaking was more common.

Fig. 4 shows the effect of hydroxypropyl- β -CD concentration on the retention of racemic dansyl leucine and dansyl valine. Note that the dansyl leucine (circles) begins to resolve at a lower CMA concentration than the dansyl valine (triangles). The enantioselectivity increases up to about 0.3 M CMA for dansyl DL-leucine and 0.4

TABLE III
SEPARATION DATA FOR DIASTEREOMERS

Compound	R_F	R_S	Mobile phase*
(1) Cinchonine	0.40	4.2	0.3 M HP- β -CD
Cinchonidine	0.23		acetonitrile-water (35:65)
(2) Quinidine	0.29	4.3	0.3 M HP- β -CD
Quinine	0.15		acetonitrile-water (35:65)
(3) 17 α ,20 α -Dihydroxy-4-pregnen-3-one	0.54	4.0	0.3 M HP- β -CD
17 α ,20 β -Dihydroxy-4-pregnen-3-one	0.40		acetonitrile-water (35:65)
(4) 20 α -Hydroxy-4-pregnen-3-one	0.37	3.3	0.3 M HP- β -CD
20 β -Hydroxy-4-pregnen-3-one	0.16		acetonitrile-water (35:65)
(5) 17 α ,20 α ,21-Trihydroxy-4-pregnene-3,11-dione	0.69	2.2	0.3 M HP- β -CD
			acetonitrile-water (30:70)
17 α ,20 β ,21-Trihydroxy-4-pregnene-3,11-dione	0.61		
(6) 11 β ,17 α ,20 α ,21-Tetrahydroxy-4-pregnen-3-one	0.63	0.8	0.3 M HP- β -CD
			acetonitrile-water (35:65)
11 β ,17 α ,20 β ,21-Tetrahydroxy-4-pregnen-3-one	0.0		
(7) N'-(Menthoxycarbonyl) anabasine	0.02	0.8	0.3 M HP- β -CD
	0.04		acetonitrile-water (35:65)
(8) N'-(Menthoxycarbonyl) 3-pyridyl-1-amipoethane	0.11	2.2	0.3 M HP- β -CD
	0.18		acetonitrile-water (35:65)

* HP- β -CD stands for the 0.6 AMS hydroxypropyl- β -CD (Table I).

** 1% Aqueous triethyl ammonium acetate (pH 7.1).

M for dansyl DL-valine (Fig. 4). It would appear from Fig. 4 that the resolution of dansyl DL-leucine may level off at higher CMA concentrations. As shown in Fig. 5, this is not necessarily the case. The enantiomeric resolution of dansyl DL-leucine increases at high CMA concentrations even though the enantioselectivity (*i.e.*, α) remains approximately constant. The reason for this is that the spots are significantly smaller (*i.e.*, better efficiency) at the higher CMA concentrations. Dansyl DL-valine does not show as pronounced an improvement in resolution at 0.4 M CMA.

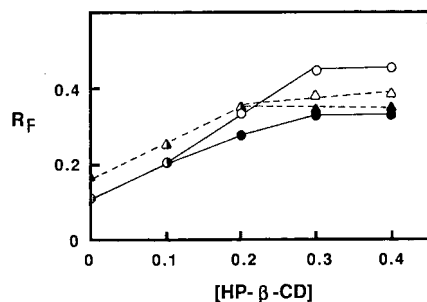


Fig. 4. Plots showing the change in R_F versus concentration of 0.6 AMS hydroxypropyl- β -CD for dansyl DL-leucine (circles) and dansyl DL-valine (triangles).

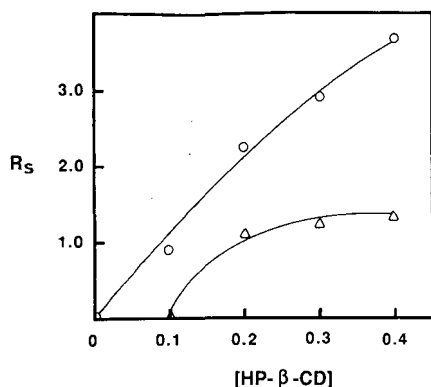


Fig. 5. Plots of resolution (R_s) versus concentration of 0.6 AMS hydroxypropyl- β -CD for dansyl DL-leucine (O) and dansyl DL-valine (Δ).

CONCLUSIONS

Hydroxypropyl- and hydroxyethyl- β -CDs can be useful CMAs for the TLC separation of enantiomers. Their increased solubility in water and hydro-organic solvents (compared to β -CD) makes them particularly convenient and useful CMAs. The 0.6 M substituted β -CD seemed to be the most effective CMA. Higher degrees of substitution increased the solubility of the base molecule, but also seemed to interfere with complexation or enantioselectivity. The use of CMAs in high-performance TLC is an area of great potential that has not been investigated adequately.

ACKNOWLEDGEMENTS

Support of this work by the National Institute of General Medical Sciences (BMT 1 R01 GM 36292-02) and Dr. Otto Huber of the Consortium für Elektrochemische Industrie GMBH is gratefully acknowledged.

REFERENCES

- 1 D. W. Armstrong, *J. Liq. Chromatogr.*, 7 (1984) 353.
- 2 D. W. Armstrong and W. DeMond, *J. Chromatogr. Sci.*, 22 (1984) 411.
- 3 W. L. Hinze, in C. J. Van Oss (Editor), *Applications of Cyclodextrins in Chromatographic Separations and Purification Methods in Separation and Purification Methods*, Vol. 10, Marcel Dekker, New York, 1981, p. 159.
- 4 D. W. Armstrong, A. Alak, K. Bui, W. DeMond, T. Ward, T. E. Riehl and W. L. Hinze, *J. Inclusion Phenomena*, 2 (1984) 533.
- 5 D. W. Armstrong, A. Alak, W. DeMond, W. L. Hinze and T. E. Riehl, *J. Liq. Chromatogr.*, 8 (1985) 261.
- 6 T. E. Beesley, *Am. Lab.*, (1985) 78.
- 7 T. J. Ward and D. W. Armstrong, *J. Liq. Chromatogr.*, 9 (1986) 407.
- 8 D. W. Armstrong and W. Li, *Chromatography*, 2 (1987) 43.
- 9 D. W. Armstrong, S. M. Han and Y. I. Han, *Anal. Biochem.*, 167 (1987) 261.
- 10 S. M. Han and D. W. Armstrong, *J. Chromatogr.*, 389 (1987) 256.
- 11 D. W. Armstrong, S. F. Yang, S. M. Han and R. Menges, *Anal. Chem.*, 59 (1987) 2594.
- 12 D. W. Armstrong, T. J. Ward, A. Czech, B. P. Czech and R. A. Bartsch, *J. Org. Chem.*, 50 (1985) 5556.
- 13 D. W. Armstrong, W. DeMond and B. P. Czech, *Anal. Chem.*, 57 (1985) 481.

- 14 W. L. Hinze, T. E. Riehl, D. W. Armstrong, W. DeMond, A. Alak and T. Ward, *Anal. Chem.*, 57 (1985) 237.
- 15 D. W. Armstrong, T. J. Ward, R. D. Armstrong and T. E. Beesley, *Science (Washington, D.C.)*, 232 (1986) 1132.
- 16 D. W. Armstrong and W. DeMond, *J. Chromatogr. Sci.*, 22 (1984) 411.
- 17 D. W. Armstrong, W. DeMond, A. Alak, W. L. Hinze, T. E. Riehl and K. H. Bui, *Anal. Chem.*, 57 (1985) 234.
- 18 R. D. Armstrong, T. J. Ward, N. Pattabiraman, C. Benz and D. W. Armstrong, *J. Chromatogr.*, 414 (1987) 192.
- 19 D. W. Armstrong, *J. Liq. Chromatogr.*, 3 (1980) 895.
- 20 W. L. Hinze and D. W. Armstrong, *Anal. Lett.*, 13 (1980) 1093.
- 21 J. Debowski, D. Sybilska and J. Jurczak, *J. Chromatogr.*, 237 (1982) 303.
- 22 J. Debowski, J. Jurczak and D. Sybilska, *J. Chromatogr.*, 282 (1983) 83.
- 23 D. Sybilska, J. Zukowski and J. Bojarski, *J. Liq. Chromatogr.*, 9 (1986) 591.
- 24 T. Takeuchi, H. Asai and D. Ishii, *J. Chromatogr.*, 357 (1986) 409.
- 25 D. W. Armstrong, L. A. Spino, S. M. Han, J. I. Seeman and H. V. Secor, *J. Chromatogr.*, 411 (1987) 490.
- 26 D. W. Armstrong, F. Y. He and S. M. Han, *J. Chromatogr.*, 448 (1988) 345.
- 27 D. W. Armstrong, *Anal. Chem.*, 59 (1987) 84A.

CHROM. 20 450

MIXED-BED ION-EXCHANGE COLUMNS FOR PROTEIN HIGH-PERFORMANCE LIQUID CHROMATOGRAPHY*

YIH-FEN MAA, FIROZ D. ANTIA, ZIAD EL RASSI and CSABA HORVÁTH*

Department of Chemical Engineering, Yale University, New Haven, CT 06520 (U.S.A.)

SUMMARY

Protein retention is investigated on high-performance liquid chromatography columns packed with mixtures of ion exchangers. Retention factors are measured at both low and high salt concentrations in the eluent and their dependence on the bed composition is found to be linear in some cases, but non-linear in others. The physical basis for the observed non-linear retention behavior has not been established and an empirical mixing rule is employed to express the dependence of protein retention on bed composition. Protein separations are carried out on the mixed-bed columns by using gradient elution with increasing salt concentration and the process is modelled mathematically. The retention times predicted by computer calculations correspond closely to the experimental findings. Optimal selection of the mixed-bed composition and the gradient steepness for the separation of four proteins is illustrated by using the window diagram technique. Although the experimental results presented here deal with electrostatic interaction chromatography of proteins only the applicability of mixed sorbents is expected to extend to all branches of liquid chromatography. It is anticipated that mixed-sorbent columns will find extensive use in the large-scale purification of biological compounds and in routine analysis.

INTRODUCTION

In liquid chromatography (LC), retention and selectivity are most conveniently adjusted to the desired value by appropriately changing the composition of the mobile phase. Whereas this practice is widespread, in certain instances the freedom to select the mobile phase composition is curtailed or the available means are insufficient to tailor retention behavior in the required fashion. Such a situation may occur in the rapidly growing field of large-scale chromatography where process design may entail the specification of a stationary phase obtained by mixing two or more sorbents in order to attain retentive properties appropriate for solving the separation problem at hand. On the other hand in analytical high-performance liquid chromatography

* Presented as part of paper No. 201 at the *10th International Symposium on Column Liquid Chromatography*, San Francisco, CA, May 18-23, 1986. The majority of papers presented at this symposium has been published in *Journal of Chromatography*, Vols. 371, 384, 385 and 386.

(HPLC) we may want to maximize the selectivity of the chromatographic system for the components of a given sample to be analyzed routinely.

Mixed stationary phases have been used in gas-liquid chromatography where it is more effective to manipulate the properties of the liquid stationary phase than those of the carrier gas¹⁻⁴. Columns with multiple stationary phases have been obtained in three ways: (a) with a series of columns, each packed with a different stationary phase, (b) by coating a mixture of liquids onto the support and (c) by packing support particles coated with different liquids in a mixed bed. Each has its parallel in LC; tandem or mixed-bed columns have been shown to offer a convenient means to manipulate stationary phase selectivity⁵ and stationary phases with mixed ligates in LC⁶ can be likened to mixed-liquid phases in gas chromatography (GC) since in both cases mixing is on the molecular scale.

Our primary concern in this study is to examine the use of columns packed with mixed ion exchangers in the linear elution chromatography of proteins. Mixed-bed columns of anion and cation exchangers were first used for desalination in 1951⁷, and are still employed for the deionization of water and other non-ionic substances. In chromatography, however, they have so far found very limited applications^{5,8,9}. We shall therefore begin with an examination of the relationship between the retention factor and the composition of binary mixed-bed columns. The relationship will then be used to predict protein retention in gradient elution on such columns and to select an optimal bed composition for the separation of acidic and basic proteins on a column packed with mixed anion and cation exchangers.

Since the primary interaction responsible for retention in ion-exchange columns often changes with increasing ionic strength in the mobile phase from electrostatic to hydrophobic¹⁰, the effect of bed composition on retention will be examined under a wide range of salt concentrations. For simplicity the studies on gradient elution and optimization will be restricted to electrostatic interaction chromatography (EIC).

EXPERIMENTAL

Instrumentation

The chromatograph was assembled from a Micromeritics (Norcross, GA, U.S.A.) Model 750 solvent delivery pump with a Model 753 ternary solvent mixer and a Model 740 control module. A Rheodyne (Cotati, CA, U.S.A.) Model 7010 sampling valve with a 100- μ l sample loop was used for sample injection. A Kratos (Ramsey, NJ, U.S.A.) Model 770R variable-wavelength detector was used to monitor the effluent at 280 nm. Chromatograms were recorded with a Shimadzu (Columbia, MD, U.S.A.) Model C-R3A integrator.

Columns

Zorbax BioSeries WCX-300 (B-WCX), SCX-300 (B-SCX), WAX-300 (B-WAX) and DEAE-300 (B-DEAE) were obtained from DuPont (Wilmington, DE, U.S.A.). According to the manufacturer, the fixed ionogenic functions are -COOH, -SO₃H, -NH₂ and -N(C₂H₅)₂ on the stationary phases B-WCX, B-SCX, B-WAX and B-DEAE, respectively. The support of these stationary phases is zirconia-treated Zorbax PSM 300¹¹, a spherical silica, having mean particle and pore diameters of

7.5 μm and 300 \AA , respectively. Three other stationary phases, H-WCX, H-WAX and H-diol, were prepared in this laboratory by using established procedures^{12,13} from Vydac silica gel (5 μm ; 300 \AA) supplied by The Separations Group (Hesperia, CA, U.S.A.) and have fixed $-\text{COOH}$, $-\text{N}(\text{C}_2\text{H}_5)_2$ and $-\text{OH}$ functions at the surface, respectively. Under typical conditions, the stationary phase particles were mixed together in a given proportion and 1.5 g of the mixture was suspended in 25 ml methanol by sonication for 1 min. The resulting slurry was packed into a 100 \times 4.6 mm I.D. No. 316 stainless-steel column with methanol as the packing solvent at 8000 p.s.i. for 20 min by using an air-driven pump (Haskel, Burbank, CA, U.S.A.).

As a test to determine whether column properties were influenced by electrostatically induced aggregation or non-uniform mixing of the ion-exchanger particles, another set of H-WCX-H-WAX mixed-bed columns was packed with a slurry of the stationary phase mixture in 20 mM aqueous phosphate buffer, pH 2.0, containing 200 mM sodium chloride. Results with these columns were found to match those obtained with columns packed with methanol slurry. The stability of the mixed-sorbent columns was tested by passing through the columns 4 l of 20 mM Tris-HCl, pH 7.0, containing 80 mM ammonium sulphate; the retention factors of proteins measured before and after this treatment differed only marginally.

Materials

Lysozyme (LYS), conalbumin (CON), and ovalbumin (OVA), all from chicken egg, α -chymotrypsinogen A (CHY) from bovine pancreas and hemoglobin (HEM) from bovine blood were purchased from Sigma (St. Louis, MO, U.S.A.). Reagent-grade ammonium sulfate, monobasic sodium phosphate, and sodium chloride were obtained from J. T. Baker (Phillipsburg, NJ, U.S.A.). HPLC-grade methanol was obtained from Fisher Scientific (Springfield, NJ, U.S.A.). Distilled water was prepared with a Barnstead unit (Barnstead, MA, U.S.A.).

Procedures

Mobile phases of appropriate salt concentrations were made by diluting a stock solution containing 0.4 M sodium chloride, 1.0 M or 2.0 M ammonium sulphate in 20 mM Tris-HCl buffer, pH 7.0, with the buffer solution. Columns were equilibrated with at least 100 ml of mobile phase before the first injection. Each protein was chromatographed at least twice, under isocratic elution conditions at a flow-rate of 1 ml/min at room temperature. Retention times, t_R , were measured at the intersection of the tangents drawn to the two inflection points of the peaks. For lack of uncharged homomorphs of the proteins, the retention time of fructose was taken as the mobile phase hold-up time, t_0 . For convenience, the retention factors of proteins eluting earlier than fructose have been reported as negative values.

A mixture of lysozyme, ovalbumin, conalbumin and α -chymotrypsinogen A was chromatographed on each of the three mixed-bed columns composed of H-WCX-H-WAX (25:75), H-WCX-H-WAX (50:50) and H-WCX-H-WAX (75:25), respectively, by a linear gradient elution. The gradient elution was run from 0.05 M to 0.3 M sodium chloride in 20 mM Tris buffer, pH 7.0, at 25°C in 30 min.

Computations

All computations were performed on a MicroVAX computer at the Depart-

ment of Chemical Engineering at Yale University. Three dimensional plots were generated using the Td3 graphics routine accessed through the Yale Computer Center.

RESULTS AND DISCUSSION

Retention factors versus bed composition

In linear elution chromatography with a mixed-sorbent column, the dependence of the retention factor, k' , on the bed composition is expected to follow the simple additivity relationship

$$k' = (1/V_M) \sum_{i=1}^N (V_{Si}K_i) \quad (1)$$

where V_{Si} is the volume of sorbent i in the column, V_M is the volume of mobile phase, K_i is the equilibrium constant for the partitioning of the elute between stationary phase i and the mobile phase and N is the number of different sorbents in the mixed-bed. As discussed in the Appendix, when the different sorbent particles have the same density, diameter and porosity, the retention factor of a given elute can be expressed as a function of the retention factors, k'_i , measured on single-sorbent columns packed in a manner identical with the mixed-sorbent column, and the individual sorbent weight fractions in the mixed-bed, w_i , according to

$$k' = \sum_{i=1}^N w_i k'_i \quad (2)$$

Since the sum of the weight fractions is unity, according to eqn. 2 the retention factor is a function of $N-1$ independent weight fractions.

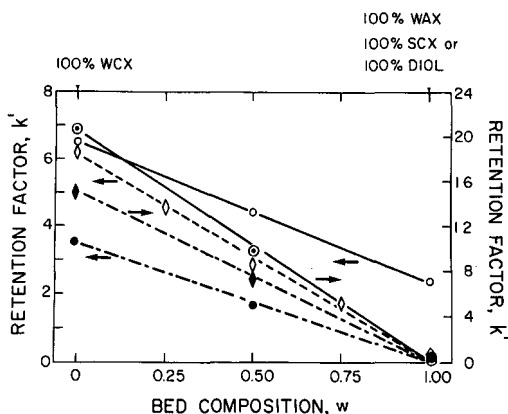


Fig. 1. Plots of retention factors against bed composition for lysozyme and α -chymotrypsinogen on columns packed with the sorbent mixtures H-WCX-H-diol (.....), B-WCX-B-SCX (—) and B-WCX-B-WAX (----) at different salt concentrations in 20 mM Tris-HCl, pH 7.0. Lysozyme: (\diamond) 0.22 M NaCl; (\blacklozenge) 0.1 M $(\text{NH}_4)_2\text{SO}_4$. α -Chymotrypsinogen A: (\circ) 0.08 M; (\bullet) 0.1 M; (\odot) 2.0 M $(\text{NH}_4)_2\text{SO}_4$. Column, 100 \times 4.6 mm I.D.; flow-rate, 1.0 ml/min; temperature, 25°C.

In this study, we shall examine protein retention on binary mixed-sorbent columns packed by the standard procedure outlined previously with stationary phases prepared from the same support. Fig. 1 shows the retention factors of two proteins plotted against the bed composition of columns packed with mixtures of either H-WCX–H-diol, B-WCX–B-SCX, or B-WCX–B-WAX. Linear behavior is observed in each case. The proteins do not interact with the H-diol phase, which acts merely as a diluent for the H-WCX. Retention data on the mixed cation-exchangers, B-WCX and B-SCX, are shown at both low and high salt concentrations. The retention *versus* bed composition relationship is linear in both cases, despite change in the retention mechanism from electrostatic to hydrophobic interactions. In these experiments the linear nature of the relationship is conserved even when the mixed sorbents carry oppositely charged groups, as with both the B-WCX–B-WAX and the B-WCX–B-DEAE mixtures.

In other cases, however, the k' *versus* w relationship is found to be markedly non-linear, as shown in Fig. 2 by plots of the retention factor against the bed composition of mixed H-WCX and H-WAX sorbents at low salt concentration in the eluent. The curves for the four basic proteins exhibit greater departures from linearity than that for ovalbumin that is acidic at the eluent pH. For the same set of columns, the non-linearity persists at high salt concentrations, as can be seen in Fig. 3.

Non-linear dependence of the retention on bed composition was also observed in the LC of organic compounds on columns packed with mixed polar adsorbents⁸. N-Alkyl substituted aromatic amines were found to adsorb more strongly on a mixture of boron oxide and silicic acid than on either sorbent alone and the magnitude of the enhanced adsorption was dependent on the particular elute. The effect was ascribed to "interactions" between the adsorbents but the precise nature of these

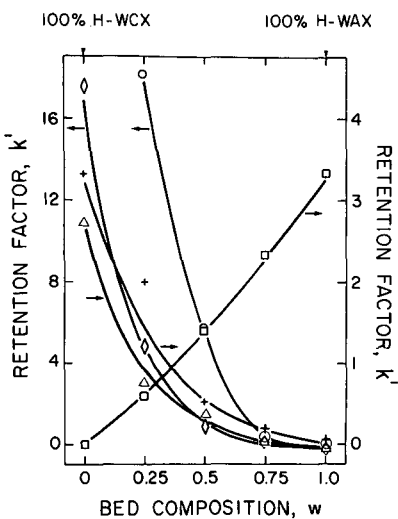


Fig. 2. Plots of retention factors against the bed composition of an H-WCX–H-WAX column at relatively low concentrations of $(\text{NH}_4)_2\text{SO}_4$ in 20 mM Tris–HCl, pH 7.0. (\diamond) Lysozyme, 80 mM; (\circ) α -chymotrypsinogen A, 30 mM; (\square) ovalbumin, 30 mM; (\triangle) hemoglobin, 10 mM; (+) conalbumin, 40 mM. Other conditions as in Fig. 1.

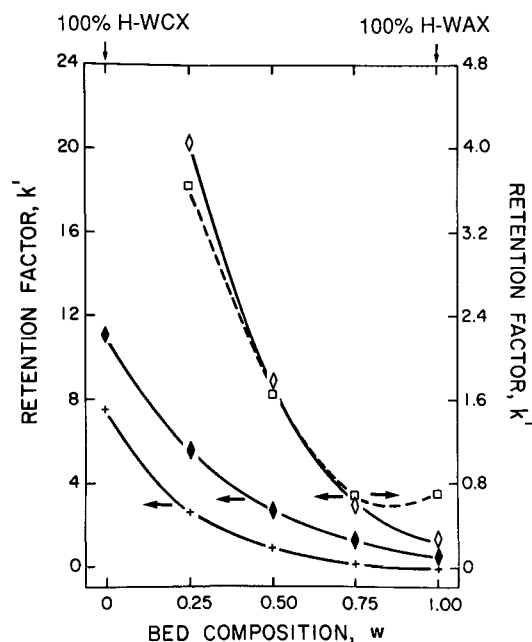


Fig. 3. Plots of retention factors against the bed composition of an H-WCX-H-WAX column at relatively high concentrations of $(\text{NH}_4)_2\text{SO}_4$ in the eluent. (\diamond) Lysozyme; (\square) ovalbumin; (+) conalbumin, all with 1.8 M salt in the eluent; (\blacklozenge) lysozyme, 1.6 M salt. Other conditions as in Fig. 1.

interactions could not be determined. Neither has the origin of the non-linearity observed in our case been discovered. The possibility of electrostatic interactions between ion-exchanger particles which carry oppositely charged functional groups is remote, since the Debye length at appreciable salt concentrations is far smaller than the particle diameter and drops sharply with increasing salt concentration, whereas the non-linearity is manifest even at high ionic strength. A similar argument precludes non-linearity due to Donnan exclusion of the proteins from the interior of like charged particles. It is also unlikely that possible small differences in porosity between the two sorbents could account for the non-linearity: they would have to differ by a factor greater than 3 to explain the data. Numerous other reasons for the observed behavior have been considered but no satisfactory explanation has been found.

An empirical mixing rule has been formulated that fits, without any adjustable parameters, the non-linear results obtained with the H-WCX-H-WAX mixed-beds. If k'_A and k'_B are the observed retention factors for the elute on columns containing only the respective stationary phase of type A and B and w_A is the weight fraction of stationary phase A in the mixture then the retention factor, k' , observed in the full range of stationary phase composition is given by

$$k' = \{w_A[k'_A/(1+k'_A)] + (1-w_A)[k'_B/(1+k'_B)]\}[1 + w_A k'_A + (1-w_A)k'_B] \quad (3)$$

Retention data calculated by eqn. 3 are compared to experimental results in Fig. 4 and the agreement is remarkably accurate. Some of the data collected, however,

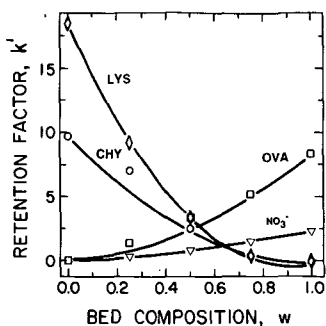


Fig. 4. Measured and predicted retention factors as a function of the bed composition in mixed H-WCX-H-WAX columns. Solid lines were calculated by using eqn. 3 and the data points were measured by using 20 mM Tris-HCl, pH 7.0, as the eluent. Lysozyme, 0.18 M NaCl; α -chymotrypsinogen A, 0.10 M NaCl; ovalbumin, 0.08 M; nitrate, 0.01 M $(\text{NH}_4)_2\text{SO}_4$.

displayed even stronger non-linearities than that predicted by this equation, and could not be reconciled with other generalized mixing rules (unpublished results), either.

Gradient elution with mixed-bed columns

The theory of retention in gradient elution has been discussed at length by several authors¹⁴⁻¹⁸ and verified experimentally for reversed-phase chromatography¹⁹ and EIC²⁰ of proteins. Here we shall put it to use for the prediction of protein retention in EIC on mixed-sorbent columns with gradient elution.

The migration of the center of an elute band down the column packed with a single sorbent is described by

$$dz/dt = u_0/(1 + V_S K/V_M) \quad (4)$$

where z is the axial position of the elute band, u_0 is the mobile phase velocity, K is the equilibrium constant for the retention and V_S and V_M are the volumes of stationary and mobile phases in the column, respectively. In gradient elution, K depends on the concentration of the mobile phase modulator—the salt in EIC—which in turn varies with time and distance along the column. The retention time, t_R , is determined by the integration of eqn. 4 with due regard for the time and position dependence of K . The term $V_S K/V_M$ may be considered the instantaneous value of the retention factor, k' , at a given axial position.

In EIC retention depends on salt concentration according to

$$\log k' = \kappa_1 - Z \log m \quad (5)$$

where m is the salt concentration in the mobile phase, Z is a characteristic number for the interaction between the elute and the stationary phase in the presence of the salt^{21,22} and κ_1 is the logarithm of the retention factor when the salt concentration is unity. Table I shows κ_1 and Z values for proteins measured on H-WCX and H-

TABLE I

EXPERIMENTALLY DETERMINED κ_1 AND Z VALUES FOR PROTEINS ON SINGLE SORBENT COLUMNS PACKED WITH EITHER H-WCX OR H-WAX ION EXCHANGERS BY USING SODIUM CHLORIDE OR AMMONIUM SULPHATE IN THE ELUENT

Protein	H-WCX				H-WAX			
	NaCl		$(NH_4)_2SO_4$		NaCl		$(NH_4)_2SO_4$	
	$-\kappa_1$	Z	$-\kappa_1$	Z	$-\kappa_1$	Z	$-\kappa_1$	Z
α -Chymotrypsinogen A	2.90	3.88	3.61	3.32	N.R.	N.R.	N.R.	N.R.
Conalbumin	3.29	2.72	6.10	3.16	4.31	2.39	4.30	1.82
Lysozyme	1.81	4.09	3.12	3.98	N.R.	N.R.	N.R.	N.R.
Ovalbumin	N.R.	N.R.	N.R.	N.R.	6.39	6.66	5.70	4.09

N.R. = Not retained.

WAX stationary phases. Each pair of values was regressed from at least four data points measured at different salt concentrations.

If a linear salt gradient is transported unchanged through a chromatographic column, the salt concentration as a function of time and distance is given by

$$m(z,t) = \begin{cases} m_s & t - (z/u_0) - \tau < 0 \\ m_s + (m_f - m_s)[t - (z/u_0) - \tau]/t_G & 0 < t - (z/u_0) - \tau < t_G \\ m_f & t - (z/u_0) - \tau > t_G \end{cases} \quad (6)$$

where it is assumed that the gradient is both preceded and followed by isocratic plateaus with the respective starting and final salt concentrations m_s and m_f , t_G is the gradient time and τ the gradient delay due to the pertinent dead volume in the system.

Eqs. 4–6 yield a first order ordinary differential equation of the form

$$dz/dt = f(z,t) \quad (7)$$

The initial condition, which reflects the time and position at which the salt gradient, delayed by a time τ , catches up with the center of the eluting band, is

$$z = u_0\tau/k'(m_s) \text{ at } t = \tau[1 + 1/k'(m_s)] \quad (8)$$

where $k'(m_s)$ is the retention factor with the starting eluent. Integration of eqn. 7 with the condition given in eqn. 8 yields the retention time of the eluite when the value of z equals that of L , the column length.

In chromatography with mixed-sorbent columns, the retention factor observed at a given salt concentration can be expressed as a function of the pertinent k' values measured on the appropriate single-sorbent columns by a mixing rule such as eqn. 2 or eqn. 3. In EIC the single-sorbent k' values for the eluites depend on the salt

concentration according to eqn. 5. A combination of eqns. 4–6 and the appropriate form of the mixing rule yields a differential equation of the form

$$dz/dt = f(w; z, t) \quad (9)$$

that expresses the movement of peaks through the column also as a function of the bed composition, w . Integration of eqn. 9 with the condition in eqn. 8 yields the retention time.

A closed form solution to such a problem is difficult, if not impossible, so we used a numerical technique—a 4th order Runge–Kutta²³ algorithm—for the integration. The procedure was terminated when the value of z exceeded the length of the column and the retention time was determined by linear interpolation between the last two time and position values.

The chromatograms in Fig. 5 illustrate the retention of four proteins, three basic and one acidic, in mixed H-WCX–H-WAX columns of different sorbent compositions under fixed gradient conditions. The retention times of the four proteins were calculated by integrating eqn. 9 with the use of the mixing rule in eqn. 3 and the corresponding values from Table I. The results are plotted against the bed composition in Fig. 6 where the pertinent experimental data points from Fig. 5 are also illustrated. The match between the calculated and measured data is quite satisfactory, considering that the mixing rule holds only approximately in some of the cases considered. Indeed, it appears that the possible sources of error, including that incurred by changes in gradient shape due to salt adsorption on the column, have either minimal effect, or compensate each other in a fortuitous manner; thus, the predictive method can be used with some degree of confidence.

Optimum bed composition

A number of optimization techniques may be used to select the bed composition most advantageous for the separation problem at hand²⁴. One is the “window diagram”, sometimes known as an “overlapping resolution map”. It is the result of a graphical procedure in which the resolution between the two least separated peaks is maximized with respect to one²⁵ or two^{26,27} variables, all others being held constant. A plot of the resolution of the least resolved peaks *versus* the variables of

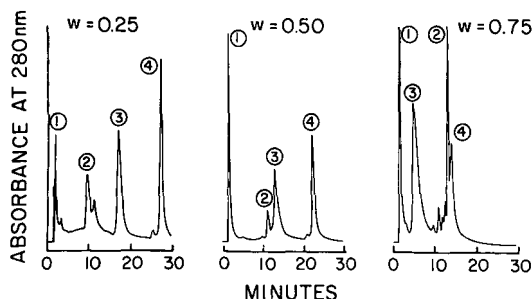


Fig. 5. Chromatograms of four proteins obtained on mixed H-WCX–H-WAX columns of different composition with gradient elution from 0.05 M to 0.3 M NaCl in 20 mM Tris–HCl, pH 7.0, in 30 min with a 3-min delay. Proteins: 1, conalbumin; 2, ovalbumin; 3, α -chymotrypsinogen A; 4, lysozyme.

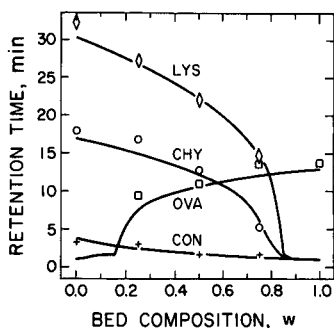


Fig. 6. Comparison of the predicted and observed dependence of protein retention on the stationary phase composition in mixed-bed columns. Solid lines were obtained by numerical integration of eqn. 9 with the use of eqn. 3 and the data from Table I. Conditions as in Fig. 5.

interest results in a surface containing a number of maxima, which, in a two-dimensional plot, may be likened to a series of "windows". The "optimum" conditions are considered to be those corresponding to the tallest window.

Whereas resolution can be readily determined in isocratic elution chromatography, it is not as easily predicted in gradient elution because there is no reliable theory to calculate band broadening. For simplicity, therefore, we have used the difference in retention times between the least separated peaks in a chromatogram, \mathcal{S} , as a measure of the separation. It is defined as

$$\mathcal{S} = \min_{j \neq i} |t_{R,j} - t_{R,i}| \quad (10)$$

where both i and j index all the peaks in the chromatogram, and the minimum is selected from all pairs of peaks. Since, in a given chromatogram, all bands have approximately the same width¹⁷ the crude measure represented in eqn. 10 suffices for our purposes.

As an illustrative example we will examine the separation of the four proteins considered previously, *vide* Figs. 5 and 6, on mixed H-WCX-H-WAX columns at pH 7. At neutral pH three of the four proteins carry a net positive and one a net negative charge. A "cathodic" ion-exchange column packed with mixed cation and anion exchangers offers a convenient means to retain each constituent of the sample, as is required in chromatographic analysis.

The search for optimum bed composition and gradient program was carried out by using the model outlined previously and the data in Table I. An additional variable was the gradient steepness G , defined as

$$G = (m_f - m_s)/t_G \quad (11)$$

For simplicity, m_s was held constant, and regions where the separation took longer than 30 min or any one of the peaks was unretained were not considered. The results are presented in Fig. 7 as a three-dimensional plot of \mathcal{S} against w and G . There are two distinct regions in which \mathcal{S} attains large values. Separation with a column con-

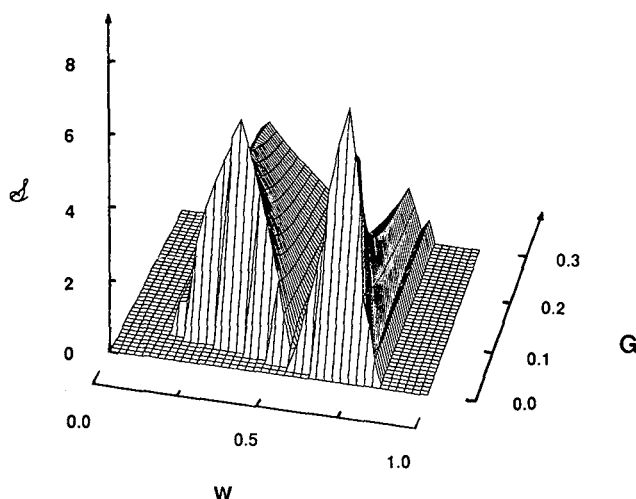


Fig. 7. Illustration of the separation of four proteins as measured by \mathcal{S} with gradient elution in mixed ion-exchanger columns as a function of the bed composition, w , and the gradient steepness, G . Other conditions as in Fig. 5. Only domains with retention time $t_0 < t_R < 30$ min are shown.

taining 75% of H-WCX and 25% of H-WAX and at a G value of approximately 0.08, which lies in a region with a high \mathcal{S} value, is illustrated in Fig. 5 ($w = 0.25$) and it is seen that the peaks are well resolved in agreement with the prediction.

Since \mathcal{S} measures only the extent of separation, other criteria may also have to be applied in the optimization process. One method of locating the optimum in such circumstances is to proceed in a stepwise manner, satisfying one criterion at a time^{24,28}. For example, in the above problem, one may wish to achieve the fastest separation by confining the search to regions of sufficiently high \mathcal{S} values in the window diagram such as in Fig. 7. The optimal value for G in our example would then be the maximum G that yields sufficiently high \mathcal{S} values. However, other means also exist to satisfy multiple criteria simultaneously and these have been discussed in the literature^{24,29}.

The optimization scheme can be extended to include more than two independent variables, *e.g.* the column length could be a third variable in the above example. Although the visual advantage of the window diagram is then lost, computer algorithms can be readily devised to find the optimum conditions³⁰. In the event that eqn. 1 holds, extension to any number of stationary phases is straightforward. When the dependence of the retention on bed composition is non-linear the task is more difficult. We have found, however, that by using a mixing rule of the form of eqn. 3 retention times in gradient elution can be predicted with reasonable accuracy even if the fit for isocratic data is not entirely satisfactory.

A more general form of this empirical equation for multiple stationary phases is

$$k' = \left(1 + \sum_{i=1}^N w_i k_i\right) \sum_i \left[w_i k_i' / (1 + k_i) \right] \quad (12)$$

where the symbols have the same meaning as in eqn. 2.

Although our discussion has so far been restricted to ion exchangers, the need for a mixing rule to facilitate the selection of the optimal bed composition is universal to any mixed-bed separation. It must be stressed that mixed beds appear to be of maximum utility in preparative applications or routine analysis. In many instances it may be more convenient to use several columns in series provided columns of appropriate dimensions and packing are readily available.

The retention behavior of proteins on mixed-bed and tandem columns was found to be similar, although with tandem columns selectivity in gradient elution was dependent on column sequence⁵. Whereas tandem columns have the advantage that they can be individually examined and replaced at will, for routine application the convenience of a single column with mixed sorbents might prove attractive.

The "general elution problem" put forward by Snyder¹⁷, refers to the fundamental difficulties in the separation under isocratic conditions of a sample having components with widely disparate retention factors. They may be partially alleviated by using an appropriate blend of stationary phases so that the retention of the light and heavy ends of the sample is increased and decreased, respectively. This approach could eliminate the need for gradient elution that requires complex instrumentation and time consuming re-equilibration of the column with the starting eluent after each run. Columns with mixed sorbents, therefore, are likely to find applications in rapid HPLC for routine analysis and *a fortiori* in process monitoring and control by ultrahigh-speed HPLC.

Other important applications for mixed-sorbent columns are expected to be found in the burgeoning field of preparative chromatography. This approach not only permits the manipulation of selectivity for separation of the desired product but also may make the use of difficult-to-remove mobile phase additives superfluous. Furthermore, mixed stationary phases may offer certain advantages in displacement^{31,32} and in other non-linear chromatographic techniques. In such cases the pertinent adsorption isotherms on multisorbents have to be evaluated by frontal chromatography³³ or other means.

Degradation of sorbents in mixed-bed columns may follow patterns different from those observed with columns packed with single sorbents as a result of intimate contact between different stationary phases. A disadvantage of a mixed-bed is that it may be difficult to determine the extent of degradation of any of the individual sorbents. Furthermore the properties of the column may change significantly upon moderate decomposition of a single stationary phase component. From this it follows that stable stationary phases are required to exploit the potential benefits of columns packed with mixed sorbents.

ACKNOWLEDGEMENT

This work was supported by Grants Nos. GM 20993 and CA 21948 from the National Institutes of Health, U.S. Department of Health and Human Resources.

APPENDIX

Consider a thin section within a uniform mixed-bed column that corresponds

to a theoretical plate. Let the total mobile phase volume and the volume of each individual sorbent in the plate be V_M and V_{Si} respectively, such that

$$\sum_{i=1}^N V_{Si} = V_S \quad (\text{A1})$$

where V_S is the total volume of the stationary phase in the plate and N is the number of individual sorbents in the mixed bed.

Let an amount of eluite equal to $C_0 V_M$ where C_0 is some arbitrary concentration be charged into the plate and allowed to equilibrate between the mobile and stationary phases. At equilibrium, the mass balance for the eluite is

$$C_0 V_M = C_M V_M + \sum_{i=1}^N C_{Si} V_{Si} \quad (\text{A2})$$

where C_M and C_{Si} are the equilibrium concentrations in the mobile phase and the sorbent i , respectively. If adsorption takes place at the sorbent surface, C_{Si} must be expressed per unit area and V_{Si} replaced by $a_{Si} V_{Si}$, a_{Si} being the surface area per unit volume of sorbent i . The results that follow, however, are not affected by this consideration.

Let it be assumed that there are no interactions between the sorbents and adsorption on each one is governed by a linear isotherm. Then, since each sorbent is individually at equilibrium with the homogenous mobile phase, the N equilibrium constants K_i are represented by

$$K_i = C_{Si}/C_M \quad (\text{A3})$$

The observed retention factor, k' , for such a mixed-bed column is given by the expression

$$k' = \left(\sum_{i=1}^N C_{Si} V_{Si} \right) / C_M V_M \quad (\text{A4})$$

Substitution of eqn. A3 in eqn. A4 yields eqn. 1.

If we define

$$\varphi_i \equiv V_{Si}/V_{Mi} \quad (\text{A5})$$

where V_{Mi} is some fraction of the mobile phase volume such that

$$\sum_{i=1}^N V_{Mi} = V_M \quad (\text{A6})$$

we can rewrite eqn. 1 as

$$k' = \left(\sum_{i=1}^N K_i V_{Si} \right) / \left(\sum_{i=1}^N V_{Si} / \varphi_i \right) \quad (\text{A7})$$

This equation can be recast in terms of the weight fractions of the individual sorbents, w_i . Since V_{Si} is proportional to w_i/ρ_i , where ρ_i is the density of sorbent i , eqn. A7 becomes

$$k' = \left(\sum_{i=1}^N K_i w_i / \rho_i \right) / \left(\sum_{i=1}^N w_i / \rho_i \varphi_i \right) \quad (\text{A8})$$

where ρ_i is the density of sorbent i . When both φ_i and ρ_i are identical for each sorbent in the mixed bed, eqn. A8 reduces to

$$k' = \varphi \sum_{i=1}^N K_i w_i \quad (\text{A9})$$

where φ is now the common value for φ_i . The terms φK_i correspond to retention factors measured on columns packed with the individual sorbents, k'_i , provided that their packing structure is identical to that of the mixed-bed column. When the different sorbent particles have equal diameter and porosity, and the respective columns are packed by the same procedure, the conditions necessary for eqn. 1 to hold are satisfied and lead to the linear mixing rule embodied in eqn. 2.

On the other hand several non-linear mixing rules can be formulated if the mobile phase is considered to be non-homogeneous, *i.e.* the composition of the mobile phase in the vicinity of the different types of sorbent particles is different. Eqn. 3 is the result of an *ad hoc* combination of two such rules.

REFERENCES

- 1 J. F. K. Huber, E. Kenndler and H. Markens, *J. Chromatogr.*, 167 (1978) 291.
- 2 G. W. Pilgrim and R. A. Keller, *J. Chromatogr. Sci.*, 11 (1973) 206.
- 3 W. H. McFadden, *Anal. Chem.*, 30 (1958) 479.
- 4 A. T. James and A. J. P. Martin, *Biochem. J.*, 50 (1952) 679.
- 5 Z. El Rassi and Cs. Horváth, *J. Chromatogr.*, 359 (1986) 255.
- 6 T. R. Floyd and R. A. Hartwick, in Cs. Horváth (Editor), *High Performance Liquid Chromatography: Advances and Perspectives*, Vol. 4, Academic Press, Orlando, FL, 1986, pp. 47–90.
- 7 F. X. McGarvey and R. Kunin, *Ind. Eng. Chem.*, 43 (1951) 734.
- 8 J. K. Carlton and W. C. Bradbury, *Anal. Chem.*, 27 (1955) 67.
- 9 S. A. Wise, L. C. Sander and W. E. May, *J. Liq. Chromatogr.*, 6 (1983) 2709.
- 10 Cs. Horváth, W. R. Melander and Z. El Rassi, presented at the 9th International Symposium on Column Liquid Chromatography, Edinburgh, July 1–5, 1985, Lecture PL3.3.
- 11 R. W. Stout and J. J. DeStefano, *J. Chromatogr.*, 326 (1985) 63.
- 12 S. H. Chang, K. M. Gooding and F. E. Regnier, *J. Chromatogr.*, 125 (1976) 103.
- 13 P. O. Larsson, M. Glad, L. Hasson, M.-D. Hansson, S. Ohlson and K. Mosbach, *Adv. Chromatogr. (N.Y.)*, 21 (1982) 41.
- 14 B. Drake, *Ark. Kemi*, 8 (1955) 1.

- 15 E. C. Freiling, *J. Am. Chem. Soc.*, 77 (1955) 2067.
- 16 P. J. Schoenmakers, H. A. H. Billiet, R. Tijssen and L. de Galan, *J. Chromatogr.*, 149 (1978) 519.
- 17 L. R. Snyder, in Cs. Horváth (Editor), *High Performance Liquid Chromatography: Advances and Perspectives*, Vol. 1, Academic Press, New York, 1980, pp. 207–316.
- 18 P. Jandera and J. Churáček, *Gradient Elution in Column Liquid Chromatography (Journal of Chromatography Library*, Vol. 31), Elsevier, Amsterdam, 1985.
- 19 M. A. Stadalius, H. S. Gold and L. R. Snyder, *J. Chromatogr.*, 296 (1984) 31.
- 20 E. S. Parente and D. B. Wetlaufer, *J. Chromatogr.*, 355 (1986) 29.
- 21 W. Kopaciewicz, M. A. Rounds, J. Fausnaugh and F. E. Regnier, *J. Chromatogr.*, 266 (1986) 3.
- 22 A. Velayudhan and Cs. Horváth, *J. Chromatogr.*, 367 (1986) 160.
- 23 R. H. Perry and C. H. Chilton (Editors), *Chemical Engineers Handbook*, McGraw Hill, New York, 5th, ed., 1983, pp. 2–59.
- 24 P. J. Schoenmakers, *Optimization of Chromatographic Selectivity (Journal of Chromatography Library*, Vol. 35), Elsevier, Amsterdam, 1986.
- 25 R. J. Laub and J. H. Purnell, *J. Chromatogr.*, 112 (1975) 71.
- 26 J. L. Glajch, J. J. Kirkland, K. M. Squire and J. M. Minor, *J. Chromatogr.*, 199 (1980) 57.
- 27 B. Sachok, R. C. Kong and S. N. Deming, *J. Chromatogr.*, 199 (1980) 317–325.
- 28 J. Krupčík, J. Mocák, A. Šimová, J. Garaj and G. Guiochon, *J. Chromatogr.*, 238 (1982) 1–12.
- 29 A. K. Smilde, A. Knevelman and P. M. J. Coenegracht, *J. Chromatogr.*, 369 (1986) 1.
- 30 R. J. Laub, J. H. Purnell and P. S. Williams, *J. Chromatogr.*, 134 (1977) 249.
- 31 J. Frenz and Cs. Horváth, *AIChEJ*, 31 (1985) 400.
- 32 Cs. Horváth, in F. Bruner (Editor), *The Science of Chromatography (Journal of Chromatography Library*, Vol. 32), Elsevier, Amsterdam, 1986, pp. 179–203.
- 33 J. Jacobson, J. Frenz and Cs. Horváth, *J. Chromatogr.*, 316 (1984) 53.

CHROM. 20 582

HYDROPHOBIC INTERACTION OF ALCIAN BLUE WITH SOLUBLE AND ERYTHROCYTE MEMBRANE PROTEINS

GIAN MARCO GHIGGERI and GIOVANNI CANDIANO

Nephrology Section, Hospital of Lavagna, Lavagna (Italy)

FABRIZIO GINEVRI

Nephrology Department, G. Gaslini Institute, Via 5 Maggio 39, Genoa (Italy)

ANTONIO MUTTI, ENRICO BERGAMASCHI and ROSSELLA ALINOVI

Institute of Clinical Medicine and Nephrology, University of Parma, Via Gramsci, Parma (Italy)

and

PIER GIORGIO RIGHETTI*

Department of Biomedical Sciences and Technologies, University of Milano, Via Celoria 2, Milan 20133 (Italy)

SUMMARY

Alcian Blue (AB), a cationic dye widely employed for monitoring negative surface charge variations on red blood cell (RBC), platelet and glomerular membranes of patients with nephrotic syndromes, was found in fact to aggregate with itself and precipitate in the pH range 7.0–7.8, *i.e.*, at the physiological pH values used for performing the binding assay between the dye and cell surfaces. This aggregation appears to be essentially hydrophobic as it is insensitive to urea but fully prevented in presence of 2% zwitterionic detergent. In addition, AB binds to most RBC membrane proteins solubilized by urea–detergent extraction, again suggesting hydrophobic interaction. AB also interacts with freely soluble proteins such as haemoglobin and myoglobin; such binding is disrupted by ethylurea and/or 2% zwitterionic detergent, typical inhibitors of hydrophobic liaisons. AB also strongly binds to myoglobin with all the negative charges blocked by esterification of the carboxyl groups, again ruling out direct interaction via surface negative charges. It is concluded that AB binding to the RBC surface can hardly monitor variations in surface charge due to sialic acid residues but, at best, variations in surface hydrophobicity.

INTRODUCTION

Alcian Blue (AB), a cationic dye possessing a bulky aromatic region (four benzene and four imidazole rings, in a haeme-like structure coordinating a central copper ion) and four positive charges due to quaternary amino groups, has recently come to play an important role in monitoring the negative surface charge changes of red blood cells (RBCs), platelets and glomerular walls in normal individuals as

compared with patients with nephrotic syndrome and focal glomerulosclerosis. Today, it is an accepted physiological mechanism that the fixed negative charges (resulting from the presence of sialic acid residues and anionic glycosaminoglycans) on the walls of the nephron provide an electrostatic barrier to the filtration of a host of negatively charged (at physiological pH values) macromolecules present in plasma (as epitomized by albumin)¹. Hence, in glomerular diseases, the enhanced excretion of albumin has been associated with the loss of such negative charges on the glomerular capillary walls, strongly diminishing such electrostatic repulsion². Therefore, the monitoring of the charge density and variation on the capillary walls could be an important tool for assessing the glomerulus function in nephrotic syndromes. The major impediment to this goal, however, comes from the difficulty in obtaining enough renal tissue for analysis.

In a search for a substitute, simple chemical test, Levin *et al.*³ noticed that AB binding to RBCs and platelets could be used as a valid alternative to direct monitoring of negative charges on the glomerulus capillary walls, as AB binding was significantly reduced in children with steroid-responsive nephrotic syndromes (SRNS). Their findings were subsequently confirmed by them⁴ and in an independent study by Boulton-Jones *et al.*⁵. On the other hand, this method has been subjected to major criticism by Feehally *et al.*⁶ and Sewell and Brenchley⁷. The first group, by repeating the same AB binding test to RBCs, was unable to reproduce the differences among control, nephrotic syndromes, membranous nephropathy and uraemic (non-nephrotic) patients, all of the tests yielding an average 85 ng of AB bound per 10⁶ RBCs. They concluded that no evidence could be found that RBC charge measurements should reliably mirror the glomerular capillary wall charge. Sewell and Brenchley⁷ reported some direct chemical tests demonstrating that AB alone, in solution in phosphate-buffered saline (PBS) at physiological pH, tends to give precipitates in the first few hours after dissolution. In addition, the presence of albumin at 1 mg/ml causes an augmented, faster precipitation. Moreover, they noted that AB (originally a textile dye) was designed to be precipitable at neutral and slightly alkaline pH values, so that textiles dipped in AB solutions would retain a permanently insoluble precipitate within their fibres. Hence they too ruled out any correlation between AB binding to RBCs and surface charge.

In this work, we have undertaken an extensive physico-chemical evaluation of the behaviour of AB alone in different solvents and in the presence of membranaceous and cytoplasmic proteins. One of the major techniques used was "electrophoretic titration curves"^{8,9}, which simultaneously monitors the behaviour of AB and proteins, either alone or in a mixture, over the pH range 3–10. Our results indicate an extensive hydrophobic interaction, with little evidence for any ionic binding.

EXPERIMENTAL

Chemicals

Myoglobin (sperm whale) was obtained from Calbiochem (La Jolla, CA, U.S.A.), ribonuclease (bovine pancreas) and lysozyme (egg white) were obtained from Sigma (St. Louis, MO, U.S.A.), sphingomyelin and Coomassie Brilliant Blue R-250 from Serva (Heidelberg, F.R.G.), Alcian Blue BGX from BDH (Poole, U.K.), N,N,N',N'-tetramethylethylenediamine (TEMED), N,N'-methylenebisacrylamide

(Bis), ammonium persulphate and 3-[(3-cholamidopropyl)dimethylammonio]-1-propanesulphonate (CHAPS) from Bio-Rad Labs. (Richmond, CA, U.S.A.), carrier ampholytes and Silane A-174 (Bind Silane) from LKB (Bromma, Sweden), urea, ethylurea and Triton X-100 from Fluka (Buchs, Switzerland) and silica TLC plates and other chemicals of analytical-reagent grade from Merck (Darmstadt, F.R.G.).

Haemoglobin preparation

Normal human adult haemoglobin was prepared according to the International Committee for Standardization in Haematology¹⁰. Thus, one volume of blood collected in heparin or EDTA was washed three times with saline (8.5 g/l of sodium chloride), then the red cells were lysed with 0.5 volume of carbontetrachloride and 1 volume of distilled water by shaking for 10 min. Red cell debris was subsequently removed by centrifugation at 4°C for 30 min at 2500 g. To the haemolysate 100 µg/ml of potassium chloride were added.

Ghost's preparation

Human erythrocyte membranes were prepared from fresh blood according to Dodge *et al.*¹¹. To obtain the electrophoretic titration curves for protein components, they were solubilized in 8 M urea and 2% Triton X-100.

Carboxyl group modification

The carboxyl groups of myoglobin were esterified by suspending the protein in methanol and adding hydrochloric acid to a final concentration of 0.1 M for 24 h at 25°C. The reaction was stopped by dilution with a large volume of ice-cold water and the excess of acid and methanol were removed by dialysis against 1 mM hydrochloric acid¹².

Electrophoretic titration curves

Electrophoretic titration curves^{8,9} were obtained in polyacrylamide gels (0.75 mm thick) supported by silanized glass plates as described by Bianchi Bosisio *et al.*¹³. The polyacrylamide gel slab (12 × 12 cm) was cast to contain 7% T, 3% C matrix and 2% Ampholines (in the following percentage ratios: 45% pH 3–10, 15% pH 4–6, 15% pH 8–9.5 and 25% pH 9–11). In some instances 8 M urea, 3% Triton X-100 or 2% CHAPS were included in the polymerization mixture; in that event the samples were also equilibrated with the same additives. The first dimension (isoelectric focusing of carrier ampholytes) was run at a constant 10 W until the steady state (800 V, 11 mA) was reached (usually 1 h). The second dimension (electrophoresis perpendicular to the pH gradient) was then run at a constant 700 V for 20 min. In both dimensions the electrode strips were impregnated with 0.2 M sodium hydroxide (cathode) and 0.2 M orthophosphoric acid (anode). pH measurements were made by cutting gel strips (4 mm) and placing them in 0.1 M potassium chloride solution at room temperature. When necessary, the gels were stained in a colloidal dispersion of Coomassie Blue in 12% trichloroacetic acid.

Electrophoretic titration curves in rehydratable gels

Some experiments were performed with ethyl- or butylurea as disaggregating agents. In these instances, owing to the polymerization inhibition of the additive, the

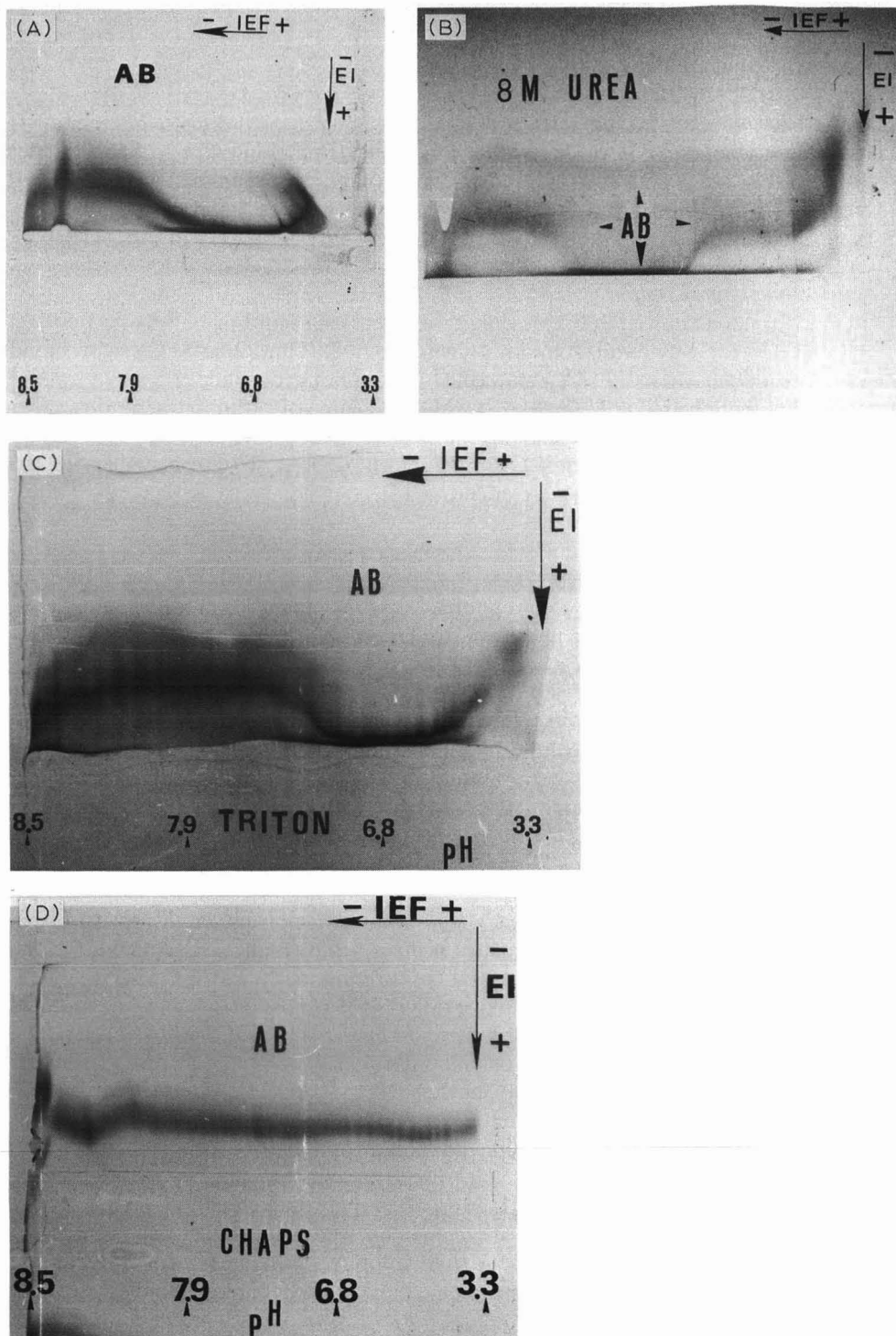


Fig. 1. Electrophoretic titration curves of AB. The gel was a 7%T, 3%C polyacrylamide containing 2% Ampholine in the pH range 3.5–10 (dimensions 12 × 12 cm, 0.75 mm thick). First dimension: focusing of carrier ampholytes alone (1 h at 800 V at the steady state). Second dimension: zone electrophoresis perpendicular to the pH gradient (constant 700 V for 20 min). (A) Titration curve of AB alone (1 mg/ml solution in 25 mM magnesium chloride; 200 μ l loaded into the trench just before the second dimension run). (B) Same as A, except that the gel and sample contained 8 M urea. (C) Same as A, except that the gel and sample were equilibrated in 3% Triton X-100. (D) Same as A, except that the gel and sample contained 2% zwitterionic detergent (CHAPS).

gels were polymerized as above, but in the absence of carrier ampholytes, washed twice in distilled water and then dried overnight. Rehydration was performed by soaking the gels in a solution containing 6 M ethylurea (or 1 M butylurea) in 2% Ampholine for 48 h at room temperature.

Thin-layer chromatography (TLC)

TLC was performed on silica plates by using chloroform–methanol–water (75:22:3) as the mobile phase. Before TLC, sphingomyelin was preincubated with AB for 1 h, extracted four times with chloroform and dried under nitrogen.

Incubations

Unless specified otherwise, AB was incubated with proteins in the presence of 1 mM magnesium chloride at 37°C for 15 min. In all instances the additives (detergents, ureas) were admixed with AB before proteins and preincubated for 5 min.

RESULTS

Electrophoretic titration curves of AB alone

We first investigated the behaviour of AB alone or in solution with different disaggregating agents with the two-dimensional technique of “electrophoretic titration curves”. Given the presence in the molecule of only quaternary and tertiary amino groups, the electrophoretic pattern of AB over the pH range 3–8 should be represented by a straight line parallel to the sample application trench in the cathodic direction, indicating constant surface charge along this titration interval. On the contrary (Fig. 1A), when run alone, AB produces a sigmoidal curve, with a flat portion (in reality a heavy precipitate against the edge of the trench) in the pH range 6.0–7.5. As AB was analysed alone, it can only be concluded that in the pH range 6–7.5 it aggregates with itself and precipitates out of solution. When the same experiment is repeated with gel and sample equilibrated in 8 M urea (Fig. 1B) a better behaviour is obtained, with two coloured lines moving out of the trench (the fastest migrating component probably representing a contaminant of AB), but there is still a heavy precipitate in the same pH range 6.0–7.5 and, in fact, additional precipitation throughout the pH range 3.0–8.5. This suggests that the AB precipitate is sparingly, if at all, hydrogen bonded. When the same experiment is repeated in the presence of non-ionic detergent (3% Triton X-100 in both sample and gel) (Fig. 1C) the migration behaviour is clearly improved, but still the precipitate around neutrality is not abolished. However, when the neutral is substituted by a zwitterionic (CHAPS) detergent (known to have a much stronger disaggregating power)¹⁴, AB now migrates as a straight line parallel to the trench, all precipitates being completely abolished (Fig. 1D). This behaviour is a clear symptom of hydrophobic interaction.

Electrophoretic titration curves of AB and proteins

We next investigated the behaviour of AB in the presence of membrane and of soluble proteins. Erythrocyte ghost proteins, solubilized according to Dodge *et al.*¹¹, were run alone by the titration curve method. As the proteins solubilized are mostly loosely bound surface antigens, with a high density of negative charges, they migrate as lines parallel to the trench, but in the anodic direction (Fig. 2A). When, however, the

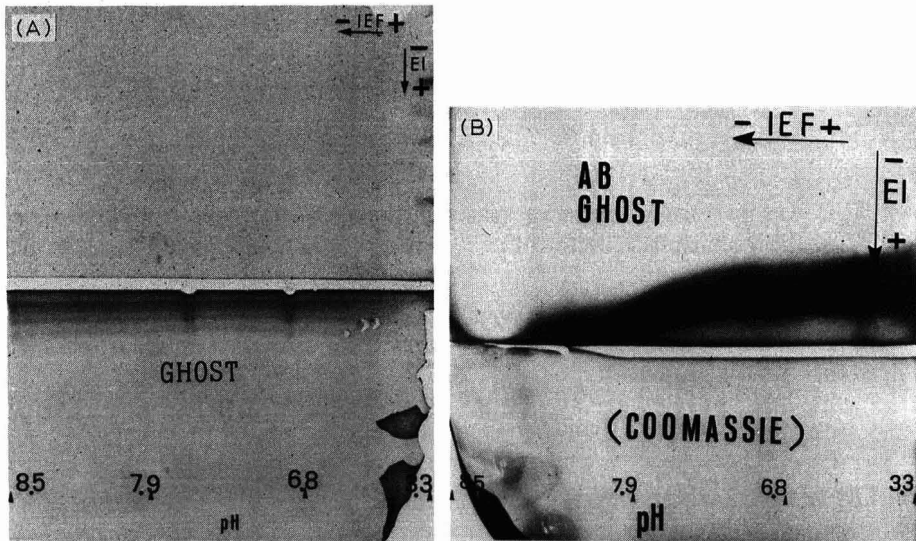


Fig. 2. Electrophoretic titration curves of erythrocyte ghost proteins in the absence and presence of AB. All other conditions as in Fig. 1. (A) 200 μ l of solubilized ghost proteins (2 mg/ml) were applied to the trench. (B) Titration curves of a mixture of ghost proteins (2 mg/ml) and AB (1 mg/ml) mixed in a 1:1 ratio (200 μ l loaded into the trench). Both gels stained with Coomassie Blue. Note that an identical pattern would be obtained in the absence of staining, indicating that all proteins are bound to AB.

same preparation is incubated with AB, this behaviour is completely reversed; all proteins seem to be coated by AB, and they all now migrate towards the cathode, producing a heavy precipitate in the pH range 8–8.5, with additional precipitates throughout the titration interval (Fig. 2B). An identical pattern was obtained in the same gel prior to Coomassie staining (*i.e.*, by visualization of the AB colour), indicating that all proteins in the mixture were bound to AB throughout the pH range 3–9.

We next investigated the behaviour of AB with soluble, hydrophilic proteins, as epitomized by myoglobin (Myo) and haemoglobin (Hb). Fig. 3 shows a typical titration curve for Myo alone in the pH range 3–9; the main component has a *pI* of 7.8 (trench cross-over point). When Myo is incubated with AB, massive precipitation occurs in the pH range 3.5–8, with only partial disaggregation above pH 8, where a blue cathodic line (free AB) and a brown anodic zone (free Myo) can be seen (in this pH range Myo begins to have a net negative charge yet, curiously, it does not bind to the positively charged AB; conversely, in the pH range 3–8, where massive coprecipitation occurs, both AB and Myo bear a net positive charge!) (Fig. 3B). Fig. 3C shows similar results with Hb, *i.e.*, strong precipitation in the pH range 3–8 and a smeared curtain of molecules in both the anodic and cathodic gel regions, due either to excess free molecules not engaged in the precipitation event or to a slowly solubilized precipitate under the electric field. Not much better results are obtained with the ternary mixture AB + Myo + Hb: the heavy Myo–Hb coprecipitate is still present in the pH range 3.5–8, with Hb tending to escape the precipitation unscathed, probably owing to a lack of free, excess AB (Fig. 3D). The situation can only be reversed in the presence of

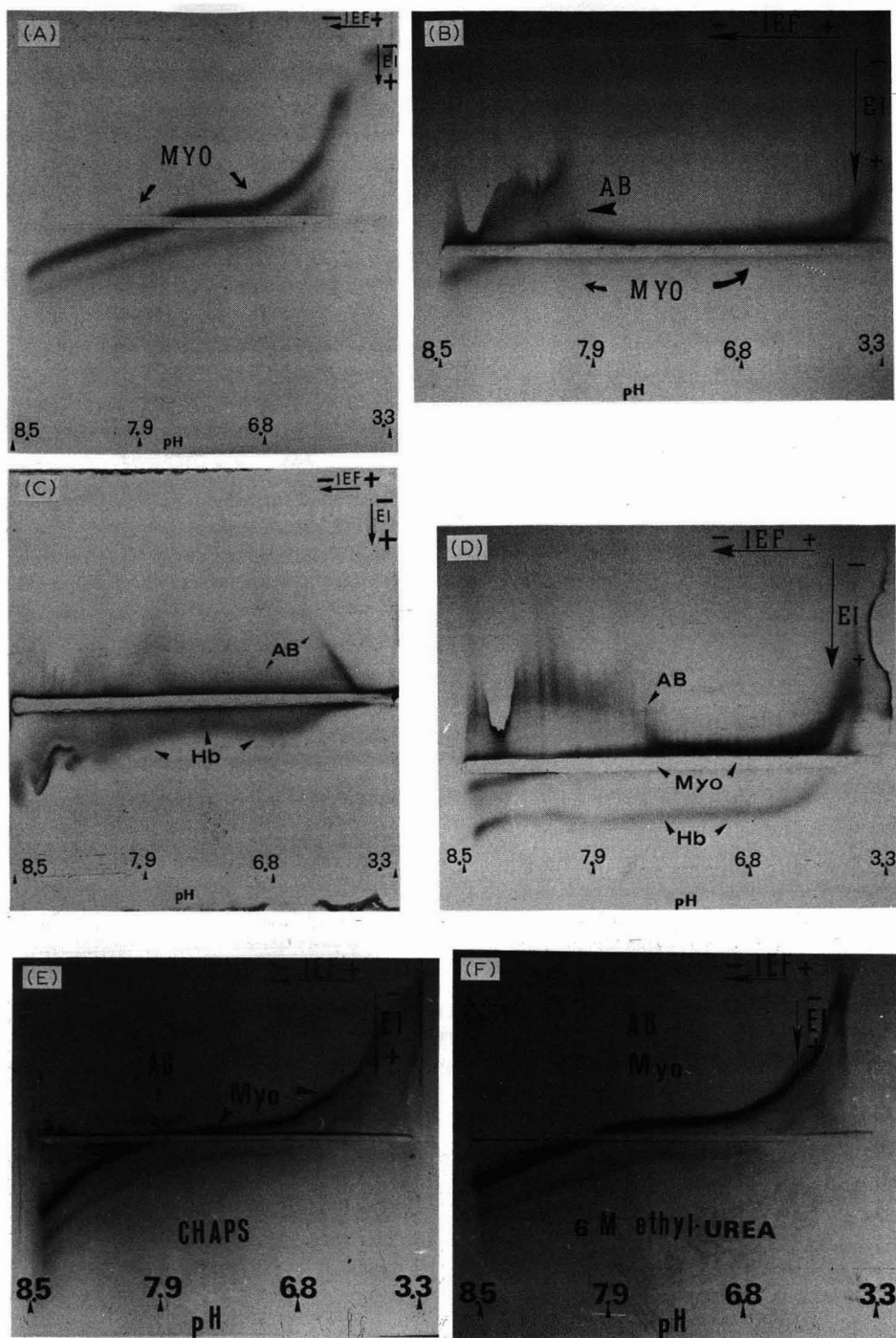


Fig. 3. Electrophoretic titration curves of myoglobin (Myo) and haemoglobin (Hb) in the absence and presence of AB and various additives. All other experimental conditions as in Fig. 1. (A) Titration curve of myoglobin alone (2 mg/ml; 200 μ l loaded); unstained gel. (B) Titration curves of a mixture of Myo (2 mg/ml) and AB (1 mg/ml) mixed in a 1:1 volume ratio (200 μ l applied); unstained gel. (C) Same as B, except that Hb was substituted for Myo. (D) Same as B and C, except that a 1:1 mixture of Myo and Hb was added to AB. (E) Same as B, except that the sample and gel were equilibrated with 2% CHAPS. Note the completely undisturbed titration curve of Myo, demonstrating complete lack of binding to AB. (F) Same as B, except that the sample and gel contained 6 M ethylurea. Note the complete disaggregation of the AB-Myo complexes.

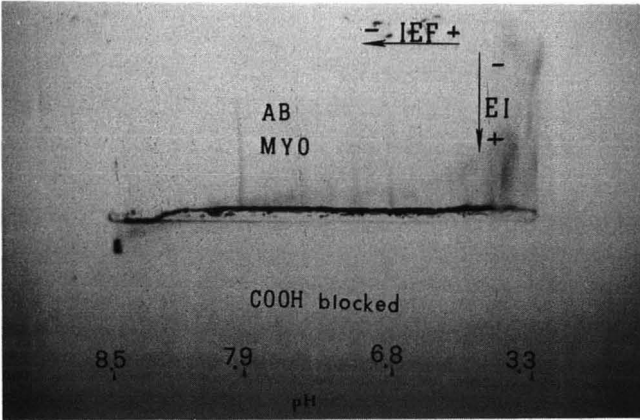


Fig. 4. Electrophoretic titration curve of a mixture of AB and myoglobin. All other conditions as in Fig. 1. A 1:1 mixture of Myo (2 mg/ml) and AB (1 mg/ml) was analysed by isoelectric focusing coupled to electrophoresis at right-angles. Myo had been previously esterified on the carboxyl groups. Note the almost complete precipitation of the AB-Myo complex, suggesting strong hydrophobic binding and stacking of the dye on the polypeptide chain.

CHAPS (Fig. 3E); now Myo gives the expected titration curve, completely undisturbed by AB (compare with Fig. 3A) while AB is probably involved in a mixed micelle with CHAPS. This again indicates hydrophobic interaction among AB and proteins. Additional evidence comes from Fig. 3F; in the presence of 6 M ethylurea (another powerful disaggregating agent)¹⁵, Myo reverts to the expected electrophoretic behaviour, completely unperturbed by the presence of AB.

As an additional check, we studied the behaviour of AB in the presence of carboxyl-esterified myoglobin. If it were true that AB interacts with negative surface charges in proteins, no binding should occur in this instance, as the protein now

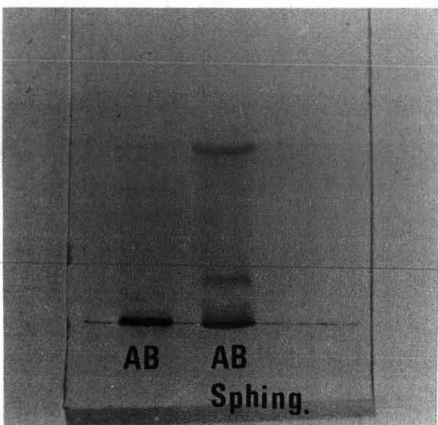


Fig. 5. TLC of AB and sphingomyelin. The chromatogram was developed with chloroform-methanol-water (75:22:3). AB, 10 µg spotted; AB-Sphing., 1:1 mixture of 10 µg each of AB and sphingomyelin. The TLC plate was not stained.

exhibits a purely positive charge. Here again, however, a mixture of AB and carboxyl blocked Myo produces a massive precipitate, even more intense than with untreated Myo (compare with Fig. 3B), extending over the entire titration interval (Fig. 4). As a final check, we studied the TLC migration of AB when admixed with a hydrophobic membrane component, sphingomyelin. In the elution system used, AB does not move from the application point, whereas in the presence of sphingomyelin it co-migrates with all the components present in it (see Fig. 5; the bands developed are not stained and they exhibit the blue colour of AB). Given the structure of sphingomyelin, it is clear that the complex of AB with it can only occur via hydrophobic interaction.

DISCUSSION

Our data cast doubt on the validity of using AB as a probe of surface charge of RBC or glomerular capillary walls, as proposed³⁻⁵. Let us examine the available data.

Behaviour of AB alone in solution

As seen in all our titration curves (Fig. 1A-D), AB alone in solution tends to aggregate and precipitate at least over a 1.5 pH unit range (in general pH 6.0-7.5, in fact up to pH 8). This aggregation appears to be caused by hydrophobic interaction, as it is insensitive to 8 M urea but completely inhibited by a zwitterionic detergent (CHAPS). The fact that the dye would precipitate was also noted by Sewell and Brenchley⁷, who reported 50% precipitation simply on standing for only 2.5 h after dissolution in phosphate-buffered saline at pH 7.4. What is even more striking is that in our titration curves the ionic strength of focused carrier ampholytes is extremely low (possibly *ca.* 1 mequiv.l⁻¹) and this should, if anything, minimize hydrophobic interaction. Conversely, under the assay conditions of Levin and co-workers^{3,4}, the high ionic strength of the medium should amplify the phenomenon of AB precipitation, as hydrophobic bonds are favoured by high salt concentration.

Behaviour of AB in the presence of proteins

Although our data for AB in the presence of ghost components would appear to favour Levin and co-workers^{3,4} hypothesis (binding to negative charges of surface proteins) (Fig. 2A and B), in reality the situation is different: the AB-ghost protein complexes completely precipitate in the pH range 8.0-8.5 and in fact give substantial precipitation throughout the titration interval (such precipitates intensify around pH 7). This is in agreement with Sewell and Brenchley⁷, who reported increased precipitation of AB in the presence of 1 mg/ml of albumin (the latter is known to bind to many hydrophobic molecules). What is even more striking is the behaviour of soluble proteins, such as Myo and Hb. The interaction with Myo goes against any expectations: if it were true that AB binds via ionic bonds, the binding should be substantial above the *pI* of Myo (*i.e.*, above pH 7.8) and should not occur at all below the *pI*, where the protein acquires an excess of positive charges. However, experimentally, the opposite is found: massive precipitation and complexing between AB and Myo occur throughout the cationic segment of the Myo titration curve, where both AB and Myo carry a positive charge and therefore, in principle, should repel each other. The same (and even more pronounced) happens with carboxyl-blocked Myo (Fig. 4): here everything is extensively precipitated in the pocket. In this last instance

Myo should have essentially no negative charges, yet the interaction is more tenacious. However, owing to the esterification of the carboxyl groups, it is certain that the overall hydrophobicity of the surface of the macromolecule is increased, and the stronger binding of AB again suggests hydrophobic interaction.

Behaviour of the complexes in the presence of detergents and alkylureas

The fact that AB alone, when run in an electrophoretic titration curve, does not aggregate or precipitate in the presence of CHAPS is indicative of hydrophobic interaction on the bulky aromatic dye surface possibly with the formation of a stack of molecules that eventually precipitate. Masking of such surfaces by incorporation in the detergent micelles abolishes this phenomenon. With protein-AB complexes, not only CHAPS but also alkylureas (ethylurea) are able to disrupt such interactions. Interestingly, asymmetrically substituted alkylureas can be regarded as simple detergents, unable to aggregate into micelles. Recently, they were utilized to inhibit hydrophobic interaction between a large protein, ferritin, and the surface of a gel containing an immobilized pH gradient¹⁶.

Behaviour of other dyes

In addition to the above data, additional evidence comes from the work of Sewell and Brenchley⁷ on the behaviour of other positively charged dyes. They noted that many cationic dyes, such as Toluidine Blue, Methyl Green, Cupreolinic Blue, Maxilon Blue TL and Ruthenium Red, do not behave like AB with respect to RBC binding. In the light of our results this is not surprising: Toluidine Blue (or the very similar Basic Blue) is composed of only three condensed aromatic rings, flanked on the outer surface by a quaternary and a primary (Toluidine Blue) or a quaternary and a tertiary (Basic Blue) amino groups. The much reduced hydrophobic area is probably sufficient to minimize or abolish completely any hydrophobic interaction with proteins.

In conclusion, we believe that AB cannot be used as a reliable indicator of negative surface charge of cells or glomerular walls, but that perhaps it could be used to probe hydrophobic patches on such surfaces. In fact, we have recently demonstrated¹⁷ that the RBC membrane of nephrotic children contains much reduced levels of phospholipids. Hence, the apparent differences in AB binding reported by Levin and co-workers^{3,4} might well be attributed to variations in the hydrophobic domains of the membrane, rather than to surface charge alterations (they clearly stated that, notwithstanding the large differences in AB binding to the RBC membranes of normal and nephrotic children, the total amount of sialic acid residues on the cell surface was the same in the two populations).

ACKNOWLEDGEMENTS

This work was supported in part by Progetto Finalizzato Biotecnologie e Biosensori, CNR, Rome, and by the Ministero della Pubblica Istruzione (MPI).

REFERENCES

- 1 W. M. Deen, M. P. Bohrer, C. R. Robertson and B. M. Brenner, *Fed. Proc., Fed. Am. Soc. Exp. Biol.*, 36 (1977) 2614-2618.

- 2 J. I. Kreisberg, D. B. Wayne and M. J. Tarnovsky, *Kidney Int.*, 16 (1979) 290–300.
- 3 M. Levin, C. Smith, M. D. S. Walter, P. Gascoine and T. M. Barratt, *Lancet*, ii (1985) 239–242.
- 4 M. Levin, D. Gibb, C. Smith, M. D. S. Walters and T. M. Barratt, *Lancet*, ii (1986) 929–929.
- 5 J. M. Boulton-Jones, G. McWilliams and L. Chandrachud, *Lancet*, ii (1986) 186–188.
- 6 J. Feehally, A. Samanta, H. Kinghorn, A. C. Burden and J. Walls, *Lancet*, ii (1986) 635–635.
- 7 R. F. Sewell and P. E. C. Brenchley, *Lancet*, ii (1986) 635–636.
- 8 P. G. Righetti, R. Krishnamoorthy, E. Gianazza and D. Labie, *J. Chromatogr.*, 166 (1978) 455–460.
- 9 P. G. Righetti, G. Gacon, E. Gianazza, D. Lostenlen and J. C. Kaplan, *Biochem. Biophys. Res. Commun.*, 85 (1978) 1575–1581.
- 10 W. F. Moo-Pen and R. M. Schmidt, *Br. J. Haematol.*, 35 (1977) 161–164.
- 11 J. T. Dodge, C. Mitchell and D. Hanahan, *Arch. Biochem. Biophys.*, 11 (1983) 119–136.
- 12 C. A. Broomfield, J. P. Roehem and H. A. Scheraga, *Biochemistry*, 4 (1965) 751–760.
- 13 A. Bianchi Bosisio, C. Locherlein, R. S. Snyder and P. G. Righetti, *J. Chromatogr.*, 189 (1980) 317–330.
- 14 D. Satta, G. Schapira, P. Chafey, P. G. Righetti and J. P. Wharmann, *J. Chromatogr.*, 299 (1984) 57–72.
- 15 P. G. Righetti, C. Gelfi and M. L. Bossi, *J. Chromatogr.*, 392 (1987) 123–132.
- 16 T. Rabilloud, J.-J. Pernelle, J. P. Wahrmann, C. Gelfi and P. G. Righetti, *J. Chromatogr.*, 402 (1987) 105–113.
- 17 S. Ginevri, G. M. Ghiggeri, G. Candiano, R. Oleggini, R. Bertelli, M. Piccardo, S. Perfumo and R. Gusmano, *Pediatr. Nephrol.*, (1988) in press.

CHROM. 20 601

PURIFICATION AND PARTIAL AMINO ACID SEQUENCE OF HUMAN URINE PROTEIN 1

EVIDENCE FOR HOMOLOGY WITH RABBIT UTEROGLOBIN

PHILIP J. JACKSON and RONALD TURNER

Unit for Cancer Research, University of Leeds, Leeds LS2 9NL (U.K.)

JEFFREY N. KEEN

SERC Sequence Unit, Department of Biochemistry, University of Leeds, Leeds LS2 9JT (U.K.)

and

ROBERT A. BROOKSBANK and EDWARD H. COOPER*

Unit for Cancer Research, University of Leeds, Leeds LS2 9NL (U.K.)

SUMMARY

We describe the purification of Urine Protein 1 (UPI), a 14–16 kDa protein which occurs in the urine of patients with renal failure, and therefore may originate from the plasma or kidney. Amino acid sequencing shows that UPI has significant homology with rabbit uteroglobin, a secretory protein of the uterus (during pregnancy) and lungs (both sexes), and previously identified only in lagomorphs (rabbits, hares, pikas). The finding of a human uteroglobin-like protein, which can be purified from a readily available source, may provide further opportunities to elucidate the, as yet, uncertain physiological functions of uteroglobin.

INTRODUCTION

Urine Protein 1 (UPI) is a small protein, with a reported molecular weight of about 20 kDa, which has been found in the urine of patients with renal failure¹. Consequently, because of its potential clinical application, a commercially produced antiserum to UPI has been available for several years (Dako, High Wycombe, U.K.).

As is the case for any urinary protein, there are several possibilities for the original source of UPI. A major source of urinary proteins, especially in renal disease, is the plasma. Proteinuria may occur as a result of damage to the glomerular charge-size barrier, indicated by the excretion of plasma proteins >40 kDa, *e.g.* transferrin (80 kDa) and albumin (67 kDa), which would normally be retained in the plasma without entering the glomerulus². Small plasma proteins (<40 kDa) do enter the glomerulus and are normally reabsorbed by the proximal tubules³. In renal tubular disease, therefore, the urinary concentration of retinol-binding protein (21 kDa)⁴ and α 1-microglobulin (27 kDa)⁵, for example, is increased. Similarly the excretion of UPI, if it does occur in the plasma, would be by this mechanism.

Alternatively, UP1 may be released into the urine by the kidney itself, reaching detectable concentrations where pathological damage is present. This is exemplified by the increased excretion of the distal tubular component, Tamm-Horsfall glycoprotein during kidney transplant rejection⁶.

A recent study suggesting that UP1 is a plasma protein^{7,8} has been corroborated in our laboratory⁹ by the finding that its excretion can be induced in healthy volunteers by experimentally inhibiting proximal renal tubular function¹⁰. However, the possibility that UP1 also occurs in the kidney cannot be ruled out since it has been detected in (a) tissues such as liver and prostate^{7,8} in addition to the plasma and (b) renal failure urine where tubular disease is not evident⁹.

Clearly, UP1 merits further study, and for this purpose we describe a protocol for the isolation of UP1 from the urine of patients with renal failure. Subsequent amino acid sequencing shows that UP1 is homologous with rabbit uteroglobin¹¹⁻¹³, a secretory protein found in high concentrations in the uterus (during pregnancy)¹¹⁻¹³ and lungs¹⁴. A uteroglobin-like protein has not been previously found in any species other than lagomorphs (rabbits, hares and pikas)^{15,16}.

EXPERIMENTAL

Materials and apparatus

Urine from patients with chronic renal failure, attending for dialysis at Leeds General Infirmary, was stored at -70°C in the presence of 0.1% (w/v) sodium azide and 5 mM disodium EDTA. Chemicals (analytical grade or equivalent) were obtained from BDH (Poole, U.K.) or Sigma (Poole, U.K.). Rabbit antiserum to UP1 was supplied by Dako.

Protein solutions were concentrated in pressure ultrafiltration cells (50 and 180 ml capacity) fitted with YM5 membranes (Amicon, Gloucester, U.K.) and dialysed in SpectraPor 3 membrane tubing (Pierce, Cambridge, U.K.).

Chromatography was carried out using a Pharmacia FPLC system with an LCC-500 controller, two P-500 pumps and a UV-M absorbance monitor with a 5-mm flow-cell. All columns (Superose 12 prep grade HR 16/50, PD-10, Mono Q HR 5/5 and Mono S HR 5/5) and DEAE Sepharose Fast Flow gel were obtained from Pharmacia (Uppsala, Sweden).

Analytical methods

Protein in concentrated urine was estimated by the trichloroacetic acid-Ponceau S method¹⁷ using the Sigma standard protein solution containing human albumin and γ -globulin.

During the purification, UP1-containing fractions were identified by counter immunoelectrophoresis¹⁸ vs. anti-UP1 antiserum in a 1-mm layer of 1% (w/v) agarose gel containing 3% (w/v) poly(ethylene glycol) 6000 (PEG), 73.2 mM Tris, 24.4 mM diethylbarbituric acid, 0.4 mM calcium lactate and 3.0 mM sodium azide, pH 8.6. The samples and antiserum were placed in 5- μl wells 1 cm apart, towards the cathode and anode, respectively, and electrophoresed for 2 h at 5 V/cm. The recovery of UP1 at each stage was monitored by radial immunodiffusion¹⁹ in agarose gel with the above composition. The purity and composition of fractions were analysed by sodium dodecyl sulphate polyacrylamide gel electrophoresis (SDS-PAGE) on Pharmacia

PhastSystem™ using pre-cast 8–25% acrylamide gradient gels. The electrophoresis and silver-staining methods were as described by Jackson *et al.*²⁰.

The *pI* of UP1 was determined by isoelectric focusing on Pharmacia Phast-System, using a pre-cast pH 4–6.5 gel²⁰.

For amino acid sequencing, UP1 (1 nmol) was dialysed *vs.* 5 mM sodium hydrogencarbonate, lyophilised and dissolved in 0.03 ml of 0.2 M sodium hydrogencarbonate, 0.25% (w/v) SDS. The remaining procedure was as described by Cavaggione *et al.*²¹. The program QUICKP was used to search the NBRF (PIR) protein sequence database (release 13.0) for UP1 homologues.

Purification of UP1

Urine containing UP1 (detected by counter immunoelectrophoresis, see above) was concentrated by pressure ultrafiltration to give 100 ml of concentrate containing 5–6 g of protein. Then 25 mM bis-tris propane was added to the urine protein concentrate and the pH adjusted to 7.0 with 50% (v/v) acetic acid. An equal volume (100 ml) of 50% (w/v) PEG was added slowly with stirring and the mixture incubated on ice for 15 min. Precipitated protein was removed by centrifugation (3500 g, 30 min) and the supernatant (containing UP1) diluted with 4 volumes of 50 mM Tris-HCl, pH 7.0. This fraction was applied in two separate batches to a DEAE Sepharose Fast Flow column (300 mm × 16 mm) at 1 ml/min, and non-bound material (including PEG) was removed by washing with 50 mM Tris-HCl, pH 7.0. Bound proteins (including UP1) were desorbed with 1.5 M sodium chloride in Tris buffer, concentrated to $A_{280} \approx 6$ and chromatographed in separate 2-ml aliquots on a Superose 12 prep grade HR 16/50 gel filtration column in 0.15 M sodium chloride, 50 mM sodium potassium phosphate, pH 7.0, at a flow-rate of 1 ml/min. UP1-containing fractions were pooled, concentrated and buffer-exchanged into 6.25 mM bis-tris propane, pH 7.5, on PD-10 desalting columns, according to the manufacturer's instructions. Aliquots (14 ml) ($A_{280} = 0.045$) were then applied separately to a Mono Q HR 5/5 anion-exchange column equilibrated with 6.25 mM bis-tris propane, pH 7.5. Protein elution was by a 20-ml 0–100% gradient of 0.35 M sodium chloride, 6.25 mM bis-tris propane, pH 9.5, flow-rate 1 ml/min. Fractions containing UP1 were pooled, buffer-exchanged into 50 mM sodium succinate, pH 4.0, and applied to a Mono S HR 5/5 cation-exchange column equilibrated with the same buffer. A 20-ml 0–100% gradient of 50 mM sodium succinate, pH 5.5 (flow-rate 1 ml/min), was used for the elution of purified UP1, which was then immediately adjusted to pH 7.5 with sodium hydroxide and dialysed *vs.* 6.25 mM bis-tris propane pH 7.5.

RESULTS

Purification of UP1

The protein composition of the UP1-containing fractions at each stage in the purification was determined by SDS-PAGE. Fig. 1a shows a typical pattern for renal failure urinary proteins where both glomerular and proximal tubular lesions are evident. Some of the proteins occurring in this complex mixture are identified in ref. 20. This pattern was considerably simplified in the supernatant after precipitation with 25% (w/v) PEG (Fig. 1b). However, Table I shows that only 52% of the UP1 in the urine protein concentrate was recovered in the supernatant, with the remainder

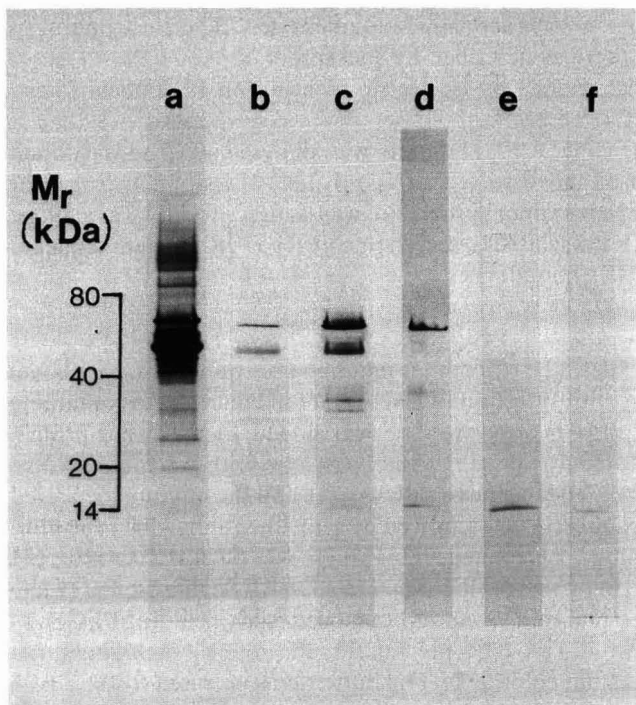


Fig. 1. Stages in the purification of UPI. Samples ($1 \mu\text{l}$) of UPI-containing fractions were analysed by SDS-PAGE²⁰ in the absence of 2-mercaptoethanol. (a) Urine protein concentrate (diluted 100-fold); (b) PEG supernatant; (c) DEAE Sepharose-bound proteins; (d) Superose 12 fraction (concentrated 100-fold); (e) Mono Q fraction; (f) Mono S fraction. Protein bands are silver-stained²⁰.

presumably trapped in the pellet of precipitated protein. A further 48% could be recovered by redissolving and re-precipitating (not accounted for in the remaining results in Table I).

The next step, anion-exchange chromatography on DEAE Sepharose, served to

TABLE I

RECOVERY OF UPI DURING PURIFICATION

UPI was estimated by radial immunodiffusion¹⁹ of 5- μl samples into agarose gel containing 0.02 ml/ml anti-UP1 antiserum. Arbitrary units were calculated from the square of the precipitin ring diameter in decimeters multiplied by the appropriate volume factor. No ring was visible in the Superose 12 fraction.

<i>Purification step/fraction</i>	<i>UPI recovered (arbitrary units)</i>	<i>Percentage of total recovered</i>
Urine protein concentrate	111	100
Poly(ethylene glycol) supernatant	58	52
DEAE Sepharose	53	48
Superose 12	—	—
Mono Q	11	10
Mono S	9	8

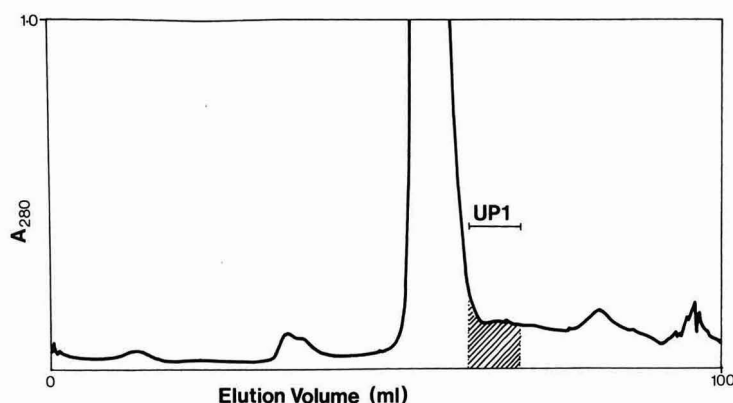


Fig. 2. Gel filtration of DEAE Sepharose-bound proteins on a Superose 12 prep grade HR 16/50 column.

(a) remove PEG, which is non-ionic, from the protein mixture and (b) concentrate the sample. The bound proteins (including UP1) were desorbed in one peak (chromatogram not shown) by using a 1.5 M sodium chloride wash. Employing a salt gradient did not fractionate the proteins to any greater extent. The concentrating effect of the DEAE Sepharose is seen in Fig. 1c, in which proteins > 80 kDa become visible (*cf.* Fig. 1b) as diffuse bands. These high-molecular-weight proteins (*e.g.* immunoglobulins) were removed by gel filtration on Superose 12 (Fig. 1d and Fig. 2) and the Mono Q fraction (Fig. 1e and Fig. 3) shows a considerable enhancement in the concentration of UP1 (at *ca.* 14 kDa). The recovery of UP1 over these two steps, however, was only about 20% (Table I) and may be explained by the accumulated loss of material over the seven gel filtration runs (and buffer exchanges) which were necessary to process the whole of the DEAE Sepharose-bound fraction.

A final purification was effected by cation-exchange chromatography on Mono S with an increasing pH gradient (4.0–5.5). UP1 eluted at pH 4.6–4.7 (Fig. 1f; chromatogram not shown) which, as expected, corresponds with its *pI* (see below). Table I shows that the overall recovery of UP1 from a single PEG fractionation of 5.6

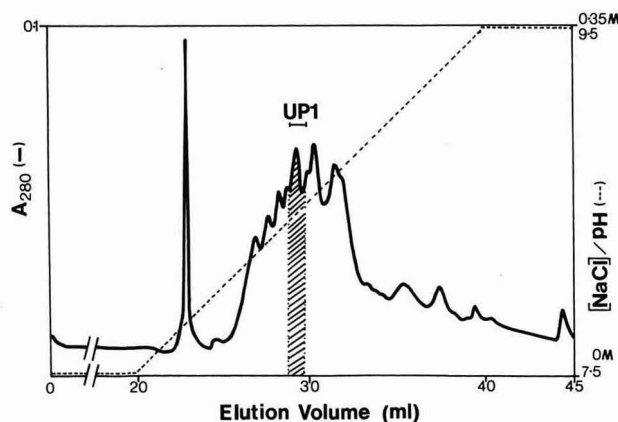


Fig. 3. Anion-exchange chromatography of the UP1-containing Superose 12 fraction on Mono Q HR 5/5.

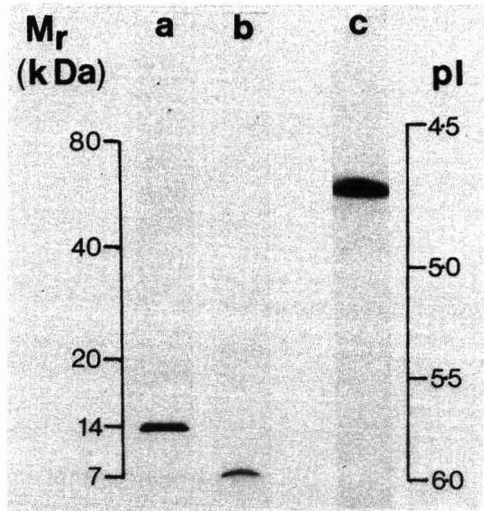


Fig. 4. Molecular weight and *pI* determinations of UPI by SDS-PAGE (8–25% acrylamide gradient) in the absence (a) and presence (b) of 2-mercaptoethanol, and isoelectric focusing (pH range 4.0–6.5) (c). Protein bands are visualised by immunoblotting vs. anti-UP1 antiserum²⁰.

g of urinary protein was 8%. The mass of UPI recovered was estimated as 0.3 mg by assuming $A_{280}^{1.0\text{g/l}} = 1.2$, the extinction coefficient of rabbit uteroglobin²² (see below).

Molecular weight and pI of UPI

Analysis of UPI by SDS-PAGE under non-reducing conditions and comparison with molecular weight standards (Pharmacia) indicated an M_r of 14–16 kDa (Fig. 4a). In the presence of 2-mercaptoethanol, the M_r of UPI decreased to 7–8 kDa (Fig. 4b), indicating that the protein is composed of two subunits of similar or equal M_r bound by disulphide bridges.

Isoelectric focusing and comparison with *pI* standards (Pharmacia) determined the *pI* of UPI as 4.7 (Fig. 4c).

Amino acid sequence of UPI

Fig. 5 shows the partial amino acid sequence (to residue 47) of UPI. A computerised search of a protein sequence database revealed that UPI has significant homology with rabbit uteroglobin.

DISCUSSION

The UPI for commercial antibody production was prepared from the urine of renal failure patients by gel filtration followed by ion-exchange chromatography on DEAE Sephadex and SP Sephadex²³. UPI has also been isolated from renal failure urine by affinity chromatography on immobilised anti-UP1 immunoglobulin^{7,8}. In our hands, neither method produced UPI of sufficient purity to give a single residue per cycle during amino acid sequencing. The complexity of the urinary protein mixture used as the source of UPI therefore merited a different protocol, which is described

											10
UP1:	Gly	Ile	Cys	Pro	Ser	Phe	Gln	Arg	Val	Ile	
	**	**	**	**		**		*	**	**	
Utg:	Gly	<u>Ile</u>	Cys	Pro	Arg	<u>Phe</u>	Ala	His	<u>Val</u>	<u>Ile</u>	
											20
UP1:	Glu	Thr	Leu	Leu	Met	Asp	Thr	Pro	Ser	Ser	
	**		**	**	*		**	**	**	**	
Utg:	Glu	Asn	<u>Leu</u>	<u>Leu</u>	Leu	Gly	Thr	Pro	Ser	Ser	
											30
UP1:	Tyr	Glu	Ala	Ala	Met	Glu	Leu	Phe	Ser	Pro	
	**	**			*			**		**	
Utg:	<u>Tyr</u>	Glu	Thr	Ser	<u>Leu</u>	Lys	Glu	Phe	Glu	Pro	
											40
UP1:	Asp	Gln	Asp	Met	Arg	Glu	Ala	Gly	Ala	Gln	
	**	*		**	*	*	**	**	*	**	
Utg:	Asp	Asp	Thr	Met	Lys	Asp	Ala	<u>Gly</u>	Met	Gln	
											50
UP1:	Leu	Lys	Lys	Leu	Val	Asp	Thr	_____			
	*	**	**	*	*	**	*				
Utg:	<u>Met</u>	Lys	Lys	Val	<u>Leu</u>	Asp	Ser	Leu	Pro	Gln	
											60
UP1:	_____										
Utg:	Thr	Thr	Arg	Glu	Asn	<u>Ile</u>	Met	Lys	<u>Leu</u>	<u>Thr</u>	
											70
UP1:	_____										
Utg:	Glu	Lys	<u>Ile</u>	Val	Lys	Ser	Pro	Leu	Cys	Met	

Fig. 5. Comparison of the partial amino acid sequence of UP1 with the complete subunit sequence of rabbit uteroglobin (Utg)¹³. Regions of exact homology are indicated by double asterisks and conservative replacements by single asterisks. Residues delineating the progesterone binding site in uteroglobin²⁸ are underlined.

here. About 0.3 mg of UP1 was recovered from 5.6 g of urinary protein. The overall yield was 8%, but this could be improved by re-extracting the PEG precipitate.

The partial amino acid sequence of UP1 indicates significant homology with rabbit uteroglobin: in the first 47 residues, 55% are identical and a further 23% conservatively replaced (Fig. 5)¹¹⁻¹³. This finding is supported by the similarities of UP1 and uteroglobin in molecular weight (both 14-16 kDa; Fig. 4a)¹² and subunit composition (both 2 × 7-8 kDa; Fig. 4b)¹². Their pI values, however, are 4.7 (UP1, Fig. 4c) and 5.4²⁴ (uteroglobin). This difference of 0.7 units may be explained by the substitution of basic residues in uteroglobin with acidic or neutral residues in UP1 (e.g. Arg 5 → Ser, Lys 26 → Glu; see Fig. 5). Nevertheless, we present the first evidence for a uteroglobin-like protein in a non-lagomorph species and suggest that this protein may be present in all mammals.

In rabbits, uteroglobin (also called blastokinin) is secreted by the endometrial cells of the uterus on induction with progesterone, either during pregnancy or

experimentally. Secretion is maximal between the fifth and tenth day of pregnancy, when uteroglobin constitutes 50% of the protein in the endometrial fluid¹¹. In addition, uteroglobin binds progesterone with high affinity ($K_d = 5 \cdot 10^{-7} M$)²⁵, implying that it acts as a carrier for its inducing steroid.

Uteroglobin has also been isolated in significant quantities from rabbit^{14,15,24} and hare^{16,26} lungs, where its secretion is induced, not by progesterone but by glucocorticoids^{14,24}. With the further finding that uteroglobin inhibits phospholipase A₂ activity²⁷, this protein also appears to be involved in the regulation of prostaglandin synthesis. Since prostaglandins mediate certain inflammatory responses, it has been suggested that the anti-inflammatory action of glucocorticoids may occur via uteroglobin, in addition to other glucocorticoid-induced proteins (*e.g.* lipomodulin, macrocortin and renocortin)²⁷.

The physiological function(s) of rabbit uteroglobin are, at present, uncertain. However, it is likely that human UP1 has the same function(s) because of the high degree of sequence homology between the two proteins. This homology even extends to those residues which, according to X-ray crystallographic data on uteroglobin²⁸, delineate the progesterone binding site (see Fig. 5).

The evidence that UP1 occurs in the plasma⁷⁻⁹ and certain other tissues, including the liver, prostate^{7,8} and possibly the kidney, suggests its widespread location in the body. This also appears to be the case for uteroglobin, which is detectable, albeit in small concentrations, in tissues other than the uterus and lungs^{15,29}.

Since studies to further elucidate the physiological functions of uteroglobin will depend on obtaining quantities of purified protein, urine from renal failure patients may provide a readily available alternative to laboratory animals.

ACKNOWLEDGEMENTS

We thank Miss Jeanette Gorst, Dako, High Wycombe, U.K., for arranging the generous donation of antiserum to Urine Protein 1. We also thank Miss Katharine Richmond for expert technical assistance.

REFERENCES

- 1 *Product List*, Dako Ltd., High Wycombe, 1987.
- 2 R. H. R. White, *Contrib. Nephrol.*, 24 (1981) 63.
- 3 W. Strober and T. A. Waldman, *Nephron*, 13 (1974) 35.
- 4 M. D. Poulak, D. Farrah, G. H. Malek, C. J. Shinnick and O. Smithies, *Biochim. Biophys. Acta*, 412 (1975) 326.
- 5 H. Yu, Y. Yanagisawa, M. A. Forbes, E. H. Cooper, R. A. Crockson and I. C. M. MacLennan, *J. Clin. Pathol.*, 36 (1983) 253.
- 6 R. H. Schwartz, J. D. Van Ess, A. G. May, E. A. Schenk and R. B. Freeman, *Transplantation*, 16 (1973) 83.
- 7 J. Ayatse, *Ph.D. Thesis*, University of Surrey, Guildford, 1987.
- 8 J. W. Wright, University of Surrey, personal communication.
- 9 P. J. Jackson and E. MacNamara, unpublished results.
- 10 D. St. J. O'Reilly, E. S. Parry and J. T. Whicher, *Clin. Chim. Acta*, 155 (1986) 319.
- 11 R. A. Popp, K. R. Foresman, L. D. Wise and J. C. Daniel, *Proc. Natl. Acad. Sci. U.S.A.*, 75 (1978) 5516.
- 12 H. Ponstingl, A. Nieto and M. Beato, *Biochemistry*, 17 (1978) 3908.
- 13 M. Atger, J.-C. Mercier, G. Haze, F. Fridlansky and E. Milgrom, *Biochem. J.*, 177 (1979) 985.

- 14 D. Fernandez-Renau, M. Lombardero and A. Nieto, *Eur. J. Biochem.*, 144 (1984) 523.
- 15 T. K. Torkkeli, K. K. Kontula and O. A. Jänne, *Mol. Cell. Endocrinol.*, 9 (1977) 101.
- 16 A. Nieto and M. Lombardero, *Comp. Biochem. Physiol.*, 71B (1982) 511.
- 17 M. A. Pesce and C. S. Strande, *Clin. Chem.*, 19 (1973) 1265.
- 18 A. Bussard, *Biochim. Biophys. Acta*, 34 (1959) 258.
- 19 G. Mancini, A. Q. Carbonara and J. F. Heremans, *Immunochemistry*, 2 (1965) 235.
- 20 P. J. Jackson, C. J. Sampson, E. H. Cooper, D. Heney and J. T. Brocklebank, *Ann. Clin. Biochem.*, 25 (1988) 319.
- 21 A. Cavaggione, R. T. Sorbi, J. N. Keen, D. J. C. Pappin and J. B. C. Findlay, *FEBS Lett.*, 212 (1987) 225.
- 22 A. Nieto, H. Ponstingl and M. Beato, *Arch. Biochem. Biophys.*, 180 (1977) 82.
- 23 J. Gorst, Dako, High Wycombe, personal communication.
- 24 T. Torkkeli, T. Krusius and O. Jänne, *Biochim. Biophys. Acta*, 544 (1978) 578.
- 25 M. Beato and R. Baier, *Biochim. Biophys. Acta*, 392 (1975) 346.
- 26 M. Soledad López de Haro and A. Nieto, *Arch. Biochem. Biophys.*, 226 (1983) 539.
- 27 S. W. Levin, J. de B. Butler, U. K. Schumacher, P. D. Wightman and A. B. Mukherjee, *Life Sci.*, 38 (1986) 1813.
- 28 J. P. Mornon, F. Fridlansky, R. Bally and E. Milgrom, *J. Mol. Biol.*, 137 (1980) 415.
- 29 H. M. Beier, H. Bohn and W. Muller, *Cell Tissue Res.*, 165 (1975) 1.

CHROM. 20 637

MASS SPECTROMETRY OF ELECTROPHORE-LABELED NUCLEOSIDES PENTAFLUOROBENZYL AND CINNAMOYL DERIVATIVES

THOMAS M. TRAINOR

Department of Chemistry and Barnett Institute of Chemical Analysis, Northeastern University, Boston, MA 02115 (U.S.A.)

ROGER W. GIESE

Barnett Institute of Chemical Analysis and College of Pharmacy and Allied Health Professions, Northeastern University, Boston, MA 02115 (U.S.A.)

and

PAUL VOUIROS*

Department of Chemistry and Barnett Institute of Chemical Analysis, Northeastern University, Boston, MA 02115 (U.S.A.)

SUMMARY

Three structurally similar deoxynucleosides (thymidine, O⁴-ethylthymidine, and 2'-deoxyuridine) were studied by mass spectrometry as pentafluorobenzyl, cinnamyl, or mixed derivatives. The purpose of the work was to define the usefulness of such derivatives for structural elucidation of deoxynucleosides. The compounds were ionized in three ways: electron capture negative ion, positive ion chemical ionization, and electron impact. For each of the derivatives examined, the combined spectra were well suited for structural elucidation purposes.

INTRODUCTION

Mass spectrometry (MS) has been shown to be particularly useful in the characterization of DNA and RNA structures through analysis of the components nucleobases, nucleosides, and nucleotides¹⁻⁵. The study of the non-volatile nucleosides has been accomplished by a variety of desorption ionization techniques, including fast atom bombardment⁶, field desorption⁷, ²⁵²Cf desorption⁸, and secondary ion MS^{9,10}. These ionization techniques permit the analysis of highly polar, thermally labile compounds directly, without the need for chemical derivatization. However, relatively large quantities of sample are normally required to carry out such experiments, typically in the microgram scale.

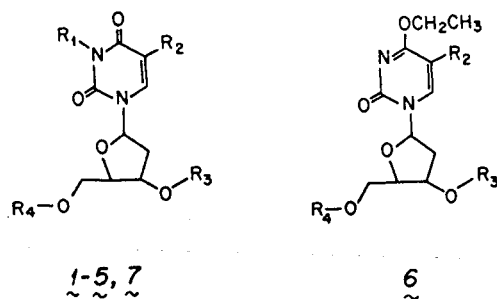
We have been interested in developing analytical methodology for the trace level detection of chemically modified nucleobases and nucleosides in physiological samples. This requires detection limits not normally associated with the aforementioned desorption MS techniques. Electron capture negative ion mass spectrometry (ECNIMS) has been shown to provide particularly low detection limits,

approaching the femtogram (10^{-15} g) level, for compounds amenable to electron capture¹¹. For compounds not inherently electrophoric, the preparation of a suitable derivative is necessary to permit efficient ionization under ECNIMS conditions¹¹⁻¹⁴. Numerous volatile derivatives of the naturally occurring and modified nucleosides have been proposed for analysis by both gas chromatography (GC)¹⁵ and MS¹⁶. These include derivatives based on acetyl¹⁷, permethyl¹⁸, alkylsilyl¹⁹, or trifluoroacetyl^{20,21} chemistry. However, very little has appeared on the preparation of electrophoric derivatives suitable for ECNIMS. Smith *et al.*²² have described the preparation of trifluoroacetyl and nitrobenzyl nucleoside derivatives. The negative ion mass spectra observed, obtained under low pressure electron impact (EI) conditions, consisted primarily of fragment ions related to the introduced electrophore, and not the original nucleoside.

Recent studies conducted in our laboratories concerning the development of volatile, chemically stable, and highly electrophoric derivatives of nucleosides^{23,24} and nucleobases^{25,26} for analysis by GC with electron capture detection (ECD) and GC-MS have provided several new approaches to nucleoside derivatization methodology. For the nucleosides, two promising derivatives are those obtained by treatment with pentafluorobenzyl bromide²³ and cinnamoyl chloride²⁴. We wish to report here the methane negative ion and positive ion chemical ionization mass spectra of several derivatives of the nucleoside thymidine, and two modified nucleosides 3-methylthymidine and 5-hydroxymethyl-2'-deoxyuridine. Presented in Table I are the structures of the seven compounds prepared for this study. Three different derivatives of thymidine 1-3, were prepared incorporating pentafluorobenzyl or cinnamoyl

TABLE I
STRUCTURES OF ELECTROPHORE-LABELED NUCLEOSIDES

CIN = COCH=CHC₆H₅; PFB = CH₂C₆F₅.



Compound	MW	R ₁	R ₂	R ₃	R ₄
1	502	H	CH ₃	CIN	CIN
2	682	PFB	CH ₃	CIN	CIN
3	782	PFB	CH ₃	PFB	PFB
4	516	CH ₃	CH ₃	CIN	CIN
5	616	CH ₃	CH ₃	PFB	PFB
6	630	—	CH ₃	PFB	PFB
7	978	PFB	CH ₂ OPFB	PFB	PFB

electrophores. Two derivatives of the modified nucleoside 3-methylthymidine, 4 and 5, were synthesized by introduction of either electrophore to the sugar hydroxyl sites. In addition, the pentafluorobenzyl derivatives of the modified nucleosides O⁴-ethylthymidine (6) and 5-hydroxymethyl-2'-deoxyuridine (7) have been prepared. As reported previously^{23,24} these derivatives have been found to be quite stable chemically, particularly in comparison to the popular silyl adducts. Moreover, the high sensitivity exhibited by these compounds by GC-ECD^{23,24} suggests possible utility for the related technique of ECNIMS.

EXPERIMENTAL

The preparation of these derivatives has been described previously^{23,24}. All mass spectra were obtained by placing approximately 100 ng of each compound in the glass tip of a direct insertion probe of the Finnigan 4021B mass spectrometer. Ion source temperature was set at 200°C and the probe was heated ballistically to 300°C. For the chemical ionization experiments, methane served as reagent gas at a source pressure of 0.30 Torr.

RESULTS

Electron capture negative ion mass spectrometry

The spectra obtained for compounds 1–7 by ECNIMS are summarized in Table II. The behavior of the derivatives in terms of fragmentation is clearly dependent on

TABLE II
METHANE ECNIMS OF ELECTROPHORE-LABELLED NUCLEOSIDES

Values in parentheses are percentages relative abundance.

Ion	<i>m/z</i>						
	1	2	3	4	5	6	7
M ⁻	502 (100)	682 (100)	782 (0.5)	516 (100)	616 (0)	630 (0)	978 (0)
(M-181) ⁻	—	501 (0)	601 (5)	—	435 (8)	449 (35)	797 (8)
b ⁻	125 (17)	125 (12)	305 (5)	139 (8)	139 (1)	153 (2)	501 (9)
Other	147* (16)	—	762 (2)	—	178** (100)	178** (100)	178** (100)
			178 (100)				196*** (80)

* C₆H₅CH=CHCOO⁻

** CH₂C₆F₄O⁻

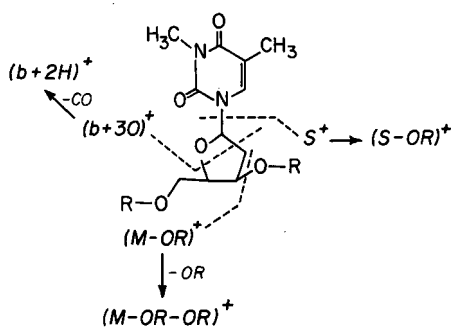
*** CHOC₆F₅⁻

the choice of added electrophore. The cinnamoyl esters 1, 2, and 4 are distinguished by the production of the molecular anion, M^- , as the base peak. Fragmentation in the spectra of these derivatives is limited; a portion of the ion current is carried by ions formed as a result of cleavage of the nitrogen-carbon glycosidic bond to give the base anion, b^- . Also formed is the complementary anion $C_6H_5CH=CHCOO^-$, m/z 147, by retention of the charge on the electrophore moiety. The high relative abundance of the radical anion M^- , created by the initial electron capture process, is most likely due to the stabilization of the charge by one or both of the cinnamoyl groups.

In contrast to the spectra of the cinnamoyl compounds, those of the derivatives which contain only the pentafluorobenzyl group, 3, 5, 6, and 7, show virtually no molecular anion, M^- . This absence of M^- , due to ionization via a dissociative electron capture process, is a common feature of ECNIMS of the pentafluorobenzyl derivatives of a variety of functionalities¹². The base peak for 5, 6, and 7 is found to be an ion at m/z 178. A probable composition for this ion is $CH_2C_6F_4O^-$, produced via either an inter-molecular nucleophilic oxygen-fluorine exchange or an intra-molecular rearrangement. Bimolecular exchange reactions have been reported previously for halogenated aromatics under methane chemical ionization conditions and may occur due to traces of oxygen in the ion source²⁷. Nevertheless, except for that of 2 (see below), the spectra of the pentafluorobenzyl derivatives studied here exhibit the fragment $(M - 181)^-$. This loss of the pentafluorobenzyl radical is quite common^{12,28,29} and provides an ion suitable for selected ion monitoring studies for trace level analyses. It is important to note that for compound 2, in which both the pentafluorobenzyl and cinnamoyl electrophores are present, the ionization is dominated by the cinnamoyl groups, yielding only M^- (100%) and b^- (12%) ions. No signal corresponding to $(M - 181)^-$ or m/z 178 was observed. Given these favorable properties of cinnamoyl-derivatized nucleosides for detection, it is unfortunate that recent work in our laboratories has revealed that 4 is a difficult solute to handle by GC.

Methane positive ion chemical ionization

The analysis of nucleosides by positive ion chemical ionization (PICI) mass spectrometry has been accomplished using both the free nucleosides³⁰ and the trimethylsilyl derivatives^{3,31}. The PICI mass spectra of compounds 1-7 are summarized in Table III. The behavior of both the cinnamoyl and pentafluorobenzyl derivatives is quite similar to that documented previously for the corresponding trimethylsilyl derivatives³. In general, the mass spectra provide both molecular weight confirmation via the MH^+ ions and details of structural features through the production of several significant fragment ions. The major fragmentation paths for these derivatives are outlined in Scheme 1. Ions indicative of the nucleobase, $(b + 2H)^+$ and $(b + 30)^+$, the sugar, S^+ and $(S - OR)^+$, and the intact nucleoside, $(M - OR)^+$ and $(M - OR - OR)^+$, are readily discernible and should aid in the structure elucidation of modified nucleosides. With the exception of compound 1, the MH^+ ion is a prominent feature for all the derivatives studied. This ion, when also considered in conjunction with the M^- or $(M - 181)^-$ ions in the ECNI mass spectra, serves to establish the molecular weight of the derivative. Chemical modifications at the sugar or base portions of the nucleoside may be ascertained by location of the appropriate fragment ions. In particular, the pair of ions $(b + 2H)^+$ and $(b + 30)^+$, separated by 28 a.m.u., are clearly featured for all the compounds studied.



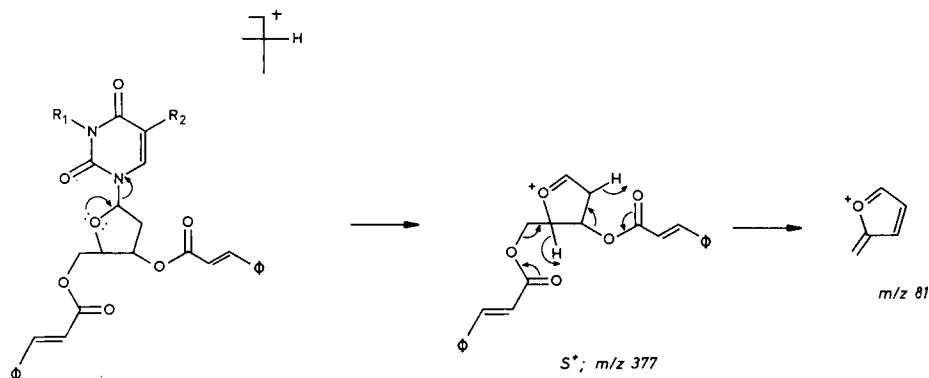
Scheme 1.

TABLE III
METHANE PICIMS OF ELECTROPHORE-LABELED NUCLEOSIDES

Values in parentheses are percentages relative abundance.

Ion	m/z						
	1	2	3	4	5	6	7
MH ⁺	503 (2)	683 (80)	783 (100)	517 (0)	617 (100)	631 (37)	979 (100)
(M-OR) ⁺	335 (9)	535 (68)	585 (12)	369 (46)	419 (11)	433 (21)	781 (68)
S ⁺	377 (40)	377 (100)	477 (25)	377 (66)	477 (14)	477 (4)	477 (19)
(S-OR) ⁺	229 (18)	229 (20)	279 (6)	229 (23)	279 (10)	279 (5)	279 (3)
(b+30) ⁺	155 (26)	335 (47)	335 (12)	169 (40)	169 (19)	183 (22)	531 (10)
(b+2) ⁺	127 (76)	307 (88)	307 (35)	141 (100)	141 (56)	155 (100)	503 (15)
Other	149 (28)	182 (15)		149 (25)	181 (12)	179 (30)	181 (20)
		131 (29)	149 (23)		131 (24)		
		81 (100)	131 (30)		81 (88)		
			81 (54)				

The spectra of the three cinnamoyl-substituted derivatives show an abundant ion of m/z 81. This ion is absent in the other derivatives studied and, most likely, can be rationalized in terms of the furan moiety depicted in Scheme 2. A similar ion has been observed in the EI mass spectra of trifluoroacetyl derivatives of nucleosides^{1,32}. The production of this ion in only the cinnamoyl derivatives is consistent with a series of six-membered ring rearrangements (Scheme 2). These processes would not be possible in the case of the pentafluorobenzyl derivatives.



Scheme 2.

Electron impact mass spectrometry

EI mass spectra were obtained for compounds 1–7 and are summarized in Table IV. As might be anticipated for these nucleosides, the spectra are composed almost solely of fragment ions, with no $M^{+\bullet}$ ions detected. The cinnamoyl esters 1, 2, and 4 are dominated by the m/z 81 ion, as discussed earlier for the PICI mass spectra. For the pentafluorobenzyl derivatives 3, 5, 6, and 7 the base peak is at m/z 181, $\text{CH}_2\text{C}_6\text{F}_5^+$. An earlier study by McCloskey³³ on the EI mass spectra of monobenzyl nucleoside derivatives reported the analogous tropylium ion at m/z 91, $\text{C}_6\text{H}_5\text{CH}_2^+$, to be the base peak.

CONCLUSION

Derivatization with electrophoric groups influences significantly the fragmentation pattern of nucleosides. In the ECNI mode, incorporation of a cinnamoyl group provides ideal conditions for formation and stabilization of a molecular anion even in the presence of a pentafluorobenzyl group. In contrast, derivatives containing a pentafluorobenzyl group alone largely form the anion $\text{CH}_2\text{C}_6\text{F}_4\text{O}^-$ with this ionization technique. On the other hand, significant fragmentation is encountered for all compounds at least under PICI and EI conditions. Together these latter spectra are well suited for structural studies.

For trace quantitative analysis, the advantages of pentafluorobenzyl derivatives of deoxynucleosides are that, for the ones examined to date, they are stable derivatives which can be detected with high sensitivity by GC–ECD²³, and certain of them give a structurally characteristic ion at $M - 181$ (loss of pentafluorobenzyl) with moderate

TABLE IV

EIMS OF ELECTROPHORE-LABELED NUCLEOSIDES

The values in parentheses are percentages relative abundance.

Ion	m/z						
	1	2	3	4	5	6	7
S ⁺	—	377 (5)	477 (4)	377 (5)	—	—	477 (2)
C ₆ F ₄ CH ₂ ⁺	—	—	181 (100)	—	181 (100)	181 (100)	181 (100)
C ₆ H ₅ CHCHCO ⁺	131 (42)	131 (40)	—	131 (30)	—	—	—
C ₆ H ₅ CHCH ⁺	103 (20)	103 (12)	—	103 (25)	—	—	—
C ₅ H ₅ O ⁺	81 (100)	81 (100)	—	81 (100)	—	—	—
Other	147 (10)	306 (8)	—	77 (16)	141 (10)	155 (30)	—
				55 (14)	55 (20)	126 (17)	
						110 (10)	
						82 (15)	
						9 (12)	
						55 (35)	

abundance (e.g. 35% for 6 relative to the base peak) under ECNI conditions, encouraging their sensitive, specific detection by GC-ECNIMS.

ACKNOWLEDGEMENTS

Financial support for this research was provided by the National Cancer Institute (Grant CA 35483) and from the Reproductive Effects Assessment Group of the U.S. Environmental Protection Agency (Grant CR 812470). Contribution No. 351 from the Barnett Institute of Chemical Analysis.

REFERENCES

- 1 C. Hignite, in G. R. Waller and O. C. Dermer (Editors), *Biochemical Applications of Mass Spectrometry*, First Supplemental Volume, Wiley, New York, 1980, pp. 527-566.
- 2 J. A. McCloskey and S. Nishimura, *Acc. Chem. Res.*, 10 (1977) 403.
- 3 J. A. McCloskey, in P. O. Ts'o (Editor), *Basic Principles in Nucleic Acid Chemistry*, Vol. I, Academic Press, New York, 1974, Ch. 4.
- 4 A. L. Burlingame, K. Straubb and T. A. Baillie, *Mass Spectrom. Rev.*, 2 (1983) 331.
- 5 J. A. McCloskey, in A. L. Burlingame and N. Castagnol (Editors), *Mass Spectrometry in the Health and Life Sciences*, Elsevier, Amsterdam, 1985, pp. 521-546.
- 6 F. W. Crow, K. B. Tomer, M. L. Gross, J. A. McCloskey and D. E. Bergstrom, *Anal. Biochem.*, 139 (1984) 243.
- 7 H. R. Schulten and H. D. Beckey, *Org. Mass Spectrom.*, 7 (1973) 861.
- 8 W. Ens, K. G. Standing, J. B. Westmore, K. K. Ogilvie and M. J. Nermer, *Anal. Chem.*, 54 (1982) 960.
- 9 C. J. McNeal and R. D. McFarlane, *J. Am. Chem. Soc.*, 103 (1981) 1609.
- 10 D. L. Slowikowski and K. H. Schram, *Nucleosides Nucleotides*, 4 (1985) 347.
- 11 K. F. Faull and J. D. Barchas, in D. Glick (Editor), *Methods of Biochemical Analysis*, Vol. 29, Wiley, New York, 1983, pp. 325-383.
- 12 T. M. Trainor and P. Vouros, *Anal. Chem.*, 59 (1986) 601.
- 13 P. Vouros and T. M. Trainor, *Adv. Mass Spectrom.*, Part B, (1985) 633.
- 14 D. F. Hunt, G. C. Stafford, F. W. Crow and J. W. Russell, *Anal. Chem.*, 48 (1976) 2098.
- 15 K. H. Schram and J. A. McCloskey, in K. Tsuji (Editor), *GLC and HPLC Analysis of Therapeutic Agents*, Marcel Dekker, New York, 1979, pp. 1149-1190.
- 16 J. A. McCloskey, A. M. Lawson, K. Tsuboyama, P. M. Krueger and R. N. Stillwell, *J. Am. Chem. Soc.*, 90 (1968) 4182.
- 17 J. Boutagy and D. J. Harvey, *J. Chromatogr.*, 156 (1978) 153.
- 18 A. P. DeLeenheer and C. I. Gelijkens, *Anal. Chem.*, 48 (1976) 2203.
- 19 M. A. Quilliam, K. K. Ogilvie, K. L. Sadana and J. B. Westmore, *J. Chromatogr.*, 196 (1980) 367.
- 20 C. F. Gelijkens, D. L. Smith and J. A. McCloskey, *J. Chromatogr.*, 225 (1981) 291.
- 21 U. I. Krahmer, J. G. Liehr, K. J. Lyman, E. A. Orr, R. N. Stillwell and J. A. McCloskey, *Anal. Biochem.*, 82 (1977) 217.
- 22 D. L. Smith, K. H. Schram and J. A. McCloskey, *Biomed. Mass Spectrom.*, 10 (1983) 269.
- 23 J. Adams, M. David and R. W. Giese, *Anal. Chem.*, 58 (1986) 345.
- 24 J. Adams and R. W. Giese, *J. Chromatogr.*, 347 (1985) 99.
- 25 G. B. Mohamed, A. Nazareth, M. J. Hayes, R. W. Giese and P. Vouros, *J. Chromatogr.*, 314 (1984) 211.
- 26 A. Nazareth, M. Joppich, S. Abdel-Baky, K. O'Connell, A. Sentissi and R. W. Giese, *J. Chromatogr.*, 314 (1984) 201.
- 27 R. C. Dougherty, *Anal. Chem.*, 53 (1981) 625A.
- 28 A. G. Netting and A. M. Duffield, *Biomed. Mass Spectrom.*, 12 (1985) 668.
- 29 R. J. Strife and R. C. Murphy, *J. Chromatogr.*, 305 (1984) 3.
- 30 M. S. Wilson and J. A. McCloskey, *J. Am. Chem. Soc.*, 97 (1975) 3436.
- 31 T. Marunaka and Y. Umeno, *J. Chromatogr.*, 221 (1980) 382.
- 32 W. A. Koenig, L. C. Smith, P. F. Crain and J. A. McCloskey, *Biochemistry*, 10 (1971) 3968.
- 33 H. T. Cory, K. Yamaizumi, D. L. Smith, D. R. Knowles, A. D. Broom and J. A. McCloskey, *J. Heterocyclic Chem.*, 16 (1979) 585.

CHROM. 20 653

COMPARISON OF THE CHROMATOGRAPHIC PROPERTIES OF STEROLS, SELECT ADDITIONAL STEROIDS AND TRITERPENOIDS: GRAVITY-FLOW COLUMN LIQUID CHROMATOGRAPHY, THIN-LAYER CHROMATOGRAPHY, GAS-LIQUID CHROMATOGRAPHY AND HIGH-PERFORMANCE LIQUID CHROMATOGRAPHY

SIHUA XU, ROBERT A. NORTON, FERRAST G. CRUMLEY and W. DAVID NES*

Plant and Fungal Lipid Group, Plant Physiology Research Unit, Russell Research Center, U.S. Department of Agriculture, 950 College Station Road, Athens, GA 30605 (U.S.A.)

SUMMARY

The chromatographic properties of approximately 100 sterols, select steroids of plant origin (sapogenins and steroidal alkaloids) and triterpenoids has been evaluated in this laboratory by monitoring their elution characteristics in adsorption (gravity column and thin-layer methods with and without the addition of silver nitrate), gas and reversed-phase high-performance liquid chromatography. The utility of each methodology to act in one or another chromatographic mode-separation, radiochemical purification, quantitation and structural elucidation, is discussed. The importance of the tilt of the -OH group at C-3 as well as the polarity, size, and shape of the rest of the molecule as it effects the hydrogen-bonding ability of the -OH group is demonstrated through changes in chromatographic behavior that result from the step-wise introduction of double bonds, methyl, bromo, oxygen, nitrogen and cyclopropyl groups into 5 α -cholestanol. An independent aid in the structure identification and quantitation of the compounds was use of a multiple-wavelength diode array detector in which different wavelengths of the UV spectrum (200-400 nm) were simultaneously monitored following passage of the sample through a reversed-phase C₁₈ column.

INTRODUCTION

There are four principal methodologies used for the chromatography of sterols, biogenetically derived steroids (steroidal alkaloids and sapogenins) and triterpenoids: gravity-flow column liquid chromatography (GCC), thin-layer chromatography (TLC), gas-liquid chromatography (GLC) and high-performance liquid chromatography (HPLC). Each chromatographic system serves a unique function in the separation, radiochemical purification, quantitation and structural elucidation of these compounds. Their chromatographic behavior is known to be influenced by the hydrogen-bonding character and other electronic attractions (*e.g.* van der Waals forces and dipole-dipole interactions) between the lipid and the adsorbent. The rate of

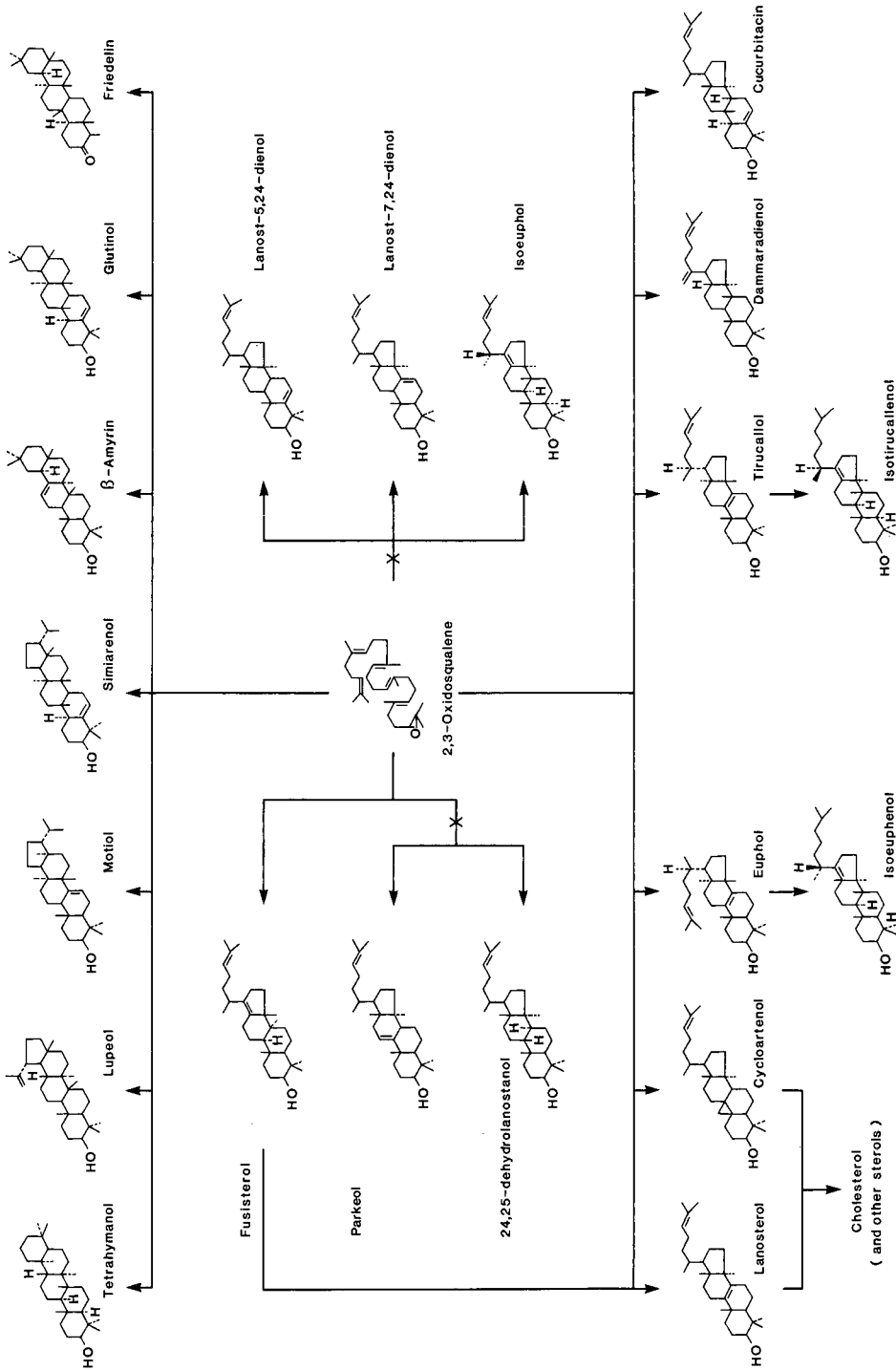


Fig. 1. Proposed routes of squalene oxide cyclization to tetracyclic and pentacyclic isopentenoids.

movement for each compound will depend on: (1) the stereochemistry and location of the polar substituents; (2) the solubility, partition coefficient and equilibrium constants of the compound in the solvent (and its polarity) used to develop the system; (3) the size and shape of the molecule; and (4) the degree of hydration and surface area of the adsorbent which affects intermolecular attraction between solvent, lipid and stationary phase. When the four systems are used in series; GCC → TLC → HPLC → GLC, not only is the probability of achieving homogeneity nearly 100% but important diagnostic information is gained about the location and geometry of select substituents and of the three-dimensional shape of the molecule as a whole.

Our interest in characterizing the chromatographic properties of steroids and triterpenoids is for several reasons. First, the physical chemistry involved in the lipid-stationary phase interaction may be similar to the kinds of associations which may be expected between these and other molecules in biomembranes. Therefore, how these compounds behave here may provide some predictive value of how they should behave in artificial and biological membranes. Second, the chromatographic behavior should reveal something about the preferred conformation of the molecule, as a result the confidence level regarding whether conformational transmission effects are realized outside of pure solution and solid state should be greatly increased. Third, to be able to predict *viz.*, to determine σ^G values, where compounds should elute in one or another system when authentic standards are not readily available for chromatography. Fourth, we have been interested for some time in the relationship between biosynthesis (Fig. 1) and function of steroids and triterpenoids throughout the evolutionary hierarchy. Because serious anomalies exist in this subject we have endeavored to prepare synthetically or isolate from natural sources numerous compounds which can be used in future metabolic, physiological and developmental studies. The chromatographic properties for many of these compounds have not before been reported in the literature (especially HPLC) and are given for the first time in this communication. In light of this volume of the *Journal of Chromatography* having been dedicated to Dr. Erich Heftmann we should like to point out at the outset that this field has evolved from the status of an art into a sophisticated science. Dr. Heftmann has, over a period of three decades, contributed much to its development¹⁻⁴. One of us (W.D.N.) had the pleasure to receive post-doctoral training (1980-1981) in this area from Dr. Heftmann. The current effort extends and compliments previous findings from this⁵⁻¹⁰ and other laboratories¹¹⁻²⁴.

EXPERIMENTAL

Nomenclature

The numbering system that we have adopted for the tetracycles is shown in Fig. 2, although it may not be applicable for all sterols (*cf.* ref. 25 which examined the sterol side chain of marine sterols). The triterpenoid numbering system is different than the steroid numbering system even though the ring systems may be similar (Fig. 2). The α/β nomenclature for the chirality at C-24 of the sterol side chain is used in this study rather than the *R/S* nomenclature. It is important to remember that reference to α/β for the stereochemistry of nuclear substituents has a different meaning than its use for diastereoisomers in the side chain¹². Unfortunately, the IUPAC system for numbering carbon atoms and rules for distinguishing the epimeric condition of chiral groups is not

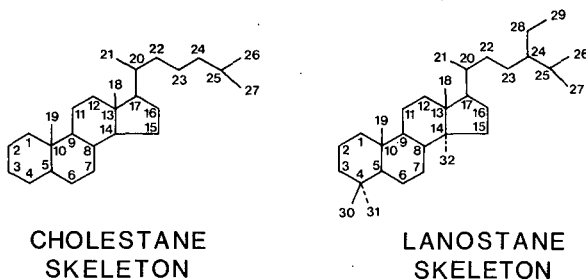


Fig. 2. Numbering system for sterols used in this study.

wholly satisfactory for the compounds examined in this study. This subject has been discussed elsewhere^{1,2}.

Chromatographic systems employed

Gravity column chromatography. GCC was performed in glass columns of varying dimensions depending on the sample load. The adsorbent (oven dried) was aluminum oxide (neutral Al₂O₃, Woelm Pharma) or silica gel (hydrated SiO₂, Mallinckrodt) having variable mesh size 60–200. An elutropic series of solvents were employed to develop the systems. For alumina GCC the material was activated with water to 3% (v/w) and the eluent composition was changed in a discontinuous manner. The step-wise gradient was diethyl ether graded in 10% increments into Skelly Solve B (mixed hexanes). For the silica gel columns the series of solvents was added in the order of increasing polarity: hexane < hexane–benzene (1:1) < benzene < diethyl ether < methanol < methanol–chloroform. For elution of nitrogen compounds, the last solvent employed was triethylamine–ethylacetate.

Thin-layer chromatography. TLC was performed on 20 × 20 cm glass plates coated with 0.25 mm Silica Gel G (Analtech). TLC plates were standardized by preeluting the plates with benzene–ether. The plates were then oven dried at 110°C for 12 h. The plates were stored in a desiccator for at least 2 h prior to use. Four solvent systems were utilized in this study: S I, benzene–diethyl ether (9:1); S II, benzene–diethyl ether (85:15); S III, ethyl acetate–triethylamine (99:1); S IV, chloroform–diethyl ether (97:3).

Silver nitrate TLC. Compounds were chromatographed on silica gel G TLC plates and impregnated with silver ion by dipping the plates in a solution of 10-g silver nitrate in 25 ml water brought up to 100 ml with methanol. Prior to use the plates were dried overnight and allowed to cool for 30 min in a desiccator containing calcium carbonate. Plates were developed once in sealed TLC tanks containing 100 ml of chloroform–anhydrous diethyl ether (97:3, v:v). Test compounds were acetylated in sealed tubes with pyridine–acetic anhydride (1:1) at 55°C for 2 h. Compounds were loaded onto TLC plates at 5 µg per spot. The chromatographed sample was visualized by spraying plates with 50% methanolic sulfuric acid and slowly charred at 60°C.

Gas-liquid chromatography. GLC was routinely performed on a Hewlett-Packard Model 5890 gas chromatograph equipped with a HP 3393A computing integrator. Operating conditions for chromatography were as follows: column temperature, 245°C; detector temperature, 300°C; injector temperature, 275°C; helium carrier gas

flow-rate 20 ml/min. Attenuator and range were normally set at 4 and 10^{-11} , respectively. Retention times are reported relative to cholesterol (RRT_c). The elution time for cholesterol was standardized at 10 min.

Reversed-phase high-performance liquid chromatography. HPLC was performed on a Hewlett-Packard Model 1090 liquid chromatograph controlled by a ChemStation equipped with a Hewlett-Packard 9000 Series 300 computer. The C_{18} column (particle size $5\ \mu\text{m}$; $110\ \text{mm} \times 4.7\ \text{mm}$ I.D. from Whatman) was interfaced with a guard column packed with Partisphere. Both columns were operated at 40°C with methanol-water (94:6, v/v) as the solvent. Flow-rate was maintained at 1 ml/min; pressure, 80 bar. Sample peak was monitored by a diode-array detector. Retention times (α_c)⁹ were relative to cholesterol. The retention time of cholesterol was maintained at about 10 min. About $10\ \mu\text{g}$ of sample was dissolved in $10\ \mu\text{l}$ of ethanol then loaded onto the column. Some compounds dropped out of solution (certain pentacycles) or failed to produce a UV response (saturated compounds). For these compounds we either changed the solvent for dissolving the compound (methanol or benzene) or increased the amount to be dissolved in the ethanol *e.g.*, sample load was increased to 100–200 μg of sample. The spectrum of each elution peak was fully characterized by continuously monitoring the absorbance between 200 and 400 nm. The UV cutoff for HPLC grade methanol and water was below 195 nm, the lowest wavelength which was used for monitoring absorption spectra of sterols. Solvents were HPLC grade (Burdick and Jackson) except for the diethyl ether, Skelly B and triethylamine which were purchased from American Scientific Products, Fisher and Eastman Kodak, respectively. The water for use in HPLC was obtained by glass distillation.

RESULTS AND DISCUSSION

Gravity column chromatography

This type of descending chromatography is usually employed as a preparative method to separate sterols from triterpenoids and to separate these polycyclic isopentenoids from other classes of lipids such as fatty acids and phospholipids. Fraction number is plotted relative to mass accumulated in test tubes. The elution profile is similar whether alumina or silica gel is the stationary phase. Preference for one system over the other may be predicated on the use of high levels of carcinogenic organic solvents such as benzene. A typical elution order is as follows: hydrocarbons (squalene) < ketones = esters < 4-monomethyl sterols < 4,4-dimethyl sterols = triterpenoids = primary long chain fatty alcohols (C_{28} – C_{32}) < 4-desmethyl sterols (cholesterol, ergosterol, etc.) < steryl glycosides = sapogenins < phospholipids < nitrogen containing sterols (elute with triethylamine). We have noted that dry-packed silica gel columns act to promote decomposition of nuclear polyunsaturated systems *e.g.* of ergosterol. The extent of decomposition (hence of recovery) and double bond rearrangements depends on the sample size to silica gel ratio and the hydration of the silica gel. Obviously, for the investigator who is unaware of this phenomenon minor compounds could be lost in the sample work-up or novel compounds could be generated from a natural source which are in fact an artifact of the chromatographic method to purify the sample.

TABLE I
RELATIVE RETENTIONS OF TEST COMPOUNDS ON VARIOUS CHROMATOGRAPHIC SYSTEMS

= not examined.

Compound	Source	System		Structure (based on 5 α -cholestanol)		
		TLC*, R _F	TLC**, R _{ST}	GC***, RRT _c	RP-HPLC [§] , α_c	
Cholestanol	Synthesis, this laboratory	0.18	1.22	1.03	1.10 (1.14)	Δ^0 -3 β -ol
Cholest-4-enol	Synthesis, this laboratory	0.25	1.12	0.96	0.93	Δ^4 -3 β -ol
Cholesterol	Steraloids	0.20 (0.47) [0.66]	1.00	1.00	1.00	Δ^5 -3 β -ol; 20R
Lathosterol	Synthesis, this laboratory	0.18 (0.43)	1.15	1.10	0.97	Δ^7 -3 β -ol
Cholest-8-enol	Synthesis, this laboratory	0.18 (0.43)	1.24	1.05	0.90 (0.93)	$\Delta^{8,9}$ -3 β -ol
Cholest-8(14)-enol	Synthesis, this laboratory	0.18	1.23	1.00	0.88	$\Delta^{8(14)}$ -3 β -ol
Cholest-14-enol	Synthesis, this laboratory	0.18	1.23	1.00	0.91	$\Delta^{14,15}$ -3 β -ol
Pregn-5-enol	W. R. Nes	0.18	—	0.16	0.18	Δ^5 -3 β -ol (no side chain)
20-Epicholesterol	W. R. Nes	0.20	—	0.93	0.84	Δ^5 -3 β -ol; 20S
(E)-17(20)-Dehydrocholesterol	W. R. Nes	0.20 (0.47)	0.25	0.94	0.64	$\Delta^{5,17(20)}$ -3 β -ol; (E)-17(20)
(Z)-17(20)-Dehydrocholesterol	W. R. Nes	0.20 (0.49)	0.19	0.86	0.61	$\Delta^{5,17(20)}$ -3 β -ol; (Z)-17(20)
Cholesta-5, (E)-20(22)-dienol	W. R. Nes	0.20	0.24	0.99	0.69	$\Delta^{5,20(22)}$ -3 β -ol; (E)-20(22)
Cholesta-5, (E)-22(23)	H. Kircher	0.20	0.44	0.92	0.81	$\Delta^{5,22(23)}$ -3 β -ol; (E)-22(23)
Zymosterol	Bakers yeast	0.20	N.E.	1.13	0.67	$\Delta^{8,24}$ -3 β -ol
Cholesta-5(Z)-22(23)-dienol	H. Kircher	0.20 (0.46)	0.33	0.90	0.74	$\Delta^{5,22(23)}$ -3 β -ol; (Z)-22(23)
Desmosterol	<i>Saprolignia ferax</i>	0.20 (0.46)	0.36	1.10	0.72	$\Delta^{5,24(25)}$ -3 β -ol
Cholesta-5,25(27)-dienol	Synthesis, this laboratory	0.21	0.17	1.07	0.78	$\Delta^{5,25(27)}$ -3 β -ol
Cholesta-8,14-dienol	Synthesis, this laboratory	0.37	0.31	1.02	0.76	$\Delta^{8,14}$ -3 β -ol
7-Dehydrocholesterol	Steraloids	0.19	0.22	1.07	0.86	$\Delta^{5,7}$ -3 β -ol
26-Homocholesterol	M. J. Thompson	0.20	—	1.35	1.12	$\Delta^{5,26}$ -Methyl-3 β -ol
Campesterol	Cactus pollen	0.20	1.04	1.29	1.11 (1.15)	Δ^5 -24 α -Methyl-3 β -ol
20(R)-n-Heptylpregn-5-en-3 β -ol	W. R. Nes	0.20	—	1.47	1.24	Δ^5 -3 β -ol
22,23-Dihydrobrassicasterol	<i>Gibberella fujikuroi</i>	0.20	1.04	1.29	1.11 (1.15)	Δ^5 -24 β -Methyl-3 β -ol
20(R)-n-Nonylpregn-5-en-3 β -ol	W. R. Nes	0.20	—	2.61	1.82	Δ^5 -3 β -ol; extended side chain
Sitosterol	Sorghum	0.20	1.04	1.60	1.28	Δ^5 -24 α -Ethyl-3 β -ol
Stigmasterol	Sorghum	0.20	0.78	1.40	1.11 (1.10)	$\Delta^{5,22(23)}$ -24 α -Ethyl-3 β -ol; (E)-22(23)

Stigmastanol	M. J. Thompson	0.18	1.23	1.62	1.29	Δ^0 -24 α -Ethyl-3 β -ol
Lophenol	H. Kircher	0.27	1.11	1.26	1.14	Δ^7 -4 α -Methyl-3 β -ol
Obtusifolol	<i>Gibberella fujikuroi</i>	0.27	—	1.49	0.96	$\Delta^{7,24(28)}$ -4 α ,14 α - Dimethyl-3 β -ol
Ergosta-4,6,22-trienone	Synthesis, this laboratory	0.37	—	1.56	0.81	$\Delta^{4,6,22}$ -24 β -Methyl-3-one
Ergosterol	<i>Gibberella fujikuroi</i>	0.19 (0.43)	0.09	1.22	0.81 (0.76)	$\Delta^{5,7,22}$ -24 β -Methyl- 3 β -ol; (E)-22(23)
Ergosterol B ₂	<i>Gibberella fujikuroi</i>	0.20	0.26	1.20	0.81 (0.71)	$\Delta^{6,8,22}$ -24 β -Methyl- 3 β -ol; (E)-22(23)
Brassicasterol	<i>Gibberella fujikuroi</i>	0.20	0.78	1.12	0.91	$\Delta^{5,22}$ -24 β -Methyl
Ergocalciferol	Sigma	0.19	—	1.10	0.60	$\Delta^{5,7,22}$ -24 β -Methyl with open B-ring
9(11)-Dehydroergosterol	Synthesis, this laboratory	0.18	0.09	1.12	0.57	$\Delta^{5,7,9(11),22}$ -24 β -Methyl- 3 β -ol; (E)-22(23)
Ostreasterol	Cactus pollen	0.20	0.12	1.26	0.87	$\Delta^{5,24(28)}$ -3 β -ol
24-Dehydropollinastanol	Cactus pollen	0.20	—	1.26	0.75 (0.71)	$\Delta^{24,9\beta,19}$ -Cyclopropyl- 3 β -ol
24-Methyldesmosterol	Synthesis, this laboratory	0.20	—	1.45	0.93	$\Delta^{5,24(25)}$ -24-Methyl-3 β -ol
Fucosterol	<i>Saprolegnia ferax</i>	0.20 (0.47)	0.40	1.62	1.03 (1.00)	$\Delta^{5,24(28)}$ -24-Ethylidene-3 β - ol; <i>cis</i> /(E)-24(28)
Isofucosterol	<i>Ulva</i> sp.	0.20	0.46	1.65	1.05 (1.00)	$\Delta^{5,24(28)}$ -24-Ethylidene- 3 β -ol; <i>trans</i> /(Z)-24(28)
Clerosterol	Codium	0.20	—	1.54	0.97	$\Delta^{5,25(27)}$ -24 β -Ethyl-3 β -ol
25(27)-Dehydroponiferasterol	W. R. Nes	0.20	0.11	1.37	0.83	$\Delta^{5,22,25(27)}$ -24 β -Ethyl-3 β -ol
14 α ,24 β -Methyl-cholest-8(9)-3-ol	M. J. Thompson	0.18	1.46	1.36	1.09	$\Delta^{8(9)}$ -14 α ,24 β -Dimethyl- 3 β -ol
Cholesterol acetate	Synthesis, this laboratory	0.70	1.00	1.41	1.99	Δ^5 -3 β -ol-acetate
Epicholesterol	Synthesis, this laboratory	0.32	—	0.97	0.87	Δ^5 -3 β -ol
Cholesterone	Synthesis, this laboratory	0.42	—	1.34	1.07 (1.02)	Δ^5 -3-one
Cholestanone	Synthesis, this laboratory	0.52	—	1.10	1.22	Δ^0 -3-one
Stigmasta-4,22-dien-3-one	Aldrich	0.38	—	1.10	1.02	$\Delta^{4,22}$ -24 α -Ethyl-3-one
Cholest-4-en-3-one	Synthesis, this laboratory	0.38	—	1.31	0.91 (0.87)	Δ^4 -3-one
24-Methylelanosterone	Synthesis, this laboratory	0.66	—	1.96	1.33	$\Delta^{8,24(28)}$ -4,4,14- Trimethyl-3-one
4,4-Dimethylcholest-5-en-3-one	Synthesis, this laboratory	0.66	—	1.27	1.48	Δ^5 -4,4-Dimethyl-3-one
4,4-Dimethylcholesta-8,14-dienol	Synthesis, this laboratory	0.31	—	1.59	1.07	$\Delta^{8,14}$ -4,4-Dimethyl-3 β -ol
20 α -Hydroxycholesterol	W. R. Nes	0.15	—	1.49	0.27	Δ^5 -3 β ,20 α -diol

(continued on p. 384)

TABLE I (continued)

Compound	Source	System		Structure (based on 5 α -cholestanol)			
		TLC*, R _F	TLC**, R _{ST}	GC***, RRT _c	RP-HPPLC§, α _c		
22-R-Hydroxycholesterol	H. Kircher	0.15	—	1.71	0.25	Δ ⁵ -3β,22R-diol	
22-S-Hydroxycholesterol	H. Kircher	0.10	—	1.70	0.21	Δ ⁵ -3β,22S-diol	
25-Hydroxycholesterol	Steraloids	0.04	—	1.63	0.28	Δ ⁵ -3β,25-diol	
26-Hydroxycholesterol	E. Heftmann	0.04	—	2.20	0.21	Δ ⁵ -3β,26-diol	
29-Hydroxyfucoesterol	T. McMorris	0.10	—	2.99	0.31	Δ ⁵ -24-Ethylidene-3β,29-diol; (E)-24(28)	
Cycloartenol	Sorghum	0.31 (0.63)	0.88	1.89	1.16	See Fig. 1	
Lanosterol	<i>Gibberella fujikuroi</i>	0.31 (0.62) [0.77]	0.86	1.65	1.04	See Fig. 1	
Lanosta-7,24-dienol	Synthesis, this laboratory	0.31	0.83	1.83	1.01	See Fig. 1	
4,4-Dimethyl-cholest-5-enol (Δ ⁵ -Lanosterol)	E. J. Parish	0.33 (0.66)	1.16	1.44	1.39	Δ ⁵ -4,4-Dimethyl-3β-ol	
24,25-Dihydrolanosterol	Synthesis, this laboratory	0.31	1.28	1.53	1.32	Δ ⁸ -4,4,14-Trimethyl-3β-ol	
24-Methyllanosterol	Synthesis, this laboratory	0.31 [0.77]	—	2.20	1.34	Δ ^{8,24(25)} -24-Methyl-3β-ol	
Agnosterol	Commercial lanosterol	0.31	—	1.56	0.86	Δ ^{7,9(11),24(25)} -4,4,14- Trimethyl-3β-ol	
24,25-Dihydroagnoesterol	Commercial lanosterol	0.31	—	1.42	1.07	Δ ^{7,9(11),4,14} - Trimethyl-3β-ol	
Lanostanol	Synthesis, this laboratory	0.31	1.28	1.92	1.44	Trimethyl-3β-ol	
24,25-Dehydrolanosterol	Synthesis, this laboratory	0.31	0.88	2.04	1.18	Δ ⁰ -4,4,14-Trimethyl-3β-ol	
Euphol	<i>Euphorbia tirucalli</i>	0.33	0.75	1.44	0.99 (1.06)	Δ ^{2,4} -4,4,14-Trimethyl-β-ol	
Tirucalol	<i>Euphorbia tirucalli</i>	0.30	0.80	1.57	1.03 (1.06)	See Fig. 1	
Isotrucalolenol	Synthesis, this laboratory	0.31	1.22	1.02	0.95	See Fig. 1	
Dammaradienol	E. Spencer	0.22	—	2.61	0.30	20β-Hydroxy-dammaradienol	
Lupeol	Sorghum	0.31	0.60	1.82	0.81	See Fig. 1	
Lupeol methyl ether	Synthesis, this laboratory	0.72	—	1.92	1.44	See Fig. 1, methyl ether	
Simiarenol	Sorghum	0.39	0.87	2.16	1.25	See Fig. 1	
Epifriedalanol	Synthesis, this laboratory	0.65	1.20	2.19	2.66	See Fig. 1; 3β-ol	
β-Amyrin	Sorghum	0.29	1.23	1.62	1.03	See Fig. 1.	
Glutinol	T. Itoh	0.42	0.88	1.85	1.03	See Fig. 1	

Friedelin									See Fig. 1
Tetrahymanol	<i>Kalmia latifolia</i>	0.39				2.33	1.42		See Fig. 1
Motiol	<i>Tetrahymena pyriformis</i>	0.29	1.29			2.50	—		See Fig. 1
α -Amyrin	Sorghum	0.28	1.09			2.43	1.50		See Fig. 1
24,25-Epimino lanosterol	Sorghum	0.31	1.23			1.79	1.13		See Fig. 1
	Synthesis, this laboratory	0.00 [0.29]	0.29			2.263	—		$\Delta^8,4,4,14$ -Trimethyl, 24(<i>RS</i>)-25-epimino-3 β -ol
25-Azalanosterol	Synthesis, this laboratory	0.00 [0.25]	0.25			1.65	—		$\Delta^8,4,4,14$ -Trimethyl-5-aza-3 β -ol
25-Aminolanosterol	Synthesis, this laboratory	0.00 [0.14]	0.14			2.34	—		$\Delta^8,4,4,14$ -Trimethyl-25-amino-3 β -ol
24,(<i>S</i>)25-Oxidolanosterol	E. J. Parish	0.23 [0.67]	0.67			2.52	0.22		$\Delta^8,4,4,14$ -Trimethyl-24(<i>S</i>)oxido; 3 β -ol
24(<i>R</i>)25-Oxidolanosterol	E. J. Parish	0.23 [0.62]	0.67			2.52	0.24		$\Delta^8,4,4,14$ -Trimethyl-24(<i>R</i>)oxido; 3 β -ol
24-Hydroxy lanosterol	Synthesis, this laboratory	0.16 [0.73]	—			2.24	0.33		$\Delta^8,4,4,14$ -Trimethyl-3 β ,24-diol
25-Hydroxy lanosterol	Synthesis, this laboratory	0.06	0.62			2.69	0.30		$\Delta^8,4,4,14$ -Trimethyl-3 β ,25-diol
24-Bromolanosterol	Synthesis, this laboratory	0.31 [0.77]	0.77			1.61	1.02		$\Delta^8,2,4,4,14$ -Trimethyl-24-bromo-3 β -ol
25-Keto,26-norcholesterol	Kurt Spira Co.	0.13	—			1.46	0.29		Δ^5 -25-One-3 β -ol
Solasodine	<i>Solanum khasianum</i>	0.02 [0.60]	—			1.88	—		See Fig. 4
Soladulcidine	E. Hefmann	0.01 [0.52]	—			1.92	—		See Fig. 4
Solanidine	E. Hefmann	0.25 [0.66]	—			1.13	—		See Fig. 4
Diosgenin	E. Hefmann	0.15 [0.67]	—			1.40	0.38		See Fig. 4
Tigogenin	E. Hefmann	0.14 [0.66]	—			1.44	0.41		See Fig. 4
Demissidine	E. Hefmann	0.07 [0.67]	—			1.12	—		See Fig. 4
25-Azacholesterol	M. J. Thompson	0.00 [0.41]	—			1.11	—		See Fig. 4
Tomatidine	D. Johnson	0.01 [0.61]	—			2.03	—		See Fig. 4
Solasodine	D. Johnson	0.19 [0.78]	—			1.18	—		See Fig. 4
Squalene	Aldrich	0.85	0.02			0.51	2.14		—
Sitosterol glycoside	<i>Solanum khasianum</i>	0.00	—			—	0.24		—
Triacotanol	Wheat	0.28	1.23			1.88	2.15		30-Carbon fatty alcohol

* Adsorption TLC; plates were developed in S I; in parenthesis, S II; in brackets, S IV.

** Silver nitrate TLC; plates were developed in S III; R_F values are relative to cholesteryl acetate; $R_{ST} = R_F(\text{compound})/R_F(\text{cholesterol})$

*** Gas-liquid chromatography was performed on 3% SE-30 packed columns operated at 245°C. Retention times are relative to cholesterol.

§ Reversed-phase HPLC was performed at 40°C with 6% aq. methanol as the eluent. Retention times are relative to cholesterol.

Thin-layer chromatography

TLC has become a multipurpose workhorse in the analysis of steroids and triterpenoids. TLC may be used not only to purify samples but the R_F value provides a clue to the compounds structural identification. Total lipid extracts of biological specimens normally contain a mixture of polycyclic isopentenoids. These compounds can be separated into various classes based on the compound's movement off the origin. Cholesterol is used as the reference marker and has an R_F of 0.18 with S I (Table I). The structural feature which most contributes to the chromatographic behavior of cholesterol in adsorption TLC is the presence of a free 3β -OH group. Addition of one or two methyls to C-4, inverting the A/B ring juncture or converting the C-3 OH to an acetoxy, methoxy, keto, or 3α -OH which occurs during routine metabolism will result in a steroid having a less polar R_F value relative to the R_F value obtained for cholesterol. The distal portion of the molecule plays less of a role in mediating the chromatographic behavior of steroids in adsorption TLC than it does in silver nitrate or reversed-phase TLC^{15,26}. Thus triterpenoids which possess geminal methyls at C-4 behave in TLC like the 4,4-dimethyl steroids (Table I) although they are structurally very different from lanosterol.

The total lipid extract is oily, as a result only bulk separations of steroids is generally achieved in the first run. In contrast to the diminished TLC sensitivity for compounds mixed in with the total lipid extract, fine-tune chromatography of the sort shown in Fig. 3 can be obtained with pure compounds. The rate of movement for each compound will depend on the hydrogen bonding strength of the polar group at C-3. The hydrogen bonding strength in turn will be influenced by the tilt of the C-3 –OH group and the proximity of double bonds, steric hindering agents (alkyl groups) and neighboring polar groups (hydroxyl, keto, nitrogen, etc.) to the C-3 –OH. Polar groups introduced into the side chain (Figs. 3 and 4) decrease the mobility of the steroid in an additive manner. The stereochemistry and position of the oxygenated function are also important to the compound's rate of movement. The polarity of the solvent can be changed to permit separation of compounds *e.g.*, nitrogen-containing steroids, which in benzene–ether failed to migrate off the origin (Table I). Good separation was achieved with triethylamine in ethyl acetate for the various nitrogen-containing steroids shown in Table I. The order of R_F values from more to less polar for the nitrogen groupings was as follows: 25-amino(tertiary amine) < 25-aza < 24,25-epimino (aziridine) < solasodane (26-azasteroid). The isomeric steroidal alkaloids at C-22, tomatidine and soladulcidine were easily separated by using S IV. The difference in migration is due to the stereochemistry of the F-ring which places the nitrogen closer or farther away from the E-ring oxygen and the stationary phase. The stereochemistry of the ring systems effect the migration of steroids and triterpenoids on TLC.

As shown in Fig. 5 the tilt of the C-3 –OH group differs between cycloartenol and lanosterol and between these steroids and cholesterol. On the assumption that the sterol interacts with the gel so that the C-18 and C-19 angular methyls are directed toward the gel (β -face binding) then the hydrogen-bond vector between the C–OH and the gel can be influenced in a predictable manner depending on the spatial orientation of the C-3 –OH group. For instance, the three-dimensional shape observed in Dreiding models and X-ray crystallographs of 3-epi and 3-keto steroids²⁷ indicate that the polar groups are directed up from the plane of the nucleus and therefore, assuming β -face binding, away from the gel. Thus, the hydrogen-bond vector is weakened and the

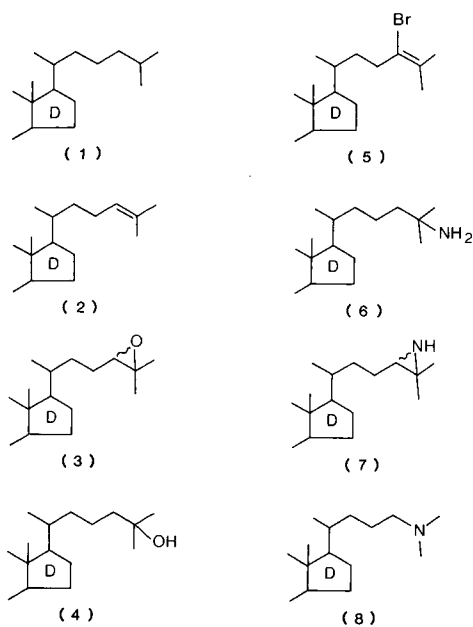


Fig. 3. Sterol side chain variations.

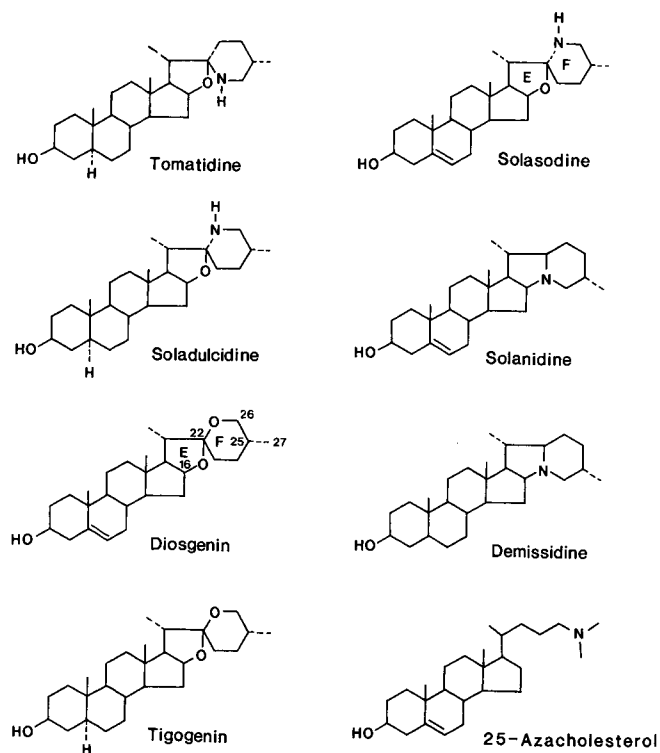


Fig. 4. Structures of steroidal alkaloids and sapogenins.

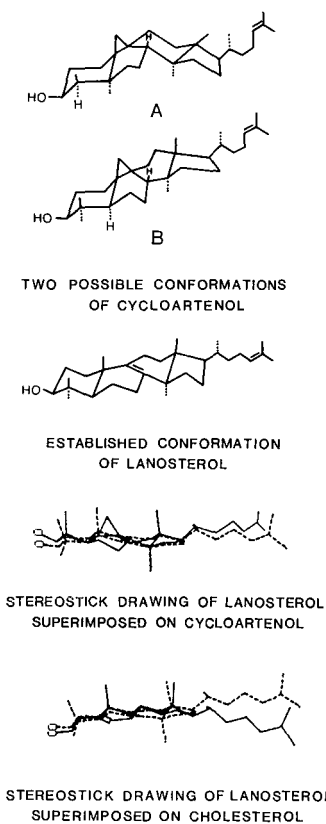


Fig. 5. Different conformations of steroids in which the tilt of the 3β -OH is observed.

compounds should and experimentally do run up the plate compared with 3β -OH sterols. The significance of conformational transmission effects on TLC behaviour is shown in the pairs of “left-handed” and “right-handed” sterols *viz.*, 20-epicholesterol–cholesterol and euphol–tirucalol, where the 20-*S* compound is slightly separated from the 20-*R* compound. Not only is the molecular volume changed by inverting the configuration at C-20 which alters the conformation of the side chain but the orientation of the 3β -OH group is changed and hence the hydrogen-bond vector (*cf.* X-ray crystallographs given in refs. 28 and 29).

Argentation chromatography

Silver nitrate TLC is a method to separate compounds based on the number and position of double bonds in the molecule. Silver nitrate on the surface of the silica gel coordinates with the double bond due to coulombic attractions between the pi electrons and the silver ion. The greater the accessibility (lack of hindrance) of the double bond to bind with the silver ion the more polar the compound's R_F value. As shown in Fig. 6 and Table I, tetrasubstituted double bonds have a small affinity for complexing with the silver ion while trisubstituted double bonds have a strong affinity for the silver ion. Double bonds in the nucleus are shielded to a greater extent than

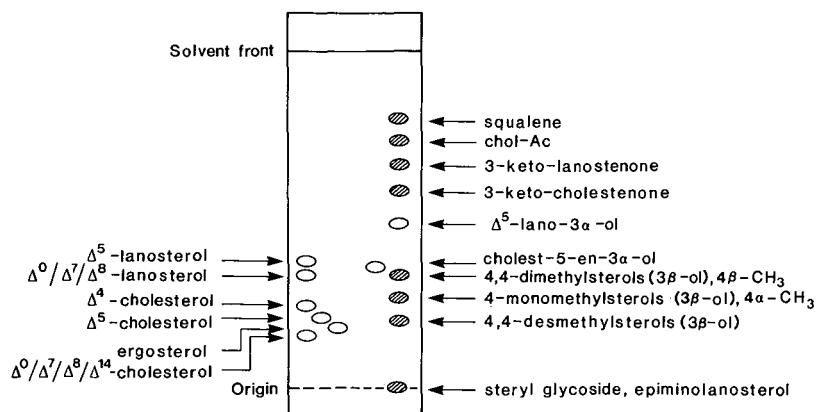


Fig. 6. Chromatographic behavior of sterols in adsorption TLC. Plates were developed with benzene-diethyl ether (9:1). Chol = cholesterol. Ac = acetate.

isolated double bonds in the acyclic side chain, therefore good separation is achieved with steroidal dienols in which one double bond is located in the nucleus and the other located in the side chain. A number of steryl acetates have been separated from one another by silver nitrate TLC³⁰⁻³³. We preferred to use the solvent system employed by Goad¹⁵ to provide a standardized silver nitrate TLC system for sterols and triterpenoids. In other studies we^{6,7} and others³⁰⁻³² have used benzene-hexane as the solvent to develop the plates. In this study we noted some variability from run to run in the R_F value of cholesteryl acetate (mean $R_F = 0.51$, $n = 7$), however the relative R_F value for each compound to the R_F value of cholesteryl acetate was constant from run to run. The order of elution based on double bond position for steroids was not directly correlatable to triterpenoids, since the triterpenoids possessed much greater nuclear

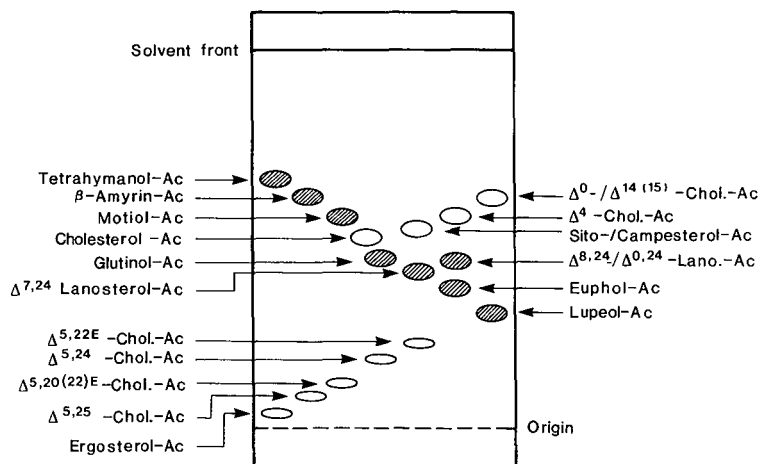


Fig. 7. Chromatographic behavior of steryl acetates in silver nitrate TLC. Plates were developed with chloroform-diethyl ether (97:3). Chol. = cholesterol; Lano. = lanosterol; Ac = acetate.

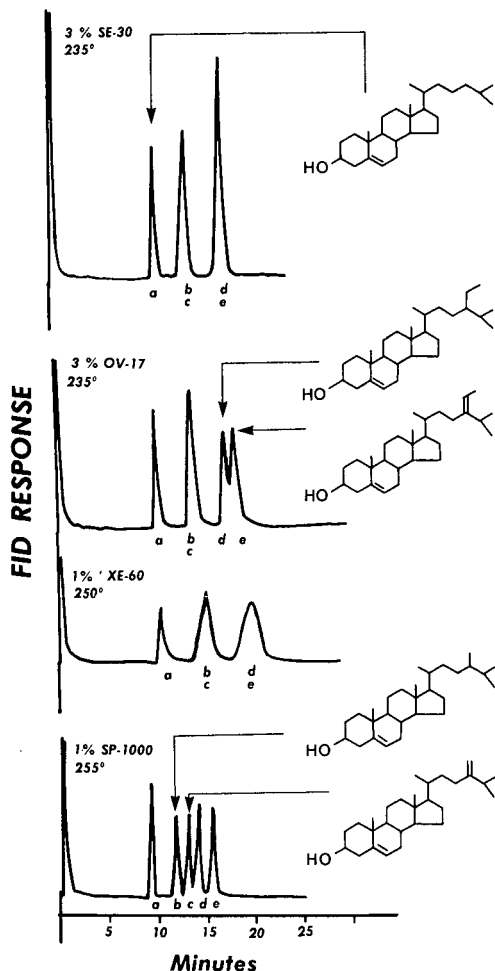


Fig. 8. Chromatographic behavior of structurally similar sterols on four GLC columns. The column packings exhibit the range of McReynolds constants from non-polar (SE-30) to polar (SP-1000).

variations and hence conformational differences due to 1–2 shifts of methyl groups and hydrogen atoms that resulted from the cyclization process (Fig. 1).

Gas-liquid chromatography

GLC is a powerful tool in structure determination and quantitation. In this study the vaporized compounds in the effluent gas were detected by a flame-ionization detector. The rate of movement for each compound in GLC was dependent on the polarity of the column packing. As shown in Fig. 8, sterols which cochromatograph on non-polar stationary phases can be separated from one another on polar stationary phases. Long polar capillary columns (100 m) where the number of theoretical plates has been greatly increased have been used to separate isomeric C-24 sterols which cannot be resolved on 6 ft. columns³⁴. Extensive correlations between structure and

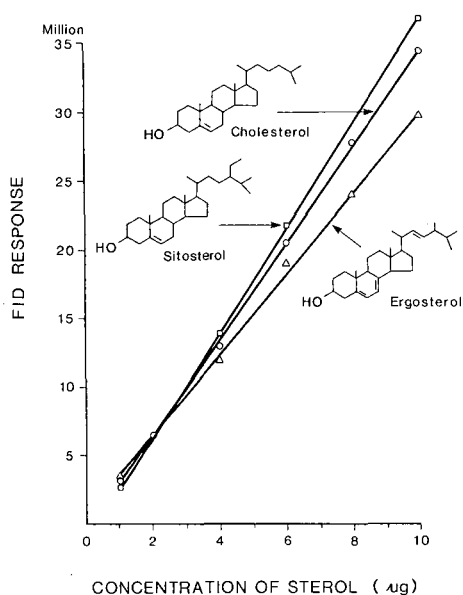


Fig. 9. Flame ionization detection (FID) in GC using 3% SE-30 packed columns to increasing concentrations of cholesterol, sitosterol and ergosterol.

retention time for sterols^{17,20,21} and triterpenoids^{17,18,35,36} have been reported using similar or the same column packings shown in Fig. 8. Because 4,4,14-trimethyl steroids, tetracyclic and pentacyclic triterpenoids possess nuclear conformations which may place angular methyl groups in spatial orientations that differ from what might be expected for such additions onto a cholestanol skeleton, it is not always possible to calculate *a priori* the retention time of the unknown steroid or triterpenoid by comparison with the features added to cholestanol (*cf.* refs. 11,19,21). For instance, the structural jump from cholestanol to lanosterol is too great to accurately calculate the RRT_c for lanosterol based on the retention time of the basal sterol structure (5α -cholestanol) and the retention factors contributed by each additional group *i.e.*, three methyls at C-4 and C-14 and two double bonds at C-8 and C-24. However, it is possible, to use the contribution factor (σ^G) when a single feature is common between pairs of structurally similar compounds. Thus, the RRT_c for the C-20 epimer of tirucalol (a tetracyclic triterpenoid) can be determined based on the retention times for the sterol pair cholesterol and 20-epicholesterol (Table I). Similarly the influence of $\Delta^0-\Delta^5$ can be determined for saponin and steroidal alkaloids based on the cholestanol-cholesterol pair of sterols.

The retention time is also influenced by the amount of the injection. While the retention time remains constant between 20 ng to 2 µg/ml solvent, as the detector response goes off scale due to an increase in the concentration of sample above 2 µg/ml, the retention time increases (in a linear manner) by as much as 0.5 min at 10 µg/ml. Furthermore, as shown in Fig. 9, the ability to quantitate sterols at the same concentration injected into the instrument becomes structurally dependent at the higher sample load. These facts should be considered at times when the investigator

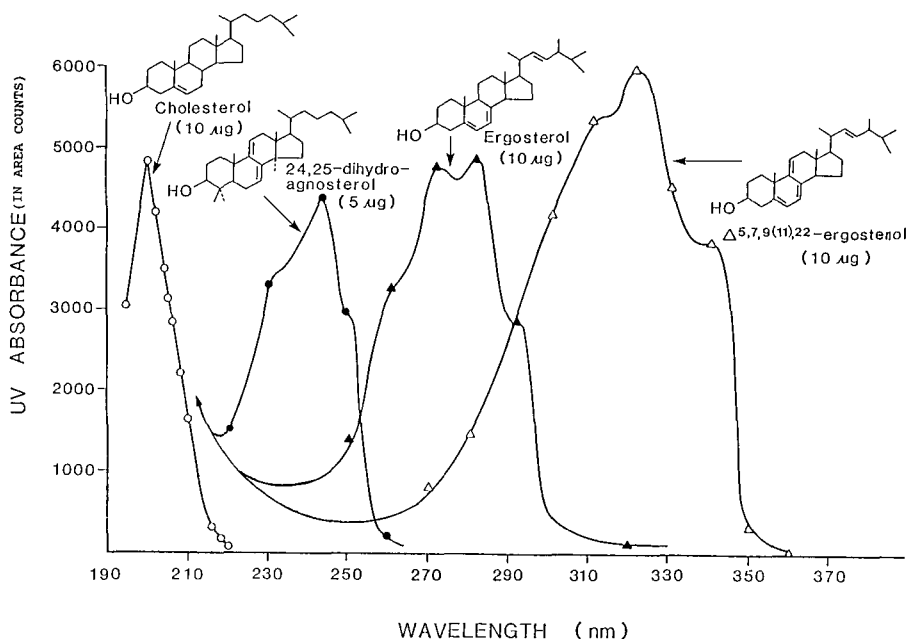


Fig. 10. Detector response at a given wavelength to the chromophore condition. The points that compose the UV fingerprints for each sterol were determined by the peak area (mAU \times time) obtained at select wavelengths between 195 and 400 nm. For 10 μ g of cholesterol monitored at 205 nm the peak area (in mAU) gave an area count of 3119. The shape of the individual curves *i.e.*, the shape between the data points, was drawn as they appeared in UV spectra obtained on the respective compound before chromatography.

has observed a major compound present in a mixture and it is off scale, then changes the attenuator to bring this peak on scale to quantify it or to obtain its RRT_c . Neither the retention time nor counts given by the computer may reflect the true RRT_c or amount of the unknown compound relative to readings based on cholesterol. It is best, as we have found, to dilute the sample and reinject it into the gas chromatograph in order to quantify the off scale peak.

Reversed-phase (RP) high-performance liquid chromatography

RP-HPLC is a recent chromatographic system that has great utility for steroid analysis. Its origin was in the lipophilic (LH-20) gravity Sephadex columns that were developed in the early part of the last decade to separate sterols differing in the number of C-24 alkyl groups and on the number of double bonds in the nucleus and side chain³⁷⁻³⁹. RP-HPLC has the advantage over the LH-20 columns in the amount of time involved for chromatography (min *versus* days) and in resolving sterols that were unseparable with the LH-20 columns. Another advantage is the ability to interface the column with a multiple-wavelength diode array detector. This detector will produce a signal for any sterol that passes through the aperture. The response or peak height measured in mAU is dependent on the amount loaded onto the column, number and kind of chromophores in the molecule *e.g.*, tetrasubstituted, trisubstituted, heteroanular, or homoanular, and on peak purity. Even though cholesterol will not be detected by UV absorbance above 220 nm (Fig. 10) all sterols including stanols exhibit

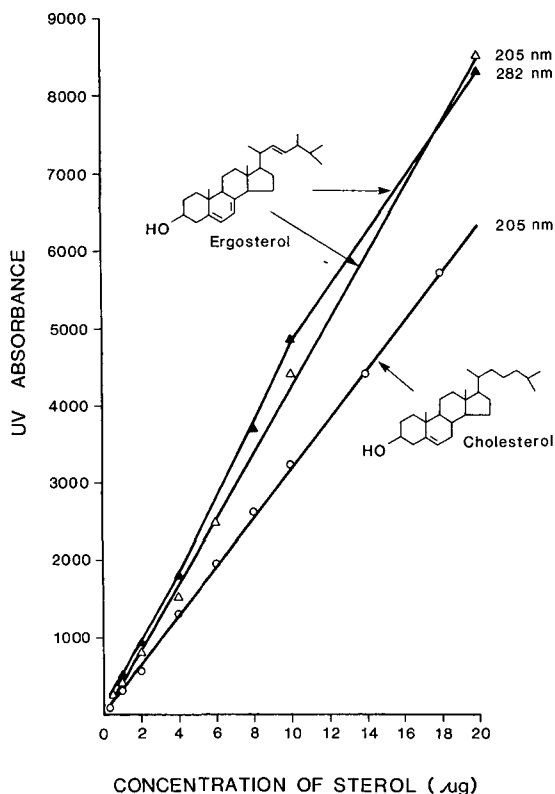


Fig. 11. UV detector response to increasing concentrations of cholesterol and ergosterol.

an end absorption spectra. Thus, the instrument can be dialed to 205 nm for routine analysis, however it should be kept in mind that similar peak heights may represent vastly different levels of sterols. As shown in Fig. 11, there is a linear response that is structurally dependent between 20 ng and 20 µg with increasing sterol concentration. In the present study we used a 10-cm C_{18} column and operated the instrument at 40°C while in earlier studies we used a 25-cm C_{18} column and operated the instrument at ambient temperature⁵⁻⁹. In our earlier studies we observed that cholesterol and lanosterol cochromatographed. However, as shown in Fig. 12 the two compounds were partially separated by elevating the operating temperature for chromatography. The compounds were distinguished by their end absorption spectra.

In addition to changing the temperature conditions other chromatographic "tricks" can be used to separate structurally similar sterols. For instance, the polarity of the eluant will influence the hydrogen bonding character of the sterol *i.e.*, the sterol will act either as a hydrogen donor or hydrogen acceptor. Therefore, it is possible to induce chromatographic frameshifts on a given set of compounds based on the use of a normal phase and reversed-phase solvents. In fact, the rate of movement of campesterol, stigmasterol, 7-dehydrocholesterol, ergosterol, 24(28)-methylene cholesterol and cholesta-5,22(*E*)-dienol relative to cholesterol is demonstrably different on C_{18} -columns eluted with acetonitrile⁴⁰, acetonitrile-water¹⁶, propanol in hexane⁴¹, methanol⁴² or methanol-water (this study).

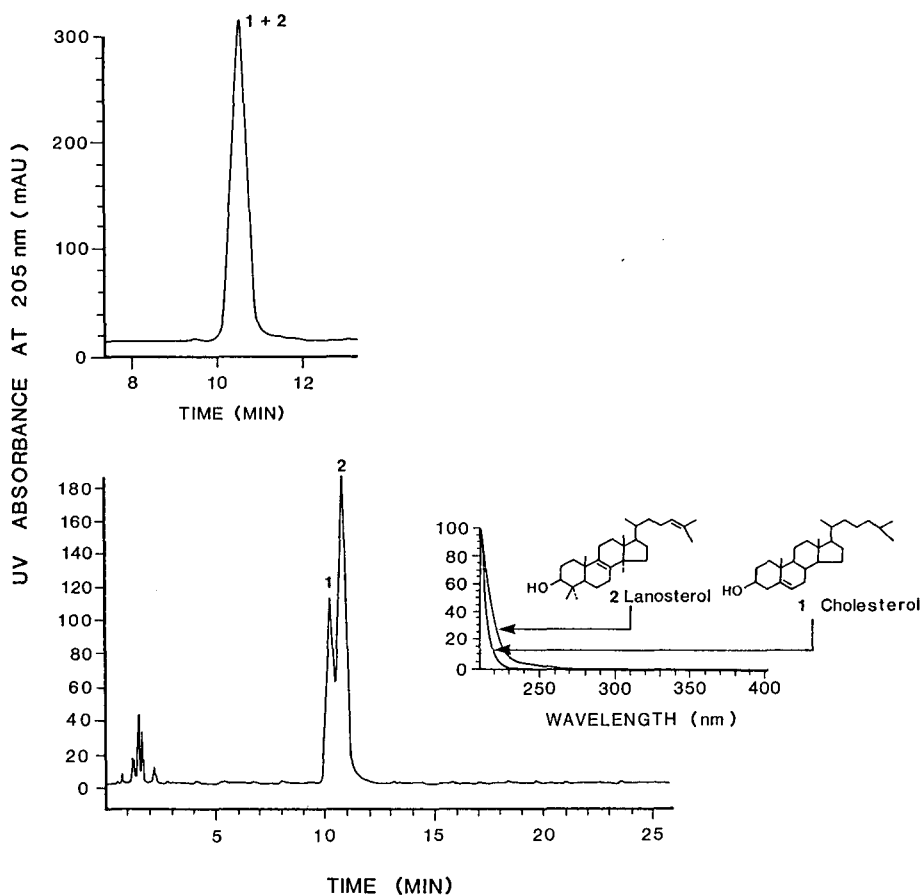


Fig. 12. Temperature dependent chromatographic separation of cholesterol and lanosterol by RP-HPLC eluted with 6% aq. methanol. (A) Column operated at 24°C; (B) column operated at 40°C.

The multiple-wavelength diode array detector was used in the purification of commercial lanosterol, a sterol mixture which contains four sterols; lanosterol, 24,25-dihydrolanosterol, agnosterol and 24,25-dihydroagnosterol⁴³. We found that neither silver nitrate TLC nor the chemical procedure of forming the dibromide alone will produce pure lanosterol as implied in the literature⁴⁴. As shown in Fig. 13 neither GLC (using the standard packed column) nor RP-HPLC in which the monitor is set at 205 nm would have indicated the presence of the impurity of 24,25-dihydroagnosterol mixed in with lanosterol. However, by monitoring several wavelengths simultaneously (Fig. 14) the presence of contaminating levels of 24,25-dihydroagnosterol in the tail of the lanosterol peak was evident. The utility of this instrumentation was demonstrated in our separation of lanosterol from the contaminant sterol by collecting the fractions corresponding to the leading edge of the peak with repeated injections using an auto injector.

We have found the C₁₈-column coupled to a multiple-wavelength diode array

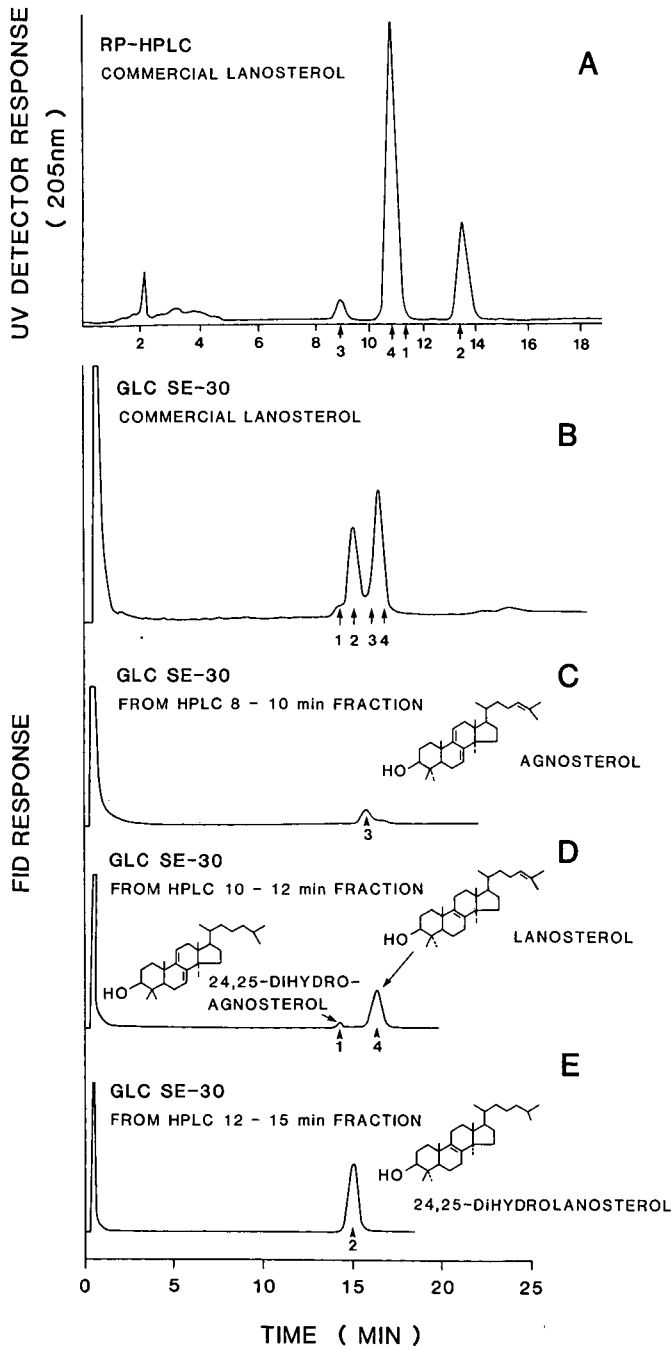


Fig. 13. Chromatograms of commercial lanosterol in RP-HPLC and GLC. The sample was fractionated by RP-HPLC and the fractions re-examined by GLC (C-E).

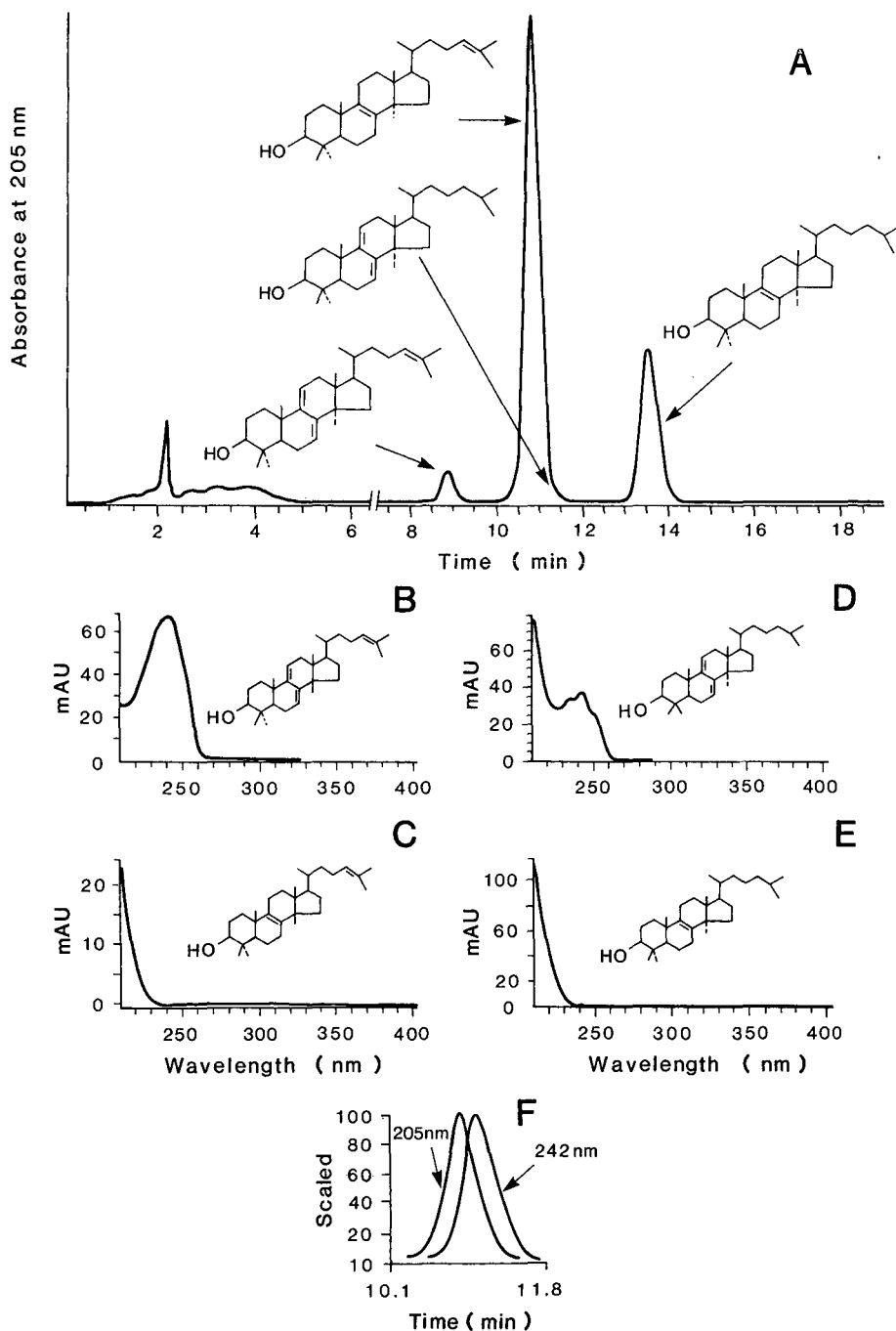


Fig. 14. Chromatogram of commercial lanosterol in RP-HPLC. UV spectra were recorded for each of the compounds eluting between 8 and 15 min. Peak purity (F) for the compound eluting between 10 and 12 min indicated two compounds with different UV spectra.

detector provides an elucidation of chemical purity which cannot be done with other chromatographic modes even GLC packed columns coupled to mass spectrometry.

CONCLUSIONS

The structural features which influence chromatographic mobility vary between adsorption and partition systems and on the polarity of each analytical system. Therefore, the way a compound behaves in TLC relative to cholesterol may be quite different in another chromatographic system. This attribute is particularly useful in the radiochemical purification of structurally similar sterols^{1,6,9,42}. Moreover, from the data compiled in Table I and consideration of molecular models of steroids and triterpenoids it should be possible to make rational choices for the chromatographic steps that will be required in the separation of a given set of compounds isolated from natural sources or prepared through chemical synthesis.

The two principal structural components that act as the chromatographic determinant are the hydrogen bonding capability of the C-3 OH-group and the stereochemistry of the molecule. For TLC, the degree of methylation at C-4 and the number and position of double bonds proximal to the -OH group affect mobility. In GLC and RP-HPLC, the methylation condition at C-4 plays a small role in the rate of movement while the flatter a sterol is the slower it moves (*cf.*, ref. 11 for a deeper discussion of this point). By comparison of the RRT_c and α_c of triacntanol and tetrahymanol the effect of cyclization of an acyclic molecule (formally with squalene) on chromatographic mobility was apparent. Interestingly, on a polar GLC column (1% SP-1000)⁴⁵, triacntanol frameshifts, to RRT_c 0.71 while tetrahymanol RRT_c remains about the same as its RRT_c on 3% SE-30 packed columns. Oxygenated and nitrogen-containing compounds such as diosgenin and solasodine will move as sterols depending on the chromatographic system employed. In general, however, the presence of polar groups has a strong effect on chromatographic mobility, but the direction and magnitude of the kind of effect depend strongly on the method. Additional double bonds in the sterol produce a more polar R_F , however, a saturation level is obtained in silver nitrate TLC after three double bonds are introduced into the molecule. In RP-HPLC we have separated sterols with base-line resolution having as many as five double bonds⁴⁶. Compounds which have a low solubility in methanol-water such as triterpenoids with very high melting points produce a broad late peak in RP-HPLC. Unfortunately, the chromatographic rules applicable for sterols may not operate for sterol-like molecules *e.g.*, triterpenoids. More data is required on the non-steroidal polycyclic isopentenoids before rules for structure-retention can be formulated as has now been constructed for sterols¹¹.

ACKNOWLEDGEMENT

We thank Dr. Jane Griffin for the stereostick drawings given in Fig. 5.

REFERENCES

- 1 E. Heftmann, S.-T. Ko and R. D. Bennett, *J. Chromatogr.*, 21 (1966) 490.
- 2 E. Heftmann, *Chromatography of Steroids*, Elsevier, Amsterdam, Oxford, New York, 1976.
- 3 E. Heftmann and I. R. Hunter, *J. Chromatogr.*, 165 (1979) 283.

- 4 E. Heftmann, in E. Heftmann (Editor), *Chromatography: Fundamentals and Application of Chromatographic and Electrophoretic Methods*. Part B. Elsevier, Amsterdam, 1983, p. 191.
- 5 P. H. Le and W. D. Nes, *Chem. Phys. Lipids*, 40 (1986) 57.
- 6 W. D. Nes, R. C. Heupel and P. H. Le, *J. Chem. Soc. Chem. Commun.*, (1985) 1431.
- 7 W. D. Nes and P. H. Le, *Pest. Biochem. Physiol.*, 30 (1988) 87.
- 8 J.-T. Lin, W. D. Nes and E. Heftmann, *J. Chromatogr.*, 207 (1981) 457.
- 9 R. C. Heupel and W. D. Nes, *J. Nat. Prod.*, 47 (1984) 292.
- 10 W. D. Nes and E. J. Parish (Editors), *Analysis of Sterols and Other Biologically Significant Steroids*, Academic Press, New York, 1988, in press.
- 11 W. R. Nes, *Methods Enzymol.*, 111 (1985) 3.
- 12 W. R. Nes and M. L. McKean, *Biochemistry of Steroids and Other Isopentenoids*, University Park Press, Baltimore, MD, 1977.
- 13 J. C. Touchstone, in C. Zweig and J. Sherma (Editors), *Handbook of Chromatography — Steroids*, CRC Press, Boca Raton, FL, 1986, 258 pp.
- 14 R. J. Rodriguez and L. W. Parks, *Anal. Biochem.*, 119 (1982) 200.
- 15 L. J. Goad, *Methods Enzymol.*, 111 (1985) 311.
- 16 J.-P. Bianchini, E. M. Gaydou, J.-C. Sigoillet and G. Terrom, *J. Chromatogr.*, 329 (1985) 231.
- 17 T. Itoh, H. Tani, K. Fukushima, T. Tamura and T. Matsumoto, *J. Chromatogr.*, 234 (1982) 65.
- 18 N. Ikekawa, *Methods Enzymol.*, 15 (1969) 200.
- 19 R. B. Clayton, *Biochemistry*, 1 (1962) 357.
- 20 E. Homberg, *Fette, Seifen, Anstrichm.*, 79 (1977) 234.
- 21 G. W. Patterson, *Anal. Chem.*, 43 (1971) 1165.
- 22 J.-T. Lin and C.-J. Xu, *J. Chromatogr.*, 287 (1984) 105.
- 23 M. J. Thompson, G. W. Patterson, S. R. Dutky, J. A. Svoboda and J. N. Kaplanis, *Lipids*, 15 (1980) 719.
- 24 G. W. Patterson, in W. D. Nes, G. Fuller and L. Tsai, (Editors), *Isopentenoids in Plants: Biochemistry and Function*, Marcel Dekker, New York, 1984, p. 293.
- 25 I. L. Stallou, J. E. Thompson, J.-H. C. and C. Djerassi, *J. Amer. Chem. Soc.*, 108 (1986) 8235.
- 26 N. J. deSouza and W. R. Nes, *J. Lipid Res.*, 10 (1969) 240.
- 27 W. L. Duax and D. A. Norton, *Atlas of Steroid Structure Vol. II*, Plenum Press, New York, 1984.
- 28 W. D. Nes, R. Y. Wong, M. Benson, J. R. Landrey and W. R. Nes, *Proc. Natl. Acad. Sci. U.S.A.*, 81 (1984) 5896.
- 29 W. L. Duax, J. F. Griffin, D. C. Rohrer and C. M. Weeks, *Lipids*, 15 (1980) 783.
- 30 D. R. Idler and L. M. Safe, *Steroids*, 19 (1972) 315.
- 31 J. A. Svoboda and M. J. Thompson, *J. Lipid Res.*, 8 (1967) 152.
- 32 H. E. Vroman and C. F. Cohen, *J. Lipid Res.*, 8 (1967) 150.
- 33 B. A. Knights, *Anal. Biochem.*, 80 (1977) 324.
- 34 R. H. Thompson, G. W. Patterson, M. J. Thompson and H. T. Slover, *Lipids*, 16 (1981) 694.
- 35 R. C. Heupel, *Phytochemistry*, 24 (1985) 2929.
- 36 B. Wilkomirski and Z. Kasprzyk, *J. Chromatogr.*, 103 (1975) 376.
- 37 P. M. Hyde and W. H. Elliott, *J. Chromatogr.*, 67 (1972) 170.
- 38 G. W. Patterson, M. W. Khalil and D. R. Idler, *J. Chromatogr.*, 115 (1975) 153.
- 39 W. R. Nes, K. Krevitz, J. Joseph, W. D. Nes, B. Harris, G. F. Gibbons and G. W. Patterson, *Lipids*, 12 (1977) 511.
- 40 J. M. Dibussolo and W. R. Nes, *J. Chromatogr. Sci.*, 20 (1982) 193.
- 41 I. R. Hunter, M. K. Walden and E. Heftmann, *J. Chromatogr.*, 153 (1978) 57.
- 42 R. C. Heupel, Y. Sauvaire, P. H. Le, E. J. Parish and W. D. Nes, *Lipids*, 21 (1986) 69.
- 43 W. R. Nes, B. C. Sekula, W. D. Nes and J. H. Adler, *J. Biol. Chem.*, 253 (1978) 6218.
- 44 F. Gautschi and K. Bloch, *J. Biol. Chem.*, 233 (1958) 1343.
- 45 W. D. Nes and T. J. Bach, *Proc. Royal Soc. Lond. B.*, 225 (1985) 425.
- 46 W. D. Nes and E. J. Parish, *Fed. Proc.*, 46 (1987) 2272.

CHROM. 20 754

QUANTITATIVE MICROANALYSIS OF BILE ACIDS IN BIOLOGICAL SAMPLES

COLLABORATIVE STUDY

FUMIO NAKAYAMA*

Kyushu University, Faculty of Medicine, Department of Surgery I, Fukuoka (Japan)

SUMMARY

The analysis of bile acids in biological samples has always presented a problem because of their complex nature and low concentration. Recently, newer analytical procedures for bile acids have become available, including enzymatic analysis, radioimmunoassay, thin-layer chromatography (TLC), gas chromatography, high-performance liquid chromatography (HPLC) and gas chromatography–mass spectrometry (GC–MS) with selected ion monitoring (SIM). However, they differ greatly with respect to specificity, sensitivity, accuracy and simplicity. On the other hand, the choice of analytical procedure differs according to the specific aims and the nature of biological samples to be analysed. These newer procedures have been compared in a double-blind fashion by distributing bile, plasma and urine samples to seven participating laboratories. GC–MS–SIM was found to be the most sensitive and reliable, but it requires other procedures for preliminary clean-up and fractionation steps. Enzymatic analysis is simple and gives small analytical errors but tends to overestimate plasma bile acids. Radioimmunoassay gives variable results but is useful as a screening procedure for large numbers of plasma samples. TLC gives reliable results for biliary bile acids in experienced hands, except for differentiation between conjugated dihydroxycholeanoic acids. HPLC, whether using derivatization or with fixed 3α -hydroxy steroid dehydrogenase detection, is suitable for the analysis of major bile acids in normal human serum but not for the identification of unknown minor peaks.

INTRODUCTION

The analysis of bile acids** in biological samples has presented problems first because of the complex nature of the bile acids present, *i.e.*, primary, such as cholic

* This paper has been prepared by F. Nakayama on behalf of the participants of the comparative study on quantitative microanalysis of bile acid analysis. The participants were: F. Nakayama, T. Hoshita, S. Ikawa, T. Osuga, T. Nambara, I. Makino and H. Miyazaki.

** In this paper, bile acids include mono-, di-, tri- and tetrahydroxycholeanoic and -choleanoic acid and -nor-bile acid and -keto-bile acid.

and chenodeoxycholic, and secondary, such as deoxycholic and lithocholic, and unconjugated and conjugated, such as glycine and taurine conjugated, sulphated and glucuronidated. Second, bile acids are present in very low concentrations in some biological samples such as plasma and urine. Therefore, the development of accurate and sensitive methods of analysis of bile acids has been the subject of intensive research. Recent advances in instrumental analysis seem to have solved the problem to some extent. At present colorimetric, spectrophotometric, paper chromatographic, thin-layer chromatographic (TLC), gas chromatographic (GC), high-performance liquid chromatographic (HPLC) and GC-mass spectrometric with selected ion monitoring (GC-MS-SIM) techniques, in order of historical development, are available. However, they differ greatly with respect to specificity, sensitivity, accuracy and simplicity. The choice of analytical procedure differs according to the specific aims and the nature of biological samples to be analysed. In this work methods of quantitative microanalysis of bile acids such as radioimmunoassay (RIA), TLC, HPLC and GC-MS-SIM were compared a double-blind fashion with respect to various biological samples such as bile, plasma and urine. Seven leading laboratories in Japan participated in the study.

EXPERIMENTAL

As no single laboratory had sufficient expertise on all the analytical procedures to be compared, a collaborative study was necessary. This study was designed to include leading laboratories specializing in bile acid research, and Kyushu University Faculty of Medicine, Department of Surgery I, Fukuoka (Professor Fumio Nakayama, Dr. Jiro Yanagisawa and Dr. Hitoshi Ichimiya), Hiroshima University School of Medicine, Department of Pharmaceutical Sciences, Hiroshima (Professor Takehiko Hoshita), Tottori University School of Medicine, Steroid Research Institute, Yonago (Professor Shiro Ikawa), University of Tsukuba School of Medicine, Department of Internal Medicine, Ibaraki (Professor Toshiaki Osuga and Dr. Yasushi Matsuzaki), Tohoku University, Pharmaceutical Institute, Department of Analytical Chemistry, Sendai (Professor Toshio Nambara and Dr. Junichi Goto), Hirosaki University School of Medicine, Department of Internal Medicine III, Hirosaki (Associate Professor Isao Makino) and Nihon Kayaku Research Institute, Tokyo, Japan (Dr. Hiroshi Miyazaki) participated.

Each laboratory was asked to perform particular analyses according to their expertise. The comparative study was carried out in a double-blind fashion. A set of the same bile, urine and plasma samples was distributed to each participating institution, identification of the samples being known only to the principal investigator (Prof. Fumio Nakayama). The bile samples used were either puncture aspirated gall-bladder bile at the time of cholecystectomy or hepatic bile collected via external drain from obstructive jaundice cases. A total of ten bile samples were distributed, of which three were prepared in triplicate from the same bile sample. As large amounts of human serum could not be obtained, frozen plasma (with sodium tartrate, citric acid and glucose added) from a blood bank and human plasma obtained at the time of plasmapheresis was used. Ten plasma samples were distributed, of which three were prepared in triplicate from the same plasma sample. Urine was obtained from by 24-h collection from patients with cholelithiasis, obstructive jaundice and gastric cancer.

Ten urine samples including three triplicate samples prepared from the same sample were also distributed.

In order to avoid the variances arising from differences in the bile acid standard used, ursodeoxycholic acid, *ca.* 99% pure by GC, obtained from Tokyo Tanabe (Tokyo, Japan) was also shipped to each participating laboratory.

Analytical procedures

Enzymatic analysis (EA). 3α -Hydroxysteroid dehydrogenase (3α -HSD) and 7α -HSD and 3β -HSD were used^{1,2}. In some cases, bile acids in plasma were analysed enzymatically after fractionation into free and glycine- and taurine-conjugated bile acids by piperidinohydroxypropyl-Sephadex LH-20 (PHP-LH-20) column chromatography³.

RIA. Glycocholic acid (GCA) and glycochenodeoxycholic acid (GCDCA) RIA methods were used, with antisera prepared in the laboratory or obtained commercially (Dainabott or Eiken Immunochemicals, Tokyo, Japan)^{4,5}.

GC. After extraction of biological samples and hydrolysis, bile acids were derivatized into either methyl ester trimethylsilyl or ethyl ester dimethylethylsilyl ethers and subjected to GC using packed^{6,7} or capillary⁸ columns. For plasma samples, solvolysis preceded hydrolysis.

TLC. After separation on thin-layer plates and colour development, free and glycine- and taurine-conjugated bile acids were quantitated densitometrically⁹.

HPLC. Bile acids in bile or plasma were extracted with a Sep-Pak C₁₈ column¹⁰ followed by fractionation on a PHP-LH-20 column into free and glycine- and taurine-conjugated bile acids. Each group was separated by HPLC with various detection systems: (1) direct UV detection, (2) prelabelling with 1-anthroyl nitrile¹¹ and (3) UV detection after passage through a 3α -HSD column¹². An ethanol extract of bile was injected directly into the HPLC instrument when profile analysis was desired¹³. The columns and separation conditions used have been described previously^{3,11-13}.

GC-MS-SIM. A capillary column gas chromatograph coupled with a multiple ion detector was used with five deuterated bile acid standards¹⁴.

Comparison of methods. Each method provides a variety of information. Therefore, in order to compare the accuracy and precision of the various methods tested, values for total bile acids, the ratio of trihydroxy- to dihydroxy-bile acids and of glyco- to tauro-bile acids and 7α -hydroxylated bile acids (cholic and chenodeoxycholic acids) were used as common denominators. Total bile acids in bile and plasma was the sum of lithocholic, deoxycholic, chenodeoxycholic, ursodeoxycholic and cholic acids for TLC, GC, HPLC, HPLC with 3α -HSD detection and GC-MS-SIM, whereas for urine it was the sum of all peaks identified as bile acids by GC and GC-MS. For RIA the values for conjugated cholic and chenodeoxycholic acids were calculated and compared.

RESULTS

Bile acids in bile

By statistical evaluation of the analysis of the triplicate samples¹⁵, the analytical errors arising from the sample preparation and those from the determination

TABLE I

TOTAL BILE ACID CONCENTRATION IN TRIPPLICATE BILE SAMPLE

C.V. = Coefficient of variation; 3 α -HSD = 3 α -hydroxysteroid dehydrogenase.

Method	Laboratory	Mean \pm S.D. (mM) (n = 3)	C.V. (%)	Variance*
3 α -HSD	C	(99.2 \pm 1.1) (n = 1)**		
	D	92.9 \pm 3.3	3.5	NS
	F	(103.9 \pm 8.2) (n = 1)**		
TLC	E	97.0 \pm 11.5	11.8	NS
GC	A	(68.9 \pm 4.3) (n = 1)**		
	E	73.3 \pm 8.0	10.9	NS
	F	114.2 \pm 16.3	14.3	S (1%)
HPLC	B	97.9 \pm 7.5	7.7	S (1%)
GC-MS-SIM	G	102.2 \pm 8.6	8.5	NS

* The analytical errors were divided into two sources, viz., sample preparation or measurement itself. S = Error during sample preparation was significant; NS = not significant.

** Single sample was used, but three determinations were made.

itself could be distinguished. The concentration of total bile acids obtained ranged from 70 to 110 mM and the inter-laboratory variations seem to be large (Table I). 3 α -HSD gave only a small inter-laboratory variation. Those obtained by TLC resembled closely those obtained by GC-MS-SIM. The coefficient of variation was also small. The underestimation by GC in laboratories A and E was considerable but could be corrected by using an appropriate internal standard.

Differences between the various analytical methods in determining the bile acid composition was evaluated using triplicate samples (Table II). With respect to the percentages of cholic acid (CA) and chenodeoxycholic acid (CDCA) compared with total bile acids (TBA), TLC was found to be inadequate because it gave a poor resolution of the conjugated dihydroxycholanoic acids present in bile, i.e., the conjugates of CDCA from deoxycholic acid (DCA). As shown in Table II, percentage of CDCA and CA in TBA ranged from 36 to 43% for CDCA and from 42 to 49% for

TABLE II

COMPOSITION OF BILE ACIDS IN TRIPPLICATE BILE SAMPLE

Tri = Trihydroxycholanoic acid; Di = dihydroxycholanoic acid.

Method	Laboratory	Mean \pm S.D. (%) (n = 3)		Tri/Di
		CDCA	CA	
TLC	E	—	48.8 \pm 3.0	1.03 \pm 0.06
GC	A	(36.8 \pm 1.5) (n = 1)*	(44.0 \pm 1.7) (n = 1)*	(0.79 \pm 0.05) (n = 1)*
	E	37.3 \pm 1.6	45.1 \pm 0.4	0.82 \pm 0.02
	F	41.9 \pm 1.4	41.9 \pm 0.8	0.73 \pm 0.02
HPLC	B	36.3 \pm 2.2	47.8 \pm 1.9	0.91 \pm 0.07
	F	37.2 \pm 0.7	44.8 \pm 1.4	0.82 \pm 0.04
GC-MS-SIM	G	42.6 \pm 0.4	49.1 \pm 0.2	0.99 \pm 0.01

* Single sample was used, but three determinations were made.

TABLE III
GLYCINE/TAURINE RATIO OF CONJUGATED BILE ACIDS IN TRIPPLICATE BILE SAMPLE

Method	Laboratory	Mean \pm S.D. ($n = 3$)	C.V. (%)	Variance*
TLC	E	4.59 \pm 0.77	16.9	NS
HPLC	B	3.07 \pm 0.25	8.1	S (1%)
	F	3.07 \pm 0.09	2.9	NS

* The analytical errors were divided into two sources, viz., sample preparation or measurement itself. S = Error during sample preparation was significant; NS = not significant.

TABLE IV
TOTAL BILE ACID* CONCENTRATION IN TRIPPLICATE PLASMA SAMPLE

Method	Laboratory	Mean \pm S.D. (μ M) ($n = 3$)	C.V. (%)	Variance**
3 α -HSD	A	(4.9 \pm 0.5) ($n = 1$) ^{§§}		
	D	7.3 \pm 0.3	4.6	NS
PHP-3 α -HSD***	B	7.0 \pm 1.6	22.9	S (1%)
	C	5.3 \pm 0.3	5.7	NS
GC	A	(0.1 \pm 0.1) ($n = 1$) ^{§§}		
HPLC-3 α -HSD [§]	C	(3.5 \pm 0.3) ($n = 1$) ^{§§}		
GC-MS-SIM	G	5.2 \pm 0.2	3.7	NS

* Sum of free, glyco- and tauro-bile acids.

** Analytical errors were divided into two sources, viz., sample preparation or measurement itself. S = Error during sample preparation was significant; NS = not significant.

*** Fractionation on PHP-Sephadex LH-20 followed by 3 α -HSD detection.

§ HPLC connected with 3 α -HSD column¹².

§§ Single sample was used, but three determinations were made.

TABLE V
TOTAL BILE ACID* CONCENTRATION IN PLASMA SAMPLE

Method	Laboratory	Mean \pm S.D. (μ M) ($n = 3$)		
		Sample S-8	Sample S-9	Sample S-10
3 α -HSD	D	16.1 \pm 0.7	14.4 \pm 0.3	19.1 \pm 0.6
HPLC-D**	B	6.7 \pm 0.1	4.0 \pm 0.1	16.7 \pm 0.2
HPLC-3 α -HSD***	C	4.6 \pm 0.1	4.1 \pm 0.6	15.1 \pm 0.0
GC-MS-SIM	F	6.0 \pm 0.3 [§]	3.2 \pm 0.1	12.3 \pm 1.1

* Sum of free, glyco- and tauro-bile acids.

** HPLC with detection of derivatized bile acid¹¹.

*** HPLC connected with 3 α -HSD column¹².

§ Including sulphated bile acid formation.

TABLE VI

DETERMINATION OF 7 α -HYDROXYLATED BILE ACIDS WITH 7 α -HYDROXYSTEROID DEHYDROGENASE (7 α -HSD) DETECTION *VERSUS* SUM OF CHOLIC AND CHENODEOXYCHOLIC ACIDS BY GC-MS-SIM

Triplicate determinations for each sample. Results in μ M.

Sample	7 α -HSD		GC-MS-SIM*	
	Laboratory A	Laboratory D	Laboratory F	Laboratory G
S-1				
S-2	3.8 \pm 1.0	4.2 \pm 0.3	—**	4.0 \pm 0.1
S-3			—	
S-4	113	98.1 \pm 3.4	—	112 \pm 1
S-5	3.9	4.2 \pm 0.1	—	3.8 \pm 0.1
S-8	—	7.9 \pm 0.3	4.9 \pm 0.1	—
S-9	—	5.3 \pm 0.2	1.8 \pm 0.1	—
S-10	—	11.3 \pm 0.3	11.7 \pm 0.9	—

* Including sulphated fraction.

** Not determined.

CA. The coefficient of variation for the percentage of CA or CDCA in the triplicate samples using the same analytical procedure was below 6.0%, much less than the 15% (Table I) in quantitative analysis by GC, HPLC and GC-MS-SIM. The minimum coefficient of variation for bile acid composition of less than 1% was found using GC-MS-SIM. Close agreement was obtained for CA/TBA and CDCA/TBA between GC in laboratories A and E and HPLC in laboratories B and F.

The trihydroxycholanoic acid/dihydroxycholanoic acid ratio varied greatly, from 0.73 by GC (laboratory F) to 1.03 by TLC (laboratory E). However, the coefficient of variation using the same method in the same laboratory on the triplicate samples was 1–8%. The glycine/taurine conjugation ratios agreed well with those obtained by the HPLC in laboratories B and F (Table III). However, the value obtained by TLC was 50% higher than those by HPLC.

Analysis of bile acids present in bile in minute amounts, *i.e.*, lithocholic (LCA) and ursodeoxycholic acids (UDCA), gave large coefficients of variation from 50 to

TABLE VII

RIA *VS.* OTHER METHODS: CONJUGATED CHOLIC ACID LEVEL IN PLASMA

Triplicate determinations. Results in μ M.

Sample	RIA (laboratory A)	HPLC-D* (laboratory B)	HPLC-3 α -HSD** (laboratory C) (n = 1)	GC-MS-SIM (laboratory F)
S-8	0.99 \pm 0.18	0.51 \pm 0.00	0.47	—
S-9	0.95 \pm 0.09	0.47 \pm 0.03	0.45	—
S-10	4.45 \pm 0.13	9.10 \pm 0.11	7.92	7.28 \pm 0.36***

* HPLC with detection of derivatized bile acid¹¹.

** HPLC connected with 3 α -hydroxysteroid dehydrogenase column¹². Single determination.

*** After group separation on PHP-Sephadex LH-20 column.

TABLE VIII

RIA VS. OTHER METHODS: NON-SULPHATED CHENOXYCHOLIC ACID LEVEL IN PLASMA

Triplicate determinations. Results in μM .

Sample	RIA* (laboratory A)	HPLC-D** (laboratory B)	HPLC-3 α -HSD*** (laboratory C)	GC-MS-SIM (laboratory G)
S-1		—	2.1	
S-2	2.4 \pm 0.9	—	2.1	3.6 \pm 0.2
S-3		—	1.5	
S-4	70.7 \pm 11.0	—	36.2	53.4 \pm 1.5
S-5	2.7 \pm 0.4	—	2.2	3.1 \pm 0.1
S-8	2.0 \pm 0.1	4.9 \pm 0.1	3.5	—
S-9	1.7 \pm 0.2	1.9 \pm 0.0	1.9	—

* RIA system detected non-sulphated fraction of unconjugated, glyco- and tauro-chenodeoxycholic acid.

** HPLC with detection of derivatized bile acid¹¹.

*** HPLC connected with 3 α -hydroxysteroid dehydrogenase column¹². Single determination only.

14% (the latter by GC-MS-SIM). It was not possible to determine LCA and UDCA quantitatively by TLC.

Plasma bile acids

Results for total bile acids in the triplicate plasma samples are summarized in Tables IV and V. The coefficient of variation was smallest with GC-MS-SIM, in-

TABLE IX

URINARY BILE ACID DETERMINATION

Triplicate determinations. Results in μM .

Sample	GC (laboratory A)	GC-MS-SIM (laboratory F)	GC-MS-SIM (laboratory G)
<i>Total bile acids in sulphated and non-sulphated fractions:</i>			
U-1	0.32*	3.10 \pm 0.44	3.80 \pm 0.08
U-2**	47.1		
U-3**	70.2	90.8 \pm 8.2	94.8 \pm 5.0
U-4	45.5	(C.V. 9%)	(C.V. 5%)
U-5	7.3	16.6 \pm 2.7	22.4 \pm 0.5
<i>Sulphated and non-sulphated CDCA:</i>			
U-1	0.20*	1.24 \pm 0.29	1.44 \pm 0.02
U-2**	5.22		
U-3**	1.53	25.2 \pm 1.3	29.6 \pm 2.1
U-4**	1.63	(C.V. 5%)	(C.V. 7%)
U-5	2.45	5.98 \pm 1.09	8.15 \pm 0.21

* Single determination

** Triplicate sample.

TABLE X

URINARY BILE ACID DETERMINATION: ENZYMATIC METHODS VS. GC-MS-SIM

Sample	Total bile acids (μM) [*]	
	Enzymatic method ^{**}	GC-MS-SIM ($n = 3$)
U-6	8.65	2.30 \pm 0.17
U-7	12.23	0.87 \pm 0.12
U-9	23.92	80.95 \pm 1.98

^{*} Sum of sulphated and non-sulphated bile acids.

^{**} Determined with 3 α -hydroxysteroid dehydrogenase (3 α -HSD), 3 α -HSD and 7 α -HSD after solvolysis.

dicating the necessity to use an internal standard to correct for the losses occurring during the sample preparation.

The 7 α -HSD method for the determination of primary bile acids, *i.e.*, CA and CDCA, was compared with GC-MS-SIM (Table VI). Analyses of triplicate samples showed that the value obtained with 7 α -HSD was comparable to those given by GC-MS-SIM but coefficient of variation was fairly large (26%) and sometimes an excessively high value was obtained (laboratory D).

The values given by RIA for triplicate samples showed good agreement with those obtained by the other methods (Tables VII and VIII). However, the values from other samples were variable by 200–50%. Therefore, the analytical error when using RIA seems to be unacceptably large.

Urinary bile acids

Enzymatic analysis (EA), GC and GC-MS-SIM were compared for the determination of urinary bile acids (Tables IX and X). In contrast to the good agreement obtained by GC-MS-SIM in two laboratories, EA gave variable results in spite of the refinement made in the clean-up steps such as inclusion of solvolysis. Therefore, EA is not suitable for the analysis of urinary bile acids (Table X).

DISCUSSION

It is relatively easy to analyse bile acids in bile as there are fewer compounds in bile that interfere with the determination. However, when bile has a high viscosity, the sampling errors could be large unless due precautions are taken, *i.e.*, a blow-out pipette should be used to minimize the error. During fractionation by methods such as PHP-LH-20 column chromatography prior to HPLC, GC or GC-MS-SIM, the use of a suitable internal standard is essential to ensure adequate reproducibility and to compensate for the sample losses during the clean-up steps. Even with a relatively simple analytical procedure such as TLC a reasonably high accuracy can be obtained, although the separation of individual conjugated dihydroxycholeanoic acids is not satisfactory. The inter-laboratory variation was relatively small when using EA, GC and HPLC. However, GC with a packed column and HPLC without specific detec-

tion are unsuitable for the determination of minor bile acids such as LCA and UDCA because the peaks are broad and even with microcomputer control the reproducibility is not satisfactory. One must resort to GC-MS-SIM for the analysis of minor bile acids.

As the concentration of bile acids in normal human serum is very low, except for GC-MS-SIM the usual analytical methods such as TLC, HPLC and GC are unsatisfactory. EA using 3 α -HSD is simple yet sensitive for the analysis of total bile acids but its major drawback is its inability to determine sulphated bile acids, which are present at levels of 10–50%¹⁶. The analytical error by EA is small, even with low concentrations such as in normal serum, compared with the other analytical procedures but tends to overestimate. Therefore, double checking by other analytical methods such as GC-MS-SIM is recommended. EA with 7 α -HSD is useful for determining primary bile acids, *i.e.*, the sum of CA and CDCA. For preliminary fractionation by PHP-LH-20 column chromatography followed by enzymatic determination with 3 α -HSD to be successful, a correlation must be made for the losses occurring in the clean-up and fractionation steps. RIA applied to conjugated CA and CDCA gave variable values compared with those obtained by other methods but is useful as a screening procedure for large numbers of samples because of its simplicity. The sensitivity of GC with a packed column was found to be insufficient for the analysis of bile acids present in normal serum at very low concentrations but is adequate for serum with a high bile acid content such as in obstructive jaundice. The use of a suitable internal standard is essential. However, GC with a capillary column and solventless¹⁴ or splitless injection mode may have sufficient sensitivity for the determination of major bile acids in serum. HPLC using UV detection is not sufficiently sensitive to be applicable to the analysis of bile acids present in normal serum. HPLC coupled with prelabelling of bile acids (HPLC-D)¹¹ was found to have sufficient sensitivity and accuracy and could be used for the analysis of bile acids present in low concentrations such as in normal human serum. With the fixed HPLC with 3 α -HSD detection, it usually gives lower values than those obtained by HPLC-D or GC-MS-SIM and the sensitivity is lower than that given by HPLC-D. However, with the use of a suitable internal standard, it may well be suitable for the analysis of major bile acids in normal human serum. However, with HPLC procedures there certain problems have to be solved such as the determination of sulphated bile acids and elucidation of the nature of unknown peaks. On the other hand, GC-MS-SIM with deuterated bile acid standards has been found to be satisfactory with regard to specificity, accuracy and sensitivity in analysing serum bile acids and is specially useful for the determination of minor bile acids and the characterization of unknown peaks. However, in order to obtain information on conjugate forms, preliminary fractionation steps by other procedures are necessary.

For the analysis of urinary bile acids, EA is totally unsuitable because of the presence of various keto bile acids. Even GC is unreliable. Satisfactory corrections cannot be made because of the complex preliminary fractionation steps involved, and the sensitivity of GC is not sufficient for the analysis of bile acids present in low concentrations in urine. Although there is a small difference in the values obtained by GC-MS-SIM in two laboratories, their coefficients of variation were less than 9%, as shown in Table IX.

Urinary bile acids are sulphated to a greater extent than serum bile acids and

some portion of urinary bile acids is glucuronidated. Unusual orientations of hydroxy and keto groups have been found to be present. Therefore, more complex but practicable preliminary clean-up and fractionation steps with good reproducibility and recovery are necessary. At present, GC-MS is the only reliable analytical procedure for urinary bile acids.

ACKNOWLEDGEMENT

This work was aided by Research Grant 56370042 (principal investigator: F. N.) from the Ministry of Education, Science and Culture, Japanese Government.

REFERENCES

- 1 F. Mashige, K. Imai and T. Osuga, *Clin. Chim. Acta*, 70 (1976) 79.
- 2 S. Ikawa, H. Kawasaki, Y. Yamanishi, T. Mura and M. Miyake, *Tohoku J. Exp. Med.*, 145 (1985) 185.
- 3 J. Goto, M. Hasegawa, H. Kato and T. Nambara, *Clin. Chim. Acta*, 87 (1978) 141.
- 4 W. J. Simmonds, M. G. Korman, V. L. W. Go and A. F. Hofmann, *Gastroenterology*, 65 (1973) 705.
- 5 I. Makino, A. Tashiro, H. Hashimoto, S. Nakagawa and I. Yoshizawa, *J. Lipid Res.*, 19 (1978) 443.
- 6 I. Makino, H. Hashimoto, K. Shinozaki, K. Yoshino and S. Nakagawa, *Gastroenterology*, 68 (1975) 545.
- 7 S. M. Grundy, E. H. Ahrens, Jr., and T. A. Miettinen, *J. Lipid Res.*, 6 (1965) 397.
- 8 W. Van der Linden, B. Katzenstein and F. Nakayama, *Cancer*, 52 (1983) 1265.
- 9 A. Kibe, T. Kuramoto and T. Hoshita, *Anal. Biochem.*, 100 (1979) 146.
- 10 K. D. R. Setchell and A. Matsui, *Clin. Chim. Acta*, 127 (1983) 1.
- 11 J. Goto, M. Saito, T. Chikai, N. Goto and T. Nambara, *J. Chromatogr.*, 276 (1983) 289.
- 12 S. Onishi, S. Itoh and Y. Ishida, *Biochem. J.*, 204 (1982) 135.
- 13 F. Nakayama and M. Nakagaki, *J. Chromatogr.*, 183 (1980) 287.
- 14 J. Yanagisawa, Y. Akashi, H. Miyazaki and F. Nakayama, *J. Lipid Res.*, 25 (1984) 1263.
- 15 G. W. Snedecor and W. G. Cochran, *Statistical Methods*, Iowa State University Press, Iowa, 5th ed., 1956, p. 237.
- 16 I. Makino, H. Hashimoto, K. Shinozaki, K. Yoshino and S. Nakagawa, *Gastroenterology*, 68 (1975) 545.

CHROM. 20 793

IMPROVED SOLID-PHASE EXTRACTION AND LIQUID CHROMATOGRAPHY WITH ELECTROCHEMICAL DETECTION OF URINARY CATECHOLAMINES AND 5-S-L-CYSTEINYL-L-DOPA

TIEHUA HUANG*, JEFFREY WALL and POKAR KABRA*

Department of Laboratory Medicine, University of California, San Francisco, CA 94143 (U.S.A.)

SUMMARY

We describe a rapid, precise, accurate liquid chromatographic procedure for determining urinary catecholamines and 5-S-L-cysteinyl-L-dopa. The catecholamines (norepinephrine, epinephrine, and dopamine) and 5-S-L-cysteinyl-L-dopa are extracted from 1.0 ml of urine together with internal standards, by using a Bond-Elut strong cation-exchange (SCX) and an affinity phenylboronic acid (PBA) extraction column in series. The eluate obtained from PBA column is then chromatographed on a reversed-phase C₁₈ column with a mobile phase containing pentane- and heptanesulfonate as ion-pair reagents. The detection is achieved with an amperometric detector set at an oxidation potential of +0.55 V. The chromatography is complete in less than 8 min for catecholamines and less than 5 min for cysteinyl-dopa. The method can measure less than 2 µg/l for catecholamines and 5 µg/l for cysteinyl-dopa. Analytical recoveries of catecholamines and cysteinyl-dopa added to urine pool ranged from 90–107%. Between run coefficient of variation ranged from 4.7 to 8%. None of the drugs and catecholamines metabolites tested interfered with the assay.

INTRODUCTION

Laboratory measurements of norepinephrine, epinephrine, dopamine and/or their metabolites are primarily useful for the diagnosis of catecholamine-secreting neurochromaffin tumors (pheochromocytomas, neuroblastomas), metabolic disorders, manic-depressive psychoses, and essential hypertension. The neurochromaffin tumors may produce excessive amounts of catecholamines or their metabolites¹. Measurement of urinary catecholamines and vinylmandelic acid is best applied to follow-up testing in patients with an elevated metanephrines or those subjects highly suspect for pheochromocytoma². Urinary 5-S-L-cysteinyl-L-dopa was recently evaluated as tumor marker for malignant melanoma and found to be a good estimate of the increased tumor burden in patients with metastases³.

Liquid chromatography with electrochemical detection (LC-ED) has gained

* Visiting scientist from Railway Medical College, Nanjing, China.

wide acceptance as a preferred method for the measurement of urinary catecholamines and 5-S-L-cysteinyl-L-dopa^{4,5}. A number of procedures utilizing cation exchange resin⁶, boric acid gel⁷, alumina⁸, alumina and boric acid gel⁹, Bond-Elut cation-exchange column¹⁰, and Sep-Pak extraction cartridges¹¹ have been used for the isolation of catecholamines from urine and plasma. A single-step extraction procedure using alumina, cation-exchange columns, or boric acid gel has proved inadequate, because endogenous peaks interfered with the catecholamine analysis^{12,13}. As a result, current LC-ED methods generally require elaborate, tedious, and time consuming sample preparation steps for LC-ED¹⁴.

Here, we describe a solid phase extraction method employing bonded phase sorbents for the isolation of catecholamines and 5-S-L-cysteinyl-L-dopa from urine. The selective isolation of catecholamines was accomplished by using two different kinds of Bond-Elut columns (strong cation exchange, and affinity mode). This chromatographic mode sequencing resulted in the selective isolation of catecholamines and 5-S-L-cysteinyl-L-dopa. The urine sample is first passed through a strong cation-exchange (SCX) Bond-Elut column which selectively retains the cationic species including catecholamines and its basic metabolites from the urine. This is followed by the elution of cationic catecholamines onto an affinity phenylboronic acid (PBA) column, where covalent bond formation with the *cis*-diol group of catecholamines takes place in a neutral or alkaline medium. Therefore, the PBA column selectively retains the *cis*-diol containing catecholamines, while other polar and non-polar cationic constituents are washed off with aqueous or polar organic solvent washes. This relatively simple, rapid and specific sample preparation scheme has dramatically improved the quality of chromatographic analysis.

EXPERIMENTAL

Apparatus

Analysis was performed on a Series 3B (Perkin-Elmer, Norwalk, CT, U.S.A.) liquid chromatograph equipped with a Model 7105 (Rheodyne, Cotati, CA, U.S.A.) injector equipped with a 150- μ l sample loop, a LC-4B electrochemical detector (Bioanalytical Systems, West Lafayette, IN, U.S.A.), a Model BD 41 (E and K Scientific Products, Saratoga, CA, U.S.A.) recorder, and a 150 \times 4.6 mm Ultrasphere ODS 5 μ m column (Beckman, San Ramon, CA, U.S.A.) maintained at 35°C in a Model LC 100 column oven (Perkin-Elmer). A Vac-Elut apparatus and Bond-Elut SCX and Bond-Elut PBA extraction columns containing 100 mg of respective bonded phases were obtained from Analytichem International, Harbor City, CA, U.S.A. The mobile phase for catecholamine analysis was prepared by dissolving 300 mg of heptanesulfonate, 100 mg of disodium salt of EDTA, 13.8 g of NaH₂PO₄ · H₂O (0.1 M), and 15 ml of acetonitrile in 1 l water. The pH of the mobile phase was adjusted to 3.0 with 0.1 M phosphoric acid. The mobile phase for 5-S-L-cysteinyl-L-dopa was prepared by dissolving 100 mg of pentanesulfonate, 50 mg of disodium EDTA, 2 ml of diethylamine, and 20 ml of acetonitrile in 1 l of water. The pH of the mobile phase was adjusted to 2.2 with 0.1 M phosphoric acid. The flow-rate for both analyses was set at 1.0 ml/min.

Reagents and standards

All inorganic reagents were analytical grade. Methanol and acetonitrile (HPLC grade) were obtained from J. T. Baker (Phillipsburg, NJ, U.S.A.). Deionized water

was used for preparing reagents and solutions. The saturated sodium carbonate solution was prepared by adding 30.0 g of sodium carbonate to 100 ml of water and shaking it vigorously. The 1 M perchloric acid solution was prepared by adding 43 ml of 11.6 M perchloric acid to 457 ml water. The 1 M hydrochloric acid solution was prepared by adding 42 ml of 12 M hydrochloric acid to 458 ml of water. The 1 M sodium hydroxide solution was prepared by dissolving 4 g of sodium hydroxide into 100 ml of water. The 1 M dipotassium hydrogenphosphate buffer was prepared by dissolving 174 g of dipotassium hydrogenphosphate to 1 l of distilled water.

The stock norepinephrine (300 $\mu\text{g/ml}$), epinephrine (100 $\mu\text{g/ml}$), dopamine (900 $\mu\text{g/ml}$), and the internal standard 3,4-dihydroxybenzylamine (100 $\mu\text{g/ml}$) were prepared by dissolving 36.5 mg of norepinephrine hydrochloride, 18.2 mg of epinephrine bitartrate, 111.1 mg of dopamine hydrochloride, and 15.8 mg of 3,4 dihydroxybenzylamine hydrobromide (Sigma, St. Louis, MO, U.S.A.) in 100 ml of 0.1 M hydrochloric acid, respectively. These standards are stable at 4°C for six months. The working standards of norepinephrine, epinephrine, dopamine, and internal standard containing 6.0 $\mu\text{g/ml}$ of norepinephrine, 2.0 $\mu\text{g/ml}$ of epinephrine, 18.0 $\mu\text{g/ml}$ of dopamine and 2.0 $\mu\text{g/ml}$ of internal standard were prepared in 0.1 M hydrochloric acid. The urine standards were prepared by adding 10, 20, 30 and 50 μl of norepinephrine, epinephrine and dopamine working standard solutions to increase the urine concentrations by 60, 120, 180 and 300 ng/ml for norepinephrine; 20, 40, 60 and 100 ng/ml for epinephrine; and 180, 360, 540 and 900 ng/ml for dopamine.

Synthesis and purification of 5-S-L-cysteinyl-L-dopa and 5-S-D-cysteinyl-L-dopa

The procedure of Agrup *et al.*¹⁵ was modified for the synthesis of 5-S-L-cysteinyl-L-dopa and 5-S-D-cysteinyl-L-dopa. The progress of the reaction was monitored by LC set up for measuring 5-S-L-cysteinyl-L-dopa, since both L-dopa and cysteinyl-dopa are detectable by electrochemical detector. The synthesis was carried in a 50 ml beaker to which 2.5 mg of tyrosinase (Sigma), 7.5 mg of L-dopa, and 10 mg of either L-cysteine or D-cysteine, were added as required. To the reaction mixture, 10 ml of 0.5 M potassium dihydrogenphosphate buffer at pH 6.5 was added and mixture stirred with a magnetic mixer. At approximately 10-min intervals, a 10- μl aliquot of this mixture, was removed and diluted with 10 ml of water, and a 10- μl aliquot was injected onto the LC. The L-dopa eluted just before cysteinyl-dopa. As the reaction progressed towards completion, the intensity of cysteinyl-dopa peak increased while L-dopa peak gradually decreased. When the reaction was complete, no more L-dopa was detectable by the LC system.

The cysteinyl-dopa was isolated from the other components of synthesis mixture by passing it through the PBA affinity columns. The PBA columns have affinity for cysteinyl-dopa and L-dopa. However, because all the L-dopa had been consumed by the excess cysteine, only cysteinyl-dopa was eluted from the affinity columns. The cysteinyl-dopa was isolated from ten PBA columns placed on the Vac Elut chamber, and activated by passing one column volume of methanol and 1 M dipotassium hydrogenphosphate buffer. The synthesis mixture (about 1 ml) was passed through each column, which was then washed with 2 volumes of water. Each column was eluted with 500 μl of 0.1 M hydrochloric acid and the eluate collected into 10 \times 75 mm collecting tubes. The contents of the ten collecting tubes were pooled and an aliquot of the pool was then injected onto LC to assess the purity of cysteinyl-dopa.

The concentration of cysteinyl-dopa was calculated from its molar absorptivity of 2800 at 292 nm. The concentrated cysteinyl-dopa was then diluted to 100 $\mu\text{g/ml}$ with 0.2 *M* hydrochloric acid containing 100 mg/l of ascorbic acid and stored frozen at -20°C until needed.

Standards for 5-S-L-cysteinyl-L-dopa analysis

A reference standard containing a solution of 200 ng/ml of 5-S-L-cysteinyl-L-dopa and 5-S-D-cysteinyl-L-dopa (internal standard) was prepared by adding 100 μl of stock 5-S-L-cysteinyl-L-dopa and 5-S-D-cysteinyl-L-dopa to 50 ml of 0.2 *M* hydrochloric acid containing 100 mg/l of ascorbic acid as preservative. The reference standard was aliquoted into 500 μl portions and frozen at -20°C for subsequent use. The standards are stable for six months when kept frozen, and two days when kept at room temperature. The working internal standard containing 200 ng/ml of 5-S-D-cysteinyl-L-dopa was prepared by diluting 1 ml of 100 $\mu\text{g/ml}$ of stock internal standard with 500 ml of 0.2 *M* hydrochloric acid containing 100 mg/l ascorbic acid. After mixing, a 0.5-ml volume was aliquoted and frozen at -20°C for subsequent use. The standard is stable for six months, when kept frozen, and two days when kept at room temperature.

Controls. The urine blank was prepared by adjusting the pH of urine above 10 with 1 *M* sodium hydroxide and allowing it to stand for few days at room temperature. This urine was analyzed for endogenous 5-S-L-cysteinyl-L-dopa and usually contained less than 10 ng/ml. For the low control (100 $\mu\text{g/l}$), 0.5 ml of 100 $\mu\text{g/ml}$ stock 5-S-L-cysteinyl-L-dopa standard was added to 500 ml of blank urine; and for high control (500 $\mu\text{g/l}$), 2.5 ml of the stock 5-S-L-cysteinyl-L-dopa standard was added to 497.5 ml of blank urine. The controls were aliquoted into 1-ml portions, and frozen and stored at -20°C . The controls are stable for six months.

Specimens. A 24-h urine sample was collected in a container with 10 ml of 6 *M* hydrochloric acid. Catecholamines and 5-S-L-cysteinyl-L-dopa are stable in acidified urine for upto a week if stored at 4°C . Patients should avoid exposure to sunlight as much as possible for two weeks preceding the collection of urine sample due to the increased synthesis of 5-S-L-cysteinyl-L-dopa by exposure to sun light.

Extraction procedure for catecholamines

To 1.0 ml of appropriate standard, control, or unknown urine into labeled 13 \times 100 mm disposable glass tube, was added 50 μl of working internal standard (3,4-dihydroxybenzyl amine) solution and 5 ml of water. The pH of the sample was adjusted to 6.5–7.0 with 1 *M* and/or 0.05 *M* sodium hydroxide. The SCX and PBA columns were placed on the top of Vac-Elut chamber and connected to a source of reduced pressure. Both columns were activated by washing them with three column volumes of 1 *M* hydrochloric acid, followed by two column washes of methanol and 0.01 *M* ammonium acetate (pH 7.3). A reservoir was placed above the activated SCX column into which urine was poured and it was connected to the vacuum source. The SCX columns were washed with two column volumes of methanol followed by two column volumes of 0.01 *M* ammonium acetate. The SCX columns were eluted with 3 \times 500 μl of 1 *M* perchloric acid. The eluate was neutralized with 400 μl of saturated sodium carbonate, and then transferred to the activated PBA column. The PBA columns were washed with two column volumes of methanol followed by two column

volumes of water. Finally, the PBA columns were eluted with $2 \times 500 \mu\text{l}$ of $0.1 M$ perchloric acid solution. The eluate was mixed, then a $40\text{--}80\text{-}\mu\text{l}$ aliquot was injected onto the LC. The column was eluted with the mobile phase at a flow-rate of 1.0 ml/min at 35°C . The detection is achieved with an amperometric detector set at an oxidation potential of $+0.55 \text{ V}$. The quantitation of catecholamines is based on the peak-height ratio of analyte to internal standard.

Extraction procedure for 5-S-L-cysteinyl-L-dopa

For each standard, control, and unknown, a SCX column was placed on the Vac-Elut chamber. The columns were activated by passing one volume of methanol and one volume of $0.1 M$ hydrochloric acid. To 0.5 ml of each standard, control, or test sample placed into a $16 \times 100 \text{ mm}$ tube was added 0.5 ml of the working internal standard. The solution was mixed briefly, then the contents of each tube was transferred onto an activated SCX Bond-Elut column. The columns were washed with one volume of $0.1 M$ hydrochloric acid. The SCX columns were removed from the Vac-Elut chamber. A set of PBA Bond-Elut columns were placed on the Vac-Elut chamber and activated with one volume of methanol and one volume of $1 M$ dipotassium hydrogen phosphate. The SCX columns were then placed in order, on top of the PBA columns, and washed with two column volumes of $1 M$ dipotassium hydrogen phosphate. The SCX columns were removed from the PBA columns, and the PBA columns were washed with water. A set of $10 \times 75 \text{ mm}$ collecting tubes were placed under the PBA columns and eluted with 0.5 ml of $0.1 M$ hydrochloric acid with 10 mg/l ascorbic acid. The collecting tubes were vortex-mixed, and an aliquot of $20 \mu\text{l}$ was injected onto the LC. The column was eluted with the mobile phase at a flow-rate of 1.0 ml/min at 35°C . The detection is achieved with an amperometric detector set at an oxidation potential of $+0.55 \text{ V}$.

RESULTS

Recovery and linearity

Catecholamines were added to an urine pool in amounts equivalent to $10\text{--}600 \mu\text{g/l}$ for norepinephrine, $4\text{--}100 \mu\text{g/l}$ for epinephrine, and $30\text{--}1800 \mu\text{g/l}$ for dopamine. A constant amount of 3,4-dihydroxybenzyl amine (internal standard) was added to each sample, which was then processed as described above. Concentrations and peak height ratios were linearly related over these ranges. The correlation coefficients were 1.000 , 0.995 and 0.998 , respectively. Analytical recoveries for catecholamines are given in Table I. Similarly, 5-S-L-cysteinyl-L-dopa was added to an urine blank pool in amounts equivalent to $31\text{--}2000 \mu\text{g/l}$, which were then processed as described above. Concentrations and peak height ratios were linearly related over this range. The correlation coefficient was 1.000 . Analytical recovery for 5-S-L-cysteinyl-L-dopa is given in Table I.

Sensitivity and precision

The minimum limit of detection for the assay is $1 \mu\text{g/l}$ for norepinephrine and epinephrine, and $2 \mu\text{g/l}$ for dopamine. The signal-to-noise ratio was >3 at these concentrations. The minimum limit of detection for 5-S-L-cysteinyl-L-dopa is $5 \mu\text{g/l}$, at a signal-to-noise ratio of 3. Repeated analysis of pooled urine samples spiked with

TABLE I
RECOVERY OF CATECHOLAMINES AND 5-S-L-CYSTEINYL-L-DOPA FROM URINE

n = 5.

Norepinephrine			Epinephrine			Dopamine			5-S-L-Cysteinyl-L-dopa		
Added ($\mu\text{g/l}$)	Recovered ($\mu\text{g/l}$)	Recovery (%)	Added ($\mu\text{g/l}$)	Recovered ($\mu\text{g/l}$)	Recovery (%)	Added ($\mu\text{g/l}$)	Recovered ($\mu\text{g/l}$)	Recovery (%)	Added ($\mu\text{g/l}$)	Recovered ($\mu\text{g/l}$)	Recovery (%)
0*	72.2	0	0*	24.3	0	0*	244	0	31.2	28	90
10	82.2	100	4	30.5	107	30	267	99	62.5	59	94
25	97.0	98	10	32.2	95	180	447	106	125	114	91
60	126	95	20	42.9	97	360	639	106	250	251	100
120	205	107	40	61.8	96	540	777	99	500	489	98
300	374	100	60	79.3	94	900	1062	93	1000	991	99
600	669	99	100	129	103	1800	2063	101	2000	1945	97

* Blank.

catecholamines at two different levels and at the endogenous levels gave within-day coefficients of variation (C.V.) ranging from 2 to 8.3%. The day-to-day C.V. values ranged from 3.4 to 7.4%. Similarly, repeated analysis of pooled urine sample including the endogenous level of 5-S-L-cysteinyl-L-dopa at two different concentrations give within-day C.V. values ranging from 1.5 to 2.5%, while day-to-day C.V. values ranged from 4.7 to 8%.

Interferences

We evaluated potential interference in this assay by chromatographing pure solutions of drugs, catecholamine metabolites and/or samples of urine containing various catecholamines and their metabolites. Drugs tested but not detected under these conditions were: acetaminophen, amitriptyline, caffeine, carbamazepine, chloramphenicol, chlordiazepoxide, diazepam, ethosuximide, gentamicin, imipramine, pentobarbital, phenobarbital, phenytoin, primidone, salicylate, secobarbital, and theophylline. The catecholamine metabolites 3,4-dihydroxyphenylalanine (DL-DOPA), DL-3-O-methyl-DOPA, 4-hydroxy-3-methoxyphenylglycol, DL- α -methyl-DOPA, 3,4-dihydroxymandelic acid, vinylmandelic acid, homovanillic acid, normetanephrine and metanephrine did not interfere with this analysis.

DISCUSSION

For LC analysis of catecholamines and 5-S-L-cysteinyl-L-dopa in urine, a preliminary extraction step is required. For this purpose, various extraction methods utilizing cation-exchange resins, adsorption chromatography on alumina and affinity chromatography on boronic acid gels have been extensively used. However, many of these extraction methods suffer from endogenous interferences and low and erratic recovery of the desired analyte from the urine. Additionally, extraction methods using thin-layer chromatography, ion-exchange resins, and adsorption on alumina are time consuming and require careful evaluation of analytical recovery.

The PBA gels have been used for the isolation of catecholamines by several investigators^{9,16,17}. Kagedal and Peterson¹⁷ isolated 5-S-L-cysteinyl-L-dopa from urine by using phenyl boronate gel with good recovery. However, further improvement in the selectivity of extraction procedure was achieved by combining phenylboronate clean-up with a cation exchange extraction. However, the clean-up procedure was slow due to the instability of bed structure at reduced or positive pressure. Bonded phase silicas are useful material as sorbents for sample preparation for several reasons. They retain rigidity under positive or reduced pressure, thereby maintaining the sorbent bed dimensions. Because of the bed stability, they allow a rapid change in solvent polarity without contraction or swelling of silica. In addition, a wide variety of selective bonded phases can be synthesized on the silica surface for the isolation/extraction of different catecholamines and their metabolites¹⁶. The key to obtaining reproducible and high recoveries of a desired analyte is to identify the right kind of bonded-phase silica that is most selective for that compound. This selectivity is dependent on the differences in affinity between the desired analyte and interferences in the matrix for the sorbent.

Extraction on bonded-phase silica columns, especially the PBA extraction column, is more selective and efficient than ion-exchange resin clean-up for catechola-

mine isolation. PBA bonded silica in its ionized form binds covalently to compounds containing vicinal *cis*-diol groups such as those found in the catecholamines. The catecholamines are then eluted from the PBA columns with strong acid. The recovery and reproducibility are excellent. There are several advantages to using bonded-phase silica extraction phases over other isolation techniques (alumina-cation-exchange resin, and boronic acid gels) for catecholamines and 5-S-L-cysteinyl-L-dopa. In addition to interference-free analysis, the extraction procedure could be adapted for batch processing by using a Vac-Elut chamber. This vacuum chamber device allowed us to process ten urine samples simultaneously in less than 20 min. Under the extraction conditions described in this report, both SCX and PBA columns can withstand two column volumes of methanol washes, so that the non-polar components could be washed off these columns without affecting the recovery of catecholamines. Another distinct advantage of this extraction protocol is that both extraction columns (SCX and PBA) can be reused for at least eight urine analyses without affecting the recovery (>90%), reproducibility (coefficient of variation <8%), and selectivity of extraction columns. The ion-pair reversed-phase chromatographic analysis of catecholamines and 5-S-L-cysteinyl-L-dopa was optimized by varying the concentration of acetonitrile, ion-pair reagent, and pH of the mobile phase. The chromatograms obtained by these procedures are illustrated in Figs. 1 and 2. The three catecholamines and the

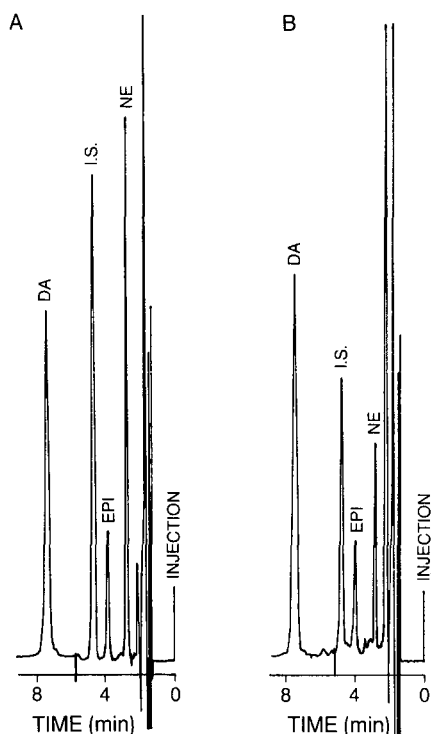


Fig. 1. (A) Chromatogram of urine standard containing 177 $\mu\text{g/l}$ of norepinephrine (NE), 48 $\mu\text{g/l}$ of epinephrine (EPI), and 224 $\mu\text{g/l}$ of dopamine (DA). (B) Chromatogram of urine sample from a patient containing 72.2 $\mu\text{g/l}$ of NE, 24.3 $\mu\text{g/l}$ of E, and 244 $\mu\text{g/l}$ of DA.

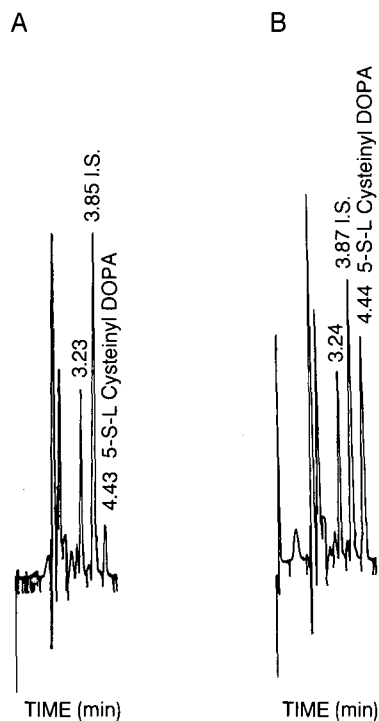


Fig. 2. Chromatograms and of patient urine samples containing (A) 40 $\mu\text{g/l}$ and (B) 198 $\mu\text{g/l}$ of 5-S-L-cysteiny-L-dopa.

internal standard are separated in less than 8 min. Similarly, 5-S-L-cysteiny-L-dopa and its internal standard 5-S-D-cysteiny-L-dopa are separated in less than 5 min.

Wu and Gornet¹⁹ compared three different extraction techniques (PBA, cation-exchange resin, and alumina) for the isolation of catecholamines from urine, and concluded that neither cation-exchange resin or alumina alone is suitable for routine use without altering the chromatographic conditions. Chromatographic interferences were observed for both cation exchange resin and alumina isolation, although the degree of interference varied from sample to sample. Both the PBA, and the combined cation-exchange resin alumina produced chromatograms with minimal interferences in most samples. However, by using both alumina and a cation-exchange step in a clean-up procedure, the recovery of catecholamines is adversely affected.

The use of silica-bonded PBA and SCX extraction columns in series helped solve many of the above mentioned problems. The major advantage of the silica-bonded phases, especially when connected to a vacuum manifold, is the shorter turn around time so that more than 80 samples can be processed in a work day. The chromatographic mode sequence (PBA in series with SCX extraction column) resulted in the selective isolation of catecholamines and 5-S-L-cysteiny-L-dopa. The combined PBA and SCX isolation scheme described by us is simple, rapid and selective for the extraction and analysis of catecholamines and 5-S-L-cysteiny-L-dopa.

REFERENCES

- 1 S. C. Chattoraj and N. B. Watts, in N. B. Tietz (Editor), *Text Book of Clinical Chemistry*, W. B. Saunders, Philadelphia, PA, 1986, p. 997.
- 2 S. E. Gitlow, M. Mendlowitz and Betrani, *Am. J. Cardiol.*, 26 (1970) 270.
- 3 G. Agrup, P. Agrup, T. Andersson, L. Hafstrom, C. Hansson, S. Jacobsson, P. E. Jonsson, H. Rorsman, A. M. Rosengren and E. Rosengren, *Acta Dermatoverner (Stockholm)*, 59 (1979) 381.
- 4 A. M. Krstulović, *J. Chromatogr.*, 229 (1982) 1.
- 5 S. Allenmark, *J. Liq. Chromatogr.*, 5, Suppl. 1 (1982) 1.
- 6 G. M. Tyce, N. S. Sharpless and C. A. Owen, *Biochem. Pharmacol.*, 21 (1972) 2409.
- 7 A. J. Speek, J. Odink, J. Schrijver and W. H. P. Scheurs, *Clin. Chim. Acta*, 128 (1983) 103.
- 8 P. T. Kissinger, R. M. Riffin, R. L. Alcorn and L. D. Rau, *Biochem. Med.*, 13 (1975) 299.
- 9 T. P. Moyer, N. S. Jiang, G. M. Tyce and S. G. Sheps, *Clin. Chem.*, 25 (1979) 256.
- 10 K. N. Frayn and P. F. Maycock, *Clin. Chem.*, 29 (1983) 1426.
- 11 D. S. Goldstein, *J. Chromatogr.*, 275 (1983) 174.
- 12 D. D. Koch and G. L. Polzin, *J. Chromatogr.*, 386 (1987) 19.
- 13 C. Lucarelli, P. Betto, G. Ricciarello, M. Giambenedeth, F. Sciarra, C. Tosticroce and P. L. Mottironi, *Chromatographia*, 24 (1987) 423.
- 14 E. Baraldi, D. Cavani, S. Seghedoni, G. Chiossi, L. Roli, A. T. Scacchatti and G. F. Baraghini, *Chromatographia*, 24 (1987) 407.
- 15 G. Agrup, L. E. Edholm, H. Rorsman and E. Rosengren, *Acta Dermatoverner (Stockholm)*, 63 (1983) 59.
- 16 L. S. Yago and T. J. Good, in P. M. Kabra and L. J. Marton (Editors), *Clinical Liquid Chromatography*, Vol. I, CRC Press, Boca Raton, FL., 1984, p. 197.
- 17 B. Kagedal and A. Petterson, *Clin. Chem.*, 29 (1983) 2031.
- 18 K. Oka, M. Sekiya, H. Osada, K. Fujita, T. Kato and T. Nagatsu, *Clin. Chem.*, 28 (1982) 646.
- 19 A. H. B. Wu and T. G. Gornet, *Clin. Chem.*, 31 (1985) 298.

CHROM. 20 489

IMMUNOAFFINITY PRE-COLUMN FOR SELECTIVE ON-LINE SAMPLE PRE-TREATMENT IN HIGH-PERFORMANCE LIQUID CHROMATOGRAPHY DETERMINATION OF 19-NORTESTOSTERONE

A. FARJAM*, G. J. DE JONG, R. W. FREI and U. A. Th. BRINKMAN

Department of Analytical Chemistry, Free University, De Boelelaan 1083, 1081 HV Amsterdam (The Netherlands)

and

W. HAASNOOT, A. R. M. HAMERS, R. SCHILT and F. A. HUF

State Institute for Quality Control of Agricultural Products, Bornsesteeg 45, 6708 PD Wageningen (The Netherlands)

SUMMARY

A liquid chromatographic column-switching system for automated sample pre-treatment and determination of the anabolic hormone β -19-nortestosterone (β -19-NT) and its metabolite α -19-nortestosterone (19-norepitestosterone) in calf urine is described. The system consists of an immunoaffinity pre-column (immuno pre-column) packed with Sepharose-immobilized polyclonal antibodies against β -19-NT, a second pre-column packed with C_{18} bonded silica and an analytical C_{18} column. Urine (25 ml) is directly loaded on the immuno pre-column, where the analytes of interest are trapped by the immobilized antibodies. Next the analytes are desorbed selectively with a solution containing an excess of the cross-reacting steroid hormone norgestrel and transferred, via the second pre-column, to the analytical column.

The recovery of β -19-NT in spiked urine samples was over 95%. The detection limit was 50 ng/l for a 25-ml urine injection. The system showed no loss of analytical performance over a 6-month period, during which about 100 samples were analysed with the same immuno pre-column. The general applicability of this sample pre-treatment method is discussed.

INTRODUCTION

The determination of trace amounts of analytes in complex samples is a well known problem area. In order to reduce the amount of interfering components and to enrich the analytes of interest sample pre-treatment is necessary in most instances. The use of small pre-columns packed with, *e.g.*, hydrophobic or hydrophilic stationary phases, ion exchangers and metal-loaded phases has gained widespread acceptance in this field¹. Immunoaffinity chromatography, however, which is based on antibody-antigen interaction and, thus, offers a highly selective retention mechanism in chromatography, has rarely been used for sample pre-treatment. The few examples found in the literature are mentioned below.

Small columns containing immobilized antibodies have been used for sample clean-up before quantification by bioassay. Gibberellins², estradiol^{3,4} and testosterone⁴ were determined in biological matrices such as plant extracts, blood plasma, milk and follicular fluid. In another study, the enantiomers of abscisic acid were purified on immunoaffinity columns before their thin-layer chromatographic separation⁵. Immunoaffinity columns have also been used in off-line sample pre-treatment for column high-performance liquid chromatographic (HPLC) analysis. An immunoaffinity column with immobilized antibodies against indole-3-acetamide has been used for the off-line purification of plant extracts prior to HPLC analysis⁶ and a similar approach has been reported for the purification and HPLC determination of cytokinins in plant extracts^{7,8}. Monoclonal antibodies have recently been used in a pre-column procedure for the clean-up of tissue extracts in combination with the HPLC determination of chloramphenicol⁹. Only a few on-line immunoaffinity sample pre-treatment systems for HPLC have been published. Phenytoin was determined by injecting a 25- μ l plasma sample on a pre-column packed with an antibody immobilized on silica (pore diameter 60 Å). The trapped phenytoin was desorbed by switching the immunoaffinity pre-column on-line with the analytical column¹⁰. A comparable system was used for the determination of cortisol in serum and urine samples¹¹.

In this paper we describe an on-line immunoaffinity sample pre-treatment procedure for HPLC, which allows both clean-up and trace enrichment by direct injection of large amounts of urine. The potential of the new technique is demonstrated for the determination of β -19-nortestosterone (β -19-NT) and its metabolite α -19-nortestosterone (or 19-norepitestosterone) (α -19-NT) in calf urine. Their structures are shown in Fig. 1. β -19-NT may be illegally used as an anabolic steroid for the growth promotion of cattle and also as a doping agent in sports. The determination of β -19-NT and α -19-NT in biological samples is extremely difficult, because in cases of abuse the concentrations in samples such as plasma, meat and urine are usually about or below 1 ppb, and also because, *e.g.*, many endogenous steroids interfere with their determination. Consequently, most existing analytical methods are cumbersome^{1,2,13}, because they consist of a combination of different analytical procedures, *e.g.*, off-line sample pre-treatment, HPLC and immunoassay. This paper demonstrates that with the help of an immunoaffinity sample pre-treatment step an automated HPLC system can be set up without the need for extensive off-line sample pre-treatment.

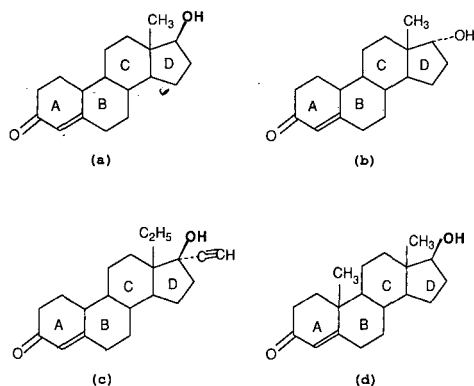


Fig. 1. Structures of (a) β -19-nortestosterone, (b) α -19-nortestosterone, (c) norgestrel and (d) testosterone.

EXPERIMENTAL

Apparatus

The set-up of the HPLC systems used is shown schematically in Fig. 2. HPLC system No. 1 consisted of two Kontron (Zurich, Switzerland) Model 410 pumps, both equipped with laboratory-made membrane pulse dampers, a Kontron MCS 670 Tracer valve switching unit, a Kontron Model 200 programmer, a Kratos (Ramsey, NJ, U.S.A.) Spectroflow 757 UV detector set at 247 nm, a Kipp & Zonen (Delft, The Netherlands) BD 40 recorder and a Kontron Anacomp Model 220 computer. The analytical column was a laboratory-packed 100 mm \times 3 mm I.D. glass column filled with 5- μ m LiChrosorb RP-18 (Merck, Darmstadt, F.R.G.), and was protected with a 10 mm \times 2 mm I.D. guard column packed with the same material. The 10 m \times 2 mm I.D. C₁₈ pre-column was packed with Baker (Deventer, The Netherlands) C₁₈ 40- μ m stationary phase.

HPLC system No. 2 consisted of a Merck-Hitachi (Darmstadt, F.R.G.) Model 655-A-11 pump for the analytical column, a Kratos Model 400 pump for sample handling, two Kratos Model Must valve-switching units, a Kratos Spectroflow 450 solvent programmer, a Merck-Hitachi L-4200 UV-VIS detector set at 247 nm and a Merck-Hitachi Model D 2000 integrator. The analytical column was a Chrompack (Middelburg, The Netherlands) 100 mm \times 3 mm I.D. glass column packed with Chromspher 5- μ m C₁₈ and protected with a Chromsep reversed-phase guard column. The C₁₈ pre-column was a 10 mm \times 2 mm I.D. Chrompack reversed-phase pre-concentration column.

For details on the immuno pre-column used in both systems, see below.

Chemicals

Sephacrose CL-6B and cyanogen bromide-activated Sepharose 4B were obtained from Pharmacia (Woerden, The Netherlands). HPLC-grade acetonitrile and

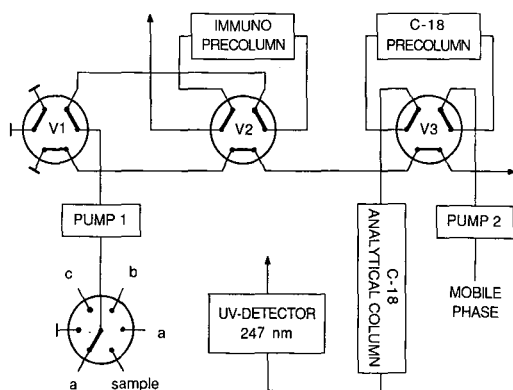


Fig. 2. Set-up of the automated HPLC system for the determination of β -19-NT and α -19-NT in urine samples. Immuno pre-column, 10 mm \times 10 mm I.D. stainless-steel column packed with Sepharose-immobilized antibodies; C₁₈ pre-column, 10 mm \times 2 mm I.D. stainless-steel column. a, Water; b, acetonitrile-water (5:95) containing 190 μ g/l of norgestrel; c, methanol-water (70:30). Mobile phase, acetonitrile-water (35:65); flow-rate of pump 1, 10 ml/min for flushing the capillaries (steps 2, 4, 6 and 8 in Table II) and 4 ml/min for all other steps; flow-rate of pump 2, 0.7 ml/min. Valves V1-V3 are all shown in position A (compare Table II).

methanol were obtained from Baker and Merck. HPLC-grade water was prepared from demineralized water using a Milli-Q (Millipore, Bedford, MA, U.S.A.) water purification system with subsequent filtration through an HPLC column filled with 40- μ m Baker C₁₈ material. The eluents were degassed under vacuum in an ultrasonic bath. β -19-NT, norgestrel (NG; see Fig. 1c) and testosterone (see Fig. 1d) were obtained from Sigma (St. Louis, MO, U.S.A.); α -19-NT was a gift from Organon (Oss, The Netherlands). Stock solutions of the steroids were prepared in ethanol (1 mg/ml) and stored at 4°C until use.

Norgestrel was purified by preparative HPLC; 1 mg of norgestrel was dissolved in 200 μ l of methanol and injected on to a Hibar (Merck) 250 mm \times 10 mm I.D. LiChrosorb RP-18 column. Acetonitrile–water (55:45) was used as the mobile phase.

All other chemicals were of analytical-reagent grade.

Antibody preparation and immobilization

Steroid hormones are too small to be immunogenic and must therefore be conjugated to a molecule large enough to elicit an immune response. In this study, a 19-nortestosterone-17 β -hemisuccinate–BSA (bovine serum albumin) conjugate, synthesized according to Kyrein¹⁴, was used for the immunization of a rabbit. The collected antiserum was purified according to the method of Steinbuch and Audrian¹⁵. The isolated IgG (immunoglobulin G) fraction was stored freeze-dried (RI-KILT batch 726-3). Cross-reactivities, as determined by radioimmunoassay, were *ca.* 70%, 20% and less than 1% for α -19-NT, NG and testosterone, respectively.

The IgG fraction was immobilized on cyanogen bromide-activated Sepharose 4B as recommended by the manufacturer¹⁶. Two different amounts of IgG were used for immobilization. In batch A 0.6 mg of freeze-dried IgG was used per ml of gel and in batch B 10 mg per ml of gel. For the latter batch the coupling efficiency was 46%, as determined by measurement (UV at 280 nm) of non-bound IgG in the coupling solution before and after immobilization. The immunosorbents obtained were stored in 0.1 M phosphate buffer (pH 7.2) containing 0.02% sodium azide.

Packing of immunoaffinity pre-columns

Laboratory made 10 mm \times 10 mm I.D. or 10 mm \times 4 mm I.D. stainless-steel columns, equipped with 5- μ m stainless-steel screens and PTFE rings as the column inlet and outlet were used. For packing the screens and PTFE rings were removed at one end and the pre-columns were connected to a vacuum facility with their closed ends. A thick slurry of immunosorbent in storage buffer was filled into the pre-column, then reduced pressure was applied in order to obtain a higher packing density, and the void thus created was packed with additional immunosorbent. The pre-column was closed under reduced pressure. Next the column was connected to an HPLC pump and flushed successively with 50 ml of 0.1 M phosphate buffer (pH 7.0), 50 ml of demineralized water and 50 ml of methanol–water (70:30) at a flow-rate of 4 ml/min (2 ml/min for the 10 mm \times 4 mm I.D. pre-column). The column was stored in methanol–water (70:30) at 4°C or at room temperature.

Determination of β -19-NT binding capacity

The binding capacity of the immunoaffinity pre-columns (immuno pre-columns) for β -19-NT was determined by pre-concentrating 16 ml of a standard solution

containing 100 $\mu\text{g/l}$ of β -19-NT and performing the analysis according to the final procedure discussed below. From the β -19-NT peak area the binding capacity was calculated by comparison with a standard loop injection. Using a 10 mm \times 10 mm I.D. pre-column the capacity was 60 ng for immunosorbent A and 340 ng for immunosorbent B when acetonitrile–water (10:90) was used for desorption. When desorption was performed with acetonitrile–water (5:95) containing 190 $\mu\text{g/l}$ of norgestrel, immunosorbent B showed a capacity of 450 ng (for an explanation, see below).

RESULTS AND DISCUSSION

Stationary phase for immobilization of antibodies

An important aspect of the design of an on-line immunoaffinity sample pretreatment system is the nature of the support material used for the immobilization of the antibodies. In order to obtain good selectivity, the support should show low non-specific interactions with the constituents of the biological samples. In this respect, polysaccharide stationary phases such as agarose are the best material available. Their only disadvantage is their compressibility, which makes them less suitable for high-pressure systems.

Experiments with the agarose gel Sepharose CL-6B, packed in a 10 mm \times 4 mm I.D. pre-column, showed that no collapse of the stationary phase occurred at flow-rates below 3.5 ml/min. The packed pre-column turned out to be stable, even when the mobile phase was switched from water to a phosphate buffer or methanol–water (70:30), or to filtered urine, and *vice versa*. In other words, agarose-based pre-columns can be loaded, flushed and desorbed without problems.

Desorption from the immuno pre-column: technical aspects

Initial experiments showed that with the agarose-based pre-column desorption could not be realized by simply switching the pre-column on-line with an analytical column (100 mm \times 3 mm I.D., 5- μm stationary phase). The agarose pre-column became blocked immediately, even if the flow-rate through the analytical column was as low as 0.7 ml/min. Probably the sudden pressure change generated by the switching caused the agarose gel to collapse. In order to circumvent this problem, a dual pre-column system was designed (Fig. 2), in which the agarose pre-column is switched in series with a second pre-column during the desorption step. The small dimensions of the second pre-column (10 mm \times 2 mm I.D.), combined with the large particle diameter (40 μm) of its C_{18} bonded silica stationary phase, result in a very low back-pressure, thereby avoiding a large pressure shock during the desorption of the agarose-based pre-column. In a second switching step, the analytes of interest are transferred from the second pre-column to the analytical column.

Desorption from the immuno pre-column: chemical aspects

Analyte desorption with aqueous solutions. For optimum performance, desorption from the large-volume immuno pre-column must be carried out with a solvent, which allows peak compression on the second, reversed-phase, pre-column. Therefore, several purely aqueous solutions were examined, which are frequently used for desorption purposes in affinity chromatography¹⁶.

None of aqueous 2.5 M sodium thiocyanate, 1 M propionic acid (pH 3.0), 0.1 M citrate buffer (pH 3.0), 0.7 M trichloroacetic acid (pH 2.3) or ethylene glycol-water (20:80) was suitable for desorption, because impurities were present in these solutions which completely obscured the β -19-NT peak in the chromatograms. Other solutions passed this test, such as 0.1 M phosphate buffer (pH 6.0 or 8.0), 0.1 M acetate buffer (pH 3.4, 4.6 or 5.7), 1 M sodium chloride and 0.1 M glycine-hydrochloric acid buffer (pH 3.0); however, they were not able to desorb β -19-NT at all; in each instance, the recovery of β -19-NT was zero. Experiments which were performed at a later stage using the final procedure showed that β -19-NT can even be pre-concentrated with good recovery from these solutions on the immuno pre-column!

The above results agree with those reported by Davis *et al.*⁷, who unsuccessfully tried to desorb low-molecular-weight plant hormones from an immunoaffinity column, using either chaotropic ions (ions which disrupt the structure of water and reduce hydrophobic interaction), high salt concentrations or changes in pH.

The various aqueous solutions, which have been successfully applied for many years for the desorption of proteins from immunoaffinity columns, obviously fail to desorb small molecules. Probably, with these solutions, the desorption of proteins is based mainly on changes in the structure of the bound protein (partial denaturation), and not on radical changes in the structure of the immobilized antibodies. This model is further supported by the fact that irreversible denaturation of the protein during the elution step is a frequently encountered problem in affinity elution. However, no case is known, so far, where the immobilized antibodies have been denatured irreversibly by these aqueous solutions. Because of their multi-point attachment to the stationary phase, the immobilized antibodies are much more resistant to denaturation and, hence, to changes in their structure, compared with free antibodies. Therefore, the elution of small molecules, that is, molecules which are not sensitive to denaturation, needs much more rigorous conditions.

Analyte desorption with aqueous solutions containing organic modifiers. In the literature, pure methanol^{6,7}, methanol-water (90:5)⁴ and acetone-water (95:5)³ have been used successfully for the desorption of low-molecular-weight compounds from an immunosorbent. In all instances the immunosorbent could be used repeatedly without a significant loss of activity.

In off-line experiments, methanol-water (70:30) was used to desorb trapped β -19-NT from the immuno pre-column; 5 ml of solution sufficed to recover β -19-NT, pre-concentrated from 16 ml of a 1 μ g/l standard solution, with a 98–100% recovery (10 mm \times 10 mm I.D. immuno pre-column). Unfortunately, this simple procedure could not be used for on-line desorption. The high methanol content did not allow the reconcentration of the desorbed analyte on the C₁₈ bonded silica pre-column. Therefore, lower organic modifier concentrations which would still allow a refocusing of analytes on the reversed-phase system were tested, first with immunosorbent A. When using dioxane-water mixtures several impurities showed up, some of which interfered with the β -19-NT peak. Good results were obtained with methanol-water and acetonitrile-water mixtures. In this study acetonitrile was preferred to methanol because it is also used as a mobile phase constituent. For on-line desorption the highest recovery was achieved by desorbing the immuno pre-column with 50 ml of acetonitrile-water (10:90). For the pre-concentration of 16 ml of a standard solution

TABLE I

RECOVERY OF β -19-NT AS A FUNCTION OF THE COMPOSITION OF THE DESORBING SOLUTION

For further explanation and details, see the text and Table II; desorption here was performed with 50 ml of solution in the back-flush mode.

Composition of the desorbing solution	β -19-NT recovery (%)
<i>Immunsorbent A (0.6 mg/ml):</i>	
Acetonitrile-water (5:95)	< 1
Acetonitrile-water (10:90)	85-90
Acetonitrile-water (15:85)	60
<i>Immunsorbent B (10 mg/ml):</i>	
Acetonitrile-water (10:90)	< 5
190 μ g/l NG in water	70
190 μ g/l NG in acetonitrile-water (5:95)	95-100
38 μ g/l NG in acetonitrile-water (5:95)	78

(1 μ g/l β -19-NT) the recoveries were 85-90% ($n=4$) (Table I; recoveries calculated by comparison with standard loop injection). The use of a lower percentage, *i.e.*, 5%, of acetonitrile gave a recovery of less than 1% β -19-NT after desorption with 50 ml of the eluent. Elution with acetonitrile-water (15:85) led to a recovery of only 60%, which was probably due to breakthrough on the C_{18} pre-column.

Using immunsorbent A, with its relatively low IgG concentration, the quoted procedure worked well with standard solutions of β -19-NT. However, in order to extend the linear detection range and to reduce the effect of cross-reacting steroids present in real samples, immunsorbent B with its higher amount of immobilized antibodies was used (binding capacity, 340 *vs.* 60 ng for a 10 mm \times 10 mm I.D. pre-column). Initial experiments with immunsorbent B, however, gave disappointing results. The recovery, which was 85-90% with immunsorbent A, dropped to less than 5% ($n = 8$) with immunsorbent B (Table I). By subsequent off-line desorption with methanol-water (70:30) it could be shown that the 95% loss of β -19-NT found with immunsorbent B was due to incomplete desorption.

The unexpected behaviour of this immunsorbent can be explained by the nature of the immobilized antibodies. Polyclonal antibodies are, in fact, mixtures of different antibodies. These antibodies (produced by different clones) may have different affinities for the antigen. If an antigen-containing solution is passed through an immunsorbent column, the antigens will first be bound by the antibodies with the highest antigen affinity. Subsequently, the antibody types with lower affinities become saturated with antigen. The phenomenon described above may be related to antigens bound to high-affinity antibodies, which are not eluted with acetonitrile-water (10:90). Because of the higher IgG content of immunsorbent B, more β -19-NT is bound to the high-affinity antibodies. This model can explain the divergent recoveries.

Immunoselective analyte desorption using a competing steroid. For quantitative desorption of β -19-NT from the immuno pre-column, a more specific principle is desired. The use of a compound with a structure similar to that of β -19-NT, which

can act as a displacer by competing for the high-affinity sites present in the immunosorbent, was tested. The synthetic steroid hormone norgestrel (NG; Fig. 1c) seemed to have a suitable structure for this purpose. On the one hand, NG has the same structure in the A and B rings as has β -19-NT, and hence is a good candidate to show a high affinity to the immunosorbent (the A and B rings are important for recognition because β -19-NT was conjugated to BSA at the opposite part of the molecule for immunization). On the other hand, in contrast to β -19-NT, NG has different substituents in the D ring (the part of the molecule which is not significant for the affinity recognition), which allows an easy HPLC separation from β -19-NT. A displacer solution of 190 $\mu\text{g/l}$ NG in water caused desorption of 70% of the trapped β -19-NT (Table I). The data in Table I clearly show the benefit of the immunoselective desorption which can be achieved with purely aqueous solutions of NG.

In principle two methods can be used to increase further the recovery of 70%: the use of larger desorption volumes or of higher amounts of NG. The disadvantages are a longer analysis time and disturbances caused by the large NG peak, respectively. A more elegant way to increase the recovery was the addition of 5% of acetonitrile to the aqueous NG-containing solution. This resulted in recoveries of 95–100%, probably owing to the reduction of non-specific interactions. Using a lower NG concentration led to inferior results (Table I).

The previous results were achieved by desorbing the immuno pre-column in the forward-flush mode. In order to reduce the desorption volume and hence to shorten the analysis time, back-flush desorption was also tested. The experimental data are given in Fig. 3. A virtually quantitative recovery was achieved with a desorption volume of 33 ml instead of 50 ml. The lower recovery for desorption volumes of over 50 ml is probably due to breakthrough on the C_{18} pre-column.

The immunoselective desorption has an additional advantage over the non-selective desorption with a high percentage of organic modifier. The competing steroid (here NG) will desorb analytes only from the antibodies for which it possesses a high affinity itself. In principle, no desorption will occur from other types of antibodies present in the immunosorbent. This is an important aspect of the present clean-up procedure, because in our case a crude IgG mixture, not purified by affin-

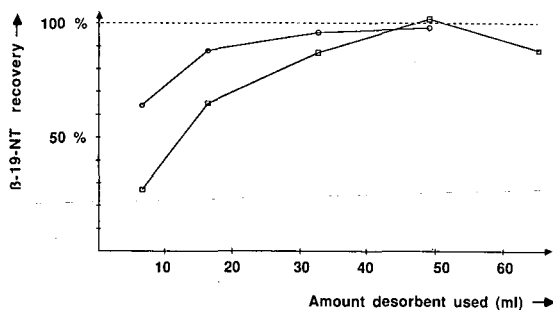


Fig. 3. Recovery of β -19-NT as a function of the amount of acetonitrile–water (5:95) containing 190 $\mu\text{g/l}$ of NG used for the transfer of analytes from the immuno pre-column to the C_{18} pre-column. A 16-ml volume of a 1 $\mu\text{g/l}$ β -19-NT standard solution was pre-concentrated and analysed according to the schedule in Table II. Forward-flush desorption (□) is compared with back-flush desorption (○). For back-flush desorption the system was set up according to Fig. 2. HPLC system No. 1 was used for the measurements.

ity-based techniques, was used for immobilization, and large amounts of antibodies of unknown specificity are present in such an immunosorbent. Further, interferences by compounds which are bound non-specifically to the stationary phase backbone, the coupling group, other immobilized proteins or even the large non-selective surface of the antibodies, will be much reduced if the selective desorption technique is utilized.

Final procedure

The final analytical procedure is summarized in Table II (also see Fig. 2). The first step involves the preconditioning of the immuno pre-column with water. Then the sample is introduced by pump 1 via the solvent selection valve. Next, the immuno pre-column is flushed with water to displace the remaining sample (urine) and to remove non-specifically bound impurities. In the following step, the C₁₈ pre-column is switched off-line with respect to the analytical column and preconditioned with water. Subsequently, the immuno pre-column, which now contains the trapped analytes, and the C₁₈ pre-column are switched in series and the transfer of the analytes is accomplished in the back-flush mode with an aqueous solution containing 190 µg of NG/l and 5% acetonitrile.

After the complete transfer of the analytes to the C₁₈ pre-column, the actual separation is started by switching the C₁₈ pre-column on-line with the analytical column; β-19-NT and NG are then separated on the analytical column. Simultaneously, the immuno pre-column is reconditioned by flushing with methanol-water (70:30). In this step NG, which saturates the immuno pre-column during the desorption step, and other compounds which are retained by non-specific interaction, are

TABLE II
SCHEDULE OF THE AUTOMATED ANALYSIS

For each valve, position A corresponds to the position shown in Fig. 2. For further explanation, see text.

Step	Event	Valve position		
		Valve 1	Valve 2	Valve 3
1	Flushing immuno pre-column (10 mm × 10 mm I.D.) with 15 ml of water	A	A	A
2	Flushing capillaries with sample	B	A	A
3	Flushing immuno pre-column with sample	A	A	A
4	Flushing capillaries with water	B	A	A
5	Flushing immuno pre-column with 15 ml of water	A	A	A
6	Flushing capillaries with water	B	A	A
7	Flushing C ₁₈ pre-column with 5 ml of water	B	A	B
8	Flushing capillaries with desorbing solution containing 190 µg/l of NG and 5% of acetonitrile	B	B	B
9	Flushing immuno pre-column and C ₁₈ pre-column in series with 33 ml of a solution containing 190 µg/l of NG and 5% of acetonitrile	A	B	B
10	Desorbing C ₁₈ pre-column by on-line switching with the analytical column	A	B	A
11	Flushing immuno pre-column with 20 ml of methanol-water (70:30)	A	A	A

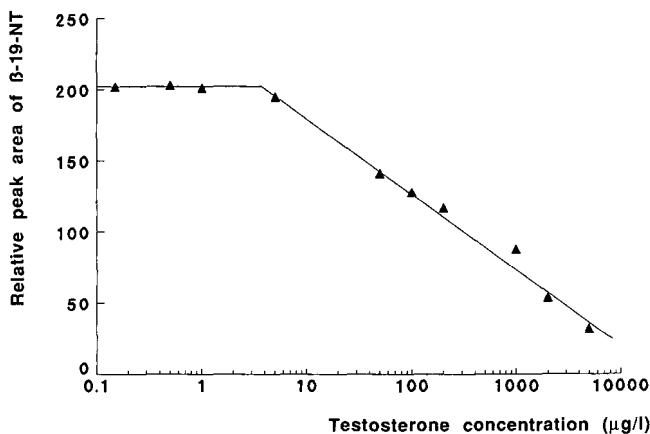


Fig. 4. Recovery of β -19-NT as a function of the testosterone concentration in the sample. A 25-ml volume of a standard solution containing 1 $\mu\text{g/l}$ of β -19-NT and the indicated concentration of testosterone was analysed according to the schedule in Table II, with a 10 mm \times 4 mm I.D. pre-column instead of the 10 mm \times 10 mm I.D. pre-column containing immunosorbent B. HPLC system No. 2 was used for the measurements.

quantitatively desorbed. Now the next analysis can be started, while the separation in the analytical column is still running.

Cross-reactivity of the immunosorbent with α -19-NT and testosterone

In cases of β -19-NT abuse, a metabolite, α -19-NT, is also present in the urine. Both compounds have the same structure in the significant A and B rings of the steroid skeleton (Fig. 1), so, as expected, pre-concentration of α -19-NT standard solutions showed the same high recovery as was achieved with β -19-NT. In other words, the immunosorbent has a similar affinity for both steroids. Fortunately, both compounds can be separated on the analytical column and hence the simultaneous determination of α -19-NT and β -19-NT creates no problems (see Fig. 8).

In addition, the structurally related steroid hormone testosterone (see Fig. 1d) occurs endogenously in urine. Concentrations of up to 2 $\mu\text{g/l}$ have been measured by us in calf urine using gas chromatography-mass spectrometry. Testosterone can interfere in the determination of β -19-NT, although the cross-reactivity of the immunosorbent for testosterone is below 1% (see Experimental). Fig. 4 shows the effect of adding increasing amounts of testosterone to standard solutions of β -19-NT (1 $\mu\text{g/l}$) on the recovery of β -19-NT. Up to a concentration of about 5 $\mu\text{g/l}$ of testosterone no effect can be seen on the recovery of β -19-NT. Higher testosterone concentrations reduce the recovery of β -19-NT, but the effect is fairly weak (note the logarithmic scale). Even with the small 10 mm \times 4 mm I.D. pre-column, packed with immunosorbent B, the recovery of β -19-NT dropped by only 10% at the high testosterone level of 10 $\mu\text{g/l}$, and by 25% at the unrealistically high concentration of 50 $\mu\text{g/l}$. This clearly demonstrates that the affinity of the immunosorbent for testosterone is much lower than for β -19-NT.

TABLE III

ANALYTICAL DATA ON THE AUTOMATED ANALYSIS OF β -19-NT-SPIKED CALF URINE SAMPLES

The samples were analysed under the same conditions as in Fig. 5.

Criterion	Level	Result
Repeatability	1 $\mu\text{g/l}$ β -19-NT ($n=3$)	1.8%
Recovery	1 $\mu\text{g/l}$ β -19-NT ($n=3$)	97%
Linearity	0.2–10 $\mu\text{g/l}$ ($n=5$)	0.9997
Detection limit	S/N* = 3:1 (from Fig. 6)	50 ng/l (1.25 ng)
Total analysis time including sample pre-treatment		45 min

* Signal-to-noise ratio.

Performance and application in spiked urine analysis

The data in Table III clearly demonstrate the potential of the method. Fig. 5 shows a calibration plot, obtained with immunosorbent B, for β -19-NT-spiked urine samples. It is linear for β -19-NT concentrations of 0.2–10 $\mu\text{g/l}$ ($r = 0.9997$). At higher concentrations the recovery rapidly diminishes, as is to be expected because the total capacity of the immuno pre-column was about 370 ng in this instance.

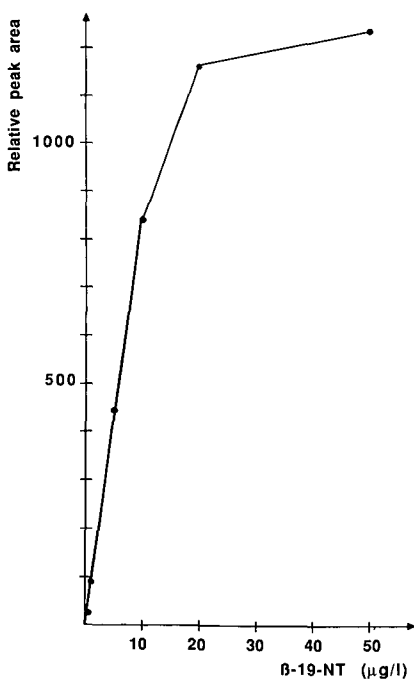


Fig. 5. Peak area as a function of the β -19-NT concentration in spiked urine. Calf urine samples were spiked with β -19-NT, diluted with an equal amount of water and filtered. An aliquot of 50 ml (containing 25 ml of urine) was loaded on immunosorbent B and processed according to the final procedure. HPLC system No. 1 was used for the measurements. The total β -19-NT capacity of the 10 mm \times 10 mm I.D. immuno pre-column was 370 ng in this instance.

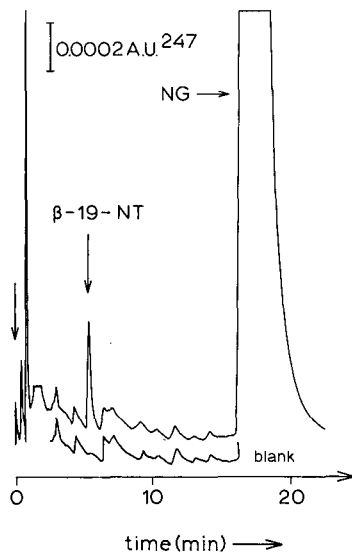


Fig. 6. Chromatogram of a calf urine sample spiked with 200 ng/l of β -19-NT and of the corresponding blank urine. The samples were filtered and diluted with an equal amount of water. An aliquot of 50 ml (containing 25 ml of urine) was loaded on immunosorbent B and processed according to the final procedure. HPLC system No. 2 was used for the measurements.

Fig. 6 shows the chromatogram of a blank calf urine and of the same sample spiked with 200 ng/l of β -19-NT; only peaks due to β -19-NT and NG are observed. In other urine samples, however, several impurities showed up, which sometimes interfered with the detection of small amounts of β -19-NT. In such an event, the interferences can be reduced by diluting the sample with water before loading it on to the system. This is demonstrated in Fig. 7a and b, where a spiked (100 ng/l) urine sample was loaded on to the system either (a) undiluted or (b) after dilution with 4 volumes of water. An inferior improvement was observed on addition of 5% acetonitrile to the urine sample before analysis (data not shown). The results of the combined approach are shown in Fig. 7c. Here the urine was spiked with 2 μ g/l of β -19-NT and 20 ml of urine diluted with 20 ml of acetonitrile–water (10:90) were loaded. The interferences were reduced to a similar extent as was reached with 4-fold dilution with water and, additionally, the analysis time was shortened considerably. Besides, even though acetonitrile was added to the sample, no decrease in recovery was observed. The chromatogram of another “dirty” urine sample, which was processed similarly and had been spiked with 0.3 μ g/l each of β -19-NT and α -19-NT, is shown in Fig. 8. The resolution of both peaks is very satisfactory.

If a sample volume of 25 ml is loaded, the detection limit for β -19-NT is 50 ng/l in spiked urine (Table III). In principle, this value can be improved by increasing the sample volume. Further, the sample can be loaded at a higher flow-rate to reduce the time of analysis. In fact, the same high β -19-NT recovery was recorded when the sample from Fig. 7b was loaded at a flow-rate of 10 ml/min instead of 4 ml/min. In other words, the antibody–antigen interaction is fast enough to permit such high flow-rates.

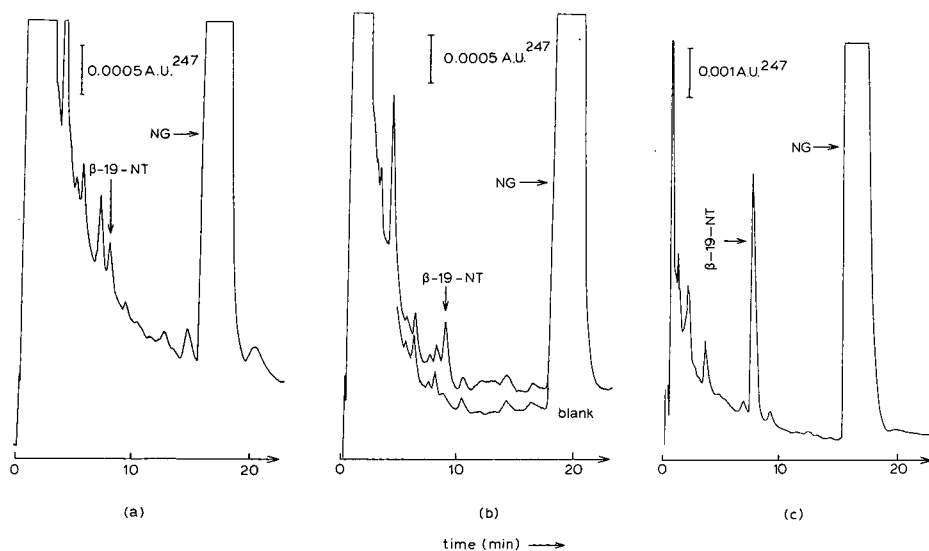


Fig. 7. Chromatograms of a spiked, and filtered, calf urine sample. (a) 36 ml of urine spiked with 100 ng/l of β -19-NT, pre-concentrated without dilution; (b) 36 ml of urine spiked with 100 ng/l of β -19-NT, diluted to 180 ml with water and pre-concentrated; (c) 20 ml of urine spiked with 2 μ g/l of β -19-NT, diluted with 20 ml of acetonitrile-water (10:90) and pre-concentrated. The analysis was performed according to the final procedure. HPLC system No. 1 was used for the measurements.

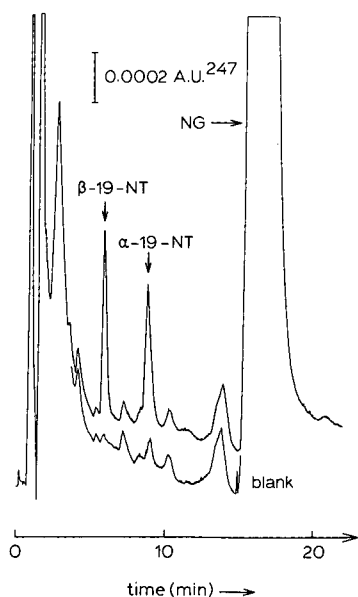


Fig. 8. Chromatograms of a calf urine sample spiked with 300 ng/l each of β -19-NT and α -19-NT and of the corresponding blank urine. The samples were filtered and diluted with an equal amount of acetonitrile-water (10:90). An aliquot of 53 ml (containing 26.5 ml of urine) was loaded and processed according to the final procedure. HPLC system No. 2 was used for the measurements.

Capacity, stability and storage of the immuno pre-columns

The capacity of the immuno pre-columns decreased slowly during their use. Over a 6-month period about 100 urine samples were analysed, using various analytical conditions, *i.e.*, testing different solvent mixtures. During this period the capacity of a 10 mm × 10 mm I.D. precolumn packed with immunosorbent B decreased from 450 to 180 ng which was, however, sufficient to determine β -19-NT in the desired concentration range. Losses were not observed during storage for, *e.g.*, 30 days, but only when the column was used for analysis. After an initial rapid decrease in capacity, the losses became much smaller once a few analyses had been carried out. Ligand leakage is probably the reason for this behaviour. It is well known that cyanogen bromide-coupled ligands are not very resistant to leakage. The use of other coupling reactions may help to improve the stability of the immunosorbent.

When not in use, the immunosorbents were stored in methanol–water (70:30) at 4°C or at room temperature. As this is the same solvent as is used in the last step of the analysis, no extra flushing step is needed to prepare the column for storage. Moreover, the addition of chemicals to prevent microbial degradation can be omitted.

CONCLUSIONS

An immunoaffinity separation is, by nature, a digital separation step rather than a continuous chromatographic procedure; that is, in principle capacity factors are close either to infinity or to zero. This is exactly what is needed in sample preparation. Because of the large retention that can be achieved in immunoaffinity chromatography, the early breakthrough of analytes that often complicates conventional pre-column procedures hardly plays a role here. In addition, the selectivity of the immunosorbent creates an extremely high clean-up efficiency.

In this paper, the potential of on-line immunoaffinity-based sample preparation for HPLC analysis has been demonstrated. The analytes of interest were concentrated on a pre-column packed with a soft immunosorbent gel displaying low non-specific interaction. The on-line desorption turned out to be a critical step and was finally performed with an almost purely aqueous solution containing a large excess of a competing steroid. The total analytical system displays considerable selectivity, which is mainly due to the pre-column antibody–antigen interaction and to the selective immunochemical desorption. At least 100 large-volume (25 ml) urine samples can be analysed without exchanging the immuno pre-column. The total time of analysis, including the automated sample pre-treatment, is about 45 min. If a large-volume autosampler or, even simpler, a multi-port solvent selection valve is available, the system can be operated unattended. The detection limit of 50 ng/l of β -19-NT for spiked urine samples is in the range required for the free drug in veterinary and doping analysis. The possibility of determining not just the free drug, but also its glucuronide and sulphate conjugates, which are present in urine at much higher concentrations, either by off-line hydrolysis or on-line by immobilized enzyme reactors, is currently being investigated. The method will also be applied to faeces, meat and bile samples.

Compared with immunoassay methods, the present system has the advantages that (i) cross-reacting compounds can be distinguished from the analytes, (ii) the

reproducibility is better, (iii) full automation can be achieved easily and (iv) more than one analyte can be determined in one run. In principle, the method can be applied to all compounds which elicit an immune response. Current research is aimed at demonstrating this. Further, combining several types of antibodies in one pre-column or, more elegantly, combining various immuno pre-columns in series, offers the possibility of determining even more analytes in just one run, and allows in principle the construction of a fully automated analytical system, the selectivity of which can be tailor-made by selecting a suitable set of immuno pre-columns. In the near future, our main attention will be focused on solving some of the analytical and technical challenges outlined here and, in addition, on investigating the mechanism of the immunoselective desorption in order to create a better model for its understanding and optimization.

ACKNOWLEDGEMENTS

This work was supported by the Dutch Foundation for Technical Science, grant No. VCH 46.0616. The National Inspection Service for Meat, Livestock and Animal Products is thanked for technical support. Organon (Oss, The Netherlands) is thanked for the gift of α -19-nortestosterone. The initial assistance of Euro-Diagnostics (Apeldoorn, The Netherlands) is highly appreciated.

REFERENCES

- 1 R. W. Frei and K. Zech (Editors), *Selective Sample Handling and Detection in High-Performance Liquid Chromatography*, Elsevier, Amsterdam, 1988.
- 2 Y. Fuchs and E. Gertman, *Plant Cell Physiol.*, 15 (1974) 629–633.
- 3 R. G. Glencross, S. A. Abeywardene, S. J. Corney and H. S. Morris, *J. Chromatogr.*, 223 (1981) 193–197.
- 4 R. Webb, G. Baxter, D. McBride, G. D. Nordblom and M. P. K. Shaw, *J. Steroid Biochem.*, 23 (1985) 1043–1051.
- 5 E. M. S. MacDonald and R. O. Morris, *Methods Enzymol.*, 110 (1985) 347.
- 6 P. Ulvskov, J. Marcussen, R. Rajagopal, E. Prinsen, P. Ruedelsheim and H. Van Onckelen, *Plant Cell Physiol.*, 28 (1987) 937–945.
- 7 G. C. Davis, M. B. Hein, D. A. Chapman, B. C. Neely, C. R. Sharp, R. C. Durley, D. K. Biest, B. R. Heyde and M. G. Carnes, *Plant Growth Substances*, Springer, Berlin, 1985, pp. 44–51.
- 8 G. C. Davis, M. B. Hein and D. A. Chapman, *J. Chromatogr.*, 366 (1986) 171–189.
- 9 C. van de Water and N. Haagsma, *J. Chromatogr.*, 411 (1987) 415–421.
- 10 B. Johansson, *J. Chromatogr.*, 381 (1986) 107–113.
- 11 B. Nilsson, *J. Chromatogr.*, 276 (1983) 413–417.
- 12 E. H. J. M. Jansen, R. H. van den Berg, G. Zomer, R. Both-Miedema, C. Enkelaar-Willemsen and R. W. Stephany, *Anal. Chim. Acta*, 170 (1985) 21–27.
- 13 C. van Peteghem, *J. Chromatogr.*, 369 (1986) 253–257.
- 14 H. J. Kyrein, *Z. Lebensm. Unters. Forsch.*, 177 (1983) 426–438.
- 15 M. Steinbuch and R. Audrian, *Arch. Biochem. Biophys.*, 134 (1969) 279–284.
- 16 *Affinity Chromatography, Principles and Methods; Product Information*, Pharmacia, Uppsala, 1983.

CHROM. 20 482

CHROMATOGRAPHY FOR DIAGNOSIS OF METABOLIC DISEASES

EGIL JELLUM

Institute of Clinical Biochemistry, Rikshospitalet, 0027 Oslo 1 (Norway)

SUMMARY

Chromatographic techniques, including computerized capillary gas chromatography-mass spectrometry and high-performance liquid chromatography with rapid scanning detection are important parts of a multicomponent analytical system designed for the diagnosis of human metabolic disorders. The usefulness of such a system is exemplified by the finding of a new case with the very rare disease hypersarcosinuria and the detection of unusual metabolites in a case of phenylketonuria.

INTRODUCTION

During the past 20 years a number of centres for the diagnosis of metabolic diseases have been established in various parts of the world¹⁻³. Various chromatographic methods, including thin-layer chromatography, gas chromatography, gas chromatography-mass spectrometry (GC-MS), high-performance liquid chromatography (HPLC) and HPLC with a computerized diode array detector, are suitable to detect and identify metabolites that are characteristic of the various diseases. The chromatography system currently used in our laboratory⁴ uses all these techniques and is capable of diagnosing over 100 different metabolic diseases.

In the present report the value of chromatography is exemplified by some recent diagnostic applications of our analytical system.

MATERIALS AND METHODS

Sarcosine (N-methylglycine), pyroglutamic acid (5-oxoproline) and BSTFA were products of Sigma (St. Louis, MO, U.S.A.). N-Nitrosomethylurea, for diazomethane production, was obtained from K&K Labs. (New York, NY, U.S.A.). N-Acetylphenylalanine was prepared from L-phenylalanine by acetylation with a mixture of acetic acid and acetic anhydride at 80°C for 1 h. All other chemicals and solvents used were commercially available products of analytical grade.

Amino acid analysis

A Kontron automatic amino acid analyser, Liquamat III (Labotron Instrumente, Zürich, Switzerland) was used for quantitative amino acid analysis, using ion-exchange chromatography and post-column ninhydrin reaction.

GC-MS analysis

The instrument used was a Hewlett-Packard 5970 mass selective detector coupled to a gas chromatograph with an automatic sample injection system (HP 5890 GC with HP 7673A 100 sample injector) and a HP 300 data system. The GC column was a 30 m fused-silica capillary column coated with SP-1000 (Supelco, Bellefonte, PA, U.S.A.). Nearly all GC peaks were identified using the mass spectral library search program supplied by Hewlett-Packard and modified in our laboratory to automatically identify *ca.* 100 organic acids known to carry specific, diagnostic information⁴. Urine samples are usually acidified, extracted with diethyl ether and methylated with diazomethane before injection into the system⁴.

RESULTS AND DISCUSSION

Unusual metabolites in a case of phenylketonuria (PKU)

Routine screening for PKU (measurement of phenylalanine in blood) recently resulted in the recognition of a newborn boy suspected of carrying this disease. As the PKU diagnosis was not certain in this case, a urine sample was submitted to our laboratory for confirmatory analysis using advanced chromatographic techniques. Amino acid analysis revealed increased urinary phenylalanine (30 times above the normal excretion) and also increased amounts of some other amino acids (not shown). Fig. 1 (top) shows the complete urinary organic acid profile as determined by GC-MS. Fig. 1 (bottom) shows the middle portion of this profile on an expanded scale. Large amounts of the typical phenylalanine metabolite, phenyllactate, were found and also considerable amounts of its oxidized form, phenylpyruvate (the latter metabolite decomposes partly at the high temperature in the GC-MS system resulting in a false low peak on the GC trace). In addition, unusually high amounts of N-acetylphenylalanine was present, indicating that the large intracellular excess of phenylalanine had undergone extensive N-acetylation in this patient. N-Acetylation is usually only a minor pathway in amino acid metabolism^{5,6}. One of the peaks (see Fig. 1) was furthermore identified as pyroglutamic acid, which was increased some 20-fold above the usual level. Pyroglutamate (5-oxoproline), a metabolite of the γ -glutamyl cycle involved in amino acid transport⁷, has previously not been reported to be elevated in PKU. From Fig. 1 (top) it is also evident that the urine contained considerable amounts of *p*-hydroxyphenyllactate, indicating reduced liver function.

These results confirmed the PKU diagnosis. The patient, however, has an atypical urinary metabolite pattern with considerable amounts of N-acetylphenylalanine and pyroglutamate in addition to the typical PKU metabolites, phenylpyruvate and phenyllactate.

Diagnosis of a case with hypersarcosinuria

Urine from a 2-year-old girl, mentally retarded and of small stature, contained large amounts of an usual peak in the amino acid chromatogram (Fig. 2). From the retention time and comparison with reference compounds it was inferred that the unknown compound might be sarcosine (N-methylglycine). The profile of urinary organic acids as determined by GC-MS of a methylated diethyl ether extract was normal (not shown). This was not surprising in view of the insolubility of sarcosine in diethyl ether. To identify the unknown compound with certainty, an aliquot (200

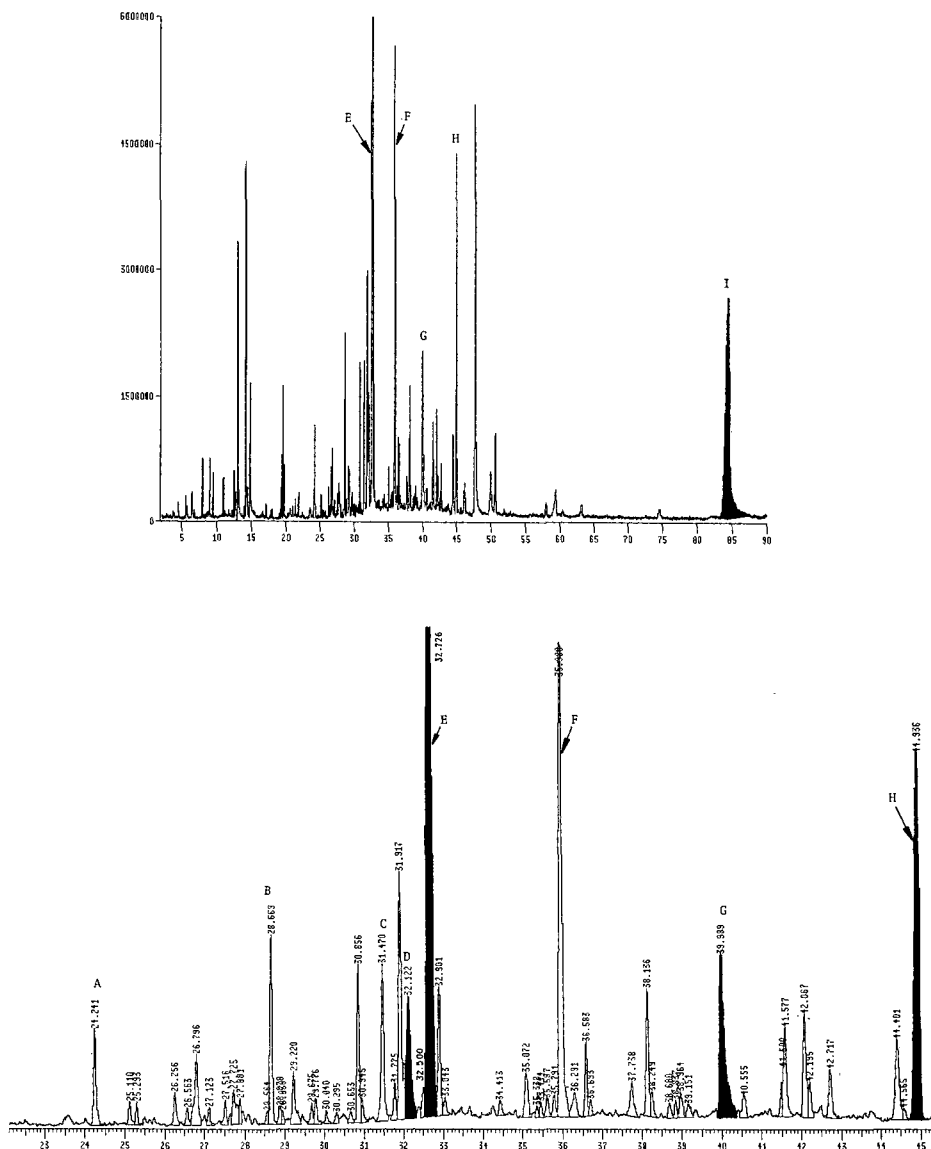


Fig. 1. Organic acid profile of urine from a patient suspected of having phenylketonuria (PKU). The sample was treated as described in the text. The fused-silica capillary column (30 m, SP-1000) was programmed from 50°C to 250°C. (Top) Complete chromatogram; (bottom) middle portion of the chromatogram on an expanded scale. Peaks: A = 3-hydroxy-3-methylglutarate; B = α -ketoglutarate; C = mandelate; D = phenylpyruvate; E = phenyllactate; F = citrate; G = pyroglutamate (5-oxoproline); H = N-acetylphenylalanine; I = *p*-hydroxyphenyllactate. Note the unusual metabolites G and H in this PKU urine.

μ l) of urine from the patient was lyophilized and the dry residue was silylated with BSTFA. This method of derivatization had to be used instead of methylation, as the glycine that is always present in urine may be methylated by diazomethane to produce

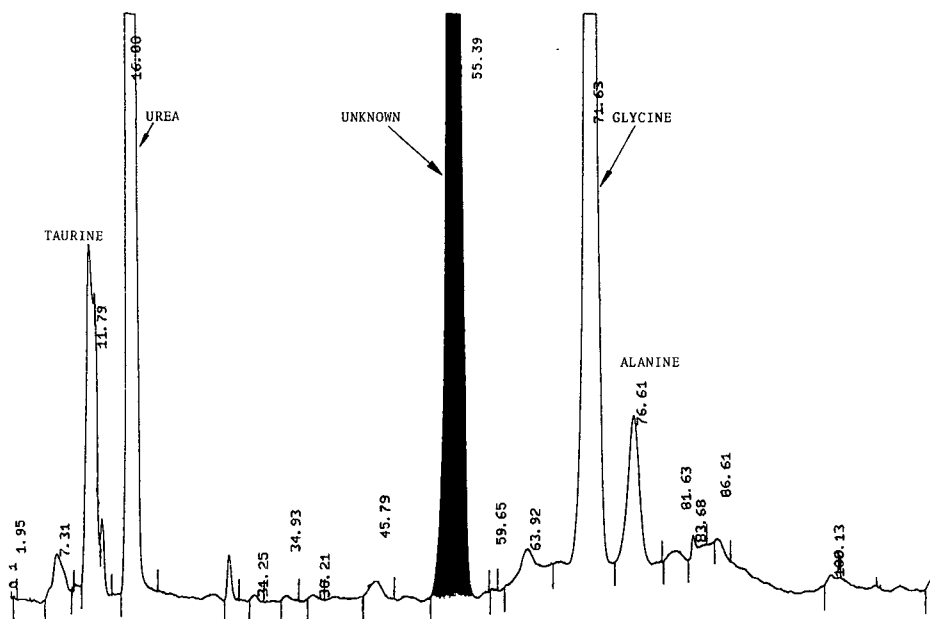


Fig. 2. Initial part of the amino acid chromatogram of urine from a two-year-old patient. Traditional ion-exchange chromatography with ninhydrin post-column reaction. Note the large amounts of an unknown compound.

sarcosine artificially. The mass spectra of the trimethylsilyl (TMS) derivatives of sarcosine are furthermore rather similar to the spectra of the TMS derivatives of alanine (not shown). Fortunately the GC retention times differ considerably, making the differentiation between sarcosine and alanine easy.

Fig. 3 (top) shows a portion of the chromatographic profile of urine from the patient. The two major peaks have identical retention times with authentic sarcosine, mono- and di-TMS derivatives, respectively (Fig. 3, bottom). Moreover, the mass spectra of the two sarcosine peaks in the patient sample were identical with the spectra of the reference compound shown in Fig. 4. It can thus be concluded with certainty that the patient excreted large amounts of sarcosine in her urine.

Hypersarcosinuria is a very rare condition⁸. Only about a dozen cases have been reported since it was first identified in 1965. The enzyme defect is located to the so-called one-carbon cycle⁸, but it is unclear whether this deficiency is responsible for the clinical condition, which appears to vary considerably in the few cases known.

CONCLUSIONS

The discovery of new metabolic disorders has often been preceded by the availability of new laboratory tests and instrumental techniques. During the first part of this century the analytical possibilities were simple chemical methods, *e.g.* the ferric chloride test, the nitroprusside reaction and other spot tests. Only a handful of metabolic diseases were recognized at that time, including PKU. A dramatic change occurred with the advent of the ninhydrin reaction and amino acid analysis by paper

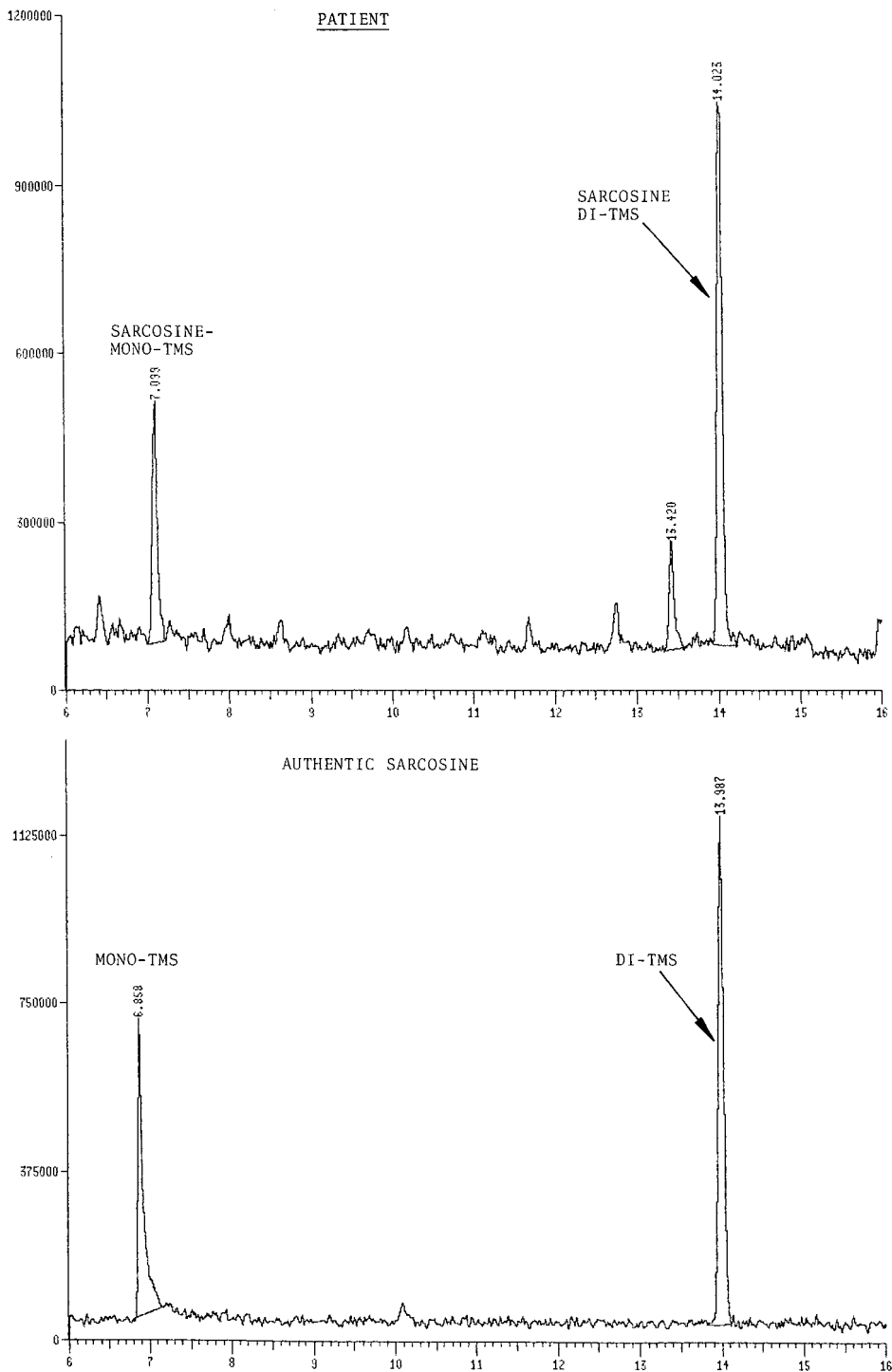


Fig. 3. (Top) Early part of the chromatographic profile of urine from the patient in Fig. 2; lyophilized urine (200 μ l) was derivatized with BSTFA before GC-MS. (Bottom) Chromatogram from GC-MS analysis of authentic sarcosine. The two peaks are the mono- and di-TMS derivatives, respectively.

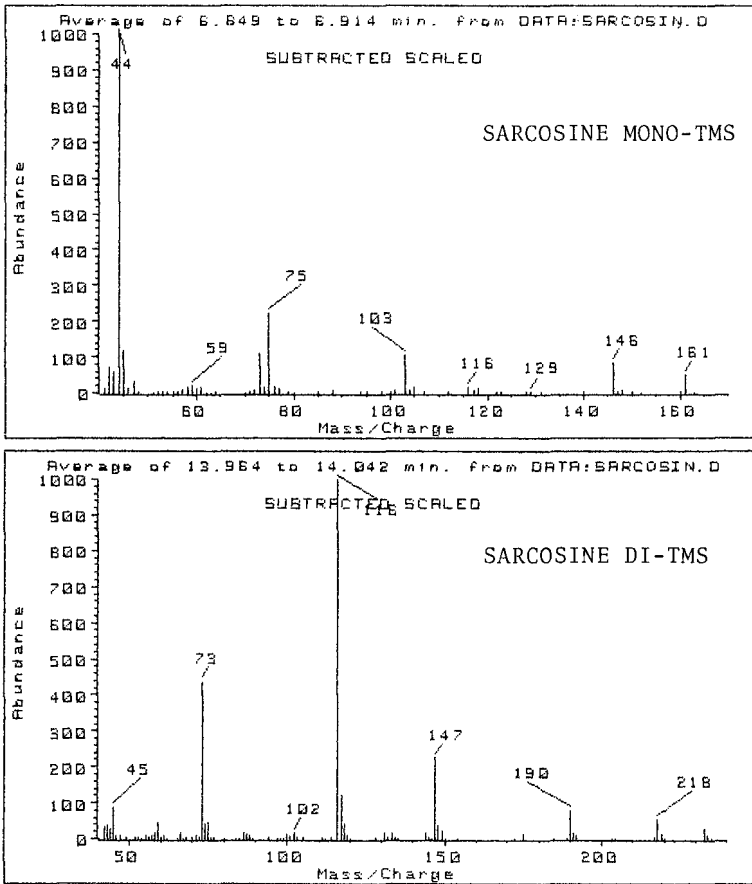


Fig. 4. Mass spectra of mono- and di-TMS derivatives of sarcosine.

and ion-exchange chromatography. Many disorders related to amino acid metabolism were soon found. During the past two decades we have witnessed the progress of GC, MS, and HPLC, and have seen how these techniques can lead to diagnosis of many new diseases.

Although modern DNA technology has been introduced for diagnostic purposes, this technique is as yet only suitable in the diagnosis of cases in which a particular disease is suspected due to inheritance. The DNA methods are therefore particularly appropriate for prenatal diagnosis in situations where the family already has a child with a known disease. The chromatographic methods, in contrast, can be used to diagnose close to one-half of all the 250–300 metabolic diseases recognized today, without knowing what to look for. It can be postulated, therefore, that chromatography, for many years to come, will continue to be a most helpful tool for diagnosing and learning more about human metabolic diseases.

REFERENCES

- 1 S. I. Goodman and S. P. Markey, *Laboratory and Research Methods in Biology and Medicine*, Alan R. Liss, New York, 1981, Vol. 6.
- 2 R. A. Chalmers and A. M. Lawson, *Organic Acids in Man*, Chapman and Hall, New York, 1982.
- 3 Z. Deyl and C. C. Sweeley (Editors), *Profiling of Body Fluids and Tissues*, *J. Chromatogr.*, 379 (1986) 1.
- 4 E. Jellum, E. A. Kvittingen, O. Thoresen, G. Guldal, L. Horn, R. Seip and O. Stokke, *Scand. J. Clin. Lab. Invest.*, 46 (suppl. 184) (1986) 11.
- 5 H. M. Liebich and C. Först, *J. Chromatogr.*, 338 (1985) 187.
- 6 E. Jellum, L. Horn, O. Thoresen, E. A. Kvittingen and O. Stokke, *Scand. J. Clin. Lab. Invest.*, 46 (suppl. 184) (1986) 21.
- 7 A. Meister, *Ann. Intern. Med.*, 81 (1974) 247.
- 8 T. Gerritsen and H. A. Weismann, in J. B. Stanbury, J. B. Wyngaarden and D. S. Fredrickson (Editors), *The Metabolic Basis of Inherited Disease*, McGraw-Hill, New York, 1978, p. 514.

CHROM. 20 497

DETERMINATION OF FATTY ACIDS AS PHENACYL ESTERS IN RAT ADIPOSE TISSUE AND BLOOD VESSEL WALLS BY HIGH-PERFORMANCE LIQUID CHROMATOGRAPHY

TOMAS HANIS*, MIROSLAV SMRZ, PAVEL KLIR and KAREL MACEK

Institute of Physiology, Czechoslovak Academy of Science, Videnska 1083, 14220 Prague (Czechoslovakia)

JOSEF KLIMA and JIRI BASE

Institute of Clinical and Experimental Medicine, Prague (Czechoslovakia)

and

ZDENEK DEYL

Institute of Physiology, Czechoslovak Academy of Science, Videnska 1083, 14220 Prague (Czechoslovakia)

SUMMARY

Twenty-two biologically relevant (6:0–22:6) saturated, monounsaturated and polyunsaturated fatty acids were separated by reversed-phase high-performance liquid chromatography after derivatization with phenacyl bromide. An optimal resolution of the critical combinations linolenic–myristic, docosahexaenoic–palmitoleic–arachidonic and palmitic–oleic acids and *cis* and *trans* isomers of octadecenoic (n9) and octadecadienoic (n9, 12) acids was achieved by continuous gradient elution with methanol–acetonitrile–water. Elution of mixtures of 6:0–22:1 fatty acids was completed within 80 min at a flow-rate of 1 ml/min. By the use of UV detection at 242 nm the detection limits for short- and long-chain fatty acids were found to be about 0.8 and 12 ng per injection, respectively. Linearity was tested up to 100 ng. The method was applied to the determination of fatty acids in rat adipose tissue and blood vessel walls of animals fed hydrogenated fat diets. The results are comparable to those obtained by gas chromatography and surpass the latter for the resolution of oleic and elaidic acids.

INTRODUCTION

Adipose tissue is the main source of blood free fatty acids, which represent the most actively metabolized pool of lipid classes. The fatty acid pattern of adipose tissue is closely related to the fatty acid composition of dietary lipids and so may reflect not only a pathological situation but also the feeding history of the animal. The latter is particularly important in nutritional experiments and in establishing adequate biological models.

Although gas chromatographic (GC) methods are traditionally used for fatty acid analyses¹, they are accompanied by some disadvantages, particularly with re-

spect to heat-labile² or short-chain fatty acids³, and moreover the separation of *cis-trans* isomers is possible only with capillary GC columns.

In order to overcome some of these shortcomings, a number of high-performance liquid chromatographic (HPLC) methods have been introduced. These methods usually offer good resolution of biologically important fatty acids^{4,5}, but the detection of underivatized fatty acids is neither sensitive nor selective because these compounds generally do not contain suitable chromophores. Absorption of underivatized fatty acids near 200 nm cannot be recommended because it is adversely affected by the properties of and frequent impurities in organic solvents, which is specifically undesirable in gradient elution.

In order to increase the sensitivity and selectivity of detection, a number of UV-absorbing or fluorescent derivatives have been prepared. Phenacyl^{3,6-12}, *p*-nitrobenzyl¹³, *p*-bromophenacyl^{14-16,25}, 2-naphthacyl^{3,17,18}, *m*-methoxyphenacyl¹⁹, *p*-phenacylazophenacyl²⁰, naphthylamine^{21,22}, pentafluorobenzyl²³, 5-dimethylamino-1-naphthalenesulphonylethanolamine²⁴, 9-diazomethylanthracene^{26,27}, 2-nitrophenylhydrazide^{28,29}, isopropylidene hydrazide³⁰, 4-bromomethyl-7-acetoxycoumarin³¹, 9,10-diaminophenanthrene³², 9-aminophenanthrene²² and 3-bromomethyl-6,7-dimethoxy-1-methyl-2(1*H*)-quinoxalinone³³ derivatives are typical examples.

Phenacyl and substituted phenacyl esters are the most commonly used compounds. They are easily prepared in quantitative yields and are stable, and so permit the determination of fatty acids even at nanogram levels^{3,9}.

Separations are usually carried out on reversed-phase columns using isocratic or gradient elution with methanol, acetonitrile and water. The order of elution is governed by the length of the fatty acid carbon chain and the number of double bonds in it³. The retention time increases with increasing chain length and decreasing number of double bonds³⁴. These opposing tendencies lead to the occurrence of several pairs of fatty acids that are difficult to separate⁷, and the separation of which may be considered a criterion of the resolution efficiency of an analytical procedure. Examples of such critical pairs are linolenic (18:3) and myristic (14:0), palmitoleic (16:1) and arachidonic (20:4) and palmitic (16:0) and oleic (18:1) fatty acids^{15,34} although difficulties with the separation of some other fatty acid pairs may also be expected. In addition, the retention of phenacyl derivatives of fatty acids on the column is affected by geometric and double-bond positional isomerism^{3,10}. The *trans* isomers are generally eluted after the corresponding *cis* isomers. Positioning of the double bond in the proximity of the carboxy group of an acid usually leads to a decrease in retention compared with an isomer of a fatty acid with the double bond shifted in the direction of the methyl end of the carbon chain¹¹. The resolution of various adjacent peaks of fatty acid phenacyl esters on reversed-phase columns is further significantly affected by the column temperature and the proportions of methanol and acetonitrile in the mobile phase.

In this work we compared various separation conditions in order to achieve an optimal resolution of biologically important fatty acids and applied the method to the determination of the fatty acid composition of rat adipose tissue and lipid components of blood vessel walls.

EXPERIMENTAL

Materials

Fatty acid standards were purchased from the following sources: caproic (6:0), caprylic (8:0), capric (10:0) and lauric (12:0) acids from Sigma (St. Louis, MO, U.S.A.), myristic (14:0), palmitic (16:0) and stearic (18:0) acids from Calbiochem (San Diego, CA, U.S.A.) and myristoleic (*cis* 14:1 n9), pentadecanoic (15:0), margaric (17:0), oleic (*cis* 18:1 n9), elaidic (*trans* 18:1 n9), linoleic (*cis,cis* 18:2 n9, 12), linoelaidic (*trans,trans* 18:2 n9,12), linolenic (all-*cis* 18:3 n9,12,15), eicosenoic (*cis* 20:1 n11), eicosadienoic (*cis,cis* 20:2 n11,14), eicosatrienoic (all-*cis* 20:3 n11,14,17), arachidonic (all-*cis* 20:4 n5,8,11,14), erucic (*cis* 22:1 n13), docosahexaenoic (all-*cis* 22:6 n4,7,10,13,16,19) acids from Serva (Heidelberg, F.R.G.). Methyl esters of these fatty acids were obtained from Supelco (Bellefonte, PA, U.S.A.). All standards were of analytical-reagent grade.

Water (silica-glass distilled) was further filtered through a Millipore 0.5- μ m filter (Millipore, Bedford, MA, U.S.A.). Acetonitrile (HPLC grade) was obtained from Aldrich (Milwaukee, WI, U.S.A.) and methanol (HPLC grade) from Merck (Darmstadt, F.R.G.), and were used without further purification. α -Bromoacetophenone was purchased from Fluka (Hauppauge, NY, U.S.A.) or prepared in the laboratory by bromination of acetophenone and recrystallization from 96% ethanol (m.p. = 50°C). Triethylamine, acetone, chloroform and diethyl ether (analytical-reagent grade), purchased from Lachema (Brno, Czechoslovakia), were redistilled under reduced air pressure before the use.

Preparation of phenacyl esters of fatty acids

Fat from adipose tissue was extracted by the method of Folch *et al.*³⁵ and saponified with 25% (w/v) potassium hydroxide in 96% ethanol. The saponification was carried out in tightly closed 125 \times 20 mm I.D. PTFE-lined screw-capped culture tubes (Corning Glass Works, Corning, NY, U.S.A.) by boiling the mixture in a water-bath for 1 h. For saponification of 0.05 g of fat, 1 ml of potassium hydroxide solution was used. After cooling and acidification to pH 2 with 3 M hydrochloric acid, free fatty acids were extracted with *n*-hexane–diethyl ether (1:1). The extraction procedure was repeated twice using 2 ml of the solvent mixture each time.

Standards of fatty acids or fatty acids released from the saponified fat (10–100 μ g) were brought to dryness under a stream of dry nitrogen and phenacyl esters were then prepared by the method described by Wood and Lee³. Except that the reaction mixture of fatty acids, phenacyl bromide (25 μ l of a 10 mg/ml solution in acetone) and ethylamine (25 μ l of a 10 mg/ml solution in acetone) was heated in a boiling water-bath for only 5 min. The excess of phenacyl bromide was reacted with acetic acid (40 μ l of a 2 mg/ml solution in acetone) and, after evaporation of solvents under a stream of dry nitrogen at 40°C, the derivatization products were reconstituted in methanol.

HPLC analyses

Analyses of phenacyl esters of fatty acids were carried out on a Spectra-Physics SP 8100 high-performance liquid chromatograph, equipped with an SP 8400 UV–VIS variable-wavelength detector and an SP 4100 computing integrator (Spectra-

TABLE I

ELUTION CONDITIONS USED FOR SEPARATION OF FATTY ACID PHENACYL DERIVATIVES

Elution mode*	Mobile phase components present			Concentration gradient, CH ₃ OH-CH ₃ CN-H ₂ O (% , v/v) (time in minutes in parentheses)**
	CH ₃ OH	CH ₃ CN	H ₂ O	
A	x		x	83:17(0-35),90:10(70),100:0(90)
B		x	x	70:30(0-40), 90:10(60),100:0(80)
C	x	x	x	40:40.5:19.5(0),80.5:0:19.5(30),90:0:10(70),100:0:0(90)
D	x	x	x	40.5:41:18.5(0), 81.5:0:18.5(28-30),90:0:10(70),100:0:0(90)
E	x	x	x	40:40.5:19.5(0),81.5:0:18.5(25-27),90:0:10(70),100:0:0(90)
F	x	x	x	40:40.5:19.5(0),81.5:0:18.5(30),90:0:10(70),100:0:0(90)
G	x	x	x	40:40.5:19.5(0),81.5:0:18.5(28-30),90:0:10(70),100:0:0(90)

* Column, 250 × 4 mm I.D., Separon SGX C₁₈, 5 μm; guard column, 50 × 4 mm I.D., Separon SGX C₁₈, 7 μm; temperature, 40°C; flow-rate, 1.0 ml/min.

** Time to reach the composition cited using a linear gradient.

Physics, Santa Clara, CA, U.S.A.). Separations were performed on 250 × 4 mm I.D. columns packed with 5-μm Separon SGX C₁₈ octadecyl-bonded spherical silica and coupled with an octadecyl 7-μm guard column (50 × 4 mm I.D.) (Tessek, Prague, Czechoslovakia).

Samples of derivatized fatty acids dissolved in methanol (1-10 μg/ml of each) were injected through a 10-μl sample loop. All solvents were degassed under vacuum and then maintained flushed with helium (99.996%) (Messer, Griesheim, Austria). The column temperature was maintained at 40°C and the eluted phenacyls were detected at 242 nm.

Elution was performed using a concentration gradient of a methanol-acetonitrile-water ternary mixture. The initial proportions of the components at the beginning of the run was 40:40.5:18.5 (v/v). The concentration of acetonitrile was then decreased linearly so that it reached 0% at 25 min while its concentration in the mobile phase was replaced with methanol at the same gradient rate. Elution was completed with a linear gradient of the methanol-water mixture so that the mobile phase usually contained 90% of methanol at 60-70 min and was 100% methanol at 90 min. The elution of phenacyl esters of 6:0-22:1 fatty acids was completed within 80 min at a flow-rate of 1 ml/min. For the detailed composition of mobile phase, see Table I, elution mode E.

GC analyses

Analyses of methyl esters of fatty acids³⁶ were performed on a Carlo Erba 2351 Fractovap gas chromatograph with a flame ionization detector (Carlo Erba, Milan, Italy) connected with a HP 3380 A integrator (Hewlett-Packard, Avondale, PA, U.S.A.). The column (2 m × 2 mm I.D.) was packed with 10% DEGS-PS on Aeropak 30 (100-120 mesh) (Supelco). The column temperature was maintained at 190°C, the injector temperature was 225°C and the detector temperature was 190°C.

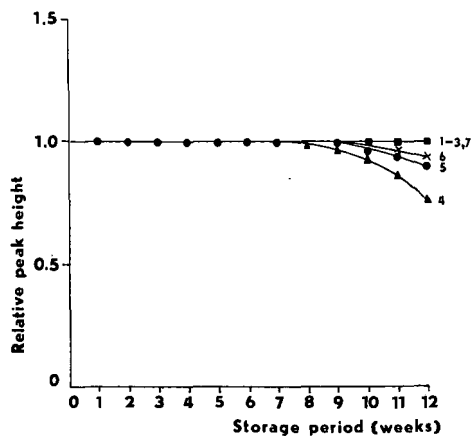


Fig. 1. Effect of storage period on relative peak heights of phenacyl esters of fatty acids. 1 = 12:0; 2 = 16:1; 3 = 18:0; 4 = 22:6; 5 = 20:4; 6 = 18:3; 7 = 18:2*cc*. Samples dissolved in methanol and stored closed in glass vials at 4°C, protected from daylight.

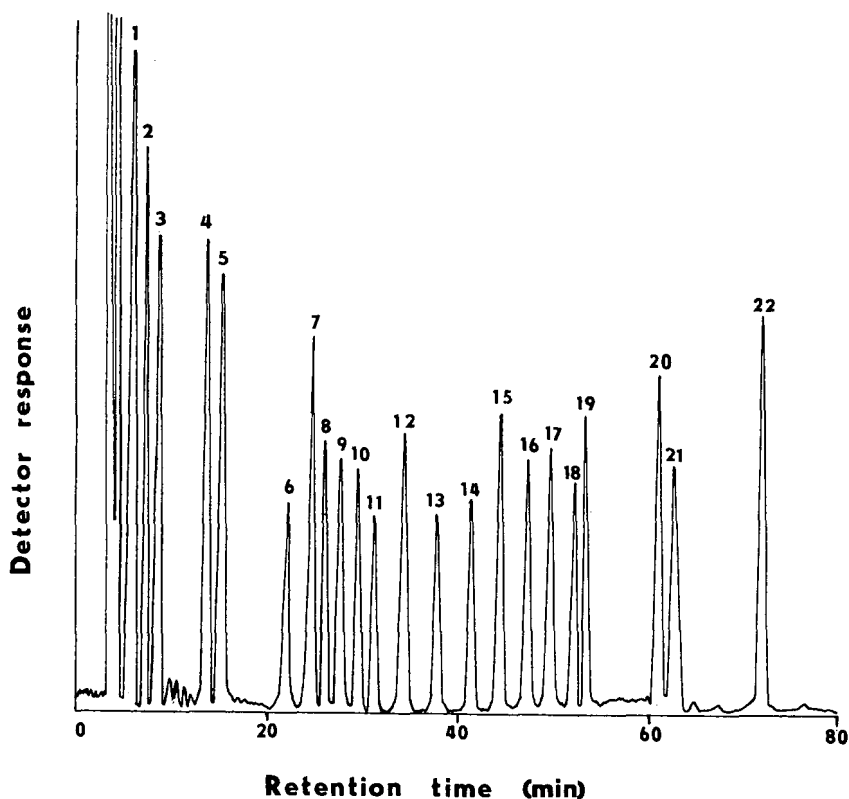


Fig. 2. HPLC of a standard mixture of fatty acid phenacyl esters (40 ng of each). Elution conditions as in Table I, elution mode E. Peaks: 1 = 6:0; 2 = 8:0; 3 = 10:0; 4 = 12:0; 5 = 14:1; 6 = 18:3; 7 = 14:0; 8 = 22:6; 9 = 16:1; 10 = 20:4; 11 = 18:2*cc*; 12 = 15:0; 13 = 18:2*tt*; 14 = 20:3; 15 = 16:0; 16 = 18:1*c*; 17 = 18:1*t*; 18 = 20:2; 19 = 17:0; 20 = 18:0; 21 = 20:1; 22 = 22:1.

TABLE II
EFFECTS OF ELUTION MODE ON RETENTION TIMES (t_R) AND RESOLUTIONS (R_S) OF SOME CRITICAL PAIRS OF FATTY ACID

Elution conditions are described in Table I. Resolution (R_S) calculated as $R_S = 2t_R/(W_1 + W_2)$, where W_1 and W_2 are the widths at the base of adjacent peaks. Individual R_S values refer to the neighbouring fatty acids. t_R = Retention time in minutes.

Elution mode	t_R 18:3	R_S	t_R 14:0	R_S	t_R 22:6	R_S	t_R 16:1	R_S	t_R 20:4	R_S	t_R 16:0	R_S	t_R 18:1
A	25.3	0	25.3	2.1	28.0	1.9	30.1	1.9	32.6	2.2	42.7	2.2	44.7
B	19.8	3.4	24.6	1.5	26.8	1.2	28.9	0	29.9	2.0	41.3	2.0	44.5
C	31.3	2.4	34.2	1.9	36.4	1.6	39.1	0.5	39.8	2.2	59.4	2.2	62.5
D	21.3	2.6	25.8	0.7	26.1	1.7	29.3	1.8	31.6	2.6	49.4	2.6	53.3
E	26.5	2.5	29.4	1.5	33.9	1.4	34.5	1.9	37.5	2.5	51.4	2.5	54.0
F	26.3	2.6	29.5	2.0	33.0	1.7	34.4	1.9	36.9	2.4	53.4	2.4	56.6
G	26.7	2.6	29.4	1.9	31.7	0.9	33.0	1.9	35.6	2.4	52.8	2.4	56.4

RESULTS

Fatty acid derivatization

Investigation of the effect of reaction time on the formation of fatty acid phenacyl esters showed that the reaction proceeded at high speed and with reproducible quantitative yields. The detector response reached its maximum value within 1 min of boiling for all of the fatty acids studied. Prolonged boiling, for up to 30 min, did not produce any additional peaks in the chromatogram or lead to an increase or decrease in the detector response.

The phenacyl derivatives of fatty acids showed good stability, as demonstrated in Fig. 1. No decreases in the HPLC peak heights were observed over a storage period of up to 8 weeks for samples dissolved in methanol and stored in closed culture tubes at 4°C and with exclusion of daylight. After that period a slight decrease in absorbance was observed with the phenacyl esters of 22:6, 20:4 and 18:3 fatty acids; however, no decrease beyond 20% relative was observed even after 12 weeks.

Resolution

A typical chromatogram of a mixture of phenacyl esters of fatty acid standards is presented in Fig. 2. The chromatographic conditions were as described under *HPLC analyses*.

Elution with a methanol-water mobile phase only failed to resolve linolenic (18:3) and myristic (14:0) acids. An acetonitrile-water mobile phase could not resolve

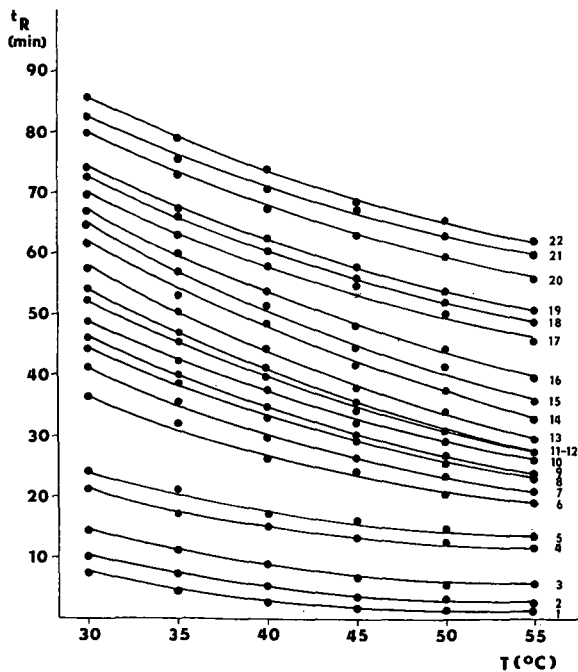


Fig. 3. Effect of column temperature on retention times of fatty acid phenacyl esters. Fatty acids as in Fig. 2. Elution mode E (Table I).

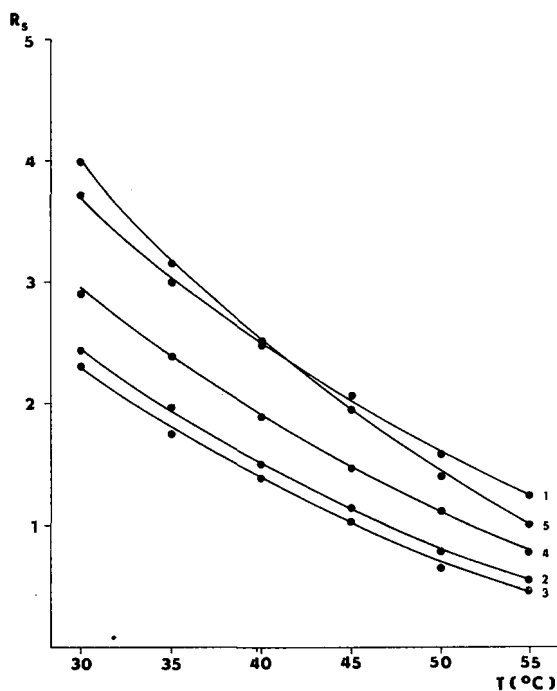


Fig. 4. Effect of column temperature on the resolution of critical pairs of fatty acid phenacyl esters. Elution mode E (Table I). Critical pairs: 1 = 18:3/14:0; 2 = 14:0/22:6; 3 = 22:6/16:1; 4 = 16:1/20:4; 5 = 16:0/18:1c.

adjacent peaks of palmitooleic (16:1) and arachidonic (20:4) acids. The retention times and resolutions of some important critical pairs of fatty acids under various elution conditions are summarized in Table II.

The effects of column temperature on the retention of some biologically important fatty acid phenacyl esters and on the resolution of their adjacent chromatographic pairs are depicted in Figs. 3 and 4. The optimal column temperature selected from these data was 40°C.

Quantitation

Calibration graphs were constructed from the chromatograms obtained by injecting 1.0, 2.5, 5.0, 10.0, 20.0, 40.0, 60.0, 80.0 and 100.0 ng of each fatty acid in a standard mixture. The ratios of the peak areas or heights were plotted against the corresponding concentrations of the fatty acid (ng per 10 μ l) and gave linear relationships over the concentration range studied. Under defined elution conditions both the measured parameters (peak heights and peak areas) gave the same results and therefore in routine analyses the peak heights were used. The linear regression equations for 22 biologically important mammalian fatty acids are presented in Table III. Identical linear equations were obtained for free fatty acid standards with those for methyl ester standards that were saponified prior to derivatization.

The detection limits for these fatty acids differ substantially depending on their

TABLE III
PARAMETERS OF THE CALIBRATION GRAPH FOR FATTY ACID PHENACYL ESTERS DETERMINED BY HPLC

Fatty acid	Abbreviation*	$x = ah + b^{**}$		r^{***}
		a	b	
Caproic	6:0	0.0025	-0.0039	0.999
Caprylic	8:0	0.0031	-0.0046	0.999
Capric	10:0	0.0038	+0.0065	0.999
Lauric	12:0	0.0037	+0.0142	0.999
Myristic	14:0	0.0078	-0.0074	0.994
Myristoleic	14:1	0.0063	+0.0106	0.998
Pentadecanoic	15:0	0.0112	-0.0021	0.996
Palmitic	16:0	0.0094	-0.0368	0.985
Palmitoleic	16:1	0.0124	-0.0053	0.998
Heptadecanoic	17:0	0.0094	+0.0448	0.973
Stearic	18:0	0.0084	+0.0547	0.981
Oleic	18:1 <i>c</i>	0.0106	+0.0607	0.987
Elaidic	18:1 <i>t</i>	0.0104	+0.0558	0.986
Linoleic	18:2 <i>cc</i>	0.0147	+0.0121	0.998
Linoelaidic	18:2 <i>tt</i>	0.0145	+0.0111	0.997
Linolenic	18:3	0.0146	-0.0084	0.998
Eicosenoic	20:1 <i>c</i>	0.0126	+0.0125	0.978
Eicosadienoic	20:2	0.0123	+0.0717	0.964
Eicosatrienoic	20:3	0.0137	+0.0147	0.996
Arachidonic	20:4	0.0122	-0.0174	0.998
Erucic	22:1	0.0073	+0.0418	0.993
Docosahexaenoic	22:6	0.0115	-0.0158	0.999

* *c* = *cis* isomer; *t* = *trans* isomer.

** x = Concentration of a fatty acid in ng per 10 μ l; h = peak height in mm. Parameters a and b calculated for the range 1–100 ng of a fatty acid in an injection volume of 10 μ l. Discrete measured concentrations were 1.0, 2.5, 5.0, 10.0, 20.0, 40.0, 60.0, 80.0 and 100.0 ng per 10 μ l ($n=5$).

*** r = Correlation coefficient.

molecular mass. Assuming a signal-to-noise ratio of 3, the limit of detection for short-chain (up to C₁₄) fatty acids was about 0.8 ng and for fatty acids with carbon chains longer than C₂₀ it was about 1.2 ng per injection. The smallest amount of fat analysed was 5 μ g.

Analytical recoveries calculated for each fatty acid from chromatograms of adipose tissue samples with and without added standard fatty acid mixture ranged from 92 to 106% with coefficients of variation in the range 1.5–6.3% ($n=5$) (Table IV).

Reproducibilities of fatty acid determinations by the proposed HPLC procedure, calculated from repeated analyses of identical adipose tissue fat samples, are presented in Table V. These results show that a given amount of each of these fatty acids can be determined accurately with a coefficient of variation of 2.1–8.2%.

The method was applied to the determination of the fatty acid composition of adipose tissue and blood vessel walls of rats fed various dietary fats (Figs. 5–8). Fatty acids were identified on the basis of the retention times of the components of the

TABLE IV

ANALYTICAL RECOVERY FOR THE DETERMINATION OF FATTY ACIDS ADDED TO RAT ADIPOSE TISSUE

<i>Fatty acid</i>	<i>Amount added (μg)[*]</i>	<i>Increase determined (μg) (n = 5)</i>	<i>Recovery (%)</i>	<i>Coefficient of variation (%)</i>
12:0	5.0	5.30 \pm 0.49	106.0	2.92
14:0	5.0	5.16 \pm 0.30	103.2	3.81
14:1	2.0	1.98 \pm 0.23	99.0	5.81
16:0	10.0	10.28 \pm 0.67	102.8	1.52
16:1	15.0	14.84 \pm 0.43	98.9	1.90
18:0	5.0	5.04 \pm 0.36	100.8	2.14
18:1c	15.0	15.20 \pm 0.67	101.3	2.41
18:1t	10.0	10.32 \pm 0.81	103.2	2.85
18:2cc	5.0	4.76 \pm 0.48	95.2	4.08
18:2tt	2.0	1.85 \pm 0.50	92.5	4.03
18:3	5.0	4.74 \pm 0.26	94.8	5.49
20:1c	2.0	1.86 \pm 0.18	93.0	4.68
20:2	2.0	1.84 \pm 0.29	92.0	3.76
20:4	2.0	1.86 \pm 0.21	93.0	6.29
22:6	2.0	1.92 \pm 0.16	96.0	2.89

* Amount of each fatty acid added to 100 μg of extracted adipose tissue fat before the saponification step.

TABLE V

REPRODUCIBILITY OF DETERMINATION OF FATTY ACIDS AS PHENACYL ESTERS IN ADIPOSE TISSUE BY HPLC

<i>Fatty acid</i>	<i>Mean[*] (μg)</i>	<i>Standard deviation (μg)</i>	<i>Coefficient of variation (%)</i>
12:0	0.28	0.08	3.00
14:0	2.78	0.23	8.20
14:1	0.30	0.10	3.33
16:0	24.54	0.55	2.24
16:1	12.30	0.55	4.47
18:0	3.18	0.28	3.81
18:1c	31.18	0.64	2.05
18:1t	15.36	0.67	4.36
18:2cc	2.08	0.43	2.67
18:2tt	2.24	0.11	4.91
18:3	1.18	0.18	5.25
20:1	0.14	0.06	3.29
20:2	0.14	0.06	3.29
20:4	0.28	0.08	3.57
22:6	0.40	0.10	2.50

* Expressed as mean amount in 100 μg of adipose tissue fat (n=5).

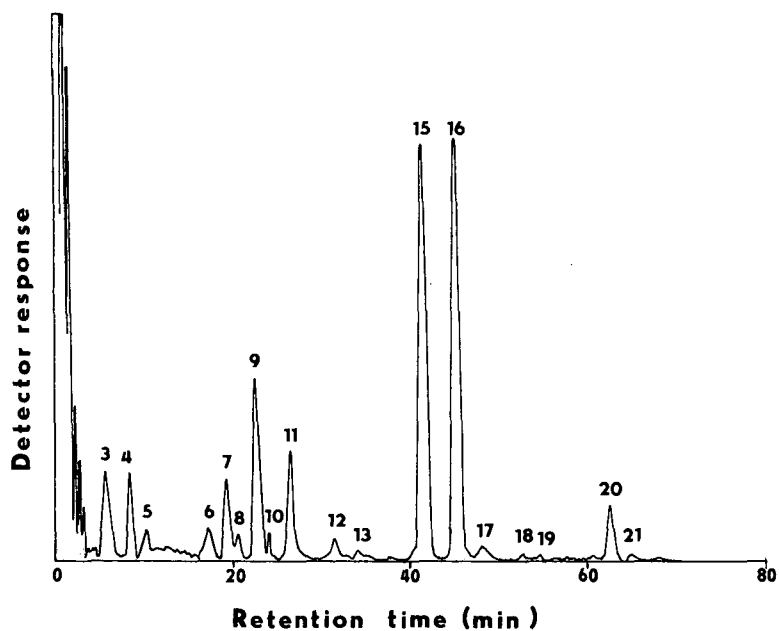


Fig. 5. HPLC of fatty acid phenacyl esters of adipose tissue of a laboratory rat fed diet A (cereal based). 100 μ g of fat per 1 ml of methanol; injection volume, 10 μ l; elution mode, E (Table I); absorbance scale, 0.04 a.u.

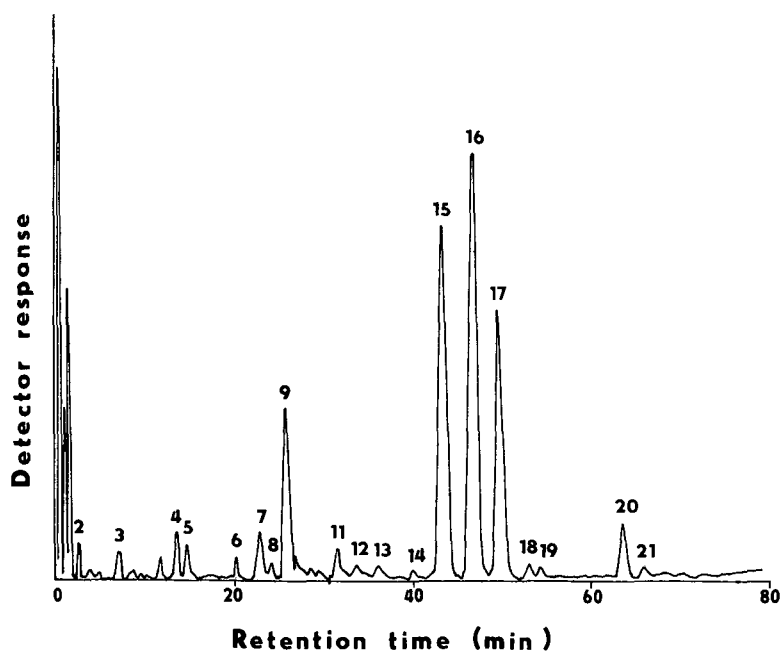


Fig. 6. HPLC of fatty acid phenacyl esters of adipose tissue of a laboratory rat fed diet B (hydrogenated vegetable oil). Conditions as in Fig. 5.

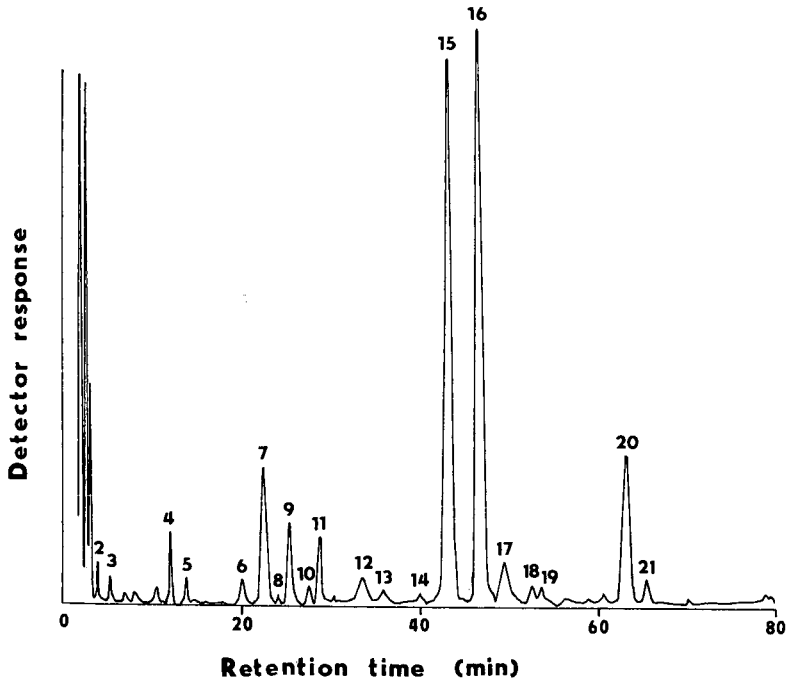


Fig. 7. HPLC of fatty acid phenacyl esters of blood vessel walls of a laboratory rat fed diet A. Conditions as in Fig. 5.

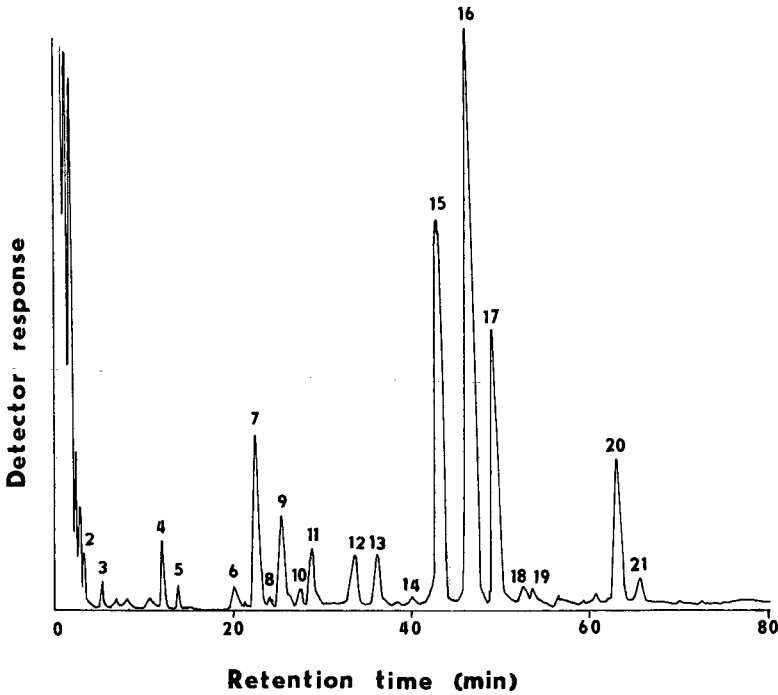


Fig. 8. HPLC of fatty acid phenacyl esters of blood vessel walls of a laboratory rat fed diet B. Conditions as in Fig. 5.

TABLE VI

COMPARISON OF HPLC AND GC RESULTS FOR DETERMINATION OF FATTY ACIDS IN ADIPOSE TISSUE FAT OF LABORATORY RATS FED DIFFERENT DIETARY FATS

Fatty acid	Concentration (% w/v)*			
	LC		GC	
	A**	B**	A**	B**
12:0	1.1	0.2	0.9	0.2
14:0	4.7	2.8	5.0	2.2
14:1	0.9	0.3	0.9	0.4
16:0	31.2	24.8	34.8	25.8
16:1	13.8	12.1	12.2	12.8
18:0	3.5	3.0	3.7	2.4
18:1 <i>c</i>	32.6	31.5	32.9	48.3
18:1 <i>t</i>	1.1	15.7	—	—
18:2 <i>cc</i>	5.7	2.1	4.7	2.2
18:2 <i>tt</i>	0.1	2.2	—	2.1
18:3	2.0	1.2	2.0	1.6
20:1 <i>c</i>	0.3	0.1	0.3	0.2
20:2	0.1	0.1	0.2	0.1
20:4	0.3	0.3	0.1	0.1
22:6	1.1	0.4	—	—

* Expressed as means of three analyses.

** A and B represent adipose tissue fat from animals fed a control diet DOS (cereal-based) and a hydrogenated fat diet, respectively.

standard fatty acid mixture. Adipose tissue fatty acids were also examined by a GC method as described under Experimental and the results of the two methods are compared in Table VI. The observed differences were slight except for 18:1 *trans* isomers, which were not resolved from the corresponding *cis* isomers by the GC method but were well resolved by the HPLC method.

DISCUSSION

Phenacyl esters of fatty acids have often been used in analytical chemistry. Recently they proved to be useful derivatives for the HPLC determination of long-chain fatty acids, both saturated and unsaturated^{3,6,7}. They can be prepared in various ways, differing mainly in the temperature and reaction time or in the presence or absence of various catalysts, for example 18-crown-6⁶. The most suitable for its simplicity and speed seems the procedure described by Wood and Lee³, which does not require a catalyst. We tested the minimum time necessary for the derivatization and found that the reaction was completed within 1 min. Further boiling did not increase or decrease the detector response. For convenience we used a 5-min reaction time.

Quenching the excess of the derivatization reagent with acetic acid is important for the successful application of this procedure³. The phenacyl esters prepared in this way exhibited very good stability; when properly stored they did not change for

about 2 months. The lowest stability was observed with phenacyl esters of polyunsaturated acids such as linolenic (18:3), arachidonic (20:4) and docosahexaenoic (22:6) acids. However, the decrease in the concentration of these acids observed after 3 months still did not exceed 20%.

The mobile phases usually used for the HPLC separation of fatty acid derivatives are acetonitrile–water^{2,3,7,9–11,24,27,29}, methanol–water^{5,6,12,14,19,23,28,30,33} and acetonitrile–methanol–water^{15,28,31,34}. Elution with acetonitrile–water is not efficient enough to separate the phenacyl derivatives of palmitoleic (16:1) and arachidonic (20:4) acids (Tables I and II), as also demonstrated elsewhere^{3,15,24}. Partial separation could be achieved with a decreased ratio of acetonitrile to water in the mobile phase, as reported by Borch⁷, but this is inconvenient owing to the substantial prolongation of the elution time (up to 4 h at a flow-rate of 2 ml/min) and the specific column requirements (90 × 0.64 cm I.D.).

Elution with methanol–water, on the other hand, cannot resolve adjacent peaks of linolenic (18:3) and myristic (14:0) acids (Tables I and II), as also reported elsewhere^{12,15,34}. Korte *et al.*¹² in addition could not resolve the phenacyl esters of oleic and elaidic acids (*cis* and *trans* isomers of 18:1 n9 acids), stearic (18:0) and *cis*-11-eicosenoic (20:1) acids and all-*cis*-4,7,10,13,16,19-docosahexaenoic (22:6) and palmitoleic (16:1) acids.

These results demonstrate the importance of the carbon chain length and the number of double bonds with respect to the solubility of phenacyl derivatives in these two solvents. Whereas in acetonitrile the number of double bonds seems to be more important for the solubility, in methanol the chain length seems more important. Utilization of the different properties of these two solvents offers some possibility for the separation of fatty acids whose differences in chain length and degree of unsaturation may make them difficult to separate with the use of either acetonitrile or methanol alone. Isocratic elution with any mixture of these solvents cannot gain from all the potential advantages of the system. As can be seen in Tables I and II, acetonitrile improves the resolution of fatty acids eluted at the beginning of the run (18:3 and 14:0), but significantly reduces the resolution of fatty acids eluted later (16:1 and 20:4 and 16:0 and 18:1). For these reasons, a ternary concentration gradient elution with acetonitrile, methanol and water seems to be the best way to optimize the separation of the phenacyl derivatives of mammalian fatty acids by reversed-phase HPLC.

In our method, the mobile phase contained acetonitrile only at the beginning of the run and the elution was then completed with an increasing concentration gradient of methanol in water (Table I, elution mode E, Fig. 1). The resolution achieved with this gradient elution and the time required seem to be better for a wider range of fatty acid phenacyl esters than reported previously^{3,7,12,14,15}. No previous paper has described the separation of 22:6 acid from palmitoleic (16:1) and myristic (14:0) acids. The resolution achieved under the chromatographic conditions suggested here is higher than 1.

The method is very suitable for the quantitation of fatty acids. The calibration graphs for both short- and long-chain fatty acids are linear over the investigated concentration range of 1.0–100.0 ng per injection. The calibration data presented in Table III demonstrate good precision and linearity.

The detection limits, close to those of fluorescence labelling methods of 0.5–2

fmol³³ or 5–1000 pmol³¹, and the good analytical reproducibility and recovery make the method suitable for a wide range of applications.

In conclusion, the method reported here demonstrates the increasing capacity of HPLC methodology to solve problems related to fatty acid analysis. This method is more efficient in the resolution of *cis* and *trans* conformational isomers of fatty acids than the usually used GC methods with packed columns, and there are no problems with derivatization of short-chain fatty acids or heat-labile polyunsaturates. Another advantage over GC methods is that the separated fatty acids are not destroyed during their detection, which enables further analyses to be performed.

REFERENCES

- 1 A. Kuksis, *J. Chromatogr.*, 143 (1977) 3.
- 2 B. Jaselskis, N. L. Stemm and W. D. Johnston, *Talanta*, 29 (1982) 54.
- 3 R. Wood and T. Lee, *J. Chromatogr.*, 254 (1983) 237.
- 4 M. I. Aveladano, M. Van Rollins and L. A. Horrocks, *J. Lipid Res.*, 24 (1983) 83.
- 5 W. M. Grogan, *Lipids*, 19 (1984) 341.
- 6 H. D. Durst, H. Milano, E. J. Kikta, Jr., S. A. Connelly and E. Grushka, *Anal. Chem.*, 47 (1975) 1797.
- 7 R. F. Borch, *Anal. Chem.*, 47 (1975) 2437.
- 8 S. Lam and E. Grushka, *J. Chromatogr. Sci.*, 15 (1977) 234.
- 9 R. Wood and T. Lee, *Fed. Proc. Fed. Am. Soc. Exp. Biol.*, 41 (1982) 1288.
- 10 R. Wood, F. Chumbler, M. Matocha and A. Zoeller, *Lipids*, 14 (1980) 789.
- 11 R. Wood, *J. Chromatogr.*, 287 (1984) 202.
- 12 K. Korte, K. R. Chien and M. L. Casey, *J. Chromatogr.*, 375 (1986) 225.
- 13 E. Grushka, H. D. Durst and E. J. Kikta, Jr., *J. Chromatogr.*, 112 (1975) 673.
- 14 T. N. Tweeten and D. L. Wetzel, *Cereal Chem.*, 56 (1979) 398.
- 15 J. Halgunset, E. W. Lund and A. Sunde, *J. Chromatogr.*, 237 (1982) 496.
- 16 P. T. S. Pei, W. C. Kossa, S. Ramachandran and R. S. Henley, *Lipids*, 11 (1976) 814.
- 17 W. Distler, *J. Chromatogr.*, 192 (1980) 240.
- 18 M. J. Cooper and M. W. Anders, *Anal. Chem.*, 46 (1974) 1849.
- 19 N. E. Bussell, R. A. Miller, J. A. Setterstrom and A. Gross, in G. L. Hawk (Editor), *Biological/Biomedical Applications of Liquid Chromatography*, Marcel Dekker, New York, 1979, p. 57.
- 20 E. Vioque, M. P. Maza and F. Millán, *J. Chromatogr.*, 331 (1985) 187.
- 21 M. Ikeda, K. Shimada and T. Sakaguchi, *J. Chromatogr.*, 272 (1983) 251.
- 22 M. Ikeda, K. Shimada, T. Sagakuchi and U. Matsumoto, *J. Chromatogr.*, 305 (1984) 261.
- 23 A. G. Netting and A. M. Duffield, *J. Chromatogr.*, 336 (1984) 115.
- 24 P. J. Ryan and T. W. Honeyman, *J. Chromatogr.*, 312 (1984) 461.
- 25 J. Weatherston, L. M. MacDonald, T. Blake, M. H. Benn and Y. Y. Huang, *J. Chromatogr.*, 161 (1978) 347.
- 26 S. A. Baker, J. E. Monti, S. T. Christian and R. D. Morin, *Anal. Biochem.*, 107 (1980) 116.
- 27 Y. Antoku, T. Sakai and H. Iwashita, *J. Chromatogr.*, 342 (1985) 359.
- 28 H. Miwa, C. Hiyama and M. Yamamoto, *J. Chromatogr.*, 321 (1985) 165.
- 29 H. Miwa, M. Yamamoto, T. Nishida, K. Nunoi and M. Kikuchi, *J. Chromatogr.*, 416 (1987) 237.
- 30 V. P. Agrawal, R. Lessire and P. K. Stumpf, *Arch. Biochem. Biophys.*, 230 (1984) 580.
- 31 H. Tsuchiya, T. Hayashi, M. Sato, M. Tatsumi and N. Takagi, *J. Chromatogr.*, 309 (1984) 43.
- 32 J. B. F. Lloyd, *J. Chromatogr.*, 189 (1980) 359.
- 33 M. Yamaguchi, R. Matsunaga, S. Hara, M. Nakamura and Y. Ohkura, *J. Chromatogr.*, 375 (1986) 27.
- 34 T. Hanis, M. Smrz, P. Klir, K. Macek and Z. Deyl, *Collect. Czech. Chem. Commun.*, 51 (1986) 2722.
- 35 J. Folch, M. Lees and G. H. Sloane-Stanley, *J. Biol. Chem.*, 226 (1957) 497.
- 36 W. Stoffel, F. Chu and E. H. Ahrens, Jr., *Anal. Chem.*, 3 (1959) 307.

CHROM. 20 521

ISOLATION OF BILE ACID GLUCOSIDES AND N-ACETYLGUCOSAMINIDES FROM HUMAN URINE BY ION-EXCHANGE CHROMATOGRAPHY AND REVERSED-PHASE HIGH-PERFORMANCE LIQUID CHROMATOGRAPHY

HANNS-ULRICH MARSCHALL, GUDRUN GREEN, BÖRJE EGESTAD and JAN SJÖVALL*
Department of Physiological Chemistry, Karolinska Institutet, Box 60 400, S-104 01 Stockholm (Sweden)

SUMMARY

A method for the isolation, separation and analysis of glucosides and N-acetylglucosaminides of non-amidated bile acids and of glycine- and taurine-conjugated bile acid glucosides from normal human urine is described. Total bile acids were extracted from 24-h collections of urine by repetitive use of Sep-Pak C₁₈ cartridges. After elution with 80% aqueous methanol, a group separation into non-amidated, glycine- and taurine-conjugated bile acids was performed by ion-exchange chromatography on Lipidex-DEAP. The glycosylated compounds were then separated from the corresponding non-glycosylated ones by high-performance liquid chromatography (HPLC) using a reversed-phase system with a linear methanol gradient. The glycosylated compounds isolated by HPLC were analysed by fast atom bombardment mass spectrometry and, after derivatization, by gas chromatography–mass spectrometry. Information about the sugar moieties of the bile acid glucosides was also obtained by treatment with different glycosidases.

INTRODUCTION

Glucosides of non-amidated*, and of glycine- and taurine-conjugated, bile acids were recently identified in normal human urine¹ using capillary gas chromatography–mass spectrometry (GC–MS) and comparisons with enzymatically prepared² reference compounds. However, the major glucosides of otherwise unconjugated bile acids did not correspond to any of the available reference compounds¹. For a detailed study including analysis by fast atom bombardment mass spectrometry (FAB–MS), it was necessary to isolate these compounds free of interfering substances. This paper describes an analytical procedure for the extraction, separation and isolation of glucosides of non-amidated, glycine- and taurine-conjugated bile acids, and of N-acetylglucosaminides of non-amidated bile acids from human urine.

* The term non-amidated is used for bile acids in which the C-24 carboxyl group is free and not linked to glycine or taurine.

EXPERIMENTAL

Solvents and reagents

All solvents and reagents were of analytical reagent grade and obtained from Merck (Darmstadt, F.R.G.) if not otherwise indicated. Chloroform, hexane, hexamethyldisilazane (Applied Science Europe, Oud-Beijerland, The Netherlands) and trimethylchlorosilane (Applied Science) were redistilled. Methanol was left with sodium hydroxide for 24 h and then redistilled twice. Pyridine was refluxed with calcium hydride, redistilled and stored over potassium hydroxide. Methoxyammonium chloride was obtained from Eastman Organic Chemicals (Rochester, NY, U.S.A.). Water was deionized and purified with a Milli Q cartridge (Millipore, Bedford, MA, U.S.A.).

Unlabelled bile acids were obtained from Steraloids (Wilton, NH, U.S.A.). Tauro[24-¹⁴C]cholic, [1-¹⁴C]glycocholic, [24-¹⁴C]cholic, [24-¹⁴C]chenodeoxycholic, [24-¹⁴C]deoxycholic and [24-¹⁴C]lithocholic acids with specific activities between 54 and 58 mCi/mmol were obtained from Amersham International (Amersham, U.K.). ¹⁴C-Labelled glucosides of taurocholic, glycocholic, cholic, chenodeoxycholic and deoxycholic acids were prepared enzymatically^{1,2}, as was hyodeoxycholic acid [¹⁴C]glucuronide³.

N-Acetylglucosaminidase from bovine kidney, α -glucosidase from bakers yeast, β -glucosidase from almonds, cholyglycine hydrolase from *Clostridium perfringens*, concanavalin A-agarose Type V-A and lentil lectin-Sepharose 4B were obtained from Sigma (Munich, F.R.G.), and *Helix pomatia* digestive juice from l'Industrie Biologique Francaise (Clichy, France). *n*-Alkane standards ranging from triacontane (C₃₀) to hexatetracontane (C₄₆) for the estimation of retention indices (RI) were obtained from Fluka (Buchs, Switzerland). Lipidex-DEAP was obtained from Packard (Downers Grove, IL, U.S.A.). Bond Elut C₂, C₈, C₁₈, CN, NH₂, SCX and PBA cartridges were obtained from Analytichem (Harbor City, CA, U.S.A.). Sep-Pak C₁₈ and Sep-Pak SIL were obtained from Waters Assoc. (Milford, MA, U.S.A.). Sep-Pak C₁₈ cartridges were washed with 5 ml methanol, 5 ml methanol-chloroform (1:1, v/v), 5 ml methanol and 10 ml water shortly before use.

Enzyme hydrolysis

Glycine- and taurine-conjugated bile acids were hydrolysed overnight at 37°C with 30 U cholyglycine hydrolase⁴. Different enzymes were tested for hydrolysis of non-amidated bile acid glycosides. Aliquots of the chromatographic fractions were treated at 25°C with 25 U α -glucosidase in 50 mM potassium dihydrogenphosphate, pH 6.8², with 25 U β -glucosidase in 50 mM sodium acetate, pH 5.0², with 2.5 U N-acetylglucosaminidase in 50 mM sodium citrate, pH 5.0⁵ or with 300 μ l of the digestive juice of *Helix pomatia* in 200 mM sodium acetate, pH 4.5⁶ or 50 mM sodium citrate, pH 3.6⁷. The incubation volume was 4 ml in all cases. After incubation, bile acids were extracted with Sep-Pak C₁₈ and rechromatographed on Lipidex-DEAP, using a column bed of 50 mm \times 4 mm (ref. 8). The non-amidated bile acids were eluted with 5 ml 0.1 M acetic acid and derivatized for GC-MS.

High-performance liquid chromatography (HPLC)

The instrument used for HPLC consisted of two LDC Constametric III pumps,

an LDC gradient Master (Laboratory Data Control, Milton Roy, Riviera Beach, FL, U.S.A.) and a Model 7125 injector Rheodyne, Cotati, CA, U.S.A.) with a 1-ml loop. The column system comprised an RP-18 guard cartridge (15 mm \times 3.9 mm; Brownlee Labs., Santa Clara, CA, U.S.A.) and a μ Bondapak C₁₈ steel column (300 mm \times 3.9 mm, particle size 10 μ m; Waters Assoc.). The samples were injected in 100 μ l 80% aqueous methanol and elution was performed with a linear gradient of 50–90% aqueous methanol containing 1% (v/v) acetic acid over a period of 80 min. The flow-rate was 1 ml/min. The radioactivity was monitored continuously, using a Trace 7140 radioactivity flow monitor (Packard Instruments).

Gas chromatography

A HRGC 4160 instrument (Farmitalia Carlo Erba, Milano, Italy) was used with a SP 4270 integrator (Spectra Physics, Darmstadt, F.R.G.). The column was a 24 m \times 0.32 mm I.D. fused-silica capillary coated with cross-linked methyl silicone (film thickness 0.25 μ m; Quadrex Corp., New Haven, CN, U.S.A.). Helium was used as the carrier gas at 50–100 kPa. The samples were injected on column as methyl ester trimethylsilyl (TMS) ether derivatives in 0.5–1 μ l hexane at 60°C. The temperature was then taken to 280 or 300°C at a rate of 30°C/min. The derivatives were prepared by methylation of the samples dissolved in 1 ml methanol–diethyl ether (1:9, v/v) with diazomethane in diethyl ether for 15 min at 4°C and converting into the TMS ethers with 100 μ l of pyridine–hexamethyldisilazane–trimethylchlorosilane (3:2:1, v/v/v) for 30 min at 60°C. The samples were taken to dryness under a stream of nitrogen and immediately dissolved in hexane.

Gas chromatography–mass spectrometry

GC–MS was carried out on a VG 7070E double-focusing mass spectrometer with an electron-impact ion source, a Dani 3800 gas chromatograph and a VG 11-250 data system (VG Analytical, Manchester, U.K.). The capillary column was directly connected and extended into the ion source. An all-glass falling-needle system was used for the injection of the samples at 270°C. After 8 min, the temperature was taken to 300°C at a rate of 15°C/min. The ionization energy was 70 eV and the trap current 200 μ A. Spectra were taken by repetitive magnetic scanning of the range m/z 800–50 at a scan rate of 2 s per decade and a resolution of 1000 (5% valley).

Fast atom bombardment mass spectrometry

FAB–MS was performed with the VG 7070E instrument equipped with a FAB ion source and an Ion Tech atom gun. A 10- μ l volume of the sample dissolved in 20 μ l methanol was applied under a slight stream of nitrogen to the FAB target already covered with the glycerol matrix. Xenon having 8.0 keV energy was used for bombardment of the sample. The spectra of negative ions were recorded in the range m/z 800–80 at a scan rate of 10 s per decade and a resolution of 1000.

Analytical procedure

A flow scheme of the method is shown in Fig. 1.

Extraction of bile acid glycosides from urine. Urine samples of 24 h were obtained from healthy humans. The urine was stored at 4°C during collection and was then analysed immediately, or frozen and stored at –20°C.

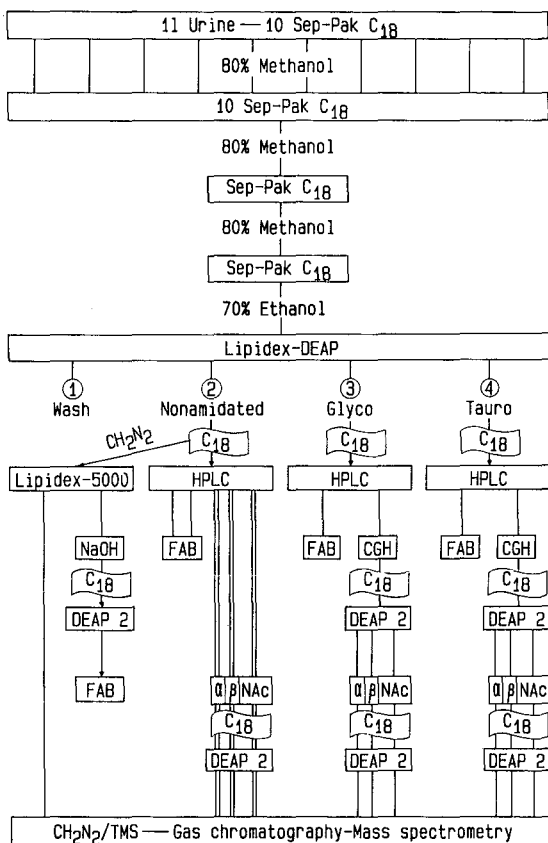


Fig. 1. Flow scheme of the analytical procedure. DEAP 2 = fraction 2 from Lipidex-DEAP containing non-amidated ("unconjugated") bile acids; C₁₈ = Sep-Pak C₁₈; FAB = FAB-MS; CGH = cholyglycine hydrolase; α = α -glucosidase; β = β -glucosidase; NAc = N-acetylglucosaminidase.

The 24-h portion of urine was filtered and $(40-50) \cdot 10^3$ dpm each of ¹⁴C-labelled taurocholic, glycocholic and cholic acids, and either cholic or chenodeoxycholic acid glucosides were added. Ten Sep-Pak C₁₈ cartridges were used for extraction of 1000 ml urine under gravity flow. Each cartridge was washed with 10 ml water and bile acids were eluted with 10 ml 80% aqueous methanol. The cartridges were then washed with 5 ml methanol and 10 ml water and used for reextraction of the eluates. The 80% aqueous methanol solution was diluted in 60 ml water and passed through the cartridges which were again washed with 10 ml water and eluted with 10 ml 80% aqueous methanol. The eluates were pooled and evaporated to about 20 ml on a rotary evaporator, and 50 ml water were added. This solution was passed through a fresh Sep-Pak C₁₈ cartridge, which was washed with 10 ml water and eluted with 10 ml 80% aqueous methanol. The eluate was again diluted in 60 ml water and extracted with another Sep-Pak C₁₈ cartridge. After washing with 10 ml water, the bile acids were eluted with 3×5 ml 70% ethanol.

Purification and separation of bile acid glycosides. The three 5-ml eluates were

applied consecutively on a 300 mm × 4 mm column of Lipidex-DEAP in 70% ethanol⁸. A nitrogen pressure of about 100 kPa gave a suitable flow-rate. After washing with 10 ml 70% ethanol, non-amidated bile acids were eluted with 25 ml 0.1 M acetic acid, glycine conjugates with 20 ml 0.3 M ammonium acetate, pH 5.0 and taurine conjugates with 20 ml 0.15 M ammonium acetate, pH 6.6, all in 70% ethanol. The three fractions were diluted in 50 ml water and extracted with Sep-Pak C₁₈. The bile acids were eluted with 5 ml methanol and the eluates were taken to dryness under a stream of nitrogen.

One fifth of the fraction containing non-amidated bile acids was methylated with diazomethane and subjected to normal-phase chromatography under gravity flow on a 60 mm × 4 mm column of Lipidex 5000 in chloroform-hexane (1:4, v/v)⁹. The sample was applied in 1 ml and rinsed into the column with 4 ml of the same solvent. After elution of methyl dihydroxycholanoates with 5 ml chloroform-hexane (3:7, v/v), and methyl trihydroxycholanoates with 5 ml chloroform-hexane (1:1, v/v), a final fraction, containing the methyl esters of bile acid glycosides, was eluted with 5 ml methanol. This fraction was divided into two parts. One part was hydrolysed for 3 h at 60°C in 2.5 ml 2 M sodium hydroxide, and bile acid glycosides were extracted with Sep-Pak C₁₈ for analysis by FAB-MS. The other part was converted into TMS ether derivatives and used for an estimation of the total non-amidated bile acid glycosides by GC-MS.

The remaining 4/5 of the non-amidated bile acids and the fractions containing the glycine and taurine conjugates were subjected to reversed-phase HPLC. ¹⁴C-Labelled taurocholic, glycocholic, cholic, chenodeoxycholic, deoxycholic and lithocholic acids, (40–50) · 10³ dpm of each, were added as markers to fractions that did not already contain these labels.

Characterization of bile acid glycosides. A 400-μl volume of each HPLC fraction of 2 ml was evaporated and methyl ester TMS ether derivatives were prepared. In the case of glycine and taurine conjugates, derivatization was preceded by treatment with cholyglycine hydrolase and rechromatography on Lipidex-DEAP. All samples were then analysed by GC. Fractions giving peaks indicative of derivatized bile acid glycosides were taken for analysis by FAB-MS and for treatment with α-glucosidase, β-glucosidase, and N-acetylglucosaminidase with analysis of the products by GC and GC-MS. One fifth of the original HPLC fractions was used for each study.

RESULTS AND DISCUSSION

Extraction.

Multiple extractions with Sep-Pak C₁₈ were required to remove pigments that would otherwise coelute with bile acids in the subsequent ion-exchange chromatography on Lipidex-DEAP. The Sep-Pak cartridges appeared to be overloaded in the first three of the four extraction steps since significant amounts of colour appeared in the effluent after passage of about two thirds of the volume to be extracted. The water wash was even more dark-coloured. However, retention of radiolabelled bile acids added to urine, including the most polar taurocholic acid, the least polar lithocholic acid and the glucosides of cholic and chenodeoxycholic acids, was better than 90% in all steps.

The original studies by Shackleton and Whitney¹⁰ indicated that one Sep-Pak C₁₈ cartridge had sufficient capacity for 95% extraction of steroid glucuronides from 100 ml urine. Obviously, the concentration of organic material in the sample is important. In the present study the total recovery of added radioactivity after the chromatography on Lipidex-DEAP was $76.4 \pm 2.1\%$ ($n = 3$) when a 24-h sample of 1 l was extracted with ten Sep-Pak cartridges. Selective losses of any of the added labelled bile acids were not observed. The recovery reached almost 100% when more dilute urine was extracted, *e.g.*, in the extraction of 1 out of 3 l collected during a 24-h period.

Group separation

The material obtained by Sep-Pak extraction is a complex mixture of amphiphilic compounds with different polarities and charges. The isolation of bile acid glycosides as individual compounds or groups would be difficult without prior separation based on the presence of other conjugating groups, *e.g.*, glycine, taurine or glucuronic acid. Ion-exchange chromatography on Lipidex-DEAP is suitable for this purpose⁸. The dimensions of the Lipidex-DEAP column as well as the volumes of the washing and buffer solutions were chosen to achieve a maximum removal of interfering substances and a minimum overlap between the bile acid groups. The column had a capacity of about 1.2 mmol for chloride ions. Although the capacity for bile acid and steroid conjugates is considerably smaller due to gel exclusion effects⁸, the size was sufficient for separation of the steroid and bile acid conjugates excreted in 24 h by healthy subjects. However, it is advisable to add ¹⁴C-labelled cholic, glycocholic and taurocholic acids to the sample to monitor the capacity and separations, particularly when pathological samples are analysed which contain larger amounts of acids.

Separation of bile acid glycosides

A number of systems were tried for the separation of glycosylated from non-glycosylated bile acids within each fraction from Lipidex-DEAP. Glycosylation did not increase the polarity to the extent expected, and a separation could not be achieved on Sep-Pak C₁₈ or Bond Elut C₁₈ cartridges eluted with water to which methanol was added in 5% increments. Similar results were obtained with Bond Elut C₂, C₈ and SCX.

Bond Elut CN and NH₂ were unsuccessfully tested in chloroform-methanol systems, and Sep-Pak SIL in the system described by Street *et al.*¹¹. Ion-pair chromatography on Lipidex 1000¹² in aqueous methanol, and reversed-phase chromatography of the acids in polar systems¹³, also did not separate glycosidic from non-glycosidic bile acids. Immobilized lectins with affinity for glucose moieties, *i.e.*, concanavalin A and lentil lectin¹⁴ failed to extract the labelled chenodeoxycholic and cholic acid glucosides from aqueous solutions containing 10% aqueous methanol. Bond Elut PBA, containing covalently linked phenylboronic acid, did not bind the glucosides from 0.1 M phosphate buffer between pH 5 and 11¹⁵, with or without 50% aqueous methanol. This is in agreement with the absence of vicinal *cis*-hydroxyl groups in a glucoside linked at C-1 to the bile acid.

Since a simple preparative method could not be established, reversed-phase HPLC was used. A wide variety of systems has been described¹⁶. For the present

purpose, high capacity and absence of buffers were important. Complete separation of individual components was not important, the main aim being to separate glycosylated from the corresponding non-glycosylated bile acids. This was achieved in a gradient of aqueous methanol containing acetic acid to suppress dissociation of all but the taurine-conjugated bile acids. The capacity of the analytical column was sufficient for separation of the entire fractions from Lipidex-DEAP without significant broadening of the peaks of the added labelled bile acids. However, a loss of about 20% was observed, the reason for which is still unclear. In an experiment where ^{14}C -labelled chenodeoxycholic acid glucoside was added alone to the urine, the recovery through the entire procedure was 68%.

Fig. 2 shows a chromatogram obtained in the separation of 5 mg material eluted in the fraction of non-amidated bile acids from Lipidex-DEAP. The peaks due to added labelled bile acids are indicated, as are the retention times of labelled glucosides of taurocholic, glycocholic, cholic and deoxycholic acids determined in separate experiments. The peak widths of the labelled bile acids were about 2 ml, and the elution volumes varied by less than 1.5 ml in different experiments, with the exception of taurocholic acid which was eluted up to 7 ml earlier when the total taurine-conjugate fraction from Lipidex-DEAP was separated. This may be due to the fact that taurine-conjugated bile acids are separated as the anions and the mobility may be affected by other compounds in the fraction.

With the bile acids studied, glucosidation increased the mobility to a lesser extent than the introduction of a hydroxyl group in the steroid skeleton. Vicinal effects or interaction with the acid group of the side chain might explain this behaviour. Alternatively, polar interactions with the bonded phase may retard the elution of the glucosylated compounds. The importance of a preliminary group separation

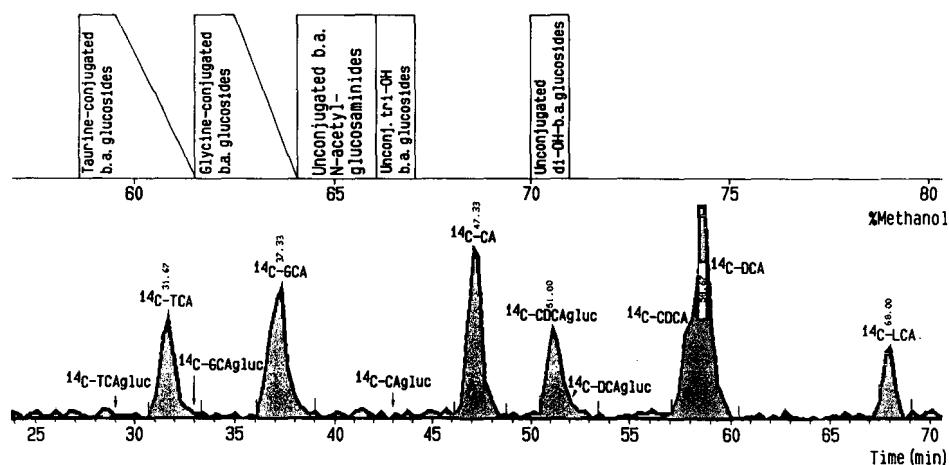


Fig. 2. Original recording of radioactivity in the HPLC separation of the non-amidated bile acid fraction from Lipidex-DEAP to which ^{14}C -labelled taurocholic (TCA), glycocholic (GCA), cholic (CA), chenodeoxycholic (CDCA), deoxycholic (DCA) and lithocholic (LCA) acids and chenodeoxycholic acid glucoside (CDCA-gluc) had been added. Retention times of other bile acid glucosides (gluc) are indicated by arrows. The ranges of elution of urinary bile acid glucosides are indicated on the line showing the methanol concentration of the gradient. The flow-rate was 1 ml/min.

on Lipidex-DEAP is obvious, especially considering the milligram amounts of interfering compounds that appear among the glycine- and taurine-conjugated bile acids. Glucuronides of neutral steroids and bile alcohols¹⁷ are found mainly in the glycine-conjugate fraction and are eluted in HPLC before 30 and after 40 ml of effluent, respectively. Part of the bile acid glucuronides⁶ and neutral steroid sulphates appear in the taurine-conjugate fraction and are eluted in HPLC before 25 and after 40 ml of effluent, respectively. The removal of bile acid glucuronides prior to HPLC is particularly important since these compounds might coelute in HPLC (hyodeoxycholic acid 6 α -glucuronide appeared at 40 ml) and give mass spectrometric fragmentation patterns similar to those of the derivatives of bile acid glucosides^{1,6}.

The elution of urinary bile acid glycosides was monitored by GC and GC-MS after removal of the glycine and taurine moieties and derivatization. Retention indices of the derivatives of intact glycosides were between 4200 and 4600¹ and in this range a search was made for fragment ions typical of derivatives of hexosides (m/z 204 and 217^{18,19}), N-acetylhexosaminides (m/z 173 and 186^{18,19}) and the steroid structure of trihydroxycholanoates (m/z 549, 459 and 369), unsaturated dihydroxycholanoates (m/z 459, 369) and dihydroxycholanoates (m/z 461, 371)⁶.

Derivatives of bile acid glycosides with retention indices between 4200 and 4400 showed fragment ions typical of derivatives of hexosides¹. Compounds giving

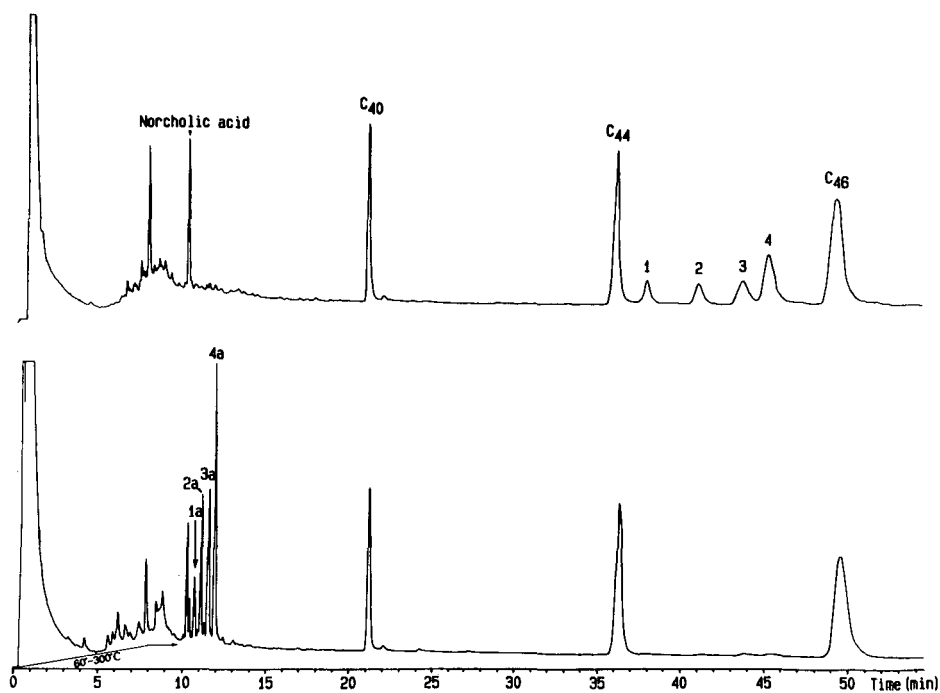


Fig. 3. GC analyses of the four major bile acid glycosides appearing at 38–42 ml of effluent in the HPLC separation of non-amidated bile acids collected from Lipidex-DEAP. Upper chromatogram: analysis of the derivatized intact conjugates. Lower chromatogram: analysis of the derivatized bile acids released by N-acetylglucosaminidase. The peak of the derivative of norcholic acid present in the original HPLC fraction appears at about 10.2 min in both chromatograms. C₄₀, C₄₄, C₄₆ = *n*-alkanes added as standards.

fragment ions typical for trihydroxy bile acid hexosides were eluted in HPLC at 42–44 ml (Fig. 2), and compounds with fragment ions typical of saturated and unsaturated dihydroxy bile acid hexosides at 50–52 ml (Fig. 2). These two groups of compounds were sensitive towards β -glucosidase.

Derivatives of bile acid glycosides with retention indices between 4400 and 4600, on the other hand, showed fragment ions typical of N-acetylhexosaminides. These compounds were eluted in HPLC at 38–42 ml (Fig. 2) and were cleaved with N-acetylglucosaminidase but not by any of the other enzymes. Fig. 3 shows the gas chromatographic analyses of material eluted at 40 ml (Fig. 2) before and after hydrolysis with N-acetylglucosaminidase. The peak areas of the derivatives of the bile acids released by the enzyme (peaks 1a–4a, Fig. 3) were about 90% of the peak areas of the derivatized N-acetylhexosaminides originally present in the fraction (peaks 1–4, Fig. 3). Norcholic acid appeared in the same HPLC fraction and could be used as an internal standard in this calculation.

The HPLC fractions were sufficiently pure for direct analysis by FAB-MS. Fractions containing taurine- and glycine-conjugated bile acid glycosides (*cf.*, Fig. 2) showed negative ions at m/z 676 and 626, consistent with the quasimolecular ions of taurine- and glycine-conjugated trihydroxy bile acid glycosides, respectively. Negative-ion FAB-MS of fractions obtained in the HPLC separation of non-amidated bile acid glycosides gave peaks consistent with quasimolecular ions of N-acetylglucosaminidase of saturated (m/z 594) and unsaturated (m/z 592) dihydroxy and saturated trihydroxy (m/z 610) bile acids (38–42 ml, Fig. 2), and peaks consistent with quasimolecular ions of glycosides of saturated (m/z 553) and unsaturated (m/z 551) dihydroxy (50–52 ml, Fig. 2) and saturated trihydroxy (m/z 569) bile acids (42–44 ml, Fig. 2). These analyses also showed that N-acetylglucosaminides of trihydroxy bile acids were eluted first, followed by those of unsaturated and then saturated dihydroxy bile acids. A detailed characterization of these compounds will be published separately.

ACKNOWLEDGEMENTS

This work was supported by the Swedish Medical Research Council (grant no. 13X-219) and Karolinska Institutet. H.-U.M. is the recipient of an education grant from the Deutsche Forschungsgemeinschaft.

REFERENCES

- 1 H.-U. Marschall, B. Egestad, H. Matern, S. Matern and J. Sjövall, *FEBS Lett.*, 213 (1987) 411.
- 2 H. Matern, S. Matern and W. Gerok, *Proc. Natl. Acad. Sci. U.S.A.*, 81 (1984) 7036.
- 3 H.-U. Marschall, H. Matern, B. Egestad, S. Matern and J. Sjövall, *Biochim. Biophys. Acta*, 921 (1987) 392.
- 4 G. Karlaganis and G. Paumgartner, *Clin. Chim. Acta*, 92 (1979) 19.
- 5 S. C. Li and Y. T. Li, *J. Biol. Chem.*, 245 (1970) 5153.
- 6 B. Almé and J. Sjövall, *J. Steroid Biochem.*, 13 (1980) 907.
- 7 A. B. Roy, in S. Bernstein and S. Solomon (Editors), *Chemical and Biological Aspects of Steroid Conjugation*, Springer, Berlin, Heidelberg, New York, 1970, pp. 75–130.
- 8 B. Almé, A. Bremmelgaard, J. Sjövall and P. Thomassen, *J. Lipid Res.*, 18 (1977) 339.
- 9 A. Bremmelgaard and J. Sjövall, *J. Lipid Res.*, 21 (1980) 1072.
- 10 C. H. L. Shackleton and J. O. Whitney, *Clin. Chim. Acta*, 107 (1980) 231.

- 11 J. M. Street, D. J. H. Trafford and H. L. J. Makin, *J. Chromatogr.*, 343 (1985) 259.
- 12 A. Dyfverman and J. Sjövall, *Anal. Biochem.*, 134 (1983) 303.
- 13 E. Nyström and J. Sjövall, *Anal. Lett.*, 6 (1973) 155.
- 14 I. J. Goldstein and R. D. Poretz, in I. E. Liener, N. Sharon and I. J. Goldstein (Editors), *The Lectins, Properties, Functions, and Applications in Biology and Medicine*, Academic Press, Orlando, 1986, pp. 33–247.
- 15 P. O. Edlund and D. Westerlund, *J. Pharm. Biomed. Anal.*, 2 (1984) 315.
- 16 T. Nambara and J. Goto, in K. D. R. Setchell, D. Kritchevsky and P. P. Nair (Editors), *The Bile Acids*, Vol. 4, Plenum, New York, London, 1988, in press.
- 17 G. Karlaganis, B. Almé, V. Karlaganis and J. Sjövall, *J. Steroid Biochem.*, 14 (1981) 341.
- 18 D. C. DeJongh, T. Radford, J. D. Hribar, S. Hanessian, M. Bieber, G. Dawson and C. C. Sweeley, *J. Am. Chem. Soc.*, 91 (1969) 1728.
- 19 P. L. Coduti and C. A. Bush, *Anal. Biochem.*, 78 (1977) 21.

CHROM. 20 718

DEVELOPMENT OF A SOLID-PHASE EXTRACTION TECHNIQUE FOR α -HUMAN ATRIAL NATRIURETIC PEPTIDE IN HUMAN PLASMA

MICHAEL A. O'FLYNN, ROGER C. CAUSON*, JOHN BROWN and SHIGERU KAGEYAMA
Department of Clinical Pharmacology, Royal Postgraduate Medical School, Hammersmith Hospital, London W12 0HS (U.K.)

SUMMARY

A reliable extraction method was developed for α -human atrial natriuretic peptide (α -hANP) using Bond Elut C₈ columns in tandem. This involved activation of the columns using methanol followed by a water wash to remove the excess methanol. Plasma (1 ml) was then added and a vacuum applied until all was drawn through. Excess protein and other endogenous compounds were removed by washing the columns with water and elution of the α -hANP was achieved with 0.75 ml acetonitrile-water-trifluoroacetic acid (80:19.8:0.2, v/v/v). Samples were evaporated under nitrogen and reconstituted in radioimmunoassay buffer ready for analysis. The recovery of α -hANP from plasma using this method was found to be 90% \pm 0.6% [mean \pm standard error of the mean (S.E.M.); coefficient of variation (C.V.) = 1.5%] which will allow more precise measurement of the peptide than is presently available. With this high precision of analysis available, having a limit of detection of 0.4 fmol/ml and a range of 0 to 32 fmol/ml, a low-dose infusion of α -hANP was conducted and the changes in plasma concentration were followed.

INTRODUCTION

The recently discovered peptide, α -human atrial natriuretic peptide (α -hANP) is released from the heart atrium. It contains 28 amino acids and is formed by peptidase cleavage of a much larger pro-peptide. It has many physiological effects including natriuresis, diuresis, kaliuresis, hypotensive effects, inhibition of adenylate cyclase¹, inhibition of aldosterone production², vasodilation³, inhibition of angiotensin II release⁴, noradrenaline and potassium-induced vasoconstriction and modulation of renal gluconeogenesis⁵. The many physiological effects of α -hANP indicate that it is important in the regulation of fluid retention, therefore precise quantitation of small changes in circulating levels of α -hANP and monitoring of physiological effects will give a more accurate indication of this peptide's role. Many methods have been published on the extraction of α -hANP using Sep-Pack C₁₈ reversed-phase extraction cartridges. Richards *et al.*⁶ quote recoveries of unlabelled peptide from plasma of 65 \pm 5% [mean \pm standard deviation (S.D.)] which could be increased to 83 \pm 5% (mean \pm S.D.) using an acidification step. Morice *et al.*⁷ quote recoveries of between

80 and 90%, however plasma α -hANP levels were not corrected for recovery. Since all other groups had concentrated on Sep-Pak extractions and considering that Analytichem produce a wider range of reversed-phase columns we decided to screen these columns and choose the best on which to base our extraction.

Morice *et al.*⁷ have attempted to demonstrate a change in circulating α -hANP levels during infusions of increasing concentrations of α -hANP (0.4, 2.0 and 10.0 pmol min⁻¹ kg⁻¹) using their extraction procedure. Since our method is more precise, we decided to repeat their work using an infusion rate of 1.2 pmol min⁻¹ kg⁻¹ to test the effectiveness of our method by monitoring plasma levels of α -hANP.

EXPERIMENTAL

Reagents and materials

All tubes used in the method were polypropylene and were obtained from Sarstedt (Leicester, U.K.). Methanol and water, both high-performance liquid chromatographic (HPLC) grade, were obtained from Rathburn Chemicals (Walkerburn, U.K.). Disodium EDTA (reagent grade) was obtained from Sigma (Poole, U.K.). Trasyol was obtained from Bayer (Newbury, U.K.). Bond Elut columns C₂ (ethyl bonded silica, catalogue number: 603101), C₈ (octyl bonded silica, catalogue number: 606101), C₁₈ (octadecyl bonded silica, catalogue number: 607101), PH (phenyl bonded silica, catalogue number: 608101), CN (cyanopropyl bonded silica, catalogue number: 613101) and CH (cyclohexyl bonded silica, catalogue number: 610101) were obtained from Jones Chromatography (Llanbradach, U.K.). The radioimmunoassay (RIA) kit (RPA 512) used was from Amersham International (Amersham, U.K.) and included the [¹²⁵I] α -hANP used to develop the extraction. The α -hANP used in the infusion was obtained from Peninsula Labs. (Merseyside, U.K.).

Apparatus

Extraction was carried out with a 10-channel Vac Elut device (Jones Chromatography). Gamma counting was carried out using a Clinigamma 1272 counter (LKB/Pharmacia; Milton Keynes, U.K.).

Sample collection and storage

Blood samples were collected into chilled polypropylene tubes containing 1 mg/ml disodium EDTA and sufficient Trasyol to give a final concentration of 1000 kallikrein inhibitor units per ml. These were centrifuged at 2000 g for 20 min at 4°C. The plasma was then separated into two 1.5-ml aliquots and stored under liquid nitrogen until analysed.

Plasma pool preparation

A plasma pool was prepared by taking 20 ml of blood from six normal human volunteers via an antecubital vein. This was centrifuged at 2000 g for 10 min at 4°C. The resultant plasma was bulked and stirred on ice for 2 min, then aliquots were taken. The aliquots were frozen in dry ice, then stored under liquid nitrogen until analysis.

Radioactivity measurements

All gamma counting was carried out using a 4-well γ -counter which was fully automated with a sample capacity of 500. Since the amount of [^{125}I] α -hANP added to each plasma was approximately 2000 cpm/ml, a counting time of 30 min was required to achieve a good precision of counting ($\chi^2 < 1\%$). This amount of radioactivity (2000 cpm/ml) is equivalent to 2 pg of unlabelled α -hANP which is within the normal range found in humans.

Selection of the column to be used in the extraction

Pool plasma was thawed and centrifuged at 2000 g for 10 min at 4°C. The supernatant was transferred to another tube. Known amounts of [^{125}I] α -hANP were added. This was then extracted on six different reversed-phase Bond Elut columns, viz. C₂, C₈, C₁₈, PH, CN and CH columns. Following activation with methanol then water, a 1-ml aliquot of plasma was applied to each column. The extracted plasma was collected and retained for γ -counting as were the wash cycles and the final eluates containing radioactive α -hANP.

Extraction procedure

Extractions were carried out using a Vac Elut device with a sample capacity of 10. The columns were first activated with 1 ml HPLC grade methanol and applying a vacuum of 35–50 kPa. The excess methanol was removed by applying 1 ml of water, again a vacuum of 35–50 kPa was applied. Plasma samples were thawed in a stream of air at room temperature (18°C) to prevent rapid thawing and were then centrifuged at 2000 g for 10 min at 4°C to ensure the isolation of platelet free plasma. Aliquots (1 ml) were then applied to a column and a vacuum of 85 kPa applied until all the plasma had been drawn through. Unretained proteins and endogenous material were removed by two 1-ml water washes using a vacuum of approximately 35–50 kPa. The α -hANP was eluted into conical polypropylene tubes using 0.5 ml of acetonitrile–water–trifluoroacetic acid (80:19.8:0.2, v/v/v), followed by a further 0.25 ml to ensure no α -hANP remained in the column and apparatus. To increase the precision of the extraction two Bond-Elut C₈ columns were connected together, this required increasing the activation volumes to 1.5 ml but the elution volume remained unchanged. Samples were then dried down under nitrogen and reconstituted in 250 μl RIA buffer (0.025 mol/l phosphate, pH 7.8). The tubes were vigorously mixed for 3 min and then assayed by RIA.

Radioimmunoassay

The RIA was carried out using the commercially available Amersham α -hANP kit. Standards used in the RIA were prepared by serial dilution of a supplied stock solution of α -hANP (640 fmol/ml). These ranged from 0 to 32 fmol/ml, thus samples may require dilution so that they lie within this range. The antibody was 100% crossreactive with α -hANP and was less than 0.3% crossreactive with atriopeptins 1, 2 and 3. For better sensitivity a disequilibrium technique was used which is only applicable to peptides with the approximate molecular weight of α -hANP or greater (3100 M_r). This method was carried out by adding antibody to reconstituted samples and prepared standards, then incubated at 4°C for up to 24 h. Next the tracer was added to all tubes and again incubated for up to 24 h, then the phase separation was

carried out. In this RIA care was also taken in the phase separation to prevent "stripping" of the antibody bound peptide by the use of a second antibody to the antibody-antigen complex. This antibody (Amerlex second antibody) was coated with magnetisable polymer particles and allowed the phase separation to be carried out without the use of a centrifuge but with an Amerlex-M-accessory (Amersham International). The supernatant was discarded and then γ -counted.

Recovery of α -hANP

Pool plasma was thawed and centrifuged at 2000 *g* for 10 min at 4°C. The supernatant was transferred to another tube to which sufficient ^{125}I was added to give 2000 cpm/ml. This was stirred on ice for 2 min and extracted and γ -counted as described above.

Optimisation of plasma volume

Pool plasma was thawed, centrifuged at 2000 *g* for 10 min at 4°C. The supernatant was divided into three different aliquots which were kept stirring on ice. [^{125}I] α -hANP was added to each aliquot to give final concentrations of 2000, 4000 and 8000 cpm/ml. These were extracted ($n = 6$ in each case) and counted for 30 min.

Volunteer study

Volunteers were recruited as part of a study involving low dose infusions of α -hANP. This had Medical Ethics Committee approval from the Royal Postgraduate Medical School and Hammersmith Hospital. This application shows the results from one male subject (age 29, weight 75 kg), who was infused for 3 h on two separate occasions with either α -hANP (1.2 pmol $\text{kg}^{-1} \text{min}^{-1}$) or 44 ml h^{-1} of 0.9% saline as vehicle. The subject was on an unrestricted salt diet, nil by mouth from 9 pm the day before being investigated. On the first day of the study the subject was seated and a cannula was inserted into an antecubital vein in both arms. One line was used for saline infusion, the other for *p*-aminohippuric acid (PAH), inulin infusion and blood sampling. On the second day of the study α -hANP was infused. The method, instrumentation and calculations used are as published in ref. 8.

RESULTS AND DISCUSSION

The impetus for carrying out this work was to devise a precise method for the extraction of α -hANP. There are currently many methods being employed^{6,7}; however, the variation in the results is large and bearing in mind that we intended to carry out a low dose infusion of α -hANP we decided to develop this method.

In the first instance the manufacturer of the reversed-phase columns had to be chosen. Since Analytichem produce an Applications Kit which includes C_2 and C_8 columns not produced by Waters Assoc. this was decided upon. The results of the initial experiments to decide which of the six columns we would use are shown in Table I. These results indicate that C_8 columns would be the most appropriate as the loss when plasma is loaded is least, while the recovery from the elution step is the highest. Another contributory factor in the choice of the C_8 column was the consistently unhindered flow. Since all samples were centrifuged at 2000 *g* for 10 min at 4°C prior to extraction to remove any precipitated fibrins flow should not have been

TABLE I
RESULTS OF PHASE SCREENING

Single Bond Elut columns were used.

Column used	Recovery				
	loaded plasma (%)	1 ml water wash (%)	1 ml water wash (%)	1 ml water wash (%)	elution (%)
C ₈	6.0	3.8	2.8	3.0	84.4
C ₁₈	11.0	3.6	2.0	2.9	80.3
C ₂	10.7	4.9	3.4	2.0	79.2
CN	11.9	3.1	6.3	3.8	75.0
PH	12.8	5.0	5.5	4.4	72.2
CH	15.8	4.0	5.7	6.9	67.5

obstructed. This may be due to the fact that Bond Elut columns are dry packed while Sep-Pak are pressure packed and exhibit better flow characteristics. The specification of the packing used is as follows; Bond Elut columns contain 40- μ m silica particle size with a porosity of 60 Å, while Sep-Pak cartridges contain 10- μ m silica particles with a porosity of 120 Å. This indicates the advantage of using Bond Elut columns as the inter-particle flow maybe increased due to larger particle size, thus high-molecular-weight proteins pass easily through the column. The lower porosity indicates a higher selectivity, as only small peptides would enter the pores, while higher porosity would facilitate entry of more contaminating peptides. For these reasons, in this methods development 100-mg Bond Elut columns were used throughout. Waters Assoc. recommend the use of positive pressure to carry out extractions using their Sep-Pak columns. As with other peptides, processing time must be kept to a minimum to avoid the introduction of error a multichannel vacuum device was employed. Since some α -hANP was lost when the plasma was applied to the activated C₈ column (Table I) we decided to connect two columns together, so that what was lost on the first would

TABLE II
RESULTS OF 1.0 ml PLASMA EXTRACTED ON C₈ COLUMNS IN TANDEM

Mean \pm S.E.M. = 90.24 \pm 0.61%.

Recovery				
loaded plasma (%)	1 ml water wash (%)	1 ml water wash (%)	1 ml water wash (%)	elution (%)
3.76	1.88	1.64	1.45	88.43
3.77	2.07	1.64	1.43	89.37
3.50	1.53	1.38	1.00	91.22
3.56	1.49	1.69	0.90	91.79
3.44	1.56	1.50	1.06	90.42
3.50	1.76	1.50	1.36	90.24

TABLE III

RESULTS OF 1.0 ml, 0.5 ml AND 0.25 ml PLASMA EXTRACTED ON BOND ELUT C₈ COLUMNS IN TANDEM*n* = 6.

<i>Plasma volume (ml)</i>	<i>C.V. (%)</i>	<i>Recovery (mean ± S.E.M.) (%)</i>
1.00	1.50	90.24 ± 0.61
0.50	1.78	94.89 ± 0.69
0.25	2.59	89.26 ± 0.95

be retained on the second. The results of this tandem extraction of 1 ml of plasma (*n* = 6) containing 2000 cpm/ml are shown in Table II. These results showed that the method had been improved by this step, primarily because the recovery from the columns was higher, 90 ± 0.6% (mean ± S.E.M.) secondly, the precision of analysis had been increased (C.V. = 1.5%) and finally, the loss from the plasma loading step had been significantly reduced. The next task in the development was to decide the volume to be used and to accurately determine the recovery. Three volumes were tested, the results of which are shown in Table III. It was concluded that the optimum volume to be used in the assay was 1 ml of plasma at this gave the lowest C.V. (1.5%).

The increased precision of this method for extraction of α -hANP is primarily due to the use of Bond Elut C₈ columns in tandem. It gives basal values (1.5–6 pg/ml for normal volunteers remaining supine for 30 min prior to determination, *n* = 25) which are significantly lower than levels published^{6,7} suggesting our method removes contaminating immunoreactive material not excluded by the previously available methods. The volume of plasma required to carry out an assay was also reduced compared to other methods which is particularly advantageous when blood loss to the subject could be detrimental as in neonates or laboratory animals, especially mice and rats.

To demonstrate the effectiveness of the extraction an infusion of α -hANP was carried out (1.2 pmol min⁻¹ kg⁻¹). The results of which are shown in Tables IV and V and graphically in Figs. 1 and 2.

TABLE IV

RESULTS OF SALINE INFUSION

Na_{ex}/GFR = Sodium excretion per unit glomerular filtration rate (GFR). Cl_{Li}/GFR = Lithium clearance per unit GFR.

<i>Time (h)</i>	<i>Aldosterone (pg/ml)</i>	<i>α-hANP (fmol/ml)</i>	<i>Na_{ex}/GFR (μmol/mol)</i>	<i>Cl_{Li}/GFR (%)</i>
0	184	2.84	1.27	14.75
1	186	2.60	1.19	19.69
2	109	2.85	0.86	13.14
3	56	2.06	0.65	13.07

TABLE V

RESULTS OF α -hANP INFUSION

Na_{ex}/GFR = Sodium excretion per unit glomerular rate (GFR). Cl_{Li}/GFR = Lithium clearance per unit GFR.

Time (h)	Aldosterone (pg/ml)	α -hANP (fmol/ml)	Na_{ex}/GFR (μ mol/mol)	Cl_{Li}/GFR (%)
0	266	3.90	1.46	12.39
1	158	20.58	1.51	45.81
2	96	41.08	1.98	31.02
3	62	57.76	2.20	43.94

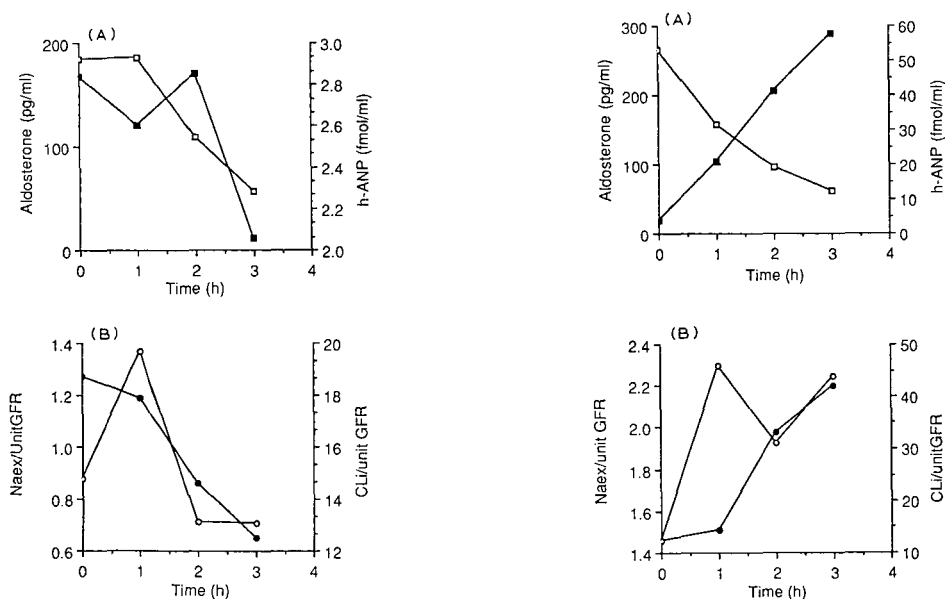


Fig. 1. (A) Graph showing the response of plasma α -hANP and aldosterone levels during an infusion of saline, (■) α -hANP and (□) aldosterone. (B) Graph showing the excretion of sodium (Na_{ex}), expressed as a fraction of the glomerular filtration rate (GFR) and lithium clearance (Cl_{Li}) again expressed as fraction of GFR, (●) Na_{ex}/GFR and (○) Cl_{Li}/GFR , respectively, during an infusion of saline.

Fig. 2. (A) Graph showing the response of α -hANP and aldosterone during an infusion of α -hANP ($1.2\ pmol\ kg^{-1}\ min^{-1}$), (■) α -hANP and (□) aldosterone. (B) Graph showing the excretion of sodium (Na_{ex}), expressed as a fraction of the glomerular filtration rate (GFR) and lithium clearance (Cl_{Li}) expressed as a fraction of GFR, (●) Na_{ex}/GFR and (○) Cl_{Li}/GFR , respectively, during an infusion of α -hANP.

CONCLUSIONS

A reliable extraction method was developed for α -hANP in human plasma using Bond Elut bonded-phase C₈ columns. This approach gave excellent recoveries (90%) and good precision of analysis (1.5% intra assay C.V.) which can be coupled with RIA and should be useful in detecting small changes in α -hANP levels with a higher degree of confidence. Sample handling is kept to a minimum and the volume of plasma required for analysis is 1 ml although this can be reduced to 0.25 ml if repeated sampling is necessary, *i.e.* in animals with a lower blood volume than man, however the analysis would not be as precise.

REFERENCES

- 1 D. M. Geller, M. G. Currie, K. Wakitani, B. R. Cole, S. P. Adams, K. F. Fok, N. R. Siegel, S. R. Eubanks, G. R. Galluppi and P. Needleman, *Biochem. Biophys. Res. Commun.*, 120 (1984) 333.
- 2 H. D. Kleinert, T. Maack, S. A. Atlas, A. Januszewicz, J. E. Sealey and J. H. Laragh, *Blood Pressure Council Supp. 1 Hypertension*, 6 (2) (1984) 1-143.
- 3 T. Obara, H. Yamada, J. Nakada and H. Endou, *Biochem. Biophys. Res. Commun.*, 129 (1985) 833.
- 4 M. B. Anand-Srivastava, R. A. Johnson, S. Picard and M. Cantin, *Biochem. Biophys. Res. Commun.*, 129 (1985) 171.
- 5 K. Atarashi, P. J. Mulrow, R. Franco-Saenz, R. Snajdar and J. Rapp, *Science (Washington, D.C.)*, 224 (1984) 992.
- 6 A. M. Richards, T. Giancarlo, G. D. McIntyre, J. Leckie and J. I. S. Robertson, *Hypertension*, 5 (1987) 227.
- 7 A. Morice, J. Pepke-Zaba, E. Loysen, R. Lapworth, M. Ashby, T. Higenbottam and M. Brown, *Clin. Sci.*, 74 (1988) 359.
- 8 J. Brown and L. Corr, *J. Physiol.*, 387 (1987) 31.

CHROM. 20 724

DIRECT ENANTIOMERIC SEPARATION OF BETAXOLOL WITH APPLICATIONS TO ANALYSIS OF BULK DRUG AND BIOLOGICAL SAMPLES

A. M. KRSTULOVIĆ* and M. H. FOUCHET

L.E.R.S. — SYNTHELABO, Recherche Analytique et Contrôle Pharmaceutique, 23/25 Avenue Morane Saulnier, 92366 Meudon la Forêt Cédex (France)

and

J. T. BURKE, G. GILLET and A. DURAND

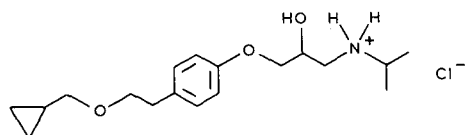
L.E.R.S. — SYNTHELABO, Pharmacocinétique et Métabolisme, 23/25 Avenue Morane Saulnier, 92366 Meudon la Forêt Cédex (France)

SUMMARY

A direct method is described for the resolution of the enantiomers of betaxolol, a novel cardioselective β -adrenergic blocking agent, using a tris(3,5-dimethylphenyl-carbamate)cellulose chiral column. An excellent resolution of the two antipodes is obtained ($R_s > 2$) with high peak symmetries. The method is simple and ideally suited to the routine control of the enantiomeric excess in the bulk drug and the analysis of the enantiomers of betaxolol in hepatocyte suspensions. With modification of the polar modifier in a hexane-based mobile phase, most commercially available β -blockers can be baseline resolved.

INTRODUCTION

Betaxolol, (\pm)-1-{4-[2-cyclopropylmethoxy]ethylphenoxy}-3-isopropylamino-2-propanol hydrochloride, is a cardioselective β -adrenergic blocking agent characterized by a high bioavailability (90%) and a long half-life of about 15 h in man¹. Its structure is



The drug, marketed as a racemic mixture under the name of Kerlone, is highly efficacious for the treatment of hypertension. The same drug substance, used for the treatment of glaucoma, is marketed under the name of Betoptic.

Most of the frequently prescribed β -blocking agents are developed and marketed as a racemic mixture, although it has been shown for some of them that the principal pharmacological effect is due to the *S*-enantiomer. Further, the hepatic oxidation of drugs such as propranolol², metoprolol³, alprenolol⁴ and bufuralol⁵ is highly stereospecific. It is therefore important to have a method for the precise and accurate

determination of the enantiomeric excess of bulk drugs obtained through resolution or enantiospecific synthesis and the determination of the metabolic disposition of racemic drugs.

Chiral stationary phases, which have been recently reviewed by Wainer⁶ and Krstulovic⁷, are becoming increasingly popular for direct enantiomeric separations. At present, there is no universal chiral bonded phase capable of separating all classes of compounds and analytical chemists are often faced with the problem of choosing the most suitable column for a particular application. The general guidelines for selection have been discussed^{6,7}.

In spite of their expense and limited efficiency, chiral stationary phases generally offer high selectivity, which results in the need for a wide range of columns when seeking the best separation conditions. The recently available tris(3,5-dimethylphenyl-carbamate)cellulose column (Chiralcel OD), developed by Okamoto's group⁸, is ideally suited to analytical and preparative separations of β -blockers^{6,8}. As the only previously reported method⁹ for resolution of enantiomers of betaxolol required a lengthy derivatization with (*R*)-(-)-1-(1-naphthyl)ethyl isocyanate, we attempted to develop a direct method needed for routine control of the bulk drug. This method was also found suitable for analysing the enantiomers of betaxolol in rat hepatocyte suspensions.

EXPERIMENTAL

Reagents and chemicals

(*R*)- and (*S*)-betaxolol were synthesized by the Chemistry Department of L.E.R.S. — SYNTHELABO. Chromatographic solvents of high-performance liquid chromatographic (HPLC) grade were obtained from Merck (Darmstadt, F.R.G.). Non-stabilized diethyl ether (Carlo Erba, Paris, France) was used for extractions of hepatocyte suspensions. The remaining chemicals were of analytical-reagent grade and were used without further purification.

Apparatus and HPLC conditions

Bulk drug analysis. The HPLC equipment used for the determination of the enantiomeric excess of the bulk drug consisted of an SP 8780XR automatic sampler (Spectra-Physics France, Les Ulis, France), a Jasco BIP-I pump (Prolabo, France) and a SpectroMonitor D variable-wavelength detector (LDC/Milton Roy, Paris, France). The detection wavelength was set at 273 nm. The column was a Chiralcel OD (250 \times 4.6 mm I.D., 10 μ m average particle size) from Daicel Chemical Industries (Sochibo, Vélizy Villacoublay, France). The column temperature was ambient (22 \pm 1°C). The mobile phase were mixtures of hexane, 2-propanol and/or ethanol and the flow-rate was 1.5 ml/min.

Analysis of hepatocyte suspensions. The need for high sensitivity and selectivity in this application necessitated the use of a fluorimeter (Jasco FP-210, Prolabo) with excitation at 270 nm and emission at 310 nm (attenuation 0.4, gain \times 1). The analytical column was protected by a 1.5-cm long Brownlee RP-18 guard column (Brownlee, Santa Clara, CA, U.S.A.). The mobile phase was hexane-2-propanol-diethylamine (87:13:0.05, v/v) at a flow-rate of 1.5 ml/min. A WISP 710B autoinjector (Waters, Paris, France) was employed for sample injection; the remaining components and

parameters of the HPLC system were the same as those used for the analysis of the bulk drug.

Sample preparation for analysing the enantiomers of betaxolol in a rat hepatocyte suspension

Betaxolol (2.5 $\mu\text{g/ml}$) was added to a suspension of rat hepatocytes ($2 \cdot 10^6$ cells/ml) prepared according to a method adapted from Guillouzo and Gurgun-Guilouzo¹⁰. Sodium hydroxide (0.1 ml, 1 M) and then 7 ml of diethyl ether were added to a 0.5-ml aliquot of hepatocyte suspension. The mixture was agitated for 15 min and then centrifuged at 4°C and 1000 g for 5 min. The aqueous phase was discarded and 6 ml of the organic phase were transferred into a clean tube containing 2 ml of 0.2 M hydrochloric acid. The compounds were then back-extracted into the acidic aqueous phase by shaking the tubes for 10 min. Following centrifugation, the organic phase was discarded and the aqueous phase was rendered alkaline by the addition of 0.25 ml of 2 M sodium hydroxide solution. The enantiomers of betaxolol were finally re-extracted with diethyl ether as described above and 6 ml of the solvent were transferred into a clean tube and evaporated to dryness under a gentle stream of nitrogen. The residue was taken up in 100 μl of hexane-isopropanol (9:1) and 50 μl were injected on to the column. Using exact volumetric transfers, the concentrations of the enantiomers were determined at different incubation times by comparing the peak areas with those obtained from the standards processed in an identical manner.

RESULTS AND DISCUSSION

Analysis of the bulk drug

Stationary phases with cellulose triesters coated on macroporous silica belong to the general category of polysaccharide sorbents. The formation of transient diastereomeric complexes with the solute molecules involves hydrogen bonding and dipole interactions. The interactive sites are located within the cavities rather than on the surface as in the Pirkle-type phases. They are used with mobile phases composed of a non-polar solvent such as hexane, modified with an alcohol or with pure polar eluents (*e.g.*, ethanol).

The use of several mobile phases was investigated for the separation of enantiomers of betaxolol on Chiralcel OD. Fig. 1 shows the separations obtained with hexane-based mobile phases containing different polar modifiers. The evolution of the chromatographic separation reflects the solubilities of the solute in the mobile phases. The best results in terms of resolution, peak symmetry and analysis time were obtained with the mobile phase hexane-2-propanol-diethylamine (87:13:0.05, v/v/v), with $R_s > 2$, asymmetry factors for the two peaks equal to 1 and a column efficiency (calculated for the *S*-isomer) of 6400 plates/m. The addition of diethylamine improved markedly the efficiency of separation and the peak symmetries (Fig. 1A and B).

In all instances, the *R*-enantiomer was eluted before the *S*-enantiomer, resulting in a high precision of the determination of the enantiomeric excess of (*S*)-betaxolol. These conditions were therefore chosen for the routine measurement of the enantiomeric purity of (*S*)-betaxolol bulk drug. Fig. 2a and b show the HPLC traces for a sample containing 0.5% of (*R*)-betaxolol with respect to (*S*)-betaxolol and a typical HPLC trace for a sample of (*S*)-betaxolol bulk drug. The concentration-response

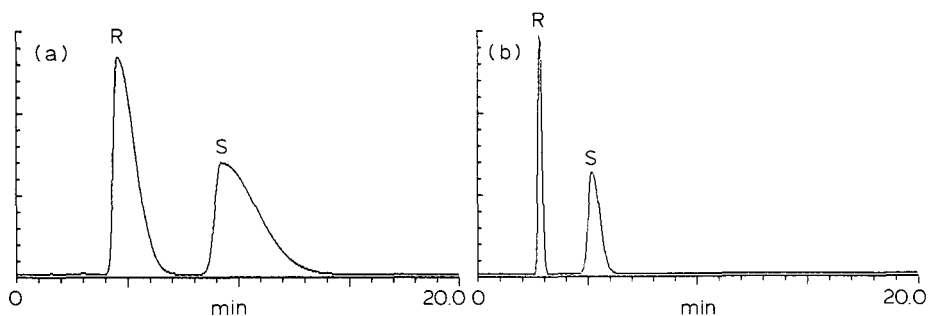


Fig. 1. Chromatograms illustrating the separation of a racemic mixture of enantiomers of betaxolol. Mobile phase: (a) hexane-2-propanol (92:8, v/v), flow-rate 1.5 ml/min, resolution $R_s = 1.77$; (b) hexane-2-propanol-diethylamine (92:8:0.05, v/v/v), flow-rate 1.5 ml/min, $R_s = 3.58$.

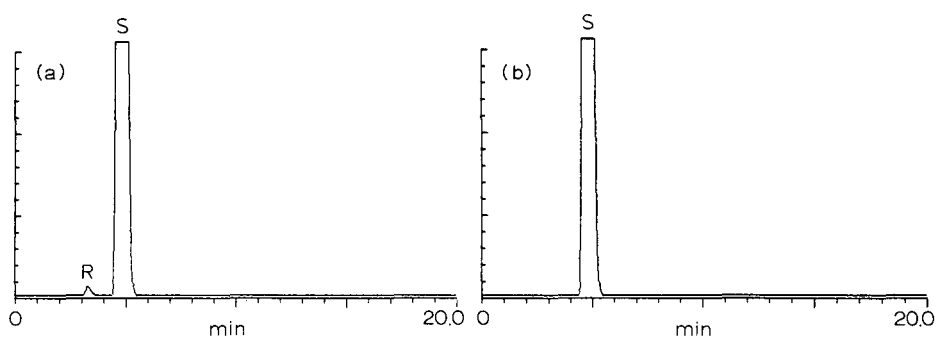


Fig. 2. Chromatograms obtained using the mobile phase hexane-2-propanol-diethylamine (87:13:0.05, v/v/v). (a) 0.5% of (*R*)-betaxolol with respect to (*S*)-betaxolol; (b) (*S*)-betaxolol bulk drug.

TABLE I

STRUCTURES OF COMMERCIALY AVAILABLE β -BLOCKERS

<chem>Ar-O-CH2-CH(OH)-CH2-NH-CH(CH3)2</chem>			
Compound	Ar	Compound	Ar
Betaxolol		Nadolol	
Propranolol		Cicloprolol	
Metoprolol		Pindolol	

curve was linear for both enantiomers in the concentration range of interest, the average within-day coefficient of variation being 0.3% and the between-day coefficient of variation 0.6%.

This column was also found useful for the analysis of other commercially available β -blockers. Their structures are shown in Table I and examples of chromatograms in Fig. 3.

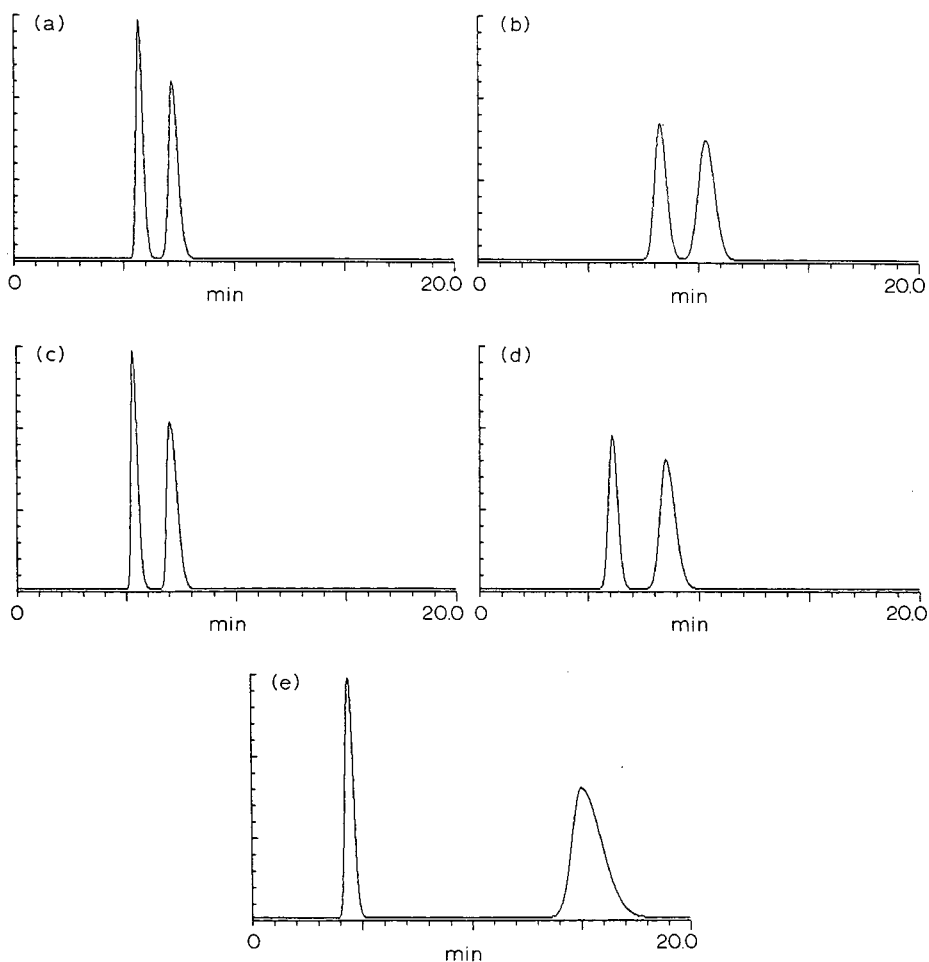


Fig. 3. Chromatograms of some commercially available β -blockers, marketed as racemates. (a) Propranolol. Mobile phase, hexane-2-propanol-ethanol-diethylamine (80:5:15:0.05, v/v/v); flow-rate, 1.0 ml/min; resolution, $R_s = 2.15$. (b) Nadolol. Conditions as in (A); $R_s = 1.68$. (c) Cicloprolol. Conditions as in (A); $R_s = 2.38$. (d) Metoprolol. Mobile phase, hexane-ethanol-diethylamine (90:10:0.05, v/v/v); flow-rate, 1.0 ml/min; $R_s = 2.26$. (e) Pindolol. Mobile phase, hexane-2-propanol-diethylamine (70:30:0.05, v/v/v); flow-rate, 1.5 ml/min; $R_s = 6.48$. Individual enantiomers were not available for assignment as the peaks. Column temperature, $22 \pm 1^\circ\text{C}$ in all instances.

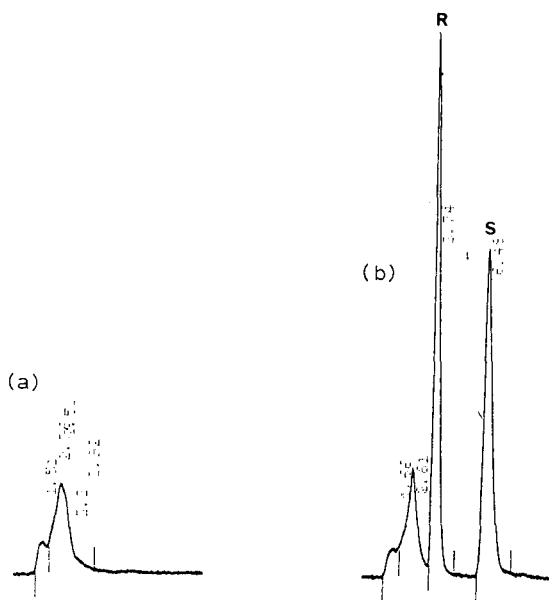


Fig. 4. Analysis of rat hepatocyte suspension; (b) suspension containing 2.5 mg/ml of betaxolol. Retention times are given in minutes.

Analysis of rat hepatocyte suspensions

The described method was applied to the determination of betaxolol in rat hepatocytes. The relative recovery of both enantiomers was essentially 100% and the absolute recovery, which depends on the volumetric transfers, was 37%. The limit of detection (signal-to-noise ratio of 3) calculated from the amount injected on to the column was approximately 5 ng for both enantiomers. The calibration graph was linear for both enantiomers in the concentration range 25–1000 mg in the tube; the mean relative residue was less than 5%. The within-day coefficient of variation was less than 2% at a concentration of 125 mg. Chromatograms of a control rat hepatocyte suspension and one, at time zero, containing equal amounts of both enantiomers (2.5 $\mu\text{g}/\text{ml}$ of betaxolol) are shown in Fig. 4a and b; no interfering endogenous peaks were detected. This chromatographic technique therefore permits the relative and absolute concentrations of the enantiomers to be followed over the incubation time (<2 h) necessary to metabolize the compounds completely. The resulting concentration–time data allows a comparison of the relative rates of hepatic metabolism of the two enantiomers; these results will be published in a subsequent paper.

In conclusion, we have developed a direct method for assessing the enantiomeric composition of betaxolol. The method is simple and precise. The column equilibration times are short and the analysis time is approximately 7 min. By changing the nature or the concentration of the polar modifier, enantiomeric separations of other β -adrenergic blocking agents can be obtained. This method has been applied to the routine determination of the enantiomeric excess of (*S*)-betaxolol and we have demonstrated its applicability to the measurement of betaxolol in rat hepatocytes. For the latter analysis it is possible to use atenolol as an internal standard as it is eluted between the

two enantiomers and is well resolved from both. Work is in progress in this area and will be reported in a forthcoming publication.

ACKNOWLEDGEMENT

We thank Dr. Alexander Wick, Director of the Chemistry Department, for his timely advice.

REFERENCES

- 1 S. J. Warrington, P. Turner, J. R. Kilborn, G. Bianchetti and P. L. Morselli, *Br. J. Clin. Pharmacol.*, 10 (1980) 449.
- 2 T. Walle, U. K. Walle, M. J. Wilson, T. C. Fagan and T. E. Gafney, *Br. J. Clin. Pharmacol.*, 18 (1984) 741.
- 3 P. Dayer, T. Leemann, J. Gut, T. Kronbach, A. Kupper, R. Francis and U. A. Meyer, *Biochem. Pharmacol.*, 34 (1985) 399.
- 4 J. Hermansson and C. von Bahr, *J. Chromatogr.*, 227 (1982) 113.
- 5 P. Dayer, R. Gasser, J. Gut, T. Kronbach, G. M. Robertz, M. Eichelbaum and U. A. Meyer, *Biochem. Biophys. Res. Commun.*, 125 (1984) 374.
- 6 I. Wainer, *Trends Anal. Chem.*, 6 (1987) 125.
- 7 A. M. Krstulovic, *J. Pharm. Biomed. Anal.*, in press.
- 8 Y. Okamoto, M. Kawashima, R. Aburatani, K. Hatada, T. Nishiyama and M. Masuda, *Chem. Lett.*, (1986) 1237.
- 9 A. Darmon and J. P. Thenot, *J. Chromatogr.*, 374 (1986) 321.
- 10 A. Guillouzo and C. Gurgun-Guillouzo, *Hepatocytes Isolés et en Culture*, John Libbey Eurotext, Montrouge, 1986.

CHROM. 20 463

HIGH-PERFORMANCE LIQUID CHROMATOGRAPHIC ANALYSIS OF THE AJMALICINE DISTRIBUTION IN ROOTS OF *CATHARANTHUS ROSEUS* LINES WITH DIFFERENT FLOWER COLOURS

MARTIN WEISSENBERG*

Department of Chemistry of Natural Products and Pesticides, Agricultural Research Organization, The Volcani Center, Bet Dagan 50 250 (Israel)

ARIEH LEVY

Department of Medicinal, Spice and Aromatic Plants, Agricultural Research Organization, The Volcani Center, Bet Dagan 50 250 (Israel)

IRIT SCHAEFFLER

Department of Chemistry of Natural Products and Pesticides, Agricultural Research Organization, The Volcani Center, Bet Dagan 50 250 (Israel)

and

ELIE C. LEVY

Rael Chemicals, Jerusalem 91160 (Israel)

SUMMARY

The distribution and yield of ajmalicine in roots were studied in three pure lines of *Catharanthus roseus* plant with different flower colours, by means of high-performance liquid chromatography. The highest levels of ajmalicine were found in the line with red-eyed flowers. In all lines, the tap root contained higher amounts of ajmalicine than the lateral roots. The implications of these findings for plant breeding and yield optimization are evaluated.

INTRODUCTION

The indole alkaloids ajmalicine (1) and serpentine (2) (Fig. 1) have been found in roots of several *Catharanthus* and *Rauwolfia* plant species¹. The minor component

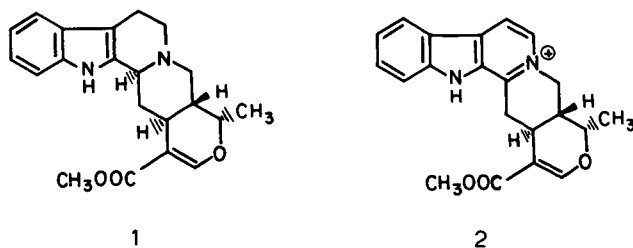


Fig. 1. The structures of ajmalicine (1) and serpentine (2).

1 is employed as a hypotensive and tranquilizing agent, whereas the major product 2, which is pharmacologically inactive, can be readily converted into 1 by reduction¹. An additional source of these derivatives might be provided by cell suspension cultures¹.

As part of a study on the production of compound 1 from *Catharanthus roseus* (L.) G. Don (Apocynaceae) roots, analytical methods were considered for the determination of 1 and 2. Previously reported procedures include thin-layer chromatography (TLC)–spectrophotometry^{2,3}, TLC–fluorimetry^{4,5,16}, densitometric TLC³ and radioimmunoassay⁴. High-performance liquid chromatography (HPLC) has also been applied to determination of compound 1 in mixtures of *C. roseus* alkaloids⁶, and in *C. roseus* roots^{3,7,16} and cell cultures^{8–13,17}.

The aim of this work was to study the distribution and yield of compound 1 in roots of *C. roseus* plants, in three pure lines with different flower colours. We report the use of reversed-phase HPLC for the estimation of this compound in the tap and lateral roots of *C. roseus* plants with white, pink and red-eyed flowers, respectively.

EXPERIMENTAL

Reference compounds and solvents

The ajmalicine used as a standard for the preparation of the calibration graph was isolated from *C. roseus*, purified and identified by comparison with an authentic sample kindly supplied by Dr. G. G. Marconi, Lilly Research Laboratories, Indianapolis, IN, U.S.A. Methanol was of LiChrosolv grade (Merck, Darmstadt, F.R.G). A solution of compound 1 in methanol (0.2 mg/ml) was used as the calibration standard.

Apparatus

Chromatographic separations were done on a Tracor 985 liquid chromatograph equipped with a Model 970 A variable-wavelength detector and a Model 951 pump, connected to an Hewlett-Packard recorder, Model 7131 A. A reversed-phase column (Alltech C₁₈, 25 cm × 4.6 mm I.D., 10 μm) was used at ambient temperature, the chromatograms being monitored at 254 nm. The mobile phase was methanol–water (8:2) containing 0.5 ml concentrated ammonium hydroxide solution per litre, the flow-rate 0.6 ml/min, the pressure 2500 p.s.i. and the recorder chart speed 0.25 cm/min.

Plant material and growth conditions

Three true breeding, unrelated pure lines, representing the three common flower types of the species were developed by two successive generations of artificial selfing of single plants with a different corolla colour: pink, white and white with a red eye in the centre¹⁴. Seeds of each line were sown separately in a greenhouse and transplanted to the field 3 weeks later. Five plants randomly sampled from each line were dug out at the end of the growing season, about 5 months after transplantation. The fresh and dry weights of the roots of each plant (drying in an oven at 60°C for 4 days) were determined, and its tap root and lateral roots were separately ground and subjected to extraction.

Extraction procedure

Dried and finely powdered plant samples (1 g) were extracted with methanol (20 ml) for 48 h at room temperature. The suspensions were filtered quantitatively and the filtrates were made up to 25 ml with methanol in volumetric flasks. Aliquots (2 ml) of the extracts were treated with sodium borohydride (*ca.* 30 mg) and kept at room temperature for 1 h for complete reduction of compound 2 to 1 (TLC evidence). The reaction mixtures were filtered quantitatively into 2-ml measuring flasks and made up to volume with methanol.

HPLC determination

Aliquots (5 μ l) of the borohydride-treated extracts were injected into the chromatograph using a sample clarification kit (Schleicher and Schüll, Dassel, F.R.G.) including a filter holder and a membrane filter disc (diameter 13 mm, porosity 0.45 μ m). The mobile phase was filtered through a membrane filter disc (diameter 47 mm, porosity 0.45 μ m; Schleicher and Schüll). The column was regenerated by washing with methanol after analyses.

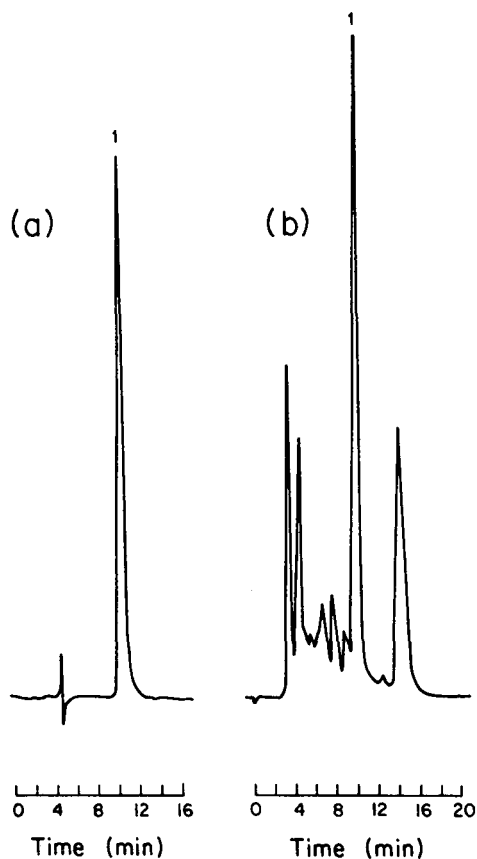


Fig. 2. Typical chromatograms of (a) standard ajmalicine (1 μ g), (b) *C. roseus* extract (100 μ g dry plant). Peak 1 = ajmalicine.

TLC-spectrophotometric determination

The assay was performed according to a published procedure², except that borohydride-treated samples prepared as described above were processed, rather than crude methanolic extracts. Following analytical TLC, the absorbances of the methanol-eluted samples were recorded at 283 nm, and their contents of compound 1 estimated with reference to a standard curve.

RESULTS AND DISCUSSION

Reversed-phase chromatography provided satisfactory resolution of compound 1 contained in borohydride-treated methanolic extracts of *C. roseus* roots, as no interfering peaks appear at a similar retention time in the chromatograms (Fig. 2). The addition of a few drops of ammonia to the mobile phase greatly improved the peak shapes, and stable baselines were obtained using isocratic elution. Virtually no differences in retention time between various batches were observed under these conditions. A linear plot was obtained of the peak height against concentration ($r = 0.995$, $y = 0.465x + 0.353$, in the range of 0.8–1.6 μg of compound 1). The recovery (mean \pm S.D.) of compound 1 from ajmalicine-fortified plant extracts was $96.6 \pm 4.0\%$ (Table I). Assays done on 1-g samples of dried plant material were found to be convenient, accurate and reproducible. The reproducibility of analyses was estimated by the coefficient of variation of a standard solution of compound 1 within four successive assays, and between fourteen assays at various time intervals (1–100 days); the coefficients were 7.66 and 19.60% within and between assays, respectively. Slightly lower recoveries were recorded when 100–500 mg of plant material were analyzed.

Previously reported methods for the determination of compound 1 in *C. roseus* roots involve the addition of water to the methanolic solution obtained following reduction with sodium borohydride, subsequent extraction of the resulting mixture with dichloromethane, and concentration of the extract to a suitable volume prior to HPLC analysis^{3,7}. Our approach suggests that the borohydride-reduced plant extracts may be injected directly into the HPLC system, thus avoiding further operations and transfers.

For comparison, several *C. roseus* roots samples were concurrently assayed by

TABLE I
RECOVERY OF AJMALICINE FROM SAMPLES OF *CATHARANTHUS ROSEUS* BY HPLC

<i>Ajmalicine (mg)</i>				<i>Recovery (%)</i>
<i>Determined in sample</i>	<i>Added</i>	<i>Calculated</i>	<i>Found</i>	
2.5	5.0	7.5	7.6	101.3
3.2	5.0	8.2	8.3	101.2
4.3	5.0	9.3	8.4	90.3
5.3	5.0	10.3	10.1	98.1
6.2	5.0	11.2	10.8	96.4
7.1	5.0	12.1	11.3	93.4
12.0	5.0	17.0	16.3	95.9

TABLE II

AJMALICINE YIELDS IN THREE LINES OF *CATHARANTHUS ROSEUS* PLANTS WITH DIFFERENT FLOWER COLOURSValues represent means \pm standard errors of five replications.

Flower colour	Root weight (g per plant)		Ajmalicine level (% of dry weight)	
	Fresh	Dry	Tap root	Lateral roots
Pink	81.9 \pm 9.6*	23.1 \pm 2.7	0.63 \pm 0.04	0.45 \pm 0.04
White	97.8 \pm 4.5	27.9 \pm 1.1	0.46 \pm 0.03	0.32 \pm 0.02
Red-eyed	109.3 \pm 3.3	31.3 \pm 2.0	0.77 \pm 0.03	0.64 \pm 0.05

the present HPLC method and by a TLC-spectrophotometric procedure², slightly modified by us for convenience and reproducibility. The values obtained by both methods are significantly correlated [$r = 0.95$; the regression line for the TLC-spectrophotometry (y) and HPLC (x) values is $y = 1.68x - 0.19$], however, the results of the TLC-spectrophotometric assays were generally higher. Admittedly, the inclusion of TLC before the spectrophotometric analysis leads to a significant increase in the errors, as well as in the assay time. The requirement of fine grinding in the sample preparation in order to ensure complete extraction is substantiated by both methods, the finely powdered samples consistently showing higher levels of compound 1 than their coarse-grained counterparts (from 1.4:1 to as much as 4:1).

The use of the present HPLC procedure pointed to significant differences between the three breeding lines in the yield of total 1, *i.e.*, naturally occurring ajmalicine and ajmalicine resulting from reduction of serpentine (Table II). The line with red-eyed flowers had the highest weights of fresh and dry roots per plant, and the highest levels of total 1 in the tap (0.77%) and in the lateral roots (0.64%). The roots of the white-flowered line displayed the lowest content of total 1, however, their fresh and dry weights were higher than those of the pink-flowered line.

The amount of total 1 in the tap root was higher than that in the lateral roots in all lines. A significant ($p < 0.01$) correlation was found between the contents of compound 1 in the two parts of the root ($r = 0.86$). Since the tap root also contributes most of the dry biomass (about 70%), the yield of total 1 in the plant is chiefly produced by this part. These results indicate that breeding and culture practices aimed at increasing the content and yield of total 1 in the species should be directed towards increasing the tap root biomass rather than that of the lateral roots.

The differences in levels of total 1 between lines with different flower colours suggest that this character might be an ideal marker for breeding cultivars of *C. roseus* with a high concentration of total 1¹⁵. Nonetheless, the linkage between the flower colour and the content of total 1 should be ascertained by genetic analysis before screening segregating populations on the flower phenotype.

In conclusion, we propose that the HPLC procedure described can be reliably applied to large screening programmes and plant selection and breeding, as well as in cell culture studies. The method involves essentially *in situ* reduction of compound 2 to 1 in crude methanolic plants extracts, which are further made up to the measuring range and directly assayed by HPLC, without prior purification steps. The assay

might also be useful in monitoring the extraction, isolation and purification of compound 1 from the plant material.

ACKNOWLEDGEMENTS

We are grateful to Dr. G. G. Marconi from Lilly Research Laboratories, Indianapolis, IN, U.S.A., for kindly sending us a sample of ajmalicine. The paper constitutes contribution No. 2318-E, 1988 series, from the Agricultural Research Organization, The Volcani Center, Bet Dagan, Israel.

REFERENCES

- 1 M. H. Zenk, H. El-Shagi, H. Arens, J. Stöckigt, E. W. Weiler and B. Deus, in W. Barz, E. Reinhard and M. H. Zenk (Editors), *Plant Cell Cultures and Their Biotechnological Applications*, Springer, Heidelberg, 1977, p. 27.
- 2 J. P. S. Sarin, R. C. Nandi, R. S. Kapil and N. M. Khanna, *Indian J. Pharm.*, 39 (1977) 62.
- 3 J. Gleye, E. Lavergne de Cervai, E. Stanislas, E. Leverd, D. Beziat and Ph. Hatinguais, *Ann. Pharm. Fr.*, 37 (1979) 217.
- 4 H. Arens, J. Stöckigt, E. W. Weiler and M. H. Zenk, *Planta Med.*, 34 (1978) 37.
- 5 J. M. Mérillon, J. C. Chénieux and M. Rideau, *Planta Med.*, 47 (1983) 169.
- 6 S. Görög, B. Herényi and K. Jovánovics, *J. Chromatogr.*, 139 (1977) 203.
- 7 E. Leverd, D. Beziat and Ph. Hatinguais, *Boll. Chim. Farm.*, 117 (1978) 27.
- 8 W. Kohl, B. Witte and G. Höfle, *Planta Med.*, 47 (1983) 177.
- 9 P. C. Roja, B. D. Benjamin, M. R. Heble and M. S. Chadha, *Planta Med.*, 49 (1985) 73.
- 10 P. Morris, *Planta Med.*, 50 (1986) 121.
- 11 D. Drapeau, H. W. Blanch and Ch. R. Wilke, *Planta Med.*, 51 (1987) 373.
- 12 J. I. Smith, N. J. Smart, W. G. W. Kurz and M. Misawa, *Planta Med.*, 51 (1987) 470.
- 13 T. Endo, A. Goodbody and M. Misawa, *Planta Med.*, 51 (1987) 479.
- 14 A. Levy, J. Milo, A. Ashri and D. Palevitch, *Euphytica*, 32 (1983) 557.
- 15 J. Milo, A. Levy, N. Akavia, A. Ashri and D. Palevitch, *Z. Pflanzenzüchtg.*, 95 (1985) 352.
- 16 U. R. Cieri, *J. Assoc. Off. Anal. Chem.*, 66 (1983) 867.
- 17 J.-P. Renaudin, *J. Chromatogr.*, 291 (1984) 165.

CHROM. 20 573

LIQUID CHROMATOGRAPHIC PROCEDURES FOR THE ANALYSIS OF COMPOUNDS IN THE SEROTONERGIC AND OCTOPTAMINE PATHWAYS OF LOBSTER HEMOLYMPH

DEBRA ANN FADOOL, STANLEY J. COBB and GABRIELLE KASS-SIMON

Department of Zoology, University of Rhode Island, Kingston, RI 02881 (U.S.A.)

and

PHYLLIS R. BROWN*

Department of Chemistry, University of Rhode Island, Kingston, RI 02881 (U.S.A.)

SUMMARY

High-performance liquid chromatography, with serial electrochemical and ultraviolet detectors, was used with a reduced activity catecholamine C₁₈ column to separate and quantify compounds important in the serotonergic and octopamine pathways in lobster hemolymph. The chromatographic mobile phase was composed of potassium dihydrogenphosphate buffer, trichloroacetic acid, sodium dodecyl sulfate, the sodium salt of ethylenedinitrilotetraacetic acid and the organic solvents, acetonitrile and methanol. The compounds serotonin, 5-hydroxyindoleacetic acid, tryptophan, 5-hydroxytryptophan, tryptamine, melatonin, octopamine and tyrosine were well resolved within 13 min. Good electrode maintenance, the use of a silica gel precolumn and careful sample preparation were necessary to give a stable baseline, high resolution of these compounds and reproducibility of retention times and peak heights. The electrochemical detector extended the range of detection to the picogram level. Because of the instability of the solutes and of the chromatographic baseline, sample preparation procedures were investigated. Deproteinization with ammonium sulfate gave the best recovery of the compounds of interest and the most stable baseline with the electrochemical detector. Peaks in the hemolymph were characterized by addition of standards, dual detection (electrochemical and ultraviolet) and the enzyme peak shift technique. With this methodology, important endogenous neurohormones in the hemolymph of lobsters can be quantitatively determined with respect to the molt cycle.

INTRODUCTION

In order to define the chemical basis for the molt-related changes in the behavior of lobsters, it is necessary to monitor changes in the concentrations of a unique group of compounds in the hemolymph of these crustaceans. Among the compounds which can act as neurotransmitters are the amines, serotonin and octopamine¹⁻⁵. Other compounds of interest are the precursors or catabolites of serotonin and octopamine: 5-hydroxyindoleacetic acid, tryptophan, 5-hydroxytryptophan, melatonin, tryptamine and tyrosine. (Figs. 1 and 2).

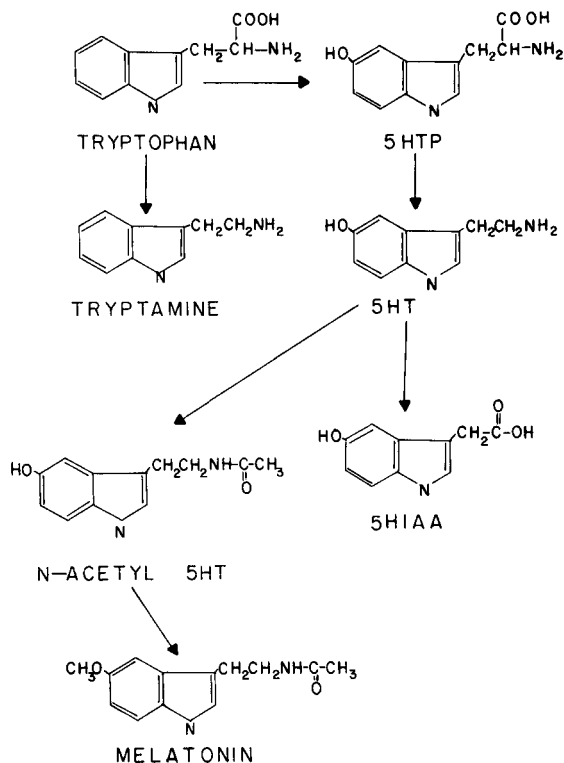


Fig. 1. Metabolic pathway of serotonin in lobster. 5HTP = 5-hydroxytryptophan, 5HT = serotonin and 5HIAA = 5-hydroxyindoleacetic acid.

However, many problems have been encountered in analyzing biological samples for this particular set of compounds. Some of the compounds are extremely labile to light or heat, others to acid. The sample volumes available are usually very small and may contain relatively large amounts of one of the compounds and only trace amounts of others; for example some of the endogenous neurohormones are present in the hemolymph in amounts as low as 10^{-10} . Moreover, some of these

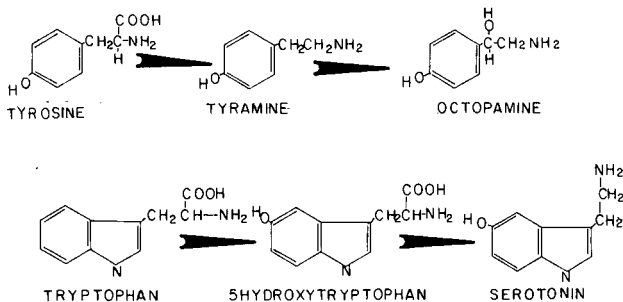


Fig. 2. Precursors in the biosynthesis of octopamine (top). Precursors in the biosynthesis of serotonin (bottom).

compounds may be present in the hemolymph in the free form and some bound to a high-molecular-weight protein or a low-density lipoprotein⁶⁻⁸.

Although good procedures for reversed-phase liquid chromatography using electrochemical detection (RPLC-ED) have been reported for the analysis of serotonin and its metabolites⁹⁻¹³, no analytical procedures have been published for the determination of trace amounts of these compounds together with octopamine. Therefore, we developed an RPLC-ED method which can be used for the analysis of any or all of these compounds. Using a solution of standards, this method gave us the required sensitivity and resolution. However, when the method was applied to samples of hemolymph, the sensitivity of the assay was reduced because of noisy baselines. In addition, some of the compounds of interest were lost in the sample preparation steps. Therefore, methods of sample preparation were also investigated in order to find the method which was most compatible with the RPLC-ED analysis. The requirements for the sample preparation method are maximum solute recovery, high degree of deproteinization and baseline stability.

EXPERIMENTAL

Instrumentation

The chromatographic instrumentation consisted of an M6000 reciprocating pump (Waters Assoc., Milford, MA, U.S.A.) equipped with a Rheodyne 7125 injection port and 6- μ l injection loop. All separations were performed on a 15 cm \times 4 mm I.D. reduced activity catecholamine analytical column of 5 μ m particle size (Perkin-Elmer, Norwalk, CT, U.S.A.) preceded by a guard column containing 30-38 μ m C₁₈ packings (Whatman, Clifton, NJ, U.S.A.). A pre-column, uniformly packed with silica gel, 37-53 μ m (Whatman), was incorporated in the system between the pump and the injector. Detection was based on a Perkin-Elmer LC15 UV detector at 254 nm in series with a Perkin-Elmer LC-17 electrochemical detector. The electrochemical detector utilized an LC-4B amperometric system with Ag/AgCl reference electrodes and glassy carbon working electrodes. A strip chart recorder and an integrator were used to obtain simultaneous signal recordings from both detection devices. The integration system used was a 3380A Hewlett-Packard (Avondale, PA, U.S.A.).

Reagents and standards

Chromatographic standards were octopamine (*d*l-aminomethyl-4-hydrobenzyl alcohol), serotonin (5-hydroxytryptamine), tryptophan, 5-hydroxyindoleacetic acid, tryptamine, melatonin and 5-hydroxytryptophan. They were obtained from Sigma (St. Louis, MO, U.S.A.). The retention times of the phenylalanine and tyrosine were also determined in an attempt to identify peaks in the lobster hemolymph. The enzymes monoamine oxidase (MAO), pyridoxal-5'-phosphate apotryptophanase and phenylethanolamine N-methyltransferase (PNMT; EC 2.1.1.28), used in peak identification, were purchased from Sigma. Trichloroacetic acid (TCA) was purchased from J. T. Baker (Phillipsburg, NJ, U.S.A.), dibasic anhydrous sodium phosphate from Matheson, Coleman and Bell (Norwood, OH, U.S.A.), ethylenedinitrilotetraacetic acid disodium salt (EDTA) from Mallinckrodt (St. Louis, MO, U.S.A.) and sodium

dodecyl sulfate (SDS) from Sigma. HPLC-grade acetonitrile and methanol were purchased from EM Science (Gibbstown, NK, U.S.A.). All the water for preparation of the eluents and standard solutions was doubly distilled, deionized and then filtered through 0.45- μm membrane filters (Millipore, Bedford, MA, U.S.A.).

Chromatographic conditions

All separations were performed isocratically at ambient temperature. The mobile phase consisted of 0.02 *M* TCA, 1.5 μM EDTA, 2.2 *mM* SDS, 0.070 *M* dibasic anhydrous sodium phosphate and 20% acetonitrile and 12% methanol as organic modifiers; a modification of the mobile phase reported by Martin *et al.*⁸. The pH of the mobile phase was adjusted to 7.4 with acetic acid–water (50:50). This solvent system was degassed with a stream of helium and pumped at a flow-rate of 0.8 ml/min.

Samples of the standard mixture, the hemolymph and the hemolymph with internal standards, respectively, were injected onto the column in 7- μl aliquots to insure that the injection loop was filled. The UV absorbance was monitored at a wavelength of 254 nm and sensitivity was varied from 0.004 to 0.064 a.u.f.s. to achieve simultaneous quantitation of the hormones present in widely varying concentrations in the hemolymph. The electrochemical oxidation was held at an applied potential of 0.90 V and sensitivity varied from 5 to 500 nA according to detection requirements of different compounds.

Standard curve and detection limits

A standard curve was prepared using both peak height and peak area *vs.* concentration of serotonin and octopamine. Concentrations ranged from 10^{-12} to 10^{-3} *M*. The lower limits of detection were determined; a signal was defined as detected if it was two times the square root of the noise.

Degradation study

To determine the stability of serotonin and octopamine to light and temperature respectively, a standard mixture of the two compounds (10^{-3} *M* in each one) was allowed to stand at room temperature and in indirect sunlight for intervals of 10 min, 20 min, 30 min, 2 h, and 24 h. After each interval, a 7- μl sample was injected onto the column. The observed peak shape was qualitatively and quantitatively compared to a control chromatogram where the sample was iced and shielded from all light. Peak height, for each interval, was also determined and compared to the control.

Hemolymph collection

Lobsters were agitated for 60 s to control effects due to variability in handling. They were then chilled for 30 min. The reduced temperature simultaneously slowed the blood clotting while minimizing degradation of the compounds of interest. Blood was drawn with claws elevated to drain blood posteriorly. A cold 18-gauge needle was inserted in the dorsal abdominal vessel between the cephalothorax and the first abdominal segment (pericardial cavity). Care was taken to draw the blood from only the immediate pericardial region, not the digestive area anteriorly adjacent. Blood was centrifuged in a Sorvall refrigerated centrifuge with a SS-34 rotor, 2500 rpm (600 *g*) for 5 min at 4°C to remove cell membranes. The supernatant (the hemolymph) was decanted off, divided into labeled vials and stored at -50°C until HPLC analysis.

Sample preparation

In preparing hemolymph for chromatographic analysis, all compounds with a molecular weight greater than 25 000 were removed. Several methods of hemolymph deproteinization were investigated to obtain optimal separation, high recovery of the compounds of interest and baseline stability. The methods investigated included deproteinization with strong acid, strong acid and heparin to facilitate precipitation of lipoproteins and stabilize the baseline^{6,7}, and "salting out" with ammonium sulfate¹⁴. Since deproteinization with saturated ammonium sulfate gave the best baselines and recovery of all the compounds of interest, only this method of sample preparation will be described.

Hemolymph (1 ml) was added to 1 ml of saturated ammonium sulfate (25°C); the tube was covered with parafilm and immediately iced (5°C). Samples were shielded from light in a black, ice container to inhibit the breakdown of serotonin, a light sensitive compound, and of octopamine, which breaks down rapidly at temperatures exceeding 10°C. Tubes were vortexed for 2 min. The samples were then centrifuged at 600 g in a Clini-Cool general purpose refrigerated bench top centrifuge (Damon, IEC Division, Needham Heights, MA, U.S.A.) at 4382 rpm for 20 min to insure complete removal of the protein precipitate and full recovery of the neurohormones. The rotating radius was 12.5 cm and the temperature of operation was 4°C.

The supernatant was poured into ultrafiltration cones (Amicon, Danvers, MA, U.S.A.) 25 000 MW, 5 ml volume capacity, dimensions of 137 × 32 mm, and operating limit of 5000 rpm. The cones were soaked in doubly distilled, deionized water for at least 1 h before use. The samples were then recentrifuged for 15 min. The filtrates were poured into labeled glass tubes which were immediately placed in the ice container. Only one sample was prepared at a time to minimize degradation of the solutes of interest.

Aliquots of the standards alone (10^{-6} M), hemolymph alone and a hemolymph-standards mixture were chromatographed before and after the sample preparation procedures to determine the effects of the ammonium sulfate treatment on the baseline and the percent loss of the compounds of interest caused by the sample preparation steps.

Peak identification

Peaks in the chromatogram of the hemolymph sample were tentatively identified by the comparison of the retention time (t_R) of the peak with that of a known compound. Second, peaks were characterized by adding sequentially known amounts of standard compounds to the hemolymph. Next, the chromatographic peaks were characterized on the basis of dual detection using both UV and electrochemical detection.

Finally serotonin, octopamine, tryptophan and 5-hydroxyindole acetic acid were identified by the enzyme peak shift technique¹⁵ which is based on the incubation of a compound with its respective degradation enzyme; thus the peak in question is shifted to its enzymatic end product. For all enzyme peak shift studies, the following samples were chromatographed: (1) standard solution, (2) standard solution plus enzyme mixture, (3) deproteinized hemolymph and (4) deproteinized hemolymph plus enzyme mixture. For the identification of serotonin, the enzyme monoamine oxidase was used; for tryptophan, apotryptophanase; for octopamine, phenylethanolamine N-methyl transferase; and for 5-hydroxyindole acetic acid, pyridoxal-5'-phosphate.

TABLE I

RETENTION TIMES AND ABBREVIATIONS OF POSSIBLE COMPOUNDS OF INTEREST

Peaks at 4.08 min (peak X), and 6.47 min (peak S) were found in the chromatograms of the samples of hemolymph from lobsters in some of the molt stages. These peaks have not yet been identified.

Compound	Abbreviation	Retention time (min)
5-Hydroxyindole acetic acid	HIAA	2.03
5-Hydroxytryptophan	HTP	2.12
Tyrosine	TYR	2.37
Tryptophan	TRP	3.13
Octopamine	OA	5.46
Melatonin	MEL	6.31
Phenylalanine	PHE	10.45
Tryptamine	TRY	11.52
Serotonin	5-HT	12.37

RESULTS

Good resolution of all the compounds of interest was achieved using isocratic elution (Table I). Temperature control was critical for the maintenance of good resolution and reproducibility of retention times. Fig. 3 shows a chromatogram of serotonin, octopamine, tryptophan, 5-hydroxytryptophan, 5-hydroxyindole acetic

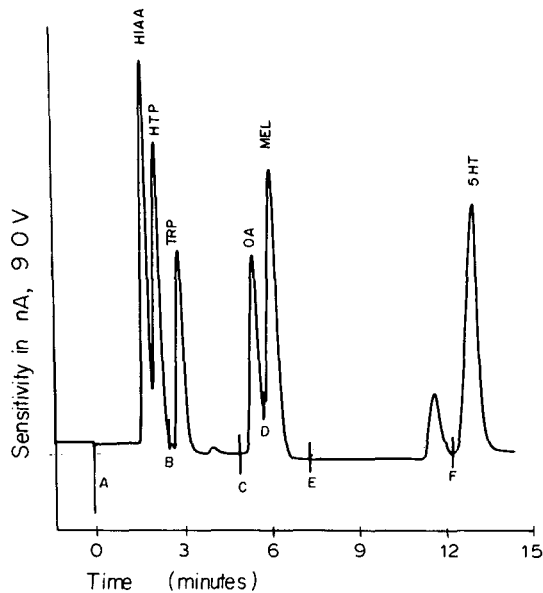


Fig. 3. HPLC-ED separation of a standard 10^{-6} M mixture of 5-hydroxyindole acetic acid (HIAA), 5-hydroxytryptophan (HTP), tryptophan (TRP), octopamine (OA), melatonin (MEL), tryptamine (TRY) and serotonin (5HT). Chromatographic conditions as described in Experimental. Sensitivity for sections of the chromatogram are: (A) 100 nA f.s., (B) 50 nA f.s., (C) 20 nA f.s., (D) 50 nA f.s., (E) 100 nA f.s., (F) 50 nA f.s.

acid, melatonin and tryptamine. There was baseline resolution of all peaks except for the octopamine and melatonin peaks.

In order to achieve optimal detection limits of all the peaks in different biological samples, the attenuation in the UV and the sensitivity of the electrochemical detector were altered throughout the separation as noted in the lettered chromatogram (Fig. 3). The stability study showed that degradation of the octopamine started within 10 min upon exposure to 25°C (room temperature) and that serotonin began to deteriorate within 10 min upon exposure to indirect sunlight. After 10, 30, and 120 min and 24 h exposure, 91.6, 95.3, 31.8 and 2.9% of the octopamine concentration remained after a standard solution was held at room temperature. When serotonin was placed in indirect sunlight, 56.0, 58.7, 32.3 and 14.7% of the control remained after 10, 20, 30, and 120 min intervals, respectively (Fig. 4).

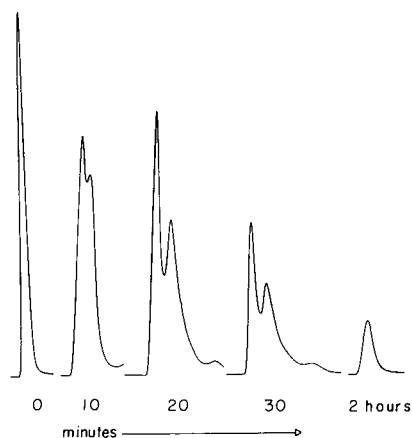


Fig. 4. Degradation of the serotonin peak upon exposure to indirect sunlight. The peak height decreased progressively with time of exposure in comparison to the peak height of the control. 500 nA f.s., applied potential 90 V. Chromatographic conditions as given in Experimental.

There was good linearity of response. Linearity is maintained down to 9 pg for octopamine when electrochemical detection was used and to 0.9 ng with UV detection ($r = 0.9996$). With the serotonin, the detection limit was 0.1 pg with ED. The limiting factor in detection with the electrochemical detector is not only the peak response but also the loss in baseline stability (Fig. 5).

The recovery of the neurohormones, octopamine and serotonin, after undergoing sample preparation and handling procedures was 98% for the octopamine and 98% for the serotonin. The recoveries were calculated on the basis of the percent difference in peak height before and after sample preparation procedures were carried out on the hemolymph samples to which known amounts of the model compounds were added. With our RPLC-ED method the relative concentrations of tryptophan, serotonin, 5-hydroxyindole acetic acid, and octopamine were monitored in seven molt stages. These peaks were identified by the enzyme peak shift technique (Fig. 6). A chromatogram of the hemolymph of a lobster in a different stage of the molt cycle

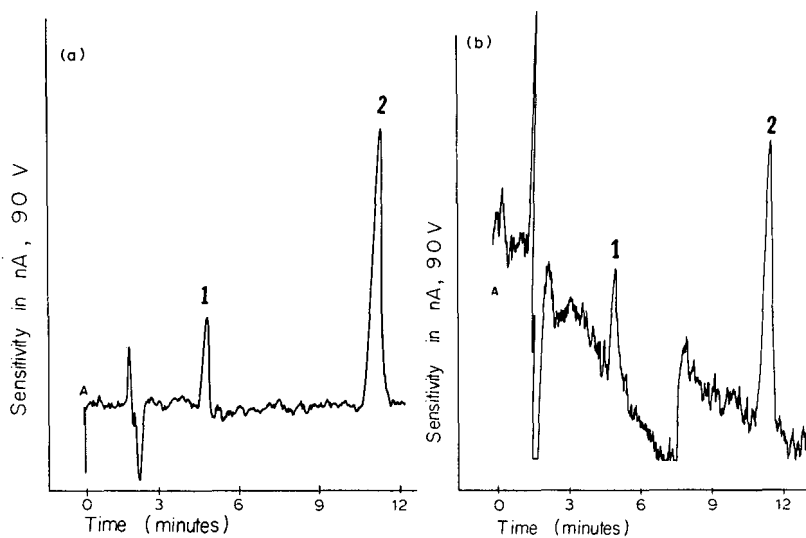


Fig. 5 (a) Detection limits for octopamine (peak 1) and serotonin (peak 2) obtained at 10 nA f.s. and a 10^{-9} M solution. (b) Chromatogram obtained using a 10^{-12} M solution when at a sensitivity of 5 nA f.s.

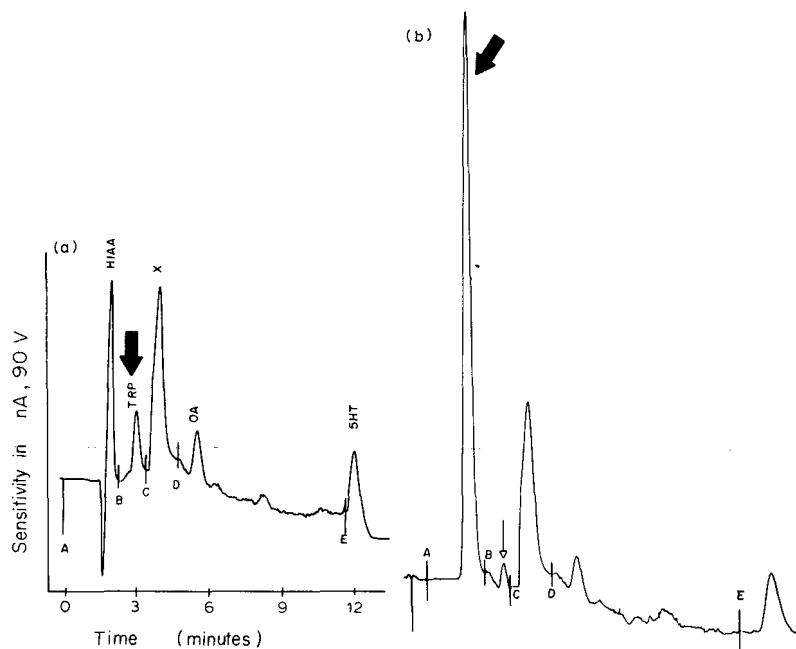


Fig. 6. Peak identification of tryptophan using the enzyme peak shift technique with the enzyme apotryptophanase. (a) Chromatogram of the hemolymph after incubation for 13 min with apotryptophanase. (b) Chromatogram of the hemolymph after incubation for 13 min with apotryptophanase. Note the increase in the HIAA and the decrease in TRP. The letters denote the sensitivity for the designated section of the chromatogram as described in Fig. 3.

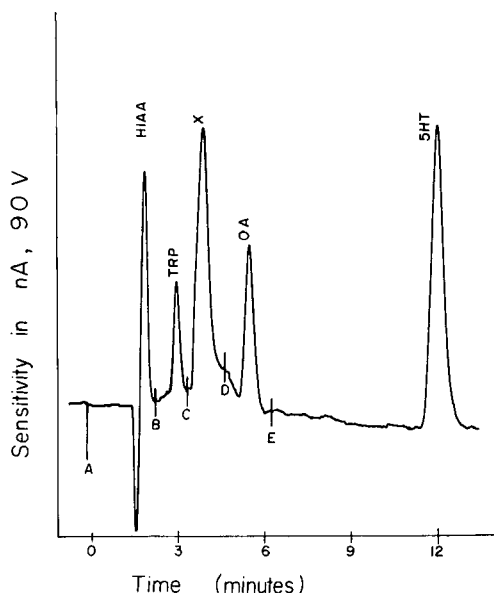


Fig. 7. Chromatograms of hemolymph from lobsters in a different molt stage from that in Fig. 6a. Note the differences in the relative amounts of TRP, 5-HT, OA and peak X in the two chromatograms. For abbreviations of the compounds, see Fig. 3. The chromatographic conditions are given in Experimental. The letters denote the sensitivity for the designated section of the chromatogram as described in Fig. 3.

than that in Fig. 6a is shown in Fig. 7. Note the relative differences in the peak heights of tryptophan, octopamine, serotonin and peak X. No tyrosine, 5-hydroxytryptophan, tryptamine, phenylalanine or melatonin were detected in any of the samples analyzed. Changes in two peaks (called peak X and peak S), which are not yet identified were observed in the hemolymph from lobsters in some of the stages of the molt cycle. Peak X had a retention time of 4.08 min and peaks S of 6.47 min. The endogenous levels of the compounds in each stage with respect to the behavioral aspect most relevant for that molt stage will be reported in the near future.

DISCUSSION

Three primary factors were found to influence the quantitation, resolution, and reproducibility of the HPLC-ED chromatograms of the compounds in the serotonergic and octopamine pathways: (1) electrode maintenance, (2) sample preparation, and (3) mobile phase composition. Electrode maintenance for both the glassy carbon working electrode and Ag/AgCl reference electrode is critical to insure peak height and shape reproducibility. Peak height is directly correlated with the oxidative properties of a compound. These properties are altered when the electrode is not properly maintained. The glassy carbon electrode must be polished weekly with aluminum oxide to prevent accumulation of contaminants which can reduce the available oxidation surface and hence cause peak height variance. The Ag/AgCl electrode must be stored in 3 M sodium chloride to prevent leakage of the chloride solution through

the seals. Leakage quickly ensues if electrodes are left overnight in the acetonitrile mobile phase. In addition the baseline is more stable and the background noise reduced when a small amount of EDTA is added to the mobile phase.

Sample preparation was also a key factor which determined the precision of the concentrations of endogenous octopamine and serotonin. Our protocol provides a high recovery of trace amounts of circulating neuroactive compounds. In order to provide better recovery than that previously reported for octopamine and serotonin, which are very labile, special care must be taken to maintain the samples at 4°C and to shield the samples from light. If these precautions are taken, good reproducibility in peak height and shape can be obtained. Even a slight delay time between processing the samples and injection of aliquots onto the column can introduce variability due to decomposition of octopamine and serotonin.

Lastly, because a complex mobile phase consisting of phosphate buffer, TCA, SDS, and organic solvents is needed to provide good peak shape as well as adequate resolution in minimum time, the column had to be washed well daily to prevent degradation of the column. In addition EDTA was required in the mobile phase to maintain electrode performance in the electrochemical detector.

Two problems were encountered when regular C₁₈ columns were used with this mobile phase: (1) strong adherence of compounds to the analytical column which produced peak tailing, and (2) breakdown of the column or reduction in column lifetime producing non-reproducible retention times and high back pressures. To alleviate these problems, the Perkin Elmer reduced activity catecholamine column was used. It provided symmetrical, reproducible peak shapes for the strongly retained compounds. Secondly, a silica gel precolumn was placed between the pump and the injector to protect the analytical column. This precolumn was repacked every two weeks with fresh silica.

The RPLC-ED method described proved to be an excellent technique to determine serotonin and its metabolites along with octopamine at the picogram level in the hemolymph of lobsters. Despite the presence of only trace amounts of the neuroactive hormones in physiological samples as well as the inherent instability of these compounds, endogenous levels of these hormones can be measured with excellent precision in minimal time if careful attention is paid to electrode and column maintenance and if chromatographic conditions as well as sample preparation and storage procedures are carefully controlled.

ACKNOWLEDGEMENTS

We thank the Perkin Elmer Corporation for the use of the electrochemical detector and for the reduced activity catecholamine column. We also thank Drs. Pamela Perrone and J. Russel Gant of The Perkin Elmer Corp. for their support, encouragement and help and Drs. Mary Jo Wojtusik and Mary Dwyer for their helpful discussions.

REFERENCES

- 1 P. D. Evans, E. A. Kravitz and B. R. Talamo, *J. Physiol.*, 262 (1976) 71.
- 2 P. D. Evans, E. A. Kravitz, B. R. Talamo and B. G. Wallace, *J. Physiol.*, 262 (1976) 51.
- 3 L. Fischer and E. Florey, *J. Exp. Biol.*, 102 (1983) 187.

- 4 S. Glusman and E. A. Kravitz, *J. Physiol.*, 325 (1982) 223.
- 5 E. A. Kravitz, B. S. Beltz, S. Glusman, M. F. Goy, R. M. Harris-Warwick, M. R. Johnston, M. S. Livingston, T. L. Schwarz, T. L. and K. K. Siwicki, *Trends Neurosci.*, 6 (1983) 345.
- 6 A. M. Krstulovic, L. Bertani-Dziedzic, S. W. Dziedzic and S. E. Gitlow, *J. Chromatogr.*, 223 (1981) 305.
- 7 L. M. Bertani-Dziedzic, A. M. Krstulovic, S. Ciriello and S. E. Gitlow, *J. Chromatogr.*, 164 (1979) 345.
- 8 R. J. Martin, B. A. Bailey and R. G. H. Downer, *J. Chromatogr.*, 278 (1983) 265.
- 9 L. A. Pachla and P. T. Kissinger, *Clin. Chim. Acta*, 59 (1975) 309.
- 10 R. Elofsson, L. Laxmyr, E. Rosengren and C. Hansson, *Comp. Biochem. Physiol.*, 71C (1982) 196.
- 11 A. M. Krstulovic, in J. C. Giddings, E. Grushka, J. Cazes and P. R. Brown (Editors), *Advances in Chromatography*, Vol. 17, Marcel Dekker, New York, 1979, pp. 279-309.
- 12 D. H. Christensen and L. C. Blank, *J. Chromatogr. Sci.*, 12 (1979) 133.
- 13 L. Larmyr, *Comp. Biochem. Physiol.*, 77C (1984) 139.
- 14 R. A. Hartwick, *J. Liq. Chromatogr.*, 2 (1979) 125.
- 15 P. R. Brown, *J. Chromatogr.*, 52 (1970) 257.

CHROM. 20654

LIQUID CHROMATOGRAPHIC ANALYSIS OF ORGANIC ADDITIVES IN COPPER PLATING BATHS

SHAUL SHOHAT and ELI GRUSHKA*

Department of Inorganic and Analytical Chemistry, The Hebrew University, Jerusalem (Israel)

and

S. GLIKBERG

Tadiran Printed Circuits, Kiriat Malachi (Israel)

SUMMARY

A new method is described for the analysis of organic additives in copper plating baths. Liquid chromatography, utilizing an ion-pair reversed-phase technique, was found to be most suited for this purpose. Ion pairing neutralizes the brightener components, thereby enabling the use of moderate conditions during analysis, *i.e.*, a pH of 4–5 and isocratic elution. Preceding the chromatography, a solid-phase extraction process was used to decrease the copper ion concentration and the acidity of the bath. Active copper plating baths were investigated and the results are given and explained.

INTRODUCTION

Electrical copper plating is one of the most important steps in the manufacture of printed circuit boards. The pattern of the copper on the board is responsible for the conductivity between the electronic components mechanically attached to the board surface. During the copper electroplating, close control is required so that neither too much nor too little copper is plated on the board or in the plated-through holes, and that the copper deposit has a bright shiny uniform appearance with high ductility and tensile strength. It has been found that the rate of electrodeposition of the copper is important in respect of efficient and repeated formation of an uniform continuous smooth layer of bright shiny metal having a controlled depth or thickness with good physical properties. Organic additives, commonly known as “brighteners” (or “copper gleam” in acidic copper baths), are used in electroplating baths to regulate the rate of metal deposition and thus to maintain control over the physical properties of the plated metal. Therefore, it is very important to be able to monitor both changes in the concentration and the chemical composition of the additives in the bath.

The concentrations of the additives fluctuate due to their electrochemical destruction during the plating process and to their inclusion in the copper plate. As the additive concentration changes, it affects the quality of the plating. If the brightener

concentration is too low, the copper electroplate becomes coarse grained or burned and powdery; if it is too high, the electroplated copper shows a burned deposit with a brittle or non-uniform surface.

Increasing demands for high reliability in the manufacture of printed circuit boards with high aspect ratios, specifically on very dense multilayer substrates, necessitate the definition control of the range of allowed concentrations of the additives in the copper plating solutions. In view of the importance of the additives, the paucity of published reports describing their analysis is most surprising. The few reports which can be found describe methods such as cyclic voltammetric stripping, high-performance liquid chromatography and ion chromatography. The oldest and most common test of additive concentration is the "Hull-cell" test which consists of a small electrodeposition cell through which a current is passed. The nature of the electroplated copper layer is monitored as function of the current density. However, this test does not provide a direct measurement of the additive concentration.

More recently, a polarographic technique known as cyclic voltammetric stripping (C.V.S.) has been used for the analysis of organic additives in baths, *e.g.*, ref. 1. The C.V.S. technique provides direct evidence of the influence of additives on the overvoltage for copper deposition. The measurement of the charge required to strip a plated deposit is indicative of the concentration of the additives. However, the C.V.S. technique is influenced by the electrolyte species, contaminant concentration, temperature and chloride concentration due to their effects on the stripping charge. Several papers and technical notes describe various modes of chromatographic analysis of the brighteners. An application note from Dionex² concerns an ion chromatographic method for the analysis of the major component in a commercial Copper Gleam solution. LeaRonal, a manufacturer of such solutions, described the reversed-phase liquid chromatographic analysis of a particular brightener solution³. The method used a solid-phase extraction step to pre-isolate the organic compounds from the acidic copper bath, a column containing a polymeric packing and step gradient elution. The resulting chromatogram was rather complex, making the quantitation difficult. Reid⁴ also described a reversed-phase liquid chromatographic system utilizing a column packed with a polymeric packing. Although he used an UV detector, most of the work employed an electrochemical detector. He monitored the concentration of brighteners in an acidic copper bath under a variety of conditions. Since the detector used was selective, only one or at most two peaks were observed.

The characterization of organic additives is difficult due to the complex nature of the bath. A typical acidic copper bath contains copper salt (15–22.5 g/l), sulphuric acid (170–230 g/l), chloride ion (30–80 ppm) and organic agents at various concentrations, usually less than 1%, depending on the system used. Therefore, the accurate analysis of the additives requires intensive pretreatment prior to the chromatographic injection. The present work examines the concentration and behaviour of the organic additives in a typical acidic copper bath.

EXPERIMENTAL

Materials

The mobile phase was prepared using 18-m Ω water and HPLC-grade acetonitrile (Bio-Lab, Jerusalem, Israel). The mobile phase components were filtered

through a 0.2- μm filter. Tetrabutylammonium hydrogensulphate was obtained from Sigma Israel (Tel Aviv, Israel). The samples of the organic additives were stored at 4°C to prevent decomposition. They, and samples from active copper plating baths, were obtained from Tadiran Printed Circuits.

The column (250 mm \times 4.5 mm I.D.) was a LiChrosorb RP-18 cartridge (Merck, Darmstadt, F.R.G.). An open column (10 mm \times 0.5 mm I.D.) packed with 40- μm reversed-phase particles was used for extraction.

The mobile phase used consisted of 91% water, 9% acetonitrile and 3 mM tetrabutylammonium hydrogensulphate.

Instrumentation

The chromatographic studies were carried out using a Series 4 liquid chromatograph (Perkin-Elmer, Norwalk, CT, U.S.A.) and either a Perkin-Elmer 85B UV-VIS detector or a Chrom-A-Scope rapid scanning UV detector and integrator (Barspec, Rehovot, Israel).

Sample preparation

It was necessary to reduce the high concentration of the copper as its strong UV absorbance obscured that of the organic components. The high acidity of the original bath is also harmful to the analytical column. In order to decrease the concentration of copper ions and of sulphuric acid in the samples from the concentrations that can be found in the bath, a solid-phase extraction process was used. A 20-ml volume of the original bath solution was passed through the extraction column followed by 3 ml water and 5 ml acetonitrile. The acetonitrile fraction was collected and its volume was adjusted to 4 ml.

RESULTS AND DISCUSSION

In this work the organic additives used were of a type commercially available in Europe, suited to work with titanium baskets and containing mainly surfactants such as sulphonic alkanes. Because of the highly ionic nature of the brightener components, they cannot be retained using conventional reversed-phase chromatography. To retard the solutes, ion-pair chromatography was used with tetrabutylammonium cations added to the mobile phase.

Fig. 1 shows a chromatogram of the additive standard as supplied. The chromatogram shows two main peaks, A and B, corresponding to two of the

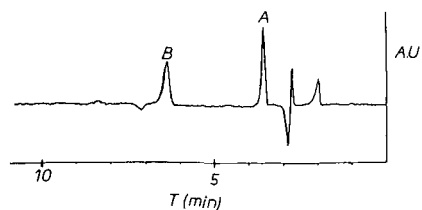


Fig. 1. Chromatogram (at 210 nm) of 7.5 ml/l of a basic additive standard showing two peaks due to the organic modifier components, A and B.

components in the organic modifier. A third component, called the "carrier" or "wetting agent", does not appear in the chromatogram since it absorbs in the UV range only below 200 nm.

Of the two other components, the second peak shows a significant decrease after bubbling of air through a sample of the brightener over an extended period, and a third peak, C, appears. The sum of the areas of peaks B and C does not equal that of the original peak B. This variation in the total peak areas might be due to the different absorption coefficient of the degradation product (peak C).

With further oxidation over 1 month, peak B decreases until it finally disappears, Fig. 2. Concurrently, there is a corresponding increase in peak C. The rate of formation of the degradation product is dependent on the rate of bubbling of air and on the temperature; when refrigerated, there is no apparent change in the second peak.

Using the Hull-cell technique, it was found that as the second component (peak B) decreases and peak C increases, the brightener solution shows a poor plating quality. This confirms the significance of the second component of the organic additive in the plating process.

Fig. 3 shows a chromatogram of the organic additive in an acidic copper bath after the solid-phase extraction. Even after the extraction process, a copper peak can still be noticed before the solvent peak. Its short retention time is due to the fact that the reversed-phase column is acting as an anion exchanger (because of the ion-pairing reagent) which will not retard the positive copper ions.

To examine the utility of the method for determination of the concentration of the additive in acidic copper baths, a calibration graph was prepared for various concentrations of the organic additive, ranging from 2.5 to 15 ml brightener per litre bath solution. Such graphs were plotted for both peak A and peak B. They were linear in this concentration range. For peak A, the relationship between the peak height and the concentration, C (in units of ml additive per litre bath solution), is:

$$\text{Height} = 0.527C - 0.239$$

The correlation coefficient is 0.9979. For the second component the equation is

$$\text{Height} = 0.899C - 0.0644$$

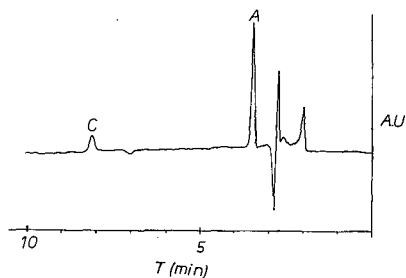


Fig. 2. Chromatogram (at 210 nm) of the same sample as in Fig. 1 after bubbling of air over an extended period. Note the disappearance of peak B and the appearance of a third peak, C.

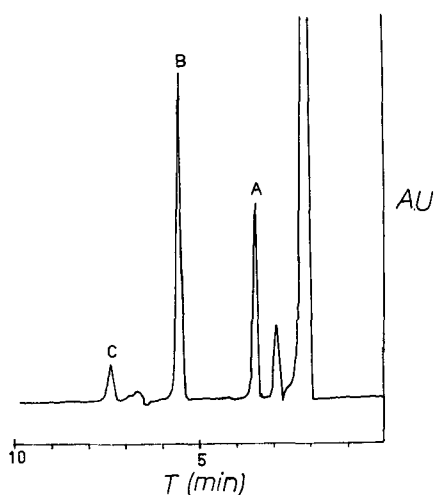


Fig. 3. Chromatogram (at 210 nm) of the organic modifier in an acidic copper bath after solid-phase extraction.

with a correlation coefficient of 0.998. The results indicate that ion-pair reversed-phase liquid chromatography can be used for quantitation of the brightener in acidic copper bath.

A chromatogram of an active bath is shown in Fig. 4. Two important points

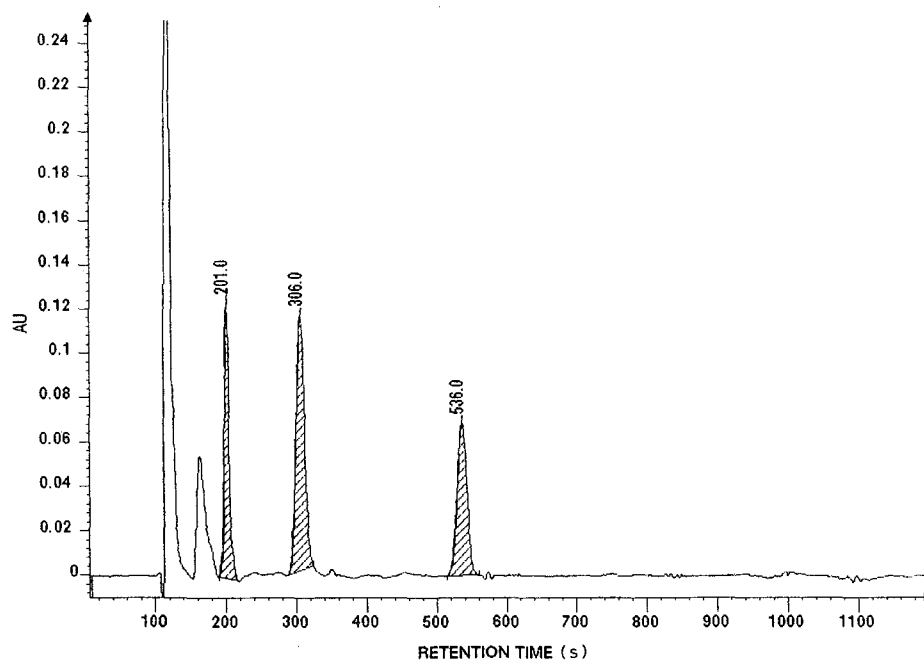


Fig. 4. Chromatogram (at 200 nm) of an active bath. Note the increased height of peak C.

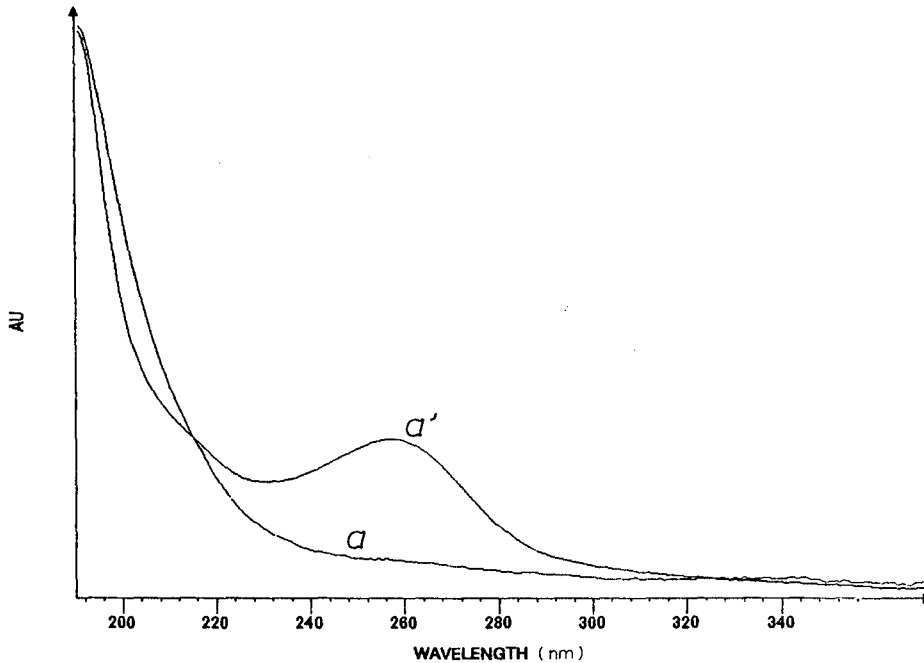


Fig. 5. Spectra of peak A in a new (a) and an activated (a') bath.

should be noted. The first is the appearance of an increased amount of the degradation product, peak C. At a first glance, it may seem that the concentrations of components B and C are equal, corresponding to their equal heights and areas. However, as mentioned above, the absorbance coefficient of the degradation product may significantly differ from that of the second component. Therefore, its relative concentration, as shown in the chromatogram, may differ from that of its source (peak B). Furthermore, the concentration of peak C seems to increase in proportion to the activation time of the bath. This is expected as new brightener is added periodically to the bath to replenish its diminishing concentration.

The second point of interest is the change in the absorbance spectrum of the first peak (peak A) in the chromatogram of the brightener before and during activation of the bath. Fig. 5 shows a spectrum, obtained with the Barspec detector, of peak A in a new bath and in an active one. An absorption peak at 260 nm appears in the spectrum of the component in an active bath. The reason for the change in the spectrum is not known at this stage of the research.

CONCLUSIONS

The liquid chromatographic method described allows the determination of the concentration of a brightener solution in an acidic copper bath, and the monitoring of changes in the composition of the brightener. The use of a rapid-scanning detector offers the possibility to monitor even more closely the changes that occur in the

brightener components. At present, we are investigating further the fate of the brightener in acidic copper baths and their effect on the quality of the plated copper.

ACKNOWLEDGEMENTS

One of us (S. Shohat) thanks Tadiran Printed Circuits for information, equipment and a scholarship to study the high-performance liquid chromatographic analysis of organic additives and impurities in copper plating baths. We thank the Barspec company for the loan of the Chrom-A-Scope detector.

REFERENCES

- 1 D. Tench and J. White, *J. Electrochem. Soc.*, 132 (1985) 831.
- 2 *Dionex's Application Update, AU111*, Sunnyvale, CA, October, 1986.
- 3 *LeaRonald's TechSpecs, 30019-HPLC*, June, 1987.
- 4 J. Reid, *PC Fab.*, November (1987) 5.

CHROM. 20 721

HIGH-PERFORMANCE LIQUID CHROMATOGRAPHY SEPARATIONS OF NITROSAMINES

III. CONFORMERS OF N-NITROSAMINO ACIDS

HALEEM J. ISSAQ*, DOUGLAS G. WILLIAMS and NICOLE SCHULTZ

Program Resources, Inc., NCI-Frederick Cancer Research Facility, P.O. Box B, Frederick, MD 21701 (U.S.A.)

and

JOSEPH E. SAAVEDRA

Bionetics Research Inc., NCI-Frederick Cancer Research Facility, P.O. Box B, Frederick, MD 21701 (U.S.A.)

SUMMARY

The separation of a selected group of N-nitrosamino acids and their *syn* and *anti* conformers by high-performance liquid chromatography using an α -cyclodextrin bonded silica gel column and a mobile phase of acetonitrile-triethylammonium acetate was achieved. The effects of mobile phase pH and concentration of acetonitrile on resolution and elution times are also reported.

INTRODUCTION

The separations of cyclic¹ and acyclic² nitrosamines by high-performance liquid chromatography (HPLC) using β -cyclodextrin and C₁₈ bonded silica columns were reported. This research deals with separation of N-nitrosamino acids and their *syn* and *anti* conformers. N-nitrosamino acids excreted in the feces and urine are used as an index of endogenous nitrosation. This is based on the findings that N-nitrosamino acids such as nitrosoproline (NPRO), nitrosohydroxyproline (NHPRO) and nitrososarcosine (NSAR), when administered orally to rats, are excreted unchanged almost quantitatively in the urine and feces³. The reaction of nitrite and creatinine forms NSAR, and NPRO can result from the reaction of the amino acid proline under nitrosating conditions⁴. Cysteine can form nitrosothiazolidine carboxylic acid (NTCA) in the presence of nitrite and formaldehyde under nitrosating conditions⁴.

Determination of N-nitrosamino acids by gas chromatography (GC) has been reported after derivatization of the carboxyl groups by methylation^{5,6} or silylation⁷. Another GC procedure was developed whereby the carboxyl group was esterified with diazomethane, and the nitroso group was oxidized with peroxytrifluoroacetic acid to give N-nitrosamino acid methyl esters. The hydroxyl group of NHPRO methylester was acylated with trifluoroacetic anhydride. The derivatives were then analyzed by

a GC utilizing an electron-capture detector⁸. In our laboratory, a GC equipped with a thermal energy analyzer (TEA) is routinely used for the determination of nitrosamines and nitrosamino acids.

Although GC with electron-capture detection (ECD) or TEA is a sensitive technique for analyzing nitrosamines and their derivatives, it may not be the best technique for the resolution of the *syn* and *anti* conformers since the analysis is carried out at above room temperature. Cryogenic thin-layer chromatography (CTLC) was successfully used for the separation of the *syn* and *anti* conformers of some dinitrosopiperazines⁹. Also, HPLC, using β -cyclodextrin and reversed-phase C₁₈ bonded silica gel columns at room temperature, was used to separate some acyclic nitrosamines and their *syn* and *anti* conformers². Iwaoka and Tennenbaum¹⁰ were able to separate the *syn* and *anti* conformers of NPRO by HPLC using a pellicular polyamide column with an eluent of 0.1% acetic acid in tetrahydrofuran. However, they were only partially, but not quantitatively, able to separate the *syn* and *anti* conformers of NSAR¹⁰. Walters *et al.*¹¹ used HPLC to separate five N-nitrosamino acids from each other but not their conformers.

This study is an extension of our previous studies^{1,2} into the use of cyclodextrin bonded packings for the separation of nitrosamines. The present study is an evaluation of the α -cyclodextrin bonded silica gel HPLC column for the separation of a group of nitrosamino acids and, where applicable, their *syn* and *anti* conformers. Also the effect of pH and percent organic modifier on resolution and retention will be studied. For these purposes, a group of five- and six-membered ring nitrosamino acids and NSAR were selected, the structures of which are shown in Fig. 1.

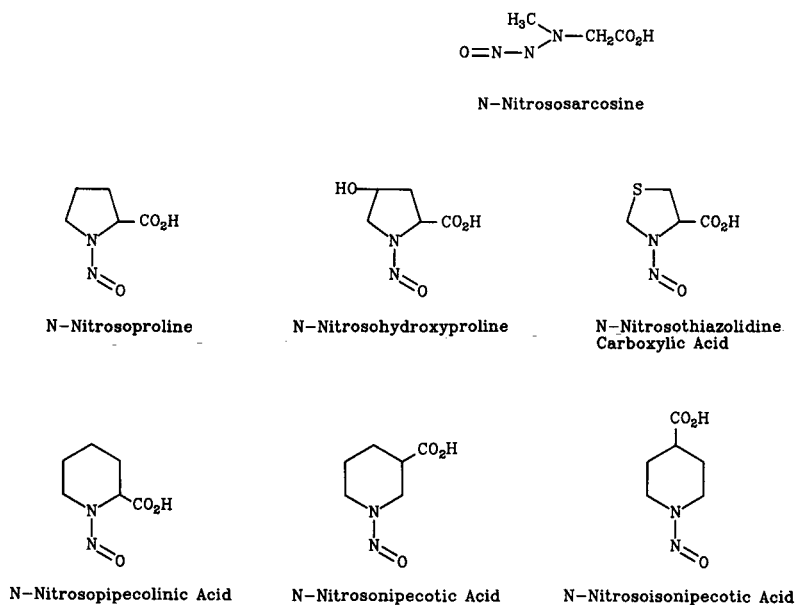


Fig. 1. Structural formulae of nitroso compounds used in this study.

EXPERIMENTAL

Materials

The nitrosamino acids used in this study, NSAR, NPRO, NHPRO, NTCA, N-nitrosopipicolinic acid (NPPC), N-nitrosoisipepicotic acid (NNPC) and N-nitrosoisonepicotic acid (NINPC), were synthesized in house by the method of Lijinsky *et al.*¹² and their structures were confirmed by elemental analysis, mass spectrometry and nuclear magnetic resonance. Acetonitrile was glass-distilled UV grade (Burdick & Jackson). Water was deionized glass distilled. The 5- μm spherical preppacked α -cyclodextrin (cyclobond III) bonded silica gel columns (150 \times 4.6 mm I.D., and 250 \times 4.6 mm I.D.) were purchased from Advanced Separations Technologies (Whippany, NJ, U.S.A.).

Apparatus

A Hewlett-Packard Model 1090 liquid chromatograph equipped with a photodiode array detector, an automatic injector, a strip chart recorder, a Hewlett-Packard Model 3392A integrator and a Hewlett-Packard Model 85 computer/controller was used.

Procedure

Solutions were prepared in water to contain approximately 0.5 $\mu\text{g}/\mu\text{l}$. A 10- μl volume of the solution was injected, unless specified. The mobile phase was made of acetonitrile-triethylammonium acetate (TEAA), which was filtered and degassed before use and maintained under helium throughout the experiment. Mobile phase flow-rate was 1.5 ml/min. Absorption was monitored at 238 nm.

The TEAA solution (0.01 M) was prepared by adding 1.4 ml triethylamine to 1.0 l of water and then titrating with acetic acid to the required pH. Throughout this manuscript TEAA will refer to a 0.01 M TEAA solution. pH measurements were made using a Fisher Accumet brand pH meter Model 750.

RESULTS AND DISCUSSION

In two previous papers we reported the separation of cyclic¹ and acyclic nitrosamines and some of their conformers² by HPLC. This work deals mainly with the separation of the *syn* and *anti* conformers of nitrosamino acids with emphasis on NSAR, NPRO, NHPRO and NTCA, which are produced endogenously.

Fig. 2 shows the separation of the *syn* and *anti* conformers of NTCA, NSAR, NPRO and NHPRO, using an α -bonded cyclodextrin column and a mobile phase of acetonitrile-TEAA (90:10, v/v) at pH 5. The figure shows base line resolution of the conformers of NHPRO, NPRO and NSAR and a good resolution, which can be quantified, of the NTCA conformers. The retention times of each pair are listed in Table I. The *syn* and *anti* conformers were determined by nuclear magnetic resonance.

The *syn* and *anti* conformers of a mixture of NPRO, NHPRO and NSAR were resolved using the same column and mobile phase, but a pH of 2.5, Fig. 3. It is not recommended to use the α -cyclodextrin column for long periods of time with low pH mobile phases. This low pH was used in order to study the effect of pH on resolution, peak position, and elution order as will be discussed later. However, Fig. 3 shows

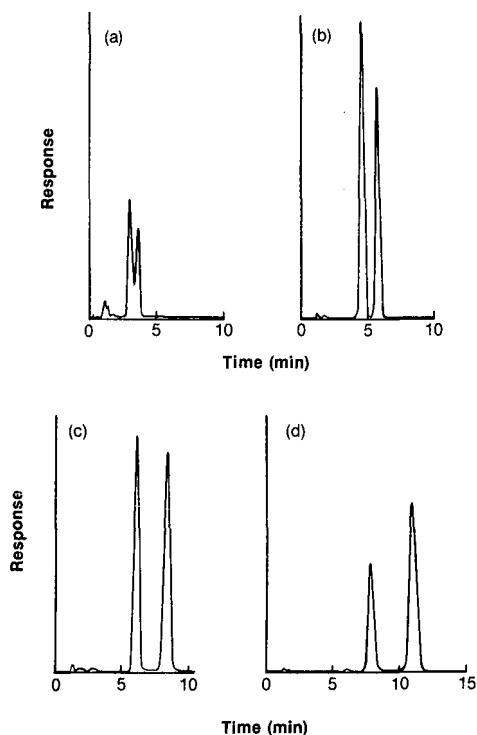


Fig. 2. Chromatograms of the separation of the *syn* and *anti* conformers of (a) NTCA, (b) NSAR, (c) NPRO and (d) NHPRO using a 150×4.6 mm α -cyclodextrin bonded column, $5 \mu\text{m}$ spherical, and a mobile phase of acetonitrile- 0.01 M TEAA, pH 5 (90:10) at a flow-rate of 1.5 ml/min. Detection was carried out at 238 nm.

a good resolution of the six conformers in the mixture. Fig. 4 shows the separation of the conformers of the five-membered ring nitrosamino acids, NTCA, NPRO and NHPRO, using a mobile phase of acetonitrile-TEAA (92:8, v/v) at pH 5. The results show a partial resolution of one of the conformers of each NPRO and NHPRO, and a quantitative resolution of the other conformers.

TABLE I

RETENTION TIMES OF THE *SYN* AND *ANTI* CONFORMERS OF NTCA, NSAR, NPRO AND NHPRO

Conditions: $15 \text{ cm} \times 4. \text{ mm}$ α -cyclodextrin bonded column, and a mobile phase of acetonitrile-TEAA (90:10, v/v), pH 5, at a flow-rate of 1.5 ml/min.

Compound	Retention time (min)
NTCA	3.11, 3.69
NSAR	4.63, 5.74
NPRO	6.04, 8.29
NHPRO	7.80, 10.92

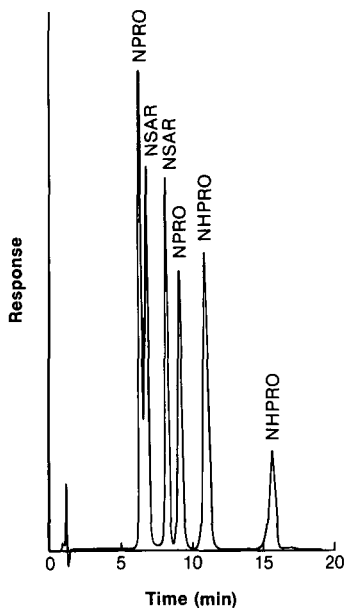


Fig. 3. Chromatogram of the separation of a mixture of NPRO, NSAR, and NHPRO. Conditions as in Fig. 2 except acetonitrile/0.01 M TEAA, pH 2.5 (80:20).

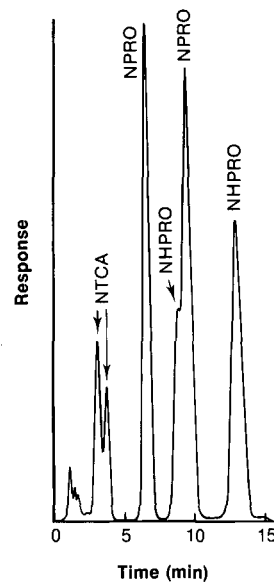


Fig. 4. Chromatogram of the separation of a mixture of five-membered ring N-nitrosamino acids. Conditions as in Fig. 2 except 92% acetonitrile.

Effect of mobile phase pH on the separation of NHPRO conformers

It was observed that the pH of the mobile phase affects not only the elution time of the nitrosamino acids but the resolution of the conformers and the shape of the peaks. For example, the *syn* and *anti* conformers of NHPRO shifted their elution positions when the pH was lowered from pH 4 to pH 3 to pH 2.75, Fig. 5. Two interesting phenomena are observed in Fig. 5: (i) at pH 4, (5a), the *anti* conformer of NHPRO eluted before the *syn* conformer. In contrast, at pH 3, (5b), the *anti* conformer eluted just after the *syn*, while the elution time of the *syn* conformer remained constant. (ii) When the pH was lowered to 2.75 (5c), the elution time of the *anti* conformer was about the same as it was at pH 3, but the *syn* conformer eluted earlier than it had at pH 3 and pH 4. This behavior may be due to the different pK_a 's of these conformers. These phenomena may be used to an advantage in order to achieve the separation of other certain mixtures of nitrosamino acids and their conformers.

Six-membered ring nitrosamino acids

Three six-membered ring amino acids, NPPC, NNPC and NINPC, were used in this study. Only two of these, NPPC and NNPC, have *syn* and *anti* conformers. The separation of the three acids is shown in Fig. 6 using acetonitrile-TEAA (90:10, v/v) at pH 5. These compounds eluted quickly at lower pH's (results not shown). The conformers of these acids were resolved, although not base line, by using a mobile phase of acetonitrile-TEAA (70:30, v/v) at pH 5 as seen in Fig. 7. It is believed based on

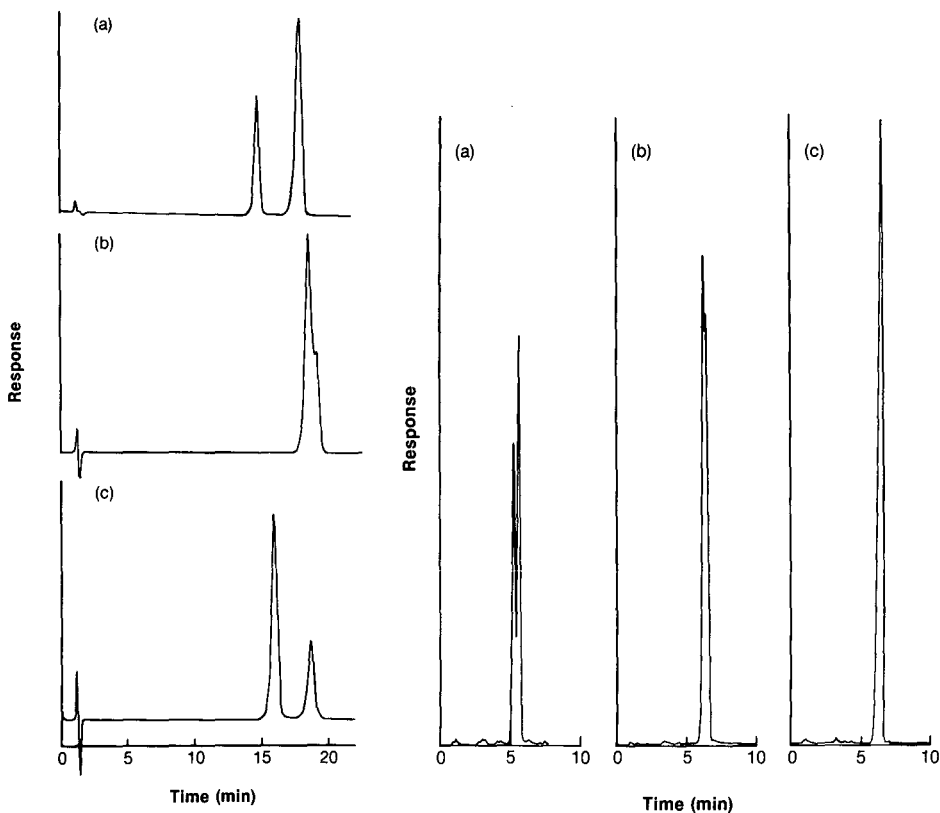


Fig. 5. Effect of pH on the separation of the *syn* and *anti* conformers of NHPRO on a 250×4.6 mm α -cyclodextrin column using a mobile phase of acetonitrile–0.01 M TEAA (80:20) at pH 4 (a), pH 3 (b) and pH 2.75 (c) and a flow-rate of 1.5 ml/min.

Fig. 6. Chromatogram of the separation of six-membered ring N-nitrosamino acids using a 150×4.6 mm α -cyclodextrin column and a mobile phase of acetonitrile–0.01 M TEAA, pH 5 (90:10) at a flow-rate of 1.5 ml/min.

previous experience⁹ that lowering the temperature of analysis will result in the complete resolution of the conformers of NPPC and NNPC. This will be dealt with in a later publication studying the effect of temperature on the HPLC separation of nitrosamines and their conformers.

Effect of organic modifier

Acetonitrile was preferred to methanol because of less back pressure (viscosity) and the shapes of the peaks were more symmetrical when acetonitrile was used in the mobile phase. The greatest effect of the percent acetonitrile in the mobile phase on the retention of the nitrosamino acids was above 70%. Below that, the compounds eluted close to the solvent front, while above that, greater retention was observed (Table II). The results in Table II show some peculiarities; in most cases, retention times increased with an increase in the volume of acetonitrile (greater than 80%) in the mobile phase

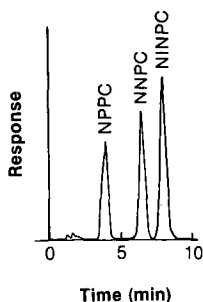


Fig. 7. Chromatograms of the separation of the *syn* and *anti* conformers of (a) NPPC and (b) NNPC. (c) Is a chromatogram of NINPC. Conditions are the same as in Fig. 6, except 70% acetonitrile.

under constant pH (NSAR, NPRO, NHPRO, NNPC and NINPC^{*}); in other cases, the retention times decreased with an increase of the volume of acetonitrile up to ~90% then increased (NTCA and NPPC). This may be due to the fact that these nitrosamine acids have different pK_a values and also different solubilities. The relatively very long retention times at 95% acetonitrile are due to the fact that these N-nitrosamino acids are more soluble in water.

TABLE II

EFFECT OF PERCENTAGE ACETONITRILE IN THE MOBILE PHASE ON THE RETENTION OF N-NITROSAMINO ACIDS IN THIS STUDY

The conditions used were: 15 cm \times 4.6 mm α -cyclodextrin bonded column, 5 μ m spherical, and a mobile phase of acetonitrile-TEAA, pH 5, at a flow-rate of 1.5 ml/min.

Compound	t_R (min)				
	Acetonitrile (%)				
	60	70	80	90	95
NSAR	4.80	4.81	4.80	5.21	9.47
	5.35	5.48	5.91	6.49	12.48
NTCA	4.38	4.01	3.62	3.48	5.54
	4.78	4.45	4.19	4.18	7.15
NPRO	5.46	5.54	5.92	6.95	14.40
	6.32	6.63	7.18	9.64	21.72
NHPRO	5.22	5.71	6.57	9.06	21.37
	5.88	6.71	8.12	12.73	33.66
NPPC*	4.99	4.41	4.15	4.45	9.08
		4.69		4.82	
NNPC*	5.31	5.31	5.90	7.76	19.74
NINPC	5.40	5.62	6.37	10.06	27.57

* NPPC and NNPC, which have two conformers, rarely had their conformers separated under these conditions. Hence, only one elution time might be listed.

CONCLUSION

The results of this study show that an HPLC system equipped with an α -cyclodextrin bonded column and an isocratic mobile phase of acetonitrile-TEAA can be used to resolve the *syn* and *anti* conformers of NSAR, NPRO, NHPRO, NTCA, NNPC and partial separation of NNPC. It was found that at lower pH (2.5) the six-membered ring nitrosamino acids eluted quickly while they were retained longer at higher pH (5.0); good resolution of the conformers of the five-membered ring nitrosamino acids were resolved at both lower pH (2.5) and higher pH (5.0) mobile phase buffers. The results also show that, in most cases, longer retention times were observed, at the same mobile phase pH with an increase in the volume of acetonitrile in the mobile phase.

ACKNOWLEDGEMENTS

This project has been funded at least in part with Federal funds from the Department of Health and Human Services under contract number N01-CO-74102. The content of this publication does not necessarily reflect the views or policies of the Department of Health and Human Services, nor does mention of trade names, commercial products, or organization imply endorsement by the U.S. Government.

REFERENCES

- 1 H. J. Issaq, J. H. McConnell, D. E. Weiss, D. G. Williams and J. E. Saavedra, *J. Liq. Chromatogr.*, 9 (1986) 1783.
- 2 H. J. Issaq, M. Glennon, D. E. Weiss, G. N. Chmurny and J. E. Saavedra, *J. Liq. Chromatogr.*, 9 (1986) 2763.
- 3 H. Oshima, J. C. Berezziat and H. Bartsch, *Carcinogenesis*, 3 (1985) 115, and references therein.
- 4 J. Casado, A. Castro, J. R. Leis, M. Mosquera and M. E. Pena, *J. Chem. Soc. Perkin. Trans. II*, (1985) 1859.
- 5 N. P. Sen, B. A. Donaldson, S. Seaman, J. R. Iyengar and W. F. Miles, in E. A. Walker *et al.* (Editors), *Environmental Aspects of N-Nitroso Compounds*, IARC Scientific Publications No. 19, IARC, Lyon, 1978, 374.
- 6 T. Ishibashi, M. Matsui and T. Kawabata, *Bunseki Kagaku (Jpn. Anal.)*, 24 (1975) 107.
- 7 G. Eisenbrand, C. Janzowski and R. Preussmann, *J. Chromatogr.*, 115(1975) 602.
- 8 T. Ishibashi, T. Kawabata and H. Tanahe, *J. Chromatogr.*, 195 (1980) 416.
- 9 H. J. Issaq, M. M. Mangino, G. M. Singer, D. J. Wilbur and N. H. Risser, *Anal. Chem.*, 51 (1979) 2157.
- 10 W. Iwaoka and S. R. Tannenbaum, *J. Chromatogr.*, 124 (1976) 105.
- 11 D. G. Walters, A. K. Mallett and R. C. Cottrell, *J. Chromatogr.*, 246 (1982) 161.
- 12 W. Lijinsky, L. Keefer and J. Loo, *Tetrahedron*, 26 (1970) 5137.

CHROM. 20 655

REVERSED-PHASE C₁₈ AND NORMAL-PHASE SILICA HIGH-PERFORMANCE LIQUID CHROMATOGRAPHY OF GIBBERELLINS AND THEIR METHYL ESTERS

JIANN-TSYH LIN* and ALLAN E. STAFFORD

Plant Development-Quality Research Unit, Western Regional Research Center, Agricultural Research Service, U.S. Department of Agriculture, Albany, CA 94710 (U.S.A.)

SUMMARY

Twenty-three gibberellins and their methyl esters were chromatographed by gradient reversed-phase C₁₈ partition and isocratic normal-phase silica adsorption high-performance liquid chromatography (HPLC). These four complementary HPLC systems allowed for the necessary separation to resolve these gibberellins. The four HPLC systems can be used to identify radioactive metabolites in metabolism studies by co-chromatography of radioactive labelled gibberellins with authentic standards using UV and radioactive flow detectors. The highest separation efficiency for these gibberellins was achieved with the reversed-phase C₁₈ HPLC of their methyl esters.

INTRODUCTION

High-performance liquid chromatography (HPLC) is now a routine procedure for the purification and separation of gibberellins, a group of plant hormones. Reversed-phase C₁₈ partition HPLC of gibberellins has been the most frequently used and reported HPLC system¹⁻⁵. The HPLC of some gibberellin derivatives have also been reported⁶⁻⁸. Very little of the C₁₈ HPLC of methyl esters of gibberellins and the silica HPLC of free gibberellins and their methyl esters have been reported.

Lin *et al.*^{9,10} have previously used both normal-phase silica adsorption and reversed-phase C₁₈ partition HPLC of twenty-six androgens (C₁₉O₂ stereoisomers) and their acetates in metabolism studies to identify radioactive metabolites by co-chromatography with standards. The four HPLC systems used complemented each other and all of the twenty-six C₁₉O₂ androgens available to us were resolved. There are more than seventy gibberellins that have been identified in plants and the fungus *Gibberella fujikuroi*, while the number of gibberellins in particular plants is limited¹¹. The structures among the twenty-six C₁₉O₂ androgens¹² are more similar than those of gibberellins¹¹. It was therefore easier to separate these gibberellins than to separate the C₁₉O₂ androgens by HPLC. We report here the separation of gibberellins using both reversed-phase C₁₈ partition and normal-phase silica adsorption HPLC of free (underivatized) gibberellins and their methyl esters. We also report here the elution properties of gibberellins in these HPLC systems.

Gas chromatography–mass spectrometry (GC–MS) has been used to detect labelled isotopic ions of the HPLC purified gibberellin metabolites when gibberellins labelled with ^{13}C , ^{14}C or ^2H were used as precursors^{13,14}. Gas chromatography–selected ion monitoring (GC–SIM) or GC–MS also has been used to identify HPLC purified radioactive metabolites without the detection of isotopic ions when the gibberellins labelled with ^3H or ^{14}C were used as precursors^{15,16}. Reversed-phase C_{18} HPLC alone without GC–MS or GC–SIM has been used to tentatively identify the radioactive metabolites¹⁷. One or more HPLC systems described here can be used to purify the metabolites with identification of the metabolites by GC–MS or GC–SIM. Gibberellins from these HPLC systems can be derivatized for GC–MS or GC–SIM identification. These four HPLC systems sequentially also can be used to identify radioactive metabolites by co-chromatography with authentic standards using UV and on-line radioactive flow detectors. The radioactive flow-detector can very accurately match the UV and radioactive peaks of a single HPLC run.

EXPERIMENTAL

A Waters Assoc. liquid chromatograph was used which consisted of two pumps (M510), a multiwavelength detector (M490), and a data and chromatography control station (M840). The injector was a Rheodyne Model 7125. The columns were a silica column (25 cm \times 0.46 cm, 5 μm , Spherisorb S5W, Alltech/Applied Science, Deerfield, IL, U.S.A.) and a C_{18} column (25 cm \times 0.46, 5 μm , Ultrasphere ODS, Beckman, San Ramon, CA, U.S.A.). Gibberellins were methylated with diazomethane. The eluents for the HPLC of free gibberellins needed 0.05% of glacial acetic acid as ion repressor, while the eluents for the HPLC of the methyl esters of gibberellins needed no glacial acetic acid. The eluent mixture for the silica HPLC of free gibberellins needs premixing, to avoid air bubble formation which interferes with UV detection. The chromatographic conditions are given in the figure legends.

RESULTS AND DISCUSSION

Results are summarized in Table I. Chromatograms from four HPLC systems are shown in Figs. 1–4 and are direct photocopies of printouts from HPLC runs. The gibberellins in Table I are arranged in the order of elution (decreasing polarity) in the C_{18} HPLC of free gibberellins. The elution orders are not the same or exactly the reverse among these four HPLC systems. Some gibberellins in Table I cannot be adequately separated by one HPLC system. However, they can be adequately separated by at least one of the three remaining HPLC systems. The C_{18} HPLC of up to 42 gibberellins has been reported¹. We include in Table I, GA_{55} , GA_{32} and GA_{54} for which HPLC results have not been reported previously^{1–5}.

The four chromatograms (Figs. 1–4) showed that the separation efficiency (theoretical plate number illustrated by peak width and retention time) in decreasing order is as follows: C_{18} HPLC of methyl esters of gibberellins (system 2) > C_{18} HPLC of free gibberellins (system 1) > silica HPLC of methyl esters of gibberellins (system 4) > silica HPLC of free gibberellins (system 3). Both C_{18} HPLC systems are very good for the separation of gibberellins. The peak widths in Fig. 2 are slightly smaller than those in Fig. 1 and therefore the separation efficiency of system 2 is the best among

TABLE I

RETENTION TIMES OF GIBBERELLINS IN HPLC

Conditions: (1) C₁₈ HPLC, free gibberellins, see Fig. 1; (2) C₁₈ HPLC, methyl esters of gibberellins, see Fig. 2; (3) silica HPLC, free gibberellins, see Fig. 3; (4) silica HPLC, methyl esters of gibberellins, see Fig. 4.

Gibberellins	Retention time (min)			
	1	2	3	4
GA ₅₅	5.03	6.64	12.21	12.57
GA ₈	5.08	7.36	11.69	12.49
GA ₃₂	6.50		12.61	12.21
GA ₃	9.38	10.32	9.34	9.73
3epi-GA ₁	9.41	11.51	12.68	12.31
GA ₁	10.51	11.41	8.99	9.24
GA ₅	17.86	18.67	5.75	4.87
GA ₂₀	18.97	19.41	5.73	4.70
GA ₃₆	20.44	24.56	4.73	3.31
GA ₁₃	20.47	26.10	6.74**	3.05
GA ₄₄ *	21.4			
GA ₁₉	22.41	23.54	5.81	3.93
GA ₅₄	22.58	22.85	5.32	4.45
GA ₃₄	22.83	22.80	4.93	4.30**
GA ₁₇	23.74	25.35	6.67**	3.89
GA ₃₇	24.07	22.94	4.84	4.38
GA ₇	24.92	23.69	4.03	3.50
GA ₄	26.07	24.60	4.00	3.36
GA ₅₃	27.81	27.34	4.96	3.13
GA ₁₄	28.17	28.64	4.36	2.74
GA ₂₄	28.86	29.91	2.90	1.84
GA ₉	29.36	27.79	2.77	2.08
GA ₂₅	29.54	31.21	3.31	1.74
GA ₁₅	29.76	27.87	3.20	2.38

* Retention time of GA₄₄ was obtained with extract from wheat seedlings²⁰.

** Broad peaks, the peak width is about twice of that of other peaks at similar retention times.

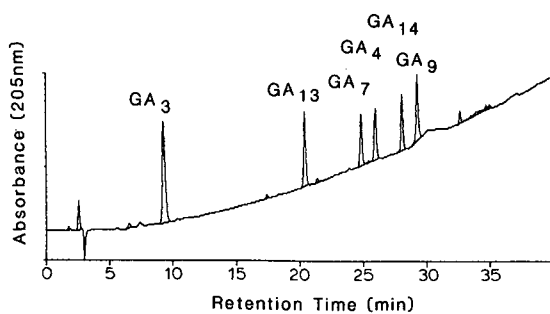


Fig. 1. Chromatogram of C₁₈ HPLC of free gibberellins (in elution order GA₃, GA₁₃, GA₇, GA₄, GA₁₄ and GA₉). The standards (about 1–5 μg each) dissolved in less than 25 μl of methanol were chromatographed on a column of Ultrasphere ODS. Eluent, linear gradient from 35% methanol in water (containing 0.05% of acetic acid) to 100% methanol (containing 0.05% of acetic acid) in 40 min; flow-rate, 1 ml/min; pressure, 3000 p.s.i.

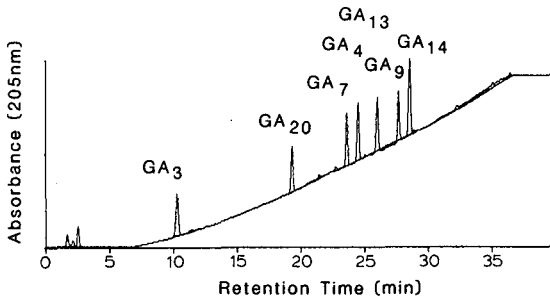


Fig. 2. Chromatogram of C_{18} HPLC of the methyl esters of gibberellins (in elution order, GA_3 , GA_{20} , GA_7 , GA_4 , GA_{13} , GA_9 and GA_{14}). The standards (about 1–5 μg each) dissolved in less than 25 μl of methanol were chromatographed on a column of Ultrasphere ODS. Eluent, linear gradient, from 40% methanol to 100% methanol in 30 min, then 100% methanol for additional 10 min; flow-rate, 1 ml/min; pressure, 3000 p.s.i.

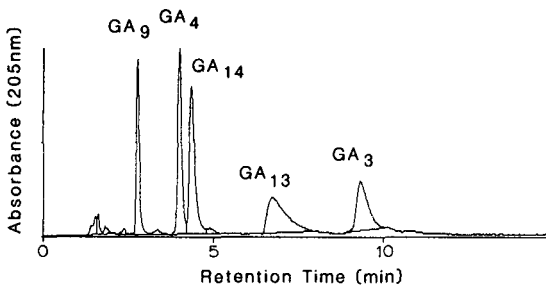


Fig. 3. Chromatogram of silica HPLC of free gibberellins (in elution order, GA_9 , GA_4 , GA_{14} , GA_{13} and GA_3). The standards (about 1–5 μg each) dissolved in less than 25 μl of the eluent were chromatographed on a column of Spherisorb S5W. Eluent, *n*-hexane-ethanol (90:10) containing 0.05% of acetic acid, pre-mixed; flow-rate, 2 ml/min; pressure, 800 p.s.i.

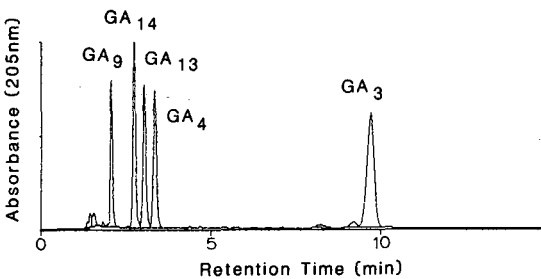


Fig. 4. Chromatogram of silica HPLC of the methyl of gibberellins (in elution order, GA_9 , GA_{14} , GA_{13} , GA_4 and GA_3). The standards (about 1–5 μg each) dissolved in less than 25 μl of the eluent were chromatographed on a column of Spherisorb S5W. Eluent, *n*-hexane-ethanol (92:8); flow-rate, 2 ml/min; pressure, 800 p.s.i.

these four HPLC systems. Even though the separation efficiency of C₁₈ HPLC of methyl esters of gibberellins (system 2) is the best among these four HPLC systems, it has only been reported previously by Birnberg *et al.*¹⁸ using acetonitrile–water as the eluent for purification. The silica HPLC of methyl esters of gibberellins has been reported^{16,18} with the retention times of GA₅₃, GA₄, GA₂₀, GA_{17/19} given¹⁶. Lin and Heftmann³ have previously reported the only silica HPLC of free gibberellins. This is adsorption chromatography and is different from the widely used silica partition chromatography¹⁹.

The factors affecting the polarity (or retention time) of gibberellins in HPLC are as follows: number of hydroxyl groups, position and orientation of hydroxyl groups, functional groups at the C-10 position, lactone form and double bond. The more polar compounds elute later from normal-phase silica HPLC and sooner from reversed-phase C₁₈ HPLC.

Some gibberellin retention properties of reversed-phase C₁₈^{1–5} and normal-phase silica³ HPLC of free gibberellins have been previously reported but not those of the other two HPLC systems. The more hydroxyl groups, the more polar the gibberellins will be and therefore will elute sooner from C₁₈ HPLC and elute later from silica HPLC for both gibberellins and the methyl esters of gibberellins. Examples of the effect of hydroxyl group on polarity in HPLC from the present study are the following pairs of gibberellins: GA₅₅ > GA₁, GA₅₄ > GA₄ (C-1β); GA₈ > GA₁, GA₃₄ > GA₄ (C-2β); 3epi-GA₁ > GA₂₀ (C-3α); GA₁ > GA₂₀, GA₄ > GA₉, GA₃₆ > GA₂₄, GA₃₇ > GA₁₅ (C-3β); GA₃₂ > GA₃ (C-12α); GA₁ > GA₄, GA₃ > GA₇, GA₁₇ > GA₂₅, GA₁₉ > GA₂₄, GA₂₀ > GA₉, GA₄₄ > GA₁₅, GA₅₅ > GA₅₄ (C-13).

The orientation and location of hydroxyl groups are also an important factor affecting the polarity of gibberellins and their HPLC retention times. The conclusions given here are derived in part from the retention times of gibberellins of Jensen *et al.*¹ which are not given in Table I. The ring A α-hydroxylated gibberellins are in general more polar than the ring A β-hydroxylated gibberellins in the C₁₈ HPLC of free gibberellins (system 1, Table I). The examples are as follows: GA₁₆ > GA₅₄ (C-1), GA₄₀ > GA₅₁ (C-2), 3epi-GA₁ > GA₁ (C-3). Based on C₁₈ HPLC of free gibberellins the polarity of gibberellins with hydroxyl groups at different locations (system 1, Table I) is, in general, 12α > 16α > 13 > 11β > 1α > 2α > 1β > 2β > 3α > 3β. Examples are as follows: 12α > 16α; GA₃₉ > GA₄₁, GA₃₁ > GA₁₀. 16α > 13; GA₁₀ > GA₂₀, (GA₄₁ < GA₂₈). 13 > 11β; GA₁ > GA₃₅. 11β > 1α; GA₃₅ > GA₁₆. 1α > 2α; GA₁₆ > GA₄₇. 2α > 1β; GA₄₇ > GA₅₄. 1β > 2β; GA₅₅ > GA₈, GA₅₄ > GA₃₄. 2β > 3α; GA₂₉ > 3epi-GA₁. 3α > 3β; 3-epi-GA₁ > GA₁. These retention properties affected by the orientation and location of a hydroxyl group of free gibberellins in C₁₈ HPLC have not been previously reported. The elution order of free gibberellins in the C₁₈ HPLC in Table I (system 1) is consistent with that of Jensen *et al.* except GA₅₃–GA₁₄.

In these four HPLC systems, C-13 hydroxygibberellins in general are more polar than the C-1β, C-2β, C-3β hydroxygibberellins. The examples are as follows: 13 > 1β; GA₁ > GA₅₄. 13 > 2β; GA₁ > GA₃₄. 13 > 3β; (GA₁₉ > GA₃₆), GA₅₃ > GA₁₄, GA₅ > GA₇, GA₂₀ > GA₄, (GA₁₇ > GA₁₃). Some examples shown here with the parenthesis are the exception only with C₁₈ HPLC of C₂₀ gibberellins (system 1). In these four HPLC systems 1β-hydroxyl gibberellins are in general more polar than 2β-hydroxyl gibberellins such as GA₅₄ > GA₃₄, GA₅₅ > GA₈.

Monohydroxygibberellins can be more polar than the dihydroxygibberellins depending on the locations of hydroxyl groups. In the C_{18} HPLC of free gibberellins (system 1), 12α -monohydroxygibberellin (GA_{31}) and 16α -monohydroxygibberellin (GA_{10}) are more polar than the dihydroxygibberellins (GA_{16} , GA_{27} , GA_{47} , GA_{34}). 13 -Monohydroxygibberellin (GA_{20}) is more polar than the dihydroxygibberellins (GA_{27} , GA_{47} , GA_{34}). In the other three HPLC systems (Table I) 13 -hydroxygibberellin (GA_{20}) is more polar than the dihydroxygibberellin (GA_{34}).

The polarity of the free gibberellins with different groups at the C-10 position in the C_{18} HPLC (system 1) is $-\text{CHO} > -\text{COOH} > -\text{CH}_3$, while in silica HPLC (system 3) $-\text{COOH} > -\text{CHO} > -\text{CH}_3$. The polarity of the methyl esters of gibberellins with different groups at the C-10 position is $-\text{CHO} > -\text{COOCH}_3 > -\text{CH}_3$ in both C_{18} and silica HPLC (systems 2 and 4). The examples are as follows: $GA_{24} > GA_{25} > GA_{12}$, $GA_{19} > GA_{17} > GA_{53}$ and $GA_{36} > GA_{13} > GA_{14}$.

The polarity of the gibberellins with γ -lactone or δ -lactone at ring A in silica HPLC of both free gibberellins and methyl esters of gibberellins (systems 3 and 4) is in general δ -lactone $>$ γ -lactone, such as $GA_{37} > GA_4$, $GA_{15} > GA_9$. The polarity of gibberellins in the C_{18} HPLC (systems 1 and 2) is γ -lactone $>$ δ -lactone when there is no hydroxyl group at ring A, such as $GA_9 > GA_{15}$, $GA_{20} > GA_{44}$, and δ -lactone $>$ γ -lactone when there is a hydroxyl group at C-3 β position, such as $GA_{37} > GA_4$, $GA_{27} > GA_{34}$, $GA_{38} > GA_1$. This retention property of γ -lactone and δ -lactone has not been previously reported.

Gibberellins with a double bond are more polar than those without the double bond in both silica and C_{18} HPLC of both free gibberellins and the methyl esters of gibberellins (systems 1-4). The examples are as follows: $GA_3 > GA_1$, $GA_7 > GA_4$, $GA_5 > GA_{20}$. The C_{18} HPLC can separate these pairs of gibberellins better than the silica HPLC.

One or more of the HPLC systems described can be used sequentially either with preparative or analytical column to purify gibberellins from plant extracts. They also can be used for identification together with GC-MS or GC-SIM. In metabolism studies using radioactive precursors, the radioactive metabolites can be identified by co-chromatography with authentic standards using the four HPLC systems sequentially.

ACKNOWLEDGEMENTS

We thank Dr. Noboru Murofushi, Department of Agricultural Chemistry, University of Tokyo, for the samples of gibberellins. J. T. Lin thanks Dr. Erich Heftmann for his intellectual stimulation and encouragement during the period of eleven co-authored papers.

REFERENCES

- 1 E. Jensen, A. Crozier and A. M. Monteiro, *J. Chromatogr.*, 367 (1986) 377.
- 2 M. Koshioka, J. Harada, K. Takeno, M. Noma, T. Sassa, K. Ogiyama, J. S. Taylor, S. B. Rood, R. L. Legge and R. P. Pharis, *J. Chromatogr.*, 256 (1983) 101.
- 3 J.-T. Lin and E. Heftmann, *J. Chromatogr.*, 213 (1981) 507.
- 4 M. G. Jones, J. D. Metzger and J. A. D. Zeevaart, *Plant Physiol.*, 65 (1980) 218.
- 5 G. W. M. Barendse, P. H. van de Werken and N. Takahashi, *J. Chromatogr.*, 198 (1980) 449.

- 6 A. Crozier, J. B. Zaerr and R. O. Morris, *J. Chromatogr.*, 238 (1982) 157.
- 7 E. Heftmann, G. A. Saunders and W. F. Haddon, *J. Chromatogr.*, 156 (1978) 71.
- 8 R. O. Morris and J. B. Zaerr, *Anal. Lett.*, 11 (1978) 73.
- 9 J.-T. Lin, D. Palevitch and E. Heftmann, *Phytochemistry*, 22 (1983) 1149.
- 10 J.-T. Lin, *LC, Liq. Chromatogr. HPLC Mag.*, 2 (1984) 135.
- 11 N. Takahashi, I. Yamaguchi and H. Yamane, in N. Takahashi (Editor), *Chemistry of Plant Hormones*, CRC Press, Boca Raton, FL, 1986, p. 57.
- 12 J.-T. Lin and E. Heftmann, *J. Chromatogr.*, 237 (1982) 215.
- 13 R. C. Heupel, B. O. Phinney, C. R. Spray, P. Gaskin, J. MacMillan, P. Hedden and J. E. Graebe, *Phytochemistry*, 24 (1985) 47.
- 14 C. G. N. Turnbull, A. Crozier, L. Schwenen and J. E. Graebe, *Planta*, 165 (1985) 108.
- 15 G. A. de Bottini, R. Bottini, M. Koshioka, R. P. Pharis and B. G. Coombe, *Plant Physiol.*, 83 (1987) 137.
- 16 S. L. Maki, M. L. Brenner, P. R. Birnberg, P. J. Davies and T. P. Krick, *Plant Physiol.*, 81 (1986) 984.
- 17 J. L. Stoddart, *Planta*, 161 (1984) 432.
- 18 P. R. Birnberg, M. L. Brenner, M. C. Mardaus, H. Abe and R. P. Pharis, *Plant Physiol.*, 82 (1986) 241.
- 19 R. C. Durley, A. Crozier, R. P. Pharis and G. E. McLaughlin, *Phytochemistry*, 11 (1972) 3029.
- 20 J.-T. Lin and A. E. Stafford, *Phytochemistry*, 26 (1987) 2485.

CHROM. 20 741

PERFORMANCE OF GRAPHITIZED CARBON BLACK CARTRIDGES IN THE EXTRACTION OF SOME ORGANIC PRIORITY POLLUTANTS FROM WATER

F. MANGANI, G. CRESCENTINI, P. PALMA and F. BRUNER*

Istituto di Scienze Chimiche, Università di Urbino, Piazza Rinascimento 6, 61029 Urbino (Italy)

SUMMARY

The use of graphitized carbon black (GCB) cartridges for the extraction of organic pollutants (pesticides, phthalates, herbicides and polynuclear aromatic hydrocarbons) from water is discussed. Recovery tests carried out by spiking either the adsorbent or the water showed that nearly 100% recoveries can be obtained in most instances with 1 ml of a suitable eluent using 50 mg of GCB (Carbopack B). Examples of analyses of actual samples by gas chromatography-mass spectrometry are also shown. Levels as low as 10 ppt can be determined.

INTRODUCTION

Sample preparation and preconcentration prior to gas chromatography and/or gas chromatographic-mass spectrometric (GC-MS) analysis of organic pollutants in water traditionally relies on liquid-liquid extraction methods. However, solid-phase extraction is becoming an emerging technique in this field, because of substantial advantages over liquid-liquid extraction: (i) the use of much smaller volumes of expensive or hazardous solvents; (ii) a shorter time and simpler facilities (very little glassware is needed); and (iii) fewer steps during sample preparation. Therefore, the risk of sample loss and introduction of artefacts is considerably reduced. In addition, the commercial availability of disposable cartridges packed with a variety of adsorbents makes the use of solid-phase extraction more attractive than in the past. XAD resins^{1,2}, porous polyurethane foams^{3,4}, Tenax^{5,6}, porous polymer beads⁷, graphitized carbon black⁸⁻¹⁴ and C₁₈ bonded phase¹⁵⁻¹⁸ have been studied as adsorbents for the extraction of several classes of organic pollutants from water.

In this work a small diameter cartridge packed with Carbopack B was studied for the recovery of some important priority pollutants such as pesticides, herbicides, phthalates and polynuclear aromatic hydrocarbons (PAHs). Carbopack B is the commercial name for a non-specific and non-porous graphitized carbon black with a surface area of about 90 m²/g. Because of the peculiar homogeneity of its surface it has been extensively used in gas-liquid-solid chromatography¹⁹⁻²³, where the surface properties are modified according to the performance needed, by adding a suitable amount of a liquid phase. Carbopack B has been already used for the sample enrichment of some organic compounds from water, air and biological fluids^{9,12,24-26}.

EXPERIMENTAL

Reagents

Pesticide-grade acetone, light petroleum (b.p. 40–60°C) and toluene from Carlo Erba (Milan, Italy) were used for sample extraction and the preparation of standards. Standard kits of pesticides, herbicides, PAHs and phthalates, 2 mm I.D. C₁₈ cartridges (Supelclean LC-18, 40 µm, 3 ml) and Carbopack B (60–80 mesh) were purchased from Supelco (Bellefonte, PA, U.S.A.). Porapak P (50–80 mesh) and Tenax TA (35–60 mesh) were obtained from Chrompack (Middelburg, The Netherlands). All capillary columns were obtained from Supelco.

Instrumentation and analysis

A Carlo Erba MRGC 5160 Mega gas chromatograph equipped with a flame ionization detector and on-column injector and a Dani 6500 gas chromatograph (Dani, Monza, Italy) equipped with an electron-capture detector and programmed-temperature vaporizer injector were used for GC analysis when recovery tests were performed.

A Hewlett-Packard 5270 quadrupole mass spectrometer (Hewlett-Packard, Avondale, PA, U.S.A.) coupled with a Hewlett-Packard 5990 gas chromatograph equipped with a split/splitless injector was used for the analysis of actual samples. The GC analysis of phthalates and PAHs was performed on an SPB5 capillary column (30 m × 0.32 mm I.D.) with a 0.25-µm film thickness and temperature programming from 90 to 120°C at 40°C/min then up to 270°C at 12°C/min. The same column was used for the analysis of herbicides but the temperature programme was 2 min at 130°C and then 4°C/min up to 230°C. The GC analysis of pesticides was carried out on an SPB 608 capillary column (30 m × 0.25 mm I.D.) with a 0.25-µm film thickness and a temperature programme of 4 min at 150°C and then 8°C/min up to a final temperature of 290°C.

The GC-MS analysis of actual samples was carried out on the SPB5 column described above using the following temperature programmes: 2 min at 100°C and then 6°C/min up to 300°C for the analysis of herbicides and phthalates and 1 min at 50°C and 10°C/min up to 300°C for the analysis of pesticides and PAHs. The mass spectrometer was used in the selected ion monitoring mode (SIM). The most intense and structurally significant ions in the mass spectra of the single compounds were monitored in this instance. Two different SIM programmes were used for pesticides, phthalates and herbicides and for PAHs. Helium was used as the carrier gas.

Apparatus and procedure

The graphitized carbon black cartridges were made of glass-lined stainless-steel tubing (6 cm × 0.3 cm I.D.) packed with 50 mg of Carbopack B (60–80 mesh), kept in place by two plugs of silanized glass-wool. Both the Carbopack B and the silanized glass-wool were previously extracted in a Soxhlet apparatus for 6 h using light petroleum-toluene (1:1).

Cartridges containing materials other than Carbopack B were prepared following the same procedure and using the same amount of adsorbent (50 mg) with the exception of the C₁₈ cartridges, which were used as received.

The apparatus used for the recovery tests and extraction of actual samples is shown in Fig. 1. The upper part of the cartridge is connected through a stainless-steel

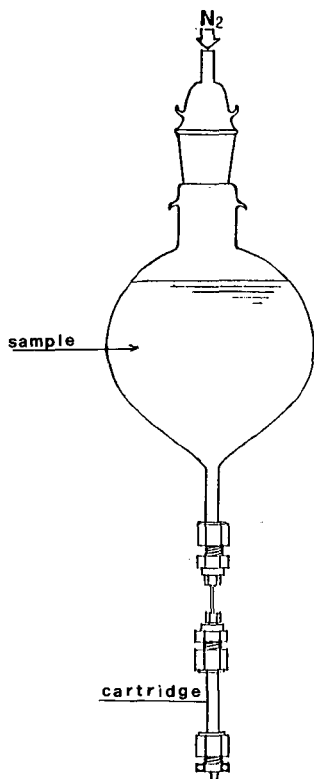


Fig. 1. Extraction apparatus.

union to a glass reservoir containing the water. A water flow-rate of 15 ml/min was ensured by applying a slight nitrogen pressure.

Recovery tests were carried out by following two different procedures. In the first, 100 μl of a standard solution in acetone containing 0.20–20 $\text{ng}/\mu\text{l}$ of the compounds of interest were placed on the top of the cartridge and the solvent was evaporated under a flow of nitrogen. A 10-ml volume of water was allowed through the cartridge, which was then dried again under a flow of nitrogen. The compounds were eluted with 1 ml of light petroleum–toluene (1:1). The choice of the elution mixture was based on previous studies carried out in this laboratory⁹. In the second procedure, 1 l of organic-free potable water was allowed through the trap, after having been spiked with 100 μl of the same standard solution according to a technique already described⁹. Also, in this instance the cartridge was dried under a flow of nitrogen and the compounds were eluted using the same solution as employed in the first procedure. The recoveries were calculated by comparing the chromatograms obtained after injection of the standard solutions and injection of the eluate from the cartridge. The recovery data are averages of three replicates and the relative standard deviation, calculated for some selected compounds with eight replicates, was 3%.

Before use, all glassware was washed with a detergent (Extran Ma 02 neutral) and thoroughly rinsed with doubly distilled water and acetone. A blank analysis with

TABLE I
RECOVERIES OF SOME CHLORINATED PESTICIDES FROM DIFFERENT ADSORBENTS

Pesticide	Recovery (%)				
	Carbopack B	Tenax	Porapak P	C ₁₈ *	C ₁₈ **
α -BHC	93	81	55	95	94
β -BHC	100	81	60	93	94
γ -BHC	100	77	51	93	—
Heptachlor	97	94	70	96	77
δ -BHC	97	94	50	96	93
Aldrin	96	88	71	88	87
Heptachlor epoxide	95	100	63	99	—
4,4'-DDE	100	87	77	93	—
Dieldrin	100	95	80	95	94
Endrin	99	89	75	94	—
4,4'-DDD	100	83	63	92	—
4,4'-DDT	100	86	55	95	83

* This work.

** Ref. 15.

the whole apparatus using 1 l of organic-free water showed no significant presence of the compounds of interest.

Thermal desorption was not tested thoroughly, but a few experiments showed that the recovery is poor in most instances and that thermal decomposition may occur with some compounds.

RESULTS AND DISCUSSION

In Table I the recoveries of twelve chlorinated pesticides from cartridges packed with five different adsorbents using only 1 ml of the extraction mixture are shown. A 50-mg amount of adsorbent was used in all instances and the recovery tests were carried out following the first procedure, *i.e.*, by placing on the top of the cartridge 100 μ l of a standard solution containing 0.50 ng/ μ l of each pesticide.

The recoveries are very low for Porapak P. Tenax TA shows a better performance, although some problems seem to exist with the elution of the benzene hexachlorides (BHCs) in general and of γ -BHC in particular. Some results obtained with Tenax GC have recently been reported⁶ using the adsorption-thermal desorption technique. Although only four compounds were tested, and a comparison is possible only for dieldrin and *p,p'*-DDE, the data are similar to those shown in Table I. Carbopack B shows the best overall recoveries with values near to 100% in most instances. Lower but still good recoveries are obtained with C₁₈. It should be noted that a double amount of adsorbent was used in this instance. The different recoveries obtained with Carbopack B and C₁₈ cannot be ascribed to the choice of the elution solvent. In fact, the data from ref. 15 show that similar values are obtained when ethyl acetate, selected after a detailed investigation, was used. The cartridge used in that work contained 200 mg of the adsorbent and 1.5 ml of ethyl acetate were used.

If organic pollutants have to be determined at trace levels it is important to

TABLE II
RECOVERIES FROM CARBOPACK B FOR DIFFERENT AMOUNTS OF PESTICIDES

Pesticide	Recovery (%)			
	50 ng	20 ng	10 ng	5 ng
α -BHC	93	93	92	92
β -BHC	100	100	100	100
γ -BHC	100	100	98	85
Heptachlor	97	98	98	96
δ -BHC	97	98	97	75
Aldrin	96	96	92	91
Heptachlor epoxide	95	95	95	93
4,4'-DDE	100	100	100	100
Dieldrin	100	100	100	100
Endrin	99	99	96	95
4,4'-DDD	100	100	86	86
4,4'-DDT	100	100	100	100

establish when irreversible adsorption becomes relevant. Table II shows the data obtained when different amounts of pesticides were placed on the top of the Carbopack B cartridge and 100 μ l of solutions containing 0.50, 0.20, 0.10 and 0.05 ng/ μ l of the single compounds were used with 1 ml of light petroleum-toluene (1:1) as eluent. It can be seen that a slight but consistent decrease in the recovery is observed when 5 ng of pesticides are desorbed. Moreover, this concerns only two compounds (γ - and δ -BHC), so that it can be safely stated that irreversible adsorption or the effect of decomposition is significant below the 5-ng level. Consequently, the use of a 50-mg Carbopack B cartridge in the extraction step allows the determination of very low levels of pesticides (5 ppt in 1 l of water).

Table III shows the recovery data for pesticides and the other classes of compounds studied, by spiking the adsorbent directly and by spiking the water. In the first instance 50 ng of pesticides and herbicides and 500 ng of phthalates and PAHs were used to spike the adsorbent. In the second, 1 l of water was spiked with the same amounts of pollutants so that the concentrations were 5 ppt for pesticides and herbicides and 50 ppt for phthalates and PAHs.

When the adsorbent was spiked, the recoveries for herbicides, phthalates and PAHs were similar to those obtained for pesticides, except for the heavier PAHs. This problem may be solved by extracting with toluene at 100°C²⁷ or by using a Carbopack with a smaller surface area. The small difference in the recoveries when the water was spiked is probably due to adsorption on the glass wall of the reservoir^{1,9,19}. The larger differences observed for di-*n*-octyl phthalate and some PAHs can be explained by the poor solubility of these compounds in water. In fact, if the cartridge was extracted with several portions of 1 ml of the eluent no appreciable amount of the compounds of interest was found after the first 1-ml fraction.

A 1-l volume of mineral water was extracted by the method described and analysed by capillary GC with flame ionization detection after storage in a plastic

* Throughout this article, the American billion (10⁹) and trillion (10¹²) are meant.

TABLE III

RECOVERIES OF PESTICIDES, HERBICIDES, PHTHALATES AND PAHs OBTAINED BY SPIKING THE ADSORBENT (A) AND BY SPIKING THE WATER (B)

2,4-DME = 2,4-dichlorophenoxy acetic acid methyl ester, 2,4,5-TME = 2,4,5-trichlorophenoxy acetic acid methyl ester, DCPA = 2,3,5,6-tetrachloroterephthalic acid dimethyl ester.

Compound type	Recovery (%)		
	Compound	A	B
Pesticides	α -BHC	93	94
	β -BHC	100	96
	γ -BHC	100	95
	Heptachlor	98	87
	δ -BHC	98	94
	Aldrin	96	90
	Heptachlor epoxide	95	97
	4,4'-DDE	100	92
	Dieldrin	100	97
	Endrin	99	99
	4,4'-DDD	100	94
	4,4'-DDT	100	95
Herbicides	2,4-DME	97	92
	Trifluralin	98	92
	Simazine	100	97
	Atrazine	96	93
	Propazine	100	97
	2,4,5-TME	96	92
	DCPA	99	98
Phthalates	Di- <i>n</i> Butylphthalate	100	100
	Butylbenzylphthalate	100	100
	Bis(2-Ethylhexyl) phthalate	100	100
	Di- <i>n</i> -octyl phthalate	100	50
PAHs	Acenaphthene	99	87
	Acenaphthylene	100	88
	Fluorene	89	89
	Phenanthrene	99	88
	Anthracene	100	87
	Fluoranthene	69	57
Pyrene	65	48	

bottle for 6 months. The presence of ethylhexyl phthalate was detected at a level of 0.6 ppb. The column and chromatographic conditions were as described under Experimental.

Water from a river near Urbino (Metauro) was analysed by GC-MS and the reconstructed ion chromatograms are shown in Fig. 2. In Fig. 2a the SIM programme was selected to detect the pesticides, phthalates and herbicides of interest. PAHs were detected in Fig. 2b by injecting another aliquot of the same sample with a suitable SIM programme. Pesticides were absent, as expected, but atrazine, phthalates and PAHs are present at ppb and ppt levels. The presence of atrazine is probably due to leaching from the nearby fields by rain water. A number of unknown peaks were detected that give a response to the m/z values in the programmes.

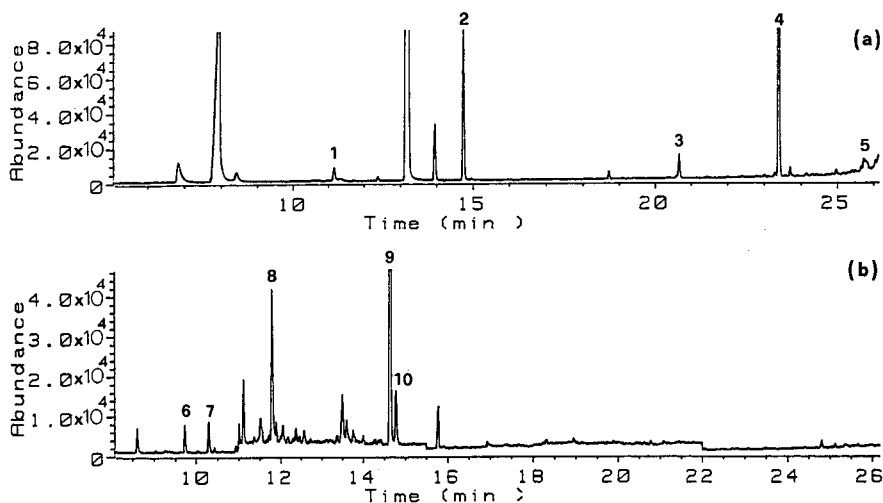


Fig. 2. Reconstructed ion chromatograms of 1 l of river water from near Urbino obtained by two injections of 2 μ l of the same light petroleum-toluene extract (1 ml) from a Carboxpack B cartridge. Chromatographic conditions: see text. (a) Pesticides, herbicides and phthalates; (b) PAHs. Concentrations (μ g/l): (1) atrazine, 0.60; (2) di-*n*-butyl phthalate, 1.40; (3) butylbenzyl phthalate, 0.60; (4) bis(2-ethylhexyl) phthalate, 4.30; (5) di-*n*-octyl phthalate, 0.30; (6) acenaphthylene, 0.01; (7) acenaphthene, 0.01; (8) fluorene, 0.05; (9) phenanthrene, 0.02; (10) anthracene, 0.02.

CONCLUSION

The extraction method presented here is very fast and allows quantitative recoveries (nearly 100%) of the compounds of interest. As a very low volume of eluent mixture is used, a high preconcentration ratio is reached (1:1000). Further, light petroleum can be eliminated in few minutes by flushing with nitrogen, so that the ratio can be as high as 1:2000. The cartridge can be reused and a large number of extractions per time unit can be carried out by a single operator. If GC-MS analysis with a quadrupole mass spectrometer is used, 10 ppt of the compounds of interest can be determined in water.

The limitations concerning the elution of the heavier PAHs can be overcome by using a graphitized carbon black with a much smaller surface area. This problem is currently under study in this laboratory.

ACKNOWLEDGEMENT

The authors thank E. Sisti for technical assistance.

REFERENCES

- 1 P. E. Strump, J. E. Wilkinson and P. W. Jones, in P. W. Jones and R. I. Frudenthal (Editors), *Carcinogenesis, Vol. 3, Polynuclear Aromatic Hydrocarbons*, Raven Press, New York, 1978, pp. 131-137.
- 2 L. K. Keith (Editor), *Advances in the Identification and Analysis of Organic Pollutants in Water*, Vol. 1, Ann Arbor Sci. Publ., Ann Arbor, MI, 1981, Section 5, pp. 293-355.
- 3 F. Uthe, J. Reinke and M. Gesser, *Environ. Lett.*, 3 (1972) 117.

- 4 M. Dressler, *J. Chromatogr.*, 165 (1979) 167.
- 5 B. Versino, H. Knöppel, M. de Groot, A. Peil, J. Poelman, H. Schauenburg, H. Vissers and F. Geiss, *J. Chromatogr.*, 122 (1976) 373.
- 6 J. F. Pankow, M. P. Ligocki, M. E. Rosen, L. M. Isabelle and K. M. Mart, *Anal. Chem.*, 60 (1987) 40.
- 7 S. Bitteur and R. Rosset, *Chromatographia*, 23 (1987) 163, and references cited therein.
- 8 A. Bacaloni, G. Goretti, A. Laganà, B. M. Petronio and M. Rotatori, *Anal. Chem.*, 52 (1980) 2033.
- 9 F. Mangani, G. Crescentini and F. Bruner, *Anal. Chem.*, 53 (1981) 1627.
- 10 R. L. Petty, *Anal. Chem.*, 53 (1981) 1548.
- 11 F. Mangani, G. Crescentini, F. Bruner and R. L. Petty, *Anal. Chem.*, 55 (1983) 793.
- 12 F. Mangani and F. Bruner, *Chromatographia*, 17 (1983) 377.
- 13 F. Bruner, G. Furlani and F. Mangani, *J. Chromatogr.*, 302 (1984) 167.
- 14 C. Borra, A. Di Corcia, M. Marchetti and R. Samperi, *Anal. Chem.*, 58 (1986) 2048.
- 15 A. W. Wolkoff and C. Creed, *J. Liq. Chromatogr.*, 4 (1981) 1459.
- 16 J. S. Andrews and T. J. Good, *Am. Lab.*, 4 (1982) 70.
- 17 E. Chaldek and R. S. Marano, *J. Chromatogr. Sci.*, 22 (1984) 313.
- 18 C. E. Rostad, W. E. Pereira and S. M. Ratcliff, *Anal. Chem.*, 56 (1984) 2856.
- 19 F. Bruner, P. Cicciooli, G. Crescentini and M. T. Pistolesi, *Anal. Chem.*, 45 (1973) 1851.
- 20 A. Di Corcia and A. Liberti, *Adv. Chromatogr.*, 14 (1976) 305.
- 21 G. Crescentini and F. Bruner, *Ann. Chim.*, 68 (1978) 343.
- 22 F. Mangani and F. Bruner, *J. Chromatogr.*, 289 (1984) 85.
- 23 A. M. Fabbri, F. Mangani, A. R. Mastrogiacomo, G. Crescentini and F. Bruner, *Chromatographia*, 23 (1987) 856.
- 24 F. Bruner, G. Bertoni and G. Crescentini, *J. Chromatogr.*, 167 (1978) 399.
- 25 F. Andreolini, A. di Corcia, A. Laganà and R. Samperi, *Clin. Chem.*, 29 (1983) 2076.
- 26 F. Andreolini, C. Borra, A. di Corcia and R. Samperi, *J. Chromatogr.*, 310 (1984) 208.
- 27 F. Mangani, A. Cappiello, G. Crescentini, F. Bruner and L. Bonfanti, *Anal. Chem.*, 59 (1987) 2066.

CHROM. 20 756

REVERSED-PHASE LIQUID CHROMATOGRAPHY OF ASTACENE

H. J. C. F. NELIS and A. P. DE LEENHEER*

Laboratoria voor Medische Biochemie en voor Klinische Analyse, Rijksuniversiteit Gent, Harelbekestraat 72, B-9000 Ghent (Belgium)

SUMMARY

Carotenoids can be efficiently separated by non-aqueous reversed-phase liquid chromatography on Zorbax ODS. However, astacene, an acidic ketocarotenoid was found to display a peculiar behaviour in that it could not be eluted from this support using mixtures of acetonitrile–methanol–dichloromethane. The importance of astacene as a degradation product of astaxanthin warranted the development of a new liquid chromatographic system. Organic acids promoted the elution of the compound, but failed to suppress the accompanying excessive peak tailing. Efficient chromatography resulted from the incorporation of bis(2-ethylhexyl) phosphate (BEHP), an acid with a high degree of lipophilicity, in the mobile phase. Optimum separation of astacene and astaxanthin was achieved using methanol-free, semi-aqueous eluents, *i.e.*, acetonitrile–water, containing 0.01–0.05 *M* BEHP. Increasing amounts of BEHP significantly reduced retention while, unexpectedly, water had little effect over the concentration range studied (1–5%). To illustrate the practical usefulness of the new system, astacene was demonstrated in a saponified extract of flower petals of *Adonis annua*.

INTRODUCTION

We have previously reported non-aqueous reversed-phase liquid chromatography (NARP) on Zorbax ODS for the separation of carotenoids¹. Typical eluents for these hydrophobic pigments contain acetonitrile as a base solvent, a non-polar modifier, usually dichloromethane, to adjust the elutropic strength and methanol to modulate the selectivity^{1,2}. Over the years this NARP system, with slight modifications, has formed the basis for the profiling and quantitation of carotenoids in a variety of biological materials, including *Artemia*³, orange juice⁴, serum⁵, bacteria⁶ and algae⁷.

• It was however soon recognized that under the standard chromatographic conditions the acidic ketocarotenoid astaxanthin failed to yield a symmetrical peak¹. This particular carotenoid is of considerable academic and practical interest because of its abundance in nature⁸ and its high economic value as a pigment in fish feeds⁹. Unlike astaxanthin, its close structural analogue astacene could not be eluted from Zorbax ODS using mixtures of acetonitrile–dichloromethane–methanol. Astacene is

readily formed as an artefact from astaxanthin or astaxanthin esters in the course of alkaline saponification¹⁰, an essential part of many isolation and analysis procedures for carotenoids. Therefore, a basic requirement of any chromatographic system for the determination of astaxanthin is its ability to include astacene and to separate both analogues.

Similar difficulties to obtain symmetrical peaks for ketocarotenoids possessing enolic hydroxyl groups are encountered in normal-phase chromatography. Derivatization, *e.g.*, acetylation of the acidic groups, is an obvious approach to suppress peak tailing¹¹. Recently, coating of the silica support with phosphoric acid has been proposed as another useful remedy¹². This can be carried out either *in situ* or by a slurry method prior to column packing. On such phosphoric acid-coated silica, astacene, semi-astacene, astaxanthin as well as three mono-*cis*-astaxanthins were readily resolved as perfectly symmetrical peaks.

We describe an alternative solution to the problem using reversed-phase chromatography with a mobile phase containing an organic, lipophilic phosphoric acid derivative. In general, reversed-phase is more attractive than normal-phase chromatography because it is more reproducible and less subject to variability.

EXPERIMENTAL

Chemicals

All-*trans*-astaxanthin and all-*trans*-astacene were gifts from Hoffmann-La Roche (Basle, Switzerland). Bis(2-ethylhexyl) phosphate (BEHP) was obtained from Fluka (Buchs, Switzerland). According to the manufacturer, the purity was approximately 50%, the remainder being mono(2-ethylhexyl) phosphate. Acetonitrile (Janssen Chimica, Beerse, Belgium), dichloromethane and methanol (both from Hoechst, Frankfurt, F.R.G.) were "chemically pure". The last two were redistilled in a spinning band apparatus. All other chemicals were reagent grade from Merck (Darmstadt, F.R.G.).

Chromatography

The HPLC system consisted of a Varian 5020 pump (Varian, Palo Alto, CA, U.S.A.), a Valco N60 valve injector (Valco, Houston, TX, U.S.A.) fitted with an 100- μ l loop, an HP 1040A multi-channel photodiode array detector, set at 470 nm and connected to an HP 9121 dual disc drive, an HP 7470A plotter (all from Hewlett-Packard, Palo Alto, CA, U.S.A.) and an SP 4100 integrator (Spectra-Physics, San Jose, CA, U.S.A.). The correct elution order of astacene and astaxanthin was verified on the basis of their absorption spectra. The columns (15 cm \times 0.46 cm I.D.) were packed with 5- μ m Zorbax ODS (DuPont, Wilmington, DE, U.S.A.) or 5- μ m Hypersil ODS (Shandon, Runcorn, U.K.). Elution was carried out with mixtures of acetonitrile-methanol-water-BEHP, the optimum mobile phase containing acetonitrile-water (97:3, v/v) and 0.05 M BEHP. The flow-rate was 1 ml/min and the temperature ambient.

Extraction of flower petals of Adonis annua

A few milligrams of flower petals of *Adonis annua* were homogenized with 3 ml of absolute ethanol in an all-glass Potter-Elvehjem tube. After addition of 0.8 ml of a

60% (w/v) aqueous potassium hydroxide solution, the mixture was saponified at 60°C for 45 min. A 3-ml volume of a 5% (w/v) sodium chloride solution was added and the carotenoids were extracted in 6 ml of diethyl ether. The organic layer was washed with water, dried over anhydrous sodium sulphate and evaporated to dryness under nitrogen. The residue was reconstituted with the chromatographic solvent and an 100- μ l aliquot was injected on the liquid chromatographic column.

RESULTS AND DISCUSSION

Chromatographic behaviour of astaxanthin and astacene in NARP

Despite their structural similarity (Fig. 1), the chromatographic behaviour of astaxanthin and astacene in NARP was thoroughly different. Using the standard eluent acetonitrile-methanol-dichloromethane, astaxanthin was mostly eluted as a badly tailing peak from new Zorbax ODS columns¹, whereas astacene did not chromatograph at all. Even a gradient to 100% dichloromethane failed to bring about elution. At first, silanophilic interactions were thought to account for the erratic chromatographic behaviour of astacene in particular. However, when Zorbax ODS, which is rich in accessible silanol groups, was replaced by Hypersil ODS, allegedly a totally endcapped material, the same phenomenon was still observed.

Effect of acids on the chromatography of astaxanthin and astacene

The addition of a small amount of formic acid to the standard eluent resulted in an astaxanthin peak with acceptable symmetry¹, although on certain batches of (used) Zorbax ODS columns efficient chromatography could also be achieved with acid-free eluents. On the contrary, although the presence of acid indeed induced the elution of astacene, the peak shape invariably remained extremely poor, both on Zorbax ODS (not shown) and Hypersil ODS (Fig. 2A). Some mineral acids were excluded for practical reasons: phosphoric acid caused a progressive (reversible) de-

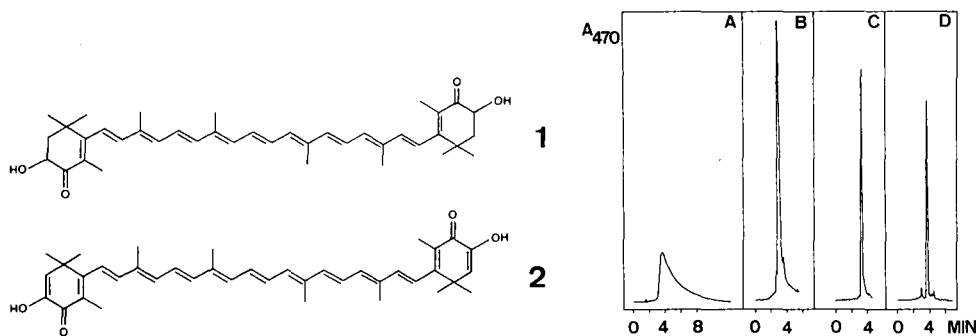


Fig. 1. Structural formulae of astaxanthin (1) and astacene (2).

Fig. 2. Chromatographic behaviour of astacene on a 5- μ m Hypersil ODS column (15 cm \times 0.46 cm I.D.) (A-C) and a 5- μ m Zorbax ODS column (15 cm \times 0.46 cm I.D.) (D) in various eluents: A, acetonitrile-methanol-dichloromethane (60:20:20, v/v/v) containing 0.2% formic acid; B, acetonitrile-methanol (80:20, v/v), containing 0.01 M BEHP; C, acetonitrile-methanol-water (79:20:1, v/v/v), containing 0.01 M BEHP; D, as C but Zorbax ODS instead of Hypersil ODS column. The flow-rate was 1 ml/min.

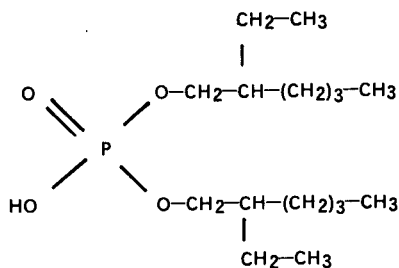


Fig. 3. Structural formula of bis(2-ethylhexyl) phosphate.

crease in column permeability, whereas sulphuric acid heavily promoted on-column carotenoid degradation. BEHP, structurally an organic phosphoric acid derivative (Fig. 3), proved to be a suitable agent to suppress peak tailing and to enhance the overall efficiency. The rationale for using this uncommon additive was the relatively strong acidity of the compound (pK_a 3.22) combined with an high degree of lipophilicity. These properties have previously underlied its use as a counter ion in ion-pair extraction of basic compounds¹³. A concentration of 0.01 *M* BEHP in an acetonitrile-methanol mixture led to a dramatic improvement of the astacene peak shape, both on Hypersil ODS (Fig. 2B) and Zorbax ODS. At the same time, however, BEHP significantly reduced the retention, which necessitated the addition of a small amount of water to neutralize this effect. Surprisingly, this further improved the peak symmetry (Fig. 2C, D). At this point, the term "NARP" is no longer applicable.

Separation of astacene from astaxanthin

For many carotenoids, the presence of methanol in a NARP eluent favourably affects resolution^{1,2}. However, in the present system it was precisely methanol which counteracted the separation of astacene from astaxanthin. The effect of the incorporation of increasing amounts of methanol in the mobile phase is illustrated in Fig. 4. A methanol-free eluent yielded near-baseline separation (Fig. 4A). The addition of 20% methanol largely nullified this resolution and the elution order was reversed (Fig. 4B). Upon incorporation of an higher methanol content in the eluent this re-

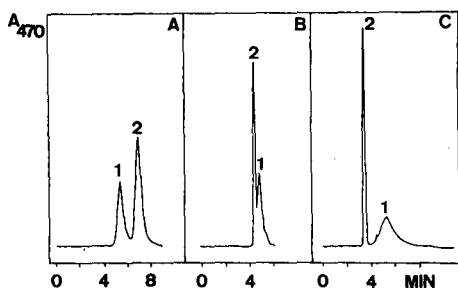


Fig. 4. Separation of astacene (1) and astaxanthin (2) on a 5- μ m Zorbax ODS column (15 cm \times 0.46 cm), eluted with different solvent mixtures: A, acetonitrile-water (98:2, v/v/v), containing 0.01 *M* BEHP; B, acetonitrile-methanol-water (78:20:2, v/v/v) containing 0.01 *M* BEHP; C, acetonitrile-methanol-water (48:50:2, v/v/v), containing 0.01 *M* BEHP. The flow-rate was 1 ml/min.

versed elution order was maintained, but astacene was no longer eluted as a symmetrical peak (Fig. 4C). A mobile phase consisting of methanol-water and 0.01 *M* BEHP still yielded a perfect astaxanthin peak, but astacene now appeared as a broad plateau. Therefore, the definitive eluent contained no methanol but only acetonitrile, water and BEHP.

Effect of eluent parameters on the retention of astaxanthin and astacene

The capacity factors, k' , of both astacene and astaxanthin were inversely related to the concentration of BEHP in the mobile phase (Table I). Unlike this pronounced effect of BEHP, the water content of the eluent influenced the retention only marginally over the concentration range studied (1–5%) (Table II), which is highly surprising considering the lipophilicity of carotenoids. It contrasts indeed with earlier observations in NARP of other non-polar compounds, in which even a minimum amount of water led to a marked deterioration of the chromatographic performance¹⁴.

Reproducibility

The results presented in Tables I and II were produced with a time interval of 2 months. It is seen that the k' values obtained with a given eluent (0.05 *M* BEHP in

TABLE I

EFFECT OF THE CONTENT OF BEHP (IN ACETONITRILE-WATER, 98:2, v/v) ON THE RETENTION OF ASTAXANTHIN AND ASTACENE

Concentration of BEHP (<i>M</i>)	k' (astaxanthin)	k' (astacene)
0.005	7.9	5.8
0.01	5.5	3.4
0.025	3.0	2.0
0.05	1.7*	1.2*
0.1	1.4	0.8

* Compare with the values in Table II.

TABLE II

EFFECT OF THE WATER CONTENT IN AN ELUENT CONSISTING OF ACETONITRILE AND 0.05 *M* BEHP (REFERRED TO THE TOTAL VOLUME) ON THE RETENTION OF ASTAXANTHIN AND ASTACENE

Concentration of water (%, v/v)	k' (astaxanthin)	k' (astacene)
1	2.3	1.6
2	2.4*	1.7*
3	2.7	2.1
4	3.1	2.5
5	3.3	2.7

* Compare with the values in Table I.

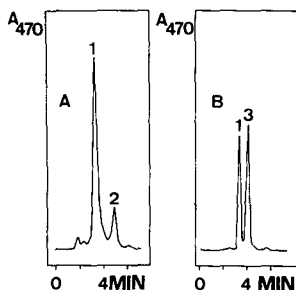


Fig. 5. (A) Chromatogram of a saponified extract of *Adonis annua* flower petals and (B) chromatogram of synthetic astacene and astaxanthin. Column: 5- μ m Zorbax ODS (15 cm \times 0.46 cm I.D.). Eluent: acetonitrile-water (97:3, v/v) containing 0.05 M BEHP; flow-rate, 1 ml/min. Peaks: 1 = astacene; 2 = unidentified; 3 = astaxanthin.

acetonitrile-water, 98:2, v/v) are different (*cf.*, the values marked with asterisks). It is significant in this respect that after this 2-month interruption the baseline separation from Fig. 4A could not at first be entirely reproduced. However, after flushing the column with dichloromethane to remove any adsorbed non-polar substances and prolonged equilibration with the mobile phase, the resolution progressively improved again.

Application

The present liquid chromatographic system could easily form the basis of analytical methods to determine astacene in a variety of organisms containing astaxanthin or astaxanthin esters. These include aquatic animals, *e.g.*, Crustacea^{8,15}, the fungus *Phaffia rhodozyma*¹⁶, a bacterium¹⁷, feathers of birds¹⁸, algae^{19,20} and the flower petals of *Adonis annua*²¹. During saponification of total lipid extracts under aerobic conditions, astaxanthin is readily converted into astacene¹⁰. To illustrate the practical usefulness of the system, astacene was demonstrated in saponified extracts of flower petals of *Adonis annua* (Fig. 5A). No trace of astaxanthin was detected. The major peak in the chromatogram was eluted in the same position as synthetic astacene (Fig. 5A and B). Confirmation of the peak identity was obtained from the corresponding absorption spectrum recorded with the photodiode array detector. As shown in Fig. 6 the spectrum did not however entirely coincide with that of synthetic astacene. The slight hypsochromic shift of the main maximum and the enhanced

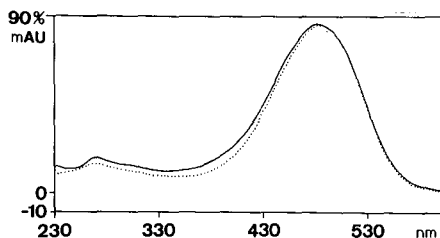


Fig. 6. Absorption spectra of peak 1 in Fig. 5A (—) and of synthetic astacene (---).

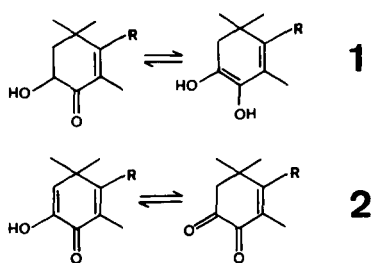


Fig. 7. Tautomeric forms of astaxanthin (1) and astacene (2).

absorption in the “*cis* peak” region suggest the presence of co-eluting *cis*-isomers of astacene²², obviously formed at the elevated temperature of the saponification. The impurity of the chromatographic peak was also indicated by its composite appearance.

CONCLUSION

To the best of our knowledge, this report presents the first example of a reversed-phase separation of astacene and astaxanthin. The different chromatographic behaviour of these compounds under various conditions, *i.e.*, in the NARP standard eluent and in the presence of BEHP–methanol, is hard to rationalize, but may be linked to the existence of different tautomeric forms (Fig. 7) and, consequently, different degrees of acidity.

ACKNOWLEDGEMENTS

This work was supported by FGWO contract 3.0048.86. H. J. C. F. N. acknowledges financial support (permanent position of Research Associate) from the Belgian Foundation for Scientific Research (N.F.W.O.).

REFERENCES

- 1 H. J. C. F. Nelis and A. P. De Leenheer, *Anal. Chem.*, 55 (1983) 270.
- 2 H. J. C. F. Nelis, M. M. Z. Van Steenberge, M. F. Lefevere and A. P. De Leenheer, *J. Chromatogr.*, 353 (1986) 295.
- 3 H. J. C. F. Nelis, P. Lavens, L. Moens, P. Sorgeloos, J. A. Jonckheere, G. R. Criel and A. P. De Leenheer, *J. Biol. Chem.*, 259 (1984) 6063.
- 4 J. F. Fisher and R. L. Rouseff, *J. Agric. Food Chem.*, 34 (1986) 985.
- 5 J. G. Bieri, E. D. Brown and J. C. Smith, *J. Liq. Chromatogr.*, 8 (1985) 473.
- 6 H. J. C. F. Nelis and A. P. De Leenheer, *Abstracts 8th Int. Symp. on Carotenoids, Boston, MA, July 27–31, 1987*, p. 9.
- 7 H. J. Nelis and A. P. De Leenheer, *Abstracts 10th Int. Symp. Microchem. Techn., Antwerp, August 25–29, 1986*, p. 133.
- 8 T. W. Goodwin, *The Biochemistry of the Carotenoids*, Vol. II, *Animals*, Chapman and Hall, London, 2nd ed., 1984.
- 9 K. L. Simpson, T. Katayama and C. O. Chichester, in J. C. Bauernfeind (Editor), *Carotenoids as Colorants and Vitamin A Precursors*, Academic Press, New York, 1981, Ch. 4, p. 463.
- 10 S. Liaaen-Jensen, in O. Isler (Editor), *Carotenoids*, Birkhäuser, Basel, Switzerland, 1971, p. 88.
- 11 G. Englert and M. Vecchi, *Helv. Chim. Acta*, 63 (1980) 1711.

- 12 M. Vecchi, E. Glinz, V. Meduna and K. Schiedt, *J. High Resolut. Chromatogr. Chromatogr. Commun.*, 10 (1987) 348.
- 13 G. Hoogewijs and D. L. Massart, *Anal. Chim. Acta*, 106 (1979) 271.
- 14 M. F. Lefevere, *Ph.D. Thesis*, Gent, 1983.
- 15 R. Castillo, G. Nègre-Sadargues and R. Lenel, in G. Britton and T. W. Goodwin (Editors), *Carotenoid Chemistry and Biochemistry*, Pergamon, Oxford, 1982, p. 211.
- 16 A. G. Andrewes, H. J. Phaff and M. P. Starr, *Phytochemistry*, 15 (1976) 1003.
- 17 H. Iizuka and Y. Nishimura, *J. Gen. Appl. Microbiol.*, 15 (1969) 127.
- 18 A. H. Brush, in J. C. Bauernfeind (Editor), *Carotenoids as Food Colorants and Vitamin A Precursors*, Academic Press, New York, 1981, Ch. 5, p. 539.
- 19 F.-C. Czygan, *Arch. Mikrobiol.*, 61 (1968) 81.
- 20 F.-C. Czygan, *Arch. Mikrobiol.*, 62 (1968) 209.
- 21 A. Seybold and T. W. Goodwin, *Nature (London)*, 184 (1959) 1714.
- 22 L. Zechmeister, *Cis-Trans Isomeric Carotenoids, Vitamins A and Arylpolyenes*, Springer, Vienna, 1962, p. 25.

Note

Potential application of thin-layer chromatography and thin-layer chromatography with flame ionization detection of cholestanol in the diagnosis of cerebrotendinous xanthomatosis

ČESTMÍR MICHALEC*

Laboratory of Protein Metabolism, Charles University Medical Faculty, 128 53 Prague (Czechoslovakia)
and

MOJMÍR RANNÝ

Research Institute of Fat Industry, Department of Organic Technology, Institute of Chemical Technology, 160 00 Prague (Czechoslovakia)

Cerebrotendinous xanthomatosis (CTX) is a rare familial sterol storage disease which results from a block in bile acid synthesis and is characterized by the accumulation of cholestanol (5α -cholestan- 3β -ol) in blood and tissues¹, particularly in the tendons and the nerve tissues. On the other hand, the concentration of cholesterol (5α -cholesten- 3β -ol) in the serum of CTX patients is usually normal or even lower than that in healthy subjects. A definite diagnosis of this disease could be made after the determination of serum cholestanol concentration. However, the amount of cholestanol in serum is much lower than that of cholesterol and, accordingly, the determination of cholestanol is difficult owing to the similarity of the molecular structures of the two compounds.

Several gas-liquid chromatographic (GLC) methods for the determination of cholestanol in serum have been reported^{2–6}. It seems that the GLC of cholestanol is not completely suitable for screening for CTX owing to an inability to analyse many samples in a limited time. Matsuoka *et al.*⁷ reported the use of high-performance liquid chromatography (HPLC) with fluorimetric detection. Recently, Iwata *et al.*⁸ described a highly sensitive HPLC method for the determination of cholesterol and cholestanol in human serum after conversion into fluorescent carbamic esters by treatment with 3,4-dihydro-6,7-dimethoxy-4-methyl-3-oxoquinoline-2-carbonyl azide.

Thin-layer chromatography (TLC) has rarely been used; *e.g.*, Kasama and Seyama⁹ developed a quantitative procedure for the determination of cholestanol in serum involving reversed-phase TLC after conversion of cholesterol to epoxides with 3-chloroperbenzoic acid. To the best of our knowledge, TLC with flame ionization detection (TLC-FID) has not previously been used.

This paper presents an improved TLC and HPTLC method and reports the use of the TLC-FID technique for the detection and determination of cholestanol in human serum.

EXPERIMENTAL

Sample preparation

A 1-ml volume of human serum was saponified with 9 ml of 1 *M* potassium hydroxide solution in 90% methanol for 30 min at 100°C. After cooling, 5 ml of water and 20 ml of *n*-hexane were added and the mixture was agitated vigorously for 2 min in a separating funnel. The upper phase was transferred into a 50-ml vessel. The lower phase was extracted twice with 20 ml of *n*-hexane. The combined upper phases were evaporated to dryness under a stream of nitrogen in a glass test-tube. The residue was dissolved in 1 ml of chloroform.

Oxidation of cholesterol with peracetic acid

A 0.5-ml volume of the chloroform extract solution was evaporated to dryness under a stream of nitrogen in a glass test-tube. To the residue 2.5 ml of 3.5% peracetic acid in methanol were added and, after thorough agitation, the reaction mixture was left for 4 h at 37°C. Subsequently, 5 ml of 2% sodium hydrogensulphite solution and 0.25 ml of 10 *M* potassium hydroxide solution were added. The oxidized sample was extracted three times with 5 ml of *n*-hexane. The hexane phases were filtered and evaporated to dryness and the residue was dissolved in 0.5 ml of chloroform.

Thin-layer chromatography

Silufol sheets (10 × 10 cm) (Kavalier Glassworks, Votice, Czechoslovakia) or silica gel 60 HPTLC plates (10 × 10 cm) (Merck, Darmstadt, F.R.G.) were used. Chromatography was carried out in *n*-heptane–ethyl acetate (60:40). The spots were located by spraying the chromatogram with a 5% solution of phosphomolybdic acid in 2-propanol or 50% sulphuric acid.

The blue spots after the reaction with phosphomolybdic acid were measured by densitometry using an ERI 10 apparatus (Zeiss, Jena, G.D.R.).

Thin-layer chromatography with flame ionization detection

An Iatroscan TH 10 Analyser Mark IV connected with a Philips PV 4850 Video Chromatography Control Centre computing system was used. The samples (1 μl of a 2% solution in chloroform) were applied on Chromarods S III (Iatron Laboratories, Tokyo, Japan) and separated by two subsequent elutions [8 min with *n*-pentane–ethyl acetate (50:50) and 30 min with *n*-pentane–ethyl acetate (90:10)]. After drying at 60–65°C, the rods were scanned in the flame ionization detector.

RESULTS AND DISCUSSION

A typical scheme for the separation of cholestanol and the oxidation products of cholesterol is given in Fig. 1 and 2.

Under above-described reaction conditions, the oxidation of cholesterol with peracetic acid proceeded quantitatively and cholestanol was not affected. We compared the oxidation reactions with 3-chloroperbenzoic and peracetic acid and the results obtained were found to be nearly identical.

Kasama and Seyama⁹ reported that on reversed-phase TLC the linearity of the coloration of cholestanol using phosphomolybdic acid was satisfactory in the

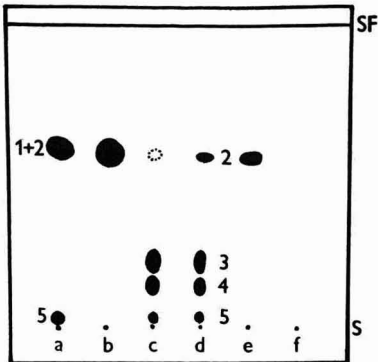


Fig. 1. TLC on Silufol sheets with *n*-hexane-ethyl acetate (60:40). (a) Standard mixture of cholesterol (1), cholestanol (2) and $3\beta,5\alpha,6\beta$ -cholestantriol (5); (b) extract of hydrolysed human serum; (c) oxidized extract of hydrolysed human serum (normal); (d) oxidized extract of hydrolysed human serum (patient with CTX) showing cholesterol epoxides, (3) and (4); (e) cholestanol standard; (f) blank extract of the reaction mixture. Detection with phosphomolybdic acid.

range 100–1000 ng when measuring with a TLC scanning densitometer at a wavelength of 630 nm. Using the same experimental conditions, we could not obtain satisfactory results. Nevertheless, in accordance with Kasama and Seyama, we can

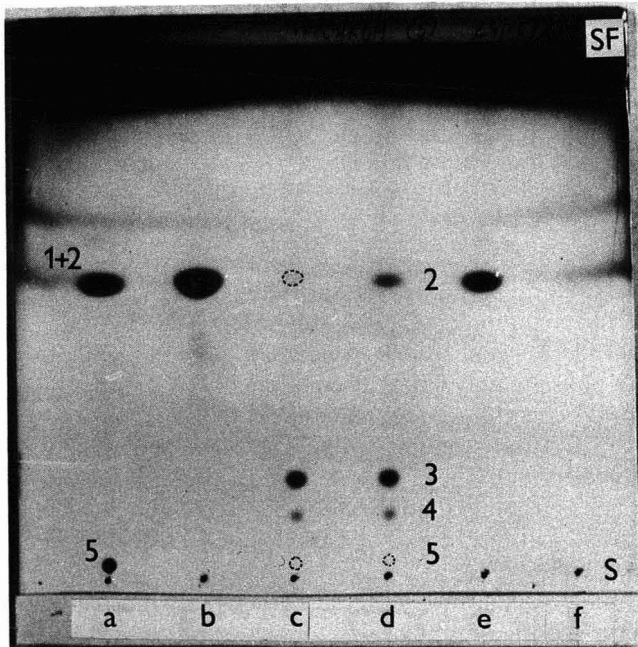


Fig. 2. HPTLC on silica gel 60 (Merck) plates with *n*-hexane-ethyl acetate (60:40). (a) Standard mixture of cholesterol (1), cholestanol (2) and $3\beta,5\alpha,6\beta$ -cholestantriol (5); (b) extract of hydrolysed human serum; (c) oxidized extract of hydrolysed human serum (normal); (d) oxidized extract of hydrolysed human serum (patient with CTX) showing cholesterol epoxides, (3) and (4); (e) cholestanol standard; (f) blank extract of the reaction mixture. Detection with 50% sulphuric acid.

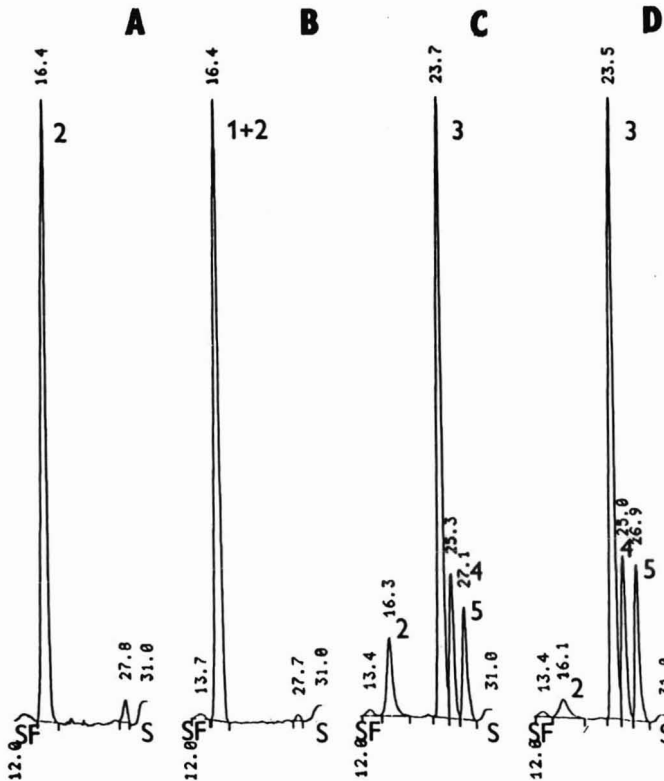


Fig. 3. TLC-FID on Chromarods S III. (A) Cholesterol standard; (B) extract of hydrolysed human serum; (C) oxidized extract of hydrolysed human serum (patient with CTX); (D) oxidized extract of hydrolysed human serum (normal). 1 = Cholesterol; 2 = cholestanol; 3-5 = products of oxidation of cholesterol.

confirm that the slope of the calibration graph varies with different plates and depends strongly on the colouring conditions.

Our results suggest that the densitometric determination of cholestanol in the TLC zone after reaction with phosphomolybdic acid can serve only as a semi-quantitative indicator of an increased concentration of cholestanol in serum.

We have found that TLC-FID is a time-saving and suitable quantitative screening method for serum cholestanol. The use of a new kind of thin layer (Chromarods S III) gives a better reproducibility than the older S II type. The separation of the cholesterol-cholestanol peak from the oxidized products is satisfactory (Fig. 3).

Further investigations on the application of these methods to biological samples are in progress and will be reported in the near future.

REFERENCES

- 1 M. Phillipart and L. van Bogaert, *Arch. Neurol.*, 21 (1969) 603.
- 2 G. Salen, *Ann. Intern. Med.*, 75 (1971) 843.

- 3 Y. Seyama, K. Ichikawa and T. Yamakawa, *J. Biochem. (Tokyo)*, 80 (1976) 223.
- 4 S. Serizawa, Y. Seyama, H. Otsuka, T. Kasama and T. Yamakawa, *J. Biochem. (Tokyo)*, 90 (1981) 17.
- 5 T. T. Yshikawa, J. B. Brazier, L. E. Stewart, R. W. Fallat and C. J. Gleuck, *J. Lab. Clin. Med.*, 87 (1976) 345.
- 6 B. J. Koopman, J. C. van der Molen, B. G. Wolthers, A. E. J. de Jager, R. J. Waterreus and C. H. Gips, *Clin. Chim. Acta*, 137 (1984) 305.
- 7 C. Matsuoka, H. Nohta, N. Kuroda and Y. Ohkura, *J. Chromatogr.*, 341 (1985) 432.
- 8 T. Iwata, M. Yamaguchi and M. Nakamura, *J. Chromatogr.*, 421 (1987) 43.
- 9 T. Kasama and Y. Seyama, *J. Biochem. (Tokyo)*, 99 (1986) 771.

CHROM. 20 525

RETENTION IN SEDIMENTATION–FLOTATION FOCUSING FIELD-FLOW FRACTIONATION USING A STEP DENSITY GRADIENT

JOSEF JANČA* and NADĚŽDA NOVÁKOVÁ

Institute of Analytical Chemistry, Czechoslovak Academy of Sciences, CS-611 42 Brno (Czechoslovakia)

SUMMARY

The previously developed method for the numerical calculation of the flow velocity profile formed in rectangular and trapezoidal cross-section channels when applying a step density gradient was used to calculate the positions of the boundaries between liquids of various density flowing in channels. The theoretical results are compared with experimental data obtained under various experimental conditions. Good agreement between the theoretical and experimental data was obtained, thus confirming the theoretical model used in the calculations and the reliability of the interpretation of the experimental retentions in terms of the densities of the fractionated solutes.

INTRODUCTION

Separation in sedimentation–flotation focusing field-flow fractionation (SFFFFF) is due to the differences in the densities of macromolecular or particulate solutes migrating through a density gradient in the direction of the external gravitational or centrifugal field forces and being focused at their isopycnic positions¹. The focused solute zones are carried by the liquid flowing along the separation channel in a direction perpendicular to the direction of the focusing forces. The shape of the cross-section of the channel determines the shape of the flow velocity profile formed in the flowing liquid under isoviscous laminar conditions. The effective separation of the focused solute zones can be achieved by choosing a suitable shape of the separation channel. Channels with modulated cross-sectional permeability were proposed in order to realize different shapes of the flow velocity profile². The usefulness of this concept was demonstrated when particles of density standards and various latexes were separated in a natural gravitational field³.

A discontinuous density gradient can be pre-formed inside the separation channel for SFFFFF. A step density gradient is established provided that the liquids of different densities enter the separation channel via the individual inflow capillaries under conditions of laminar flow⁴. The form of the separation channel cross-section affects the flow velocity pattern inside.

A method for the numerical calculation of the flow velocity distributions formed in rectangular and trapezoidal cross-section channels under the conditions

of a step density gradient was developed recently⁵. It can be used if the liquids of different viscosities forming the step density gradient are applied in SFFFFF. Several typical examples of the flow velocity profiles were calculated for various conditions simulating real experiments⁵.

The shape of the flow velocity profile and the position of the boundaries between the liquids of different viscosity should be known for the quantitative evaluation of the experimental retention data.

The retention ratio, R is defined as

$$R = v_R / \langle v \rangle \quad (1)$$

where v_R is the average linear velocity of the longitudinal migration of the focused zone of the solute carried by flow and $\langle v \rangle$ is the average linear longitudinal velocity of the flow of the bulk liquid inside the channel.

General theoretical relationships describing the retention and dispersion in focusing FFF for various cross-section channels (rectangular, trapezoidal and parabolic) were derived previously⁶. The theory assumed a constant gradient of focusing forces in the region of the focused zone and isoviscous flow conditions.

If several liquids of different densities are used to form the step density gradient inside the channel, the flow velocity profile reflects the differences in the viscosities of individual liquid layers and the gradient of focusing forces also has a more complicated shape. This has to be taken into account if the retention ratio measured experimentally for a given solute is considered as a fundamental parameter from which the density of the fractionated sample is to be evaluated.

The aim of this work was to verify experimentally the previously developed method for the numerical calculation of the flow velocity profile⁵ and to establish the reliability of the interpretation of the experimental retention ratios in terms of the densities of the fractionated solutes. In order to avoid mathematical difficulties in data treatment, simplified model experimental conditions were designed. However, the experimental conditions were chosen in such a way that the resulting conclusions would be generally valid.

THEORY

Focusing forces

The force acting on the solute particles or macromolecules undergoing focusing by sedimentation–flotation processes is coordinate dependent:

$$F(\varphi) = Vg(d\rho/d\varphi)(\varphi_{\max} - \varphi) \quad (2)$$

where V is the molar volume of the solute species, $d\rho/d\varphi$ is the density gradient, g is the gravitational or centrifugal acceleration, φ is the dimensionless coordinate in the direction of the focusing forces and φ_{\max} is the coordinate of the maximum concentration of the zone, *i.e.*, the focusing point for which $F(\varphi_{\max}) = 0$. The coordinate system used in this paper is shown in Fig. 1 for both rectangular and trapezoidal cross-section channels. At equilibrium the flux of the solute due to focusing forces is just balanced by the flux due to the diffusion in the direction of the φ axis:

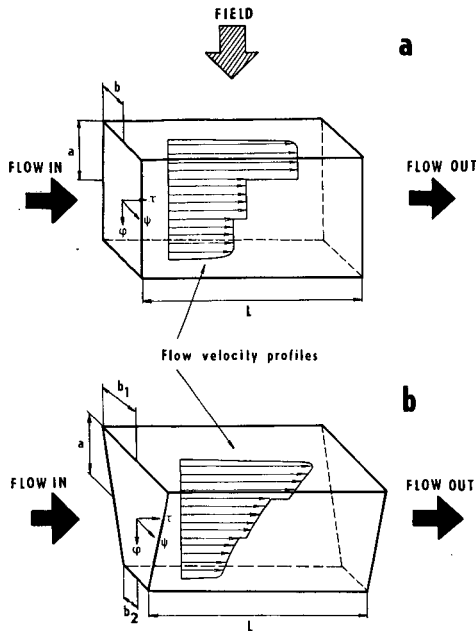


Fig. 1. Schematic representation of (a) rectangular and (b) trapezoidal cross-section channels with flow velocity profiles formed under step density gradient conditions with defined coordinate system.

$$D(dc/d\varphi) = u(\varphi)c \quad (3)$$

where D is the diffusion coefficient and c is concentration. The velocity of solute migration under the influence of the focusing forces, $u(\varphi)$, is given by

$$u(\varphi) = F(\varphi)/f \quad (4)$$

and the friction coefficient f is defined by

$$f = R^0T/D \quad (5)$$

R^0 being the universal gas constant and T the absolute temperature. The gaussian distribution for the focused zone of the solute along the φ axis is obtained by substituting from eqns. 2, 4 and 5 in eqn. 3 and solving the first-order differential eqn. 3:

$$c(\varphi) = c(\varphi_{\max}) \exp[-Vg(d\rho/d\varphi)(\varphi - \varphi_{\max})^2/2R^0T] \quad (6)$$

The first simplifying condition based on eqn. 6 can be formulated. The average velocity of movement of the focused zone due to the longitudinal flow can be approximated by the streamline velocity at the position of maximum concentration in the focused zone, φ_{\max} . This approximation holds for narrowly focused solute zones.

Shape of the flow velocity profile

The most practical shapes of the flow velocity profiles are those formed in the fluid flowing inside the rectangular or trapezoidal cross-section channels under laminar and isoviscous flow conditions. The distribution of the flow velocities is influenced by non-isoviscous flow if a continuous or a step density gradient is applied. The relationship describing the mean flow velocity of the liquid averaged across the rectangular or trapezoidal cross-section channel thickness, $\bar{v}(\varphi)$, normalized relative to the velocity in the centre line $\varphi = 0$) of the channel, has been derived²:

$$\bar{v}(\varphi) = \frac{b^2(\varphi)L}{b^2(0)l(\varphi)} \left\{ \frac{1 - \frac{\cosh[\sqrt{3} A(\varphi)\varphi]}{\cosh[\sqrt{3} A(\varphi)]}}{1 - \frac{1}{\cosh[\sqrt{3} A(0)]}} \right\} \quad (7)$$

where $b(\varphi)$ is a φ coordinate-dependent half-thickness of the channel (see Fig. 1), $A = a/b(\varphi)$ is an aspect ratio (see Fig. 1), L is the length of the flow streamline at the centre line of the channel and $l(\varphi)$ is the length of the flow streamline at the given coordinate φ . The actual shape of the flow velocity profile can be calculated using eqn. 7 for given geometric dimensions of the fractionation channel and for isoviscous conditions of the flow.

When a discontinuous (*i.e.*, step) density gradient is applied, a numerical method has to be used to calculate the shape of the flow velocity profile and the positions of the boundaries between the individual liquid layers of different densities and viscosities. The method of numerical calculation, described in detail in a previous paper⁵, is based on the mass balance equations. For example, the total volumetric flow-rate q of three liquids of different densities and viscosities is the sum of the flow-rates of the individual liquids:

$$q = q_1 + q_2 + q_3 \quad (8)$$

For non-isoviscous conditions a series of equations have been derived⁵:

$$\frac{\mu_1 q_1}{\mu_2 q_2} = \frac{\sum_{j=1}^{m'} \frac{b_{1j}^3}{l_{1j}}}{\sum_{j=m'}^{n'} \frac{b_{2j}^3}{l_{2j}}} \quad (9a)$$

$$\frac{\mu_1 q_1}{\mu_3 q_3} = \frac{\sum_{j=1}^{m'} \frac{b_{1j}^3}{l_{1j}}}{\sum_{j=n'}^{o'} \frac{b_{3j}^3}{l_{3j}}} \quad (9b)$$

$$\frac{\mu_2 q_2}{\mu_3 q_3} = \frac{\sum_{j=m'}^{n'} \frac{b_{2j}^3}{l_{2j}}}{\sum_{j=n'}^{o'} \frac{b_{3j}^3}{l_{3j}}} \quad (9c)$$

The left-hand sides of eqns. 9a–c are known and can be designated LHS_{12} , LHS_{13} and LHS_{23} , respectively. Correspondingly, the summation terms on the right-hand sides can be designated S_1 , S_2 and S_3 , respectively, and rewritten

$$LHS_{12} = S_1/S_2 \quad (10a)$$

$$LHS_{13} = S_1/S_3 \quad (10b)$$

$$LHS_{23} = S_2/S_3 \quad (10c)$$

Further

$$S_1 + S_2 + S_3 = \sum_{j=1}^m \frac{b_{1j}^3}{l_{1j}} + \sum_{j=m}^n \frac{b_{2j}^3}{l_{2j}} + \sum_{j=n}^o \frac{b_{3j}^3}{l_{3j}} \quad (11)$$

The value of the right-hand side of eqn. 11, which describes the isoviscous flow conditions, is known. The numerical integration limits m , n and o have the meaning of the positions in φ coordinate of boundaries between different liquids but of identical viscosity. Consequently, eqns. 10a, 10b, 10c and 11 can be solved numerically to find S_1 , S_2 and S_3 and the required m' and n' values that determine the numerical integration limits satisfying the above system of eqns. 10a–11. The m' and n' integration limits in this instance have the meaning of the position in φ coordinate of the boundaries between the liquids of different viscosity. The linear velocities of the two liquid layers at their boundary can be calculated for known m' and n' positions from the corresponding flow-rates at these boundaries.

Retention

For the classical field-flow fractionation method, the retention ratio, R , as defined by eqn. 1, can acquire values between 1 and 0 for unretained and completely retained solutes, respectively. This is so in view of the fact that the solutes always are or are not retarded owing to retention, and can therefore never move by flowing at an average longitudinal velocity higher than the average velocity of the fluid flow.

The situation is completely different for focusing field-flow fractionation. Here the solutes can be focused at any lateral position inside the separation channel and, consequently, can move at linear longitudinal velocities higher than the average linear velocity of the liquid flow. In these instances, the retention ratio can acquire values higher than 1, according to both the established flow velocity profile and the position of the focused zone. The relationship describing the retention ratio for isoviscous liquid flow conditions was derived previously⁶ for a rectangular cross-section channel:

$$R = (3/2)(1 - \varphi_{\max}^2 - \sigma^2) \quad (12)$$

where σ is the standard deviation of the gaussian focused zone expressed as a fraction of the total width of the channel in the direction of coordinate φ , which means in

the direction of the focusing forces. Similarly, the relationship for a trapezoidal cross-section channel and isoviscous conditions was derived⁶:

$$R = \frac{3}{3 + \tan^2\alpha} \left[(1 + \varphi_{\max}\tan\alpha)^2 + 2\sigma^2\tan^2\alpha \right] \quad (13)$$

where α is the angle between the two opposite walls of the trapezoidal cross-section channel.

The calculation of the retention ratio for non-isoviscous flow under step density gradient conditions is more complicated. The focused zones should be so narrow in the direction of the focusing field that they will move longitudinally by the flow virtually in a single streamline. The position of the streamline is identical with a sharp boundary between the two liquids of various density and thereby various viscosity. If both diffusion and convection between the two liquids of various density are neglected, then the distribution of velocities in both rectangular and trapezoidal channels is stepwise, as illustrated schematically in Fig. 1. The linear velocity of the movement of the solute zone focused at the boundary between the layers of different densities averaged across the channel thickness, \bar{v}_R , will lie between the linear velocities of the streamlines adjoined from both sides to this boundary. The average linear velocity of the liquid in the channel, $\langle v \rangle$, normalized with respect to the centre, can be calculated numerically from the relationship

$$\langle v \rangle = \frac{\sum_{j=1}^{o'} v_j b_j \delta}{\sum_{j=1}^{o'} b_j \delta} \quad (14)$$

where δ is the increment of the distance between the streamlines. The retention ratio R can be calculated by substituting these linear velocities into eqn. 1. Despite a certain indefiniteness of the mean velocities of the focused zone movement at the boundary, \bar{v}_R , the retention ratios R can, with application of the step density gradient, acquire only discrete values. The determination of the position of the focused zone in the step density gradient from experimentally found R values and thereby the determination of the solute density are therefore obviously possible.

The experimental part of this work was aimed at the verification of the theoretical analysis presented above.

EXPERIMENTAL

Experimental verification of a mathematical model of flow and retention was performed by using a discontinuous density gradient and a gravitational force of 1 g acting on particles.

A rectangular channel was cut in Teflon foil, 0.84 mm thick, inserted between two glass plates, 3 mm thick and 40 × 400 mm. The channel itself had the dimensions 20 × 350 × 0.84 mm. The channel was equipped with three openings with capillaries for the inlet of density media and a fourth opening with a capillary served to let the media out from the channel. The trapezoidal channel was composed of a sandwich

of two Teflon foils with rubber in the middle that was inserted between the two glass plates, 3 mm thick and 40 × 400 mm. The channel itself, cut in the sandwich, was 350 mm long and 20 mm wide. The difference in the channel thickness between the upper and lower walls was approximately 0.27 mm. The channel was again equipped with openings for the inlet and outlet of the density media. The channels were clamped mechanically between two Perspex plates with a system of screws. A complete channel of this design is illustrated in Fig. 2.

An LD 2 linear displacement feeder (Development Workshops, Czechoslovak Academy of Sciences, Prague, Czechoslovakia) was used to pump simultaneously three solutions of various densities. It was equipped with three injection syringes whose pistons moved at the same linear velocity. The flow-rate of each density medium was determined by the diameter of the piston of the injection syringe used.

Solutions of sucrose (Lachema, Brno, Czechoslovakia) of various concentrations and Percoll solutions (Pharmacia, Uppsala, Sweden) diluted to the required concentrations were used as density media. Solutions of two densities were always prepared. Pure distilled water and 0.15 *M* sodium chloride solution were used as the topmost layers of the step density gradient in combination with sucrose and Percoll solutions, respectively. The concentrations of sucrose solutions were 6% and 14% (w/w). The 6% solution of sucrose was coloured with bromophenol blue so that the positions of individual boundaries of the density layers in the channel might be observed. The position of the boundary between the layers of different densities of Percoll solutions was determined with the aid of cross-linked dextran coloured density standards (Pharmacia). The densities of individual media were determined at a given temperature pycnometrically and the viscosities with an Ubbelohde viscometer. The heights of individual coloured density layers in the channel were read from millimetre paper fixed on the glass plate forming one of the channel walls. The measurements were performed at 22 or 23.5°C.

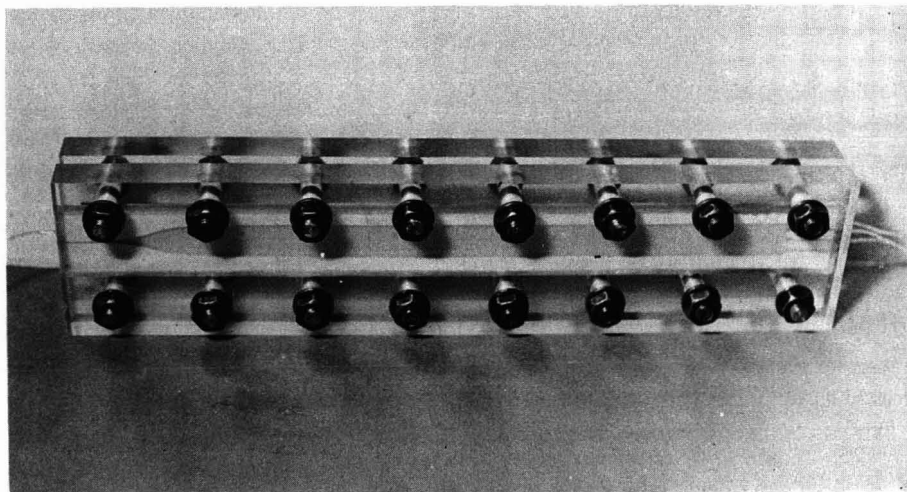


Fig. 2. Channel for SFFFFF using a step density gradient in a natural gravitational field.

RESULTS AND DISCUSSION

As foils or the sandwich could be pressed unequally during the assembly of the channels, the real thickness of the channels was checked by microscopic measurements. The real half-thicknesses of the rectangular channel cross-section were determined as $b_1 = 0.396$ and $b_2 = 0.405$ mm, and the half-thicknesses of the trapezoidal channel cross-section were $b_1 = 0.462$ mm and $b_2 = 0.595$ mm. These values were used in all the calculations.

Physico-chemical characteristics, *i.e.*, density and viscosity, of all the density media used are given in Table I.

Injection syringes used in the linear injector permitted the adjustment of certain discrete flow-rate ratios of the individual density media. The adjustment of the linear velocity of the movement of injection syringe pistons was continuous. In all the following experiments, the total flow-rate of all three density media in the channel and the ratio of the flow-rates of individual media from the highest density, *i.e.*, from the lowest layer, were known.

The initial experiments were designed to verify qualitatively the shape of the velocity profile formed in the channels of rectangular and trapezoidal cross-sections under isoviscous flow conditions. Distilled water was pumped through each channel only in the central inlet capillary (one of the three vertically arranged inlet capillaries). At a certain moment, water was replaced with bromophenol blue solution and the coloured zone formed in the channel indicated the shape of the velocity profile. The experiments were photographed. Fig. 3a, b and c illustrate various phases of the movement of the coloured zone in the channel of rectangular cross-section. The zone formed in this way is, in agreement with theoretical assumptions, axially symmetrical. The slight asymmetry in Fig. 3c is due to the fact that even a small difference between the densities of pure water and the dyestuff solution results in slow sedimentation of this solution. The finding that the asymmetry in the zone shape increased with time after the flow had been stopped confirmed the sedimentation of the dye solution. Fig. 4a, b and c show various phases of the movement of the coloured zone in the channel of trapezoidal cross-section. The zone formed is, in agreement with theory,

TABLE I

DENSITIES AND VISCOSITIES OF THE DENSITY MEDIA USED AT DIFFERENT TEMPERATURES

Density medium	Density (g/cm^3)		Viscosity ($mPa s$)	
	22°C	23.5°C	22°C	23.5°C
Water	0.9978	0.9974	0.960	0.927
0.15 M NaCl	1.0027	1.0016	1.031	0.928
6% sucrose (coloured)	1.0220	—	1.123	—
14% sucrose	1.0460	—	1.445	—
Percoll I	1.1023	1.1020	1.596	1.535
Percoll II	1.1223	1.1220	1.845	1.776

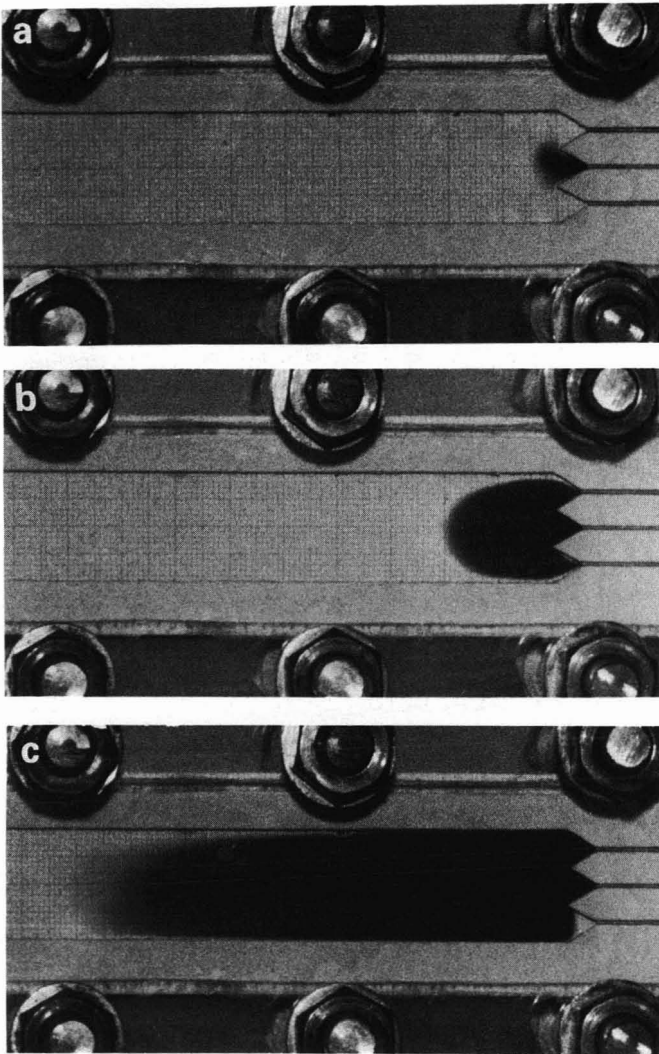


Fig. 3. Various phases of the movement of the coloured zone in a rectangular cross-section channel under isoviscous conditions.

axially asymmetrical, the most rapid streamlines being in the upper and wider section of the channel.

The aim of the following experiments was to determine the positions of the boundaries in both channels with the flow of liquids of different viscosities and at various flow-rate ratios and to compare the experimental values with the theoretical calculation. All the results obtained with the use of sucrose and Percoll solutions as density media in the channels of both rectangular and trapezoidal cross-sections are presented in Table II. For illustration, the formation of sharply separated layers of sucrose solutions in the channels of rectangular and trapezoidal cross-sections is

TABLE II
EXPERIMENTAL AND THEORETICAL POSITIONS OF THE BOUNDARIES BETWEEN THE LAYERS OF DIFFERENT DENSITY MEDIA FLOW-
ING IN CHANNELS OF RECTANGULAR AND TRAPEZOIDAL CROSS-SECTIONS UNDER VARIOUS CONDITIONS

Channel	Density medium	Temperature (°C)	Total flow- rate, q ($\mu\text{l}/\text{min}$)	Relative flow-rates, $q_1:q_2:q_3$	Relative positions of boundaries			
					Theory		Experiment	
					Lower	Higher	Lower	Higher
Rectangular	Sucrose solutions + water	22	1500	1:1:1	0.41	0.71	0.36	0.71
Rectangular	Sucrose solutions + water	22	1360	1.54:1.54:1	0.31	0.67	0.30	0.66
Trapezoidal	Sucrose solutions + water	22	1500	1:1:1	0.49	0.77	0.50	0.75
Trapezoidal	Sucrose solutions + water	22	488	1.54:1:1	0.43	0.69	0.45	0.77
Trapezoidal	Sucrose solutions + water	22	1360	1.54:1.54:1	0.39	0.73	0.40	0.70
Rectangular	Percoll solutions + 0.15 M NaCl	22	122	1.54:1:1	0.37	0.68	0.36	0.64
Trapezoidal	Percoll solutions + 0.15 M NaCl	23.5	122	1.54:1:1	0.46	0.75	0.47	0.70

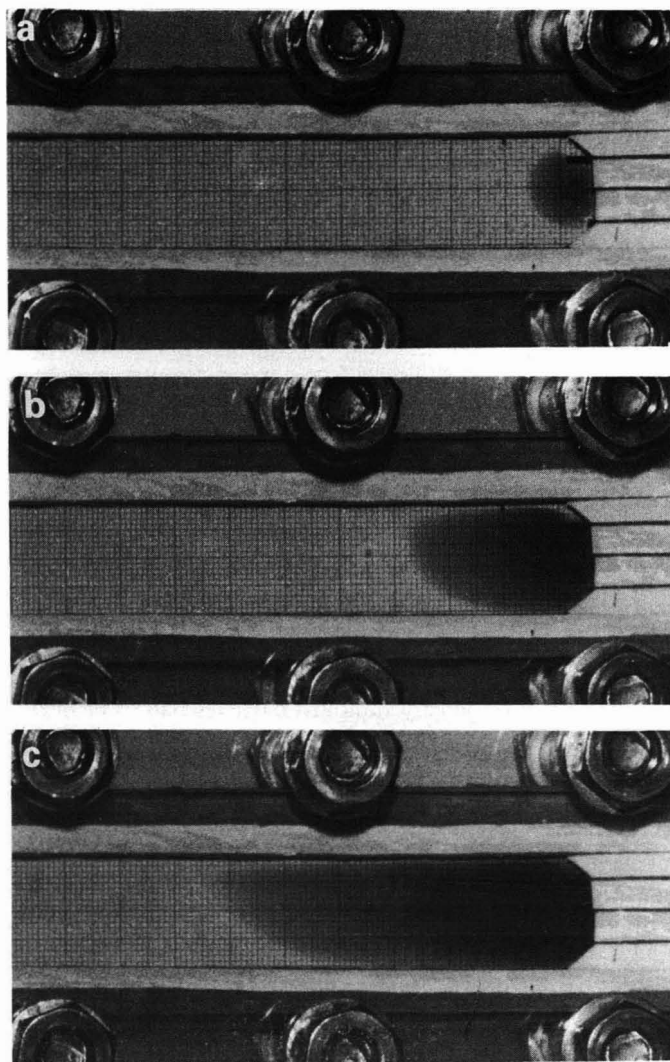


Fig. 4. Various phases of the movement of a coloured zone in a trapezoidal cross-section channel under isoviscous conditions.

shown in Figs. 5 and 6, respectively. In both instances the sucrose solution in the middle layer is coloured.

The relative position of the boundary was calculated as the ratio of the distance of this boundary from the lower channel wall to the total channel width in the vertical direction.

It follows from both the experimental results and the calculated boundary positions presented in Table II that very good agreement was obtained between the theoretical and experimental data in the channels of both types under various experimental conditions. The average deviation of the experiment from the theory,

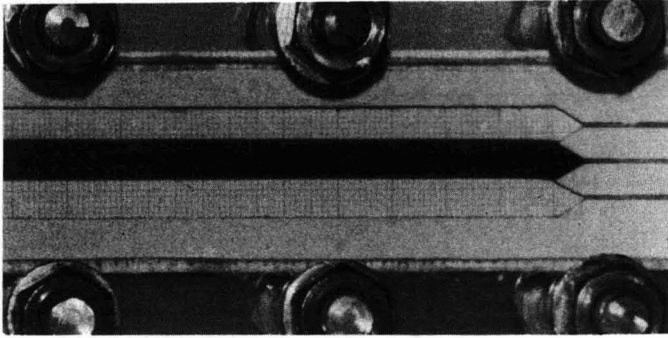


Fig. 5. Coloured layers of sucrose solutions of different density formed in a rectangular cross-section channel ($q = 1500 \mu\text{l}/\text{min}$; $q_1 : q_2 : q_3 = 1 : 1 : 1$).

calculated from all the experimental and theoretical data, is 4.4% relative. Most of the experimental data show, within the given range, a negative deviation from the theoretically calculated values of boundary positions. The deviation, probably systematic, cannot be explained.

Further experiments were carried out to verify whether the experimentally found retentions lie within the range of the theoretically calculated values. This task was made difficult by two factors. The first complication, of experimental character, was due to the fact that the movement of density standard particles had to be evaluated visually directly in the channel. The use of the photometric detector was prevented by the sedimentation of the density standard particles (the average particle size was in the range 100–200 μm) in the detector cell, which resulted in its plugging.

Particle movement was thus evaluated in such a manner that the relative axial position in the direction of the flow of the most rapid particles focused at one of the boundaries was measured with respect to the axial position in the direction of the flow of the most rapid particles focused at the other boundary. The ratio of these

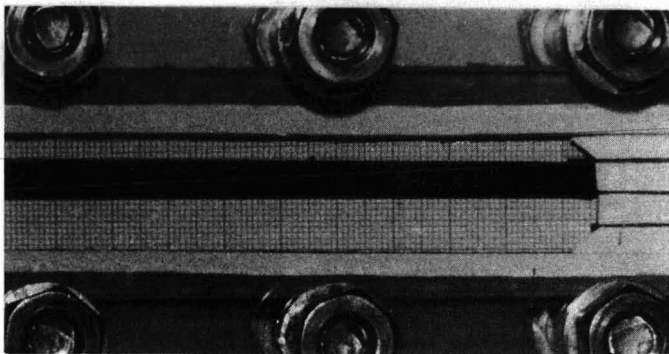


Fig. 6. Coloured layers of sucrose solutions of different density formed in a trapezoidal cross-section channel (flow-rates as in Fig. 5).

distances then specified the relative retention, $r_{1,2}$, defined for two solutes 1 and 2 by the relationship

$$r_{1,2} = R_1/R_2 \quad (15)$$

The second complication follows from the accepted simplification by which the velocity of the two streamlines adjoining the boundary changes stepwise. This transition will obviously be continuous. The particles of finite dimensions will reach the streamlines of various linear velocities. The real longitudinal velocity of the focused zones will therefore lie between the two extreme velocities at the boundary, as mentioned above. From the quantitative viewpoint, it is therefore expedient to establish whether the experimentally found relative retentions correspond to the relative retentions calculated theoretically from linear velocities lying in the middle of the interval at the boundary of the layers of various densities. The experimental and the theoretical results presented in Table III indicate the relative retentions of the both studied density standard particles. In agreement with theory, higher relative retentions were obtained by the fractionation in the trapezoidal cross-section channel than in the rectangular type. It is further obvious from the experimental values of the relative retentions that the relative velocity of the movement of the both focused zones is constant along the channel. Further experiments not shown in Table III also confirmed these findings. It will undoubtedly be possible to achieve a better agreement if analytical separations by SFFFFF are performed in a classical arrangement, *i.e.*, with the detector at the end of the separation system, thereby permitting the exact determination of the retention volumes of individual focused zones.

It can be concluded that this study has demonstrated good agreement between the experimental results and the theoretical calculations, particularly with regard to the position of the boundary between the layer of the liquids of various densities

TABLE III

RELATIVE RETENTIONS OF TWO SAMPLES OF DENSITY STANDARDS ($\rho_1 = 1.076 \text{ g/cm}^3$, $\rho_2 = 1.120 \text{ g/cm}^3$) IN PERCOLL ($q = 122 \text{ } \mu\text{l/min}$, 1.54 : 1 : 1, 22°C) FOUND EXPERIMENTALLY AND CALCULATED THEORETICALLY FOR CHANNELS OF RECTANGULAR AND TRAPEZOIDAL CROSS-SECTIONS

<i>Channel</i>	<i>Focussed zone</i>	<i>Position of the focused zone front in axial direction (mm), and relative retention</i>				
Rectangular	Upper	50	100	150	200	250
	Lower	48	93	140	187	231
	Relative retention	1.04	1.08	1.07	1.07	1.08
	Theoretical average relative retention	1.38				
Trapezoidal	Upper	50	100	150	200	250
	Lower	47	89	132	177	222
	Relative retention	1.06	1.12	1.14	1.13	1.13
	Theoretical average relative retention	1.63				

flowing through the channel in SFFFFF under conditions of the application of a step density gradient.

Subsequent studies will be aimed at the applications of SFFFFF using a step density gradient to smaller particles and to particles of different characters.

REFERENCES

- 1 J. Janča, *Makromol. Chem. Rapid Commun.*, 3 (1982) 887.
- 2 J. Janča and V. Jahnová, *J. Liq. Chromatogr.*, 6 (1983) 1559.
- 3 J. Chmelik and J. Janča, *J. Liq. Chromatogr.*, 9 (1986) 55.
- 4 J. Janča and N. Nováková, *J. Liq. Chromatogr.*, 10 (1987) 13.
- 5 J. Janča, *J. Chromatogr.*, 404 (1987) 23.
- 6 J. Janča and J. Chmelik, *Anal. Chem.*, 56 (1984) 2481.

CHROM. 20 419

HIGH-PERFORMANCE LIQUID CHROMATOGRAPHIC ANALYSIS OF THE ALKALOID SPECTRUM IN THE ROOTS AND CAPSULES OF THE SPECIES AND HYBRIDS OF *PAPAVER* SECTION *OXYTONA*

JUDITH MILO, ARIEH LEVY and DAN PALEVITCH*

Department of Medicinal, Spice and Aromatic Plants, Agricultural Research Organization, The Volcani Center, Bet Dagan 50 250 (Israel)

and

GIDEON LADIZINSKY

Department of Field Crops, The Hebrew University of Jerusalem, Faculty of Agriculture, Rehovot (Israel)

SUMMARY

A reversed-phase high-performance liquid chromatographic method was developed for the simultaneous quantitation of the alkaloids of *Papaver* species in section *Oxytona*: salutaridine, thebaine, oripavine, alpinigenine, isothebaine and orientalidine. The concentrations of the alkaloids were compared in roots and capsules of the species *P. bracteatum*, *P. orientale* and *P. pseudo-orientale* and their interspecific hybrids. The alkaloid spectrum was similar for the two parts of each plant, and significant correlations were found between the concentration of each alkaloid in the roots and in the capsules. The importance of the results for the screening of plant populations and for breeding purposes is discussed.

INTRODUCTION

The species of the section *Oxytona*, *Papaver bracteatum*, *P. orientale* and *P. pseudo-orientale*, have aroused increased interest due to the pharmacological properties of some of their alkaloids, particularly thebaine, found in *P. bracteatum*^{1,2}. This alkaloid is the natural precursor of codeine and can be converted also into other drugs³. Various chromatographic systems for the separation and determination of *Papaver* alkaloids have been described⁴⁻¹². However, none is adequate for the simultaneous quantitation of the main alkaloids of the *Oxytona* species, namely, isothebaine, alpinigenine, oripavine, orientalidine and thebaine (Fig. 1). Such a method is needed for studies of the interspecific hybrids expected to have the alkaloid spectrum of both parents.

Most chemical studies with *Papaver* species have employed capsules for the alkaloid analysis, and other plant parts were investigated only in a few cases¹³. So far, no comparative and systematic screening of the main alkaloids present in the capsules and roots of the three species of the section *Oxytona* and their hybrids has been reported. Studies of the thebaine content in the roots and capsules of *P. brac-*

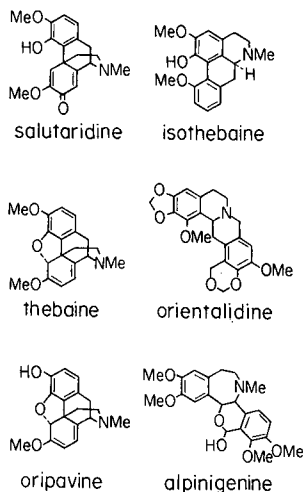


Fig. 1. Structures of the major alkaloids of *Papaver* species of section *Oxytona*. Me = methyl.

teatum plants from different origins have been reviewed¹⁴. The thebaine and oripavine concentrations in roots and capsules of *P. bracteatum*, *P. orientale* and their F₁ hybrid were compared¹⁵, and the alkaloid content in various parts of *P. orientale* and *P. pseudo-orientale* was studied^{16,17}.

In the present study an improved high-performance liquid chromatographic (HPLC) procedure adapted to distinguish between the predominant alkaloids of the species of the section *Oxytona* was developed. This method was further used for the analysis and comparison of the alkaloid spectrum in the roots and capsules of *P. bracteatum*, *P. orientale*, *P. pseudo-orientale* and their interspecific hybrids.

EXPERIMENTAL

Plant material

The plant populations used were: a breeding line of *P. bracteatum* (PB) selected for early flowering and high thebaine, from an original accession from Iran (P.I. 381442); a *P. orientale* (PO) accession (P.I. 376815) from Iran and two accessions of *P. pseudo-orientale* (PPO) one from Iran (P.I. 375952) and the other from the U.S.S.R. (P.I. 372772). For each accession the identification of the species was confirmed by determination of the chromosome number (PB, $2n = 14$; PO, $2n = 28$; PPO, $2n = 42$) and morphological characters. From each species, F₁ and F₂ hybrids, five to ten plants were examined. The capsules and roots of each plant were collected and analysed separately. For a detailed description of the growing conditions and the interspecific crosses see Milo *et al.*¹⁸.

Extraction of the alkaloids

A modified method of Fairbairn and Helliwell¹¹ was used for the extraction. Exactly 250 mg of dried powder plant material were extracted with 20 ml of 5% aqueous acetic acid at room temperature for about 18 h. The solution was filtered

and 7 ml of hexane were added. The aqueous fraction was made alkaline with ammonium hydroxide, and extracted with 3 × 15 ml chloroform–2-propanol (3:1). The pooled extracts were evaporated to dryness under reduced pressure. The residue was dissolved in 2.5 ml of methanol and filtered through a RC 55, 0.45- μ m membrane filter (Schleicher & Schull, Dassel, F.R.G.).

High-performance liquid chromatography

A Tracor liquid chromatograph was used and included a Model 951 pump unit, a 980 A solvent programmer, a 970 A detector and a computing integrator Model CI-10B (LDC/Milton Roy). The reversed-phase HPLC was carried out on a LiChrosorb Superspher[®] RP-18 column (Merck, particle size 4 μ m, 125 mm × 4 mm I.D.). Separation of the alkaloids was accomplished at 25°C by the mobile phase 5% 2-propanol, 40% acetonitrile, 55% water with 1% ammonium carbonate. The solvent flow-rate was 1 ml/min and detection was at 280 nm. All the solvents used (methanol, 2-propanol, acetonitrile, water) were of HPLC grade. Thin-layer chromatography (TLC) was performed as described previously^{1,2}. For alkaloid quantitation, a linear correlation ($r = 0.999$) was observed between the sample concentration and the HPLC-integrated peak area, in the range of 0.01–1.0 mg/ml for each alkaloid.

Reference compounds

Samples of the various purified alkaloids were generous gifts from Dr. L. A. Anderson (School of Pharmacy, University of London, U.K.) and professor D. Lavie (The Weizman Institute of Science, Israel). The identity of the alkaloids was confirmed by co-chromatography with references in both TLC and HPLC.

RESULTS AND DISCUSSION

Two reversed-phase HPLC procedures for the alkaloid separation were evaluated. The first method used a 250 mm × 4 mm RP-18 column with a gradient solvent programme: A, 60% water with 1% ammonium carbonate, 30% acetonitrile and 10% methanol; B, 80% acetonitrile and 20% methanol. The programme started with solvent A for 20 min, and then 5% of solvent B per min were added; under these conditions, good separation with the following retention times was obtained: oripavine, 19 min; alpinigenine, 22 min; isothebaine, 27 min and thebaine, 37 min.

In order to avoid the use of the gradient programme and to shorten the analysis time, a second procedure was elaborated as described in the Experimental section. The chromatogram of the standard alkaloids is shown in Fig. 2. Most of the previously reported HPLC methods were developed for the analysis of the opium alkaloids^{4–7}.

We present herewith a rapid and sensitive method which is well suited for quantitative studies and for genetic analysis of *Papaver* alkaloids in interspecific hybrids in the section *Oxytona*. In some of the chromatograms, other unidentified peaks were obtained, indicating that this method might be appropriate for the separation of additional alkaloids. The accuracy of the assay was evaluated from six replications of a mixture (0.1 mg/ml) of the three major alkaloids and from four replicated samples of a bulk plant material from PO. In the mixture, the average and standard

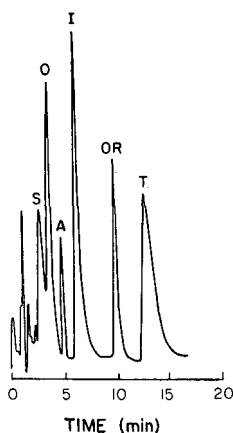


Fig. 2. Chromatogram of an artificial mixture of purified alkaloids. Column: LiChrosorb C_{18} (RP) Superspher $4 \mu\text{m}$. Eluent: 2-propanol–acetonitrile–water (5:40:55) with 1% ammonium carbonate; flow-rate, 1 ml/min. Detection: 280 nm. Salutaridine = S; oripavine = O; alpinigenine = A; isothebaine = I; orientalidine = OR; thebaine = T.

deviation ($\cdot 10^3$) of the integrated areas were: oripavine, 144.7 ± 5.2 ; isothebaine, 236.9 ± 25.2 and thebaine, 224.4 ± 21.2 . In the plant sample, the average and standard deviation of the concentrations of these alkaloids were: 0.097 ± 0.009 , 0.019 ± 0.007 and 0.065 ± 0.01 respectively.

It was found that the alkaloid spectra of the roots and capsules were similar in each plant for each species (Fig. 3) and hybrid (Fig. 4) examined. However, quantitative differences in the various alkaloids were observed between the two parts of each plant. The chemical spectra of the three species are consistent with those reported in other studies^{13,19}. Significant correlations ($p = 0.05$) were found between the contents of each major alkaloid in the capsules and in the roots for the entire plant population. The correlation coefficients were 0.65, 0.60 and 0.82 for isothebaine, oripavine and thebaine, respectively. The concentrations of the major alkaloids isothebaine, thebaine and oripavine in the different parents and hybrids are shown in Table I. The distribution of the different alkaloids in the roots and capsules followed different patterns in the three species and hybrids.

In PB only thebaine was found; its content in the capsules was significantly much higher than in the roots, 2.15 and 0.92%, respectively. This feature was found also in plants from the population of F_2 (PB \times PPO) having thebaine as the predominant alkaloid. In PO the total alkaloid concentration was low, oripavine and thebaine being the major alkaloids. No significant differences between roots and capsules were detected for these compounds. Isothebaine was the major alkaloid in PPO and its content in the capsules was higher than in the roots. However, the accession from Iran (PPO 31) showed a higher content (0.72% in the capsules) and a larger variation compared with the second accession (PPO 82) from the U.S.S.R.

In the F_1 hybrid (PB \times PO) only oripavine and thebaine were present; in some plants an additional unidentified peak was observed, see Fig. 2. The oripavine content in capsules (0.51%) and roots (0.49%) was much higher in this hybrid than in the PO parent (0.09%); on the other hand, the thebaine concentration was much lower

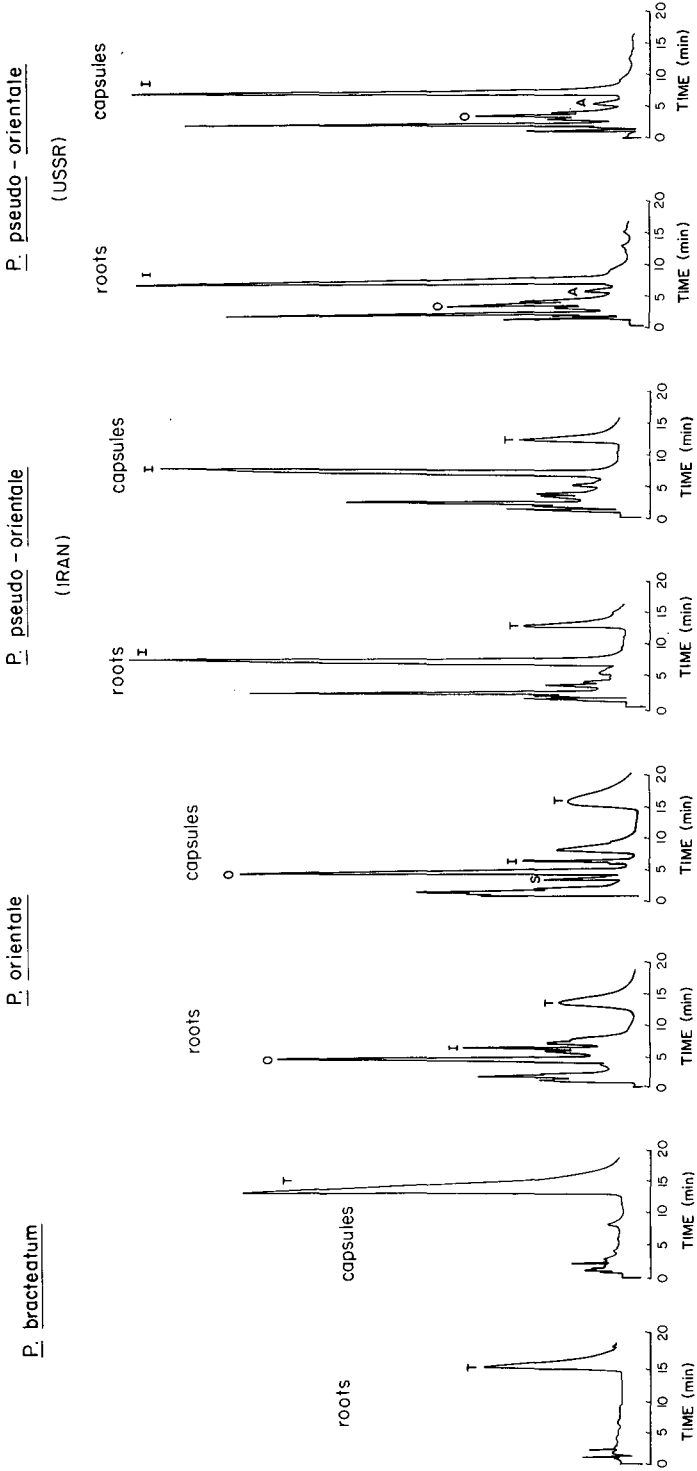


Fig. 3. Typical chromatograms of extracts from roots and capsules of *Papaver bracteatum*, *P. orientale* and *P. pseudo-orientale*. Other details as in Fig. 2.

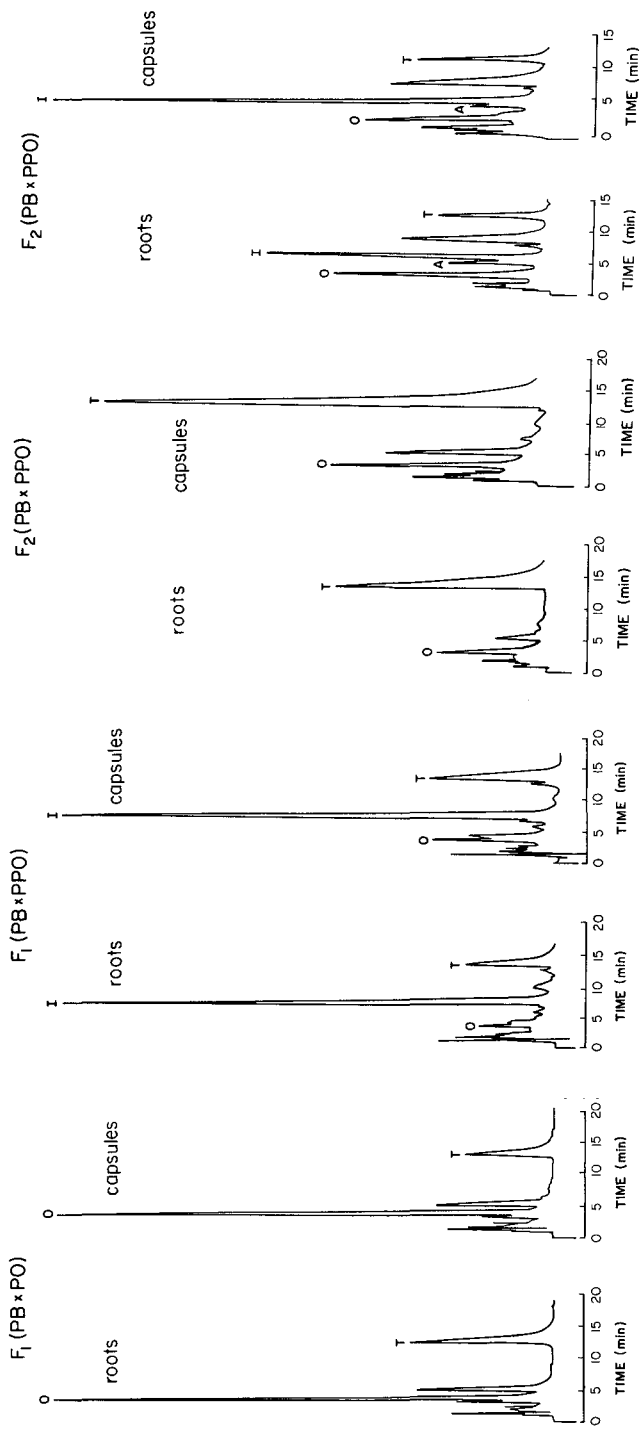


Fig. 4. Chromatograms of extracts from roots and capsules of interspecific hybrids between *Papaver bracteatum* (PB), *P. orientale* (PO) and *P. pseudo-orientale* (PPO). Other details as in Fig. 2.

TABLE I

CONTENT OF THE MAJOR ALKALOIDS (% DRY WEIGHT) IN CAPSULES AND ROOTS OF *PAPAVER BRACTEATUM* (PB), *P. ORIENTALE* (PO), *P. PSEUDO-ORIENTALE* (PPO) AND THEIR HYBRIDS

Species or hybrid	Isothebaine		Thebaine		Oripavine	
	Capsules	Roots	Capsules	Roots	Capsules	Roots
PB			2.15* (1.24-3.75)	0.92 (0.45-1.23)		
PO	0.03 (tr-0.09)	0.001 (tr-0.003)	0.06 (0.02-0.13)	0.07 (tr-0.16)	0.09 (0.02-0.13)	0.09 (0.08-0.09)
PPO 31	0.72 (0.08-1.38)	0.41 (0.003-0.65)	0.007 (tr-0.02)	0.004 (tr-0.01)	0.03 (0.004-0.04)	0.03 (0.01-0.05)
PPO 82	0.33 (0.27-0.41)	0.20 (0.17-0.24)	0.04 (tr-0.08)	0.04 (tr-0.07)	0.05 (tr-0.1)	0.06 (0.03-0.09)
F ₁ PB × PO			0.07 (0.09-0.11)	0.14 (0.08-0.23)	0.51 (0.30-0.70)	0.49 (0.26-0.78)
PB × PPO ₃₁	0.11 (0.01-0.21)	0.16 (0.08-0.27)	0.07 (0.06-0.08)	0.07 (0.05-0.11)	0.04 (0.02-0.05)	0.02 (0.01-0.05)
F ₂ PB × PPO ₃₁	0.16 (0.06-0.20)	0.09 (0.07-0.12)	0.26 (0.07-0.59)	0.15 (0.06-0.24)	0.07 (tr-0.13)	0.08 (0.01-0.18)

* The values are means from 5-10 plants; under each value, the range is given in parentheses. tr = Traces, <0.003% of dry weight.

than that of PB. Similar patterns have been reported¹⁵; however, the low alkaloid content of PO in our study might result from differences in growing conditions or in the origin of the plant populations.

The alkaloid spectrum of the F₁ hybrid (PB × PPO 31) was similar to that of the PPO 31 parent. No significant differences between capsules and roots were obtained. When compared with the parents, the oripavine concentration of this hybrid (0.04%) was similar to PPO, its isothebaine content was reduced and thebaine (0.07%) was higher than in PPO but much lower than in PB.

A wide range of alkaloid spectra was observed in the plants of the segregating generation F₂ (PB × PPO); however, the similarity between roots and capsules of each plant remained.

The constancy of the alkaloid spectrum in the roots and capsules, and the significant correlations found between the content of each alkaloid in these parts, show that chemical screening could be conducted on either capsules or roots. The use of capsules, however, requires a long growth period of the plants, until flowering and capsule maturation. Indeed, the species of the section *Oxytona* require cold for flowering or are biannual^{14,20}; moreover, the plant biomass obtained from the capsules is much lower than that available from the roots. So far, chemical analysis has been performed mainly on capsules¹³. The findings of the present work and the

previous considerations show that the roots can be exploited to advantage in the chemical screening of these species and hybrids in breeding and genetic studies of the alkaloids' accumulation. Using roots for the chemical analysis therefore enhances the selection process for a desired alkaloid spectrum by reducing the growth period of the plants and the generation time.

ACKNOWLEDGEMENTS

This research forms part of the Ph.D. thesis of J. Milo to be submitted to the Hebrew University of Jerusalem, and was supported in part by grant No. I-368-81 from the US-Israel Binational Agricultural Research and Development Fund (BARD). We thank Professor D. Lavie for his suggestions on the manuscript. The paper constitutes contribution No. 2243-E, 1987 series, from the Agricultural Research Organization, The Volcani Center, Bet Dagan, Israel.

REFERENCES

- 1 J. W. Fairbairn and F. Hakim, *J. Pharm. Pharmacol.*, 25 (1973) 353.
- 2 M. Seddigh, G. D. Joliff, W. Calhoun and J. M. Crane, *Econ. Bot.*, 36 (1982) 433.
- 3 L. F. McNicholas and W. R. Martin, *Drugs*, 27 (1984) 81.
- 4 K. R. Khanna and S. Sudhir, *Planta Med.*, 52 (1985) 157.
- 5 L. W. Doner and A.-F. Hsu, *J. Chromatogr.*, 253 (1982) 120.
- 6 C. Y. Wu and J. J. Wittich, *Anal. Chem.*, 49 (1977) 359.
- 7 S. H. Hansen, *J. Chromatogr.*, 212 (1981) 229.
- 8 F.-F. Wu and R. H. Dobberstein, *J. Chromatogr.*, 140 (1977) 65.
- 9 P. G. Vincent, W. R. Gentner, F. J. E. M. Koppers and A. Salemink, *J. Pharm. Sci.*, 68 (1979) 87.
- 10 D. W. Smith, T. H. Beasley, R. L. Charles and H. W. Ziegler, *J. Pharm. Sci.*, 62 (1973) 1691.
- 11 J. W. Fairbairn and K. Helliwell, *J. Pharm. Pharmacol.*, 27 (1975) 217.
- 12 D. Lavie, J. Rothman, A. Levy and D. Palevitch, *Phytochemistry*, 18 (1978) 2011.
- 13 H. G. Theuns, R. H. A. M. Janssen and A. Salemink, *Rec. Adv. Bot. Hort. Pharmacol.*, 2 (1987) 57.
- 14 H. Böhm, *Pharmazie*, 36 (1981) 660.
- 15 H. Böhm and H. Nixdorf, *Planta Med.*, 48 (1983) 193.
- 16 J. Slavik, K. Picka, L. Slavikova, E. Taborska and F. Veznik, *Collect. Czech. Chem. Commun.*, 45 (1980) 914.
- 17 E. Schlittler and J. Müller, *Helv. Chim. Acta*, 31 (1948) 1119.
- 18 J. Milo, A. Levy, G. Ladizinsky and D. Palevitch, *Theor. Appl. Genet.*, 72 (1986) 524.
- 19 J. D. Phillipson, A. Scutt, A. Baytop, N. Özhatay and G. Sariyar, *Planta Med.*, 43 (1981) 261.
- 20 P. Goldblatt, *Ann. Mo. Bot. Gard.*, 61 (1974) 264.

CHROM. 20 460

REVIEW

MICELLAR, INCLUSION AND METAL-COMPLEX ENANTIOSELECTIVE PSEUDOPHASES IN HIGH-PERFORMANCE ELECTROMIGRATION METHODS

JIRÍ SNOPEK

Department of Analytical Chemistry, Charles University, Albertov 2030, 128 40 Prague 2 (Czechoslovakia)

IVAN JELÍNEK

Research Institute for Pharmacy and Biochemistry, Kouřimská 17, 130 60 Prague 3 (Czechoslovakia)

and

EVA SMOLKOVÁ-KEULEMANSOVÁ*

Department of Analytical Chemistry, Charles University, Albertov 2030, 128 40 Prague 2 (Czechoslovakia)

CONTENTS

1. Introduction	571
2. High-performance electromigration techniques	572
3. Pseudophases	573
3.1. Micellar pseudophases	574
3.2. Inclusion pseudophases	576
3.2.1. Cyclodextrins	576
3.2.2. Crown ethers	578
3.3. Enantioselective metal-complex pseudophases	580
4. Application of pseudophases in high-performance electromigration methods	581
4.1. High-performance capillary zone electrophoresis and its modifications	581
4.2. Capillary isotachopheresis	581
5. Conclusions	588
6. Summary	588
References	588

1. INTRODUCTION

In recent years much effort has been devoted to the development of separation methods especially in the field of analytical chemistry. Since the sixties, the progress in chromatography and related methods has been nearly explosive, connected with the rapid accumulation of experimental material and new information. The present stage can be characterized by the following trends: (1) efforts to improve the separation efficiency and speed of analysis leading to the development and application of high-performance techniques; (2) in order to achieve the widest possible applicability, new hybrid methods involving two or more formerly independent separation methods have been employed; (3) improvement in the separation of structurally related compounds and isomers, especially optical isomers (enantiomers) with the aid of various chiral discriminators.

These trends are increasingly evident in the electromigration methods (EMMs). The latest and very promising topic is the development of various pseudophases¹ which substantially extend the application of EMMs towards various types of isomers and, on the other hand, to non-electrolytes.

The aim of this review is to cover the most promising modern trends and to characterize the present stage in the utilization of micellar, inclusion and enantioselective metal-complex formation for the creation of pseudophases. This approach may help to characterize better the newly formed types of EMMs.

2. HIGH-PERFORMANCE ELECTROMIGRATION TECHNIQUES

The trend in modern electromigration methods can be characterized by a high resolution and sensitivity achieved in a short time. A major factor in performance of the system is its ability to dissipate the Joule heat generated by high potentials and currents.

The first method in a planar arrangement dates from 1951, when Michl² showed how paper electrophoresis (PE) could be speeded up by the use of high potentials (approx. 50 V/cm) and pointed out that the diffusion phenomena in the separation process could thus be considerably decreased. It was possible to separate amino acids, polypeptides, organic acids and metal ions in about 20 min whereas 1–12 h were previously necessary. A rapid electrophoretic method that can yield good separation within a few minutes involving an extremely simple arrangement called “high-performance paper electrophoresis” has been developed by Lederer³. Some new and promising elements appeared in his experimental arrangement. The use of a sandwich type separation compartment (paper between two glass plates) minimizes the evaporation of solvent, contributes to a stabilization of the thermal conditions and thus improves substantially the reproducibility of the method.

The introduction of open-tubular capillaries into EMMs represented great progress in the instrumentation. In the past years, high-voltage (HV) or high-performance capillary zone electrophoresis (HPCZE) have become powerful tools for the separation of ionic as well as neutral substances with remarkable efficiency^{4–7}. Capillary columns permit high potential fields to be employed to yield high-speed and high-performance separation. A major factor in the performance is the ability of the capillary tubing system to dissipate the Joule heat. In this way, diffusion is decreased and zone-broadening effects are minimized.

The first successful high-performance separation of metal ions in capillary zone electrophoresis mode was carried out by Hjertén⁴. The separation was achieved in about 2–3 min for simple and in 10–20 min for more complicated mixtures, respectively.

A similar acceleration, based on the use of an HV power supply was developed in capillary isotachopheresis (ITP)⁸. The use of an high electric field strength increases the self-sharpening effect which represents an efficient counteraction to diffusion, convection and electroendosmosis.

The use of aqueous–organic and organic media^{9–11} may extend the applicability and efficiency of HPCZE and/or ITP methods to a wide range of compounds which have about the same effective mobilities and *pK* values and/or are only slightly soluble in water.

As a combination of HPCZE and sodium dodecyl sulphate polyacrylamide gel electrophoresis (SDS-PAGE)¹², high-performance capillary SDS-PAGE (HPC-SDS-PAGE) has been developed¹³. This method may serve as an example of a non-micellar technique used for the separation and molecular weight determination of peptides and proteins. The SDS is able in general to disrupt all non-covalent bonds. In the case of proteins all multiple non-covalently linked chains are broken and free valences are saturated by SDS. The protein mixture is denatured and the SDS-polypeptide complexes created are separated via sieving through the polyacrylamide gel matrix¹⁴.

The apparatus for HPCZE may be adapted for isoelectric focusing (IEF). Rapid and reproducible high-performance IEF experiments with human haemoglobin and transferrin were successfully performed in glass capillaries¹⁵. The experiments confirmed that the IEF resolution under a pH gradient in the capillary separation compartment is very efficient but requires a special postseparation technique for on-line UV detection. This could be achieved either by pumping the zones past the stationary UV detector or by electrophoretic elution.

Electroosmosis, usually performed in a device for HPCZE with extremely thin capillaries¹⁶ or in a commercial capillary ITP device¹⁷, represents a transition between the electrophoretic and liquid chromatographic methods. The electroosmotic effect in thin open tubes is used for pumping the mobile phase. The method could be used in principle for separations of both charged and uncharged species. The resolution of uncharged species depends mostly on their size differences. These differences are usually very small and, consequently, the technique is not very useful for the separation of neutral compounds.

Recently, Terabe *et al.*¹⁸ introduced micellar solubilization into HPCZE and first reported the so-called "micellar electrokinetic capillary chromatography" (MECC). The technique combines many of the operational principles and advantages of micellar liquid chromatography¹ and HPCZE. The surfactant is added to the mobile phase in a concentration above its critical micellar concentration (CMC). The micellar pseudophase formed provides an effective mechanism especially for the separation of neutral hydrophobic compounds. They are resolved in harmony with their partitioning between the mobile phase and the hydrophobic interior of the micelles. An electroosmotic flow of the solvent enables the transport of solutes, including neutral ones, through the separation compartment. The electrokinetic separation seems to be applicable to a variety of non-polar and polar slow migrating solutes. It seems to be limited by the solubility of the solutes in water since the addition of an organic solvent causes a disintegration of the micellar pseudophase.

3. PSEUDOPHASES

There are many possibilities of using the micellar, inclusion and enantioselective complexing phenomena in the electromigration methods. Intensive research in this field was stimulated mainly by the requirement of the resolution of various isomeric compounds, which do not differ in their mobilities and pK values.

In recent years, the interest in chiral separations has grown considerably. The resolution of enantiomers by EMMs, in comparison with chromatographic methods, has just started and is still sporadic. The first successful attempts to separate optical

isomers were made in paper electrophoresis¹⁹, HPCZE²⁰ and capillary isotachopheresis²¹, respectively.

3.1. *Micellar pseudophases*

The utilization of surface-active agents (surfactants) substantially alters the possibilities and limitations of EMMs and gives rise to the existence of newly modified ones. Most EMMs employ the extraordinary ability of surfactants to form organized aggregates (micelles) and thus may be classified as micellar techniques. Some of the earlier methods do not require the presence of an aggregated surfactant and belong to the non-micellar type. As an excellent example of the widely used non-micellar EMMs, SDS-PAGE¹² must be mentioned, where the presence of the surfactant in micellar form is undesirable. Sometimes it is quite impossible to differentiate micellar and non-micellar techniques because the separation process can be mediated simultaneously by the presence of the micellar and monomeric form of the surfactant.

Many reviews and articles describe the properties of surfactants and their behaviour in aqueous and non-aqueous solutions and propose possible structures for the micelles created^{1,22}. Only some fundamental properties of micellar systems, most important for applications in EMMs, will be mentioned here.

The surfactants are amphiphilic molecules containing both hydrophobic and hydrophilic parts. Depending on the charge of the polar "head" group, the surfactant molecule can be classified as anionic, cationic, zwitterionic or non-ionic. The apolar hydrophobic part of the molecule is usually formed by a long alkyl chain, except for some biological surfactants like molecules, namely bile salts, which differ substantially in their structure and micelle formation mechanism²⁴ and thus must be classified separately.

As suggested above, the surfactants may exist in the form of aggregates when their concentration in solution exceeds the CMC. The CMC value and aggregation number depend on various physicochemical parameters. In EMMs the dependence of the CMC upon the pressure is not significant and may be neglected, but the influence of temperature may substantially alter the separation process. Plots of CMC *vs.* temperature, for the commonly utilized ionogenic surfactants, exhibit a minimum between 20 and 30°C. Dramatic changes in CMC may occur when some electrolytes are added to the surfactant–water system²². It can be concluded that an increase in ionic strength often results in an increase in the aggregation number and a decrease in the CMC. Both water-soluble and -insoluble organic solvents may play a significant role in micelle formation^{24,25}. Short-chain alcohols added to aqueous micellar systems enhance the micelle formation by decreasing the CMC, if the alcohols are present in low concentration. At higher concentrations they prevent the micelle formation. The organic solvents which are able to form strong hydrogen bonds with water molecules, acetone, dioxane, acetonitrile, tetrahydrofuran, etc., inhibit the formation of micelles. The addition of water immiscible organic solvents like long-chain alcohols or alkanes can either enhance or inhibit micelle formation depending on the concentration of surfactant present in the solution and amount of the organic additive.

The structural description of micellar systems demonstrates the difficult prob-

lem which has not yet been solved in detail. Many simplified models, which contribute to the understanding of micelle properties, have appeared in the literature. The simplest radial model of a normal aqueous micelle²⁶⁻²⁸ proposes an approximately spherical geometry with all hydrophobic chains in the central core and head hydrophilic groups situated on the surface (see Fig. 1). This oldest model may serve to explain the solubilization hydrophobic and electrostatic interactions between micelles and solutes in the separation process. Experimental observations, which confirmed a significant contact between water and the hydrocarbon chains of a normal micelle, resulted in the proposal of new and more complicated models. The Menger model of a normal micelle²⁹⁻³³ supposes that the hydrocarbon chains are extended to the surface and may interact directly with the solvent. The Fromherz model³⁴ represents an highly organized spherical system with both the hydrocarbon chain portions and the head hydrophilic groups exposed to the solvent. The similar Dill model³⁵⁻³⁷, developed recently, is much less structural but again there is a considerable amount of hydrocarbon exposed at the surface of the micelle. These models enable a better explanation of the interspatial surface interactions between micelles and solutes in the separation process.

The shape of micelles depends on the surfactant concentration in the solution. The theoretical models propose a roughly spherical shape for a normal micelle. An increase in the surfactant concentration may result in the formation of other types of aggregates^{22,29}. Initially, a transition from spherical to rod-like or cylindrical micelles may be observed. Still higher surfactant concentrations lead to the formation of liquid crystalline aggregates^{1,22,38}.

The utilization of reversed micellar systems^{22,39,40} is connected with the use of apolar organic media. Promising results with reversed micelles in liquid chromatography methods could not be simply transferred to EMMs due to the necessity of using apolar systems with great electric resistance. The only technique which could be compared to the use of reversed-phase liquid chromatography was published by Walbroehl and Jorgenson⁴¹. The solvophobic interaction between a non-polar solute and a tetraalkylammonium ion utilized is similar to that between a solute and a reversed phase.

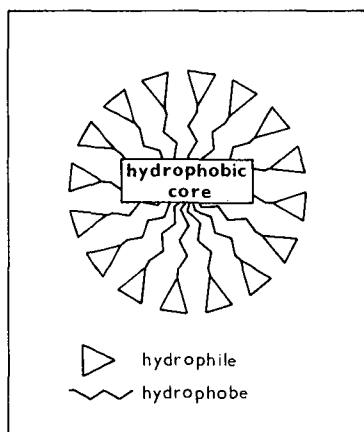


Fig. 1. Radial model of the micelle.

The use of surfactants as pseudophases in EMMs is based on the partitioning of the solute between the micellar phase and the solvent which is a fast dynamic equilibrium process. The distribution constant is defined by the equation

$$K_D = [S]_m/[S]_s$$

where $[S]_m$ = solute concentration in the micellar phase and $[S]_s$ = solute concentration in the solvent phase, respectively.

For diluted solutions the distribution constant may be related to the solute-surfactant binding constant, K_b

$$K_b = [S \cdot M]/[S][M]$$

where $[S]$, $[M]$ and $[S \cdot M]$ are the concentrations of the uncomplexed solute, the micellar pseudophase and the surfactant-solute "complex", respectively, by the use of the equation⁴²

$$K_b = (K_D - 1) \cdot \bar{v}$$

where \bar{v} = molar volume of the surfactant in the organized surfactant medium.

As mentioned above, the association rate of the majority of solutes with the surfactant is very rapid and therefore a direct proportionality between the binding constant, K_b , and the stability of the associated solute-surfactant complex can be assumed. The structural differentiation, based on the use of the micellar pseudophase, depends directly on the differences in binding constants of the solutes.

3.2. Inclusion pseudophases

Inclusion complexes are molecular compounds of characteristic structural arrangements, in which one compound (the host molecule) spatically encloses another (the guest molecule) or at least part of it. The inclusion phenomena have found the widest use in separation methods, *e.g.*, in chromatography^{22,43-46}. In EMMs, increasing attention has recently been paid to the formation of inclusion compounds of cyclodextrins or its derivatives^{21,47-55} and crown ethers^{47,56-59}. Both types of compounds are utilized as inclusion pseudophases.

3.2.1. Cyclodextrins

Cyclodextrins (also known as Schardinger dextrins, cycloglucopyranoses, cycloamyloses, cycloglucans)¹ are cyclic oligosaccharide molecules built up of D-(+)-glucopyranose units, bonded via α -(1,4) linkages, with all glucose units in a Cl(D) chair conformation (Fig. 2A). Their structure is unique in that it resembles a truncated cone with both ends open (Fig. 2B). The top of the torus corresponds to the more open side which is rimmed with secondary hydroxyl groups on carbons 2 and 3 of each glucose unit, all rotated to the right. The smaller opening of the cones is rimmed with the more polar primary hydroxyl groups on carbon 6 of the glucose unit. The interior of the cyclodextrin (CD) cavity contains two rings of C-H groups with a ring of glycosidic oxygens in between. Their surface is relatively hydrophilic,

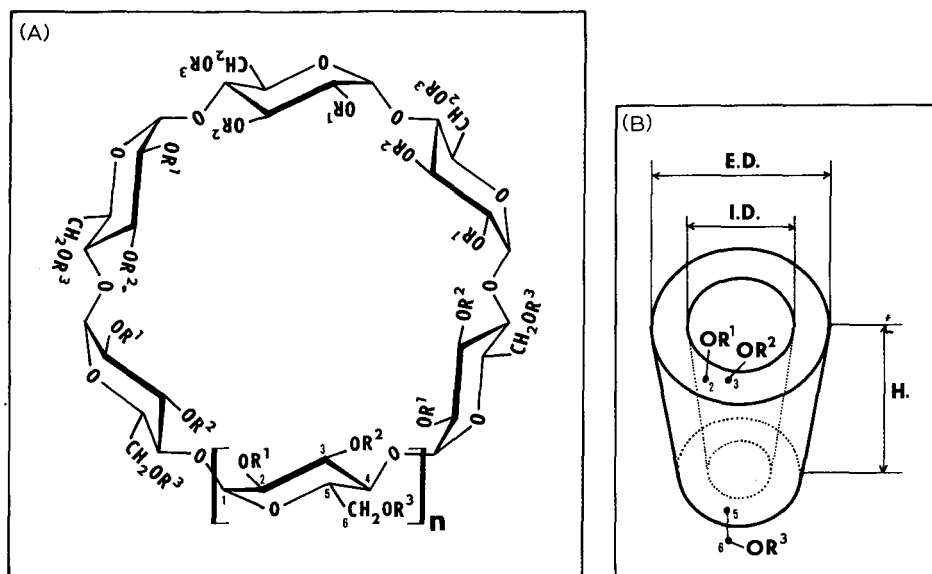


Fig. 2. Chemical structure (A) and schematic model (B) of cyclodextrin and/or its derivatives. For n , H , I.D., E.D. values and R^{1-3} substitution see Table I.

therefore the CDs are soluble in water. Their cavity, however, is of apolar character. Useful physical data and properties are given in Table I.

The exceptional properties of CDs have been described in many papers, reviews^{1,43,44,60} and monographs^{22,45,46,61-64}. The remarkable property of CDs, its

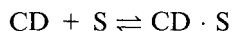
TABLE I
CHARACTERISTICS OF CYCLODEXTRINS^{1,43,60,61}

	Cyclodextrin		
	α	β	γ
$R^1 = R^2 = R^3^*$	H	H	H
Number of glucose units	6	7	8
n^*	1	2	3
Molecular weight	972.86	1135.01	1297.15
Diameter of cavity, I.D.* (nm)	0.47-0.52	0.60-0.64	0.75-0.83
Diameter of outer periphery, E.D.* (nm)	1.46 ± 0.04	1.54 ± 0.04	1.75 ± 0.04
Height of cavity, H^* (nm)		(for all) 0.79-0.80	
Volume of cavity (nm ³)	0.176	0.346	0.510
pK _a range of hydroxyl groups		(for all) 12.1-12.6	
Solubility in water at 25°C (g/100 ml)	14.50	1.85	23.20
Number of water molecules taken up by cavity	6	11	17
Melting point (K)	551	572	540
Specific rotation, $[\alpha]_D^{25}$	150.5 ± 0.5	162.5 ± 0.5	177.4 ± 0.5

* For meaning of abbreviations see Fig. 2.

derivatives and/or polymers is their ability selectively to include a wide variety of guest organic and inorganic molecules or ions into their hydrophobic cavity.

The formation of inclusion compounds of CDs is a spontaneous process with a negative Gibbs energy. It can be described by an equilibrium



characterized by an equilibrium constant, K_b , defined by the relationship

$$K_b = [\text{CD} \cdot \text{S}]/[\text{CD}][\text{S}]$$

where $[\text{CD} \cdot \text{S}]$, $[\text{CD}]$ and $[\text{S}]$ are the equilibrium molar concentrations of the inclusion compound, cyclodextrin and guest, respectively. The K_b values indicate the stabilities of the inclusion compounds and the possibilities for the separation of related compounds.

The relative stabilities of the CD inclusion compounds are governed by factors such as hydrogen bonding, hydrophobic interactions (Van der Waals interactions), solvation effects (in liquid media) and the space-filling ability of the molecule. Depending on the size and geometry of the guest molecule, in relation to the dimensions of the CD cavity, substantial differences in binding behaviour can be observed for series of structurally related solutes and optical isomers. This is the basis of the use of CDs in the separation process, including EMMs.

For completeness, some other properties of CDs which may play a significant role in the separation process must be mentioned. Except for inclusion phenomena, the micellar pseudophase formation may occur in water solutions, using derivatized cyclodextrin. The methylated cyclodextrins are known to be extremely soluble in both water and organic solvents, less hygroscopic and highly surface active^{65,66}. Their behaviour in aqueous solutions is very similar to that of non-ionic surfactants.

3.2.2. Crown ethers

The crown ethers belong to the group of synthetic macrocyclic polyethers which are able to form stable inclusion complexes with various inorganic and organic cations. Many papers and several monographs, published during the past two decades, have been devoted to aspects of the synthesis and utilization of crown ethers⁶⁷⁻⁷¹. In this review we shall limit the discussion to a brief description of their properties and their use in EMMs as selective pseudophases.

Crown ethers may be classified in general as synthetic macrocyclic compounds containing some electron-donor heteroatoms (O,N,S) in the cyclic structure. This definition includes not only the cyclic oligomers of epoxyalkanes but also derived aromatic and alicyclic crown ethers, thia- and aza-crown ethers which contain sulphur and nitrogen atoms in the ring, respectively.

The structure of a common crown-ether skeleton, with oxygen atoms only, is given in Fig. 3, and the cavity diameters of the simple crown ethers are given in Table II. Many aromatic and alicyclic crown ethers, derived from this fundamental skeleton, with different dimensions and complexation ability, have been synthesized. The crown compounds, *e.g.*, with aromatic or alicyclic units in the fundamental skeleton, are, in comparison to crown ethers of the basic structure, much less soluble in aqueous solutions.

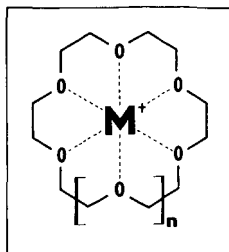


Fig. 3. Chemical structure of a crown-metal (M^+) complex, *e.g.*, $n=1$ for 18-crown-6- M^+ , $n=2$ for 21-crown-7- M^+ , etc.

Many crown ethers synthesized are able to form complexes not only with metal ions but also with organic nitrocompounds, aryldiazonium salts, amines and nitriles in their ionic forms. The complex formation is based on ion-dipole interactions between the host and guest molecules. The most important factors influencing the stability of crown complexes are summarized in the following paragraphs.

The complex formation depends strongly on the relationships between the cavity diameter and the size of the host ion. The maximum stability is obtained when the cation diameter is comparable with the dimensions of the cavity.

The number, geometrical position and geometrical symmetry of oxygen-donor atoms in the ring are of great importance. The higher is the number of oxygen atoms which lie in the same plane, the more stable is the complex created. A symmetrical arrangement of oxygen atoms is favourable for the stability of the complex.

The partial negative charge of oxygen atoms present in the macrocycle, together with the neighbouring aliphatic carbon atoms, increases the stability of the complex. The presence of aromatic rings in the crown structure decreases the negative charge on the oxygen atoms, thus the stability of the complex is decreased.

Steric hindrance of the polyether ring decreases the stability of the complex formed. On the other hand, the introduction of an optically active group into the crown ether has great significance, especially for the separation of optically active organic compounds. An efficient liquid chromatographic separation of various chiral amino acids has been achieved recently⁷⁴⁻⁷⁶.

TABLE II

CROWN ETHER CAVITY DIAMETERS^{68,72,73}

A, From Corey-Pauling-Koltur atomic models; B, from Fisher-Hirschfelder-Taylor atomic models; C, from X-ray crystallographic data.

Name	Internal diameter (nm)		
	A	B	C
14-Crown-4	0.12	0.15	—
15-Crown-5	0.17	0.22	0.172-0.184
18-Crown-6	0.26	0.32	0.268-0.286
21-Crown-7	0.34	0.43	—
24-Crown-8	0.4	—	—

Solvation affects substantially the size of the included cation and thus the stability of the complex. It can be concluded that higher solvation of the cation means a less stable complex.

The utilization of crown ethers in EMMs has been restricted to improvement in the separation of alkaline and alkaline-earth metals. The rapid progress in the synthesis of enantioselective crown ethers opens up new possibilities in the separation of enantiomers.

Although the fundamentals of the cyclodextrin and crown-ether inclusion phenomena are rather different, both separation processes can be expressed similarly in terms of complex equilibria between the solvent and pseudophase.

3.3. Enantioselective metal-complex pseudophases

The utilization of enantioselective metal complexes represents one of the oldest approaches to the solution of chiral resolution. The so-called ligand-exchange phases for the separation of enantiomers were introduced in liquid chromatography by Davankov *et al.*⁷⁷⁻⁷⁹. An amino acid, such as L-proline, attached to the support material, and Cu^{2+} present in the mobile phase were used for the formation of ternary diastereomeric complexes of different stabilities with the racemic amino acids to be separated and thus an effective chiral resolution was achieved. This technique remains one of the most effective means of separating underivatized amino acid racemates.

The diastereomeric ternary complex formation, described above, is theoretically applicable to the resolution of sample molecules with two polar correctly spaced groups which can simultaneously act as ligands for the central metal ion. Therefore, especially α -amino acids with their NH_2 and COOH groups are very suitable for both formation of the enantioselective phase and its utilization as a solute. The structural differentiation of the typical diastereomeric ternary complex, formed by two amino acids as ligands for the central metal ion, is shown in Fig. 4.

The experiments with enantioselective metal complexes were recently transferred to EMMs. The chiral pseudophase may be obtained simply by adding complex-forming components to the support electrolyte without the need of its immobilization. Chiral Cu^{2+} -L-histidine and Cu^{2+} -aspartame pseudophases were successfully used in HPCZE^{20,80}. Studies of chiral complexes of Co^{3+} and Cr^{3+} with amino acids, cyclohexanediamine and oxalate as ligands were performed in HPPE^{19,81-85}. The detailed description of their behaviour in chiral support electrolytes may help to extend the number of chiral complexes which are of potential use as enantioselective pseudophases.

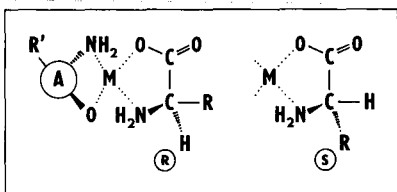


Fig. 4. Schematic model of amino acid chiral resolution by means of amino acid (A)-metal (M) complexes. R = R-enantiomer and S = S-enantiomer.

4. APPLICATION OF PSEUDOPHASES IN HIGH-PERFORMANCE ELECTROMIGRATION METHODS

The pseudophases described allow a widening of the application range of modern high-performance electromigration methods towards various types of structural isomers (positional, optical, geometrical, etc.) and even uncharged organic compounds. In some cases such modification of the electrophoretic system results in the introduction of quite a new method of separation, *e.g.*, micellar electrokinetic chromatography. The number of theoretical and application contributions, described in the literature, indicates the increasing interest in EMMs.

4.1. HPCZE and its modifications

Most attention has been paid to the application of micellar pseudophases in this area. The modification of HPCZE which utilizes many of the operational principles and advantages of micellar liquid chromatography is frequently called micellar electrokinetic capillary chromatography (MECC). In this method a surfactant is added above its CMC, thereby affording an effective mechanism for the separation of both neutral and charged solutes. The separation of neutral solutes is based simply on their differential partitioning between the electroosmotically pumped aqueous mobile phase and the hydrophobic interior of the micelles, which are charged and moving at a speed slower than the mobile phase due to electrophoretic effects. Charged solutes are not only distributed between the micellar and liquid phases, but are simultaneously separated electrophoretically according to their mobilities. The superposition of the two phenomena may either enhance or deteriorate the separation efficiency. The electrophoretic velocity of charged species must be smaller than the electroosmotic flow in the opposite direction, otherwise there is no possibility to detect and thus quantify the moving zone.

The use of other types of pseudophases in electrokinetic chromatography is based on the same principles mentioned above and may further extend its application area. The use of 2-O-carboxymethyl- β -CD as a pseudophase permits the distribution process between the mobile phase and the CD cavity. This modification seems to be advantageous especially for the separation of neutral aromatic isomers.

The creation of a metal-complexing pseudophase in the support electrolyte, *e.g.*, of the Davankov type, enables the diastereomeric chiral discriminating complex formation between the pseudophase and the solutes. The enantiomeric resolution of positively and negatively charged solutes can be achieved in principle.

The applications of pseudophases in HPCZE, described in literature, are summarized in Table III.

4.2. Capillary isotachopheresis

The use of pseudophases in capillary ITP is in the development stage. Most attention has been paid to the utilization of macrocyclic ionophores such as crown ethers and cyclodextrins. The mechanism of the separation process in ITP differs from that in CZE. The electroendoosmotic flow, which plays a significant role in CZE, is minimized here and we may presume that the uncharged inclusion pseudo-

TABLE III

APPLICATION OF PSEUDOPHASES IN HPCZE

Abbreviations used: β -Ala = 3-alanine, C = capillary, coumarin 540 A = tetrahydro(trifluoromethyl)benzopyrazolizin-11-one, β -CMCD = 2-O-carboxymethyl- β -cyclodextrin, CTAC = cetyltrimethylammonium chloride, D = detection, DE = device, DTAB = dodecyltrimethylammonium bromide, E = electrolyte, EACA = 6-aminocaproic acid, GD = Girard derivative, $(h_i)_{rel}$ = relative step height, HEC = hydroxyethylcellulose, His = L-histidine, HPMC = hydroxypropylmethylcellulose, LE = leading electrolyte, MES = morpholinoethanesulphonic acid, NBD = 7-nitrobenzofurazan, *n*-CA = *n*-caproic acid, PTH = phenylthiohydantoin, PU = potential units, PVA = poly(vinyl alcohol), STS = sodium tetradecyl sulphate, TBAB = tetrabutylammonium bromide, TBAC = tetrabutylammonium chloride, TE = terminating electrolyte, TEA⁺ = tetraethylammonium, Tris = tris(hydroxymethyl)aminomethane, Val = L-valine.

<i>Pseudophases</i>	<i>Conditions</i>	<i>Compounds separated</i>	<i>Notes</i>	<i>Refs.</i>
SDS	E: borate-phosphate buffer (pH 7.0) C: silica tubing (650 or 900 mm \times 0.05 mm I.D.) D: UV (270 nm)	Acetylacetone, phenol, <i>o</i> -, <i>m</i> -, <i>p</i> -cresols, chlorophenols, xlenols, <i>p</i> -ethylphenol	Max. theoretical plate number 400 000 for <i>p</i> -ethylphenol and xlenols (height equivalent to a theoretical plate of 1.9–3.6 μ m)	18
SDS, STS	E: borate-phosphate buffer (pH 7.0) C: silica tubing (500 mm \times 0.05 mm I.D.) D: UV (210 nm)	Methanol, resorcinol, phenol, <i>p</i> -nitroaniline, nitrobenzene, toluene, 2-naphthol, Sudan III	Fundamental characteristic of MECC; the mathematical description of capacity factor, resolution, effective plates and peak capacity; Range of retention times of electrically neutral solutes are limited between elution time of water, t_0 , and that of the micelle, t_{mc}	86
SDS, DTAB	E: borate-phosphate buffer (pH 7.0) C: fused-silica tubing (650 mm \times 0.05 mm I.D.) D: UV (260 nm)	22 PTH-amino acids	Comparative measurements with anionic SDS and cationic DTAB were performed	87
SDS	E: borate-phosphate buffer (pH 6.0–9.0) C: fused-silica tubing (650 mm \times 0.05 mm I.D.) D: UV (220 nm)	Chlorinated phenols (mono-, di-, tri-, tetra-, penta-), phenol, Yellow OB	The capacity factor of chlorinated phenols, which were partially ionized under given conditions, decreases with increasing pH	88
SDS	E: borate-phosphate buffer (pH 5.0–9.0) C: fused-silica tubing (650 mm \times 0.05 mm I.D.) D: UV (210 nm)	Methanol, resorcinol, phenol, <i>p</i> -nitroaniline, nitrobenzene, toluene, 2-naphthol, Sudan III	Coating of polymers polyethylene glycol 20M (DB-WAX), methylsilicone (DB-1) on the inner wall of fused-silica tubing; effect of pH and concn. of SDS on electrokinetic migration were investigated	89

TABLE III (continued)

<i>Pseudophases</i>	<i>Conditions</i>	<i>Compounds separated</i>	<i>Notes</i>	<i>Refs.</i>
SDS	E: phosphate-borate buffer C: 25–75 μm I.D. D: laser-excited fluorescence	B ₆ vitamin and its five metabolites	Determined in human urine; efficiency as high as 60 000 theoretical plates/m; limits of detection are less than 1 pg injected	90
SDS	E: borate-phosphate buffer C: fused-silica (1 m \times 75 μm I.D.) D: UV (280 nm)	Theobromine, hypoxanthine, theophylline, caffeine, uric acid, xanthine	Effect of injection procedures on efficiency in MECC; 240 000 theoretical plates/m are reported for caffeine	91
SDS, CTAC	E: soln. Na ₂ HPO ₄ C: fused-silica (650 mm \times 0.05 mm I.D.) D: fluorescence (488 nm/540 nm)	NBD-ethylamine, - <i>n</i> -propylamine, - <i>n</i> -butylamine, -cyclohexylamine, - <i>n</i> -hexylamine, coumarin 540A	Inside wall of the column is silanated by trimethylchlorosilane. The effect of 2-propanol on diminution of solute-wall interaction and separation efficiency was studied	92
SDS	E: borate-phosphate buffer (pH 7.0) C: quartz (700 mm \times 0.05 mm I.D.) D: UV (206 nm)	Phenol, PTH-alanine, 4-nitroaniline, di-, triglycine, (<i>S</i>)- <i>cis</i> -verbenol, GD of nonanol and undecanol, (<i>E</i>)-9-dodecen-1-ol, (<i>8E</i> , 10 <i>E</i>)-8,10-dodecadien-1-ol, 1- and 2-naphthol	Inside wall of the column coated by Sylgard 184 (dimethylpolysiloxane RTV). The experimental device was constructed utilizing the components of capillary ITP	93
SDS	E: phosphate buffer (pH 7.0–11.0) C: fused silica (800 mm \times 0.1 mm I.D.) D: UV (214 nm)	Acetylsalicylic acid, caffeine, <i>p</i> -acetamidophenol, salicylamide, <i>o</i> -ethoxybenzamide	Ethyl <i>p</i> -aminobenzoate was used as the internal standard for on-column detection. Column efficiency: 70 000–130 000 theoretical plates.	94
SDS	E: borate-phosphate buffer (pH 7.0) C: fused silica (650 mm \times 0.05 mm I.D.) D: UV	Chlorinated phenols (mono-, di-, tri-, tetra-, penta-), methanol, Yellow OB, resorcinol, <i>p</i> -nitroaniline, nitrobenzene, 2-naphthol	Phenol was used as internal standard. Reproducibility of retention times, peak area and peak heights for repeated injection of constant amounts of samples is presented.	95
SDS (+ Zn ²⁺ , Mg ²⁺ , Cu ²⁺)	E: borate-phosphate buffer (pH 7–9) C: fused silica (500–850 mm \times 0.05 mm I.D.) D: UV (260 nm)	Eight bases, nucleotides, 18 oligonucleotides	Combination of low concentration of divalent metals and SDS micelles is demonstrated.	96
SDS	E: Na ₂ HPO ₄ solutions C: fused silica (750 mm \times 0.025, 0.075 and 0.10 mm I.D.) D: fluorescence (480/540 nm)	NBD-cyclohexylamine, ethylamine	Effects of the applied voltage, column dimensions, concentration of buffer and surfactant on the separation efficiency were studied.	97

(Continued on p. 584)

TABLE III (continued)

<i>Pseudophases</i>	<i>Conditions</i>	<i>Compounds separated</i>	<i>Notes</i>	<i>Refs.</i>
SDS	E: borate-phosphate buffer (pH 8.4–8.9) C: fused silica (685 mm × 0.06 mm I.D.) D: UV (256 nm)	Fourteen normal and modified deoxyribonucleosides, deoxyribomononucleotides, ribonucleoside and pyrimidine	The number of theoretical plates: 370 000–540 000 (highly dependent on the solute concentration). The dependence of the applied voltage and electroinjection time on the separation efficiency was studied.	98
SDS	E: phosphate buffer (pH 6.95–7.0) MES buffer (pH 6.05) C: fused silica (879 mm × 0.026 mm I.D. and 651 mm × 0.052 mm I.D.) D: amperometric	Dopamine, norepinephrine, epinephrine, catechol, 4-methyl- and 4-ethylcatechol	New type of detection for MECC was developed. The detection limit was less than 20 fmol. The number of theoretical plates was more than 400 000.	105
β -CMCD β -CD	E: phosphate buffer (pH 7.0) C: silica tubing (650 mm × 0.05 mm I.D.) D: UV (210 nm)	Acetophenone, anisole, methyl-, ethyl-, propyl-, butyl-benzoate, cresols, nitroanilines, chloroanilines, dinitrobenzenes, nitrophenols, xylydines, xlenols	Host-guest interactions between β -CMCD and the solute operates as distribution process. This concept extends the utilization of specific interactions in electrokinetic chromatography. The number of theoretical plates are 120 000–130 000.	55
Cu^{2+} -L-histidine complex	E: L-histidine, CuSO_4 , ammonium acetate (pH 7–8) C: fused silica (750 mm × 0.075 mm I.D.) D: laser fluorescence (325 nm)	Ten enantiomers of DL-dansyl amino acids	Chiral recognition is explained by mixed chelate complexation to form two diastereomeric, ternary complexes. Replacement of L- by D-His in the support E reverses the migration order of the D- and L- amino acids.	20
Cu^{2+} -aspartame complex STS	E: aspartame, CuSO_4 , ammonium acetate (pH 7.5) C: fused silica (1 m × 75 μm I.D.) D: laser-induced fluorescence (325/550 nm)	Eighteen racemic dansylated DL-amino acids	Aspartame = dipeptide L-aspartyl-L-phenylalanine methyl ester. The separation is based on the diastereomeric interaction between DL-amino acids and chiral Cu^{2+} -aspartame complex present in the support electrolyte. Effect of electrolyte composition, pH and temperature are described as well as linearity and sensitivity of response. Micellar (STS) electrolyte solution has been employed in order to increase the differentiation of neutral amino acids.	80

TABLE III (continued)

<i>Pseudophases</i>	<i>Conditions</i>	<i>Compounds separated</i>	<i>Notes</i>	<i>Refs.</i>
			Review, univ. microfilms, etc.	99-104
Mixed micelles didecyl-L-Ala + SDS	E: Sodium acetate, SDS, <i>N,N</i> -didecyl-L-Ala, Cu ²⁺ , 10% glycerol C: 800 mm × 0.075 mm I.D. D: UV (260 nm)	Dansylated D,L-threonine, -methionine and -leucine	Overviews several aspects of HPCZE and presents chiral resolution of dansylated amino acids using a chiral metal chelate micelle.	104

TABLE IV
APPLICATION OF PSEUDOPHASES IN ITP

For abbreviations used, see Table III. HEPES = N-2-hydroxyethylpiperazine-N'-2-ethanesulfonic acid.

<i>Pseudophases</i>	<i>Conditions</i>	<i>Compounds separated</i>	<i>Notes</i>	<i>Refs.</i>
α -CD 18-crown-6 (12-crown-4 and 15-crown-5)	DE: Shimadzu IP-2A C: 40 mm × 1 mm I.D. + 150 mm × 0.5 mm I.D. LE: 5 mM <i>p</i> -toluenesulphonic acid, 0.01% Triton X-100 TE: 5 mM TBAB	Li ⁺ , Na ⁺ , K ⁺ , Rb ⁺ , Cs ⁺ , NH ₄ ⁺ , TEA ⁺ , Mg ²⁺ , Ca ²⁺ , Sr ²⁺ , Ba ²⁺ , I ⁻ , Cl ⁻ , Br ⁻ , ClO ₄ ⁻ , Fe(CN) ₆ ³⁻ , Fe(CN) ₆ ⁴⁻	TEA ⁺ was used as an internal standard. Li ⁺ , Mg ²⁺ , Ca ²⁺ and TEA ⁺ do not interact with 18-crown-6. 12-crown-4 and 15-crown-5 were practically without any effect on the electrophoresis. 2% α -CD allowed the otherwise impossible separation of I ⁻ in the presence of Cl ⁻ and Br ⁻ . 1% α -CD allowed the separation of ClO ₄ ⁻ in the presence of ferri- and ferro-cyanide.	47
β -CD	DE: Shimadzu IP-2A C: 40 mm × 1 mm I.D. + 150 mm × 0.5 mm I.D. LE: 10 mM HCl, β -Ala (pH 3.6) TE: 10 mM <i>n</i> -CA	<i>o</i> -, <i>m</i> -, <i>p</i> -Iodobenzenesulphonate, toluenesulphonate, naphthalene-mono- and disulphonate	The dependence of PU values on β -CD concentration in the LE was studied.	49
β -CD	DE: Shimadzu IP-2A C: 40 mm × 1 mm I.D. + 150 mm × 0.5 mm I.D. I.D. Acidic electrolyte systems (pH 3.5-4.0)	<i>o</i> -, <i>m</i> - and <i>p</i> -Substituted benzenesulphonic acids (BSA):NH ₂ -, OH-, MeO-, EtO-, Me-, Cl-, I-; naphthalene-sulphonic acids (NSA)	Me-, Cl-, I-BSA and NSA can be separated effectively in the LE with β -CD.	50

(Continued on p. 586)

TABLE IV (continued)

<i>Pseudophases</i>	<i>Conditions</i>	<i>Compounds separated</i>	<i>Notes</i>	<i>Refs.</i>
α -CD	DE: Shimadzu IP-2A C: 150 mm \times 0.5 m I.D. LE: 10 mM HCl or acetic acid + potassium acetate (1:1), 0.01% PVA TE: 5 mM (<i>p</i> -methylbenzyl)trimethylammonium bromide or 1-naphthylamine hydrochloride	Li ⁺ , Na ⁺ , K ⁺ , TEA ⁺ (<i>o</i> -, <i>m</i> - and <i>p</i> -methylbenzyl)-trimethylammonium ions, (<i>o</i> - and <i>p</i> -nitrobenzyl)-trimethylammonium ions, (<i>m</i> -, <i>p</i> - and <i>o</i> -, <i>p</i> -dimethylbenzyl)trimethylammonium ions, quaternary pyridinium ions	Li ⁺ , Na ⁺ , K ⁺ , TEA ⁺ = calibration ions. The evaluation of the binding equilibrium constants between α -CD and investigated ions.	48
α -, β - and γ -CD	DE: LKB Tachophor 2127 C: 400 mm \times 0.5 mm I.D. or 520 mm \times 0.5 mm I.D. LE: 5 mM HCl + EACA (pH 4.3–4.8) or β -Ala (pH 3.5–4.0), 0.2% HPMC TE: 5 mM MES or <i>n</i> -CA	Related penicillins (sulbactam, its synthetic intermediates and alkaline degradation product)	Comparative measurements with D-glucose and starch were carried out to confirm the role of the cyclic structure of CD for separation improvement. The most important factors are: CD ring diameter, pH and CD concentration in LE.	51
α -, β - and γ -CD	DE: LKB Tachophor 2127 C: 400 mm \times 0.5 mm I.D. LE: 5 mM HCl, EACA (pH 4.7), 0.2% HPMC TE: 5 mM MES	<i>o</i> -, <i>m</i> -, <i>p</i> -Halogenobenzoic acids: F-, Cl-, Br- and I-	The dependence of (h_i) _{rel} values on the concentration of CDs, CD cavity diameter and size of substituents was demonstrated.	52
β -CD	DE: LKB Tachophor 2127 C: 400 mm \times 0.5 mm I.D. LE: I, 5 mM sodium acetate, acetic acid (pH 5.5), 0.2% HPMC; II, 5 mM HCl, His (pH 5.0), 0.2% HPMC TE: I, 10 mM EACA; II, 5 mM MES	Naftidrofuryl and its synthesis intermediates positional isomers	The study of axial and equatorial inclusion complex formation in both cationic and anionic ITP mode. The possibility of quantitative evaluation and purity control of final substances is demonstrated.	53
β -CD, diMe- β -CD, triMe- β -CD	DE: LKB Tachophor 2127 C: 370 mm \times 0.5 mm I.D. or 250 mm \times 0.5 mm I.D. LE: I, 5 mM sodium acetate, acetic acid (pH 5.48), 0.2% HEC; II, 5 mM Ba(OH) ₂ , Val (pH 9.69), 0.2% HEC TE: I, 10 mM β -Ala; II, 20 mM Tris	Ephedrine alkaloid enantiomers	Chiral ITP resolution of pseudoephedrine is demonstrated. The dependence of the chiral resolution quality on the type and concentration of CD was studied.	21

TABLE IV (continued)

<i>Pseudophases</i>	<i>Conditions</i>	<i>Compounds separated</i>	<i>Notes</i>	<i>Refs.</i>
β -CD, diMe- β -CD	DE: LKB Tachophor 2127 C: 370 mm \times 0.5 mm I.D. LE: 5 mM sodium acetate, acetic acid (pH 5.5), 0.2% HEC TE: 10 mM β -Ala	Ketotifen and its polar intermediate	The discovery of ketotifen enantiomers; the dependence of maximum racemate loads on the type and concentration of CD in the LE was studied. The possibility of ketotifen's quantitative evaluation is confirmed by statistically processed calibration data.	54
α , β - and γ -CD, diMe- β -CD, triMe- β -CD	DE: LKB Tachophor 2127 C: 230 mm \times 0.5 mm I.D. or 370 mm \times 0.5 mm I.D. LE: 5 mM HCl + His (pH 6.4), 0.4% HEC TE: 10 mM HEPES + Tris (pH 8.3)	17 bile acids	The study of solubilization and structural differentiation effect on CDs.	106
18-crown-6	DE: LKB Tachophor 2127 C: 200 mm \times 0.8 mm I.D. LE: 10 mM HCl TE: 10 mM Tris or TBAC	Li ⁺ , Na ⁺ , K ⁺ , Rb ⁺ , Cs ⁺ , NH ₄ ⁺ and lysine	The simultaneous determination of metal ions in 18-crown-6-modified LE. Simplified mathematical model for the evaluation of stability constants for 1:1 crown-metal complexes is presented. The monitoring of lysine neutralization with KOH was performed.	56,57
18-crown-6	DE: non-commercial LE: CsNO ₃ , HNO ₃ (pH 4.4-4.5) 0.05% PVA TE: 5 mM acetic acid	Na ⁺ , K ⁺ , Cs ⁺ , Ca ²⁺ , Sr ²⁺ , Ba ²⁺ , Pb ²⁺ , Al ³⁺	The method for metal ion analysis in glass is demonstrated.	58

phase does not migrate and acts simply as a pseudostationary phase. This experimental arrangement is advantageous especially for the separation of rapidly migrating organic ions. The deliberate use of micellar and enantioselective metal-complex pseudophases for the improvement of separation has not been reported.

Crown ethers were utilized for the selective retardation of inorganic ions, especially for the differentiation of alkaline and alkaline-earth metals.

Cyclodextrins seem to be useful especially in the area of structurally related organic compounds and also inorganic anions. In ITP the cyclodextrins are free in the solution and therefore inclusion complex formation should be the main resolution mechanism. The increasing number of cyclodextrin derivatives, which are commercially available, greatly extend the application area of ITP to organic isomeric compounds, including enantiomers, in their cationic as well as anionic forms. Several other parameters affect the resolution, such as the concentration of the pseudophase, pH value and type of counter ion. The possible applications of ionophore pseudophases are summarized in Table IV.

5. CONCLUSIONS

The use of various pseudophases in EMMs represents one of the most promising approaches to increasing the resolution power of the latter and the extension of their applications especially to organic molecules. The application of new types of pseudophases is determined by the rapid progress in the theory of inclusion and micellar phenomena and steadily increasing number of suitable carrier molecules and tenzides.

The utilization of pseudophases enables the introduction of another important factor which may contribute to improvement in separations. The experience with micellar pseudophases has enabled to the applicability of electromigration methods to be extended to uncharged organic molecules. The use of inclusion pseudophases significantly improves the differentiation of structurally related organic solutes. There is no sharp boundary between micellar and inclusion pseudophases. It was experimentally confirmed that derivatized cyclodextrins form organized systems in aqueous solutions and thus may act also as micellar pseudophases.

The use of optically active pseudophases is the only way of separating enantiomers. Promising results with cyclodextrins in ITP has demonstrated their usefulness as chiral discriminators for the separation of aromatic solutes. Copper–amino acid complexes were utilized for the separation of various α -amino acids in capillary electrophoresis. New possibilities exist for the use of newly synthesized chiral crown ethers and chiral micellar systems in high-performance electromigration methods.

SUMMARY

An overview of important trends in electromigration methods, with emphasis on development of highly efficient techniques and application of various complex-forming discriminators, is presented. The fundamental characteristics of micellar, inclusion and metal-complex pseudophases and their utilisation in high-performance electromigration methods are discussed in detail. Their advantages are demonstrated on numerous practical examples.

REFERENCES

- 1 D. W. Armstrong, *Sep. Purif. Methods*, 14 (1985) 213.
- 2 H. Michl, *Monatsh. Chem.*, 82 (1951) 489.
- 3 M. Lederer, *J. Chromatogr.*, 171 (1979) 403.
- 4 S. Hjertén, *Chromatogr. Rev.*, 9 (1967) 122.
- 5 F. E. P. Mikkers, F. M. Everaerts and T. P. E. M. Verheggen, *J. Chromatogr.*, 169 (1979) 11.
- 6 J. W. Jorgenson and K. DeArman Lukacs, *Anal. Chem.*, 53 (1981) 1298.
- 7 S. Hjertén, *J. Chromatogr.*, 270 (1983) 1.
- 8 F. M. Everaerts, J. L. Beckers and T. P. E. M. Verheggen, *Isotachophoresis*, Elsevier, Amsterdam, 1976.
- 9 J. L. Beckers and F. M. Everaerts, *J. Chromatogr.*, 51 (1970) 339.
- 10 Y. Walbroehl and J. W. Jorgenson, *J. Chromatogr.*, 315 (1984) 135.
- 11 S. Fujiwara and S. Honda, *Anal. Chem.*, 59 (1987) 487.
- 12 L. R. Sherman and J. A. Goodrich, *Chem. Soc. Rev.*, 14 (1985) 225.
- 13 A. S. Cohen and B. L. Karger, *J. Chromatogr.*, 397 (1987) 409.
- 14 A. Chrambach, in V. Neuhoff and A. Maelicke (Editors), *Advanced Methods in the Biological Science*, VCH Verlagsgesellschaft, Weinheim, 1985, Ch. 15, p. 177.

- 15 S. Hjertén and M.-D. Zhu, *J. Chromatogr.*, 346 (1985) 265.
- 16 T. Tsuda, K. Nomura and G. Nakagawa, *J. Chromatogr.*, 248 (1982) 241.
- 17 T. Tsuda, *J. High Resolut. Chromatogr. Chromatogr. Commun.*, 10 (1987) 622.
- 18 S. Terabe, K. Otsuka, K. I. Chikawa, A. Tsuchiya and T. Ando, *Anal. Chem.*, 56 (1984) 111.
- 19 H. Yoneda and T. Miura, *Bull. Chem. Soc. Jpn.*, 43 (1970) 574.
- 20 E. Gassmann, J. E. Kuo and R. N. Zare, *Science, (Washington, D.C.)*, 230 (1985) 813.
- 21 J. Snopek, I. Jelinek and E. Smolková-Keulemansová, *J. Chromatogr.*, 438 (1988) 211.
- 22 W. L. Hinze and D. W. Armstrong (Editors), *Ordered Media in Chemical Separation, ACS Symp. Ser.*, 342), American Chemical Society, Washington, DC, 1987.
- 23 D. W. Armstrong, *Am. Lab. (Fairfield, Conn.)*, 13 (1981) 14.
- 24 C. A. Burton, L. H. Gan, F. H. Hamed and J. R. Moffatt, *J. Phys. Chem.*, 87 (1983) 336.
- 25 M. Manabe, Y. Tanizaki and H. Watanabe, *Niihama Kogyo, Koto Semmon Gakko Kiyō, Rikogaku Hen*, 19 (1983) 50; *C.A.*, 98 (1983) 204875x.
- 26 G. S. Hartley, *Trans. Faraday Soc.*, 31 (1935) 31.
- 27 G. S. Hartley, *Q. Rev. Chem. Soc.*, 2 (1948) 152.
- 28 P. Mukerjee and J. R. Cardinal, *J. Phys. Chem.*, 82 (1978) 1620.
- 29 F. M. Menger, *Acc. Chem. Res.*, 12 (1979) 111.
- 30 F. M. Menger, J. M. Jerkunica and J. C. Johnston, *J. Am. Chem. Soc.*, 100 (1978) 4676.
- 31 F. M. Menger and B. J. Boyer, *J. Am. Chem. Soc.*, 102 (1980) 5936.
- 32 F. M. Menger and J. M. Bonicamp, *J. Am. Chem. Soc.*, 103 (1981) 2140.
- 33 F. M. Menger, K. S. Venkatasubban and A. R. Das, *J. Org. Chem.*, 46 (1981) 415.
- 34 P. Fromherz, *Chem. Phys. Lett.*, 77 (1980) 460.
- 35 K. A. Dill and P. J. Flory, *Proc. Natl. Acad. Sci. U.S.A.*, 77 (1980) 3115.
- 36 K. A. Dill and P. J. Flory, *Proc. Natl. Acad. Sci. U.S.A.*, 78 (1981) 676.
- 37 K. A. Dill, D. E. Koppel, R. S. Cantor, J. D. Dill, D. Bendedouch and S.-H. Chen, *Nature (London)*, 309 (1984) 42.
- 38 H. Wennerstrom and B. Lindman, *Phys. Rep.*, 52 (1979) 1.
- 39 H. F. Eicke, *Pure Appl. Chem.*, 53 (1981) 1417.
- 40 N. J. Muller, *J. Colloid Interface Sci.*, 63 (1978) 383.
- 41 Y. Walbroehl and J. W. Jorgenson, *Anal. Chem.*, 58 (1986) 479.
- 42 I. V. Berezin, K. Martinek and A. K. Yatsiminsky, *Russ. Chem. Rev.*, 42 (1973) 778.
- 43 E. Smolková-Keulemansová, *J. Chromatogr.*, 251 (1982) 17.
- 44 E. Smolková-Keulemansová and S. Krýsl, *J. Chromatogr.*, 184 (1980) 347.
- 45 D. Sybilska and E. Smolková-Keulemansová, in J. L. Atwood, J. E. D. Davies and D. D. Mac Nicol (Editors), *Inclusion Compounds*, Vol. 3, Academic Press, London, Orlando, San Diego, San Francisco, New York, Toronto, Montreal, Sydney, Tokyo, Sao Paulo, 1984, p. 173.
- 46 E. Smolková-Keulemansová, in D. Duchêne (Editor), *Cyclodextrins and Their Industrial Uses*, de Santé, Paris, 1987.
- 47 M. Tazaki, M. Takagi and K. Ueno, *Chem. Lett.*, 5 (1982) 639.
- 48 M. Tazaki, T. Hayashita, Y. Fujino and M. Takagi, *Bull. Chem. Soc. Jpn.*, 59 (1986) 3459.
- 49 N. Kuramoto, *Chem. Express*, 1 (1986) 343.
- 50 N. Kuramoto and K. Asao, *Osaka-Furitsu Kogyo Gijutsu Kenkyusho Hokoku* 88, (1986) 18, *C.A.*, 106, (1987) 188186z.
- 51 I. Jelinek, J. Snopek and E. Smolková-Keulemansová, *J. Chromatogr.*, 405 (1987) 379.
- 52 J. Snopek, I. Jelinek and E. Smolková-Keulemansová, *J. Chromatogr.*, 411 (1987) 153.
- 53 I. Jelinek, J. Dohnal, J. Snopek and E. Smolková-Keulemansová, *J. Chromatogr.*, 435 (1988) 496.
- 54 I. Jelinek, J. Snopek and E. Smolková-Keulemansová, *J. Chromatogr.*, 439 (1988) 386.
- 55 S. Terabe, H. Ozaki, K. Otsuka and T. Ando, *J. Chromatogr.*, 332 (1985) 211.
- 56 F. S. Stover, *J. Chromatogr.*, 298 (1984) 203.
- 57 F. S. Stover, *J. Chromatogr.*, 368 (1986) 476.
- 58 F. M. Everaerts and J. W. Venema, *Isotachophorese als Mogelijke Analyse Methode voor "Glasgemengen"*. Report, Technical University, Eindhoven, 1987.
- 59 F. M. Everaerts, personal communication.
- 60 S. Krýsl and E. Smolková-Keulemansová, *Chem. Listy*, 79 (1985) 919.
- 61 J. Szejtli, *Cyclodextrins and their Inclusion Complexes*, Akademiai Kiados, Budapest, 1982.
- 62 F. Cramer, *Einschlussverbindungen*, Springer, Berlin, Göttingen, 1954.
- 63 L. Mandelcorn, *Non-Stoichiometric Compounds*, Academic Press, New York, 1964.

- 64 M. L. Bender and M. Komiyama, *Cyclodextrin Chemistry*, Springer, Berlin, Heidelberg, New York, 1978.
- 65 K. Uekama and T. Irie, in D. Duchene (Editor), *Cyclodextrins and Their Industrial Uses*, de Santé, Paris, 1987.
- 66 K. Uekama, personal communication.
- 67 C. J. Pedersen, *J. Am. Chem. Soc.*, 89 (1967) 7017.
- 68 C. J. Pedersen, *J. Am. Chem. Soc.*, 92 (1970) 386.
- 69 C. J. Pedersen, *J. Am. Chem. Soc.*, 92 (1970) 391.
- 70 C. J. Pedersen and J. K. Frensdorf, *Angew. Chem.*, 84 (1972) 16.
- 71 M. Hiraoka, *Crown Compounds —their Characteristics and Applications*, Elsevier, Amsterdam, Oxford, New York (Russian translation, Moscow, Mir, 1986).
- 72 K. D. Pedersen and Ch. K. Frensdorf, *Usp. Khim.*, 42 (1973) 493.
- 73 N. K. Dalley, in R. M. Izatt and J. J. Christensen (Editors), *Synthetic Multidentate Macrocyclic Compounds*, Academic Press, New York, London, 1978, Ch. 4, p. 207.
- 74 L. R. Sousa, G. D. Y. Sogah, D. H. Hoffman and D. J. Cram, *J. Am. Chem. Soc.*, 100 (1978) 4569.
- 75 G. D. Y. Sogah and D. J. Cram, *J. Am. Chem. Soc.*, 101 (1979) 3035.
- 76 T. Shinbo, T. Yamaguchi, K. Nishimura and M. Sugiura, *J. Chromatogr.*, 405 (1987) 145.
- 77 V. A. Davankov and S. V. Rogozhin, *J. Chromatogr.*, 60 (1971) 280.
- 78 V. A. Davankov, S. V. Rogozhin, A. V. Semechkin and T. P. Sachkova, *J. Chromatogr.*, 82 (1973) 359.
- 79 V. A. Davankov, A. A. Kurganov and A. S. Bochkov, *Adv. Chromatogr.*, 22 (1983) 71.
- 80 P. Gozel, E. Gassmann, H. Michelsen and R. N. Zare, *Anal. Chem.*, 59 (1987) 44.
- 81 L. Ossicini and C. Celli, *J. Chromatogr.*, 115 (1975) 655.
- 82 S. Fanali and L. Ossicini, *J. Chromatogr.*, 212 (1981) 374.
- 83 S. Fanali, V. Cardaci and L. Ossicini, *J. Chromatogr.*, 265 (1983) 131.
- 84 S. Fanali, L. Ossicini and T. Prosperi, *J. Chromatogr.*, 318 (1985) 440.
- 85 S. Fanali, P. Masia and L. Ossicini, *J. Chromatogr.*, 403 (1987) 388.
- 86 S. Terabe, K. Otsuka and T. Ando, *Anal. Chem.*, 57 (1985) 834.
- 87 K. Otsuka, S. Terabe and T. Ando, *J. Chromatogr.*, 332 (1985) 219.
- 88 K. Otsuka, S. Terabe and T. Ando, *J. Chromatogr.*, 348 (1985) 39.
- 89 S. Terabe, H. Utsumi, K. Otsuka, T. Ando, T. Inomata, S. Kuze and Y. Hanaoka, *J. High Resolut. Chromatogr. Chromatogr. Commun.*, 9 (1986) 666.
- 90 D. E. Burton, M. J. Sepaniak and M. P. Maskarinec, *J. Chromatogr. Sci.*, 24 (1986) 347.
- 91 D. E. Burton, M. J. Sepaniak and M. P. Maskarinec, *Chromatographia*, 21 (1986) 583.
- 92 A. T. Balchunas and M. J. Sepania, *Anal. Chem.*, 59 (1987) 1466.
- 93 Z. Prusík, V. Kašička, S. Staněk, G. Kuncová, M. Hayer and J. Vrkoč, *J. Chromatogr.*, 390 (1987) 87.
- 94 S. Fujivara and S. Honda, *Anal. Chem.*, 59 (1987) 2773.
- 95 K. Otsuka, S. Terabe and T. Ando, *J. Chromatogr.*, 396 (1987) 350.
- 96 A. S. Cohen, S. Terabe, A. J. Smith and B. L. Karger, *Anal. Chem.*, 59 (1987) 1021.
- 97 M. J. Sepaniak and R. O. Cole, *Anal. Chem.*, 59 (1987) 472.
- 98 K. H. Row, W. H. Griest and M. P. Maskarinec, *J. Chromatogr.*, 409 (1987) 193.
- 99 K. Hattori, *Bio Ind.*, 4 (1987) 327; *C.A.*, 107 (1987) 167984p.
- 100 Y. Walbroehl, *Theoretical and Practical Aspects of Electrokinetic Separation Techniques in Open Tubular Capillaries*, Univ. Microfilms Int., Univ. North Carolina, Chapel Hill, NC, U.S.A.; Order No. DA 8628270, 1986; *C.A.*, 106 (1987) 108504p.
- 101 D. E. Burton, *Development and Application of Micellar Electrokinetic Capillary Chromatography*, Univ. Microfilms Int., Univ. Tennessee, Knoxville, TN, U.S.A.; Order No. DA 8713452, 1987; *C.A.*, 107 (1987) 171953v.
- 102 M. J. Sepaniak, D. E. Burton and M. P. Maskarinec, *ACS Symp. Ser.*, 342 (1987) 142.
- 103 J. H. Knox and I. H. Grant, *Chromatographia*, 24 (1987) 135.
- 104 A. S. Cohen, A. Paulus and B. L. Karger, *Chromatographia*, 24 (1987) 15.
- 105 R. A. Wallingford and A. G. Ewing, *Anal. Chem.*, 60 (1988) 258.
- 106 J. Snopek, E. Smolková-Keulemansová, I. Jelínek, J. Dohnal, J. Klinot and E. Klinotová, *J. Chromatogr.*, in press.

CHROM. 20 492

USE OF A DOUBLE-DETECTOR SYSTEM FOR THE MEASUREMENT OF MOBILITIES IN ZONE ELECTROPHORESIS

J. L. BECKERS, Th. P. E. M. VERHEGGEN and F. M. EVERAERTS*

Laboratory of Instrumental Analysis, Eindhoven University of Technology, P.O. Box 513, 5600 MB Eindhoven (The Netherlands)

SUMMARY

A double-detector system with which mobilities can be determined by capillary zone electrophoresis is described. Ionic species are detected by two detectors, mounted at a fixed distance from each other. In zone electrophoresis the velocity of an ionic species is proportional to its mobility. The time needed for an ionic species to pass both detectors is reversely proportional to that mobility, provided that the electric field strength is constant. From the ratio of the times required by a sample ionic species and a standard ionic species (with a known mobility) to pass from the first to the second detector, the mobility of the sample ionic species can be calculated. During the analyses parameters such as temperature, pH and ionic strength are constant, which simplifies the calculations substantially. From experiments with some standard ionic species, mobilities have been obtained comparable to those in the literature with a relative standard deviation of about 1%.

INTRODUCTION

Mobilities have often been determined with electrophoretic methods, such as isotachopheresis (ITP) and zone electrophoresis (ZE). In ITP, all ionic species migrate in their respective zones with an equal velocity v if the steady state has been reached. Hereby an electric field strength E is created, determined by their effective mobilities m according to

$$v = mE \quad (1)$$

Using a conductivity detector, an isotachopherogram will be obtained in which the step heights contain information concerning the conductivity of the zones and, from this, mobilities can be calculated. Because the pH, temperature and concentrations vary in the different zones, corrections for, *e.g.*, activities must be calculated in an iterative manner.

Several workers have successfully determined mobilities using ITP data^{1–7}. Although absolute mobilities and pK values could be calculated from thermometric ITP data, using the concept of the isoconductor⁸, it appeared to be more difficult to

obtain reproducible and accurate data using ITP conductivity data. Although a conductivity detector (a.c./d.c. mode) has superior qualities with regard to analytical applications, not pure zone conductivities but impedances are measured with a conductivity detector whereby, *e.g.*, double layers and the coating play an important part. Sometimes the step heights vary substantially on adding certain non-conducting surface-active additives whereas the zone conductivities can be considered to be nearly equal⁹.

In ZE, all ionic species also migrate with a velocity $v = mE$. If retention times are measured for ionic species ($t_{R,i}$) and a standard ionic species ($t_{R,Si}$) with a known mobility (m_{Si}), the effective mobilities (m_i) can be calculated by the following relation:

$$m_i = t_{R,Si} m_{Si} / t_{R,i} \quad (2)$$

assumed the E gradient to be constant. In this way ionic species can be identified in ZE.

In capillary ZE (CZE) the sample is often introduced by means of an injection valve or by dipping one end of the capillary tube in the sample solution, whereby the sample is introduced using a gravity flow or by electromigration*.

After sampling, in the first stage of the ZE separation process the sample concentration must be adjusted to that of the background electrolyte by means of a moving boundary procedure. An advantage of this procedure is that diluted sample solutions will be concentrated¹¹. However, after this procedure the sample ought to be eluted by the background electrolyte until a nearly constant E gradient is created. Only from this moment can we really speak of zone electrophoresis and only from this moment can we use the retention times properly. Because this first stage in CZE can last tens of seconds, retention times measured from the beginning of the analysis often differ considerably¹² and inaccurate mobilities can result.

In order to cope with these problems, the use of a so-called double-detector system (DDS) is introduced in this paper, with which mobilities can be determined and ionic species can be identified. Using a DDS it is only of importance that at the time of detection, for both detectors, all components are separated and migrate zone electrophoretically. By detecting the zones with two detectors mounted at a fixed distance from each other, the mobilities can be determined related to a standard ionic species by

$$m_i = m_{Si} t_{Si} / t_i \quad (3)$$

where t_{Si} and t_i are the times required by the standard and sample ionic species to migrate from the first to the second detector.

* It must be borne in mind that in electromigration the sample introduced does not have the same composition as the original sample solution, because this sample introduction follows a moving boundary procedure¹⁰. By applying electroosmotic flow this effect is often negligible.

THEORETICAL

In order to optimize the positions of the measuring electrodes of a ZE apparatus we simulated the ZE process for the separation of four cations by means of a numerical solution of the basic transport equation:

$$\frac{dc}{dt} = - \frac{d(mEc)}{dx} + D \cdot \frac{d^2c}{dx^2} \quad (4)$$

where c is the concentration of the ionic species and x is the position in the separation tube.

The electric field strength was calculated from the electric current density i by

$$i = E \sum_j c_j m_j F \quad (5)$$

whereby F is the Faraday constant. The conditions of the simulation are given in Table I. The values for the capillary diameter, electric current and mobilities of the background electrolyte ionic species are chosen arbitrarily.

The diffusion constant D was calculated using the equation¹³

$$D = mkT/ez \quad (6)$$

where k is the Boltzmann constant, T is the absolute temperature and ez is the charge of the ionic species.

Concentration effect of the sample

In order to concentrate the sample in a narrow band, a very dilute sample (0.00025 M) is introduced into the capillary tube over a length of 8 mm. The concentration effect of the sample was simulated and shown in Fig. 1 for one of the sample ions, K^+ , after 0.1 and 1.0 s.

It can be clearly seen that a concentration by a factor of about 10 occurs,

TABLE I
CONDITIONS FOR THE SIMULATION OF A ZONE ELECTROPHORETIC SEPARATION
Electric current, 20 μA ; capillary diameter, 0.25 mm I.D.

Species	Ion	Concentration (M)	Mobility ($10^5 \text{ cm}^2/V \cdot s$)
Background electrolyte	M^+	0.01	30
	X^-	0.01	20
Sample ions	K^+	0.00025	76.2
	Na^+	0.00025	51.9
	Li^+	0.00025	40.1
	TEA^+	0.00025	33.0

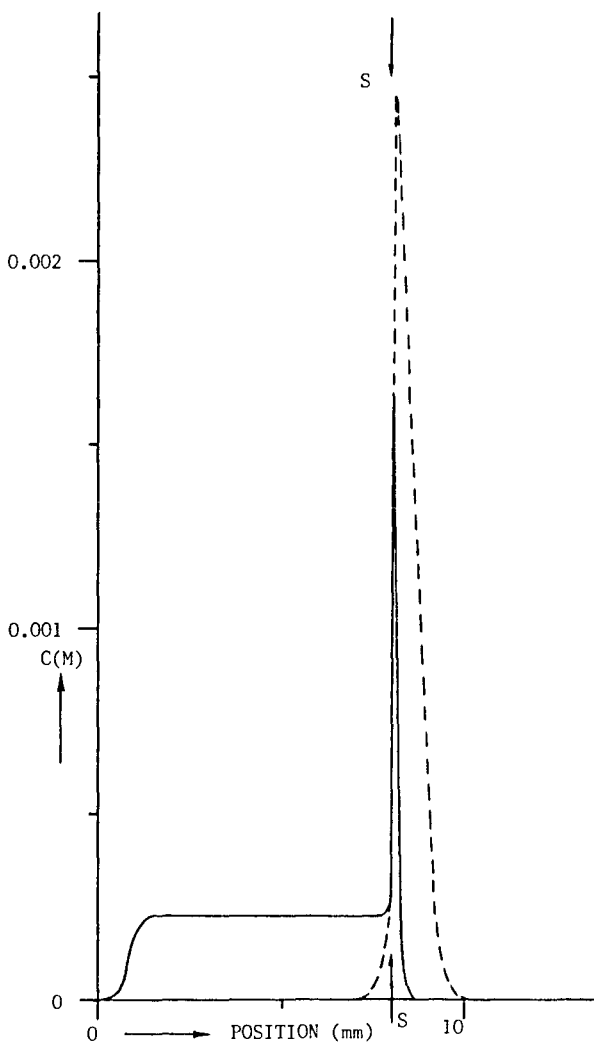


Fig. 1. Concentration effect for one of the ionic species (K^+) in the sample in the zone electrophoretic simulation. The sample is introduced at a concentration of $0.00025 M$ and is concentrated to about $0.0025 M$ beyond the sampling point S . The concentration profiles are given after 0.1 and 1 s (dotted line) of the separation. On the horizontal axis the position in the capillary tube is given (in mm), the original position of sampling being between 0 and 8 mm.

which means that the sample band will be about 0.8 mm in length. It is remarkable that the concentration effect occurs beyond the position of injection S , which means that a large E gradient exists at the position of sampling according to Kohlrausch's law. For this reason a larger diameter in our apparatus was chosen at the position of sampling in order to decrease this effect. Further, the concentration profiles (see Fig. 1) are diffuse at the front side and steep at the rear side as the sample ionic species have a higher mobility than the background electrolyte ionic species M^{+11} .

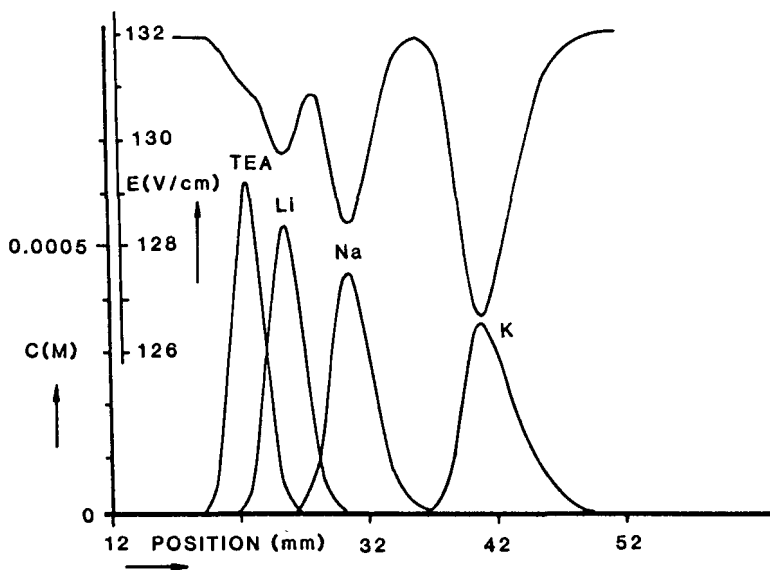


Fig. 2. Concentration profiles and E gradient for the simulation of a zone electrophoretic separation of four cations after 36 s. On the horizontal axis the position in the capillary tube is given in mm. The original position of sampling lies between 0 and 8 mm.

Length of the capillary tube

Because the length of the capillary tube must be chosen in such a way that all ionic species migrate in a zone electrophoretic way (*i.e.* the E gradient must be constant within, *e.g.*, 1%), the minimal distance between the sampling point and first detector was determined by means of a simulation. In Figs. 2 and 3 the concentration

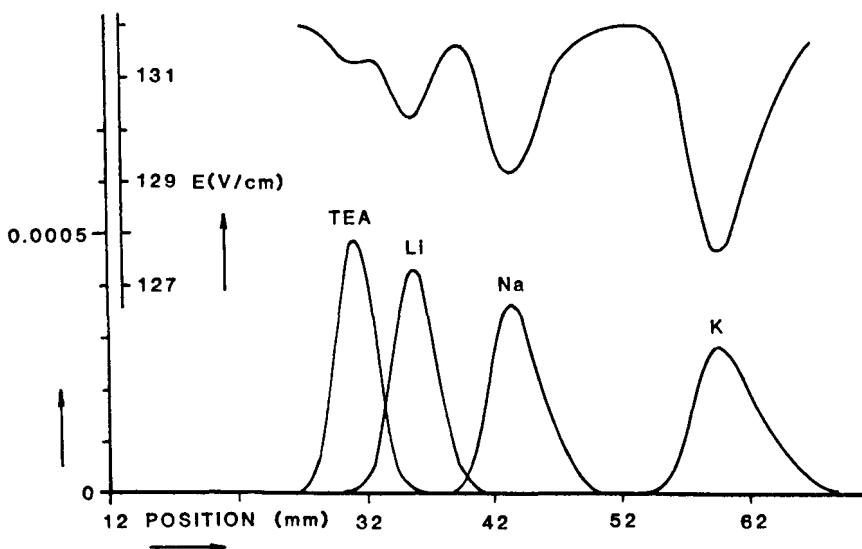


Fig. 3. Concentration profiles and E gradient for the simulation of a zone electrophoretic separation of four cations after 55 s. See Fig. 2 for further details.

profiles and E gradient as a function of the position in the capillary tube after 36 and 55 s are given (see Table I). It must be noted that although the last two zones are almost separated, the E gradient shows only a slight indication of the presence of two ionic species. Further, the K^+ zone shows a large difference in E gradient although its concentration is the lowest of the four cations. This means that the E gradient is strongly dependent on both the concentrations in the zones and the difference between the mobilities of the ionic species and the background ions.

From Figs. 2 and 3 it can be concluded that by about 3 cm from the sampling point (at position 38) all sample ionic species have been separated.

EXPERIMENTAL

In order to examine the utility of the principle of the DDS, analyses were performed with a separation and detection unit constructed as described elsewhere¹⁴. The capillary tube has an I.D. of 0.25 mm and contains three sets of measuring electrodes. The distance from the sampling point to the first electrode set is about 3 cm and the distances between the electrode sets are about 10 mm. The sample is introduced into a broadened part (0.55 mm I.D.) of the capillary tube. The sampling volume is about 2.4 μ l.

In the electrode compartments the electrolyte solution contacts Pt-Ir electrodes. For detection we used a.c. electronics¹⁵, which appears to be sufficiently stable at low noise levels¹¹. For the determination of mobilities we used the described apparatus with all valves closed so that the linear electroendosmotic flow would be eliminated. Using an open capillary tube, usually with very narrow bore capillaries, the determined velocity of the ionic species will be the sum of the electric field strength-induced velocity and the electroendosmotic flow velocity.

RESULTS

The apparatus was constructed in order to check if mobilities can be measured with sufficient accuracy. The separation capability is small because of its dimensions. Therefore, separations can be carried out of about four ionic species that have sufficient differences in their mobilities such as K^+ , Na^+ , Li^+ and TEA^+ for cation separations. Chloride, formate, acetate, propionate and *p*-aminobenzoate were chosen for the anion separations. For dilute samples good separations could be obtained, even at the first detector.

For both anion and cation separations we used as a background electrolyte a solution of 0.01 *M* morpholinoethane sulphonic acid (MES) and 0.02 *M* histidine at pH 6.4. The mobilities of the ions in this solution are low, so a large E gradient can be obtained at a low current density. All experiments were carried out at a constant electric current of 10 μ A.

For the experiments we used the first and the third electrode set (both equipped with a.c. measuring electronics) as the DDS. The E gradient was measured with d.c. potential gradient electronics connected to the second set.

In the first instance we measured the effect of the concentration of the sample ions. Symmetric peaks could be obtained for concentrations of about 10^{-5} *M* and lower. At these concentration levels it could be concluded from the second detector

TABLE II

MIGRATION TIMES AND CALCULATED "ABSOLUTE" MOBILITIES FOR THE CATIONS K^+ , Na^+ , Li^+ AND TEA^+ USING THE DDS

Migration time* (mm)				Calculated mobility ($10^5 \text{ cm}^2/V \cdot s$)			
K^+	Na^+	Li^+	TEA^+	K^+	Na^+	Li^+	TEA^+
36.3	53.7	68.7	82.2	76.78	51.90	40.57	33.91
36.5	53.7	68.0	82.4	76.36	51.90	40.99	33.82
36.0	52.7	67.9	81.4	75.98	51.90	40.28	33.60
43.7	63.5	82.5	99.3	75.42	51.90	39.95	33.19
43.2	63.7	82.2	99.3	76.53	51.90	40.22	33.29
43.2	63.0	82.2	99.0	75.69	51.90	39.78	33.03
43.4	63.2	82.5	99.2	75.75	51.90	39.76	33.07
41.3	60.3	77.3	92.8	75.78	51.90	40.49	33.72
40.5	59.9	76.3	91.2	76.76	51.90	40.74	34.09
41.3	59.2	76.8	91.8	74.39	51.90	40.01	33.47
35.2	52.2	67.8	82.4	76.97	51.90	39.96	32.88
36.1	53.9	69.5	84.5	76.20	51.90	39.58	32.55
35.1	51.7	67.8	82.1	76.45	51.90	39.58	32.68
35.5	52.4	66.8	80.7	76.61	51.90	40.71	33.70

* Required to pass from the first to the second detector, taken from the electropherograms in millimeters.

that the fluctuations in the E gradient were less than about 1.5% for the most mobile ionic species K^+ and even less for the others.

In the Tables II and III the migration times (in mm) required to pass the DDS are given for both cations and anions. Of course, using a DDS, retention times are of no importance.

TABLE III

MIGRATION TIMES AND CALCULATED "ABSOLUTE" MOBILITIES FOR THE ANIONS CHLORIDE (I), FORMATE (II), ACETATE (III), PROPIONATE (IV) AND p -AMINO-BENZOATE (V) USING THE DDS

Migration time (mm)					Calculated mobility ($10^5 \text{ cm}^2/V \cdot s$)				
I	II	III	IV	V	I	II	III	IV	V
40.3	56.4	76.5	88.5	104.8	78.68	56.22	41.45	35.83	30.26
42.9	59.0	80.6	94.0	111.2	77.88	56.62	41.45	35.54	30.04
43.4	59.9	82.0	95.0	112.0	78.32	56.74	41.45	35.78	30.35
43.0	59.3	82.0	94.8	113.0	79.04	57.32	41.45	35.85	30.08
42.2	59.0	81.3	94.2	110.8	79.86	57.12	41.45	35.77	30.41
42.7	59.0	81.5	93.5	111.2	79.11	57.26	41.45	36.13	30.38
41.8	56.8	79.0	90.8	107.8	78.34	57.65	41.45	36.06	30.38
42.4	58.5	81.2	93.7	110.7	79.38	57.53	41.45	35.92	30.40

TABLE IV

MOBILITIES DETERMINED BY THE USE OF A DDS IN ZONE ELECTROPHORESIS

The values for the cations and anions are averages from 14 and 8 experiments, respectively (see Tables II and III). For literature values, see refs. 4 and 13.

Ionic species	Average mobility ($10^5 \text{ cm}^2/\text{V} \cdot \text{s}$)			Standard deviation ($10^5 \text{ cm}^2/\text{V} \cdot \text{s}$)
	Measured	After correction for pH	From literature	
K^+	76.12	76.12	76.2	0.66
Na^+	51.90	51.90	51.9	0.00
Li^+	40.19	40.19	40.1	0.44
TEA^+	33.36	33.36	—	0.46
Chloride	78.83	78.83	79.1	0.60
Formate	57.06	57.23	56.6	0.46
Acetate	41.45	42.40	42.4	0.00
Propionate	35.86	36.96	37.1	0.17
<i>p</i> -Aminobenzoate	30.29	31.29	31.6	0.14

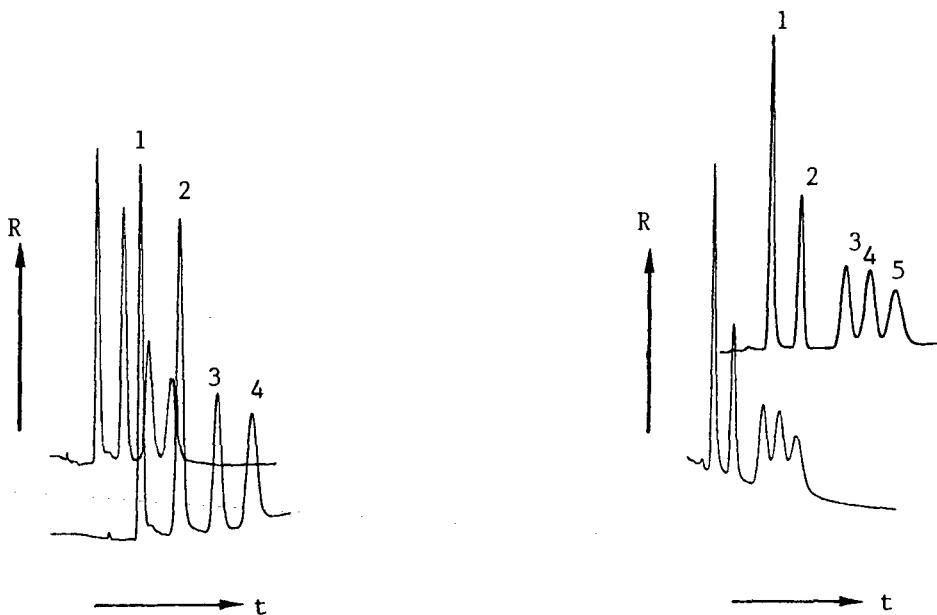


Fig. 4. A zone electropherogram for the separation of the four cations, (1) K^+ , (2) Na^+ , (3) Li^+ and (4) TEA^+ (tetraethylammonium), with the use of a DDS. The detector response R correlates with increasing conductivity.

Fig. 5. A zone electropherogram for the separation of five anions, (1) chloride, (2) formate, (3) acetate, (4) propionate and (5) *p*-aminobenzoate, using a DDS. The detector response R correlates with increasing conductivity.

In practice, the "effective mobilities" measured, are related to the absolute mobilities by

$$m_{\text{eff},i} = \alpha_i \gamma_i m_{0,i} \quad (7)$$

where $m_{\text{eff},i}$ is the effective mobility, α_i is the dissociation constant, γ_i is the activity coefficient and $m_{0,i}$ is the absolute mobility. In order to calculate the effective mobilities of all ionic species from the migration times using eqn. 3, we have to know the effective mobility of one of the ionic species, which can be considered as a standard. For the cation separations Na^+ and for the anion separations acetate ions were taken as standards.

In a zone electrophoretic system (*i.e.*, at constant ionic strength, pH and temperature) for monovalent, fully ionized species the activity coefficients and dissociation constants can be considered to be equal. This means that using the absolute mobility of the standard ionic species (eqn. 3) the absolute mobility of the sample ionic species can be obtained at that temperature.

Further, all ionic species show a very similar dependence of their absolute mobilities on temperature (about 2% per °C). Therefore, using the absolute mobility of the standard at 25°C, the absolute mobilities at 25°C of the sample ionic species can be obtained. To check this, the first experiments were carried out with the apparatus thermostated at 25°C. The results were identical with and without thermostating.

For weak anions we used as the standard acetic acid ($\text{p}K_a = 4.756$) and calculated its mobility with a correction for the pH. The calculations of "absolute" mobilities obtained in this way are given in the Tables II and III. It is remarkable that, although the migration times differ considerably, the calculated mobilities fit very well. Differences in migration time can be caused by pressures in the system due to the use of syringes to introduce the sample and background electrolyte. Using a peristaltic pump or gravity flow to fill the compartments more constant migration times were obtained.

In Table IV the average determined "absolute" mobilities are compared with those in the literature. For the weak anions a correction was made for the influence of the pH of the system.

In Figs. 4 and 5 examples of zone electrophorograms are given for a cation and an anion separation, respectively, obtained with the DDS.

CONCLUSION

Using a DDS in CZE, ionic mobilities can be determined with values comparable to those given in the literature with a relative standard deviation of about 1%. A great advantage over the ITP determination of mobilities is that in CZE parameters such a temperature, pH and ionic strength are nearly constant, which simplifies substantially the calculations. The question of whether a DDS can be used for identification in ZE depends on the stability and sensitivity of the measuring electronics, especially with the use of longer capillary tubes. Of course, a double-beam laser or a double-beam UV system can be used as a DDS.

REFERENCES

- 1 Y. Kiso and T. Hirokawa, *Chem. Lett.*, (1979) 891.
- 2 T. Hirokawa and Y. Kiso, *J. Chromatogr.*, 252 (1982) 33.
- 3 T. Hirokawa, M. Nishine and Y. Kiso, *J. Chromatogr.*, 252 (1982) 49.
- 4 T. Hirokawa, M. Nishino, N. Aoki, Y. Kiso, I. Sawamoto, T. Yagi and J.-I. Akiyama, *J. Chromatogr.*, 271 (1983) D1-D106.
- 5 J. Pospíchal, M. Deml, Z. Žemlová and P. Boček, *J. Chromatogr.*, 320 (1985) 139.
- 6 J. Pospíchal, M. Deml and P. Boček, *J. Chromatogr.*, 390 (1987) 17.
- 7 I. Hoffmann, R. Muenze, I. Dreyer and R. Dreyer, *J. Radioanal. Chem.*, 74 (1982) 53.
- 8 J. L. Beckers, *J. Chromatogr.*, 320 (1985) 147.
- 9 F. M. Everaerts and P. J. Rommers, *J. Chromatogr.*, 91 (1974) 809.
- 10 Z. Deyl (Editor), *Electrophoresis—A Survey of Techniques and Applications, Part A: Techniques*, Elsevier, Amsterdam, 1979, p. 155.
- 11 F. E. P. Mikkers, F. M. Everaerts and Th. P. E. M. Verheggen, *J. Chromatogr.*, 169 (1979) 1.
- 12 F. E. P. Mikkers, F. M. Everaerts and Th. P. E. M. Verheggen, *J. Chromatogr.*, 169 (1979) 11.
- 13 P. W. Atkins, *Physical Chemistry*, Oxford University Press, Oxford, 1981.
- 14 Th. P. E. M. Verheggen, J. L. Beckers and F. M. Everaerts, 452 (1988) 615.
- 15 F. M. Everaerts, J. L. Beckers and Th. P. E. M. Verheggen, *Isotachopheresis, Theory, Instrumentation and Applications*, Elsevier, Amsterdam, 1976.

CHROM. 20 668

CAPILLARY ZONE ELECTROPHORESIS

QUANTITATIVE STUDY OF THE EFFECTS OF SOME DISPERSIVE PROCESSES ON THE SEPARATION EFFICIENCY

F. FORET, M. DEML and P. BOČEK*

Institute of Analytical Chemistry, Czechoslovak Academy of Sciences, Leninova 82, CS-611 42 Brno (Czechoslovakia)

SUMMARY

The contributions of diffusion, Joule heating, sampling and electroosmotic flow to the dispersion of zones separated by capillary zone electrophoresis were evaluated theoretically and verified experimentally. The theoretical model predicts that an optimum electric field strength, E , exists at which the number of theoretical plates, N , is a maximum. Both open and closed capillaries were considered and a simple formula was derived for the calculation of a maximum with a given experimental arrangement. The theoretical efficiency curves, N vs. E , were calculated and compared with those obtained experimentally in capillaries of various I.D.'s and filled with background electrolytes of various conductivities. The possibilities of minimization of some dispersion factors are discussed.

INTRODUCTION

Capillary zone electrophoresis (CZE) is one of the most rapidly developing electrophoretic techniques. Its most attractive feature is the simplicity of the experimental arrangement and the speed and efficiency of the separation. For the quantitative description of the separation efficiency, the concept of the number of theoretical plates has been proposed¹ and is currently used in a similar way as in chromatography. The number of theoretical plates, N , depends on the working conditions, the electric field strength, E , being of key importance since it controls the migration velocity. Jorgenson and Lukacs² regarded diffusion as the exclusive dispersion factor and obtained a linear dependence of N on the voltage, V , across the capillary. For low values of E the theoretical and experimental data are in good agreement. Several authors³⁻⁶, however, have reported the existence of a maximum in the experimental dependence of N vs. V and tried to explain it in a qualitative way by means of the Joule heat effects.

In gel electrophoresis, the theory concerning the dispersion due to temperature gradients and the prediction of the existence of such maxima has been published and

verified experimentally⁷. In CZE, the theory concerning the Joule heat effects was published many years ago⁸, however no comparison of the theoretical and experimental curves, $N = f(E)$, has been published till now.

The theory and discussion given here accounts for the dispersion caused by diffusion, the initial sample pulse width, the Joule heat and the electroosmotic flow in both open and closed capillaries of various I.D.'s. Moreover, a new relationship has been derived which describes the maximum in the curve of $N = f(E)$ and thus the optimum working conditions for a separation.

THEORETICAL

Plate numbers

The electrophoretic separation of ionic substances is based on their different speeds of migration in an electrolyte column across which an electric voltage is applied. During this process the zones of the various substances are not only separated but they are also continually broadened due to a series of dispersive factors, e.g., diffusion, convection, etc.

To obtain good separation of two substances with similar mobilities, minimization of the dispersion is of key importance. For the description of the separation efficiency the number of theoretical plates was introduced¹ as

$$N = L^2/\sigma^2 \quad (1)$$

where L is the migration distance and σ^2 is the variance of the concentration distribution in the zone.

The number of theoretical plates required for the complete separation (resolution, $R = 1$) of two separands is¹

$$N_{\text{req}} = 16 \cdot \frac{1}{(\Delta v/\bar{v})} \quad (2a)$$

where Δv is the difference in their migration velocities and \bar{v} is their average velocity. If the movement of a separand is caused only by electromigration, then eqn. 2a can be written in the form

$$N_{\text{req}} = 16 \cdot \frac{1}{(\Delta u/\bar{u})} \quad (2b)$$

where Δu is the difference in their effective mobilities and \bar{u} is their average mobility.

The variance (total) can be assumed to be the sum of the variances due to particular sources of dispersion

$$\sigma^2 = \sigma_I^2 + \sigma_D^2 + \sigma_E^2 + \sigma_T^2 + \sigma_{E_0}^2 + \sigma_0^2 \quad (3)$$

where the right-hand terms represent the contributions of injection, diffusion, electromigration, temperature profiles due to Joule heat, electroosmosis and other effects, respectively.

Except for σ_1^2 , the variances are directly proportional to the analysis time, the constants of proportionality being the respective dispersion coefficients, D_i . The total variance of the sample distribution is expressed by the relationship

$$\sigma^2 = \sigma_1^2 + 2t \sum_i D_i \quad (4)$$

where t is the migration time. It can be expressed as

$$t = L/v \quad (5)$$

where v is the velocity of the respective migrating zone.

The first four terms on the right-hand side of eqn. 3 represent the effects inherent to the principle of the method and can never be suppressed to zero; however, their influence upon the separation efficiency can be controlled by appropriate design of the instrument and selection of the working conditions.

Dispersion effects

(i) The injection term is related to the shape of the initial sample pulse. In an ideal case, the sample is introduced into the separation capillary as a rectangular pulse. For a sample pulse of width l , the input variance is constant^{8,9}:

$$\sigma_1^2 = l^2/12 \quad (6)$$

In order to obtain highly efficient separation, in practice it is necessary to keep the width of the initial sample pulse smaller than 1% of the length of the separation capillary.

(ii) The diffusion term in eqn. 3 can be calculated from the Einstein equation

$$\sigma_D^2 = 2D_D t \quad (7)$$

where D_D is the diffusion coefficient.

(iii) Electromigration dispersion is related to changes in the local electric field strength in the migrating zone with respect to that in the background electrolyte¹⁰. It can be minimized by decreasing the difference between the mobility of the separand and that of the background electrolyte constituent of the same sign, or by decreasing the concentration in the separated zones. Usually the electromigration dispersion is negligible when the concentration of the separated ions is more than two orders of magnitude lower than that of the background electrolyte¹⁰. In such a case the use of extremely sensitive detectors is necessary.

(iv) The Joule heat affects the dispersion of zones via the effects of the temperature gradients formed. The capillary is cooled only on its outer surface and the temperature difference between the solution in the centre and the inner wall can be several degrees even in very narrow capillaries. Since the mobility of most ions increases by 2% per 1 K, ions located near the wall of the capillary move slower than those in the centre and the migrating zone broadens. The dispersion caused by this

temperature effect increases with increasing Joule heat and, thus, with the voltage applied across the capillary. The exact temperature profile in the tubular column can be described by Bessel functions¹¹, however, it can be closely approximated by simple parabolic functions^{12,13}.

For such a case the dispersion coefficient due to the Joule heat can be expressed in the form⁸

$$D_T = \frac{\kappa^2 \delta^2 u^2 E^6 R^6}{3072 D \lambda_T^2} \quad (8)$$

where κ is the conductivity of the background electrolyte, δ the temperature coefficient of the mobility of the separand, R the radius of the separation capillary, D the diffusion coefficient of the separand and λ_T the thermal conductivity of the background electrolyte.

(v) The effects of electroosmosis on the performance of CZE can be described as follows. Between the inner wall of the capillary and the electrolyte solution an electric double layer is always formed which can be characterized by its zeta potential and which is manifested by electroosmotic movement of the liquid in the capillary when an electric field is applied. The velocity of this flow is proportional to the zeta potential according to the Helmholtz–Smoluchowski equation

$$v = -\frac{\varepsilon \zeta E}{\eta} \quad (9)$$

where ε is the permittivity of the solvent, ζ the zeta potential and η the viscosity of the background electrolyte. With respect to the effects of electroosmosis upon the dispersion and migration of zones, two cases must be distinguished:

Open capillary. In the case of a capillary with open ends and a constant zeta potential along its axis, the electroosmotic flow has almost a piston character and its contribution to the dispersion of the migrating zone is small^{14–16}. Thus, especially for low electroosmotic velocities, $D_{E_0} \rightarrow 0$. However, the analysis time is strongly influenced by electroosmosis in this case.

The migration velocity of a zone is given by the sum of the electrophoretic migration and the electroosmotic flow

$$v = (u + u_{E_0})E \quad (10)$$

where u_{E_0} represents the constants on the right-hand side of eqn. 9, *i.e.*

$$u_{E_0} = -\frac{\varepsilon \zeta}{\eta} \quad (11)$$

Hence, in open capillaries, the electroosmosis can contribute only to the transport of separands by either increasing or decreasing the overall migration velocity according to the sign of the zeta potential. However, in the case of non-uniformly charged walls of the capillary, local turbulences can occur causing irreproducible dispersion¹⁷.

Closed capillary. In the case of a closed capillary, *e.g.*, by a semipermeable membrane, the electroosmotic flow near the wall of the capillary is balanced by the opposite flow in the centre, causing continual dispersion of the sample zone during the migration¹⁸. The dispersion coefficient due to the electroosmotic flow in a closed capillary can be expressed in the form⁸:

$$D_{E_0} = 1/48 \cdot \frac{R^2 \varepsilon^2 \zeta^2 E^2}{D \eta^2} \quad (12)$$

Separation efficiency vs. electric field strength

As mentioned above, the cases of open and closed capillaries must be clearly distinguished.

Open capillary. After the substitution of the respective dispersion coefficients ($D_{E_0} = 0$) and rearrangement of eqn. 1, one obtains

$$N = \frac{A_1 E}{B_1 E^6 + F_1 E + H_1} \quad (13)$$

where $A_1 = 1536(u + u_{E_0})LD\lambda_T^2$, $B_1 = \delta^2 \kappa^2 u^2 R^6$, $F_1 = 128 D \lambda_T^2 l^2 (u + u_{E_0})/L$ and $H_1 = 3072 D^2 \lambda_T^2$.

The electric field strength at the maximum of efficiency ($\partial N / \partial E = 0$) is:

$$E_{\max} \approx 2.92 \sqrt[3]{\frac{D \lambda_T}{\delta \kappa u}} \cdot \frac{1}{R} \quad (14)$$

The maximum efficiency for $l \Rightarrow 0$ is then

$$N_{\max} \approx 0.82(u + u_{E_0}) \frac{L}{R} \sqrt[3]{\frac{\lambda_T}{D^2 \delta \kappa u}} \quad (15)$$

which represents the maximum theoretical efficiency accessible for a given capillary, background electrolyte and separand mobility. Obviously, the higher is u_{E_0} the higher is N_{\max} . However, in this case, N_{req} is given by

$$N_{\text{req}} = 16 \cdot \frac{u + u_{E_0}}{\Delta u} \quad (16)$$

and the ratio N_{\max}/N_{req} is independent of u_{E_0} . Hence, in open capillaries, the electroosmotic flow will displace the efficiency curves upwards, but the higher plate numbers thus obtained are not effective for the separation, since all migrating zones, together with the background electrolyte, are transported only along the capillary¹⁹. The mutual separation of zones is based on the relative difference in effective mobilities.

Closed capillary. Closed capillaries prevent hydrodynamic movement of the solutions inside, and, thus, no care need be taken about the levels of the solutions in the electrolyte chambers. As the electroosmotic flow does not contribute to the transport of the separand, the migrating time is determined only by the electrophoretic mobility of the separand. On the other hand, electroosmosis contributes to the dispersion of the moving zone with the dispersion coefficient expressed by eqn. 12. The resulting expression for the separation efficiency in a closed capillary is

$$N = \frac{A_2 E}{B_2 E^6 + C_2 E^2 + F_2 E + H_2} \quad (17)$$

where $A_2 = 1536 u L D \eta^2 \lambda_T^2$, $F_2 = 128 D \lambda_T^2 \eta^2 l^2 u / L$, $C_2 = 64 R^2 \epsilon^2 \zeta^2 \lambda_T^2$, $B_2 = \eta^2 \delta^2 \kappa^2 u^2 R^6$ and $H_2 = 3072 D^2 \eta^2 \lambda_T^2$.

To derive the expression for the optimum E corresponding to the maximum N , the procedure based on $\partial N / \partial E = 0$ can again be employed. However, in contrast with the case of the open capillary, the relationship for the optimum E has implicit form and can be solved only numerically.

The dependence $N = F(E)$ for the closed capillary is shown in Fig. 1. Here, for a given capillary, background electrolyte and separand mobility, the value of the zeta potential is chosen as a parameter. The curve at zero zeta potential is identical for both a closed and an open capillary with completely deactivated walls. It is seen that very high plate numbers can be reached, but in closed capillaries it is necessary to decrease the zeta potential to less than 2 mV. This can usually be done either by deactivation of the capillary surface or by use of additives to the background electrolyte as in capillary isotachopheresis²⁰.

EXPERIMENTAL

Equipment

The experiments were carried out in laboratory made equipment, see Fig. 2, consisting of Perspex electrolyte chambers with electrodes (E1, E2) connected to

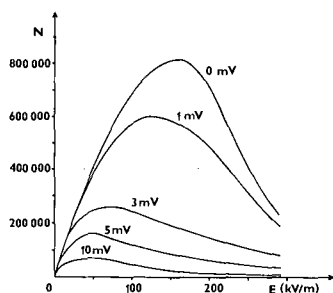


Fig. 1. Calculated dependences of the separation efficiency, N , on the intensity of the electric field, E , with parametrically chosen values of the zeta potential in mV. Closed capillary: $0.5 \text{ m} \times 0.1 \text{ mm}$ I.D. Conductivity of the background electrolyte: 0.05 S/m . Other parameters used for the calculation are listed in Table I.

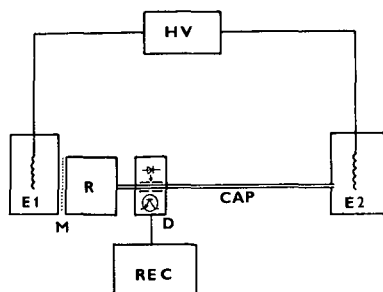


Fig. 2. The experimental equipment used. For details see text.

a high-voltage power supply (HV) and the refluxing block (R) to which capillaries (CAP) of various lengths and diameters can be connected. A cellophane membrane (M) placed between the refluxing block and the electrolyte chamber prevented the hydrodynamic flow inside the capillary. A laboratory-made optical on-column VIS absorbance detector (D) was employed where a light emitting diode (LED) and a phototransistor were used as the source and detector, respectively. The detector signal was recorded by a line recorder (REC). An high-voltage power supply (16 kV, 500 μ A), developed originally for capillary isotachopheresis²¹ and enabling simultaneous measurement of the voltage and current, was used. Soft glass capillaries of desired diameter were kindly provided by Drs. K. Tesařík and K. Janák from this Institute. To obtain high electric field strengths with the high voltage power supply used, the separation capillaries had to be a bit shorter than those currently used. The length of each capillary tested was 160 mm, with the detector situated 118 mm from the injection point in all experiments. The capillary was cooled by an air fan at room temperature.

Chemicals and electrolytes

Triethylamine and caproic acid were of analytical reagent grade (Lachema, Brno, Czechoslovakia). Night blue and hydroxypropylcellulose (HPC) were from Lachema and EGA-Chemie (Steinheim/Albuch, F.R.G.), respectively. Methyl green for microscopy (Fluka, Buchs, Switzerland) was used as a sample. The stock solution of HPC was purified on a mixed-bed ion exchanger; other chemicals were used without further purification.

The background electrolytes consisting of 0.002 or 0.008 *M* triethylamine + caproic acid to pH 4.9 with the additives 0.1% HPC and $5 \cdot 10^{-5}$ *M* night blue were used in all experiments. The sample solution was $2 \cdot 10^{-4}$ *M* methyl green in the background electrolyte diluted with water 1:5. The sample was introduced into the capillary by the electromigration technique², where the respective electrolyte chamber E₂ was replaced by a beaker containing the sample solution and a small current (1–5 μ A) was applied for 10 s. Thus, since the capillary was closed at the opposite end by the membrane M, the sample was introduced by electromigration only. Due to the adjustment of concentrations when crossing the stationary concentration boundary between the background electrolyte and the sample solution, methyl green was concentrated into a sharp initial pulse in the capillary, the length of which was 1 mm. The capillary was rinsed and filled with fresh background electrolyte for each new experiment.

RESULTS AND DISCUSSION

Preliminary isotachophoretic experiments were done to find the sample having the same effective mobility as the ion of the background electrolyte with the same sign, to avoid electromigration dispersion, and, the buffering counter ion having low mobility to minimize the electrolytic conductivity and thus the excessive production of Joule heat. Methyl green (ionic mobility $ca. 34 \cdot 10^{-5} \text{ cm}^2/\text{V s}$) and triethylamine (ionic mobility $ca. 33 \cdot 10^{-5} \text{ cm}^2/\text{V s}$) were finally selected as the separand and the background electrolyte constituent, respectively. The pH of the background electrolyte was set to 4.90 using caproic acid (ionic mobility $30.2 \cdot 10^{-5} \text{ cm}^2/\text{V s}$, $pK_a = 4.86$)²². For the suppression of the electroosmotic flow, 0.1% HPC was added to the background electrolyte.

In the first experiments, severe zone tailing due to the adsorption of the methyl green zone onto the capillary walls was observed. Neither the use of fused-silica capillaries nor silylation of the capillary walls brought about substantial improvement. Then the competitive adsorption²³ of a substance which binds to the capillary walls more strongly than does the separand was examined. The addition of $ca. 10^{-5} \text{ M}$ of night blue to the background electrolyte was found to eliminate the tailing completely, see Fig. 3, and this system was adopted for further measurements.

As the detected peaks were symmetrical, the number of theoretical plates was calculated using the formula $N = 5.545 (l/w_{1/2})^2$, where l is the distance of the peak from the start on the record and $w_{1/2}$ is the width at half height. Each measurement was repeated five times and average values were plotted. The relative standard deviation was less than 10%. A typical example of the detector trace is shown in Fig. 4.

The theoretical and experimental dependences of N vs. E in capillaries of various inside diameters are shown in Fig. 5a,b. The concentration of the background electrolyte with respect to triethylamine was 0.008 M and its conductivity 0.04 S/m in

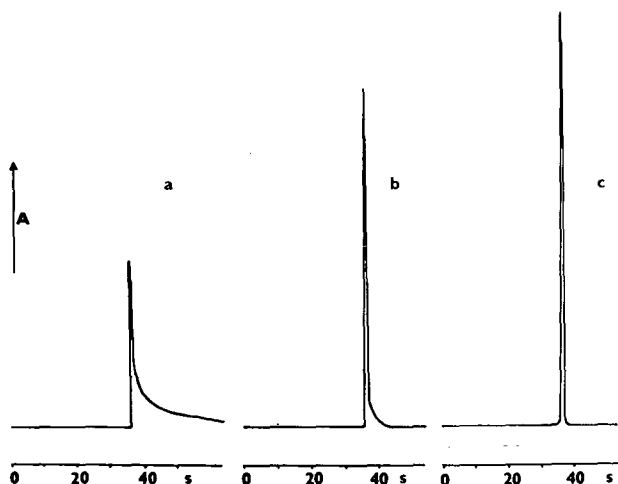


Fig. 3. The elimination of zone tailing by competitive adsorption. (a) Without additive; (b) 10^{-5} M night blue added to the background electrolyte; (c) $2 \cdot 10^{-5} \text{ M}$ night blue added to the background electrolyte. A = Absorbance at 640 nm.

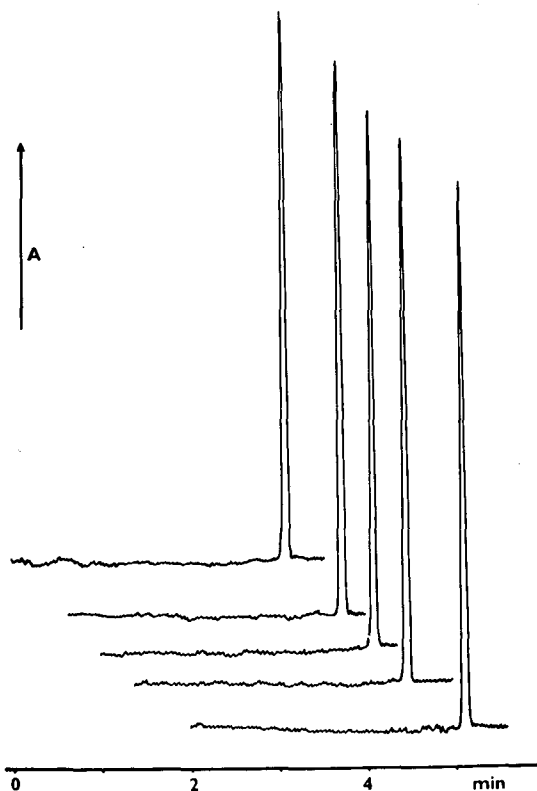


Fig. 4. An example of a set of measurements used for the calculation of N . Capillary: 0.2 mm I.D. Conductivity of the background electrolyte: 400 $\mu\text{S}/\text{cm}$, 18 kV/m.

the case of Fig. 5a, and 0.002 M and 0.01 S/m in the case of Fig. 5b. The numerical values of the constants used for the calculation are listed in Table I. In accord with experiments published by Lukacs and Jorgenson²⁴, it is clearly demonstrated that the smaller is the inside diameter of the capillary the higher are the plate numbers. An additional increase in the separation efficiency can be achieved by lowering the conductivity of the background electrolyte, *e.g.*, by decreasing its concentration. A decrease in the background electrolyte concentration and the use of very narrow capillaries makes higher demands on the detection system. In our case the limited sensitivity of the detector prevented measurements with capillaries narrower than 0.1 mm since the reproducibility of the plate number reading drastically decreased due to detector noise. For the same reason, experimental data measured in an 0.125 mm I.D. capillary filled with a low conductivity electrolyte are not included.

Though the experimental values plotted in Fig. 5 do not exactly fit the theoretical curves, the agreement between the theory and experiment is good, especially in the case of low conductive background electrolyte. The theoretical and experimental values of plate numbers and electric field strengths in the maxima of the efficiency curves are compared in Table II. It should be noted that the shape of the theoretical curves strongly depends on the value of zeta potential chosen for computing (see Fig. 1). Its

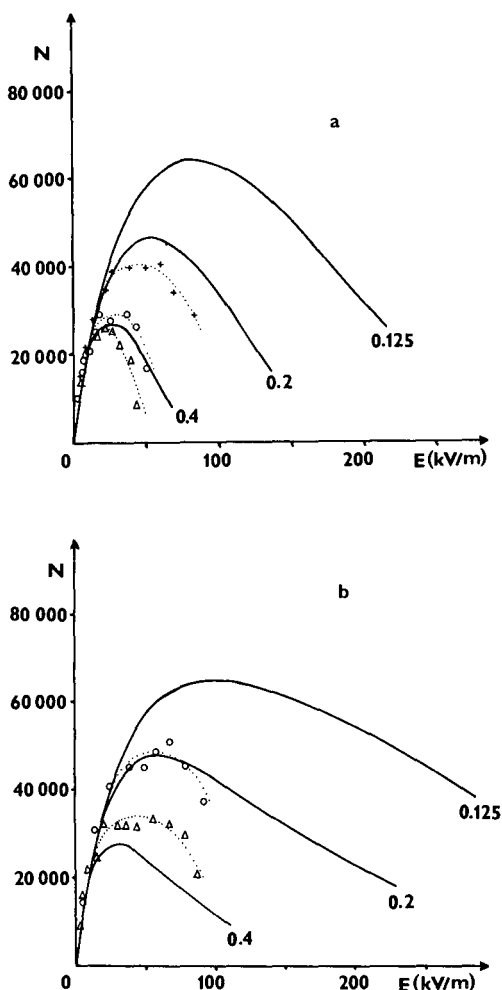


Fig. 5. The dependences of N versus E for background electrolyte conductivities (a) 0.04 and (b) 0.01 S/m. The internal diameter of the separation capillary (in mm) is marked on each theoretical curve. The experimental points are: +, 0.125 mm; O, 0.2 mm and Δ , 0.4 mm I.D.

actual value is hardly accessible during the run and in our case a value of 1.5 mV was adopted as the result of comparing our preliminary measurements with literature data²⁰. Moreover, due to the elevation of the mean temperature inside the capillary most parameters which are assumed constant during the calculations, may show variability. However, we can say that in our case, when using closed capillaries, dispersion due to electroosmosis is dominant, dispersions due to sampling, temperature gradients, electromigration and residual adsorption representing only minor contributions.

In the present capillary electrophoretic practice, the electric field strengths rarely exceed 50 kV/m and, thus, usually the plate numbers lie in the linear part of the

TABLE I

NUMERICAL VALUES OF CONSTANTS USED FOR THE CALCULATION OF PLATE NUMBERS

<i>Constant</i>	<i>Numerical value</i>
λ_T	0.6 W/m K
δ	0.024
ε	$7.12 \cdot 10^{-10}$ C ² /J m
η	0.001 kg/m s
u	$34 \cdot 10^{-9}$ m ² /V s
L	0.118 m
D	$8.8 \cdot 10^{-10}$ m ² /s
l	0.001 m
κ	0.04, 0.01 S/m
R	0.625, 0.1 and $0.2 \cdot 10^{-3}$ m

efficiency curve. The efficiencies thus obtained reach several hundreds of thousands of plates per metre of the separation capillary. By appropriate selection of the background electrolyte with respect to the electromigration dispersion and Joule heat as discussed previously, even higher efficiencies should be reached using high electric field strengths. The experiments presented here confirm that, even in relatively wide-bore capillaries, efficiencies of hundreds of thousands of plates per metre of the separation capillary can be reached if the separation conditions are selected carefully^{9,25}.

However, in practice, when multicomponent samples are to be analysed, the optimum separation conditions for each of the analytes of interest will rarely be achieved simultaneously and a compromise must be looked for. Another practical problem is the selection of the capillary diameter. The use of wide-bore capillaries makes low demands on the detection sensitivity, but on the other hand it makes high demands on the cooling of the capillary since the Joule heat production is proportional to the square of the capillary diameter. As mentioned above, the temperature difference between the centre and the inner wall of the capillary can be several degrees. This temperature difference is determined mainly by the thermal conductivity of the

TABLE II

THEORETICAL AND EXPERIMENTAL NUMBERS OF THEORETICAL PLATES AND ELECTRIC FIELD STRENGTHS AT THE MAXIMUM OF THE EFFICIENCY CURVE

<i>Capillary I.D. (mm)</i>	$\kappa = 0.01$ S/m				$\kappa = 0.04$ S/m			
	<i>Theory</i>		<i>Experiment</i>		<i>Theory</i>		<i>Experiment</i>	
	<i>N</i>	<i>E (kV/m)</i>	<i>N</i>	<i>E (kV/m)</i>	<i>N</i>	<i>E (kV/m)</i>	<i>N</i>	<i>E (kV/m)</i>
0.4	27 600	29	34 000	56	27 100	26	26 000	26
0.2	47 400	58	50 000	67	46 700	53	29 000	38
0.125	65 000	92	—	—	64 000	58	40 000	40

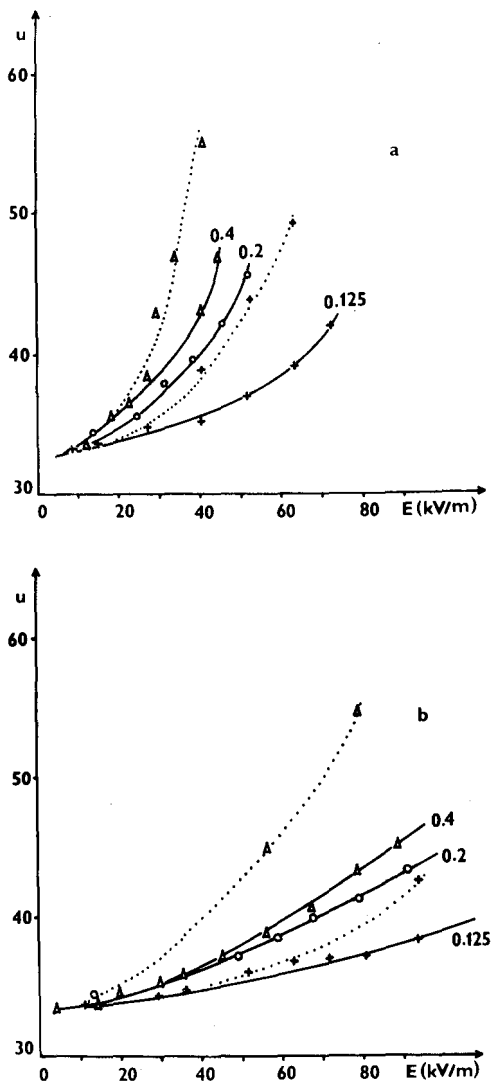


Fig. 6. The experimental dependences of the electrophoretic mobility of methyl green (in 10^{-5} $\text{cm}^2/\text{V s}$) on the intensity of the electric field used. The diameter of the separation capillary (in mm) is marked on each curve. The conductivity of the background electrolyte was (a) 400, (b) 100 $\mu\text{S}/\text{cm}$. The dotted lines represent the experiments in non-cooled capillaries.

background electrolyte and contributes significantly to the dispersion of zones as described in the Theoretical.

The diameter of the capillary also plays an important role in the elevation of the mean temperature of the background electrolyte. The mean temperature can be estimated by employing the experimental dependence of the separand mobility on the intensity of the electric field used. These dependences are shown in Fig. 6. Given the fact that the mobility increases by 2.4% per K, the mobility rise in Fig. 6 represents the

mean temperature elevation up to 50°C. This is in good agreement with data we obtained by thermocouple measurement of the temperature of the outside capillary wall and with published data²⁶. It is seen that the mobility increase and thus the temperature elevation is less pronounced in narrow-bore capillaries and when cooling is applied.

REFERENCES

- 1 J. C. Giddings, *Sep. Sci.*, 4 (1969) 181.
- 2 J. W. Jorgenson and K. D. Lukacs, *Anal. Chem.*, 53 (1981) 1298.
- 3 T. Tsuda, G. Nakagawa, M. Sato and K. Yagi, *J. Appl. Biochem.*, 5 (1983) 330.
- 4 K. D. Lukacs, *Thesis*, Univ. North Carolina, Chapel Hill, 1983.
- 5 M. J. Sepaniak and R. O. Cole, *Anal. Chem.*, 59 (1987) 472.
- 6 K. H. Row, W. H. Griest and M. P. Maskarinec, *J. Chromatogr.*, 409 (1987) 193.
- 7 H. C. Cox, J. K. C. Hessels and J. M. G. Teven, *J. Chromatogr.*, 66 (1972) 19.
- 8 R. Virtanen, *Acta Polytech. Scand.*, No. 123 (1974) 7.
- 9 H. H. Lauer and D. McManigil, *Trends Anal. Chem.*, 1 (1986) 11.
- 10 F. E. P. Mikkers, F. M. Everaerts and Th. P. E. M. Verheggen, *J. Chromatogr.*, 169 (1979) 1.
- 11 J. F. Brown and J. O. N. Hinckley, *J. Chromatogr.*, 109 (1975) 218.
- 12 S. Hjertén, *Chromatogr. Rev.*, 9 (1967) 122.
- 13 P. Boček, *Top. Curr. Chem.*, 95 (1981) 131.
- 14 M. Martin and G. Guiochon, *Anal. Chem.*, 56 (1984) 614.
- 15 M. Martin, G. Guiochon, Y. Walbroehl and J. W. Jorgenson, *Anal. Chem.*, 57 (1985) 561.
- 16 T. Tsuda, K. Nomura and G. Nakagawa, *J. Chromatogr.*, 248 (1982) 241.
- 17 J. L. Anderson and W. K. Idol, *Chem. Eng. Commun.*, 38 (1985) 93.
- 18 T. W. Nee, *J. Chromatogr.*, 105 (1975) 231.
- 19 J. W. Jorgenson and K. D. Lukacs, *Science (Washington, D.C.)*, 222 (1983) 266.
- 20 J. C. Reijenga, G. V. A. Aben, Th. P. E. M. Verheggen and F. M. Everaerts, *J. Chromatogr.*, 260 (1983) 241.
- 21 M. Deml, P. Boček and J. Janák, *J. Chromatogr.*, 109 (1975) 49.
- 22 T. Hirokawa, M. Nishino, N. Aoki, Y. Kiso, Y. Sawamoto, T. Yagi and J.-I. Akiyama, *J. Chromatogr.*, 271 (1983) D1.
- 23 H. H. Lauer and D. McManigill, *Anal. Chem.*, 58 (1986) 166.
- 24 K. D. Lukacs and J. W. Jorgenson, *J. High Resolut. Chromatogr. Chromatogr. Commun.*, 8 (1985) 407.
- 25 F. E. P. Mikkers, F. M. Everaerts and Th. P. E. M. Verheggen, *J. Chromatogr.*, 169 (1979) 11.
- 26 S. Terabe, K. Otsuka and T. Ando, *Anal. Chem.*, 57 (1985) 834.

CHROM. 20 496

SIMPLE SAMPLING DEVICE FOR CAPILLARY ISOTACHOPHORESIS AND CAPILLARY ZONE ELECTROPHORESIS

Th. P. E. M. VERHEGGEN, J. L. BECKERS and F. M. EVERAERTS*

Laboratory of Instrumental Analysis, Eindhoven University of Technology, P.O. Box 513, 5600 MB Eindhoven (The Netherlands)

SUMMARY

A simple sampling device for isotachophoresis and zone electrophoresis is described, whereby the sample solution is introduced directly into a broadened part of the capillary tube by two feeders, placed perpendicularly to the capillary tube. The advantage of this sampling device is that with the absence of moving parts, automation of the sample introduction can be carried out in a simple way, cleaning is simple and the device is inexpensive. Experiments showed that a reproducibility of less than 2% can be obtained, including the day to day variations using different sample solutions.

INTRODUCTION

The sampling methods usually applied in capillary isotachophoresis (ITP) and capillary zone electrophoresis (CZE) are: injection with a syringe, via a septum, in an injection block, injection valves, with/without a sample loop, and dipping one end of the capillary tube into the sample solution, whereby the sample is introduced by (a) the gravity flow or (b) electroendosmosis and/or electromigration.

The best way of sampling in CZE is to introduce a representative aliquot of a sample, concentrated as much as possible in a narrow band and without mixing with the background electrolyte¹. However, none of the methods mentioned above was appropriate for this purpose. The use of a syringe can cause reading errors, especially for small amounts of sample, and a great disadvantage is the mixing of the sample with the background ionic species so that the sample cannot be introduced in a narrow band. In ITP this is of no importance because of the self-correcting effect of the zone boundaries.

A sample valve is¹, in fact, the most suitable sampling method for CZE. With a sample valve a known volume of a representative aliquot of the sample can be introduced without mixing with the background electrolyte. Using a sample valve in CZE it was very difficult, however, to avoid impurities coming from the "dead volumes" (*i.e.*, impurities coming from the liquid films) between moving parts because in CZE very small amounts of ionic species can be detected.

When a gravity flow², electroendosmosis or electromigration^{3,4} is applied an

unknown volume is introduced so that an internal standard has to be used for quantitative analyses. In electroendosmosis and electromigration, moreover, the sample introduced often does not have the same composition as the original sample (see Discussion). Applying pulse injections with splitting techniques⁵ can be considered as electromigration with the advantage that a representative aliquot of the sample is taken.

In this paper a simple sampling device for capillary ITP and CZE is described, whereby the sample solution is introduced directly into part of the capillary tube by means of two feeders, perpendicular to the capillary tube. The sample can be introduced without mixing with the background electrolyte. With the absence of moving parts cleaning is simple. An advantage, as obtained with the use of a valve, is the concentration effect of dilute sample ionic species⁶.

EXPERIMENTAL

In order to examine the utility of this new sampling device, an apparatus was constructed as shown in Fig. 1. A cast capillary block C is connected between the electrode compartment A₁ and the sampling device SD. In the electrode compartments A₁ and A₂, the electrolyte solutions contact the Pt-Ir electrodes E. The capillary tube (0.25 mm I.D., separation length 6 cm) contains measuring electrodes M connected with a.c. electronics⁷. The sampling device SD consists of a broadened part of the capillary tube (0.55 mm I.D.) connected with two feeders (0.4 mm diameter), perpendicular to the capillary tube.

The electrolyte solutions are introduced using valves 1 and 3 and the drain 2. Valves 5 and 6 are used for complete rinsing of the electrode compartments. The sample can be introduced via valve 4 and the drain 2.

In first instance, the experiments were carried out with a closed valve, connected to drain 2. All data presented in this paper, however, were measured with drain 2 open, because identical results were obtained.

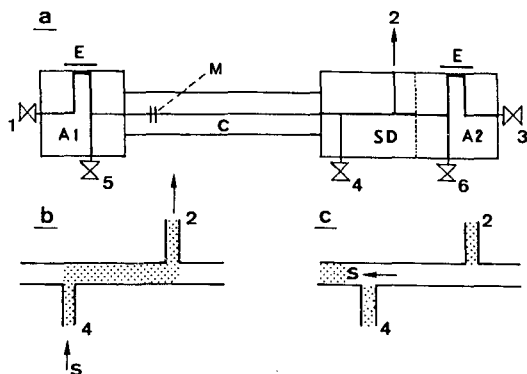


Fig. 1. (a) Schematic diagram of electrophoretic equipment with sample device (for further explanation, see text). (b) Sample device during sampling (S = sample). (c) Sample device after a certain time (S = sample).

RESULTS

In order to study the feasibility, accuracy and reproducibility of the new sampling method, two questions have to be answered. The first is whether the sample device (SD) has a constant volume independent of the mobilities and concentrations of the sample components and the exact value of this SD volume. It is possible that, although no electric field gradient over the feeders exists, sample components from the feeders may diffuse into the capillary tube when the sample has already left the sampling position. This means that these sample ions, in the ITP mode, will be found in the terminating zone (with a very high electric field gradient) by means of which some of the sample ionic species can reach their own sample zones. This effect will lead to a greater zone length for high ionic mobilities and high concentrations.

The second question is whether reproducible and linear calibration graphs can be obtained for each sample component in both the ITP and CZE modes.

Determination of the volume of the sample device

For the determination of the SD volume, the fact has been used that equal amounts of ionic species always need equal times to pass a detector, whatever capillary diameters may be used in ITP analyses, provided that an equal electric current is applied.

Because in ITP the equation

$$E = j\sigma \quad (1)$$

holds, where j is the electric current density in A/cm², σ is the specific resistance in Ω cm and E is the electric field gradient in V/cm, the concentration of a specific sample zone is always constant if the same leading electrolyte is used. If, for example, the cross-sectional area of the capillary tube is increased, then the zone length decreases in proportion. Because the electric current density j decreases in a similar way, the zone velocity decreases, hence the time needed for the zone to pass the detector remains the same. This can also be formulated in another way, as follows. In order that a specific amount of a sample can pass a detector, a specific quantity of charge Q has to be transported. The quantity of transported charge will always be:

$$Q = It \quad (2)$$

Working at a constant electric current I a specific quantity of charge Q will pass in an equal time t . This fact was used to determine the volume of the sampling device.

Several different volumes of a sample solution were introduced into an ITP apparatus equipped with a capillary tube of 0.2 mm I.D. and an injection block. The sample volumes were introduced with a syringe and the volumes were read off under a microscope. Using the corresponding zone lengths a calibration graph was constructed.

The same sample solution was then introduced by the SD into the apparatus described in Fig. 1, and an ITP experiment was carried out using the same leading electrolyte and the same electric current. From the measured zone length the SD

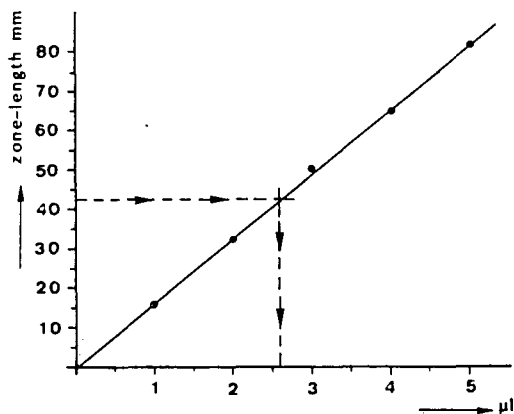


Fig. 2. Calibration graph for glutamate (0.001 *M*) in a leading electrolyte system at pH 6 (0.01 *M* hydrochloric acid + and 0.02 *M* histidine). The sample was introduced with a syringe and an injection block. From the zone length obtained using the sample device (SD) its volume can be obtained (dotted line).

volume can be obtained using the calibration graph for the ITP apparatus with injection block (see Fig. 2). This was carried out for different electrolyte systems and different sample solutions and the values obtained are given in Table I. It can be concluded from Table I that for ionic species with high ionic mobilities, a larger sample volume is found using the SD.

In order to establish whether the SD volume is also dependent on the concentration of the sample ionic species, the experiments were repeated with both apparatus for glutamate at different concentrations. The results are given in Table II, from which it can be concluded that the SD volume also depends on the concentration of the sample ionic species.

TABLE I

ZONE LENGTHS MEASURED WITH ITP EQUIPMENT WITH AN INJECTION BLOCK AND WITH THE SD FOR IONIC SPECIES AT A CONCENTRATION OF 0.001 *M*, AND CALCULATED SD VOLUMES

The leading electrolytes were 0.01 *M* hydrochloric acid + 0.02 *M* histidine at pH 6 and 0.01 *M* hydrochloric acid + 0.02 *M* ϵ -aminocaproic acid at pH 4.4. The terminator was MES. From the calibration graphs obtained with the injection block data and the zone length of the SD, the SD volume was calculated. The electric current was 25 μ A.

Ion	pH	Zone length using injection block (mm)					Zone length using SD (mm)	SD volume (μ l)
		1 μ l*	2 μ l*	3 μ l*	4 μ l*	5 μ l*		
Nitrate	6	13.7	24.4	36.7	48.3	59.1	34.1	2.80
Propionate		13.0	26.1	38.9	52.2	64.3	35.2	2.71
Glutamate		15.3	32.4	48.5	65.5	80.6	42.0	2.60
Nitrate	4.4	13.5	24.9	36.0	49.1	60.4	34.3	2.82
Propionate		12.7	25.6	37.4	52.0	64.3	33.5	2.61
Glutamate		14.8	31.6	46.7	62.7	77.3	39.5	2.54

* Injection volume.

TABLE II
AS TABLE I FOR GLUTAMATE SOLUTIONS OF DIFFERENT CONCENTRATIONS

Concentration (<i>M</i>)	Zone length using injection block (mm)					Zone length using SD (mm)	SD volume (μ l)
	1 μ l*	2 μ l*	3 μ l*	4 μ l*	5 μ l*		
0.005	79.5	162.5	244.3	323.0	416.3	206.1	2.54
0.001	16.1	32.6	50.1	64.8	81.4	42.5	2.60
0.0005	8.1	16.1	24.4	33.5	40.2	21.6	2.65

* Injection volume.

The diffusion of sample ionic species from the feeders into the capillary tube cannot explain these two effects. The results in Table I, *viz.*, larger effective SD volumes for ionic species with high mobilities, agree with the possibility of diffusion from the feeders, but the results in Table II, *viz.*, higher effective SD volumes for smaller sample concentrations, do not. The explanation for the latter may possibly be that introducing low concentrations of sample ionic species means that the terminator solution at the original position of sampling will also have a low concentration according to Kohlrausch's law⁸. Hence high electric field strengths and high temperatures will result, which may be responsible for the larger effective SD volumes. The differences in SD volumes are, however, only a few percent.

Calibration

In order to check the reproducibility and linearity of the SD we measured the zone lengths for glutamate and acetate in an electrolyte system at pH 6 for several concentrations. The different concentrations were prepared by dilution of two different prepared standard solutions. The results are given in Table III, from which it can be concluded that linear calibration graphs were obtained with good reproducibility for the ionic species (see Table IV).

In order to check whether the calibration graphs are affected by the presence of other ionic species in the sample, we prepared several mixtures of acetate and glutamate and used the measured zone lengths to determine their concentrations in the sample mixture using the calibration graphs. In all instances the differences were less than about 2%.

To compare the results obtained with an injection block and the new SD, in Table IV all data for the calibration graphs are given. The results of a regression analysis are given, *viz.*, the regression coefficient and the constants *a* and *b* according to the equation

$$Y = aX + b \quad (3)$$

where *Y* is the zone length (mm) and *X* is the volume injected (μ l) or the concentration (*M*).

From Table IV it can be concluded that the regression coefficients for the new sample device are better than those for the injection block. Although we used the average value of the zone length from five experiments for the new SD, it must be

TABLE III

ZONE LENGTHS FOR SEVERAL CONCENTRATIONS OF ACETATE AND GLUTAMATE MEASURED USING THE SD

All zone lengths were measured five times on different days. The leading electrolyte was 0.01 *M* hydrochloric acid + 0.02 *M* histidine at pH 6. The terminator was MES. The electric current was 25 μ A.

<i>Ion</i>	<i>Concentration (M)</i>	<i>Zone length (mm)</i>					<i>Average zone length (mm)</i>	<i>Standard deviation (mm)</i>
Acetate	0.0005	15.3,	15.4,	15.6,	15.7,	15.3	15.46	0.162
	0.001	30.5,	31.2,	30.1,	30.8,	31.1	30.74	0.403
	0.0015	44.9,	45.5,	44.7,	44.8,	44.6	44.9	0.316
	0.002	61.3,	60.3,	60.4,	59.3,	60.3	60.32	0.634
	0.0025	73.5,	74.3,	73.0,	73.0,	73.0	73.36	0.508
	0.005	144.3,	146.4,	143.6,	146.5,	144.3	145.02	1.196
	0.010	144.4,	144.4,	144.4,	144.0,	141.0	143.64	1.329
Glutamate	0.0005	294.8,	298.1,	297.4,	296.6,	296.9	297.76	1.104
	0.001	21.6,	21.4,	21.5,	21.9,	21.9	21.66	0.206
	0.001	42.3,	42.1,	42.1,	42.9,	42.2	42.32	0.299
	0.001	42.1,	42.4,	42.1,	42.1,	42.1	42.16	0.120
	0.002	83.6,	83.5,	83.0,	83.2,	83.5	83.36	0.224
	0.0025	103.4,	105.0,	104.6,	104.7,	105.0	104.54	0.592
	0.005	206.9,	209.9,	202.6,	205.2,	204.0	205.72	2.523
	0.005	202.7,	203.0,	202.7,	202.7,	205.3	203.28	1.017
	0.010	411.1,	407.1,	411.4,	407.4,	410.6	409.52	1.873

TABLE IV

CORRELATION COEFFICIENT AND THE CONSTANTS *a* AND *b* FOR THE REGRESSION ANALYSIS OF ALL CALIBRATION GRAPHS

<i>Apparatus</i>	<i>pH</i>	<i>Ion</i>	<i>Constant a (mm/μl)</i>	<i>Constant b (mm)</i>	<i>Correlation coefficient</i>
Injection block*	6	Nitrate	11.47	2.03	0.99950
		Propionate	12.87	0.29	0.99980
		Glutamate	16.19	0.0	0.99945
	4.4	Nitrate	12.18	0.0	0.99805
		Propionate	12.83	0.0	0.99899
		Glutamate	15.55	0.0	0.99948
Injection block**	6	Glutamate (0.005 <i>M</i>)	83.41	-5.11	0.99925
		Glutamate (0.001 <i>M</i>)	16.28	0.16	0.99940
		Glutamate (0.0005 <i>M</i>)	8.16	-0.02	0.99827
SD***	6	Acetate	29409.6 [§]	0.18	0.99954
		Glutamate	40752.2 [§]	1.53	0.99995

* Results in Table I.

** Results in Table II.

*** Results in Table III.

§ mm · mol⁻¹ · l.

borne in mind that all these experiments were carried out with different electrolyte solutions and on different days so that these deviations include all possible errors such as those coming from the sample device, day to day variations, the use of different stock solutions and the non-linearity of the calibration graphs.

From the foregoing experiments it can be concluded that the new SD has an effective volume that is dependent on the effective mobilities and concentrations of the sample ionic species. Calibration graphs, for the different ionic species, however, show a linear relationship between zone length and concentration of ionic species, independent on their mobilities and unaffected by the presence of other sample ionic species.

The dimensions of the feeders and the sampling channel were chosen arbitrarily. The choice of the optimal dimensions of the SD is under investigation, especially for the use of narrow-bore capillaries ($50\ \mu\text{m}$).

In order to study the possibilities of automation, some experiments were carried out in which all electrolyte solutions and the sample were introduced by aspiration, using a simple peristaltic pump connected to drain 2. The results were identical with those obtained in the manual experiments, which means that the SD can be used for the automation of analyses.

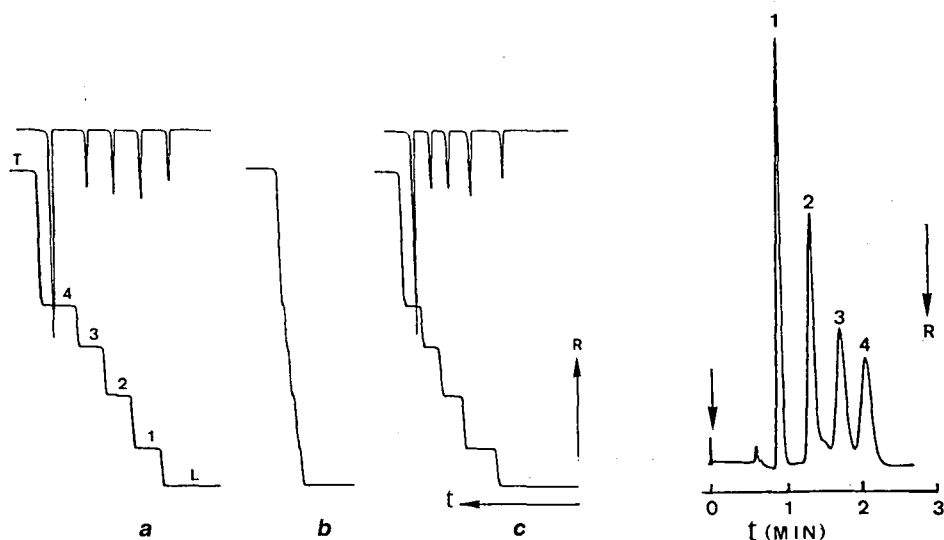


Fig. 3a. Isotachopherogram for the separation of (1) formate, (2) acetate, (3) benzoate and (4) glutamate. The leading electrolyte L was $0.01\ M$ hydrochloric acid + and $0.02\ M$ histidine at pH 6. The concentrations of the sample ionic species were $5 \cdot 10^{-4}\ M$. The terminator T was 2-(N-morpholino)ethanesulphonic acid (MES). The electric current was $25\ \mu\text{A}$. (b) As (a) with sample concentrations of $5 \cdot 10^{-5}\ M$. (c) As (b) with electromigration sampling.

Fig. 4. Electropherogram for the zone electrophoretic separation of (1) formate, (2) acetate, (3) benzoate and (4) glutamate. The concentrations of the sample ionic species were $2.5 \cdot 10^{-5}\ M$. The background electrolyte was $0.01\ M$ MES + $0.02\ M$ histidine at a pH 6.4. The electric current was $25\ \mu\text{A}$.

DISCUSSION

Using the new sampling device a known amount of sample ionic species can be introduced and it has advantages over other sampling techniques in which a known sample is introduced. Compared with injection by a syringe this method has the advantage that there is no mixing with other electrolyte solutions, in either the ITP or the CZE mode. Compared with sampling valves the advantage is the absence of rotating parts. Compared with methods applying electromigration it has the advantage of introducing a representative aliquot of the sample (trapping⁹ or splitting⁵ have a similar advantage). To demonstrate the effect of applying electromigration for sampling three ITP experiments were carried out with the equipment described in Fig. 1, from which the isotachopherograms shown in Fig. 3 were obtained. Fig. 3a shows the separation of formate, acetate, benzoate and glutamate anions in a system of pH 6 and with concentrations of the sample ionic species of $5 \cdot 10^{-4} M$. The separation was repeated with the same anions at concentrations of $5 \cdot 10^{-5} M$ (Fig. 3b) and the zone lengths are scarcely visible. In a third experiment (Fig. 3c) the sampling was carried out by electromigration, a dilute sample of $5 \cdot 10^{-5} M$ flowing through the SD for 30 s with application of an electric current. Although large zone lengths could be obtained, it can clearly be seen that no representative sample aliquot was introduced. The sample introduction follows a moving boundary procedure whereby larger amounts of ionic species with high mobilities are introduced.

With the same sample solution of concentrations $2.5 \cdot 10^{-5} M$ a zone electrophoretic experiment was also carried out and the electropherogram is shown in Fig. 4. The peaks are clearly visible, showing that very dilute samples easily can be handled using CZE. Further, the SD gives much greater possibilities of automating the sampling procedure both for ITP and CZE.

REFERENCES

- 1 F. E. P. Mikkers, F. M. Everaerts and Th. P. E. M. Verheggen, *J. Chromatogr.*, 169 (1979) 11.
- 2 A. Tsuda, K. Nomura and G. Nakagawa, *J. Chromatogr.*, 264 (1983) 385.
- 3 J. W. Jorgenson and K. DeArman Lukacs, *J. Chromatogr.*, 218 (1981) 209.
- 4 J. W. Jorgenson and K. DeArman Lukacs, *Science*, 222 (1983) 266.
- 5 M. Deml, F. Foret and P. Böcek, *J. Chromatogr.*, 320 (1985) 159.
- 6 F. E. P. Mikkers, F. M. Everaerts and Th. P. E. M. Verheggen, *J. Chromatogr.*, 169 (1979) 1.
- 7 F. M. Everaerts J. L. Beckers and Th. P. E. M. Verheggen, *Isotachopheresis, Theory, Instrumentation and Applications*, Elsevier, Amsterdam, 1976.
- 8 J. L. Beckers, Th. P. E. M. Verheggen and F. M. Everaerts, 452 (1988) 591.
- 9 F. E. P. Mikkers, *Thesis*, Eindhoven University of Technology, 1980, p. 142.

CHROM. 20 488

SEPARATION OF α -KETO ACIDS BY CAPILLARY SUPERCRITICAL FLUID CHROMATOGRAPHY AS THEIR QUINOXALINOL DERIVATIVES

P. A. DAVID and M. NOVOTNY*

Department of Chemistry, Indiana University, Bloomington, IN 47405 (U.S.A.)

SUMMARY

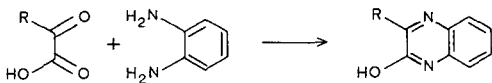
α -Keto acids were derivatized with *o*-phenylenediamine to produce a nitrogen-containing quinoxalinol. The derivatives were analyzed by capillary supercritical fluid chromatography (SFC) with nitrogen thermionic detection. The quinoxalinols were analyzed without additional silylation as is required for efficient gas chromatographic analysis. α -Keto acids were also extracted from human urine and converted to the corresponding quinoxalinols. Simultaneous pressure and temperature programming was employed to optimize chromatographic efficiency. The nitrogen thermionic detector used demonstrated linearity over 3–4 orders of magnitude. A sensitivity of 1 pg N/s was obtained for 3-benzylquinoxalinol at a signal-to-noise ratio of 4:1.

INTRODUCTION

During the last several years, supercritical fluid chromatography (SFC) has been under extensive development as an effective method for the analysis of non-volatile and thermally labile compounds. For difficult separations, capillary SFC has been primarily applied to relatively non-polar mixtures originating from fossil fuels, plastics and fatty materials. Applications of SFC to polar substances, such as various biochemical compounds, natural products, or pharmaceuticals, remain uncommon due to the relatively poor solvating capacities of the conventional mobile phases (*e.g.*, carbon dioxide or nitrous oxide).

In order to extend the scope of SFC toward polar solutes, three general approaches appear feasible: (a) exploring the mobile phases with appreciable dipole moments (*e.g.*, ammonia or sulfur dioxide); (b) using a polar retention modifier; and (c) improving the solute's solubility in a mobile phase through chemical derivatization. Although all three approaches merit exploration, the sample derivatization is particularly attractive if the formed derivatives become sufficiently soluble in "comfortable" mobile phases such as carbon dioxide or nitrous oxide. This has recently been demonstrated with silylated oligosaccharides¹ and biological conjugates of steroid metabolites and bile acids².

The present communication deals with yet another example of a biologically important class of compounds, α -keto acids. The reaction of these compounds with *o*-phenylenediamine is known to proceed quantitatively, forming quinoxalinols:



While this derivatization scheme was initially proposed for gas chromatographic (GC) studies³, the restrictions of volatility are a problem. Such a difficulty is not experienced in SFC. An additional advantage of this solute derivatization approach is the incorporation of two nitrogen atoms into the structure, which facilitates highly sensitive detection by a nitrogen-sensitive thermionic detector.

EXPERIMENTAL

Apparatus

The supercritical fluid chromatograph was a home-made instrument as described previously⁴. A Brownlee Labs. micropump (Applied Biosystems, Santa Clara, CA, U.S.A.) with software version G, was used as the source of mobile phase. The mobile phase employed was SFC grade nitrous oxide (Scott Specialty Gases, Plumsteadville, PA, U.S.A.). The nitrous oxide cylinder also contained 1100 p.s.i. of helium head pressure to facilitate rapid filling of the pump without externally cooling the pump heads. Injection was accomplished via an electrically actuated high-pressure valve with an internal sample loop volume of 0.06 μ l (Valco Instruments, Houston, TX, U.S.A.). The capillary columns were 10 m \times 50 μ m I.D. The fused-silica inner surface was deactivated prior to coating through treatment with polymethylhydro-siloxane (85 cSt) (Petrarch Systems, Bristol, MA, U.S.A.)⁵. The column was statically coated with a 0.25- μ m film of SE-30 at 50°C, and the stationary phase was crosslinked three times with azo-*tert.*-butane (Alfa Products, Danvers, MA, U.S.A.)⁶.

Pressure restriction for the operation of a flame detector was accomplished by forming an integral restrictor⁷ directly at the end of the coated column. The detector was a modified Perkin-Elmer Sigma 3 nitrogen-phosphorus detector. Polarization voltage, bead heating current and signal amplification were provided by a Perkin-Elmer stand-alone nitrogen-phosphorus detection electrometer (Perkin-Elmer, Norwalk, CT, U.S.A.). The rubidium silicate thermionic source was prepared according to the procedure of Lubkowitz *et al.*⁸. Beads containing 1.6% B₂O₃, 12.4% Na₂O, 74.0% SiO₂, 12.0% Rb₂O exhibited optimum sensitivity and lifetime. Typical detector operating conditions were: heating block temperature, 300°C; polarizing voltage, -250 V; bead heating current, 2.5 A; 1.0 ml/min hydrogen flow; 100 ml/min air flow.

Derivatization procedure

All α -keto acid standards were obtained in the free acid form (Sigma, St. Louis, MO, U.S.A.). Milligram amounts of the α -keto acid standards were dissolved in 2 ml of 4 *N* hydrochloric acid. To this solution 2 ml of a 1% solution of *o*-phenylenediamine in 2 *M* hydrochloric acid was added. The reaction was performed at 70°C for 1 h. The resultant quinoxalinols precipitated upon cooling and were collected by vacuum filtration. The filtrate was recrystallized from a 70% ethanol solution.

α -Keto acids were extracted from normal urine by a procedure similar to that reported by Langenbeck *et al.*⁹. After collection, 4 mg of sodium dithionite was added per ml of urine to stabilize aromatic α -keto acids¹⁰. A 20-ml aliquot of a 24-h urine

collection was acidified to pH 2 with 12 M hydrochloric acid. Urinary acids were extracted three times with 4 ml of ethyl acetate and twice with 4 ml of diethyl ether. The combined extracts were evaporated to dryness. The residue was dissolved in 0.5 ml of 4 M hydrochloric acid, and 1 ml of 1% *o*-phenylenediamine in 2 M hydrochloric acid was added to the solution. The reaction proceeded for 1 h at 70°C. After reaction was completed, the solution was saturated with 1.5 g of ammonium sulphate. The quinoxalinols were extracted three times with 5 ml of chloroform. The combined extracts were evaporated to dryness under a stream of dry nitrogen. The residue was reconstituted in 50 μ l of acetone.

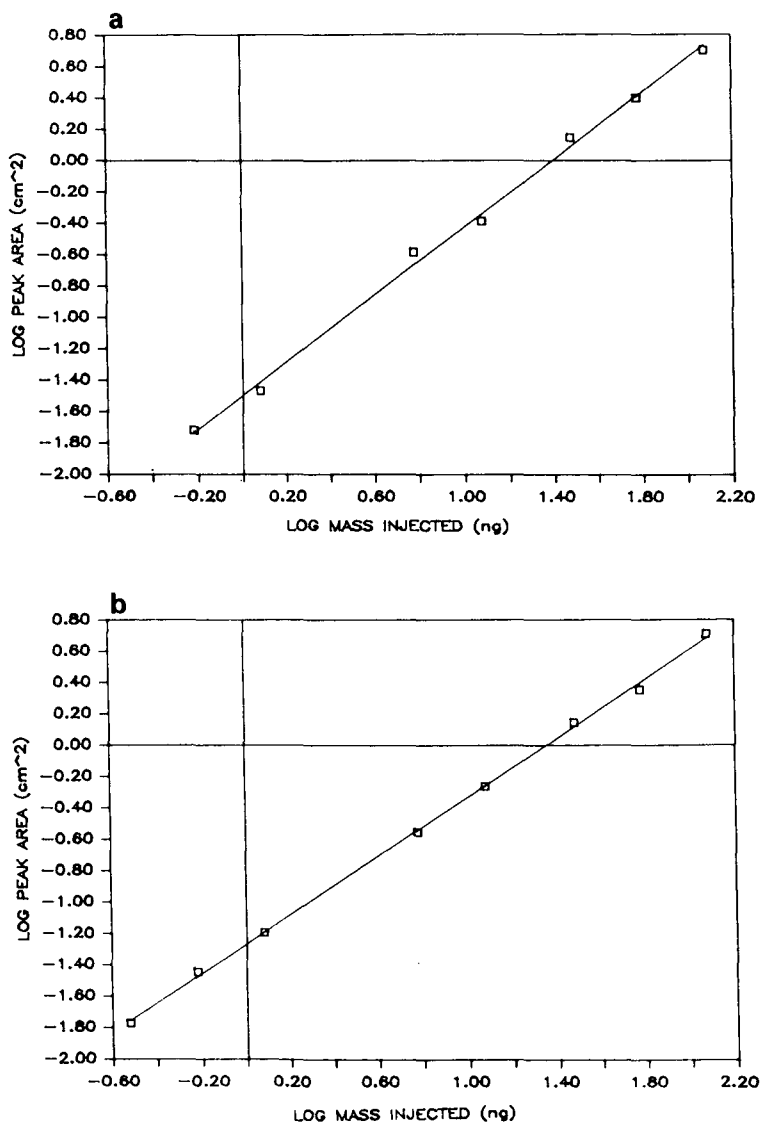


Fig. 1. Linearity of thermionic detector response. (a) *n*-Hexylquinoxalinol, (b) 3-benzylquinoxalinol.

RESULTS AND DISCUSSION

Calibration curves for both an aliphatic and aromatic α -keto acid quinoxalinol are shown in Fig. 1. Each point plotted was the average of five peak area measurements at each concentration. All peak area measurements had a relative standard deviation (R.S.D.) of 4% or less. Throughout the calibration study, a constant background bead current of 10 pA was maintained to improve the reproducibility of the detector response. Background current was controlled by making fine adjustments in the bead heating current.

Fig. 1a shows the calibration curve for *n*-hexylquinoxalinol from α -ketoctanoic acid. The response was linear over 3–4 orders of magnitude with a correlation coefficient of 0.9984. The slope of the log–log plot was 1.071. The sensitivity for *n*-hexylquinoxalinol was 2.0 pg N/s at a signal-to-noise ratio of 3:1.

Fig. 1b shows the calibration curve for 3-benzylquinoxalinol formed from phenylpyruvic acid. The detector response was linear over the same range as above, with a correlation coefficient of 0.9995. The slope of the log–log plot was 0.936. A sensitivity of 1.0 pg N/s was obtained for 3-benzylquinoxalinol at a signal-to-noise ratio of 4:1.

As shown in Fig. 2, quinoxalinol derivatives of aliphatic α -keto acids were

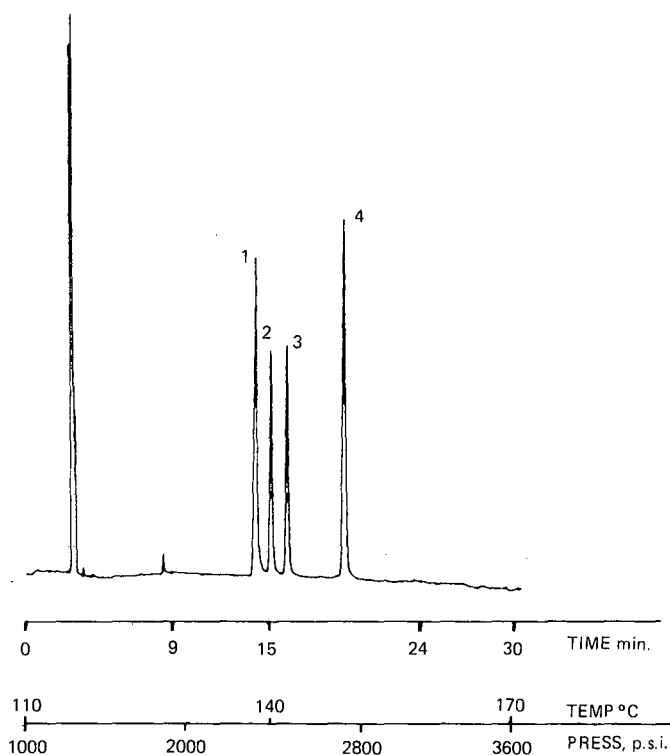


Fig. 2. Standard chromatogram of aliphatic quinoxalinols. Peak identification: (1) methylquinoxalinol from pyruvic acid; (2) ethylquinoxalinol from α -ketobutyric acid; (3) *n*-propylquinoxalinol from α -ketovaleric acid; (4) *n*-hexylquinoxalinol from α -ketoctanoic acid.

analyzed by capillary SFC without silylation of the remaining hydroxyl group as is required for efficient GC analysis^{9,10}. Each peak corresponds to approximately 3 ng of quinoxalinol injected on column. Resolution was optimized through a simultaneous temperature/pressure program. At high mobile phase pressure (density) the solute diffusion coefficient (D_m) decreases, leading to a corresponding loss of efficiency. Fields and Lee¹¹ have shown that chromatographic efficiency in SFC decreases by nearly 75% during a density programmed run. To partially offset the efficiency loss at higher mobile phase densities, higher column temperatures can be used. The increase in

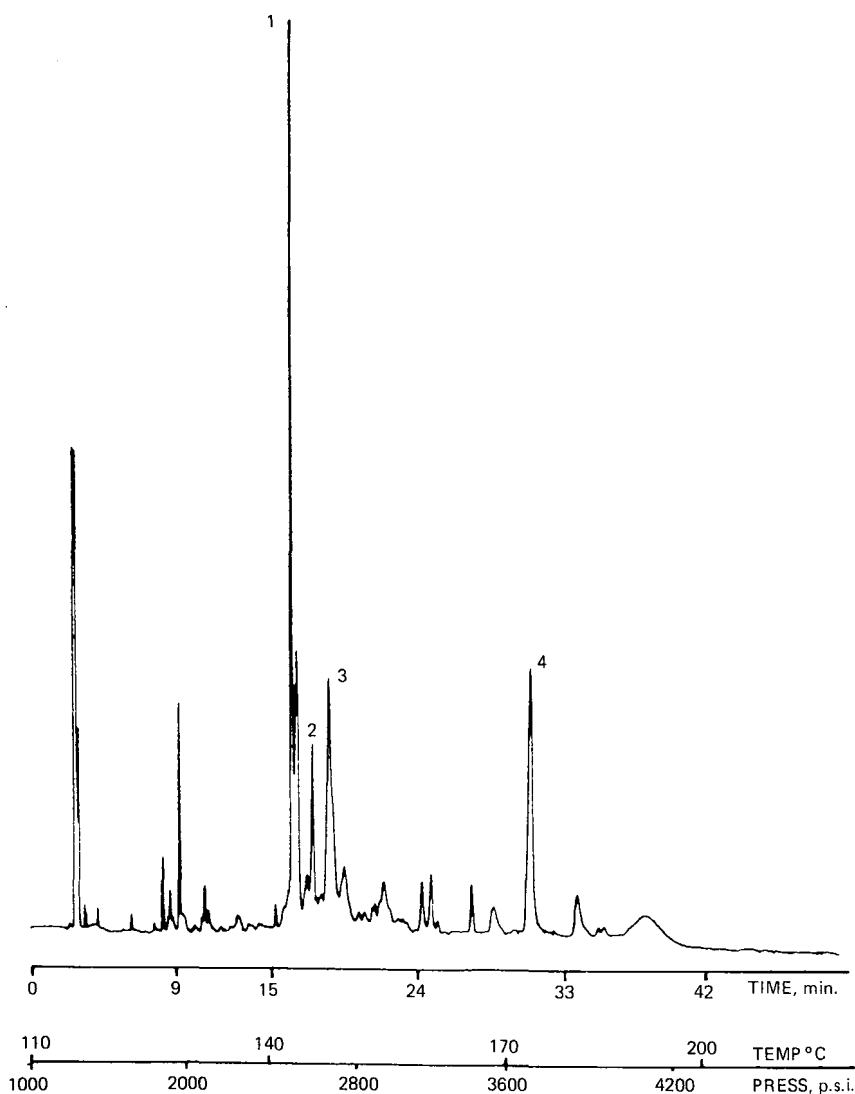


Fig. 3. Chromatogram of quinoxalinol derivatives of human urinary α -keto acids. Peaks tentatively: (1) methylquinoxalinol; (2) ethylquinoxalinol; (3) *p*-propylquinoxalinol; (4) 3-benzylquinoxalinol.

operating temperature enhances separation through two effects: (1) an increase in the mobile phase diffusion coefficient; and (2) an increase in solute volatility which corresponds to a decrease in capacity factor (k'). In both the standard and urinary quinoxalinol chromatograms (Figs. 2 and 3) a slow temperature ramp of 2°C/min was initiated at injection to enhance efficiency.

The chromatogram of urinary α -keto acids is shown in Fig. 3. Peaks were tentatively identified by retention time comparison with standard quinoxalinols. Peaks corresponding to aliphatic, aromatic and dicarboxylic α -keto acid derivatives are evident in the chromatogram. The aliphatic region of the chromatographic profile occurs at 15–25 min, while the aromatic quinoxalinols elute approximately 30 min after injection. The two broad chromatographic zones eluting after 33 min have tentatively been assigned to the carboxyquinoxalinols of α -ketoglutaric and α -keto-adipic acids. These derivatives contain a free carboxylic acid moiety which increases their polarity and consequently decreases their solubility in supercritical nitrous oxide. Therefore, these compounds are more susceptible to irreversible interaction with the residual surface silanols which have not been deactivated in the column coating process. The calibration curve for the quinoxalinol from α -ketoglutaric acid exhibited non-linearity for the lower mass range. This result is indicative of irreversible interaction occurring in the analysis of the carboxyquinoxalinol. These interactions can result in a broadened chromatographic peak profile. Two possibilities exist to improve chromatographic efficiency for the carboxyquinoxalinols: (1) the use of a more inert capillary column with a greater stationary film thickness (0.5–1 μm), or (2) the addition of a polar mobile phase modifier to enhance the solvent strength of supercritical nitrous oxide. Our preliminary results indicate that the nitrogen thermionic detector shows negligible loss of sensitivity or selectivity with mixed supercritical mobile phases containing up to 10 mol% of an organic solvent such as methanol or isopropanol.

The consequence of increased supercritical mobile phase solvent strength is a decreased solute retention. To maintain resolution of the early eluting peaks in the urine chromatogram, mobile phase modification must occur only at the end of the analysis. Therefore, the composition of the mobile phase must be programmed in a manner analogous to gradient elution in high-performance liquid chromatography¹².

The efficiency of capillary SFC combined with sensitive and selective thermionic detection is ideal for the analysis of biologically important compounds existing in complex physiological matrices. Additional derivatization reactions which incorporate heteroatom-containing moieties into the compounds of biochemical interest are under investigation. Minor detector modifications allow selective thermionic response to other heteroatoms besides nitrogen. The sensitivity and selectivity of the thermionic detector response can thus be exploited in the analysis of other biologically important compounds.

ACKNOWLEDGEMENTS

This work was supported by Grant No. CHE 8605935 from the National Science Foundation and a grant-in-aid from Dow Chemical Company.

REFERENCES

- 1 T. L. Chester and D. P. Innis, *J. High Resolut. Chromatogr. Chromatogr. Commun.*, 9 (1986) 209–212.
- 2 C. Borra, F. Andreolini and M. Novotny, *Anal. Chem.*, in press.
- 3 U. Langenbeck, H.-U. Möhring and K.-P. Dieckmann, *J. Chromatogr.*, 115 (1975) 65–70.
- 4 M. Novotny and P. David, *J. High Resolut. Chromatogr. Chromatogr. Commun.*, 9 (1986) 647–651.
- 5 C. L. Woolley, R. C. Kong, B. E. Richter and M. L. Lee, *J. High Resolut. Chromatogr. Chromatogr. Commun.*, 7 (1984) 329–332.
- 6 B. W. Wright, P. A. Peaden, M. L. Lee and T. J. Stark, *J. Chromatogr.*, 248 (1982) 17–34.
- 7 E. J. Guthrie and H. E. Schwartz, *J. Chromatogr. Sci.*, 24 (1986) 236–241.
- 8 J. A. Lubkowitz, B. P. Semonian, J. Galobardes and L. B. Rogers, *Anal. Chem.*, 50 (1978) 672–676.
- 9 U. Langenbeck, A. Hoinowski, K. Mantel and H.-U. Möhring, *J. Chromatogr.*, 143 (1977) 39–50.
- 10 U. Langenbeck, A. Mench-Hoinowski, K.-P. Dieckmann, H.-U. Möhring and M. Petersen, *J. Chromatogr.*, 145 (1978) 185–193.
- 11 S. M. Fields and M. L. Lee, *J. Chromatogr.*, 349 (1985) 305–316.
- 12 C. R. Yonker and R. D. Smith, *Anal. Chem.*, 59 (1987) 727–731.

Author Index

- Alinovi, R., see Ghiggeri, G. M. 347
Antia, F. D., see Maa, Y.-F. 331
Armstrong, D. W.
—, Faulkner Jr., J. R. and Han, S. M.
Use of hydroxypropyl- and hydroxyethyl-de-
rivatized β -cyclodextrins for the thin-layer
chromatographic separation of enantiomers
and diastereomers 323
Barkley, R. M., see McNamara, E. A. 75
Base, J., see Hanis, T. 443
Beckers, J. L.
—, Verheggen, Th. P. E. M. and Everaerts, F. M.
Use of a double-detector system for the mea-
surement of mobilities in zone electrophore-
sis 591
—, see Verheggen, Th. P. E. M. 615
Beerabee, M., see Jack, D. B. 257
Berg, J. H. M. van den, see Tipker, J. 227
Bergamaschi, E., see Ghiggeri, G. M. 347
Bergh-Swart, J. K. van den, see Tipker, J. 227
Boček, P., see Foret, F. 601
Borówko, M.
— and Jaroniec, M.
Studies of adsorption and partition effects in
liquid chromatography with mixed mobile
phases 131
Brinkman, U. A. Th., see Farjam, A. 419
Brooksbank, R. A., see Jackson, P. J. 359
Brown, J., see O'Flynn, M. A. 469
Brown, P. R., see Fadool, D. A. 491
Bruner, F., see Mangani, F. 527
Burford, R. P., see Haken, J. K. 37
Burke, J. T., see Krstulović, A. M. 477
Candiano, G., see Ghiggeri, G. M. 347
Causon, R. C., see O'Flynn, M. A. 469
Cobb, S. J., see Fadool, D. A. 491
Cooper, E. H., see Jackson, P. J. 359
Crescentini, G., see Mangani, F. 527
Croteau, R. B., see Satterwhite, D. M. 61
Crumley, F. G., see Xu, S. 377
Davankov, V. A.
—, Kurganov, A. A. and Ponomareva, T. M.
Enantioselectivity of complex formation in li-
gand-exchange chromatographic systems with
chiral stationary and/or chiral mobile phas-
es 309
David, P. A.
— and Novotny, M.
Separation of α -keto acids by capillary super-
critical fluid chromatography as their quinox-
alinal derivatives 623
Dawkins, J. V.
—, Gabbott, N. P., Lloyd, L. L., McConville, J.
A. and Warner, F. P.
Reversed-phase high-performance liquid
chromatography with a C₁₈ polyacrylamide-
based packing 145
De Jong, G. J., see Farjam, A. 419
De Leenheer, A. P., see Nelis, H. J. C. F. 535
Deml, M., see Foret, F. 601
Deyl, Z., see Hanis, T. 443
Durand, A., see Krstulović, A. M. 477
Egestad, B., see Marshall, H.-U. 459
El Rassi, Z., see Maa, Y.-F. 331
Everaerts, F. M., see Beckers, J. L. 591
—, see Verheggen, Th. P. E. M. 615
Fadool, D. A.
—, Cobb, S. J., Kass-Simon, G. and Brown, P.
R.
Liquid chromatographic procedures for the
analysis of compounds in the serotenergic and
octopamine pathways of lobster hemo-
lymph 491
Farjam, A.
—, De Jong, G. J., Frei, R. W., Brinkman, U. A.
Th., Haasnoot, W., Hamers, A. R. M., Schilt,
R. and Huf, F. A.
Immunoaffinity pre-column for selective on-
line sample pre-treatment in high-perform-
ance liquid chromatography determination of
19-nortestosterone 419
Faulkner Jr., J. R., see Armstrong, D. W. 323
Fisher, D. H.
— and Giese, R. W.
Determination of 5-methylcytosine in DNA
by gas chromatography-electron-capture de-
tection 51
Floyd, T. R.
—, Sagliano Jr., N. and Hartwick, R. A.
Analysis of short alkylsilane bonded silica gel
high-performance liquid chromatographic
stationary phases using hydrofluoric acid di-
gestion and headspace analysis by capillary
gas chromatography 43
Foret, F.
—, Deml, M. and Boček, P.
Capillary zone electrophoresis. Quantitative
study of the effects of some dispersive process-
es on the separation efficiency 601
Fouchet, M. H., see Krstulović, A. M. 477
Frei, R. W., see Farjam, A. 419
Gabbott, N. P., see Dawkins, J. V. 145

- Ghiggeri, G. M.
 —, Candiano, G., Ginevri, F., Mutti, A., Bergamaschi, E., Alinovi, R. and Righetti, P. G.
 Hydrophobic interaction of Alcian Blue with soluble and erythrocyte membrane proteins 347
- Ghodbane, S.
 — and Guiochon, G.
 Effect of mobile phase flow-rate on the recoveries and production rates in overloaded elution chromatography. A theoretical study 209
- Giese, R. W., see Fisher, D. H. 51
 —, see Trainor, T. M. 369
- Gillet, G., see Krstulović, A. M. 477
- Ginevri, F., see Ghiggeri, G. M. 347
- Glikberg, S., see Shohat, S. 503
- Görög, S.
 —, Herényi, B., Nyéki, O., Schön, I. and Kisfaludy, L.
 Determination of impurity profiles in drugs and related materials. II. Detection and quantification of a diastereomeric impurity in the peptide RGH-0205 (Arg-Lys-Asp) 317
- Golombek, F.
 — and Schwedt, G.
 Methyl green-coated column for separation of inorganic anions by ion chromatography 283
- Goto, J.
 —, Miura, H., Inada, M., Nambara, T., Nagakura, R. and Suzuki, H.
 Studies on steroids. CCXXXVIII. Determination of bile acids in liver tissue by gas chromatography-mass spectrometry with negative ion chemical ionization detection 119
- Green, G., see Marshall, H.-U. 459
- Groen, C. P., see Tipker, J. 227
- Grushka, E., see Shohat, S. 503
- Guiochon, G., see Ghodbane, S. 209
- Haasnoot, W., see Farjam, A. 419
- Hais, I. M.
 Tswett's letter to Claparède on tropism and taxes 5
- Haken, J. K.
 — and Smith, R. J.
 Dispersion and selectivity indices of alkyl and alkenyl benzenes 31
- , Harahap, N. and Burford, R. P.
 Quantitative determination of dicarboxylic acids and polyols in silicone-polyester resins 37
- Hamers, A. R. M., see Farjam, A. 419
- Han, S. M., see Armstrong, D. W. 323
- Hanis, T.
 —, Smrz, M., Klir, P., Macek, K., Klima, J., Base, J. and Deyl, Z.
 Determination of fatty acids as phenacyl esters in rat adipose tissue and blood vessel walls by high-performance liquid chromatography 443
- Harahap, N., see Haken, J. K. 37
- Hartwick, R. A., see Floyd, T. R. 43
- Hawker, J. L., see Jack, D. B. 257
- Herényi, B., see Görög, S. 317
- Hongxin, H., see Peichang, L. 175
- Horvath, Cs., see Maa, Y.-F. 331
- Huang, T.
 —, Wall, F. and Kabra, P.
 Improved solid-phase extraction and liquid chromatography with electrochemical detection of urinary catecholamines and 5-S-L-cysteiny-L-dopa 409
- Huf, F. A., see Farjam, A. 419
- Inada, M., see Goto, J. 119
- Issaq, H. J.
 —, Williams, D. G., Schultz, N. and Saavedra, J. E.
 High-performance liquid chromatography separations of nitrosamines. III. Conformers of N-nitrosamino acids 511
- Jack, D. B.
 —, Hawker, J. L., Rooney, L., Beerah, M. Lobo, J. and Patel, P.
 Measurement of the distribution coefficients of several classes of drug using reversed-phase thin-layer chromatography 257
- Jackson, P. J.
 —, Turner, R., Keen, J. N., Brooksbank, R. A. and Cooper, E. H.
 Purification and partial amino acid sequence of human urine protein. I. Evidence for homology with rabbit uteroglobin 359
- Janča, J.
 — and Nováková, N.
 Retention in sedimentation-flotation focusing field-flow fractionation using a step density gradient 549
- Jaroniec, M., see Borówko, M. 131
- Jelínek, I., see Snopek, J. 571
- Jellum, E.
 Chromatography for diagnosis of metabolic diseases 435
- Johansson, M.
 — and Westerlund, D.
 Effects of system peaks in ion-pair reversed-phase liquid chromatography for noscapine and metabolites 241
- Jong, G. J. de, see Farjam, A. 419
- Kabrà, P., see Huang, T. 409
- Kageyama, S., see O'Flynn, M. A. 469

- Kass-Simon, G., see Fadool, D. A. 491
Keen, J. N., see Jackson, P. J. 359
Kersten, B. R.
— and Poole, C. F.
 Considerations for using the solvent selectivity triangle approach for stationary phase characterization 191
Kisfaludy, L., see Görög, S. 317
Klima, J., see Hanis, T. 443
Klir, P., see Hanis, T. 443
Krstulović, A. M.
—, Fouchet, M. H., Burke, J. T., Gillet, G. and Durand, A.
 Direct enantiomeric separation of betaxolol with applications to analysis of bulk drug and biological samples 477
Krull, I. S., see Lookabaugh, M. 295
Kuksis, A., see Myher, J. J. 93
Kurganov, A. A., see Davankov, V. A. 309
Ladizinsky, G., see Milo, J. 563
Lederer, M.
 Some considerations on the 'charge' on a metal ion in ion-exchange Chromatography 265
Leenheer, A. P., De, see Nelis, H. J. C. F. 535
Levy, A., see Milo, J. 563
—, see Weissenberg, M. 485
Levy, E. C., see Weissenberg, M. 485
Lin, J.-T.
— and Stafford, A. E.
 Reversed-phase C_{18} and normal-phase silica high-performance liquid chromatography of gibberellins and their methyl esters 519
Lloyd, L. L., see Dawkins, J. V. 145
Lobo, J., see Jack, D. B. 257
Lookabaugh, M.
— and Krull, I. S.
 Determination of nitrite and nitrate by reversed-phase high-performance liquid chromatography using on-line post-column photolysis with ultra violet absorbance and electrochemical detection 295
Maa, Y.-F.
—, Antia, F. D., El Rassi, Z. and Horváth, Cs.
 Mixed-bed ion-exchange columns for protein high-performance liquid chromatography 331
McConville, J. A., see Dawkins, J. V. 145
Macek, K., see Hanis, T. 443
McNamara, E. A.
—, Montzka, S. A., Barkley, R. M. and Sievers, R. E.
 Superconductor metal oxide catalyst in a chemiluminescence chromatography detector 75
Mangani, F.
—, Crescentini, G., Palma, P. and Bruner, F.
 Performance of graphitized carbon black cartridges in the extraction of some organic priority pollutants from water 527
Marai, L., see Myher, J. J. 93
Marshall, H.-U.
—, Green, G., Egestad, B. and Sjövall, J.
 Isolation of bile acid glucosides and N-acetylglucosaminides from human urine by ion-exchange chromatography and reversed-phase high-performance liquid chromatography 459
Martin, M.
—, Thevenon, G. and Tchaplá, A.
 Comparison of retention mechanisms of homologous series and triglycerides in non-aqueous reversed-phase liquid chromatography 157
Martire, D. E.
 Unified theory of adsorption chromatography: gas, liquid and supercritical fluid mobile phases 17
Matsuura, S., see Niwa, T. 85
Michalec, Č.
— and Ranný, M.
 Potential application of thin-layer chromatography and thin-layer chromatography with flame ionization detection of cholestanol in the diagnosis of cerebrotendinous xanthomatosis 543
Milo, J.
—, Levy, A., Palevitch, D. and Ladizinsky, G.
 High-performance liquid chromatographic analysis of alkaloid spectrum in the roots and capsules of the species and hybrids of *Papaver* section *Oxytona* 563
Miura, H., see Goto, J. 119
Montzka, S. A., see McNamara, E. A. 75
Mori, S.
 Interchangeable use of aqueous and organic solvents in a hydrophilic poly(vinyl alcohol) gel column 137
Mutti, A., see Ghiggeri, G. M. 347
Myher, J. J.
—, Kuksis, A. and Marai, L.
 Identification of the more complex triacylglycerols in bovine milk fat by gas chromatography-mass spectrometry using polar capillary columns 93
Nagakura, R., see Goto, J. 119
Nagatsu, R., see Niwa, T. 85
Nakayama, F.
 Quantitative microanalysis of bile acids in biological samples. Collaborative study 399
Nambara, T., see Goto, J. 119

- Nelis, H. J. C. F.
 — and De Leenheer, A. P.
 Reversed-phase liquid chromatography of as-tacene 535
- Nes, W. D., see Xu, S. 377
- Niwa, T.
 —, Takeda, N., Tatematsu, A., Matsuura, S., Yoshida, M. and Nagatsu, R.
 Migration of tetrahydroisoquinoline, a possible parkinsonian neurotoxin, into monkey brain from blood as proved by gas chromatography-mass spectrometry 85
- Norton, R. A., see Xu, S. 377
- Nováková, N., see Janča, J. 549
- Novotny, M., see David, P. A. 623
- Nyéki, O., see Görög, S. 317
- O'Flynn, M. A.
 —, Causon, R. C., Brown, J. and Kageyama, S.
 Development of a solid-phase extraction technique for α -human atrial natriuretic peptide in human plasma 469
- Palevitsch, D., see Milo, J. 563
- Palma, P., see Mangani, F. 527
- Patel, P., see Jack, D. M. 257
- Peichang, L.
 — and Hongxin, H.
 Expert system for chromatography 175
- Ponomareva, T. M., see Davankov, V. A. 309
- Poole, C. F., see Kersten, B. R. 191
- Ranný, M., see Michalec, Č. 543
- Rassi, Z. El, see Maa, Y.-F. 331
- Righetti, P. G., see Ghiggeri, G. M. 347
- Rooney, L., see Jack, D. B. 257
- Saavedra, J. E., see Issaq, H. J. 511
- Sagliano, Jr. N., see Floyd, T. R. 43
- Satterwhite, D. M.
 — and Croteau, R. B.
 Applications of gas chromatography to the study of terpenoid metabolism 61
- Schaeffler, I., see Weissenberg, M. 485
- Schilt, R., see Farjam, A. 419
- Schön, I., see Görög, S. 317
- Schultz, N., see Issaq, H. J. 511
- Schwedt, G., see Golombek, F. 283
- Shohat, S.
 —, Grushka, E. and Glikberg, S.
 Liquid chromatographic analysis of organic additives in copper plating baths 503
- Sievers, R. M., and see McNamara, E. A. 75
- Sjövall, J., see Marshall, H.-U. 459
- Smith, R. J., see Haken, J. K. 31
- Smolková-Keulemansová, E., see Snopek, J. 571
- Smrz, M., see Hanis, T. 443
- Snopek, J.
 —, Jelínek, I. and Smolková-Keulemansová, E.
 Micellar, inclusion and metal-complex enantioselective pseudophases in high-performance electromigration methods 571
- Stafford, A. E., see Lin, J.-T. 519
- Suzuki, H., see Goto, J. 119
- Takeda, N., see Niwa, T. 85
- Tatematsu, A., see Niwa, T. 85
- Tchapla, A., see Martin, M. 157
- Thevenon, G., see Martin, M. 157
- Tipker, J.
 —, Groen, C. P., Van den Bergh-Swart, J. K. and Van den Berg, J. H. M.
 Contribution of electronic effects to the lipophilicity determined by comparison of values of log *P* obtained by high-performance liquid chromatography and calculation 227
- Trainor, T. M.
 —, Giese, R. W. and Vouros, P.
 Mass spectrometry of electrophore-labeled nucleosides pentafluorobenzyl and cinnamoyl derivatives 369
- Turner, R., see Jackson, P. J. 359
- Van den Berg, J. H. M., see Tipker, J. 227
- Van den Bergh-Swart, J. K., see Tipker, J. 227
- Verheggen, Th. P. E. M.
 —, Beckers, J. L. and Everaerts, F. M.
 Simple sampling device for capillary isotachopheresis and capillary zone electrophoresis 615
- , see Beckers, J. L. 591
- Vouros, P., see Trainor, T. M. 369
- Wall, F., see Huang, T. 409
- Warner, F. P., see Dawkins, J. V. 145
- Weissenberg, M.
 —, Levy, A., Schaeffler, I. and Levy, E. C.
 High-performance liquid chromatographic analysis of the ajmalicine distribution in roots of *Catharanthus roseus* lines with different flower colours 485
- Westerlund, D., see Johansson, M. 241
- Williams, D. G., see Issaq, H. J. 511
- Xu, S.
 —, Norton, R. A., Crumley, F. G. and Nes, W. D.
 Comparison of the chromatographic properties of sterols, select additional steroids and triterpenoids: gravity-flow column liquid chromatography, thin-layer chromatography, gas-liquid chromatography and high-performance liquid chromatography 377
- Yoshida, M., see Niwa, T. 85

PUBLICATION SCHEDULE FOR 1988

Journal of Chromatography and Journal of Chromatography, Biomedical Applications

MONTH	J	F	M	A	M	J	J	A	S	O	N	D
Journal of Chromatography	435/1 435/2 435/3 436/1	436/2 436/3	437/1 437/2	438/1 438/2	439/1 439/2 440 441/1	441/2 442 443	444 445/1 445/2 446	447/1 447/2 448/1	448/2 448/3 449/1	449/2 450/1 450/2 450/3 452	The publication schedule for further issues will be published later.	
Bibliography Section		460/1		460/2		460/3		460/4		460/5		460/6
Cumulative Indexes, Vols. 401-450												451
Biomedical Applications	424/1	424/2	425/1 425/2	426/1 426/2	427/1	427/2 428/1	428/2 429	430/1	430/2 431/1	431/2	432	433 434

INFORMATION FOR AUTHORS

(Detailed *Instructions to Authors* were published in Vol. 445, pp. 453-456. A free reprint can be obtained by application to the publisher, Elsevier Science Publishers B.V., P.O. Box 330, 1000 AH Amsterdam, The Netherlands.)

Types of Contributions. The following types of papers are published in the *Journal of Chromatography* and the section on *Biomedical Applications*: Regular research papers (Full-length papers), Notes, Review articles and Letters to the Editor. Notes are usually descriptions of short investigations and reflect the same quality of research as Full-length papers, but should preferably not exceed six printed pages. Letters to the Editor can comment on (parts of) previously published articles, or they can report minor technical improvements of previously published procedures; they should preferably not exceed two printed pages. For review articles, see inside front cover under Submission of Papers.

Submission. Every paper must be accompanied by a letter from the senior author, stating that he is submitting the paper for publication in the *Journal of Chromatography*. Please do not send a letter signed by the director of the institute or the professor unless he is one of the authors.

Manuscripts. Manuscripts should be typed in double spacing on consecutively numbered pages of uniform size. The manuscript should be preceded by a sheet of manuscript paper carrying the title of the paper and the name and full postal address of the person to whom the proofs are to be sent. Authors of papers in French or German are requested to supply an English translation of the title of the paper. As a rule, papers should be divided into sections, headed by a caption (*e.g.*, Summary, Introduction, Experimental, Results, Discussion, etc.). All illustrations, photographs, tables, etc., should be on separate sheets.

Introduction. Every paper must have a concise introduction mentioning what has been done before on the topic described, and stating clearly what is new in the paper now submitted.

Summary. Full-length papers and Review articles should have a summary of 50-100 words which clearly and briefly indicates what is new, different and significant. In the case of French or German articles an additional summary in English, headed by an English translation of the title, should also be provided. (Notes and Letters to the Editor are published without a summary.)

Illustrations. The figures should be submitted in a form suitable for reproduction, drawn in Indian ink on drawing or tracing paper. Each illustration should have a legend, all the legends being typed (with double spacing) together on a *separate sheet*. If structures are given in the text, the original drawings should be supplied. Coloured illustrations are reproduced at the author's expense, the cost being determined by the number of pages and by the number of colours needed. The written permission of the author and publisher must be obtained for the use of any figure already published. Its source must be indicated in the legend.

References. References should be numbered in the order in which they are cited in the text, and listed in numerical sequence on a separate sheet at the end of the article. Please check a recent issue for the layout of the reference list. Abbreviations for the titles of journals should follow the system used by *Chemical Abstracts*. Articles not yet published should be given as "in press" (journal should be specified), "submitted for publication" (journal should be specified), "in preparation" or "personal communication".

Dispatch. Before sending the manuscript to the Editor please check that the envelope contains three copies of the paper complete with references, legends and figures. One of the sets of figures must be the originals suitable for direct reproduction. Please also ensure that permission to publish has been obtained from your institute.

Proofs. One set of proofs will be sent to the author to be carefully checked for printer's errors. Corrections must be restricted to instances in which the proof is at variance with the manuscript. "Extra corrections" will be inserted at the author's expense.

Reprints. Fifty reprints of Full-length papers, Notes and Letters to the Editor will be supplied free of charge. Additional reprints can be ordered by the authors. An order form containing price quotations will be sent to the authors together with the proofs of their article.

Advertisements. Advertisement rates are available from the publisher on request. The Editors of the journal accept no responsibility for the contents of the advertisements.

Automatic Methods of Analysis

by **M. VALCÁRCEL** and **M.D. LUQUE DE CASTRO**,
*Department of Analytical Chemistry, University of Córdoba,
Córdoba, Spain*

(Techniques and Instrumentation in Analytical Chemistry, 9)

This new book gives a comprehensive overview of the state of the art of the automation of laboratory processes in analytical chemistry. The topics have been chosen according to such criteria as the degree of consolidation, scope of application and most promising trends.

The book begins with the basic principles behind the automation of laboratory processes, then describes automatic systems for sampling and sample treatment. In the second part the principal types of analysers are discussed: continuous, batch and robotic. The third part is devoted to the automation of analytical instrumentation: spectroscopic, electroanalytical and chromatographic techniques and titrators. The last part presents examples of the application of automation to clinical chemistry, environmental pollution monitoring and industrial process control.

The text is supplemented by 290 figures and 800 literature references. It is written primarily for those directly involved in laboratory work or responsible for industrial planning and control, research centres, etc. It will also be useful to analytical chemists wishing to update their knowledge in this area, and will be of especial interest to scientists directly related to environmental sciences or clinical chemistry.

CONTENTS:

1. Fundamentals of Laboratory Automatic
2. Computers in the Laboratory.
3. Automation of Sampling.
4. Automation in Sample Treatment.
5. Automatic Continuous Analysers: Air-Segmented Flow Analysers.
6. Automatic Continuous Analysers: Flow-Injection Analysis.
7. Automatic Continuous Analysers: Other Automatic Unsegmented Flow Methods.
8. Automatic Batch Analysers.
9. Robots in the Laboratory.
10. Automation of Analytical Instrumentation: Spectrometric Techniques.
11. Automation of Analytical Instrumentation: Electroanalytical Techniques.
12. Automation of Analytical Instrumentation: Chromatographic Techniques.
13. Automatic Titrators.
14. Automation in Clinical Chemistry.
15. Automation in Environmental Pollution Monitoring.
16. Process Analysers.

1988 xii + 560 pages
US\$ 131.50 / Dfl. 250.00
ISBN 0-444-43005-9



ELSEVIER SCIENCE PUBLISHERS

P.O. Box 211, 1000 AE Amsterdam, The Netherlands
P.O. Box 882, Madison Square Station, New York, NY 10159, USA